UNCLASSIFIED

AD 268 353

Reproduced
by the

ARMED SERVICES TECHNICAL INFORMATION AGENCY
ARLINGTON HALL STATION
ARLINGTON 12, VIRGINIA



UNCLASSIFIED

NOTICE: When government or other drawings, specifications or other data are used for any purpose other than in connection with a definitely related government procurement operation, the U. S. Government thereby incurs no responsibility, nor any obligation whatsoever; and the fact that the Government may have formulated, furnished, or in any way supplied the said drawings, specifications, or other data is not to be regarded by implication or otherwise as in any manner licensing the holder or any other person or corporation, or conveying any rights or permission to manufacture, use or sell any patented invention that may in any way be related thereto.

268353

62-1-5
XEROX

PROCEEDINGS OF THE SEVENTH SAGAMORE
ORDNANCE MATERIALS RESEARCH CONFERENCE

MECHANICAL AND METALLURGICAL BEHAVIOR OF SHEET MATERIALS

CATALOGED BY ASTIA
AS AD No.
268 353

Conducted at
SAGAMORE CONFERENCE CENTER
RACQUETTE LAKE, NEW YORK
August 16 to 19, 1960

Contract No. DA-30-069-ORD-2566

Co-sponsored by the

ORDNANCE MATERIALS RESEARCH OFFICE

and

THE OFFICE OF ORDNANCE RESEARCH
of the
U.S. ARMY

ASTIA
DEC 26 1961
TIPDR

Arrangements by



SYRACUSE UNIVERSITY RESEARCH INSTITUTE

Met E 661-611/F

Best
Available
Copy

PROCEEDINGS

of the

SEVENTH SAGAMORE ORDNANCE MATERIALS RESEARCH CONFERENCE

MECHANICAL and METALLURGICAL BEHAVIOR

of

SHEET MATERIALS

Conducted at
Sagamore Conference Center
Raquette Lake, New York
August 16 to 19, 1960

Contract No. DA-30-069-ORD-2566

Co-sponsored by the
ORDNANCE MATERIALS RESEARCH OFFICE
and the
OFFICE of ORDNANCE RESEARCH
of the
U.S. ARMY

Arrangements by
Syracuse University Research Institute, Syracuse 10, N.Y.



Dr. George Sachs

IN MEMORIAM

Dr. George Sachs was a key figure in initiation and development of the Sagamore Ordnance Materials Research Conference Series of which this conference was the seventh. Its success and popularity are due, in no small measure, to the driving force and imagination of Dr. Sachs. His knowledge and experience contributed greatly to the development of excellent programs. These conferences which attracted participants from this country and abroad are recognized as among the most informative and popular in the United States. Dr. Sachs' own vigorous participation in the discussions and presentations gave all who were "exposed" to him an opportunity to appraise and appreciate his genius as well as his geniality.

Dr. Sachs death on 29 October 1960, leaves a large void in the scientific community. However, his presence will long be felt in the many committees on which he has served and the conferences in which he has participated not only by the memory of him, but also by the frequent references which will be made to his voluminous technical publications.

The proceedings of this, the Seventh Sagamore Ordnance Materials Conference are respectfully dedicated to the memory of Dr. George Sachs by all those who have been priviledged to know and work with him in the Sagamore Ordnance Materials Research Conferences.

The Seventh Sagamore Conference Committee

PREFACE

The papers and proceedings assembled in this report were presented at the Seventh Sagamore Ordnance Materials Research Conference which was held at Syracuse University's Adirondack Conference Center near Raquette Lake, New York, from August 16th to the 19th, 1960. Syracuse University Research Institute made the arrangements for conducting this conference with the assistance of the Adirondack Conference Center staff under Contract No. DA-30-069-ORD-2566 (modification No. 1). The conference was co-sponsored by the Ordnance Materials Research Office and the Office of Ordnance Research, U.S. Army. The general planning and operations were transacted through a committee composed of representatives of the contracting parties, with Dr. George Sachs of Syracuse University Research Institute as Chairman of the Conference Committee.

This research conference was the seventh of a series devoted to subjects on materials of primary interest to the U.S. Army Ordnance Corps. The intent was to provide governmental and associated non-governmental groups with an up-to-the-minute, correlated picture of the status of present utilization and the future of high strength sheet materials. Special consideration was given to the mechanical and metallurgical behavior of the alloys not only in the form of flat sheet but also in all fabricated forms which typify thin-walled pressure vessels.

The scope of this conference included a definitive analysis of sheet material problems and the influences that fabrication techniques have on the mechanical and metallurgical characteristics. Correlation of basic material properties, the results of laboratory tests and service behavior at temperatures from -100 to +500 F were the prime concern. The lectures and discussions presented helped to clarify the sheet material situation and suggested possible future research programs in order that the ultimate goal of utilization of high strength materials be attained and in order that laboratory tests to predict service behavior be established.

A total of 40 persons consisting of outstanding investigators in this field contributed definitions of problems, advanced theories and presented results of recent work. This group was made up from government agencies, industry, universities and research institutes. Papers were presented by 15 representatives of government, 8 from universities and research institutes and 17 from private industry.

The conference proceedings include the manuscripts and prepared discussions submitted by the speakers and the discussions from the attendees, as tape recorded and transcribed by Technocopy Incorporated of New York City. These discussions were corrected by the participants dur-

ing or shortly after the conference. Some portions of these discussions and the related questions and answers have been deleted at the request of the authors. The manuscripts, discussions and other material were compiled, edited and prepared for publication by J. V. Latorre, Conference Secretary and other members of the Syracuse University Metallurgical Research Laboratory staff with the assistance of A. F. Jones of the Ordnance Materials Research Office.

The Committee is greatly indebted to all those contributing to the success of this conference, and particularly to the speakers and moderators for their efforts to summarize voluminous data in their fields and their contributions of preprints and manuscripts ready for reproduction.

The attendees were welcomed by Dr. R. A. Galbraith, Dean of the College of Engineering at Syracuse University; Dr. J. L. Martin, Director of the Ordnance Materials Research Office at Watertown, Massachusetts; and Dr. John Dawson, Chief Scientist of the Office of Ordnance Research at Durham, North Carolina. The main dinner speaker was John Stack, Assistant Director of the Langley Research Center, National Aeronautics and Space Administration, Langley Field, Virginia who gave an interesting and challenging talk on "Prospects and Problems for the Supersonic Commercial Air Transport."

The Committee commends the Technocopy representatives for their execution of the difficult task of accurately and completely recording and transcribing the discussion. The Committee also commends Syracuse University's Adirondack Conference Center under Dr. Robert Snow and the Food Service Department for providing the excellent facilities at the Sagamore Conference Center.

The continued active interest and support in the conduct of these conferences by Dr. J. L. Martin, Director of the Ordnance Materials Research Office and Col. G. Taylor, Commanding Officer of the Office of Ordnance Research is also appreciated.

by the Conference Committee

R. Beeuwkes, Jr.	Ordnance Materials Research Office
W. F. Brown, Jr.	National Aeronautics & Space Administration
J. Burke	Ordnance Materials Research Office
A. Jones	Ordnance Materials Research Office
J. V. Latorre	Secretary Syracuse University Research Institute
N. L. Reed	Ordnance Materials Research Office
G. Sachs	Chairman Syracuse University Research Institute

TABLE OF CONTENTS

	Page
PREFACE	IV
PROGRAM	IX
SESSION I: REQUIREMENTS OF HIGH STRENGTH SHEET MATERIALS	
Moderator: G. Sachs, Syracuse University Research Institute, Syracuse, New York	
1. "Material Problems in Solid Fuel Case Design and Manufacture," G. Sachs	I-1
2. "Army Requirements," J. Burke	I-39
3. "High Strength Sheet and Plate in Navy Equipment," T. F. Kearns	I-43
4. "Air Force Developments for High Strength Material," P. L. Hendricks	I-57
5. "Experience With Ultra High Strength Forgings in Aircraft Structures," G. Wald	I-61
6. "Need for Basic Information," R. Beeuwkes, Jr.	I-84
SESSION II: MATERIALS, THEIR PROPERTIES AND CHARACTERISTICS	
Moderator: S. V. Arnold, Watertown Arsenal, Watertown, Mass.	
1. "Materials, Their Properties and Characteristics," S. V. Arnold	II-1
2. "A Modern High-strength Steel for Ordnance Applications," C. M. Carman	II-31
3. "High Alloy Ferritic Steels for Ordnance Applications," R. C. Powell	II-59
4. "Titanium Alloys for Solid Rocket Casings," W. H. Sharp	II-71
5. "Cold Rolled Stainless Steel," J. F. Watson, J. L. Christian	II-79
6. "Strain Hardening Properties of High Strength Sheet Materials," F. Larson, J. Nunes	II-101
Discussion	II-167
SESSION III: EFFECTS OF FABRICATION VARIABLES	
Moderator: W. A. Backofen, Massachusetts Institute of Technology, Cambridge, Mass.	
1. "Influence of Fabrication History on Mechanical and Metallurgical Behavior of Sheet Materials," W. A. Backofen	III-1
2. "Defects, Surface Finishes, and Hydrogen Embrittlement," C. E. Spaeth	III-[illegible]

		Page
3.	"Effects of Forming," W. J. Wilson	III-39
4.	"Aus-Shear Forming of Low Alloy Steel Cylinders," E. S. Jones	III-63
5.	"The Effects of Procedural Variables on the Properties of Butt Welds," C. M. Adams	III-83
6.	"Fusion Welding High Strength Titanium Sheet," C. E. Hartbower	III-101
	Discussion	III-129

SESSION IV: FRACTURE, CRACK INITIATION AND PROPAGATION
Moderator: V. Weiss, Syracuse University Research Institute, Syracuse, N. Y.

1.	"Fracture, Crack Initiation and Propagation," V. Weiss	IV-1
2.	"Behavior of a Brittle Metal," J. G. Sessler	IV-33
3.	"Characteristics of Fracture Appearance of Steels and Titanium Alloys," J. E. Srawley	IV-43
4.	"Plastic Zone Near a Crack and Fracture Toughness," G. Irwin	IV-63
5.	"Crack Arrest in Thin-Walled Pressure Vessels," J. Bluhm	IV-79
6.	"Slow Crack Extension Preceding Unstable Fracture, H. T. Corten	IV-115
7.	"Embrittlement by Liquid Metals," W. Rostoker	IV-159
	Discussion	IV-169

SESSION V: MECHANICAL SCREENING TESTS
Moderator: W. F. Brown, Jr., National Aeronautics & Space Administration, Lewis Research Center Cleveland, Ohio

1.	"Mechanical Screening Tests," W. F. Brown, Jr.	V-1
2.	"Standardization of Test Procedure for Tear Resistance of Metallic Sheet Material," T. J. Stapleton	V-41
3.	"Dynamic Notched Screening Test," A. J. Brothers, H. Martens	V-79
4.	"Instrumented Bend Tests Applied to Pressure Vessel Reliability," R. McPhee, K. E. Muszar, G. R. Sippel, G. L. Vonnegut	V-83
5.	"The Effect of Specimen Geometry on Determination of Elongation in Sheet Tensile Specimens," E. B. Kula, N. H. Fahey	V-105
6.	"The Use of Shear-Cracked Specimens for Evaluation of Sheet Materials," J. D. Morrison, J. R. Kattus	V-127
7.	"Screening Tests for Notch Toughness of Sheet," E. W. Brady	V-141
	Discussion	V-144

SESSION VI: MECHANICAL MODEL TESTING
Moderator: A. Hurlich, Convair Astronautics, San Diego, California

1.	"Mechanical Model Testing," A. Hurlich	VI-1

Page

2. "Hydrodynamic Testing of Thin-Walled Cylinders," K. H. Abbott VI-11
3. "Evaluation of Biaxial Properties of Rocket Motor Case Material Using Sub-Scale Specimens," G. K. Bhat, D. V. Lindh VI-23
4. "The Correlation of Laboratory Specimen and Strip Wound Pressure Vessel Tests," R. J. Voth VI-55
5. "Full Scale Pershing Motor Case Burst Tests (Titanium and Steel)," C. A. Tidwell, Jr. VI-73
6. "Model (Subscale) Testing and Significance," E. C. Schneider VI-75
7. "Rocket Casing Behavior Predicted by Laboratory Tests," J. D. Marble VI-89
8. "Simulated Service Evaluations of Steels for Solid-Propellant Missile Motor Cases," K. E. Caine, J. M. Hodge, R. D. Manning, W. J. Murphy, H. J. Nichols, H. M. Reichhold VI-91
Discussion VI-93

DINNER SPEAKER:

"The Materials Problems of the Supersonic Transport", Appendix A
John Stack

LIST OF ATTENDEES Appendix B

TECHNICAL PROGRAM

Tuesday, August 16, 1960

5:00 p.m.

Opening by Conference Chairman:
Prof. Dr. George Sachs,
Associate Director
Syracuse University Research Institute

Welcoming Addresses:
For Syracuse University:
Dr. Clark D. Ahlberg, Vice President
for Administration & Research

For Ordnance Materials Research Office:
Dr. J. L. Martin, Director
Watertown, Massachusetts

For Office of Ordnance Research:
Col. George Taylor, Commanding Officer,
Dr. John Dawson, Chief Scientist

7:00 p.m.

SESSION I

REQUIREMENTS OF HIGH STRENGTH SHEET MATERIALS

Moderator:

G. Sachs, Syracuse University Research Institute, Syracuse, New York
"Material Problems in Solid Fuel Case Design and Manufacture"

Lectures:

J. Burke, Ordnance Materials Research Office, Watertown, Mass.
"Army Requirements"

T. F. Kearns, Bureau of Naval Weapons Washington, D.C.
"High Strength Sheet and Plate in Navy Equipment"

P. L. Hendricks, Wright Air Development Division, Wright Patterson Air Force Base, Ohio
"Air Force Developments for High Strength Material"

G. Wald, Lockheed Aircraft Corp., Burbank, California
"Experience With Ultra High Strength Forgings in Aircraft Structures"

R. Beeuwkes, Jr., Ordnance Materials Research Office, Watertown, Mass.
"Need for Basic Information"

Paper to be presented by L. Schapiro

Wednesday, August 17, 1960

8:30 a.m.

SESSION II
MATERIALS, THEIR PROPERTIES AND CHARACTERISTICS

Moderator:

S. V. Arnold, Watertown Arsenal Watertown, Mass.
"Materials, Their Properties and Characteristics"

Lectures:

C. M. Carman, Frankford Arsenal Philadelphia, Pennsylvania
"A Modern High Strength Steel for Ordnance Applications"

R. C. Powell, Pratt & Whitney Aircraft Corp., East Hartford, Connecticut
"High Alloy Ferritic Steels for Ordnance Applications"

W. H. Sharp, Pratt & Whitney Aircraft Corp., East Hartford, Conn.
"Titanium Alloys for Solid Rocket Casings"

J. F. Watson, J. L. Christian
Convair Astronautics, San Diego, Calif.
"Cold Rolled Stainless Steel"

F. R. Larson, J. Nunes
Watertown Arsenal, Watertown, Mass.
"Strain Hardening Properties of High Strength Sheet Materials

Discussion

7:00 p.m.

SESSION III

EFFECTS OF FABRICATION VARIABLES

Moderator:

W. A. Backofen, Massachusetts Institute of Technology, Cambridge, Mass.
"Influence of Fabrication History on Mechanical and Metallurgical Behavior of Sheet Materials"

Lectures:

C. E. Spaeth, Pratt & Whitney Aircraft Corp., East Hartford, Conn.
"Defects, Surface Finishes and Hydrogen Embrittlement"

W. J. Wilson, Kaiser Fleetwings
Bristol, Pennsylvania
"Effects of Forming"

E. S. Jones, Flight Propulsion Laboratory Department, General Electric Co.
Cincinnati, Ohio
"Aus-Shear Forming of Low Alloy Steel Cylinders"

C. M. Adams, Massachusetts Institute of Technology, Cambridge, Mass.
"The Effects of Procedural Variables on the Properties of Butt Welds"

C. E. Hartbower
Watertown Arsenal, Watertown, Mass.
"Fusion Welding High Strength Titanium Sheet"

Discussion

Thursday, August 18, 1960

8:30 a.m.

SESSION IV

FRACTURE, CRACK INITIATION AND PROPAGATION

Moderator:

V. Weiss, Syracuse University Research Institute, Syracuse, N.Y.
"Fracture, Crack Initiation and Propagation"

Lectures:

J. G. Sessler, Syracuse University Research Institute, Syracuse, N.Y.
"Behavior of a Brittle Metal"

J. E. Srawley, Naval Research Laboratory, Washington, D.C.
"Characteristics of Fracture Appearance of Steels and Titanium Alloys"

G. Irwin, Naval Research Laboratory, Washington, D.C.
"Plastic Zone Near a Crack and Fracture Toughness"

J. Bluhm, Watertown Arsenal Watertown, Mass.
"Crack Arrest in Thin-Walled Pressure Vessels"

H. T. Corten, University of Illinois, Urbana, Illinois
"Slow Crack Extension Preceding Unstable Fracture"

W. Rostoker, Armour Research Foundation, 10 West 35th St. Chicago, Illinois
"Embrittlement by Liquid Metals"

Discussion

3:00 p.m.

SESSION V

MECHANICAL SCREENING TESTS

Moderator:

W. F. Brown, Jr., National Aeronautics & Space Administration, Lewis Research Center, Cleveland, Ohio
"Mechanical Screening Tests for Sheet Alloys"

Lectures:

T. J. Stapleton, Lockheed Aircraft Corp. Burbank California
"Standardization of Test Procedure for Tear Resistance of Metallic Sheet Material"

A. J. Brothers, General Electric Co. Schenectady, N. Y.
H. Martens, Jet Propulsion Laboratory Pasadena, California
"Dynamic Notched Screening Test"

R. McPhee, K. E. Muszar, G. R. Sippel, G. L. Vonnegut, Materials Research Lab. General Motors Corporation
"Instrumented Bend Tests Applied to Pressure Vessel Reliability"

E. B. Kula, N. H. Fahey
Watertown Arsenal, Watertown, Mass.
"The Effect of Specimen Geometry on Determination of Elongation in Sheet Tensile Specimens"

J. D. Morrison, J. R. Kattus, Southern Research Institute, Birmingham, Alabama
"The Use of Shear-Cracked Specimens for Evaluation of Sheet Materials"

E. W. Brady, Aerojet General Corp., Solid Rocket Plant, Sacramento, California
"Screening Tests for Notch Toughness of Sheet"

Discussion

Friday, August 19, 1960

8:30 a.m.

SESSION VI

MECHANICAL MODEL TESTING

Moderator:

A. Hurlich, Convair Astronautics
San Diego, California
"Mechanical Model Testing"

Lectures:

K. H. Abbott, Watertown Arsenal
Watertown, Mass.
"Hydrodynamic Testing of Thin-Walled Cylinders"

G. K. Bhat, D. V. Lindh
Mellon Institute, Pittsburgh, Pa.
"Evaluation of Biaxial Properties of Rocket Motor Case Material Using Sub-Scale Specimens"

R. J. Voth, Ryan Aeronautical Co.
San Diego, California
"The Correlation of Laboratory Specimen and Strip Wound Pressure Vessel Tests"

C. A. Tidwell, Jr., Marshall Space Flight Center, National Aeronautics & Space Administration, Redstone Arsenal
Huntsville, Alabama
"Full Scale Pershing Motor Case Burst Tests (Titanium and Steel)"

E. C. Schneider, Pratt & Whitney Aircraft, E. Hartford, Conn.
"Model (Subscale) Testing and Significance"

J. D. Marble, Flight Propulsion Laboratory Dept., General Electric Co., Cincinnati, Ohio
"Rocket Casing Behavior Predicted by Laboratory Tests"

K. E. Caine, J. M. Hodge, R. D. Manning,
W. J. Murphy, H. J. Nichols,
H. M. Reichhold, U. S. Steel Corp.
Applied Research Lab., Monroeville, Pa.
"Simulated Service Evaluations of Steels for Solid-Propellant Missile Motor Cases"

Discussion

DINNER SPEAKER:

"The Materials Problems of the Supersonic Transport",
John Stack, NASA Langley Research Center

LIST OF ATTENDEES

FIRST SESSION

"Requirements of High Strength Sheet Materials"

MATERIAL PROBLEMS IN SOLID FUEL CASE DESIGN AND MANUFACTURE

By
George Sachs
Syracuse University

INTRODUCTION

0.0 The introductory lecture for this conference will present an abstract of the problems facing the designer and manufacturer of large diameter pressure vessels having small wall thickness. This discussion will concern primarily the material and strength requirements for the cylindrical portion of the vessel. It is this part of the vessel where the strength-to-weight ratio of the material used is of greatest significance for the weight of the entire structure.

The problems encountered in producing a solid fuel rocket motor case which will survive the service stresses are very complicated. The materials used can be considered as semibrittle or brittle. The properties depend greatly on a number of design parameters and on the history of the material from alloying to assembling. The individual problems encountered will be dissected and, I hope, cured by the many experts in the various sessions. The objective of my lecture is to introduce these problems and attempt to assemble them into a coherent story.

1. SERVICE REQUIREMENTS

The service requirements for a solid fuel motor case are threefold, namely:

1.1 The vessel must withstand during service, a single pressure cycle without either (a) yielding or (b) bursting. It is the peak load at the very beginning for which the vessel is designed. At this load, the circumferential stress in the cylinder should be equal to or a certain value below the yield strength of the material. Using the yield strength determined by means of a tensile test, a factor of safety between 1.00 and 1.15 is used by different designers.

There also should be a certain margin of safety between the design stress and the ultimate burst strength of the vessel. This second factor of safety is between 1.25 and 1.50.

1.2 Each vessel is subjected to a proof pressure test to insure that it will conform to the yield strength requirement. It is loaded to the design stress. Any vessel which passes this test is considered as usable.

Occasionally the proof test is repeated several times. No particular benefit can be ascribed to this procedure of repeated proof testing. Loading-unloading cycles to high stresses may take some ductility and, if the ductility is low, some strength out of the vessel. In general, therefore, proof testing damages metallic materials.

1.3 A limited number of vessels are subjected to destructive testing, determining the burst pressure and the nominal (circumferential) ultimate burst strength.

Occasionally the yield strength of a vessel derived from such tests has been reported. However, just what the yield strength of a pressure vessel is, has not been clearly defined. Theoretical concepts postulate that the vessel when loaded to its 0.2 percent yield strength should expand permanently in circumference by a value that exceeds 0.2 percent.

However, a volume change of 0.2 percent is frequently used as a measure of yielding, and this corresponds to an average change in diameter of only 0.1 percent.

1.4 In addition, it has been proposed that the fracture mode should be specified. There may be some merit to a ductile appearing failure, consisting of a single or branched longitudinal crack, rather than to a brittle fragmentation of the case. However, it is difficult to visualize how such a subjective criterion can be fully controlled.

2. GENERAL MATERIAL PROBLEMS

2.1 Any one metallic material under consideration for a motor case is generally characterized by two criteria obtainable from a tensile test; namely, the 0.2 percent tensile yield strength and the (ultimate) tensile strength. In addition, only alloys which show sufficient ductility in tension to allow the load to pass through a maximum before failure are in use at present.

2.2 The tensile and yield strength determine the potential of a material in the form of a pressure vessel.

However, the relations between these values and the yield and the ultimate strength in bursting are complex, for a variety of reasons.

2.3 It is frequently doubtful whether the condition of the material of the tension specimen and the vessel are identical.

2.4 All theoretical and experimental evidence available clearly indicates that for identical materials the values in bursting should differ from those in tension.

Also, this deviation is expected to be different for the yield strength than for the ultimate strength.

2.5 Premature failure of a metal may occur in bursting, because the ductility of a vessel is generally lower than that of a tension test specimen.

2.6 This is caused in part by the biaxial state of stress in the pressurized vessel as contrasted with the uniaxial state of stress in the tension test.

To date, no definite evidence exists on the embrittling effect of this particular biaxiality on the ductility of high strength material.

2.7 Other factors which can generally be classified as "stress raisers" exist, further reduce the ductility of a high strength material.

To evaluate the sensitivity of a metal in this respect, one of several types of notch tests are generally used.

2.8 In addition, the fact that the structure of the material may be nonuniform enters into the picture. This applies, for example, to the unfavorable effect of the highly stressed welds and weld affected zones, as well as to the favorable effect of decarburization of steels.

3. YIELD STRENGTH

3.1 A fundamental approach to the problem of vessel strength can be applied only to isotropic or nondirectional metal products. In the case of a vessel it may be satisfactory to consider a material which possesses the same yield and ultimate strength for longitudinal and circumferential specimens*.

3.2 The fundamental effect of biaxiality on the yield strength (F_y) is the subject of various "plasticity conditions."

The frequently preferred "distortion energy" hypothesis predicts, for the stress ratios 2/1 and 1/2, a yield strength value of 1/16 times that for uniaxial tension, and for the stress state 1/1 the same yield strength as in tension.

Another theory, the maximum shearing stress theory, predicts equal yield strength values in all biaxial states, including 2/1 and 1/2.

For biaxial conditions, the two theories are usually represented by a square and an ellipse respectively, with the two principal stresses as coordinates, (see Fig. 1).

3.3 Extensive tests on a variety of materials primarily on small scale tubular specimens, subjected to combined longitudinal stress and internal pressure, have been conducted since 1926 to test the effects of biaxiality on yield strength (1, 2, 3)**. The results of these tests

---

* These two tests are termed uniaxial tension and may be alternatively characterized by the symbols 1/0 and 0/1 respectively. The stress state in the cylindrical portion of a closed vessel is characterized by the longitudinal tension being one half of the circumferential tension. It is given the symbol 1/2. It is also called plane strain state because the length of the case remains practically constant. The symbol 2/1 applies to a condition of plane strain, where the longitudinal tension is twice the circumferential tension. The tension in a pressurized sphere are equal in all directions and its symbol is 1/1. This state of stress is also called balanced biaxial stress state.

** Numbers refer to bibliography at end of text.

are generally between those predicted by the two theories mentioned in 3.2 (4).

Recently, such tests have also been extended to 4340 and D-6-A steels having various hardness (5). The D-6-A steel, in particular, was found to be nearly nondirectional. The yield strength values, F_y, derived from these tests are given in Fig. 2. The tubular specimens in this investigation were machined from bar stock, 2 in. OD, 2 in. cylindrical length and 0.050 in. wall thickness. Because of the relatively thick wall, a correction of 2-1/2 percent should be added to the measured values for the stress states 1/1 and 1/2, and of 1-1/4 percent for the stress states 2/1 and 0/1. These are derived from the distortion energy hypothesis. The average yield strength values derived from these tests are also shown in Fig. 1 with the longitudinal yield strength as ordinate and the circumferential stress as abscissae.

Fig. 1 and Fig. 2 confirm the conclusion derived from previous investigations that neither of the two plasticity theories quantitatively explains the dependence of yield strength F_y, on biaxiality (F_{ty} is the uniaxial yield strength in the longitudinal direction).

The ratio F_y/F_{ty} for the stress ratio 2/1 and 1/2 is found to be close to 1.12.

The ratio F_y/F_{ty} for the stress ratio 1/1 appears also to be greater than 1.0. The data in Figures 1 and 2 yield a value of 1.02, but considering the strain equivalent to 0.2 percent offset in uniaxial tension may change this value.

3.4 Burst tests on small and full size motor cases have been performed in a number of instances, but only a few investigators have provided yield strength values for the cylindrical portion.

These were generally compared with those obtained by tension tests on small specimens. There is some question whether the material, as well as the definition of yield strength in the two types of tests had been identical.

One of these investigations yields a ratio F_y/F_{ty} between 1.04 and 1.23 with an average value of 1.12 (6). Other reported data (see 4.8) give values for this ratio between about 0.95 and over 1.3.

4. ULTIMATE STRENGTH

4.1 The ultimate burst strength of a ductile vessel is a very complex material characteristic. In order to evaluate its significance and to establish ratios between the ultimate strength in bursting and in uniaxial tension, not only biaxiality but also the stress strain characteristics of the particular material need to be considered.

These relations have been explored theoretically and to a limited extent also experimentally.

4.2 In order to analyze the effect of a particular material its stress-strain curves for various biaxialities should be known. The various plasticity theories have been extended in this respect, and numerous investigations have shown that the true tensile stress required to produce equivalent strains depends on biaxiality in much the same manner as the yield strength, (2, 3, 7, 9, 10). This means, that the ratios reported for yield strength at different biaxialities also apply approximately to higher stresses, for any equal value of equivalent or effective strain defined by the theories, Fig. 3 and Fig. 4. The two theories yield slightly different relations, but this is of little significance for the problem under consideration.

The stress-strain curves reported for D-6-A steel also appear in conformance with the results of the earlier tests, see Fig. 5.

4.3 The parallelity of the true-stress versus effective strain curves is not maintained if conventional rather than the true stresses are considered. The factors which transform true stress into conventional stress are different for different biaxialities.

Conventional tension stresses generally rise with increasing strain less than the true stress and pass through or terminate near a flat maximum, see Fig. 5.

4.4 The existence of such maxima, which are usually associated with strain localization or "necking" is quantitatively explained by the theory of tensional instability (11, 12). This theory predicts that the burst strength is reached at lower strains than the tensile strength (13). Its result is that a deduction in strength should be made when comparing ultimate burst strength with tensile strength. This deduction depends on the strain hardening capacity of the material. This problem has been extensively studied for both pressurized tubes, spheres and bulges (14-21).

Although the existence of pressure maxima and localized bulging are not established, the slope of conventional stress-strain curves appears clearly to be less steep for conditions of bursting than for those leading to tensional failure, see Fig. 5. Of particular in-

terest here is the difference between the curves for plane strain, or the stress states 2/1 and 1/2.

Tests to determine the validity and accuracy of the theory of tensional instability have apparently been performed only on bulges (18, 19).

4.5 The tests on 4340 and D-6-A steel tubes (22) permits the evaluation of the tensional instability effect for high strength steels. The results of the tests on D-6-A, Fig. 6 and Fig. 7, lead to the following ratios between the ultimate strength for a certain biaxiality, F_u, and that in tension, F_{tu}, and the differences between these and the yield strength ratios F_y/F_{ty}:

Stress State	F_u/F_{tu}	F_y/F_{tu}	$F_y/F_{tu} - F_u/F_{tu}$
1/0	(1.0)	(1.0)	(0)
2/1	1.105	1.115	0.010
1/1	1.00	1.02	0.02
1/2	1.08	1.12	0.04

These small scale tests yield an average value for the burst strength of a closed cylinder about 8 percent above the tensile strength. For the stress state 1/1, corresponding to a pressurized sphere, the tests indicate a burst strength equal to the tensile strength.

In agreement with the theory, the values for bursting in plane strain (1/2) are found to be slightly smaller, by 2 to 3 percent, than those for the same tensional stress state (2/1).

Furthermore, the ultimate strength ratios for conditions of bursting are found to be slightly below the respective yield strength ratios. This also agrees with theory.

4.6 Numerous burst tests have been performed on full size rocket cases and model vessel in high strength steel and titanium which are described in other parts of these proceedings.

A comparison of the (ultimate) burst strength values with the tensile strength of presumably identical material leads to ratios between 0.95 and 1.25.

Although the low values may be attributed to premature failures, no explanation can be given for the frequently observed very high values.

5. STRESS CONCENTRATION SENSITIVITY

5.1 Numerous failures have been encountered in the development and proof testing of motor cases. These are explained by the stress concentration sensitivity of ultra high strength steel. This phenomenon is the biggest obstacle to utilizing the strength potential of these steels and other alloys, such as titanium alloys, i.e. the practical use of materials having maximum (yield) strength-to-weight ratios.

5.2 Steels of the type used in motor cases, however, perform satisfactorily in the form of forgings for landing gear and other parts. Premature failures in these structures are prevented by combinations of rigidly observed design, manufacturing and fabricating rules.

In addition, notch tensile tests have been developed prior to these applications of such steels and are being used for screening and control purposes.

The present limit of applicability of ferritic steels for forgings is a tensile strength of about 290 ksi or a yield strength of about 270 ksi.

In contrast, the same steel types are used in motor cases heat treated to a yield strength of only 200 ksi or slightly higher, in order to avoid premature failures.

5.3 Many laboratory tests have been suggested to guard against such failures and to evaluate and screen materials for this purpose. However, it is only very recently that the real sources of the difficulties begin to become established and that, a critical analysis of possible screening and design tests is possible.

5.4 The tests in use and under consideration are predominantly tensile tests on flat, one to three inch wide specimens provided with some type of center notch or edge notch.

The only type of center notches investigated are cracks produced by various methods. These simulate the highest possible stress concentrations.

Edge notches can also be made extremely sharp without undue difficulties. Test results on specimens having a width of only one inch indicate that they respond basically in the same manner to the sharp edge notch as center-cracked specimens (23).

The radius of an edge notch can also be machined readily to any desired value, simulating a corresponding stress concentration (24).

5.5 It is to be expected, but it has not been sufficiently explored, that bend tests on notched specimens yield basically the same information as notch tension tests. This is suggested by the simple relation obtained from such tests on round specimens, Fig. 8 (25). In fact, according to these tests, the notch bend test appears to be more sensitive than the notch tensile test in the strength range of particular interest.

5.6 Bend tests on unnotched specimens have also been suggested and it is claimed that their results relate to vessel performance (26). It must be kept in mind, however, that the plane strain state which characterized a closed pressurized cylinder develops only in relatively wide bend specimens, as discussed in paragraph 8.5.

5.7 Particular attention in the literature has been given to the significance of the data derived from precracked or sharply notched specimens (23). A large amount of such data has been and is continuously being generated, and its value for screening purposes appears well established.

However, the physical significance of such numerical data, as well as its merits for design purposes is a very controversial matter.

5.8 More recently, the response of different materials to stress concentrations of various magnitude is also finding considerable interest and practical application.

6. GRIFFITH THEORY

6.1 A design philosophy which has governed various applications of metallic materials is the "fail-safe" concept. In the case of an extended load-carrying sheet part without the possibility of stress relief the fail-safe concept would require that the design stress for this structure not exceed its strength in the presence of cracks which may exist in this structure.

This concept has been expanded to limit the use of materials to those possessing a maximum resistance to crack propagation. This requirement is identical or nearly identical to that of maximum strength for sharply notched specimens.

6.2 The basis of all evaluation of strength data for cracked and sharply notched specimens is Griffith's theory for completely brittle materials. This theory postulates that the gross strength, σ, of an infinite body sufficiently apart from a crack having a length 2c is

$$\sigma = A/\sqrt{c} \qquad (6.21)$$

where **A** is a compound material constant containing the surface tension and elastic constants.

The conclusions which can be derived from this equation are easily visualized from a log-log plot of σ versus $\sqrt{c}$, Fig. 9a.

6.3 Griffith's theory has serious deficiencies.

The most obvious of these is that it extrapolates to extremely high strength for very small cracks.

To reconcile Griffith's concept with the fact that the strength of a material is limited, it has been proposed that a perfectly sound material should contain cracks of a certain length. This concept is not proven and not generally accepted.

6.4 To explain the rather high energy required to fracture metallic materials, plasticity corrections have been applied to Griffith's equation (Weiss, Session 4 of these Proceedings). The simplest of these increases the constant **A** in the equation to account for the additional energy of plastic deformation (28). The value of **A** can be determined by a single test.

6.5 A somewhat more refined correction uses a material constant, such as the yield strength, in addition to a constant which corresponds to that in Griffith's equation. Although such modifications have been based on consideration of the stress state near the crack tip, the knowledge of elastic-plastic theories is not sufficiently advanced to allow any rigorous or convincing approximate treatment of this problem. Also, Griffith's approach circumvents the stresses and should not be mixed with any stress calculations and stress concentration concepts.

Apparently no attempt has been made to date to test the full implications of these concepts.

7. NOTCH STRENGTH AND STRESS CONCENTRATION

7.1 The theory of finite stress concentrations, as presented most completely in Neuber's book (29), offers an alternate and flexible approach to the strength problem of notch sensitive materials.

In order to arrive at strength rather than stress values, the theory should be combined with some theory of strength, such as the maximum (principal) stress theory. Both of these concepts are well established and supported by tests.

This combination postulates, for a brittle material, that the net or notch strength, σ_N:

$$\sigma_N = \sigma_u \mid K_e \tag{7.11}$$

where σ_u is the tensile strength of the (brittle material) and K_e is the stress concentration factor determined by elasticity theory.

7.2 Considering the same case as Griffith, of an infinite plate with an elliptical notch having a length 2c, it is necessary to assign an end radius, r, to this notch. The stress concentration is then:

$$K_e = 1 + 2\sqrt{c/r} \tag{7.21}$$

Inserting in equation (7.21) the strength becomes:

$$\sigma = \sigma_N = \sigma_u \mid K_e = \frac{\sigma_{ii}}{1 + 2\sqrt{c/r}} \tag{7.22}$$

A comparison of equation (7.22) in Fig. 9b with Griffith's equation in Fig. 9a shows that the trend of both is equal for large crack lengths, but that the former is more realistic for small crack length values, as it extrapolates to the material strength.

7.3 Equation (7.11) can also be represented as a straight line under 45 degrees in a log-log plot of σ_N versus K_e, Fig. 10, theoretical.

Experiments on very brittle metals indicate that these respond to stress concentration in good agreement with equation (7.22), see Fig. 10.

7.4 However, this agreement does not extend to very high stress concentrations. The limited information available at present indicates that if K_e is larger than about 10, the notch strength remains nearly constant.

The inability of metals to retain extremely high stress concentrations has already been recognized by Neuber. He suggested that this can be formally accounted for by adding a material constant 2η to the radius r, or using instead of r,

$$r' = r + 2\eta$$

7.5 The notch strength of commercial alloys is generally considerably greater than that expected and observed for brittle materials.

The most significant deviation from the elastic stress concentration theory is that such a material possesses the ability to relax stress concentration up to a certain limit.

7.6 A general increase in notch strength can be obtained theoretically, by replacing the elastic stress concentration K_e, by a value K_p reduced by the plastic flow in the notch*

$$K_p = 1 + (K_e - 1) \qquad \frac{\varepsilon_e}{\varepsilon_t} = e(K_e - 1) + 1 \tag{7.61}$$

where ε_e is the elastic strain at failure, ε_p is the plastic strain or ductility of the metal under the stress conditions present in the notched section,

$$\varepsilon_t = \varepsilon_e + \varepsilon_p \text{ , and } \quad e = \varepsilon_e \mid \varepsilon_t \text{ .}$$

Examples of the relations resulting from these corrections of the stress concentration concept are illustrated in Fig. 10. In this graph, the value 2η is assumed to be 0.0035 in. and ε_e is varied between 0 (completely plastic) and 1.0 (completely elastic).

7.7 Equations (7.11) and (7.61) contain several material constants. These are known to depend on numerous parameters. Close agreement between theoretical concepts and experimental data, therefore, cannot be expected until these effects are fully established for the materials under consideration.

8. NOTCH STRENGTH, BIAXIALITY AND DUCTILITY

8.1 The properties of metallic materials are generally observed to be very diversified and impossible to fit completely into a rigid set of rules. This also applies to stress concentration effects.

Material characteristics depend on numerous variables and the laws which govern them are virtually unknown for high strength materials. The major variables which influence their properties are the following:

---

* Equation (7.61) is similar to that used by Hardrath and Ohman (30) for approximating the measured change in stress concentration on plastically straining specimens provided with stress raisers.

(a) Biaxiality and triaxiality
(b) Temperature
(c) Strain rate
(d) Section size
(e) Stress gradient

8.2 Biaxiality is possibly the most important of these. The cylindrical portion of a vessel is subjected to a stress state, which, as far as is known to date, possesses a minimum ductility. On the other hand, if small scale tests on flat specimens are performed, the degree of biaxiality may differ considerably depending on the specimen geometry. In order to understand fully the significance of a notch test it should be first clarified how the notch strength may be affected by biaxiality.

8.3 The notch sensitivity of titanium alloys, illustrated in Fig. 10 comes as close as can be expected to a uniform behavior. Their notch strength versus stress concentration curves at room and low temperatures form a simple family of curves.

A comparison of these curves with those theoretically developed in Fig. 10, however, indicates distinct differences in two respects, namely:

(a) The notch strength is larger than the tensile strength at low stress concentrations.

(b) The change from these high values to low values at high stress concentrations is more abrupt than indicated in the theoretical curves.

(c) In addition, it is noted that these effects develope within a limited range of stress concentration. In the present tests this range appear to be below $K = 8$.

8.4 To explain the differences, it should be understood that the uniaxial stress state in a smooth tensile test is replaced by a complex condition in a notched section. In particular, biaxiality is developed in the notch bottom and triaxiality inside of the metal. These result generally in two effects, namely:

(1) An increase in the resistance to plastic flow and, therefore, in the strength of a ductile material.

(2) A decrease in ductility and, therefore, increase in notch sensitivity.

8.5 Biaxiality in the notch bottom increases as the notch radius decreases. Triaxiality inside of the specimen is probably closely related to the biaxiality and should follow the same trend.

From the analogy of the stress gradients in a notched tension and in a smooth bend specimen, it can be expected that the limiting condition of plane strain is reached if the notch radius is less than about 1/8 of the metal thickness (see Weiss, Session 4 of these Proceedings).

8.6 Both biaxiality and triaxiality reduce the ductility of a metal.

The increase in these quantities with increasing stress concentration, therefore, explains both major discrepancies between the test data and the stress concentration effects predicted on the basis of a constant ductility, namely:

(a) That the actual notch strength first gradually increases with stress concentration.

(b) That the notch strength rather suddenly decreases for a comparatively small increase in stress concentration.

8.7 The effect of biaxiality on ductility has been determined in a number of instances, by two different methods.

Tests on tubes, subjected to combined axial stress and internal pressure, can be conducted to yield a controlled degree of biaxiality, as already discussed in paragraph 3.3.

The results of earlier tests of this type are not quite clear, because of large scattering (31, 32). The more recent tests by Fitzgibbon and Goodman (22), however, reveal that the ductility of high strength steels in the plane strain state is greatly reduced from the uniaxial value.

8.8 In bend tests on flat specimens, biaxiality is present at the center of the convex surface, Fig. 11. It increases from uniaxiality to plane strain as the width-to-thickness ratio of the specimen becomes larger (34).

The ductility decreases in relation to the biaxiality. For aluminum alloy and soft steel the ductility for plane strain, i.e. for wide specimens, is found to be roughly one half of the tensile ductility.

8.9 Another possible method of studying the effect of biaxiality on ductility is bulging. Plane strain occurs in a bead and balanced biaxial stress occurs in a spherical bulge.

9. EFFECTS OF TEMPERATURE, STRAIN RATE, SECTION SIZE AND STRESS GRADIENT

9.1 For many metals, a small change in biaxiality, as well as in various other basic parameters is associated with a rather small change in ductility.

This explains the comparatively smooth appearance of the notch strength versus stress concentration curves for most titanium alloys.

9.2 Ferritic steels, however (and a number of other metals) are known to exhibit very large changes in ductility for small changes in a critical temperature or strain rate.

Fig. 12 illustrates that the transition temperature of an ultra high strength steel also depends greatly on the stress concentration factor (24). The basic variable is then presumably the degree of biaxiality as discussed in paragraph 8.5.

9.3 Such a shift in transition temperature is equivalent to an abrupt change in notch strength, as the stress concentration is changed only slightly. This explains the irregularities and inconsistencies frequently observed on sheet steels in this respect.

9.4 Regarding the effects of other basic parameters, very little is known for high strength materials.

9.5 The strain rate effect is considered to be tied in with temperature. Increased strain rate is considered to be equivalent to a (slight) reduction in test temperature.

9.6 The section size effect for notched specimens may be also considered as an effect of stress gradient.

It may be mentioned that the effect of specimen width, for either a highly brittle material or for semibrittle ultra high strength steels, Fig. 13, is found to be considerably smaller than to be expected from any theory of the effects of section size available at present.

This applies particularly to attempts of fitting the section size effect into Griffith's theory. This hypothesis never intended to cover the section size effect. (It has been considered for glass, assuming that cracks are present and that they differ in length for different section sizes).

10. MATERIAL PROBLEMS

10.1 This paper is devoted primarily to the performance of the metallic materials which are used to date for rocket fuel cases. These are the heat treatable ferritic steels, having a tensile strength level well above 200 ksi and generally known under the name "ultra high strength steels."

The metallurgical developments leading to improved performance of such steels concern the entire range of alloy chemistry and product technology.

The two targets of such developments are:

(1) A maximum (yield) strength-to-weight ratio

(2) A minimum notch sensitivity

10.2 Properly produced steel sheet is characterized by nearly identical properties in the various directions.

Another group of potential rocket case materials, the heat treated titanium alloys, exhibits low directionality properties. They possess properties slightly superior to those of the ultra high strength steels. This, applies both to their strength-to-weight ratio and to their notch sensitivity, Fig. 14, and particularly also to their notch sensitivity at low temperatures.

10.3 There also exists a variety of potential homogeneous and composite materials for this application. Some of these appear to possess a potentiality considerably superior to those of ferritic steels and titanium alloys.

However, all these materials exhibit directional properties. The information available to date for their basic strength properties is very limited, and no attempts have been yet made to analyze its significance for pressure vessel strength.

10.4 As far as the nondirectional materials in use or under consideration are concerned, it appears that their potentialities are clearly limited.

Substantial increases in yield strength of ferritic steels and titanium alloys by variations in chemistry, fabrication or heat treating are accompanied by a rapid increase in notch sensitivity, Fig. 14.

10.5 Present efforts are devoted to three areas, namely:

(a) To obtain comparatively small increases in yield strength, with other properties being kept substantially constant.

(b) To obtain an improved structure which reduces notch sensitivity.

(c) To develope fabricating procedures which either eliminate and reduce stress concentrations or which reduce the response of the metal to stress concentration.

10.6 Regarding the yield strength of heat treated steels, it may be pointed out that the strongest ultra high strength steels possess a yield strength which is exceptionally low in comparison to their tensile strength. This should leave a considerable margin for improvement.

However, it appears that very little is known about chemical and other factors which determine the yield strength characteristics of steels, and about possible procedures which may increase the yield-strength-to-tensile-strength ratio.

10.7 Structural improvements of steels have been effected by numerous measures. These range from vacuum melting to various closely controlled forming, heat treating and welding operations.

The result of these fabricating procedures is frequently a homogeneous structural and mechanical condition.

10.8 The problem of evaluating the effects of deviations from a homogeneous and isotropic condition has found little attention.

The suitability of notch tests, for example, for predicting the performance of steel vessels with a decarburized surface appears to be questionable. Tests on specimens machined from vessels in steels decarburized by different amounts (Murphy, Session 6 of these Proceedings) indicate, according to Fig. 15, that the vessel strength well correlates with notch strength, if the steel is only slightly decarburized. However, severe decarburization which leads to higher vessel strength, only slightly increases the notch strength of specimens which are decarburized at the flat surfaces but not at the notch surface.

11. LOW CYCLE FATIGUE

11.1 A general phenomenon observed in testing strong materials is failure on repetition of a load cycle below that carried on the previous test without any indication of damage. This phenomenon is called Low Cycle Fatigue.

Such premature failures have been also observed on proof testing motor cases, where the proof test was performed more than once.

11.2 The general explanation for such failures is, according to present concepts, a gradual deterioration of the metal under repeated loading. It is assumed, hereby, (a) that the load cycle is associated with plastic deformation and (b) that at each load cycle, a portion of the ductility of the metal is consumed.

11.3 In regular fatigue tests on uniform smooth specimens this effect is hidden. The metal appears to be strengthened by the first few cycles and generally fails only after a considerable number of cycles if the load is slightly below its strength.

However, tests on notched specimens of notch sensitive materials clearly show a considerable decrease in fatigue strength at a few cycles (25).

11.4 Further information on low cycle fatigue is rather limited. Apparently, only one investigation by Padlog and Rattinger (33), is directly applicable to steel cases.

This data, although rather incomplete, appears to reveal several facts of general significance, namely:

(a) At low cycles a pressurized tubular section possesses a considerable lower fatigue life than a flat specimen.

(b) This difference is about the same as that between a smooth and a notched flat specimen, while at higher cycles the smooth tube possesses higher fatigue strength.

(c) Notching has a comparatively small effect on the low cycle fatigue strength of tube.

(d) Consequently, the low cycle behavior of notched tube and sheet differs considerably less than that of smooth specimens.

11.5 Several investigators are now concerned with fatigue crack propagation in sheet. The results obtained to date concern slow crack movements leading to failure at comparatively large numbers of cycles.

ACKNOWLEDGEMENT

Most of the recent work on steels and titanium alloys at Syracuse University mentioned in this paper has been performed under a contract with the Navy Bureau of Aeronautics (now Bureau of Naval Weapons). The results shown in Fig. 14 were obtained on a contract with Materials Central, Wright Air Development Division.

The concepts presented in the paper were developed in co-operation with Prof. V. Weiss and Mr. J. Sessler of Syracuse University, and with Dr. O. Hoffman and Dr. L. Schapiro of Lockheed's Missiles and Space Division in Palo Alto, California.

BIBLIOGRAPHY

1. W. Lode, Tests on the Effect of the Intermediate Principal Stress on the Yield Strength, Zeitschrift Physik, Vol. 36, p. 913 (1926).

2. M. Ros and A. Eichinger, The Failure Condition of Solid Bodies for Static Straining, Eidgenossische Materialpruefungsanstalt Zuerich, Rep. No. 172 (1949).

3. J. Marin, J. H. Faupel, V. L. Dutton and M. V. Brossman, Biaxial Plastic Stress-Strain Relations for 24ST Aluminum Alloy, Nat. Adv. Comm. Aero., TN 1536 (1948).

4. G. Sachs, Contribution to the Derivation of the Plasticity Condition, Zeitschrift Verein Deutscher Ingenieure, Vol. 72, p. 134 (1928).

5. Goodman et al (Space Technology Laboratories, Inc.), Testing Materials in Biaxial Stress Fields, AFBMD - TR - 60 - 45 and TR 60 - 109 (1960).

6. Caine et al, (U.S. Steel Applied Research Laboratory), (May 1960), Simulated Service Evaluations of Steels for Solid-Propellant Missile Motor Cases, Proc. 7th Sagamore Res. Conf. (1960) in print.

7. E. A. Davis, Increase in Stress with Permanent Strain and Stress-Strain Relations in the Plastic State for Copper Under Combined Stresses, Trans. Ham.Soc.Mech.Eng.,Vol. 65, p. A-187 (1943).

8. E. A. Davis, Yielding and Fracture of Medium Carbon Steel Under Combined Stresses, J. Applied Mechanics, Fo. 12, p. 13 (1945).

9. W. R. Osgood, Combined Stress Tests on 24ST Aluminum Alloy Tubes, J. Applied Mechanics, Fol. 14, p. 147 (1947).

10. C. C. Chow, A. W. Dana and G. Sachs, Stress and Strain States in Elliptical Bulging, J. Metals, Vol. 1, 3, p. 49 (1949).

11. G. Sachs, Tension Test, Zeitschrift Verein Deutscher Ingenieure, Vol. 72, p. 734 (1928).

12. G. Sachs and J. D. Lubahn, Failure of Ductile Metals in Tension, Trans. Am.Soc.Mech.Eng., Vol. 68, p. 271 (1946).

13. G. Espey, Instability of Thin-Walled Tubes Subjected to Internal Pressure, Trans.Am.Soc.Mech.Eng., Vol. 68, p. 281 (1946).

14. W. F. Brown and G. Sachs, Strength and Failure Characteristics of Thin Circular Membranes, Trans.Am.Soc.Mech.Eng., Vol. 70, p. 241 (1948).

15. W. F. Brown and F. C. Thompson, Strength and Failure Characteristics of Metal Membranes in Circular Bulging, Trans.Am.Soc.Mech.Eng., Vol. 71, p. 575 (1949).

16. R. Hill, A Theory of the Plastic Bulging of a Metal Diaphragm by Lateral Pressure, Phil. Mag. (7), Vol. 41, p. 1133 (1950).

17. H. W. Swift, Plastic Instability Under Plane Stress, J. Mechanics Physics Solids, Vol. 1, p. 1 (1952).

18. P. M. Mellor, Stretch Forming Under Fluid Pressure, J. Mechanics Physics Solids, Vol. 5, p. 41 (1956/57).

19. P. B. Mellor, Plastic Instability in Tension, Engineer, p. 517 (1960).

20. N. A. Weil, Approximation to Plastic Behavior of Circular Membranes, Proc. ASCE, Paper No. 1139, Vol. 83 (1957).

21. N. A. Weil, Bursting Pressures and Safety Factors for Thin-Walled Vessels, J. Frau Klin Inst., Vol. 265, p. 97 (1958).

22. D. P. Fitzgibbon and J. Goodman, Pressure Vessel Design Criteria, Contract AF 04 (647)-309, Semi-annual Reports (1960).

23. Fracture Testing of High-Strength Sheet Materials; A Report of a Special A.S.T.M. Committee; A.S.T.M. Bulletin, p. 29-51, Jan. and Feb. (1960).

24. G. Sachs and J. G. Sessler, Effect of Stress Concentration on the Tensile Strength of Titanium and Steel Alloy Sheet at Various Temperatures, Am.Soc.Test.Mat., Preprint 76a (1960).

25. G. Sachs and G. Scheven, Relation Between Direct-Stress and Bending Fatigue of High-Strength Steels, Proc.Am.Soc.Test.Mat., Vol. 57, p. 667 (1957).

26. D. K. Hanink and G. R. Sippel, A Bend Test for Toughness, Metal Progress, Vol. 78, p. 89 (1960).

27. A. A. Griffith, The Phenomenon of Rupture and Flow in Solids, Phil. Trans.Roy.Soc., Series A, Vol. 221, p. 163 (1921).

28. E. Orowan, Reports Progr. in Physics 12, 185 (1948/49).

29. H. Neuber, Kerbspannungslehre, Springer Verlarg (1958).

30. H. F. Hardrath and L. Ohman, A Study of Elastic and Plastic Stress Concentration Factors Due to Notches and Fillets in Flat Plates, NACA TN 2566 (1951).

31. E. Siebel and F. F. Maier, Effect of Multiaxial Stress State on the Ductility of Metallic Materials, Zeitschrift Verein Deutscher Ingenieure, Vol. 77, p. 1345 (1933).

32. E. G. Thompson and J. E. Dorn, The Effect of Combined Stresses on the Ductility and Rupture Strength of Magnesium-Alloy Extrusion, J. Aero.Sci., Vol. 11, p. 125 (1944).

33. J. Padlog and I. Rattinger, Low Cycle Fatigue Strength of Pressurized Components, Am.Soc.Test.Mat., (Pres. at San Francisco Oct. 1959) (1960).

34. G. S. Sangdahl, E. L. Aul and G. Sachs, An Investigation of the Stress and Strain States Occurring in Bending Rectangular Bars, Proc.Soc.Exp. Stress Analysis, Vol. 6, p. 1 (1948).

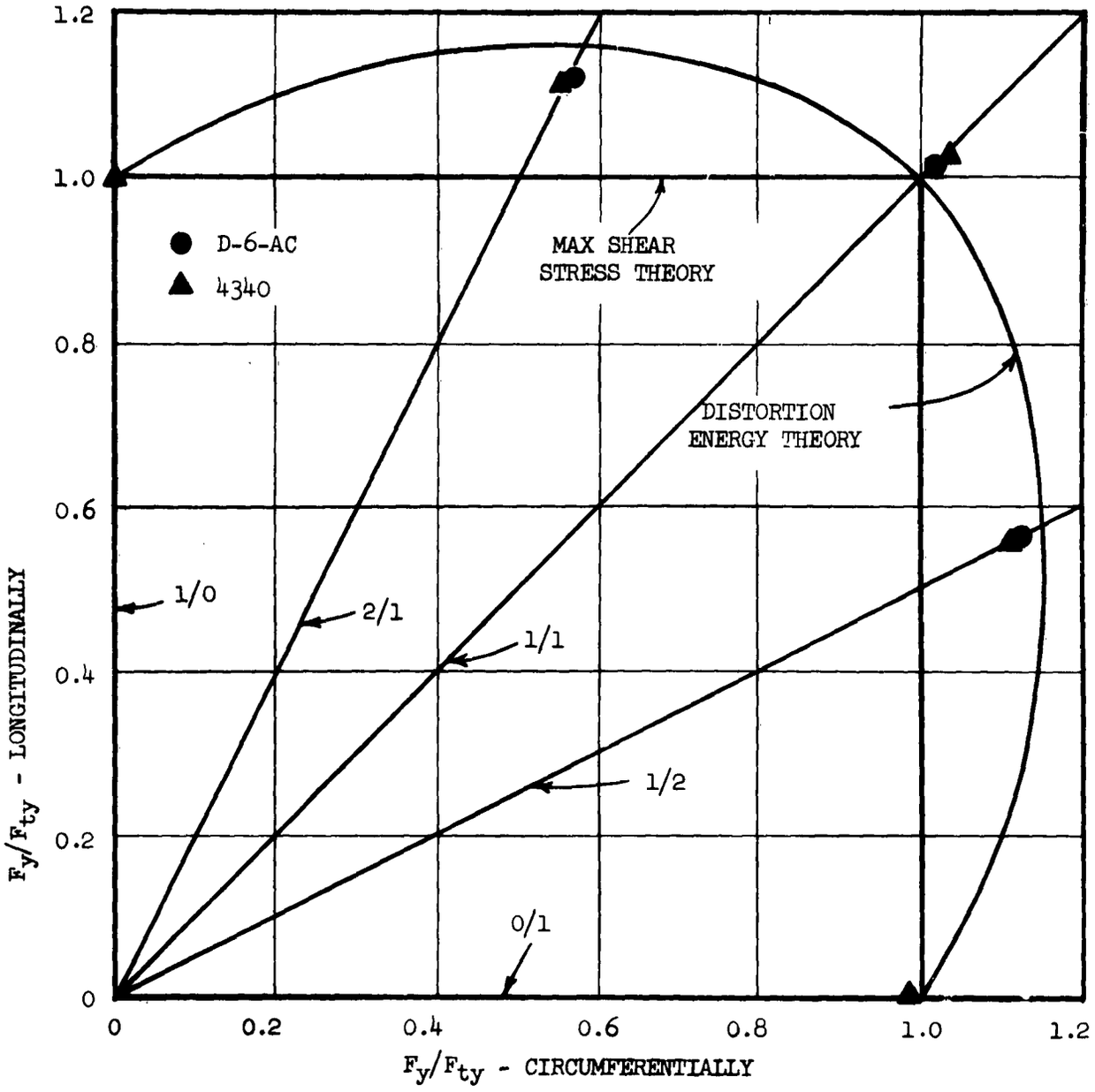


FIG.1 YIELD STRENGTH DATA FOR STEEL CYLINDERS IN COMBINED LONGITUDINAL AND CIRCUMFERENTIAL TENSION
(DATA BY FITZGIBBON-GOODMANN 1960)

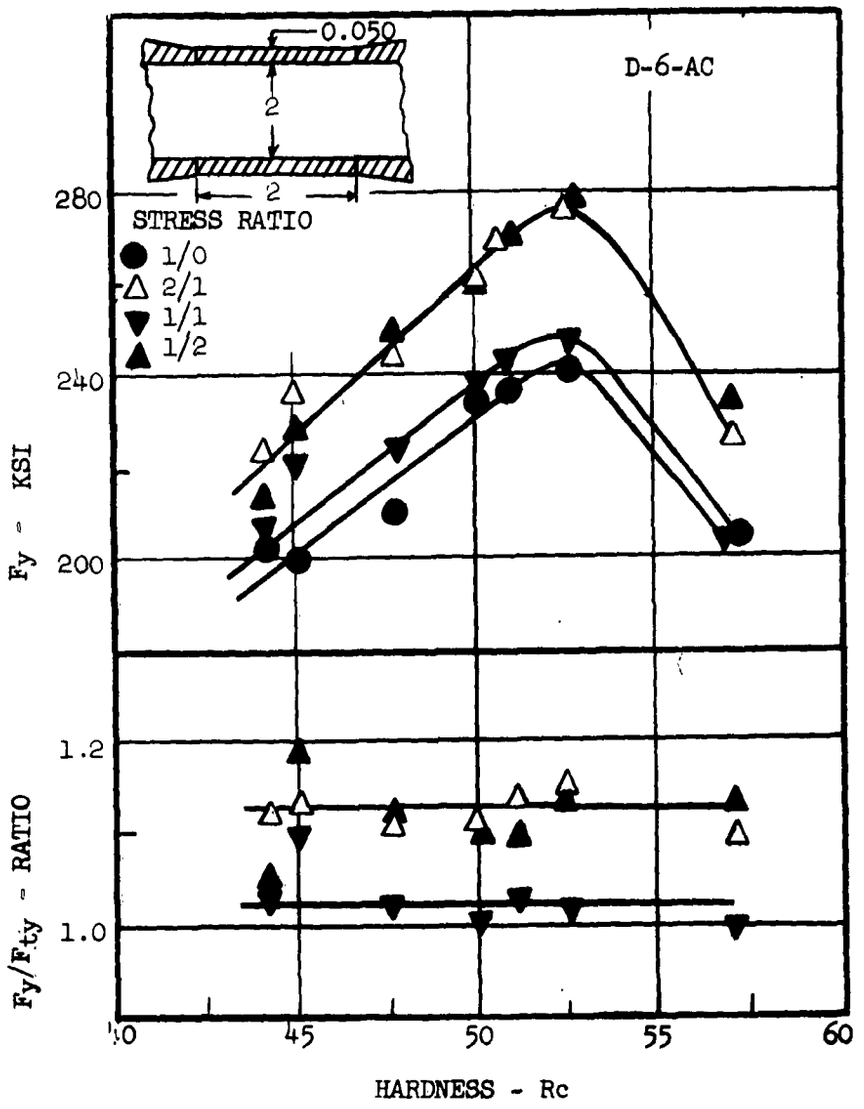


FIG.2 YIELD STRENGTH VALUES FOR D-6-AC STEEL TUBES UNDER COMBINED TENSION AND PRESSURE (DATA BY GOODMAN ET AL 1960)

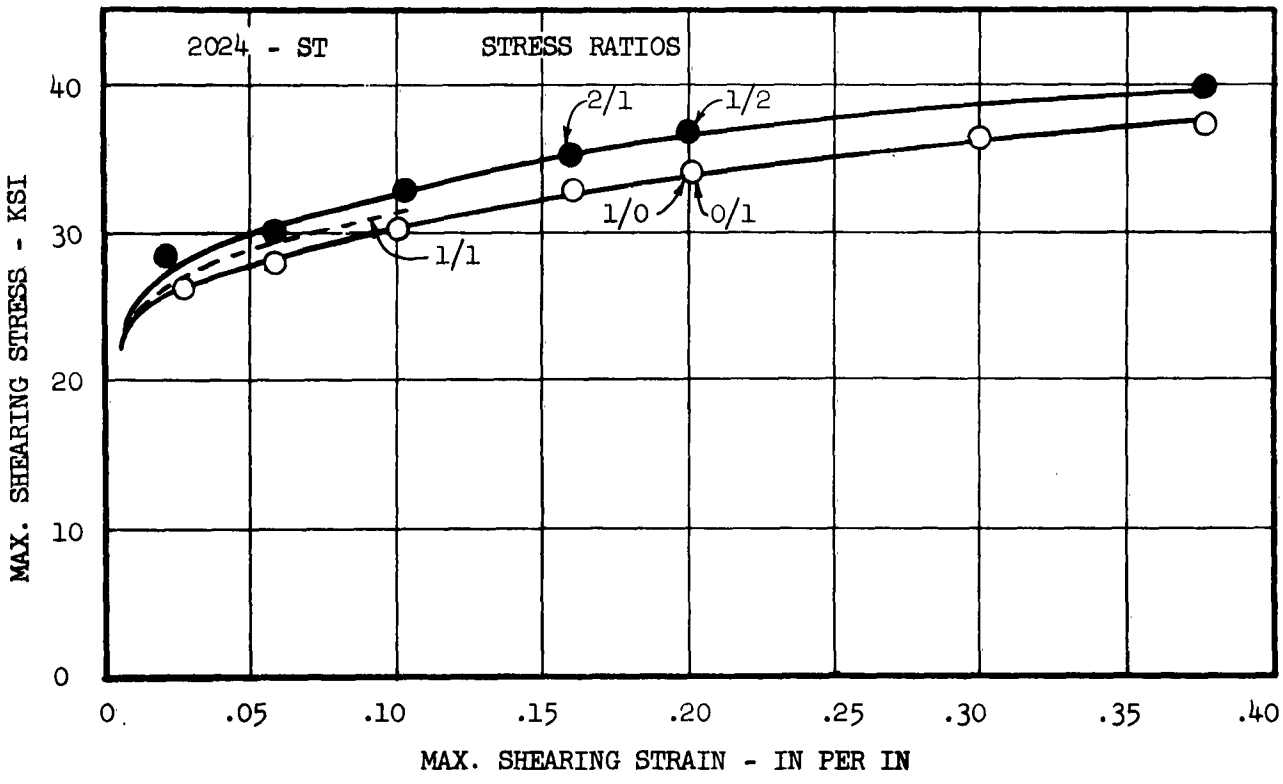


FIG. 3 TRUE STRESS - TRUE STRAIN CURVES FOR VARIOUS BIAXIALITIES FROM TESTS ON ALUMINUM ALLOY TUBES (OSGOOD 1947)

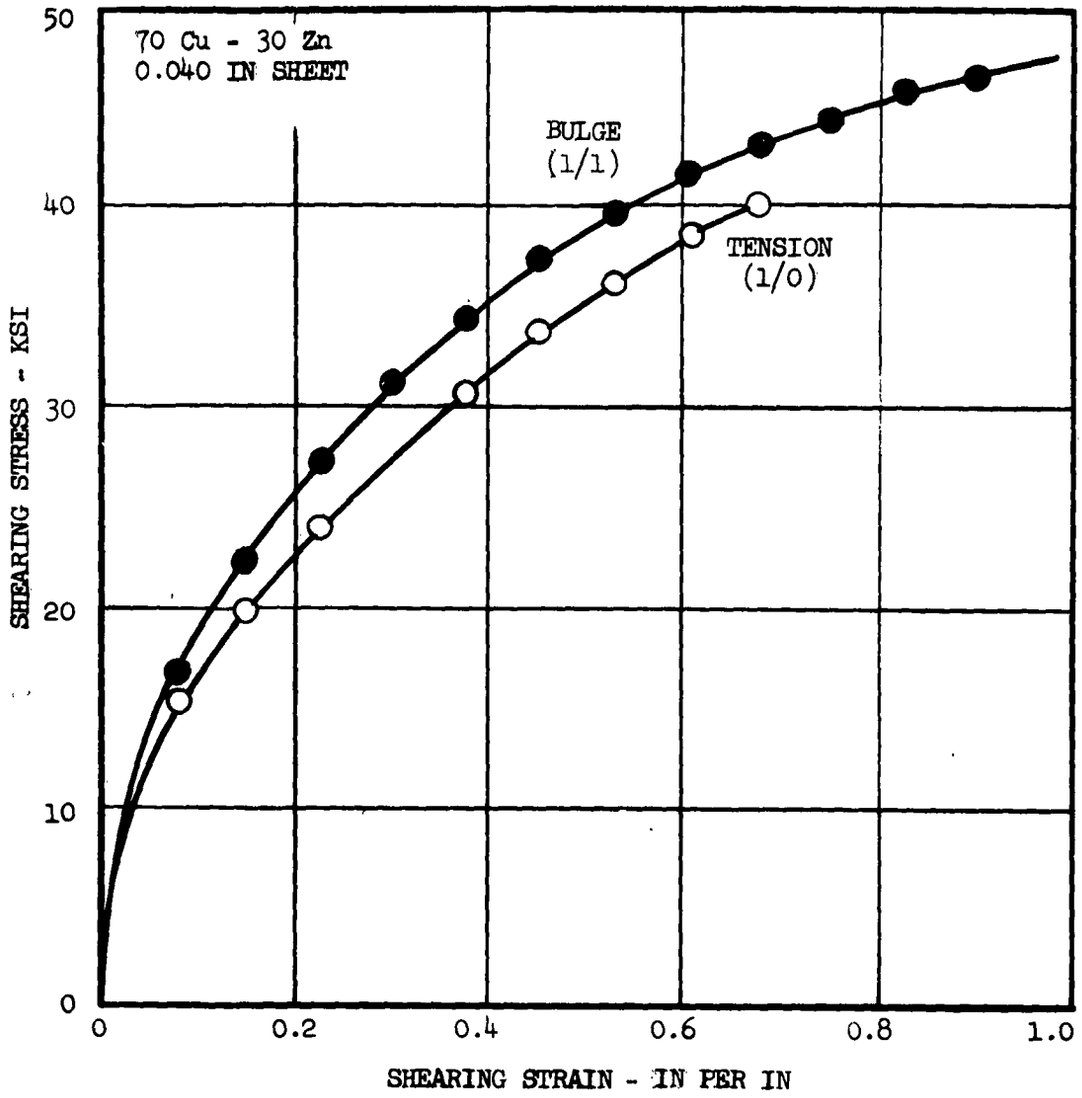


FIG. 4 STRESS STRAIN CURVES FOR BRASS IN TENSION AND BULGING (DANA-CHOW-SACHS 1949)

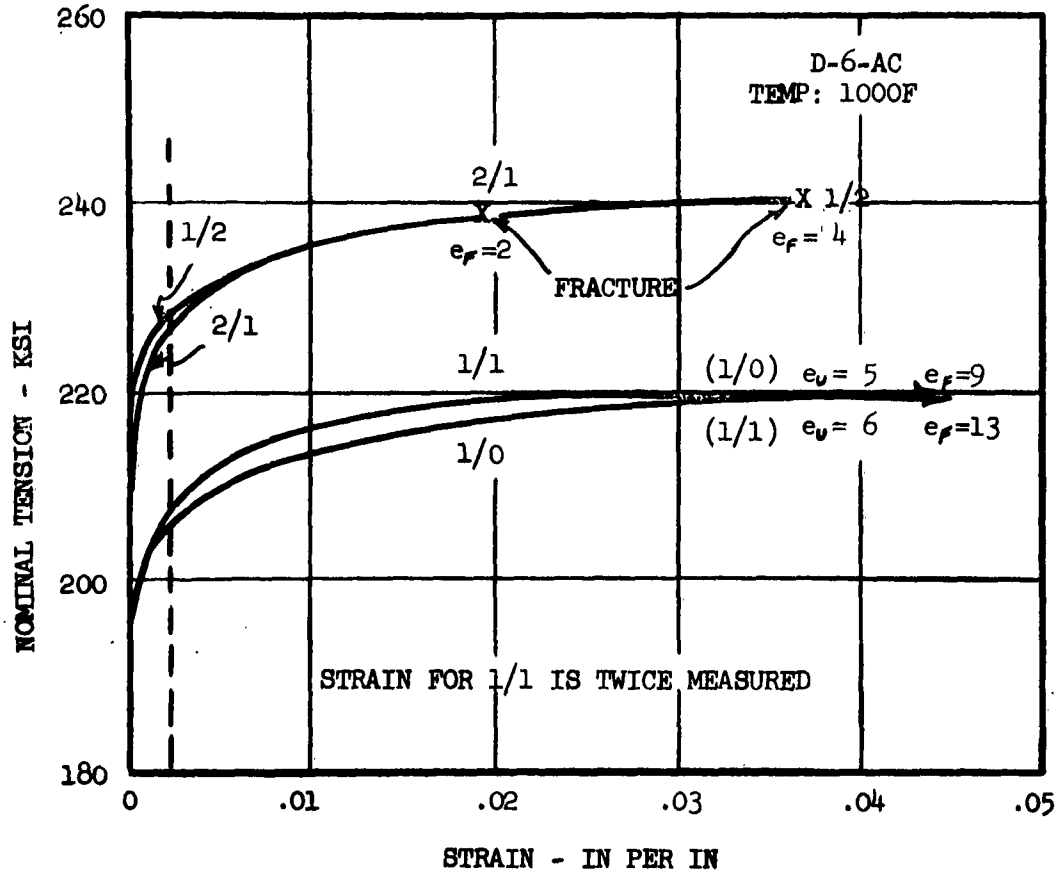


FIG.5 CONVENTIONAL STRESS - STRAIN CURVES FOR D-6-AC STEEL TUBES UNDER COMBINED TENSION AND PRESSURE (DATA BY FITZGIBBON-GOODMAN 1960)

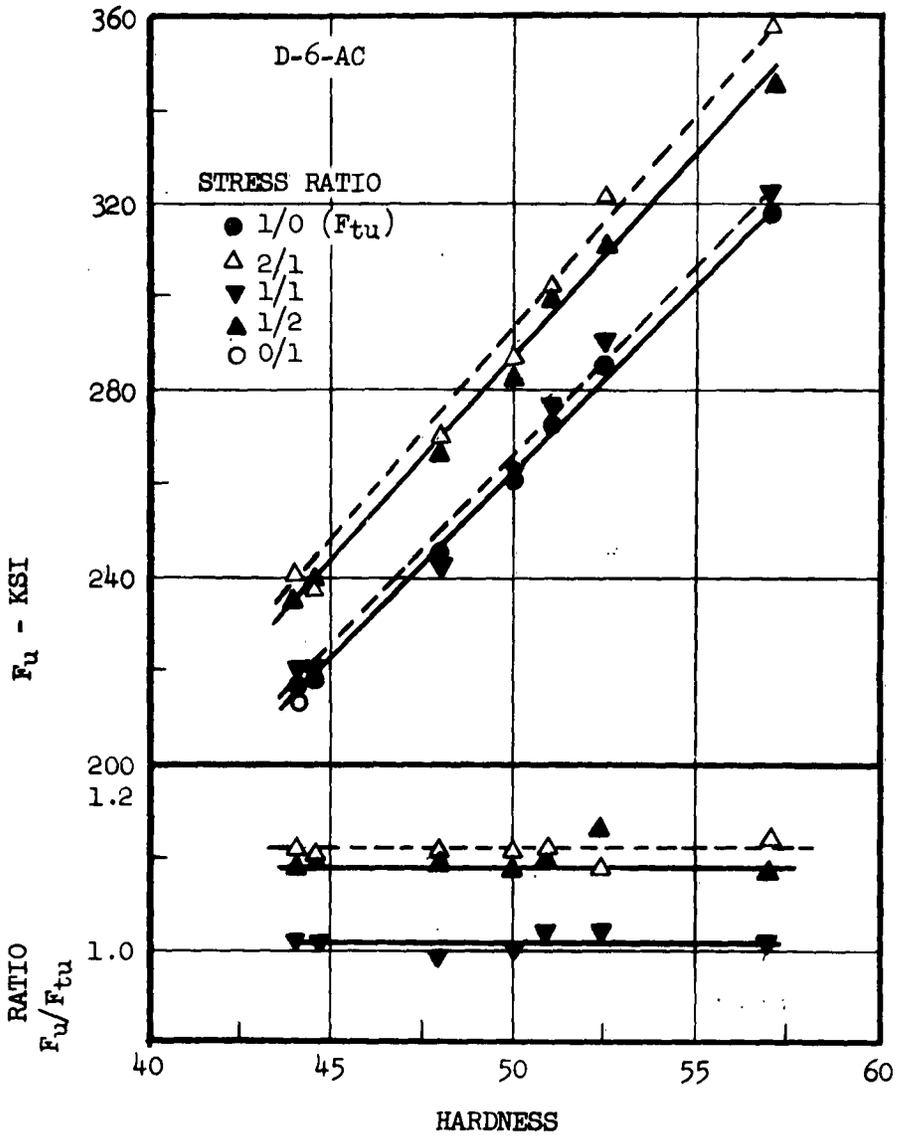


FIG. 6 ULTIMATE STRENGTH VALUES FOR D-6-AC STEEL TUBES UNDER COMBINED TENSION AND PRESSURE (DATA BY FITZGIBBON-GOODMAN 1960)

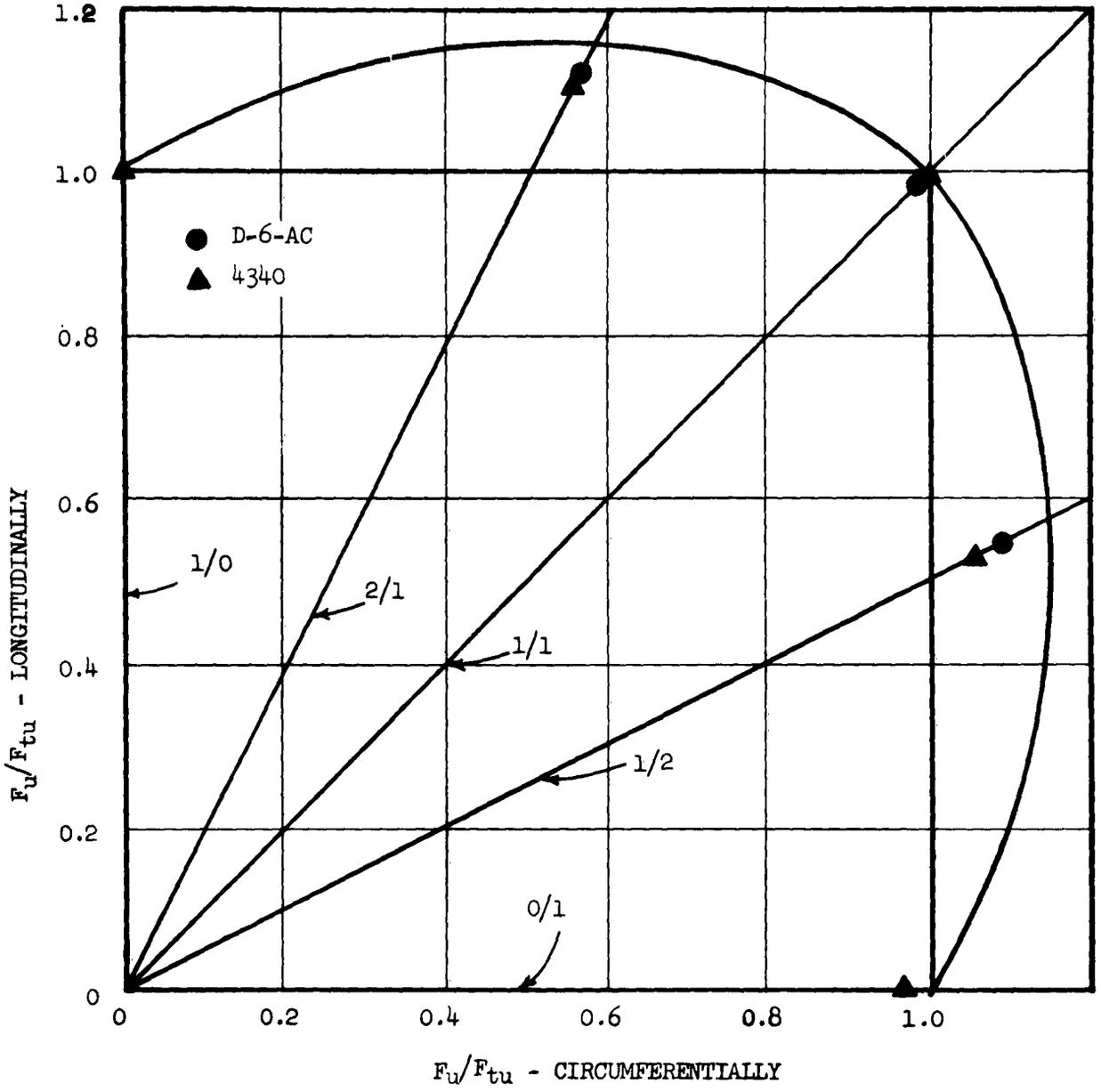


FIG. 7 ULTIMATE STRENGTH DATA FOR STEEL CYLINDERS IN COMBINED LONGITUDINAL AND CIRCUMFERENTIAL TENSION (DATA BY FITZGIBBON-GOODMAN 1960)

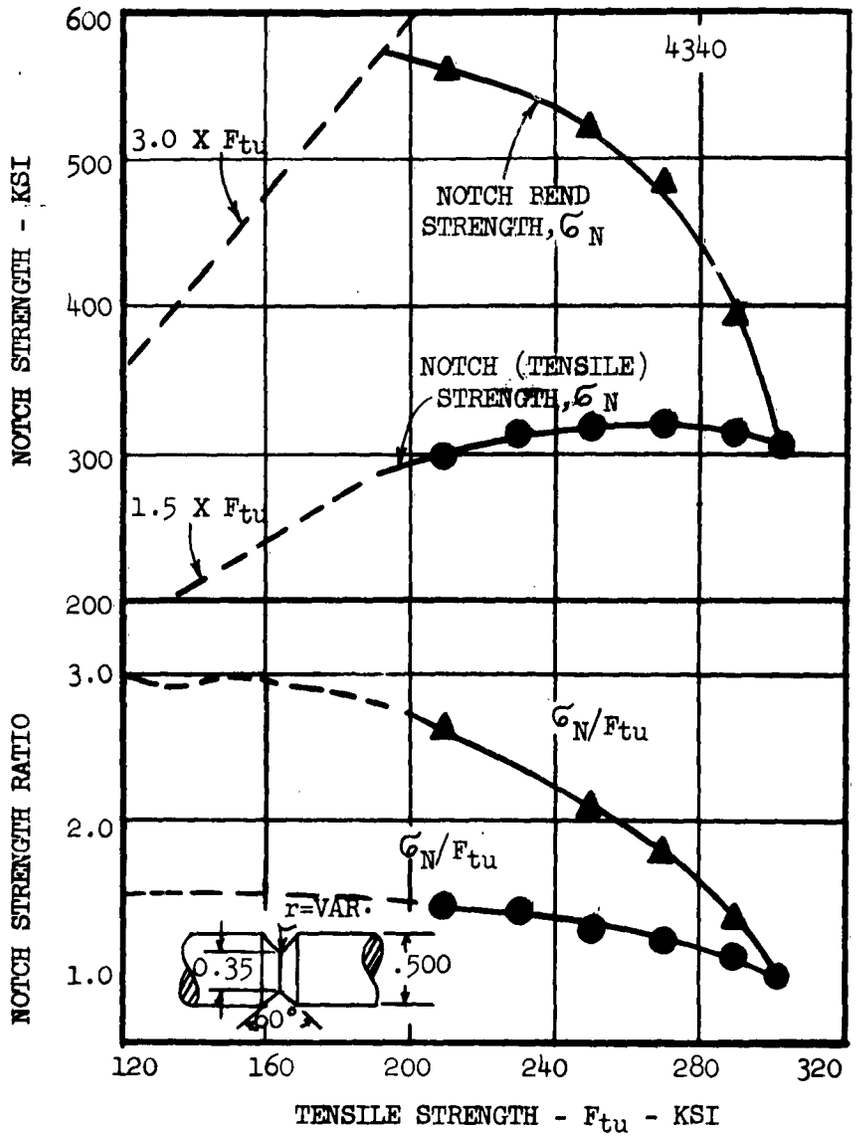


FIG. 8 RELATION BETWEEN NOTCH BEND STRENGTH AND NOTCH TENSILE STRENGTH OF 4340 STEEL
(DATA BY SCHEVEN-SACHS 1957)

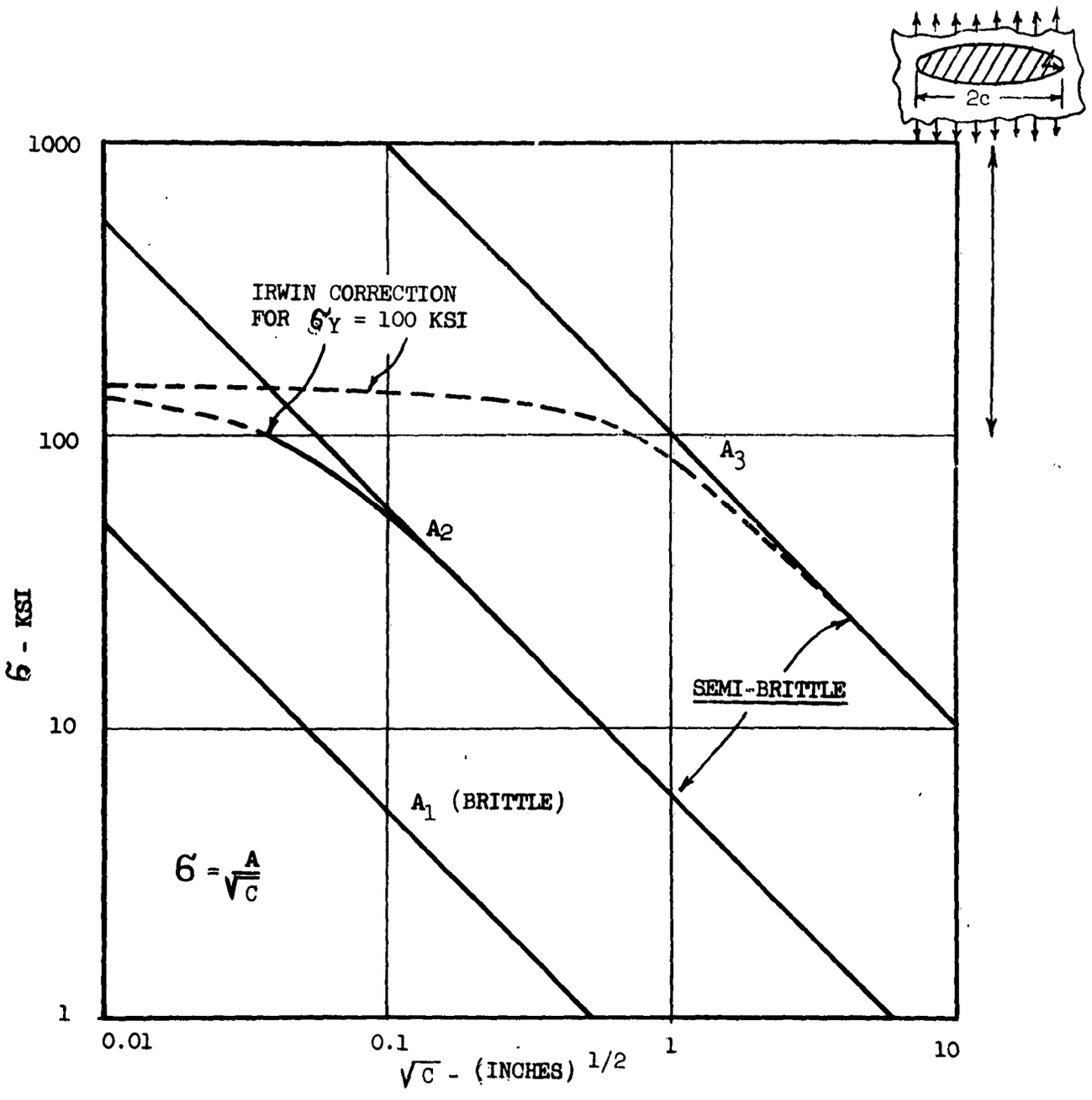


FIG. 9a GRAPHIC REPRESENTATION OF SUGGESTED RELATIONS BETWEEN STRENGTH OF AN INFINITE PLATE WITH AN ELLIPTICAL CRACK OR HOLE

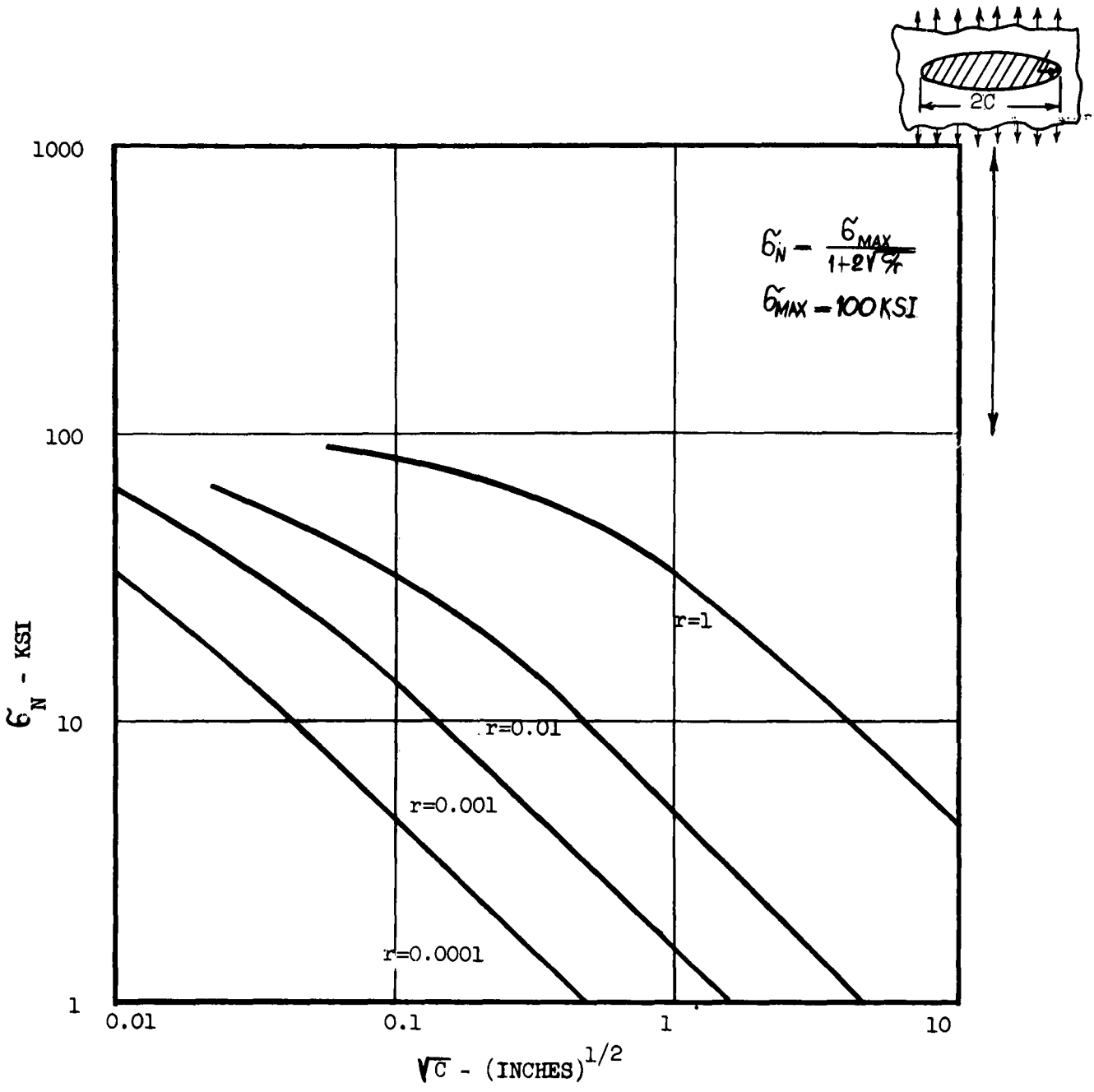


FIG. 9b GRAPHIC REPRESENTATION OF SUGGESTED RELATIONS BETWEEN STRENGTH OF AN INFINITE PLATE WITH AN ELLIPTICAL CRACK OR HOLE

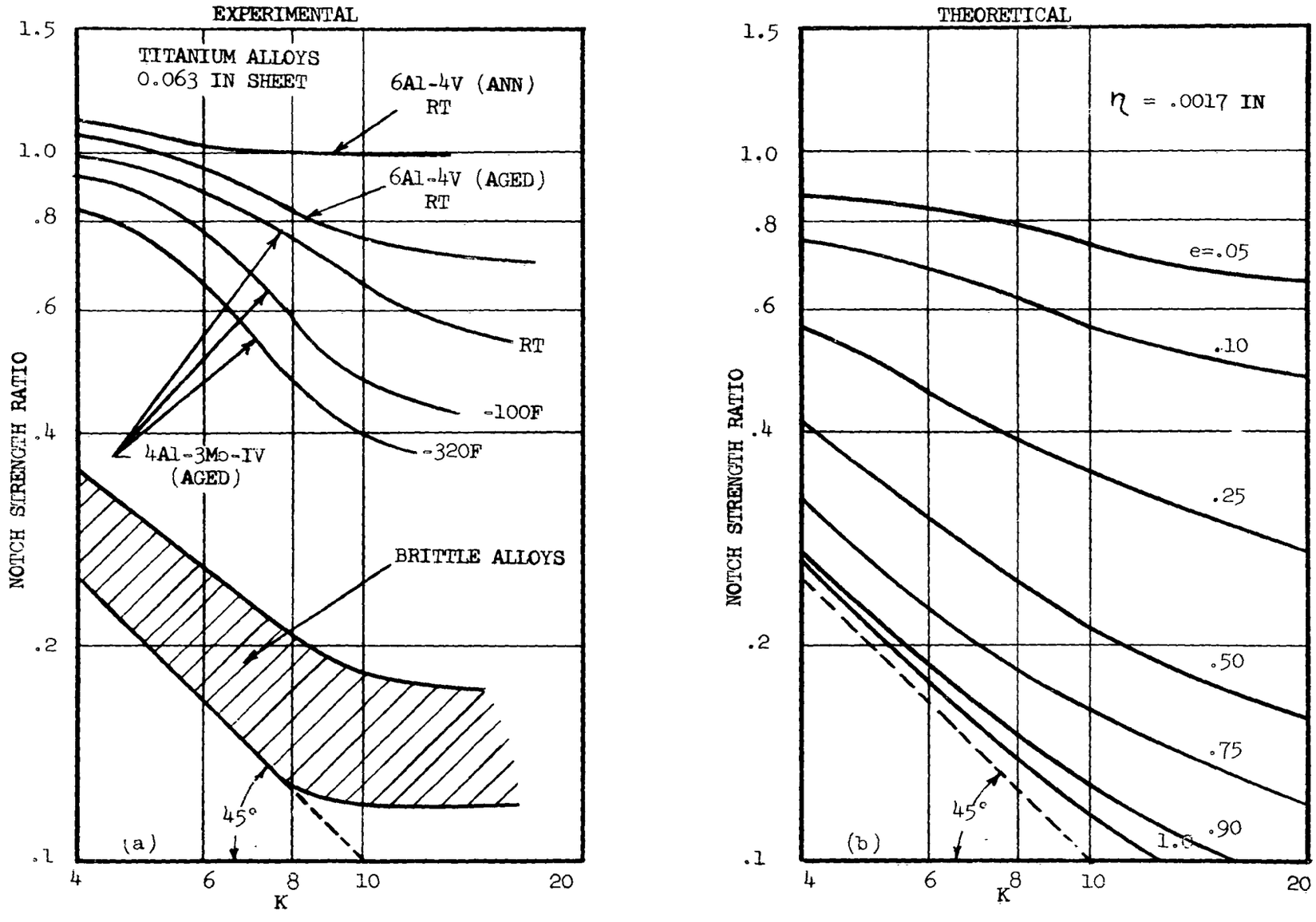


FIG. 10 COMPARISON OF EXPERIMENTAL CURVES AND THEORETICAL CURVES (LOG-LOG REPRESENTATION)

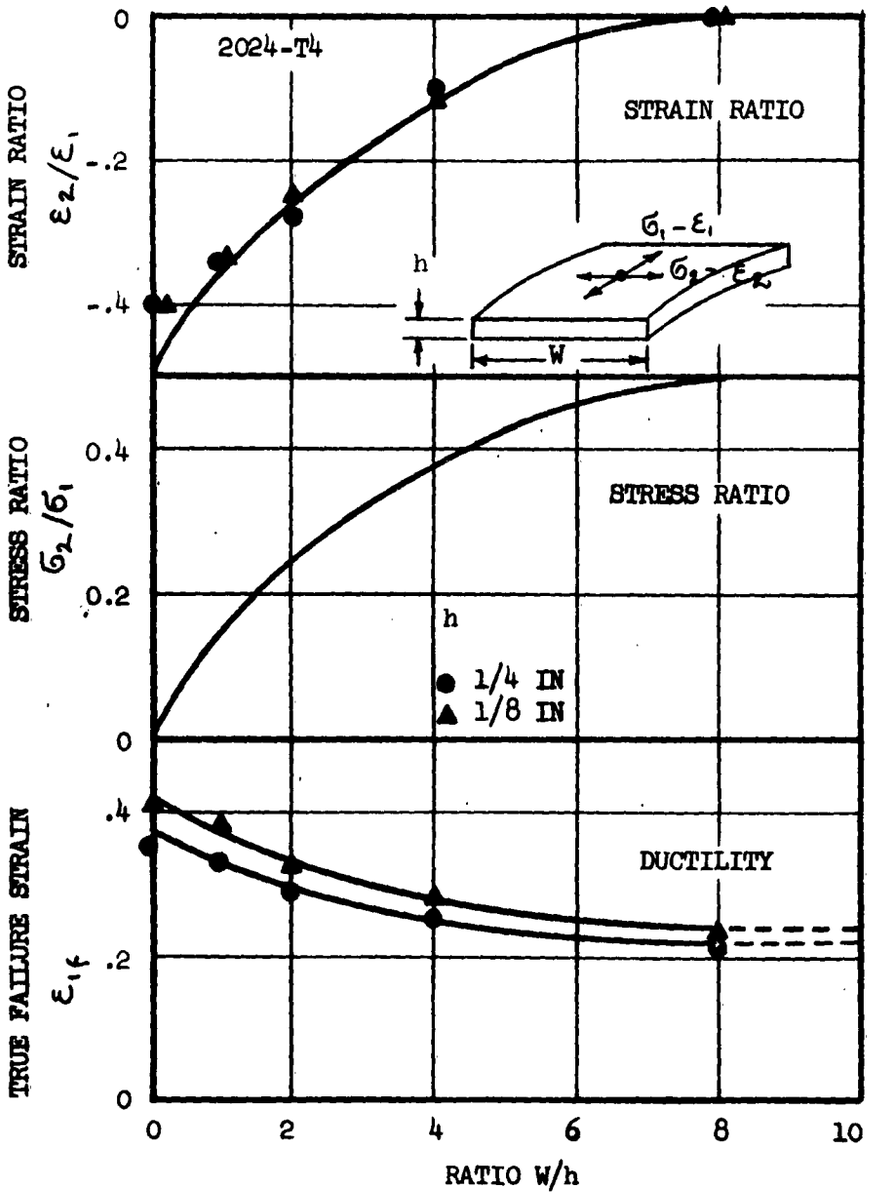


FIG. 11 EFFECT OF WIDTH TO THICKNESS RATIO OF BENT ALUMINUM ALLOY SPECIMENS ON STRAIN RATIO, STRESS STATE AND DUCTILITY (SANGDAHL-AUL-SACHS 1948)

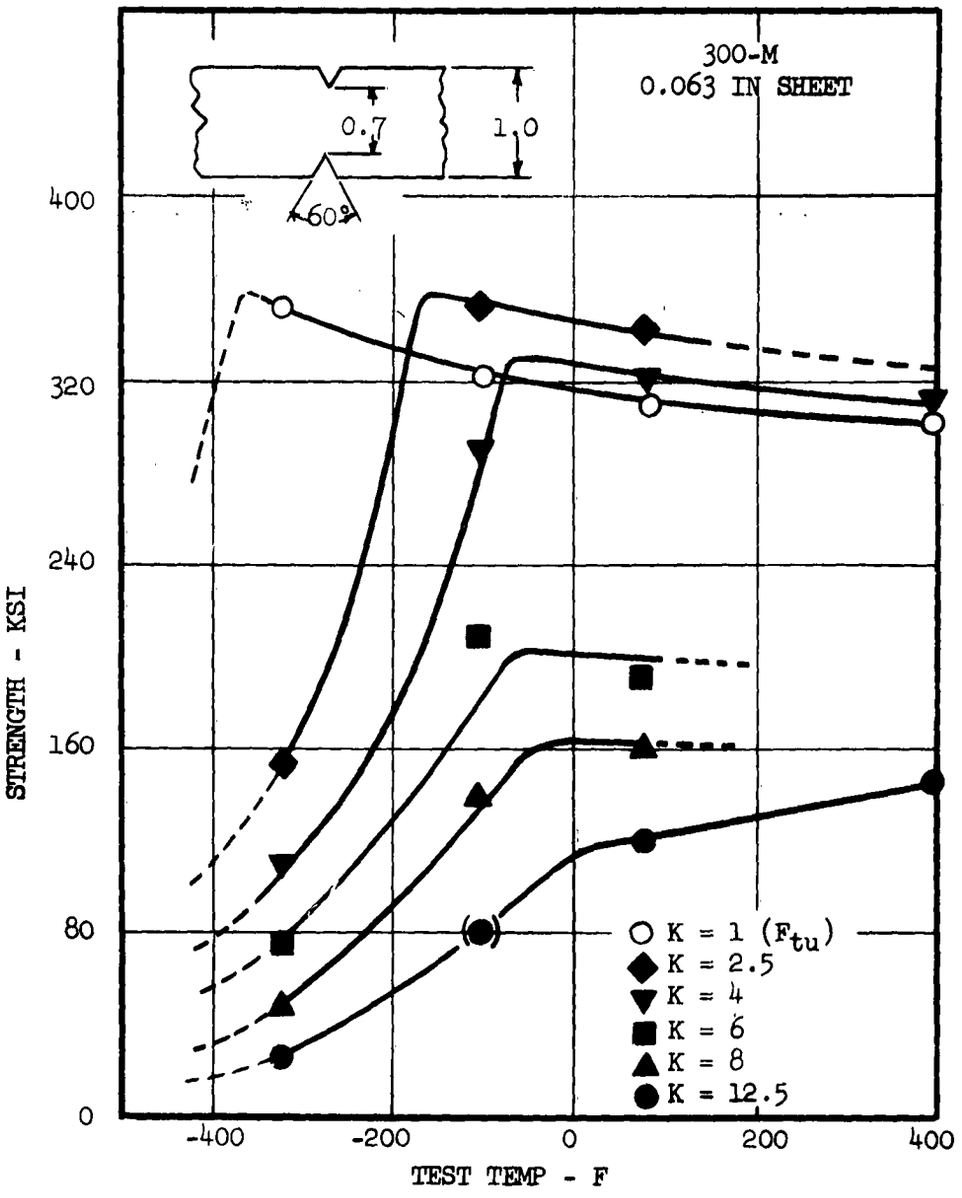


FIG. 12 EFFECTS OF TEST TEMPERATURE AND STRESS CONCENTRATION ON NOTCH STRENGTH OF 300-M STEEL
(SACHS-SESSLER 1960)

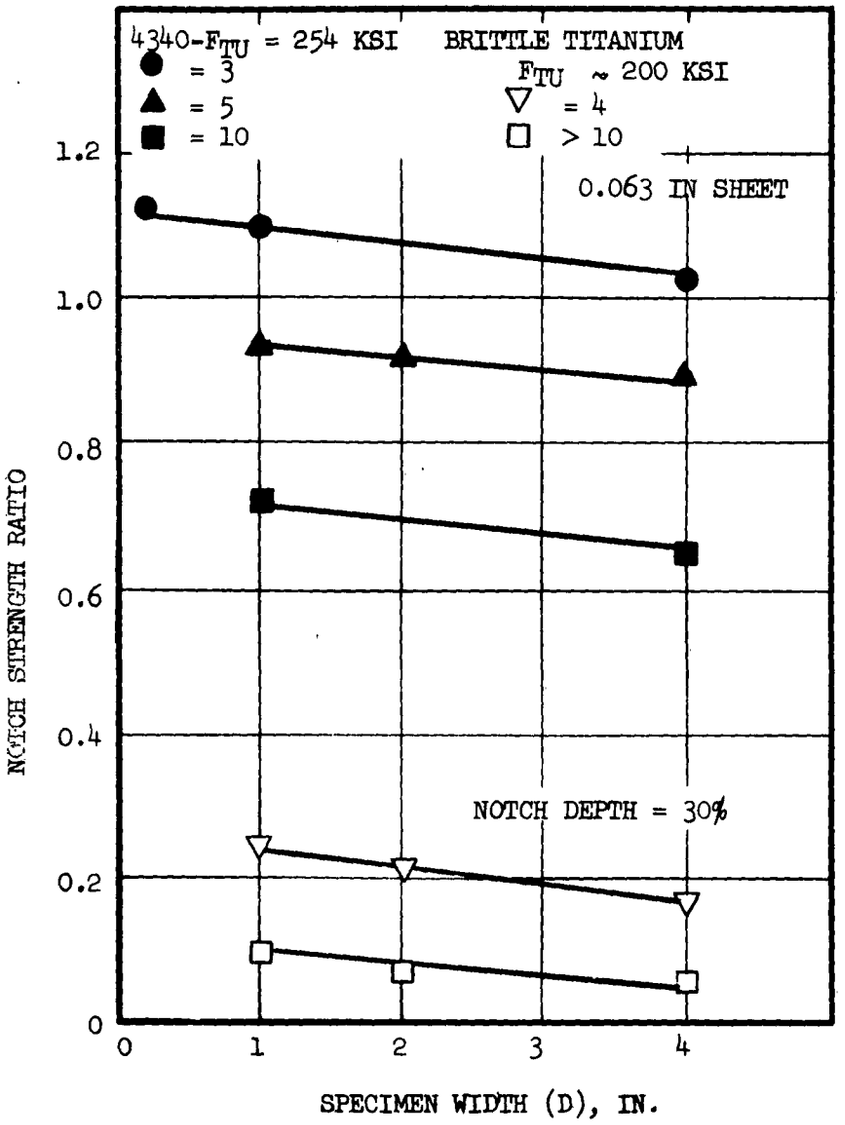


FIG. 13 COMPARISON OF WIDTH EFFECT FOR HIGH STRENGTH 4340 STEEL AND A BRITTLE TITANIUM ALLOY

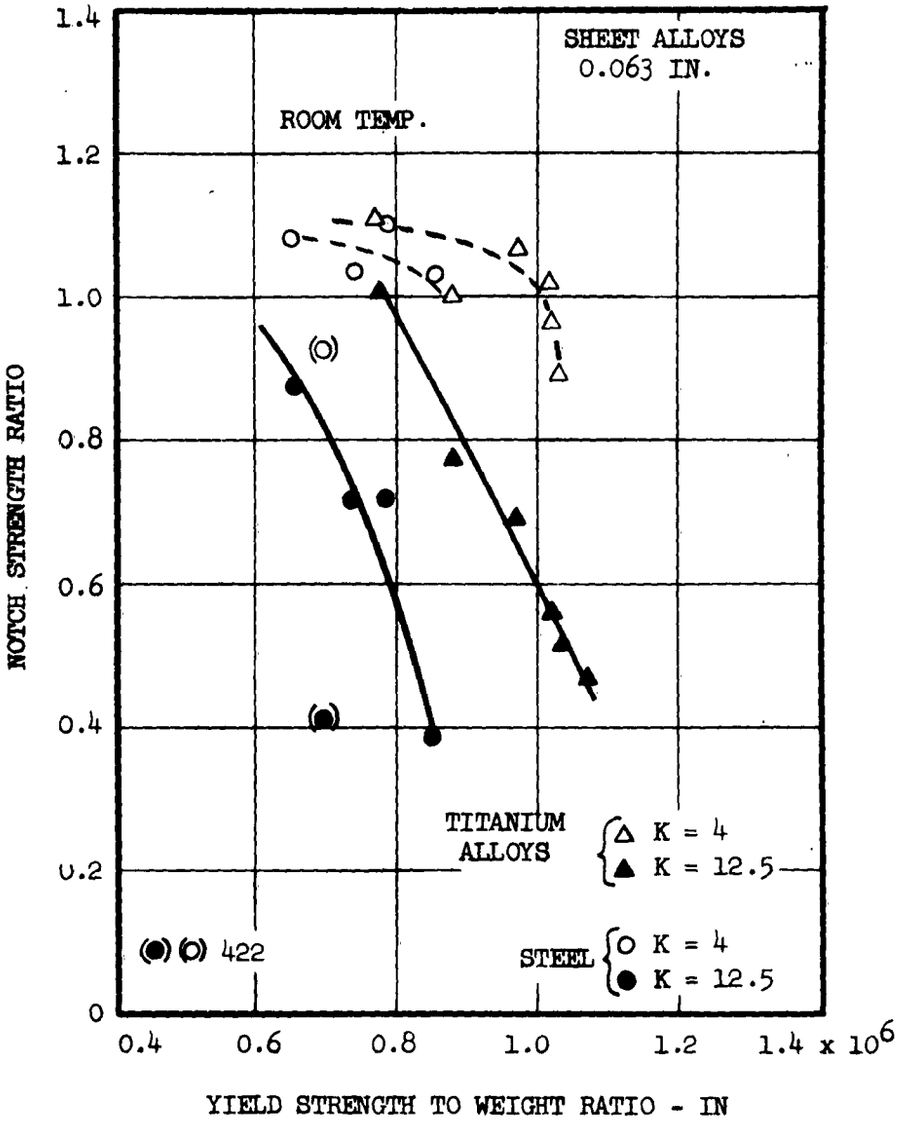


FIG. 14 COMPARISON OF THE NOTCH STRENGTH RATIOS OF FERRITIC STEELS AND TITANIUM ALLOY FOR EQUAL YIELD STRENGTH TO WEIGHT

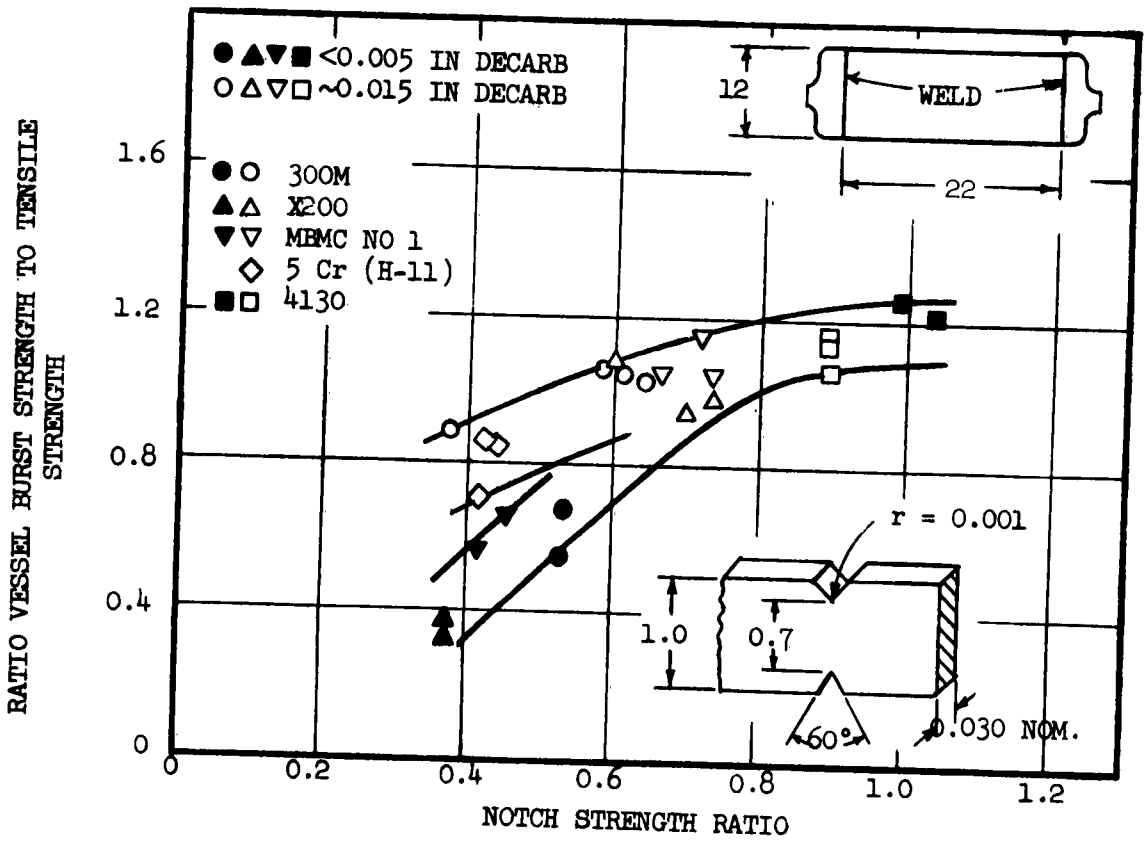


FIG. 15 RELATION OF BURST STRENGTH TO NOTCH STRENGTH CHARACTERISTICS OF SPECIMENS CUT FROM VESSELS (CAINE ET AL 1960)

ARMY REQUIREMENTS

JOHN J. BURKE

Ordnance Materials Research Office

The three Services are concerned with the problems associated with conducting modern warfare. As a result, the problems each encounters in the use of high strength sheet materials are similar although subtle differences do exist. Since the problems are associated, we have a large community of interest in the behavior of sheet materials and thus the probability that some of the difficulties will be eliminated in the near future is increased.

When one looks back over the years and considers the requirements of the Army in our early history, one finds such expressions as "keep your powder dry" and "don't fire until you see the whites of their eyes"; how uncomplicated it was to wage war at Lexington and Bunker Hill. However, the world has changed and so have the Army requirements. Today we have the responsibility of equipping an Army that must be transportable quickly to any area of the Globe, must be prepared to fight a decisive war, and must be able to carry its own supplies of fuel, food, and ammunition. The heart of the problem is mobility; light-weight, compact equipment.

The Army has many problems to solve in order to have an instantaneous retaliatory fighting Group. However, one of the most urgent problems is that associated with high strength sheet material. It must appear ironic to the layman on being informed that the Stanley Steamer had a boiler constructed by a roll and weld procedure and in addition was wire wrapped that today, in 1960, one of the most serious limiting factors in the construction of missiles is the fabrication of a case to retain the propulsion pressures.

This conference has been set up to bring together some of the best minds in the field of research to consider in detail and to take a hard look at the problems in the use of sheet materials. It is quite apparent that the problems relating to sheet materials encompass a wide spectrum -- from the preparation of the materials from the raw state -- through the working of the metal -- fabrication -- joining -- testing, etc., until it ends up as a component that conforms and operates as the design calls for. During the next few days, many of the problems relating to sheet materials will be explored in depth.

Perhaps it would be appropriate to state the Ordnance Corps philosophy as it pertains to materials. The Ordnance Corps feels that once the requirements of a certain application of a material are determined and appropriate test procedure set up to assure compliance, then industry should have the freedom of selecting the appropriate material and treatments. This approach has been used in numerous procurement actions and has proven to be a very feasible method. However, this state of affairs has not, as yet, been reached for high strength sheet materials for missile applications.

When one asks what the Army requirements in sheet material are, he is asking a question that is rather difficult to answer in ten minutes. The Army uses sheet materials in a number of items that extend from its grass roots use in body armor and helmets to missiles and rocket applications. A few of the uses in the Services are high strength/light weight pipes, thin sheets stiffened by dimpling, material for use in vertical take-off craft or craft that hover a few feet off the ground and can skim over the terrain. In addition, we have the use of sheet material in bridges, landing mats, and numerous other applications. However, the problems relating to sheet materials for missiles, rockets and erecter launchers are perhaps the most severe from a weight-load consideration.

The requirements or boundary conditions of a material are dictated by how an Army must operate. Thus high strength sheet material for missiles or rockets must possess certain properties that would not be critical for other Army uses.

The Army has a strong interest in solid propellant missiles, the basic reason being that it is a weapons system that offers instantaneous retaliatory capability while circumventing the problems of storage and handling associated with liquid propellant systems

The next consideration is the weight of the inert parts of the missile. For every decrease in weight of these parts, substantial gains are made in the range or payload of the missile. The principle areas where savings in weight may be realized are the combustion chamber section including the forward and aft enclosure bulkheads, the nozzle section and the vector control devices.

The motor casing is subjected to a pattern of stresses due to the combustion of the fuel and those imposed due to flight. The skin temperature usually does not exceed 300-400°F while the fuel burning temperature is around 4000-5000°F and lasts for a time interval of a few seconds to around 90 seconds.

The requirements of the Army for sheet materials for use in missiles may now be stated. Broadly speaking, at present we want motor casings with a strength/density ratio of around 1,000,000. However, once this goal has been firmly reached, our requirements will be raised. This is necessary to assure the development of more efficient weapons systems.

Having a high strength/light weight material is not enough. The material must be reliable in all aspects which are many and contingent on freedom from flaws, possession of high fracture toughness, good corrosion resistance, and formability and joinability.

The best candidate materials today are steel, titanium alloys and certain reinforced plastics. In order that these candidates qualify as rocket materials, it is necessary to develop their high strength potential. This is being done by conventional heat treatment, alloy development and by plastic working of the material.

One of the Army programs being carried out in this area covers a study of the effects of mechanical and thermal processing on high strength steels, including the effect of retained austenite and stress induced martensite on mechanical properties. The effects of prestraining and aging are also being investigated.

The less conventional methods being studied are thermal-mechanical sequence, flow tempering, composites, etc. "Flow Tempering", which is a combination of cold working and tempering applied to quenched or isothermally treated steels is a typical program. The steels so treated are then tested to determine the effect of the process on their strength, ductility and toughness.

The next step in the development of a missile would be forming. The basic methods used to form the sheet material into a motor casing are the roll and weld metal, the use of mechanical ring forgings or roll forming a forged pre-form. Under investigation are spinning, deep drawing, wire wrap, strip wrap and the other novel methods with which we are all familiar. I might mention a couple of the Army's programs; one covers the development of ultra-high strength rocket cases by cryogenic stretch forming of annealed stainless steels. Another one is to develop high strength rocket motor cases utilizing interlocked titanium wire.

Equally important are the methods by which the components are joined together. The weld joint efficiency should be better than 90 percent. However, there have been cases when it has been necessary to accept values somewhat lower and to compensate by design changes.

The Army has a program investigating the effects of joint width on the properties of electron beam weld using certain titanium alloys.

A second investigation is concerned with the nature and distribution of micro and macro cracks and porosity in high strength weld metals, and the effects of such flaws on mechanical properties. The causes of such flaws are being investigated and attempts to eliminate them carried out.

Testing of the welds of the motor casings has presented some formidable difficulties. I might mention that the Army is investigating the use of infrared techniques for examination of the welded joints in thin sheet material. It is hoped that the technique can be extended to examination of the complete motor case.

Finally, we are supporting work on the mechanics of fracture. At present, steels with a yield strength of 225,000 psi or greater present problems of low fracture toughness aggravated by potential fracture centers. In this regard, there is a definite need for more basic knowledge about strain hardening and fracture mechanisms. The Army would like to be able to use steels with a 300,000 psi yield strength and still have sufficient toughness and ductility.

Titanium alloys and especially some of the newer all-beta alloys give promise of exceeding a strength/density ratio of over 1,000,000. However, there are other problems associated with the use of titanium that will be discussed at this conference.

Therefore, meeting of the Army requirements is contingent upon development of materials, control of processing, fabrication, understanding the fracture process and, finally, test methods and specifications of properties. The program scheduled for the next few days should place these problems in their right perspective and should provide some insight on possible solutions.

HIGH STRENGTH SHEET AND PLATE IN NAVY EQUIPMENT

T. F. Kearns
Head, Metals Branch
Bureau of Naval Weapons

The Navy, in the performance of its assigned missions in national defense, operates a very wide variety of equipment. The ships and submarines at sea, aircraft and related equipment with the carrier task groups, in anti-submarine patrol and reconnaissance, the complement of missiles needed for naval purposes and, more recently, activity in the space field as well as the amphibious and ground equipment needed by the U. S. Marine Corps present an extremely broad and varied series of requirements for materials of construction in sheet or plate form.

The breadth and variety of the Navy requirements makes it completely impracticable to attempt a listing, even in outline form, for presentation at this conference in any reasonable amount of time. Moreover, since the interests both of the Army and of the Air Force are in many cases identical with ours, when similar equipment is being discussed, there would be considerable duplication should an extensive listing of requirements be attempted. The following information, therefore, represents merely examples of Navy requirements selected to illustrate specific needs.

Strength Considerations - The requirement which commands first attention in practically all structural material development is tensile strength. This is usually spoken of as a strength/weight ratio because in so many structural applications, where low weight is at a premium, it is in fact the strength/weight ratio rather than strength, per se, which is significant. However, this is not always the case. Figure 1 illustrates a trend in airfoil shape that has been in progress for many years. In an airfoil which is a cantilever beam we are not at liberty, as the beam depth decreases, to judge materials solely on a strength/weight basis inasmuch as the effectiveness of the material varies with its distance from the neutral axis. In some of the very thin wings we find that materials with lower strength/weight ratios are actually more efficient than lower density materials of higher strength/weight ratio. In addition to the matter of structural efficiency we are frequently space-limited wherein materials of the highest possible tensile strength per se are required. The fittings which attach the very thin airfoil to adjacent structure are examples of these applications.

In the last several years, as emphasis in flying vehicles has shifted from manned aircraft to missiles, there has been not the slightest decrease in the pressure exerted by design engineers on the materials fraternity to make available to them construction materials of even higher strength/weight capabilities. The Polaris missile is typical of the end-items involved. At the present time alloy steel of 200,000 psi yield strength is a typical case construction material. However, the pressure for higher strength/weight materials of construction will inevitably force an increase in this figure. The driving force behind this requirement is simple and is illustrated in Figure 2. It is, in fact, even more important in missile construction than it was in the construction of manned aircraft that materials with the very highest capabilities be available for design use.

In another field, that of the submarine, the Navy would profit greatly from an increase in sheet/plate material performance. In a typical vehicle the material concerned is that which forms the pressure hull. A submarine is so designed, by location of internal stiffeners and bulkheads, that the critical mode of failure of the pressure hull is compression yielding. For operational purposes there are considerable advantages to be attained from an increase in the maximum operating depth capability of submarines and the Navy, therefore, has a requirement for submarines with this capability. Figure 3 indicates what this means in terms of material parameters. The numbers have been omitted to keep this presentation unclassified. However, the advantage of a high compressive yield strength/weight ratio in hull material should be apparent.

Sheet and plate materials for use in the very high temperature regimes encounter, generally, a somewhat modified set of materials parameters. Perhaps the most significant change from the customary lower temperature parameters is the entry of time as a major variable. Short-time properties, stress-rupture strengths and creep strengths become determinants of material performance.

There has been so much said and written on the need for improved high temperature materials that repetition here would serve no purpose. However, in the area of very short time properties, there is one point that seems to deserve greater emphasis than it is currently being accorded. This concerns the heat treatment condition in which materials are tested for very short time (seconds) properties. In most evaluation and testing programs designed to examine the short-time high temperature properties of materials we find that the materials are being tested in heat treatment conditions which represent desirable long-time service conditions. Aluminum alloys fully aged, steels fully heat-treated etc. by procedures established not for short-time but for

long time performance. It is not clear how great an advantage may be attainable through tailoring the heat treatment to maximize short-time performance. However it would certainly seem worthy of consideration and this avenue of approach is suggested as one means of attaining the improved sheet materials required by the Navy for short-time high temperature service.

Fabrication Considerations - The requirements that are placed on the developers and producers of materials are, by no means, limited to strength characteristics. In the production of sheet material itself matters of sheet size and of tolerances may become very important weight determining considerations. As sheet becomes wider and thinner variations in thickness become more significant and estimates of over 10% weight saving in thin sheet metal structures, possible by reduction of thickness tolerances, have been made. In addition to the rolling operation it appears that the trend in requirements for the sheet metals needed for future Navy equipment will require a rather broad series of advances in sheet material fabrication and quality control techniques. In this area, vacuum and similar melting for higher quality ingot production, improved breakdown procedures particularly for the more refractory materials and the establishment of precise technical limits at each stage of sheet production are required to insure the production of the high quality, uniform, reproducible sheet products needed for future equipment.

Forming and joining of sheet or plate into end items also constitutes an area in which the Navy sees a need for considerable advancement. The welding of large sections of thin high strength sheet for missile casing has received considerable attention. In the case of the deep-diving submarine we have a similar welding problem. However, in this case the material thickness may be several inches and heat treatment after welding completely impracticable. Requirements for new and improved welding techniques arise also from the introduction of new alloy systems into the construction material portfolio. Molybdenum, tungsten and beryllium together with the high strength titanium alloys all create welding problems for which solutions must be found. You may be interested in the weld, shown in Figure 4, made by ultrasonic welding between two QMV beryllium sheets. This process, which was developed under Navy sponsorship, is typical of the unusual fabrication techniques for which we see a need in fabricating future high strength sheet materials.

Resistance to Environment - As one might expect, the Navy, operating over, in and under salt water, places considerable emphasis on the subject of corrosion and its prevention. As those of you who have spent any time aboard Naval vessels are aware, the chipping hammer is in full operation. Recent trends in design in the flying vehicle field, introducing higher and higher strength alloys, have increased the sensitivity of our equipment to corrosion damage. At the end of World

War II operational aircraft outer skins were clad aluminum alloy approximately .064 inch thick. Today they may be milled from bare high strength aluminum alloy plate several inches thick. The resultant elimination of the protective cladding and of the increase in thickness of the material during heat treatment produces an increased sensitivity to intergranular and stress corrosion. Unfortunately, many of the light alloys which exhibit improved mechanical properties are also more susceptible to corrosion and stress corrosion cracking. Laboratory and exposure tests of the precipitation hardening stainless steels have also indicated a sensitivity of these alloys to stress corrosion cracking.

The mere fact that a material is sensitive to corrosion or stress corrosion need not preclude its use in Naval equipment. However, there is a logistic penalty for poor corrosion resistance which the Navy must pay for use of materials of this type. Corrosion resistance must therefore be accorded an important place among Navy requirements in sheet materials.

A phenonemon which complicates the corrosion resistance picture in the high strength steel area is that of hydrogen embrittlement. Figure 5 shows typical results of hydrogen damage to steel in the 260-280,000 psi UTS range as a result of cyanide cadmium plating. These are unnotched C ring specimen results showing typical delayed fractures, the time to fracture varying with the applied stress. Considerable effort has been expended on the development of electrolytic application techniques for corrosion protective platings for high strength steels with only partial success. On steels at strength levels of over 240,000 psi UTS the Navy does not believe that electrodeposited cadmium or zinc coatings can be reliably depended upon to be free of possible hydrogen embrittlement damage and lists among its requirements in the high strength steel area a reliable means of applying a protective metallic coating which will eliminate the cost and application disadvantages of the alternative sprayed or vapor deposited coatings.

Lest the elimination of the metallic protective coating appear attractive as a means of eliminating the hydrogen embrittlement problem, we have found that 4340 steel at a strength level of 260-280,000 psi will crack in a few days in salt spray under an applied stress of 80% of the yield strength. We need not resolve here the question of whether this is a hydrogen embrittlement or a stress corrosion failure or whether there is any difference between the two. The need for a metallic protective coating which will withstand rough usage and will prevent corrosion of high strength steels remains.

At elevated temperatures the problem of high temperature oxidation is encountered. This becomes most serious at temperatures

above 1800°F when, for reasons of strength, we are forced to leave the nickel and cobalt base super alloys and employ the refractory metals.

There are available, as a result of many years work, several coatings which will prevent oxidation of molybdenum alloys at temperatures from 2000-3000°F for times varying from several hundred hours to a few hours respectively. However, when the complications of forming, joining, drilling and rivetting or welding of assemblies, the presence of faying surfaces, abrasive conditions and thermal shock in service are added, there still remains a need for much better protective coatings for molybdenum alloys than those now available.

Although niobium does not, as does molybdenum, have a volatile oxide, it is very rapidly attacked by oxygen at high temperatures. Whereas considerable alloy development effort in molybdenum has failed to produce an oxidation resistant alloy it is yet too early in niobium-base alloy development to be completely pessimistic on this score. A coating development, which some of you may not have seen, was released this Spring by the Navy and is illustrated in Figure 6. This is a specimen of niobium which was coated with zinc and exposed for some twenty (20) hours at 1800°F after having been milled deeply enough through the center section to remove completely the zinc coating in the 3/8" slot area. The zinc coating appears to be effective in preventing both surface oxidation and oxygen pick-up, as indicated by hardness measurements, at temperatures up to about 2100°F, and its self-healing ability is outstanding.

One of the complications which arises in a search for a coating which will prevent oxidation of tungsten at high temperatures is the very limited number of possible systems available. Tungsten, due to its high density, is structurally competitive only at the highest temperatures. In many applications, such as in rocket nozzles, the environmental temperatures will approach the melting point of tungsten itself. The requirement that an oxidation protective coating have a melting point of the order of that of tungsten itself is quite effective in eliminating broad classes of materials from consideration.

Beryllium and Vanadium - Recent results obtained in an alloy development program on vanadium base alloys have indicated the availability of very attractive possibilities in that system. In an alloy of V-20% Cb-5% Ti short time tensile strength of 75,000 psi at 1800°F, 50,000 psi at 2000°F and 35,000 psi at 2200°F have been attained. With densities of about 6.2 and apparently good ductility and weldability, the vanadium system appears to be one of increased interest for the future.

We are all aware of the interest and activity in the area of beryllium alloys and of the very attractive density and rigidity properties available in this alloy system. In this area, work sponsored by the Bureau of Naval Weapons has demonstrated what we believe is the first evidence of significant basal plane ductility. A single crystal with basal plane orientation 20° off-parallel with the applied stress was pulled in tension and achieved a reduction of area of about 20% before failure. Extensive basal plane slip was indicated by both microscopic and x-ray diffraction measurements. The crystal was very pure, resulting from a five (5) pass zone refining in very pure argon. This work is continuing and, we believe, indicates the possibility of developing truly ductile beryllium alloy sheet.

The above examples are cited to emphasize the Navys need not only for improved materials and techniques in the alloy systems of which we are now constructing equipment but also in new systems such as beryllium and vanadium in which an extensive technology remains still to be developed.

Crack Propagation and Failure - It is apparent from the presentations scheduled at this Sagamore conference that the subject of crack propagation and failure will receive extensive attention. It is, in fact, a field of great importance and of extensive current activity.

The remarks which have been and will be made by representatives of the other services should cover adequately the significant requirements of the Navy in this area.

However, there is a thought in this area which might well receive more attention than it is currently being accorded.

Figure 7 is a plot of some missile case burst test results showing a decrease in load carrying capacity of the case wall as the depth of defects increases. This case was, no doubt, designed on the basis of yield strength as the controlling material parameter. The assumption that a structure will not yield, much less fail, at a stress lower than its yield strength underlies most structural design. We know, of course, that this is not true for many materials, particularly at very high strength levels. We know that cracks, or defects, may propagate and cause structural failure at stress levels well below yield strengths.

It would appear that the materials fraternity has a task here, in cooperation with the design engineers, not only to select and verify more meaningful structural performance criteria, which it is now doing, but also to lend the fullest cooperation in the necessary task of translating this information into design practice. The latter step will probably require a deliberate concerted effort by materials

people. It will require the measurement and reporting of the meaningful criterion, as a matter of course, in standard property data tabulations. It will require on the part of the materials people a detailed acquaintance with the subject of crack propagation and a good knowledge of the significance and limitations of the failure criterion. The universities, finally, must play their part by so modifying the instruction of future design engineers that rational design practice for the conditions under which crack propagation failure is a hazard becomes a part of the thinking of future engineers.

As one step in this vein the Navy has conducted a series of tests of an aircraft wing, the lower skin of which was constructed of a single large 7075-T6 integrally stiffened plate. Laboratory tests had indicated that catastrophic failure by crack propagation might be expected at stresses on the order of 25,000 psi. As you will see, from the high speed motion pictures taken of these tests, the full-scale structure tests confirmed quite well (28,000 psi) the results predicted in the laboratory.

AIRFOIL TRENDS
15%
1935 TO 1945
THICKNESS RATIO = 0.15
10%
1945 TO 1955
THICKNESS RATIO = 0.10
4%
1955 TO →
THICKNESS RATIO = 0.04
RAZOR BLADE
THICKNESS RATIO = 0.038

FIG. 1

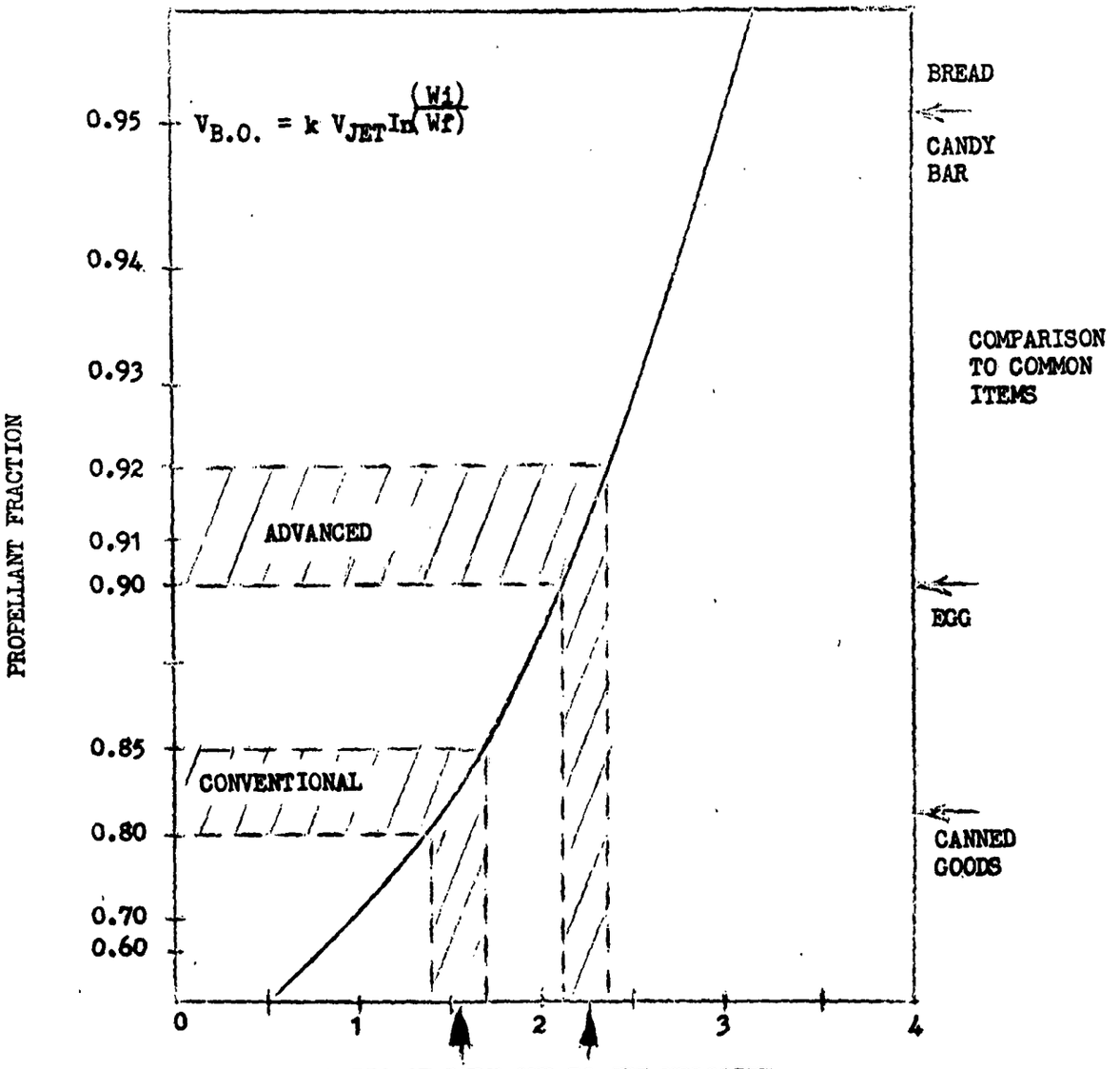


FIG. 2 RATIO OF BURN-OUT TO JET VELOCITY

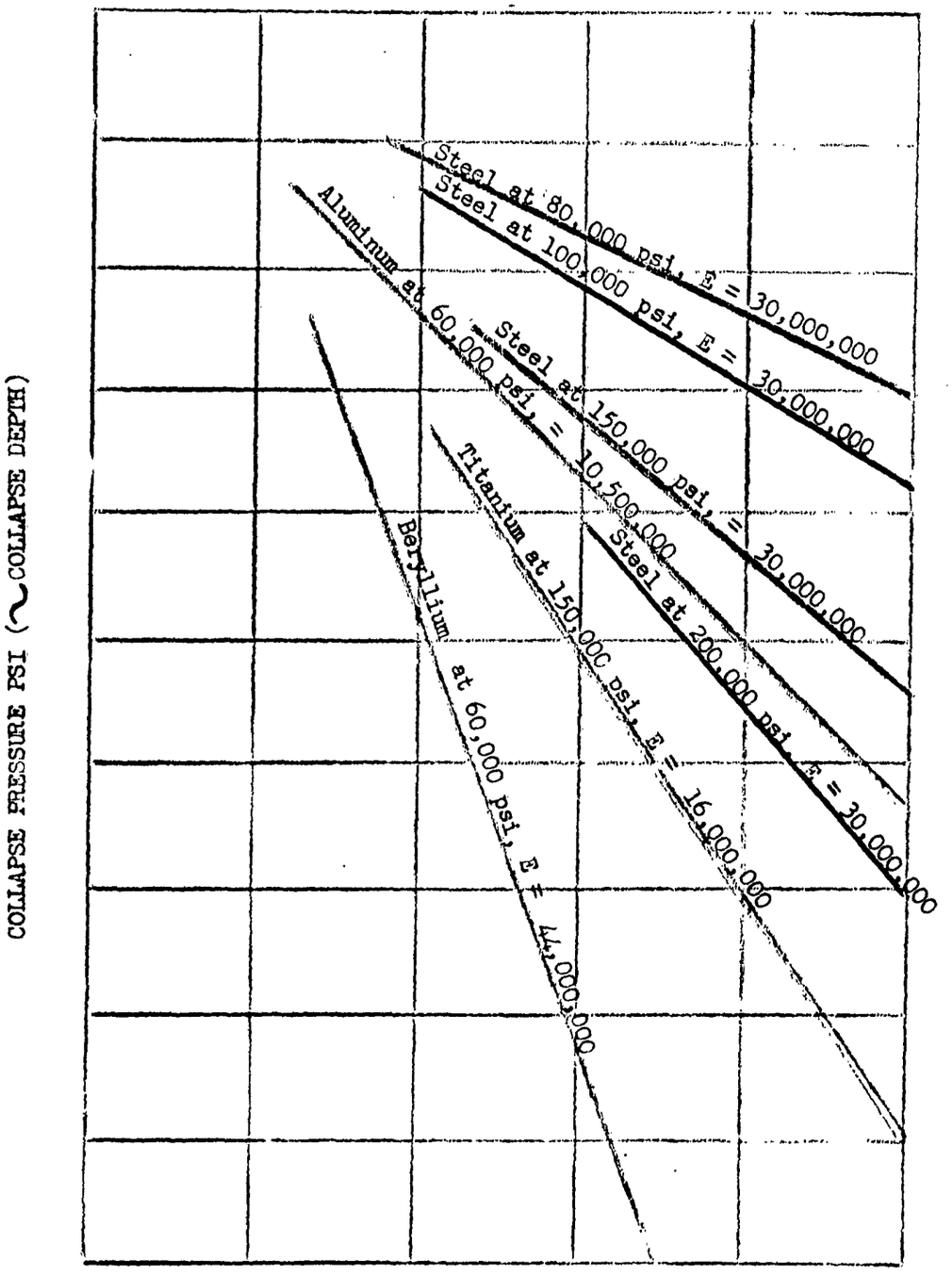


FIG. 3 WEIGHT OF PRESSURE HULL
WEIGHT OF DISPLACEMENT



FIG. 4

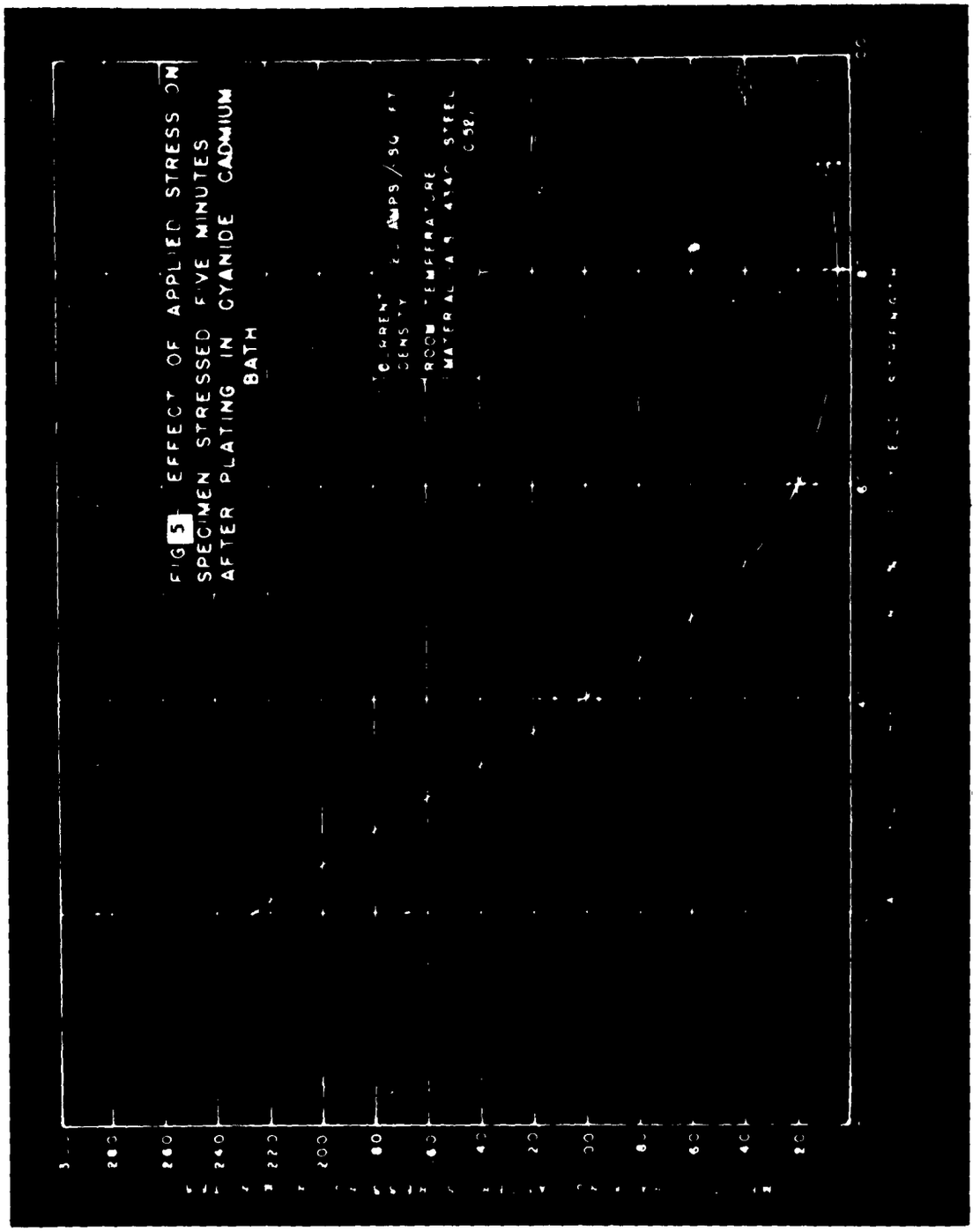

FIG 5 EFFECT OF APPLIED STRESS ON
SPECIMEN STRESSED FIVE MINUTES
AFTER PLATING IN CYANIDE CADMIUM
BATH

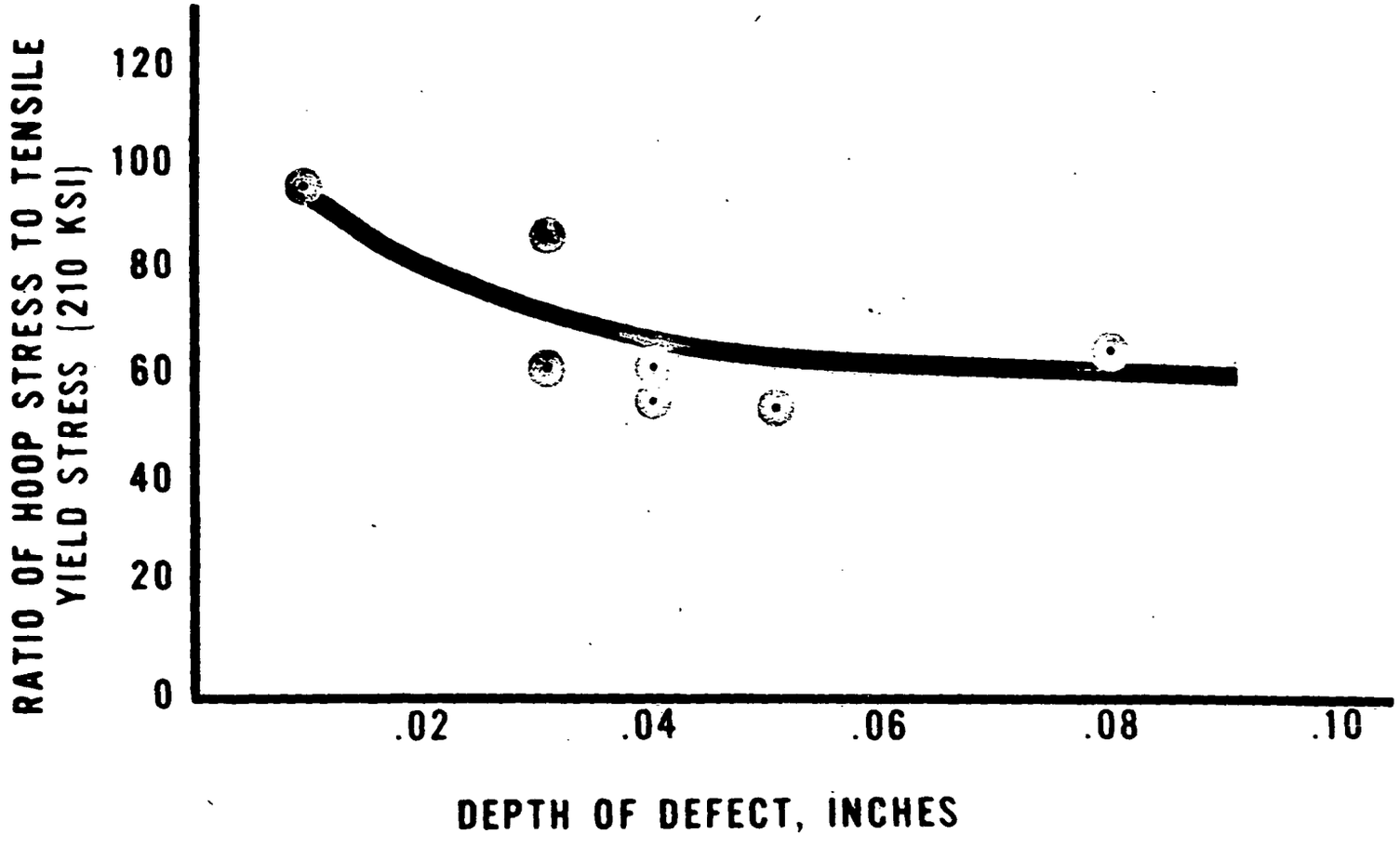
FIG. 5



FIG. 6

FIG. 7

DEPTH OF PRIOR DEFECT WHICH INITIATED FRACTURE OF STEEL WELDED CASES RELATED TO RATIO OF HOOP STRESS TO UNIAXIAL YIELD STRENGTH OF THE WALL MATERIAL



AIR FORCE DEVELOPMENTS FOR HIGH STRENGTH MATERIAL

by

Paul L. Hendricks
Wright Air Development Division
Wright-Patterson Air Force Base, Ohio

Of the various areas requiring high strength sheet material, perhaps one of the most important areas of application is the solid propellant rocket motor case. Although there are various materials under consideration for this application, only high strength steels and titanium alloys will be considered in this brief presentation.

The primary concern currently is the development and utilization of steel and titanium alloys with high strength to weight ratios for application at ambient and moderately elevated temperatures. While strength to weight ratios are of prime importance, there are other secondary characteristics which the material must also possess in order to take advantage of the high strength to weight ratios obtainable in steel and titanium alloys. The present state of the art has produced materials with high strength to weight ratios; however, a lack of knowledge as to the control of factors that influence such secondary characteristics as notch toughness, corrosion resistance, etc., have placed severe limitations on the strength levels at which steel and titanium alloys may be used. Even when a better understanding is obtained regarding the control of secondary characteristics, the modulus of elasticity of these materials may be a controlling factor. Since it is unlikely that the modulus can be substantially increased, it appears that one may not be able to take full advantage of high strength to weight ratios obtainable since buckling may become a factor below a certain thickness.

With regard to Air Force developments in steel and titanium alloys, it appears that the obtaining of materials with high strength to weight ratios does not represent the major problem. The greater problem seems to be a lack of understanding of the factors that control secondary characteristics and other factors, such as joining, that will ultimately control the extent to which currently available materials may be utilized. As one considers all the factors involved in the utilization of high strength to weight ratio materials, the required Air Force developments become increasingly complex and cannot be stated in relatively simple terms. Let us now consider briefly some of the required areas of research and development necessary for making possible the utilization of high strength steel and titanium alloys.

Recent failures of solid propellant rocket cases by brittle fracture have resulted in the development of a number of test methods for evaluating the fracture toughness or brittle fracture tendencies of alloy sheet steel and titanium alloys at high strength levels. Experience has shown that none of the standard tests, such as uniaxial tensile tests, are suitable for application to high strength sheet materials. A discussion of various tests currently in use is beyond the scope of this

paper; however, it should be mentioned that these tests involve tensile loading of center and edge notched specimens, bending of flat notched specimens, impact loading of notched specimens, bulging of unnotched, notched, and welded specimens, and combinations of tensile loading and internal pressurizing of cylindrical specimens. In light of available information, none of these tests has been recognized as a standard test and correlation of test data with pressure vessel performance has been limited. Studies currently under way should produce information as to the relative usefulness of each test in evaluating fracture toughness of sheet material. There still remains, however, the problem of determining the relationship between such factors as alloy composition, heat treatment, welding, fabrication techniques, and the fracture toughness of sheet materials.

One of the principal areas of interest to the Air Force is therefore the relationship of microstructure in steel and titanium alloys to fracture toughness. This is an area that is relatively complex in nature since there are a number of factors, all of which have an influence either directly or indirectly on the microstructure. It is felt that to date primary interest has been centered on obtaining results on different alloys using one or more of the many fracture toughness tests recently developed and few known attempts have been made to correlate fracture toughness with microstructural conditions. The study of microstructure as related to fracture toughness is considered to be a prime area requiring intensive investigation. An investigation of microstructural conditions on a gross scale is not deemed adequate to provide the information necessary for an intelligent approach to utilization of high strength sheet materials. It appears that an intensive study of microstructures requiring the use of such tools and techniques as electron transmission and electron microscopy to delineate microstructures on a fine scale, including sub-structure, will be requisite for such an investigation. The use of such an approach to a study of the relationship between microstructure and fracture toughness is expected to yield valuable information regarding the utilization of high strength sheet materials in such applications as pressure vessels.

Increasing requirements for higher strength to weight ratio materials demands that an investigation and evaluation of unique processing techniques to obtain strengths greater than those available through regular heat treating or conventional techniques be accomplished. Examples of these techniques are the so called "Aus-Forming" process which has been successfully applied to certain steels and strain aging techniques which may be applicable to both high strength steels and titanium alloys under certain conditions. There is also the possibility that a knowledge of the unfluence of microstructural conditions may suggest methods of improved heat treating which will result in improved strength and fracture toughness characteristics.

The ever increasing trend toward sheet materials with higher strengths requires that the joining problem be given adequate attention. One of the prime considerations, therefore, as to the fabricability of a material is its weldability. Not only must the material be capable of being welded, but the resulting joints must have strength properties similar to those of

the base material; otherwise, any advantage of high strength is lost. In addition to considerations of strength, the weld joint must be sound and free from porosity, cracks, and other types of flaws which might result in stress concentrations and thus promote premature failure. It is also apparent that the weld metal's resistance to crack propagation is of great importance. With regard to high strength steels, most of them can be welded; however, the big problem is to obtain welds that are serviceable in pressure vessels. The production of rocket motor cases from steel would be greatly enhanced if methods could be developed for producing satisfactory longitudinal welds. In fact, the welding of high strength steels for rocket motor cases is a problem of such proportions that many manufacturers will go to great trouble and expense in order to keep the use of welds in such structures to a minimum. There is also no universal answer to the problem of welding high strength steels since the answer will no doubt vary, depending upon the composition in question. It does appear, however, that there will be certain basic information obtainable relative to welding that will be applicable in all instances. An example of such information could conceivably be a knowledge of the relation of factors contributing to the response of the weld to subsequent heat treatment.

The utilization of welds in titanium alloys poses a quite different and a difficult problem. There are two primary reasons why titanium alloys are difficult to weld by common welding processes such as gas fusion welding and arc welding with active gases:

1. Titanium and titanium alloys are extremely reactive when heated to welding temperatures and readily react with air and most elements and compounds, including all known refractories.

2. The ductility and toughness of titanium welds are reduced by the presence of small amounts of impurities, especially carbon, hydrogen, nitrogen, and oxygen.

In spite of their high reactivity and low tolerance for impurities, certain assemblies can be readily joined by spot, seam, flash, and pressure welding. These welds, however, are not always considered adequate for application in pressure vessels. It therefore is readily apparent that research in the welding of titanium alloys is a necessity if these materials are to be given serious consideration for application in rocket motor cases.

For materials that obtain high strengths through the use of unique processing techniques, joining represents a major problem. Welding may or may not be possible, depending upon the details of the operation involved. For materials in this category, a new approach to joining may be necessary.

In light of the many developments that have taken placed in obtaining steel and titanium alloys with higher strength and with an increase in knowledge pertaining to factors that influence notch toughness, programs in alloy development may become increasingly important. Many of the increases in strength have been obtained by applying new techniques to existing alloy systems. These systems may not represent

the optimum compositions insofar as obtaining materials with the desired service characteristics is concerned. It seems very feasible that the development of new compositions tailored to meet conditions found necessary for optimum service performance may be highly desirable.

As has been previously mentioned, one of the principal problems in the utilization of high strength materials is failure by brittle fracture on pressure testing. This problem has been complicated by the fact that materials used and welds produced in pressure vessels often contain flaws that escape present inspection techniques. These flaws have been observed in many instances at the origin of brittle fracture in many failed pressure vessels. In material sensitive to brittle fracture, the larger flaws may initiate brittle fracture during pressure testing. In materials with adequate toughness, pressure testing may develop the crack to some size at which no further extension occurs; whereas in materials with inadequate toughness, rapid propagation of the crack may occur, resulting in brittle fracture. Since many of the flaws, subsequently determined to be points of initiation of brittle fracture, have not been detectable using present techniques, there seems to be a requirement for the development of new and improved inspection techniques which are capable of detecting the various types of flaws which are known to contribute to brittle fracture.

Desirable Air Force developments for high strength materials may be summarized as follows:

1. A knowledge of the factors that control or influence the notch toughness of high strength materials.

2. A simple test upon which the service performance of high strength materials can be predicted.

3. Weldments capable of giving adequate performance under stress systems found in pressure vessels.

4. Investigation and evaluation of unique processing and improved heat treatments resulting in higher strength materials.

5. The development of alloys tailored to various processing techniques capable of meeting present service requirements.

6. The development of adequate inspection techniques to insure reliability of performance in high strength materials.

These developments should result in the production of pressure vessels fabricated from high strength materials with a high degree of reliability and performance.

EXPERIENCE WITH ULTRA HIGH STRENGTH FORGINGS IN AIRCRAFT STRUCTURES

George G. Wald, Research Specialist
Lockheed Aircraft Corporation, California Division
Burbank, California

Introduction

It has now been more than ten years since Lockheed initiated their investigation of ultra high strength steel. As a result of that investigation it was determined that 4340 steel heat treated to 260-280 ksi level was eminently suitable as an aircraft structural material. The first application of this ultra high strength steel to critical aircraft components followed in 1953 on modifications of the main and nose landing gear of Lockheed's 1049 series commercial Constellation Transports. A sketch of the main landing gear is shown in Fig. 1 to illustrate the type of parts heat treated to the 260-280 ksi level. The high heat treat parts include 1) the main cylinder; 2) the attachment bolts in the upper and lower drag links; 3) the upper drag links; 4) the torque arms; 5) the axle; and 6) the piston (not shown). Three of these parts including the main landing gear cylinder, piston and axle are shown in Figs. 2, 3 and 4 respectively. This same gear was also successfully used on military versions of the Lockheed Constellation seeing both Air Force and Navy service.

Since that time ultra high strength steel has been employed for the landing gear of the 1649, a long range version of the Constellation and the C130 Hercules Transport for miscellaneous pins, bolts and fittings for our F-104 Starfighter and more recently for the main and nose landing gear components of Lockheed's Electra prop-jet transport.

Fig. 5 shows a photo of the Electra main landing gear. The main cylinder, piston, side braces, trunion arms and the torque arms (not shown) are fabricated from high heat treat steel.

Lockheed's service record has shown a minimum of difficulties with all these components. Thus, it is the purpose of this paper to review the basic considerations, permitting exploitations of such material for aircraft structural components and the special design and manufacturing controls required.

Establishment of Structural Integrity

In the early application of steel to aircraft parts the tensile strength was limited to approximately 200 ksi, even though higher strength could be easily obtained by simple modification of heat treatment. Probably the most important single factor influencing this failure to make use of the potential high strength characteristics of alloy steel was the fear of excessive brittleness. However, the increasing demand of the airframe designer for improved structural efficiency forced a number of

aircraft manufacturers to re-evaluate the behavior of ultra high strength steels under the design and service conditions normally encountered in aircraft.

Lockheed, in making this evaluation, relied principally upon investigation of the tensile, notch tensile and notch fatigue characteristics. The stress concentrations employed were typical of the maximum normally encountered in aircraft design. Studies were conducted on specimens representing the complete range of sizes encountered or anticipated in aircraft design. Thus, test coupons were fabricated from small bars and from forgings ranging up to 12 inches in diameter. Both longitudinal and transverse grain directions were studied. The evaluation of these coupons was supplemented by investigation of the fatigue and impact behavior of a typical aircraft component.

Contrary to the general belief at that time, the toughness characteristics of 4340 at high strength levels were found to be entirely satisfactory. The notched fatigue strength increased with increasing static tensile strength. This was true throughout the entire range investigated, except for the low cycle range of the curve for specimens having a notch which produced an effective elastic stress concentration factor K_t of 3.0. In this low cycle region of the K_t-3.0 curve, the fatigue strength remained substantially constant as the static strength was increased.

Fig. 6 shows the improvement found at three levels of stress concentration on longitudinal specimens fabricated from two inch bar under completely reversed axial loading (R=-1).

Similarly notch tensile tests indicated that static notch sensitivity, although slightly greater at 260-280 ksi than at 180-200, was satisfactory for aircraft design.

Following these tests a complete analysis was made:

1. To determine design characteristics including compression yield, shear, bearing, modulus of elasticity, column allowables, bending allowables, torsional properties, bursting characteristics, and impact properties.

2. To determine fabrication characteristics.

3. To establish heat treating and processing procedures.

4. To determine the effect of mill variables and various manufacturing operations upon these properties.

No attempt will be made to review details of the complete investigation now, since the work was amply documented at the time (1) (2) (3). Instead, the remainder of this paper will be devoted to the design considerations and manufacturing limitations imposed on the use of ultra high strength steels.

Design Considerations

As already indicated, our analyses of the behavior of high strength steels under typical aircraft structural conditions indicated that it would not be substantially different from that of the moderate strength steels when applied to landing gear and similar aircraft parts. Thus, the rules for good design at the high heat treat level are only an extension of those required for good design at the more conventional heat treat levels. These concepts of good design have been well known for many years by all of us. However, since they are frequently overlooked or compromised, a few are summarized for review.

1. The first design rule is the proper application of the philosophy of exotic sweeps and gentle transitions. A glance at the notch tensile behavior of high strength steels shown in Fig. 7 demonstrates the vital necessity for adherence to this rule. Full strength of steels may be developed where adequate radii are provided - - see typical curve for K_t of 1.6 and 3. However, this is not always possible at high stress concentrations. The notch tensile strength is affected by many factors. These include type of steel, quality of steel, method of heat treat, strength level, size of product, degree of reduction from ingot, grain direction, type and size of specimen being tested and temperature of testing. These factors are superimposed on the normal testing variables; the most important of which is eccentricity of loading. As a consequence, there is considerable scatter in notch tensile data. This scatter is greater at high stress concentrations than at low. A few typical curves are presented here to illustrate the effect of some of the variables noted. The effects of increased stress concentration, specimen size, and grain direction were taken from the work of Klier, Muvdi and Sachs (4). Note that the transverse grain direction is as deleterious at $K_t = 3$ as at $K_t = 10$. The detrimental effect of specimen size is shown at $K_t = 10$.

2. The second rule is to lower the stress level at critical intersections. This is illustrated in Fig. 8 which shows a representative section of the axle piston intersection on a nose landing gear. Here, in addition to providing reasonable radii, the critical transition area is "beefed up" to reduce the operating stress level. Since this area is only a small portion of the whole gear, the overall weight is only slightly affected. The need for this restriction results from the uneven distribution of loading in transition areas. The load tends to be funneled through stiffer members resulting in high local stresses. Thus, the mean stress must be lowered to avoid premature failure.

3. A third rule which is difficult to apply to landing gear components but is important as a design consideration is the maintenance of straight load paths to minimize eccentricities. While this may not always be possible, designs are made to approach this goal as much as practical. Therefore, in areas of reinforcement, usually in the vicinity of fittings and joints, material

is gradually added equally on both sides of the load path centerline. The tension stresses resulting from even small eccentric loadings very often greatly exceed the tension stress due to the primary axial loads. Thus, load carrying ability and fatigue life may be greatly reduced. This effect has been dramatically illustrated by the work of Sachs and Klier in a number of papers.

Their recent work on the effect of eccentric loading on the notch tensile behavior of 4340 heat treated in the 260-280 ksi range (4) is illustrated in Fig. 9. The eccentrically loaded specimens only carried 40% of those concentrically loaded at $K_t = 3$ and only 30% at $K_t = 10$.

4. A fourth rule is to limit the degree of exploitation of the maximum static strength of the material for design conditions where the normal repeated loads are nearly equal to the maximum load on the part. The need for such a restriction is readily apparent on examination of any S-N curve where it is evident that the number of load applications that can be sustained, when high loads are applied, are relatively low. It is also obvious that such a restriction would have to be applied to conventional as well as high heat treat parts. Typical parts on which this restriction would apply would be those on which loads result from hydraulic or other pressure systems.

5. Fifth--Lockheed has preferred to use flash and pressure weld designs and to avoid the use of fusion welds for critical aircraft components. This preference is based upon the fact that pressure and flash weldments are produced by automatic methods wherein reproduction of proven welding procedures can be reliably expected. Residual stresses introduced during flash and pressure welding are low because of the uniformity of the heating and cooling processes; thus, cracking of hardenable alloys such as 4340 is no problem. In contrast, fusion welds are made progressively; thus, high restraint with resultant high residual stresses are realized and cracking becomes quite probable. To overcome this cracking tendency, exacting preheat, postheat and stress relief treatments must be employed. Because of the human element in these and other controlling practices the welds are more subject to inconsistencies. Thus, we do not say you cannot fusion weld but that the exacting process control requirements of the welding procedure results in greatly reduced reliability.

6. The sixth rule is to avoid grinding wherever possible. Since the grinding process involves severe localized temperature differentials, ground parts are subject to high residual tensile stresses, grind cracks, and the generation of untempered martensite. In addition, parts not cracked during grinding are still susceptible to the formation of cracks during subsequent processing. As a result, considerable difficulty has been experienced in the grinding of ultra high strength steels and extreme care has been required to avoid grind cracks. In order to reduce this difficulty to a minimum, Lockheed specifications prohibit the use of grinding except where specifically authorized by engineering

drawing. Even localized rework, i.e. removal of surface defects such as tool marks and magnetic indications is accomplished with a rotary carbide burr rather than by grinding.

Where grinding has been permitted, Lockheed requires parts to be baked in order to temper any martensite generated due to localized overheating and lightly shot peened to remove high surface residual tensile stresses.

7. The seventh rule is to consider the effect of surface conditions on part performance. The effect of surface condition on fatigue properties was dramatically demonstrated early in Lockheed's investigation during fatigue evaluation of a standard aircraft drag strut damper piston shown by Fig. 10.

Tests were being conducted at both the 180-200 ksi and 260-280 ksi strength levels. At the 180-200 ksi level failure occurred in the radii under the piston head. However, two of the specimens heat treated to 260-280 failed in the shank with failure originating at the as heat treated inner surface. This indicated that the decarburized surface was more critical than the stress concentration at the shoulder. These findings were confirmed by evaluation of standard fatigue specimens heat treated to produce varying depths of decarburization.

Fig. 11 presents the results of these tests. It will be noted that the as heat treated surface reduces fatigue more than a stress concentration of $K_t = 3.0$. This loss in properties occurred with .003 decarburization as well as with .030 decarburization. The effect of as-forged surfaces is even more deleterious as shown by the work of Hankins and Becker (5).

The design rule for parts which are critical in fatigue is that as-forged and as heat treated surfaces must be removed by machining However, where machining after heat treatment is not practical, the deleterious effect of decarburization can be largely overcome by shot peening. The effectiveness of shot peening for restoration of fatigue resistance has been demonstrated by studies at Lockheed as shown.

8. The eighth rule is to orient principal stresses in the favorable grain direction. The work of Klier, Muvdi and Sachs, shown in Fig. 7, on the "Effect of Stress Concentrations on Tensile Strength" illustrated the adverse effect of transverse grain direction on notch tensile properties and ductility. Similarly, our studies of the properties of large landing gear axle and fulcrum forgings and prolongation from production forgings confirmed these results. Our concern for the integrity of these parts was allayed to a great degree when we realized that loads in the transverse direction were low and of a minor nature. Thus, we instituted the practice of designing parts to insure the maintenance of major loads in favorable grain directions including the use of notes on engineering drawings to indicate the grain directions required. Our service experience has shown that this practice has been

extremely satisfactory.

Materials, Process and Fabrication Controls

In addition to the design considerations already noted, Lockheed has instituted a number of special material, process and fabrication controls. These requirements are based upon both Lockheed tests and upon a thorough review of work done by other investigators as reported in the general literature, government reports, and vendor studies. These items have been previously reported, however, they are briefly summarized for review.

Material Controls

Although there are many other steels which could be used for highly heat treated parts Lockheed has employed 4340. This steel has the advantage of being a standard analyses with many years of production experience available. Thus, most normal mill problems have been resolved. Three new controls had to be superimposed on normal practices.

1. Hardenability - The minimum hardenability requirements of the military specifications had to be employed rather than the old AISI minimim to insure both attainment of the 260-280 ksi level and to obtain tempered martensite in lieu of intermediate transformation structures for the section sizes employed.

2. Quality - Quality standards had to be established to control the cleanliness of the steel being used. When Lockheed first initiated its use of high heat treat steel, specifications normally called for "Aircraft Quality." However, on investigation it was found that there were as many interpretations of what this meant as there were steel procedures. As a result of this investigation, Lockheed drafted their own quality standard for inspection based upon the frequency and severity of nonmetallic inclusions similar to that used by a number of other manufacturers of critical parts. At the same time Lockheed brought the subject before the AISI Steel Bar Committee during a joint session with the AMS division of the SAE at New Orleans. At this time, work was initiated to reach agreement between AISI and the AMS Division of the SAE so that AMS specifications could be developed defining Aircraft Quality. Recently, AMS 2300 and 2301 have been released describing these requirements.

3. Grain Flow - The first production forging from a forging die is cross-sectioned and examined metallographically to be certain that the grain flow in critical areas is in favorable directions as required by engineering drawings. This must be done prior to initiating the production of these forgings.

Heat Treatment

The standard Lockheed heat treatment for 260-280 ksi includes several pertinent features as follows:

1. Normalizing prior to heat treatment to level out steel mill

processing variables and provide a good structural base for furthur processing.

2. Austenitizing for longer times to permit more complete solution of carbides at the lower temperatures used to obtain more desirable properties.

3. Control of section size to insure formation of tempered martensitic structure throughout the cross-section.

4. Adequate quench to minimize retained austenite or intermediate transformation products.

5. Long time tempering to permit adequate transformation of martensite and reduction of retained austenite at the low temperature employed. Such treatment is required to obtain the optimum yield strengths and ductility of which these high strength steels are capable. Fig. 12 shows the improvement in yield obtained in Lockheed tests (2). The fact that the tensile strength dropped 23 ksi while the yield increased 18 ksi with longer tempering time indicates the unstable nature of the structure resulting from the use of short tempering times.

6. Stabilization of retained austenite to preclude its later transformation to untempered martensite.

7. Atmosphere control to prevent carburization and limit decarburization.

Stress Relief

Lockheed requires stress relief of ultra high strength parts after every fabrication operation which may induce high residual tensile stresses such as grinding and straightening. Recognizing the fact that the low temperatures used are not adequate for major reductions of the induced stress level, parts are shot peened subsequent to the stress relief operations to develop favorable surface residual stress patterns.

Flash Welding

It was necessary to refine the mechanical and electrical setting used for the lower heat treat levels and to provide closer control of the tubing tolerances in order to develop the full strength of the weldments at the 260-280 ksi strength level. To assure machine operation between these closer limits, requirements for oscillographic recording of the critical variables were established. The oscillographic records of production runs are compared with those obtained during qualification of the particular machine settings and part.

Finishing

Special cleaning and plating procedures had to be developed to minimize hydrogen embrittlement. The use of standard acid and alkaline cleaning baths to prepare the surfaces for plating has been prohibited. Clean surfaces, as a base for cadmium plating, are now obtained by vapor degreasing and blast cleaning or by a sequence of anodic clean, electro hone and immersion in

the plating bath, depending upon the plating process being used. Where parts have been immersed in an embrittling bath they must be baked and recleaned in accordance with the requirements discussed above before plating.

Normal cadmium plate procedures were found to be entirely inadequate because of the high degree of hydrogen embrittlement found in plated parts. Consequently, an extensive research and development program was initiated at Lockheed to establish a non-embrittling plating procedure. As a result of this work, three procedures were approved for the cadmium coating of ultra high strength steel parts.

1. The first is vacuum metallizing which is completely non-embrittling but expensive and limited in the size of part which can be processed.

2. The second is the controlled deposition of a thin cadmium film at high current densities. Hydrogen is formed during deposition, however, the cadmium film is porous and does not act as a barrier to hydrogen outgassing during subsequent baking operations.

3. The third is a modified cyanide bath developed by the Lockheed Chemical and Metallurgical Research Department which reduces the degree of embrittlement during plating sufficiently to permit use of parts without baking. A review of the work at Lockheed and that of other investigators has indicated that the various mechanical properties are affected to differing degrees by the presence of hydrogen.

The most sensitive property as shown by Fig. 13, illustrating the typical effects of H_2 Conc., is the notch stress rupture or static fatigue strength. This behavior pattern, i.e. delayed failure under high continuous loads accounts for the majority of failures which have been observed during fabrication and service of parts at the 180-220 ski heat treat levels and of springs heat treated to higher strength levels.

It should be noted that the notch tensile strength is not affected until moderate amounts of hydrogen are introduced. The position of the knee in this curve will be affected by degree of stress concentration. At higher stress concentrations the knee will be shifted to lower hydrogen concentration. Indications are that reduction of area follows the same path as the notch tensile strength. The least sensitive measurement is the tensile strength which was unaffected even by deliberate hydrogen charging using conventional cathodic cleaning procedures. Standard cadmium plating procedures frequently result in reduction of notch tensile as well as of stress rupture strength.

On the other hand, cadmium plating, in accordance with current Lockheed specifications, requires qualification and periodic check to determine that tensile reduction of area is unaffected and that notch stress rupture specimens can withstand a stress of 75% of the notch tensile strength for 200 hours without failure. In the original evaluation of these processes it was also demonstrated that the notch tensile strength was unaffected.

Standard chrome plating procedures result in the introduction of considerable quantities of hydrogen, however, baking has been an effective means of relief. The following special requirements have been imposed to preclude difficulties.

1. All areas to be chrome plated must be peened prior to plating.

2. Chrome plating is prohibited in transition area or radii.

3. All chrome plated parts must be baked 24 hours.

Inspection

To insure compliance with the above requirements, close liaison was maintained between engineering, manufacturing and inspection personnel. Special Quality Assurance procedures were established and processing limited to those sources which had proven their ability to meet our requirements.

Summary

In summary, the design and manufacturing controls required for the successful use of 4340 steel heat treated to 260-280 ksi strength level in aircraft components have been outlined. It was emphasized that this analysis only applied to the materials and design service conditions evaluated. The use of this or similar alloys in the form of sheet or plate in other applications at this strength level would require a comparable program to analyze and evaluate behavior characteristics and performance of these products under the design conditions proposed.

Acknowledgement

The findings presented in this report are a result of the collective effort of many groups and individuals within Lockheed Aircraft Engineering Department. In particular, the author wishes to acknowledge the work of various people in the Engineering Research Laboratory, Structural Methods Department, Project Structures, and co-workers in the Production Engineering Department whose contributions and assistance have made this article possible.

References

(1) "Ultra High Strength Steels for Aircraft Structures", M.A. Melcon, Product Engineering, October 1953.

(2) "Processing of Highly Heat Treated Steel", G. G. Wald, SAE SP120, March 1953, Symposium Ultra High Strength Steels in Aircraft Applications.

(3) "Critical Design Factors for High Strength Steel", H.J. Well and M.V. Ward, Machine Design, October 1953.

(4) "The Static Properties of Several High Strength Steels", E.P. Klein, B.B. Muvdi and G. Sachs, Proceedings, Am. Soc. Testing Mats., Vol. 57, p. 715 (1957).

(5) "The Fatigue Resistance of Unmachined Forged Steels", Hankins and Becker, J. of Iron and Steel Inst., No. II, Vol. CXXVl, p. 205-236 (1932).

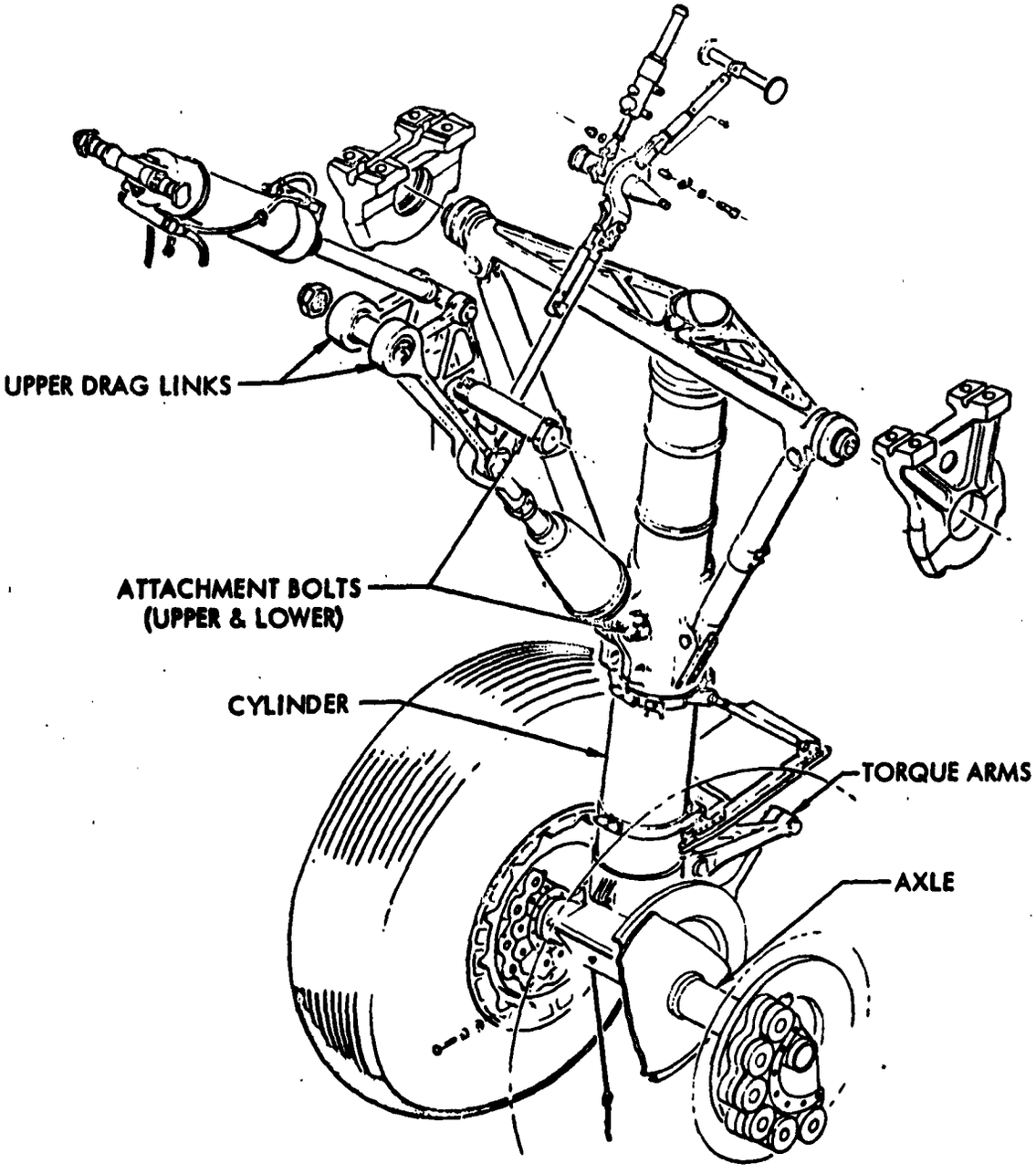


FIG. 1 MAIN LANDING GEAR ASSEMBLY
MODEL 1049

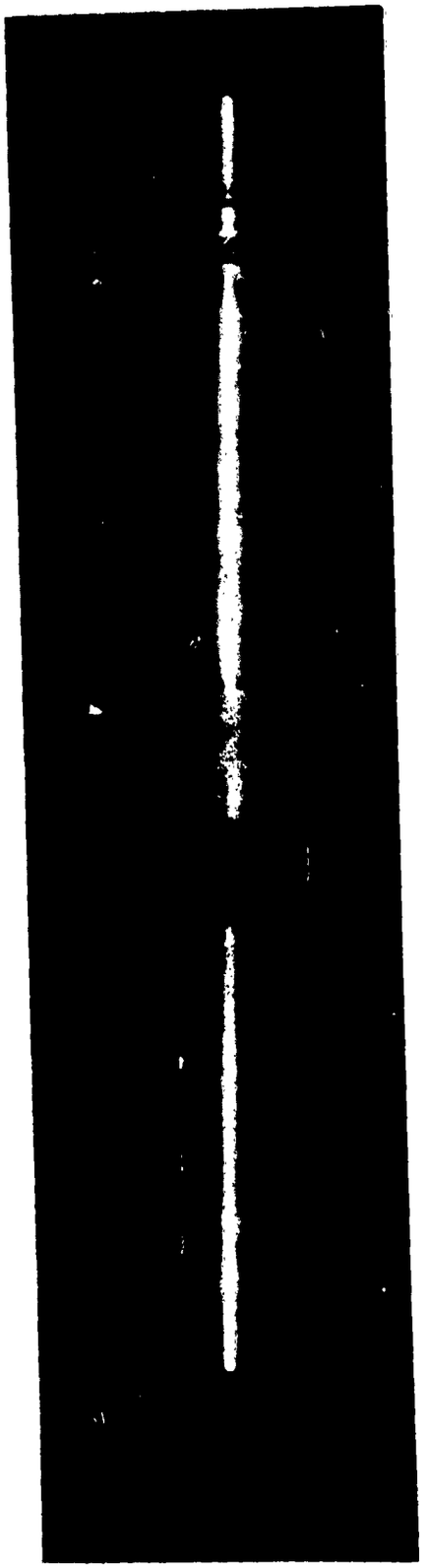


FIG. 2 MAIN LANDING GEAR CYLINDER



FIG. 3 MAIN LANDING GEAR PISTON

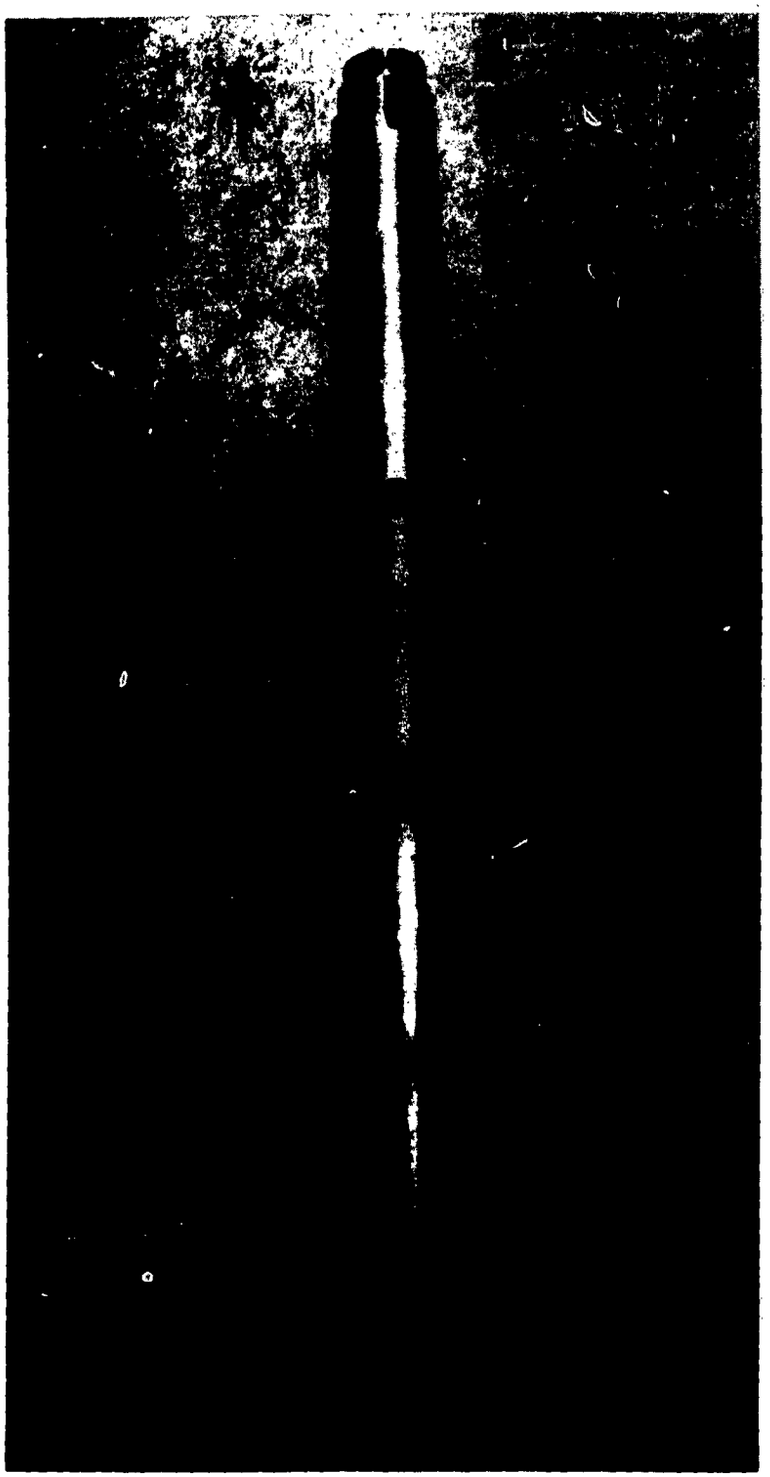


FIG. 4 MAIN LANDING GEAR AXLE

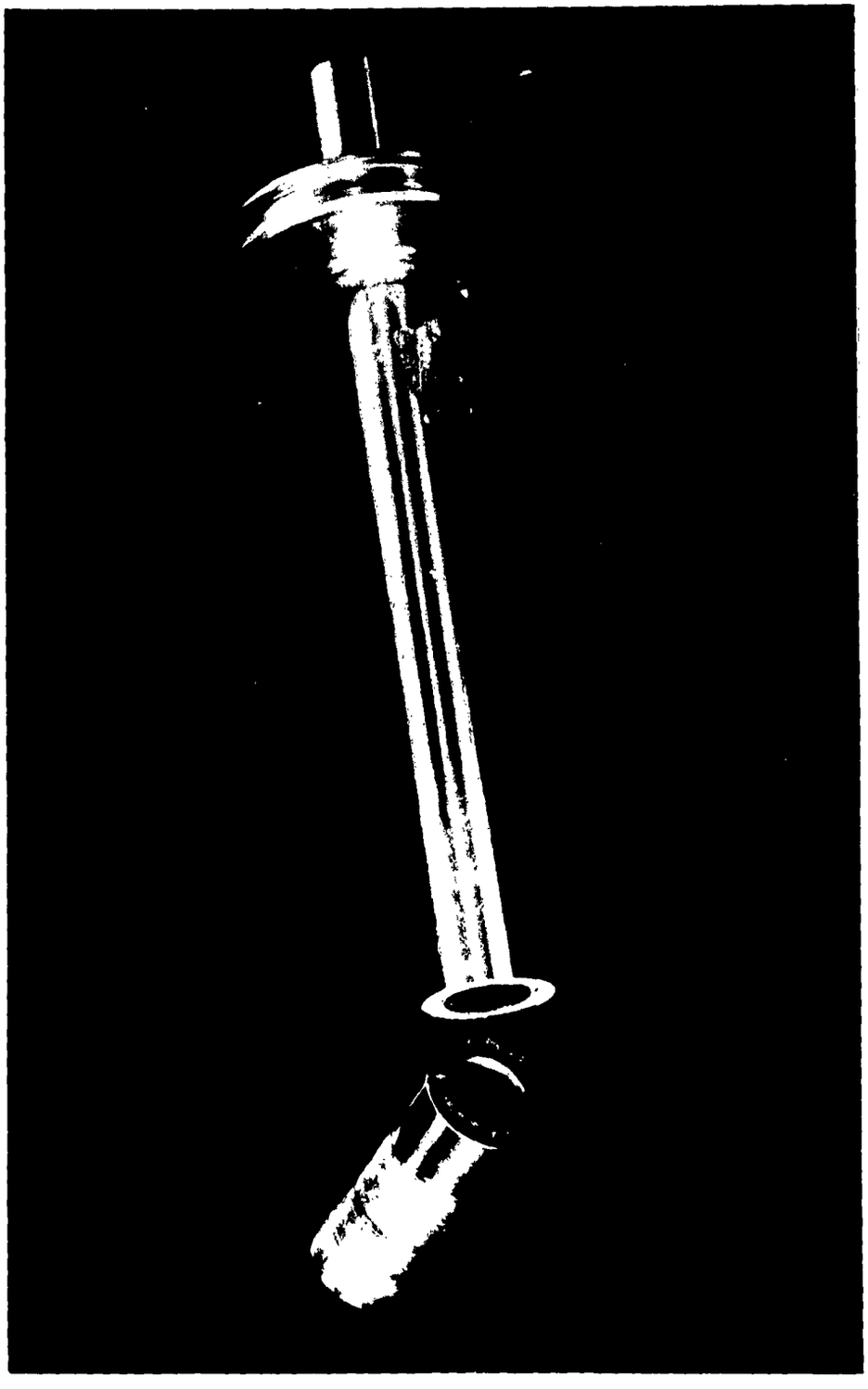


FIG. 5 MAIN LANDING GEAR ASSEMBLY - ELECTRA

ENDURANCE LIMIT OF 4340 STEEL AT VARIOUS STRENGTH LEVELS FOR THREE DIFFERENT STRESS CONCENTRATIONS

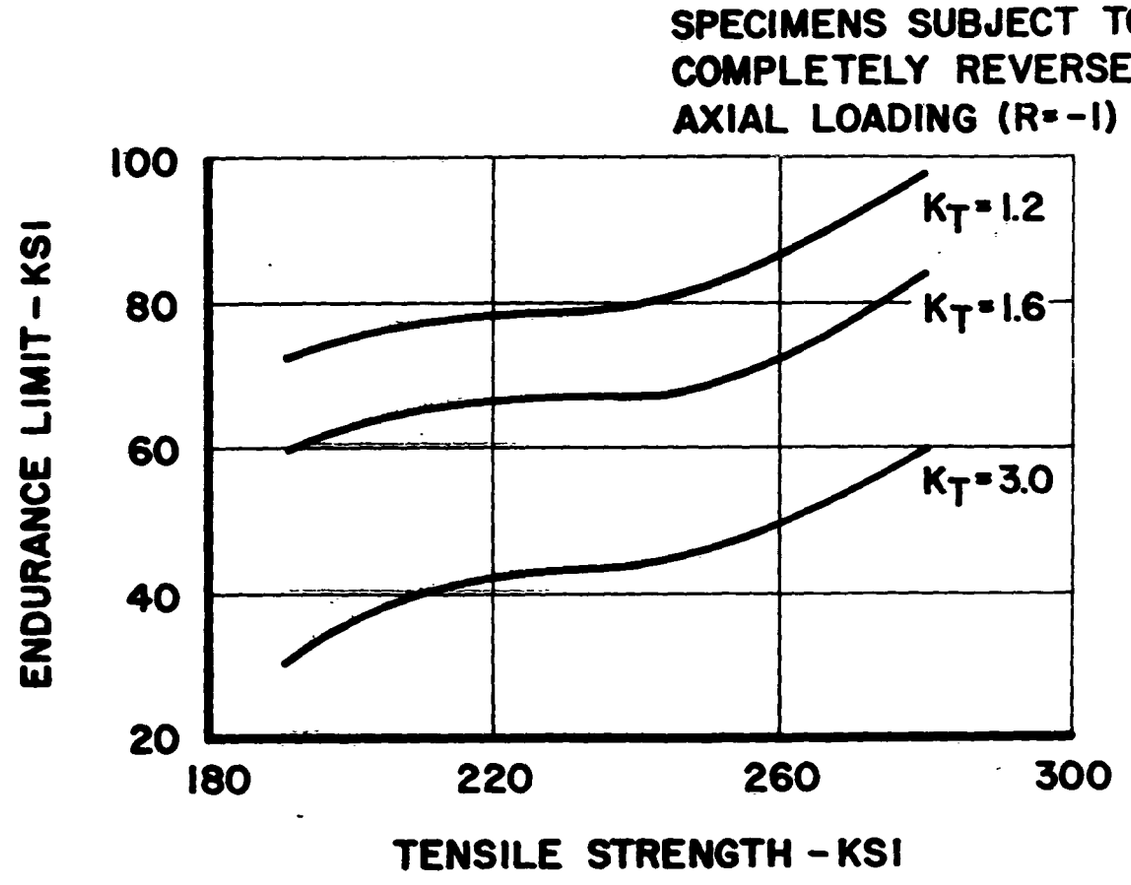


FIG. 6

EFFECT OF STRESS CONC. AND SIZE ON NOTCH TENSILE STRENGTH

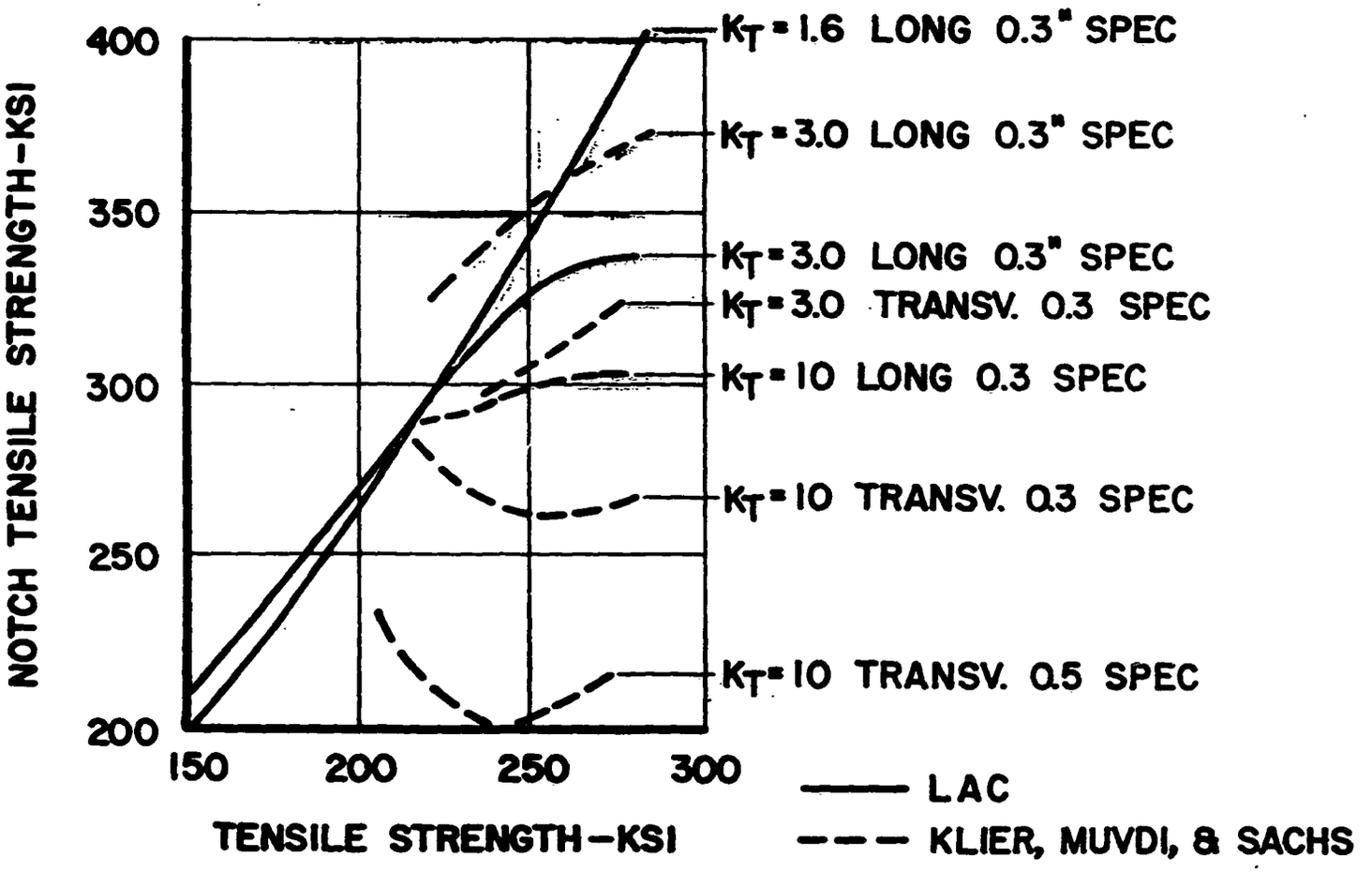


FIG. 7

PISTON ASSM. SHOCK STRUT. - N.L.G.
HEAT TREAT 260-280KSI

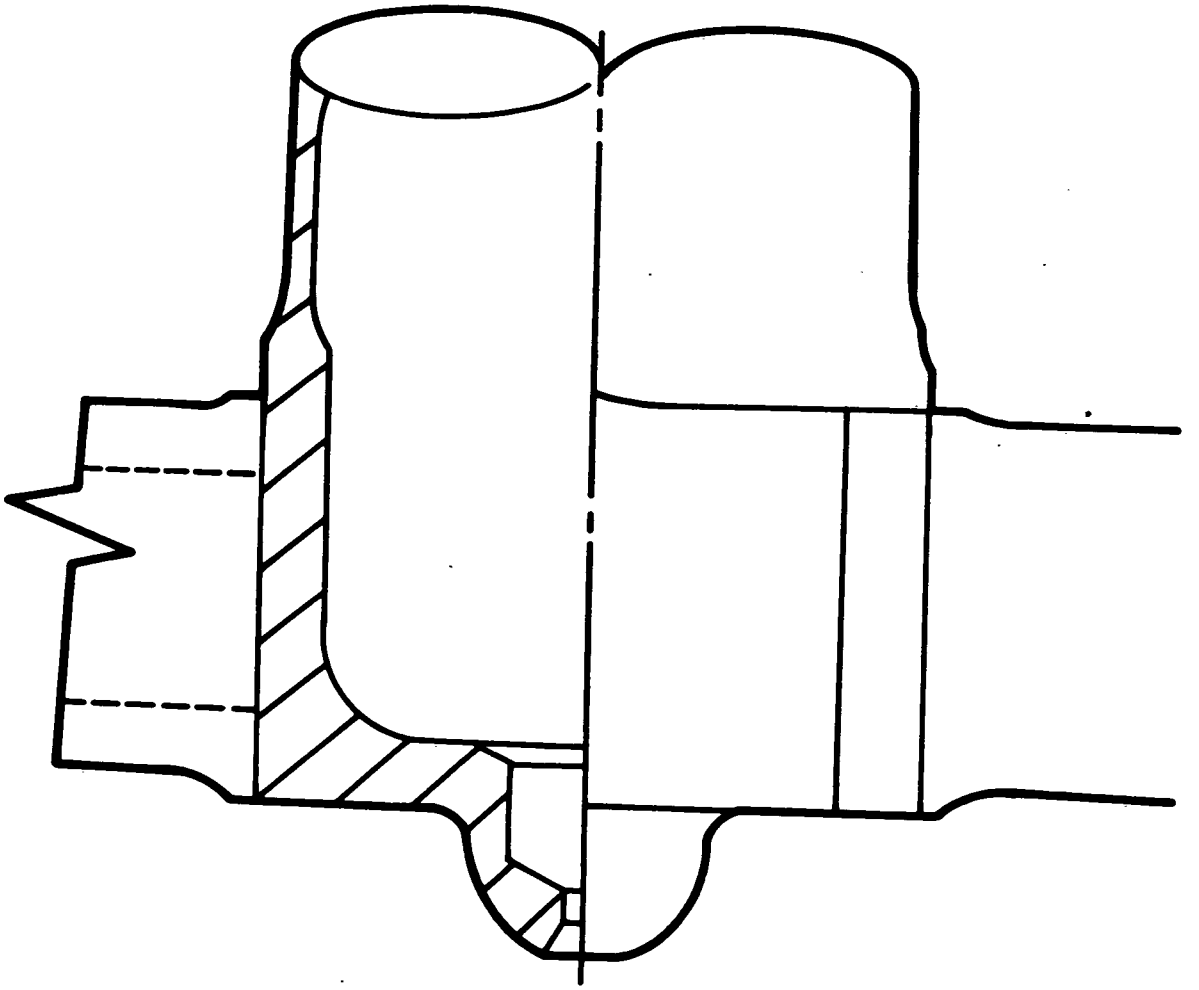


FIG. 8

EFFECT OF ECCENTRICITY OF LOADING ON NOTCH TENSILE STRENGTH OF 4340 AT 260-280KSI (1)

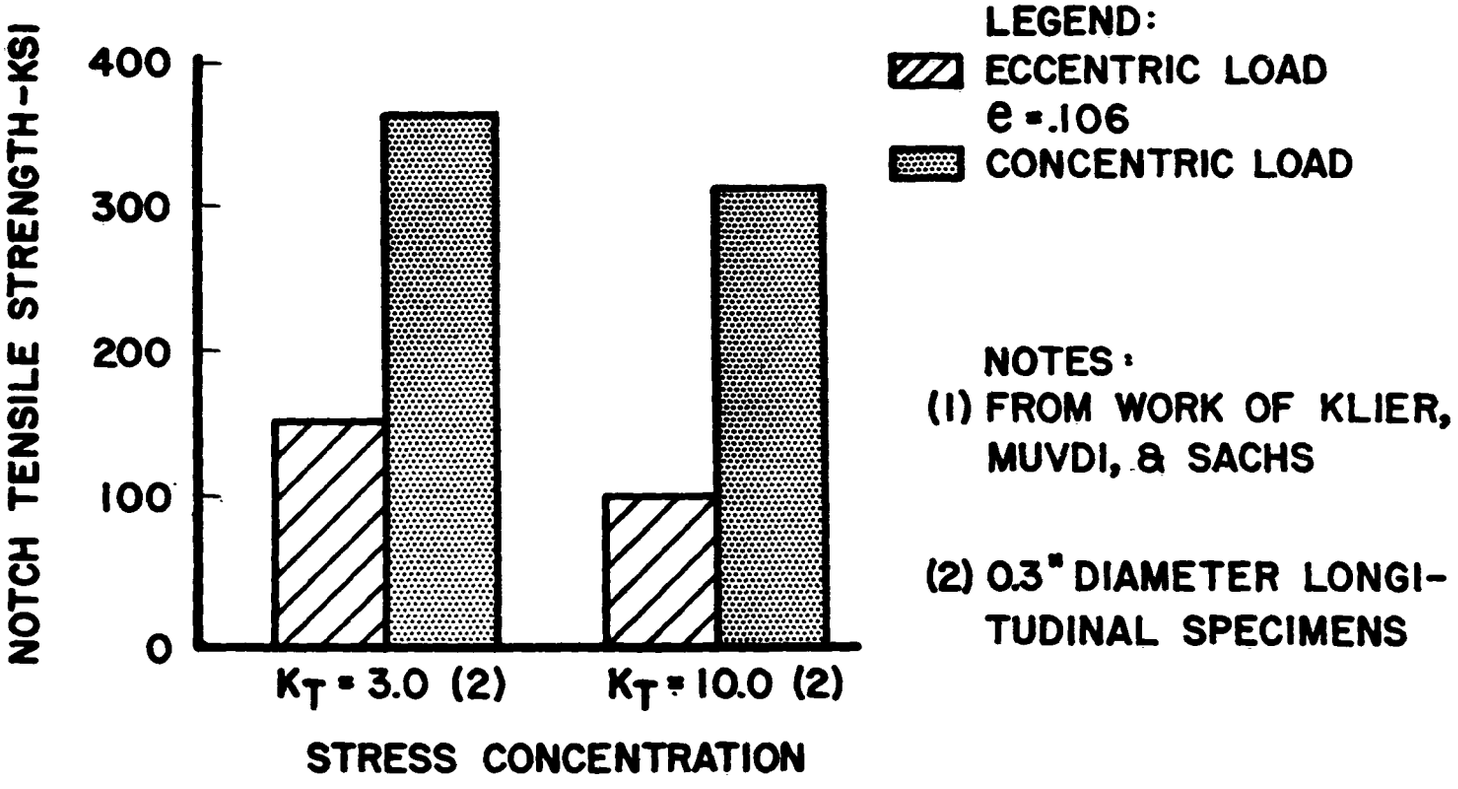


FIG. 9

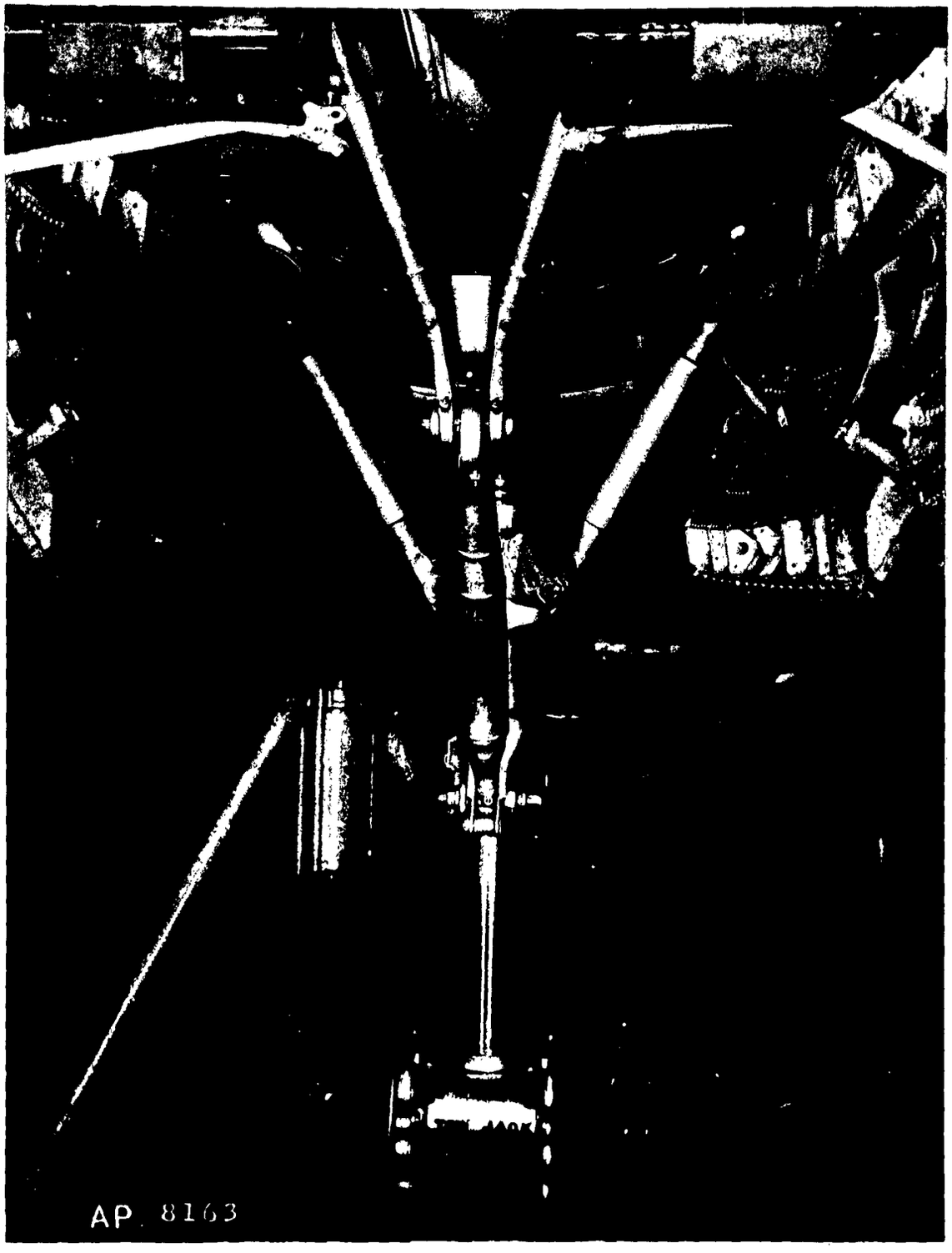


FIG. 10 FATIGUE FAILURE DRAG STRUT DAMPER PISTON TEST

EFFECT OF DECARBURIZING & PEENING ON FATIGUE

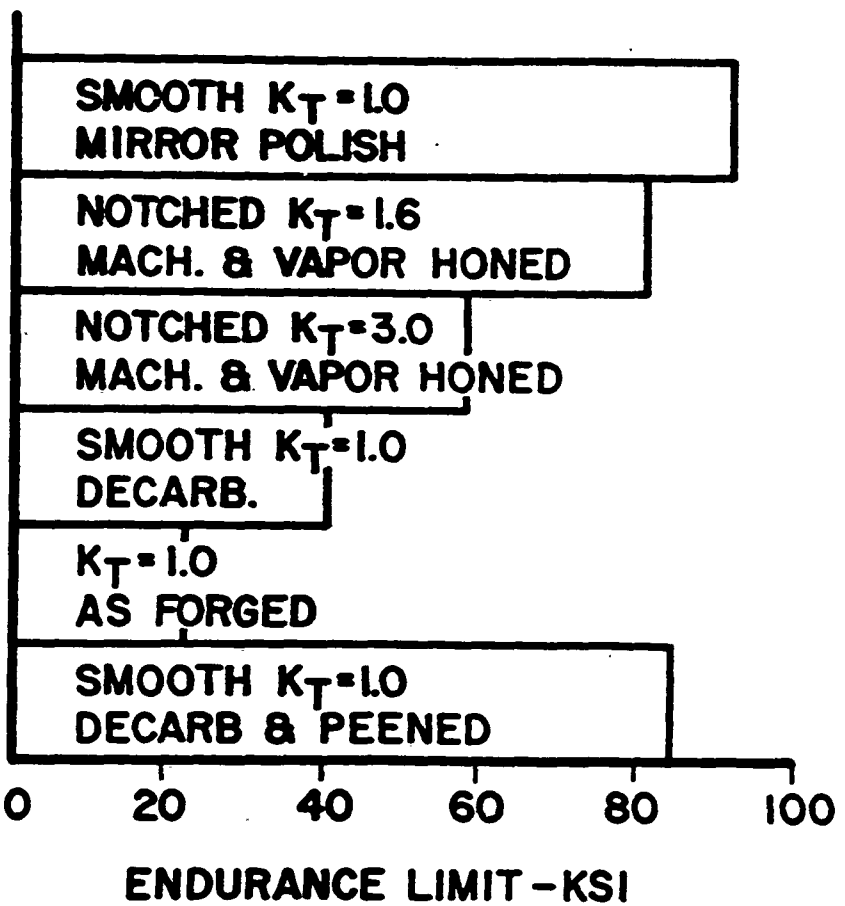


FIG. 11

EFFECT OF TEMPERING TIME ON TENSILE PROPERTIES

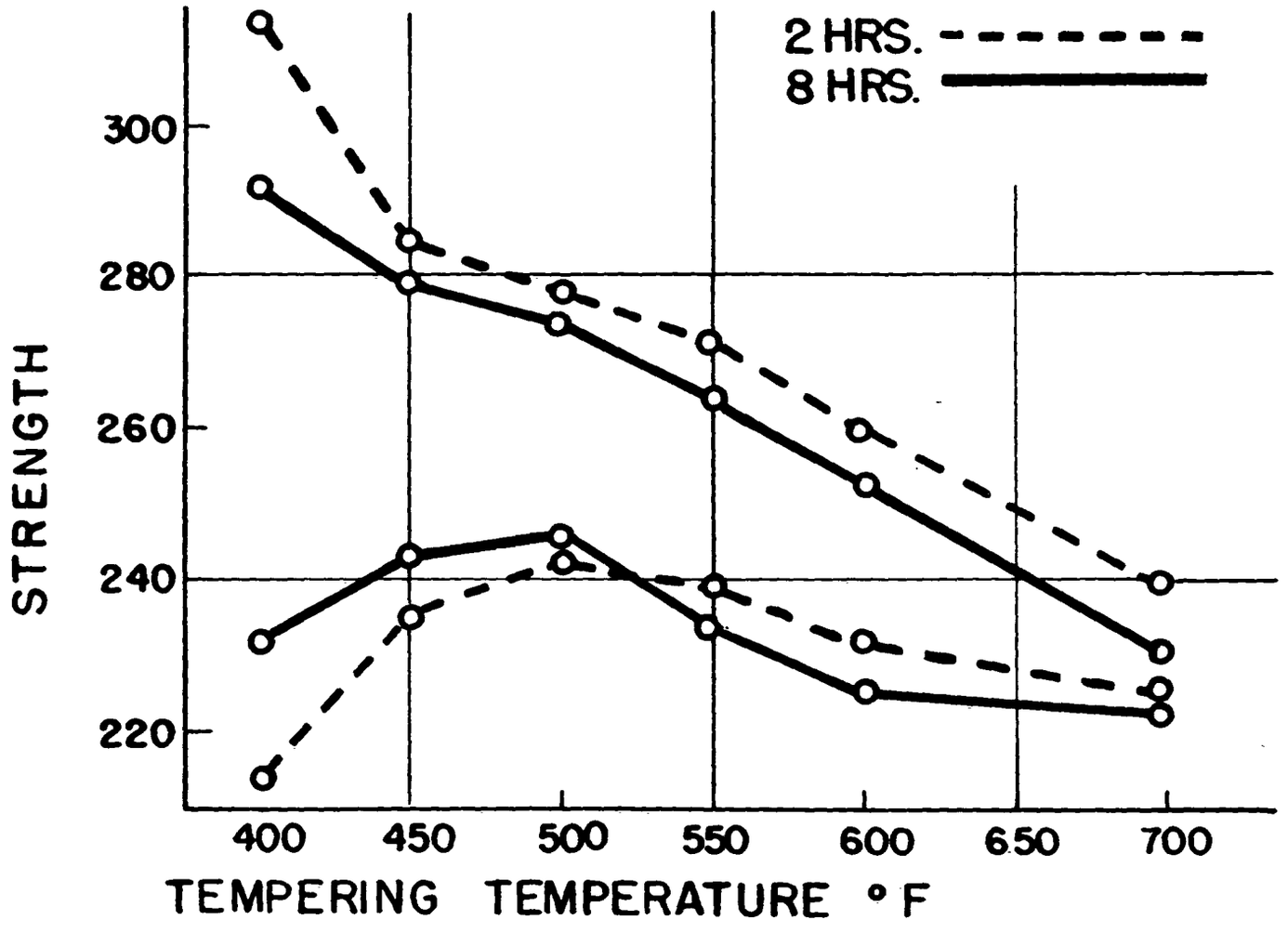


FIG. 12

EFFECT OF ECCENTRICITY OF LOADING ON NOTCH TENSILE STRENGTH OF 4340 AT 260-280KSI (1)

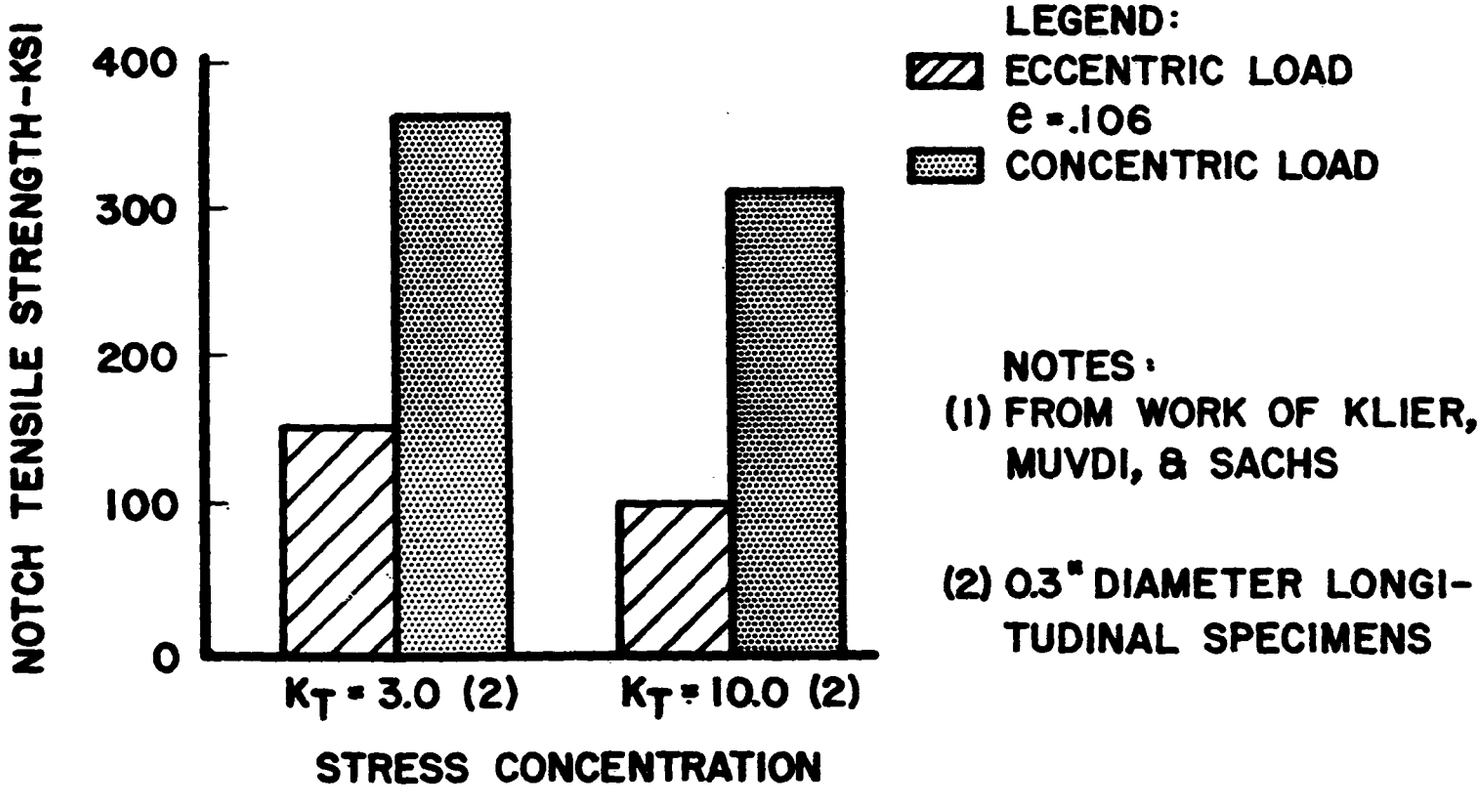


FIG. 13

SECOND SESSION

"Materials, Their Properties and Characteristics"

Materials, Their Properties and Characteristics

S. V. Arnold*

The subject of this session is, ostensibly, "Materials, Their Properties and Characteristics". I'm sure such an imaginative title, for which I bear no responsibility, persuaded many of our number to catch some extra sack time. I was tempted to change it to "Metals for Modern Monolithic Motor Cases" just to increase sales appeal and to indicate that we were having no truck with reinforced plastic jobs or ribbon wrap. Not that we're casting aspersions on these fine latter materials--our field was just a little large and we wanted to narrow it down is all.

The rocket motor case is typically cylindrical in configuration (see Figure 1). This fact imparts a difference in principal stresses in the sidewall, the circumferential stress being twice the axial. This situation does not maintain in the head and tail closure sections where the ratio is nearer unity. There are, of course, zones where the closure sections blend with the cylindrical side wall where an intermediate situation prevails. But the interesting feature, insofar as we're concerned, is that 2:1 ratio in the side wall. Sophisticated designers will take advantage of this by utilizing directional qualities of the case metal and by orienting structural features in such manner as to minimize stress concentrations. The rolling direction of the strip from which the Atlas is fabricated is oriented circumferentially. Axially disposed weld beads were avoided in the Pershing motor so that these discontinuities would not be stressed transversely when the case is pressurized.

Now that we have mentioned weld beads it may be well to remark that, as yet, there is no truly monolithic modern metal motor case--they're all composed of separate components welded together. Quite possibly other methods of joining are feasible, but they have not achieved importance to date. And so we have to live with mother-in-law. In selecting an alloy for the motor case, we have to consider its weldability; that is, the compatibility of weld properties with requirements of joint design. Because welding all high strength sheet alloys raises problems in various sorts and sizes most case designers take considerable pains to minimize the length of welds.

The Pratt and Whitney design for the Pershing motor is a fine example of minimized welding. There are two circumferential girth welds; that's all. The head and tail closure sections are contour machined from cupped forgings. In this way the need to weld in igniter and thrust reversal bosses is ob-

*Watertown Arsenal Laboratories

viated. The cylindrical portion is machined from a flow-turned ring-rolled forging. When we consider the comparative ease with which the case could be formed and assembled from sheet, if welds were 100% efficient, the penalty for avoiding them is apparent.

But let us for the moment assume that welds could be eliminated completely--and maybe they will be if OMRO's development program with Lyons, Inc. for a one-piece case proves successful--what materials limitations would face us then? We might pursue the strength/density ratio a little further before some other secondary characteristic provides the next barrier. Stress corrosion? Notch sensitivity? They may work in concert. There has been precious little work done to compare specimen tests with pressure vessel tests when the latter were free of weld beads. The next correlation, between weld-free pressure vessel and weld-free full-scale burst tests, has not, of course, been possible. Some of the available weld-free pressure-vessel data are shown in the next figure, (see Figure 2).

You have no doubt heard that scatter of burst stress values increased with strength of the case metal and certainly there are quantities of data for welded pressure vessels which bear this out. However, when welds are absent and care is exercised to eliminate flaws from other sources, this point is not well established. If we take this particular set of data and analyze it statistically with regard to the premise that scatter increases with mean hoop stress for each pair of data, it turns out that we can accept this premise with only 61% confidence. If we plot percent deviation from the mean versus mean hoop stress for each pair of data, (see Figure 3) it becomes apparent that the premise is indeed questionable. We can, therefore, take an opposite tack and argue that these data show promise for cases constructed of metal with a steel equivalent of 250 ksi yield strength. Surely, the metal might be "brittle as glass", but as long as the case performed consistently, would it matter? Well, of course, that "consistency" is a big assumption. It includes babying the case right up to the moment of firing lest some inadvertent scratch provide the assiduously avoided defect that will cause failure. But, even if we were willing to take such trouble, would it serve our purpose?

We hear a great deal about critical crack length that which will propagate catastrophically under the extension forces engendered by operating pressure. The concept is useful, because obviously one cannot tolerate

such a defect in the motor case. Unfortunately, however, it is only part of the story because sub-critical defects propagating during testing or in storage can attain the critical size. True, defect propagation during storage hasn't been established as a problem, but propagation during pressure cycling is another matter.

Such propagation is essentially a fatigue phenomenon. Let us examine some data from current work of Carpenter at Swarthmore (see Figure 4). These results derive from test of center-notched 3-inch wide sheet tensile specimens of Mellon Steel (4137 + 1% Co and Si) heat treated to circa 230,000 psi yield strength. The driving force, G, defined as shown, was maintained constant at selected values while crack length was measured as a function of the number of loading cycles. The essentially linear relation is apparent. The crack grows a certain amount on each cycle, the amount determined by the driving force. We note that the increment of growth decreased sharply with driving force. Extrapolation suggests that a driving force less than 25 ipsi would not propagate the crack at all. If these cycles to failure are plotted against driving force the aspect of finite fatigue is evident (see Figure 5).

The data show that a <u>constant</u> driving force will cause a crack in a selected material to increase by a certain increment on each loading cycle. The increment increases with driving force. If we plot the size of increment versus driving force, (see Figure 6) we find the meager data suggest a hyperbolic relation, if we give credence to all three points. The seeming difficulty of maintaining a constant driving force when the crack is growing rapidly makes the value of this datum somewhat questionable, however. It is possible, therefore, that a linear relationship maintains--which would support the idea that propagation does not occur below this 25 ipsi level. As a matter of fact, Carpenter did not observe growth of the .75-inch starting crack after 10 cycles at G = 40 ipsi.

If a minimum driving force, G_g, is necessary to promote crack growth on cyclic loading, it is evident that there exists a minimum length of crack which can be grown at a selected level of stress. The maximum operational stress will define the <u>smallest</u> crack which will grow on cycling at the minimum driving force G_g. It would be nice, of course, to exclude all cracks possessing growth potential from the motor case, but the smaller of these may very well escape detection (or be so prevalent as to obviate

control). If, however, we determine crack growth behavior under various driving forces, it may be feasible to accept cracks of a size which will not propagate to the critical length during the planned seqvence of testing and final firing. Carpenter may apparently entertain some such idea, for he calculates a "sub-critical driving force" under which his specimen may be cycled at least three times without propagating his starting crack length to the critical dimension. To me, three cycles seem rather too few, but the principal is clear.

Now the rate of crack growth under a given driving force will vary with a number of factors, notably; material, geometry, and temperature. This can be illustrated by a simple experiment of several years ago (see Figure 7) wherein we determined the number of blows to break Charpy "V" specimens of a particular steel at various temperatures. Of course, the number of blows depended upon their energy and the temperature. Without becoming involved in the difference of fracture mechanisms, I point the evident fact that the number of loading cycles--that is, number of blows--decreased sharply at a transition temperature. Here again you see the aspect of finite fatigue. Probably we could have found a minimal energy of blow to initiate and propagate fracture; below this value the entire energy of the blow would have been absorbed in elastic deformation of the specimen and machine parts.

But the important feature here is the role of temperature. We should know how temperature affects the rate of crack growth in our motor case metals.

Another way we could reduce rate of crack growth would be to reduce the driving force, G. Since G is a function of the nominal stress, which in turn is determined by the internal pressure of the motor, there is not much hope in this direction unless we wish to downgrade performance. But there is a situation where the nominal stress does not provide the entire driving force, i.e., when residual stresses are present. By relieving residual stress, we can reduce locally high driving forces.

It's surprising how residual stress augments the nominal (applied) stress and thereby greatly modifies crack initiation and propagation. In some recent work in WAL we ran a simple experiment which illustrates this point. We bent Charpy "V" specimens over a fulcrum positioned against the notch as shown (see Figure 8) until a permanent set was induced. During

the bending operation the metal at the base of the notch was upset in compression, but, when the load was released, elastic recovery placed the notch base in tension. By inducing bend angles of sufficient magnitude, sufficient tension would be created upon elastic recovery to form a crack at the base of the notch. Precise bending allowed us to control crack length and likewise to induce the maximum residual stress at the notch base which could be withstood without formation of a crack. By breaking these specimens in an impact testing machine in the conventional manner, it was possible to observe the effect of these various conditions. The next figure (see Figure 9) shows several interesting features:

1. Above the transition temperature, performance is essentially unaffected by residual stress alone or by the presence of tensilely-stressed cracks at the base of the notch.

2. The presence of a tensilely-stressed crack at the base of the notch will seriously impair impact strength below the transition temperature.

3. High residual tensile stress at the base of the notch will also impair impact strength below the transition temperature and can be as effective in this regard as a tensilely-stressed crack.

In this particular instance where specimens of AISI 4340 quenched and tempered to 165,000 psi were tested, these pretreatments do not seem to have affected the transition temperature. Nor did they for specimens of the same steel at 130,000 psi. At 215,000 psi strength level the picture was less certain, both because the transition curve differed in character and because control of crack initiation was more difficult.

To check the effect of prior stress (simulating residual stress) upon impact energy, the contraption shown in the next figure (see Figure 10) was constructed. It enables us to stress the notch of a psuedo-Charpy "V" specimen in controlled amounts and to strike the stressed specimen with impact blows from a drop weight. The breaking energy is determined by cut-and-try with limited combinations of impact energy corresponding to four heights of drop one foot apart and three weights of 1, 2, and 5 lbs. Accordingly, breaking energies are bracketed rather than determined precisely. Nevertheless, the picture to date is enlightening (see Figure 11). The steel specimens for these data were heat treated to 230,000 psi yield strength (to match our better motor case steels) and prestressed to 0%,

50%, 75%, and 100% of the proportional limit. The degree of prestressing obviously raises the transition temperature. Beyond this we cannot state with certainty until our curves are more exactly defined.

These findings are similar to those reported by Kihara and Masubuchi who tested plate weldments with residually stressed crack starters (see Figure 12). Their results are summarized in the following plot (see Figure 13). The authors define the conditions for partial and complete fracture with and without residual stress at a sharp notch. You will observe that the weldment ignores the presence of sharpy notches and residual stress above the transition temperature. Below this temperature the notch substantially reduces the applied stress to failure. A residually stressed notch, moreover, caused failure at applied stresses well below the yield point of the base metal. If a residual stress promoted crack initiation at low values of applied stress, the cracks would not run to failure, but would quit after a short distance. It was then necessary to raise the applied stress to yield level in order to complete failure. On the other hand, if residual stresses were not sufficient to promote cracking until higher orders of applied stress were reached, cracking once started proceeded to failure.

This behavior, Kihara and Masubuchi concluded, was attributable to relief of the residual stresses by formation of limited cracks. I think we can explain their observations by assuming that cracks initiating under the combined action of residual and applied stress must grow to a size critical for the latter alone in order to propagate continuously to failure. If the added impetus of residual stress is exhausted before this size is reached, the applied stress cannot continue rapid propagation of the crack.

Our Japanese friends concluded that relief of residual stresses by plastic deformation in the ductile temperature region offered a considerable benefit, even though this might bring about limited crack propagation. They conducted the following experiment (see Figure 14) in which specimens were subjected to pre-loads above the transition temperature before testing to failure at a lower temperature. They found that this procedure assured fracture stresses at the lower temperature <u>at least equal</u> to the preload stress applied at the higher temperature. It would seem reasonable, therefore, to proof test rocket motor cases in this fashion. To be sure, the pressure medium would have to be heated in order to get most of our popular motor case steels above the transition region, but this is not insuperable.

(However, I disclaim any responsibility, if some of our operators get boiled in oil.) By proof testing above the transition temperature range we pay the least penalty for relieving localized residual stress. If cracks form in the process, their propagation will be minimal. Some stresses, which would have initiated cracks at lower proving temperatures, will be alleviated by local plastic deformation at the high temperature.

Let us now consider another factor in fracture behavior of sheet metals which has had rather scant attention: gage. Probably many of you have assumed that the fracture energy is directly proportional to gage. This is not a good generality. The next Figure (see Figure 15) compares sheet of 1100-F and 2024-T4 aluminum alloys. You will note that impact energy is proportional to gage in the stronger, relatively brittle 2024-T4. However, this does not hold strictly true for the weaker and highly ductile 1100-F. In brittle fracture, energy absorption is directly related to fracture surface area, ergo to sheet gage in specimens of constant width. In ductile fracture another factor, the volume of plasticity deformed metal adjacent to the fracture surface, contributes to the absorbed energy. This factor is not linearly related to gage.

In moderate to high strength steels, however, the relationship is sufficiently close to linear that we can think in this fashion as a matter of convenience. This slide shows the relation for a steel of 110,000 psi tensile strength. I think we can agree that the relation is essentially linear over the gage range for sheet products, the upper limit for which is usually accepted as .250 inch.

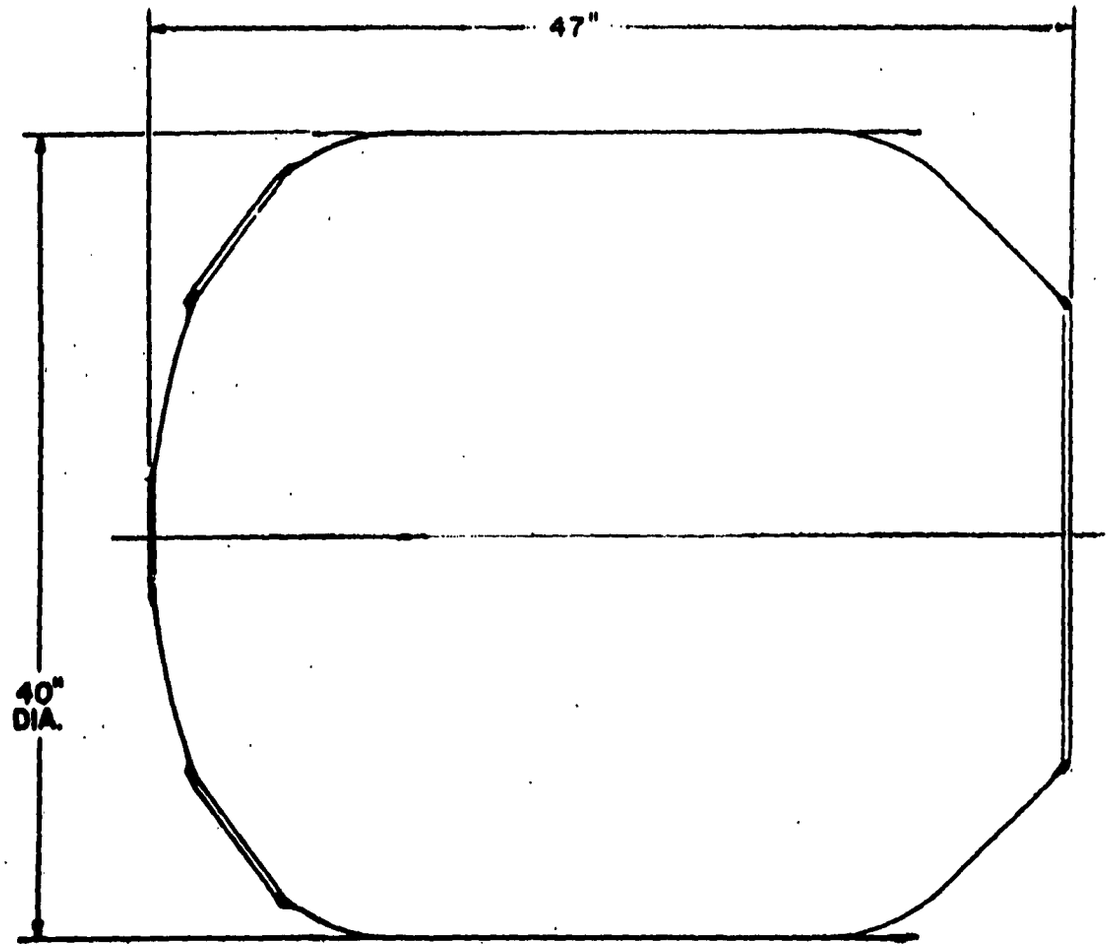
With steel sheet, abrupt variation of fracture mode with temperature must be considered. This transition, we find, is also influenced by gage, as this curve (see Figure 16) illustrates. Accordingly, it develops that the designer must evaluate gage not only for load capacity and stiffness, but also for its effect on toughness. The next figure (see Figure 17) shows this rather clearly. For a service at -150°C there is good reason for the designer to avoid sheet of this particular steel great than 1/8 inch in gage.

What is the effect of strength level on this behavior? The next figure (see Figure 18) shows us conventional impact energy transition curves for simulated sheet machined and ground from AISI 4340 quenched and tempered to 165,000 and 210,000 psi tensile strength. These same data replotted to reveal the effect of gage show an interesting pattern (see Figure 19).

Those of you with telescopic vision will note the subscripts by the various symbols--these represent the percent of fibrous fracture for the respective specimens. At a selected temperature a linear relation of impact energy to gage prevails, if the fracture is completely ductile, i.e. 100% fibrous. Likewise, if the fracture is predominantly brittle as at lower selected temperatures, energy is linearly related to gage. Over an intermediate range of temperatures the mode of fracture will change from completely ductile to partially ductile as gage increases. The pattern at a lower strength level is similar with fracture transitions occuring at lower temperatures and/or heavier gages as would be expected (see Figure 20).

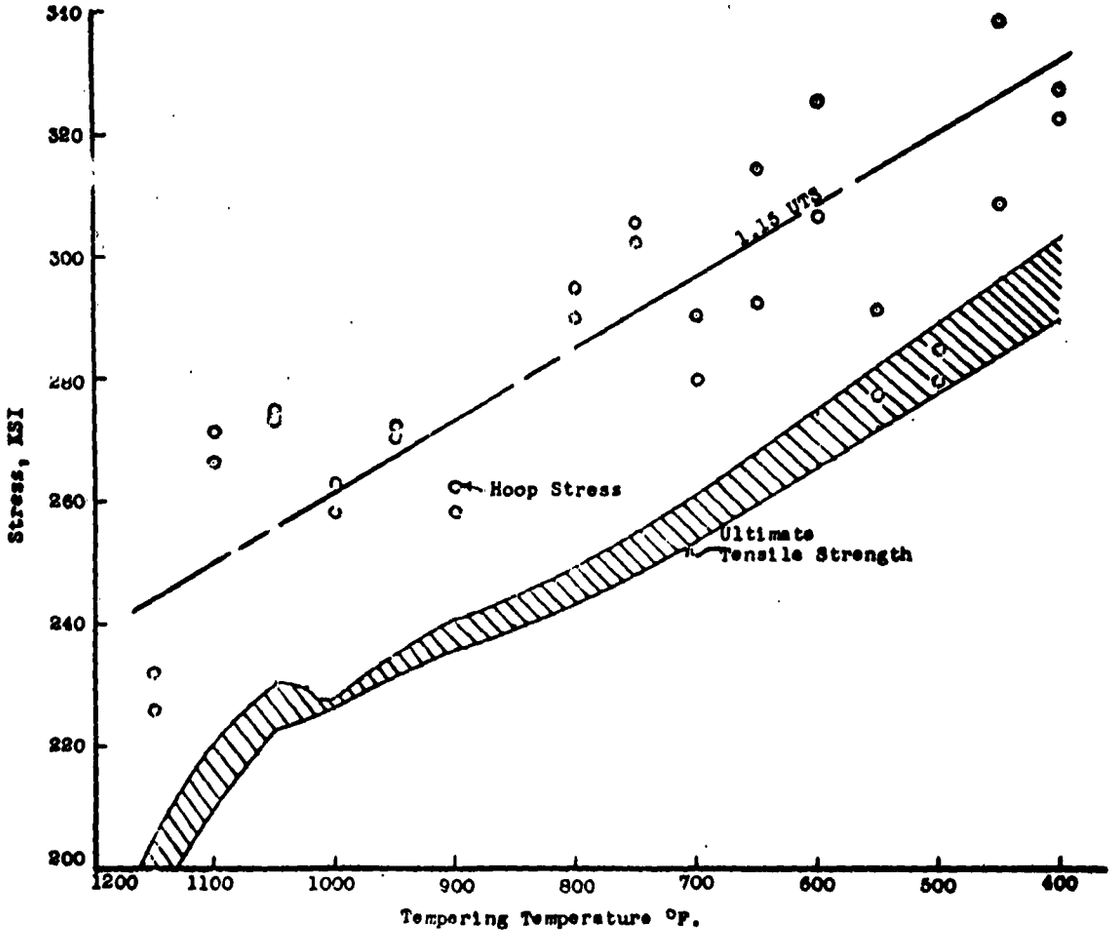
Now that we are thinking in terms of gage, let us consider how toughness will vary with gage and strength level. Back in 1949 Baeyertz, Craig, and Sheehan developed some data which show that impact strength of heat treated AISI 4340 in fully ductile fracture varies inversely as a linear function of hardness over the range R_c 31-46. Converting hardness to strength allows the plot shown in the next figure (see Figure 21). If we assume that impact strength increases proportionately with section thickness (which, we have seen, is essentially correct for sheet of 4340 within the ductile range of gage and temperature), we can calculate the increase in impact energy corresponding to the substitution of a weaker and thicker sheet for a stronger and thinner one of the same load bearing capacity. Further calculation (see Figure 22) shows increase in impact energy as a function of tensile strength decrease, gage increase and weight increase, all on a percentage basis. It is evident that the motor case designer can obtain a substantial improvement in toughness, that is, greater resistance to crack propagation and increased tolerance for defects, by recourse to heavier gages at lower strength levels. However, he need not follow this practice throughout his design--and, indeed weight limitation would not permit this--he can confine the heavier sections to those areas where defects cannot consistently be avoided. Weld beads are typical defect areas. Some case designs (see Figure 1), such as this one which we saw previously, incorporate "reinforced" sections in the vicinity of the girth weld beads. I cannot say whether the various matters we have discussed were considered in developing this particular case; probably they were not considered in quite the same fashion. As you will hear, this design has proven very successful. I should like to think that we can do still better. Thank you.

LARGE MOTOR CASE



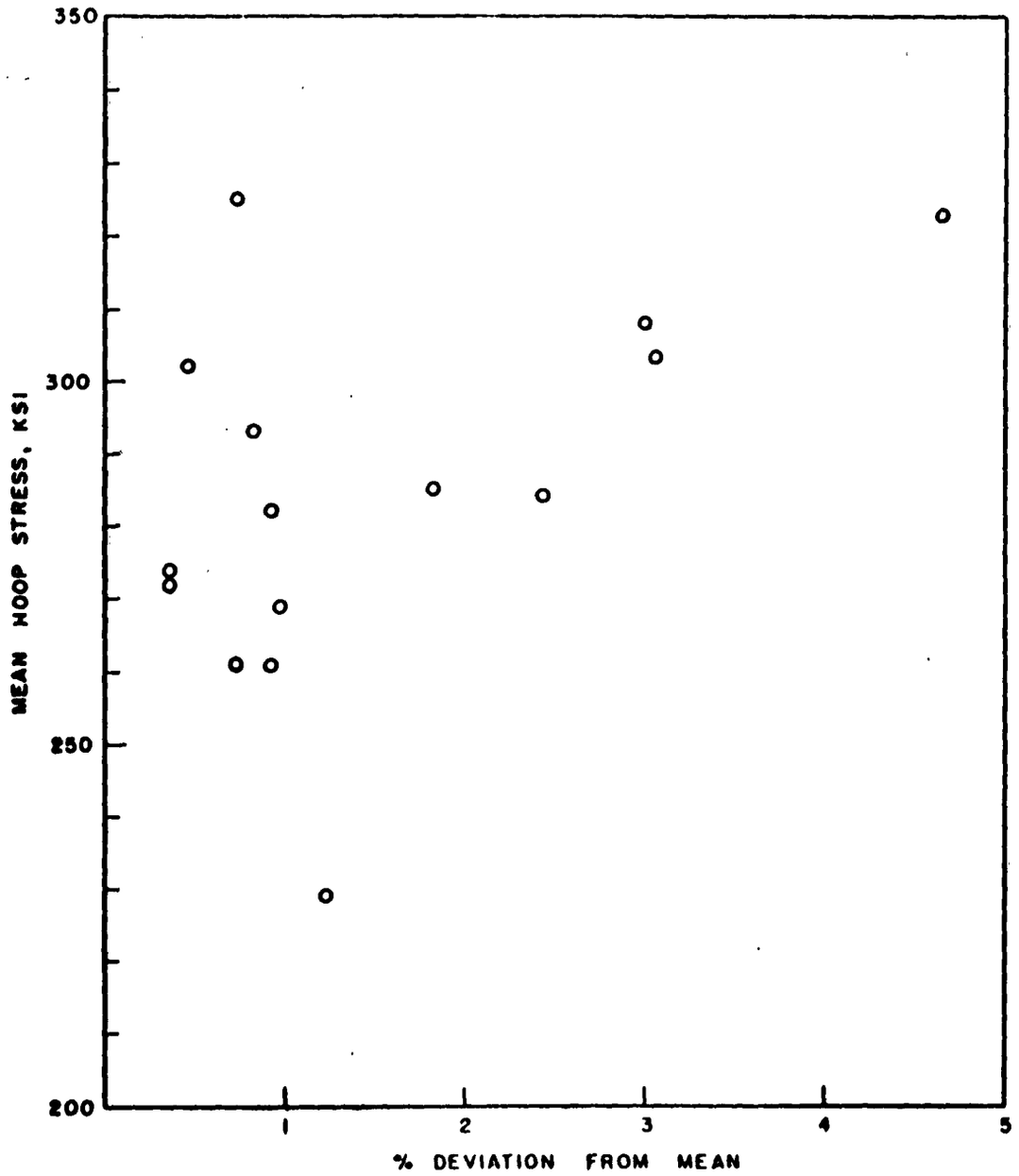
PRATT & WHITNEY AIRCRAFT
DIVISION OF UNITED AIRCRAFT CORPORATION

FIGURE 1



BURST DATA ON LADISH D6aC CYLINDERS (AEROJET-GENERAL)

FIGURE 2



MEAN HOOP STRESS VS % DEVIATION FROM THE MEAN I BURST TEST DATA ON LANDISH D6aC CYLINDERS. (AEROJET-GENERAL)

FIGURE 3

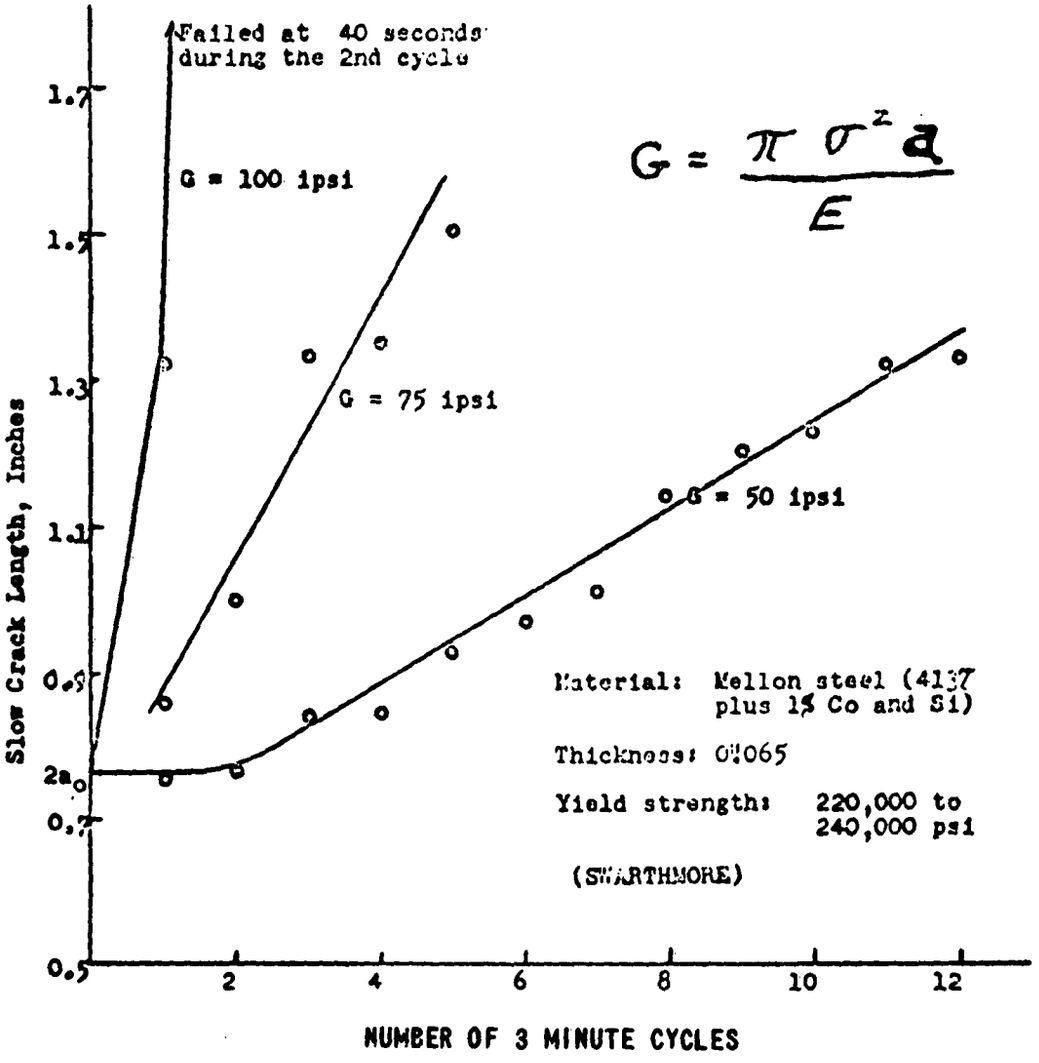

Failed at 40 seconds during the 2nd cycle
G = 100 ipsi
G = 75 ipsi
G = 50 ipsi
$G = \frac{\pi \sigma^2 a}{E}$
Material: Mellon steel (4137 plus 1% Co and Si)
Thickness: 0.065
Yield strength: 220,000 to 240,000 psi
(SWARTHMORE)
Slow Crack Length, Inches
$2a_o$
1.7
1.5
1.3
1.1
0.9
0.7
0.5
2
4
6
8
10
12
NUMBER OF 3 MINUTE CYCLES

FIGURE 4

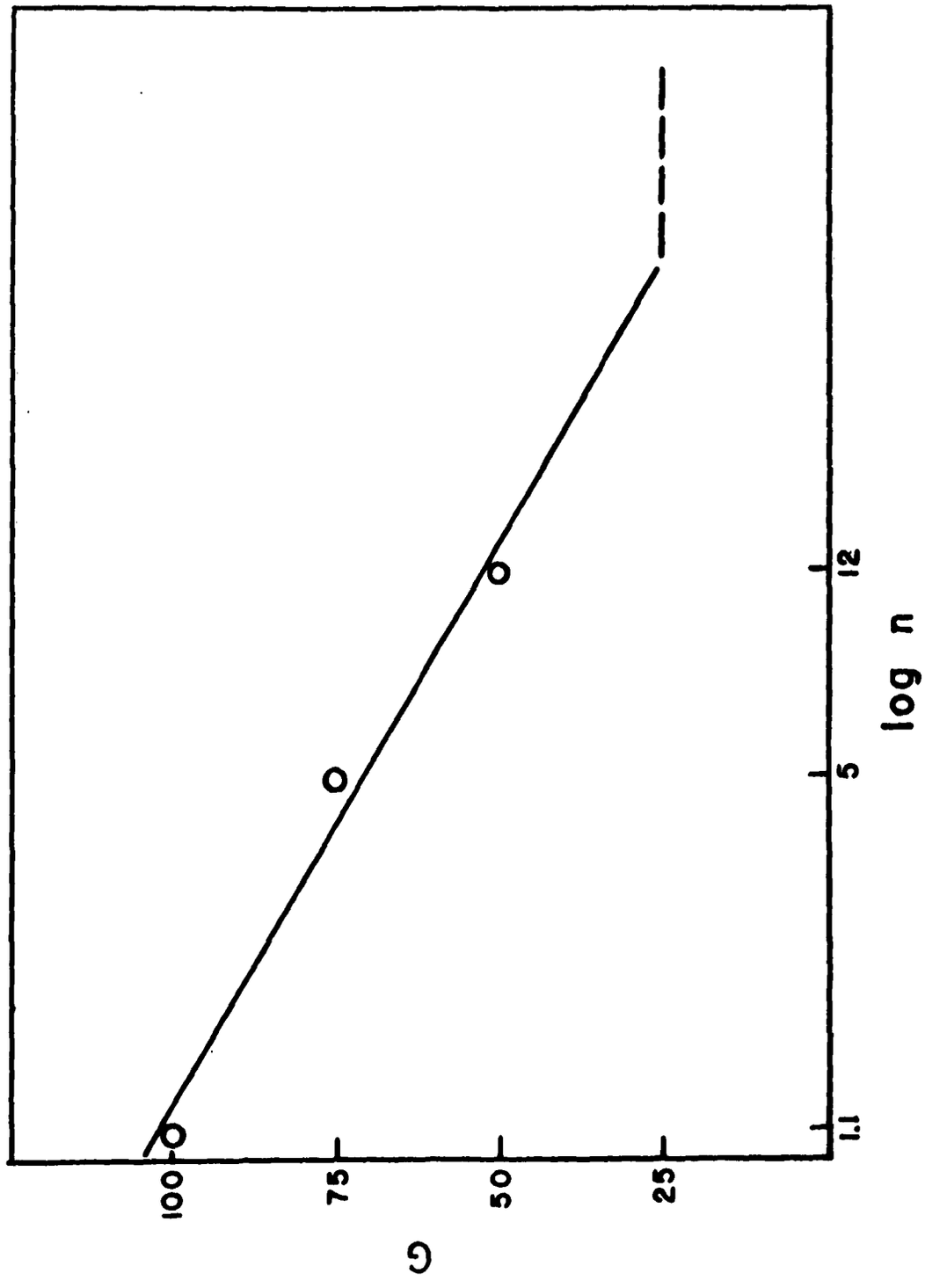


FIGURE 5

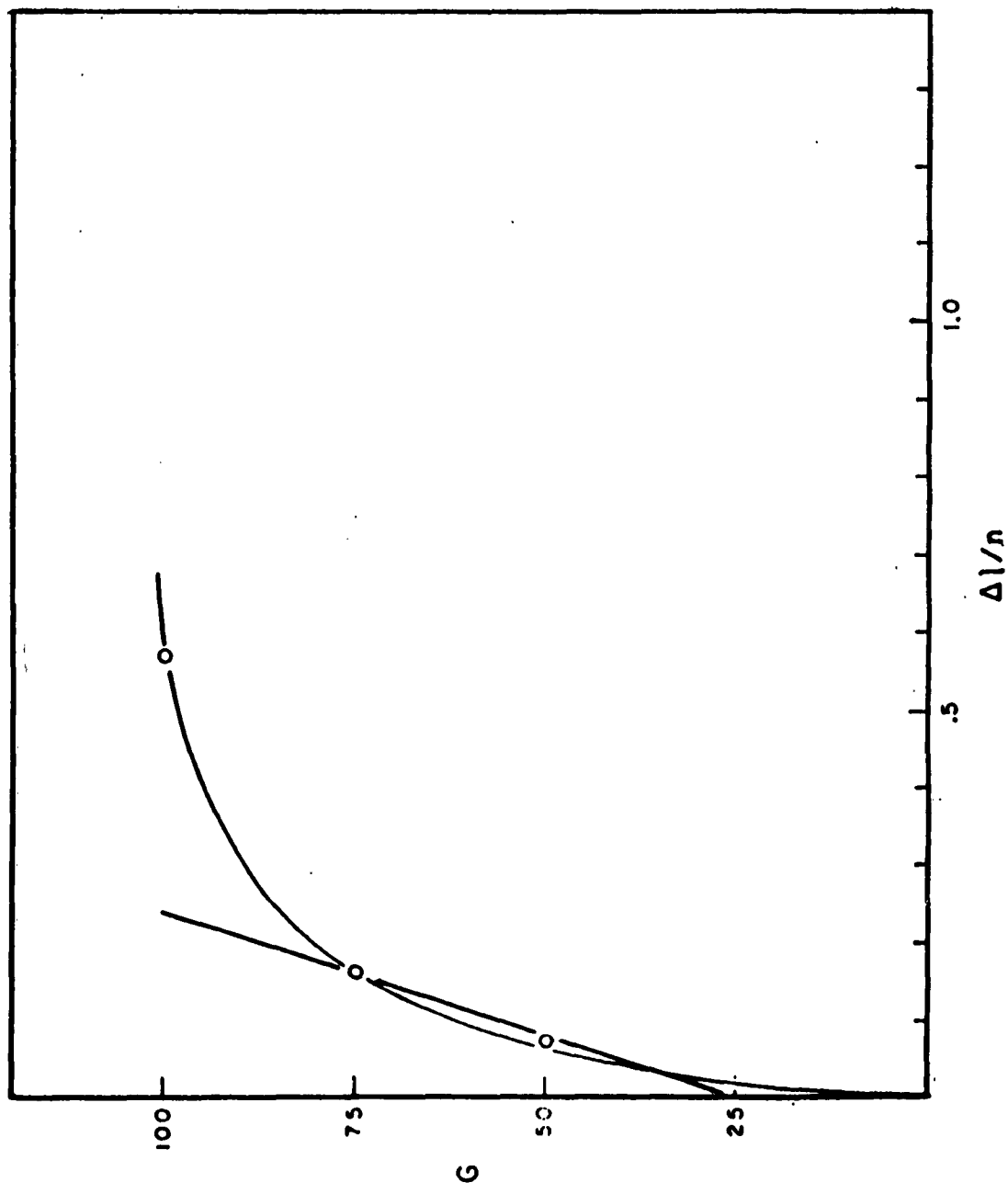
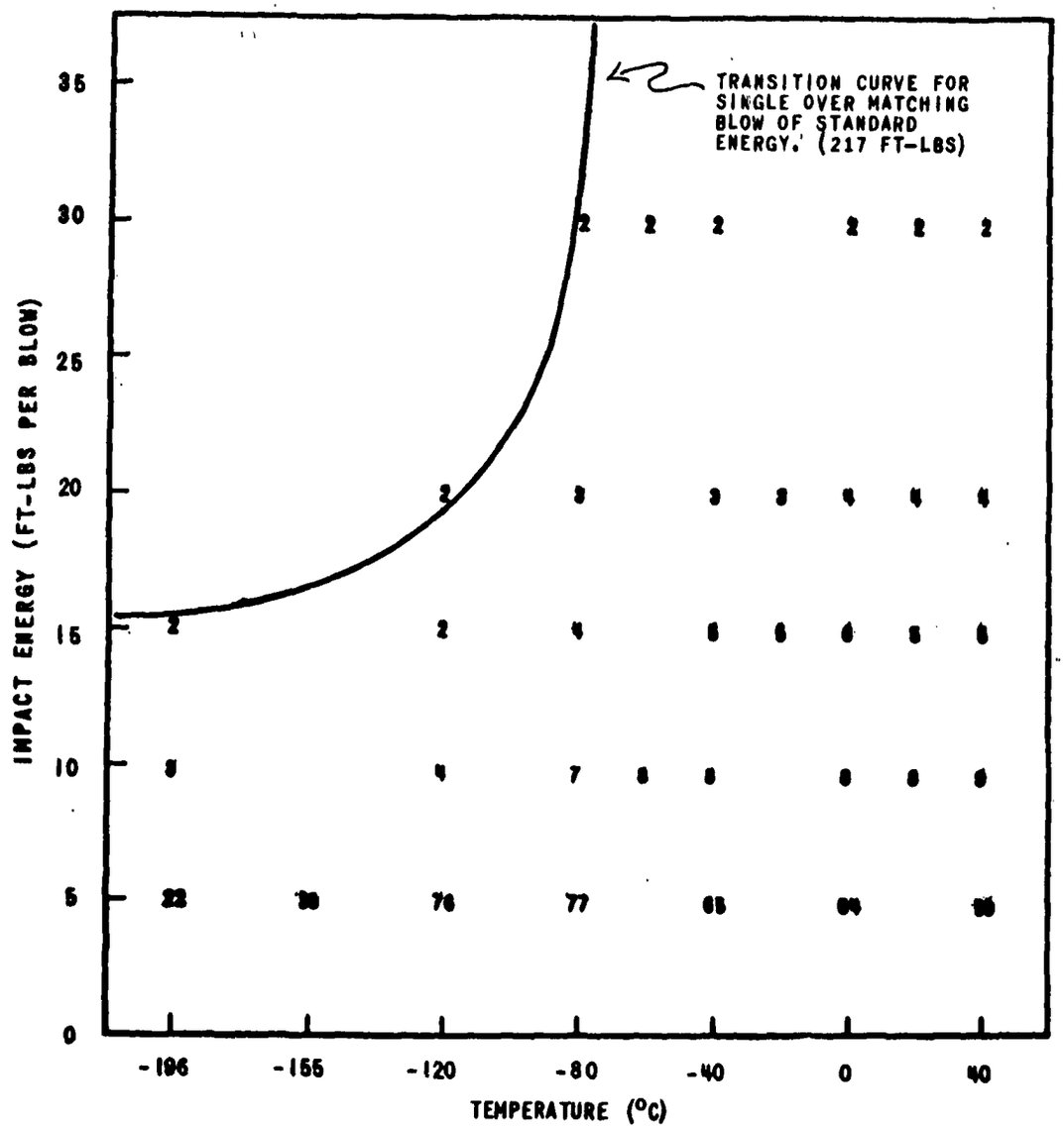


FIGURE 6



NUMBER OF BLOWS TO EFFECT COMPLETE FRACTURE, IMPACT ENERGY PER BLOW VS TEST TEMPERATURE

FIGURE 7

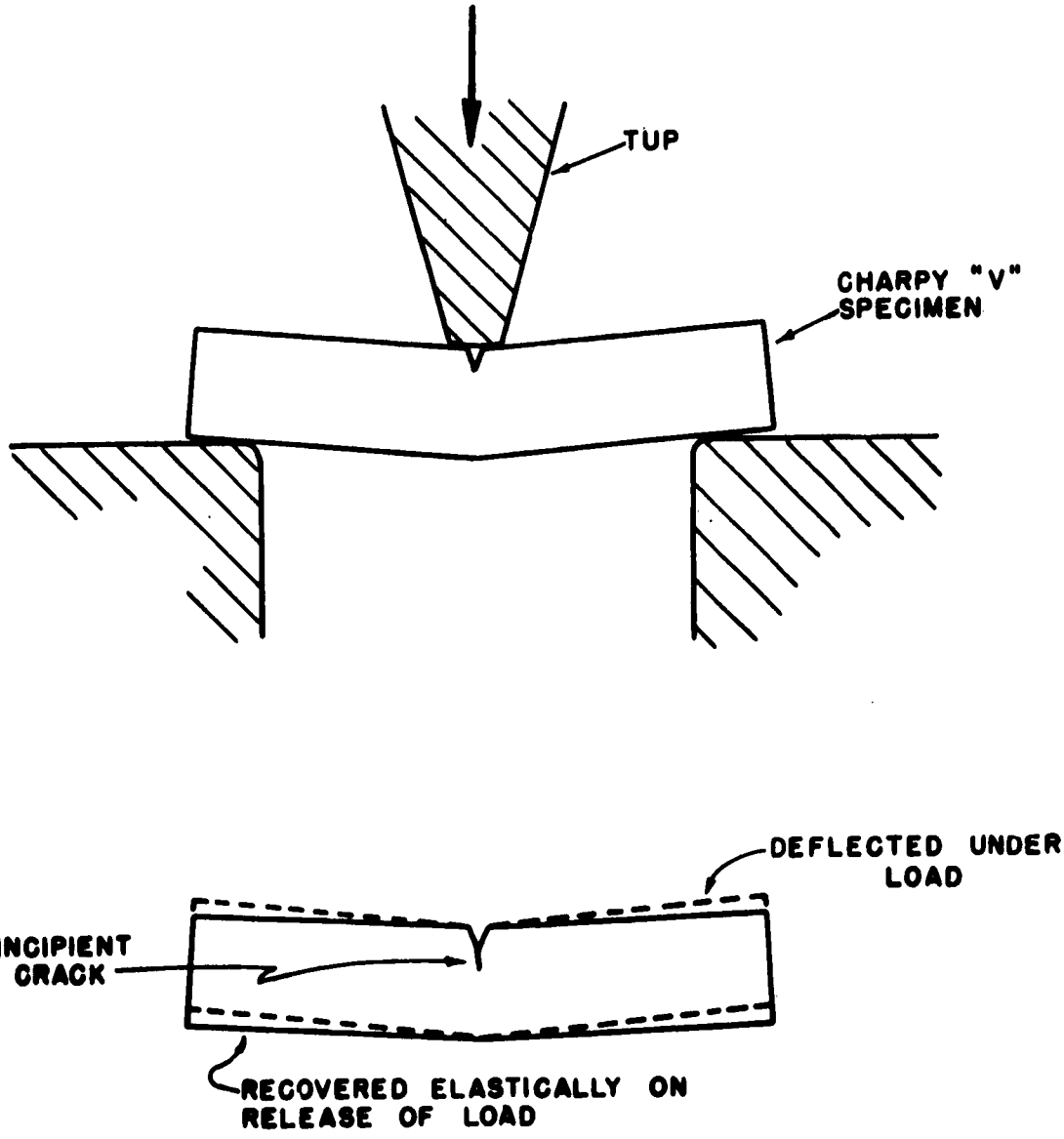

TUP
CHARPY "V"
SPECIMEN
DEFLECTED UNDER
LOAD
INCIPIENT
CRACK
RECOVERED ELASTICALLY ON
RELEASE OF LOAD

FIGURE 8

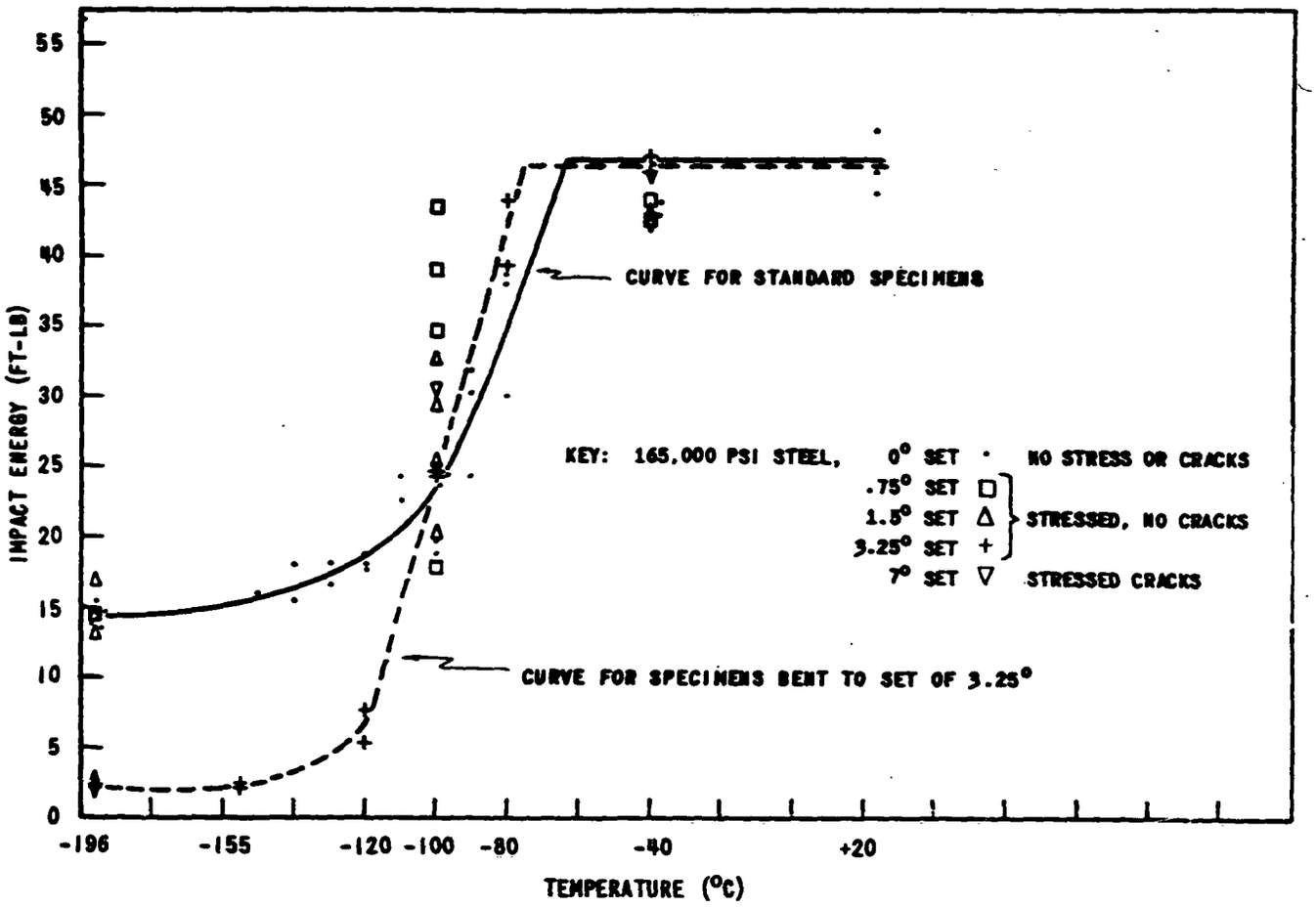


FIGURE 6

INFLUENCE OF RESIDUAL TENSILE STRESS AND TENSILELY-STRESSED CRACKS AT THE BASE OF THE NOTCH UPON TOUGHNESS OF CHARPY V SPECIMENS OF AISI 4340 STEEL QUENCHED AND TEMPERED TO 165,000 PSI TENSILE STRENGTH.

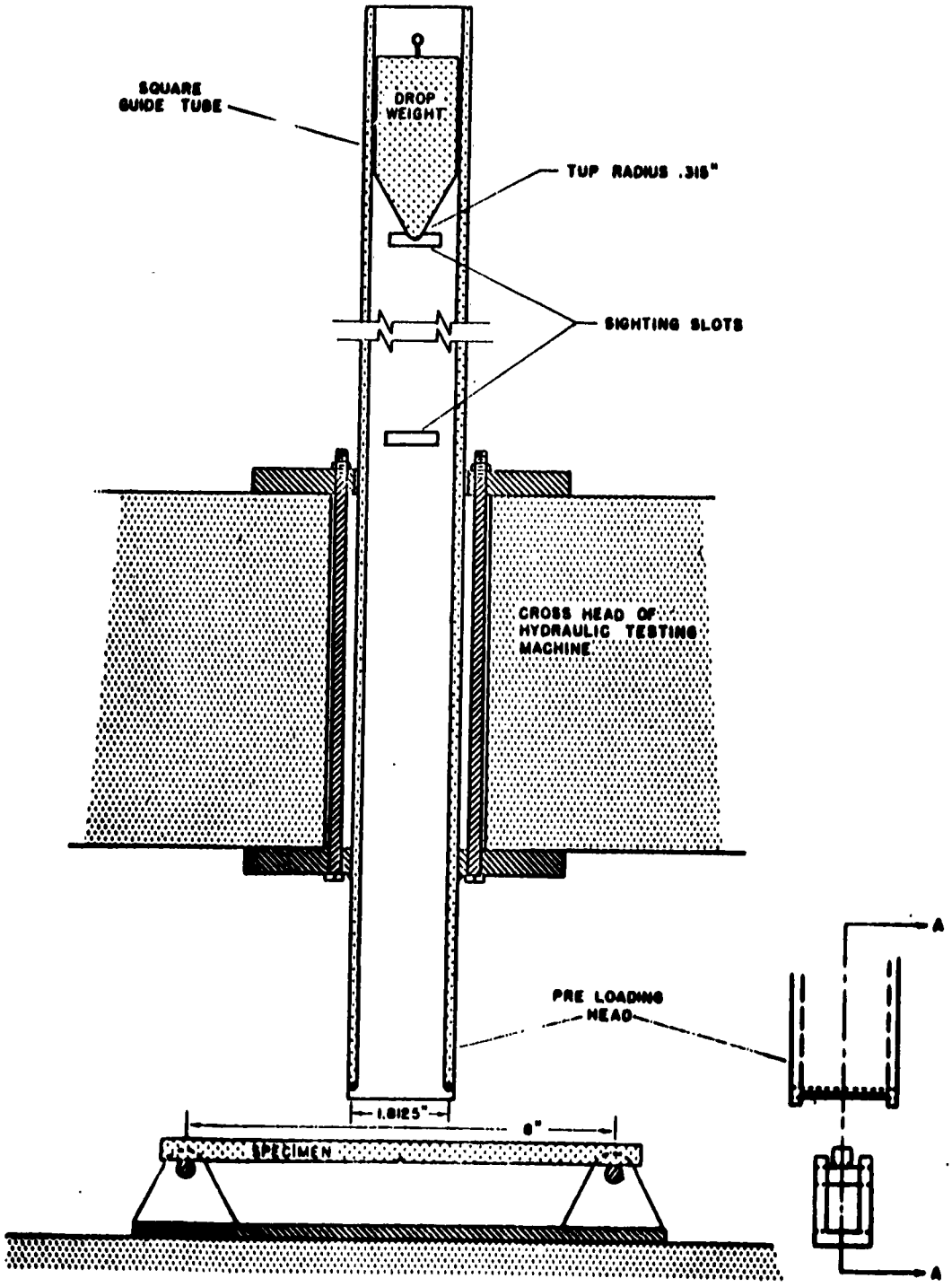
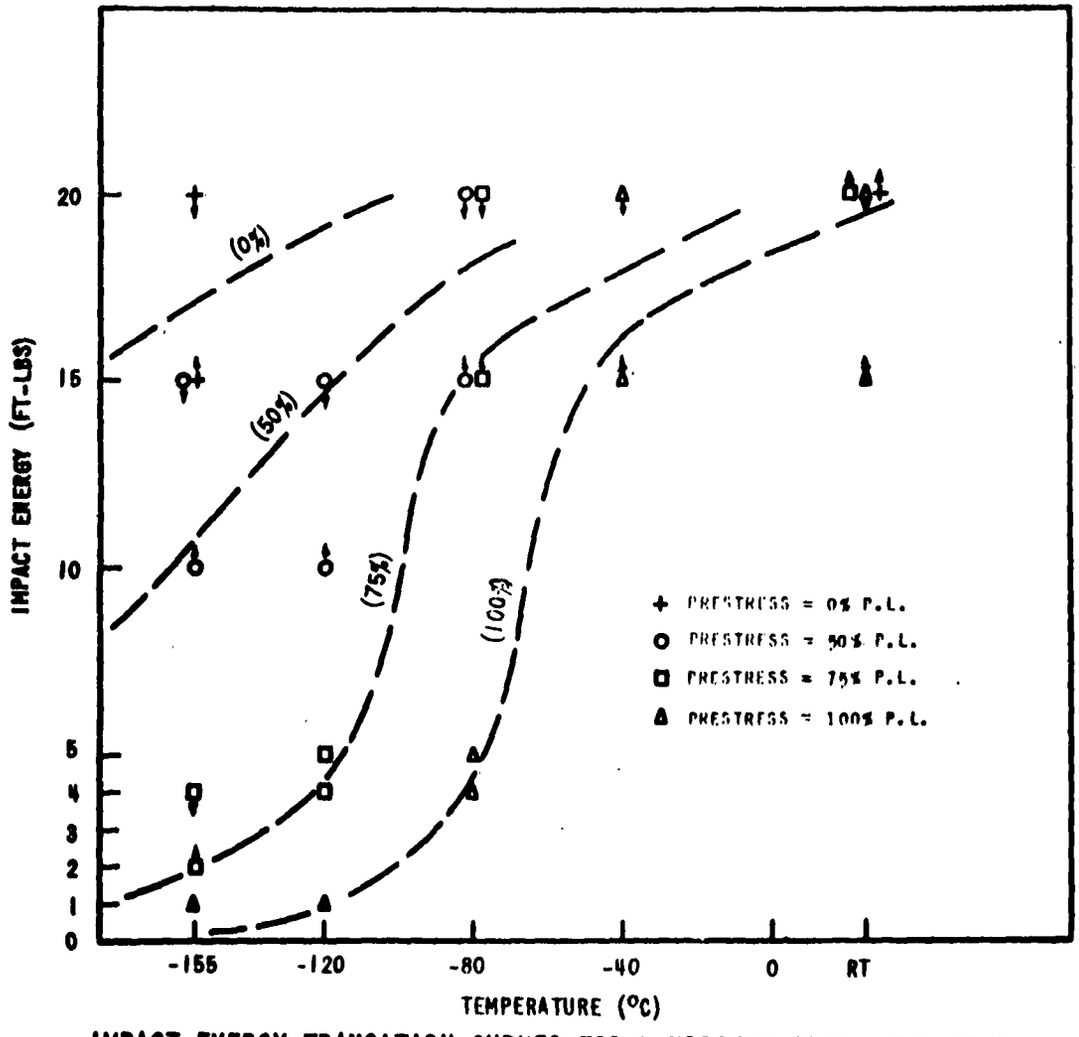

SQUARE GUIDE TUBE
DROP WEIGHT
TUP RADIUS .315"
SIGHTING SLOTS
CROSS HEAD OF HYDRAULIC TESTING MACHINE
PRE LOADING HEAD
A
A
1.8125"
8"
SPECIMEN

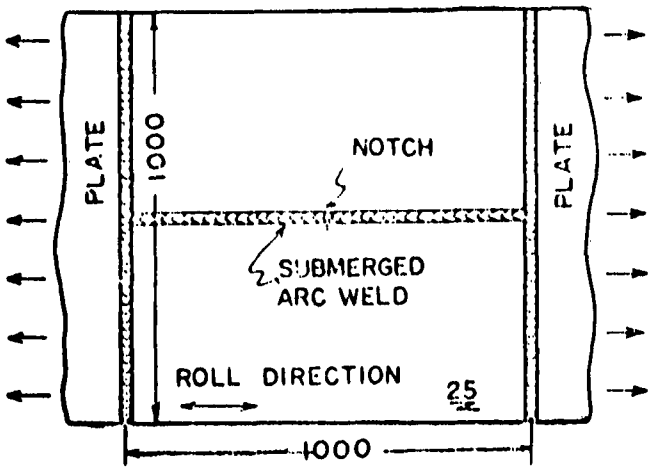
FIGURE 10



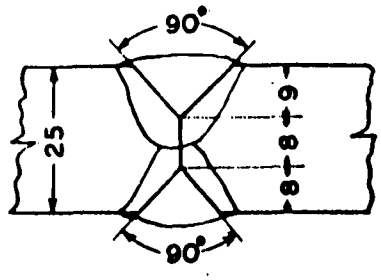
IMPACT EVERGY TRANSITION CURVES FOR V-NOTCHED SPECIMENS OF 230,000 PSI YIELD STRENGTH STEEL PRESTRESSED TO VARIOUS PERCENTAGES OF THE PROPORTIONAL LIMIT

FIGURE 11

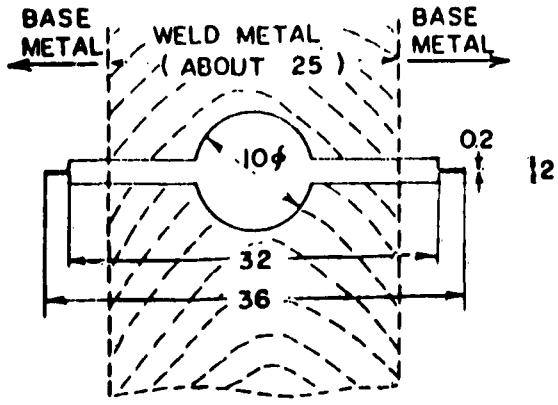
A - TEST SPECIMEN



B - JOINT PREPARATION

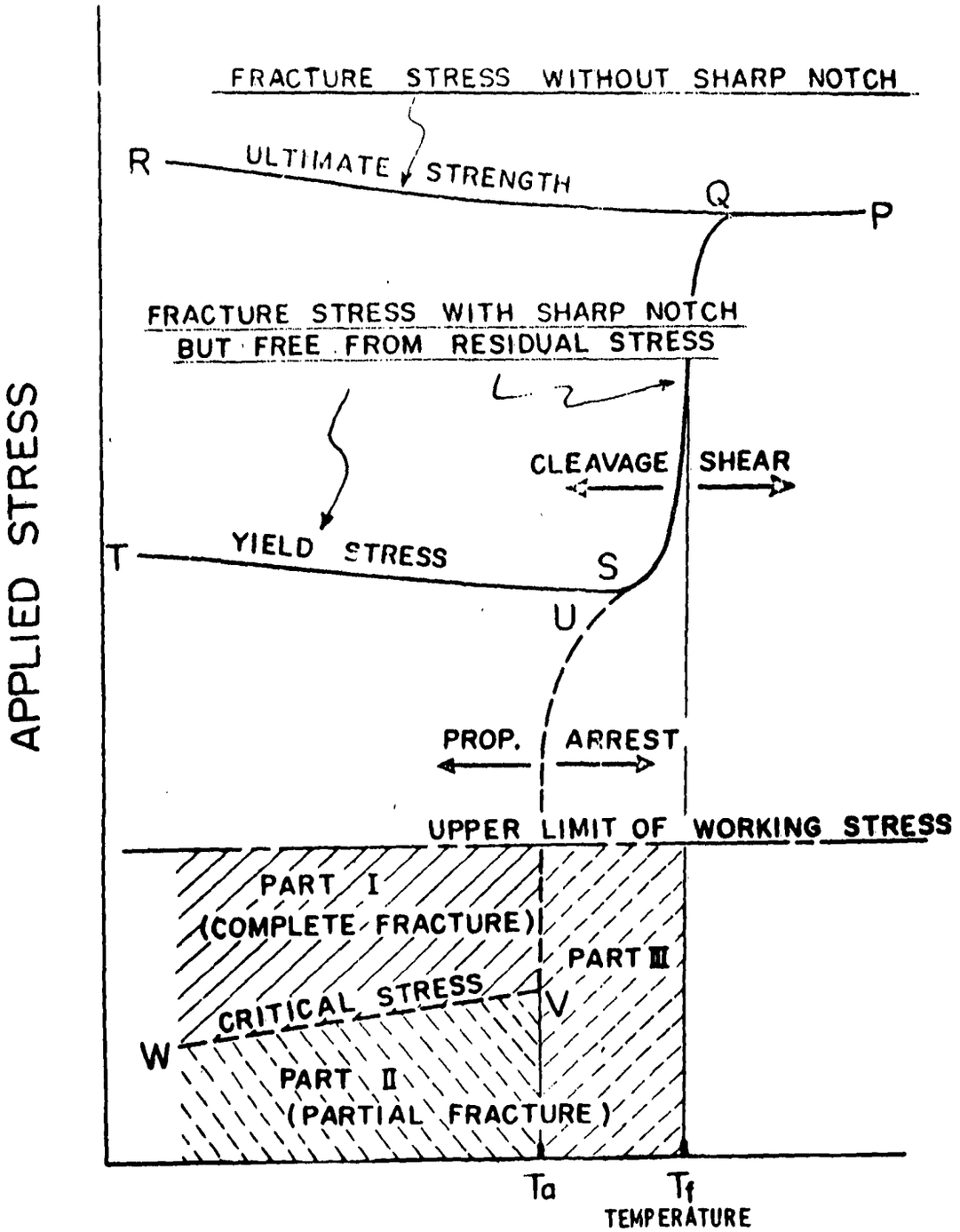


C - NOTCH DETAILS (PLAN)



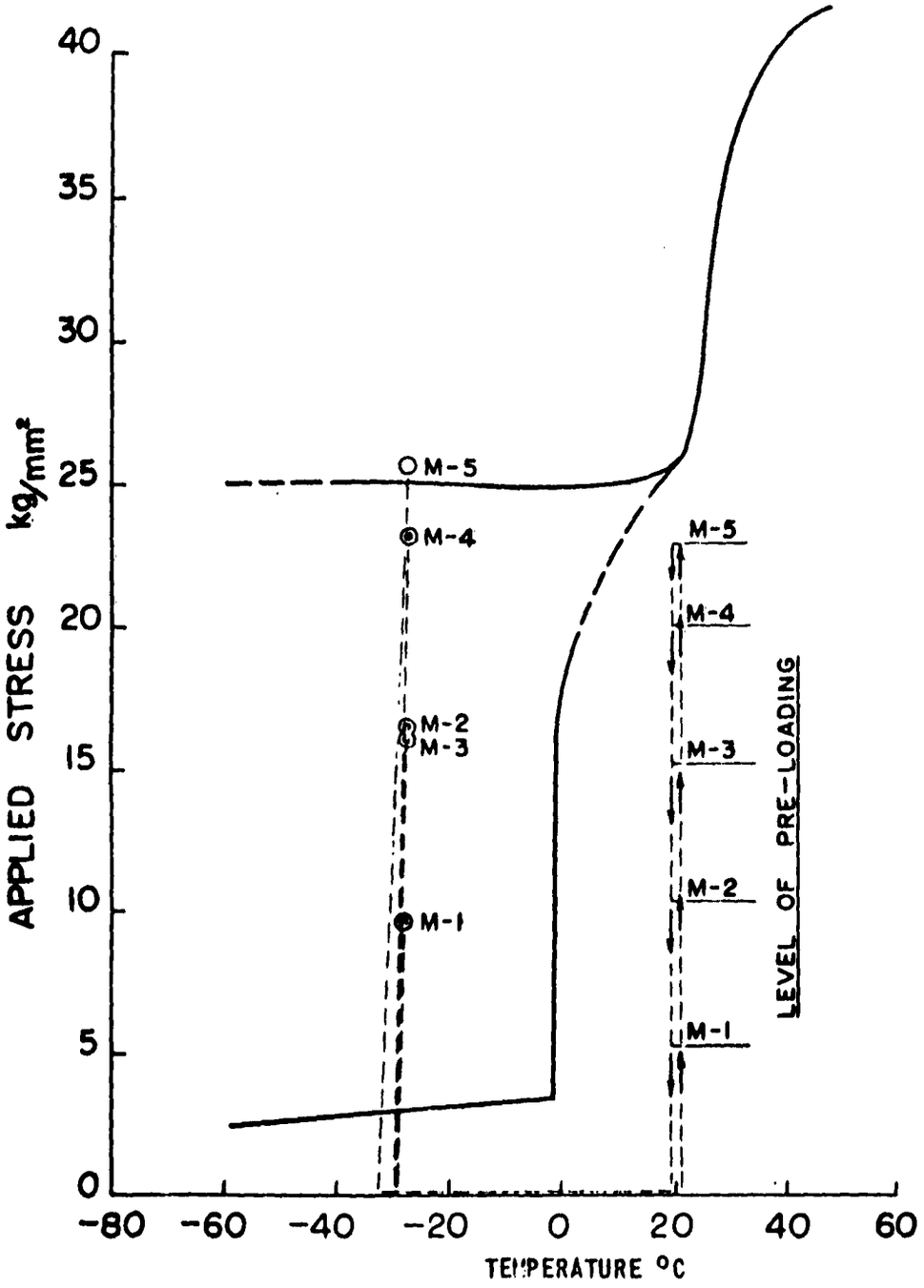
SPECIMEN USED IN SECOND SERIES OF TESTS
(All dimensions in mm)

FIGURE 12



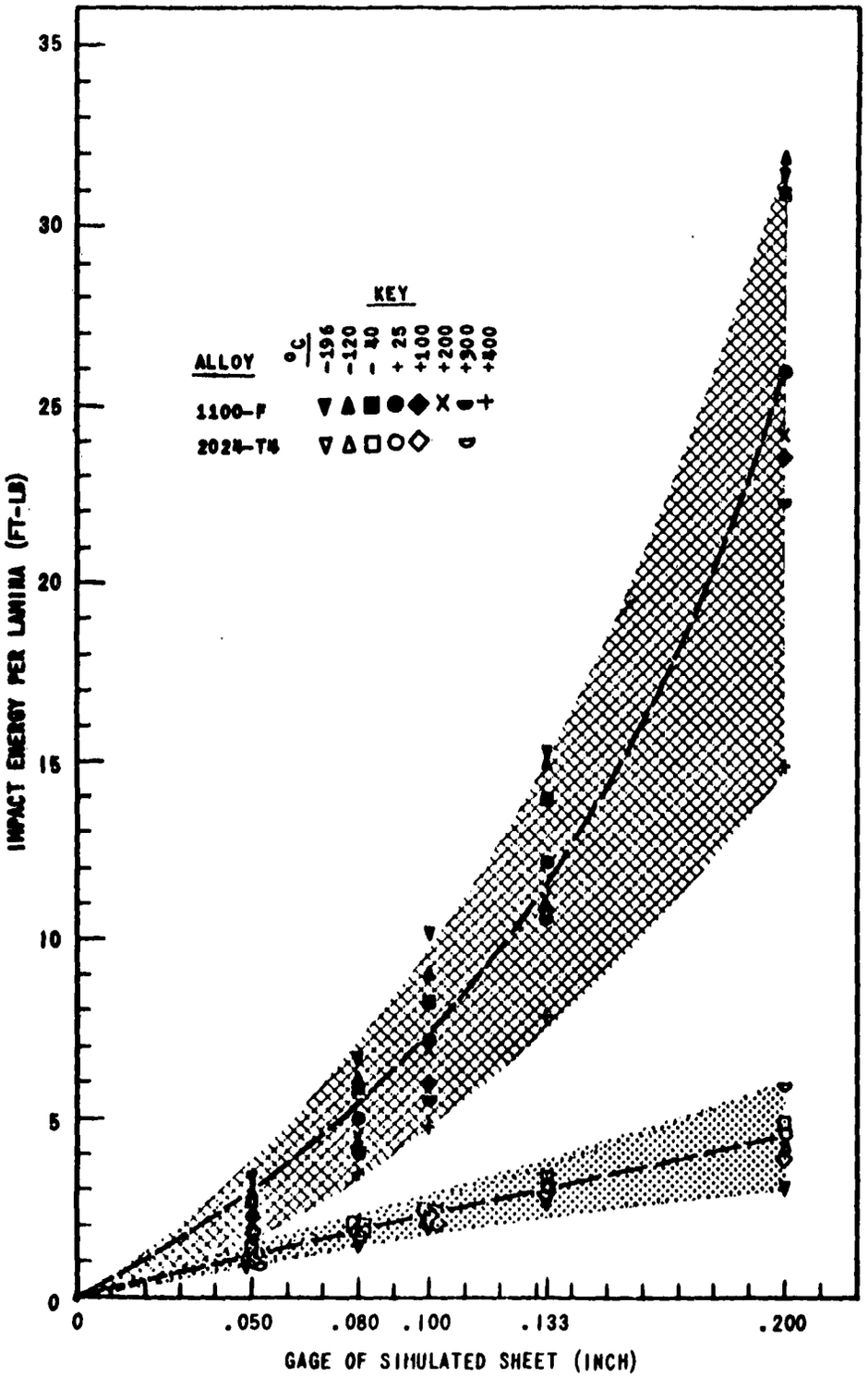
SCHEMATIC FIGURE ON FRACTURE STRENGTH OF WELDED PLATE AND EFFECT OF RESIDUAL STRESS ON IT

FIGURE 13



EFFECT OF PRELOADING ON FRACTURE STRENGTH

FIGURE 14



IMPACT ENERGY OF SIMULATED SHEET VERSUS GAGE, COMMERCIALLY PURE ALUMINUM, 1100-F, AND ALLOY 2024-T4.

FIGURE 15

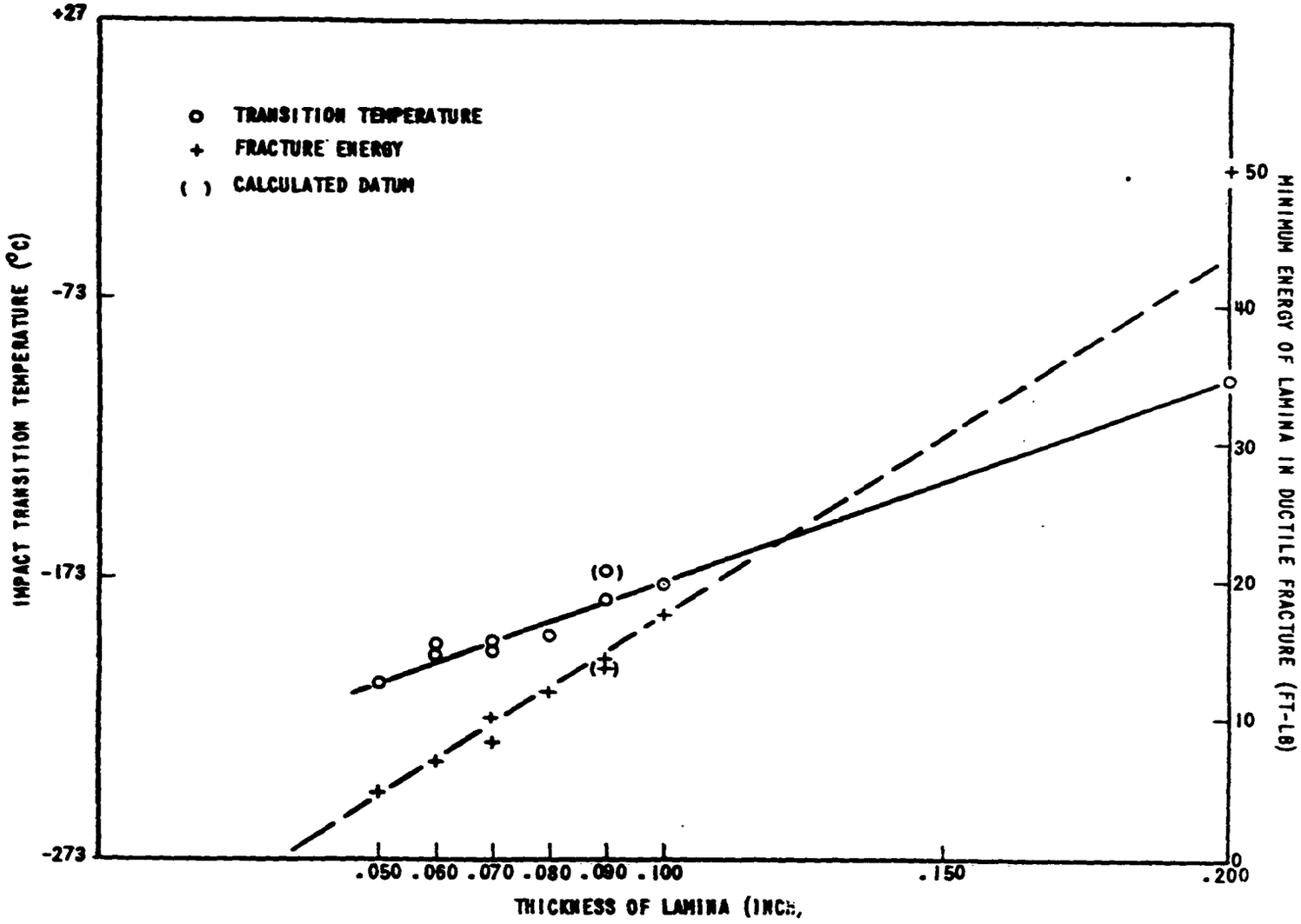


FIGURE 16

IMPACT BEHAVIOR OF SIMULATED SHEET MACHINED FROM HEAT-TREATED LOW ALLOY STEEL BY LAMINATED CHARPY TEST

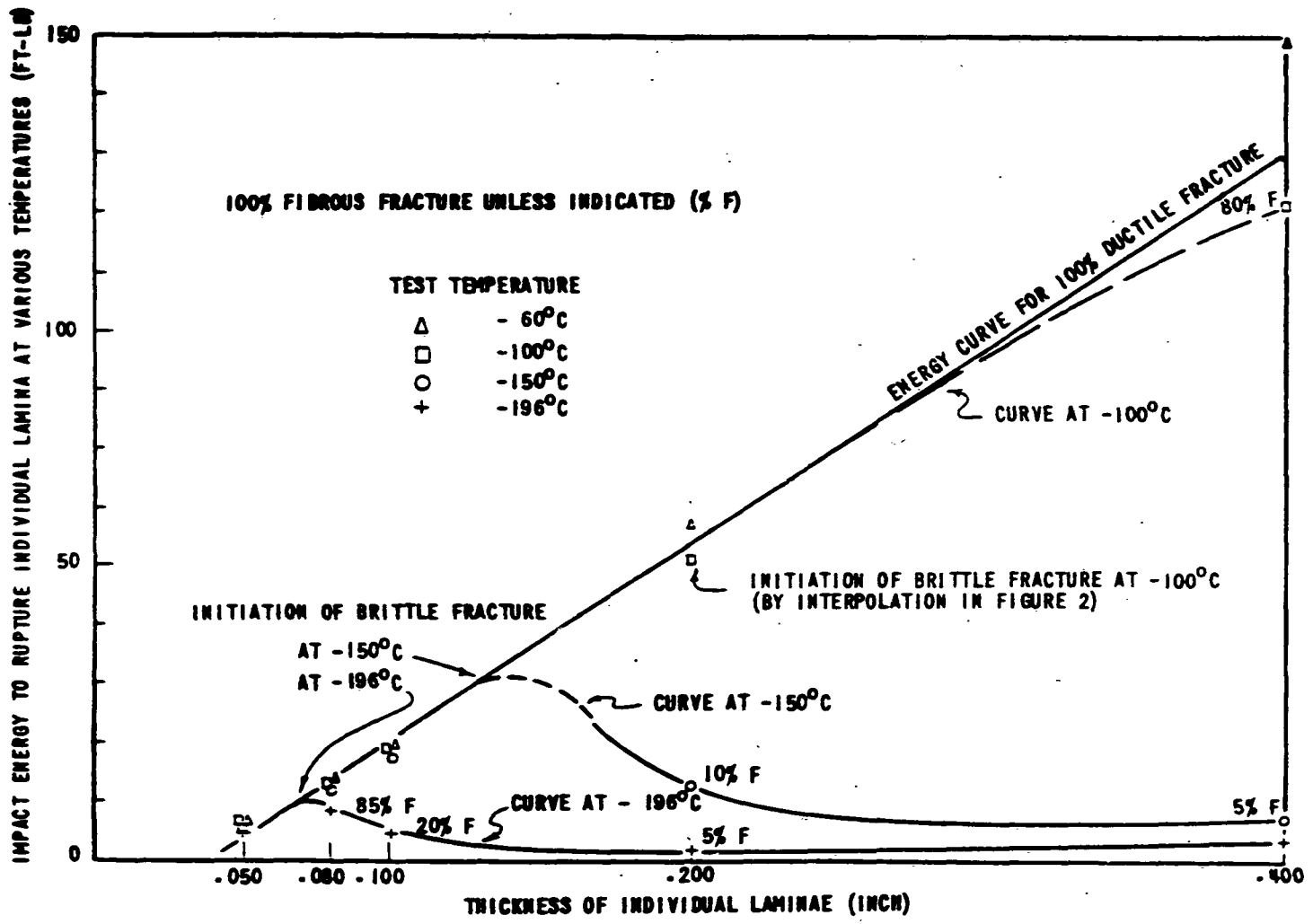
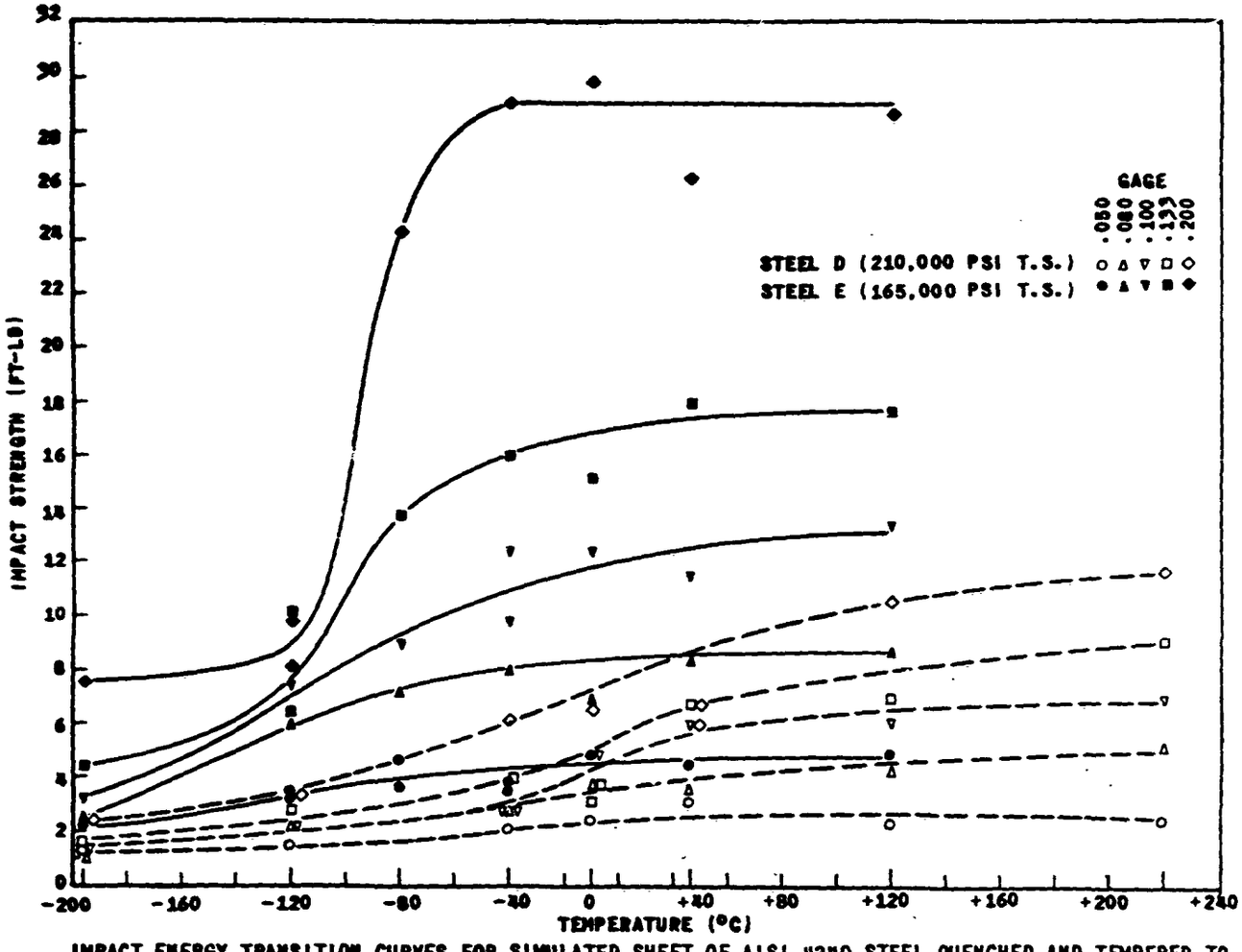


FIGURE 17

DUCTILE/BRITTLE BEHAVIOR VERSUS SHEET (LAMINA) THICKNESS BY LAMINATED CHARPY TEST OF SIMULATED SHEET MACHINED FROM HEAT-TREATED LOW ALLOY STEEL



IMPACT ENERGY TRANSITION CURVES FOR SIMULATED SHEET OF AISI 4340 STEEL QUENCHED AND TEMPERED TO 210,000 PSI AND 165,000 PSI TENSILE STRENGTH. THE SHEET CHARPY V SPECIMEN WAS USED.

FIGURE 18

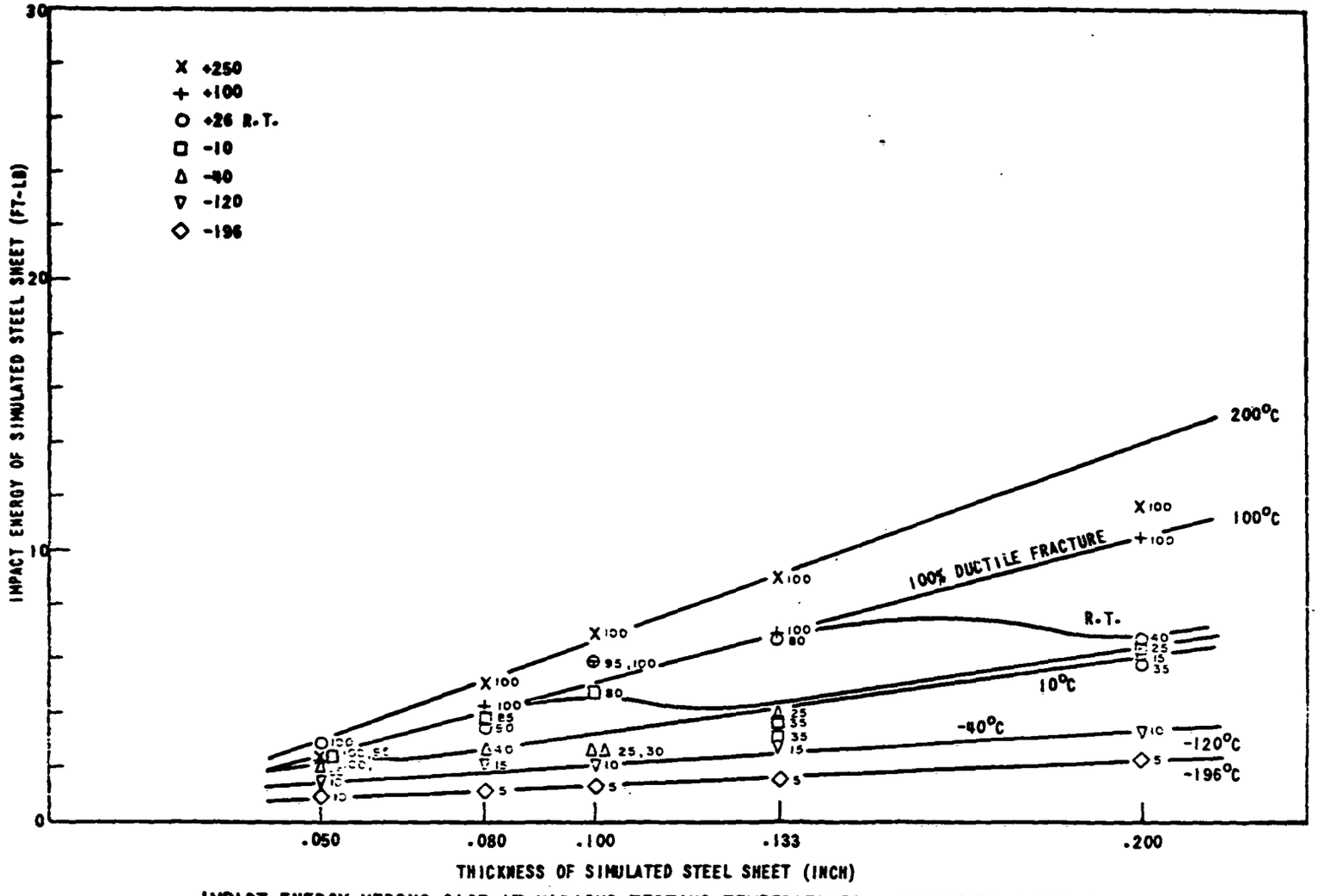


FIGURE 19

IMPACT ENERGY VERSUS GAGE AT VARIOUS TESTING TEMPERATURES. SIMULATED SHEET OF AISI 4340 QUENCHED AND TEMPERED TO 210,000 PSI TENSILE STRENGTH (STEEL D).

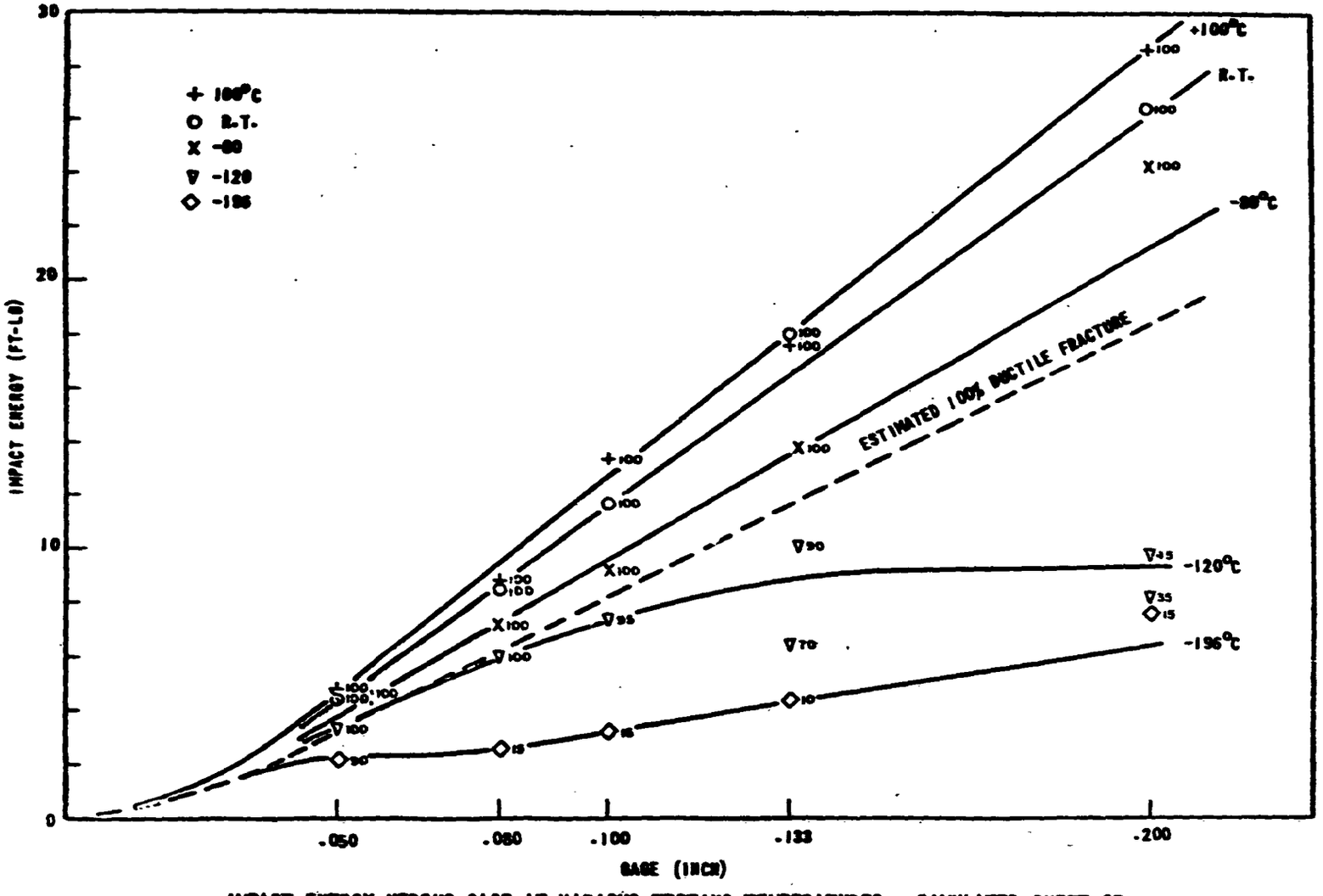


FIGURE 20

IMPACT ENERGY VERSUS GAGE AT VARIOUS TESTING TEMPERATURES. SIMULATED SHEET OF AISI 4340 QUENCHED AND TEMPERED TO 165,000 PSI TENSILE STRENGTH (STEEL E).

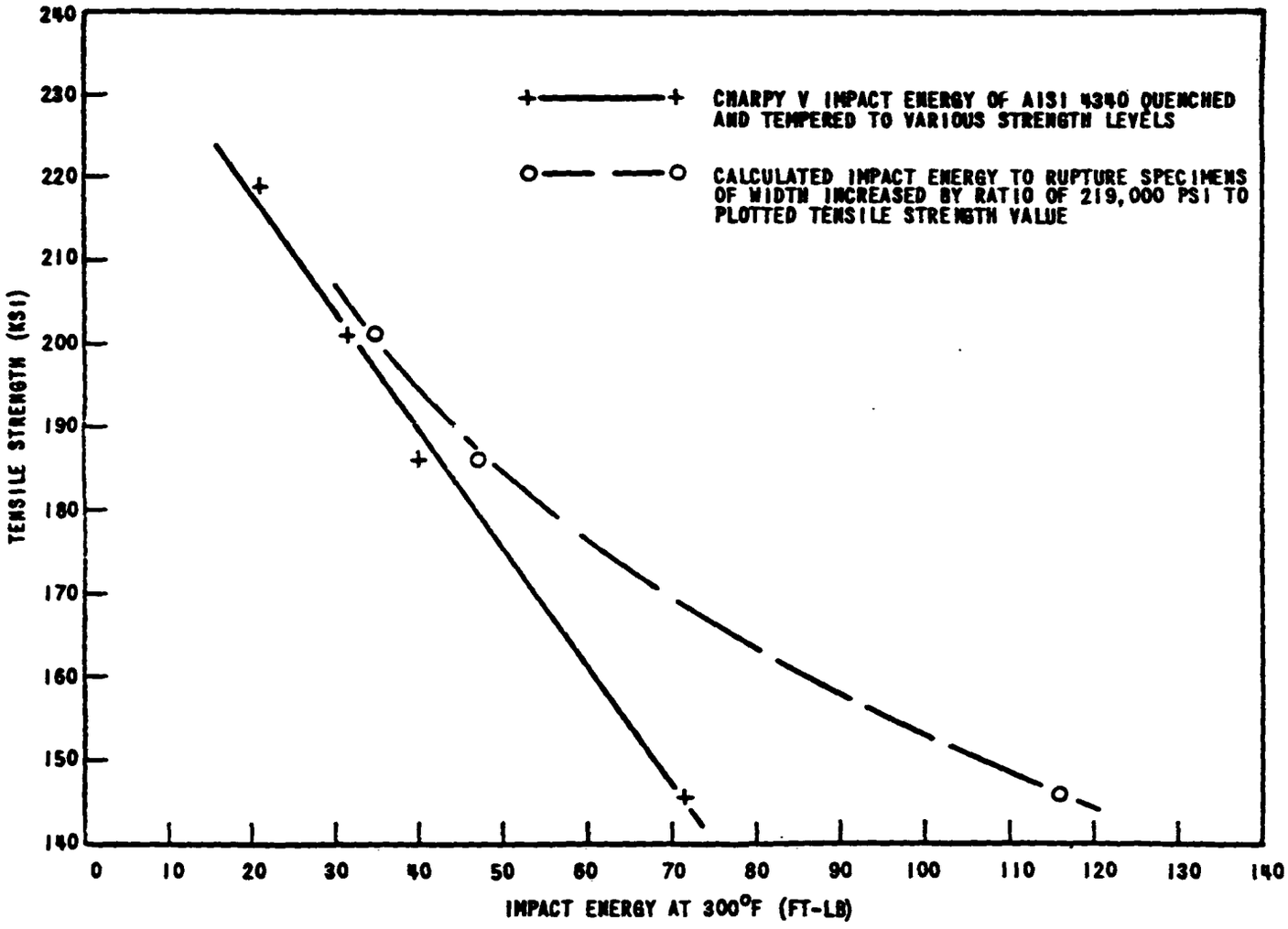


FIGURE 21 TENSILE STRENGTH VERSUS IMPACT ENERGY FOR QUENCHED AND TEMPERED AISI 4340 BAR STOCK; CALCULATED IMPACT ENERGY OF THICKER SECTIONS SUBSTITUTED ON EQUIVALENT STRENGTH BASIS FOR 219,000 PSI MATERIAL.

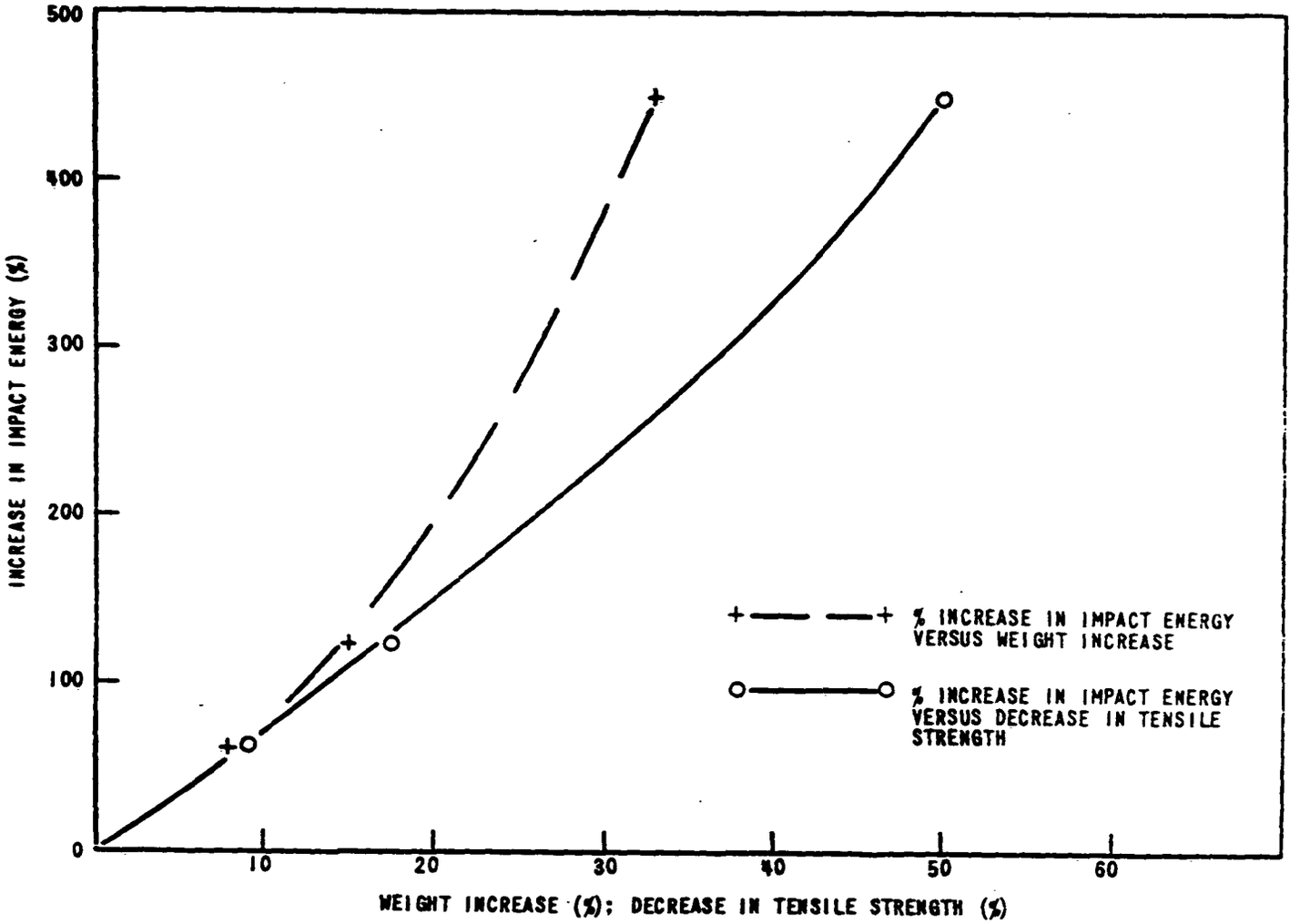


FIGURE 22

INCREASE IN IMPACT ENERGY VERSUS DECREASE IN TENSILE STRENGTH AND INCREASE IN WEIGHT WITH REFERENCE TO FIGURE 9

A Modern High-strength Steel for Ordnance Applications

Carl M. Carman*

Modern recoilless rifle developments needed a high-strength, low-alloy steel having a high-yield strength to reduce the weight of the weapon. To make the weight reduction worthwhile, a minimum yield strength of 200,000 psi at 0.10% offset, corresponding to approximately 220,000 psi yield strength at 0.20% offset, was required. In addition to these high-strength values, a high degree of fracture toughness under plane strain conditions is necessary to guarantee slow crack propagation through the wall. The same is required under plane stress conditions to insure slow failure once a crack has penetrated the wall. Since these weapons must fire many rounds, a good finite fatigue life in the presence of high-stress concentrations, plus reasonable high-temperature strength values, imposes additional requirements.

Examination of these specifications, plus the fact that the recoilless rifle wall is only approximately 0.100 inch thick, shows that the problems encountered in recoilless rifle service are very similar to those encountered in missile design. The similarity between these problems is heightened by the consideration being given to using roll ring forgings, flow turning, and hydrospinning for missile parts. In fact, the problems encountered in recoilless rifle service may be more severe since this is a many shot device.

A survey was made of the commercially available high-strength steels and it was found that those with sufficient strength were deficient in ductility and those with adequate ductility were low in strength.

These results indicated that maximum toughness, ductility and resistance to tempering at slightly elevated temperature were developed by the high-silicon steels tempered at 600° F. Also, it was found that the carbon content should be as low as possible, consistent with the desired strength level, to obtain highest values of fracture toughness. Based on these general principles, the following composition was developed by Frankford Arsenal for recoilless rifle service: 0.30/0.35 C, 0.75/1.00 Mn, 0.80/1.00 Cr, 1.50/2.00 Ni, 0.40/0.60 Mo, 0.08/0.12 V, and 1.40/1.70 Si. This steel was designated by Frankford Arsenal as 4330V (Mod + Si) steel.

The steel was melted as a one-ton induction furnace heat and was press-forged to a one-inch square bar from a thirteen-inch ingot. The various samples were normalized from 1700° F, oil quenched from 1625° F, and were tempered for four hours at the various temperatures. The tensile properties of this steel as a function of tempering temperature are given in Table I and Figure 1.

Attention is directed to the broad plateau in the yield strength and tensile strength curves for tempering between 450° and 650° F. This indicates a relative insensitivity of strength to tempering temperature over this temperature range. The phenomenon has been explained in terms of the start of the third stage of tempering by Alstetter, Cohen and Averbach.(1)

---

* Frankford Arsenal

Fracture Toughness Considerations

As desirable as these tensile properties are, they give no indication of the material behavior in the presence of high-stress concentrations, which is considered of the utmost importance for these applications. Although there is no theory which completely describes and predicts the fracture toughness of a material, the Griffith-Irwin [2,3,4] theory of fracture most nearly fulfills these requirements.

To study the material behavior under conditions of plane strain, circumferentially notched rounds, 0.505-inch and 0.750-inch diameter specimens, were used and are shown in Figure 2.

* In Figure 3, the fracture toughness values for plane strain fracture K_{IC} [1] and the notch strength are plotted as a function of tempering temperature. It will be observed that the notch strength and plane strain fracture toughness show a minimum after tempering in the temperature range of 750° to 950° F. This is attributed to embrittlement which normally occurs in alloy steels after tempering at 600° F. The effect of high-silicon content is to raise the tempering temperature at which this embrittlement may occur.

Both the edge notched plate tensile specimen described by Sachs [5] and Brown [6] and the centrally notched plate specimen described by Irwin and Kies were used to study fracture toughness under conditions approaching plane stress. These specimens are shown in Figure 4.

In Figure 5 the crack propagation fracture toughness values (K_{c_1} and K_{c_2}) for 4330V (Mod + Si) steel are plotted as a function of tempering temperature. These values follow the same general trend as that reported for the plane strain fracture toughness values and, of course, for the same reasons.

Although these fracture toughness values have meaning by themselves, it is helpful to compare these values with those for other widely used high-strength steels. The tensile strength, yield strength, notch strength, and plane strain fracture toughness, K_{IC}^*, of Airsteel X200 are plotted as a function of tempering temperature in Figure 6. Similar data are presented for 300-M and D6A steels in Figures 7 and 8.

These results show that, in general, the 4330V (Mod + Si) steel has slightly higher values of K_{IC}^* than the other steels investigated. Actually there is no great difference in K_{IC}^* values among these high-strength steels. The values range from 60,000 psi $\sqrt{\text{in.}}$ to 80,000 psi $\sqrt{\text{in.}}$ when they are heat treated to their maximum strengths.

Comparisons of crack propagation fracture toughness, K_{c_1}, of 4330V (Mod + Si) steel, D6A, Airsteel X200, H11 and 300-M are shown in Figure 9. These tests were made in accordance with ASTM standards.

1* Denotes corrected for plastic zone.
A factor of $\sqrt{2}$ was used in the analysis to allow for some strain hardening.

Table I

Tensile Properties of 4330V (Mod + Si) Steel

Tempering Temperature °F	Yield Strength (0.10% Offset) psi	Yield Strength (0.20% Offset) psi	Tensile Strength (psi)	Elong. (%)	Red. of Area (%)
350	181,000	199,000	279,000	13.2	36.0
450	198,500	213,000	267,000	13.0	42.8
	207,000	221,000	270,000	12.0	41.5
550	222,000	232,000	265,000	12.4	41.0
	207,000	220,000	266,000	12.4	43.7
600	207,000	219,500	263,000	12.2	43.4
	206,500	220,000	261,500	13.5	48.0
650	208,000	221,500	261,000	11.9	41.0
	209,000	220,000	258,000	13.2	50.4
750	190,000	198,500	238,500	14.5	45.8
	187,000	197,000	237,500	14.1	43.7
850	173,000	185,000	231,000	13.0	39.8
	176,000	187,000	233,000	14.2	41.5
950	181,000	192,500	221,000	15.8	46.3
1050	186,000	190,500	210,000	14.2	41.5

The 4330V (Mod + Si) steel showed very high values of fracture toughness at the low tempering temperatures, which is consistent with the principal of minimum carbon content associated with the strength level. In addition to the evidence presented in this Figure, the specimens of 4330V (Mod + Si) steel tempered at the lower tempering temperatures showed considerable necking. Comparison at the 220,000 psi yield strength level shows that the 4330V (Mod + Si) steel has higher values of fracture toughness than either the D6A or the Airsteel X200.

The 300-M steel tempered at 600° F failed by what is now considered low-energy shear, but did show higher fracture toughness than the other high-strength steels. The H11 steel showed fairly low values of fracture toughness under the conditions tested.

Transition Temperature Effects in Notch Testing

Another technique of comparing materials is by notch testing at a series of subzero temperatures, as suggested by Srawley and Beacham.[7] In these tests the crack propagation fracture toughness values decrease with decreasing temperature and the fracture mode shows a transition from shear to flat fracture. In this respect, these tests show behavior very similar to that exhibited by the more familiar "V" Notch Charpy impact test.

Transition temperature results for the 4330V (Mod + Si) steel, 300-M steel, AMS 6434 steel, and AMS 6434 CEVM (consumable electrode vacuum melted) steel, both longitudinal and transverse, are shown in Figure 10.

The transition effects of AMS 6434 CEVM and AMS 6434 are shown in the top two sections of this figure. The drop off in K_{c_3} in the longitudinal direction occurs at -150° F for the AMS 6434 CEVM and at -100° F for the AMS 6434. In the transverse direction, this drop off occurs at -100° F for the AMS 6434 CEVM and the K_{c_3} appears to fall gradually with temperature for the AMS6434. It also appears that the directionality is less pronounced for the AMS6434 CEVM steel.

The 4330V (Mod + Si) steel shows transitional behavior similar to that exhibited by the AMS6434 steel. The room temperature K_{c_3} and -150° F K_{c_3} compare favorably with the values for AMS 6434 and AMS 6434 CEVM at a lower yield strength. It should be noted, however, that the percentage of shear in the fast fracture decreases more rapidly with decreasing temperature for the 4330V (Mod + Si) steel than the AMS 6434 steel.

The properties of the 300-M steel decrease very rapidly with decreasing temperature and the steel becomes relatively brittle at -40° F.

Burst Tests

These various tests indicate the probable behavior of this steel under multiaxial stresses but do not fully demonstrate its behavior under service conditions. To determine this probable behavior, model sections of a 90 mm recoilless rifle were made. These model sections were loaded

hydrostatically to failure by Watertown Arsenal. A modified type of Bridgeman seal was used to seal the ends.

The bending moments induced by the change in section induced extensive bulging (Figure 11) and precluded analysis of the load-strain curves by the simple pressure vessel formula. Elasticity theory was used to analyze the load-strain curves in terms of combined stress. This analysis is as follows:

$$E\epsilon_T = \sigma_T - \nu(\sigma_L + \sigma_R)$$
$$E\epsilon_L = \sigma_L - \nu(\sigma_R + \sigma_T)$$
$$E\epsilon_R = \sigma_R - \nu(\sigma_T + \sigma_L)$$

Since we are considering only the outer fibers the radial stress is zero. The equations then reduce to the following:

$$\sigma_L = \frac{E}{1-\nu^2}(\epsilon_L + \nu\epsilon_T)$$
$$\sigma_T = \frac{E}{1-\nu^2}(\epsilon_T + \nu\epsilon_L)$$

The Von Mises criterion was used to calculate the combined stress. The equation is as follows:

$$\sigma_C^2 = \sigma_L^2 - \sigma_L\sigma_T + \sigma_T^2$$

The analysis was applied at the 0.10% yield point and the calculated combined value compared with the uniaxial yield strength. These results are given in Table II.

These values closely approach the uniaxial values of yield strength. A more detailed plastic analysis would probably give higher values.

Fracture initiation and propagation in these vessels was by shear.

Table II

Hydrostatic Test Values

Test Chamber Number	Internal Pressure for Yielding (psi)	Hydrostatic Yield Stress (psi)	Uniaxial Yield Strength (psi)
2B	6,600	185,000	206,000
1C	6,370	215,000	

Fatigue Properties

Since recoilless guns are designed to last for at least 1000 rounds, there is considerable interest in the low cycle-high stress portion of the fatigue curve. Two types of specimens were used for this portion of the investigation. One is the standard R. R. Moore rotating beam fatigue specimen and the other is a notched rotating beam type specimen having a stress

concentration of $K^t = 6.7$. Stresses were selected so as to induce failure before 10^5 cycles were reached. These results are shown in Figure 12.

It will be observed that the introduction of the sharp notch reduced the fatigue life by a factor of 35. However, even at a high-stress level the notched specimens had a life greater than 1000 cycles.

In addition to these tests, specimens were stressed at 125,000, 100,000, and 80,000 psi and were run for 80, 60, 40, and 20 per cent of the cycles required for failure. These specimens were heat tinted and broken in tension. After fracturing, the area not cracked in fatigue was measured. The results are shown in the lower right hand corner of Figure 12. These data show that, as the stress level is raised, the percentage of uncracked area increases at the higher life percentages.

Temper Embrittlement

Since either in firing or during processing the steel may accidentally be subjected to a thermal cycle tending to produce classic temper embrittlement, the susceptibility of this steel should be determined. To determine this susceptibility, 100 V-notch Charpy impact specimens were machined. Fifty of these specimens were subjected to a thermal cycle devised by Powers and modified by Low (Table III) to develop embrittlement. The remaining samples were water-quenched after tempering at 1100° F for one hour.

Table III

Power's Embrittling Cycle as Modified By Low

Temper 1100° F for 1 hour
Furnace cool to 1000° F and hold 15 hours
Furnace cool to 975° F and hold 24 hours
Furnace cool to 925° F and hold 48 hours
Furnace cool to 875° F and hold 72 hours
Air cool to room temperature

The specimens were tested over the temperature range from room temperature to -320° F. The results are shown in Figure 13.

Based on the energy absorbed it may be concluded that the material is sensitive to classic temper embrittlement. This contention is supported by metallographic examination as shown in Figure 14.

Elevated Temperature Properties

Since these weapons may reach fairly high temperatures during firing, the degradation of the tensile properties with increasing temperature is quite important in design. Standard 0.505-inch diameter tensile specimens

were machined, heat treated, and tested over the temperature range from room temperature to 1000° F. Transverse test values were obtained by Watertown Arsenal. These results are shown in Figure 15. The yield and tensile strength values show the usual decrease with increasing temperature and are relatively insensitive to direction. The transverse reduction of area and elongation are less than the longitudinal values, per expectations.

Commercial Production

Two twenty-ton basic electric arc furnace heats of this steel have been melted for fabrication into larger caliber recoilless weapons. The compositions of these heats are given in Table IV.

In order to assist in further industrial procurement, standard transverse 0.357-inch diameter tensile specimens were machined from the gun forgings. These specimens were oil quenched from 1650° F and were tempered over the temperature interval from 450° to 750° F. The tensile test results are shown in Figures 16 and 17. Each point represents the average of six individual tests. The same general trend of yield and tensile strength will be observed, as in the case of the longitudinal specimens. The tensile strength of Heat No. 21L482 was somewhat lower than that of Heat No. 21K631, as would be anticipated from the carbon contents. These results show that the mechanical properties are reproducible from heat to heat, and ballistic testing of the weapons shows that good service may be expected.

Areas for Future Work

The Griffith-Irwin fracture theory will satisfactorily characterize the fracture behavior of material very well and provides a quantitative measure of fracture toughness (K_c and $\mathcal{G}_c$). The fracture toughness may also be used to compare materials. In addition, this theory offers the promise of being able to predict the maximum size of flaw which may be tolerated before the fracture becomes unstable. From our present state of knowledge, it appears that the most important application will remain the last to be exploited, namely, the maximum flaw size. Although this size may be calculated, subcritical flaws will grow to critical size in just a few cycles and research is needed in this area. The effect of biaxial stress systems on crack initiation and propagation needs further research.

Table IV

Chemical Analysis of Twenty-Ton Heats of 4330V (Mod + Si) Steel

	% Element by Weight								
Heat No.	C	Mn	S	P	Cr	Ni	Mo	V	Si
21K631	0.34	0.98	0.005	0.015	0.95	1.82	0.42	0.14	1.37
21L482	0.31	0.87	0.004	0.007	0.87	1.74	0.45	0.10	1.45

Acknowledgement

The author wishes to thank Dr. Irwin and his staff at the Naval Research Laboratory and Mr. W. F. Brown, Jr., of National Aeronautics and Space Administration for their help and encouragement and Miss Marie Dougherty of the Engineering Mechanics Branch, Frankford Arsenal, for her assistance with the experimental work.

References

1. Alstetter, C. J., Cohen, M., and Averbach, B. L., "The Effect of Silicon on the Tempering of High Strength Steels" WADC Report 59-57

2. Irwin, G. R., "Fracture Mechanics" First Symposium on Naval Structural Mechanics, Stanford University, 11 - 14 April 1958

3. Irwin, G. R., Kies, J. A., and Smith, H. L., "Fracture Strengths Relative to Onset and Arrest of Crack Propagation" Paper presented before ASTM, Boston, Massachusetts, April 1958

4. Irwin, G. R., "Plastic Strain Zone Correction" NRL Technical Memorandum #77

5. Sachs, G., Sessler, J. G., Pray, R. F., and Yeh, T. H. "Relations Between the Notch Tensile Strength of Cylindrical and Prismatic Specimens of Titanium Alloys Heat-Treated Steels" ASME Journal of Basic Engineering, June 1960

6. Epsey, G., Jones, M. H., and Brown, W. F.,Jr., "The Sharp Notch Tensile Strength of Several High Strength Sheet Alloys" Proceedings ASTM vol. 59, p. 837 (1959)

7. Srawley, J. E., and Beacham, C. D., "Crack Propagation Tests of Some High Strength Sheet Steels" NRL Report No. 5263, Naval Research Laboratory, Jan. 10, 1959

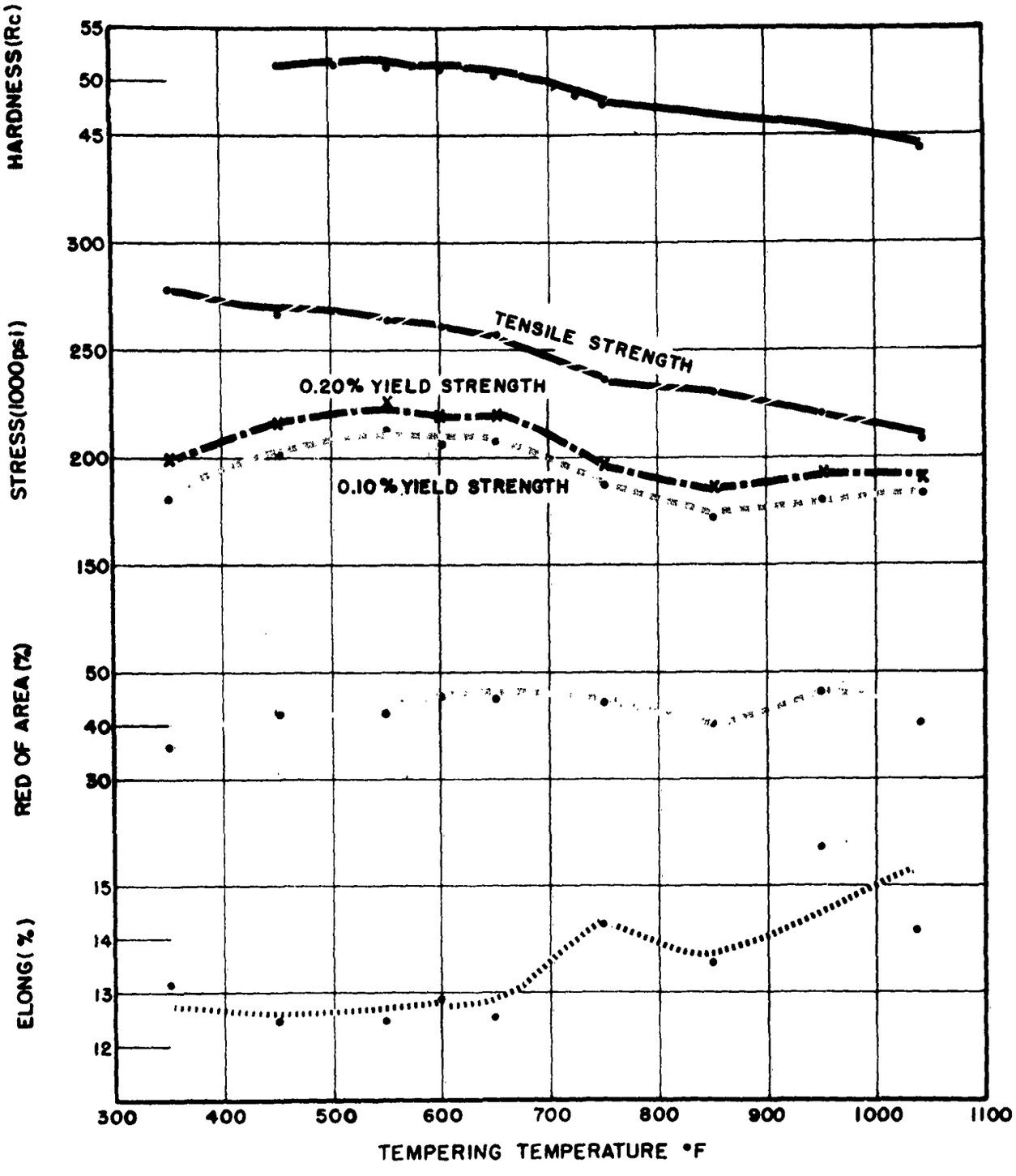
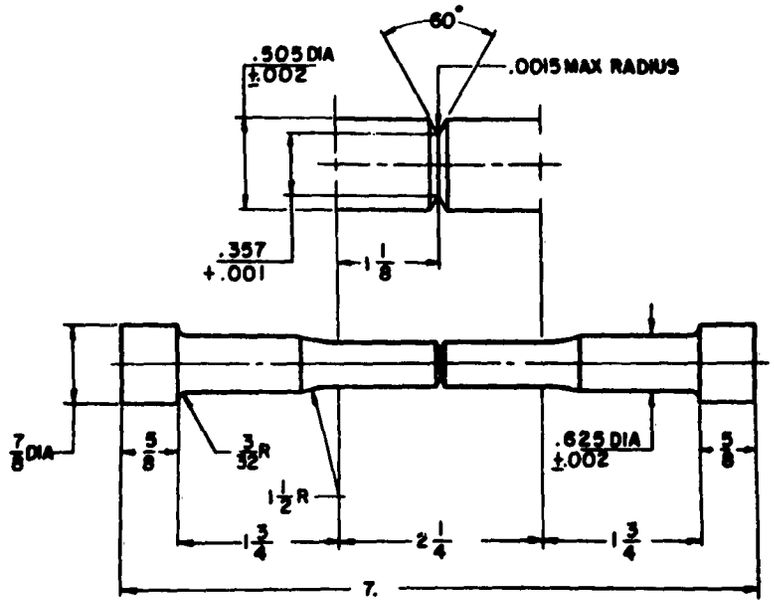


Fig. 1. Tensile properties of 4330V (Mod + Si) steel as a function of tempering temperature



ALL FINISHED SURFACES ARE TO BE GROUND

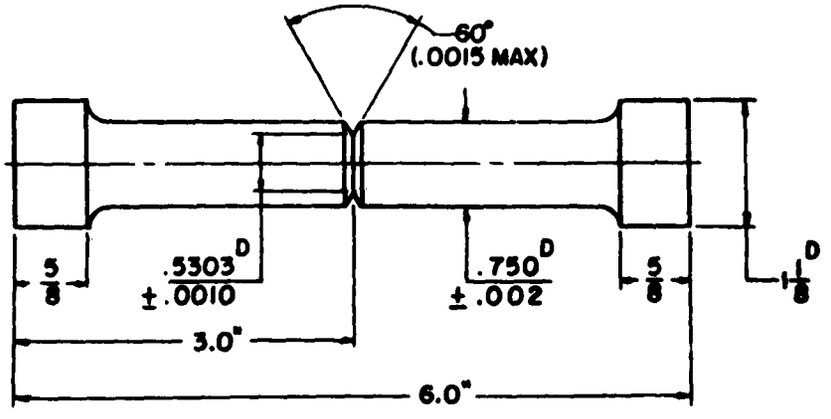


Fig. 2. Circumferentially notched tensile specimens

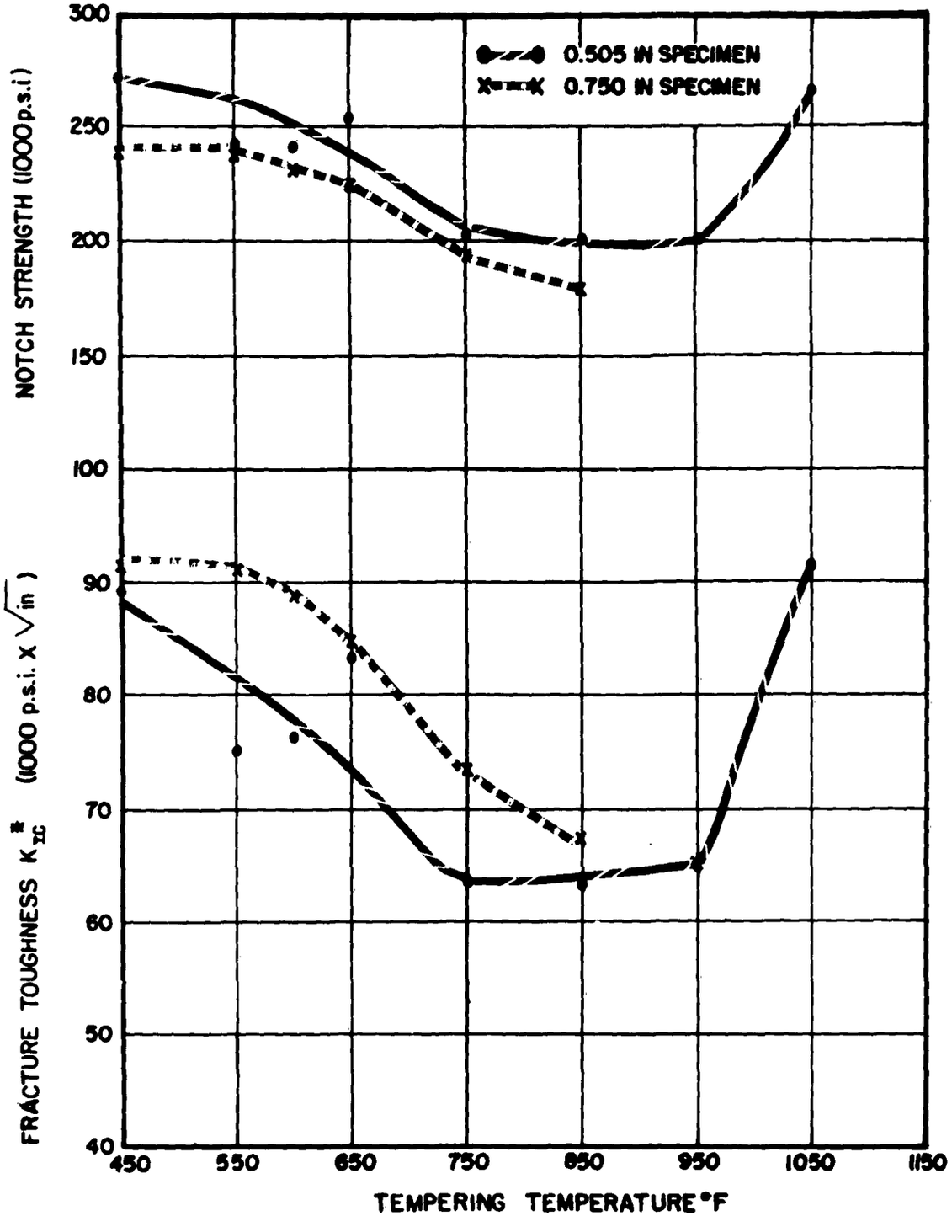
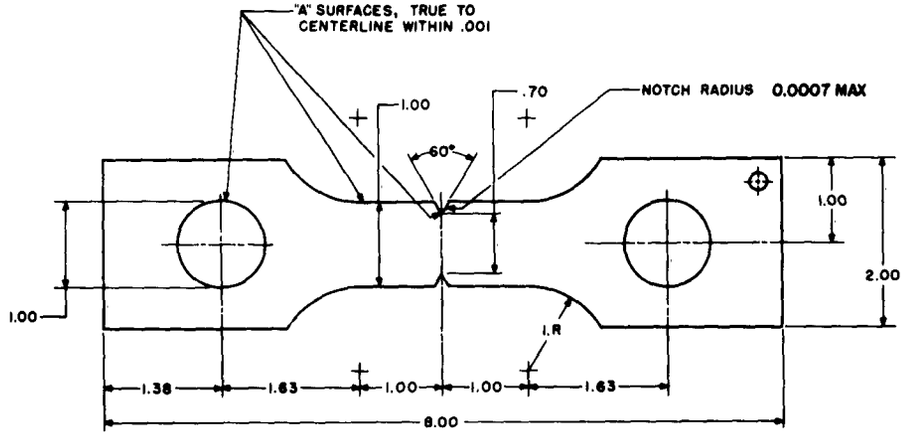


Fig. 3. Notched tensile strength and K_{IC} values of 4330V (Mod + Si) steel as a function of tempering temperature



NOTCH SPECIMEN

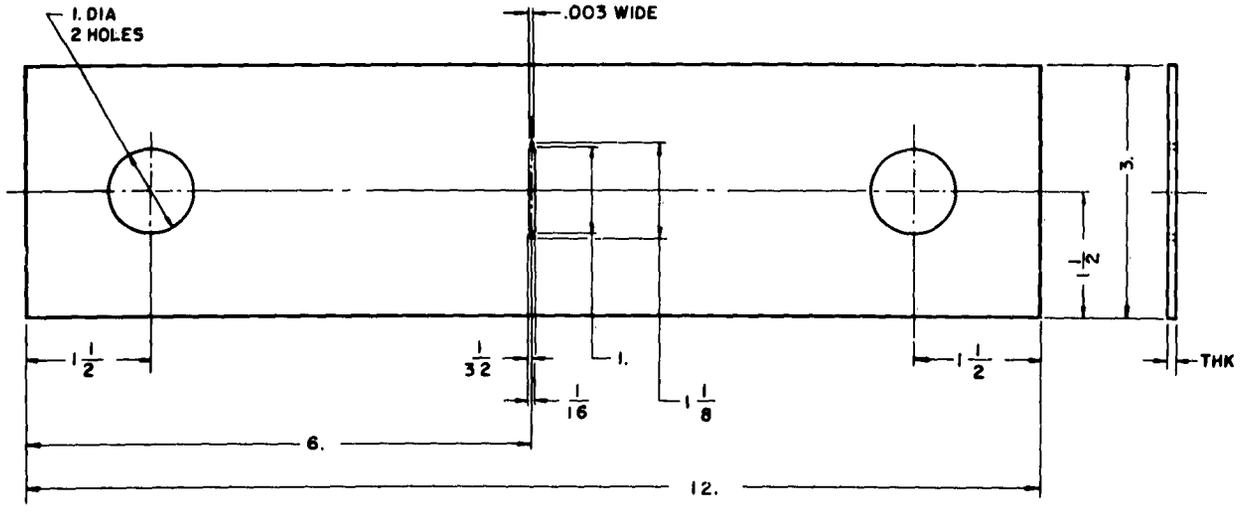


Fig. 4. Notched sheet tensile specimens

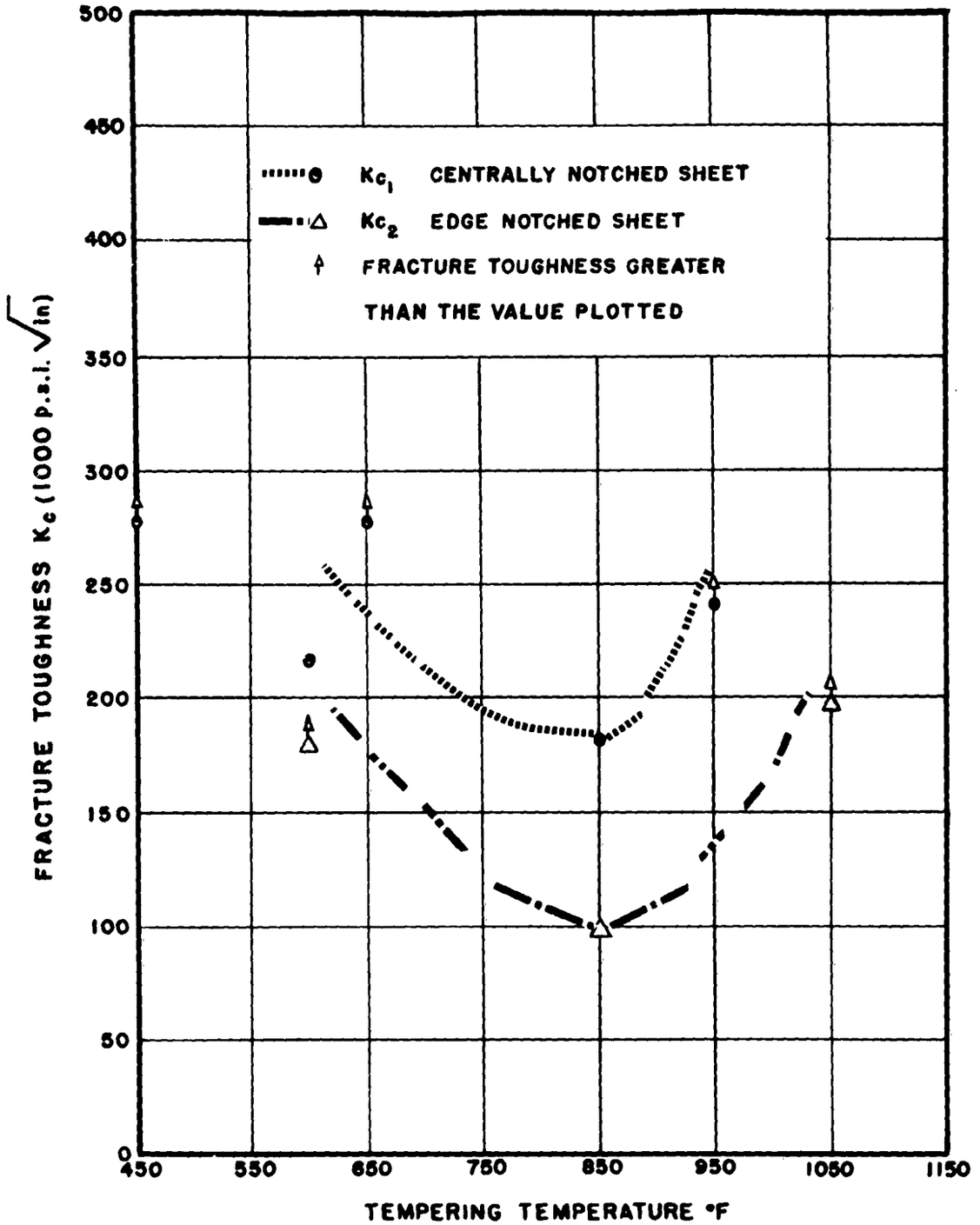


Fig. 5. Crack propagation fracture toughness values of 4330V (Mod + Si) steel as a function of tempering temperature

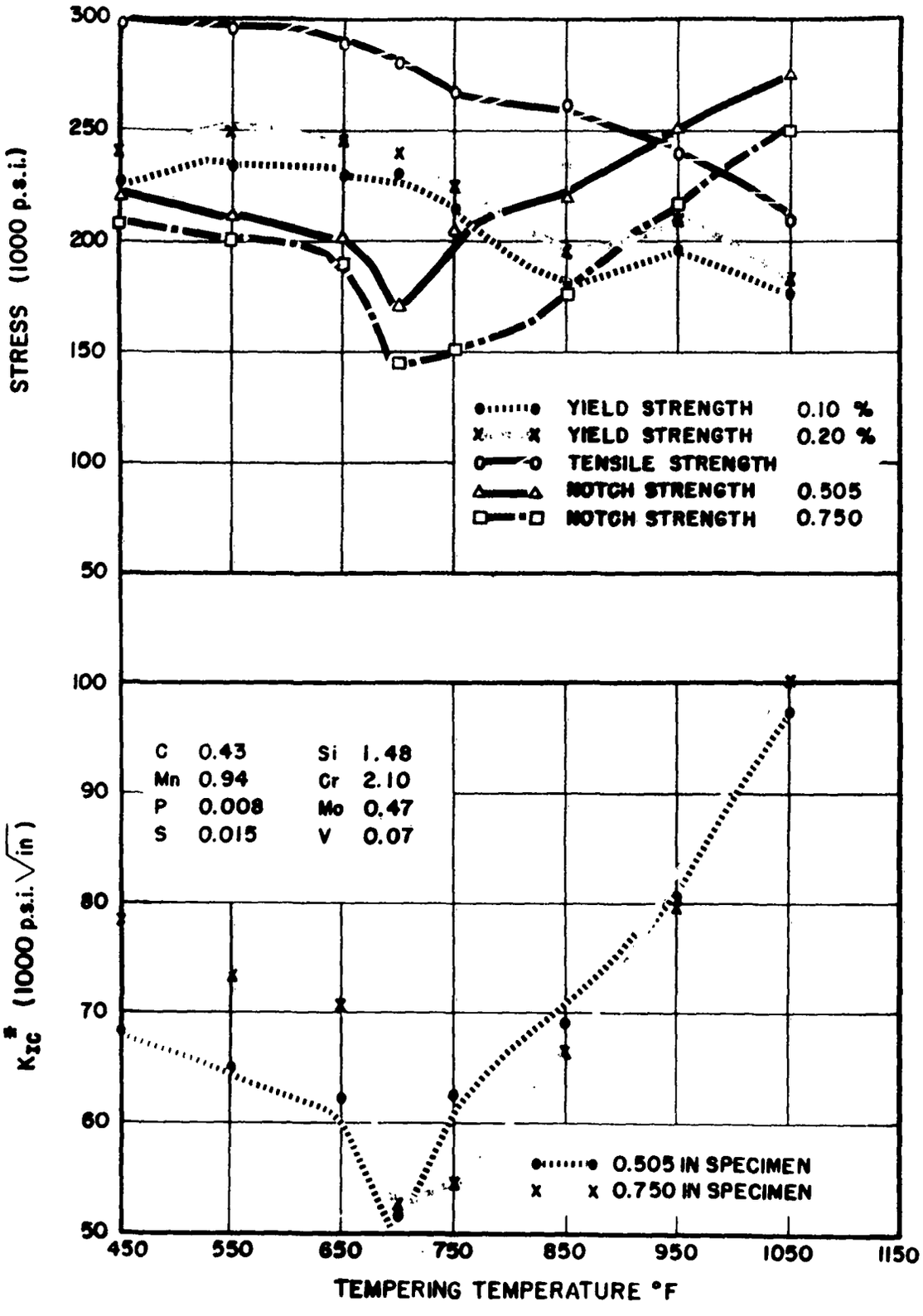


Fig. 6. Notched tensile strength and K_{IC} values of Airsteel X200 as a function of tempering temperature

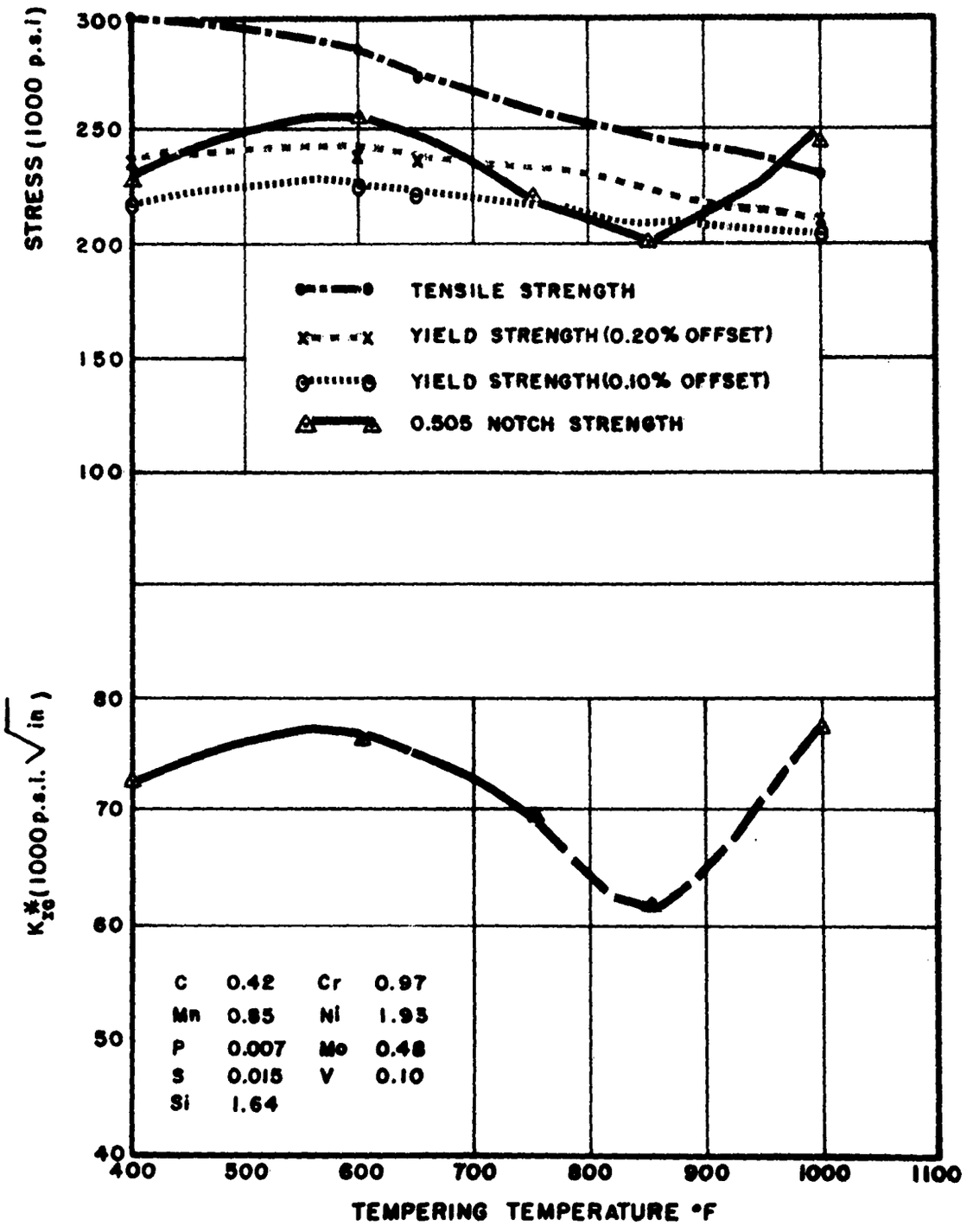


Fig. 7. Notched tensile strength and K_{IC} values of 300-M steel as a function of tempering temperature

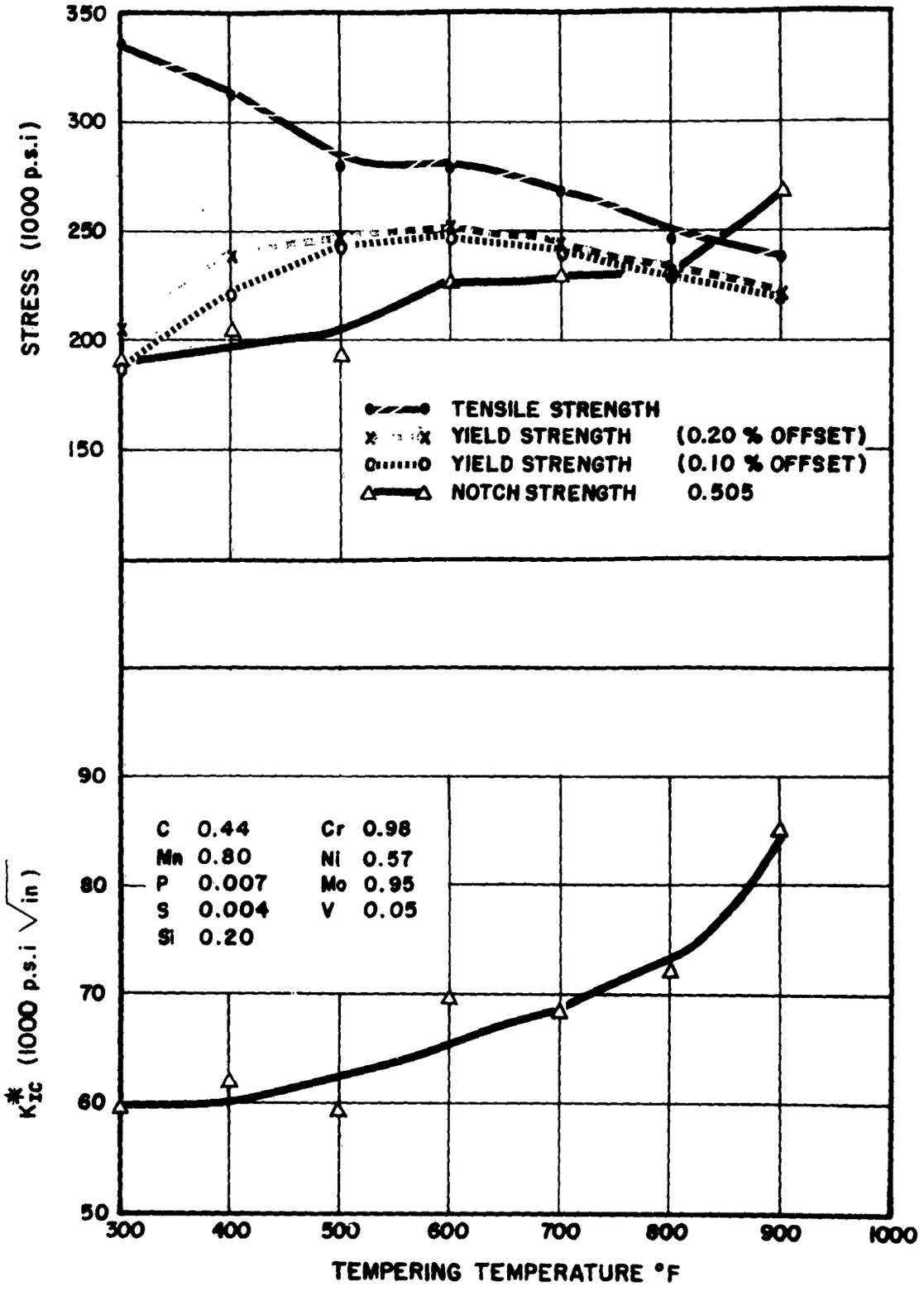


Fig. 8. Notched tensile strength and K_{IC} values of D6A steel as a function of tempering temperature

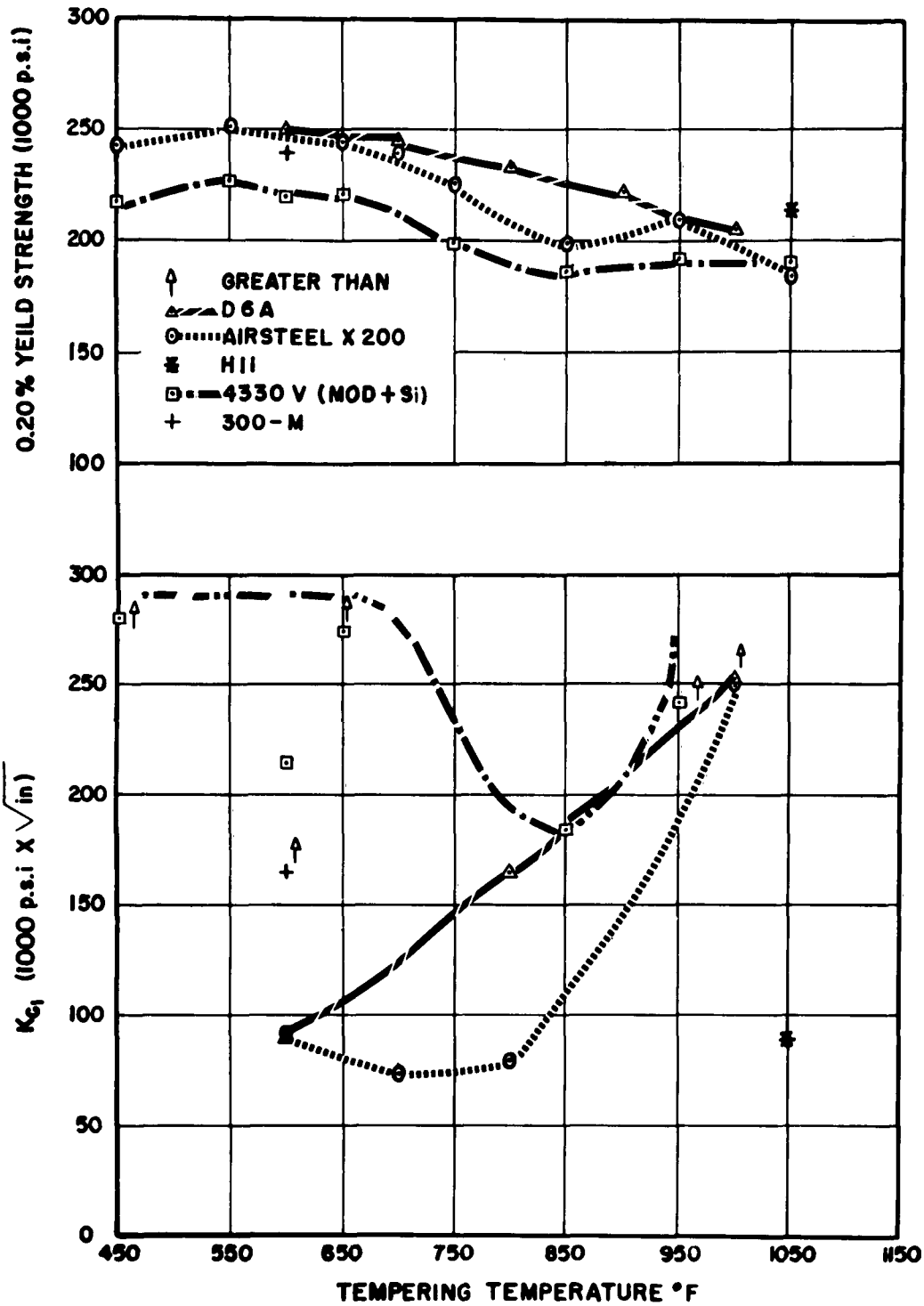


Fig. 9. Crack propagation fracture toughness values of 4330V (Mod + Si), D6A, Airsteel X200, H11, and 300-M steels as a function of tempering temperature

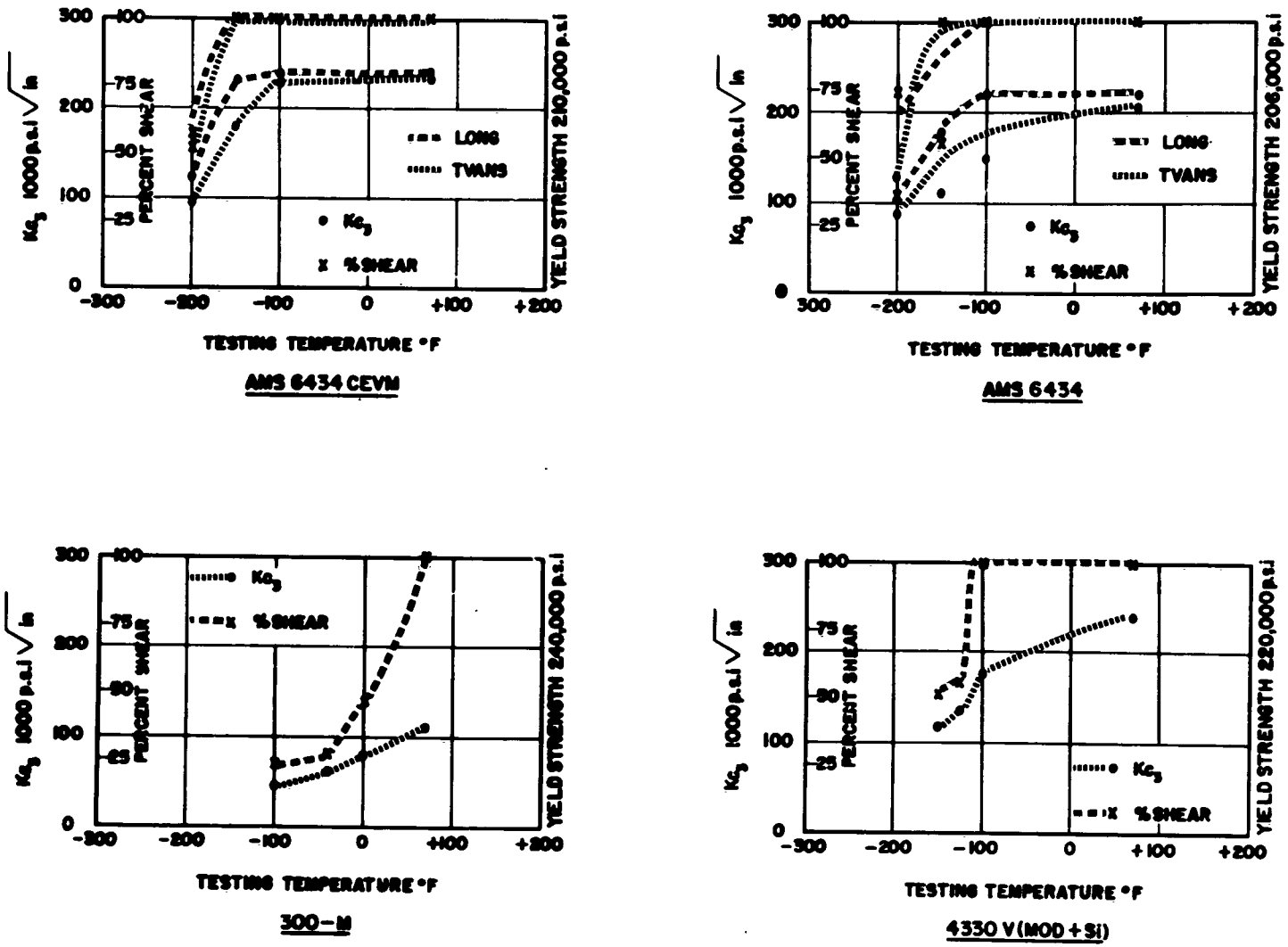


Fig. 10. Transition effects for 4330V (Mod + Si), 300-M, AMS6434, and AMS6434 CEVM steels



Fig. 11. Fracture test specimen of 4330V (Mod + Si) steel

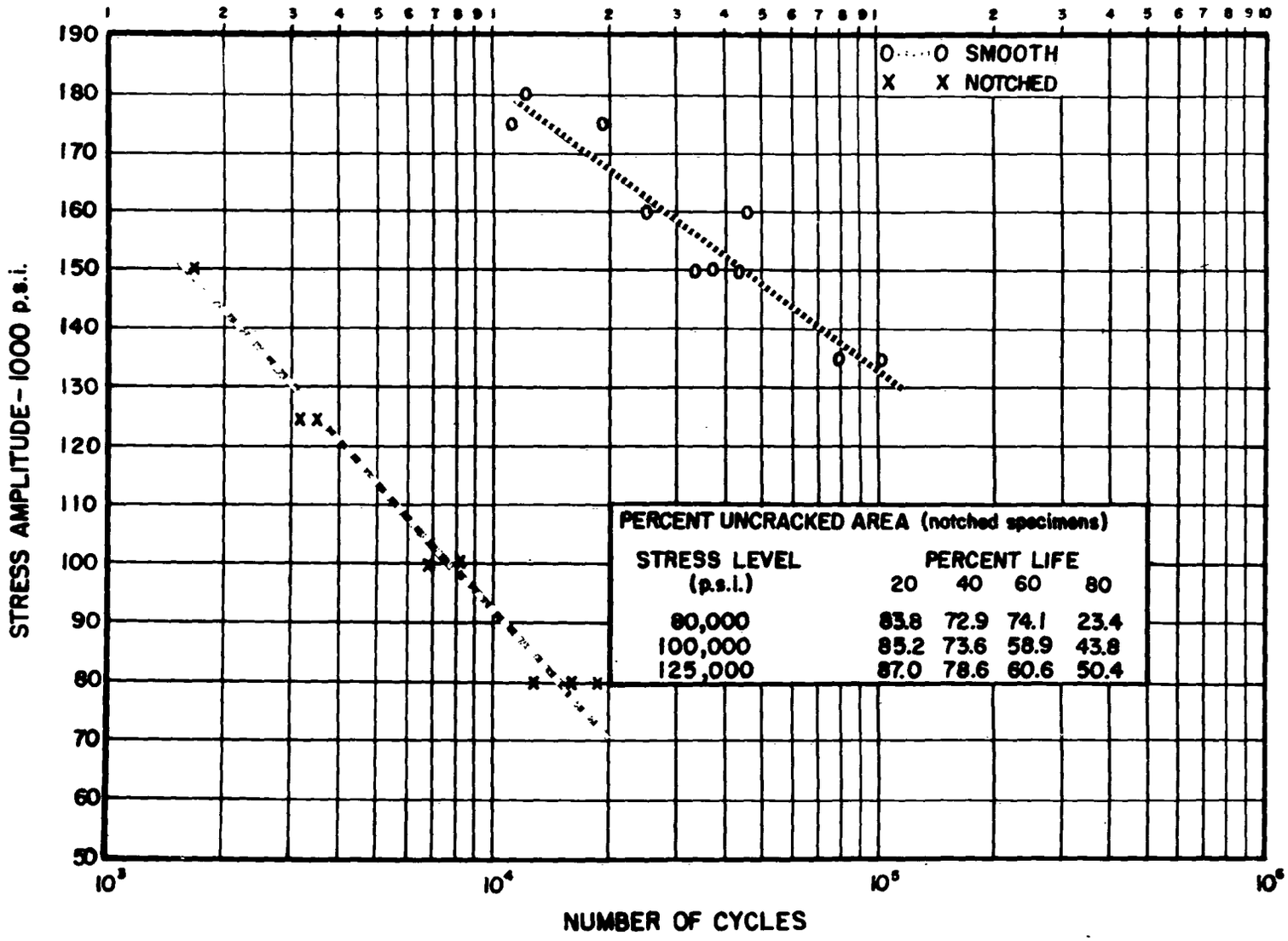


Fig. 12. Fatigue test results for 4330V (Mod + Si) steel

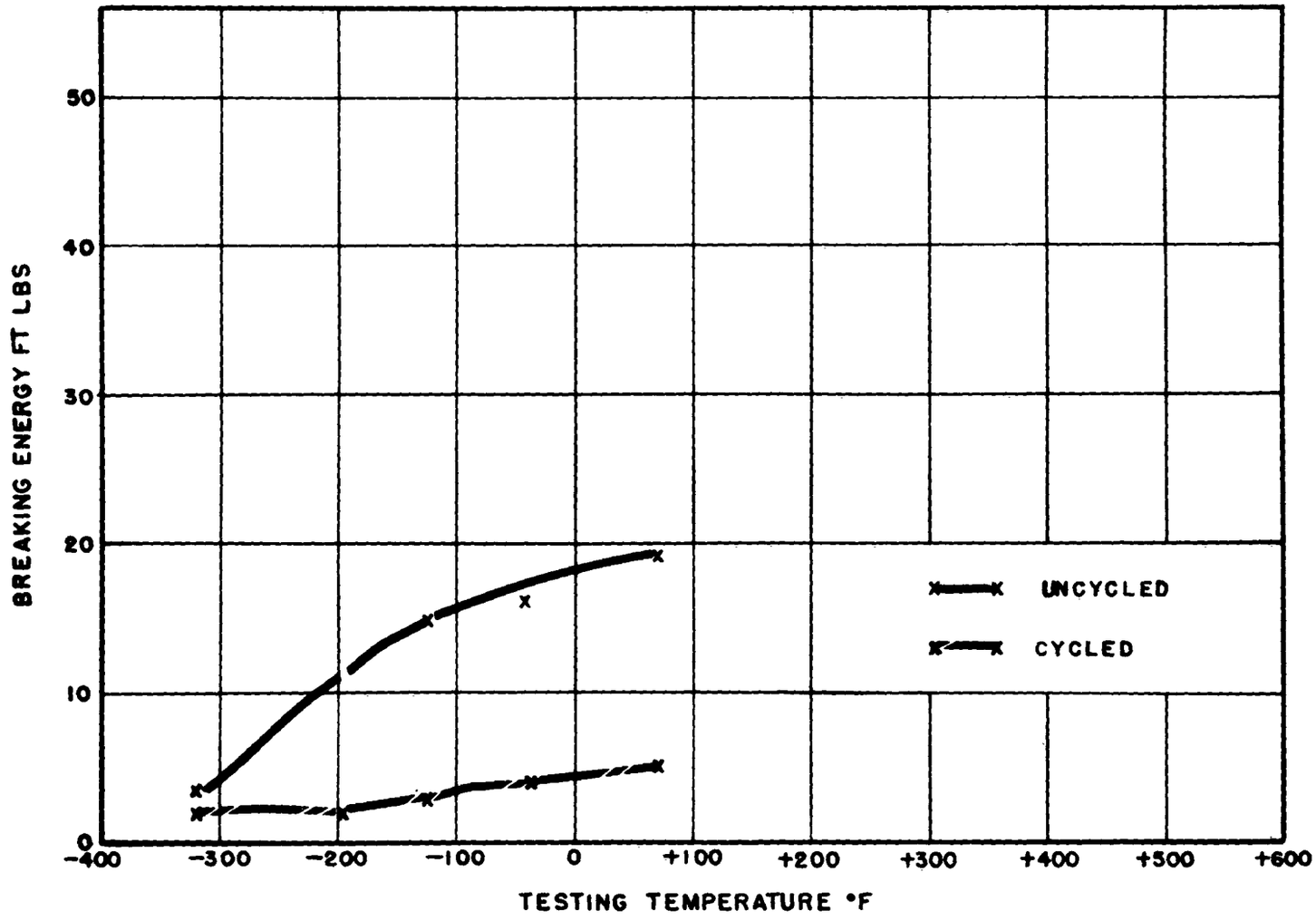


Fig. 13. Impact test results showing classic temper embrittlement of 4330V (Mod + Si) steel



Fig. 14. Structure in temper embrittled 4330V (Mod + Si) steel

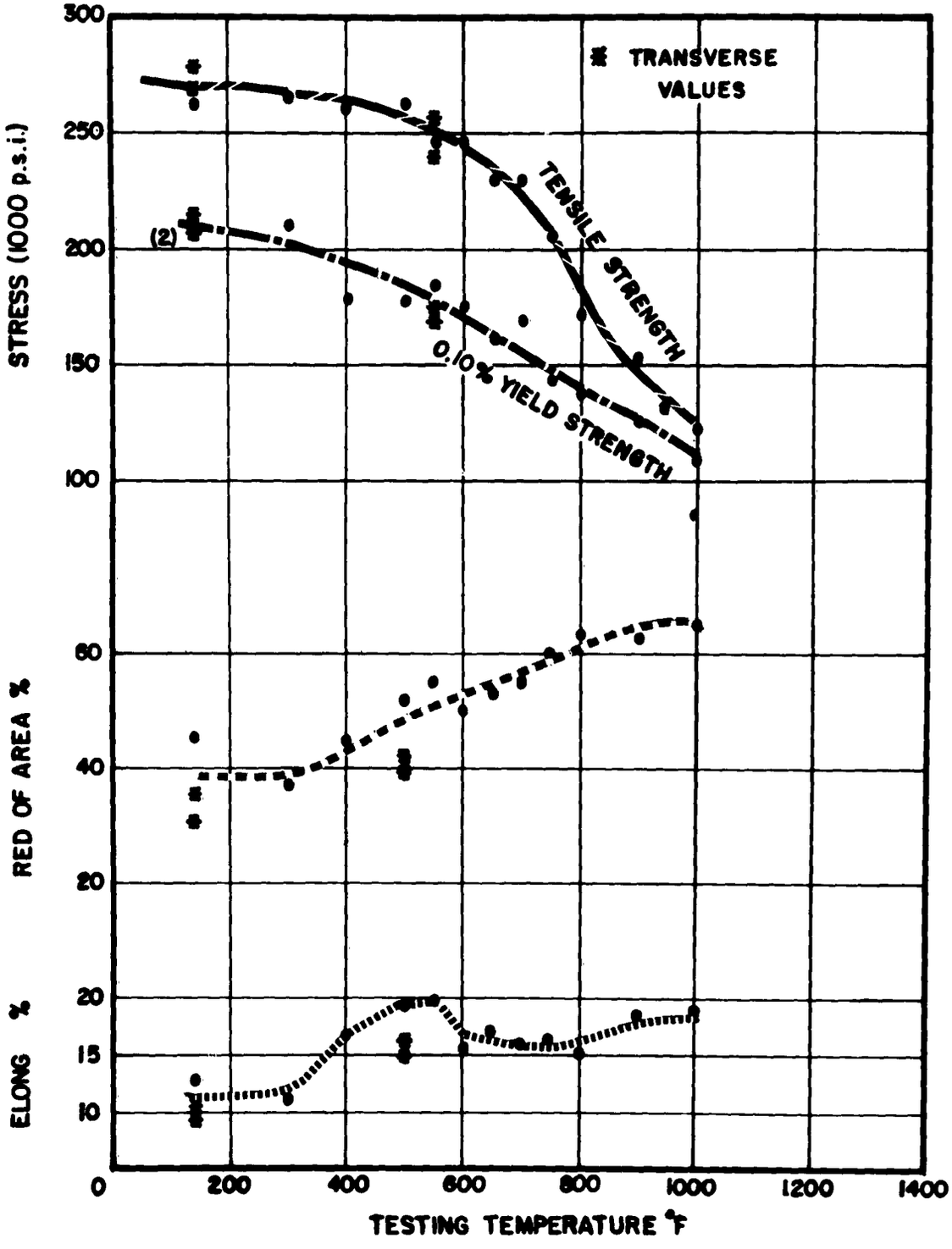


Fig. 15. Elevated temperature tensile properties of 4330V (Mod + Si) steel

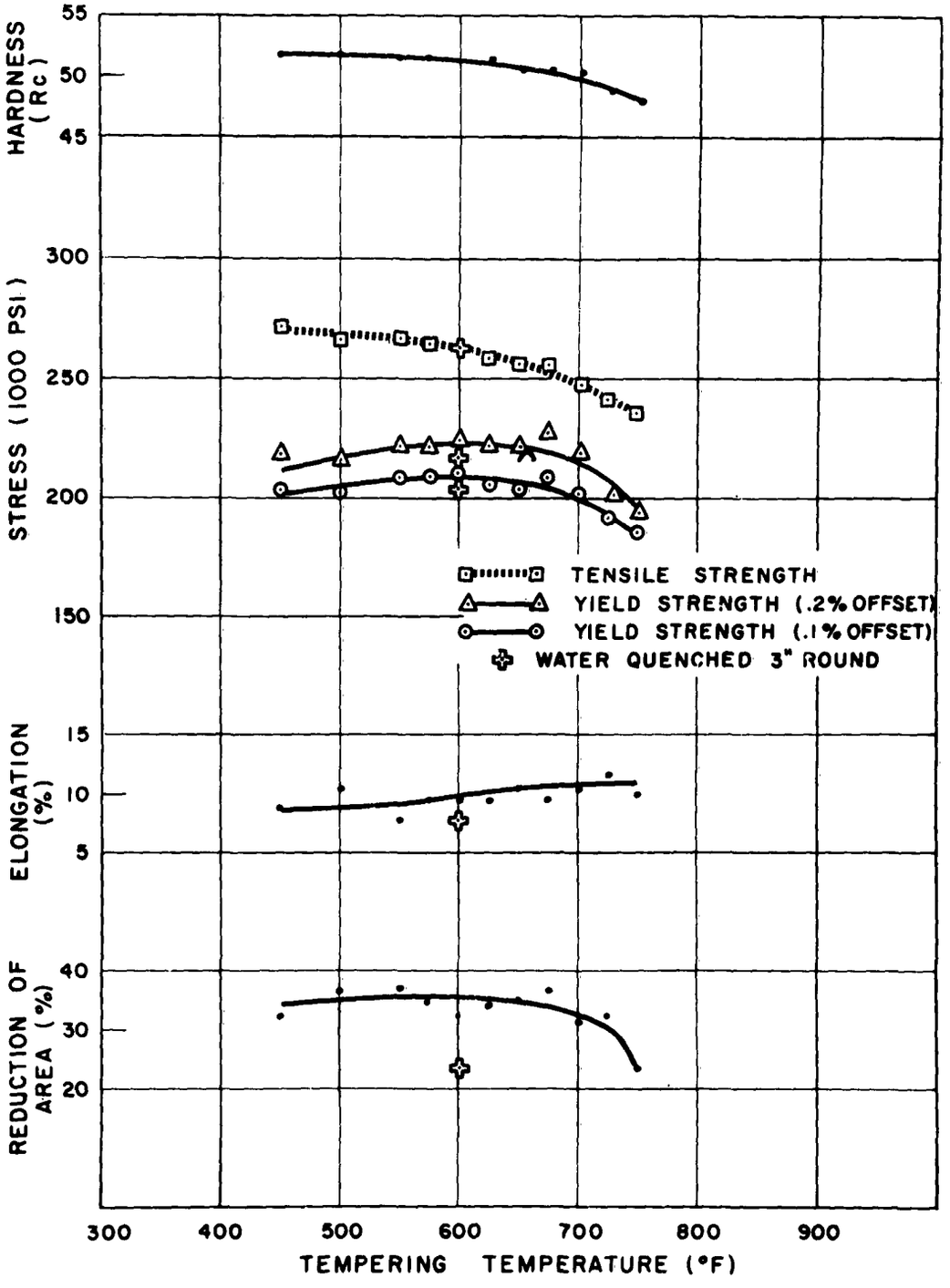


Fig. 16. Transverse tensile values for 4330V (Mod + Si) steel. Heat 21K631

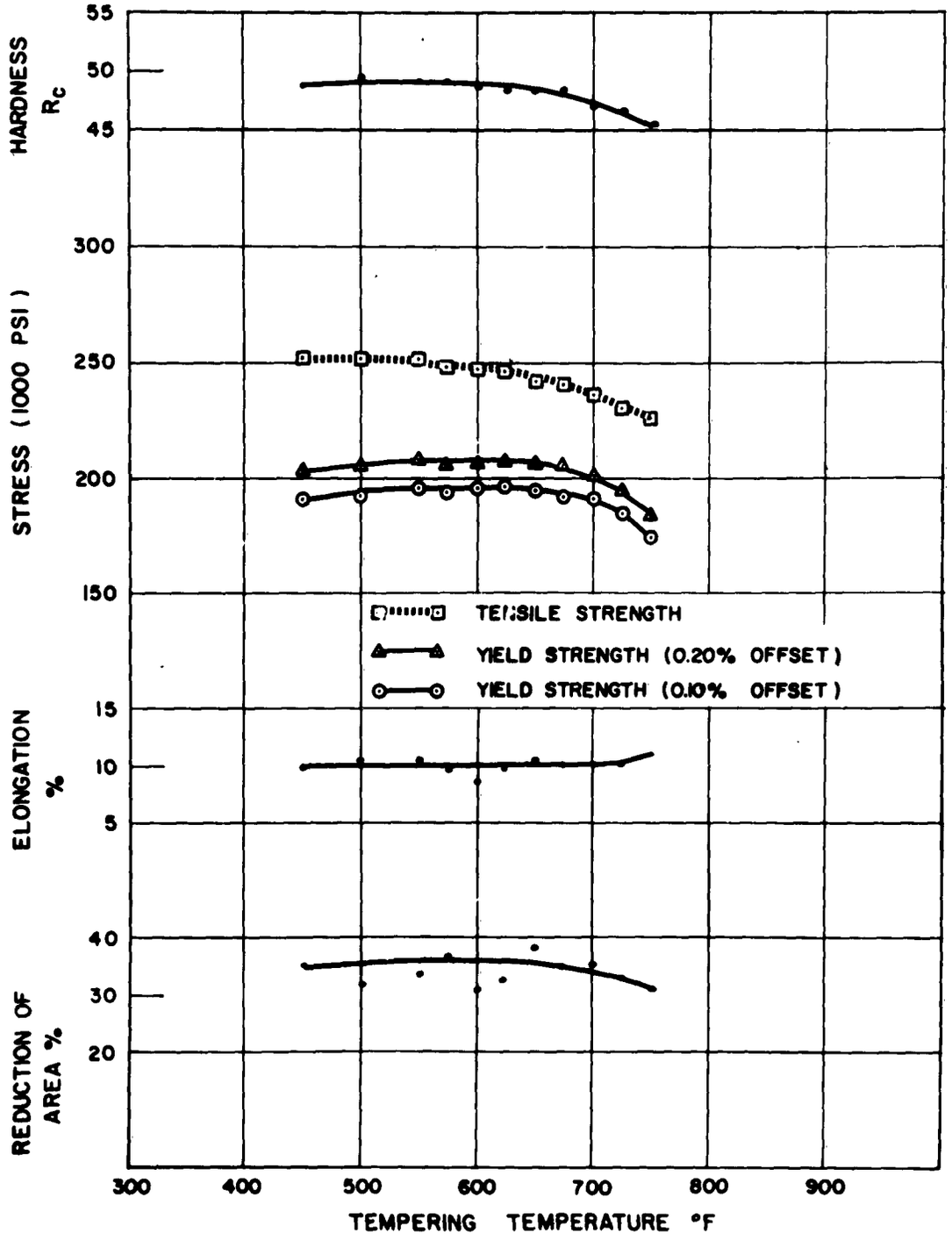


Fig. 17. Transverse tensile values for 4330V (Mod + Si) steel. Heat 211482

High Alloy Ferritic Steels for Rocket Casings

By R. C. Powell
Pratt and Whitney Aircraft
East Hartford, Conn.

The high alloy ferritic steels offer a number of advantages for use as high strength solid fuel rocket case materials. These include deep air-hardening capability, providing ease of heatreatment and minimizing distortion problems; a high tempering temperature, providing adequate stress-relief of welded assemblies; good weldability, without the necessity for special techniques such as preheating; and good machinability and flow-turning characteristics.

The first table shows the chemical composition of a number of high alloy ferritic steels which might be considered for high strength pressure vessels. H-11 is a 5% chromium hot work die steel with extreme deep hardening characteristics, which has been evaluated extensively as a missile case material. It will be noted that the carbon content of the H-11 weld wire is somewhat lower than the parent material, to minimize the problem of weld cracking. Unimach II is a more highly alloyed modification of H-11. Greek Ascoloy and Crucible 422 are modified 12% chromium stainless steels with excellent air hardenability, moderate corrosion resistance, and good weldability.

The next table shows typical tensile properties for these steels. The properties of H-11 are shown at two strength levels, approximately 220,000 psi and 240,000 psi yield strength, at which full-scale rocket cases have been fabricated. Unimach II, with somewhat higher carbon and alloy content, provides the possibility of somewhat higher properties, but the higher carbon will also tend to increase welding problems.

The modified 12% chromium martensitic stainless steels, with their lower carbon contents, have somewhat lower tensile properties than the 5% chromium steels. While they possess good over-all corrosion resistance, they are sensitive to stress-corrosion when tempered in the secondary hardening range. Therefore, for application in

corrosive environments, these alloys should be tempered below 700F, in which condition they have shown no evidence of stress-corrosion attack. The lower tempering temperature, however, limits strength levels to the bottom of the property ranges shown.

In the evaluation of steels at these high strength levels, considerable emphasis has been placed on notch toughness and notch-tensile testing. The notch-tensile strength of H-11 steel has been explored over a range of stress concentration factors, but the majority of our testing has been done using sheet specimens with a 0.022" notch radius (Kt=4) and 0.005" notch radius (Kt=8). The next figure shows a plot of smooth tensile properties versus notched tensile strength of H-11, as influenced by hardness. It will be observed that the notched tensile strength reaches a maximum of slightly over 200,000 psi at Rockwell "C" 48-52. Superimposed on this plot are points representing the realized bursting stresses for H-11 pressure vessels, both sub-scale and full-scale. (The squares represent short time burst tests on 9.4" diameter sub-scale pressure vessels, the triangles show sustained load sub-scale tests. The circles represent full-scale 40" diameter cases pressure tested to destruction, and the diamond a 40" x 70" full-scale case which was burst tested). It will be noted that the failure stresses are above the notched ultimate strength (at Kt=8) in all cases, and that the majority of the failures occurred at stress levels above the uniaxial smooth tensile strength. It is apparent that with sound processing, strengths considerably in excess of the theoretical notched tensile strength can be obtained. However, this depends on rigorous control of material quality, machining, and welding to avoid introducing notches, and proper heattreatment to minimize notch sensitivity. It might be mentioned that one of the full-scale cases was tested at -36F.

It has been demonstrated, by bend tests, impact tests, and burst tests on both sub-scale and full-size pressure vessels that surface decarburization has a definite

beneficial effect on both ductility and notch sensitivity of steels at high strength levels. The bend tests shown in the following figure were performed on H-11 steel, welded and unwelded, with 0.002-0.004" decarburization. A skin of partial decarburization controlled to a thickness of 0.002-0.008" can make the difference between ductile and brittle behavior in these steels. It is considered significant that an experimental full-scale 40" x 70" case containing decarburized flow-turning surface laps up to 0.006" deep, nevertheless sustained a wall stress of 269,000 psi before rupture. The next figure shows such a decarburized layer on H-11 steel. It should be noted that the decarburizing of the 5% chromium steels is somewhat more sluggish than of the lower alloy high strength steels, and this permits more precise control of the degree and depth of the partially decarburized layer.

In using steels at high strength levels, control of material quality, particularly cleanliness, is especially important. Large or concentrated non-metallic inclusions and segregation can have an adverse effect on fabrication. This is particularly true when flow-turning is used for generating cylindrical sections. In addition, large inclusions may act as stress-raisers in thin wall sections. For these reasons, the use of vacuum melted steel is considered mandatory for this application, at the high strength levels used. The next figure compares air-melted H-11 steel with the same composition produced by the vacuum consumable electrode melting process. Inclusions similar to those shown at the left, if critically located, could have an adverse effect on flow-turning quality, or on toughness.

Considerable experience has now been gained in the manufacture of full-scale H-11 steel solid fuel rocket cases, particularly at the 200,000-220,000 psi yield strength level. With careful processing, rigorous quality control, and heatreatment to produce a protective skin of decarburization, such cases can be made to withstand repeated pressurizing to levels well above the uniaxial yield strength, with bursting strengths approaching and beyond 300,000 psi. At this strength level, such cases still possess considerable ductility, as evidenced by the following figure. This

shows a 40" diameter, 0.068" wall full-scale rocket motor case which was burst at ambient temperature. Calculated wall stress at failure was approximately 305,000 psi. Note the bulging of the case, indicating considerable ductility under multi-axial stress. A higher strength levels the high alloy ferritic steels show a declining toughness and reduced notch strength; this same trend is shown by the lower alloy high strength steels. But even at the 240,000 psi yield strength level improved design and careful fabricating and heatreating practice permit the manufacture of pressure vessels which can withstand cyclic testing at stresses to the yield strength, and show high burst strength from 275,000 psi to over 300,000 psi.

In summary, it can be stated that the high alloy ferritic steels, particularly the 5% chromium hot work die steels, can be fabricated into pressure vessels capable of repeated loading to high stress levels, and showing extremely high burst strengths. In order to realize these properties, careful design and strict control of material quality, processing and inspection are required.

CHEMICAL COMPOSITION OF HIGH ALLOY FERRITIC STEELS FOR ROCKET CASINGS

	C	Si	Cr	Ni	Mo	W	V
H-11	.40	.90	5.00	—	1.30	—	.50
H-11 WELD WIRE	.34	.90	5.00	—	1.30	—	.50
UNIMACH II	.50	1.00	5.00	1.50	1.40	—	1.00
GREEK ASCOLOY	.18	.40	13.00	2.00	—	3.00	—
422	.23	.40	12.00	.90	1.00	1.00	.25

II-63

M-5207
8-2-60

PRATT & WHITNEY AIRCRAFT
DIVISION OF
UNITED AIRCRAFT CORPORATION

Fig. 1

TYPICAL TENSILE PROPERTIES OF HIGH ALLOY FERRITIC STEELS

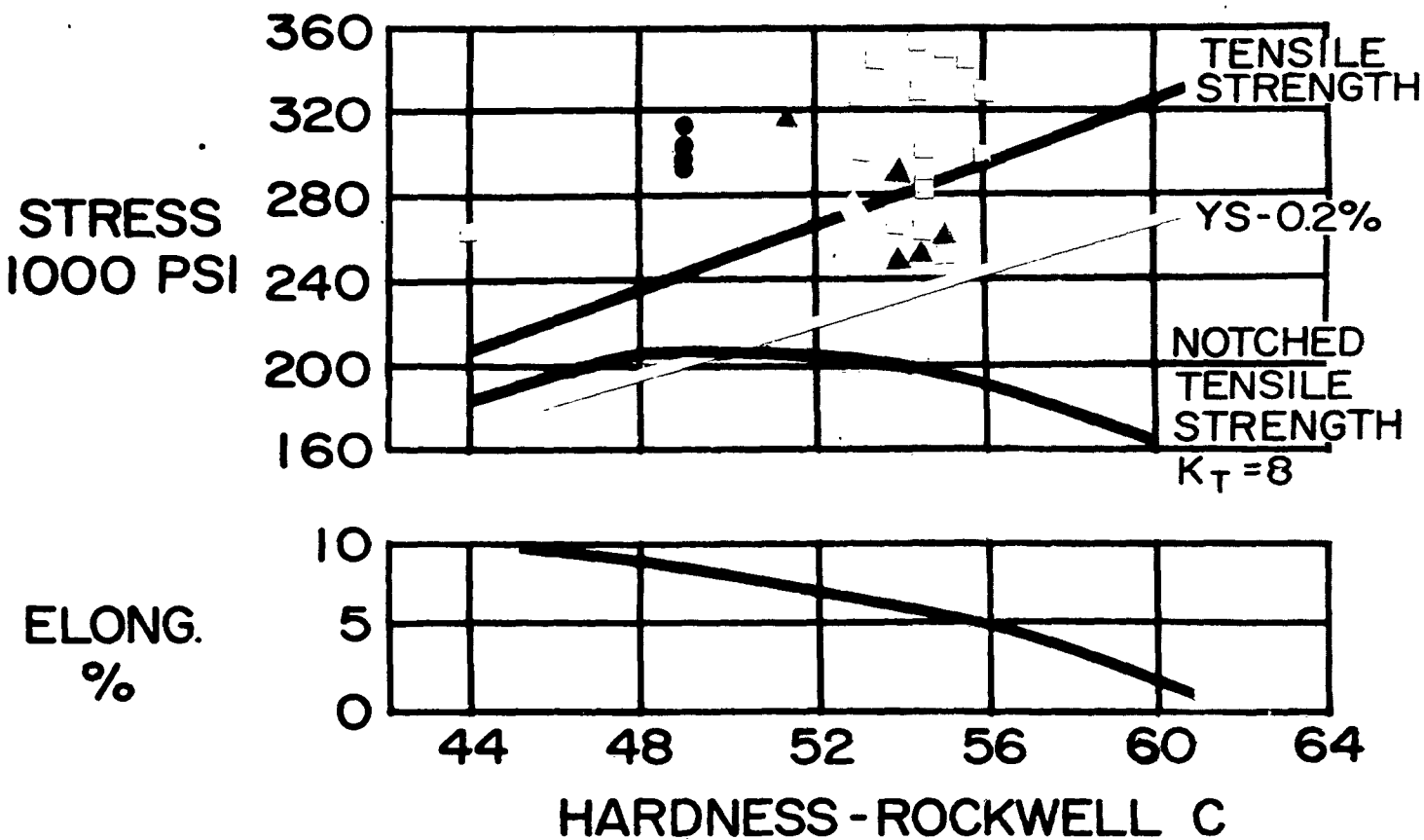
STEEL	TEMPERING TEMP.	HARDNESS RC	U.T.S. PSI x 10^{-3}	Y.S.(0.2%) PSI x 10^{-3}	ELON. %
H-11	1050-1100 F	46-50	235-260	210-225	6-9
H-11	1000-1050 F	50-54	260-310	225-245	5-7
UNIMACH II	1000-1050 F	52-58	270-320	230-250	4-8
GREEK ASCOLOY	650-900 F	44-46	200-225	165-185	9-12
422	600-900 F	46-49	245-280	170-210	4-6

M-5208
8-2-60

PRATT & WHITNEY AIRCRAFT
DIVISION OF
UNITED AIRCRAFT CORPORATION

Fig. 2

BURST STRENGTH OF H-11 PRESSURE VESSELS AND TENSILE PROPERTIES AT VARIOUS HARDNESS LEVELS



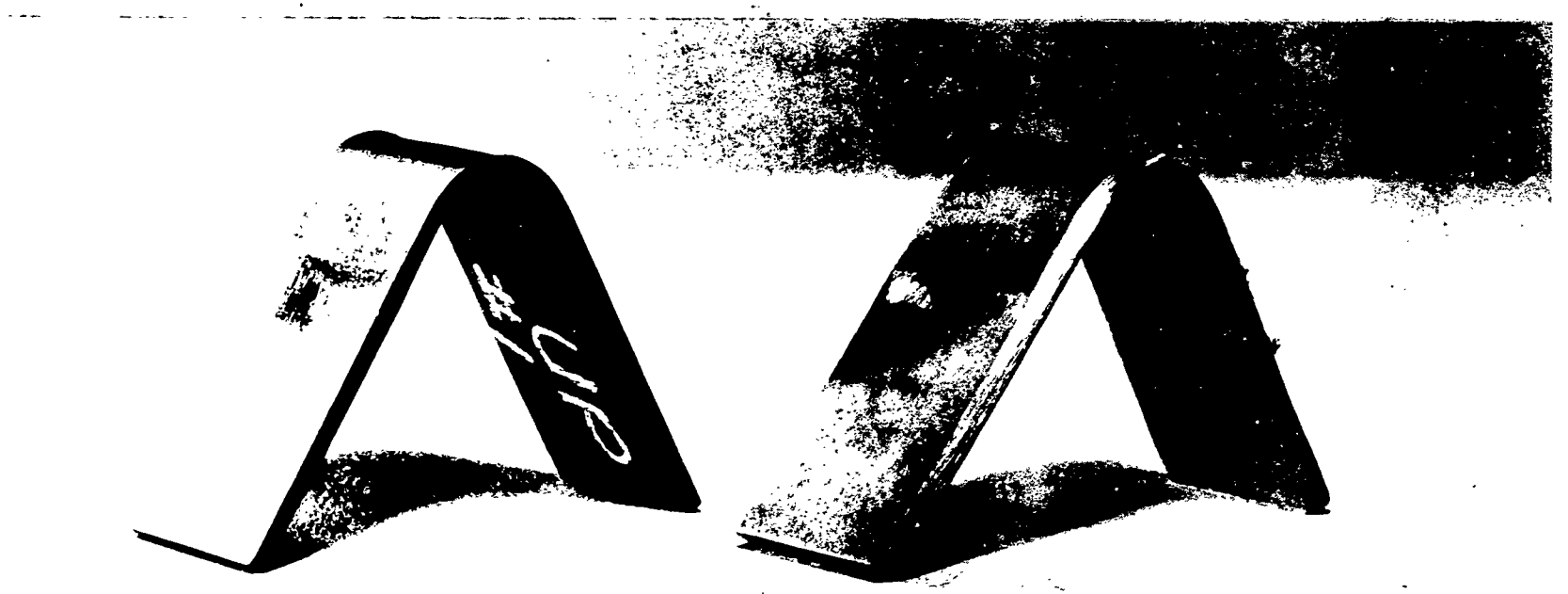
PRATT & WHITNEY AIRCRAFT
DIVISION OF
UNITED AIRCRAFT CORPORATION

M-5209
8-2-60

II-65

Fig. 3

H-11 STEEL HARDENED TO R_c 48-50 BENT OVER 10 T DIAMETER THROUGH 105°



WELDED SPECIMEN PARENT METAL

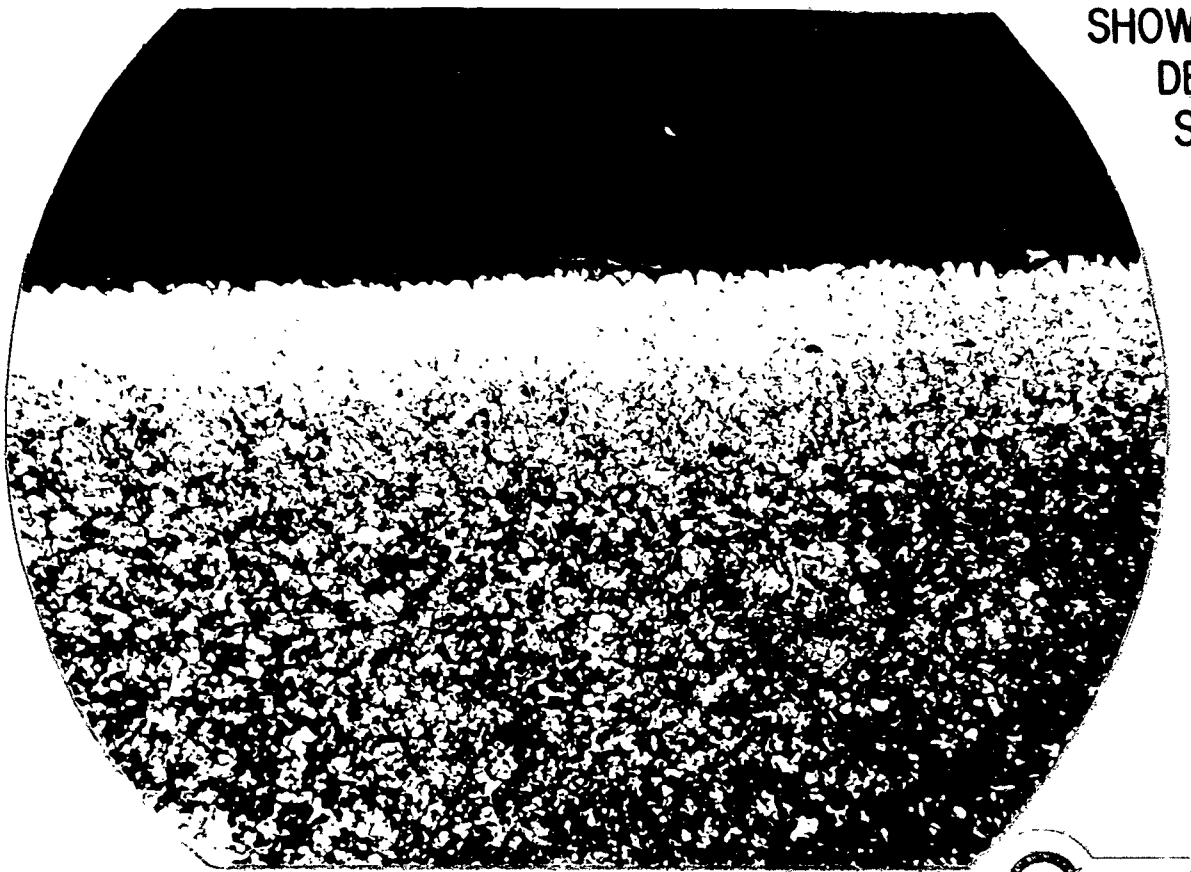
M-5210
8-2-60

PRATT & WHITNEY AIRCRAFT
DIVISION OF
UNITED AIRCRAFT CORPORATION

Fig. 4

MICROSTRUCTURE OF HARDENED & TEMPERED H-11 STEEL PRESSURE VESSEL

SHOWING PARTIALLY DECARBURIZED SURFACE LAYER 0.003" DEEP



M-2638
6-4-60 REV

PRATT & WHITNEY AIRCRAFT
DIVISION OF
UNITED AIRCRAFT CORPORATION

Fig 5

H-11 STEEL
VACUUM CONSUMABLE
ELECTRODE MELTED
ASTM INCLUSION
RATING:
LESS THAN A1

H-11 STEEL
AIR MELTED
ASTM INCLUSION
RATING:
A2 - A3
PRATT & WHITNEY AIRCRAFT
DIVISION OF
UNITED AIRCRAFT CORPORATION

Fig. 6

FULL-SCALE
H-11 STEEL
ROCKET MOTOR
CASE

SHOWING
APPEARANCE
AFTER BURST TEST

PRATT & WHITNEY AIRCRAFT
DIVISION OF
UNITED AIRCRAFT CORPORATION

M-5205
8-2-65

Fig. 7

TITANIUM ALLOYS FOR SOLID ROCKET CASINGS

by W. H. Sharp
Pratt & Whitney Aircraft, East Hartford, Conn.

The two titanium alloys under consideration for solid fuel rocket motor cases are the 6Al - 4V and Beta (B-120 VCA) alloys. By reason of extensive experience with 6-4 in aircraft and aircraft engines, one could call it the 4340 of titanium alloys available today. It can be readily forged; in the solution treated, quenched and aged condition 6-4 develops tensile minima of YS 155,000, TS 170,000 and elongation 5%. Fusion welding is best accomplished employing commercially pure titanium filler under inert gas. Looking for a modest gain in strength/weight over today's alloy steel rocket casings, the 6Al - 4V alloy is a good choice. Certainly if high fracture toughness at high strength/weight ratios were the sole criterion, 6-4 would take precedence over the steels. 6-4 is a good engineering material, and we have endorsed it by using it widely in aircraft engines.

In looking for a material with substantially higher strength/density values than the more optimistic values for steels, we decided upon VCA (Beta) titanium alloy containing 13V - 11Cr - 3Al as having great potential. Certainly after having made and tested all manner of forgings, rolled rings, subscale pressure vessels and, finally, after having made several full scale rocket motor cases, we are ever more hopeful about its potential.

VCA, at this stage of development, is more difficult to forge than 6-4. VCA forgings heatreated to high strength levels can be expected to machine somewhat more difficultly than the lower strength 6-4. Welding of VCA is not easy but one must bear in mind that it took some years to come up with dependable fusion welds in 6-4. With respect to cold flow (flow turning or shear spinning), the beta alloy, as was anticipated, appears to be far better than the alpha-beta alloy. At present VCA cylinders can be generated by cold reductions of 40% without intermediate annealing whereas 6-4 does not appear to respond to cold flow turning. 6-4 cylinders will have to be machined from oversize hot rolled cylinders unless flow turning at elevated temperatures or flow turning solution treated material becomes practicable.

Looking at some of the mechanical properties of VCA components targeted for yield strength levels of 180,000 psi minimum affords a good picture of progress made thus far:

Figure 1 shows the tensile properties of the front closure from the first VCA full scale motor case. This forging was made by Wyman Gordon Company. They upset 14 in. diameter x 35 in. high billet into biscuits 5 in. thick at a temperature range of 1700 - 1800 F. Biscuits were then heated to approximately 1400 F and further upset to a 54 in. diameter x 1-1/2 - 2 in. thick pancake. After rough machining to remove forging scale, the pancake was heated to 1300 - 1400 F and hydraulically pushed through a draw ring by a punch with a contour of the front end closure. As may be seen, the warm work in the 1300 to 1400 F range has caused a favorable response to the subsequent aging at 900 F for 60 hours. The aging times at 900 F for warm

worked forgings have varied from 11 to 60 hours. We have noted a reduction of strength of 15,000 psi at the polar location of the forgings, and have recently learned that the effect is principally due to segregation.

Properties of the rear closure (Figure 2) used in the first 2nd stage case show a somewhat higher level of properties than obtained in the front closure. The explanation for the 10,000 psi higher yield strength lies in aging time of 30 hours. Material was from the same source, the same heat; the forging was made by the same technique as the front and was aged at 900 F. It is observations of this sort which will permit us to exercise the control over VCA required for high strength rocket casings.

Figure 3 gives the properties obtained in the flow turned cylindrical section from the first 2nd stage rocket case. The cylinder was made as follows:

The Ladish Company upset 14 in. billet at 1850 F. The center of the upset was punched out to form a doughnut; the doughnut was heated to 1850 F and rolled into a 40 in. diameter cylinder approximately 15 inches in length. The rolled ring was finish machined to a 39 in. plus diameter 12 in. long flow turning blank which was flow turned at room temperature in two flow turning passes, of about 40% reduction each, to a 22 in. long cylinder of the same diameter. Between flow turning passes there was an anneal at 1325 - 1400 F for 15 minutes. The flow turned cylinder was given an abbreviated aging cycle of 850 F for 30 minutes, considerably less than the warm worked forgings by reason of the vastly greater response of cold worked VCA to aging. In Figure 3 note the directionality present in the cylinder caused by flow turning: Strength in the circumferential direction is of the order of 10,000 psi higher than in the axial direction, a characteristic which is not undesirable inasmuch as the ratio of circumferential (or hoop) stresses to axial stresses are of the order of 2:1 in rocket cylinders. We have noted similar directionality effects in flow turned and aged steels of the precipitation hardening types such as AM 350 and 17-7PH.

As is well known, the fracture toughness of a material -- the resistance to fracture that a material exhibits in the presence of a defect or crack -- has become an important consideration in the rating of steels and titanium alloys. In studying the fracture toughness of 6Al - 4V and VCA, H. E. Romine of the U.S. Naval Weapons Laboratory has reported (in Technical Memorandum T-14/60) 6-4 at a yield strength level of 150,000 psi to have a G_c value of about 1200 for the base metal and 650 - 700 for the weld (no filler metal was used). VCA heatreated to a yield strength of 200,000 psi, gave G_c values of 170 for the base metal; the weld zone gave average values of 124. Both 6-4 and VCA test panels were submitted by the same source and heatreated and welded (by the TIG method) under comparable conditions.

Through the courtesy of Dr. Romine we have recently obtained Gc values from the first full scale rocket motor case. Values on circumferential specimens from the cylinder were 625 and 681. Welds, produced with VCA filler, gave values of 177 - 252 inch pounds/inch^2. Figure 4 shows the specimens from which G_c values for base metal and welds were obtained. Although it is not quite cricket to draw favorable conclusions from a comparison of G_c values on 200,000 psi material as opposed to 180,000 psi (for the cylinder), it certainly is valid to say that the fracture toughness of the full scale case at 180,000 psi appears adequate inasmuch as the critical crack length tolerance for .080 inch thick

material is 2.1 - 2.4T. The fracture toughness values for the welds, on the other hand, would suggest that further development of welding technique is needed. The relative lack of shear in fast fractures through VCA welds argues for an improvement. VCA welds tend to be coarse grained and to show grain boundary precipitate. Under the OMRO development program, we hope to ameliorate these two conditions to provide welds of higher strength and toughness.

Comparing the circumferential uniaxial yield strength of 180,000 psi of the first case with the 0.2% biaxial yield strength of 200,000 psi shows that biaxial loading confers an 11% increase. Based upon our experience with VCA pressure vessels, the 11% is just above the kick-up range of 8 - 10% for yield strength and 11 - 13% for ultimate strength. This is in the same league as the biaxial kick-up found in 6-4. The inherent 15 - 25% superior strength of VCA (the density differences taken into account) over 6-4, coupled with an equal biaxial kick-up, makes for an attractive material.

The burst strength values of pressure vessels plotted against chronological vessel number (Figure 5) emphasize that burst strengths well in excess of 200,000 psi are definitely attainable.

In conclusion, the successful manufacture and pressure testing of a full scale rocket case demonstrates the great potential of VCA as a material.

TENSILE PROPERTIES (70F) OF FRONT CLOSURE

SPECIMEN	DIRECTION	LOCATION	U.T.S.	Y.S. (0.2%)	Y.S. (0.02%)	%El.
FC-A	TANGENTIAL	BETWEEN IGNITER & THRUST REVERSAL BOSSES	197.2 KSI	183.2 KSI	139.0 KSI	5.0
FC-B	"	"	193.4	185.8	162.8	5.0
FC-D	"	"	187.4	181.2	165.8	5.0
FC-H	"	BETWEEN THRUST REVERSAL BOSS AND SKIRT	192.7	185.6	164.8	6.0
FC-L	"	"	190.8	181.6	165.0	5.0
FC-6	RADIAL	"	193.8	183.0	163.0	7.0

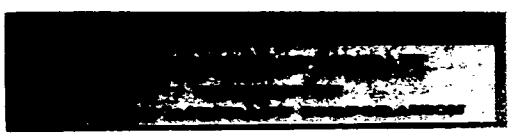


Fig. 1

TENSILE PROPERTIES (70F) OF REAR CLOSURE

SPECIMEN	DIRECTION	LOCATION	U.T.S	Y.S.(0.2%)	Y.S.(0.02%)	%El.
RC 4	RADIAL	MIDWAY BETWEEN FLANGE AND SKIRT	208.2 KSI	193.5 KSI	165.0 KSI	5.0
RC 5	"	"	208.2	196.5	172.9	5.0
RC 6			209.2	194.9	175.0	6.5
RC 8	"	"	206.0	188.8	153.5	6.0
RC-B	TANGENTIAL	ADJACENT TO FLANGE	204.5	193.0	175.0	6.0



[redacted]

Fig. 2

TENSILE PROPERTIES (70F) OF CYLINDER SECTION

SPECIMEN	DIRECTION	LOCATION	U.T.S	Y.S.(0.2%)	Y.S.(0.02%)	%El.
C-1	CIRCUMFERENTIAL	FRONT	188.0 KSI	181.2 KSI	151.5 KSI	4.0
C-5	"	CENTER	195.8	183.0	153.2	5.0
C-13	"	REAR	195.5	188.5	163.5	6.0
AF-1	AXIAL	FRONT	185.2	176.5	157.6	8.0
AC-1	"	CENTER	185.2	174.6	150.2	7.5

PRATT & WHITNEY AIRCRAFT
DIVISION OF
UNITED AIRCRAFT CORPORATION

Fig. 3

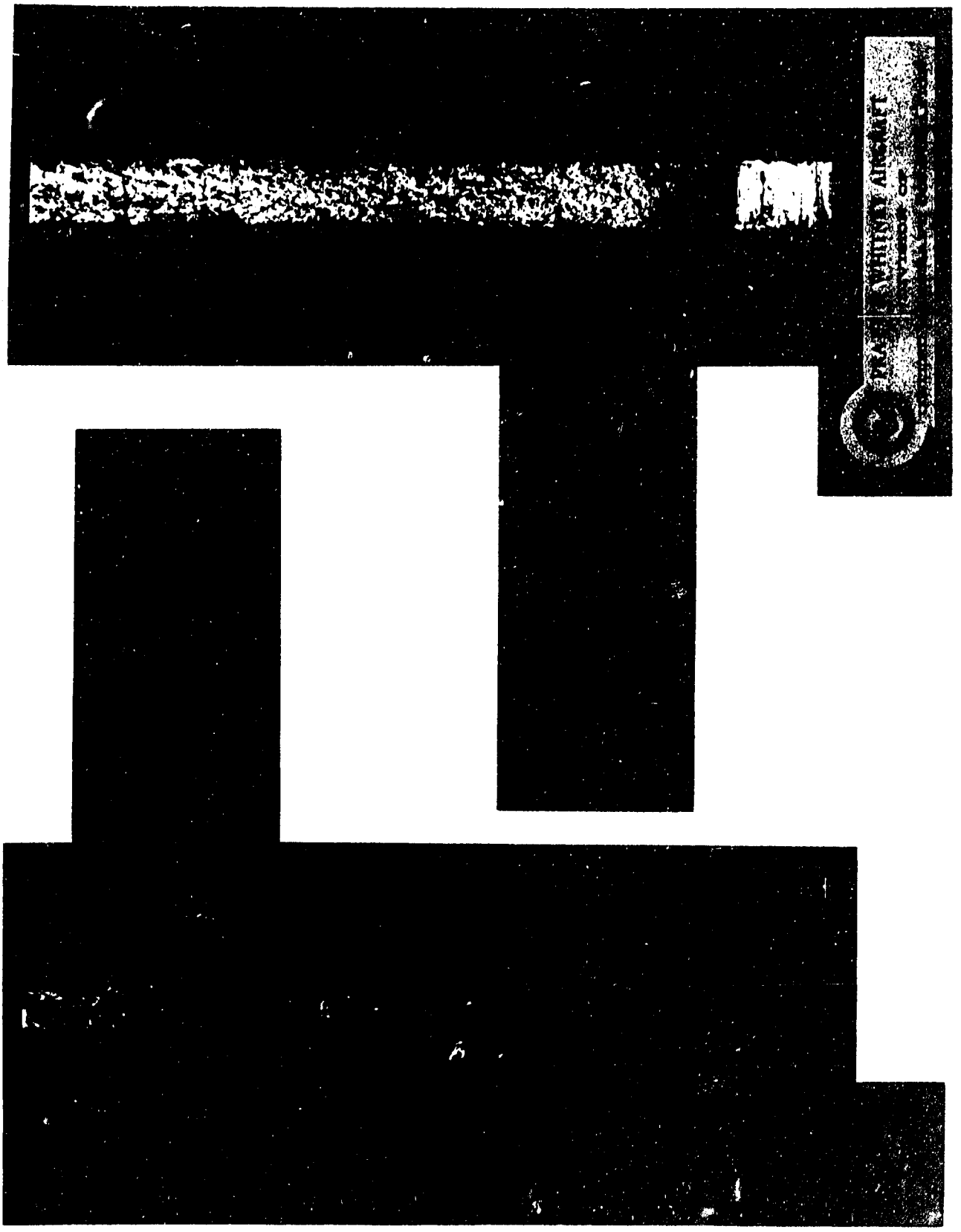


Fig. 4

BURST STRESSES

SUBSCALE PRESSURE VESSELS OF VCA TITANIUM ALLOY

Fig. 5

COLD ROLLED STAINLESS STEEL

J. F. Watson
J. L. Christian

Convair-Astronautics
Division of General Dynamics Corp.

The cold-rolled austenitic stainless steels have assumed an important position in missile and space vehicle applications where they are used as skins and other highly stressed structural members at temperatures ranging down to -423°F (the boiling point of hydrogen). In the cold-rolled condition, this alloy class exhibits an outstanding combination of properties which suits it for structural application in missiles and space vehicles utilizing cryogenic propellants. The critical nature of structural weight and pressure integrity in pressurized cryogenic propellant tanks requires a material having an optimum combination of high strength/density ratio, weldability, and resistance to brittle fracture of cryogenic temperatures, as well as adequate formability and corrosion resistance. The AISI type 300 series austenitic stainless steels are used for this type of application due to their excellent weldability and toughness at low temperature and their moderately high strength/density ratios which improve markedly at lower temperatures.

The use of cold work to improve the tensile strengths of the AISI type 300 series stainless steels has been described by Krivobok (1), Krivobok and Talbot (2), and Krivobok and Lincoln (3), This improvement in properties resulting from cold work is due to two effects; the strain hardening induced in the austenite lattice by cold rolling, and the strain-induced transformation of austenite to the harder martensite phase. The first of these effects is approximately the same in all of the 300 series stainless steels; i.e., equivalent amounts of cold reduction will result in approximately the same amount of strain-induced strengthening of the austenite. The second of these effects, strain-induced transformation of austenite to martensite, differs widely between the various alloys of the 300 series, and exhibits its greatest effect in the least stable steels (4) (5). Stability (i.e., resistance to transformation) is a function of chemistry, temperature, tensile stress, and prior lattice strain (6) (7) (8) (9) (10). Nickel is the major austenite stabilizing element in the grade of stainless steel, as evidenced by the relatively low stability exhibited by type 301 which contains 7 percent nickel and the high stability of type 310 containing 20 percent nickel. The other alloys of this class, such as the 302 and 304 ELC reported herein, fall between these two extremes because of their intermediate nickel contents (about 8 percent). Second-order effects of chemistry on austenite stability are due to variations in the interstitial carbon and nitrogen contents of the various alloys because these elements

also act as austenite stabilizers. The effect of chemistry on the M_s temperature for this grade of steel has been reported by Eichelman and Hull (11) as follows:

$$M_s\ (°F) = 75(14.6 - Cr\ wt\ \%) + 110(8.9 - Ni) + 60(1.33\ 0\ Mn) + 50(0.47 - Si) + 3000\ (C.068 - C + N)$$

Low temperatures and high tensile stresses are also known to promote the transformation of austenite to martensite (12)(13), and thus the low temperature tensile tests performed in this investigation favored this reaction for all alloys and tempers studied. For any given alloy, the cold rolled tempers generally exhibit greater stability than the annealed temper because the effect of prior lattice strain acts to retard the transformation. This prior lattice strain tends to impede the martensite reaction due to the crystallographic nature of this reaction which involves an instantaneous atomic shear mechanism that occurs most easily in a strain-free lattice. Thus, annealed material (such as that associated with welded joints) would tend to be more susceptible to this reaction than would the cold-rolled base metal.

AISI Type 301

These considerations explain why type 301 stainless steel, the least stable of the 300 series, exhibits the greatest increase in tensile strength for a given percentage cold reduction for any alloy of this class. Figure 1 shows that extra-full-hard (about 60 percent cold rolled) type 301 has tensile and yield strengths of about 220 and 200 ksi, respectively, accompanied by an elongation of about 5 percent at 78°F. The limiting factor in this strengthening process is the low elongation and toughness associated with the even harder tempers. For example, type 301 cold rolled 78 percent has a tensile strength of 300 ksi at 78°F, but its low toughness (as measured by notched tensile ratios) and low elongation makes it suitable for missile applications which require a high order of resistance to brittle failure.

This consideration of toughness becomes even more critical at lower temperatures, because the strain-induced martensite exhibits a ductile-to-brittle transition at subzero temperatures and reduces the toughness of the alloy drastically. In this study toughness was measured by notched/unnotched tensile ratios (stress concentration factor, $K_t = 6.3$) rather than by Charpy V-notch tests because no fully reliable impact test for thin sheet has yet been devised. The stress concentration factor of 6.3 was chosen because notched/unnotched tensile tests at this level of notch acuity have correlated with axial fatigue tests of complex welded joints over the temperature range of from 78° to -423°F (14).

Within certain well defined limits, the data obtained in this study on type 301 were in general accord with other data describing the behavior of face centered cubic materials at low temperature (15). This typical

behavior of face centered lattices is characterized by relatively large increases in tensile strength with decreasing temperature, the retention of toughness at low temperature. The magnitude of the increase in tensile and yield strengths has been found to depend on the degree of cold work in the sample prior to testing. In general, increasing amounts of cold work reduce the magnitude of the increase in tensile and yield strength. Wessel for example, found that the tensile strength of annealed nickel, which is face centered cubic, increased fivefold between 1110°F and -423°F, compared to a twofold increase in yield strength between the same temperatures (15). In contract to this behavior, Wessel observed a 46 percent increase in the tensile strength of body centered cubic annealed beta brass between 70°F and -423°F compared to a 240-percent increase in yield strength between the same temperatures. In cold-worked alloys smaller percentage changes would be expected, although the relative changes would remain the same.

Outside of the well defined limits mentioned above, anamolous behaviors were observed in the cold-worked 301 stainless steels which were found to have been caused by a sold-state transformation of austenite (face centered cubic) to martensite (body centered tetragonal). This austenite-to-martensite reaction, which had a strong influence on all of the properties studied, is known to be favored by both low temperature and high tensile stress (6). In this study, martensite was found to be formed both during cold work at room temperature, and during tensile testing at low temperature. The microstructure containing martensite formed under these two separate conditions apparently had somewhat different properties.

The yield stress data of Figure 1 (301-60-percent cold-rolled) show a relatively large (about 25 percent) increase between 70°F and -320°F which is not characteristic of face centered alloys, especially in the cold-worked tempers. This condition (i.e., increases in yield strength which equal increases in tensile strength) strongly suggests that some other common metallic structures (h.c.p. and b.c.c.) are know to exhibit relatively large increases in yield strength with decreasing temperature (15). Furthermore, the large increases in yield strength associated with the samples possessing greater degrees of cold work would indicate that the more highly cold-worked samples contain more of the non-face centered phase. This is in accordance with other work which has shown that increasing amounts of cold reduction result in larger amounts of martensite, and is confirmed by Magne-gage and x-ray diffraction studies obtained in this study.

The relatively high notched/unnotched tensile ratios that occur at -423°F where elongation values are relatively low show that elongation is not a measure of toughness, or notch sensitivity. Until recently, many investigators have been using the terms ductility and toughness interchangeably, when actually they measure two distinctly different parameters. Elongation, which is a measure of ductility, describes the ability of a material to deform plastically

under conditions of slowly applied loads in the absence of notches or other stress conceptrations. Toughness, which may be measured by Charpy V-notch impact strength, notched/unnotched tensile ratios, and various tear tests, is a measure of resistance to failure under conditions of impact loading and stress concentrations, such as notches, rivet holes, inclusions, sharp re-entrant corners, etc. Combinations of impact loads, stress concentrations, and low temperature form the severest type of toughness test, and are all present in a Charpy V-notch test conducted at low temperature. The correlation of these variables (i.e., strain rate, notch acuity, and temperature) has been made for steels by Wallace et al (16), and these concepts may be extended to other alloy systems.

The data of Table I, which pertains to both longitudinal and transverse tests, shows that the transverse notch/unnotch tensile ratios are somewhat lower than the corresponding longitudinal ratios under all conditions of cold work and temperature. This difference becomes more pronounced in areas where brittle failure tends to occur (i.e., at -423°F in 40- and 60 percent cold-worked samples and at all temperatures in the 78-percent cold-worked material). This greater embrittlement in the transverse direction is believed to be primarily due to preferred orientation effects resulting from the large amounts of cold work introduced into this alloy during cold rolling rather than from oxide or silicate stringers, because microscopic examination has shown this steel to be relatively free of nonmetallic inclusions. However, second order reasons for this behavior may be associated with the microstructure of the steel. In the transverse notched coupons, the crack occurs in the direction of rolling. Cracks are more readily initiated and propagated in the rolling direction than the transverse notch/unnotch tensile ratio in severely cold-worked metal would be expected to be somewhat lower than the corresponding longitudinal value. Similar behavior has been observed by other investigators in type 301 and 304L cold-worked austenitic stainless steels.

The data of Figure 2 show that an optimum amount of cold work occurs at about 60-percent reduction in order to obtain high notch/unnotch ratios. Reduction beyond this amount results in excessive low temperature embrittlement due to the presence of large amounts of martensite formed by cold work at room temperatures, while lesser amounts of cold work do not introduce enough defects into the lattice to impede the austensite-to-martensite reaction (which results from low temperature and high strain during deformation). The resulting large amounts of martensite which occur again lead to embrittlement as measured by the notch/unnotch ratio..

Absolute measurements of percent martensite were not attempted for several reasons. The Magne-gage technique was not used quantitatively because suitable calibration standards were not available. The x-ray diffraction technique was not used quantitatively due to the large degrees of preferred orientation present in the cold-worked samples. Metallographic calibration of the Magne-gage and x-ray techniques was not possible due to the extremely distorted microstructures which were not amenable to normal metallographic techniques

for determining percent martensite. The martensite could not be discerned in the structure of the severely cold rolled steel even at 1000 diameters. Finally, volumetric measurements did not yield suitable sensitivity. One promising method of determing percent martensite is a calibration of the Magne-gage with compacts of mixed powders (mounted in very small amounts of Bakelite) containing known amounts of a forromagnetic phase such as ferrite, and a paramagnetic phase such as austenite, and making the assumption that alloying effects present in the stainless steel would not affect the results significantly. Another promising method is to bend an annealed sample of type 301 at low temperature (-320°F) so that varying amounts of martensite are formed around the bend radius. These areas can be subjected to a microscopic lineal analysis to determine the amount of martensite present, and then the Magne-gage can be calibrated directly. Both of these techniques are being developed.

The behavior of the other 300 series stainless steels reported herein can be interpreted in terms of the well-known behavior of austenite (face centered cubic) between 78° and -423°F, and then deviations from this behavior can be explained in terms of the presence of low carbon martensite (body centered tetragonal) in the austenite matrix. It was found that all of the factors which control the stability of austenite were operative to some degree in this study (i.e., chemistry, temperature, tensile stress, and degree of prior lattice strain).

AISI TYPE 302

For example, type 302 stainless steel exhibits tensile strengths at 78°F of 178 and 205 ksi when cold rolled 40- and 60-percent, respectively, with corresponding elongations of 7- and 3- percent. The toughness at 78°F in both cases is excellent as indicated by a notched/unnotched tensile ratio of about 1.07 in both cases. These facts are all in accord with the behavior of stable austenite; i.e., moderate increases in tensile strength with cold work and good toughness, which is associated with the face centered crystal structure at all temperatures. The stability of this steel results in very little formation of martensite during the tensile test at 78°F, as shown by a low Magne-gage ratio at 78°F. However, at lower temperatures deviations from the typical behavior of austenite occur, and can be correlated with the occurence of the austenite-to-martensite reaction as measured by Magne-gage ratios at -320° and -423°F. Although this steel is relatively stable under the influence of tensile stress at 78°F, the combined effect of low temperature and tensile stress causes large amounts of martensite to form at -320° and 423°F. This formation of martensite causes the decrease is notched/unnotched tensile ratio at -320° and 423°F.

AISI TYPE 304ELC

Type 304ELC stainless steel cold rolled 50-percent also exhibits the typical properties of face centered cubic austenite at 78°F, and then deviates from them at -320° and -423°F. At 78° and -100°F this alloy exhibits moderately high yield and tensile strengths, and has good toughness as shown by a notched/unnotched tensile ratio of 1.09 at both temperatures (see Table II and Figure 3). Magne-gage readings confirm that no martensite is formed during tensile testing at 78° and -100F. At -320°F however, the Magne-gage shows that large amounts of martensite have been formed during tensile testing. In this case, however, the notched/unnotched tensile ratio remains at 1.04, which is not in accord with previous data on types 301 and 302 which showed that the formation of martensite caused embrittlement at low temperture. It is believed that in this extra low carbon steel (0.023 percent C) the martensite formed during tensile testing is of such a low carbon content that the embrittling effects associated with higher carbon martensites are greatly reduced. At -320°F this sample exhibits 33-percent elongation in conjunction with the formation of large amounts of martensite which leads further support to this hypothesis. At -423°F this steel fractures after 1-percent elongation, and this behavior is accompanied by a notched/unnotched tensile ratio of 1.09, a tensile strength of 279 ksi which is about 30 ksi greater than that exhibited at -320°F, and a Magne-gage ratio of about unity which shows that almost no martensite was formed during the tensile test. The microstructure of the fracture surface (tested at -423°F) shows that a small amount of martensite did form during tensile testing and acted as the locus of the fracture. The Magne-gage did not measure this martensite due to its very small volume and its location in a narrow strip along the edge of the fracture.

AISI TYPE 310

The data for type 310 cold-rolled stainless steel (Figure 4) are in accord with the typical behavior of fully stable austenite over the temperature range of from 78° to -423°F. No deviations from typical behavior (i.e., moderate increases in strength with increasing cold reduction and good toughness at low temperature) occur, and this structural correlation is confirmed by Magne-gage ratios which show that no martensite is formed during tensile testing at all cryogenic temperatures. The fully austenitic cold-rolled structure retains excellent toughness over the range of from 78° to -423°F.

AISI TYPE 301-N

An additional steel studied in this program was type 301-N which has chemistry similar to type 301 with the exception that 0.10 to 0.15-percent nitrogen is added and nickel is reduced from 7 to 6 percent. According to the work of Eichelman and Hull (11), the effect of this change in chemistry is to lower the M_s temperature

(i.e., to increase austenite stability) by 289°F, compared to type 301. (This calculation yields M_s temperatures of -54° and -343°F for annealed types 301 and 301-N, respectively.) However, Magnegage ratios indicate that more martensite forms during tensile testing in type 301-N than in type 301 (see Figure 23). In view of previous data which show that the 301-N should be more stable than type 301, it appears that the effect of interstitial content(i.e., carbon and nitrogen) on the stress-induced martensite reaction overshadows the austenite stabilizing effect of the chemistry present in type 301-N on the temperature-induced martensite reaction.

A further result of this experimental program was the correlation of the notched/unnotched tensile ratio with the axial fatigue properties of complex welded joints. While some materials retain useful ductility and toughness at low temperatures, the metallurgical changes produced in and around weld zones may result in low-temperature embrittlement of weld joints, and seriously impair the utility of such metals for cryogenic temperature applications. It has therefore proved necessary to conduct relatively large-scale costly tests of complex test specimens and fabricated components before it it is possible to insure that materials can be satisfactorily employed at extremely low temperatures.

In developing the Atlas missile for the U.S. Air Force, Convair-Astronautics conducted extensive tests of base materials and welded joints at room and at liquid nitrogen (-320°F) temperatures. Ten-foot diameter prototypes of liquid oxygen and fuel tanks were constructed and subjected to hydraulic fatigue and rupture tests at both temperatures, the liquid oxygen tanks being filled with liquid nitrogen during test.

Axially loaded tensile and fatigue-test specimens incorporating welded joints similar to those on the tanks were designed which closely reproduced the strength and fatigue properties of the large test tanks at both temperatures. As a result, these axially loaded tensile and fatigue test specimens, having test area widths of approximately 4 in. and gage lengths of 20 in., have been standardized for the evaluation of candidate materials for large, thin-skinned, lightweight propellant tanks. More recently, the same techniques were successfully applied to the evaluation of materials for large liquid hydrogen fuel tanks.

The axial fatigue test of welded joints at liquid hydrogen temperatures, while extremely useful and discriminatory, is both costly and time consuming, requiring several thousand cycles of test, extending over a one- to two-day period per specimen, with specimens immersed in liquid hydrogen throughout the test. The notched/unnotched tensile ratio reported herein is a simpler, less costly test with equal or superior discrimination capabilities and can be used to rapidly screen candidate materials being considered for cryogenic applications.

Tests performed to date at Convair-Astronautics have demonstrated that axially loaded fatigue tests on welded joints of a number of extrahard, cold-rolled stainless steels of Type 300 series tested at temperatures in the range of +70° to -423°F correlate with notched/unnotched ratios obtained from tensile tests of small-base metal specimens at corresponding test temperatures in alloys 301, 301-N and 310 in the cold rolled condition. Table III contains data developed at Convair-Astronautics in evaluating materials for use in the Atlas missile and Centaur upper stage.

Table III demonstrates the correlation between the notched/unnotched strength ratios, and the fatigue resistance of complex welded joints tested at various temperatures. The fatigue tests were performed at high stress levels, approaching 90% of the nominal yield strengths of the materials. Thus, the number of cycles to failure are relatively low. High operational stresses are characteristic of missile design where minimum weight structures are of paramount importance.

Table III shows that when the notched/unnotched ratio is unity or higher, the fatigue resistance is high; when the ratio drops below unity, the fatigue resistance also declines. Fatigue tests are performed at a uniform stress level (a maximum of 144,000 psi) at all temperatures, whereas the strengths of the materials increase with decreasing temperature. Thus, it should be expected that, if materials retain their resistance to brittle fracture, the fatigue resistance will increase with decreasing temperatures. The fact that this does not always occur indicates the embrittlement which is apparent in Type 301-N steel at -320°F and in Type 301 at -423°F. The notched/unnotched ratios of both materials at the respective temperatures are less than unity.

If materials remain ductile at reduced temperatures, their fatigue resistance increases with decreasing temperature if the fatigue stress level remains constant since the strength of materials increases with decreasing temperature. Note that the fatigue life of welded joints in Type 301 cold-rolled steel is 2671 cycles at -320°F as compared to 934 cycles at +70°F when fatigued cyclically from 0 to 140,000 psi stress. The static tensile strengths of these same joints increased from approximately 210,000 psi at +70°F to approximately 250,000 psi at -320°F; thus, while the fatigue stress at room temperature was 70% of the tensile strength, the fatigue stress at -320°F was reduced to 58-percent of the tensile strength, hence the increased fatigue life.

The correlation of notched/unnotched tensile ratio with cycles to failure in axial fatigue tests of complex welded joints in type 301, 60-percent cold rolled, is shown in Table III. It is seen that a decrease in the notched/unnotched tensile ratio from 0.99 to 0.92 between -320°F and -423°F is accompanied by a decrease in cycles to failure in axial fatigue tests from 2093 cycles to 633 cycles (at the same stress level of 140,000 psi) between the same

temperatures. Thus a moderate condition of embrittlement exists in this alloy at -423°F, and the severity of the service application (stress level, stress concentrations, etc.) will determine if this alloy can be used. For example, Table III shows that for a lower stress level in the axial fatigue test (from 140,000 psi to 120,000 psi), the average cycles to failure increase from 633 cycles to 1964 cycles at -423°F. This threefold increase in fatigue life is due to the steep slope of the S-N curve in the low cycle, high stress range.

This condition of embrittlement also manifests itself in the spread of experimental data obtained from repetitive tests. Table III shows this effect in the ± 3 sigma tabulation of cycles to failure in axial fatigue tests. These limits (i.e., ± 3 sigma) mean that in an infinite series of identical tests, the cycles to failure would fall within the given limits 99.9 percent of the time. It is seen that both lower temperatures and higher stress levels contribute to more brittle behavior, as indicated by wider ± 3 sigma levels.

Where better fatigue life for a given stress level is desired, a more stable steel (i.e., one in which the austenite to martensite reaction does not occur) would be specified. Such a steel is AISI type 310 CRES, which was tested in the 40-, 60- and 75-percent cold rolled conditions.

In the 75-percent cold rolled condition this alloy sacrifices some strength at 78°F as compared to extra full hard type 301 to obtain complete stability. However, the increased strength of 310 at lower temperatures exceeds the room temperature strength of type 301. Thus where the steel is stressed only at low temperature, type 310 imposes no weight penalty where room temperature properties are the basis of design allowables. This stability of type 310 is reflected by the higher fatigue life of this material in the welded joint at -423°F. After 2000 cycles (0-140,000 psi) at -423°F, only one small crack had appeared. Based on prior experience in fatigue tests where final failure occurs after 50-percent or more of the number of cycles at which the first crack initiates, it can be conservatively estimated that the fatigue life of this material will be at least 3000 cycles at -423°F; this compares with 633 cycles for the 301 CRES at -423°F.

SUMMARY

This study has shown that the most promising cold rolled austenitic stainless steels for cryogenic applications in missiles and space vehicles are type 301, 60 percent cold rolled; type 310, 75-percent cold rolled; and to a lesser extent, type 304ELC, 50-percent cold rolled. The type 301 exhibits moderate tendencies toward brittle behavior at -423°F, and in those applications where maximum resistance to brittle behavior is required, types 310 or 304ELC are recommended although a small tensile strength penalty

occurs. Type 301 possesses the highest yield and tensile strength of any alloy of the 300 series for a given degree of cold work. However, the solid state phase transformation of austenite to martensite which occurs in this alloy (under the combined effects of high tensile stress and low temperature) and accounts for the high tensile strength also causes a moderate condition of embrittlement in this alloy at -423°F, due to the brittle nature of the martensitic phase. Type 310 however, remains fully stable (i.e., austenitic) under all conditions of tensile stress and low temperature, and for this reason remains tough at all cryogenic temperatures. However, because of this stable austenitic structure, the yield and tensile strengths of type 310 are slightly lower than those of type 301. Thus the choice between types 301 and 310 depends on the severity of the application; i.e., stress level, temperature, occurance of shock type loads, and presence of stress concentrations such as rivet holes, sharp re-entrant corners, etc. Type 310 is recommended for the more severe service conditions.

Austenitic stainless steels of AISI types 301, 302, 304ELC, 310 and 301-N exhibit mechanical properties between 78° and -423°F that are structure dependent, and the dependence of this structure on chemistry, temperature, tensile stress, and prior deformation is in general accord with previous investigations which have measured the effects of each of these variables on structure, or more specifically, the austenite to martensite transformation.

Type 301 cold rolled stainless steel exhibits low temperature mechanical properties that are dependent upon both the original austenitic structure and upon martensite induced by combinations of low temperature and plastic strain. Reductions in tensile strength and elongation between -320°F and -423°F are indicative of the occurrence of the austenite to martensite transformation at these temperatures. These reductions are accompanied by decreasing notch/unnotch tensile ratios, which are an index of embrittlement. The solid state transformation of austenite to martensite was confirmed and measured by both magnetic and x-ray diffration techniques. Heliarc butt welded joints exhibit a much larger percentage increase in tensile strength between 70°F and -320°F than did the cold worked tempers. The weldments also exhibit embrittlement between -320°F and -423°F, as shown by decreases in tensile strength between these temperatures, accompanied by large scatter in the test data.

The behavior of fully stable alloys such as AISI type 310 at cryogenic temperatures is in accord with the generalized behavior of face centered cubic metals. This behavior includes the retention of toughness at low temperatures (i.e., high notched/unnotched tensile ratios) and moderate increases in yield and tensile strength with decreasing temperature for cold-worked tempers. The behavior of the unstable alloys at cryogenic temperatures is dependent upon the amount and composition of martensite formed during both cold rolling at room temperature and tensile testing at cryogenic temperatures.

Increasing amounts of martensite generally act to increase tensile and yield strengths and decrease toughness at any given temperature, although the magnitude of these effects is strongly dependent upon interstitial content. Thus, type 304ELC forms large amounts of martensite during tensile testing at -320°F, yet retains good toughness (notched/unnotched tensile ratio of 1.04) due to the low carbon content (0.023-percent) of this alloy. Type 301-N, which undergoes transformation during tensile testing at -320°F, displays much more brittle behavior than type 301 due to its high interstitial content (0.13-percent N and 0.10-percent C). Alloys commonly regarded as stable at 78°F (i.e., type 302) are subject to the austenite-to-martensite transformation at -320° and -423°F, with resulting brittle behavior as measured by low notched/unnotched tensile ratios. The magnitude of this effect is dependent upon the degree of cold work at room temperature, prior to tensile testing at low temperature. Generally, an optimum degree of cold work exists (such as 60-percent in type 301) which yields maximum toughness during tensile testing at low temperature.

Type 304ELC, like type 310, remains tough at -423°F although it forms some martensite during tensile testing at -423°F. This martensite does not behave in a brittle manner due to the low carbon (.03-percent maximum) content of this alloy. However, other investigators have reported various toughnesses for this alloy at low temperature, and the discrepancies appear to be related to variations in chemistry occurring in this alloy, within the allowable limits. Thus, since type 304ELC has about the same strength as type 310, and can vary quite widely in toughness depending on its chemical composition, type 310 would be recommended in preference to type 304ELC. If type 304ELC can be cold rolled to higher strength levels, and the effects of chemical content on toughness accurately determined, it may offer more promise for cryogenic application.

Type 302 has lower strength than type 301, and lower toughness at low temperature than type 310 or 304ELC, and for these reasons doe not show promise for low temperature application. Type 301-N becomes quite brittle at -320°F due to its high carbon and nitrogen content, and is not suited for cryogenic application.

The variation of the yield strength/density and tensile strength/density ratios with temperature for the alloys studied in this program, as well as some of the more promising nonferrous alloys have been calculated, and the most promising of these alloys are shown below in order of decreasing strength density ratios. Notched/unnotched tensile ratios are included to indicate why some alloys, such as 7178-T6 aluminum, which have high strength/density ratios at low temperature cannot be used in structural applications due to their notch sensitivity.

TEST TEMP	MATERIAL	F_{ty}/density in x 10^6	F_{tu}/density in x 10^6	Notched/ Unnotched Tensile Ratio
78° F	7178-T6 Aluminum	.83	.90	1.02
	A110AT Titanium	.70	.74	1.34
	301 CRES 60% cold rolled	.64	.76	1.08
	304ELC 50% cold rolled	.55	.61	1.09
	310 CRES 75% cold rolled	.53	.60	1.10
-320°F	A110AT Titanium	1.14	1.22	1.15
	301 CRES 60% cold rolled	.86	1.10	.95
	310 CRES 75% cold rolled	.74	.84	1.11
	304ELC 50% cold rolled	.65	.87	1.04
-423°F	A110AT Titanium	1.43	1.52	.97
	7178-T6 Aluminum	1.11	1.23	.51
	301 CRES 60% cold rolled	1.00	1.10	.94
	310 CRES 75% cold rolled	.87	.97	1.01
	304ELC 50% cold rolled	.80	.96	1.09

In those cases where transverse notched/unnotched tensile ratios were lower than the longitudinal values, both preferred orientation caused by cold rolling, and the presence of elongated inslusions such as oxides, silicates and supphides were believed to be contributing to this effect. The relative magnitude of these effects could not be measured. Types 301 and 302 were relatively clean, but exhibited lower transverse notched properties, especially at low temperature. Type 304ELC was exceptionally clean, and had good and about equivalent transverse and longitudinal properties. Type 310, however, was relatively dirty and yet still had good and about equal transverse and longitudinal properties. These data suggest that inclusions occurring in structures containing both austenite and martensite (e.g., types 301, 302, and 304ELC) decrease the transverse notched properties by acting as stress concentrations in the more brittle martensite. In fully austenitic structures (e.g., type 310) it appears that inclusions have little effect on transverse notched properties. Further study of this effect is needed, and it is recommended that vacuum induction melted and consumable electrode melted type 301 be prepared and tested in both the longitudinal and transverse directions at 78°F, -100°F, -320°F, and *423°F.

Notched/unnotched tensile ratios obtained in this study have been found to correlate with cycles to failure in axial fatigue tests of complex welded joints obtained as part of prior work done Atlas and Centaur contracts. This correlation is significant because it offers a means of substituting the relatively rapid and inexpensive notched/unnotched test for the costly and time consuming axial fatigue tests of comple welded joints.

BIBLIOGRAPHY

1. V. N. Krivobok: "Properties of Austenitic Stainless Steels at Low Temperatures", Nat'l Bur. of Std. Circular 520, Washington D. C., 1952.

2. V. N. Krivobok and A. M. Talbot, "Effect of Temperature on The Mechanical Properties, Characteristics, and Processing of Austenitic Stainless Steel", Proc. ASTM, vol. 50, 1950.

3. Krivobok, V. N., and Lincoln, R. A., "Austenitic Stainless Alloys", Trans. ASM, 25, 1937, p. 637.

4. Cina, B., "Effect of Cold Work on the Gamma-Alpha Transformation in some Fe-Ni-Cr. Alloys", J. Iron and Steel Inst., 177, 1954, p. 406.

5. Ziegler, N. A., and Brace, P. H., "Hardening of Austenitic Stainless Steels by Mechanical Working at Sub-Zero Temperatures", Trans. ASTM, 50, 1950, p. 86.

6. G. W. Powell, E. R. Marshall, and W. A. Backofen, "Strain Hardening of Austenitic Stainless Steel", Trans. ASM, vol. 50, p. 478.

7. S. A. Kulin and M. Cohen, "On the Martensite Transformation at Temperatures Approaching Absolute Zero", J. Met., vol. 188, Sept 1950, p. 1139.

8. Post, C. B., and Eberly, W. S., "Stability of Austenite in Stainless Steel" Trans. ASM, 39, 1947, p. 868.

9. McAdam, D. J., Geil, G. W., and Cromwell, F. J., "Influence of Low Temperatures on the Mechanical Properties of 18-8 Cr.-Ni-Steel" Trans. ASM, 41, 1949, p. 609-645.

10. Kurdyumov, G. V., and Maksimova, O. P., "Kinetics of the Austenite-to-Martesite Transformation at Low Temperatures" Kodlady Adad. Nauk SSSR, 61, 1948 #1 p. 83. (Brutcher Translation #2187).

11. Anonymous, "Low Temperature Bibliography for the Field of Cryogenics", (with eight supplements), Engineering Division, A. D. Little Inc. 1958.

12. T. Angel, "Formation of Martensite in Austenitic Stainless Steels", J. Iron and Steel Inst., May 1954, p. 165.

13. H. C. Fiedler, B. L. Averbach and M. Cohen, "The Effect of Deformation on the Martensite Transformation in Austenitic Steels", Trans. ASM, vol. 47, 1955, p. 267.

14. Watson, J. F., and Hurlich, A., "A Proposal for the Development of Tests to Evaluate the Toughness of High-Strength Sheet Alloys and the Fatigue Resistance of Welded Joints at Extreme Subzero Temperatures", Convair-Astronautkcs Report AZM-094, 26 October, 1959.

15. Wessel, E. T., "Some Exploratory Observations of the Tensile Properties of Metals at Very Low Temperatures", Trans. ASM, 49, 1957, p. 149.

16. Wallace, et.al., "Impact Tests Help Engineers Specify Steel", SAE Journal, March 1951, pp. 24-28.

TABLE I

Mechanical Properties of 60 Percent Cold-Rolled 301 Stainless Steel Sheet

.023" Thick, Washington Steel Co., Heat #48112, Coil 36125

TEST TEMP	DIRECTION	F_{ty}	F_{tu}	e	NOTCHED T.S.		NOTCHED/ UNNOTCHED TENSILE RATIO		HELIARC* BUTT WELD T.S.	WELD ELONG	JOINT EFF
		ksi	ksi	%	Kt=6.3	Kt=3.2	"A"	"B"	ksi	%	%
+78°F	Long.	203	212	5	230	229			151	4	
	"	200	212	6	231	231			154	4	
	"	203	212	5	230	231			154	4	
	"	201	208	5	229	232					
	"	194	212	5	231	229					
	Avg	200	212	5	230	231	1.08	1.08	153	4	72
+78°F	Tran.	180	223	8	216	226			150	4	
	"	180	223	7	216	220			151	4	
	Avg	180	223	8	216	223	.97	1.00	151	4	68
-320°F	Long.	250	313	23	297	303			287	15	
	"	-	314	23	293	300			287	15	
	"	246	313	22	292	303			287	15	
	"				290	304					
	"				295	300					
	Avg	248	313	23	293	302	.94	.96	287	15	92
-320°F	Tran.	225	319	17	233	291			282	11	
	"	223	315	18	280	286			284	12	
	"				272						
	Avg	224	317	18	276	289	.87	.91	283	12	89
423°F	Long.	-	312	14	331	326			227	6	
	"	291	309	14	316	349			233	2	
	"	-	330	2	-	352			355	4	
	"	284	315	2	-	367			265	3	
	Avg	291	317	8	323	342	1.02	1.08	238	4	75
-423°F	Tran.	277	335	8	219	273			251	2	
	"	292	335	8	242	307			187	1	
	"	266	333	9	219						
	Avg	285	335	8	227	290	.68	.87	214	2	64

*Heliarc butt weld; x-rayed; roll planished; no doubler reinforcement

TABLE II

Mechanical Properties of 50 Percent Cold-Rolled 304 ELC Stainless Steel Sheet

.012" Thick, Rodney Metals Heat #33251

TEST	DIRECTION	F_{ty} ksi	F_{tu} ksi	e %	NOTCHED T.S. ksi (Kt=6.3	NOTCHED/ UNNOTCHED TENSILE RATIO	HELIARC* BUTT WELD T.S. ksi	WELD ELONG %	JOINT EFF %
+78°F	Long.	158	174	6	191		90.3	2	
	"	156	174	6	192		90.0	2	
	"	158	177	5	188		88.2	2	
	Avg	158	176	6	191	1.09	89.5	2	51
+78°F	Tran.	153	190	4	209		83.0	1	
	"	153	192	5	207		87.6	1	
	Avg	153	191	5	208	1.09	85.3	1	45
-100°F	Long.	191	196	4	214		150	2	
	"	181	199	5	216		151	3	
	"	186	199	5	216		149	3	
	Avg	186	198	5	216	1.09	150	3	76
-100°F	Tran.	184	217	7	240		149	3	
	"	180	215	6	243		148	2	
	Avg	182	216	7	242	1.12	149	3	69
-320°F	Long.	192	250	32	261		221	4	
	"	184	250	35	262		222	4	
	"	193	253	33	263		221	3	
	Avg	187	251	33	262	1.04	221	4	88
-320°F	Tran.	190	256	38	301		223	2	
	"	189	254	36	299		226	3	
	Avg	190	255	37	300	1.18	224	3	88
-423°F	Long.	-	276	1	304		259	4	
	"	231	285	2	302		263	4	
	"	-	276	1	303		267	4	
	Avg	231	279	1	303	1.09	263	4	94
-423°F	Tran.	233	305	1	317		284	4	
	"	233	304	2	322		282	4	
	Avg	233	305	2	320	1.05	283	4	93

*Heliarc butt weld; roll planished; no doubler reinforcement

TABLE III

Correlation of Base Metal Notched/Unnotched Tensile Ratios with Fatigue Properties of Complex Welded Joints[a] of Cold Worked Stainless Steel Sheet. 1.020- in. Thick

MATERIAL	TEST TEMP	NOTCHED/ UNNOTCHED TENSILE RATIO (Kt = 6.3) LONG.	TRANS.	CYCLES TO FAILURE IN AXIAL FATIGUE TESTS[b] 0 to 140,000 psi AVG	± 3 d	0 to 120,000 psi AVG	± 3 d
Type 301 CRES 60-percent cold-rolled	+78	1.05	0.97	934[e]	776 1123	-	-
	-320	0.99	0.87	2671[e]	2066 3444	-	-
	-423	0.92	0.68	633[e]	196 2004	1964	765 4650
Type 310 CRES 75 percent cold-rolled	+78	1.10	0.97	-	-	-	-
	-320	1.11	1.07	1855[g]	-	-	-
	-423	1.11	1.03	2000[c]	-	-	-
Type 301-N CRES 60-percent cold-rolled	+78	1.06	0.94	632[f]	497 800	-	-
	-320	0.95	0.87	327[f]	17 3503	-	-

[a] Weld joints 3-1/2 in. wide, 20-in. gauge length, 38-in. overall length. Mid-section contains heliarc butt-weld joint, roll planished and reinforced with 4-in. wide doubler resistance spot welded with four rows of spots on each side of the butt weld. All sections 0.020-in. thick.

[b] Fatigue test of weld joint consists of axially loading and unloading between 0 and 140,000 psi in tension at a rate of 6 cpm.

[c] Test stopped after 2000 cycles after which one small crack was evident in heat-affected zone of one of resistance spot welds in outer row of spots. Based on prior experience in fatigue tests where final failure occurs at 50-percent or more of the number of cycles in which crack initiates, it can be estimated that fatigue life is in the order of 3000 cycles.

TABLE III (Continued)

[d] A statistical analysis which means that in an infinite series of identical tests, the cycles to failure would fall within the given limits 99.9 percent of the time.

[e] Average of three tests

[f] Average of five tests

[g] Average of two tests

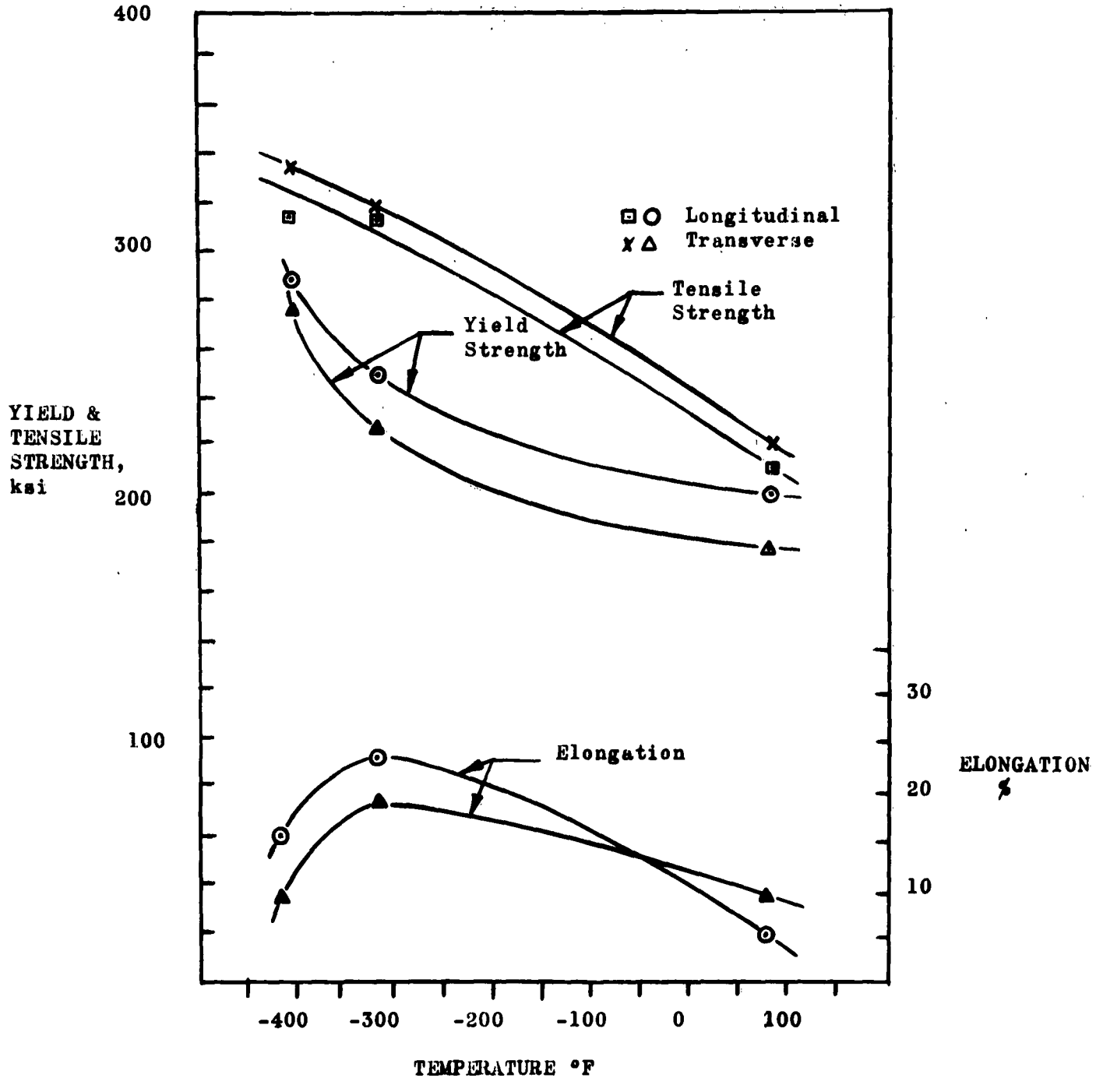


Fig. 1. Yield and tensile strength (ksi) and elongation (%) vs. temperature (°F) for 60% cold-rolled 301 CRES, .023" thick.

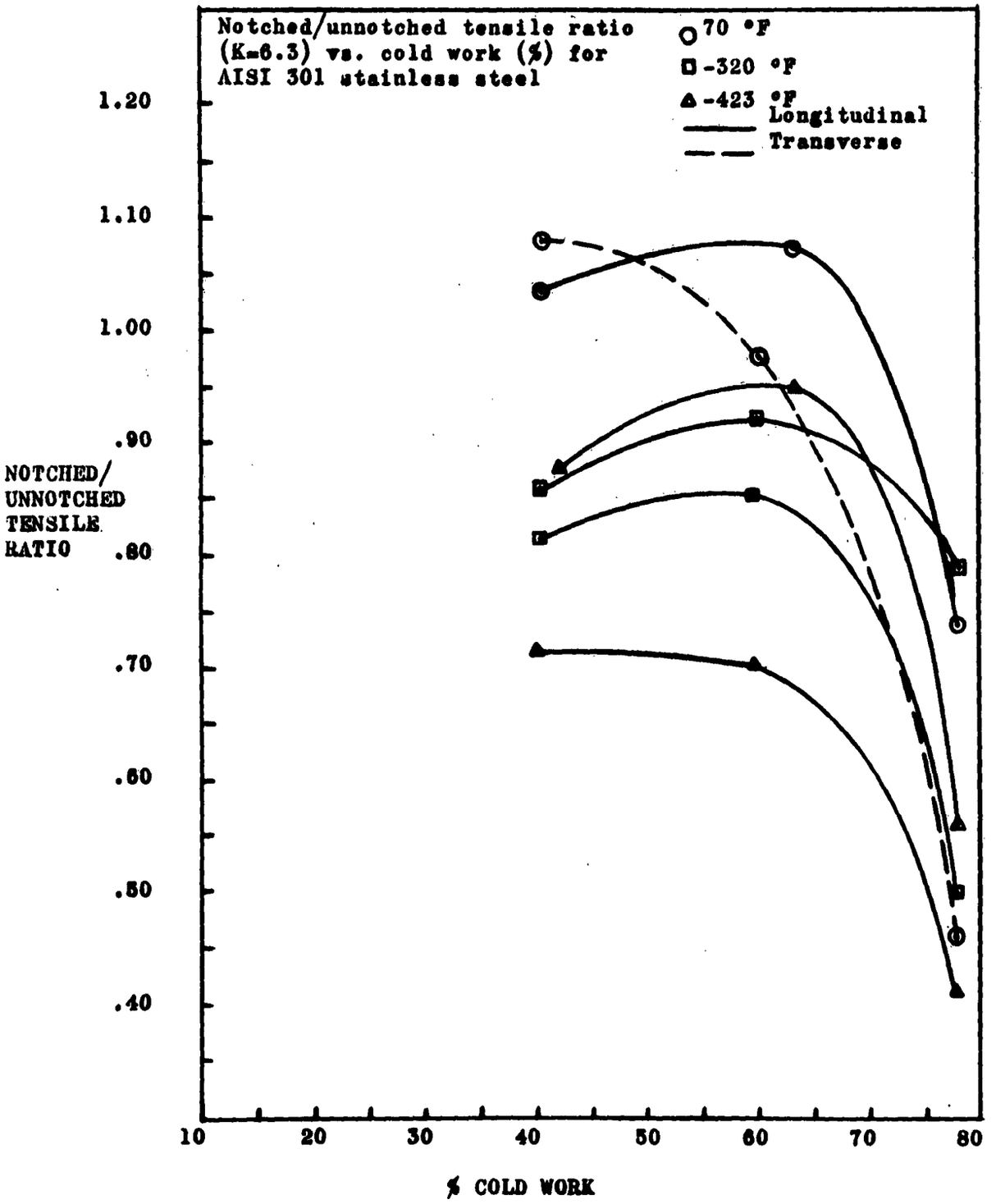


Fig. 2. Notched/unnotched tensile ratio (K_t=6.3) vs. cold work (%) for 301 CRES.

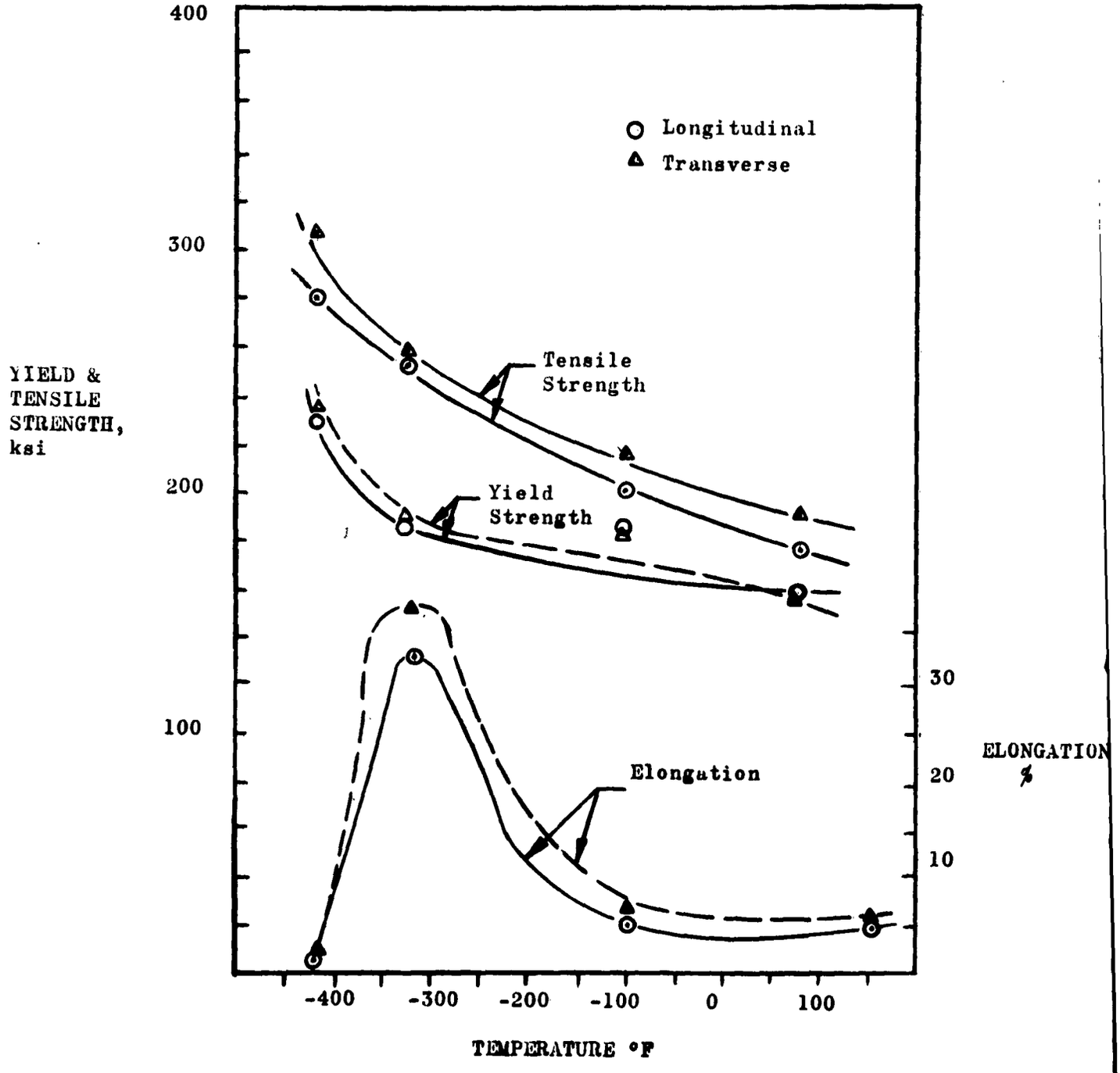


Fig. 3. Yield and tensile strength (ksi) and elongation (%) vs. temperature (°F) for 50% cold-rolled 304 ELC CRES.

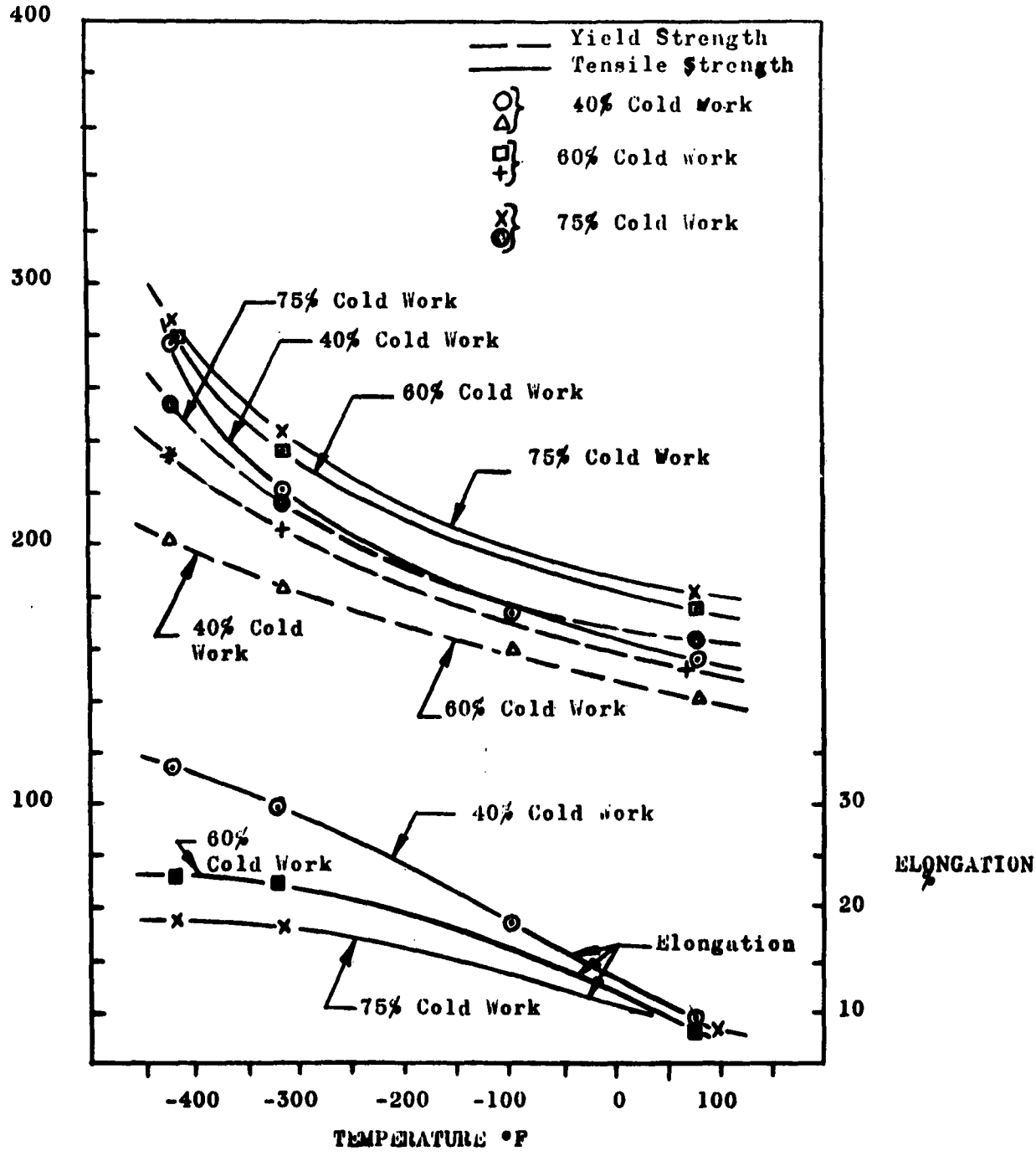


Fig. 4. Yield and tensile strength (ksi) and elongation (%) vs. temperature (°F) for cold-rolled 310 CRES.

STRAIN HARDENING PROPERTIES OF HIGH STRENGTH SHEET MATERIALS

by

Frank Larson
John Nunes
Watertown Arsenal Laboratories

INTRODUCTION

Recent interest in high strength to weight ratio materials in sheet form for certain missile applications has provided the impetus for the initiation of many new programs.[1] The inability to predict service behavior, particularly failure loads, has been the cause of great concern. The majority of these programs[2] have resorted to mechanical tests, most of which involve the testing of notched specimens or other means of providing a strain concentration, because it is known that these high strength materials are particularly sensitive to discontinuities. In many cases these notch or bending tests are supplemented by standard tension tests where the conventional engineering properties are determined. Although these tests are certainly useful for screening purposes, it is not possible to obtain the basic deformation properties. Clearly, it is important to determine the fundamental plastic flow characteristics for at least some of these materials.

The tension test, where simultaneous load and minimum area measurements are made, provides a means of determining true stress-strain properties.[3] From such tests a curve can be established depicting true stress (σ) or flow stress as a function of true strain (ϵ). The rate of stress increase with strain ($d\sigma/d\epsilon$) is then a measure of the strain hardening properties but varies with strain and hence is complicated. The often used power relation[4] gives a convenient single-valued quantity termed the strain hardening exponent (n). It is this basic property of strain hardening which plays such an important part in the strength and ductility of structures.

The strain gradients that develop during plastic deformation as a result of discontinuities, heterogeneous properties or nonuniform stress systems are a function of the strain hardening properties of the material being deformed. This has been demonstrated for the necking case[5,6] where the principle tensile load passes through a maximum. The importance of the strain hardening properties is particularly well known in the plastic working of metals.

Knowledge of the fundamental plastic flow of steels at high strength levels is extremely limited. The majority of true stress-strain testing has been confined to low strength ductile conditions and Gensamer[7] has summarized these results for steels up to a hardness level of about 40 R_c.

Relatively little work[8,9] has been carried out above this hardness presumably because of testing difficulties.

Although there has been quite widespread use and interest in true stress-strain testing during the last 15 years, testing of sheet materials has not been too extensive. The procedure becomes a bit more complicated and the test data reduction to curves quite time consuming. For sheet, it is necessary to measure two principle strains at the minimum section, in the width (ϵ_w) and thickness (ϵ_t) directions, rather than only the minimum diameter as for round bars. Procedures based on length measurements have been used, but these are not considered too satisfactory because they are only usable up to the limit of uniform elongation, and it has been shown that the deformation of sheet materials is far from homogeneous even in the "uniform range". This is probably due to the heterogeneous properties of the material, constraints from the radius on the ends of the specimen, dimensional variations in the gage length particularly in the thickness direction. Truly there is a need for improvement of testing techniques.

The problem of the measurement and the meaning of ductility has always been a difficult one particularly in sheet metal. Low ductilities encountered in high strength materials aggravate this situation. A fairly recent review[10] on this subject has been made and illustrates some of the salient problems. The true stress-strain testing invalidates many of the criticisms of engineering ductility measurements and provides a fundamental flow curve. From this flow curve and a proper theory of plasticity, it should be possible to predict the behavior in other geometric configurations.

The measurements of transverse thickness and width strains can provide information about mechanical anisotropy. The effect of the directional properties in plastic flow is far from being clear, but it is evident that in certain cases it can be extremely important.[11-14] Investigations into the anisotropic behavior of sheet have shown that this is a difficult problem and considerable further work is necessary. The techniques applied in this program lend themselves quite well to a measurement of mechanical anistropy and results will be shown for steel and titanium alloys where the mechanical anisotropy is small and very large, respectively.

MATERIALS AND PROCEDURE

Since the prime objective of this program was to provide basic plastic flow information on materials of high strength levels, it was felt that most of the investigation should center around currently available materials where possible and these are listed with their chemical analysis in Table I. In that there were many variables that were examined, such as heat treatment, testing temperature, specimen orientation, etc., description of the entire program can be best made via Tables II and III.

The tension tests were conducted on a 30,000 pound capacity Tinius

Olsen mechanical testing machine at a constant head speed to give a strain rate of .01 "/" per minute. Continuous load, width, and thickness measurements necessary for the computation of true stress-strain data were obtained. The load was detected by a strain gage dynamometer which was placed in series with the test specimen. The width and thickness measurements were made employing a principle similar to that described by Powell et al.[15] The main feature of this apparatus is a strain gaged cantilever beam aligned parallel to the specimen axis for the detection of dimensional changes of the test bar. The entire fixture is free to move vertically searching the full length of the tension specimen. Whereas Powell was testing round bars, he used a single pair of cantilever arms and chose to search for the minimum section manually. To test sheet specimens, it became necessary to add a second pair of sensing arms, 90° from the original pair, thereby enabling the measurement of both width and thickness changes in the same horizontal plane. Because of difficulties in searching for minimum section (WXT), it was necessary to abandon manual scanning. The assembly was motorized and provided with limit switches so that the sensing arms could be driven at a constant pre-selected speed, from a variac control, up and down the specimen. The test set-up is pictured in Figure 1. The signals from the dynamometer, the width gage, and the thickness gage are then fed into a strain gage oscillographic recorder. Since the recorder chart runs at a pre-selected constant speed, and the deformation is small for each scan, the resulting curve is essentially the specimen profile. The specimen width and thickness profile are then repeated continuously along with the load as the specimen deforms. A typical record is shown in Figure 2. The adjacent records of specimen profile are actually mirror images for one is for the up and the next is for the down probe. For measurement of yield strength at room temperature, the width and thickness probe was retracted to an up position and a standard snap-on sheet extensometer was used. To check the load readings from the dynamometer and obtain yield strength values at other than room temperature, an autographic load versus cross-head displacement record was employed.

RESULTS

True stress-strain curves are shown in Figures 3 through 14 which illustrate the effects of heat treatment and testing temperature for the various steel alloys. Comparative properties of several titanium alloys tested at room temperature, are listed in Table IV. In the vicinity of maximum load, the steel specimens showed the formation of a shear band across the width. The geometry of this shear band along with the measuring technique used gives rise to a computed width strain which is smaller than the maximum and thereby in error. Since the neck forms in the thickness direction first[16], the thickness strain seems to be more homogeneous and the measurement more representative of the maximum strain in that direction. Plots of width versus thickness strain were constructed to check this and assuming constant anisotropy they seem to indicate these ideas are correct. There is a linear width to thickness strain region from initial yielding

up to the vicinity of maximum load and then a break occurs and the width strain increases at a lesser rate. Illustrated in Figure 15 is a representative plot of width versus thickness strain. Because of the uncertainty of the width strain measurements, the true stress-strain curves were drawn with solid lines from yielding up to this inflection in the width versus thickness strain plot and then dotted to fracture. Incidentally, none of the titanium specimens tested showed this pronounced shear band behavior, and plots of width versus thickness strain remained reasonably linear from yielding to the vicinity of fracture. These graphs of width versus thickness strain were also used for the determination of the mechanical anisotropy values which are tabulated in Table V.

Since the strain rate influences strength and ductility of metals, tests should be run at a constant true strain rate from initial yielding through fracture. As previously mentioned, these tests were run at a constant head speed so as to give an approximate starting strain rate of .01 "/" per minute, and it is well known that the strain rate varies considerably, especially during nonuniform extension, so it is worthwhile to examine this for this specimen geometry. The instrumentation used in this program provides an excellent means for determining the strain as a function of time from which the strain rate may be obtained. An illustrative graph of the longitudinal strain versus the strain rate is shown in Figure 16. The longitudinal strain used is the strain in the minimum section. Superimposed on this plot is the constant strain rate line which, of course, would be a horizontal line and the theoretical strain rate (assuming uniform deformation) for a constant crosshead speed. The curves illustrate quite dramatically strain rate variation even during the so-called uniform strain region.

DISCUSSION

Summary plots that illustrate general trends for certain selected strength, strain hardening, and ductility parameters were constructed. To enable comparisons between various alloys, heat treatment, and testing temperature, these parameters were chosen to reflect the basic behavior or point out significant differences in the various materials. Two strength measuring parameters were used, the true stress at a strain of 0.04 and at fracture. The true stress at a strain of 0.04 (about 4% elongation) was used because residual stresses and retained austenite make the determination of stresses at lower strains much less certain and reflect only special cases. The true stress at fracture that is reported is the final instantaneous load divided by the final minimum cross sectional area supporting that load to just prior to the rapid drop in load. For ductility, the true compressive transverse strain in the thickness direction was employed. This appeared to be more significant because those specimens that broke with some ductility as evidenced by necking, seemed always to have the origin of the fracture at the minimum and in the center of the thickness dimensions of the bar but might be located nearly any location across

the width. The strain hardening properties were measured by the strain hardening exponent in the well known power law. The strain hardening exponent was determined by measuring the slopes of the log-log plots of true stress-strain. Many of these plots did not yield a single straight line, but it was possible to develop several regions of different straight lines and these are reported as different strain hardening exponents. This behavior is fairly well known for titanium, and for the stress induced martenistic transformation. The upward curvature of the log-log plots after maximum load, due to triaxial Bridgeman stresses and/or increased strain rate were not measured or reported. Therefore, only the strain hardening properties at or prior to maximum load were studied.

Figures 17 and 18 illustrate the above described properties for the two chemically similar materials, Vasco Jet 1000 and Crucible 56, as influenced by tempering temperature. Both of the strength parameters follow the trends that would be expected. The true stress at fracture for both alloys seems to be nearly equivalent at about 370,000 psi up to a tempering temperature of about 900°F and then drops abruptly with increasing temperature. The flow stress at true strain of 0.04 follows a similar trend although there seems to be a slight secondary hardening peak in the region of this 900°F temperature. The true transverse thickness strain at fracture shows an increase with increasing tempering temperature with a definite minimum valley apparently associated with the secondary hardening peak at 900°F. There are two regions of strain hardening in the specimens tempered below 1100°F. The first region (n) of very high strain hardening existed at low strain, and x-ray determinations indicated this to be associated with about 6% retained austenite. The higher strain hardening of the as-quenched and tempers up to 300°F may be connected with residual stresses. Further work needs to be done to study these effects in the low strain range more thoroughly. The strain hardening properties, measured in the region of maximum load, seems to be an unsystematic function of tempering treatment with a peak occurring in the 900°F region and generally increasing at the high tempering temperature.

Figure 19 illustrates the effect of aging temperature upon these same properties for the AM 350 Alloy. The stress parameters especially the true stress at fracture increase with increasing aging temperature having a peak in the vicinity of 900°F and then decreasing with increasing temperature. The strain hardening properties of this alloy are quite interesting and different from that of the prior alloys. Strain hardening is similar to that observed for stainless steel where it is low during the initial straining, increases to a high value while the austenite is transforming to martensite, and then falls to a low value when the strain induced martensitic reaction is complete. The strain hardening of the AM 350 at low strains follows slow decrease with increasing aging temperature and has a valley around 1000°F. However, the strain hardening properties in the vicinity of maximum load behaves quite erratically and is probably due to the unknown effect of aging temperature upon the subsequent stability of the austenite to plastic deformation. That is, some of the specimens

at certain aging treatments did not show any evidence of the strain induced martensitic reaction at any strain, other specimens reached maximum load during this martensitic transformation, and finally, in some specimens, maximum load occurred when the martensitic reaction was complete. These effects in this alloy are more pronounced in the low temperature tests and will be discussed later. It is particularly interesting to see that the fracture ductility of this alloy follows the same general trend with aging as does the strain hardening properties at maximum load.

The effect of testing temperature for three preselected tempering temperatures for Vasco Jet 1000 of 700, 1000, and 1300°F were studied. These properties are illustrated in Figures 20 through 22. The strength parameters generally increase with decreasing testing temperature. The true stress at fracture seems to increase with decreasing temperature until brittle behavior is encountered. When the true stress at fracture decreases, the true strain at fracture increases abruptly. The strain hardening properties do not seem to vary greatly with temperature.

The low temperature properties of AM 350 were also studied at three preselected aging treatments of 850, 900 and 1050°F and are illustrated in Figures 23 through 25. Here, like the previous material, the strength parameters increase with decreasing testing temperature. The true strain at fracture decreases with decreasing testing temperature, the 850°F aged specimen being quite brittle at liquid nitrogen testing temperature. Strain hardening showed three regions that are characteristic of the stainless steels forming strain induced martensite. For the 850°F aging treatment, the material seemed most resistant to this transformation being completely stable at room temperature and not completing the reaction at low temperatures (i.e. log-log plots did not show decrease in strain hardening after the high rate associated with the austenite to martensite reaction). The strain hardening properties (except for the 850°F) seemed to be relatively insensitive to testing temperature. The rate of strain hardening for the different aging treatments seemed to be very nearly the same. The strain hardening exponent for the initial deformation of the martensite-austenite mixture was about 0.05 for the stage where austenite is transforming to martensite about 0.20 and for the final stage about 0.13. These values did not change appreciably with testing temperatures.

Illustrated in Figure 26 are the low temperature properties of AM 355 which had been cold worked 30%. Here is an abrupt transition from a ductility to brittle type of fracture as is evidenced by the drop in fracture strain from 0.25 approximately to 0.02 between temperatures of -130° and -155°C. There is an even more abrupt drop in fracture stress over the same temperature range of approximately 120,000 psi from 440,000 psi. There was no apparent variation of the strain hardening properties with temperature for this material.

The effect of low temperature upon the mechanical properties of 3/4 hard and 301 stainless steel are shown in Figure 27. The flow stress at

a true strain of 0.04 does not vary appreciably with testing temperature. The true stress at fracture, however, increases dramatically with decreasing testing temperature, an effect previously noted for face centered cubic metals[1]. This has been attributed to the increased strain hardening properties at the lower temperatures. It can be seen from this figure that the true strain at fracture does not change greatly with temperature so that the effect of the large amount of strengthening associated with the strain induced martensite transformation is felt. Here it is interesting to note that the strain hardening increases very rapidly to a fairly constant value (about 0.90) as the temperature of testing is decreased.

As mentioned before, the titanium alloys tested for this program at room temperature showed no shear band formation detectable either visually or by the construction of width versus thickness strain plots. The actual true stress-strain plots have been illustrated in Figure 6. The pertinent strength and ductility parameters are tabulated in Table IV. In comparison to the steel, it can be seen that the strain hardening properties are quite similar. The log-log plots of the true stress-strain results for these specimens showed only one slope, contrary to what has been previously reported. Various conventional mechanical property relationships were examined for these alloys without much success. Strain hardening may be thought of as the material's ability to resist localized plastic deformation, and it was believed that there there should be some relationship between fracturing properties and strain hardening. This fact is very nicely illustrated in Figure 28 for titanium and titanium alloys. As the strain hardening exponent increases, the true strain at fracture increases.

Measurements of the mechanical anisotropy for the various materials studied in this program were made and are tabulated in Table V. To determine this mechanical anisotropy, plots were constructed of the true transverse compressive strain in the width versus thickness directions, and the slope of these curves was measured and recorded. This is the ratio of the width to thickness strain and is a measure of mechanical anisotropy of the material under this stress system. The steels showed very little anisotropy with the principle strain in the thickness direction always being equal or slightly larger than the width direction giving ratios of 1.0 to about 0.8. The AM 355, which was cold rolled, was an exception and had a very low value of about 0.5. The various titanium alloys, which are known to be anisotropic even in large section sizes, were found to be quite variable. The ratios for titanium varied from about 7.2 to 0.2. It is evident that this strong anistropy is a preferred crystallographic orientation effect, whereas for the steels, it could be a mechanical effect due to the specimen geometry or a mechanical fibering.

Measurements in this program are measurements of what may be called normal anisotropy; that is, the ratio of two principle strains, one perpendicular and one in the plane of the sheet. Tests which compare the anisotropy in the plane of the sheet only, do not necessarily reveal anisotropy for it is important to measure all three directions for a complete picture.

CONCLUSIONS

Through the use of suitable instrumentation, it is possible to measure the principle strain in the width and thickness dimensions on sheet specimens, thereby developing more basic plastic flow and fracture properties of these sheet materials. The deformational properties of high strength steels appear quite heterogeneous, which is probably due to their low strain hardening properties. Shear band formation, which results from a neck in the thickness direction, was prevalent in the high strength steels but not in the titanium alloys.

With the exception of the AM 355 alloy, the steel showed only slight anisotropy with the ratio of width to thickness strains being somewhat smaller than one. However, the titanium alloys showed a high degree of anisotropy with width to thickness strains ranging from about 7.2 to 0.2.

The behavior at low testing temperatures for these materials is similar to that which has previously been reported. The strength parameters generally increase with decreasing temperature until brittle fracture occurs. The ductility decreases gradually and then abruptly when brittle fracture ensues with decreasing test temperature.

The fracture properties seem to be related to the strain hardening properties indirectly. Correlating these two properties directly is somewhat difficult because of the influence of other variables, particularly in the steel. For the titanium alloys, the fracture ductility seems to be directly related to the strain hardening properties.

Retained austenite was found to affect the rate of strain hardening in the 5% chromium steels, producing a very low yield strength and thereby a very high initial rate of strain hardening. X-ray studies showed about 6% retained even after sub-zero cooling and multiple tempering. Mechanical property measurement showed that this retained austenite persisted up to tempering temperatures of 1100°F. It appeared from these tests that a minimum in ductility exists for this and the AM 350 at the 900°F tempers so this should be avoided. From consideration of the retained austenite it would appear that 1100°F temper would be desirable, however, it may be that a slightly lower temper could be used if a longer tempering time is employed. The 600°F to 700°F tempering range appears to yield nearly maximum strength with excellent ductility and if some method could be devised to get rid of the retained austenite, which when strained transforms to martensite and can produce severe embrittling effects, this lower tempering range would provide some very desirable properties.

Finally, considerations of the directional properties, especially the normal anisotropy, led to the conclusion that, sheet, specially processed and then oriented in the components with regard to principle maximum stress fields, should give rise to superior performance.

APPENDIX A

Definitions of Symbols used in the Text

σ	=	True stress at minimum cross section
σ_f	=	True fracture stress
$\sigma_{.04}$	=	True stress at a strain of 0.04
n_{ml}	=	Strain hardening exponent at maximum load
n_1 & n_2	=	Strain hardening exponents other than maximum load Where: $\sigma = s_1\epsilon^n$
ϵ	=	Strain of $\epsilon_w + \epsilon_t$
ϵ_{f-t}	=	Fracture strain in the thickness direction
ϵ_t	=	Thickness strain
ϵ_w	=	Width strain

REFERENCES

1. Symposium "Testing and Evaluation of Materials for Solid Propellant Rocket Motor Casing" National Academy of Sciences, National Research Council, Washington, D. C. MAB-156, Feb 1959.

2. CAMPBELL, J. E., and ACHBACK, W. P., "Current Tests for Evaluating Fracture Toughness of Sheet Metals at High Strength Levels," DMIC Report 124, Jan 28, 1960, Battelle Memorial Institute.

3. LUDWIK, P., "Elements der technologiachen Mechanik," Berlin, 1909, Julius Springer.

4. HOLLOMON, J. H., "Tensile Deformation," Trans. AIME 162, 1945, p. 268.

5. SACHS, G., and LUBAHN, J. D., "Failure of Ductile Metals in Tension," Trans ASME 68, 1946, p. 271.

6. ESPEY, G., "Instability of Thin-Walled Tubes Subjected to Internal Pressure," Trans ASME 68, 1946, p. 281.

7. GENSAMER, M., "Strength and Ductility," Trans. ASM 36, 1946, p. 30.

8. READ, T. A., MARCUS, H., and GAUGHEY, J. M., "Plastic Flow and Rupture of Steel at High Hardness Levels, " Fracturing of Metals - ASM Book, 1948, p. 228.

9. KLENGER, L. J., CHOW, C. C., and SACHS, G., "Flow and Fracture Characteristics of a Die Steel at High Hardness Levels," Trans. AIME 185, 1949, p. 927.

10. RUDNICK, A., and CARLSON, R. L., "The Influence of Sheet Thickness on the Tensile Properties of Metal Sheet," DIMC Memo No. 5., Jan 23, 1959, Battelle Memorial Institute.

11. LANKFORD, W. T., SNYDER, S. C., and BAUSHER, J. A., "New Criteria for Predicting the Press Performance of Deep Drawing Sheets," Trans. ASM 42, 1950, p. 1197.

12. HAZLETT, T. H., ROBINSON, T. A., and DORN, J. E., "An Evaluation of a Theory of Plastic Flow in Anisotropid Sheet Metals," Trans. ASM 42, 1950, p. 1326.

13. BOURNE, L., and HILL, R., "On the Correlation of the Directional Properties of Rolled Sheet in Tension and Cupping Tests" Philosophical Magazine 41, 1950, p. 671.

14. KRUPKOWSKI, A., and KAWINSKI, S., "The Phenomenon of Anisotropy of Annealed Polycrystalline Metals," Journal Institute of Metals, July, 1949, p. 869.

15. POWELL, G. W., MARSHALL, E. R., and BACKOFEN, W. A., "A Diameter Gage and Dynanometer for True Stress-Strain Tension Tests at a Constant True Strain Rate," Proceedings ASTM 55, 1955, p. 797.

16. ARONOFSKY, J., "The Formation of a Necked Region and Fracture Along an Oblique Line in Flat Tensile Bars," Proceedings of Applied Mechanics, June, 1951, p. 521.

TABLE I

LIST OF MATERIALS, SHEET GAGES AND CHEMICAL ANALYSIS

Materials	Specimen Dimensions* Thickness	Width	Nominal Composition (wt. - %) C	Mo	Si	Mn	Cr	Ni	N	Al	V	Ti	Fe
Steel													
Vascojet 1000	0.127	0.372	0.40	1.30			5.00				0.50		
Crucible 56	0.091	0.450	0.40	2.50	1.00	0.55	3.25				0.33		
AM 350	0.057	0.272 0.305	0.10	2.75	0.25	0.80	16.5	4.30	0.10				
AM 355	0.071	0.321	0.10	2.30	0.60	0.80	15.0	4.20	0.09				
301 S.S.	0.107	0.367	0.08 to 0.20		1.00		16.0 to 18.0	6.00 to 8.00					
Titanium	**Thickness**	**Width**											
4Al-3Mo-1V	0.059	0.500	.045	3.07					0.09	3.85	0.96		
6Al-4V	0.129	0.501								6.0	4.0		
4Al-4V	0.138	0.501								4.0	4.0		
2.5Al-16V	0.056	0.500	.025						.025	2.79	15.8		
Rc 150B	0.131	0.499	.05	4.8			4.66						4.6
Rc 130B	0.127	0.501				4.0				4.0			
Rc 55	0.126	0.501										99.2	
Ti-100A	0.126	0.502										99.0	

**Thickness variations were a maximum of ± .003 inch.*
Width variations were a maximum of ± .004 inch.
Reduced gage section of 2.75 inches.

TABLE II

OUTLINE OF PROGRAM

Material*	Heat Treatment	Test Temperature (°C) R.T.	-40	-80	-105	-130	-155	-196
Vascojet 1000	1450°F Preheat --- 1800°F 20 min. in salt Air cooled -- Quenched Liq. N_2 1 hrs. - Double Temper 1 hr. at 500, 600, 700, 900, 950, 1000, 1050, 1100, 1200 and 1300°F Air cooled.	A	B	B	B	B	B	B
Crucible 56	1500°F Preheat --- 1875°F 1 hrs. in salt Air cooled - Quenched Liq. N_2 3 hrs., 4 hrs. at 200, 300, 400, 500, 600, 700, 800, 900, 1000, 1050, 1100, 1150 and 1200°F Air cooled, Double Temper	A						
AM 350	1710°F 15 min. Air cooled Quenched in Liq. N_2 3 hrs. Temper at 400, 600, 800, 850, 900, 1000, 1050, and 1100°F in salt Air cooled	A	C	C	C	C	C	C
AM 355	1710°F Solutionized Cold Rolled at 30%	D	D	D	D	D	D	D
301 S.S.	As received 3/4 Hard	D	D	D	D	D	D	D
All titanium tested	As received	D						

All materials tested in the longitudinal direction parallel to the rolling direction.

A All Tempers

B 700, 1000, & 1300°F Tempers

C 850, 900, & 1050°F Tempers (no test for 1050°F at -196°C)

D As Received Condition — All tests

TABLE III

COOLANTS USED FOR DIFFERENT TEST TEMPERATURES

Room Temperature	Tested in still air
-40° and -80°C	Alcohol mixed with dry ice
-105, -130 and -155°C.	Isopentane cooled by liquid N_2
-196°C	Liquid N_2

TABLE IV

ROOM TEMPERATURE TENSION PROPERTIES OF TITANIUM MATERIALS TESTED

	True Stress-Strain Properties						Engineering Properties	
Material	$\sigma_{.04}$	σ_{ml}	σ_f	ϵ_{ml}	ϵ_{f-t}	n_{ml}	Y.S. 0.2%	U.T.S.
Rc 150B	162,000	-----*	174,100	----*	.079	.065	154,400	158,600
Rc130B Ht. 23471	160,000	176,100	203,800	.112	.171	.104	136,800	157,600
Ht. B23321	150,000	168,400	190,800	.123	.168	.107	137,300	148,900
6Al - 4V	137,600	141,600	170,900	.058	.098	.070	123,800	133,500
4Al - 4V	136,600	150,900	157,600	.091	.107	.088	115,000	137,900
2.5Al - 16V	122,500	134,400	145,300	.100	.173	.098	105,700	118,600
4Al-3Mo - 1V	101,000	103,600	150,300	.051	.107	.074	98,600	99,700
Ti 100A	100,300	114,000	130,000	.112	.173	.112	83,100	102,100
Rc 55	72,000	82,000	103,300	.109	.221	.126	56,000	72,900

**Specimen Broke before Maximum Load.*

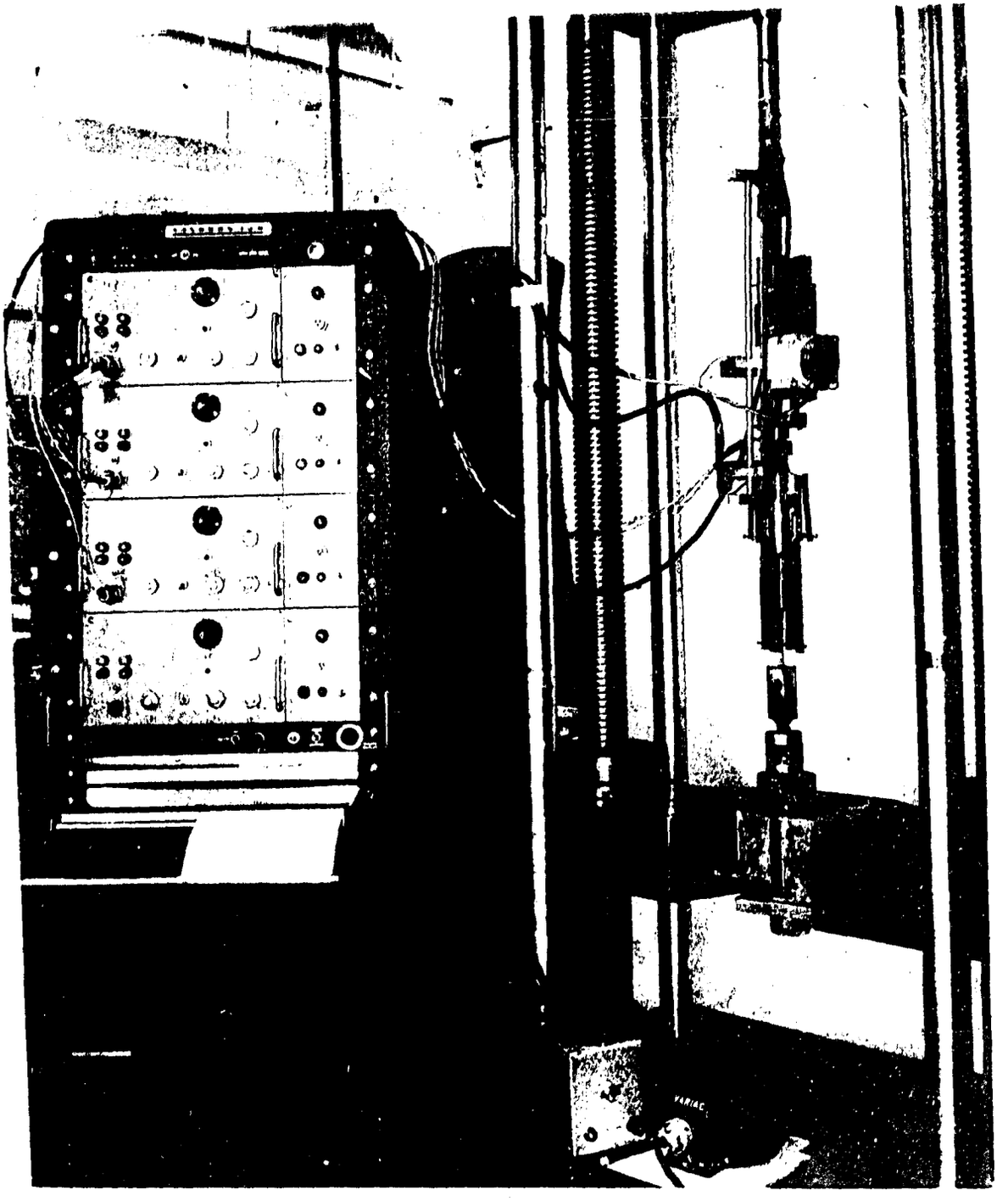
TABLE V

MECHANICAL ANISOTROPY VALUES FOR THE VARIOUS MATERIALS TESTED AT ROOM TEMPERATURE

Material		
Steel	Titanium	R*
	4Al-3Mo-1V	7.20
	6Al-4V	3.62
	Rc130B	** 1.38
	Rc 55	1.34
	Ti-100A	1.13
Vascojet 1000		** 0.95
301 SS		0.94
AM 350		**0.93
Crucible 56		**0.80
	4Al-4V	0.72
AM 355		0.48
	2.5Al-16V	0.46
	Rc150B	0.23

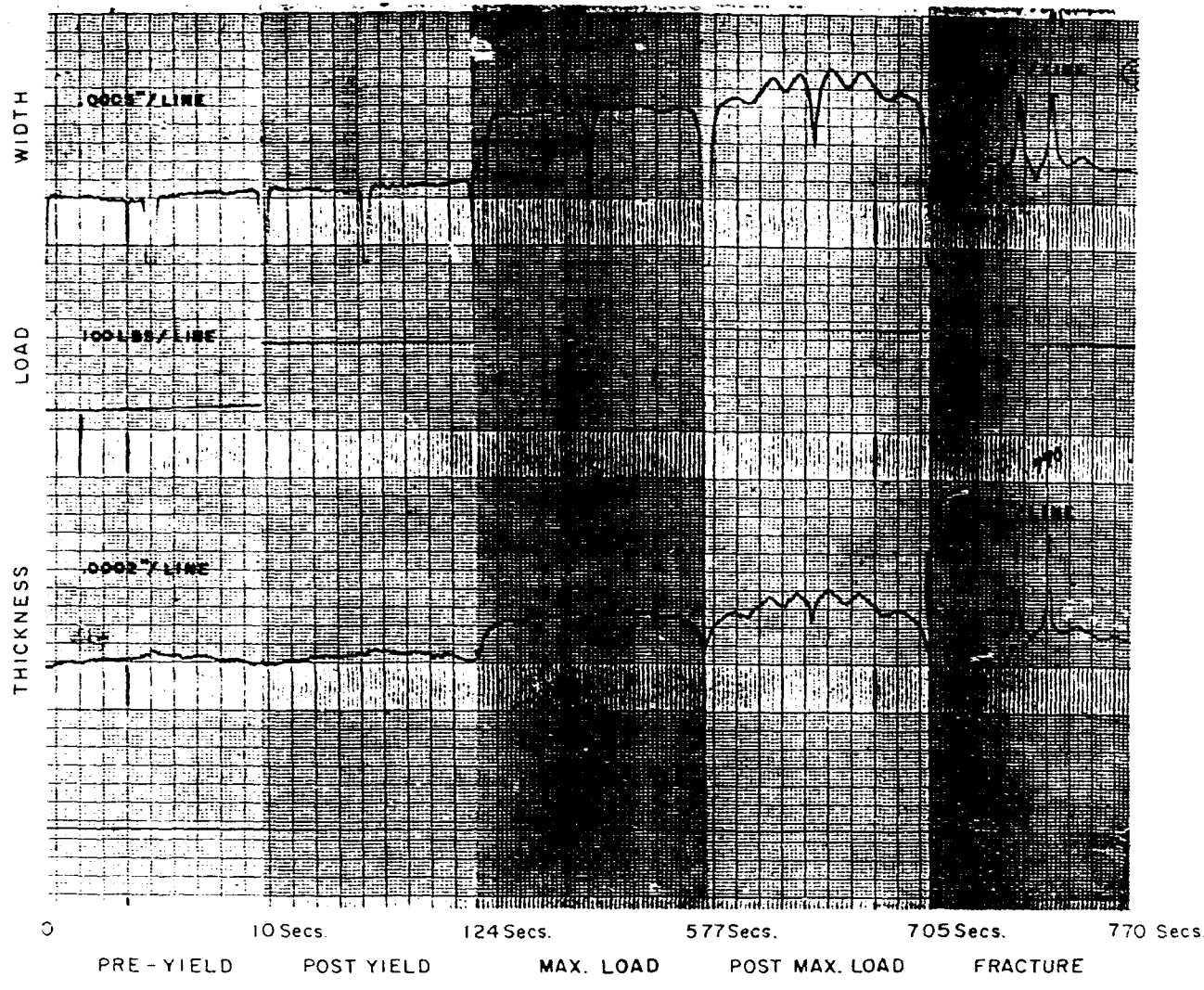
*$R = \epsilon_w / \epsilon_t$ where: $\epsilon_w = R\,\epsilon_t$

**Average values taken from more than one test.



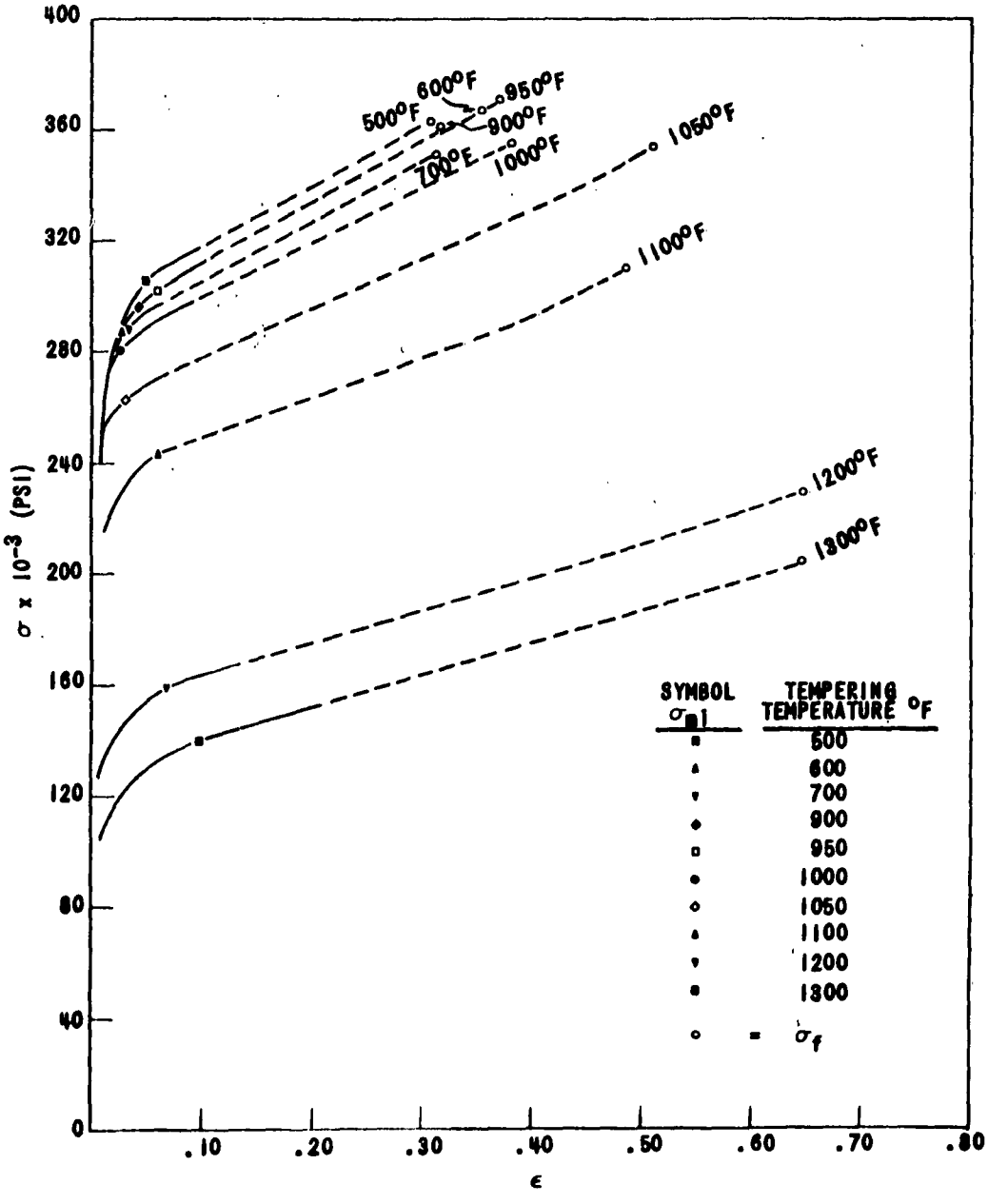
TEST SET-UP

FIGURE 1



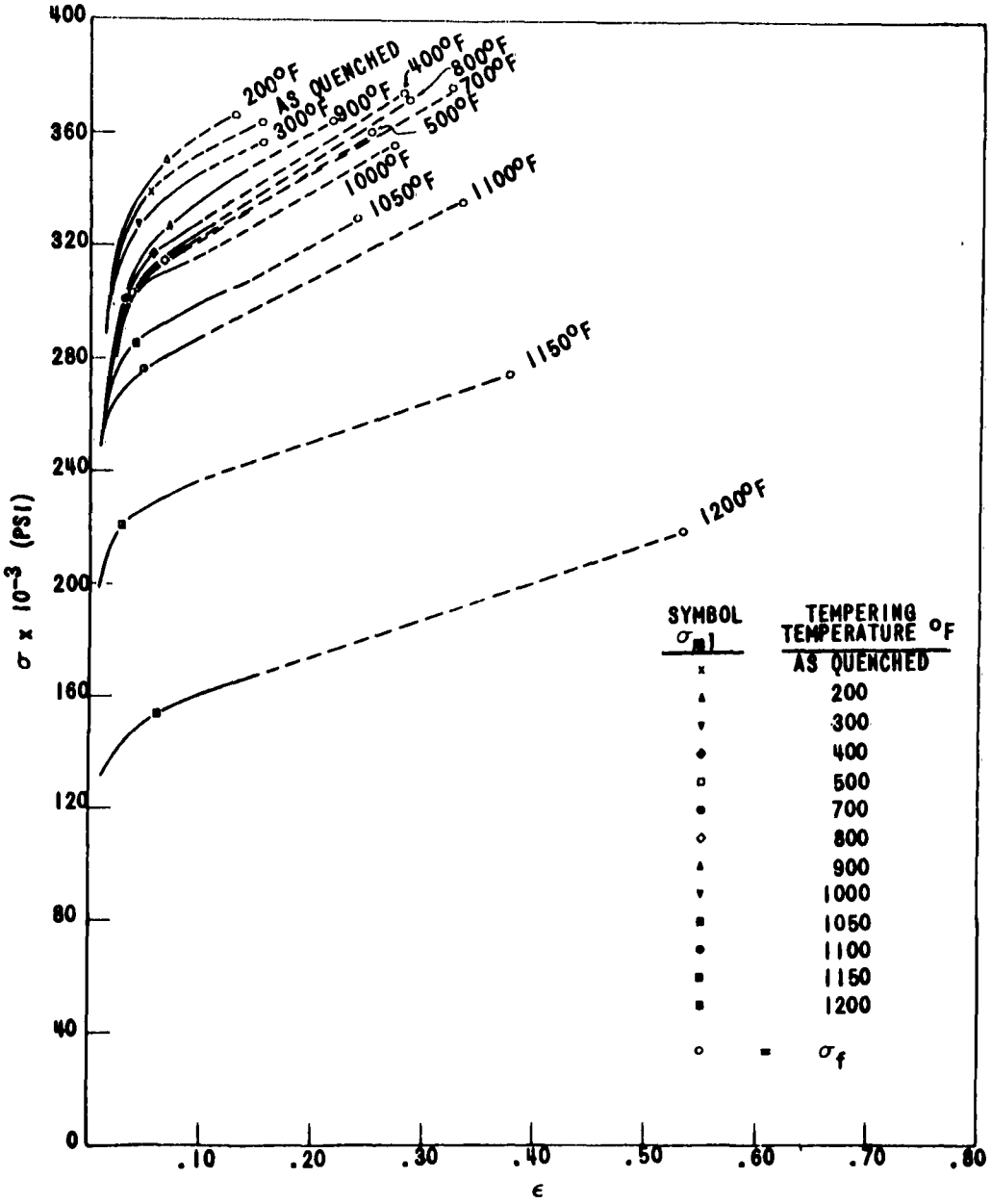
TYPICAL TEST RECORD (SEGMENTS OF FULL CURVE SHOWN AT VARIOUS TIME INTERVALS FOR AM350 AT 1100°F AGE)

FIGURE 2



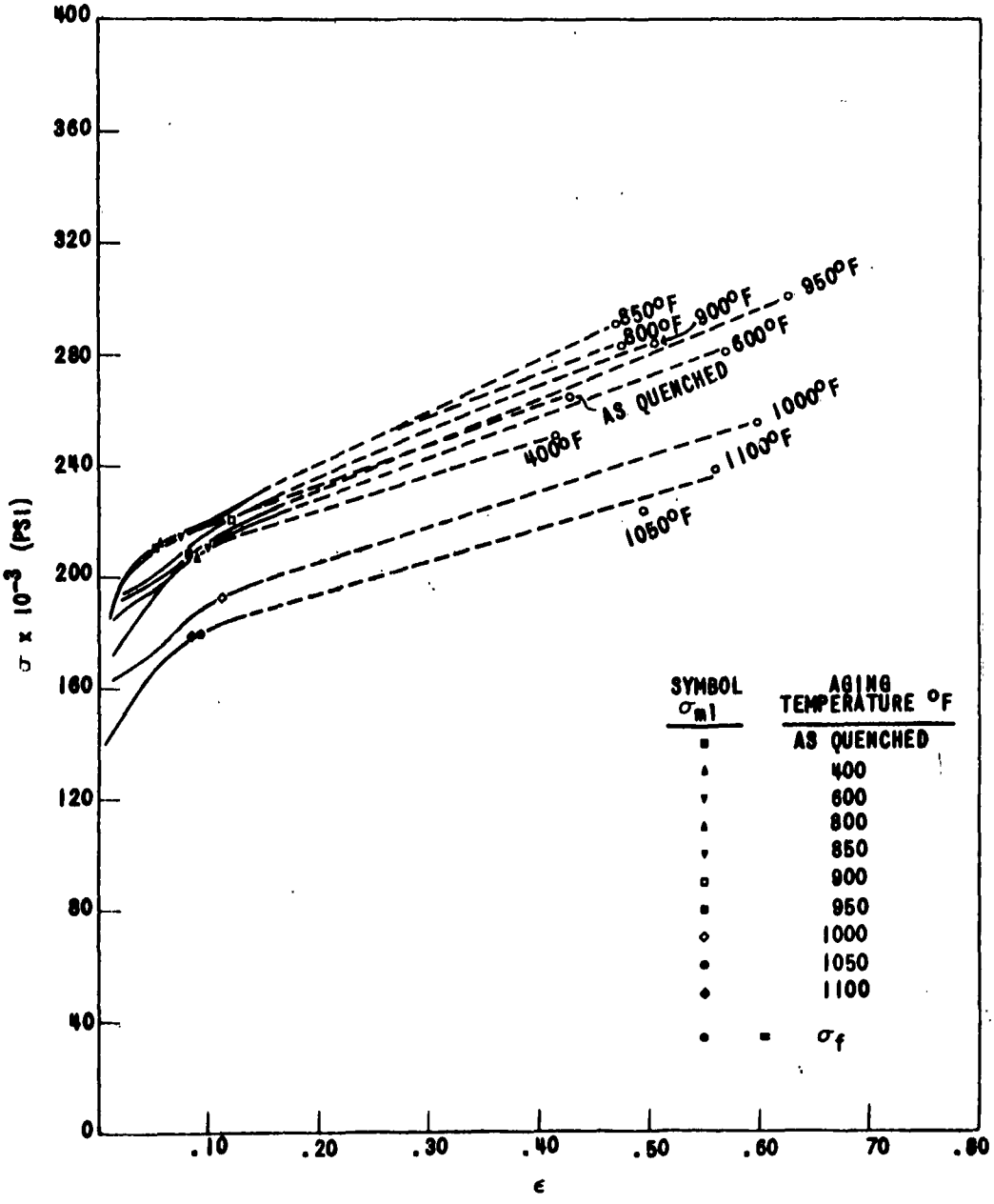
ROOM TEMPERATURE TRUE STRESS-STRAIN CURVES FOR VASCOJET 1000 AT VARIOUS TEMPERED CONDITIONS

FIGURE 3



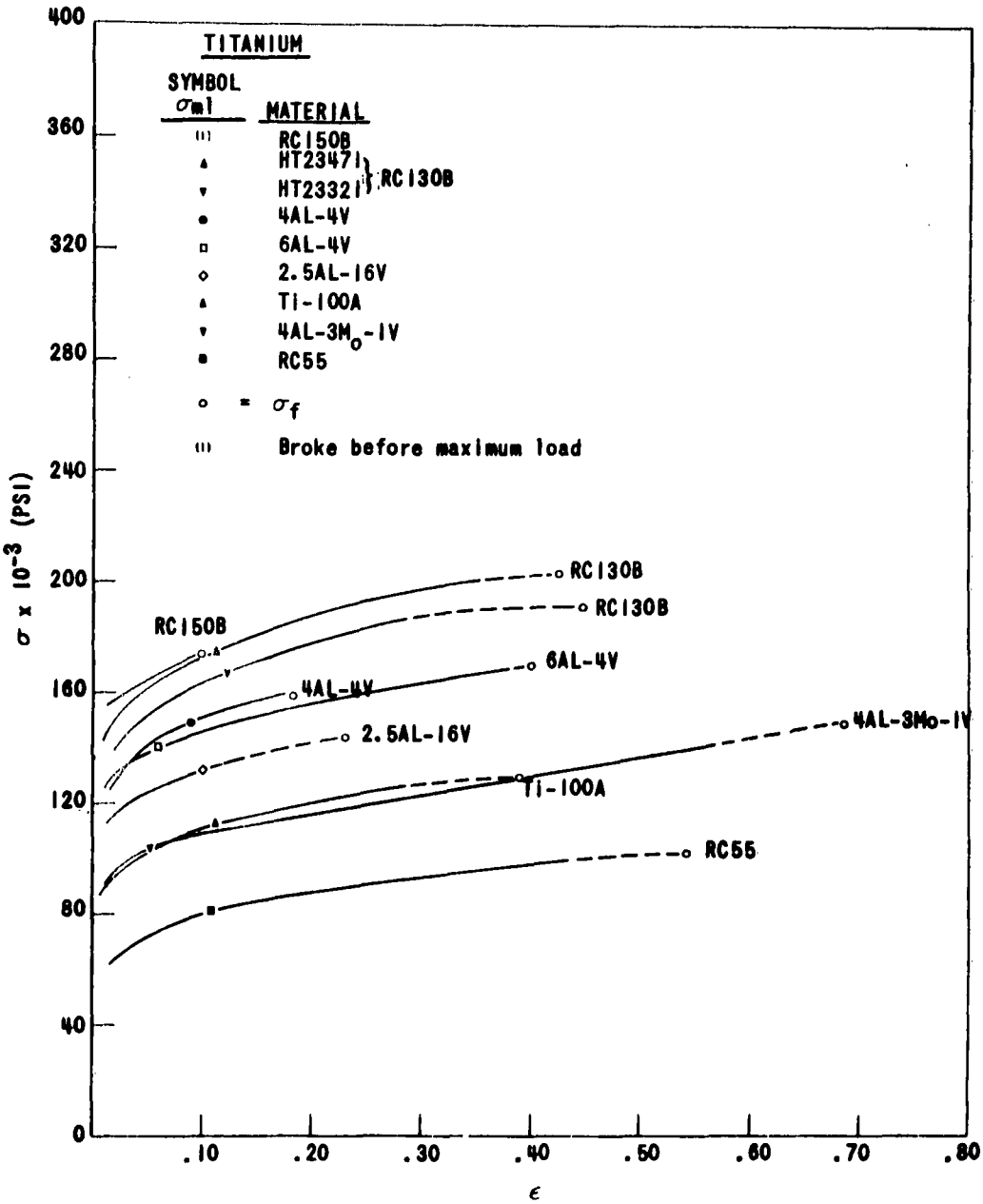
CRUCIBLE 56 TEMPERATURE TEMPERED STRESS-STRAIN CURVES FOR AM350 AT VARIOUS AGED CONDITIONS

FIGURE 4



ROOM TEMPERATURE TRUE STRESS-STRAIN CURVES FOR AM350 AT VARIOUS AGED CONDITIONS

FIGURE 5



ROOM TEMPERATURE TRUE STRESS-STRAIN CURVES FOR "AS RECEIVED" TITANIUM MATERIALS TESTED

FIGURE 6

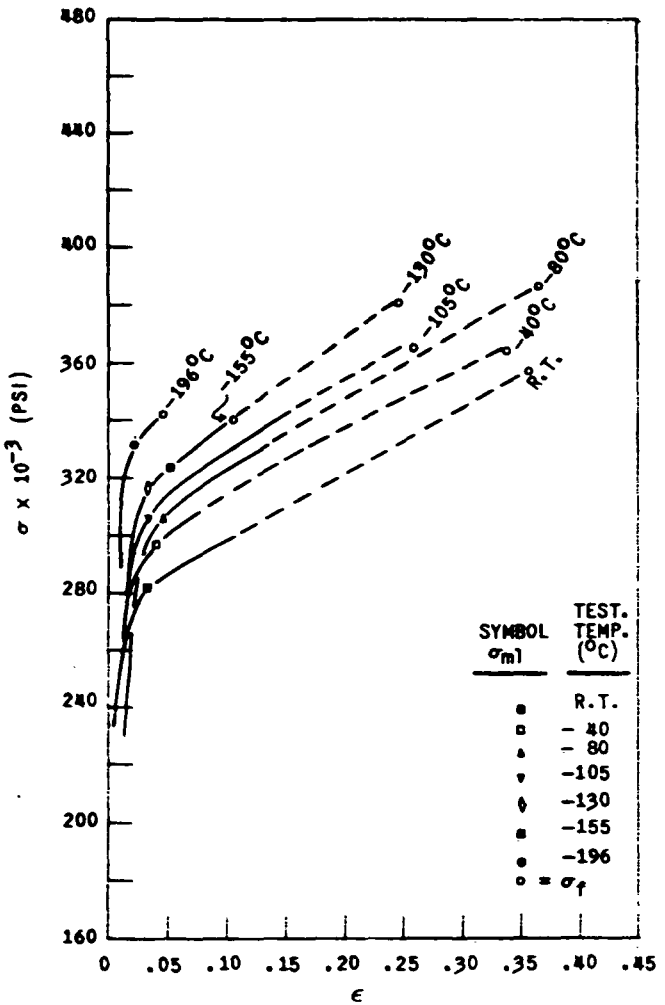


FIGURE 7: TRUE STRESS-STRAIN CURVES OF VASCOJET 1000, TEMPERED AT 700°F, AT TEMPERATURES OF R.T. TO —196°C

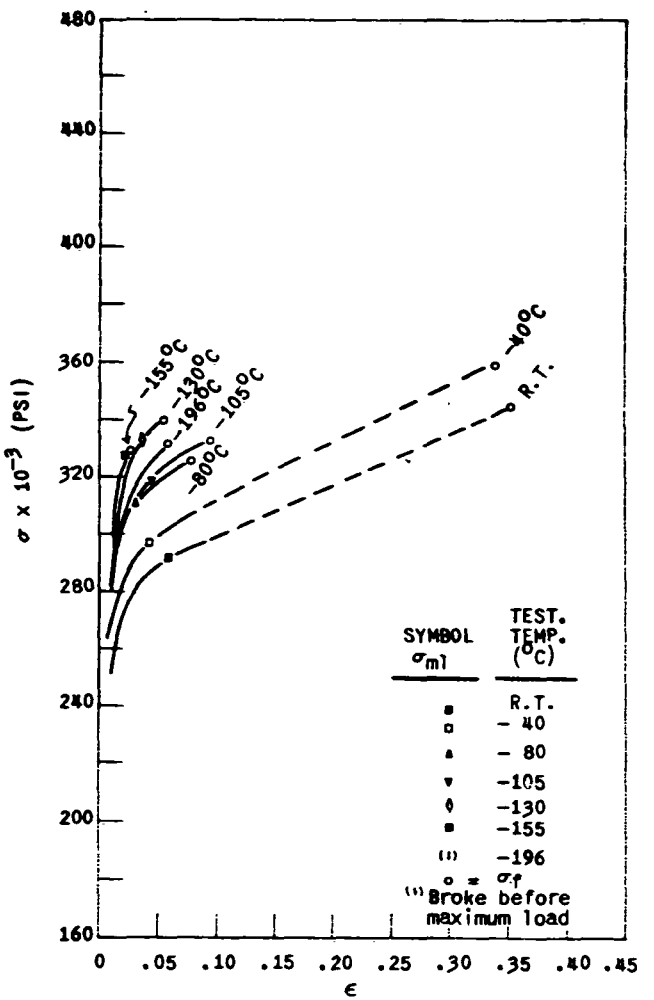
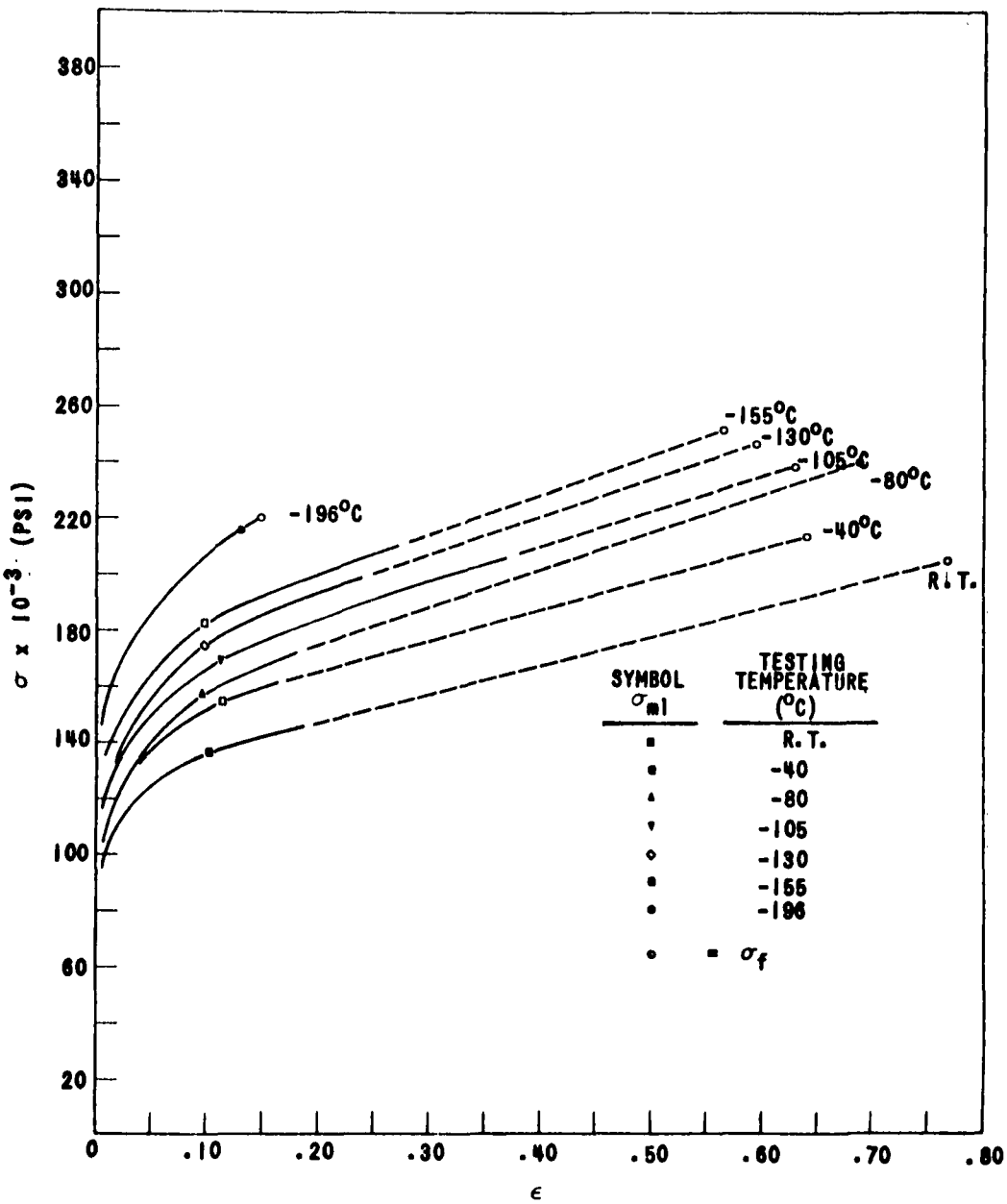


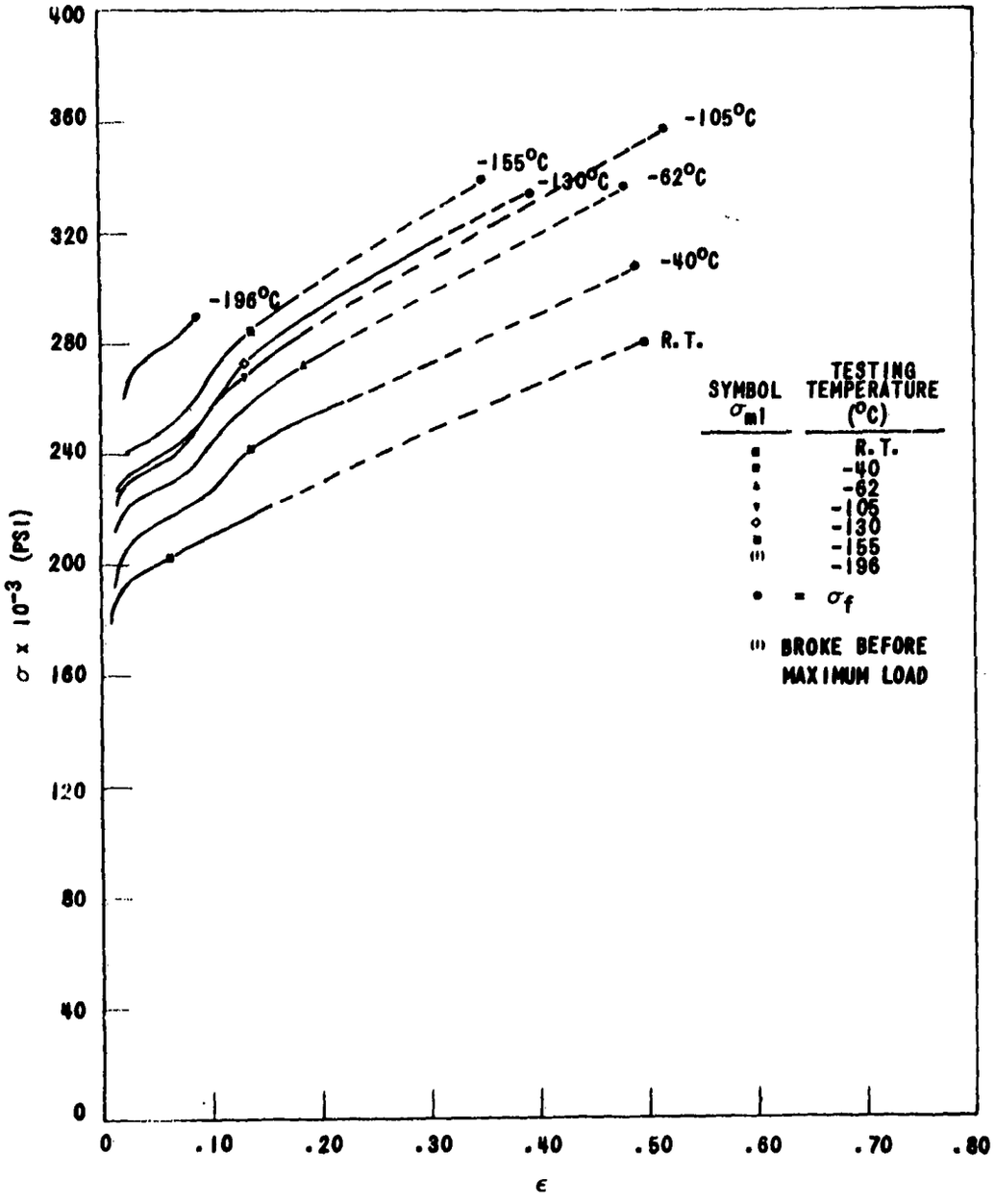
FIGURE 8: TRUE STRESS-STRAIN CURVES OF VASCOJET 1000, TEMPERED AT 1000°F, AT TEMPERATURES OF R.T. TO —196°C

FIGURES 7 & 8



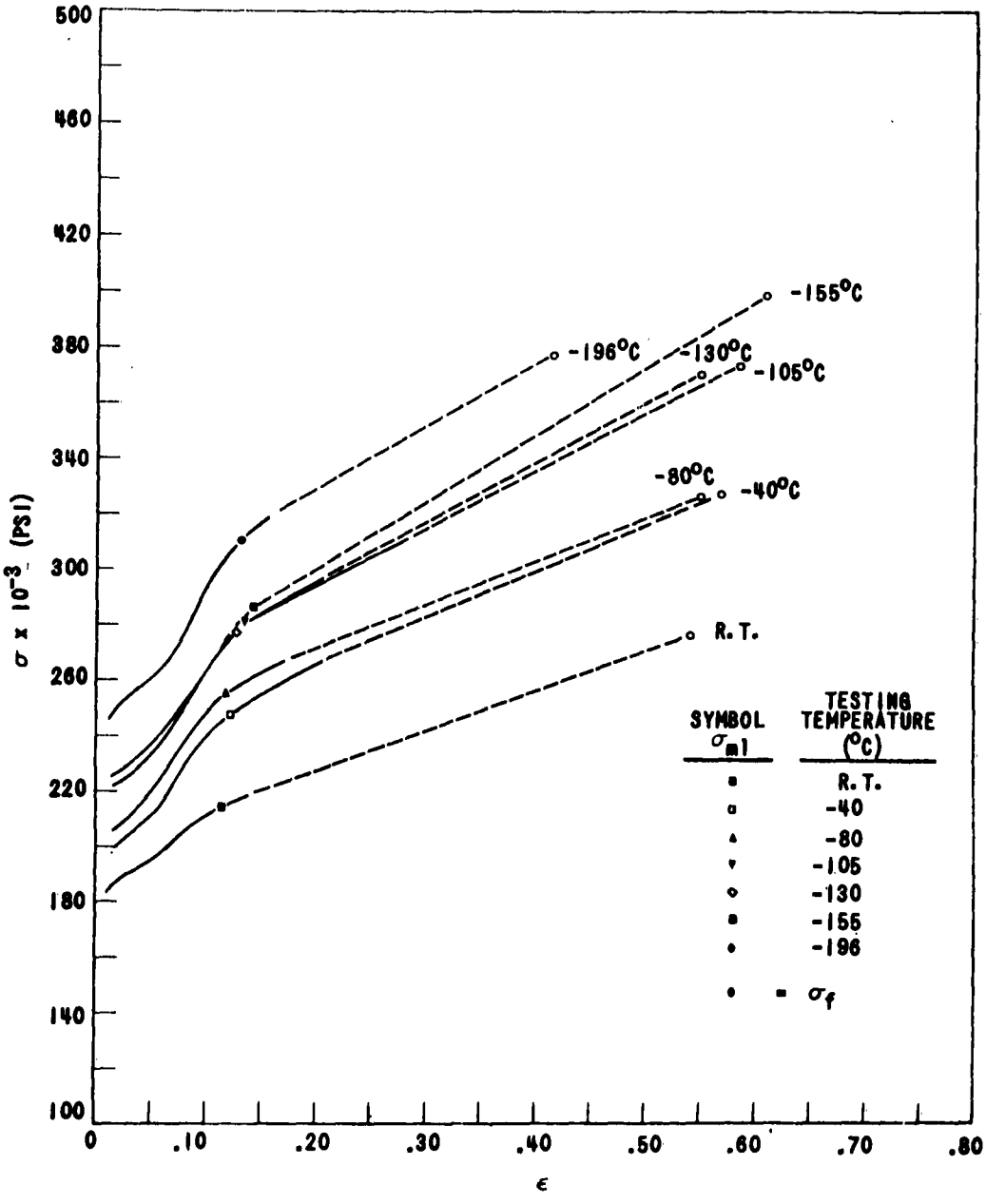
TRUE STRESS-STRAIN CURVES OF VASCOJET 1000, TEMPERED AT 1300°F, AT TEMPERATURES OF R.T. TO -196°C

FIGURE 9



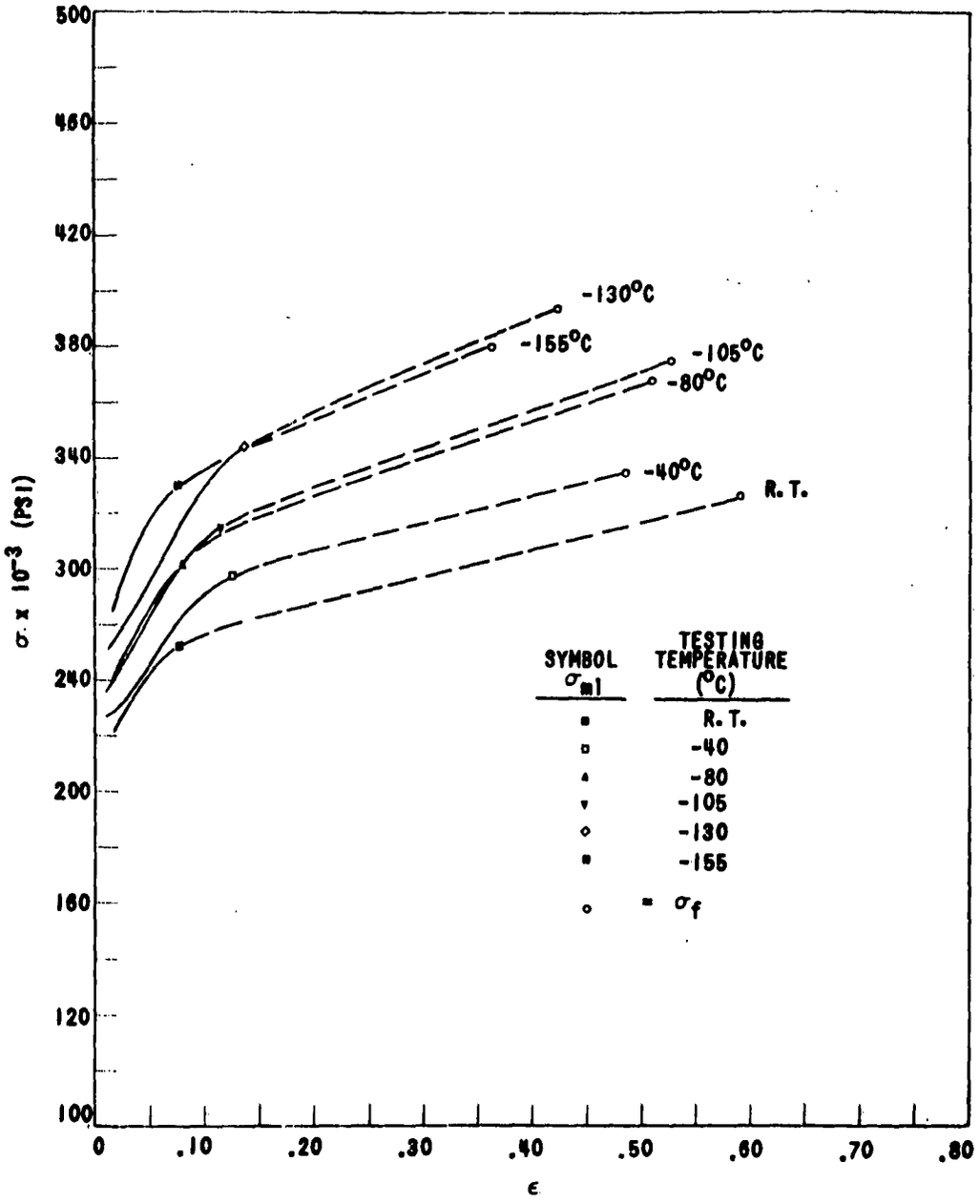
TRUE STRESS-STRAIN CURVES OF AM350, AGED AT 850°F AT TEMPERATURES OF R.T. TO -196°C

FIGURE 10



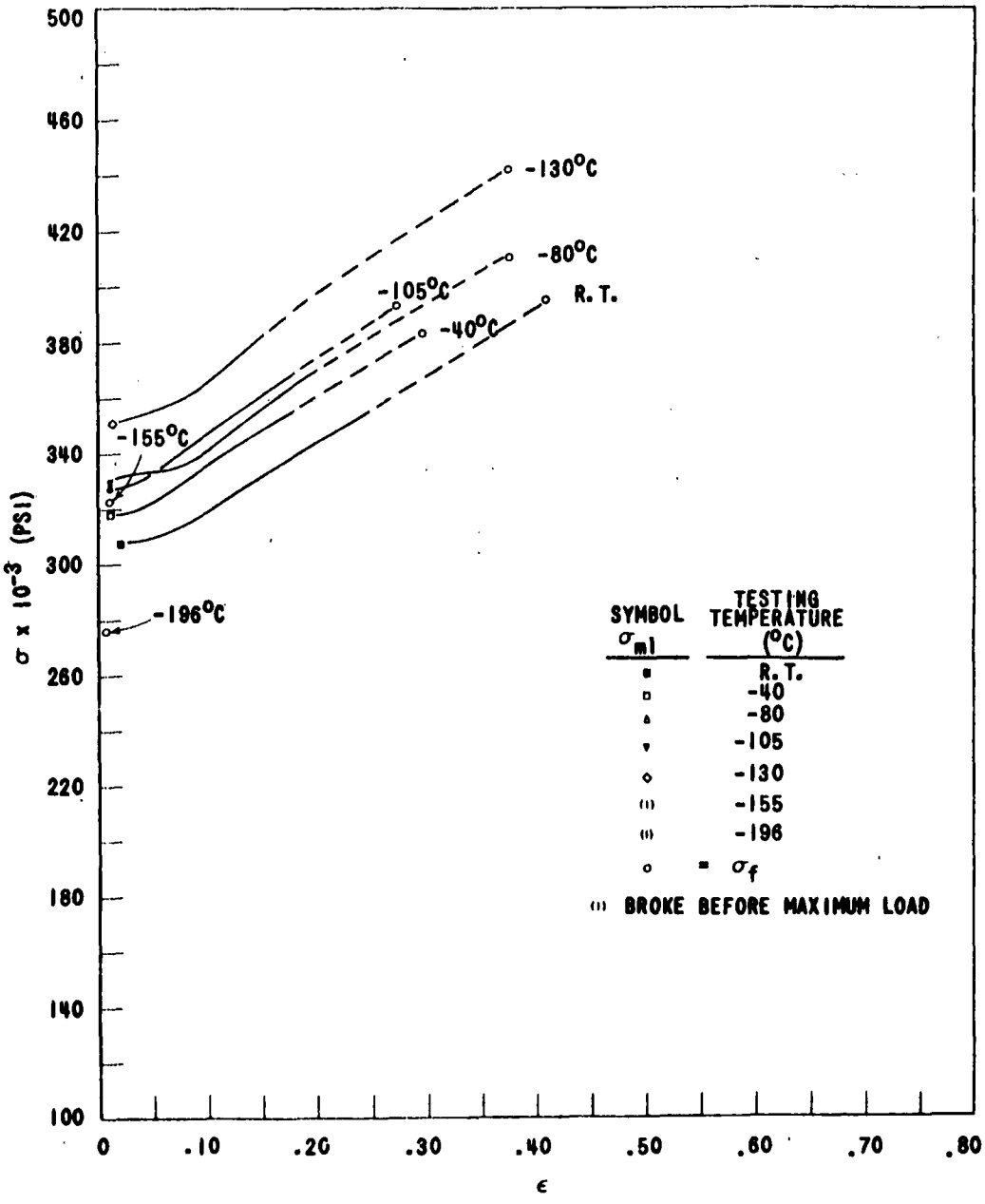
TRUE STRESS-STRAIN CURVES OF AM350, AGED AT 900°F, AT TEMPERATURES OF R.T TO -196°C

FIGURE 11



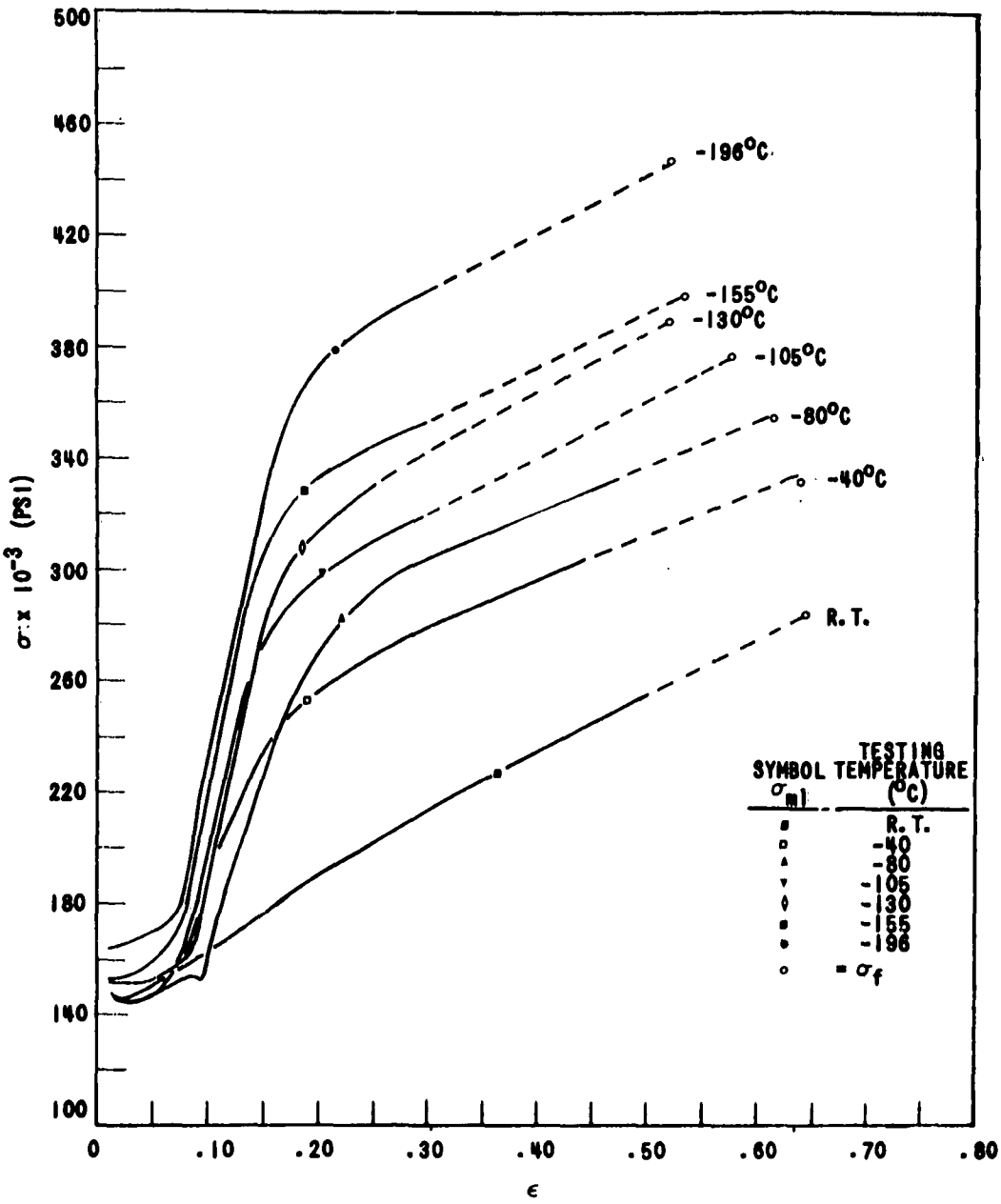
TRUE STRESS-STRAIN CURVES OF AM350, AGED AT 1050°F, AT TEMPERATURES OF R.T. TO -155°C

FIGURE 12



TRUE STRESS-STRAIN CURVES OF AM355 AT TEMPERATURES OF R.T. TO -196°C

FIGURE 13



TRUE STRESS-STRAIN CURVES OF 301 STAINLESS STEEL AT TEMPERATURE OF R.T. TO -196°C

FIGURE 14

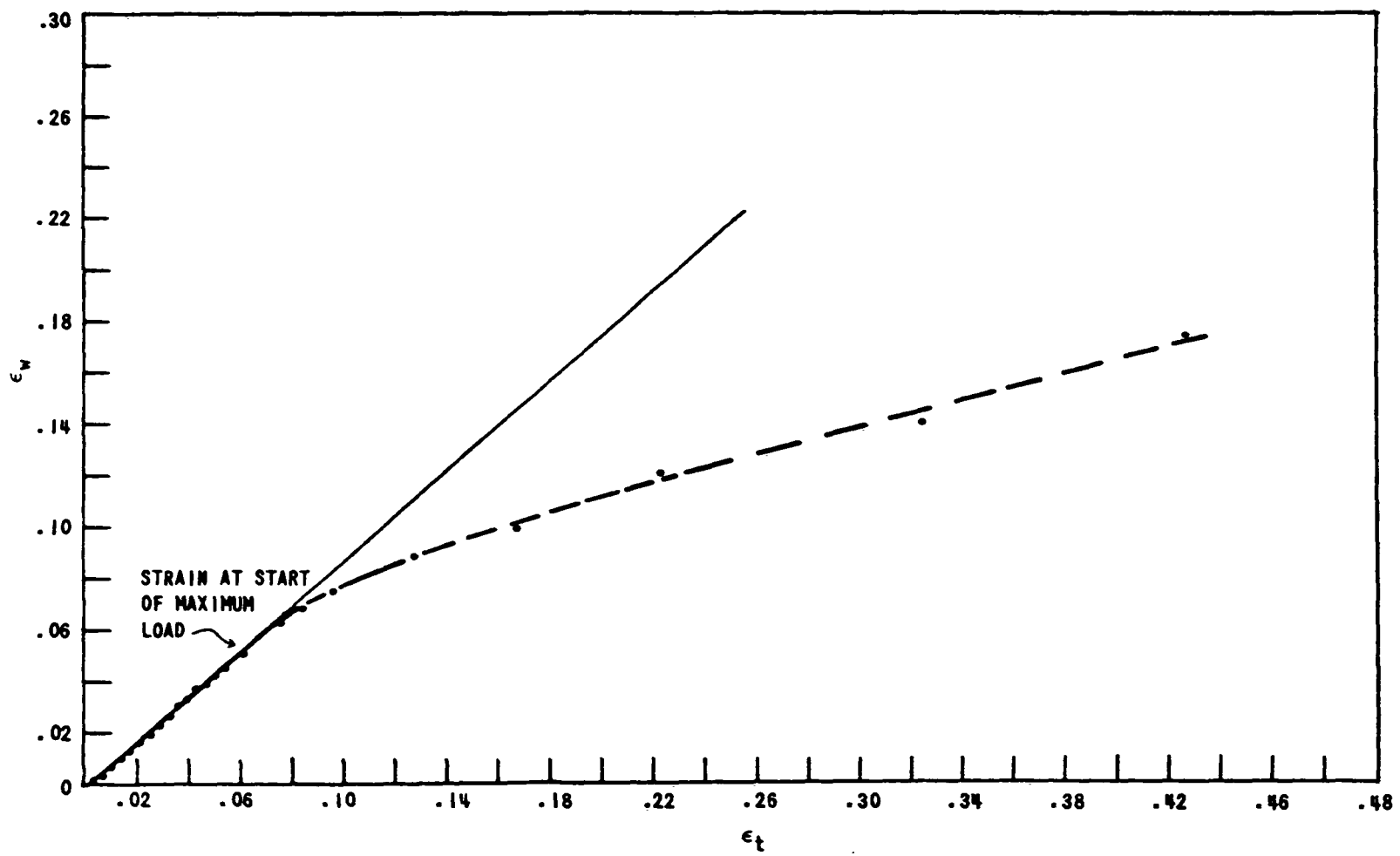
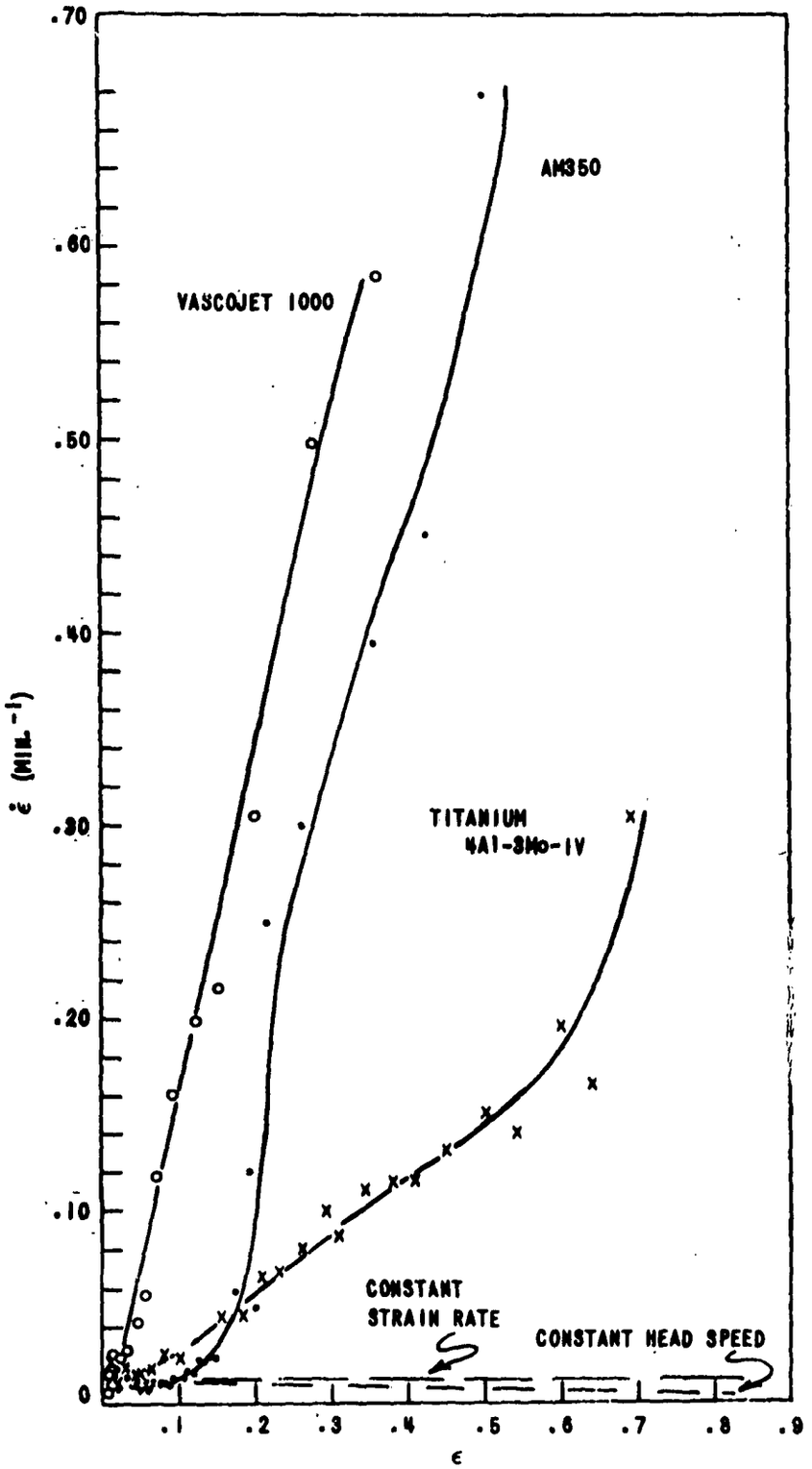


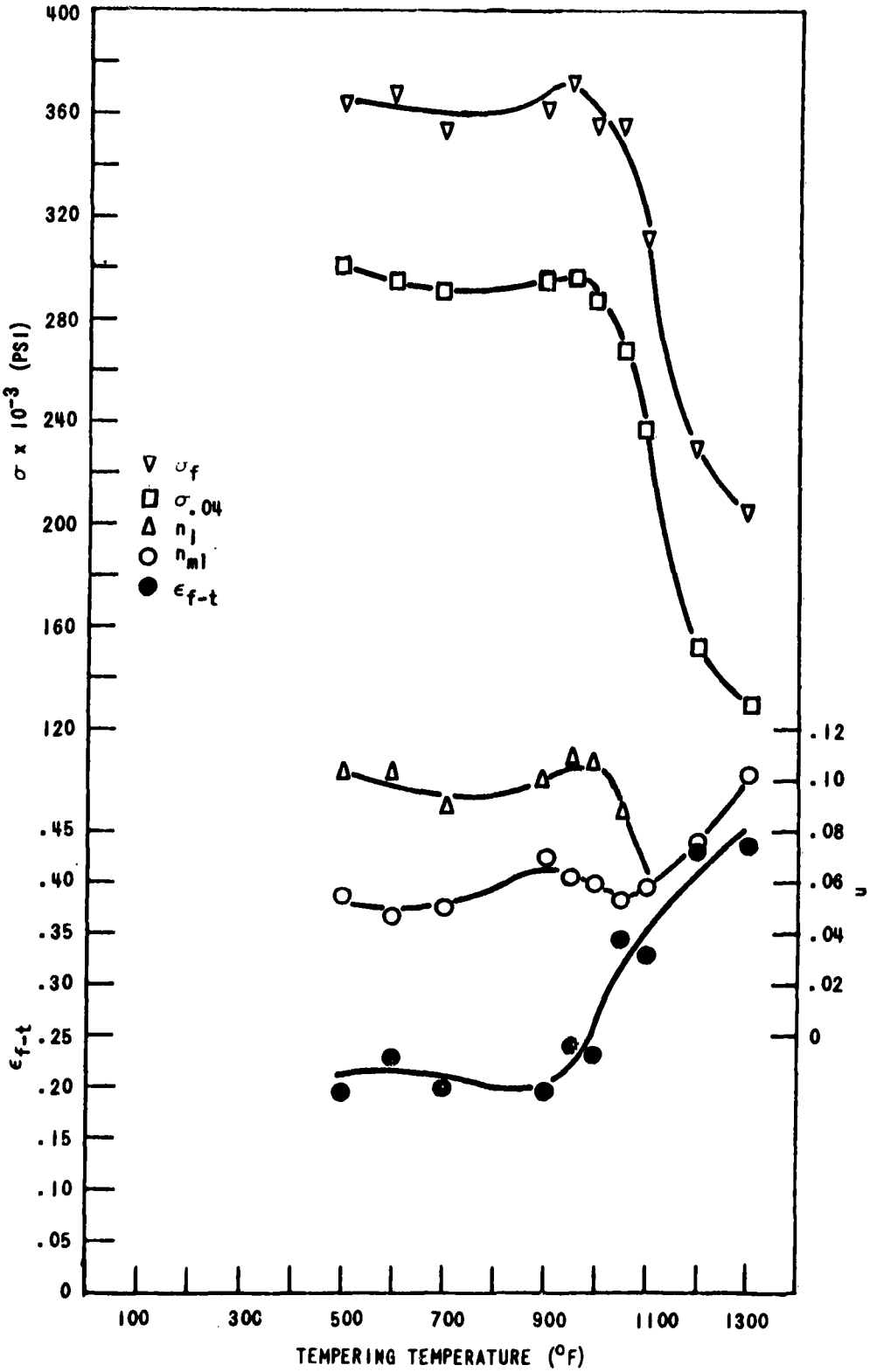
FIGURE 15

WIDTH STRAIN VERSUS THICKNESS STRAIN FOR AM350, AGED AT 1000°F AND TESTED AT ROOM TEMPERATURE



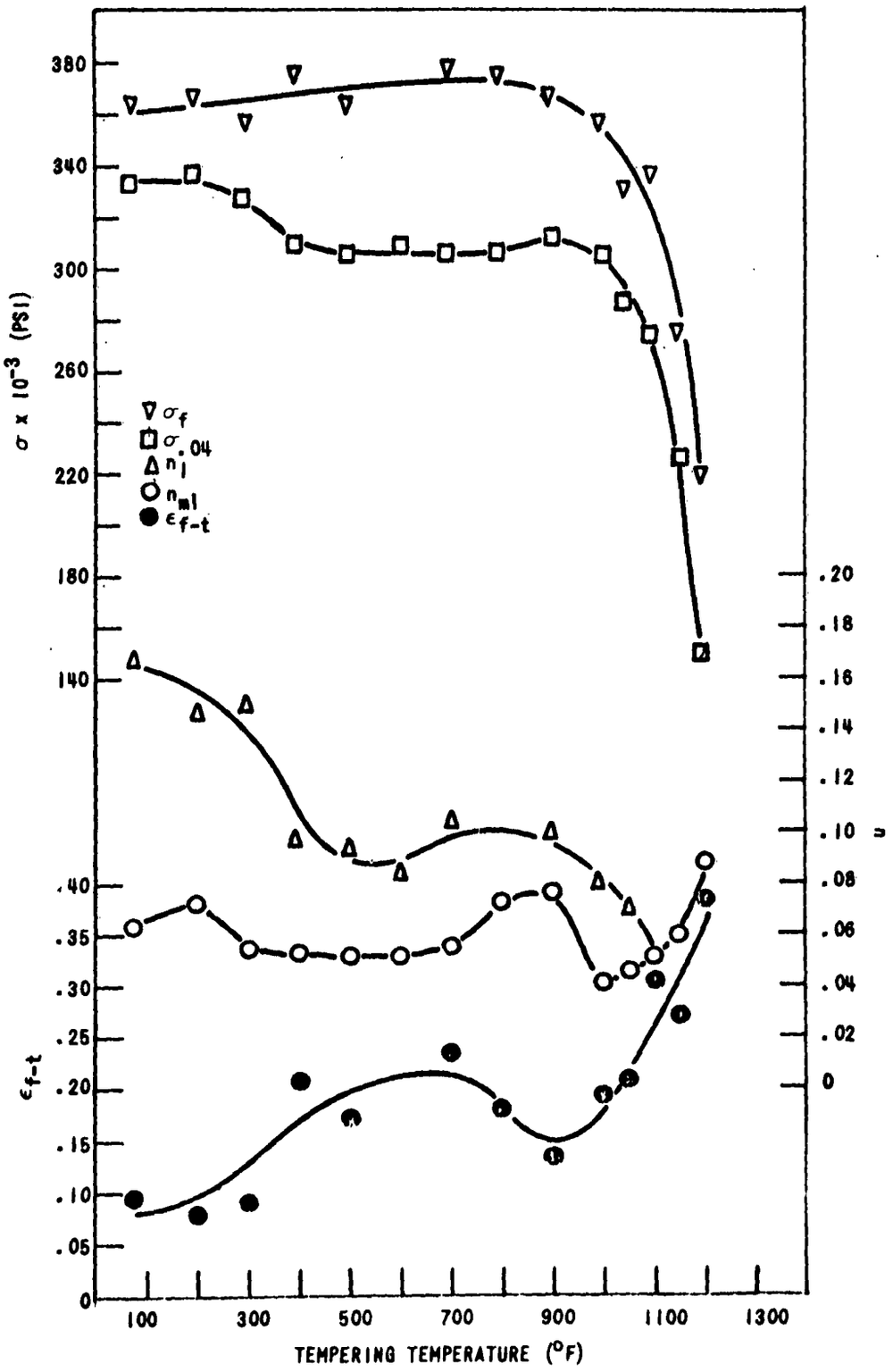
STRAIN RATE VERSUS STRAIN FOR ROOM TEMPERATURE TESTS OF VASCOJET 1000, 700°F TEMPER - AM350, 900°F AGE - Ti-4Al-3Mo-1V AS RECEIVED CONDITION

FIGURE 16



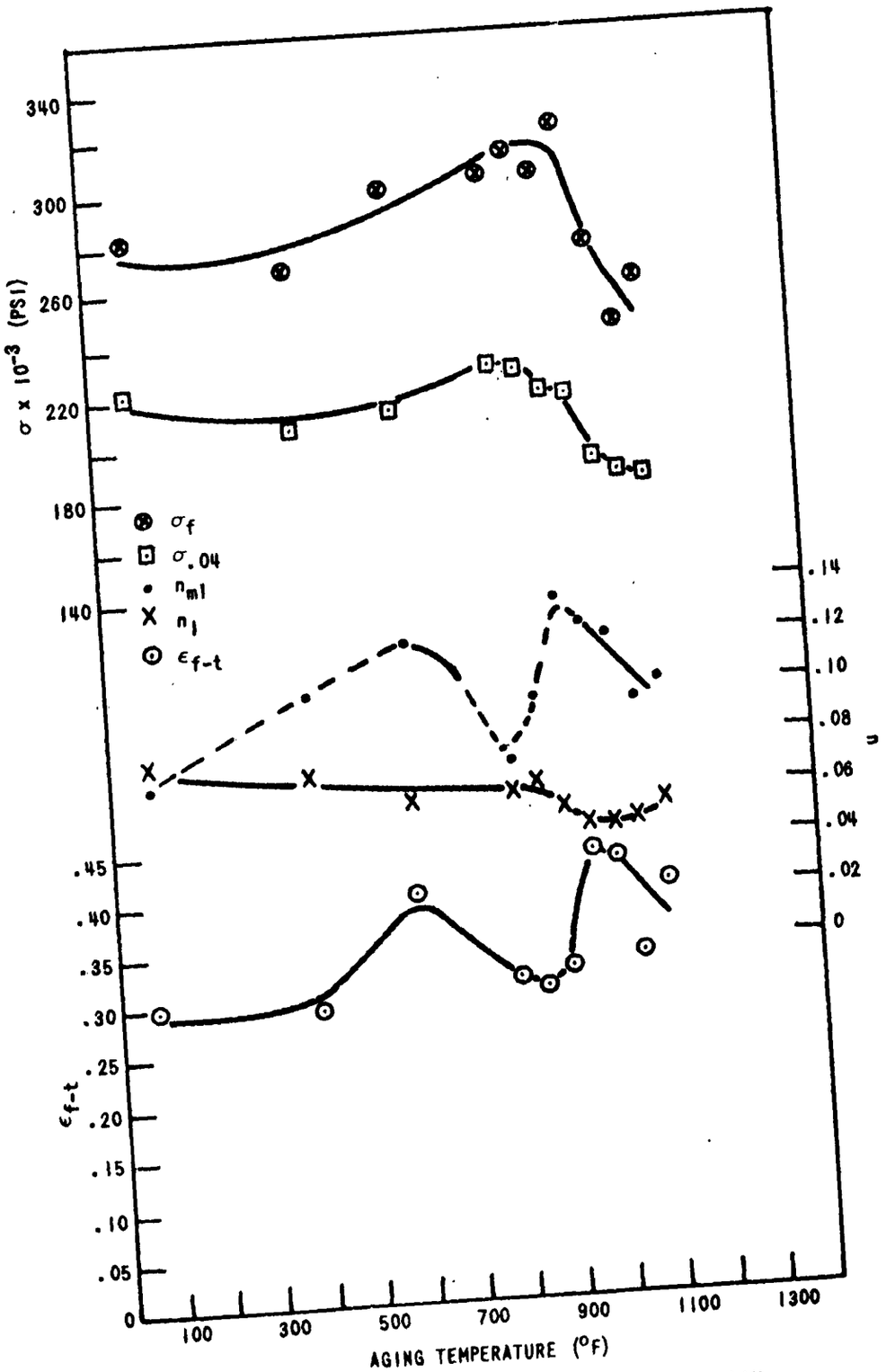
SELECTED ROOM TEMPERATURE TRUE STRESS-STRAIN PROPERTIES OF VASCOJET 1000 VERSUS TEMPERING TEMPERATURES

FIGURE 17



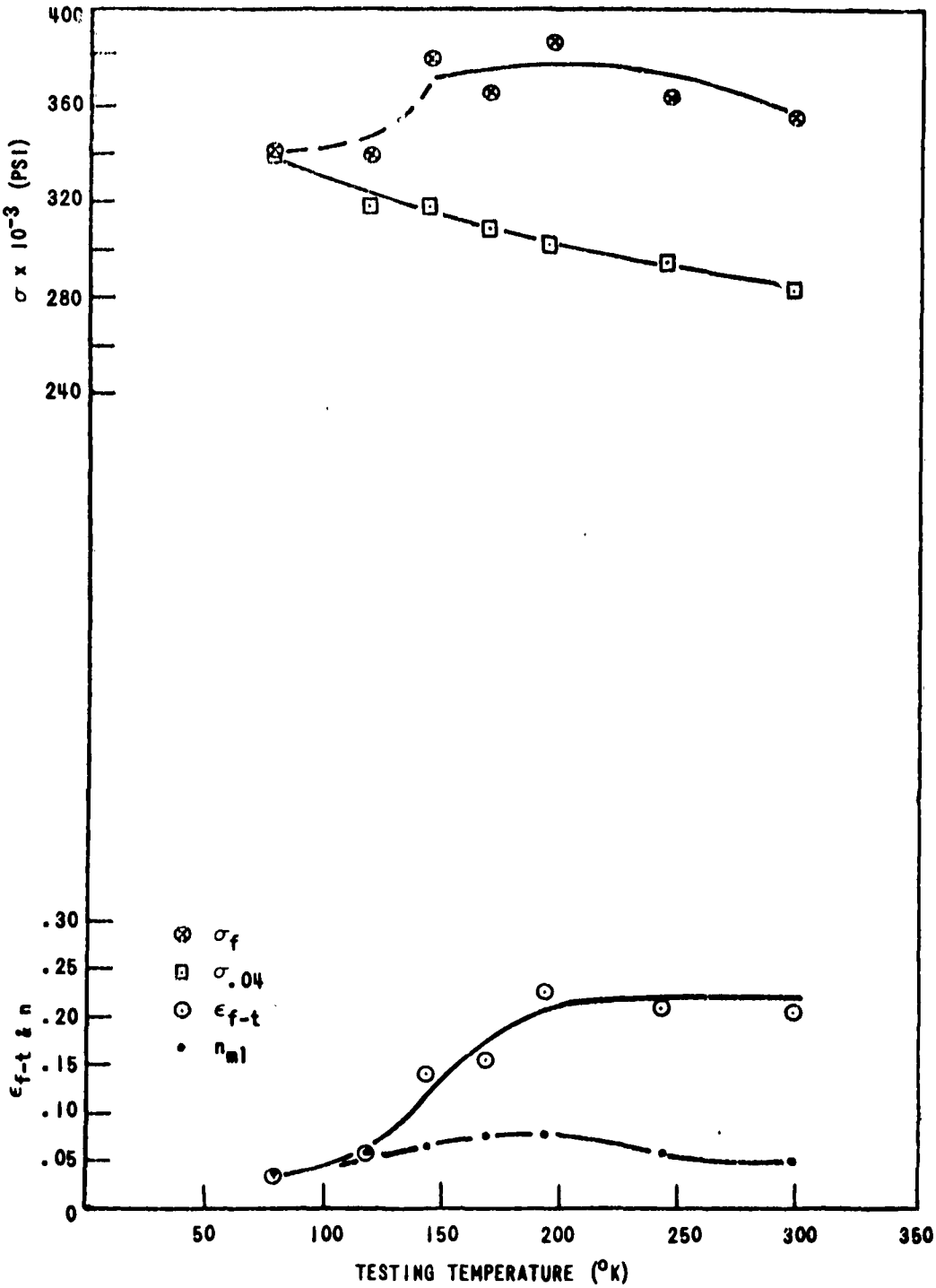
SELECTED ROOM TEMPERATURE TRUE STRESS-STRAIN PROPERTIES OF CRUCIBLE 56 VERSUS TEMPERING TEMPERATURE

FIGURE 18



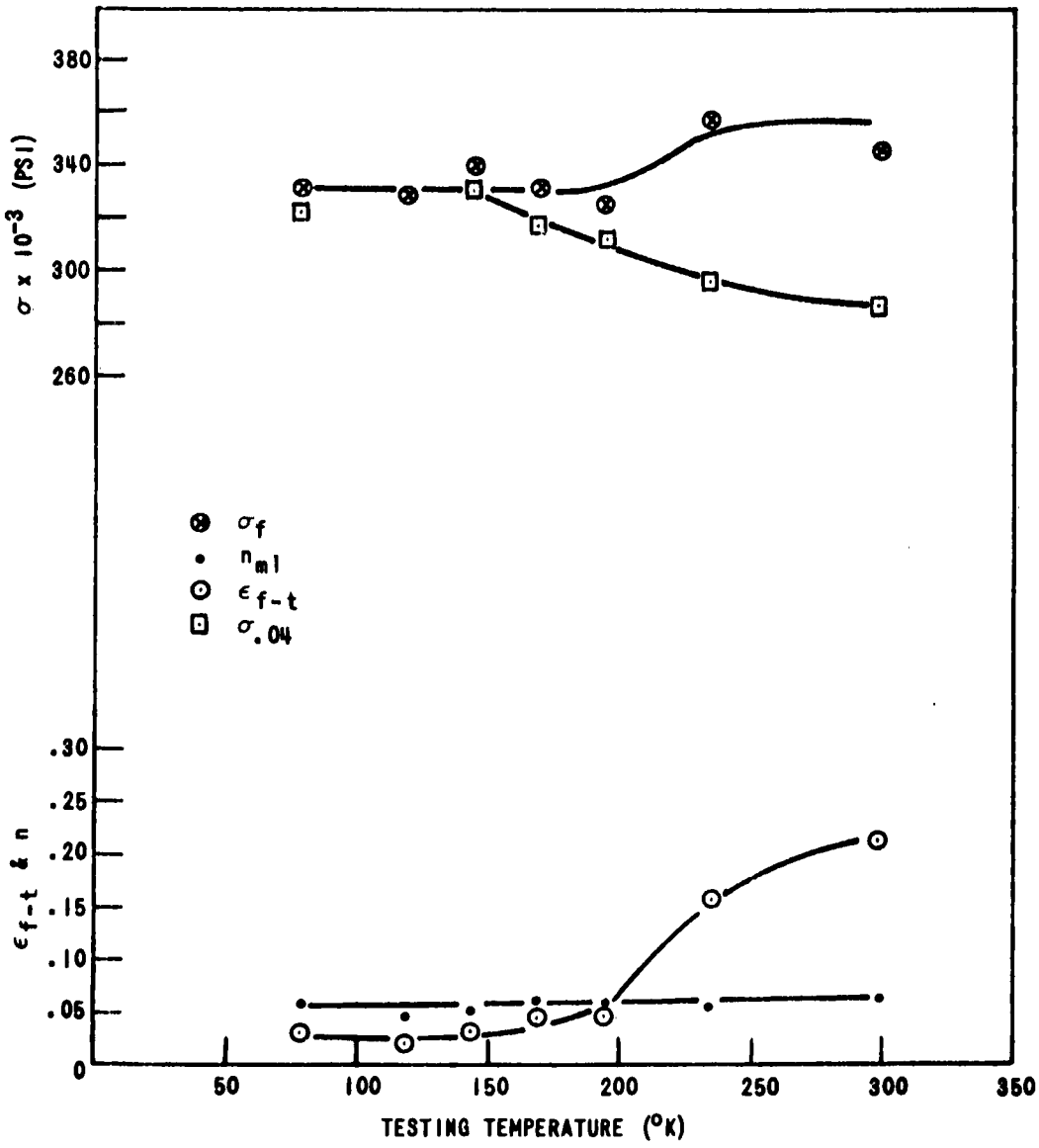
SELECTED ROOM TEMPERATURE TRUE STRESS-STRAIN PROPERTIES OF AM350 VERSUS AGING TEMPERATURE

FIGURE 19



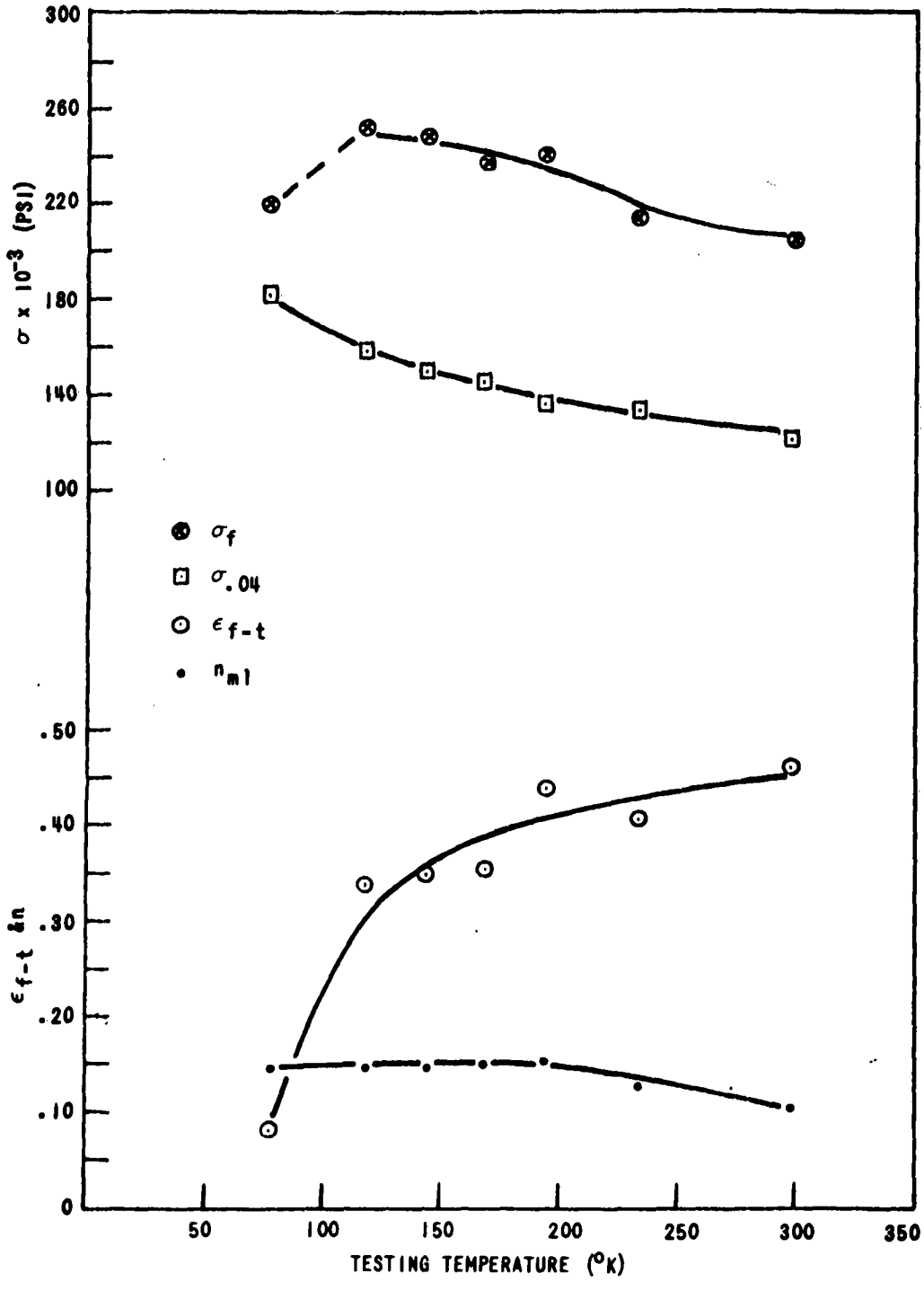
LOW TEMPERATURE TRUE STRESS-STRAIN PROPERTIES OF VASCOJET 1000, TEMPERED AT 700°F

FIGURE 20



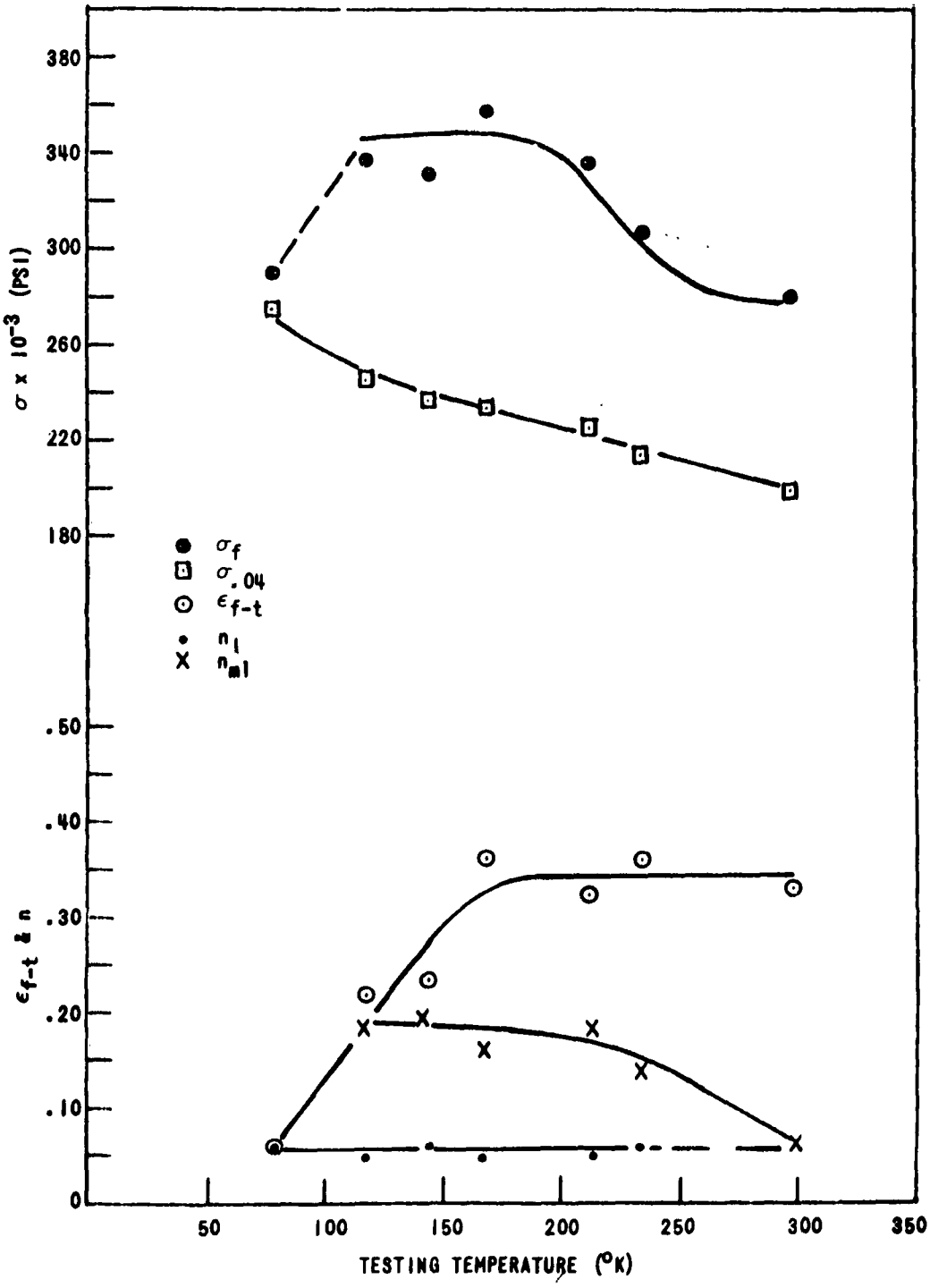
LOW TEMPERATURE TRUE STRESS-STRAIN PROPERTIES OF VASCOJET 1000, TEMPERED AT 1000°F

FIGURE 21



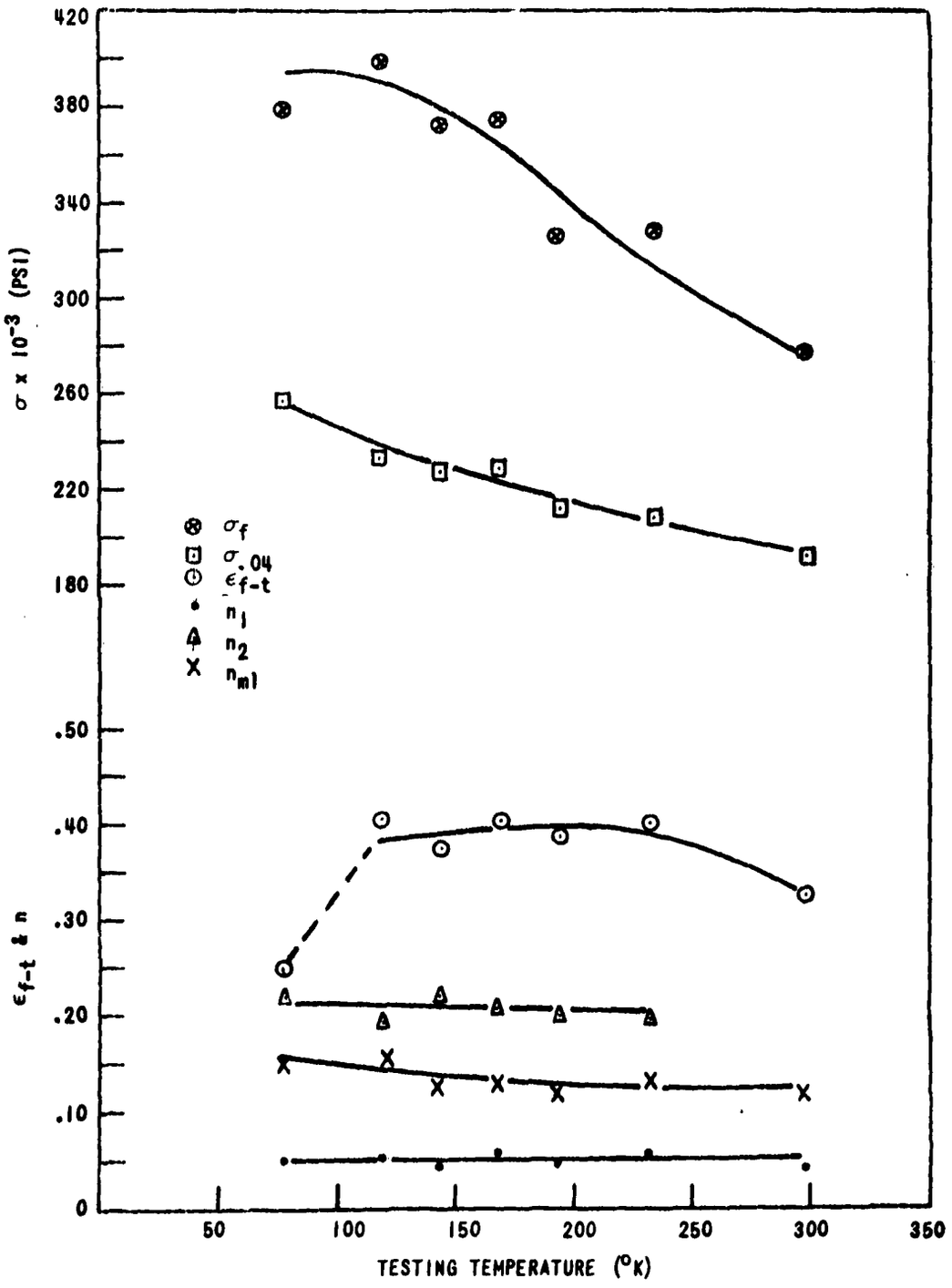
LOW TEMPERATURE TRUE STRESS-STRAIN PROPERTIES OF VASCOJET 100C, TEMPERED AT 1300°F

FIGURE 22



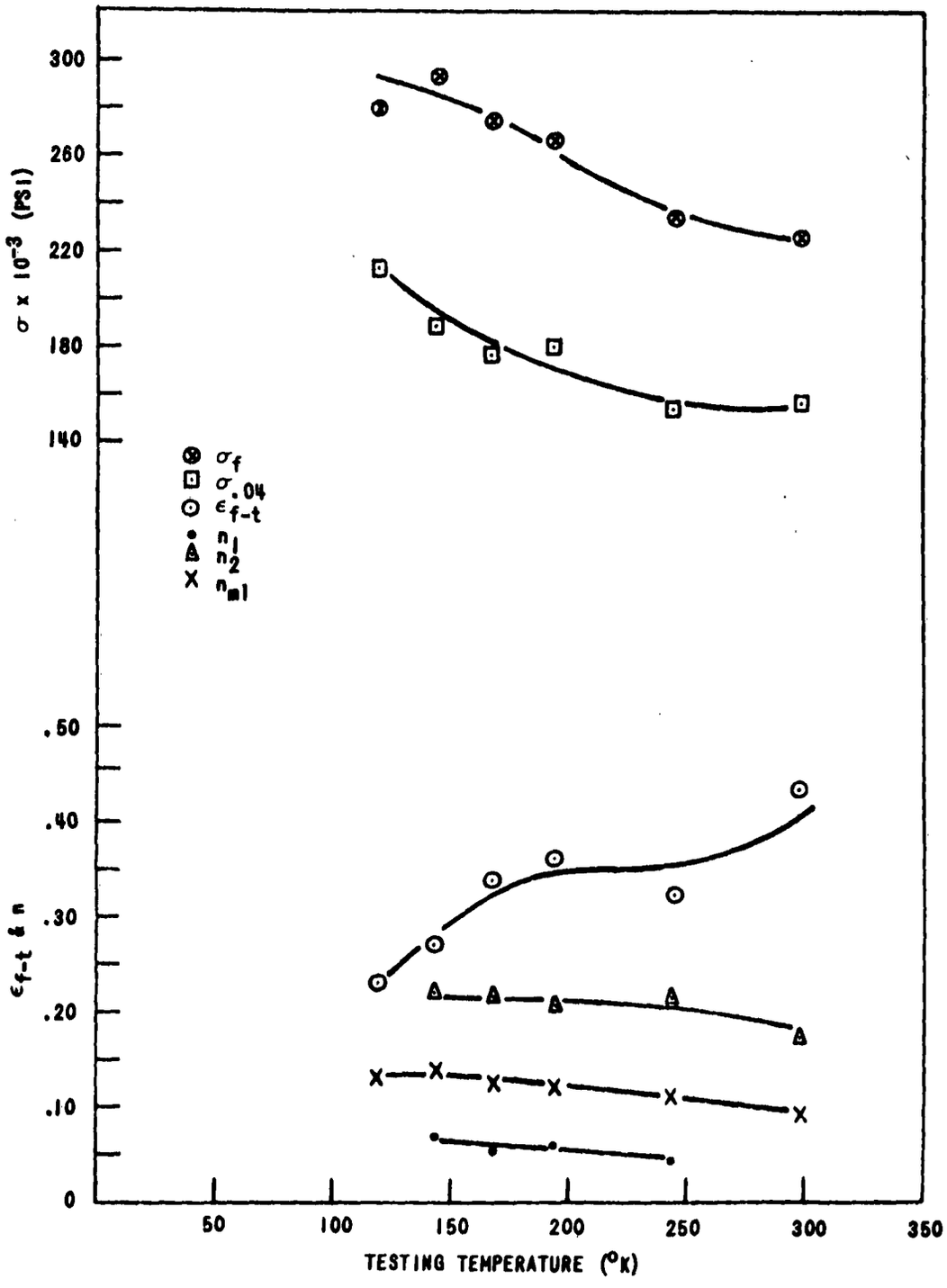
LOW TEMPERATURE TRUE STRESS-STRAIN PROPERTIES OF AM350, AGED AT 850°F

FIGURE 23



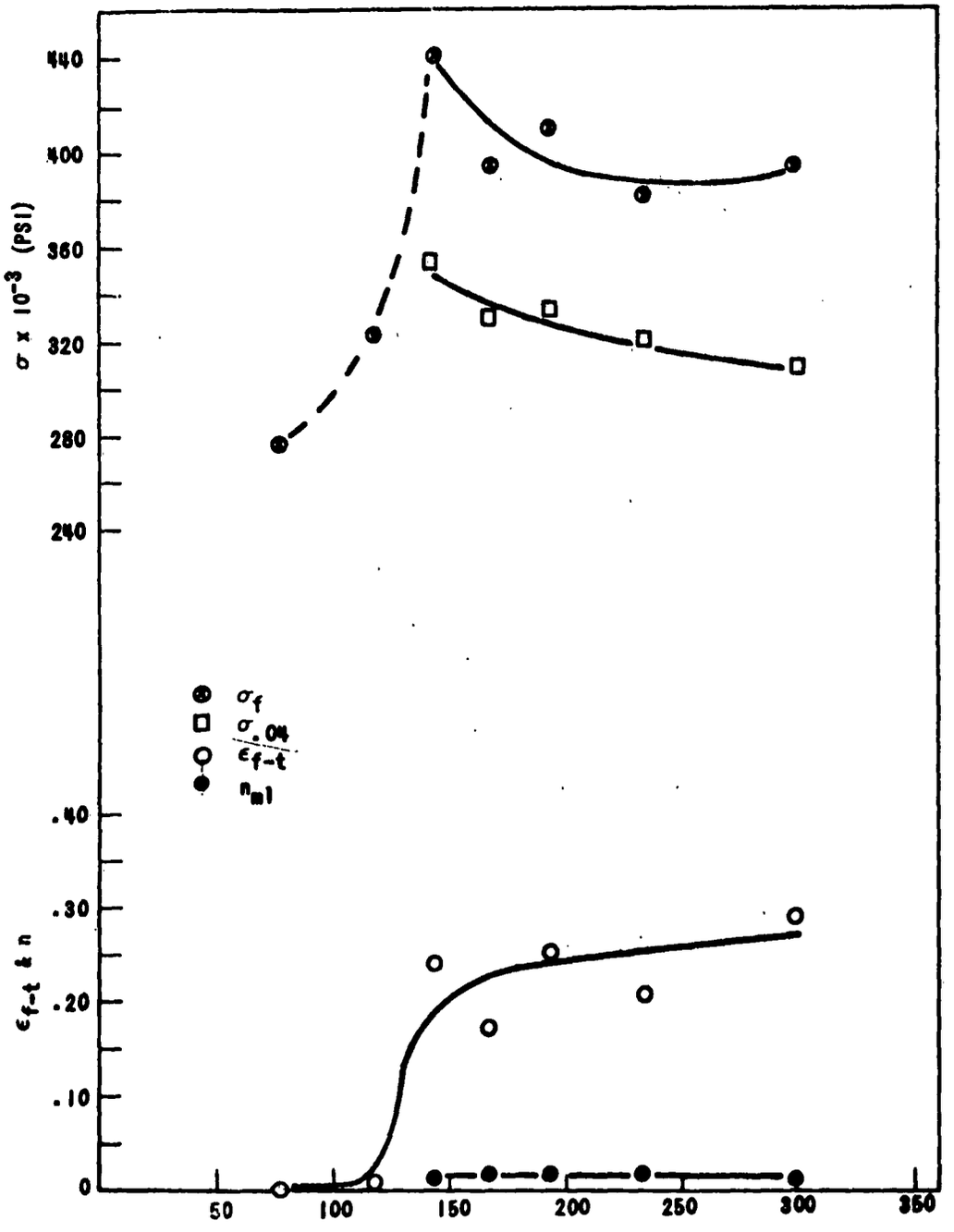
LOW TEMPERATURE TRUE STRESS-STRAIN PROPERTIES OF AM350, AGED AT 900°F

FIGURE 24



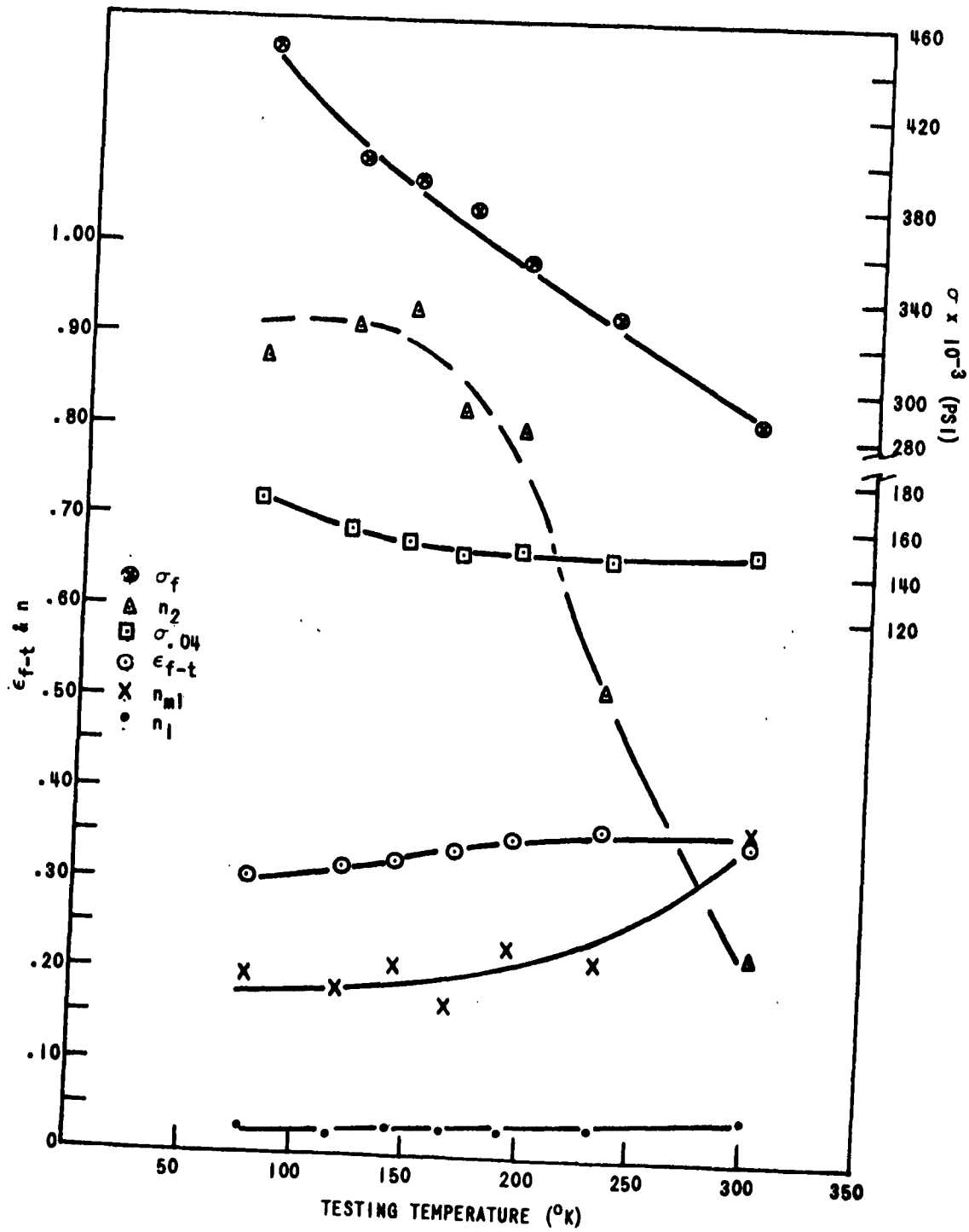
LOW TEMPERATURE TRUE STRESS-STRAIN PROPERTIES OF AM350, AGED AT 1050°F

FIGURE 25



LOW TEMPERATURE TRUE STRESS-STRAIN PROPERTIES OF AM355, COLD WORKED 30 PERCENT

FIGURE 26



LOW TEMPERATURE TRUE STRESS-STRAIN PROPERTIES OF 301 S.S. 3/4 HARD CONDITION AS RECEIVED

FIGURE 27

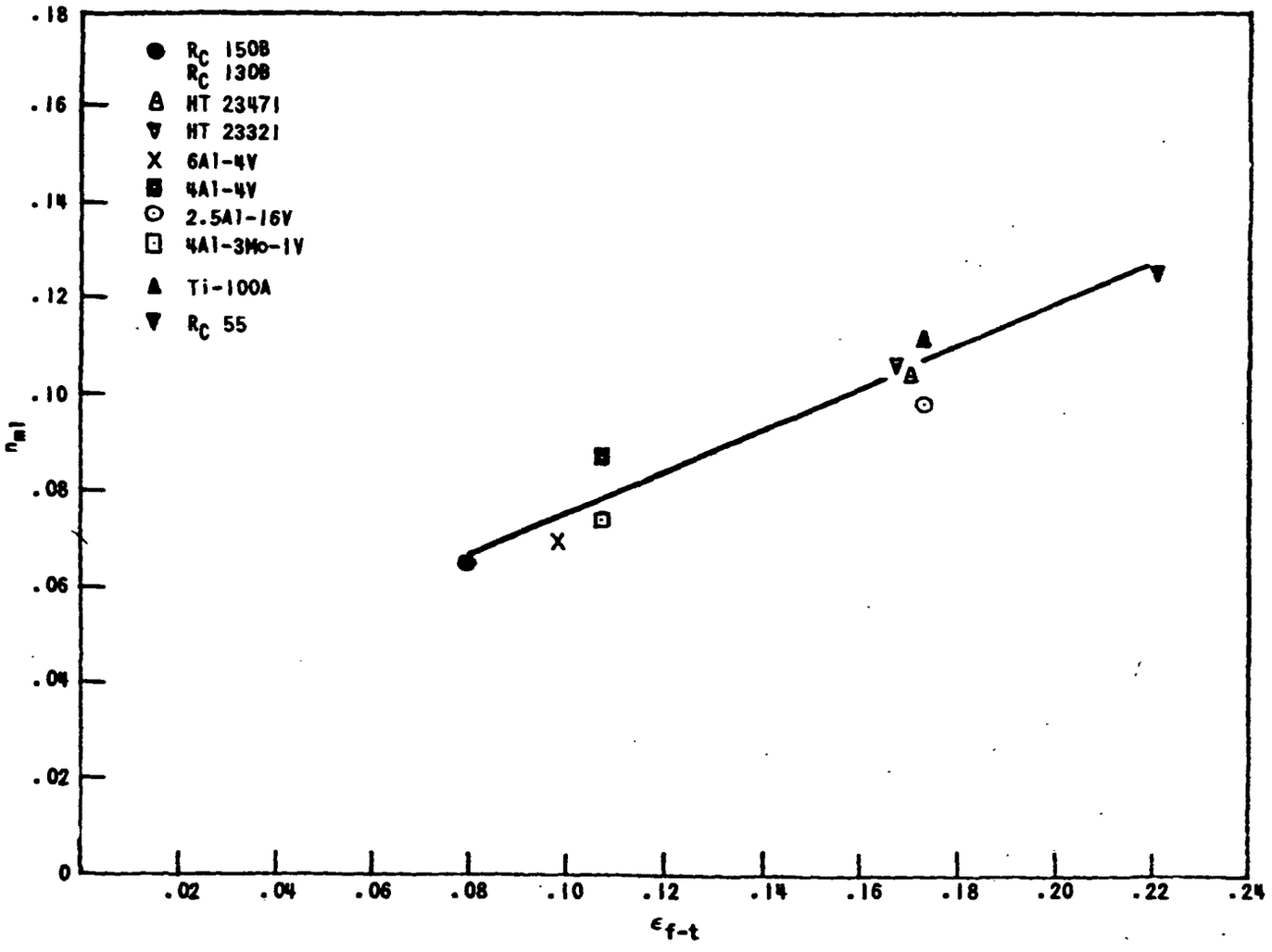


FIGURE 28

STRAIN HARDENING EXPONENT (n_{m1}) AS A FUNCTION OF FRACTURE STRAIN (ϵ_{f-t}) FOR TITANIUM MATERIALS TESTED AT ROOM TEMPERATURE

THE EFFECT OF HEAT TREATMENT UPON THE NOTCH TOUGHNESS OF HIGH STRENGTH TITANIUM ALLOY SHEET

DONALD A. CORRIGAN

Watertown Arsenal Laboratories

Introduction

The notch toughness of high strength sheet materials is a poorly understood phenomenon of much recent interest. Along with related welding problems, the lack of notch toughness limits the utilizable strength of presently available engineering materials. An area that has received little systematic study is the effect of heat treatment upon the notch toughness of high strength commercial titanium alloys. This report includes information on the effect of heat treatment upon the notch tensile behavior of Ti-3Al-13V-11Cr(B120VCA), Ti-2Fe-2Cr-2Mo (Ti-140A), Ti-5Al-1.5Fe-1.4Cr-1.2Mo (Ti-155A), and Ti-4Al-3Mo-1V.

Before presenting the data, it seems desirable to discuss the significance of notch tensile strength and the often used notch strength -- ultimate tensile strength ratio. The notch strength is defined as the maximum load reached in the test divided by the cross-sectional area under the notch. Incorporated in this measurement are at least four distinctly different possible load limiting mechanisms. These are:

1. Initiation of a crack at the notch tip, slow propagation followed by instability and rapid propagation, a load limiting mechanism similar to that in the G_c test. Here the crack propagation resistance of the material is the notch strength limiting property.

2. Rapid crack propagation immediately following initiation of a natural crack at the notch tip. The condition for rapid propagation is more than met upon crack initiation and the load is limited by the resistance of the material to crack initiation.

3. Slow crack propagation, followed by a load maximum prior to rapid propagation. Here, the slow crack propagation reduces the load carrying cross section of the specimen faster than work hardening increases load carrying capability. This mechanism is similar to that encountered in G_c tests of highly ductile materials such as pure titanium and stainless steels.

4. Gross yielding and plastic instability, a mechanism in which the notch has little or no effect.

For equivalent notch strengths, raising the tensile strength reduces the notch ratio. If mechanism 2 is controlling, the notch raio is of little meaning. A notch ratio of 1.0 or greater implies mechanism 4 is probably load limiting.

The above discussion indicates that the notch strength can be a measure of any of several phenomena. The edge notch tensile test, however, offers a most convenient method for qualitatively evaluating a largenumber of heat treatments where little is known about notch toughness effects.

Materials

The titanium alloys employed in this investigation were received as 1/16" hot rolled hand mill sheet. Compositions are listed below:

Alloy	C	N	H	Fe	Al	V	Cr	Mo
Ti-3Al-13V-11Cr	.012	0029	.004	.26	2.8	13.7	10.4	---
Ti-140A	.016	.010	.005	2.0	---	----	2.3	1.9
Ti-4Al-3Mo-1V	.021	.017	.013	.12	4.2	3.1	----	0.9
Ti-155A	.013	.013	.090	1.3	5.2	----	1.4	1.2

The Ti-140A sheet was mill annealed while the other sheets were received from the mill in the solution treated condition.

Experimental Procedure

Single conventional and duplicate edge-notched tensile tests were used to measure the notch tensile behavior of the titanium alloys. All specimens were taken parallel to the final direction of rolling. The notch tensile specimen was similar to that recommended by the ASTM Committee on Fracture Testing of High-Strength Sheet Materiels[1] i.e., it was pin loaded, 1" wide with .15", 60° edge notches, with .001" maximum notch root radii. Testing was performed in conjunction with the recommendations of the committee.

All specimens were heat-treated in air as 3" x 9" blanks, grit blasted and pickled in a solution of 2%HF-30%HNO_3 in hot tap water for fifteen minutes. This cleaning technique has been shown to minimize contamination and have no deleterious effect upon notch tensile strength.

Results and Discussion

The heat-treatments studied, and the smooth and notch tensile data obtained for the four titanium alloys are presented in Tables I-IV. To facilitate discussion of these results, each alloy will be considered individually before comparisons are made among the different alloy systems.

Ti-3Al-13V-11Cr

Basic Metallurgy - This alloy is entirely beta phase when received from the mill in the annealed condition. Upon simple aging, at all practical transformation temperatures, this alloy undergoes the following reaction:

$$\beta \longrightarrow \alpha + \beta \longrightarrow \alpha + \beta + TiCr_2$$

TTT diagrams are avaiable in the literature.[2,3] The exact positions of the $\beta/\alpha+\beta$ and $\alpha+\beta/\alpha+\beta+TiCr_2$ lines are a function of both chemistry and residual strain, and therefore will vary from heat-to-heat and with sheet processing technique. It has been suggested that the omega phase may also be a beta decomposition product, but because of the inherent difficulty of determining the existance of this phase it has not been included in the published TTT diagrams. Omega is believed to be chiefly responsible for the low ductility found in high strength sheet after single aging treatments. Duplex aging treatments have been developed for this alloy[3] on the theory that the elimination of the omega phase will result in improved ductility with only a small strength decrease.

Notch Tensile Results - Figure 1 shows a plot of notch strength vs. yield strength for material aged at 800°F and 900°F for various times. Notch strength appears to decrease linearly with increasing yield strength. Figure 2 shows the as received, 1000°F and 1100°F single aged and multiple aged results superimposed upon the relation obtained in Figure 1. It appears that high temperature aging results in the precipitation of brittle intermetallic compounds in times less than 20 hours, and that the brittleness is emphasized as aging times are increased. Short time aging reduced notch strengths without significant yield strength increases. Solute redistribution prior to generalized precipitation has been noted in this alloy.[2] Of the duplex aging treatments used, the low temperature aging followed by short time high temperature aging appeared the best. The other multiple aging treatments offered no improvement upon single aged notch strengths.

Ti-4Al-3Mo-1V

Basic Metallurgy - A TTT for this alloy quenched from high in the alpha-beta field is available in the literature.[2] The as-quenched structure consists of small primary alpha particles in a matrix of beta which has partially transformed to martensite. Aging results in the reaction:

$$(\alpha) + \beta + \alpha' \longrightarrow (\alpha) + \beta + \alpha$$

Lowering the solution temperature will increase the amount of primary alpha and lower the M_s temperature, thereby decreasing the alpha prime-beta ratio in the matrix of the microstructure.

Notch Tensile Results - Figure 3 shows a plot of notch strength vs. yield strength for Ti-4Al-3Mo-1V solution treated at 1650°F or 1450°F and subsequently aged at temperatures from 900-1100°F for various times. For a given yield strength level the higher solution temperature offers higher notch strength. This effect is more lucidly demonstrated in Figure 4. Here NTS/UTS is plotted versus strength. This plot eliminates the ambiguity inherent at low yield strengths where notch sensitivity is low and where notch strength tends to increase with increasing strength level. For a given notch ratio there is at least a 10 ksi strength advantage afforded by the higher solution temperature. Air cooling from 1650°F, followed by low temperature aging, gave notch tensile results comparable to those obtained by water quenching from the lower solution temperature.

Ti-140A

Basic Metallurgy - The physical metallurgy of this alloy has not been studied as thoroughly as the two previous alloys because Ti-140A is not one of the DOD Titanium Sheet Rolling Program alloys. There is no alpha strengthener in this alloy, and for this reason, processing and heat treating temperatures tend to be lower than other commercial alpha-beta alloys, and attendant microstructures finer. The hardening mechanism in this alloy is the simple reaction:

$$(\alpha) + \beta \longrightarrow (\alpha) + \alpha + \beta$$

At lower aging temperatures the brittle omega phase is also likely to be a decomposition product.

Notch Tensile Results - Figure 5 shows a plot of NTS/UTS vs. yield strength for material solution treated at 1480°F or 1350°F and aged for various times at temperatures between 800°F - 1100°F. The higher solution temperature again affords higher strength for a given notch ratio. The heat treatment response of this alloy upon air cooling is apparently quite good, one treatment giving a notch strength of 143 ksi, at 147 ksi yield and 157 ksi tensile strength. Aging at 800°F after the 1480°F solution temperature resulted in an extremely brittle structure, which may mean omega is present in the structure.

Ti-155A

Basic Metallurgy - This alloy is a moderately beta stablized alpha-beta alloy with an alpha strengthener. The M_s temperature of this alloy is apparently below room temperature.[4] The hardening mechanisms are not well known, but much of the discussion of the metallurgy of Ti-140A is probably applicable to this alloy.

Notch Tensile Results - Figure 6 shows a plot of .2% yield strength vs. notch strength for this alloy solution treated at 1450°F or 1650°F followed by subsequent aging. The effect of solution temperature is not as well defined in this alloy, but the trend again is that higher solution treating temperatures give higher notch strengths for a given yield strength level. Longer times at the aging temperature appear to improved notch strength with little or no loss in yield strength. All notch strengths for this alloy, however, were low, with no NTS/UTS as high as 0.9.

Comparison Between The Alloys

Table V summarizes the best notch values obtained as a function of yield strength level in 10 ksi increments. It can be seen that in the range 130-160 yield, alloy Ti-140A gives both highest notch strength and best notch ratio. Notch results fall off drastically above 160 ksi for this alloy, and no other alloy offers high notch strength above this yield strength level.

The data contained in Table VI clearly point out that tensile ductility is not an accurate measure of notch toughness. It seems clear that alloy type, heat treatment and attendant microstructure, as well as tensile properties must be considered as important factors in notch sensitivity.

Conclusions

1. Distinct differences in notch strength exist between different titanium alloys of equivalent strength.

2. Distinct differences in notch strength exist between different microstructural configurations, of equivalent strength level, in a given alloy.

3. In the important yield strength region of 130-160 ksi, alloy Ti-140A appears to be less notch sensitive than the other alloys tested in this investigation.

4. For the alpha-beta titanium alloys, higher alpha-beta solution temperatures, followed by aging, appear to produce less notch-sensitive structures for a given strength level.

5. Uniaxial tensile elongation is not necessarily an accurate measurement of notch sensitivity.

General Considerations

The purpose of this investigation has been to evaluate the effect of a large number of heat treatments upon the notch toughness of a number of titanium alloys. It should be emphasized that the effective toughness of a material is a function of many parameters, both mechanical and metallurgical, e.g., microstructure, section size, loading rate. It should also be pointed out that the notch tensile test gives a qualitative measure of the effect of many of these variables, but notch strength can be a measure of any of the previously noted failure mechanisms. A recent experiment has shown this point quantitatively. Ti-140A heat treated to a yield strength of 160 ksi and notch strength of 140 ksi gave a reproducible K_c value of approximately 74 ksi in. Using the analysis made available by the ASTM Committee on Fracture Testing of High Strength Sheet Materials,[1] self propagation of a natural crack in an edge notch tensile test should occur at any notch stress value above 120 ksi, a value 20 ksi below the measured value of notch tensile strength. Alloy Ti-155A of approximately equivalent K_c gave notch strengths of only 75 ksi. The former is an example of notch strength limited by resistance to crack initiation, the latter by resistance to crack propagation.

This investigation has served as a starting point for the study of notch toughness in titanium alloy sheet. Additional work is planned which will include a more complete series of tests in the more informative and promising areas. For the Ti-3Al-13V-11Cr alloy, the effect of duplex aging treatments, especially the low-high type, will be more fully studied. The effects of cold working followed by subsequent aging have been shown to improve tensile ductility levels and this will also be studied. The proper use of either of these techniques may improve toughness, and allow the utilization of this alloy, with its many attractive characteristics, without loss of reliability.

REFERENCES

1. ASTM Bulletin - Fracture Testing of High-Strength Sheet Materials - A Report of a Special Committee. - Jan and Feb 1960

2. DMIC Report #46G, Oct 19, 1959 - Time-Temperature, Transformation Diagrams of the Titanium Sheet Rolling Program Alloys. - Defense Metals Information Center, Battelle Memorial Institue, Oct 19, 1959

3. DMIC Report #110, 17 April 1959 - The All-Beta Titanium Alloy - Defense Metals Information Center, Battelle Memorial Institute

4. G. A. Lenning et al - TMCA - The Determination of the effect of heat treatment on the elevated temperature stress-stability of titanium alloys - WADC Technical Report 57-630 Feb. 1958.

TABLE I

EFFECT OF HEAT TREATMENT UPON

CONVENTIONAL AND MECHANICAL NOTCH PROPERTIES

Ti-3Al-13V-11Cr

HEAT TREATMENT	.2% Y.S. (ksi)	UTS (ksi)	%El. (2")	NTS (ksi)	Ave. NTS (ksi)	NTS/UTS
As Received	128	131	22.0	145 146	145	1.11
900°F(2 hrs)AC	126	134	27.0	134 131	133	0.99
900°F(20 hrs)AC	156	173	9.0	101 107	104	.60
900°F(100 hrs)AC	185	204	6.0	70 74	72	.35
800°F(2 hrs)AC	128	139	20.0	131 131	131	.94
800°F(100 hrs)AC	168	190	8.5	91 102	97	.51
1000°F(1 hr)AC	127	136	20.0	127 129	128	.94
1000°F(20 hrs)AC	150	169	10.5	104 104	104	.61
1000°F(50 hrs)AC	157	173	5.0	78 79	78	.45
1000°F(100 hrs)AC	157	172	4.5	61 62	61	.35
1100°F(1 hr)AC	128	133	24.0	115 135	125	.93
1100°F(20 hrs)AC	134	150	13.0	104 105	104	.70
1100°F(50 hrs)AC	135	148	6.5	85 85	85	.57
1100°F(100 hrs)AC	136	146	4.0	70 70	70	.48
1200°F(4 hrs)AC + 900°F(72 hrs)AC	161	182	7.0	89 90	90	.49

TABLE I (Cont)

EFFECT OF HEAT TREATMENT UPON

CONVENTIONAL AND MECHANICAL NOTCH PROPERTIES

Ti-3Al-13V-11Cr

HEAT TREATMENT	.2% Y.S. (ksi)	UTS (ksi)	%El. (2")	NTS (ksi)	Ave. NTS (ksi)	NTS / UTS
900°F(48 hrs)AC + 1100°F(2 min)AC	161	179	9.5	113 112	113	.63
1200°F(2 hrs)AC+ 900°F(48 hrs)AC+ 1100°F(2 min)AC	154	173	8.5	104 108	106	.61
900°F (100 hrs)AC	179	199	7.0	78 75	77	.38
900°F(100 hrs)AC	179	200	5.5	83 81	82	.41
900°F(100 hrs)AC	175	194	4.5	81 85	83	.43

TABLE II

EFFECT OF HEAT TREATMENT UPON

CONVENTIONAL AND MECHANICAL NOTCH PROPERTIES

Ti-4Al-3Mo-1V

HEAT TREATMENT	.2% Y.S. (ksi)	UTS (ksi)	%El. (2")	NTS (ksi)	Ave. NTS (ksi)	NTS/UTS
As Received	91	141	17.0	114 110	112	.79
1800°F(1/4 hr)WQ	128	152	2.5	138 133	135	.89
1700°F(1/4 hr)WQ	113	136	4.0	127 117	122	.89
1650°F(1/4 hr)WQ	95	145	14.5	115 113	114	.79
1600°F(1 hr)WQ	87	143	13.0	110 108	109	.76
1550°F(1 hr)WQ	76	135	15.0	104 103	104	.77
1500°F(1 hr)WQ	81	134	13.5	105 105	105	.78
1450°F(1 hr)WQ	102	130	13.5	116 119	118	.91
1400°F(1 hr)WQ	108	128	11.5	129 128	129	1.01
1650°F(1/4 hr)WQ + 900°F(2 hrs)AC	156	202	4.5	112 100	106	.52
1650°F(1/4 hr)WQ + 900°F(7 hrs)AC	181	201	4.0	92 101	97	.48
1650°F(1/4 hr)WQ + 900°F(24 hrs)AC	177	199	2.5	87 100	93	.47
1650°F(1/4 hr)WQ + 1000°F(2 hrs)AC	178	200	4.5	97 108	103	.51
1650°F(1/4 hr)WQ + 1000°F(7 hrs)AC	169	190	4.5	102 109	105	.55
1650°F(1/4 hr)WQ + 1000°F(24 hrs)AC	169	182	8.0	123 114	119	.65
1650°F(1/4 hr)WQ + 1100°F(2 hrs)AC	163	177	7.5	124 130	127	.72

TABLE II (Cont)

EFFECT OF HEAT TREATMENT UPON

CONVENTIONAL AND MECHANICAL NOTCH PROPERTIES

Ti-4Al-3Mo-1V

HEAT TREATMENT	.2% Y.S. (ksi)	UTS (ksi)	%El. (2")	NTS (ksi)	Ave. NTS (ksi)	NTS/UTS
1650°F(1/4 hr)WQ + 1100°F(7 hrs)AC	151	165	3.0	133 115	124	.75
1650°F(1/4 hr)WQ + 1100°F(24 hrs)AC	141	153	8.5	145 136	140	.92
1450°F(1/4 hr)WQ + 900°F(2 hrs)AC	135	163	8.5	116 115	115	.71
1450°F(1/4 hr)WQ + 900°F(7 hrs)AC	140	160	3.0	114 108	111	.69
1450°F(1/4 hr)WQ + 900°F(24 hrs)AC	132	159	6.0	121 118	120	.75
1450°F(1 hr)WQ + 1000°F(2 hrs)AC	129	150	6.5	137 138	137	.92
1450°F(1 hr)WQ + 1000°F(7 hrs)AC	128	145	7.0	136 110	123	.85
1450°F(1 hr)WQ + 1000°F(24 hrs)AC	127	146	12.5	147 137	142	.97
1450°F(1 hr)WQ + 1100°F(2 hrs)AC	125	145	8.0	135 136	135	.93
1450°F(1 hr)WQ + 1100°F(7 hrs)AC	126	140	11.0	138 138	138	.98
1450°F(1 hr)WQ + 1100°F(24 hrs)AC	119	134	11.0	125 134	129	.97
1800°F(1/4 hr)AC	138	153	2.5	118 114	116	.76
1650°F(1/4 hr)AC	133	159	7.0	124 141	133	.83
1500°F(1/4 hr)AC	108	132	13.0	123 118	120	.92
1650°F(1/4 hr)AC + 900°F(2 hrs)AC	142	161	3.5	114 124	119	.73
1650°F(1/4 hr)AC + 900°F(7 hrs)AC	135	154	2.0	122 123	122	.80
1650°F(1/4 hr)AC + 900°F(24 hrs)AC	134	155	5.0	130 141	135	.87

TABLE III

EFFECT OF HEAT TREATMENT UPON

CONVENTIONAL AND MECHANICAL NOTCH PROPERTIES

Ti-140A

HEAT TREATMENT	.2% U.S. (ksi)	UTS (ksi)	%El. (2")	NTS (ksi)	Ave. NTS (ksi)	NTS / UTS
As Received	114	134	22.5	125 129	127	.94
1600°F(1/4 hr)WQ	VERY BRITTLE			23 61	42	----
1480°F(1/4 hr)WQ	143	146	1.0	112 119	116	.79
1440°F(1/4 hr)WQ	156	160	1.5	115 113	114	.71
1400°F(1/4 hr)WQ	160	165	9.5	147 131	139	.84
1350°F(1 hr)WQ	136	145	15.0	145 142	143	.98
1300°F(1 hr)WQ	130	139	16.5	140 139	140	1.00
1350°F(1 hr)WQ + 800°F(2 hrs)AC	171	184	1.0	69 59	64	.35
1350°F(1 hr)WQ + 800°F(7 hrs)AC	150	176	4.0	111 114	112	.64
1350°F(1 hr)WQ + 800°F(24 hrs)AC	152	173	10.0	117 118	117	.67
1350°F(1 hr)WQ + 900°F(2 hrs)AC	149	173	13.0	118 118	118	.68
1350°F(1 hr)WQ + 900°F(7 hrs)AC	135	155	18.5	124 128	126	.81
1350°F(1 hr)WQ + 900°F(24 hrs)AC	136	155	15.0	133 128	130	.84
1350°F(1 hr)WQ + 1000°F(2 hrs)AC	135	148	15.0	141 142	142	.95
1350°F(1 hr)WQ + 1000°F(7 hrs)AC	130	142	19.0	139 137	138	.97

TABLE III (Cont)

EFFECT OF HEAT TREATMENT UPON

CONVENTIONAL AND MECHANICAL NOTCH PROPERTIES

Ti-140A

HEAT TREATMENT	.2% Y.S. (ksi)	UTS (ksi)	%El. (2")	NTS (ksi)	Ave. NTS (ksi)	NTS/UTS
1350°F(1 hr)WQ + 1000°F(24 hrs)AC	127	138	20.0	134	134	.97
1350°F(1 hr)WQ + 1100°F(2 hrs)AC	124	136	15.0	136 136	136	1.00
1350°F(1 hr)WQ + 1100°F(7 hrs)AC	124	134	21.0	132 131	131	.98
1350°F(1 hr)WQ + 1100°F(24 hrs)AC	116	126	21.0	125 126	126	1.00
1480°F(1/4 hr)WQ + 800°F(2 hrs)AC	SHATTERED DURING SHEARING					
1480°F(1/4 hr)WQ + 800°F(2 hrs)AC	SHATTERED DURING SHEARING					
1480°F(1/4 hr)WQ + 800°F(24 hrs)AC	SHATTERED DURING SHEARING					
1480°F(1/4 hr)WQ + 900°F(2 hrs)AC	157	164	7.5	146 145	146	.89
1480°F(1/4 hr)WQ + 900°F(7 hrs)AC	141	154	10.5	140 137	138	.90
1480°F(1/4 hr)WQ + 900°F(24 hrs)AC	145	157	10.0	149 144	147	.94
1480°F(1/4 hr)WQ + 1000°F(2 hrs)AC	156	165	9.0	159 146	152	.92
1480°F(1/4 hr)WQ + 1000°F(7 hrs)AC	147	159	13.0	154 154	154	.97
1480°F(1/4 hr)WQ + 1000°F(24 hrs)AC	133	145	15.5	147 144	145	1.00
1480°F(1/4 hr)WQ + 1100°F(2 hrs)AC	139	148	13.5	153 148	150	1.02
1480°F(1/4 hr)WQ + 1100°F(7 hrs)AC	133	144	15.5	143 140	141	.98
1480°F(1/4 hr)WQ + 1100°F(24 hrs)AC	124	134	14.0	136 133	134	1.00

TABLE III (Cont)

EFFECT OF HEAT TREATMENT UPON

CONVENTIONAL AND MECHANICAL NOTCH PROPERTIES

Ti-140A

HEAT TREATMENT	.2% Y.S. (ksi)	UTS (ksi)	%El. (2")	NTS (ksi)	Ave. NTS (ksi)	NTS / UTS
1600°F(1/4 hr)AC	---	168	----	45 70	58	.34
1480°F(1/4 hr)AC		SHATTERED DURING SHEARING				
1400°F(1/4 hr)AC	175	178	1.5	104 91	97	.54
1480°F(1/4 hr)AC + 900°F(2 hrs)AC	147	157	9.0	143 136	139	.89
1480°F(1/4 hr)AC + 900°F(7 hrs)AC	147	157	10.0	145 142	143	.91

TABLE IV

EFFECT OF HEAT TREATMENT UPON

CONVENTIONAL AND MECHANICAL NOTCH PROPERTIES

Ti-155A

HEAT TREATMENT	.2% Y.S. (ksi)	UTS (ksi)	%El. (2")	NTS (ksi)	Ave. NTS (ksi)	NTS/UTS
As Received	141	149	13.5	132 127	129	.86
1800°F(1/4 hr)WQ	138	157	2.5	90 84	87	.55
1700°F(1/4 hr)WQ	82	129	5.5	66 76	71	.55
1650°F(1/4 hr)WQ	80	164	10.0	75 79	77	.47
1600°F(1 hr)WQ	79	145	8.5	77 77	77	.53
1550°F(1 hr)WQ	129	150	8.5	116 120	118	.78
1500°F(1 hr)WQ	138	146	8.5	130 125	127	.87
1450°F(1 hr)WQ	136	148	13.0	132 119	125	.84
1400°F(1 hr)WQ	139	150	12.5	134 131	133	.88
1650°F(1/4 hr)WQ + 900°F(2 hrs)AC	SHATTERED DURING SHEARING					
1650°F(1/4 hr)WQ + 900°F(7 hrs)AC	SHATTERED DURING SHEARING					
1650°F(1/4 hr)WQ + 900°F(24 hrs)AC	---	196	0	75 77	76	.39
1650°F(1/4 hr)WQ + 1000°F(2 hrs)AC	194	211	4.0	76 68	72	.34
1650°F(1/4 hr)WQ + 1000°F(7 hrs)AC	188	196	3.0	80 68	74	.38
1650°F(1/4 hr)WQ + 1000°F(24 hrs)AC	190	192	2.5	111 107	109	.57
1650°F(1/4 hr)WQ + 1100°F(2 hrs)AC	182	184	4.0	101 97	99	.54

TABLE IV (Cont)

EFFECT OF HEAT TREATMENT UPON

CONVENTIONAL AND MECHANICAL NOTCH PROPERTIES

Ti-155A

HEAT TREATMENT	.2% Y.S. (ksi)	UTS (ksi)	%El. (2")	NTS (ksi)	Ave. NTS (ksi)	NTS/UTS
1650°F(1/4 hr)WQ + 1100°F(7 hrs)AC	174	175	4.5	100 112	106	.60
1650°F(1/4 hr)WQ + 1100°F(24 Hrs)AC	164	164	3.0	114 98	106	.64
1450°F(1 hr)WQ + 900°F(2 hr)AC	159	181	6.5	97 98	98	.54
1450°F(1 hr)WQ + 900°F(7 hrs)AC	164	184	7.0	97 93	95	.52
1450°F(1 hr)WQ + 900°F(24 hrs)AC	166	185	6.5	99 101	100	.54
1450°F(1 hr)WQ + 1000°F(2 hrs)AC	167	182	9.5	87 93	90	.49
1450°F(1 hr)WQ + 1000°F(7 hrs)AC	161	176	9.0	107 105	106	.60
1450°F(1 hr)WQ + 1000°F(24 hrs)AC	160	175	9.0	104 109	107	.61
1450°F(1 hr)WQ + 1100°F(2 hrs)AC	155	169	10.5	112 110	111	.65
1450°F(1 hr)WQ + 1100°F(7 hrs)AC	147	159	10.5	120 114	117	.74
1450°F(1 hr)WQ + 1100°F(24 hrs)AC	144	156	11.5	123 112	117	.76
1800°F(1/4 hr)AC	160	164	2.5	103 107	105	.64
1650°F(1/4 hr)AC	167	178	3.0	101 101	101	.57
1650°F(1/4 hr)AC + 900°F(2 hr)AC	163	178	3.0	103 101	102	.57
1650°F(1/4 hr)AC + 900°F(7 hrs)AC	---	176	0	78	78	.44
1650°F(1/4 hr)AC + 900°F(24 hrs)AC	---	178	0	61 62	61	.34

TABLE V

MAXIMUM NOTCH VALUES FOR

VARIOUS YIELD STRENGTHS

.2% Yield Strength Level	Maximum Notch Strength Alloy	Value (ksi)	Maximum Notch Ratio Alloy	Value
Up to 120 ksi	Ti-4Al-3Mo-1V	129	Many over 1	
120 ksi to 130 ksi	Ti-3Al-13V-11Cr	145	Ti-3Al-13V-11Cr	1.11
130 ksi to 140 ksi	Ti-140A	150	Ti-140A	1.02
140 ksi to 150 ksi	Ti-140A	154	Ti-140A	.97
150 ksi to 160 ksi	Ti-140A	152	Ti-140A	.96
160 ksi to 170 ksi	Ti-4Al-3Mo-1V	127	Ti-4Al-3Mo-1V	.72
170 ksi up	Ti-155A	110	Ti-155A	.60

TABLE VI

COMPARISON OF SAMPLE NOTCH STRENGTH

AND TENSILE DUCTILITY VALUES

Alloy	.2% Yield (ksi)	UTS (ksi)	%El. (2")	Notch Strength (ksi)	Ratio
Ti-140A	156	165	9.0	152	.92
Ti-140A	157	163	7.5	146	.89
Ti-3Al-13V-11Cr	150	169	10.5	104	.61
Ti-155A	155	169	10.5	111	.65

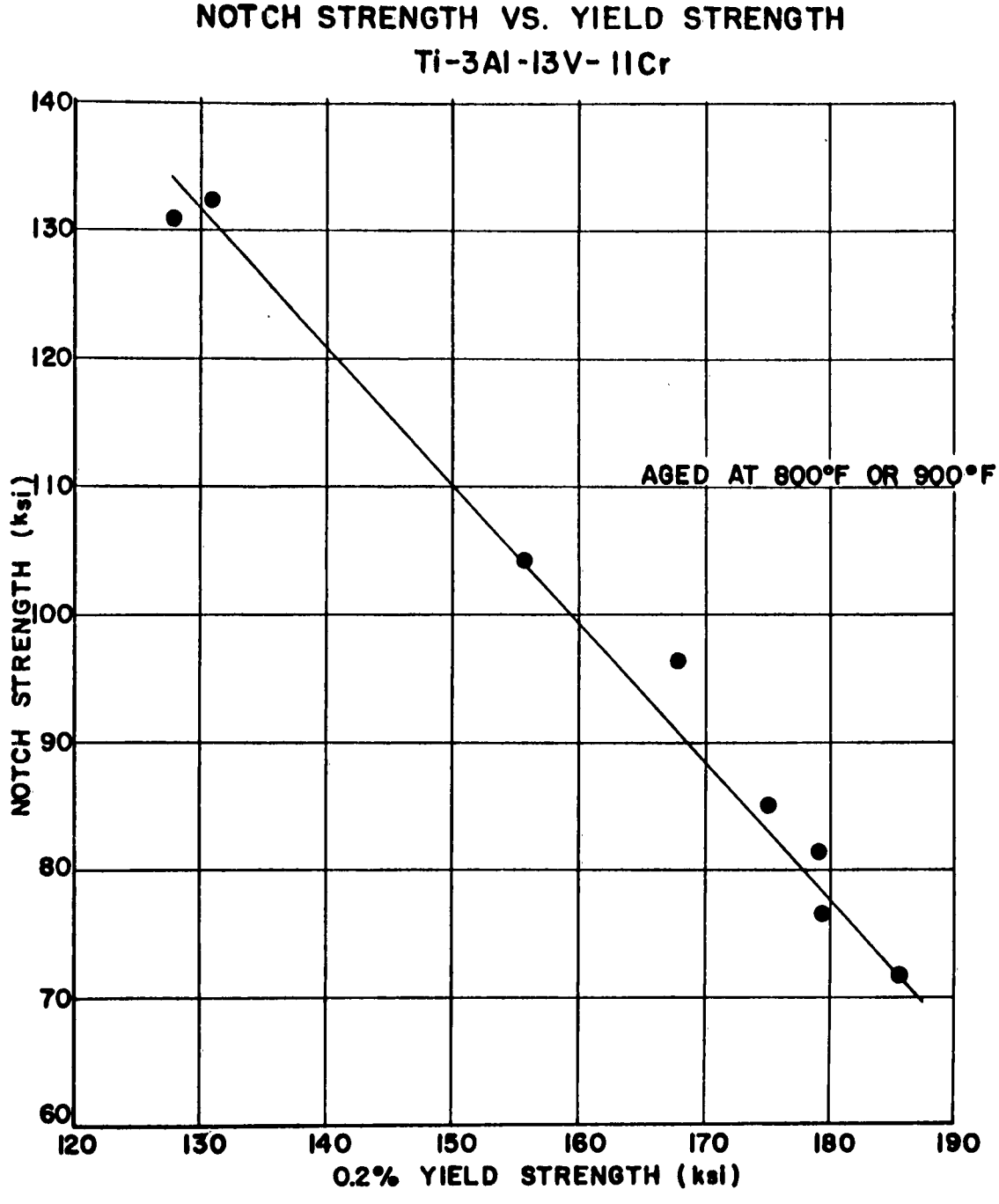

NOTCH STRENGTH VS. YIELD STRENGTH
Ti-3Al-13V-11Cr
AGED AT 800°F OR 900°F
NOTCH STRENGTH (ksi)
0.2% YIELD STRENGTH (ksi)
140
130
120
110
100
90
80
70
60
120
130
140
150
160
170
180
190

FIGURE 1

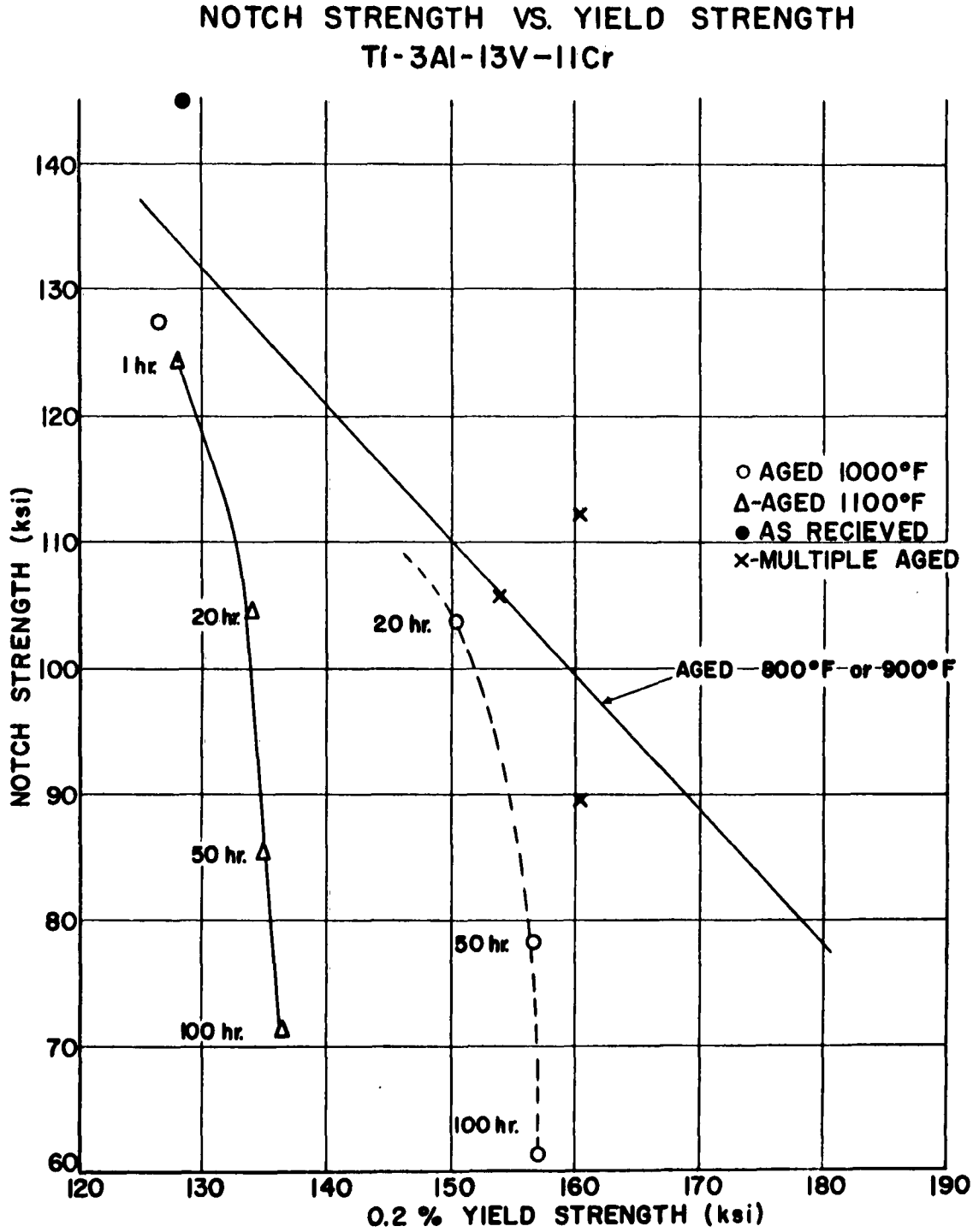

NOTCH STRENGTH VS. YIELD STRENGTH
Ti-3Al-13V-11Cr
NOTCH STRENGTH (ksi)
0.2 % YIELD STRENGTH (ksi)
140
130
120
110
100
90
80
70
60
120
130
140
150
160
170
180
190
1 hr.
20 hr.
50 hr.
100 hr.
20 hr.
50 hr.
100 hr.
o AGED 1000°F
Δ-AGED 1100°F
● AS RECIEVED
×-MULTIPLE AGED
AGED—800°F-or-900°F

FIGURE 2

NOTCH STRENGTH VS. YIELD STRENGTH
Ti-4Al-3Mo-1V

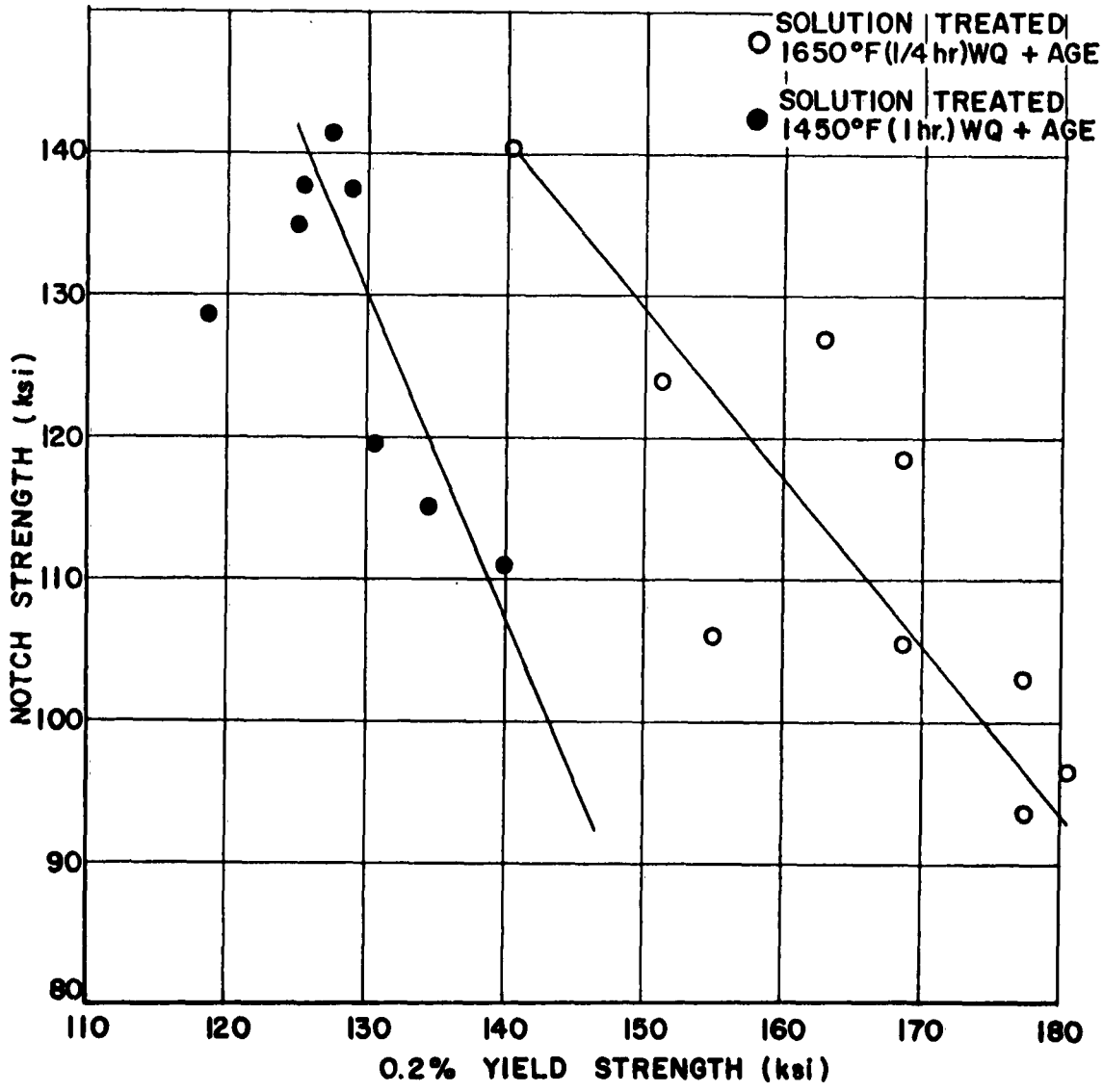


FIGURE 3

$\frac{NTS}{UTS}$ VS. YIELD STRENGTH

Ti - 4Al - 3Mo - 1V

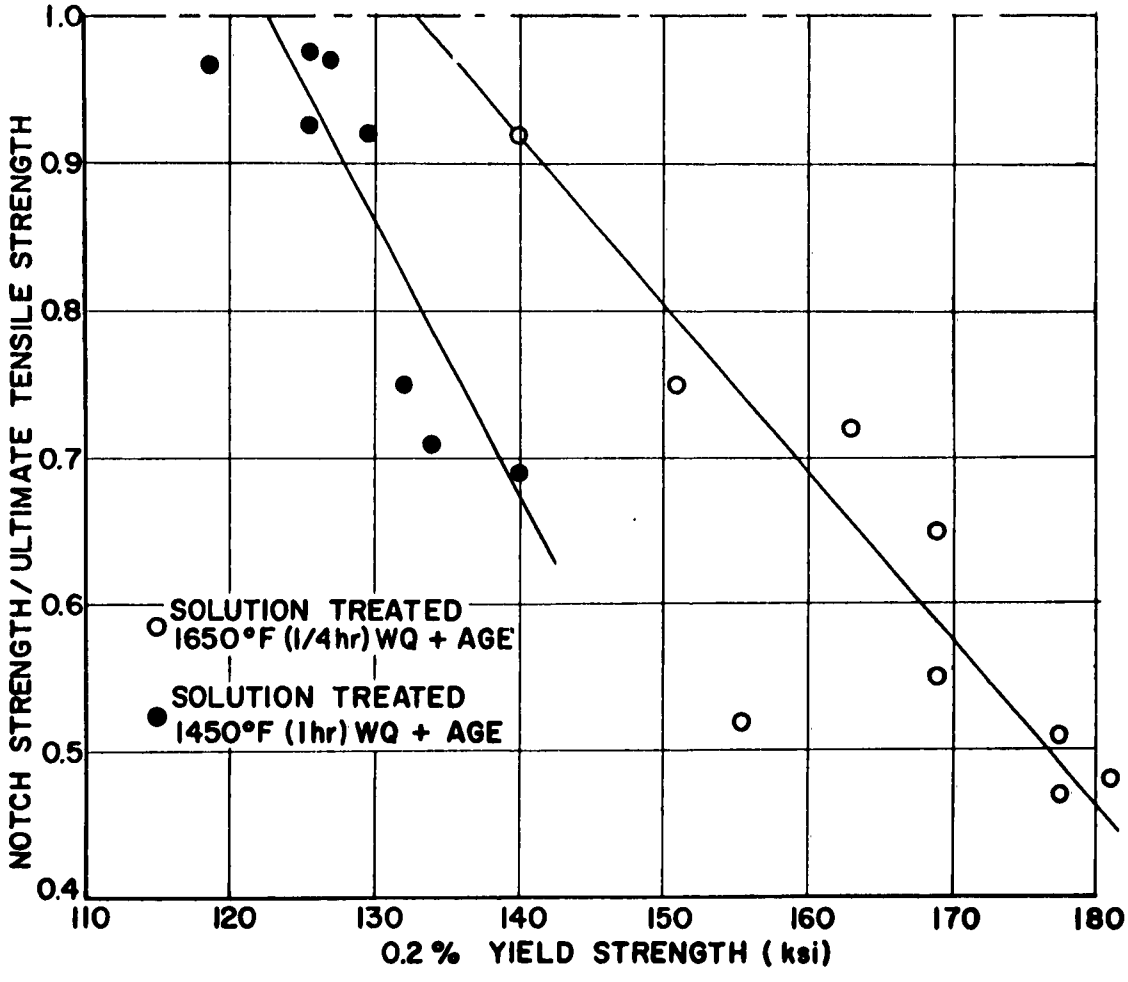


FIGURE 4

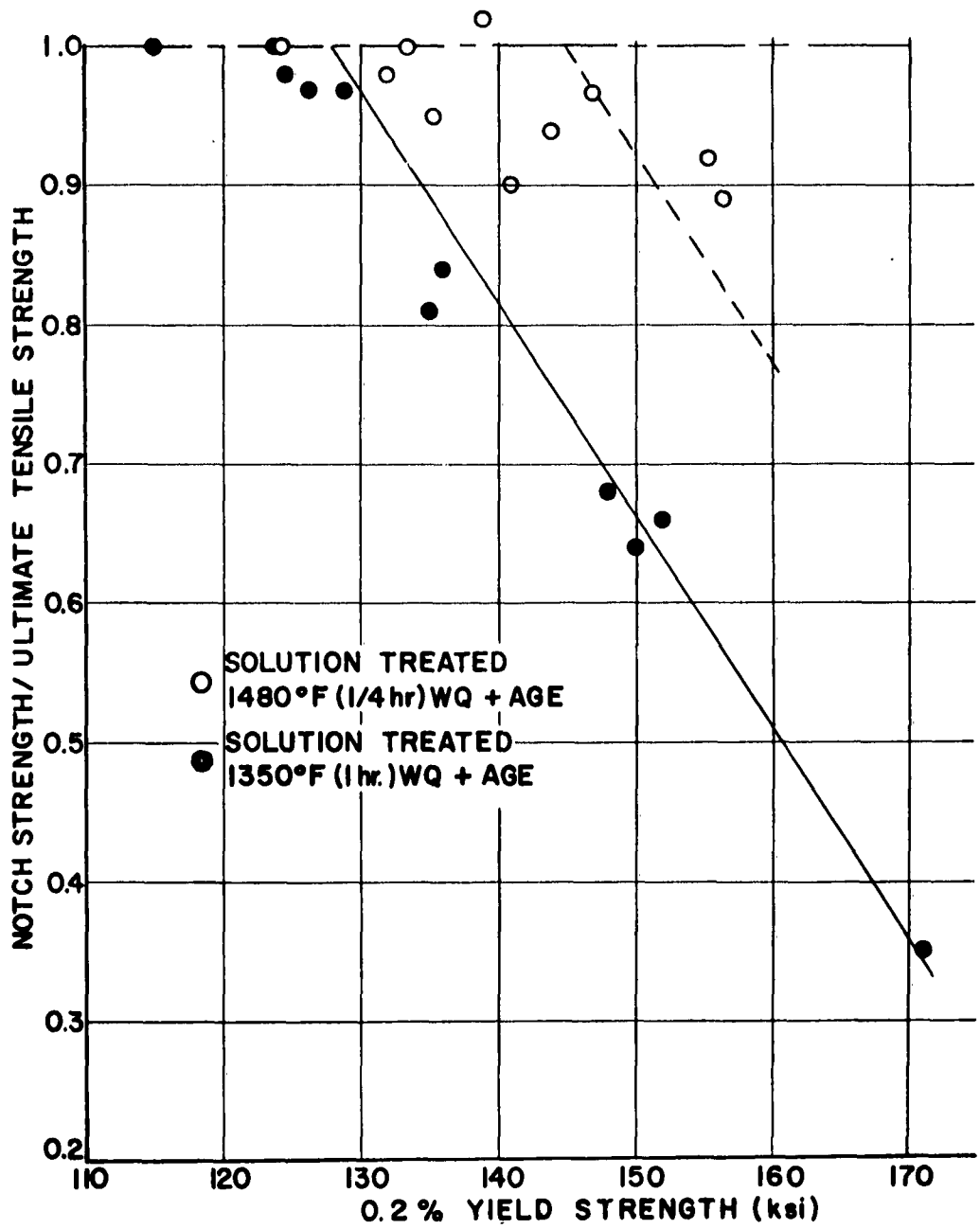

NTS/UTS VS. YIELD STRENGTH
Ti-140A
NOTCH STRENGTH/ ULTIMATE TENSILE STRENGTH
1.0
0.9
0.8
0.7
0.6
0.5
0.4
0.3
0.2
110
120
130
140
150
160
170
0.2 % YIELD STRENGTH (ksi)
SOLUTION TREATED
1480°F (1/4 hr) WQ + AGE
SOLUTION TREATED
1350°F (1 hr.) WQ + AGE

FIGURE 5

NOTCH STRENGTH VS. YIELD STRENGTH

Ti-155A

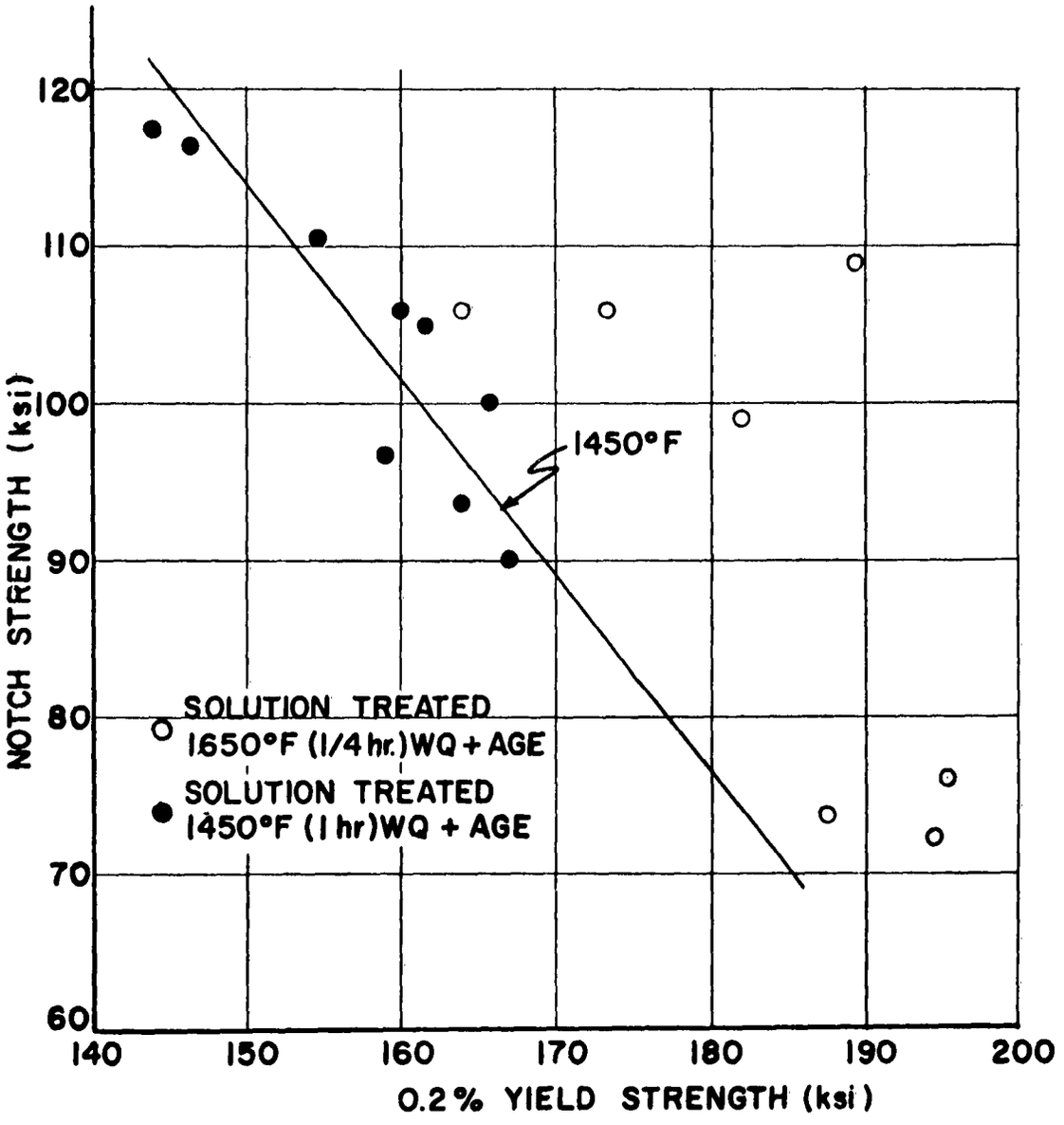


FIGURE 6

E. R. Mertz I would like to ask Mr. Powell if in the first test he illustrated, he made correction for bulging? I noticed appreciable bulging and found that making corrections for the bulge resulted in a considerable reduction in burst strength.

R. C. Powell Calculations were made to try to estimate the effect of bulging on the absolute burst test values as originally recorded, and I think there was a maximum effect of about 20,000 psi. As I recall, maximum correction lowered stresses to around 282,000 psi. This was not true for all cases. In some cases where there was little bulging, little if any correction was necessary.

V. Weiss I would like to ask Mr. Arnold a question. How are these impact tests on sheet specimens obtained and finally reported? I believe you took stack sheet specimens and notched them. Did you divide the impact energy that you obtained by the number of specimens to get the impact energy for one sheet specimen?

S. V. Arnold No. This particular group of data were obtained using a single thickness Charpy specimen of dimensions which were conventional except that the thickness corresponded to the gauge under investigation. This design works very well in gauge thickness where buckling does not occur during the fracture process.

W. F. Brown I'd like to make a comment which I'll direct to Jack Hamaker of the Vanadium Alloys Steel Company and to you Mr. Powell. This has to do with the effect of decarburization increasing the toughness of H-11. This puzzles me a bit. We and Jack Hamaker have results which show the toughness of this steel increases with increasing carbon content, and there is enough data now so that we believe we are not fooling ourselves in any way. Our results cover carbon contents from about 0.23 to about 0.43 percent and a range of tempering temperatures. There is no question that the toughness increases with increasing carbon content though it did level off at about 0.38 carbon. Jack Hamaker, in a similar investigation, used impact tests and obtained essentially the same results. Now these data seem to be in contradiction to the reported increase in toughness due to decarburization.

R. C. Powell This effect of decarburization is something that we noted a long time ago, observing SAE type alloy steels and it doesn't seem to be confined to any particular grade of steel. The effect was measured by the bend test as illustrated, and also by impact tests on notched Charpy specimens, decarburized vs not decarburized; after tempering at 1000 and 1100 F. In each case we showed a distinct improvement in the impact strength for the decarburized specimen.

W. F. Brown — We made a carbon investigation for 300-M and it was found - as expected - that the toughness increases at a given strength level with decreasing carbon content. The H-11 showed the reverse effect.

J. Hamaker — The degree of decarburization is, I believe, the critical point here. I think Mr. Powell's photomicrographs show that there is still a good bit of carbon in there; in fact, the surface layer probably doesn't go below 0.30%. There definitely is increased ductility with lower carbon as shown in smooth bar tests. Thus, where localized, bending stresses are obtained in vessels, a small amount of decarburization might well be helpful. Our data did not clearly define the critical carbon content between 0.30 and 0.40 percent but indicated that severe decarburization is harmful.

A. Hurlich — I think the effect of decarburization can be attributed to the fact that in any normal heat-treated steel you will find some grain boundary oxidation or defects that open up maybe two or three grains deep. The effect of decarburization is to reduce the effect of the stress concentrations provided by these grain boundary defects and give you a tougher material which is capable of a little deformation at the surface and therefore obviates the dangers inherent in these very minute surface defects.

W. F. Brown — The point that I'm trying to make is that according to our results there should be more not less sensitivity to surface defects if H-11 is decarburized. The lower carbon material has less tougness, not the other way around.

H. Bernstein — We have no data on the effect of decarb on H-11 steel as determined by central notch tests. U. S. Steel has the best data we've seen to date on X200. It shows a really spectacular increase in fracture toughness and resistance to crack propagation by means of the central notch test on decarburized X200 steel. We have observed the same thing on AMS 6434. This may be chemistry-sensitive. It is quite possible that H-11 is a different beast but we have no data to support it. I do not think there is enough difference between H-11, AMS 6434, AMS200 to give you this marked change in fracture behavior, but this has not been substantiated because we do not have any data on it.

N. L. Reed — This is a question for Mr. Powell. You show a burst full size motor case. Can you tell us whether you examined that for decarburization?

R. C. Powell — The case was not examined by us for decarburization, but according to the test pieces that were heat-treated along with it and should be representative of the case, the depth of decarb ranged between 0.002 to 0.005 inches.

F. Richmond — We have done quite a bit of work on H-11 and our results are exactly contrary to Mr. Brown's in that we get a very significant increase in

toughness (at least as measured by the instrumented bend test) by reducing the carbon to about 0.30 to 0.35 percent and heat-treating to get the same yield strength as for 0.40 percent carbon. With the lower carbon H-11 we have been able to obtain 240,000 psi yield strength with parameter values of 1 or greater in the instrumented bend test. We are very much concerned with the fact that Mr. Brown and others have recently shown that H-11 reacts differently than most other alloys in regard to the effects of carbon on toughness. I do not have the data with me but we do have a report in preparation and will be happy to circulate it to anyone who is interested. It is possible that Mr. Brown and others have missed the effect we noted because of a lack of data in this critical range or because of other differences in their materials. We definitely feel that lower carbon is quite beneficial in H-11.

W. F. Brown We also have looked into consumable electrode-vacuum melted versus standard air melted H-11. Fracture toughness measurements were made at 0.35 carbon level over a range of tempering temperatures. We were always careful to know the carbon content of the heat-treated sheet and compared CEVM with air melt at the same carbon level. The data show very little difference between consumable electrode-vacuum melted and air melted material. Now, I would like to ask Mr. Powell why he thinks that the consumable electrode-vacuum melted material is necessary? Do you have data to show consumable electrode-vacuum melted material should be used or is it used only to be on the safe side?

R. C. Powell Our choice of vacuum melted material is predicated on fabrication as well as on the properties of the finished product. I have mentioned that we flow-turned the cylindrical section, and we have considerable evidence based on flow-turning of high temperature alloys. In martensitic stainless steels, non-metallics can be a serious detriment to flow-turning quality. We have seen some difficulties with air-melted H-11. You can have a clean heat of air-melted H-11, and consumed electrode-vacuum melting is no guarantee of cleanliness. Nevertheless, we feel, to be on the safe side, we will go with the vacuum melted product.

D. W. Kinsey I'd like to ask Mr. Brown what order of magnitude of partial decarburization he was examining for the results which might reverse their field? Our impression is that decarb, when you are at .001, .002 or .003 inches, is probably normal for at least roll and weld construction with sheet coming from the producer and being heat-treated at the fabricator's plant, is typical of what we would call the undecarburized condition. This is opposed to .010 or .015 inches which is the order of magnitude which I think has been examined for improvements in burst test performance.

W. F. Brown The sheet we investigated was not decarburized but we had sheet from different heats that varied in carbon content.

H. Bernstein I think the only way we can resolve this to my satisfaction is to get some decarburized sheets and run some center notch fracture toughness tests on it.

P. R. Kosting Is this decarburization process carried out in a high oxidizing atmosphere?

R. C. Powell The control of partial decarburization can be achieved by either controlling the dew point of an endothermic gas atmosphere, or by using an exothermic type atmosphere with needed amounts of propane added to the gas atmosphere.

L. Schapiro I would like to say something with regard to H-11, and although it is not pertinent to the discussion on decarb, I think it is important to get it into the record. It might also give Mr. Brown an added thing to worry about. I would like to call your attention to the fact that the photograph that was shown by Mr. Powell on the H-11 burst case showed a nice watermelon type burst rather than the fragmented burst that I believe we have all seen from other people on H-11. This is an added difference resulting from the controlled decarb heat-treatment, the difference between watermelon and fragmented bursts.

J. Hamaker We have reviewed quite a few burst tests during the past few years. In most cases bad decarburization from poor heat-treat control appeared to be the only consistent contributing factor. Since Mr. Brown, Mr. Klier, and ourselves have all come up with the same answer, there appears to be a definite correlation.

L. Schapiro In this regard I think it is very important for everyone to make themselves very clear on just how much decarb they are speaking about. The amount of decarb that Mr. Hamaker was referring to, I believe, was considerably in excess of the amount that Mr. Powell was describing. This is very important.

J. Sheehan We have recently obtained data at Armour Research that tend to support Bill Brown's result. We melted a series of heats of 2 percent Cr steel having carbon contents of 0.24, 0.30, 0.40, and 0.50 per cent. Using the center-notch tensile test we found increasing G_C values as the carbon content decreased from 0.50 to 0.30 percent but with the 0.24 percent carbon content there was an anomalous reversal to very low G_C values. At the moment we cannot explain this behavior, however, we hope to be able to draw better conclusions on the effects of carbon content after the results of our decarburization studies on these same steels have been obtained.

C. M. Carman I would like to ask Mr. Powell if he shouldn't be thinking a little different about this. I noticed that with the titanium alloys you get large improvements in fracture toughness after the flow-turning operation. We have seen lots of H-11 specimens and have broken a few of them ourselves, but never had such good results as were indicated by your burst tests. Could it be conceivable, for an idea at least, that the flow-turning has more to do with improving the structural properties of this material than the decarb?

R. C. Powell Theses cases are heat-treated after flow-turning which obviates a good deal of the original directionality that has been put in by working. It is possible that the flow-turning does have something to do with the high burst stresses. We have not considered this.

C. M. Carman Are your titanium cases heat-treated after flow-turning also?

R. C. Powell They are aged after flow-turning.

P. Wallace Regarding decarburization I just want to introduce another factor that some people might want to take into consideration. There are heat-treatment variables which can be very critical at times. The amount and nature of residual stresses are function of thermal and constitutional changes that are taking place in a metal during heat-treatment. The effects of these residual stresses are more pronounced on carburized surfaces but they also must be effective on decarburized surfaces. Whether this decarburized surface is in tension or compression is determined by heat-treatment variables in addition to chemistry, mass, configuration, and so forth.

W. P. Achbach With respect to the work by Pratt and Whitney and U. S. Steel and that work by NASA (Brown) and Vanadium Alloys (Hamaker) on decarburization and alloy carbon content, I should like to point out that at a carbon level somewhere around 0.25 percent (depending upon the remainder of the steel chemical composition), we have what is called low-carbon martensite which, if you look at it under high magnification has a blocky appearance. At carbon levels over about 0.25 percent an ascicular type of martensite prevails which has a predominantly needle-like appearance. A gradient in structure from blocky to ascicular probably prevails inthe decarburized skin, Mr. Powell is talking about. There is a basic difference between studies on the effect of carbon content on the behavior of sheet, and studies on the effect of a decarburized layer at the root of a notch on the behavior of the sheet, both with respect to stress distribution, stress gradient, and flow characteristics.

D. W. Kinsey I think most of Aerojet's data will show that .002 or .003 inches of partial decarb will not do this job. To get back to Mr. Brown's original statement, in line with the work at Armour, we have run a series of 3 percent chromium, 1 1/2 percent silicon steels at various carbon levels through fracture toughness studies. Many of you have seen this data. At 0.35 and 0.36 percent carbon, everything else being essentially constant, we got G values in excess of a thousand. Where we went to 0.42 percent carbon, the G value dropped down to less than 400. I am of the opinion that in this type of steel the crossover point therefore must be somewhere between 0.36 and 0.42 percent. As Bill indicated, 0.38 still was of that magnitude. I think this is bracketing, now, the cross-over point on section carbon as opposed to the theorists who like the surface decarb as a method of improving the notch toughness.

J. W. Sweet Mr. Arnold, in regard to your work on the effects of residual tensile stress, have you considered shot peaning to observe the amount of improvement that might occur in the notch sensitivity?

S. V. Arnold No, my study has been concerned with residual tensile stresses in combination with a notch. It is not immediately apparent how one could shot pean the base of sharp notches such as have been incorporated in the specimens I have employed.

K. H. Abbott We, at Watertown Arsenal Labs, initially planned to present another paper here on the notch-unnotch tensile properties, as a function of solution treating temperatures, aging temperature and time for two titanium alloys. One is Ti 140A and the other is the B120 VCA. The data is not ready since the final tests are being conducted this week. The data consists of notch-unnotch tensile ratios with the ASME standard edge notch specimen with a .001 in. radius notch. For the Ti 140A, for example, at .2 percent yield strength levels of about 140 to 150 thousand psi, notch-unnotch ratios of approximately 1 were obtained. All of the possible practical solution treating and aging temperatures and times were included.

A. Hurlich Last night, Dr. Beeuwkes gave an equation on the effects of missile performance by reduction in weight, showing that you could get very significant improvements and range by decreasing your weight just a few pounds, and then he asked how meaningful is this and how much advantage can be taken of it. I'd like to answer that and also bring out a point that pertains to the last presentation. In the Atlas where we use the cold rolled stainless steels, by virtue of the fact that our cold rolling is achieved on the Sendzimir mill, we are buying material on a production basis that is cold rolled to about a third or a half of the AISI thickness tolerance. Consequently, at .015 inches we are buying material that has a plus or minus .0005 inches thickness tolerance; at .020 inches we are buying at plus or minus .0008 inches thickness tolerance. This is one of the very direct advantages of purchasing material that is cold worked to final gages. You can have a very close thickness tolerance control, and this is very significant for the weight control and range performance of long range missiles. In the Atlas missile, although the exact details are classified, the variation in weight from missile to missile is within a relatively small number of pounds, and therefore the range is very carefully controlled and also maximized by keeping the weights down to an absolute minimum consistent with the yield strength and the design allowable strength levels of the materials employed. This is a very important point that should not be lost sight of since we are dealing with thin sheet materials. It is possible to control the thickness and weight of thin sheet materials much more precisely than many companies care to do commercially. Five or six years ago we went out to buy the Atlas skin material and only one company made an attempt to meet the requirements. Today about six or seven companies have qualified to meet the requirements to produce materials to this close gauge control and I think there is a definite move in industry to provide thickness tolerances that are much better than normal commercial practices.

J. D. Marble I have a question for Frank Larson. In this thickness to width strain anisotropy, what was the effect of the actual thickness of the sheets? Also, do you consider the large differences in the different titanium alloys to be an effect of the different phase structure?

F. R. Larson We did not study too many different sheets thicknesses. We were limited, primarily because of time, to study only what we had available or only what we could get quickly, and these were all in the range of .050 to .100 inch thickness so that I could not say from our test data. Offhand one would feel that the thinner the material the greater the normal anisotropy should be, possible from mechanical fibering and crystallographic orientation which is predominantly the effect in titanium alloys. In titanium alloys the effect primarily comes from texture of a crystallographic nature.

N. L. Reed I have a question for Frank Larson. Frank in your table 5 you show that the R-value for the 4Al - 3Mo - 1V is better than 7, and for 6Al - 4V is better than 3. Have you tested V120 VCA, or are you planning to. The second part of the question is, if you haven't done that would you guess if the R-value is going to be high or is it unreasonable to make any estimates at this time?

F. R. Larson I do not like to speculate a great deal on it, except to say that people have done a lot of longitudinal and transverse tests, and said, well this sheet is very isotropic. Further, they have compared their longitudinal and transverse properties from uniaxial tension tests to those for biaxial stress states which actually have different strain conditions. So the uniaxial cases in longitudinal transverse tests cannot tell you a great deal about how something would be resistant thinning, which I believe is the primary thing we are interested in. We would like to study this behavior in titanium a little more systematically, because the effect in titanium undoubtedly comes from a crystallographic texture. Crystallographic texture is developed by the prior thermal-mechanical history of the material. People attempted to reduce it a few years ago by cross-rolling the material. This cross-rolling does not get rid of the normal anisotropy so I think, we have to really dig in and study a little bit more about the normal anisotropy because this is really the thing that makes the difference in the behavior of the material under a multiaxial stress condition.

E. S. Jones I have a question for Mr. Sharp. Would you like to comment on the relative fracture toughness of beta titanium at about the 180,000 to 185,000 psi yield strength level versus H-11 at the 240,000 psi yield strength level?

W. H. Sharp Just based upon what I know of fractured toughness of H-11 and other steels at the 240,000 psi level, they are not very good to say the least. B-120 VCA at a strength level of 180,000 psi certainly would appear to be at all odds better than the steels. Now what is going to happen to B-120 VCA at say 200,000 or 210,000 psi I think, is something that has to be watched very closely. I would say that B-120 VCA is definitely tougher at an equivalent strength level.

L. Schapiro Mr. Carman, when you showed us a picture of a cylinder which was pressurized, you commented that the yield and the burst on that cylinder were about

comparable with the uniaxial properties. The question, I have to ask you is, was that cylinder made from a tube or was it made from a bar that was machined out and how was the uniaxial specimen taken?

C. M. Carman It was made from a seamless tube. The round bar specimens for the uniaxial properties were taken from the billet from which we made the tube.

W. F. Brown I would like to give a little more information on the question of titanium versus steel. Mr. Jones asked about the comparative fracture toughness of beta titanium alloy and H-11. You can find that data in an ASTM paper we presented at the 1960 annual meeting. Fracture toughness values are plotted as a function of yield strength to density and as a function of tensile strength to density. These plots show Mr. Sharp's answer to be essentially correct. However, the fully heat-treated condition of either the titanium or steel is not very tough, but the titanium does seem to have an edge.

J. E. Srawley In connection with what Bill Brown just said, I think you have to bear in mind that if you compare the yield strength to density ratios, you also have to compare the K_c to density ratios. You should not compare the K_c for titanium with K_c for steel on the basis of equal yield strength to density ratio unless you do the same thing for K_c value. What is important in fracture toughness is actually the ratio of K_c to the stress level, which is presumably proportional to the yield strength of the material used in the application. This is to the advantage of the titanium alloy.

H. Bernstein A question for Mr. Sharp. How do you intend to get equivalent toughness and strength in your closures and domes for the B-120 VCA case? You are going to get strength and toughness in the cylindrical section by cold working and partial aging. You will have unheat-treated welds. How about domes and closures?

W. H. Sharp I must say that we have not checked the toughness of the domes of the B-120 VCA assemblies. This is something we will do in the future. I think the effect of warm work on the dome coupled with appropriate aging will result in fracture toughness characteristics of a similar order. This is a guess. If we are able however, to attain a structure in the domes that compares favorably with the structure of the flow-turned cylinder, then we will come up with comparable toughness characteristics.

H. Bernstein Do you intend to match the strength of the domes and closure with the sidewalls? Will the yield strengths equivalent?

W. H. Sharp The indications are now that the end closures will be but slightly inferior to the cylinder.

S. V. Arnold With regard to this matter of determining the notch toughness of the head sections, this is no easy trick. If you consider the finshed section, you will realize that this is curved so that taking a meaningful specimen would be rather difficult.

E. R. Mertz I would like to ask Mr. Larson for his comments on the possibility of sub-zero cooling as a means of transformation of retained austenite. We too are concerned with the retained austenite in some of these steels and would like to hear some opinions in this regard.

F. R. Larson We found in the materials that we tested of the H-11 type, that most of the retained austenite was thermally stable. In other words, we did sub-zero cooling, I don't recall the actual temperatures, (the treatments are in the paper) and try as we may, we found that we had about five to six per cent retained austenite still left. It was apparent that this retained austenite was quite thermally stable. On the other hand, the points that I would like to make are the adverse effect of retained austenite of lowering your yield strength and the embrittling effect of the transformation of the retained austenite revealed possibly on proof testing. Another point is that this retained austenite is quite stress-sensitive, so that a very small strain completely transforms any retained austenite that you might have. If we could make a vessel thermally treated to get rid of the majority of retained austenite then stress this to a few percent strain followed by a subsequent tempering operation, we might utilize a lowered tempering temperature and a higher strength. That was the main point I tried to get across.

R. C. Powell We have not observed any difficulties with the H-11 five percent chromium steel which we could associate with retained austenite. The double tempering, particularly beyond the peak of the secondary hardening range, seems to have gotten us beyond any point where we would have difficulties. One analysis where we have seen a retained austenite problem in sub-scale pressure vessels has been with 300-M.

J. Hamaker I just wanted to add that manufacturers of aircraft components, including primary carry-through structures, landing gear, and so forth, have checked out the retained austenite content of H-11 modified and, with the multiple tempering that you're using, find less than 1 percent on X-ray studies. That is even after tempering at 1000 F to 300,000 psi ultimate strength.

THIRD SESSION

"Effects of Fabrication Variables"

INFLUENCE OF FABRICATION HISTORY ON MECHANICAL AND METALLURGICAL BEHAVIOR OF SHEET MATERIALS

by

Walter A. Backofen*

Introduction

An urgent need to improve technology in the field of manufacturing from high-strength sheet has inspired much new experiment and development. One result has been a more or less parallel surge in reports and paper-publication, particularly over the past two years, from such sources as the DMIC, MAB, various symposia, fracture conferences, and society meetings. There is no question about the value of this output; however it might be weighed and criticized, it gives a rather clear picture of interlocking problem areas with fabrication somewhere near the middle, spilling over into others that the Conference will consider.

Many different kinds of deformation processing, joining, and heat treatment are under trial, depending upon design, materials, and convictions of sponsoring as well as fabricating groups. Innovation is very much a trademark of the field, which is a fact made plain by any sampling of activity such as: the shear spinning of a metastable phase, adhesives joining or pressure welding without fusion, intentional decarburization of high strength steel, non-mechanical machining, etc.

Fabrication, or processing in general, has two broad objectives: One is to change a material's shape so as to meet specified size, form, and tolerance; the other is to regulate material composition and structure and in so doing to control properties and behavior. An over-all competitive economy is usually a related objective. But there are at least two reasons why it is somewhat less than clear how to make an argument here for economy in establishing processing programs: These are the initial boundary conditions set on costs in budget planning and the fact that performance of finished devices may be so critical. The key problem of property control makes it essential to examine processes first for effects on material structure and general behavior.

---

* Associate Professor of Metallurgy, Metals Processing Laboratory, Massachusetts Institute of Technology, Cambridge, Massachusetts.

Obviously the shape-changing objective has to be realized; but in doing so, service behavior ought not to be put in jeopardy, and, ideally, there should even be an assist towards still higher performance. Welding is of special interest in this connection for the welding advocate generally includes economy in his argument. Yet welding as practiced is basically a means for shape control, not material improvement; and it does introduce the risk of structural damage. These features, both strong and weak, in the case for welding are more than evident and give good incentive to bolster the over-all position of such processing.

Effects of Fabrication

The effects of processing are naturally easier to state than their control. Nevertheless there is some value in simply collecting effects into three broad categories to show that in most cases they may act through changes in:

1. Flaw distribution

2. Fracture toughness

3. Strength level

Fracture Toughness: The idea is central to the entire range of problems at hand and is now under almost constant discussion. One of the basic starting points in this whole field has long been the possibility of fracture because a crack under stress acquires a critical length at which it propagates rapidly or unstably without change in stress. This length becomes smaller as stress increases, and the important parameter determining the stress:crack-length relationship is fracture toughness (generally designated as G_c for the plane stress case of a thin sheet with a crack through the thickness). The value of the fracture toughness is fixed when the amount of stored-up elastic strain energy drained away with a unit of crack extension just matches what is needed to produce the new crack surface. The important detail is that this "sink" for the stored energy consists almost entirely of plastic-deformation work in a more-or-less thin volume of strained material at the head of the crack.

The conclusion to this story, which has been told so many times, is the formula in the Figure giving the condition for unstable growth of a crack of length, l, in a material with Young's modulus, E, under

a mean stress, σ. For all of its retelling, it still suggests a straightforward way of summing up interactions among problem areas of fabrication, metallurgical control, inspection, and testing, and pointing out, as well, the effects of fabrication.

A Graphical View of Fracture Conditions: The relationship between critical crack length and applied stress is shown schematically for different levels of fracture toughness in the Figure. Curves are ended on the right with vertical drops when the yield stress, σ_y, is reached, if this is to be the maximum allowable stress. The l-σ coordinates define an "operating point" for a particular region in a device that is cracked and under load; location of this point relative to the appropriate G_c curve for the region indicates something about how imminent fracture may be. Many such points can be plotted, of course, with different l-σ-G_c combinations, and that one becomes critical which first satisfies the instability criterion.

The preferred conditions for service quite clearly are high G_c and a position well below the curve as far to the right as allowed by σ_y, which also ought to be high. Arbitrary specification of G_c is obviously naive since its control remains a basic materials problem, influenced also by section geometry. There are other factors, too, that badly complicate such a simple point of view. Even if G_c were not in question, there would be no way of knowing that a point did in fact lie safely below the line unless crack dimensions were also known, which underscores the inspection problem. In addition, G_c of a given material is likely to vary with strength level, dropping more or less rapidly as σ_y increases; this compounds the problem by lowering the ceiling on tolerable flaw size still further. Since there are practical lower limits to the length of crack that can be detected, a potential "fracture area" for service is indicated although very schematically. Any inspection limit, e.g. the horizontal line, bounds this area at top; the lower edge lies more or less along the G_c curve and may be well below if loading history, as in proof testing, causes the growth of an initially subcritical crack into one that will run unstably. No such area is to be found only for material "C" since now σ_y is reached, with general yielding, above the limiting line.

Fabrication effects the crack-length coordinate while design and service conditions fix the other (σ); fabrication further effects the important boundary conditions of fracture toughness and strength level.

The direction to follow, then, is evident even if the details of a route are not.

1. Fabrication without flaws but disposition of any that cannot be avoided in such a way as to do the least harm.

2. Development of high fracture toughness and strength levels, with fabrication being practiced ideally so as to contribute but at least not to produce any impairment.

3. Inspection to insure that operation in a potential fracture area is not attempted.

Some Sources of Flaws: Something of a semantics problem is posed in cataloguing flaws. Distinctions tend to be made between cracks, pores, scratches, grooves, pits, etc., while origins are generally traced to transformation and thermal-stress cracking (as in welding and heat treating), to different forms of surface mutilation (such as laps, tool marks, incipient wrinkles in sheet drawing, weld-bead discontinuities), to corrosion, and to bulk plastic straining. Some, but hardly all, of the possible ways for producing such flaws are understood and have been discussed at length many times. The last entry in this list is of interest for it seems not to be as widely recognized as others. Nonetheless, it is well established that plastic deformation at any stage of processing may lead to a breaking up of brittle components of microstructure and separation over inclusion-matrix interfaces because of a weakness at these places coupled with the dissimilar plastic properties of the phases involved.[1]

Some Variables Effecting Fracture Toughness: There should be some benefit by way of higher fracture toughness in a large plastic "sink" around the crack tip into which stored elastic strain energy can drain. The capacity of this "sink", measured in terms of G_c, can be increased by meeting two conditions:

1. Large deformation work per unit volume, which would be variable throughout the total volume but favored by large plastic strain and high flow stress;

2. Large total plastic volume.

Fracture with low energy absorption, or low fracture toughness, could be expected if either condition is not satisfied. A sharp decrease in plastic strain because of a basic change in fracture mechanism, e.g. from ductile to cleavage, would preclude meeting the first. Also, a localization of strain, even if the strain were large, could mean small total volume and a violation of the second.

Therefore, a material's plastic properties, which would be affected by fabrication history, become important to fracture-energy absorption. In particular, a higher and over-all more persistent rate of strain hardening (to large plastic strain) should be useful because then plastic strain ought to penetrate deeper into material at the crack tip to give a larger, more absorbent, volume.[2] Accordingly it might be profitable to pay more attention to the interrelationships between strain-hardening characteristics and structure, particularly at high-strength levels, as these are influenced by the various joining, heat treating, and deformation processing operations.

When the stress-strain curve can be fitted with a "power-law" equation, the exponent is a good indicator of how rapidly the hardening rate falls off with straining. As a rough approximation, this strain-hardening exponent tends to decay exponentially with rising strength level, so that hardening rate is generally found to drop rather quickly at strength levels of current interest. The implication, therefore, is that attempts at control would probably be concerned with fairly subtle variations.

Unfortunately, there have been many examples to show that welding may also be a source of fracture-toughness impairment. A variety of structural changes can be responsible, and some of these are sure to be discussed later on. Weld strength might be depressed because of enlarged grain size, over-aging, or local recrystallization, perhaps aggravated by an accompanying drop in fracture strain from segregation, grain-boundary film formation, aging effects, etc.

Another aspect of fracture toughness is the anisotropy than can be found in high strength sheet. Values tend to be larger when cracking occurs across, in contrast to along, a well-defined rolling direction, and in some cases a measurement made in the one direction will be several times that in the other. Certainly the basic reason is structural anisotropy produced by the earlier processing. There are implications in its presence both for fabrication and for speculation about fracture mechanism.

In the first place, it may be a factor in the problem of correlating uniaxial-load property measurements and biaxial-stress test results. Depending upon stress ratio, various fracture paths with different G_c values can be imagined under the biaxial loading, so that there would be value in good information about the anisotropy when attempting to relate working direction to service loading.

An explanation of this anisotropy might include several structural details. Two of particular interest are, first, the mechanical fibering caused by alignment through prior deformation of inclusions, extra phases in general, unwelded cavities, etc., and, second, the texture from preferred crystallographic orientation. The latter is known to effect plastic flow characteristics while mechanical fibering is associated very closely with fracture. From considerable work on the ductile-brittle transition in low-carbon steel, it also seems quite clear that strong fracturing anisotropy --- whether this is measured in terms of a stress, fracture strain or reduction of area in tension, or energy absorption in notched specimens --- is encountered when fracture occurs by a non-cleavage mechanism.[3] The implication, then, is that a mechanism of cleavage in the usual crystallographic sense may not operate at very high strength levels either, even though energy absorption should be relatively low, when there is a pronounced fracture-toughness anisotropy.

The picture has a certain consistency. If fracture toughness is related to plastic properties, it ought to reflect a change in the strain hardening curve. Such a change could be related in turn to many things, including texture and mechanical fibering. The one should have greater effect on the over-all curve shape; the other ought to be much more potent in acting to terminate the curve, depending upon direction of measurement, and thus regulate plastic work for fracturing. These are simply two more fabrication variables, and their development is another effect that might be brought under still closer control and used to better advantage. One possible, even unsuspected, advantage may be found at the moment during the through-thickness (plane strain) propagation of a small crack; it could be argued that a fiber distributed in the plane of a sheet might help to offset the basically lower fracture toughness associated with this condition of propagation.

A final and well-recognized source of impairment to fracture toughness is residual stress, whichever one of many possible origins it might have. These would include the various deformation processes (roll forming, shear spinning, deep drawing, machining, etc.), heat treatment, welding (because of mismatch, peaking, etc.), and even hydrogen embrittlement as it has been discussed by Shank, et al.[4]

Controls

The real difficulty lies in the next and obviously necessary step of specifying procedures and controls to insure the objectives of proper mechanical form, properties, and behavior.

In the control of flaws, of all kinds, there are problems attached to every approach. In deformation processing, any strain-induced porosity may be countered and anisotropy regulated in part at least with cleaner, more homogeneous, i.e. vacuum melted, materials.

However, the problems facing an advocate of assembly by welding are notoriously severe. Some such fabrication may be essential from a practical point of view, but it still has its beginning in a state that must never be allowed to recur and that is one of loose pieces; all of which vaguely suggests what faced the king's horses and men in the Humpty Dumpty story. Ideas about how to improve this position by operating on fusion and heat-affected zones, thermal history, design of filler material, etc. can be anticipated in what follows.

To meet such problems, there is the much discussed trend in motor-casing design, as the example of the minute, away from welds in highly stressed locations. Current practices on newer designs are being developed around deformation processes such as forging, shear spinning and deep drawing. The more highly stressed (longitudinal) welds are eliminated and, with machining, bosses and skirts may be made integral. Still other developments in progress based on deep drawing and shear spinning, or flow-turning, are aimed at fully integral cases. A somewhat different viewpoint is held by devotees of wrap processes. Now circumferential joints would be basic to design but made innocuous with sufficient overlap and some method of joining such as resistance welding, adhesive bonding, brazing, or even mechanical interlocking. A potential advantage is construction from thin, narrow, strip with the high-toughness direction strategically disposed and possibly strengthened (if steel) through some thermal-mechanical process such as "ausforming" (or, what is probably very similar, low temperature rolling of metastable austenitic steel). It is interesting to note that a closely similar design based on wrapped sheet metal was tried about 100 years ago for the somewhat lower pressure application of black-powder cartridge cases.[5]

Each approach can be characterized in much greater detail by its own particular set of problems such as tolerance control, forming limits, machining requirements, welding set-up and processing costs. Competetive positions are strongly influenced by the interactions at this level, but they are issues that could hardly be brought up in detail here.

In regulating fracture-toughness and strength-level, the basic concern is with structure and chemistry. Weld-zone microstructure and composition; surface carburization or decarburization, retained austenite, temper embrittlement after heat treatment; uniformity of initial microstructure as it influences response to heat treatment; structures from cold or "warm" working operations to produce strengthening -- all of these fit in here.

The broad practical goals to be reached have been identified many times: great strength with light weight and high fracture toughness. The major problem areas where the interference originates are at least roughly mapped out. Interlocking is clear and one area well surrounded by others is fabrication. Its peculiar importance rests on a potential for action in two rather different ways: with control it can assist, yet without control it may seriously impair progress towards these goals.

References

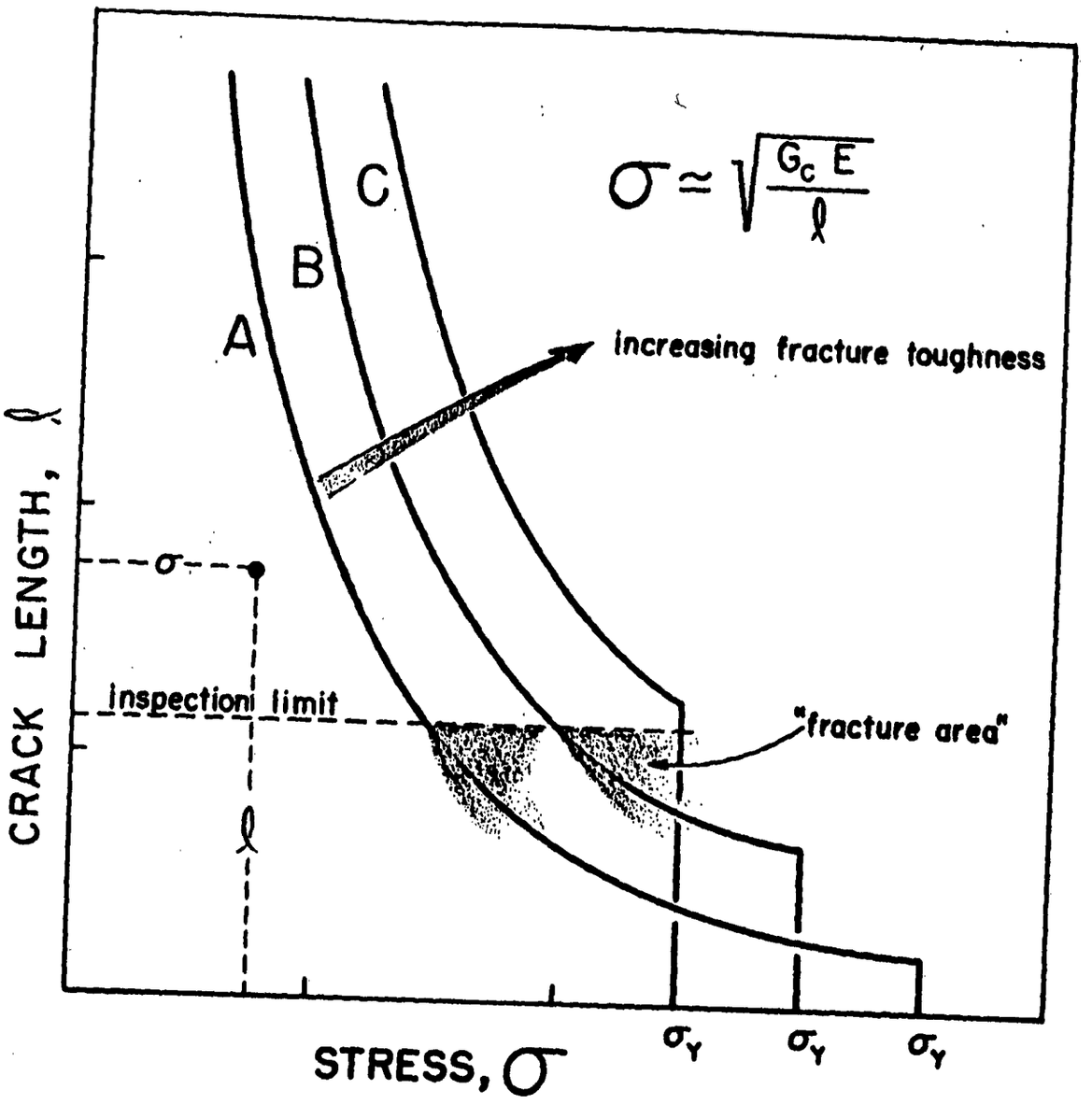
1. W. A. Backofen, "Metallurgical Aspects of Ductile Fracture", Conference on Fracture of Engineering Materials, ASM, Troy, N. Y., August 1959, to be published.

2. M. Gensamer, "Strength and Ductility", Transactions ASM, 36, 1946, p. 30.

3. F. de Kazinczy and W. A. Backofen, "Effect of Rolling Conditions on Brittle Fracture", Transactions, ASM, 52, 1960.

4. M. E. Shank, C. E. Spaeth, V. W. Cooke and J. E. Coyne, "Rocket Motor Cases and Delayed Failures", Pratt & Whitney Aircraft Div. United Aircraft Corporation, Rocket Motor Case Symposium, September 29, 1959.

5. U. S. Patent 40,988, December 15, 1863.


$\sigma \simeq \sqrt{\frac{G_c E}{\ell}}$
A
B
C
increasing fracture toughness
CRACK LENGTH, ℓ
σ
Inspection limit
ℓ
"fracture area"
STRESS, σ
σ_Y
σ_Y
σ_Y

DEFECTS, SURFACE FINISHES, AND HYDROGEN EMBRITTLEMENT

C. E. Spaeth
Senior Design Engineer
Pratt & Whitney Aircraft
East Hartford, Conn.

ABSTRACT

A report is presented of the design, fabrication, and testing of full scale (40 in. diameter, 6 ft. long) solid fuel rocket motor cases capable of operation at 240,000 psi tangential stress. An H-11 consutrode vacuum remelted steel, hardened to 270,000 psi tensile strength, was employed. Failure, originating in parent material, of a full scale motor case, and subsequent investigation showed that water used in hydrostatic testing can initiate hydrogen induced fracture. To substantiate this conclusion, characteristics of this mode of failure are contrasted with characteristics produced in experiments dealing with stress corrosion.

The merits of partial decarburization as a surface treatment are discussed. It is concluded that flo-turned rocket motor cases of H-11 to operate at stress levels of 240,000 psi are both feasible and practical. As a demonstration of feasibility, cyclic tests to 220,000 and 240,000 psi were performed on two full scale cases, using oil as the pressurizing fluid. These motor cases not only retained their integrity, but in addition suffered no perceptible yielding.

INTRODUCTION

The effect of fabrication variables upon the performance of sheet materials used in pressure vessels is effectively illustrated by data obtained during the course of rocket motor case development and production at the author's company. The data reduced to simplest terms is presented as Figure 1, which shows the relationship of pressure vessel burst strength to the uniaxial 0.2% offset yield strength of the material involved. This method of presentation is chosen because it gives quantitative information concerning the loss in strength due to fabrication variables, and it shows that deterioration in pressure vessel performance need not occur accompanying a material yield strength increase from the 200,000 psi range to a level of 240,000 psi. A break in slope around 200,000 psi and a premature failure branch have been recognized by G. R. Irwin[1] and others as associated with low fracture toughness. While there is no disagreement with this insight into the problem, Figure 1 emphasizes that low fracture toughness is not apparent in pressure vessel burst strength performance except as fabrication defects or phenomena such as hydrogen embrittlement are also present. Failures on the lower branch to the right of the peak must be termed premature, while failures on the upper branch represent material capability.

Premature failures may be divided into two categories according to whether the failure is time dependent or occurs immediately upon application of pressure. If failure occurs prematurely and without delay, then a defect of critical proportions must have existed in the vessel as manufactured. A method of dealing with surface defects will be discussed. Time dependent failures and their prevention will also be discussed.

The burst test results constituting the upper branch curve in Figure 1 were obtained subsequent to the investigations described in the present paper. The consistency of results from cases tempered to the same strength level is noteworthy as is the fact that failure stress increased steadily with increase in uniaxial yield strength level over the range covered by the data.

DESIGN, MATERIAL, AND FABRICATION

Figure 2 shows the various portions of the full size casing before assembly. The main longitudinal section is seamless, having been flowturned into a cylinder from a solid seamless ring forging of the same internal diameter. The ellipsoidal head on the right of the photograph has been machined from a forging and the base of the attachment skirt is integral with it. The left-hand closure in Figure 2 is forged and machined out of a single piece. The large closure flange (see left side of Figure 2) is integral with this ellipsoidal head. Only girth welds are needed to assemble these details into cases approximately 40 inches in diameter and 6 feet long.

Following the decisions concerning the basic design criteria for the vessel considerable thought was given to the choice of material from which to manufacture it. On the basis of information concerning strength, ductility, and toughness then available, as well as ease of fabrication, an H-11 composition was chosen. H-11 material is essentially a 5% Cr toolsteel with 0.42% C, 0.29% Mn, 0.96% Si, 5.17% Cr, 1.35% Mo, and 0.52% V. In order to get the cleanest and highest quality material

possible, consutrode remelted stock was employed. One of the major factors in picking an H-11 steel was the success achieved in a pilot series of pressure vessels 9.5 in. in diameter and approximately 14 in. long, with wall thicknesses in the cylindrical portion of approximately 0.040 in. The cylindrical portion consisted of two sections integral with hemispherical heads. They were hydroformed and had no longitudinal welded seam. The two halves were joined with a girth weld. Failures originating at welds were encountered in hydrostatic tests of some of the earlier test vessels. These difficulties were corrected.

Another series of vessels failed at very high stress levels with the origins of failure being in no way connected with welds, but rather being in the parent metal. Figure 3 shows a subscale vessel after failure. The fracture origin indicated by the arrow is in parent metal 1.50 in. from the circumferential closure weld.

TEST OF EXPERIMENTAL FULL SCALE CASE

The vessel had been designed for a material with a minimum yield strength level of 235,000 psi and a tensile strength of 270,000 psi nominal. Following manufacture the vessel was set up in a test rig and hydrostatically tested, using water as the fluid, at a temperature of 70°F. It was tested in successive steps over a period of one hour to a maximum wall stress of 46,200 psi in a tangential direction. Several days later it was filled with glycerine which had been heated to a temperature of 360°F. The hot glycerine was employed because there was at that time a specification requiring a 360°F test. Stress was held at 188,000 psi for a period of three minutes. Finally, several months later, a third series of tests was performed at room temperature, again employing water as the hydrostatic fluid. Tests were successfully performed at stress levels of 61,700 psi, 154,000 psi, and 216,000 psi. As the fourth test in this series was being run to reach a stress level of 220,000 psi, premature fracture occurred when the vessel had reached only 185,000 psi. This was considerably lower than the previous successful test. Catastrophic failure occurred, with the shattering results shown in Figure 4. The water had been in the vessel 57 minutes in this final test series.

INVESTIGATION OF FAILURE

An investigation was immediately started to determine why the vessel, having survived previous tests at higher stress levels, had failed at a level of 185,000 lbs. per square inch tangential stress in the cylindrical portion. As a first step in the investigation the pieces were reassembled. Examination of the many feet of fracture surface showed that chevron or herringbone markings, usually found in brittle failures of carbon plate steel structures at relatively low stress levels[8], were present in the casing. The apices pointed back to the direction from which the failure had come. While the crack pattern was very complex, it was clear that all markings led back to a single origin of fracture as shown in Figure 5. The origin was clearly shown to be in a pit in the inner cylindrical surface. This pit was one of many in a small area which had been ground superficially to remove a slight defect. Fracture markings fanned out from this pit in both directions, as shown in Figure 6. It was also noted that a shear lip was present along the edges of the fracture except at the pit. These last two features are typical of catastrophic brittle failures at much lower stress levels and in much softer materials.[8]

Standard tensile tests were performed on specimens machined from the fragments in the axial direction of the cylinder. It was seen that the tensile strength was somewhat over 270,000 psi and the yield strength at 0.2% offset was 236,000 psi in one case and 240,000 in another. Obviously, then, the general structure of the vessel had adequate strength to withstand hydrostatic tests of greater pressures than were employed at or before the time of failure.

EFFECT OF PARTIAL DECARBURIZATION

In the course of the failure investigation evidence of the advantage of partial surface decarburization was brought to light (Figure 7). On the left is a view of a plane parallel to the inner surface of the vessel which exhibited a superficial defect at this location. The inset shows a right section through a portion of the defect. Of particular interest is the lighter colored beach-like area, which is the zone of intentional partial decarburization. It is noteworthy that this zone encases the tip of the lap, thereby constituting a barrier to the progress of the fissure into and through the high strength core material that lies beyond. The results of bend tests of H-11 material at this strength level had shown dramatic improvement due to decarburization, which led to this treatment for the case.

THE EFFECT OF HYDROGEN IN STEEL

At this point it would be well to discuss some of the recent research work that has been carried on concerning the nature of hydrogen embrittlement, cracking, and delayed failure in steel. Much work has been performed in this area in recent years. Some of the most significant has been carried out by Troiano[2-7] and his co-workers and by Sachs.[10,11] No complete review of theories of hydrogen embrittlement and associated delayed failure will be attempted here. For such a review the reader is referred to References 2, 5, and 11. Theoretical and experimental developments pertinent to the present problem, however, will be briefly covered.

It has long been known that if specimens containing small amounts of hydrogen in solution are tested by conventional methods they may display the normal properties of strength and ductility. Yet delayed failure in the same material will occur under long time loading in the presence of a stress concentration. If the delayed failure tests are performed for a steel of given tensile strength (as measured in smooth specimens) with fixed concentration of hydrogen in solution and fixed notch acuity of the test specimen, three characteristics are revealed. First, there is an upper stress level corresponding to the notch tensile strength of the material for short-time loading. Second, there is a static fatigue or lower limit of stress below which failure will not occur in any length of time. Third, there is an intermediate range of stress over which delayed failure takes place[5]. These features are shown in Figure 8, which is after Troiano[5]. It has been further demonstrated that under stress in the presence of a stress concentration such as a notch or void hydrogen will diffuse to the point of maximum triaxiality of stress. Thus the process involved is not one of classical diffusion, but rather diffusion in the presence of a stress gradient. For a sharply notched specimen the point of maximum triaxiality lies close to the surface near the root of the notch. For rounded notches the point of maximum triaxiality of stress lies increasingly away from the surface of the stress concentration. After the period of incubation the crack initiates at this point and propagates

both outward to the surface of the stress concentration and inward. This is shown in Figure 9.

WATER AS A CAUSE OF FAILURE DURING HYDROTEST

As stated earlier, all cracks were traced to a single origin and at this location there were a number of corrosion pits. (See Figure 10.) An edge of one of these is shown highly magnified at the left hand edge of Figure 11. In this photograph also are cracks which can be presumed to resemble the one that reached critical size and led to catastrophic failure. One crack, marked by an arrow, clearly extends into the pit itself. However, the portion of this crack that is most widely opened is somewhat removed from the pit surface. The portion of the crack that extends into the pit surface is rather narrow. Just above this there is another crack which does not open into the pit surface. At 500 diameters the comparatively large crack is seen to be separated from the pit by about 0.005 in. The adjacent crack is connected with the pit by a narrow, discontinuous region. The more open portion of the crack is separated from the pit surface by about 0.005 in. The features described are typical of the pitted regions in the large fractured casing. They are also very similar to those taken from the experimental work of Troiano.

The role postulated for the water was two-fold. First, it provided the pit which in turn provided the essential triaxiality of stress; and, second, it was a medium for electrolysis which released the essential hydrogen. A more complete discussion of the latter effect may be found in Reference 12.

A program of investigation to support or refute the hypothesis was immediately launched. Six sub-sized test vessels exactly like those previously employed were manufactured for testing. Again the material was H-11 analysis, but air melted stock. The hydrogen content was 1.5 ± 0.1 parts per million prior to fabrication of the small vessels. Heat treat and fabrication procedures were as used in the large casing.

Hydrostatic tests were run on each of these vessels. The details are given in Table I. The first in the series, Vessel No. 14, was stressed tangentially at the thinnest section of the wall to 201,500 psi for 60 minutes and 224,000 psi for 53 minutes, at the end of which time it fractured. The origin of failure was on the inside cylindrical surface about 1-1/2 inches from the central girth weld. The origin was in parent metal. The pressurizing fluid had been water. Examination of the origin showed a dark area which extended into the thickness of the material about one-quarter of its thickness, or roughly about 0.010 inch. Chevron markings were developed away from the point of origin and a shear lip was present everywhere except at the point of origin. The fracture is shown in Figure 12. The darker area at the origin is typical of hydrogen-initiated failures. It is well illustrated in References 6 and 11. It is caused by the fact that slow, hydrogen-induced crack propagation has a finer texture than the surrounding fracture area which propagates at high velocity.

The second vessel in the series, No. 15, was also pressurized with water. It was loaded seven successive times at different stress levels and for different times, as indicated in Table I. The fractured vessel was shown reassembled in Figure 5

and the surface of fracture is shown in Figure 12. It will be seen that the origin of fracture was some distance removed from the welded joint and was in the parent metal. Again, the dark area typical of hydrogen-induced fracture was present. A third vessel, No. 16, was also pressurized with water. It carried a sustained tangential wall stress of 255,000 psi for 840 minutes. Following this it was loaded to 256,000 psi tangential wall stress for 135 minutes, whereupon it fractured. Again, the origin of fracture was in the parent metal at a point removed by about 1-1/2 inches from the circumferential weld. As shown in Figure 12, there was also the dark area at the origin, indicating fracture originating from hydrogen. Shear lips appear along the edges of fracture except at the origin.

The next vessel to be tested, No. 21, was coated inside with Ochre Heresite primer (AMS 5108) to protect it from electrolytic attack by the water. It sustained a maximum tangential stress of 241,000 psi in the cylindrical portion for 810 minutes. Following this it carried a stress of 262,000 psi for one minute before fracturing. The fracture originated in parent metal on the inside surface about 1-7/8 inches from a weld. The area containing the origin of fracture was badly bulged (see Figure 13). It will be noted that there is no discolored area at the origin of fracture, and in fact the fracture origin has a shear lip running alongside it, indicating that fracture must have initiated beneath the surface, probably at some sort of inclusion. Analysis of the material for hydrogen content indicated that it contained 3.2 parts per million. Subsequent check of the hardness of vessel No. 21 showed it to be R_c55, indicating that it had been inadvertently tempered at too low a temperature, probably 950° - 1000°F. All other vessels had a hardness of R_c 50-51. This would indicate vessel No. 21 to have a higher tendency to crack initiation from mechanical causes(13) such as inclusions.

The fifth vessel in the series to be tested, No. 22, was again coated on the inside with primer. The pressurizing medium was water. However, in this test the vessel itself was submerged in a water bath with the outside unprotected. It sustained a maximum tangential stress in the cylindrical portion of 218,000 psi for 870 minutes and of 240,000 psi for 75 minutes, following which it fractured. The origin of fracture was in the parent metal 2-7/8 inches from the weld. It is of the greatest significance that the fracture originated on the outside surface of the vessel, which was submerged in water and unprotected. As seen in Figure 14, there is the dark area typical of hydrogen-induced fracture at the origin. There is also a relatively smooth pit at the origin about 0.0025 inches deep. The average hydrogen content of the steel was found to be 2.0 parts per million.

The final vessel in the series, No. 25, was coated both inside and outside with primer. It was cycled four times for three minutes each time to 264,000 psi with water as the pressurizing medium and a water bath on the outside. Following this it was held at 264,000 psi for 585 minutes. It was then held at 264,000 psi for 240 minutes, at 275,000 psi for 525 minutes, and again at 275,000 psi for 135 minutes with rest periods. See Table I. After this the water was removed from both inside and outside and it was pressurized with oil. It was held at 275,000 psi for 435 minutes. Following this the pressure was increased each hour in steps over a period of 810 minutes. Failure occurred at 318,000 psi after 45 minutes at this stress level. The fracture surface is shown in Figure 15. Interestingly

enough, the mode of failure through the cylindrical section was largely shear, except for a small tensile progression at the failure origin. There was no evidence of a discolored area at the failure origin, indicating that the failure had not been hydrogen-induced. See Figure 15.

The results of the foregoing delayed failure tests are recapitulated in Figure 16. Here the average local stress level at the failure origin in each case is plotted against the time to fracture. The local stress level was determined on the basis of the thickness of material at the fracture origin. The vessels had a slightly uneven thickness in the cylindrical portion. The fracture origin in no case occurred at the point of thinnest section. It is the maximum tangential stresses at the point of thinnest section that are reported in Table I. Because of this difference the stresses in Figure 16 are slightly less in value than those appearing in Table I. The fact that the fracture origin in the small vessels was usually between one and two inches from the weld is indicative of secondary bending stresses caused by weld thickening. The actual stress here may therefore be higher than is indicated by Figure 16. None of the fracture origins was in a heat-affected zone.

TESTS OF ADDITIONAL FULL SCALE ROCKET CASINGS

Following the completion of the foregoing series of tests, two full size solid fuel rocket casings, as shown in Figure 2, were hydrostatically tested. The pressurizing fluid employed was oil. They were cycled four times from zero stress to a tangential stress level of 220,000 psi and held 5 minutes in each cycle. They were then cycled four times to a stress level of 240,000 psi and held for 5 minutes in each cycle. The vessels retained their integrity and subsequent detailed examination showed that they had suffered no damage.

DISCUSSION AND CONCLUSIONS

In the tests of the full size and sub-size vessels two facts are clear. First, if a vessel is free of fabrication defects failure can be induced at high tangential stresses in the parent metal of the cylindrical section away from weld areas and changes of contour, providing the metal is not allowed to come in contact with an electrolytic solution. This is seen in test vessels No. 21 and 23, protected from electrolytic action. The stress levels at which they failed were higher than any of those in vessels No. 14, 15, 16, and 22 which were exposed to water during testing. Second, it is possible to transfer the origin of the fracture from the inside to the outside surface, as in Vessel No. 22, by protecting the inside and exposing the outside to an electrolytic solution, even though it be a weak electrolyte such as tap water. This argument is reinforced by the appearance of the fracture origins. In the vessels exposed to an electrolyte the origins showed the local darkening typical of hydrogen induced failures. In the protected vessels, No. 21 and 23, there was no evidence of this. In the case of No. 21 the fact that the shear lip is present alongside the origin demonstrated that the failure was subsurface in origin and therefore could not be connected with electrolytic action.

Stress corrosion cracking also is a possible cause of delayed failure, but in the instances cited there is ample evidence to indicate hydrogen embrittlement. When hydrogen embrittlement is not a factor, stress corrosion in martensitic steels is predominantly intergranular in character (14, 15). The failures induced during hydrostatic testing were characterized by a zone of slow crack propagation exhibiting a dark appearance attributable to the fine texture of transgranular progression. This feature is therefore indicative of hydrogen embrittlement.

When hydrogen embrittlement is not a factor, stress corrosion in martensitic steels is commonly characterized by a many-branched system of cracks (14, 15). On the other hand, when heavy cathodic charging is introduced into the experiments, hydrogen embrittlement predominates and branching disappears (15). The absence of branching in the failures encountered in the present work would therefore indicate involvement with hydrogen embrittlement.

While not conclusive, the observed tendency for cracks to originate at a definite distance from pits is a further indication of hydrogen embrittlement as shown by Troiano(5) and discussed heretofore in the present paper.

The conclusions drawn as a result of these investigations may be summarized as follows:

1. In the absence of avoidable defects, burst strengths in excess of 500,000 psi can be attained consistently using material heat treated to 240,000 psi yield strength.

2. Hydrogen embrittlement can lower the burst strength by 150,000 psi or more owing to the low fracture toughness of the material.

3. Any crack of the same size and orientation as the hydrogen induced crack would be equally damaging.

4. Hydrotesting with oil is an effective preventative measure against hydrogen embrittlement provided the motor case is not loaded with hydrogen prior to hydrotest.

5. Surface decarburization is effective as a means of preventing the catastrophic spread of certain classes of defects.

BIBLIOGRAPHY

1. G. R. Irwin, Notes for meeting of ASTM Committee, New York, March 24, 1959.

2. J. G. Morlet, H. H. Johnson, and A. R. Troiano, "A New Concept of Hydrogen Embrittlement in Steel", WADC Technical Report 57-190, March 1957.

3. W. H. Frohmberg, W. J. Barnett, A. R. Troiano, "Delayed Failure and Hydrogen Embrittlement in Steel", Trans. ASM 47, pp. 892-923 (1956).

4. W. J. Barnett and A. R. Troiano, "Crack Propagation in the Hydrogen-Induced Brittle Fracture of Steel", Journal of Metals, April 1957, pp. 486-494.

5. E. A. Steigerwald, F. W. Schaller, and A. R. Troiano, "Effect of Temperature on the Static Fatigue Characteristics of Hydrogen Embrittled 4340 Steel", WADC Technical Report 58-178, April 1958.

6. H. H. Johnson, J. G. Morlet, and A. R. Troiano, "Hydrogen, Crack Initiation, and Delayed Failure in Steel", Transactions of the Metallurgical Society of AIME, 212, No. 4, August 1958, pp. 528-536.

7. P. Blanchard and A. R. Troiano, "Delayed Failure and Notch Tensile Properties of a Vacuum Melted 4340 Steel", WADC Technical Note 58-176, Sept. 1958.

8. M. E. Shank, "A Critical Survey of Brittle Failure in Carbon Plate Steel Structures other than Ships", Bulletin No. 17, Welding Research Council, January 1954.

9. R. H. Raring, J. A. Rinebolt, "Static Fatigue of High Strength Steel", Trans. ASM 48, pp. 198-212 (1955).

10. E. P. Klier, B. B. Muvdi, V. Weiss, G. Sachs. Discussion to Reference 9.

11. E. P. Klier, B. B. Muvdi, and G. Sachs, "The Response of High-Strength Steels in the Range of 180,000 to 300,000 psi to Hydrogen Embrittlement from Cadmium-Electroplating", ASTM Preprint 78 (1958).

12. M. E. Shank, C. E. Spaeth, V. W. Cooke, and J. E. Coyne, Metal Progress, 76, 74-82 (1959).

13. G. B. Espey, M. H. Jones, W. F. Brown, Jr., "Preliminary Report on Sharp Notch and Smooth Tensile Characteristics for a Number of Ultra High Strength Sheet Steel Alloys", Preprint for ASTM meeting (June 1959).

14. H. J. Noble, W. H. Sharp, Steels and Protective Treatments for use up to 1000°F, SAE Transactions (1956).

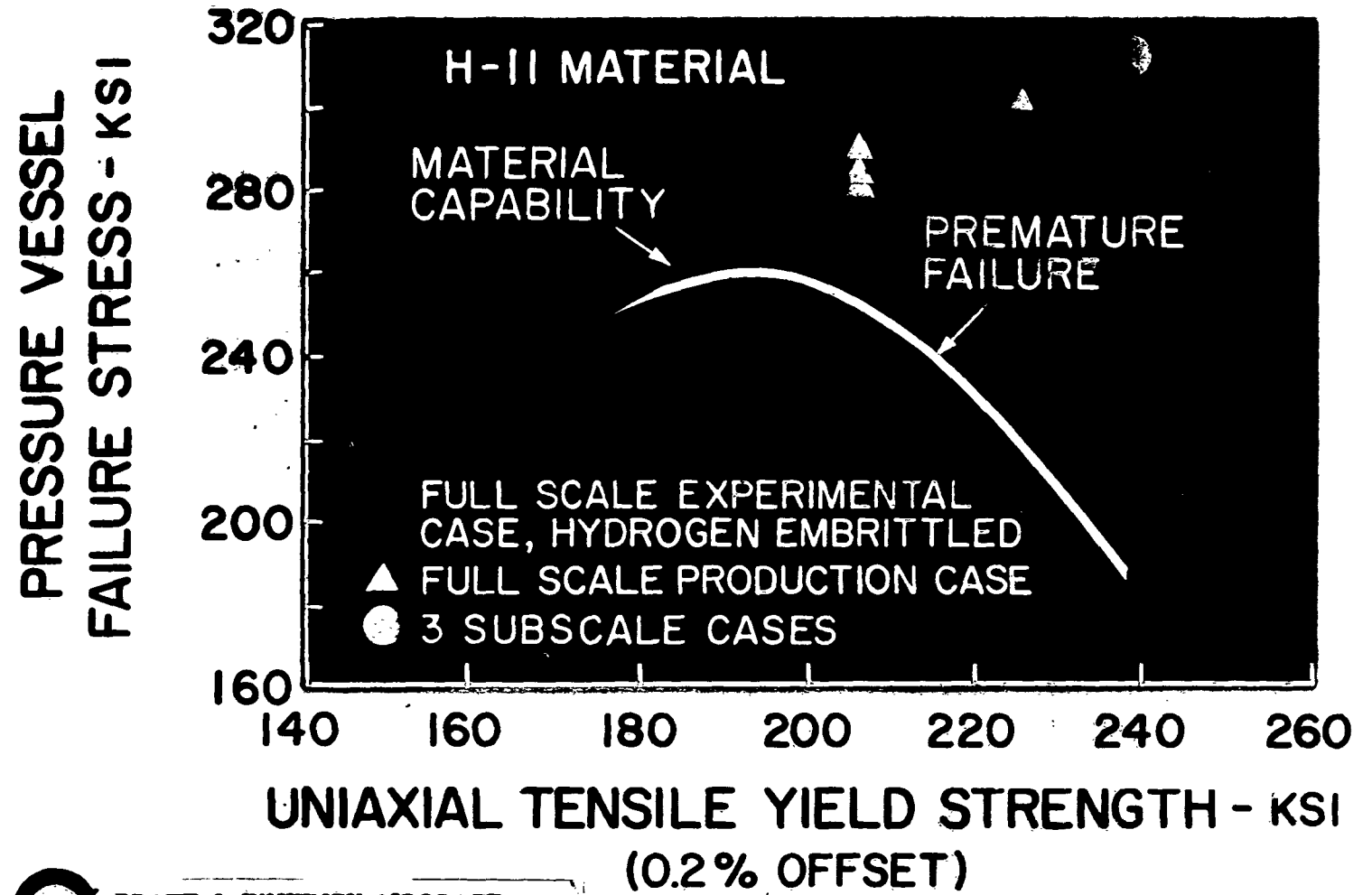
15. E. H. Phelps, A. W. Loginow, "Stress Corrosion of Steels for Aircraft and Missiles", Applied Research Laboratory, United States Steel Corporation, Monroeville, Pennsylvania.

Table I . Sub-size Vessels Burst-Tested in Delayed Failure to Demonstrate Effect of Hydrogen Charging. All H-11 Air Melted Stock**. Stresses are tangential, based on thinnest wall section of cylinder.

No.	Remarks	Type of Test	Tangential Burst Strength-psi	Origin of Failure	Pressurizing Fluid	Comments	Average Hydrogen Content - ppm
14	no protection	sustained Load 201,500 psi - 60 min. 224,000 psi 53 min.	224,000	Inside cylindrical surface in parent metal about 1-1/2 in. from weld.	Water	Dark area typical of hydrogen induced fracture at origin of fracture.	---
15	"	sustained load 275,000 psi 1 sec. 206,000 5 min. 252,000 5 min. 172,000 180 min. 172,000 420 min. 229,000 420 min. 252,000 16 min.	252,000	" "	Water	" "	---
16	"	sustained load 235,000 psi 840 min. 256,000 135 min.	256,000	" "	Water	" "	---
21	Inside coated with Herisite Primer (AMS 3108)	sustained load 241,000 psi 810 min. (Depressurized. Water left in.) 262,000 psi 1 min.	262,000	Inside cylindrical surface in parent metal about 1-7/8 in. from weld	Water	No discolored area at origin of fracture	3.2±0.1
22	Inside coated with Herisite Primer (AMS 3108) Outside submerged in water bath	sustained load 218,000 psi 870 min. (Depressurized. Water left in.) 240,000 psi 75 min.	240,000	Outside cylindrical surface in parent metal 2-7/8 in. from weld.	Water	Dark area typical of hydrogen induced fracture at origin. Origin at relatively smooth pit 0.0025 in. deep	2.0±0.1
23	Inside & outside coated with Herisite Primer (AMS 3108). Tempered in vacuum to reduce hydrogen. *Vessel immersed in water for tests so marked.	sustained load 4 cycles of 3 min. ea. to 264,000 psi 264,000 psi 585 min. * (57.4 hrs. rest. Water drained.) 264,000 psi 870 min. * (14.25 hrs. rest. Water drained.) 264,000 psi 240 min. * 275,000 psi 345 min. * (8.75 hrs. rest. Water drained) 275 000 psi 135 min. * (8.0 hrs. rest.) 275,000 psi-435 min, following which pressure increased hourly in steps over 810 min. Failure at 318,000 after 45 min.	318,000	Inside surface of cylinder in parent metal approximately 2-3/4 in. from weld.	Water Oil	No discolored area at origin of fracture	9.6±0.1

**Initial stock contained 1.3 ppm of hydrogen prior to fabrication.

SHEET MATERIAL PERFORMANCE AS AFFECTED BY PRESSURE VESSEL FABRICATION VARIABLES



PRATT & WHITNEY AIRCRAFT
DIVISION OF
UNITED AIRCRAFT CORPORATION

M-5221
6-9-60

III-22

FIG. 1

Exploded Assembly of the Full Size Vessel. Central Cylindrical section is flowturned with no longitudinal seams. Piece at the left is a closure for test purposes. The dome-shaped head at the left has the closure flange integral with the shell. The skirt on the ellipsoidal head at the right is integral with the shell portion. The extended skirt section at the far right is then welded to the skirt on the ellipsoidal head.

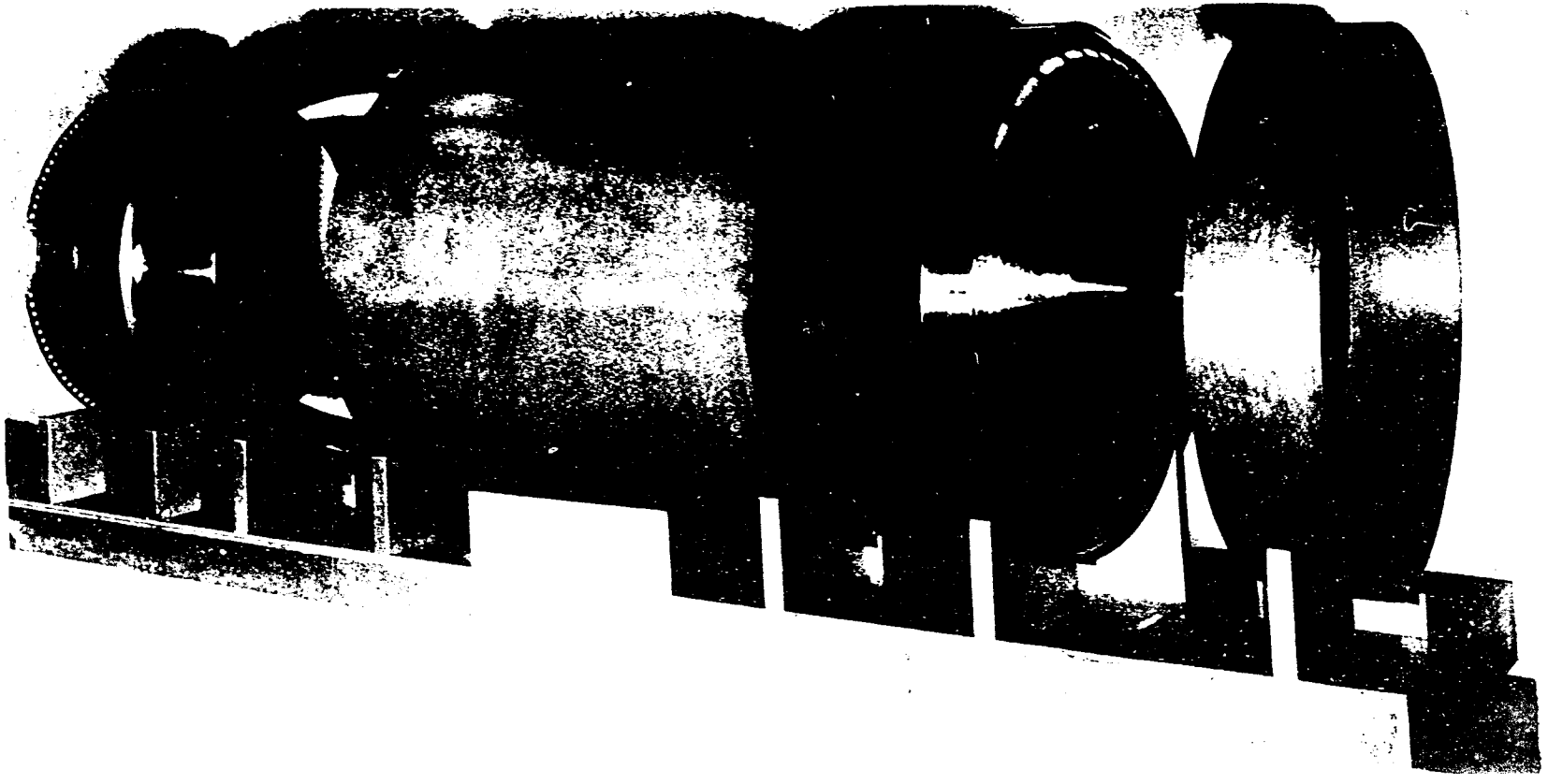
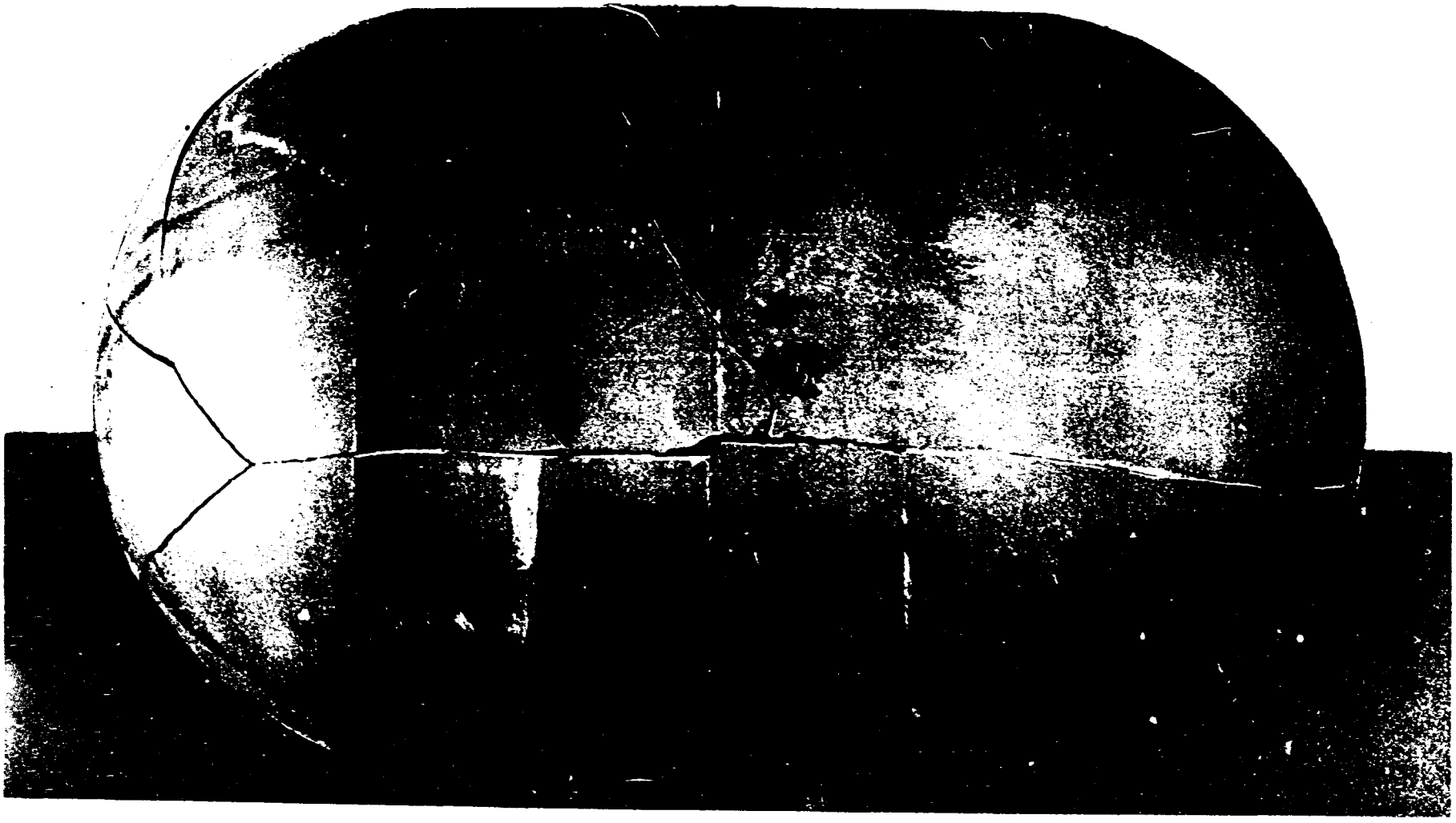


FIG. 2



Test Vessel No. 15, which burst at 252,000 psi maximum tangential wall stress in the cylindrical portion. Arrow indicated location of failure origin. It is in parent metal about 1-1/2 inches from the weld.

Fig. 3

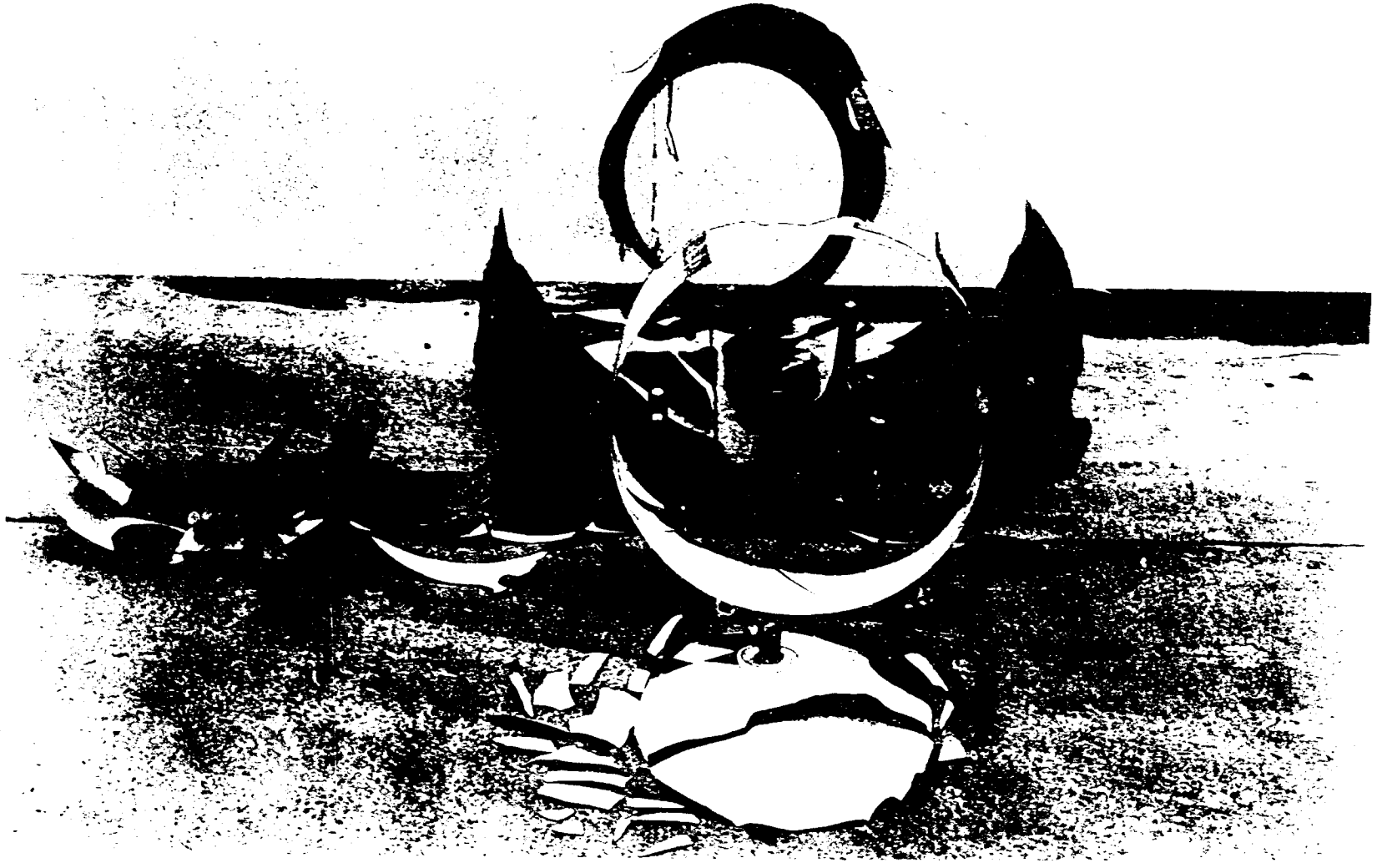
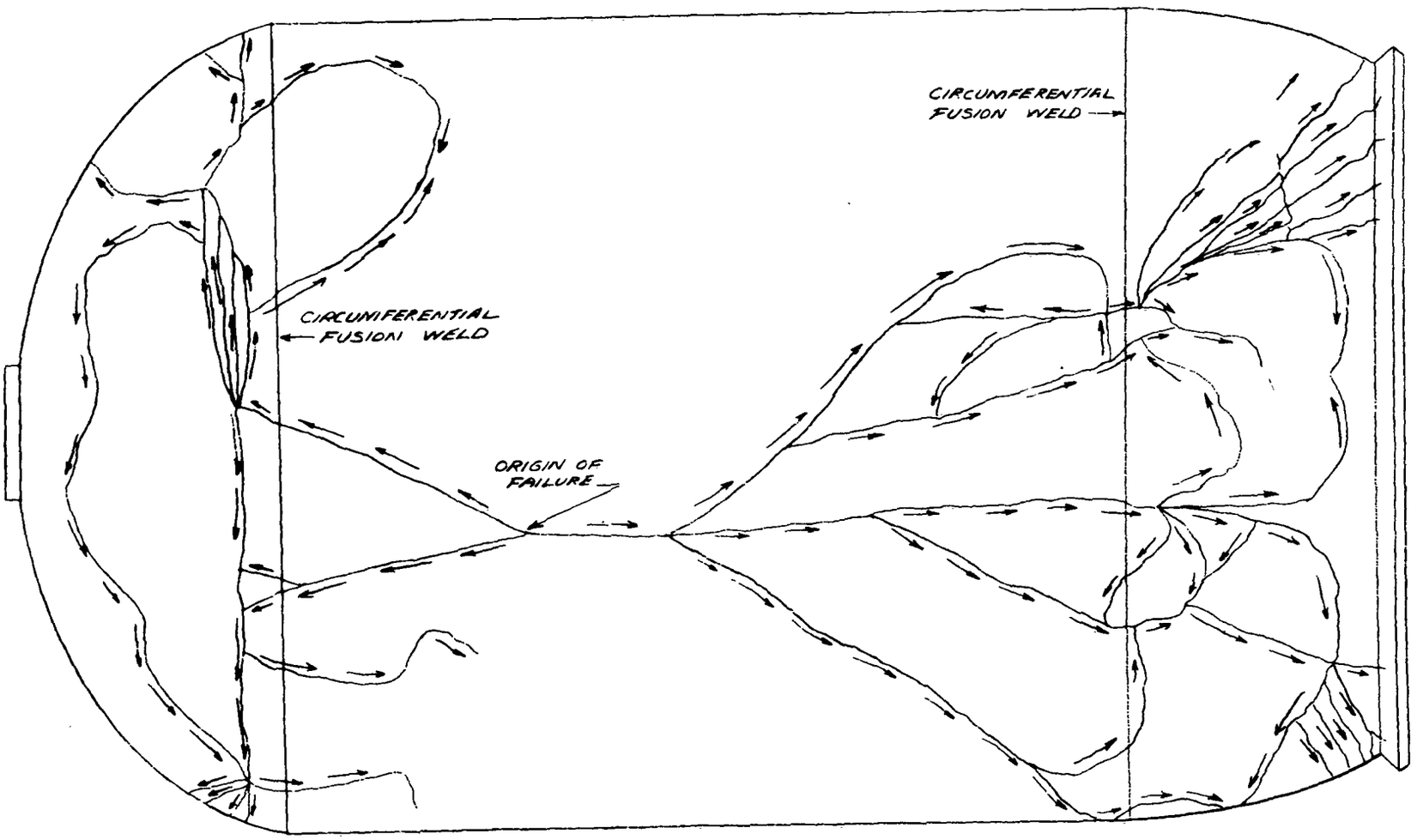


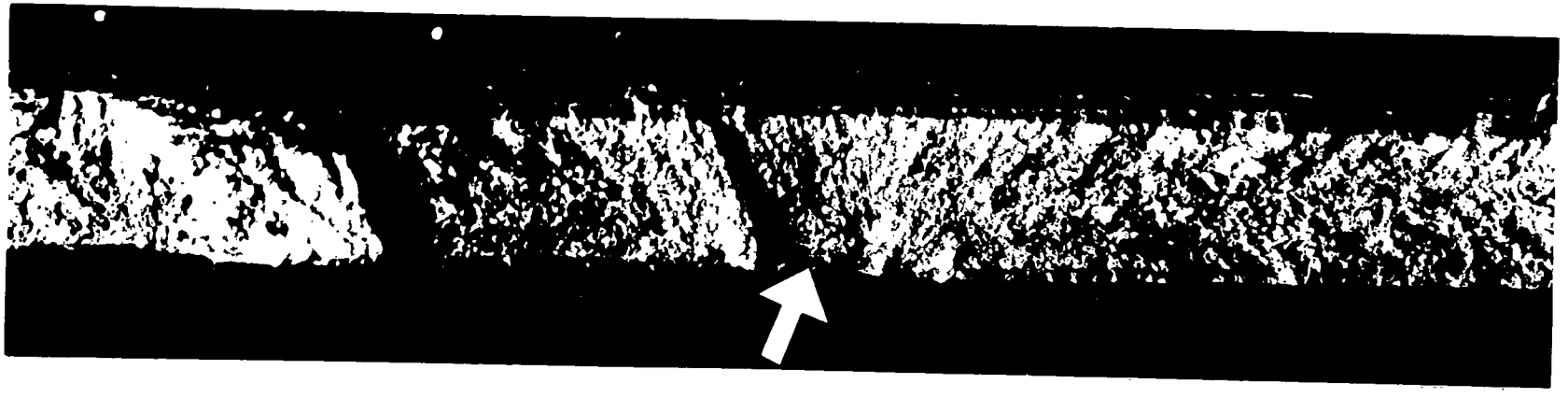
Fig. 4 Remains of the full scale missile casing after failure. The cylindrical objects resting on the central portion of the fractured pieces are weights used to hold them in position for the photograph.



Map of the Outer Surface of the Full Scale Missile Casing, showing the fracture pattern as determined from fracture surface markings. The arrows indicate the direction of fracture propagation.

P-11426

Fig. 5



Surface of fracture at the origin in the full scale rocket casing. The exact origin of failure is at the inner surface of the cylindrical wall section in the pitted region mentioned in the text. Note the pitting at the origin of failure indicated by the arrow. All fracture markings fan out from this point, and toward the right of the figure have developed into chevron markings. A shear lip is present everywhere except at the exact point of origin. This origin was approximately 12 inches from the nearest circumferential fusion weld.

Fig. 6

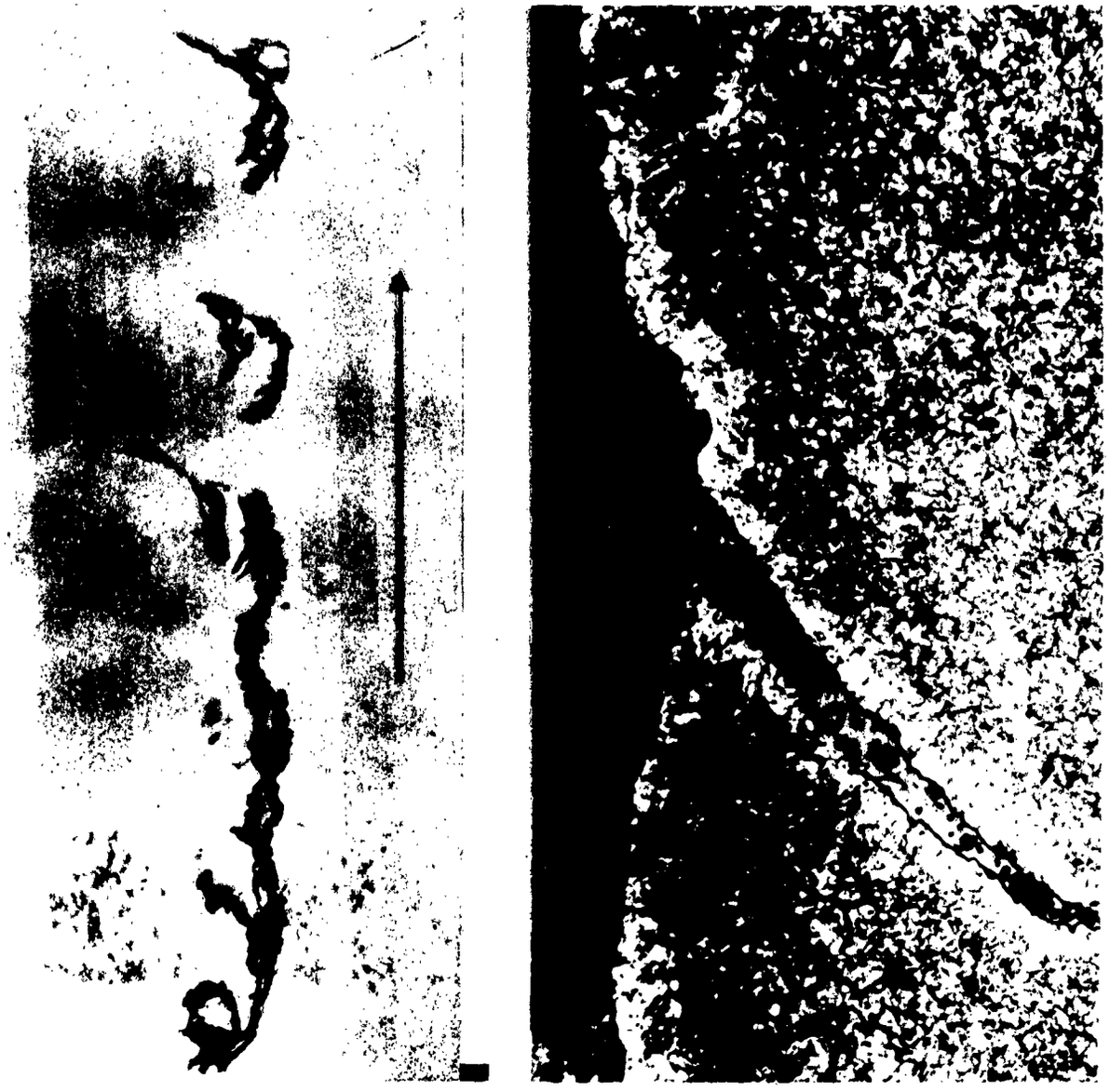
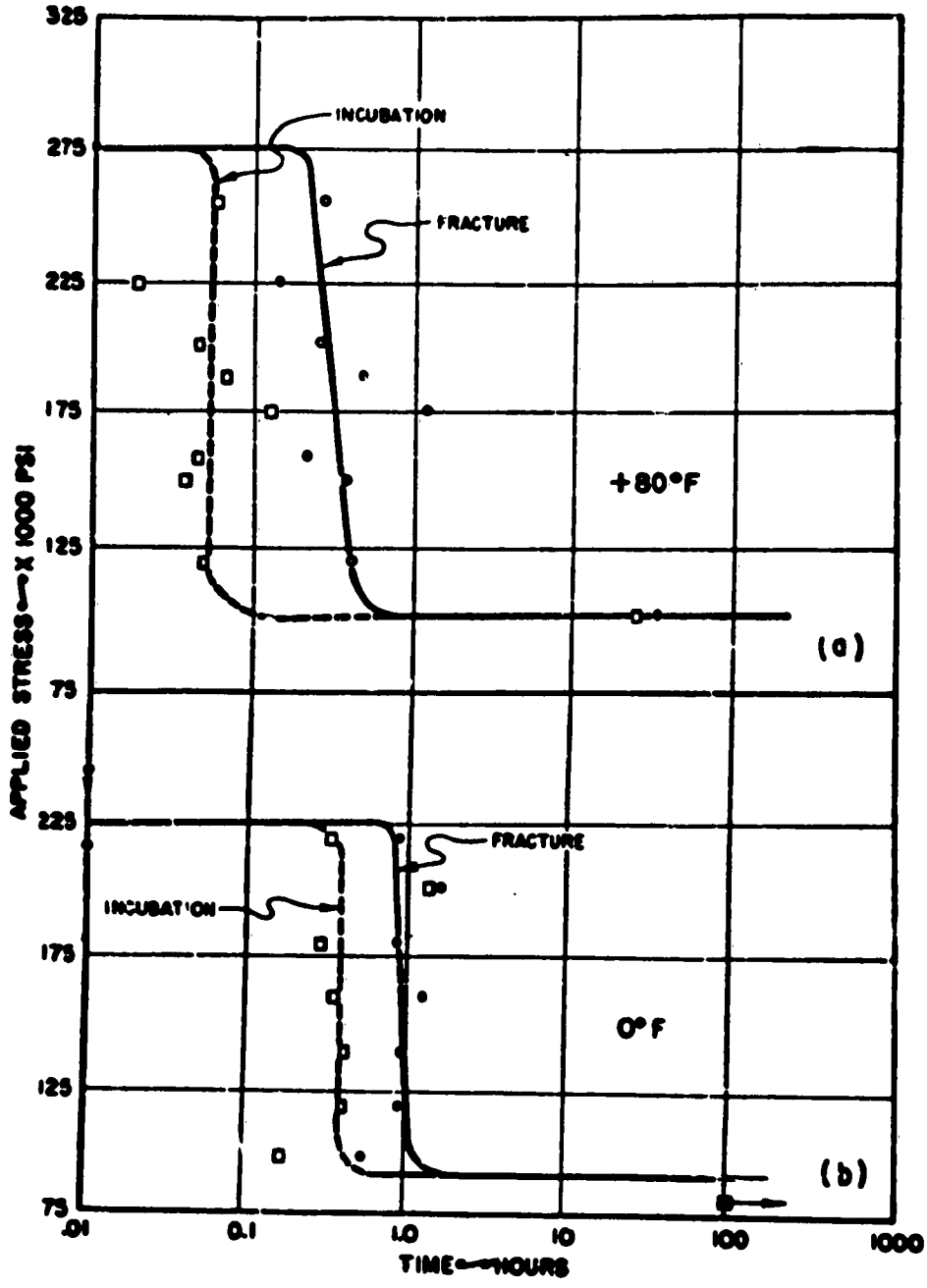


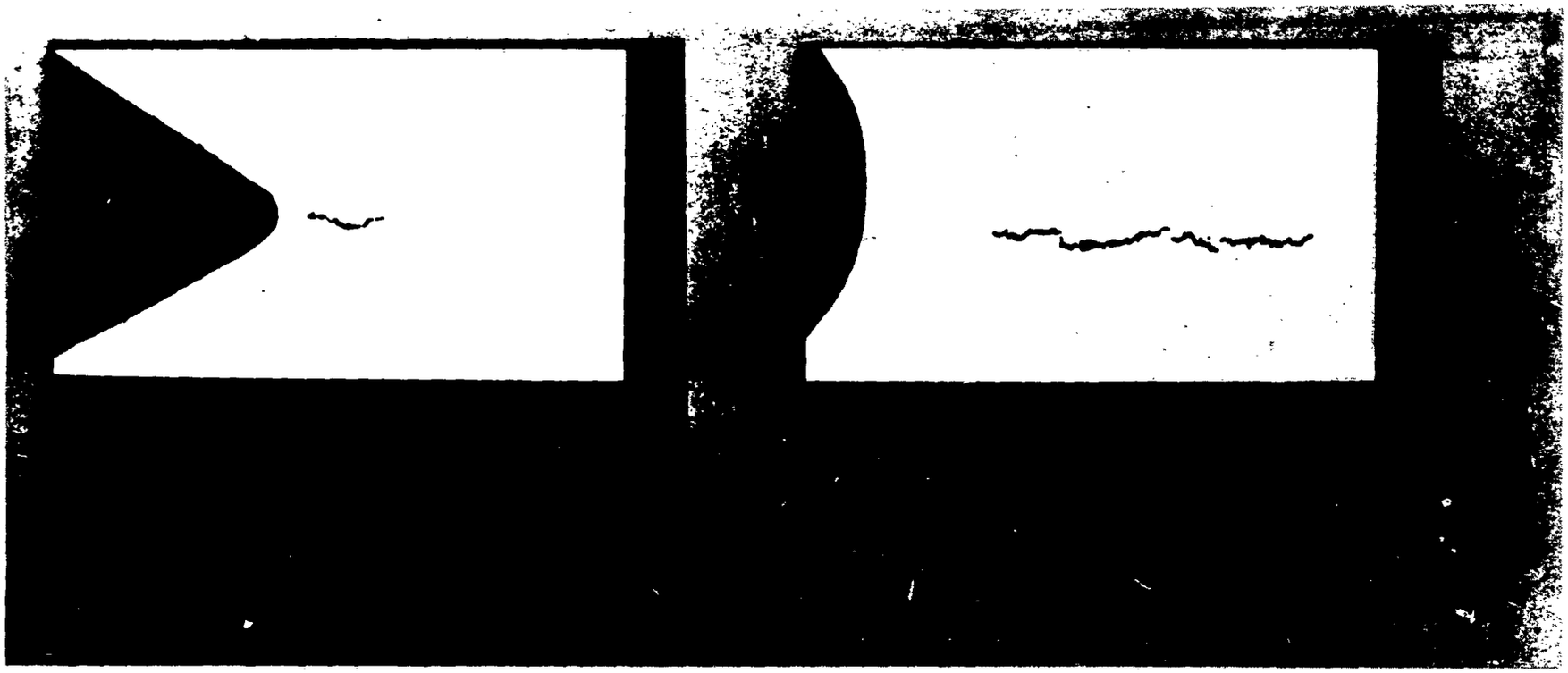
Fig.7—Section Parallel to Inner Surface of Fractured Full-Scale Rocket Casing. Defect indicated by magnetic particle inspection following failure is shown. Direction of material movement in flow-turning is shown by arrow. Defect has the appearance of being a lap formed in the surface in the metal forming process. Unetched. 75 X. Inset shows transverse section of similar defect at 500 X, nital etch. Depth of this defect is about 0.006 in. Decarburization indicates that the defect was present prior to completion of manufacture.

Fig. 7



Static Fatigue Curves for Hydrogenated High Strength Steel Specimens Tested at Various Temperatures as Indicated. The specimens were cylindrical and contained sharp notches. The material was AISI 4340 aircraft quality steel heat treated to a smooth tensile strength of 230,000 psi. After Troiano[5].

Fig. 8



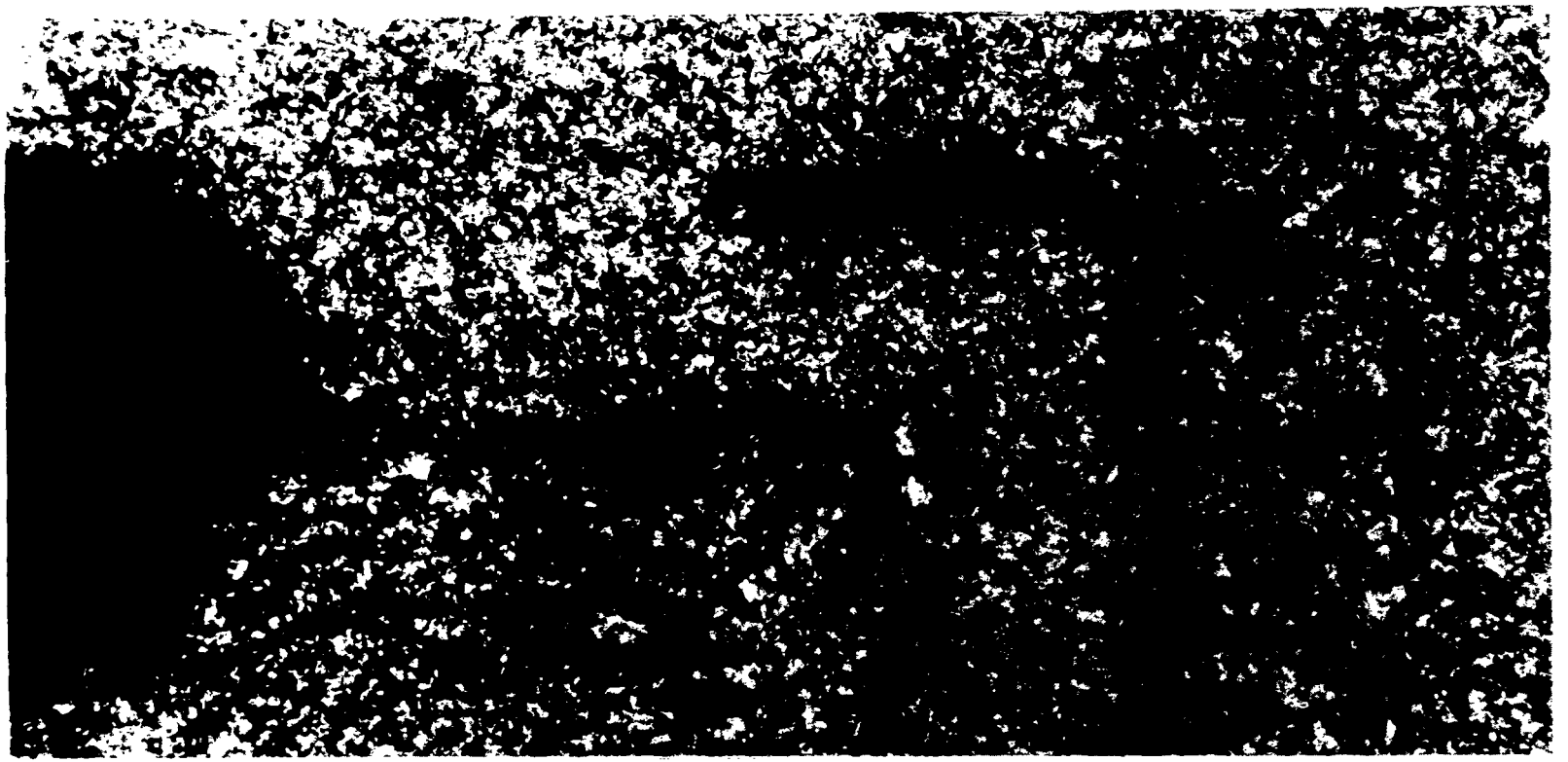
Cracks observed by Troiano[6] in notched specimens sectioned after static loading. Specimens had been hydrogenated, cadmium plated, and baked at 300°F. Longitudinal section. 100X. In the sharply notched specimen, the area of maximum manality is near the notch root surface and the initial crack forms here. In the rounded notch the area of maximum triaxiality is further from the crack. The cracks then travel outward to the surface and inward to the interior of the specimen.

FIG. 9

Section parallel to the inner surface of the full scale fractured rocket casing. This shows the region of the pit, also seen in Fig. 10. The entire vessel had been decarburized deliberately to a depth of .005 in. yet there is no decarburization along the pits or cracks. 1% nital etch. 500X.



Fig. 10



Section parallel to the inner surface of the full scale fractured rocket casing. This shows the region of the pit, also seen in **Fig. 10.** The entire vessel had been decarburized deliberately to a depth of .005 in. yet there is no decarburization along the pits or cracks. 1% nital etch. 500X.

Fig. 11

FRACTURED SURFACES OF TEST VESSELS 14, 15, 16,
PRESSURIZED WITH WATER. FRACTURE ORIGINATED FROM
THE INSIDE SURFACE AND DISPLAYS AT THE ORIGIN THE
DARK AREA TYPICAL OF HYDROGEN INDUCED FRACTURE.
PRATT & WHITNEY AIRCRAFT
DIVISION OF UNITED AIRCRAFT CORPORATION

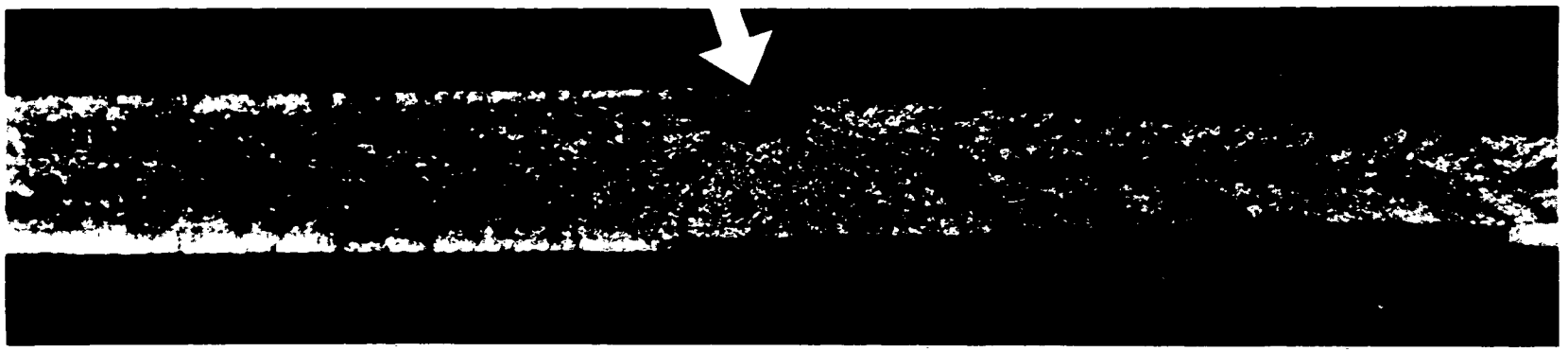
FRACTURED SURFACES OF TEST VESSELS 14, 15, 16, PRESSURIZED WITH WATER. FRACTURE ORIGINATED FROM THE INSIDE SURFACE AND DISPLAYS AT THE ORIGIN THE DARK AREA TYPICAL OF HYDROGEN INDUCED FRACTURE.
PRATT & WHITNEY AIRCRAFT
DIVISION OF UNITED AIRCRAFT CORPORATION

Fig. 12



Fracture of test vessel No. 21, which had been coated with primer on the inside to prevent contact with water. This had been subjected to sustained loading and fractured at a stress of 262,000 psi. The origin of the fracture was in parent metal about 1 7/8 inches from the nearest weld. It will be noted that there is no discolored area at the origin of fracture and that shear lip is seen along both edges of the fractures surface, even at the origin. This is indicative of the fact that fracture started under the surface. There is no discolored area indicative of hydrogen induced failure. Fracture origin is near the inside surface. 10X.

Fig. 13



Fracture surface of test vessel No. 22. This had been coated with primer on the inside and pressurized with water, while at the same time the outside surface was bathed in water. Failure was at 240,000 psi maximum tangential stress after sustained loading. The origin of fracture was at the outside where it was exposed to water. Shear lip existed everywhere but in this location. The origin was in parent metal 2 7/8 in. from the nearest weld and displays the dark area typical of hydrogen induced fracture. There is a pit at the point of origin. 16X.

Fig. 14

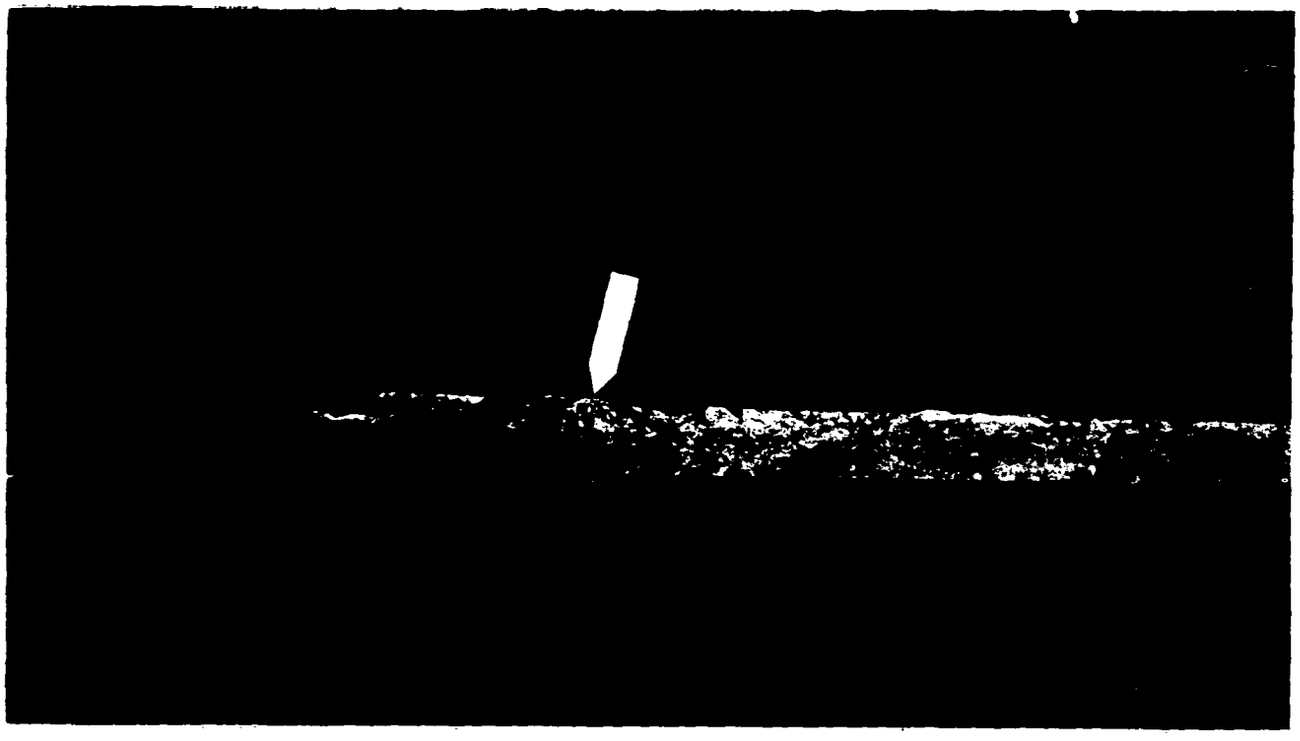
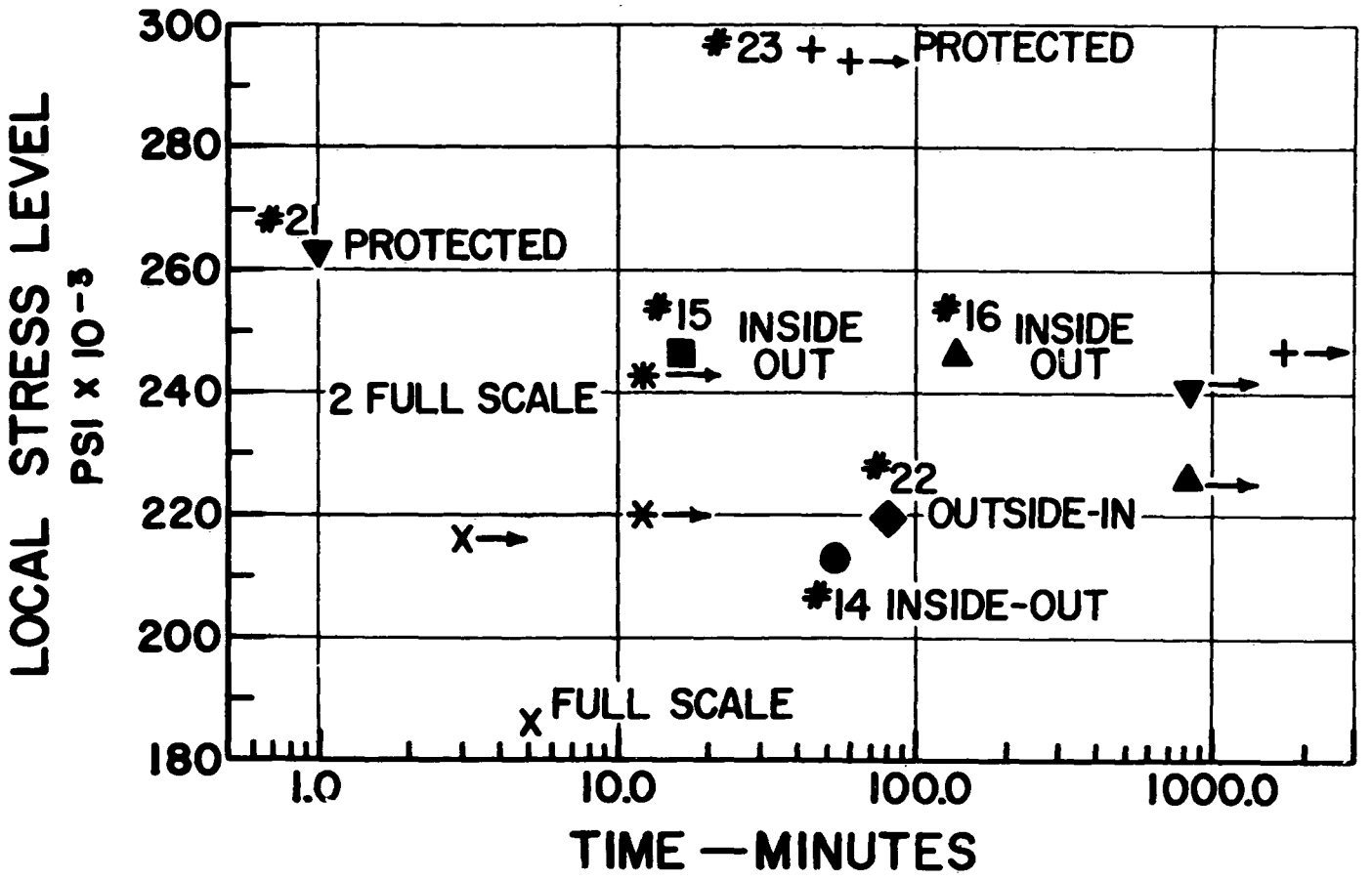


Fig. 15

Fracture surface of test vessel No. 23. This had been coated inside and outside with primer. This vessel had been stressed for a total of 2800 minutes above 264,000 psi maximum tangential wall stress. It finally fractured at a stress of 318,000 psi after 45 minutes at this level. Initially the vessel had been pressurized with water, later with oil. Fracture of the vessel was mostly in the shear mode. There was no discolored area at the origin of fracture, indicating that fracture had not been hydrogen induced. 10X.



Resume of delayed failure test results, showing the local stress level at the origin of failure, plotted against the time to delayed failure. The stress levels here indicated are slightly lower than those shown in Table I, inasmuchas the test vessels never failed at the thinnest section. Repeated use of the same symbol signifies repeated test of the vessel. Arrow signifies vessel not failed.

Fig. 1

EFFECTS OF FORMING

INTRODUCTION

Generally, materials are developed and manufactured to achieve the desired strength and ductility with a minimum of attention to the requirements for processing. The material manufacturers usually assert that fabrication processes are diversified, that it would be impossible to anticipate all fabrication factors influencing the mechanical and metallurgical behavior.

Recognition of this fact necessitates that the fabricator explore the effects of various fabrication techniques to justify the practices, determine the results obtained and establish processing precautions and criteria for material selection. This is especially significant in the missile industry which employs new materials and processes. The performance requirements of high strength-weight ratio motor cases demands material designed to meet the needs of fabrication processes employed, as well as the strength and toughness required to insure reliability. By evaluation of formed parts, the properties are substantiated and material parameters established.

MATERIAL AND SHAPES INVESTIGATED

This was accomplished on various spun components including the cylinder and head illustrated in Figure 1. The forming was accomplished by cold spinning, without the employment of external heat, utilizing the Hydrospin equipment illustrated in Figure 2. The parts selected for test represented the production spinning technique to be employed. In the procurement of material, it was anticipated that a clean, fine grain, spheroidized structure would be required and this was substantiated on 13" test cylinders. The material used to fabricate the parts was AMS-6428 and AMS-6434 modified as follows:

Chemical Composition

		Check Analysis
Carbon	0.35 - 0.40	±0.02
Manganese	0.60 - 0.85	±0.03
Silicon	0.20 - 0.35	±0.02
Phosphorus	.025 Max	-
Sulphur	.025 Max	-
Chromium	0.65 - 0.90	±0.03
Nickel	1.65 - 2.00	±0.05
Molybdenum	0.30 - 0.40	±0.02
Vanadium	0.17 - 0.23	±0.02

Condition

Sheet - Hot finished, spheroidized annealed, pickled and oiled to a hardness of R_b 95 max. and 85% minimum spheroidized structure.

Forging - Rough machined, spheroidized annealed and oiled to R_b 95 max. and 85% minimum spheroidized structure.

Mechanical Properties

Yield Strength (0.2% Offset)	210,000 psi min.
Elongation (% in 2 inches)	6% min.

Transverse specimens air or oil cooled from 1625 ± 25°F and tempered for two (2) hours minimum at approximately 500°F.

OBJECTIVE

It was desired to determine the tensile strength and microstructure of spun material and to evaluate the effects of various reductions and surface tool marks. It was also desired to explore the condition of spun welds and establish the effect of cold work on the weld.

SELECTION OF SPECIMENS AND THERMAL TREATMENT

Consequently, specimens were obtained from the head and cylinders as illustrated in Figure 3.

This provided specimens of different reductions from the head, transverse and parallel to the tool marks. Specimens from the cylinders were also transverse and parallel to the tool marks. In addition, specimens were obtained transverse and parallel to the weld. The angular location of the weld is due to spinning. The preform weld is straight across the cylinder.

The heat treatment cycle employed was 1650°F held for twenty minutes in Argon atmosphere, quenched in 400°F salt and held five minutes followed by air cool and tempered at 475°F for two (2) hours.

A summary of specimen types is indicated in Table I.

PROPERTIES OF VARIOUS SHAPES

The mechanical properties of specimens from the center dome are shown in Table 2. There is very little or no reduction in this area. Similarly the properties of specimens from the half-radius, approx. 20% reduction and full radius, approx. 43% reduction are shown in Table 3 and 4. The data indicates the reduced areas have a lower "as-spun" yield strength than the unspun areas, whereas the ultimate strength and elongation was essentially unaffected.

The properties of specimens from the spun forged cylinder are shown in Table 5. Specimens 7TF through 12TF were the only specimens tested with the tool marks left on the surface. The data does not conclusively show a difference in tensile strength between specimens obtained transverse to, and parallel to, the tool marks. A slight decrease in yield strength is indicated on specimens whose surface contains the tool marks in a transverse direction when compared with otherwise similar specimens whose surface has been ground smooth.

The properties of specimens from the sheet material rolled and welded cylinder are shown in Tables 6 and 7. The data indicates no significant difference in tensile strength between parent metal specimens and welded specimens in either the "as-spun" or "as-spun and heat treated" condition. Similarly, no significant difference was observed in the tensile elongation, except in the heat treated specimens obtained parallel to the spin tool marks. In this case a slight decrease in elongation was observed in the welded specimens compared to the parent metal specimens.

The average tensile results for various conditions tested are shown in Table 8.

WELDING ASPECTS

The longitudinal weld was made by the tungsten inert gas process in accordance with the schedule shown in Figure 4.

It should be noted that is is an oscillation weld utilizing a cam-driven mechanism to oscillate the arc and wire feed simultaneously during the welding operation. This technique is employed to produce a completely sound weld. It is important to have the weld as relatively free of imperfections as the parent material in view of the extent of cold working. The oscillation equipment is illustrated in Figure 5.

Analysis of the microstructure reveals an appreciable difference between the weld and base metal in the "as-spun" condition shown in Figures 6 and 7, respectively. However, the cold working has acted to refine the weld structure. For comparison purposes, the microstructure of a weld prior to cold working is shown in Figure 8. In the hardened and tempered condition, the weld is homogenized and refined and appears very similar to the hardened and tempered base metal.

The effect of the spinning on the weld is to produce a structure comparable to the base metal providing essentially a relatively homogeneous fabrication.

STRUCTURE OF VARIOUS SHAPES

The microstructure of specimens obtained from the heat at full radius, half radius, and dome areas are very similar as shown in Figures 9, 10, and 11. However, the "as spun" specimens obtained from the cylinders exhibited

a slightly elongated grain structure shown in Figure 12 which was eliminated by heat treatment. This was reflected in the ductility measurements. The "as-spun" head specimens exhibited less loss of ductility than the "as spun" specimens from the cylinders.

There is no significant difference between the microstructure of base metal specimens obtained transverse and parallel to the spin tool marks shown in Figures 13 and 14. However, the "as-spun" weld structure is coarser in the transverse specimen, Figure 15, than the parallel specimen, Figure 16.

ADDITIONAL SUBSTANTIATING INVESTIGATIONS

Evaluation of welded and spun cylinders was also conducted on X200 material using 13" development cylinders. Figure 17 illustrates the specimen locations, and Table 9, the results obtained. This work was supplemented by destructive pressure tests of longitudinally welded cylinders in a restrained jig. No weld failures were encountered.

Similar tests were conducted on AMS-6434 modified, 13" development cylinders. Figure 18 illustrates the destructive failure.

TOUGHNESS

Supplementing this work, it is important to evaluate the sensitivity of spun material to the presence of notches. Fortunately this type of testing has received considerable attention from the onset of the missile chamber program. Various types of tests have been conducted on basic material, forms and types. Numerous investigations have reported results on high strength spun material.

The results of work utilizing the center notch tensile test has been summarized by Warga (1) in Table 10.

MATERIAL EVALUATION

In seeking the best material for this process, consideration was given to both ring forgings and welded sheet preforms and both have been used to fabricate cylindrical sections. Each form presented problems which had to be overcome to avoid a deleterious effect on the basic material. Rolled and welded sheet is the simplest to fabricate. Sheet material may be obtained with a low inclusion count to exact chemical composition. The sheet receives considerable work to produce the pre-spinning thickness and it responds well to spheroidizing. However, the mill rolling can produce surface imperfections which are enlarged or ruptured in the spinning operation. Careful surface inspection before and after spinning is mandatory to eliminate defective surface conditions. A rupture which occurred on the I.D. surface of spun sheet material is illustrated in Figure 19. In this case, the failure progresses the length of the cylinder approx. 3" from, and parallel to, the longitudinal weld. The weld was unaffected as shown in Figure 20.

MATERIAL CRITERIA

Ring forgings may be procured to exact chemical composition with a low inclusion count, but there appears to be a greater variation in the cleanliness. Forgings are made 3.00" thick, roughly machined to 1.00" and final machined to the desired preform thickness. Spheroidizing is accomplished in the as-forged and rough-machined condition. Use of the forging eliminates the longitudinal weld and permits accurate control of the preform thickness.

However, different mill practices can produce variations in the forging structure which affect the final product. The amount of work the forging receives is significant and the heat treating procedure must be accorded special consideration to condition the structure for spinning. Figure 21 illustrates a mixed non-homogeneous structure that is unsatisfactory. Figure 22 illustrates a structure with insufficient spheroidization. Figures 23 and 24 illustrate the desired and minimum acceptable structures respectively.

When attempts were made to spin unacceptable structures, ruptures such as illustrated in Figure 25 were encountered. Extensive control of structure is required, necessitating sampling forgings at each end and respheroidizing when required.

The strict requirements for structure are alleviated to some extent when an interpass stress relieve is employed. However, the material presented for spinning should be missile quality compatible with the product to be manufactured, and the process controlled to eliminate deleterious effect.

In addition to meeting the normal specification requirements, the material must be designed to meet the requirements of spinning. It should be fine grained, consumable electrode, vacuum remelted, or equivalent, clean material with the following micro inclusion rating.

	Thin	Heavy
A	1-1/2	1
B	1	0
C	1/2	0
D	1-1/2	1

Forgings should preferably comply with magnetic particle inspection frequency-severity rating of .5 and 1.0 per square inch of surface respectively, utilizing the test procedure illustrated in Figure 26. It should be sufficiently worked to provide a homogeneous structure with a minimum of 85% spheroidization and maximum hardness of 95 R_b.

SUMMARY

The effect of forming by mechanical spinning is to provide a cold worked homogeneous structure. A thermal treatment is required prior to further processing to relieve the stresses introduced by cold working. No deleterious effect is observed, providing the material is acceptable for spinning. Material not specifically designed for spinning may have conditions which are detrimental and reflect adversely on the process. The reliability of longitudinal welds in cylinders is enhanced by spinning.

REFERENCES

(1) J. J. Warga - "The Use of the Center Notch Tensile Test to Evaluate Rocket Chamber Materials", American Society of Mechanical Engineers, Metals Engineering Division Los Angeles, California, April 25-29, 1960 (Preprint).

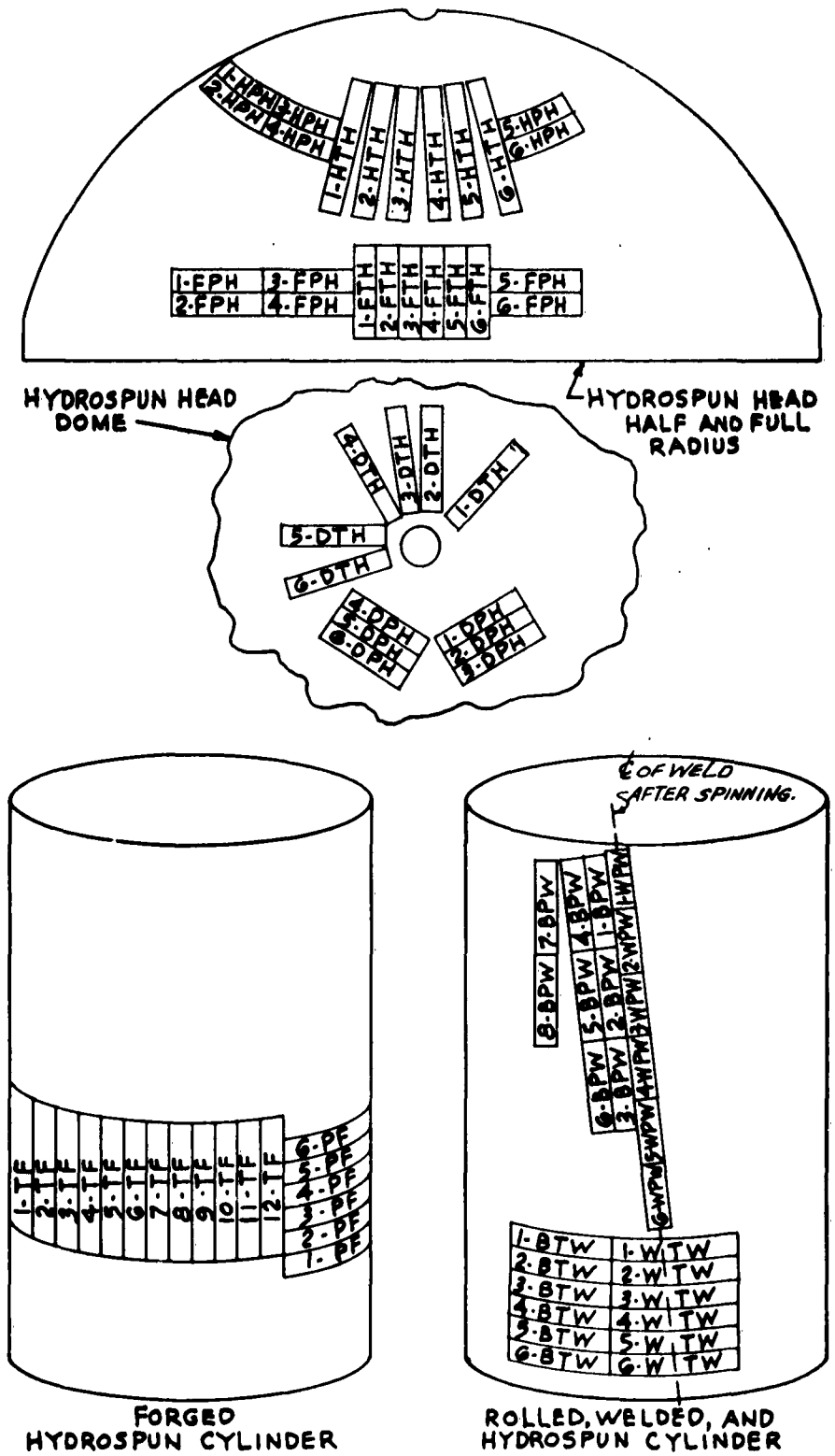


FIGURE - 1



FIGURE - 2

FIGURE - 3 LOCATION OF SPECIMENS

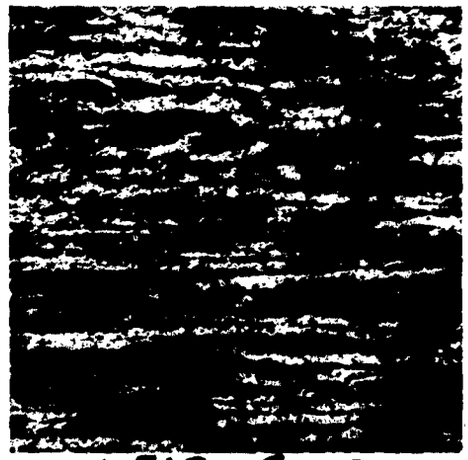


MATERIAL	AMS - 6434 - MOD.		
JOINT TYPE	"V" BUTT		
	1/16" - LAND 45° CHAMFER		
WIRE TYPE	17-22		
WIRE SIZE	.045"		
ELECTRODE TYPE	2% THOR TUNGSTEN		
ELECTRODE SIZE	1/8"		
PASS NO.	1	2	3
TRAVEL SPEED (IN./MIN.)	5	10	10
WELD CURRENT (AMP.)	160	180	180
ARC VOLTAGE (VOLTS)	10.5	11.0	12.5
WIRE FEED (IN./MIN.)	20	30	30
OSCILLATION WIDTH (IN.)		3/32	1/8
RATE OF OSCILLATION	100 CYCLES PER MINUTE		
PREHEAT 450°F ± 50°F POSTHEAT 1050°F ± 50°F - 10 MINUTES			

AUTOMATIC OSCILLATING WELD SCHEDULE
FIGURE 4



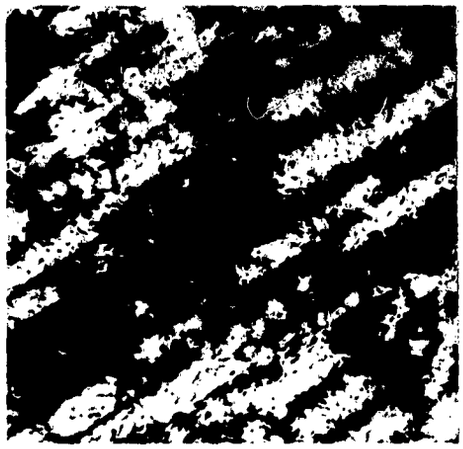
FIGURE - 5



NITAL-FIG.-6 200X



NITAL FIG.-7 200X



NITAL FIG.-8 200X



VILLE FIG.-9 1000X

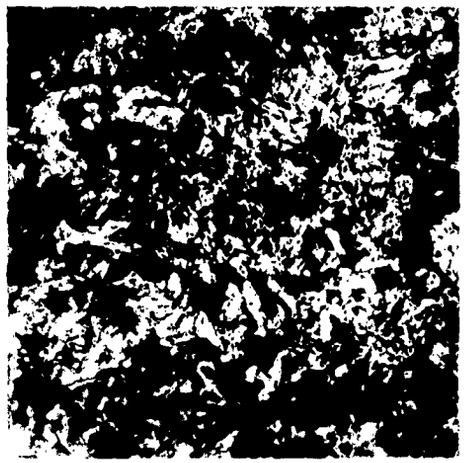


FIG.-10
VILELLA'S 1000X

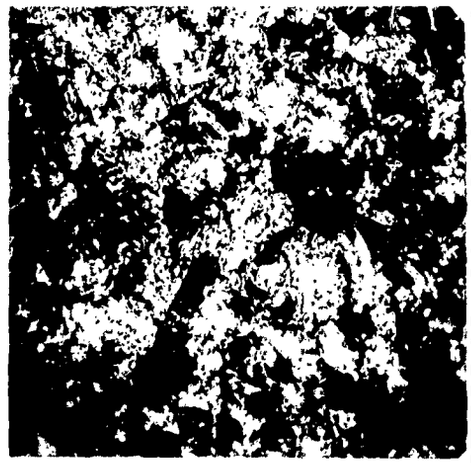


FIG.-11
VILELLA'S 1000X

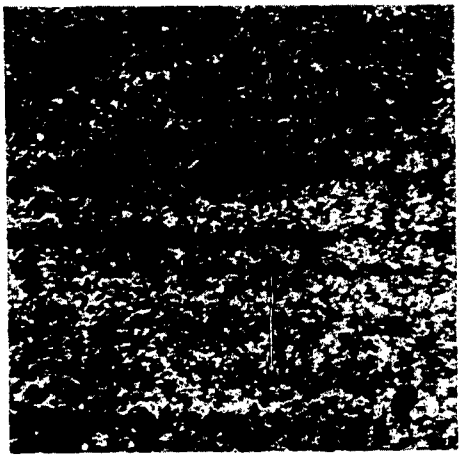


FIG.-12
VITAL 200X

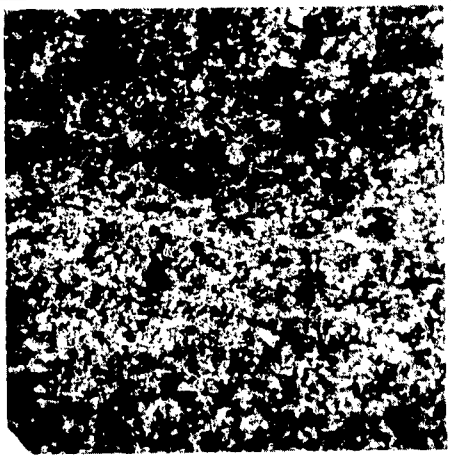


FIG.-13
VILELLA'S 1000X



VILELLA'S FIG.-14 1000X

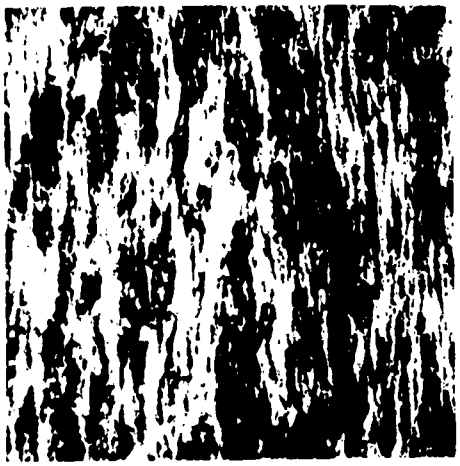


FIG.-15
NITAL 130X

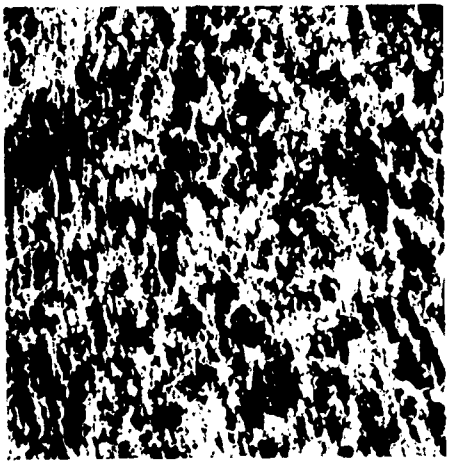
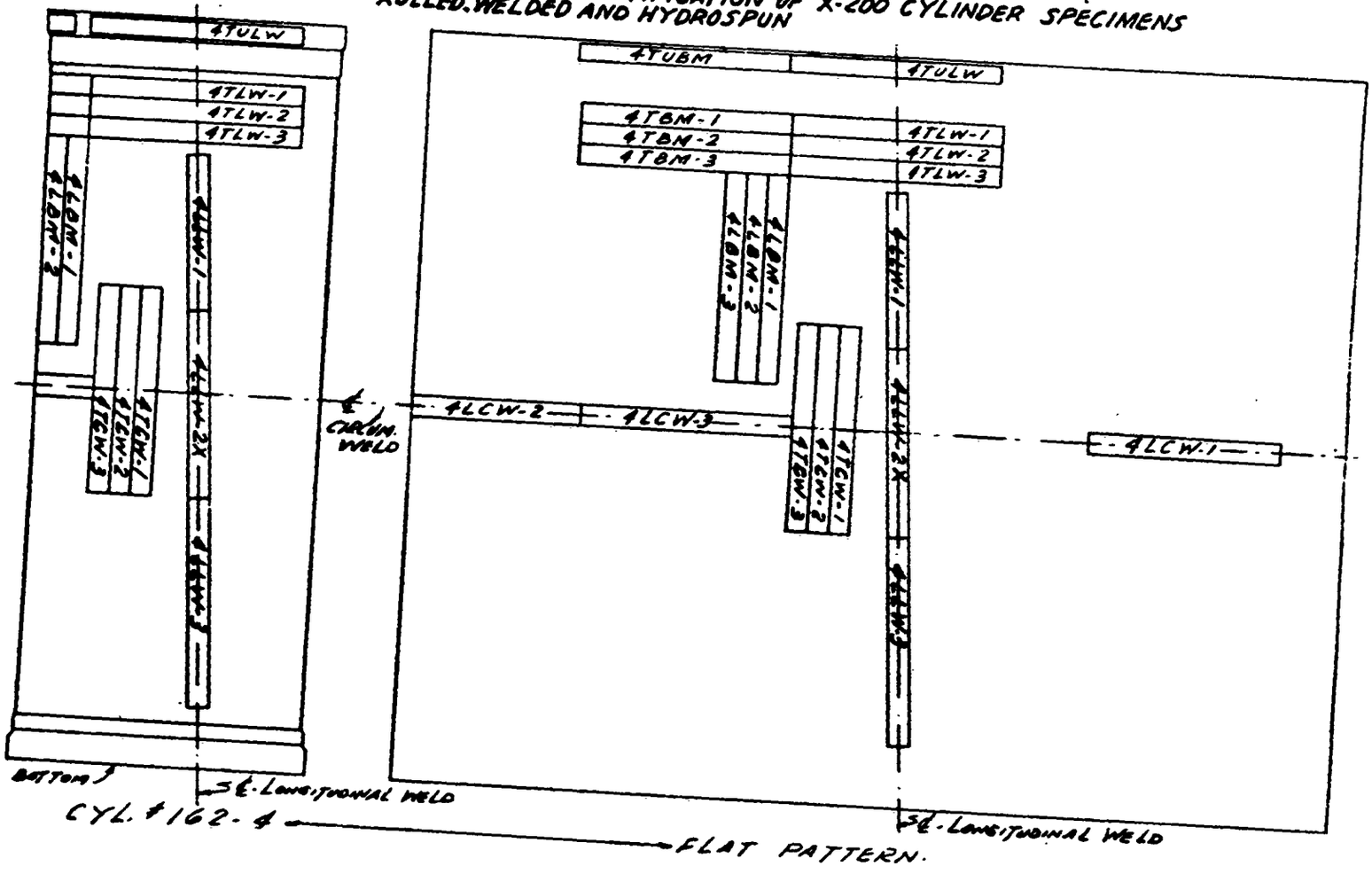


FIG.-16
NITAL 130X

FIGURE-17 LOCATION AND IDENTIFICATION OF X-200 CYLINDER SPECIMENS ROLLED, WELDED AND HYDROSPUN



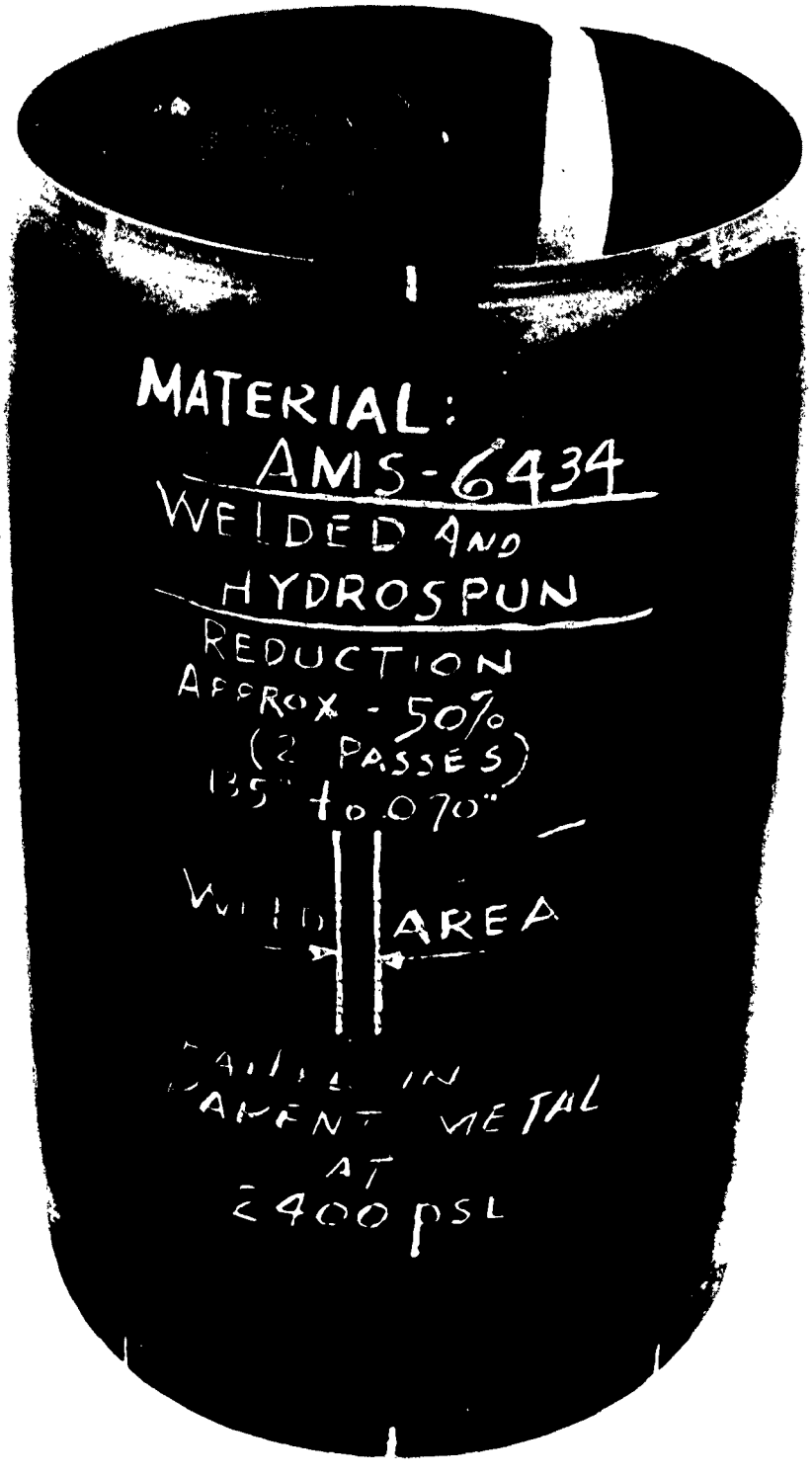

MATERIAL:
AMS-6434
WELDED AND
HYDROSPUN
REDUCTION
APPROX - 50%
(2 PASSES)
135" to 070"
AREA
AT
≥400 PSI

FIGURE - 18

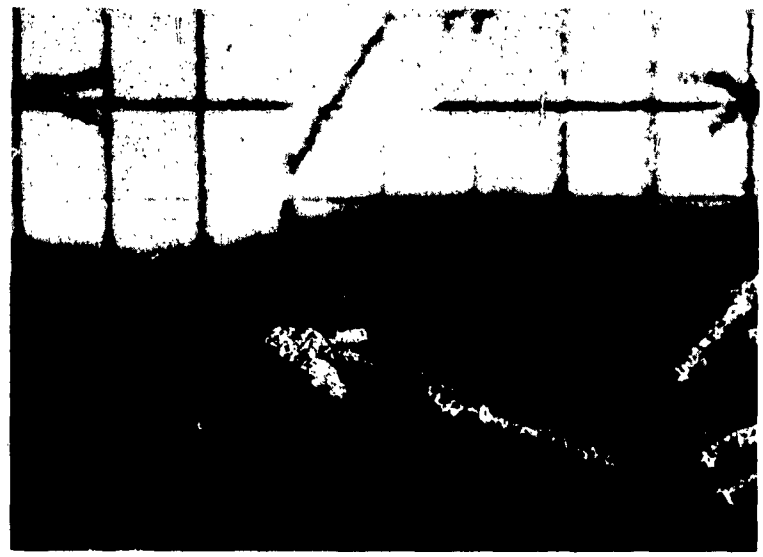


FIG. -19

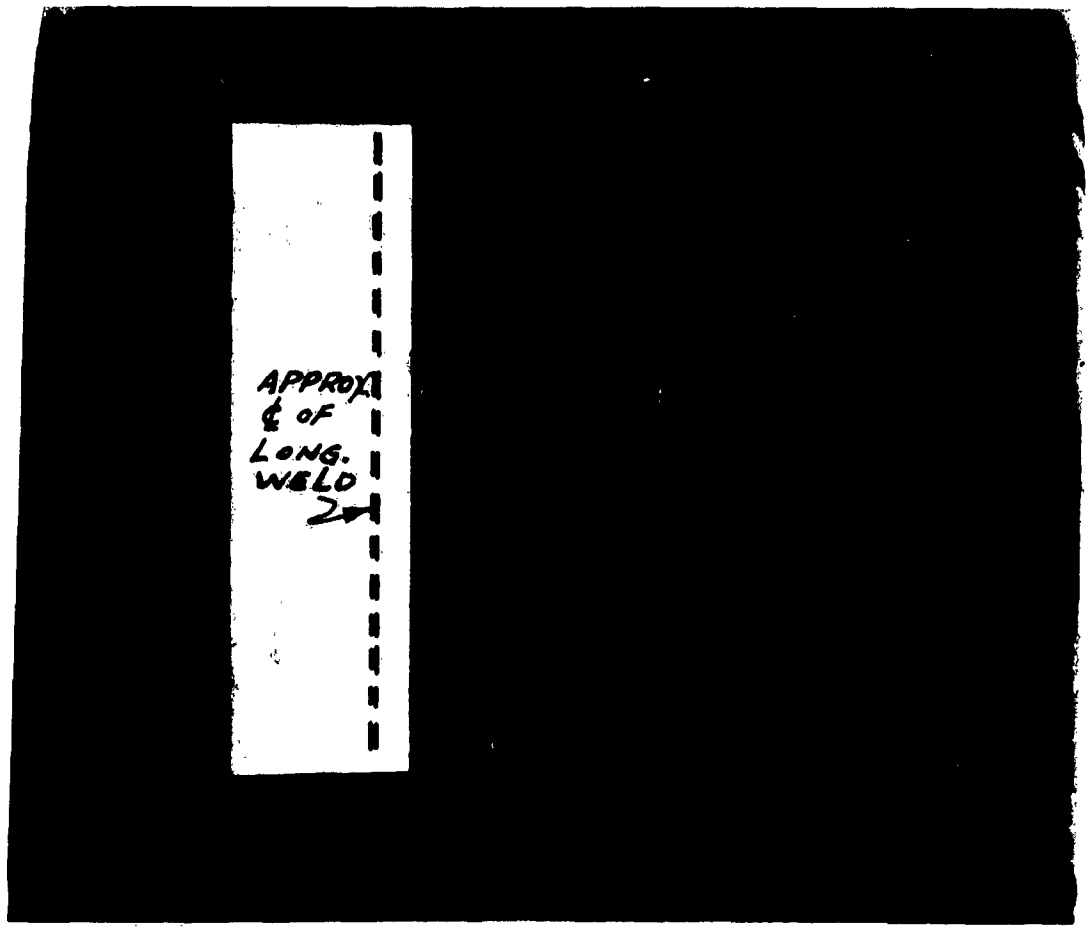


FIG. - 20

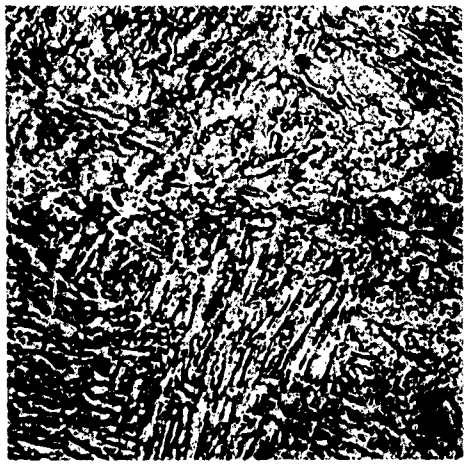


FIG.-21
4% NITAL 500X

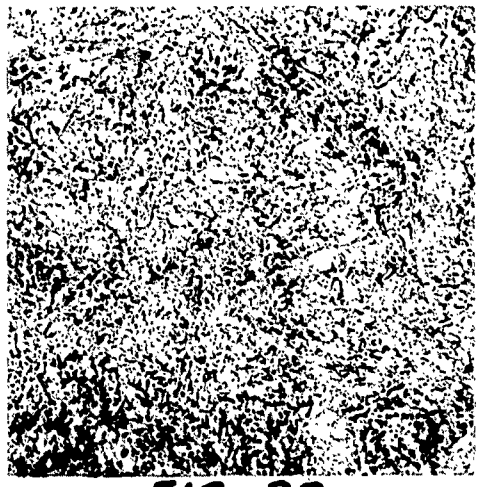


FIG.-22
4% NITAL 500X

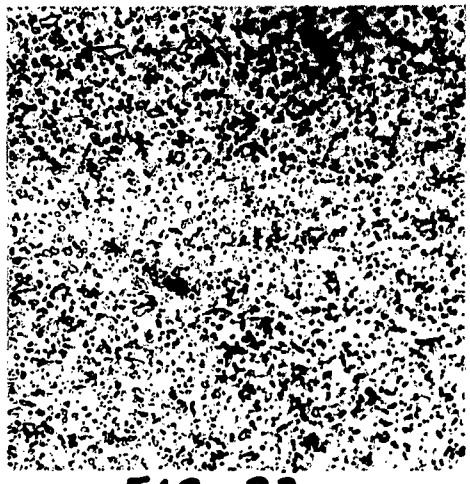


FIG.-23
4% NITAL 500X

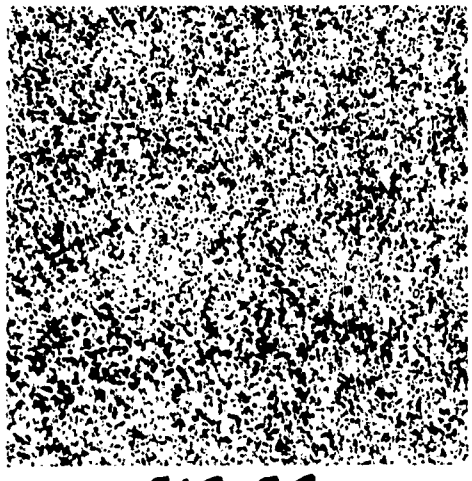


FIG.-24
4% NITAL 500X

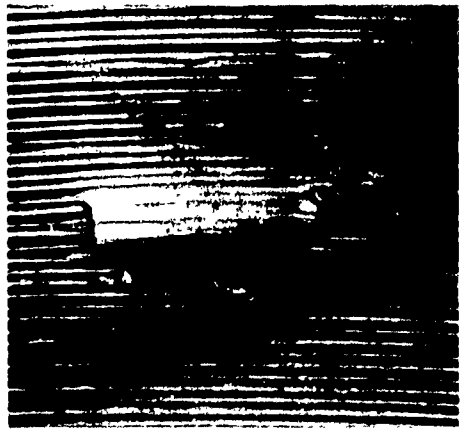


FIG.-25

FIGURE 26 - FREQUENCY - SEVERITY TEST PROCEDURE

MATERIAL SHALL BE FORGED AND MACHINED, TO THE SPECIMEN CONFIGURATION SHOWN BELOW, TO A SURFACE FINISH OF 40 MICRO-INCHES MINIMUM AND MAGNETIC PARTICLE INSPECTED USING A CIRCULAR WET CONTINUOUS METHOD WITH A CURRENT OF 1,000 AMPERES PER INCH OF THICKNESS. RECORD THE NUMBER AND SIZE OF INDICATIONS FOUND ON EACH BAR AND CALCULATE THE FREQUENCY-SEVERITY RATING AS FOLLOWS:

FREQUENCY = NUMBER OF INDICATIONS PER SQUARE INCH. DIVIDE TOTAL NUMBER OF INDICATIONS BY SURFACE AREA (IN SQ. IN.) INSPECTED.

SEVERITY = THE TOTAL SUM OF THE NUMBER OF INDICATIONS TIMES THE SEVERITY FACTORS DIVIDED BY THE NUMBER OF SQUARE INCHES OF THE SURFACE AREA INSPECTED.

SEVERITY FACTORS

Length of Indications (Inch)	Severity Factor
1/64 - 1/32 incl.	2
Over 1/32 - 1/16 incl.	4
Over 1/16 - 1/8 incl.	16
Over 1/8 -	256

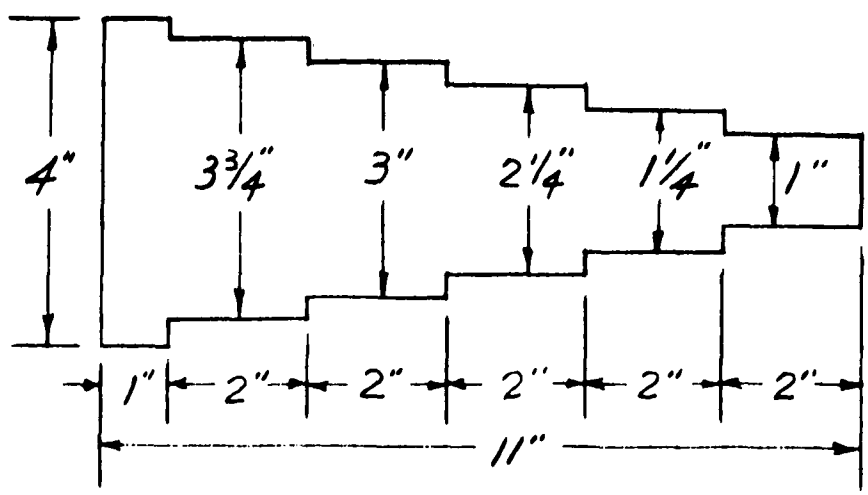


TABLE - 10

* EFFECT OF SHEAR SPINNING ON FRACTURE TOUGHNESS

MATERIAL	CONDITION	THICK. (IN.)	Y.S. (KSI)	NET SECTION STRESS (KSI)	FRACTURE ENERGY (IN. LBS./SQ. IN.)
4340	UNSPUN (L)	.085	185.	192 - 214	946 - 1167
	SPUN-RADIAL	.094	186.	192 - 201	904 - 1050
	SPUN-AXIAL	.094	186.	198 - 206	973 - 1091
AMS-6434	UNSPUN (L)	.095	190.	192 - 212	920 - 1100
	SPUN-RADIAL	.092	195.	190 - 203	931 - 1000
	SPUN-AXIAL	.092	194.	186 - 204	890 - 1060

STRESS RELIEVED AND HEAT TREATED.

* - "THE USE OF THE CENTER NOTCH TENSILE TEST TO EVALUATE ROCKET CHAMBER MATERIALS" - (1)

TABLE - 9 MECHANICAL PROPERTIES - 13" CYLINDER ROLLED, WELDED (LONG. AND CIRCUMF. WELDS) AND HYDROSPUN MATERIAL - X-200.

SPEC. No.	DESCRIPTION OF SPECIMENS SEE FIGURE - 17 - FOR LOCATION	YTS .2% OFF. KSI	UTS KSI	ELONG % IN 2"	R_c	LOCATION OF FRACTURE
4LLW-1	LONGITUDINAL WELD SPEC. ON LONG. WELD	241.6	287.5	7.5	54.0	
4LLW-2X	LONGITUDINAL SPEC. AT INTERSECTION OF WELDS	236.6	281.2	5.0	53.0	
4LLW-3	LONGITUDINAL WELD SPEC. ON LONG. WELD	235.8	283.5	6.0	53.0	
4TLW-1	TRANSVERSE SPEC. ON LONG. WELD	240.7	283.9	6.0	53.0	BASE METAL
4TLW-2	" " " "	235.5	275.2	6.0	51.0	BASE METAL
4TLW-3	" " " "	237.0	274.4	5.5	51.0	WELD
4LCW-1	WELD SPEC. LONG. TO CIRCUMF. WELD	228.5	276.1	6.0	52.0	
4LCW-2	" " " "	240.7	283.7	* 4.5	53.0	
4LCW-3	" " " "	234.0	278.4	5.5	52.0	
4TCW-1	WELD SPEC. TRANS. TO CIRCUMF. WELD	226.6	272.7	* 5.0	50.0	BASE METAL
4TCW-2	" " " "	230.7	267.8	* 5.5	49.0	BASE METAL
4TCW-3	" " " "	237.2	282.0	* 5.5	50.0	BASE METAL
4LBM-1	LONGITUDINAL BASE METAL SPEC.	233.6	277.5	* 5.5	52.0	
4LBM-2	" " " "	232.8	280.6	6.0	53.0	
4LBM-3	" " " "	232.9	282.7	6.0	53.0	
4TBM-1	TRANS. OR CIRCUMF. BASE METAL SPEC.	233.7	278.8	* 6.0	52.5	
4TBM-2	" " " "	235.1	279.1	* 6.0	52.5	
4TBM-3	" " " "	234.6	280.1	* 6.0	52.5	
4TULW	UNSPUN WELD SPEC. TRANS. TO LONG. WELD	255.0	290.2	6.0	51.0	BASE METAL
4TUBM	UNSPUN BASE METAL SPEC. CIRCUMFERENTIAL	248.3	289.5	6.0	52.0	

HEAT TREATMENT: ALL SPECIMENS

1. NORMALIZE - HEAT TO 1740° ± 10° F. - HOLD AT TEMP. FOR 30 MIN. - AIR COOL.
2. TEMPER - " " 1300° ± 10° F. - " " " " 60 " - " "
3. HARDEN - " " 1740° ± 10° F. - " " " " 45 " - " "
4. TEMPER - " " 725° ± 5° F. - " " " " 2 HOURS - " "
5. ARGON ATMOSPHERE USED FOR STEPS 1, 2 AND 3.

* - FRACTURED LESS THAN 25% OF GAGE LENGTH FROM DATUM POINT.

TABLE - 8 MECHANICAL PROPERTIES
AVERAGE - ALL CONDITIONS - SEE FIGURE-3 FOR LOCATION.

CONDITION DIRECTION TO TOOL MARKS TEST DATA		"AS SPUN" PARALLEL YTS KSI	"AS SPUN" PARALLEL UTS KSI	"AS SPUN" PARALLEL ELONG. % IN 2"	"AS SPUN" TRANSVERSE YTS KSI	"AS SPUN" TRANSVERSE UTS KSI	"AS SPUN" TRANSVERSE ELONG. % IN 2"	HEAT TREATED PARALLEL YTS KSI	HEAT TREATED PARALLEL UTS KSI	HEAT TREATED PARALLEL ELONG. % IN 2"	HEAT TREATED TRANSVERSE YTS KSI	HEAT TREATED TRANSVERSE UTS KSI	HEAT TREATED TRANSVERSE ELONG. % IN 2"
HYDRO SPUN HEAD	DOME HALF RAD.	127.6	149.8	12.3	117.6	144.8	12.5	227.1	269.8	5.5	228.5	272.0	6.0
	FULL RAD.	109.7	139.3	13.3	105.3	140.3	12.8	225.0	268.5	6.3	221.4	262.6	6.0
		111.2	143.7	13.7	104.1	148.4	13.0	229.0	273.3	6.0	238.8	285.4	5.7
HYDRO-SPUN FORGED CYL.	GROUND SMOOTH	126.4	152.0	5.5	129.6	149.2	3.3	217.4	261.7	5.7	218.2	257.6	4.2
	TOOL MARKS				120.7	150.1	5.2				214.8	257.7	3.8
ROLLED, WELDED AND SPUN CYL.	BASE METAL	136.2	161.4	5.0	134.5	156.7	4.2	209.8	253.0	5.7	203.9	246.5	5.7
	WELD METAL	137.1	164.4	4.8	136.8	159.1	4.3	210.3	250.7	4.5	203.4	245.9	5.5

TABLE - 6 MECHANICAL PROPERTIES ROLLED, WELDED AND HYDROSPUN CYLINDER - PARENT METAL

SPEC. No.	% RED.	GAGE IN.	YTS .2% OFF. KSI	UTS KSI	ELONG. % IN 2"	Rc
1-BTW	68	.070	139.0	161.9	5.0	31.0
2-BTW		.070	132.9	161.4	5.0	
3-BTW		070	136.8	161.0	5.0	
AVER.			136.2	161.4	5.0	
1-BPW		.066	132.9	157.9	4.0	31.0
2-BPW		.067	134.3	156.7	4.5	
3-BPW		.068	136.4	155.4	4.0	
AVER.			134.5	156.7	4.2	
4-BTW		.069	207.8	251.5	5.5	47.0
5-BTW		.069	207.7	250.7	6.5	
6-BTW		.068	214.0	256.8	5.0	
AVER.			209.8	253.0	5.7	
4-BPW		.065	203.1	247.7	5.5	48.0
5-BPW		.066	205.2	246.2	6.0	
6-BPW		.067	203.3	245.5	5.5	
AVER.			203.9	246.5	5.7	
7-BPW		.067	133.2	154.8	4.0	
8-BPW	68	.066	206.6	250.0	5.5	

TABLE - 7 MECHANICAL PROPERTIES ROLLED, WELDED AND HYDROSPUN CYLINDER WELD METAL

SPEC. No. *	% RED.	GAGE IN.	YTS .2% OFF. KSI	UTS KSI	ELONG. % IN 2"	Rc
1-WTW	68	.069	138.1	162.8	4.5	30.0
2-WTW		.069	136.6	166.2	5.0	
3-WTW		.069	136.6	164.2	5.0	
AVER.			137.1	164.4	4.8	
1-WPW		.066	137.9	159.8	4.5	32.0
2-WPW		.066	135.2	159.4	4.5	
3-WPW		.067	137.3	158.2	4.0	
AVER.			136.8	159.1	4.3	
4-WTW.		.067	209.2	250.7	4.5	48.0
5-WTW		.067	212.6	252.5	4.5	
6-WTW		.068	209.2	249.3	4.5	
AVER.			210.3	250.7	4.5	
4-WPW		.066	204.5	247.7	5.5	47.0
5-WPW		.066	203.8	242.4	5.5	
6-WPW	68	.066	201.8	247.7	5.5	
AVER.			203.4	245.9	5.5	

* SPECIMENS No. 1, 2 & 3-WTW BROKE IN BASE METAL
" " 4, 5 & 6-WTW " " WELD.

THE SPECIMENS DESIGNATED - WPW HAVE A SPUN WELD COINCIDING WITH THEIR LONGITUD. AXIS AND OCCUPYING APPROX. 75% OF THE CROSS SECTIONAL AREA IN THE GAGE LENGTH.

TABLE - 4 MECHANICAL PROPERTIES HYDROSPUN HEAD FULL RADIUS

SPEC. No.	% RED.	GAGE IN.	YTS .2% OFF. KSI	UTS KSI	ELONG. % IN 2"	R_c
1-FPH	39	.086	112.0	143.2	13.0	30.0
2-FPH	43	.081	112.5	142.4	14.0	
3-FPH	39	.087	106.1	145.6	14.0	
AVER.			111.2	143.7	13.7	
1-FTH	43	.080	106.2	148.2	12.5	30.5
2-FTH	43	.081	100.5	146.4	13.0	
3-FTH	43	.081	105.5	150.7	13.5	
AVER.			104.1	148.4	13.0	
4-FPH	43	.081	229.4	271.8	6.0	51.5
5-FPH	39	.086	230.4	274.2	6.0	
6-FPH	43	.081	227.3	274.0	6.0	
AVER.			229.0	273.3	6.0	
4-FTH	43	.080	237.5	299.4	6.0	52.5
5-FTH	43	.081	240.1	279.0	5.5	
6-FTH	43	.081	238.8	277.9	5.5	
AVER.			238.8	285.4	5.7	

TABLE - 5 MECHANICAL PROPERTIES HYDROSPUN CYLINDER FORGED

SPEC. No.	% RED.	GAGE IN.	YTS .2% OFF. KSI	UTS KSI	ELONG. % IN 2"	R_c
1-PF	50	.090	130.3	152.6	5.5	31.5
2-PF	↑	.091	125.8	151.0	5.5	
3-PF		.090	123.1	152.4	5.5	
AVER.			126.4	152.0	5.5	
1-TF		.086	127.6	148.0	3.0	31.5
2-TF		.085	131.4	149.5	3.5	
3-TF		.086	129.9	150.1	3.5	
AVER.			129.6	149.2	3.3	
7-TF		.090	121.1	150.4	4.5	30.5
8-TF		.091	119.3	149.9	6.0	
9-TF		.091	121.7	150.0	5.0	
AVER.			120.7	150.1	5.2	
4-PF		.090	217.3	261.6	4.0	51.0
5-PF		.090	219.5	262.6	7.0	
6-PF		.089	215.4	260.0	6.0	
AVER.			217.4	261.4	5.7	
4-TF		.082	219.6	257.9	4.5	50.5
5-TF		.083	218.3	258.4	4.5	
6-TF		.083	216.8	256.6	3.5	
AVER.			218.2	257.6	4.2	
10-TF		.092	210.5	258.7	5.0	51.0
11-TF		.092	215.8	256.5		
12-TF	↓	.090	218.2	257.8	3.5	
AVER.	50		214.8	257.7	4.3	

TABLE-1 SUMMARY OF SPECIMENS
SEE FIGURE-3 FOR LOCATION

FORM, CONDITION AND LOCATION		MICRO SPECIMENS* - PARALLEL AS SPUN	MICRO SPECIMENS* - PARALLEL HEAT TREAT.	MICRO SPECIMENS* - TRANSVERSE AS SPUN	MICRO SPECIMENS* - TRANSVERSE HEAT TREAT.	TENSILE SPECIMENS - PARALLEL AS SPUN	TENSILE SPECIMENS - PARALLEL HEAT TREATED	TENSILE SPECIMENS - TRANSVERSE AS SPUN	TENSILE SPECIMENS - TRANSVERSE HEAT TREATED
HYDRO-SPUN AFT HEAD	DOME	1-DPH	2-DPH	1-DTH	2-DTH	1,2,3-DPH	4,5,6-DPH	1,2,3-DTH	4,5,6-DTH
	HALF RAD.	1-HPH	2-HPH	1-HTH	2-HTH	1,2,3-HPH	4,5,6-HPH	1,2,3-HTH	4,5,6-HTH
	FULL RAD.	1-FPH	2-FPH	1-FTH	2-FTH	1,2,3-FPH	4,5,6-FPH	1,2,3-FTH	4,5,6-FTH
FORGED HYDRO-SPUN CYL.	GROUND SMOOTH	1-PF	2-PF	1-TF	2-TF	1,2,3-PF	4,5,6-PF	1,2,3-TF	4,5,6-TF
	WITH SPIN MARKS							7,8,9-TF	10,11,12-TF
ROLLED, WELDED AND HYDRO-SPUN CYL.	BASE METAL	1-BPW	2-BPW	1-BTW	2-BTW	1,2,3-BTW	4,5,6-BTW	1,2,3,7-BPW	4,5,6,8-BPW
	WELD METAL	1-WPW	2-WPW	1-WTW	2-WTW	1,2,3-WTW	4,5,6-WTW	1,2,3-WPW	4,5,6-WPW

* LOCATION OF MICRO-SPECIMENS NOT SHOWN ON FIGURE 3.

TABLE - 2 MECHANICAL PROPERTIES HYDROSPUN HEAD DOME AREA

SPEC. No.	% RED.	GAGE IN.	YTS .2% OFF. KSI	UTS KSI	ELONG. % IN 2"	R_c
1-DPH	NONE	.098	125.5	149.0	13.0	31.5
2-DPH		.095	128.9	150.5	12.0	
3-DPH		.096	128.4	149.9	12.0	
AVER.			127.6	149.8	12.3	
1-DTH		.095	121.6	147.4	12.5	31.0
2-DTH		.096	117.9	143.6	12.5	
3-DTH		.097	113.4	143.3	12.5	
AVER.			117.6	144.8	12.5	
4-DPH		.097	228.3	271.2	5.5	51.5
5-DPH		.097	226.8	270.6	6.0	52.0
6-DPH		.097	226.3	267.5	5.0	
AVER.			227.1	269.8	5.5	
4-DTH		.097	227.6	271.3	6.0	51.5
5-DTH		.096	228.6	272.4	6.0	
6-DTH	NONE	.097	229.3	272.2	6.0	
AVER.			228.5	272.0	6.0	

DATA REPRESENTS SPECIMENS OBTAINED NEAR THE DOME OF THE HYDROSPUN HEAD AS SHOWN IN FIGURE - 3 AND WERE SUBJECTED TO LITTLE OR NO REDUCTION.

TABLE - 3 MECHANICAL PROPERTIES HYDROSPUN HEAD HALF RADIUS

SPEC. No.	% RED.	GAGE IN.	YTS .2% OFF. KSI	UTS KSI	ELONG. % IN 2"	R_c
1-HPH	23	.137	110.8	138.8	14.0	29.0
2-HPH	16	.153	111.1	140.2	14.0	
3-HPH	23	.130	107.1	139.0	12.0	
AVER.			109.7	139.3	13.3	
1-HTH	20	.103	104.6	140.6	13.5	29.0
2-HTH	20	.101	106.2	140.3	13.0	
3-HTH	20	.099	105.0	140.0	12.0	
AVER.			105.3	140.3	12.8	
4-HPH	16	.148	226.0	271.9	7.0	52.5
5-HPH	23	.133	224.8	265.4	6.0	
6-HPH	16	.152	224.2	268.2	6.0	
AVER.			225.0	268.5	6.3	
4-HTH	20	.102	218.4	261.7	6.0	52.5
5-HTH	20	.102	228.2	263.1	6.0	
6-HTH	20	.099	217.7	263.1	6.0	
AVER.			221.4	262.6	6.0	

DATA REPRESENTS SPECIMENS OBTAINED AT APPROX. THE HALF RADIUS OF THE HEAD WHICH IS A THICKENED AREA. THE TRANSVERSE SPECIMENS FROM THIS AREA WERE SURFACE GROUND TO PRODUCE PARALLEL SURFACES AND RESULTED IN THE GAGE OF THE TRANSVERSE SPECIMENS (HTH) BEING THINNER THAN THE PARALLEL SPECIMENS (HPH).

AUS-SHEAR FORMING OF LOW ALLOY STEEL CYLINDERS

E. S. Jones, General Electric Company
Flight Propulsion Laboratory Department, Cincinnati Ohio

Background:

The need for higher strength materials for use in pressure vessels such as rocket cases has provided a great stimulus to development of high strength steels. While the aircraft industry uses steels with strengths well in excess of 200,000 psi, the demands of the rocket industry are such that much stronger materials could be put to good use.

The 1954 article by Lips and Van Zuilen[1] touched off a wave of interest in the process of warm working steels in the metastable austenitic condition to achieve high strengths. Several investigators have reported (2, 3, 4 and 5) the results of such studies, among the more active being those of the Ford Motor Company. A summary of the more recent activities in the warm working of steels in the metastable austenitic temperature region has recently been published.[6]

Under sponsorship of the Navy Bureau of Ordnance (now the Bureau of Weapons), the General Electric Co., Flight Propulsion Laboratory Department, undertook to apply the process to the shear forming of low alloy steel cylinders, hereafter referred to as aus-shear forming. The objectives of this work were to:

1. Demonstrate feasibility of applying the process to thin walled cylindrical shapes.
2. Explore the effect of processing variables.
3. Evaluate the strength and ductility of cylinders produced by such methods.

It is the purpose of this paper to report the results of this study, and to assess the potential of the process.

EXPERIMENTAL APPROACH

Aus-Shear Forming Equipment:

The basic roll forming equipment used in this study was a modified vertical turret lathe. For warm roll forming all tooling was especially designed and built to withstand elevated temperatures. The 6" diameter mandrel and rollers were made of M-50 high speed tool steel, tempered 100°F above the expected maximum operating temperature. The mandrel was drilled to accommodate three (3) electrical cartridge heaters and these provided the primary source of heat. Slip rings were positioned below the hardened mandrel to supply power to the heaters. To balance convection and radiation heat losses, a hinged shell containing several electrical strip heaters partially surrounded the mandrel. A thermocouple inserted into the mandrel and connected to a controller in the heating element circuit provided automatic control of the mandrel temperature. Figure 1

shows a schematic view of the mandrel and roller arrangement. Although it was expected that the work roll would require heating, this proved unnecessary, since it reached forming temperature very soon after contact with the blank. Temperature checks of the blank in process and of the mandrel were made with a contact pyrometer or with Tempilstik.

Considerable modification to the original tooling was required as the experiments progressed. It was necessary to increase the strength and rigidity of the equipment in order to obtain the desired amount of warm working. As originally designed, no tailstock was used for the shear forming. However, the force required to deform the steels being studied - even in the austenitic condition - required that a tailstock be added. With increasing experience, it was possible to achieve reductions up to 75% in a 6" diameter cylinder having a ¼" thick wall. Figure 2 shows the equipment in its final form.

The blanks were austenitized in a 15 KW induction heating unit. A 5-turn coil was designed to give uniform rapid heating of the blanks. Inconel X sheet stock was placed around the inner and outer diameters of the blank during heating to help minimize scaling. Wire filled asbestos cloth and transite were used to minimize heat losses. An optical pyrometer was used to measure temperatures during the austenitizing cycle.

Adequate water and oil quenching facilities were available where required for roll-formed parts. A large forced air furnace was used for tempering the cylinders.

Selection of Steels:

Three commercially available steels were chosen for study. These are shown below, together with the analyses of the heats:

Material	%C	Mn	Si	Ni	Cr	V	Mo	S	P
Halcomb 218	.36	.36	1.13	--	5.00	.33	1.30	.019	.015
LaBelle HT	.42	1.34	2.21	--	1.32	.28	.36	.016	.016
Super Tricent	.54	.83	2.11	3.63	.90	.13	.49	.005	.013

Halcomb 218 is representative of the H-11 class (5% Cr) of tool steel, while the LaBelle HT and Super Tricent are medium carbon low alloy steels. The nickel content of the latter was of interest, since it was believed that Ni would have a beneficial effect on the transformation characteristics. All of these steels exhibited TTT characteristics thought to be favorable to aus-shear forming, ie, a deep-bay region with a sufficiently broad range of temperature and time such that severe deformation could be accomplished without encountering non-martensitic transformation during deformation. The TTT curves for Super Tricent and LaBelle H.T. are shown in Fig. 3.

Cylinder Pre-form Preparation:

Ring forgings of air melted Halcomb 218, LaBelle HT, and Super Tricent were procured from commerical sources. These were machined to 6"I.D.,

¼" wall, and 4½" long cylindrical pre-forms. The exact I.D. for each type of pre-form was varied due to slight differences in thermal expansion in the three steels. A clearance of .020" to .025" was allowed for fitting pre-forms (cold) on the mandrel. All blanks were magnafluxed after machining and were found to be of good quality.

All ring forgings were given a spheroidizing heat treatment prior to being austenitized in the induction heater, (preparatory to aus-shear forming). This spheroidizing treatment resulted in hardnesses below $R_c 25$.

Aus-Shear Forming Procedure:

In order to reach the desired reduction, many experiments in the rate of feed, mandrel rpm, force applied, roller configuration, number of passes etc, were made. Concurrently, several methods of temperature control and measurement were being tested. Due to equipment limitations, 65% to 70% was the maximum practical reduction which could be consistently achieved.

The procedure finally adopted for the detailed variable study was.

1. Austenitize the ring forging in the induction heater at 2000°F, hold at 2000°F ($\pm$ 10°F) for 7 to 8 minutes, the temperature being measured with an optical pyrometer.
2. Place the hot ring forging on the mandrel heated to the desired aus-shear forming temperature. Allow the blank to cool to the mandrel temperature, and measure the ring forging temperature with a contact pyrometer or Tempilstiks
3. Make the first roll-forming pass at .040"/rev.feed and 20 rpm. Check cylinder temperature and size after first pass.
4. Make the second pass at .020"/rev.feed and 20 rpm. Check the cylinder temperature.
5. Remove the cylinder from the mandrel as rapidly as possible and oil quench or air cool as required.
6. Double temper the cylinder immediately after cooling to room temperature. Cool to room temperature between the first and second temper cycles.

CYLINDER EVALUATION RESULTS

After completing the preliminary equipment development and material handling phase, a comprehensive study of the critical variables was undertaken. This consisted of a study of three deformation temperatures, and three tempering temperatures, on each of the three previously mentioned steels. A total of 27 cylinders were thus prepared (9 of each of the three steels). In all instances, aus-shear forming reductions were approximately 65 to 70%, this being the maximum possible with the equipment (available at that time).

Tensile Specimen Preparation:

After aus-shear forming of the 6" dia. cylinders, they were double tempered and longitudinal sheet tensile specimens were cut from the cylinder walls, parallel to the cylinder axis. All specimens were ground to final size to eliminate the curvature in the strips and to avoid the necessity of straightening by mechanical means. Final specimen size was 6" overall length x 1" gage length x 0.08" thickness x 0.24" gage width.

Tensile tests at room temperature were performed in triplicate. Some difficulty was experienced in testing several of the cylinders due to the extremely high strength, and the geometry of the test bars. Fracture sometimes occurred outside of the gage length of the specimens, making it difficult to obtain either strength and/or elongation measurements.

Tensile Properties:

The results of the tensile tests are tabulated in Tables I, II, and III.

Considering first the properties of the Halcomb 218 cylinders (Table I) the cylinders aus-shear formed at 900°F appear to show the best combination of strength and ductility. Tempering at 1000°F gave these average properties:

UTS	0.2% Y.S.	% Elong.	TS/YS Ratio
393,000	282,000	6.0	1.4

While higher single tensile or yield strength levels were obtained from other processing temperature conditions, those cited above are the best average (of three tests) properties.

The high ratio of TS/YS suggests that a large amount of retained austenite was present in these cylinders. Tempering at 1100°F reduced the TS/YS ratio for cylinders deformed at each of the three temperatures studied. With respect to ductility, this steel is relatively insensitive to changes in processing parameters, the elongation of all specimens being 4 to 7%.

Data on conventionally heat treated Halcomb 218 sheet strip (different heat) have these strength values:

UTS	0.2% Y.S.	% Elong.
285 - 295 ksi	225 - 235 ksi	5

Comparing these strengths with those obtained from the aus-shear formed cylinders (above), it is evident that the yield strength was increased by nearly 25%, without sacrifice of ductility.

Considering next the LaBelle H.T. cylinders (Table II) it is apparent that this steel is quite sensitive to cracks under the conditions investigated. Where "cracks" are denoted in the Table, the cylinders generally shattered into multiple pieces during aus-shear forming, immediately after removal from the mandrel, or sometime prior to tempering. For the 800 F deformation temperature, and either 600 or 700°F tempering these properties resulted:

UTS	0.2% Y.S.	% Elong.	TS/YS Ratio
388 - 338 ksi	352 - 325 ksi	5-9	1.1 - 1.05

Here the TS/YS ratio suggests that much less austenite was retained. The high incidence of cracked cylinders also indicates the possibility of strain induced transformation taking place during the aus-shear forming. This is discussed at greater length in the subsequent section on "Mechanism Studies".

Data on conventionally heat-treated LaBelle H.T. (different heat) sheet strip gave these strength values:

UTS	0.2% Y.S.	% Elong.
270 - 300 ksi	240-245 ksi	5-6

Comparing these data with the results of cylinder specimen tests (above) the yield strength was increased by nearly 50% by aus-shear forming, while equivalent ductility was retained.

Finally considering the Super Tricent cylinders (Table III), those aus-shear formed at 900°F and tempered at 700°F show excellent combinations of strength and ductility, as shown by these average values:

UTS	0.2% Y.S.	% Elong.	TS/YS Ratio
341 ksi	293 ksi	13.0	1.16

The properties of conventionally heat treated Super Tricent sheet strips are:

UTS	0.2% Y.S.	% Elong.
290 - 310 ksi	235 - 255 ksi	10 - 15

Thus the yield strength resulting from aus-shear forming has been increased by about 20% while ductility is substantially equivalent.

There are several observations one can make from these data:

1) A deformation temperature of 700°F results in excessive stresses, possibly due in part to strain-induced transformation, which causes cracked cylinders.

2. The relatively high TS/YS ratio, combined with high ductility, suggests the presence of appreciable retained austenite.
3. Tempering temperatures of at least 700°F are required to complete the temper reactions and produce high yield strengths.
4. Refrigeration after aus-shear forming to transform retained austenite would probably result in additional strength increases, at the expense of ductility.

From the standpoint of both yield strength and ductility, these properties of cylinders processed in the above described manner are quite remarkable. This is particularly evident when one compares the aus-shear formed properties with those generally reported for the conventionally heat treated condition. However, such comparisons should be made with caution, since specimen geometry, heat analysis, etc, are usually not comparable.

Microstructure:

The microstructures of all of these aus-shear formed materials were quite similar, and representative photomicrographs are shown in Figure 4. The structures shown were taken from the longitudinal axis of cylinders deformed about 65-70%. The fibrous nature of these structures is the result of the deformation which takes place during the aus-shear forming.

The electron photomicrographs (6000X) show the very fine martensitic needle size achieved by the process. There appears to be no unusual carbide precipitation or dispersion, at least at this magnification. It has been suggested that the refinement of the martensitic needle size is a major contributor to the strengthening achieved through aus-shear forming. This is discussed at greater length in the section on "Mechanism Studies".

Reproducibility Study:

Three additional Halcomb 218 cylinders (6" dia.) were aus-shear formed to determine the reproducibility of properties between cylinders. As described previously, the cylinders were austenitized for about 10 minutes at 2000°F, and were then transferred to the heated mandrel. A deformation temperature of 900°F was used. The three cylinders were each aus-shear formed in two passes to approximately 50-60% reduction in thickness, and were then removed from the mandrel and allowed to air cool to room temperature. Following this, the cylinders were double tempered at 1000°F. Each cylinder then had one tensile specimen (6" long x 3/8" gage width x 2" gage length) prepared from it, parallel to the cylinder axis. The results of the tensile tests are shown below:

REPRODUCIBILITY DATA - HALCOMB 218 CYLINDERS

Cylinder No.	% Reduction	Time on Mandrel (Min.)	T.S. psi	0.2% YS psi	% Elongation in 1"	% Elongation in 2"
A	53	31	303,000	249,000	7	5.5
B	60	36	377,000	279,000	7	5
C	62	35	395,000	293,000	8	6

These tests indicate that the aus-shear forming process, as carried out under the previously described conditions, is quite sensitive to process variables, and results in a rather large spread in strengths between cylinders. Additional study is needed to define more accurately the processing variable limits which must be observed in order to minimise these differences in properties.

MECHANISM STUDIES

The encouraging results from the cylinder property evaluation, coupled with the results of work being reported by other investigators, prompted the initiation of studies to investigate the basic reason for the strengthening. By so doing, it was hoped that process optimization and control could be facilitated.

Specimen Preparation:

For expediency as well as economy, the mechanism study was conducted on specimens aus-rolled by laboratory rolling mills. Plate, approximately 3/8" thick, of vacuum induction melted Super Tricent and LaBelle H.T. was utilized at the starting material in this study. The analyses of these materials are shown below:

Material	%C	Cr	V	Mo	Si	Ni	Mn	P	S
Super Tricent	0.53	0.9	0.1	0.4	2.2	3.6	0.7	.012	.009
LaBelle H.T.	0.43	1.2	0.3	0.4	2.0	---	1.0	.012	.013

Two heating furnaces, located in close proximity to the rolling mill, were used to austenitize and then heat at lower temperatures for aus-rolling. Reductions in thickness of between 65 and 90% were studied, these usually being achieved in 3-10 rolling passes, with about 5 minutes reheating between passes. During rolling the strips were checked between each pass for magnetic response with a strong Alnico bar magnet. After rolling to the desired thickness reduction the strips were oil quenched. Specimens were then either immediately tempered, or were first refrigerated for 8 hours in liquid nitrogen, and then single tempered for one hour at either 600 or 700°F. Tensile specimens were prepared in the longitudinal (to rolling) direction, and were surface ground to remove any possible surface decarb.

Tensile Test Results:

The results of tensile tests on the aus-rolled material are shown in Tables IV and V.

Super Tricent

Over the range of aus-rolling temperatures investigated (800 - 1250°F) this alloy showed only a "weak" to "mild" magnetic response during deformation, indicating slight strain-induced transformation (Table IV). Deformation temperatures of 800 or 1000°F were effective in increasing the

yield strength. Refrigeration also increased yield strength compared with non-refrigerated specimens, indicating considerable retained austenite. However, refrigeration also resulted in a corresponding decrease in ductility.

Based on magnetic characteristics, it would appear that Super Tricent is fairly insensitive to strain-induced transformation, and that in the region of 800 - 1000°F, a nearly completely austenitic structure was being deformed in the aus-rolling process.

LaBelle H.T.:

In contrast to the response of the Super Tricent, this alloy showed a decidedly greater magnetic response over the range of temperatures studied. (Table V). Aus-rolling for 75% reduction at 1000°F resulted in yield strengths of 350-360 ksi, somewhat higher than Super Tricent aus-rolled equivalent degrees. Refrigeration was again effective in increasing yield strength.

The magnetic response of LaBelle during aus-rolling suggests that a portion of the deformation was accomplished on a structure consisting of both austenite and strain-induced martensite. Warm working of such a duplex structure is thought to be partially responsible for the higher strengths that were achieved. Furthermore, this also suggests that steels which respond to this type of strain-induced transformation may exhibit the greatest strengthening potential, as contrasted to steels which are not subject to strain-induced transformation.

Interpretation of Results:

The data contained in Tables IV and V may be interpreted in several ways; however, it is felt that a discussion of the differences in magnetic response between the two steels is appropriate.

It is evident that generally similar tensile properties were obtained in aus-rolled sheet, compared to the properties of aus-shear formed cylinders. Referring once more to Table II, it may be observed that several LaBelle H.T. cylinders cracked during processing. Based on the degree of strain-induced transformation encountered in aus-rolling of LaBelle strip, it seems likely that a similar strain-induced transformation occurred during LaBelle cylinder aus-shear forming. If substantial transformation took place during the initial roll-forming pass, then a duplex (austenite + martensite) structure was probably deformed during the second roll-forming pass. It is believed that this condition should be avoided, since quenching of such a structure following the completion of aus-shear forming could result in unequal distribution of internal stresses and consequent initiation of cracks. Since this susceptibility to cracks was not evident in the Super Tricent cylinders (at deformation temperatures above 700°F), one might suspect that it would be more desirable to aus-shear form cylinders from a steel which does not undergo extensive strain-induced transformation.

Based on the data from this study, combined with the results of other investigations, it seems likely that the following strengthening mechanisms are each partially responsible for the high strengths obtained during aus-shear forming:

1. Refinement of the martensitic needle size through deformation of the austenitic structure.
2. Strain hardening of transformation products.

Opposing these strengthening mechanisms is the effect of retained austenite, which tends to promote higher ductility at the expense of high strength.

FUTURE OUTLOOK

The data reported herein serves to illustrate that the aus-shear forming process can be used to make cylindrical shapes that possess very high yield strength, combined with good ductility, from certain steels.

To be economically justifiable, aus-shear forming should be reserved for strengthening steels above and beyond that which can be achieved through heat treatments alone. Steels are being developed currently which can be heat treated to yield strength levels of 275 to 300 ksi, with appreciable ductility. Therefore, it seems likely that aus-shear forming of pressure vessels will probably be used to achieve yield strengths in excess of 300 ksi.

While feasibility has been demonstrated, there remains much to be learned before the aus-shear forming process can be applied to the manufacture of hardware. Optimizing steel compositions, controlling deformation temperatures and directionality effects, developing aus-shear forming equipment and techniques, and a knowledge of the limiting process variables all must be investigated in much more detail. When studies of this type have been completed, it should be possible to produce hardware with reliable properties.

ACKNOWLEDGEMENTS

The author wishes to acknowledge the contributions of W.F. Zimmerman and E. N. Bamberger for the data relating to the aus-shear formed cylinders. Dr. W. H. Chang supplied the data obtained during the mechanism study, and was most helpful in interpreting the results.

Appreciation is also expressed to the Navy Bureau of Weapons, Special Projects Office, for sponsoring the work and for permission to publish the results.

REFERENCES

1. E. M. H. Lips and H. Van Zuilen, "Improved Hardening Technique", Metal Progress, August 1954, pp 103-104.

2. D. Gullotti, E. Eichen, and J. W. Spretnak, "Development of New Mechanisms and Techniques for Obtaining Steels in the Ultrahigh Strength Range", WADC-TR-56-555, AD 130755, May, 1957, pp 49

3. D. J. Schmatz and V. F. Zackay, "Mechanical Properties of Deformed Metastable Austenitic Ultra-High Strength Steels," Trans. ASM, 51, 1959, pp 476-488; discussion, 488-494

4. E. B. Kula and J. D. Dhosi, "Effect of Deformation Prior to Transformation on the Mechanical Properties of 4340 Steel", Trans, ASM Vol. 52, 1960, pp 321

5. J. C. Shyne, V. F. Zackay and D. J. Schmatz, "The Strength of Martensite Formed from Cold-Worked Austenite", Trans. ASM, Vol 52, 1960, pp 346.

6. "Development of High Strength Steels by Working of Metastable Austenite", Defense Metals Information Center Memo #39, Nov 30, 1959.

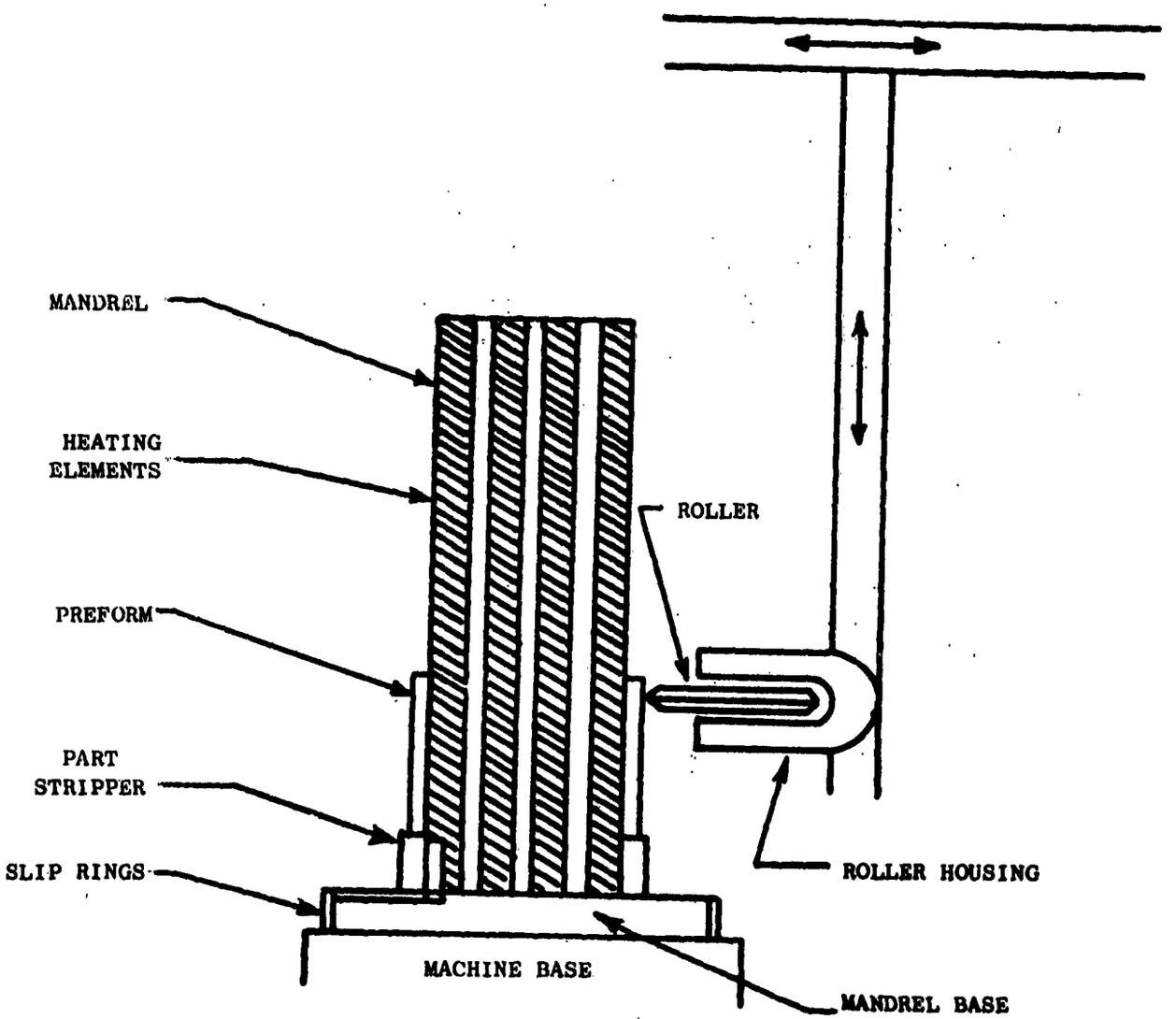


FIGURE 1.

SCHEMATIC VIEW OF TOOLING FOR AUS-SHEAR FORMING

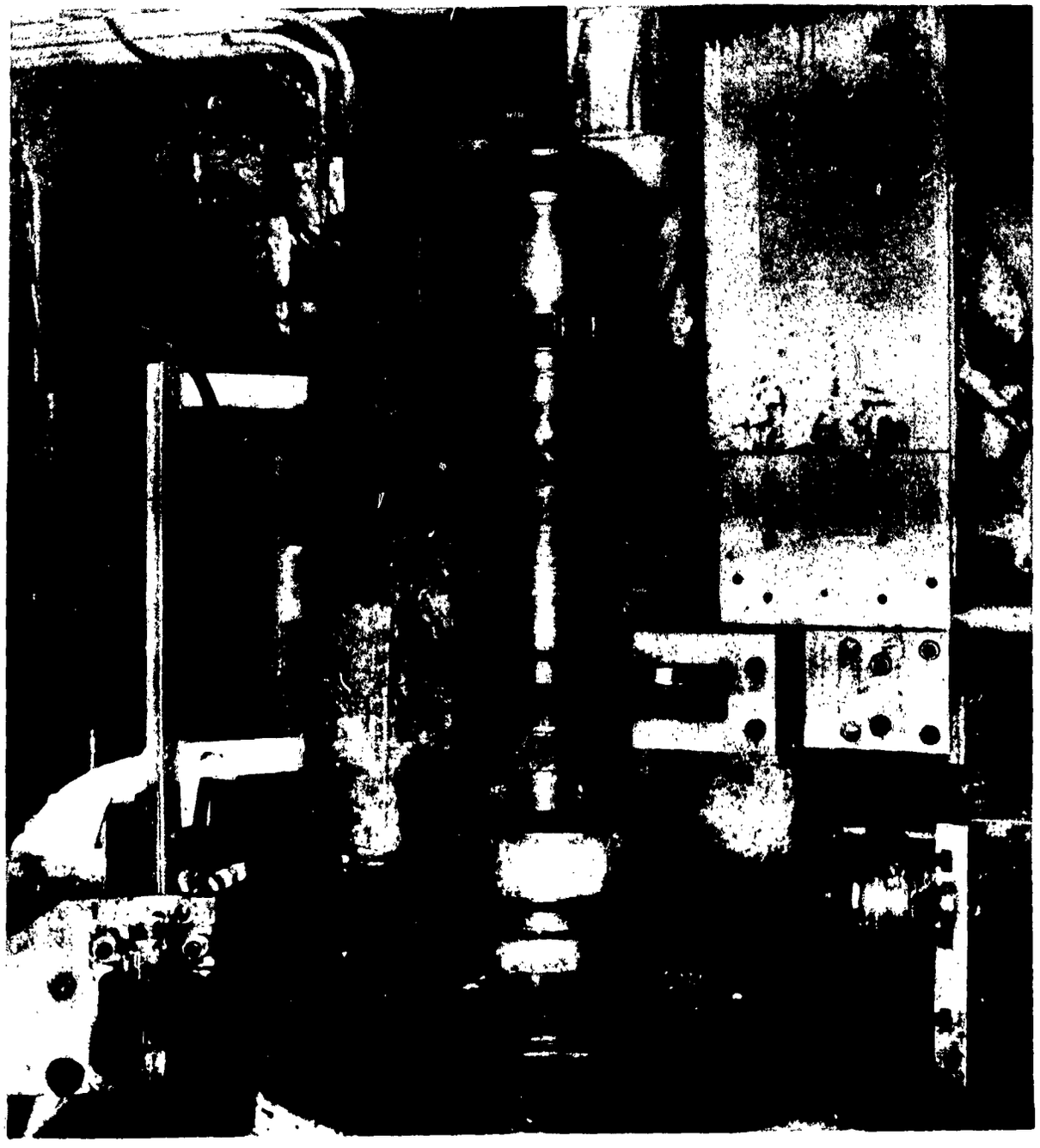


Figure #2

Aus-shear forming equipment as finally modified (Guard heater out of position).

FIG. 3 TTT CURVES FOR SUPER TRICENT AND LABELLE H.T.

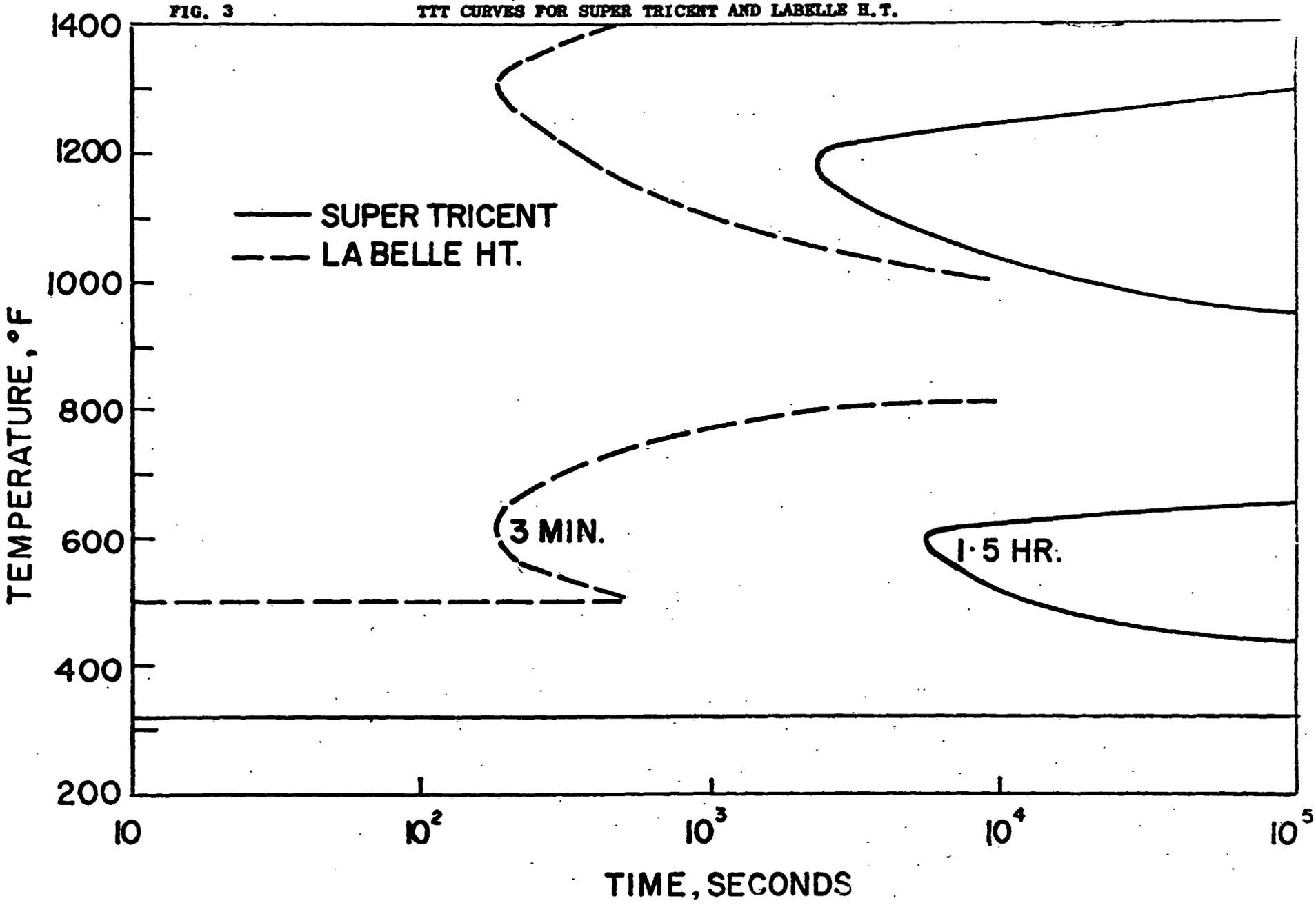
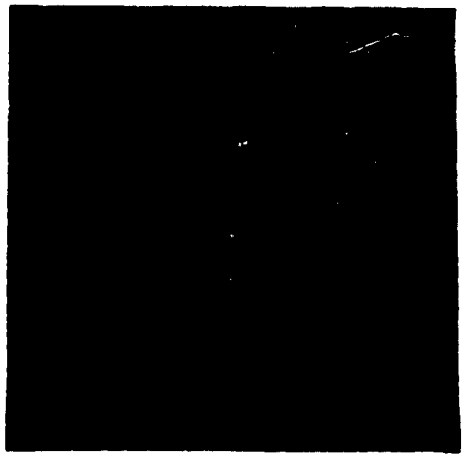


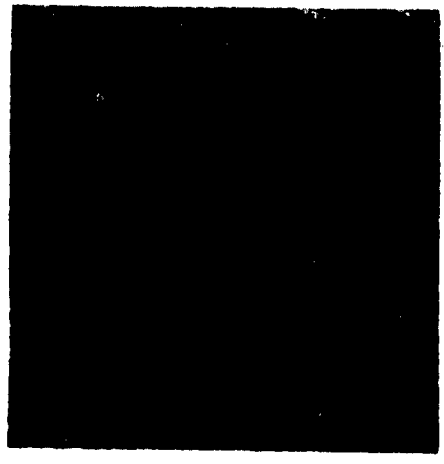
FIGURE 4

REPRESENTATIVE PHOTOMICROGRAPHS OF AUS-SHEAR FORMED CYLINDER SPECIMENS

LABELLE H.T.

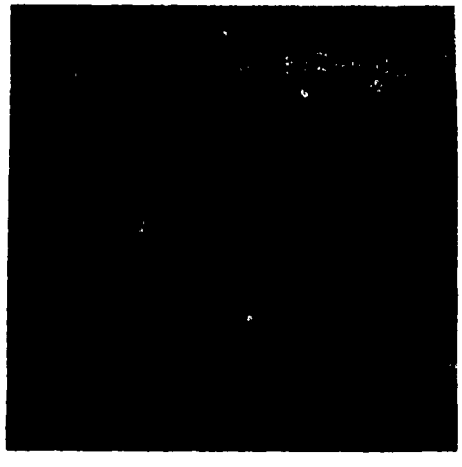


250 X



6000 X

HALCOMB 218



250 X



6000 X

TABLE I

Room Temperature Tensile Properties of Aus-Shear Formed Halcomb 218 Cylinders

Cylinder No.	Mandrel Temperature	Tempering Temperature	UTS ksi	0.2% Y.S,ksi	% Elongation(in 1 inch)
1	800F	900F	*	247	*
			405	248	7.0
			*	284	*
9	800F	1000F	354	275	5.0
			380	276	5.0
			385	313	6.0
4	800F	1100F	300	272	6.0
			306	281	5.0
			255	232	5.5
2	900F	900F	394	273	6.0
			365	275	-
			346	266	5.0
7	900F	1000F	393	284	5.0
			391	272	6.0
			395	291	6.0
6	900F	1100F	286	254	5.0
			290	260	5.0
			291	268	6.0
3	1000F	900F	413	284	5.0
			412	265	4.0
			*	256	*
8	1000F	1000F	345	265	6.0
			352	298	6.5
			344	275	7.5
5	1000F	1100F	286	260	7.0
			283	260	6.5
			271	251	6.5

All cylinders were shear-formed 60-70% reduction in thickness
Strain rate .005"/"/min. to yield.

* Broke in tab.

TABLE II

Room Temperature Properties of Aus-Shear Formed LaBelle H.T. Cylinders

Cylinder No.	Mandel Temperature	Tempering Temperature	UTS ksi	.2% Yield, ksi	% Elongation
3	700F	400F	-	Cylinder Cracked	-
7	700F	600F	-	Cylinder Cracked	-
4	700F	700F	340	241	15.5
			324	247	15.0
			*	237	*
2	800F	400F	-	Cylinder Cracked	-
3	800F	600F	388	351	5.0
			-	350	-
			373	352	5.0
5	800F	700F	338	326	9.0
			343	325	5.0
			350	328	7.0
1	900F	400F	*	281	*
			370	284	8.0
			374	298	9.0
9	900F	600F	-	Cylinder Cracked	-
6	900F	700F	-	Cylinder Cracked	-

All cylinders were shear-formed 60-70% reduction in wall thickness
Strain rate .005"/"/min. to yield.

* Broke in tab.

TABLE III

Room Temperature Properties of Aus-Shear Formed Super Tricent Cylinders

Cylinder No	Mandrel Temperature	Tempering Temperature	UTS ksi	0.2% Yield, ksi	% Elongation	Rc Hardness
7	700F	400F	-	Cylinder Cracked	-	-
8	700F	600F	348	237	13.0	56-57
			360	231	14.5	57.5-59
			364	230	15.0	56.5-58
9	700F	700F	-	Cylinder Cracked	-	-
6	800F	400F	293	189	*	59.0-60.5
			269	195	*	59.5
			332	204	*	59-60
2	800F	600F	361	206	12.5	57
			368	-	15.0	57
			358	202	14.0	56.5
3	800F	700F	309	276	2.0	56-59
			334	281	4.0	59.5
			327	289	7.0	59.5
1	900F	400F	388	212	12.0	60
			332	235	-	60
			380	222	10.0	58-59
4	900F	600F	334	270	7.0	56-57
			338	265	15.0	57.5
			331	199	10.0	57
5	900F	700F	343	300	10.0	58.5
			342	290	13.0	59.5-60
			339	288	15.0	59-60

All cylinders were aus-shear formed 60-70% reduction in wall thickness Strain rate .005"/"/min. to yield.

** Broke in tab.

TABLE IV SUPER TRICENT DATA - AUS-ROLLED SHEET

Rolling T	% Red & No. of Passes	(1) Magnetic	(2) Refrig.	(3) Temper	Rc	Tensile Properties T.S	Y.S.	% El. (in 1")
1250°F	75 - 3	N-W-W	-100°F/8 hrs.	600°F		317	279	4.0
			-100°F/8 hrs.	700°F		303	217	4.0
	89 - 8	N-W-M	-100°F/8 hrs.	600°F		266	212	7.5
			-100°F/8 hrs.	700°F		252	220	4.0
1000°F	72 - 2	W-M	None	600°F		341	296	14
	(36 min) *		-100°F/8 hrs.	600°F	60.5	365	333	4($\frac{1}{2}$")
			-100°F/8 hrs.	700°F	59.5	359	343	-
	79 - 3	N-W-M	-100°F/8 hrs.	600°F		358	320	5
	(17 min)*							
	88 - 5	W-M	-100°F/8 hrs.	600°F		367	337	5.5
	(61 min)*							
800°F	75 - 3	N-W	As Rolled	—		366	151	6.5
	(10 min) *		-100°F/8 hrs	600°F		344	314	6
			-100°F/8 hrs	700°F		344	321	4
	85 - 8	W-M	As Rolled			367	248	9.5
	(70 min) *		-100°F/8 hrs.	600°F		362	347	1.0
			-100°F/8 hrs.	700°F		361	358	2.0

* Total Heating Time.

(1) N = Non-magnetic; W = Weakly magnetic; M = Mildly magnetic; V = Very magnetic.

(2) -100°F/8 hrs (liq. N_2)

(3) Single temper for one (1) hour.

TABLE V LABELLE H.T. DATA - AUS-ROLLED SHEET

Rolling T	% Red. & No. of Passes	(1) Magnetic	(2) Refrig.	(3) Temper	Rc	Tensile Properties T.S.	Y.S.	% El. (in 1")
1250°F	76 - 3 (38 min)*	V	-	As Rolled		151	126	10
	89 - 8 (61 min)*	W-V	-	As Rolled		158	135	12
1000°F	75 - 3 (32 min)*	N-M-V	-100°F/8 hrs.	600°F	60.0	367	353	4(½")
			-100°F/8 hrs.	700°F	59.0	351	351	2(1")
	75 - 5 (33 min)*	N-M-V	None	600°F	-	341	322	4
			-100°F/8 hrs.	600°F	61.0	379	363	4
			-100°F/8 hrs.	700°F	59.5	361	354	3
	90 - 10 (90 min)*	N-W-M	-100°F/8 hrs.	600°F	-	334	326	4
			-100°F/8 hrs.	700°F	-	320	300	5
800°F	65 - 4 (20 min)*	M-V	As Rolled	-	-	294	220	16
			-100°F/8 hrs.	600°F	55	289	266	17
			-100°F/8 hrs.	700°F	54	284	265	20

* Total Heating Time.

(1) N = Non-magnetic; W = Weakly magnetic; M = Mildly magnetic; V = Very magnetic.

(2) -100°F/8 hrs

(3) Single temper for one (1) hour

THE EFFECTS OF PROCEDURAL VARIABLES ON THE PROPERTIES OF BUTT WELDS

By

Clyde M. Adams, Jr.,
Associate Professor of Metallurgy
M.I.T. - Cambridge, Mass.

I. INTRODUCTION

In the fabrication of shaped structures from sheet material, the various welding processes play an obvious and important part. When these structures are to be of unusually high strength, it becomes an objective of welding to preserve properties as well as to generate shape. In this sense, welding has become regarded as a negative factor in the solid propellant motor case industry in that welding can and too often does weaken the entire structure, but can never homogeneously strengthen it. In a thin-skinned pressure vessel, a weld which is stronger and tougher than the surrounding structure contributes nothing to the overall strengthening of the vessel, whereas a weld which is softer or more brittle quite definitely weakens the entire unit. As a processing technique, welding cannot have the primary function of beneficiation of structures and properties; one must be content with the aim of leaving the properties of the sheet material as good as they were before welding.

This gloomy view of welding, as a process where strength can be lost but never gained, has lent impetus to the adoption of shaping procedures such as spinning and deep drawing, which processes do operate on the entire metallurgical structure, as alternative fabrication techniques. Of even greater significance has been the almost inherent variability associated with the welding process which has militated strongly against its use in fabrication of ultra high strength rocket motor cases.

However, there are very pursuasive technical as well as economic arguments for continued study and development of welding for such demanding areas as motor case fabrication. For example, tooling is generally simpler and less expensive for welding than for other shaping techniques. The flexibility of the process with respect to short production runs, accomodation of design changes during production runs, or the generation of unusually large shapes, is unexcelled. In addition, the cost and form of the starting material offer many advantages. Many alloys can reach a condition of higher

strength when processing includes hot and/or cold rolling into sheet form than by any other route. Thus, while it is true that spinning and deep drawing plastically operate on an entire structure and thereby accord promise of homogeneity, these processes may not always be best suited to the generation of optimum mechanical properties. If the manipulation and control of the welding process ever reaches the station of true reliability, there is every reason to hope that thin-skinned pressure vessels could be welded more cheaply and at least as strong and tough as those produced by more specialized techniques, largely because welding takes advantage of a processing history in rolled sheet which is often identified with the best mechanical properties a given material has to offer.

Reliability in welding will have to be preceded by a deeper understanding of the interplay of thermal, metallurgical, and mechanical phenomena which are involved. Much more systematic study of the relation of processing variables to resulting structures and properties is needed to accompany the recent advances in the gadgetry and mechanistics of welding.

II. HEAT FLOW

Fusion welding is primarily a thermal process. The cooling rates and distributions of peak temperatures associated with moving arcs have much to do with the resulting structures and properties and the genesis of defects. When heat flow from a single weld pass in relatively thin sheet material is considered, there are two governing relationships which quite describe the thermal situation insofar as the development of metallurgical structures is concerned. Of primary interest is the distribution of peak temperatures expressed as a function of distance from the weld fusion line. The following equation gives the maximum or peak temperature, T_p, experienced at a point in the heat affected zone as a function of distance, r, from the weld:

$$\frac{1}{T_p - T_o} = 4.13 \rho C_p \left(\frac{V}{M q}\right) t r + \frac{1}{T_m - T_o}$$

(Equation 1)

where T_m, T_o = melting temperature and initial (uniform) temperature, respectively.

ρ, C_p, t = density, specific heat, and thickness, respectively, of material being welded.

V = arc travel speed.

r = distance from weld fusion boundary

q = arc power

μ = arc-to-plate heat transfer efficiency, usually the order of 0.9.

Equation (1) is plotted for a variety of 5000 series aluminum alloys in Figure 1 with experimental peak temperature determinations superposed. Equation (1) is especially useful in that knowledge of thermal conductivity is fortunately not required, and data on density and specific heat are generally available. When a welding process involves a novel heat source, or the properties of the material are not well known, experimental determinations of peak temperature distribution can readily and accurately be made using temperature sensitive lacquers in transverse stripes across the weld as depicted in Figure 2. Whatever the metal, plotting in terms of the coordinates of Figure 1 will always lead to a straight line correlation for the particular material and process combination being used.

With materials such as high strength steels, in which structures are sensitive to cooling rate as well as to peak temperatures, the following relation is often useful, especially in correlating preheat requirements with sheet thickness and arc energy input:

$$\frac{dT}{d\theta} = 2\pi K \rho C_p \left(\frac{Vt}{\mu q}\right)^2 (T - T_o)^3$$

(Equation 2)

where $\frac{dT}{d\Theta}$ = cooling rate in the weld.
T = temperature at which cooling rate is to be determined, usually selected in the critical range between 900 and 1400°F for most steels.
T_o = initial or preheat temperature
K = thermal conductivity of material being welded.

These equations are not only descriptive of the weld thermal regime, but give a clearer idea of the extent to which process variation can modify structural effects. For example, it is often stated that high arc travel velocity will automatically generate narrow heat affected zones and high cooling rates. Equations (1) and (2) show it is the ratio of arc power to arc velocity which is significant, and if increased velocity is accompanied with increased amperage as is often the case, there will be little influence on peak temperature distribution or cooling rate, and therefore upon either the width or structure of the heat affected zone. On the other hand, in comparing different processes, energy inputs may be quite different. For example, high voltage electron beam is characterized by a much lower total energy input than an arc, and heat affected zones may be significantly narrower as a result.

Equations (1) and (2) are particularly useful to the research worker for making quantitative correlations between structures and procedures in fusion welding.

III. WELD METAL STRUCTURES

Arc deposited metal has a structure which is directly influenced by the thermal regime described by Equations (1) and (2), but the relationships of structure to properties and of procedure to structure are not nearly so well understood for the weld metal itself as for the heat affected zone. The cooling and solidification rates are so high that weld metal structures must be treated as unique to the processing field. Arc deposits freeze more rapidly than the most severely chilled thin walled castings, and fine dendritic structures are produced such as shown in Figure 3 for 2014 aluminum alloy. It is felt the same basic type of structure prevails in other alloy systems including the steels, but in many of these, the solidification details and distribution of alloying elements are so obscured by subsequent solid state transformation that dendrite configurations are difficult to resolve.

Different alloy systems give somewhat different textures than that shown in Figure 3. For example, nickel-rich alloys invariably exhibit side branching from long rod-like dendrites. All systems studied to date have in common very fine dendrite structure and dispersion of solute concentrations or secondary phases. In fact it begins to appear that arc deposition accords greater macroscopic chemical homogeneity than any other processing technique. The scale of microsegregation and dendrite spacing is the order of a few microns, and very brief solutionizing or austenitizing treatments will beget almost complete homogeneity. One relationship which has been observed between weld metal structures and thermal conditions is reflected in Figure 4 which shows the effects of arc energy input on dendrite dimensions. As would be expected, more rapid freezing produces finer dendrites, and the quantitative theoretical prediction that spacing should be proportional to the square root of arc energy input is fairly well confirmed by experiment. The effect of dendrite spacing on speed of solutionizing is evident in Figure 5 which shows the response of 2014 arc deposits to short solutionizing treatments. Of interest are (a) the magnitude of the solutionizing times, 5 and 15 minutes, and (b) that for very low energy arc deposits, solidification rates and dendrite fineness are such that 5 minutes accomplishes complete solutionizing, while with higher energy inputs, 15 minutes are required. To achieve this same degree of homogeneity (as reflected in strength or hardness) a casting requires solutionizing for a period the order of one week. Thus, it hardly seems proper to refer to weld metal as exhibiting a "cast" structure; the structures of arc deposits are as different from castings as wrought material, and a new "set of rules" will be required to describe their structures and properties.

IV. COMPOSITE PROPERTIES OF WELDS

When the structures in weld metal and heat affected zones are linked together in transverse loading, the resulting overall strength and deformation pattern depend not only on individual plasticities and strengths of the critical regions, but their mutual constraints. One important and poorly understood factor influencing composite properties is that chemically identical arc deposited and wrought material are mechanically different, especially as relates to their post yield plastic behavior.

Cold worked aluminum-magnesium (5000 series) alloys have received much study in connection with the overall plastic and strength properties of welded joints. Hardness distributions typical of cold worked material which has been welded are shown in Figure 6. Increasing arc energy input has the effect of widening the heat affected zone in conformance with Equation (1) and decreases the centerline hardness of the fusion zone, a property which apparently depends upon dendrite spacing. The dependence of minimum fusion zone hardness on arc energy input for various 5000 series combinations is shown in Figure 7, and other hardness distributions are shown in Figure 8. From a metallurgical point of view it it is of interest that hardness distributions shown in Figures 6 and 8 do not correspond in any obvious way to the plastic behavior of the same welds under simple transverse tension. Consider a weld of matching chemistry in fully annealled 5154 plate which exhibits essentially no hardness variation across the weld (Figure 8); the weld, heat affected, and base metal zones are all of about the same hardness. When tested in transverse tension, the strain is concentrated within the weld metal to a marked extent (Figure 9). Another feature common to strain distributions in these alloys are the minima observed in the heat affected zones immediately adjacent to the weld metal; there seems to be a constraint to flow in the region of the fusion zone boundary.

With some hardenable steels, exactly the opposite behavior is observed. With matching chemistry and heat treatment, weld metal in steels such as 4130 exhibits less plastic flow under transverse loading than does the surrounding wrought material.

These observations are offered to emphasize the need for further basic research into the properties of arc deposits and the problems involved in matching mechanical behavior of arc deposits with chemically similar wrought material.

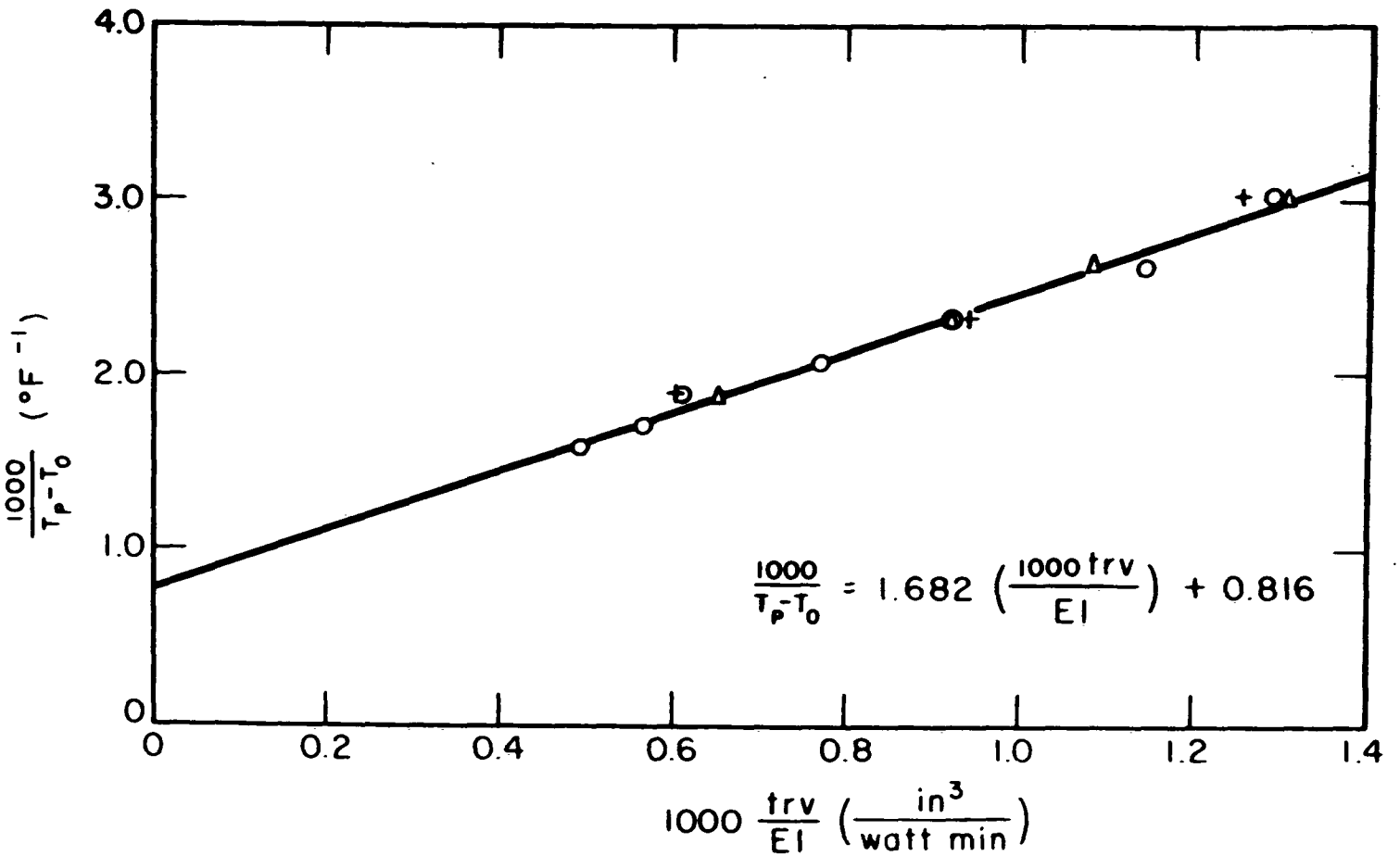
V. WELDING STRESSES AND CRACKING

In addition to modifying metallurgical structures, the fact of welding imposes strains upon these structures with consequences which depend upon the strength and plasticity of the weld and heat affected zones. There is a critical interplay between the strength of the deposit itself and the loading or cracking of material in either the fusion or heat affected zones of the weld. With hardenable steels, cooling rate not only has a bearing on structures and their ability to withstant plastic strain, but also influences the rate with which

thermal contraction imposes loads on the weld and the temperature at which the weld accepts the greatest amount of plastic strain. In general, high arc energy inputs and high preheat temperatures promote (1) greater overall strain, (2) higher strain rate, and (3) straining takes place at relatively higher temperatures. In the limit, with very high preheat or interpass temperatures, sufficiently large strains may be imposed before solidification is complete to cause hot cracking in the weld metal itself. Since these same variables influence the structures produced, the relationship of filler composition, weld thermal variables and resulting stresses, strains, and cracks, are only vaguely understood. Some of the dependencies which have been observed for hardenable steel are shown in Figures 10 and 11. In Figure 10, the effect of deposit strength on the incidence of cracking is shown for a weld which was restrained from lateral contraction during and after welding. The strong filler produced higher separating forces and earlier initiations of cracking than did the soft filler. Preheat avoids cracking even with a high strength filler, and insufficient preheat has the effect of imposing a delay to the initiation of cracking over that observed when no preheat is used; these effects are shown in Figure 11. These phenomena threaten to be the most difficult of all in the welding field to rationalize, because of the complicated and simultaneous ways in which thermal variables influence mechanical and metallurgical responses. The development and tailoring of filler metal alloys for joining high strength crack sensitive steels will certainly benefit from more clear understanding of the multiplicity of events which accompanies the deposition of an arc weld.

VI. CONCLUSION

There is strong need for basic phenomenalogical research into thermal, mechanical, and metallurgical reactions associated with and, in some ways, peculiar to arc welding. Arc welding is a fundamentally complicated process, many aspects of which are only qualitatively understood, but it is here to stay, and will always be of importance in the fabrication of high strength structures from sheet materials.



PEAK TEMPERATURE DISTRIBUTION IN ARC WELDING ALUMINUM

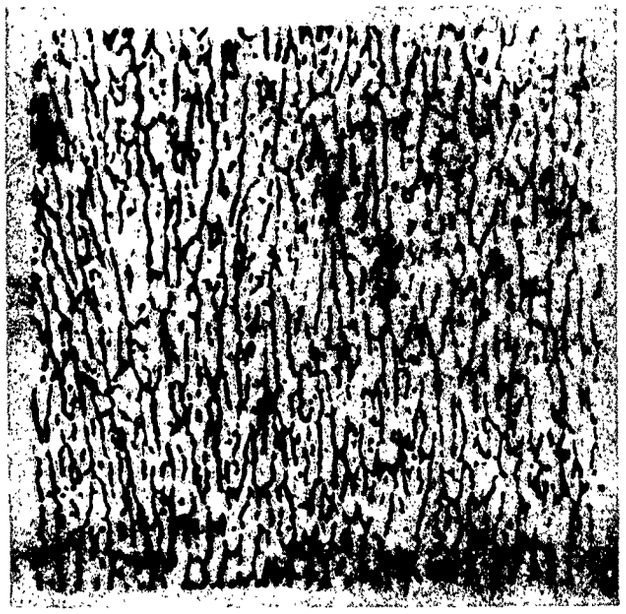
RECIPROCAL OF PEAK TEMPERATURE RISE IN PLOTTED AS A FUNCTION OF: DISTANCE, r, FROM THE FUSION ZONE; PLATE THICKNESS, t; VELOCITY, V; VOLTAGE, E; AND AMPERAGE, I. EXPERIMENTAL POINTS ARE FROM 5000 SERIES ALLOY WELDS.

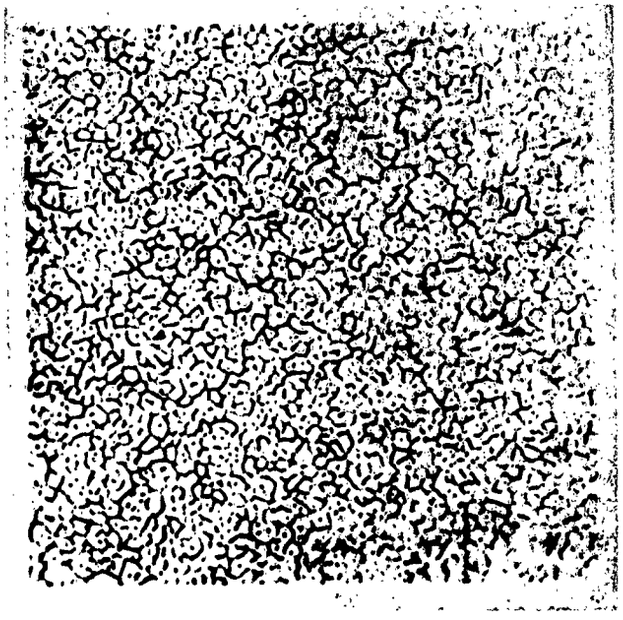
FIGURE 1



PHOTOGRAPH SHOWING THE RESPONSE TO WELDING HEAT OF LACQUERS WHICH ARE SENSITIVE TO VARIOUS TEMPERATURES

FIGURE 2





ARC DEPOSIT IN 2014 ALUMINUM ALLOY

TOP: PARALLEL TO WELD AND PERPENDICULAR TO PLATE SURFACE

BOTTOM: PARALLEL TO PLATE SURFACE

ENERGY INPUT: 9300 JOULES/INCH

MAGNIFICATION 300X KELLER'S DOUBLE ETCH

FIGURE 3

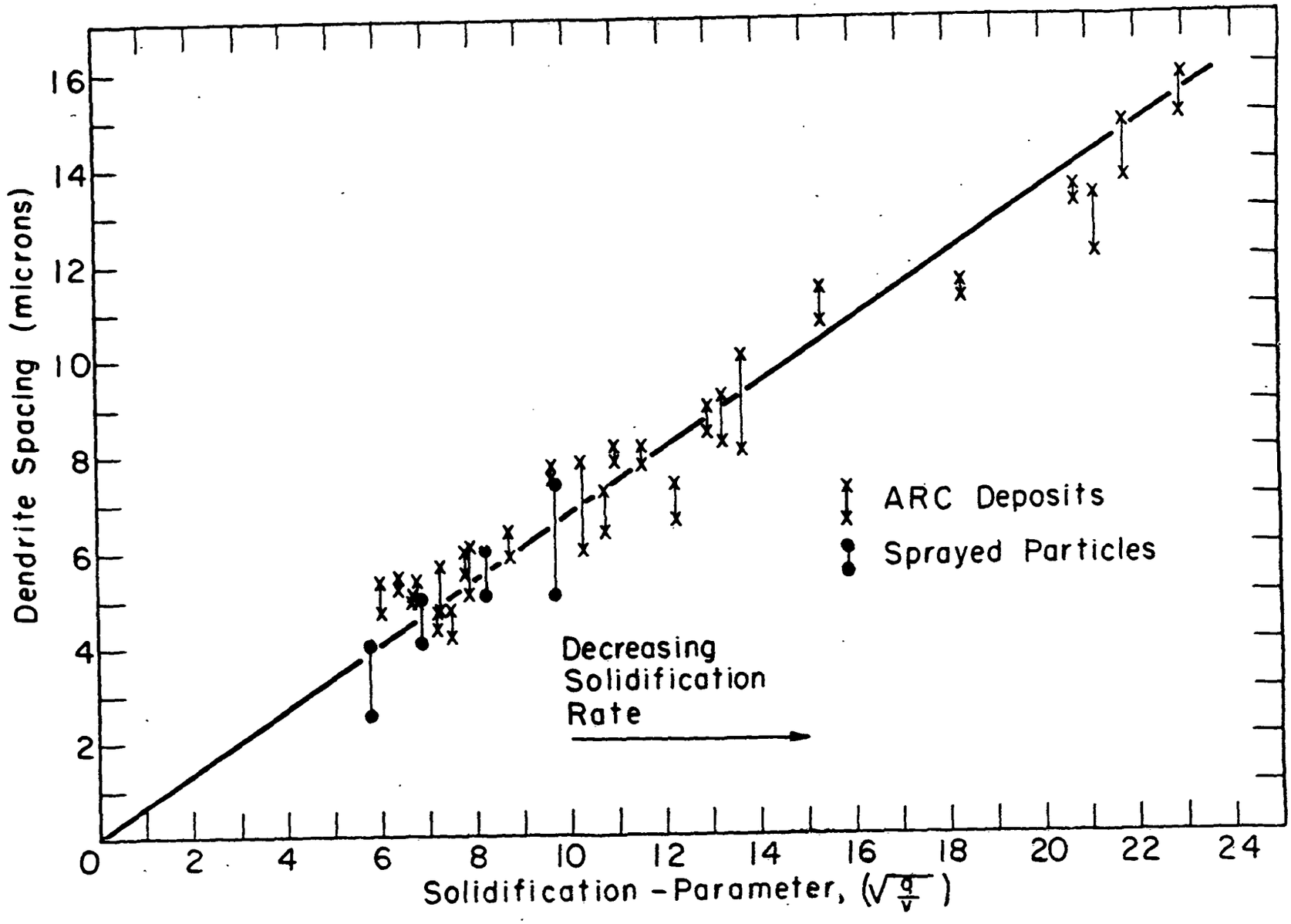
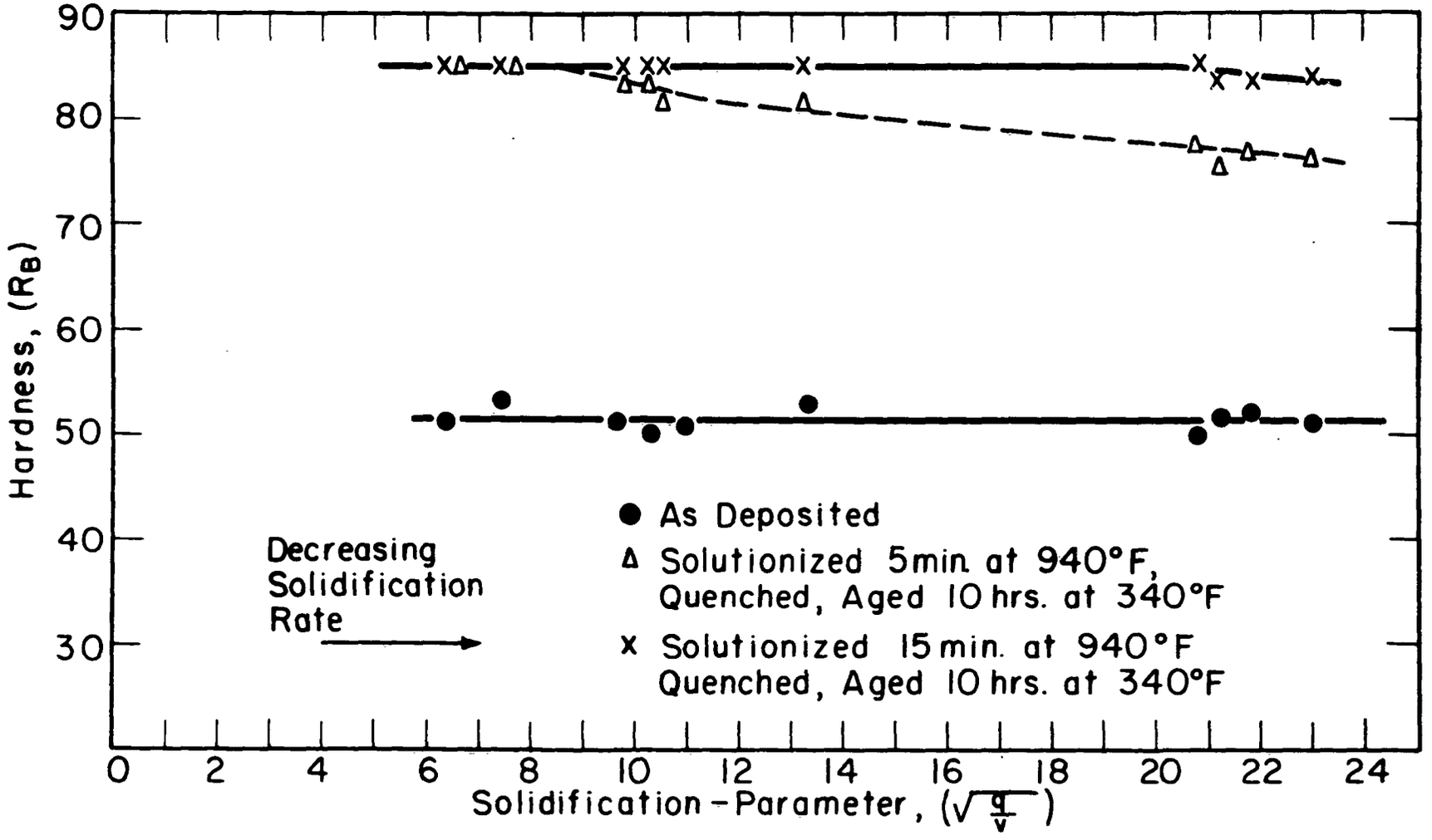


FIGURE 4

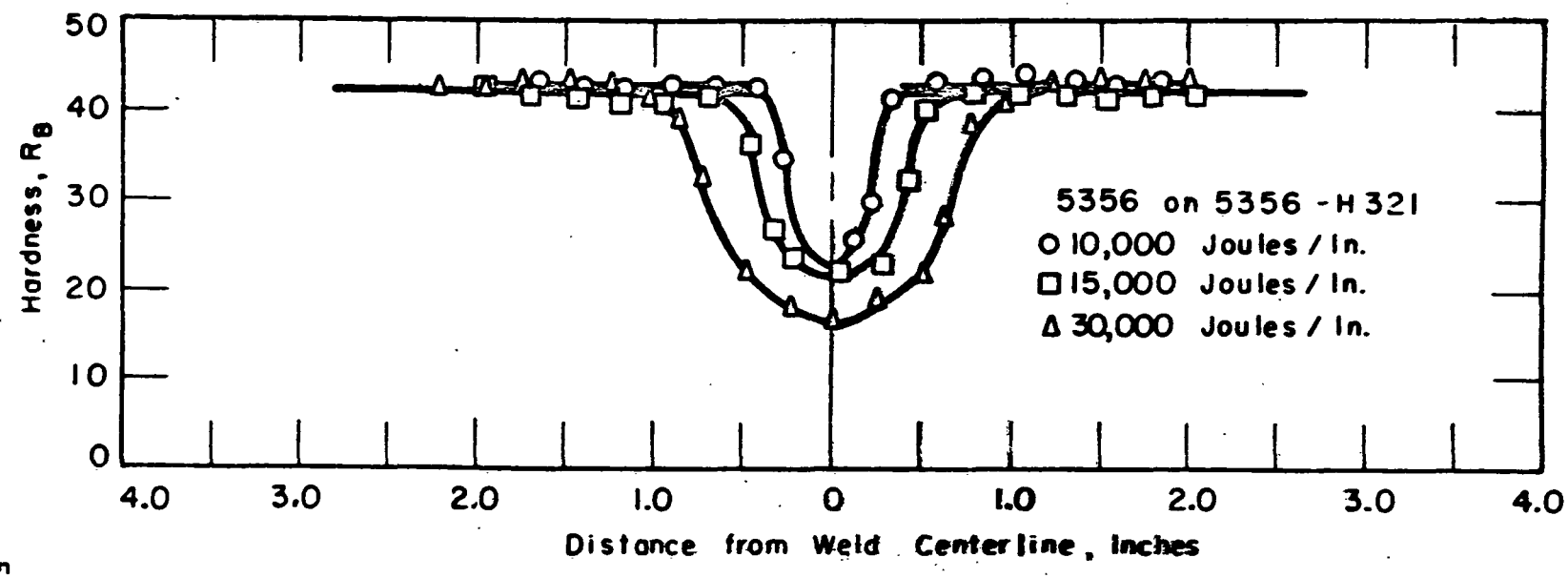
EFFECT OF ARC ENERGY INPUT ON DENDRITE SPACING IN 2014 ALUMINUM ALLOY



III-94

FIGURE 5

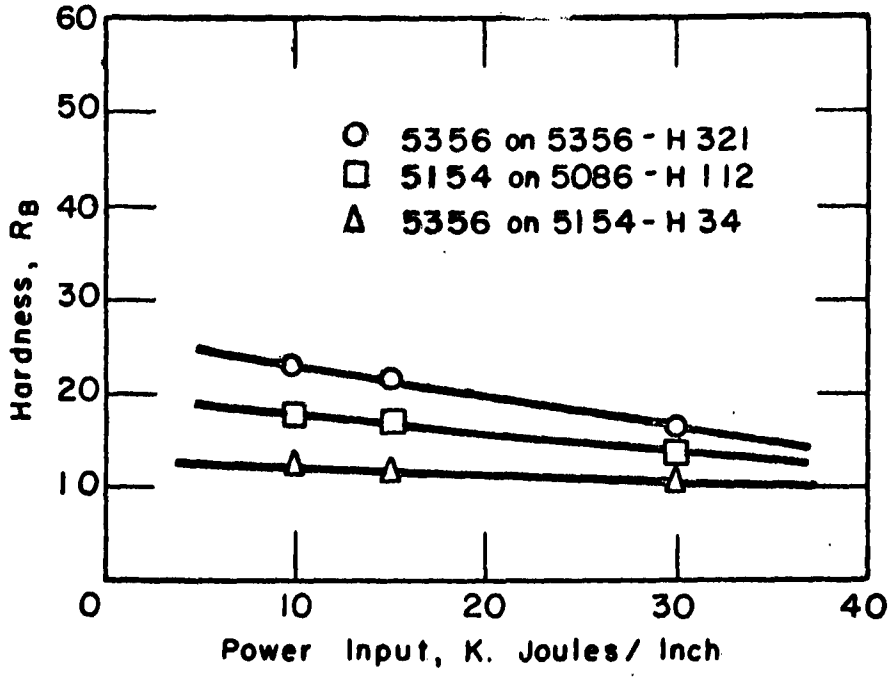
EFFECT OF ENERGY INPUT ON RESPONSE TO HEAT TREATMENT OF 2014 ARC DEPOSITS



III-95

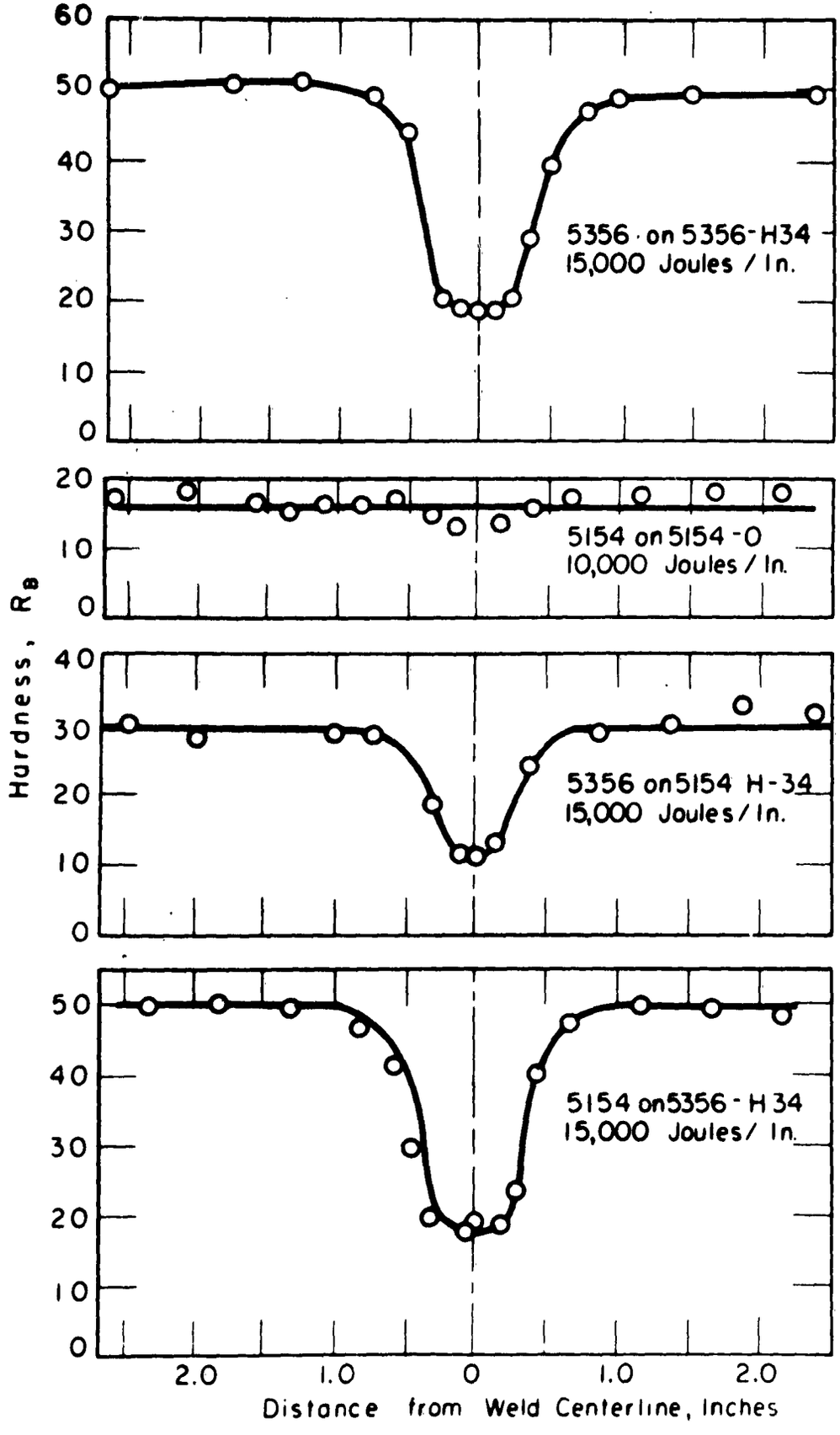
FIGURE 6

TRANSVERSE WELD HARDNESS DISTRIBUTIONS IN WORK HARDENED 5356 ALUMINUM ALLOY



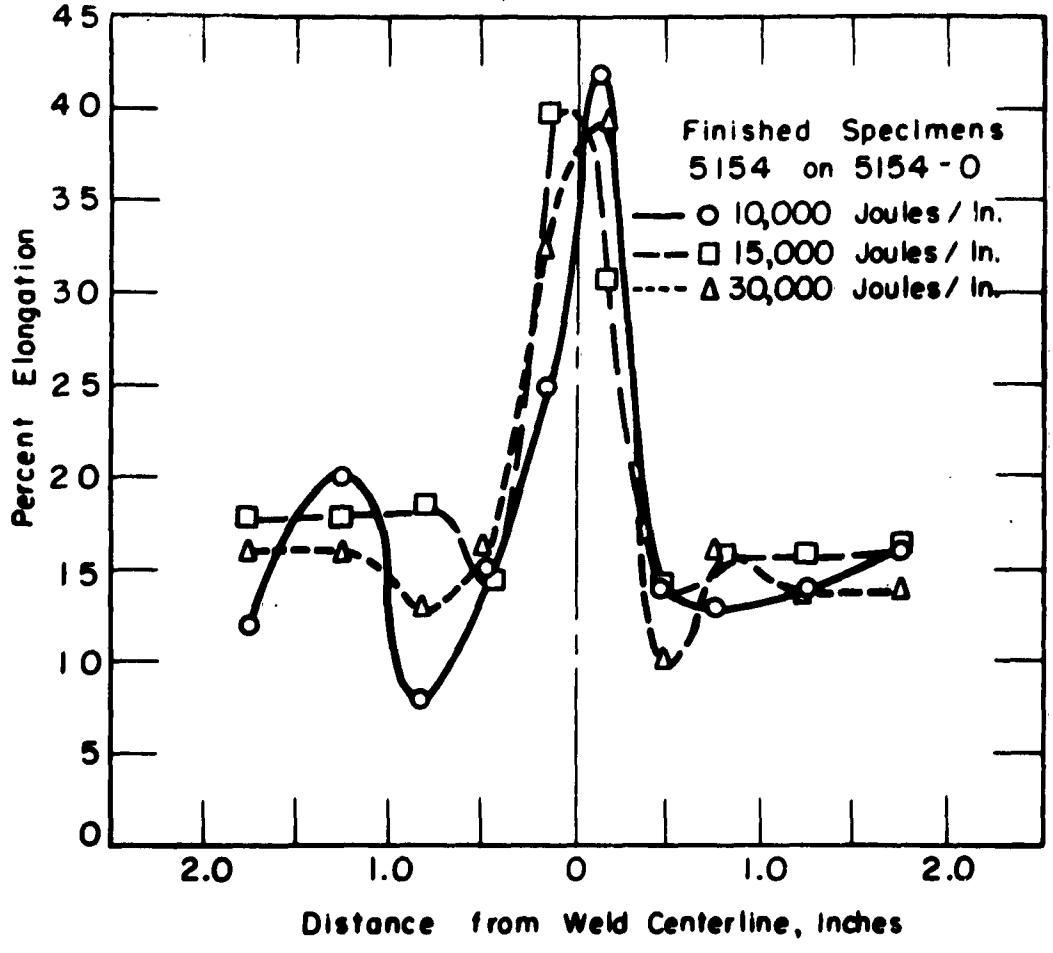
THE EFFECT OF ARC ENERGY INPUT ON CENTERLINE HARDNESS IN THE WELD METAL

FIGURE 7



TYPICAL TRANSVERSE WELD HARDNESS DISTRIBUTIONS IN 5000 SERIES ALUMINUM ALLOYS

FIGURE 8



STRAIN DISTRIBUTIONS OBSERVED IN TRANSVERSE TENSILE TESTING ANNEALED AND WELDED 5154 ALUMINUM ALLOY

FIGURE 9

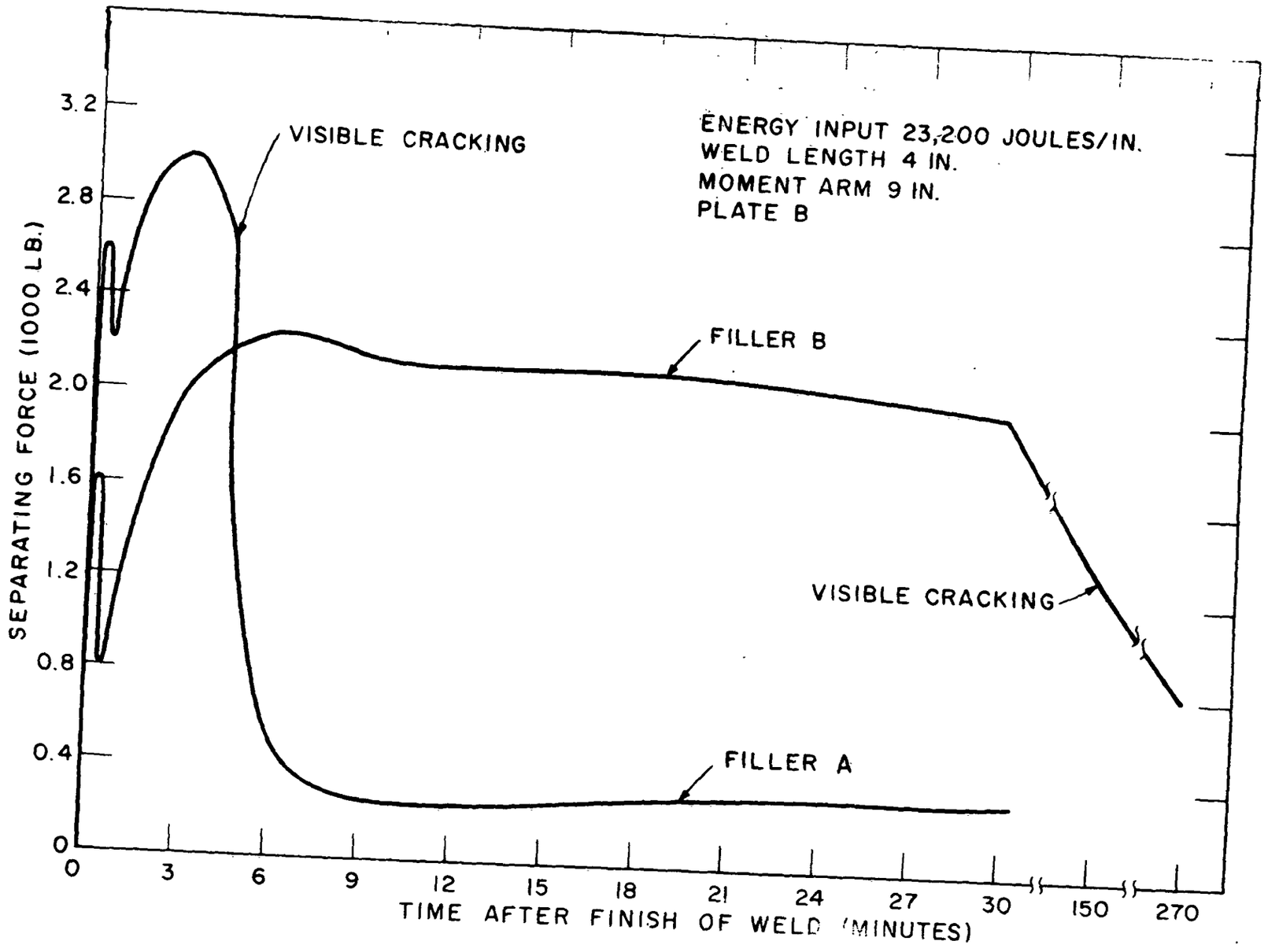
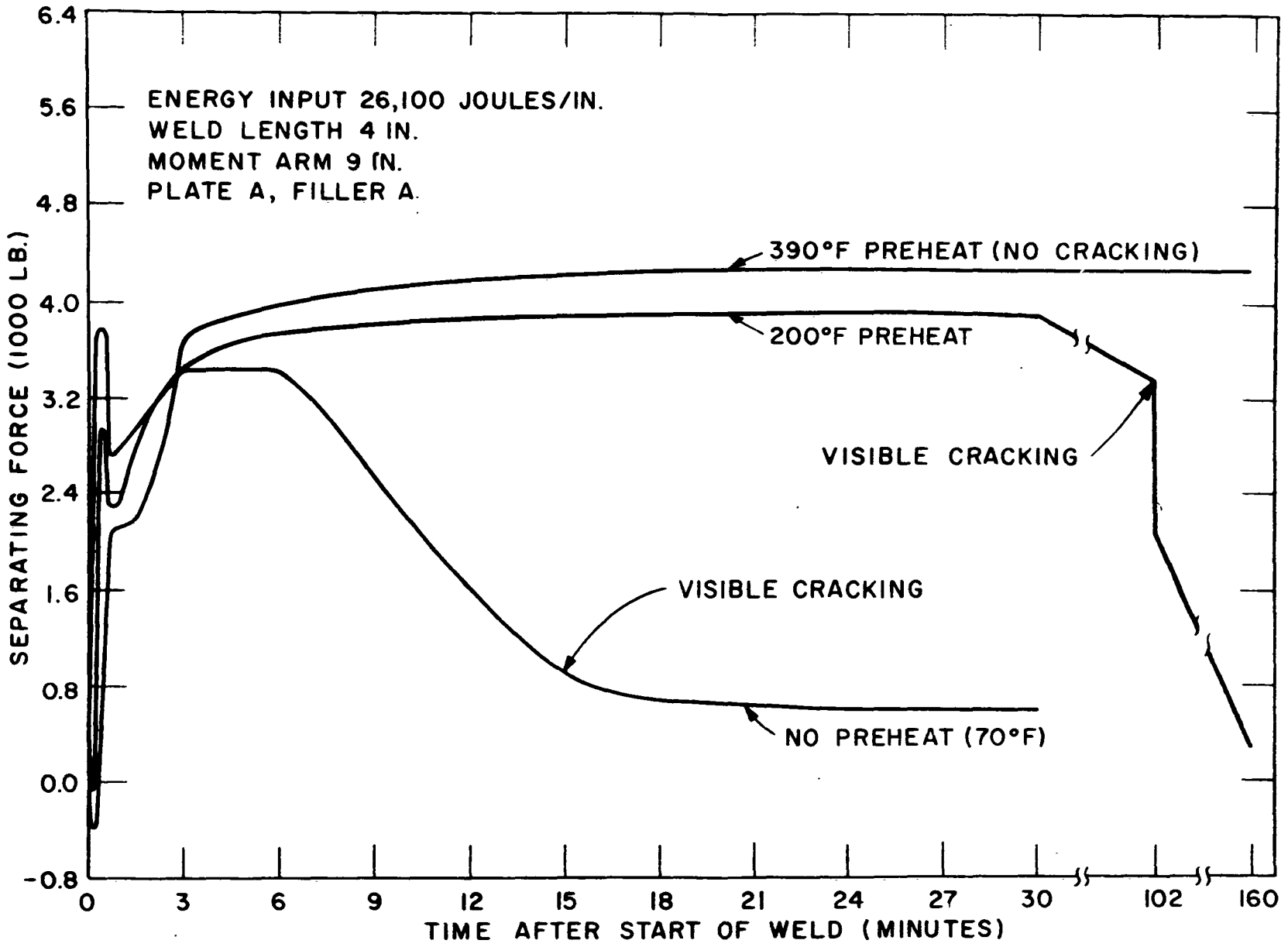


FIGURE 10

EFFECT OF FILLER HARDNESS ON TIME DELAY IN WELD CRACKING
FILLER A CONTAINS 0.30% CARBON AND FILLER B, 0.08% CARBON; USED IN WELDING 0.30% CARBON, MANGANESE - MOLYBDENUM STEEL.



EFFECT OF PREHEAT ON THE INCIDENCE AND TIME DELAY OF CRACKING
FILLER A CONTAINS 0.30% CARBON AND FILLER B, 0.08%
CARBON: USED IN WELDING 0.30% CARBON, MANGANESE-MOLYBDENUM STEEL

FIGURE 11

FUSION WELDING HIGH-STRENGTH TITANIUM SHEET

by

Carl E. Hartbower*

ABSTRACT

The welded strength, ductility and toughness of three DOD Titanium Alloy Sheet Rolling Program Materials in various conditions of heat treatment are compared using low-energy inert-gas-shielded consumable-electrode (MIG) welds made with Watertown Arsenal Laboratories' procedure and high-energy inert-gas-shielded non-consumable-electrode (TIG) welds made with more-or-less typical industrial procedure. The principal difference between the Watertown Arsenal Laboratories' procedure and industrial procedure is that Watertown Arsenal Laboratories uses as low an energy input and as high an inert-gas flow rate as is consistent with good practice; whereas, industry uses relatively high energy input and low gas-flow rates.

Welding in the solution-treated condition and then aging after welding gave good tensile properties in all three composition types. The tensile properties were competitive (on a strength/weight basis) with steel at 240,000 to 280,000 psi yield strength regardless of the welding process used. Tensile ductility of all welds in the aged condition was low, with very little uniform elongation. However, fracture toughness did not correlate with tensile elongation. The low-energy MIG procedure gave consistently satisfactory fracture toughness in the welded-and-aged condition in all three alloys; whereas, TIG resulted in a severe embrittlement in the welded-and-aged Ti-2.5Al-16V alloy. In the high-strength welded-and-aged condition, G_c values of 800 to 1800 in-lb/in^2 were obtained with the MIG procedure.

- - - - - - - - - -

*Mr. Hartbower is Chief of the Metals Joining Branch, Watertown Arsenal Laboratories.

- - - - - - - - - -

The opinions or assertions contained herein are the private ones of the authors and are not necessarily to be construed as official or reflecting the views of the Department of the Army.

- - - - - - - - - -

This is a condensed version of a paper entitled "Low-Energy Fusion Welding of Titanium Alloys" by C.E. Hartbower; M.M. D'Andrea, Jr.; and G.M. Orner, scheduled for publication in The WELDING JOURNAL in 1961.

INTRODUCTION

An earlier study* of the feasibility of welded titanium sheet for missile applications found that (1) as-welded tensile properties were generally satisfactory with the exception of low tensile ductility in some of the materials investigated; (2) 100% tensile joint efficiencies were consistently obtained in welding mill-annealed sheet alloys and (3) notch sensitivity appeared to be a problem, particularly after welding, with marked variations in notch sensitivity from heat-to-heat in a given composition type.

The overall objective of this investigation was to determine the welded strength, ductility and toughness of three Department of Defense Titanium Alloy Sheet Rolling Program Materials in various conditions of heat treatment using both low-energy inert-gas-shielded consumable electrode (MIG) and high-energy inert-gas-shielded non-consumable electrode (TIG) processes.

About two years ago, it was observed that the procedures generally used by industry in welding titanium sheet are radically different from those used by the Metals Joining Branch of Watertown Arsenal Laboratories in three respects:

(1) First, Watertown Arsenal Laboratories uses the consumable electrode process (MIG) wherever possible; whereas, industry tends to use the tungsten-inert-gas process (TIG) even for plate 1/4 to 1/2 inch thick.

(2) Second, Watertown Arsenal Laboratories uses as low an energy input as possible; whereas, industry with the TIG process at low travel speeds usually uses relatively high energy inputs.

(3) And third, Watertown Arsenal Laboratories uses a high inert-gas flow-rate (100 cfh or higher of Helium + Argon mixture); whereas, industry generally uses about 20 cfh of argon.

- - - - - - - - - -

*Reference: "Feasibility of Titanium for Welded Missiles" by C.E. Hartbower, G.M. Orner and D.M. Daley, The WELDING JOURNAL, Vol. 38(9), p. 345-s, September 1959 (WAL TR 401/301, August 1958).

When it was first realized that industrial practice was generally different from that of the Watertown Arsenal Laboratories, the matter was discussed with people in industry in an attempt to find out why there are such marked procedural differences. The concensus seemed to be that most industrial applications involved manual welding and, therefore, practical considerations dictate TIG with relatively slow arc-travel speeds. The low gas-flow stem from economical considerations and a desire to avoid turbulent gas flow.

The welding conditions used by Watertown Arsenal Laboratories had evolved from several years of titanium welding research. The principal argument was that low-energy welding with fast arc-travel speeds and high gas-flow rates assure less general heating of the weldment, faster cooling rates, and shorter times at elevated temperature - all of which are necessary conditions to minimize air contamination when welding titanium in open air (Watertown Arsenal Laboratories has never used a chamber).

Thus, a secondary objective was to compare the mechanical properties and chemistry of low energy MIG welds made with Watertown Arsenal Laboratories procedure, with high-energy TIG welds made with more-or-less typical industrial procedure.

The sheet alloys investigated were taken from the DOD Titanium Alloy Sheet Rolling Program* and consisted of 1/8-inch thick Ti-6Al-4V, Ti-2.5Al-16V and Ti-4Al-3Mo-1V sheet. Both unalloyed and matching filler wire were used in welding Ti-6Al-4V; only unalloyed wire was used in welding Ti-2.5Al-16V and Ti-4Al-3Mo-1V. (A detailed listing of heat numbers and chemistry may be found in Table VIII).

EXPERIMENTAL PROCEDURES

Welding

Table I summarizes the conditions used for MIG and TIG welding. The conditions for TIG welding were selected to be representative of those generally used by industry and the MIG welding conditions are those recommended by the Metals Joining Branch of the Watertown Arsenal Laboratories. Basically, the difference between the two procedures was that the low-energy MIG welding was done in one pass at a travel speed of 75 in/min (in 1/8-in. thick sheet) with a high gas-flow rate of

---

*Reference: DMIC Report 46 H dated 1 June 1960.

150 cfh (He+A) issuing from the torch; whereas, the high-energy TIG welding was done in two passes at a travel speed of only 10 in./min and a gas-flow rate of only 20 cfh (Argon).

Preparatory to welding, the joint edges for most of the weldments were cold degreased and then wire brushed. Late in the investigation, because of excessive porosity, there was a change in procedure; viz., after cold degreasing and wire brushing, the edges were pickled just prior to welding.

Table II presents the various heat treatments and welding-heat treatment sequences investigated. Note that in addition to welding the materials in the solution-treated condition and then testing in the as-welded condition, the materials were also aged before and after welding.

Testing

Various mechanical tests were conducted to provide a basis for comparing the three composition types, the various conditions of heat treatment, and the MIG and TIG welding procedures. Tensile data were obtained with the ASTM standard rectangular tension test specimen E8-57T. Welds were tested both longitudinal and transverse to tensile loading. The longitudinally welded specimens included both heat-affected base metal and deposited weld metal (the weld deposits were approximately 3/8-in. wide at the face; the tensile specimens were 1/2-in. wide). To determine the distribution of plastic flow in and around the welds and fractures, a photo-grid (0.05-in. spacing) was used on the tensile-specimen surfaces. Tests were made with weld reinforcement both on and machined off.

A variety of fracture-toughness tests were conducted. Among the tests that are generally accepted as meaningful is the Irwin-Kies G_c test. G_c is generally determined by means of a centrally notched tensile specimen, with the notch mechanically sharpened at the ends. In this investigation the G_c tensile specimen contained a transverse weld with the notch centered on the weld. In addition to the G_c tensile test for fracture toughness, V-notch Charpy tests were conducted. It has been demonstrated that the V-notch Charpy impact test using a single-thickness edge-notched specimen may be used for testing sheet in thicknesses down to about 40 mils*. One of the principal advantages of the Charpy test over the G_c test is that the Charpy can be conducted readily over a range

* - - - - - - - - -
Reference: G.M. Orner and C.E. Hartbower "An Engineering Evaluation of Notch Sensitivity in High Strength Sheet Materials" WAL Report TR 405.1/1 dated March 1960; also a condensed version in The WELDING JOURNAL, Vol. 39(4), p.147-s (April 1960).

of testing temperatures at both slow and impact rates of loading. The principal disadvantage of the Charpy when tested with a standard 10-mil radius V-notch is that fictitiously high energy values are sometimes obtained in brittle materials. In fact, when using the standard Charpy V-notch and fracture is brittle, there is an elastic-energy loss that in some instances is so large percentagewise that it overshadows all other sources of energy absorption combined*. Charpy specimens with natural cracks have been tested in some weld-base metal combinations to eliminate the problem of excess elastic-strain energy. Moreover, by separating the energy to initiate cracking from the energy to propagate cracking, it is possible to assess fracture toughness in terms of energy per unit of fracture-surface area (in-lb/in^2). Tests of precracked Charpy specimens provide data that are directly proportional to G_c data obtained from center-notched tensile tests.

EXPERIMENTAL RESULTS

Tensile tests, Ti-6Al-4V

Tensile data were obtained using the ASTM standard rectangular tension test specimen E8-57T. Table III presents the data for Ti-6Al-4V transversely welded by the MIG and TIG processes using both unalloyed and matching filler wire. Note at the top of the table, as a basis of comparison, data are included for unwelded sheet.

With mill-annealed sheet in the as-welded condition, failure always occurred in the base metal beyond the weld heat-affected zone (HAZ). As would be expected, there was little or no difference between the solutionized-and-welded and the solutionized-aged-and-welded conditions. Aging after welding, on the other hand, produced a decided strength advantage. Note that the tensile joint efficiencies obtained with unalloyed and matching (6Al-4V) filler wire were not significantly different. Particularly noteworthy is the slight difference between MIG and TIG test results. In general, the tensile elongation values as measured over a two-inch gage length were poor for both the MIG and TIG welded with both unalloyed and matching filler wire.

- - - - - - - - - - -

*Reference: Sagamore Conference, 5th Session Paper "DYNAMIC NOTCHED SCREENING TESTS" discussion by Orner and Hartbower.

It should be noted in connection with Table III and the following tables, that 140,000 psi yield strength in titanium is competitive with steel at approximately 240,000 psi on a strength/weight basis.

Table IV presents the data for Ti-6Al-4V using longitudinally welded test specimens. With the weld oriented parallel to the direction of tensile (uniaxial) loading, weld metal, HAZ and base metal are forced to strain the same; whereas, in a transversely welded test specimen, practically all of the strain can occur in the weld-joint component having the lowest flow strength. Thus, in the longitudinally welded tensile specimens, both deposited weld metal and heat-affected base metal are under test (the deposits were approximately 3/8-in. wide at the weld face, in a 1/2-in. wide test section).

The results obtained with the longitudinally and transversely welded tensiles were very nearly the same - with two exceptions; viz., (1) the TIG welds with unalloyed filler had substantially lower yield strengths than any other conditions tested, and (2) the tensile elongation values were substantially lower in the transversely welded tests.

In the case of the transversely welded tensiles (Table III), it will be noted that most of the failures occurred at the weld fusion line. Fusion-line porosity was evident in the fracture surfaces of all such specimens. In the case of the MIG welds, the porosity (as noted by X-ray) consistently occurred at the fusion line; whereas, the TIG welds were characterized by general porosity, with fine linear porosity associated with the root gap location. The fact that both the MIG and the TIG procedures, as widely different as they were, were attended by porosity, suggested that the problem was the result of some procedural variable common to both processes.

In the final stages of the WAL's investigation, an attempt was made to eliminate porosity by pickling after cold degreasing. This change in procedure was high successful in elininating porosity from both the MIG and TIG welds. It is very interesting that although the fracture location changed from the fusion line (with porosity) to the weld metal (see data columns with asterisks in Table III), there was only a slight improvement in tensile ductility when porosity was eliminated.

In September 1959, the Jet Propulsion Laboratory reported the use of Ti-6Al-4V in the 4th stage of a successful lunar-probe flight. In the R&D preceeding fabrication of the actual motor case, JPL encountered weld porosity in spite of scrupulous cleaning techniques. Five motor cases with known areas of weld porosity were hydrostatically tested to rupture. In no case could fracture be associated with the porosity. Several other cases which contained weld porosity (rejectable by radiographic standards) were proof tested and statically fired successfully*.

Because the tensile elongation measured over a 2-in. gage length was so low in the transversely welded tensile tests, a grid was photographically reproduced on a number of tensile specimens to determine the distribution of plastic deformation in and around the weld and fracture. Figure 1 shows the distribution of strain in mill-annealed Ti-6Al-4V sheet containing a transverse joint in the as-welded condition. The location of the weld is indicated by a rectangular block on the abscissa; distance is measured from the location of fracture. Note the large values of elongation measured over a very short gage length (grid spacing 0.05 in.) in the vicinity of the fracture (approximately 50% as compared with 11% elongation over a 2-in. gage length). Figure 2 shows a very different situation when the material is aged either before or after welding. Practically all of the plastic deformation occurred in the weld joint, with little or no uniform elongation. It will be shown later that these low values of tensile elongation do not correlate with notch toughness. With the weld longitudinal (Figure 3), there was generally more uniform elongation; however, with matching filler wire there was a definite trend toward less ductility.

Tensile tests, 4Al-3Mo-1V

Table V presents the data for Ti-4Al-3Mo-1V transversely and longitudinally welded by the MIG and TIG processes using unalloyed filler wire. Note that the tensile properties were approximately the same as those obtained with welds in Ti-6Al-4V sheet. One difference between Ti-6Al-4V and Ti-4Al-3Mo-1V is noteworthy; viz., that the Ti-4Al-3Mo-1V gave approximately the same strength regardless of whether the material was aged before or after welding. As in the case of Ti-6Al-4V, note that the MIG and TIG processes resulted in approximately the same strengths.

* Reference: JPL Report 30-8 "Welded Titanium Case for Space-Probe Rocket Motor" by Brothers, Boundy, Martens and Jaffe, September 1959.

Tensile tests, Ti-2.5Al-16V

Table VI presents the data for Ti-2.5Al-16V transversely and longitudinally welded by the MIG and TIG processes using unalloyed filler wire. Note that if useful strengths are to be realized, the weldments must be aged after welding. A comparison between the unwelded tensile results in the solution-treated condition and the solutionized-and-welded and the solutionized-aged-and-welded conditions shows that welding in effect was a solutionizing treatment. Note that again the TIG and MIG processes developed comparable strengths, and that in the aged condition, the welds are competitive with steel at approximately 280,000 psi yield strength.

Fracture toughness tests

Tensile tests indicated little or no difference between the MIG and TIG welding procedures. The next consideration was that of fracture toughness. Among the tests that are generally accepted as meaningful is the Irwin-Kies G_c test. In this investigation a 6-inch wide G_c tensile specimen was notched in the deposited weld metal. Ink staining was used to define the length of the crack prior to fast fracture. Because of the narrowness of the weld joint, the propagating fracture was free to run either in the weld metal or in the HAZ.

It is interesting to note, as a basis of comparison, that DMIC report 118 dated 12 October 1959, discussing materials for construction of motor cases for the Polaris missile, stated that a G_c value of 1000 has been set as a tentative minimum for rocket case base materials. Weld joints in AMS 6434 steel at a yield strength of approximately 200,000 psi were observed to have G_c values in the range of 500 to 800.

Table VII presents the G_c tensile data for the three materials investigated. Note that with the exception of the aged-and-welded 4Al-3Mo-1V and the TIG welded-and-aged 2.5Al-16V, the G_c values were very promising (as compared with the G_c values usually obtained in steel at strength levels in excess of 220,000 psi yield). Note that in three weld-base metal combinations, the MIG welds were decidedly superior to the TIG welds; in two combinations, the MIG and TIG welds were approximately equivalent; and in the two remaining combinations investigated, the TIG welds were decidedly superior to the MIG welds.

Porosity appears to have had a more definite effect on fracture toughness than on tensile properties. For example, MIG-welded 6Al-4V in the welded-and-aged condition gave a G_c of 1356 in-lb/in^2 with porosity; without porosity (chemically cleaned preparatory to welding) the G_c was 1822 in-lb/in^2. Likewise, in the case of the TIG-welded 6Al-4V in the annealed-and-welded condition, with porosity the G_c was 763 in-lb/in^2 and without porosity the G_c was 1341 in-lb/in^2. The loss of toughness was not so great in the case of TIG-welded 6Al-4V in the annealed-and-welded condition when matching (6Al-4V) filler wire was used; the G_c value dropped from 820 with no porosity (pickled) to 706 in-lb/in^2 with general porosity. There was one instance of pickled welds tested in duplicate where one weld had very small porosity along the fusion line and the other was free of porosity; the weld with porosity had a G_c of 762 in-lb/in^2 and the porosity-free weld had a G_c of 1020 in-lb/in^2. Lacking complete chemical analysis of the welds made with and without pickling, it is quite possible that the difference in fracture toughness was due to higher interstitial content in the welds which were not pickled rather than porosity per se. Whatever the cause, the G_c data available from welds made with and without pickling of the joint edges preparatory to welding indicated an increase of 100 to 500 in-lb/in^2 as a result of the pickling operation.

It was demonstrated in earlier work that the V-notch Charpy impact test, using a single-thickness edge-notched specimen, may be used for testing sheet in thicknesses down to about 40 mils. The experimental work upon which this observation is based has been published as a WAL Report TR 405.1/1 dated March 1960, entitled "An Engineering Evaluation of Notch Sensitivity in High-Strength Sheet Materials" and in a condensed version published in The WELDING JOURNAL, Vol. 39(4), p.147-s (April 1960). Since WAL Report 405.1/1 was prepared, additional development work has been done which indicates a direct proportionality between notched-tensile G_c values and precracked V-notch Charpy impact* in a wide variety of strengths and composition types.

Table VII presents fracture toughness data obtained from precracked V-notch Charpy specimens for comparison with G_c tensile results. Charpy fracture toughness is expressed in terms of energy absorbed per unit of fracture-surface area (W/A), in-lb/in^2).

* - - - - - - - - - -

Reference: ORNER and HARTBOWER, Metals Joining Branch, 12th, 13th and 14th Progress Reports on Notch Sensitivity in High Strength Sheet, dated 16 May, 30 September and 10 November 1960.

Note that the Charpy results confirmed the trends indicated by the G_c tests with regard to the relative toughness of MIG and TIG welds.

Figure 4 presents precracked Charpy transition curves for Ti-6Al-4V welded-and-aged with matching and unalloyed fillers. Note that the results are consistent with G_c in that they show MIG to be superior to TIG with unalloyed filler but not with matching filler. In examining this figure and the following figures, it should be recalled that a precracked V-notch Charpy value of 2 ft-lb is equivalent to a G_c of approximately 900 in-lb/in^2.

Likewise, precracked V-notch Charpy tests of Ti-4Al-3Mo-1V in the weld-and-aged condition correlated well with G_c tensile results. Figure 5 indicates that MIG and TIG welds in Ti-4Al-3Mo-1V heat M8012 in the aged condition are about equivalent; in fact TIG appears slightly better. However, a second heat of 4Al-3Mo-1V again indicated the MIG to be decidedly superiod to the TIG procedure.

Figure 6 which presents the precracked Charpy transition curves for Ti-2.5Al-16V weld-and-aged using both MIG and TIG shows the MIG weld to be decidedly superior to the TIG weld. Again, the results correlated well with G_c (see Table VII).

Chemistry, Dilution and Grain Growth

It was anticipated that the TIG welds, because of the slow arc-travel speed, relatively slow cooling rates and general heating, would have higher interstitial content than the MIG welds. Chemical analysis of randomly selected MIG and TIG weld deposits did not substantiate this (Table VIII). In some instances the TIG welds actually appeared to have lower interstitial content; however, the differences between MIG and TIG were neither marked nor consistent. One fact was clear; viz., that the TIG welds because of greater base-metal melting, had substantially higher substitutional alloy content than the MIG welds. This would be expected to have an effect on mechanical properties, particularly in the case of the Ti-2.5Al-16V alloy. (Alpha-beta weld deposits generally have excellent toughness if the substitutional alloy content is held in the range of 1 to 4 percent).

Another marked difference between the MIG and TIG welds as produced in this investigation is in the grain size of the weld deposits. The grain size of the TIG welds was very much larger than that of the MIG welds (Figure 7). This would be expected to result in greater toughness in the MIG welds.

SUMMARY AND CONCLUSIONS

The welded strength, ductility and toughness of three DOD Titanium Alloy Sheet Rolling Program Materials are compared using low-energy inert-gas-shielded consumable-electrode (MIG) welds made with Watertown Arsenal Laboratories' procedure and high-energy inert-gas-shielded non-consumable-electrode (TIG) welds made with more-or-less typical industrial procedure. The principal difference between the WAL and industrial procedures is that Watertown Arsenal Laboratories uses as low an energy input and as high an inert-gas flow rate as is consistent with good practice; whereas, industry uses relatively high energy input and low gas-flow rates.

The three sheet alloys investigated were Ti-6Al-4V, Ti-4Al-3Mo-1V and Ti-2.5Al-16V in each of the three conditions of heat treatment; viz., (1) solution-treated, welded and tested, (2) solution-treated, aged, welded and tested and (3) solution-treated, welded, aged and tested. In addition to the above conditions, Ti-6Al-4V was also tested in the annealed-and-welded condition.

The mechanical tests used for evaluating the weldability of the three processes were (1) the tensile test (unnotched), (2) tensile ductility as measured in a photogrid at 0.05-in. spacing, (3) the centrally notched G_c tensile test and (4) the edge-notched Charpy impact test. Chemistry of weld deposits and metallography were also employed in comparing the two welding processes.

The most noteworthy observations were as follows:

(1) The tensile strength of all three alloys was very good when aged after welding. All three alloys had yield strengths in the range of 140,000 to 160,000 psi which is competitive (on a strength/weight basis) with steel at 240,000 to 280,000 psi regardless of the welding process used. There was, in fact, very little difference, strength-wise, between welds made with the MIG and TIG procedures.

(2) The 2.5Al-16V alloy was completely unsatisfactory, strengthwise, unless aged after welding. When solution-treated, welded and tested, and when solution-treated, aged, welded and tested (i.e., tested in the as-welded condition), the 2.5Al-16V alloy had yield strengths of less than 90,000 psi. Apparently, welding was highly effective in solutionizing this alloy.

(3) The tensile ductility of all welds in the aged high-strength condition was low, with very little uniform elongation; Photogrids showed the deformation to occur as unstable plastic flow. Porosity, at first suspected of causing the low ductility proved to have only a slight effect in lowering the elongation values.

(4) Fracture toughness did not correlate with tensile elongation. In several instances, alloys with only 3 to 4 percent tensile elongation had excellent fracture toughness.

(5) There were marked heat-to-heat variations in "weldability". In other words, there were marked variations in the fracture toughness of welds deposited in different heats of a given composition type, even with a given electrode and welding process.

(6) Because of heat-to-heat variations, comparison between the MIG and TIG procedures was not conclusive. However, the trend of results favor the low-energy high-gas-flow MIG procedure. In general, the fracture toughness of the MIG welds was higher than that of the TIG welds. The exceptions where TIG gave higher values than MIG generally occurred in welds that were adequately tough (in the neighborhood of 1000 G_c) with either process.

It is concluded from this study that the titanium sheet alloys investigated offer a highly attractive combination of strength and toughness for rocket and missile structures that can be aged after welding. Because of the marked variations in fracture toughness that occur from heat to heat and from one welding process to another, it is essential that a meaningful test for fracture toughness be employed. The G_c notched tensile test or the precracked V-notched Charpy test are recommended. The latter is particularly useful as a screening test because (1) the test permits rapid evaluation of a large number of metallurgical variables and testing conditions with a minimum expenditure of time, money and materials; (2) the test is easily and economically conducted over a wide range of testing temperatures; and (3) the test is sufficiently sensitive to reveal changes in specimen brittleness as influenced by composition and heat treatment.

TABLE I

TITANIUM WELDING CONDITIONS

	INERT - GAS - SHIELDED	
	TUNGSTEN ARC (TIG)	CONSUM. ELECTRODE (MIG)
SHEET THICKNESS, IN.	0.125	0.125
JOINT DESIGN*	SQ. BUTT	SQ. BUTT
ROOT OPENING, IN.	0	0.032
FILLER DIAM., IN.	1/32	1/32
NUMBER OF PASSES	2	1
AMPERES**	245 S.P.	250 R.P.
VOLTS	14	36
ARC TRAVEL, IPM	10	75
ENERGY INPUT, JOULES/IN.	20,800	7,200
PRIMARY GAS. CFH	20A	125 He + 25A
TRAILING GAS, CFH	50A	60A
NOZZLE I.D., IN.	1.0	1.0
W-ELECTRODE, IN.	3/32	-
ARC-LENGTH, IN.	0.095	-
CONTACT-TUBE HGT., IN.	-	1/2

*JOINT PREPARATION: BLANCHARD-GROUND EDGES, COLD DEGREASED, AND WIRE BRUSHED. JOINT BACKED WITH GROOVED COPPER BAR.

**POWER SOURCE: DC RECTIFIER (500 AMP CAPACITY) WITH DROOPING CHARACTERISTIC.

19-066-771/ORD-60

TABLE II

WELDING - HEAT TREATMENT SEQUENCE

6AL-4V	MILL ANNEALED (AS REC'D)-WELDED-TESTED
	SOLUTION TREATED-WELDED-TESTED
	SOLUTION TREATED-AGED-WELDED-TESTED
	SOLUTION TREATED-WELDED-AGED-TESTED
4AL-3Mo-1V and 2.5AL-16V	SOLUTION TREATED(AS REC'D)-WELDED-TESTED
	SOLUTION TREATED-AGED-WELDED-TESTED
	SOLUTION TREATED-WELDED-AGED-TESTED

TITANIUM HEAT TREATMENTS
(PERFORMED AT WATERTOWN ARSENAL)

6AL-4V	SOLUTION TREATED AT 1750°F(±10°) FOR 15 MIN.-W.Q.
	AGED AT 900°F(±5°) FOR 24 HOURS-A.C.
4AL-3Mo-1V and 2.5AL-16V	AGED AT 925°F(±10°) FOR 24 HOURS-A.C.

19-066-766/ORD-60

TABLE III

6Al-4V TITANIUM TRANSVERSELY WELDED

CONDITION	REIN-FORCE-MENT	FRACTURE LOCATION	YIELD 0.2% OFFSET	ULTIMATE STRENGTH	ELONG. % in 2"	R.A. %	JOINT EFFICIENCY YLD	JOINT EFFICIENCY ULT
UNWELDED BASE MATERIAL								
Mill Annealed		Unwelded	136,000	137,000	12	37		
Solution Treated		Unwelded	139,000	166,000	7	21		
Solution Treated-Aged		Unwelded	161,000	173,000	2	7		
MIG - UNALLOYED FILLER								
Mill Annealed-Welded	Off	BM	129,000	130,000	11	34	95	95
Sol.Tr.-Welded	Off	FL	131,000	141,000	2	19	94	85
Sol.Tr.-Aged-Welded	Off	FL	135,000	139,000	2	13	84	80
Sol.Tr.-Welded-Aged	Off	FL	141,000	145,000	3	14	88	84
	Off	WM*	138,000	144,000	3	20	86	83
TIG - UNALLOYED FILLER								
Mill Annealed-Welded	On	BM	128,000	136,000	8	32	94	99
Sol.Tr.-Welded-Aged	On	FL-HAZ	149,000	159,000	2	11	92	92
	Off	WM*	144,000	150,000	3	17	89	87

TABLE III (Continued)

CONDITION	REIN-FORCE-MENT	FRACTURE LOCATION	YIELD 0.2% OFFSET	ULTIMATE STRENGTH	ELONG. % in 2"	R.A. %	JOINT EFFICIENCY YLD	JOINT EFFICIENCY ULT
MIG - MATCHING FILLER								
Mill Annealed-Welded	Off	BM	135,000	136,000	11	37	99	99
Sol.Tr.-Welded	Off	FL	143,000	157,000	2	9	103	95
Sol.Tr.-Aged-Welded	Off	FL	147,000	157,000	2	11	91	91
Sol.Tr.-Welded-Aged	Off	FL	158,000	161,000	2	12	98	93
	Off	FL-WM*	156,000	165,000	3	12	97	95
TIG - MATCHING FILLER								
Mill Annealed-Welded	On	BM	129,000	132,000	8	37	95	96
Sol.Tr.-Welded-Aged	On	FL	145,000	159,000	2	12	90	92
	Off	WM*	143,000	154,000	4	18	89	89

- - - - - - - - - -

*X-ray clear - pickled before welding to eliminate porosity.

TABLE IV

6Al-4V TITANIUM LONGITUDINALLY WELDED

CONDITION	REIN-FORCE-MENT	YIELD 0.2% OFFSET	ULTIMATE STRENGTH	ELONG. % IN 2"	R.A. %	JOINT EFFICIENCY YLD	JOINT EFFICIENCY ULT
UNWELDED BASE MATERIAL							
MILL ANNEALED	UNWELDED	136,000	137,000	12	37		
SOLUTION TREATED	UNWELDED	139,000	166,000	7	21		
SOLUTION TREATED - AGED	UNWELDED	161,000	173,000	2	7		
MIG - UNALLOYED FILLER							
MILL ANNEALED - WELDED	OFF	120,000	132,000	10	32	88	96
SOL.TR.-WELDED	OFF	136,000	152,000	7	25	98	92
SOL.TR.-AGED-WELDED	OFF	131,000	152,000	2	15	81	88
SOL.TR.-WELDED-AGED	OFF	146,000	155,000	7	28	91	90
TIG - UNALLOYED FILLER							
MILL ANNEALED - WELDED	OFF	96,000	122,000	8	30	70	82
SOL.TR.-WELDED-AGED	OFF	128,000	150,000	8	16	80	87
MIG - MATCHING FILLER							
MILL ANNEALED - WELDED	OFF	125,000	148,000	8	15	92	104
SOL.TR.-WELDED	OFF	142,000	157,000	4	9	102	95
SOL.TR.-AGED-WELDED	OFF	142,000	157,000	4	9	88	91
SOL.TR.-WELDED-AGED	OFF	158,000	166,000	4	14	98	96
TIG - MATCHING FILLER							
MILL ANNEALED - WELDED	OFF	126,000	148,000	5	9	93	104
SOL.TR.-WELDED-AGED	OFF	145,000	156,000	9	15	90	90

19-066-756/ORD-60

TABLE V

4AL-3Mo-1V TITANIUM TRANSVERSELY WELDED

CONDITION	REIN-FORCE-MENT	FRACTURE LOCATION	YIELD 0.2% OFFSET	ULTIMATE STRENGTH	ELONG. % IN 2"	R.A. %	JOINT EFFICIENCY YLD	JOINT EFFICIENCY ULT
UNWELDED BASE MATERIAL								
SOLUTION TREATED		UNWELDED	136,000	143,000	16	50		
SOLUTION TREATED - AGED		UNWELDED	174,000	194,000	6	29		
MIG - UNALLOYED FILLER								
SOL.TR.-WELDED	OFF	BM	116,000	141,000	13	55	85	99
SOL.TR.-AGED-WELDED	OFF	FL-WM	149,000	155,000	1	15	86	80
SOL.TR.-WELDED-AGED	OFF	FL-WM	142,000	147,000	2	14	82	76
TIG - UNALLOYED FILLER								
SOL.TR.-WELDED-AGED	OFF	WM	142,000	156,000	2	10	82	80

4AL-3Mo-1V TITANIUM LONGITUDINALLY WELDED

MIG - UNALLOYED FILLER								
SOL.TR.-WELDED	OFF		133,000	156,000	6	20	98	109
SOL.TR.-AGED-WELDED	OFF		135,000	158,000	6	18	78	81
SOL.TR.-WELDED-AGED	OFF		137,000	152,000	4	21	79	78
TIG - UNALLOYED FILLER								
SOL.TR.-WELDED-AGED	OFF		134,000	156,000	6	6	77	80

19-066-754/ORD-60

TABLE VI

2.5Al-16V TITANIUM TRANSVERSELY WELDED

CONDITION	REIN-FORCE-MENT	FRACTURE LOCATION	YIELD 0.2% OFFSET	ULTIMATE STRENGTH	ELONG. % in 2"	R.A. %	JOINT EFFICIENCY YLD	JOINT EFFICIENCY ULT
UNWELDED BASE MATERIAL								
Solution Treated		Unwelded	70,000	109,000	16	28		
Solution Treated-Aged		Unwelded	177,000	187,000	5	14		
MIG - UNALLOYED FILLER								
Sol.Tr.-Welded	Off	FL-HAZ	69,000	105,000	7	31	99	96
Sol.Tr.-Aged-Welded	Off	FL-HAZ	81,000	115,000	1	23	46	62
Sol.Tr.-Welded-Aged	On	FL-HAZ	165,000	173,000	2	4	93	92
	Off	FL-WM	157,000	160,000	2	10	89	86
	On	BM	171,000	180,000	5	23	96	96
TIG - UNALLOYED FILLER								
Sol.Tr.-Welded-Aged	Off	WM	167,000	176,000	2	8	94	94

2.5Al-16V TITANIUM LONGITUDINALLY WELDED

MIG - UNALLOYED FILLER								
Sol.Tr.-Welded	Off		64,000	109,000	9	34	92	100
Sol.Tr.-Aged-Welded	Off		87,000	130,000	4	24	49	70
Sol.Tr.-Welded-Aged	On		147,000	158,000	4	-	83	84
TIG - UNALLOYED FILLER								
Sol.Tr.-Welded-Aged	Off		148,000	163,000	4	8	84	87

TABLE VII

FRACTURE-TOUGHNESS TEST RESULTS
(Transversely welded with unalloyed filler, except as noted)

Sheet Material	Heat Number	Test Condition	G_c (in-lb/in^2) MIG	G_c (in-lb/in^2) TIG	Precracked Charpy (in-lb/in^2) MIG	Precracked Charpy (in-lb/in^2) TIG
Ti-6Al-4V	M4789	annealed-welded	1170(4)	763(3)		
		welded-aged	1822(2)*	1392(2)*	2410(5)*	1605(4)*
Ti-6Al-4V (with 6-4 filler)	M4789	annealed-welded	726(3)	706(2)		
		welded-aged	1020(1)*	1415(2)*	991(5)**	1483(3)*
Ti-4Al-3Mo-1V	M8174	aged-welded	418(5)	434(4)		620(6)
	M8012	welded-aged	865(2)	1010(2)	1113(4)	1186(3)
Ti-2.5Al-16V	T22162	welded-aged	960(4)	316(3)	1190(6)	465(4)

*Data from chemically cleaned (pickled) porosity-free welds.
**Chemically cleaned, with slight porosity.
Data are average values; the number in parenthesis is the number of tests conducted.

TABLE VIII

CHEMICAL ANALYSIS OF SELECTED HEATS AND WELDS
(percent by weight)

	Heat	Carbon	Oxygen	Hydrogen	Nitrogen	Aluminum	Vanadium	Molybdenum
WIRE CHEMISTRY								
1/32" Ti55A	M7935	0.013	0.136	0.0058	0.011			
1/32" Ti-6Al-4V	M2789	0.025	0.140	0.0071	0.018	6.02	3.99	
BASE-METAL CHEMISTRY								
Ti-6Al-4V	M4789	0.022	0.092	0.0042	0.012	5.98	4.03	
	M4790	0.020	0.107	0.0038	0.018	6.05	4.00	
Ti-4Al-3Mo-1V	M8012*	0.022		0.010	0.010	4.1	1.0	3.0
	M8011*			0.007	0.013	4.4	0.9	2.9
	M8168*	0.024	0.109	0.008	0.013	4.1	1.0	2.9
	M8174M*	0.020		0.007	0.011	4.0	0.9	3.1
Ti-2.5Al-16V	T22162*	0.06		0.0069	0.010	3.13	15.62	
	M23372*	0.02		0.0119	0.018	2.51	15.85	

* Producer's Laboratory Report

TABLE VIII (Continued)

WELD-METAL CHEMISTRY**		Carbon	Oxygen	Hydrogen	Nitrogen	Aluminum	Vanadium	Molybdenum
Ti-6Al-4V (unalloyed wire)								
	MIG	0.009(1)	0.123	0.0023	0.016	3.57	2.27	
	TIG	0.014	---	---	0.020	3.31	3.53	
Ti-6Al-4V (matching wire)								
	MIG	0.028	0.124	0.0080	0.031	5.93	3.96	
	TIG	0.018	0.127	0.0047	0.020	5.84(1)	3.95	
Ti-4Al-3Mo-IV (unalloyed wire)								
	MIG	0.014(1)	0.135	0.0049	0.016	2.39	0.55	1.60
	TIG	0.019	0.144	0.0075	0.039	3.51	0.85	2.69
Ti-2.5Al-16V (unalloyed wire)								
	MIG	0.045(1)	0.139	0.0153	0.019	1.67(1)	8.88	
	TIG	0.033	0.151	0.0056	0.021	2.34	14.00	

- - - - - - - - - -

*Producer's Laboratory Report

**Values are the average of two or more determinations, except as designated by (1).

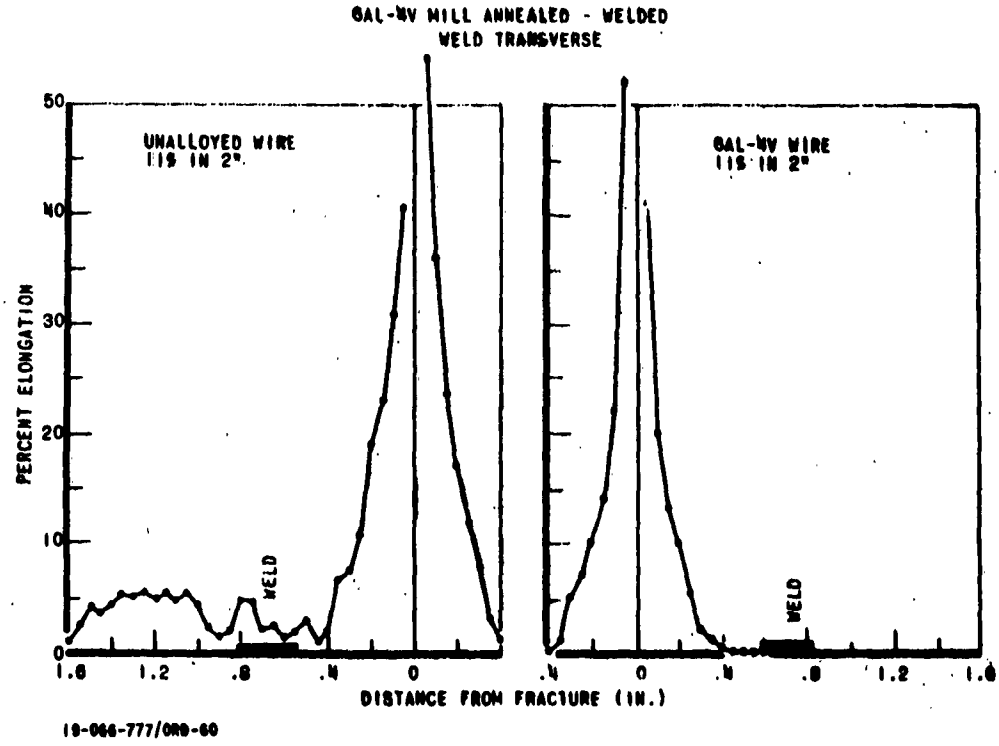


FIGURE 1 - DISTRIBUTION OF STRAIN IN TRANSVERSELY WELDED MILL-ANNEALED 6AL-4V TITANIUM SHEET TENSILE SPECIMENS.

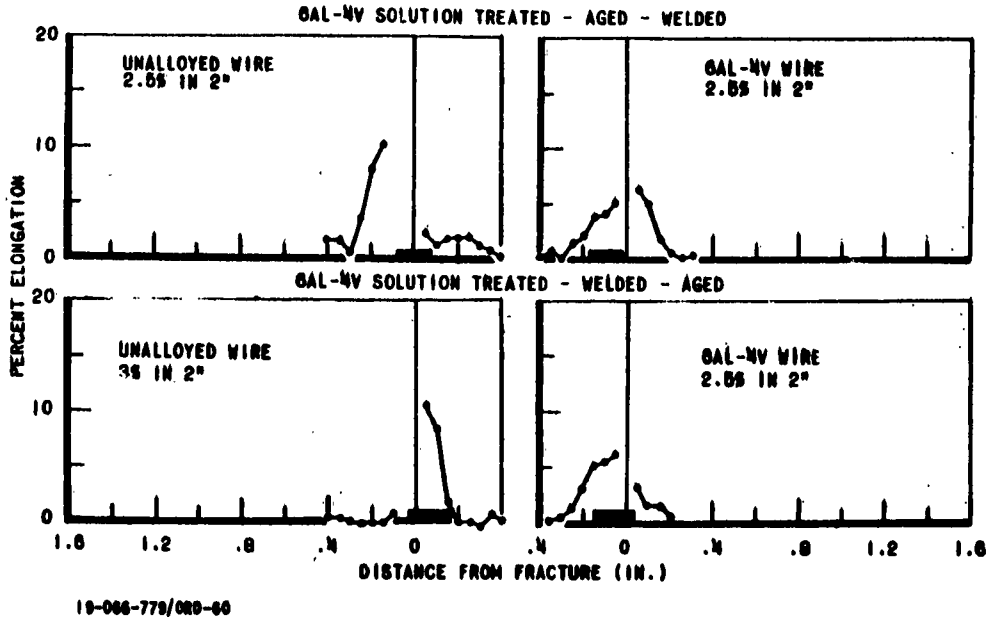


FIGURE 2 - DISTRIBUTION OF STRAIN IN TRANSVERSELY WELDED 6AL-4V TITANIUM SHEET TENSILE SPECIMENS AGED BEFORE AND AFTER WELDING.

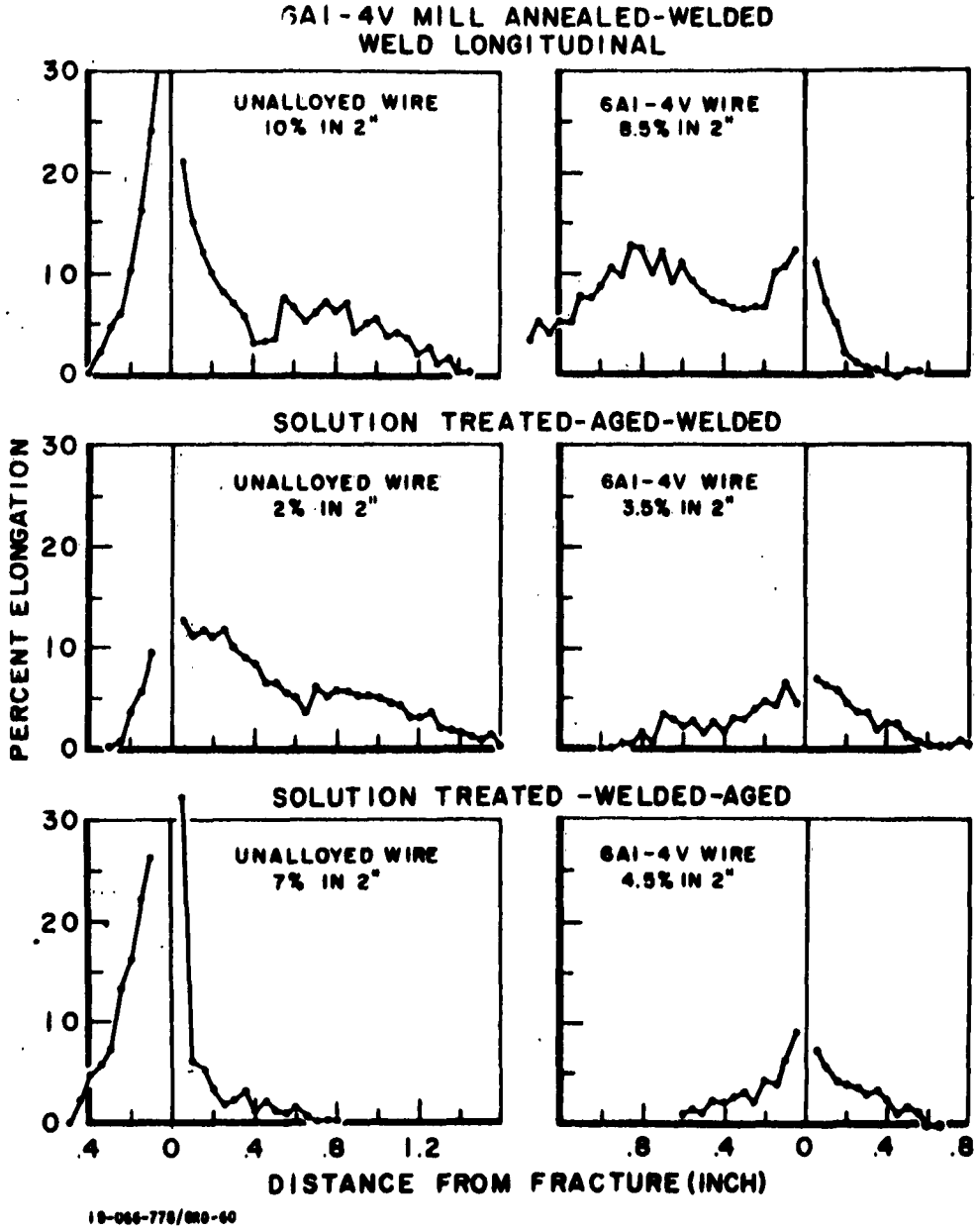


FIGURE 3 - DISTRIBUTION OF STRAIN IN LONGITUDINALLY WELDED 6AL-4V TITANIUM SHEET TENSILE SPECIMENS IN VARIOUS CONDITIONS.

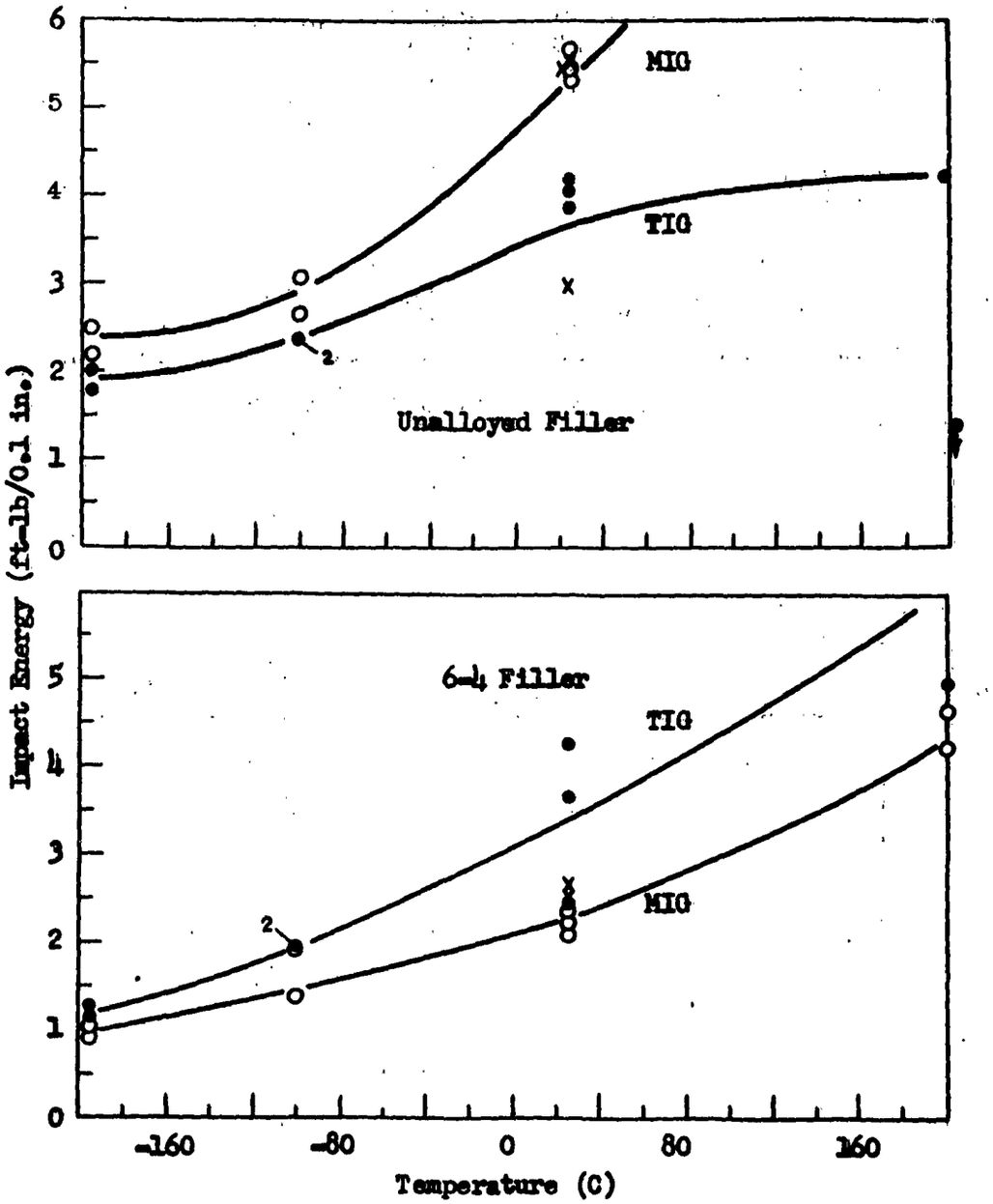


FIGURE 4 - ENERGY-TEMPERATURE TRANSITION CURVES FOR 6AL-4V TITANIUM SHEET IN THE WELDED-AND-AGED CONDITION. The Charpy specimens were precracked by means of a preliminary low-energy blow, or by fatigue(x). An energy value of 2 ft-lb/0.1-in. is equivalent to a G_c of approximately 900 in-lb/in^2. Heat M4789.

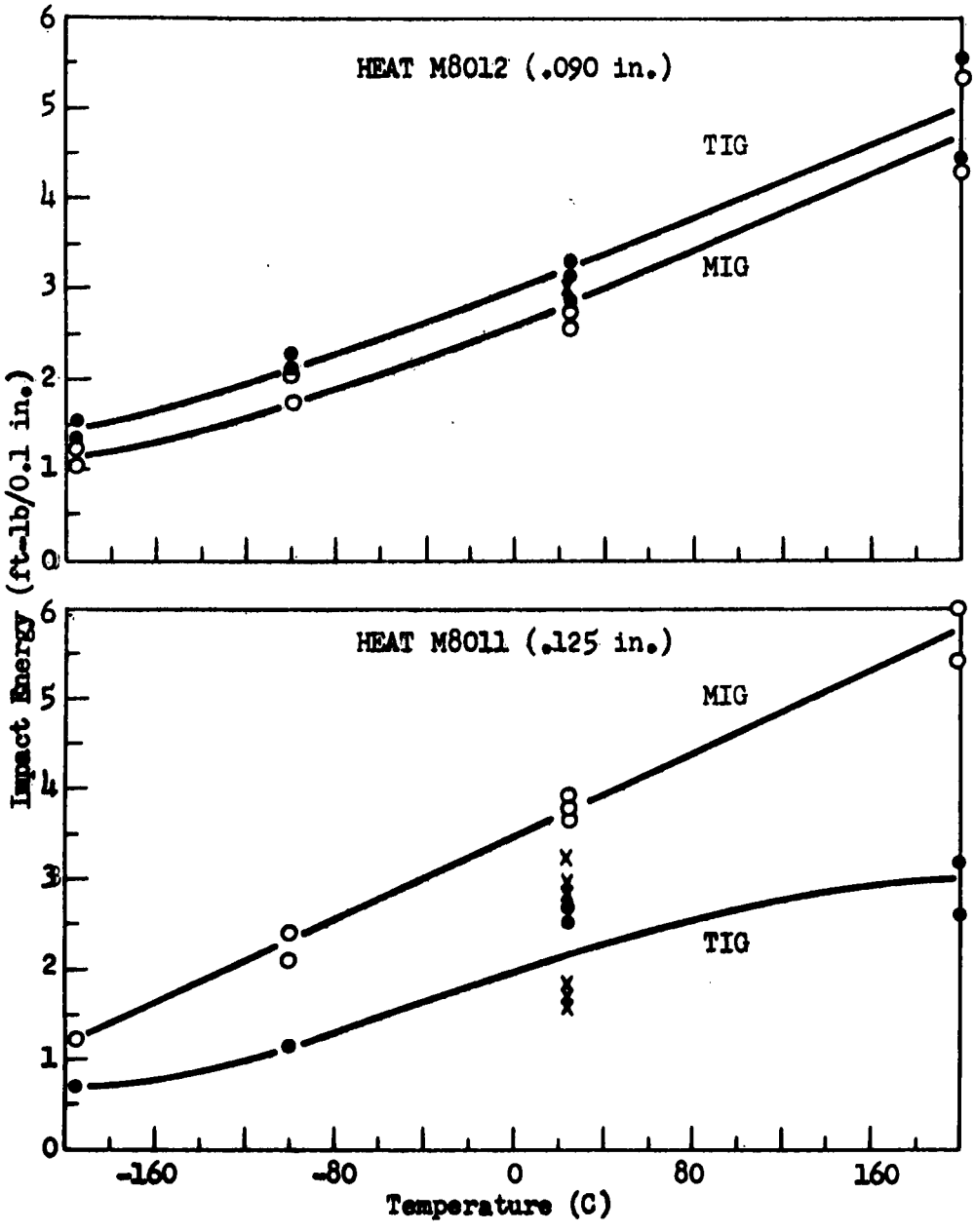


FIGURE 5 - ENERGY-TEMPERATURE TRANSITION CURVES FOR 4AL-3MO-IV TITANIUM SHEET IN THE WELDED-AND-AGED CONDITION. The Charpy specimens were precracked by means of a preliminary low-energy blow, or by fatigue (x). An energy value of 2 ft-lb/0.1 in. is equivalent to a G_c of approximately 900 in-lb/in^2.

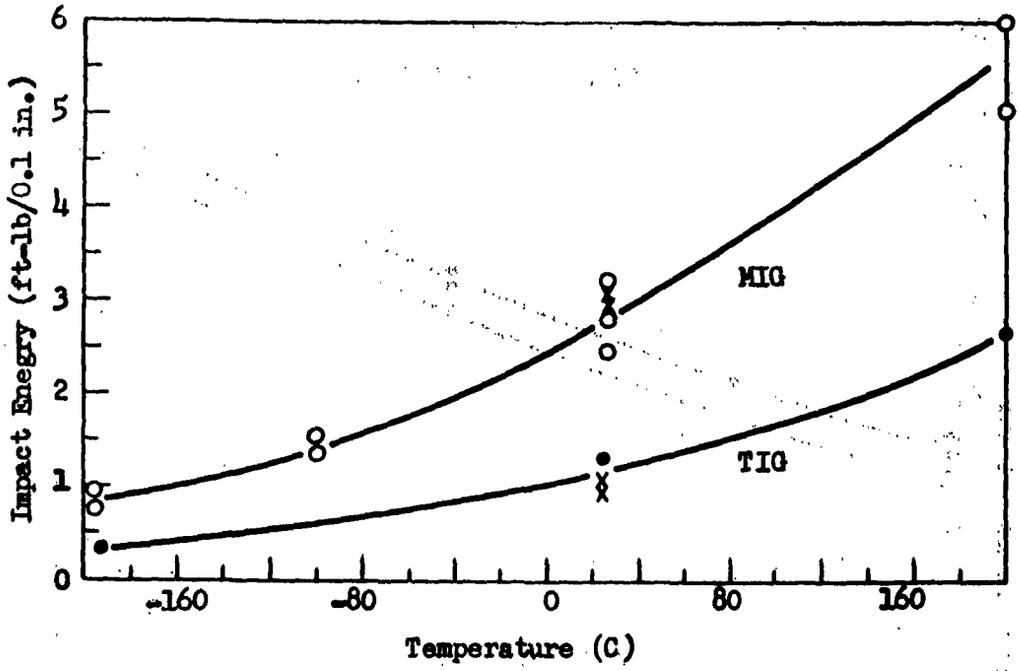


FIGURE 6 - ENERGY-TEMPERATURE TRANSITION CURVES FOR 2.5AL-16V TITANIUM SHEET IN THE WELDED-AND-AGED CONDITION. The Charpy specimens were precracked by means of a preliminary low-energy blow, or by fatigue (x). An energy value of 2 ft-lb/0.1-in. is equivalent to a G_c of approximately 900 in-lb/in^2. Heat T22162.

PREPARED DISCUSSION - THIRD SESSION

Discussion of Paper

"Aus-Shear Forming of Low Alloy Steel Cylinders"

by
E. S. Jones

prepared by
J. C. Hamaker

In comparing the H-11 type steel, tempered at 900-1100 F with the two low alloy steels, tempered at 400-700 F, the author concludes that the comparatively high ratio of TS/YS for the H-11 is due to the presence of retained austenite in the steel. We would like to point out that an alternate, very possible explanation may lie in the fact that the higher tempering temperatures used for the H-11 resulted in greater relief of the warm working stresses and thereby lower yield strength. The effect of raising stress relief temperatures by about 300 F in the 700-1000 F range is well known in the cold working of ferrous materials. The fact that the H-11 steel retained such a high ultimate strength (over 400,000 psi), despite the 300 F higher stress relief and tempering temperature, is indeed remarkable and a tribute to the effectiveness of the austempering operation. Actually, the H-11 material with an Ms temperature of 525 F during conventional heat treatment, should retain less austenite than the two other higher carbon, lower alloy steels, and has the added advantage of transforming this austenite by the conditioning mechanism afforded by its much higher tempering temperature. Of course, these reactions may be changed considerably by the ausforming operation; it would be interesting to see actual X-ray diffraction data on the relative retained austenite contents of the three steels after the ausforming and tempering operations have been completed.

PREPARED DISCUSSION - THIRD SESSION

Discussion on Session Topic

"Effects of Fabrication Variables"

prepared by
R. J. Voth

Adhering strictly to the literal translation of the title of this particular session, which is "Effects of Fabrication Variables", the one variable of strip wound cylinders which I could cover in the 3 to 5 minutes which the moderator has alloted me, is that of wrap angle. In the early stages of the development by the Ryan Company of strip-wound motors, three particular or basic types of configurations were considered. The first of those three, not necessarily in the order of preference is the geodetic wrap cylinder. It is merely a cylindrical shell in which the strip materials are helically wound, first one layer in one direction, then the second layer placed in the opposite direction. A second configuration is that of unidirectional wrapping, and that is a series of layers all in the same direction except that the second layer is displaced from that of the first layer, and so on until you get a sufficient number of layers to achieve the thickness desired. The third configuration is that which has been described by the gentleman from the Budd Company, and that is the coil wrap in which a single layer is wrapped upon itself as a scroll a sufficient number of times to give you a completed cylinder. Then resistance welds are placed through these laminates at various points in order to complete the pressure bottle. Naturally, this configuration has no wrap angle. The variations on the unidirectional configuration I intended to cover in my paper on Friday, which leaves us with a geodetic configuration and one of the many problems thereof is that of wrap angle.

It can be seen that if the two to one biaxial load distribution on an element with unit lengths sides in this particular type of a case were vectorially added, that there should be an angle at which you could wrap these shells which would result in a stable cylinder without any bonding being placed between the subsequent layers. Pursuing this line of thought, a two to one ratio will give you an angle of some 26 degrees of wrap angle between a line normal to the cylinder axis and the angle of wrap. This is not the true angle at which pure tension results in the strip because we have neglected the elemental shear stresses which must be transferred between adjacent strips. If we consider these elemental shear stresses, then this angle is not 26 degrees but it is closer to 36 degrees or 35 degrees and 15 minutes.

Figure 1 is the result of computations made regarding the variation in wrap angle. The percentage of PR over T hoop stress versus wrap angle is shown. If you were to have pure hoops you would have of course a tension in those strips of 100 percent of the hoop stress. At the angle of 26 degrees you will find that the stress in the direction of the strip is about 1.42 times the hoop stress. At the 35 degrees and 15 minutes angle where the shear transfer between adjacent strips becomes zero, the stress in the direction of wrap is one and a half times the hoop stress. Similar strip wound

cylinders were constructed at two angles of 26 and 36 degrees to prove out this analytical development.

Figure 2 shows the chamber pressure plotted against stress. We have a line of 1.42 times the hoop stress for a cylinder of 26 degrees and 6 minutes with no attachment between subsequent layers. Strain gage measurements give us a tension in the strip direction corresponding to the solid line, PR over T stress, again the dotted line here and the measurement by strain gage plotted in the solid line. Axial stress PR over 2T is plotted as the dotted line with the strain gage measurements following. The relatively good agreement is apparent.

In Figure 3, the 35 degrees and 55 minutes geodetic cylinder test is shown with a line plotted one and a half times the hoop stress and the tension in the direction of the ribbon plotted; PR over T stress, string gage reading adjacent to it. PR over 2T, the axial stress and the strain gage measurement.

In conclusion I can say that this is an extremely interesting problem with many variables other than those shown. The significant point regarding wrap angle is that the increase in stress to 1-1/2 times the hoop stress cannot be tolerated and that bending of the laminates is essential to convert the stress distribution shown in the Figure to that of a monolithic case.

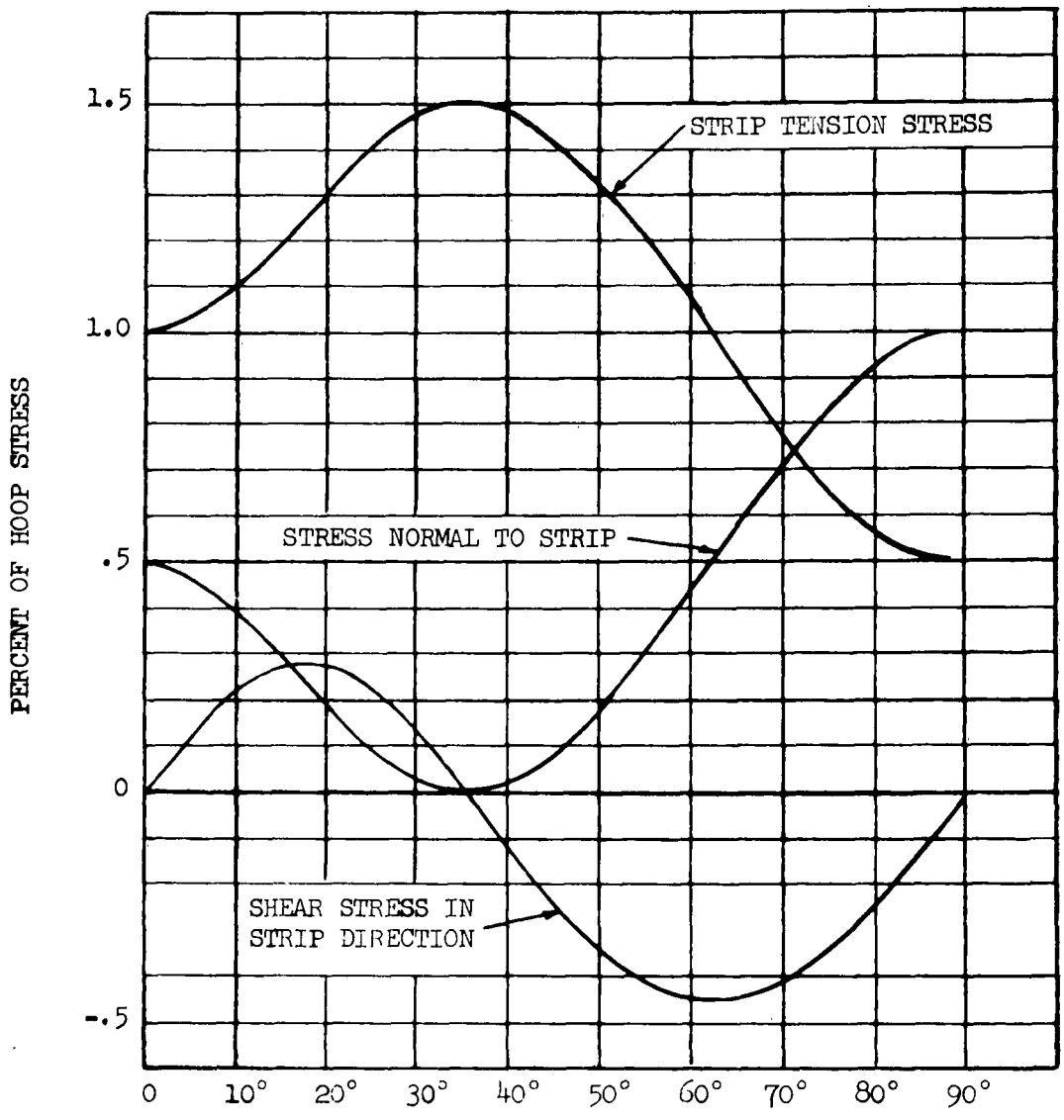


Figure 1 Stress Distribution In A Geodetic Wrapped Cylinder
(No Attachment Between Successive Layers)

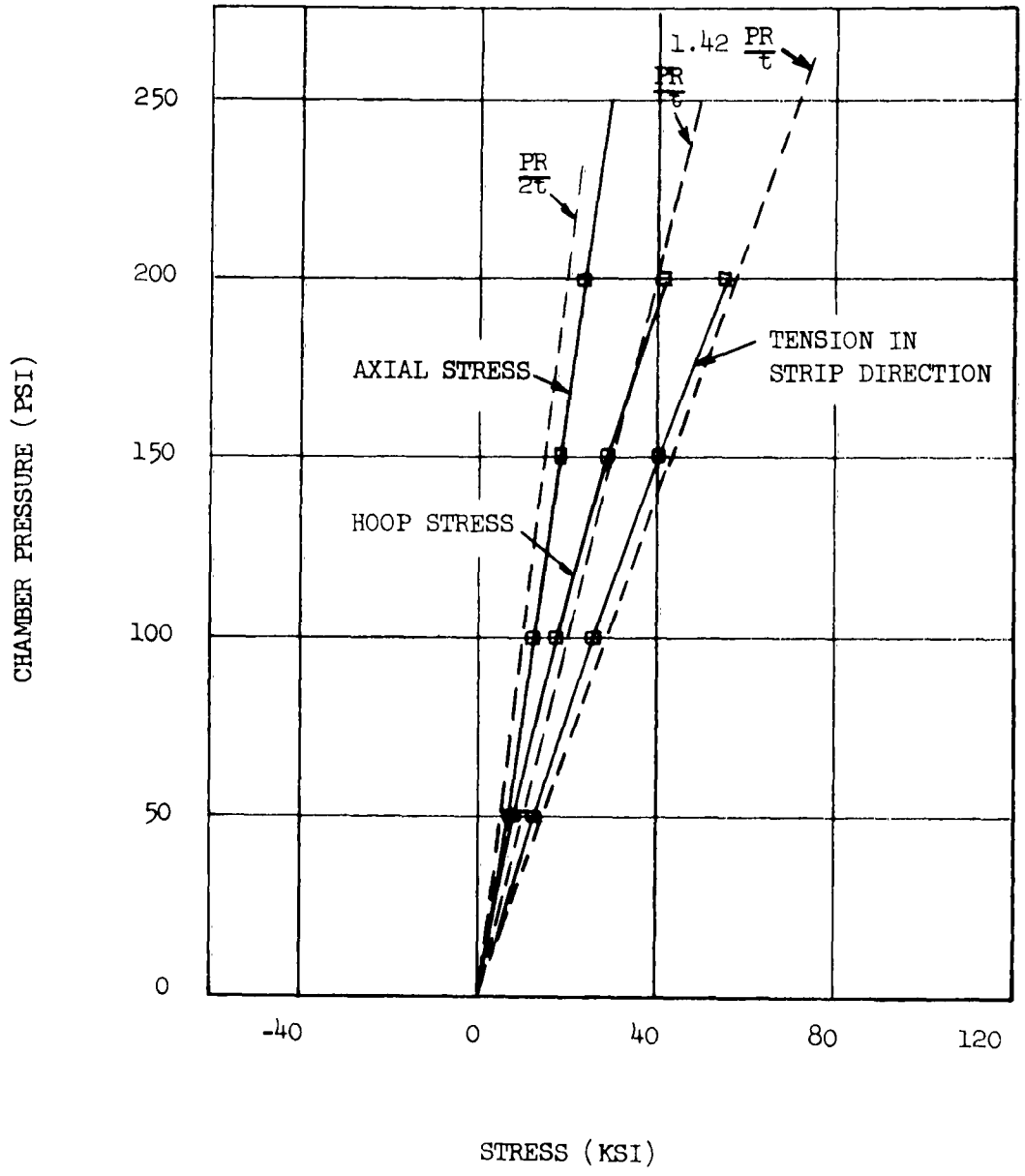


Figure 2 Strain Gage Readings of 26° 6' Geodetic Cylinder
(No Attachment Between Layers)

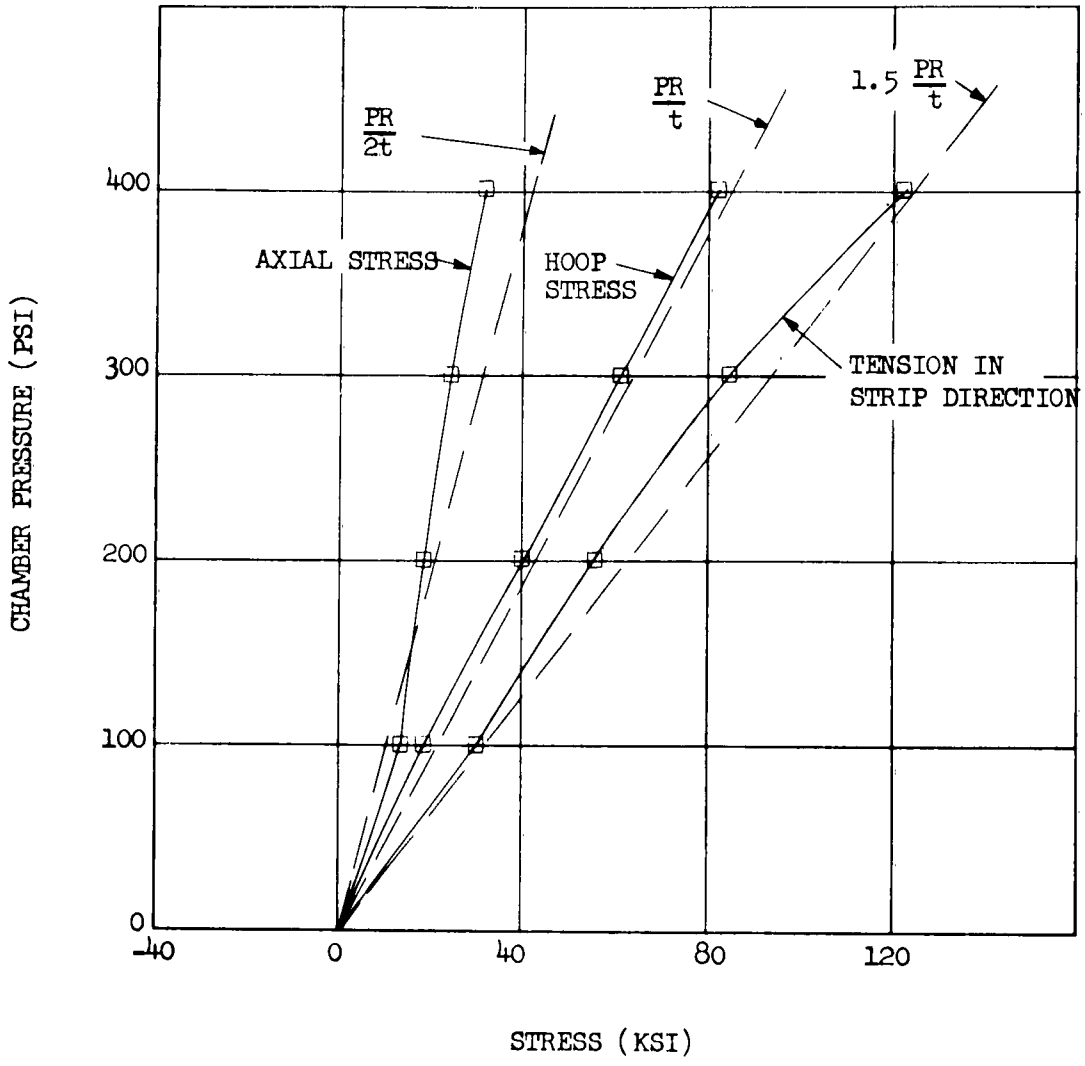


Figure 3 Strain Gage Readings of 35° 55' Geodetic Cylinder
(No Attachment Between Layers)

PREPARED DISCUSSION - THIRD SESSION

Discussion on Session Topic

"Effects of Fabrication Variables"

prepared by
H. A. Jahnle

The papers presented so far in this conference have emphasized low alloy steels, H-11 steels and titanium alloys. I would like to discuss briefly the development of wrapped cases, made from strain hardened and tempered stainless steels, which are being studied by the Budd Company.

Consider a flat sheet of AM 355 cold worked and tempered to a strength of 250,000 to 350,000 psi. The length of the sheet is twice the circumference of the cylindrical portion of the case. The gage is one-half the final thickness desired and the width is equal to or a fraction of the cylinder length.

This sheet is wrapped about a mandrel to obtain a two-layered cylinder, and the overlapping ends are resistance welded together, as shown in Figure 1. The resistance welded areas are annealed and the joint will have a lower strength than the parent material. A joint of a helical pattern would increase the efficiency. By experiment, this pattern is obtained and a chevron joint developed. This chevron represents elements of the helix. Joints having 90 to 100 percent of parent material strength are obtained.

Field welds are also placed at points determined by experiment to make the two sheets act together in bending and axial loading. The optimum spacing and number of such welds must be determined to provide maximum resistance to internal pressure and bending.

Individual cylinders are leak tested prior to assembly.

Cylinders are joined together by arc welding and with the use of a resistance welded doubler. This is shown in Figure 1 also. The doubler is used for additional strength.

The arc weld joint is prepared by seam welding the ends of the cylinder followed by machining. The arc weld nugget is then superimposed on the resistance welds.

Cylindrical portions are then welded to the headers which are made of a forgeable or deep drawing steel. This steel must be compatible to AM 355 and our tests so far have emphasized PH 15-7 Mo. Other steels are being considered.

The header is hardened prior to welding and the joint area is again annealed. The necessary strength is obtained by a combination of increased base metal thickness and doublers. These basic ideas are shown in Figure 2. As you can imagine, there are several possible combinations.

Figure 3 is a subscale model showing field welds and the chevron joint.

Figure 4 shows a one segment, 65" diameter case being prepared for test.

Figure 5 contains some test results of subscale bottles which have been made. It should be noted that the lowest hoop stress at burst has been 232,000 psi and the highest has been 296,000 psi. More important is the ratio of hoop stress to material strength. This indicates possible hoop stresses in full size bottles of 320,000 psi. There have been no failures in the chevron joint.

Our biggest problem has been in the headers. Several full-scale cases have been tested with all failures occurring in the heads.

One other advantage of this procedure is in its flexibility. Almost any size cylinder can be made without regard to heat treating facilities. This also allows on-the-site assembly of very large cases which cannot be easily transported.

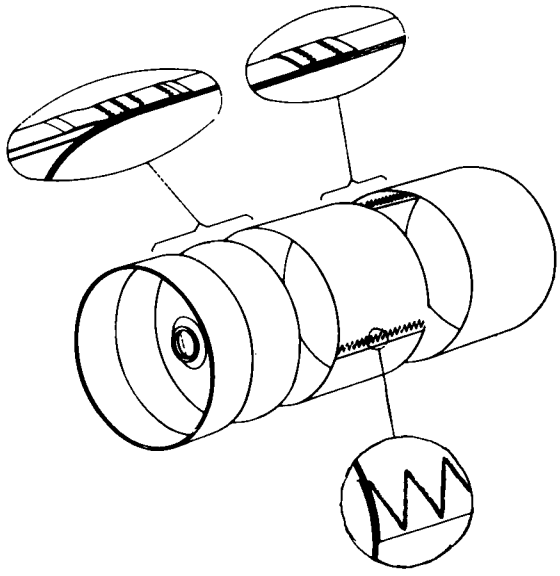


Figure 1. Rocket Motor Case Construction Showing Double Wrap Shell

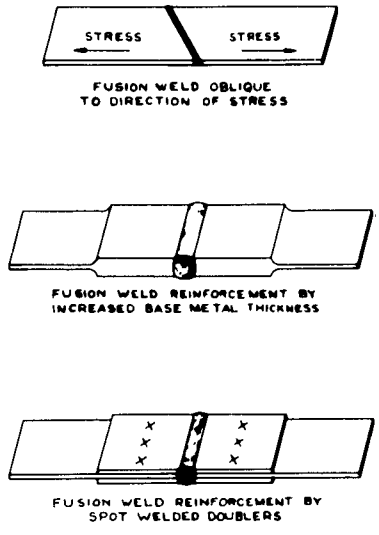


Figure 2. Basic Joint Designs

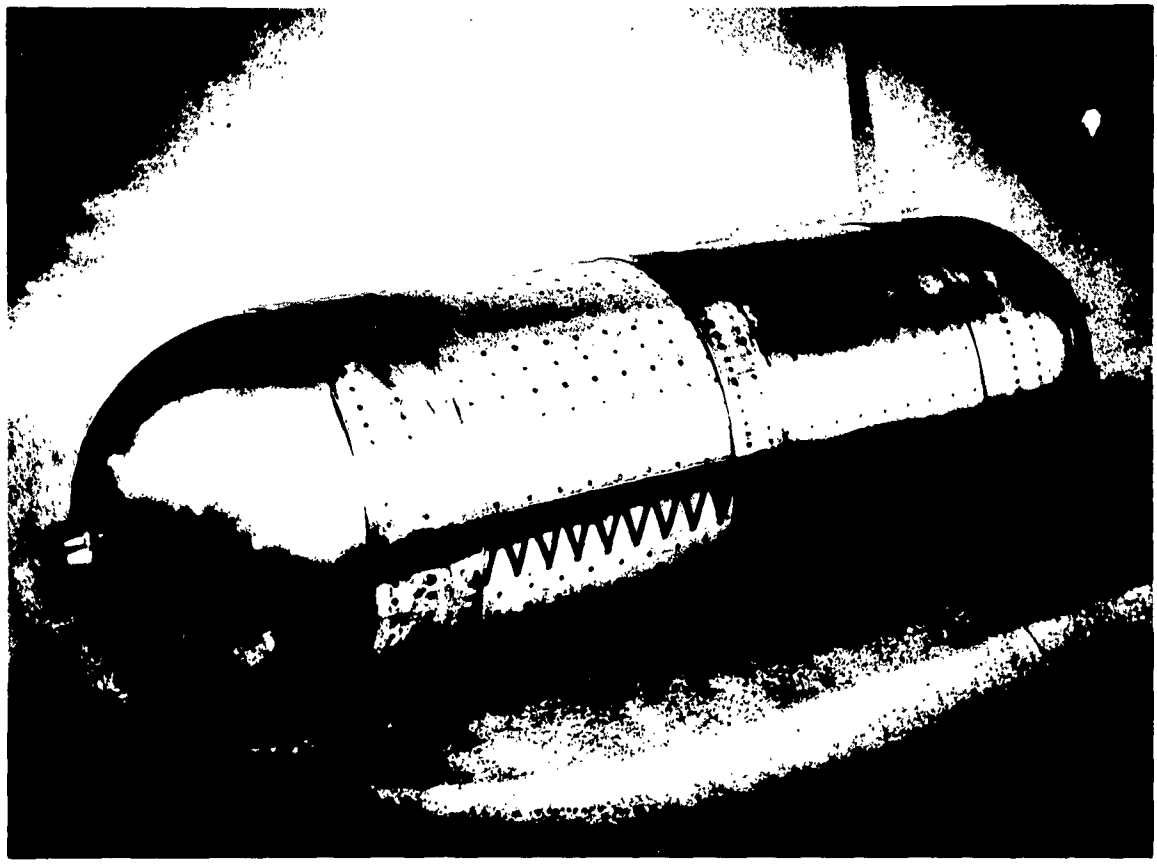


Figure 3. Subscale Model Showing Field Welds and Chevron Joint



Figure 4. One Segment Case (65-inch diameter)

THE BUDD CO.

SUB SCALE TEST RESULTS

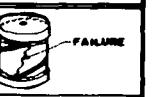
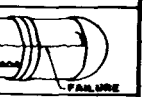
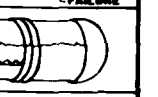
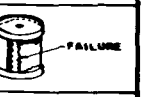
CYLINDER															HEADS							
								MATERIAL DATA								MATERIAL						
DRAWING NO.	TEST PURPOSE	OUTSIDE DIA. (IN.)	LENGTH (IN.)	NO. OF SECT'S	LAP JOINT TYPE	FIELD WELD SPACING	NO OF WRAPS	TYPE	TEMPER	COIL NO.	GAGE	YIELD 2% STRESS	ULTIMATE TENSILE STRENGTH	% ELONG.	PURPOSE & CONFIGURATION	TYPE	TEMPER	GAGE	P.S.I. BURST PRES.	K.S.I. CYL. HOOP STRESS	CYLINDER BURST ST. U.T.S.	
095-SK-495	BURST TEST	10 5	12 0	1	HELICAL LAP RESIS. WELDED	NONE	1	301 SS.	F.H.	GK	.014	L 285000 286000 297000 T 271000 268000	L 297000 293000 303000 T 302000 302000	L 1.0 T 2.0 2.0	CLOSE OFF FLAT PLATE	TANK PLATE		1.0"	708	292	$\frac{292}{298}$ = .980	
095-SK-497	BURST TEST	10 5	12 0	1	CHEVRON 1.0 PITCH 1 5 RISE	NONE	1	301 SS	F.H.	GK	.014	L 285000 286000 297000 T 271000 268000	L 297000 293000 303000 T 302000 302000	L 1.0 T 2.0 2.0	CLOSE OFF FLAT PLATE	TANK PLATE		1.0"	750	280	$\frac{280}{298}$ = .940	
095-SK-510	BURST TEST	10 5	12 0	1	HELICAL RESIS WELDED	NONE	3	301 S.S.	FH	KO	.005	L 308000 T 283000 283000	L 328000 T 327000 327000	L 0.5 T 1.0 1.0	CLOSE OFF FLAT PLATE	TANK PLATE		1.0"	770	270	$\frac{270}{328}$ = .824	
162-SK-710	BURST TEST	10 4	9.75	2	CHEVRON .75 PITCH 1.13 RISE	LONG. .75 TRANS. .28	2	AM 355	SCCRT	OP	.014	L —— T 278000 282000 283000	L 299000 299000 298000 282000 T 289000 289000	L 1.0 .5 1.0 T 2.0 3.0	DUMMY PLATE CLOSE OFF HEMISPHERE	TANK PLATE AM 355		1.0" 0.50	1300	242	$\frac{242}{299}$ = .810	
162-SK-731	BURST TEST	10 1	10.25	2	CHEVRON .88 PITCH 1.33 RISE	LONG. .88 TRANS. .28	2	AM 355	SCCRT	OP	.014	L —— T 278000 282000 283000	L 299000 299000 298000 282000 T 289000 289000	L 1.0 .5 1.0 T 2.0 2.0	DUMMY HEMISPHERE DUMMY	17-7PH 17-7PH		.063 .063	1500	273	$\frac{270}{299}$ = .903	
193-SK-753	BURST TEST	10.2	12.5	1	CHEVRON .88 PITCH 1.33 RISE	LONG. .87 TRANS. .28	2	AM 355	SCCRT	PA	.012	L —— T 336000 337000	L 351000 351000 T 343000 343000	L 5.0 T 2.5	CLOSE OFF FLAT PLATE	TANK PLATE		1.0	1380	296	$\frac{296}{351}$ = .843	
231-SK-1068	BURST TEST	10.2	8.0	1	CHEVRON .88 PITCH 1.33 RISE	LONG. .88 .090 DIA. TRANS. .62	2	AM 355	SCCRT	PO	.014	L —— T 310000 315000 308000	L 324000 327000 328000 311000 T 314000 311000	L 0.75 1.00 0.50 T 2.00 ——	DUMMY ELLIPSOID OF REV. 1.6:1 RAT. ACTIVE	304 S.S. 17-7PH	D.S. RH1050	.064 .032	1500	268	$\frac{268}{326}$ = .822	
231-SK-1069	BURST TEST																		1550	276	$\frac{276}{326}$ = .846	
231-SK-1069	BURST TEST	10.2	8.0	1	CHEVRON .88 PITCH 1.33 RISE	LONG. .88 .090 DIA. TRANS. .62	2	AM 355	SCCRT	PO	.014	L —— T 310000 315000	L 324000 327000 328000 311000 T 314000 311000	L 0.75 1.00 0.50 T 2.00 ——	DUMMY ELLIPSOID OF REV. 1.6:1 RAT. ACTIVE	304 S.S. 17-7PH	D.S. RH1050	.064 .032	1310	232	$\frac{232}{326}$ = .713	

Figure 5. Tabulation of Test Results

P. L. Hendricks I would like to direct a question to Mr. Spaeth. In the successive testing of motor cases through pressurization, it appears that there is definitely the possibility of producing strain induced martensite from the retained austenite usually present. Martensite formed in this manner would be untempered, and because of its brittle nature, highly undesirable. Do you know of any instances where failure during pressure testing could be related to the presence of such untempered martensite and secondly do you have any information as to what effect the stresses produced by repeated pressurization have upon the properties of the tempered martensite already present?

C. E. Spaeth In answer to the first question, the determination of retained austenite for the pressure vessels involved in my discussion was made and found to be extremely small. I do not think, from our experience, that we have seen any significant effects of cycling causing further transformation of untransformed austenite to martensite. We have cycled many of our pressure vessels approaching hundreds of times in the process of getting to the burst pressure, each time returning to zero pressure. It has not been our experience that what we would understand to be failure, resulted from transformation and then a subsequent loading, over stressing untempered martensite.

S. V. Arnold I understand that you have tested pressure vessels made of other steels than H-11. The H-11 steel heat-treated by the recommended practice, as I understand it, has very little retained austenite. Would your findings apply to the pressure vessels of other steels as well?

R. C. Powell The one steel in which we observed positive retained austenite effects was 300 M. We found a significant increase in the yield strength following cold treatment and further tempering.

P. Stark In response to Mr. Hendrick's question concerning the possible effects of proof testing on tempered martensite, I would like to call his attention to the work done by E. T. Stephenson and M. Cohen on AISI 4340 steel which is to be published in the ASM Transactions. They found that prestraining tempered martensite by small amounts followed by retempering, results in a type of mechanical instability upon reloading in tension. The strength-to-yield ratio for these prestrained and retempered specimens is: approximately unity and the elongation to fracture occurs with decreasing loads. The maximum load is greater than the value observed in a continuous tensile test. Although the phenomenon was observed in AISI 4340, it is possible that it also occurs in hot work die steels. Thus, a small amount of plastic deformation occurring in localized regions during proof testing and subsequent tempering

at ambient temperatures could result in the failure of rocket motor cases.

The above also includes answers to questions by Mr. Schapiro asking for a definition of "Mechanical Instability", and the amount of deformation encountered.

N. L. Reed I have a question for Dr. Adams. You outlined some programs that might be undertaken. I believe you did not speak of the possibility of improving the strength of a weld by hot deformation or by hot working. Is it now conceivable that we can do something along this line, or are we wasting our time if we think that we can improve properties of welds by hot working?

C. M. Adams Any study directed to possible benefication of welds is not a waste of time. Hot-working is certainly one of the possible techniques which deserves attention as is cold plastic deformation of welds. I do not know whether you have reference to such things as the hydro-spinning of welds or the expansion of tubing.

N. L. Reed I just wondered if you felt that in the university programs, attention should be given to hot deformation or warm deformation of weld materials.

C. M. Adams Some systematic work in this area should be undertaken. With respect to the unusual combinations of properties reflected in fusion zones, these seem related, at least in part, to the extreme chemical homogeniety of fusion zones, a degree of homogeniety not realized in other forms of the same material. Since plastically "squashing" the fusion zone presumably would not "unmix" it in any way, it would still potentially have unusual response to heat treatment, and so forth. This deserves a deeper explanation than it has had to date. However, I think the big need is for further work relating chemistry to properties in these unusually homogeneous structures.

L. Schapiro Mr. Jones, you have described to us the aus-forming of open-end cylinders. Rumors have reached the West coast that GE has aus-formed closed-end cylinders. If this is true, would you tell us something about it?

E. S. Jones To my knowledge, such rumors are not true. That would be a large step forward in the state of the art, and will not come for a while yet unless some fairly large sums of money can be spend on such a development.

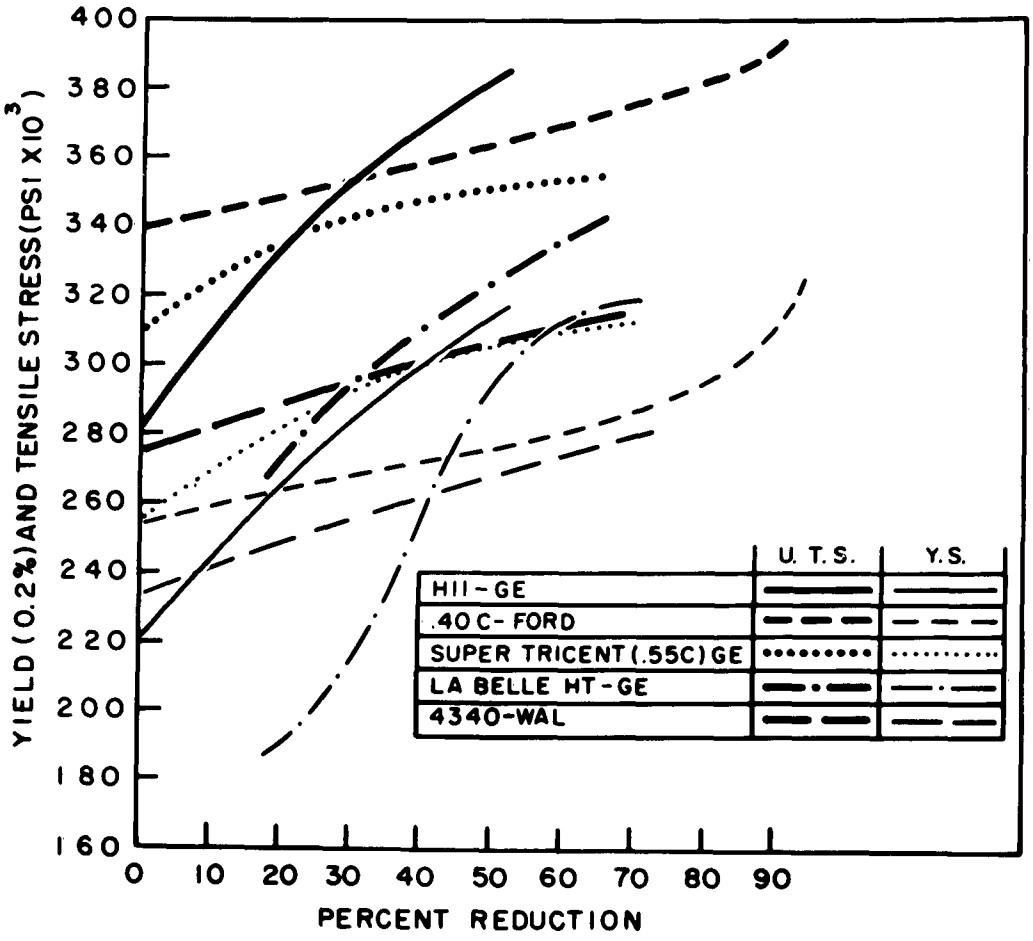
A. Hurlich I want to ask Mr. Jones a question regarding the aus-shear forming of Super Tricent. He was quite proud of the fact that he has attained 12 or 15 percent of elongation and said that this is something that would be much better than the Halcomb or HT Steel where he got 6 or 7 percent elongation. I would like to ask him two questions: First, what is the significance of elongation, secondly, why is 12 percent elongation better than 6 percent elongation in a structure that would fail after probably 1 percent elongation.

E. S. Jones I think you are right. The significance of the elongation ductility is certainly over-shadowed by the now known lack of notch-toughness at that strength level. Recently we have done more work with a modification of Super Tricent at about that same strength level, and have found that the $K_t = 5$ notched properties were quite low, of the order of .5 to .6. I do not know whether present casing designs can tolerate that sort of notch sensitivity or not. I suspect they cannot.

H. Bernstein I want to comment on the hydro-spin process with particular reference to Mr. Wilson's talk. It has been said elsewhere that the hydro-spin process is self-inspecting. Well, this just is not so. The failure which Mr. Wilson showed us was a second stage Polaris motor case in which, fracture started at a tear on the inside surface. It was not present in the sheet. This particular cylinder was hydro-spun from a rolled and welded blank, and the sheet was inspected before it was rolled and welded, and then spun into the full size section. Unfortunately, there was no inspection after the hydro-spinning. We know from the scale of the surface, as Mr. Wilson observed, that this flaw was present prior to heat-treatment. It was present in the hydro-spun blank and it could have been found by inspection. The only reason that I want to stress this is that no process is self-inspecting, and the product of any fabrication procedure like hydro-spinning or welding must be inspected to ensure reliability of the pressure vessel.

W. J. Wilson I simply concurr with that. I do not think we have reached the point where we can waive our inspection steps.

E. B. Kula I would like to introduce some data in support of the conclusions reached by Mr. E. S. Jones. On the figure are shown some examples of the strength increases that can be obtained by aus-shear forming, ausforming, austenrolling, or whatever name is given to the process of forming martensite and/or other transformation products in cold rolled austenite.



Examples of Strength Increases Obtained
by Aus-shear Forming

Tensile strength and 0.2 percent yield strength are plotted versus percent reduction. Data shown are for Halcomb 218 (H-11), LaBelle HT, and Super Tricent taken from a pamphlet published by the General Electric Company* about a year ago, a 0.40 percent C steel from some results from Ford, and 4340 steel from work at Watertown Arsenal Laboratories. These results are taken from published work, and hence are not compared at the same tempering temperature.

Note that the curves for the .40 C steel and the 4340 are parallel, i.e. the same amount of strengthening per unit reduction was achieved. The 4340 steel was deformed by single pass rolling at 1000 F, and no strain induced transformation occurred during rolling (A similar curve for rolling at 1550 F, above the critical temperature, could have been plotted). There is reason to believe that the .40 C steel used by Ford did not show any transformation during rolling. The slopes of these curves then can be interpreted as representing the strength increase that can be obtained by forming martensite in cold-rolled austenite.

The Super Tricent shows a slope slightly greater than the previous two steels. As was pointed out in the paper, there were indications that a small amount of strain induced transformation occurred during rolling. The LaBelle HT and Halcomb 218 show the greatest slopes, and these are the steels which gave the greatest indications of strain induced transformation. As Mr. Jones pointed out, the strengthening here is partially accounted for by strain hardening of the transformation products.

The conclusions to be drawn from this are rather obvious. The highest strengths can be obtained where there is isothermal transformation and further cold work of the transformation products. This may be accompanied by reduced ductility and toughness. If isothermal transformation products can be avoided, the highest strengths can be achieved in steels having the highest heat-treated strength.

Finally, I would like to ask Mr. Jones a question concerning directionality. He reported inferior notch sensitivity in the transverse direction. Does he feel that this directionality is a result of aus-shear forming or would he expect to find similar directionality if the material had been heat-treated after shear forming? I ask this question, since in our work at Watertown Arsenal, we found that there was a significant difference between ductility and impact toughness in the longitudinal and transverse directions after austenrolling 50 percent, but that this difference existed even in the normal heat-treated condition, without any rolling. A relatively small change in the yield and tensile strength could be attributed to the preferred orientation developed during rolling.

* "Cases and Nozzles for Solid Propellant Rocket Motors", Rocket Engine Section, General Electric Company.

E. S. Jones That is a good point, we did not check this and I might add that the initial work was done on air melted material and the later work that we have done has been on vacuum arc melted material which I am sure is a good deal cleaner. I guess I cannot really substantiate this with actual data, but microstructural observations indicate that the shear forming does produce a highly fiberous structure. When you test with the fiber direction, the orientation of your notch will be across fibers. You should expect less notch sensitivity here than in the case where you take a specimen transverse to the rolling direction, and if you notch this, fracture is likely to follow right along grain (or fiber) boundaries. So I still think that the directionality effect will increase with the degree of fibering which is the result one would of course expect with increasing reduction by shear forming. If you only do 50 percent shear forming reduction, notch sensitivity will be less pronounced than if you do 80 to 90 percent.

J. F. Watson I would like to direct this question to Mr. Spaeth regarding your hydrogen embrittlement hypothesis occurring during hydrostatic test. I feel uneasy about this hypothesis if it is based only on the similarity in appearance between a crack in your sample, and cracks in other samples known to be hydrogen embrittled. Do you have supporting data, or do you plan confirming experiments such as varying the pH of the solution and obtaining correlations of burst pressure with hydrogen ion concentration, or better yet, analyzing for hydrogen in that volume of the sample believed to be embrittled?

C. E. Spaeth There was supporting evidence, but we have not done nor do we plan to do supporting tests involving the alkalinity or acidity of the pressurizing fluid. I think this answers your question, but I would enlarge just slightly on some of the important parts. The failure exhibited a dark appearance under macroscopic examination and this observation relates to another observation by Troiano that there is a very smooth trans-granular nature to the fractures over that region which was a slow fracture in contrast with the subsequent region which occurs at a catastrophic rate. Whereas a stress corrosion failure, the other thing it might have been, is an intergranular affair in the martensitic steel. Also these cracks were not branched, and a feature of cracks in martensitic steels when they occur by stress corrosion, is a branched crack. These branches can be made to disappear and the failure becomes a single crack if a cathodic charging is used. When cathodic charging is used, the failure is due to hydrogen embrittlement, and you get a single crack as opposed to a branched intergranular crack. So on the basis of these additional factors which I deleted from my privious resume, we are satisfied with the hydrogen explanation.

T. H. Burns I would like to address my question to Dr. Hartbower. Have you done any electron beam welding of titanium?

C. Hartbower No, we have not. There is in existence an Ordnance Materials Research Office contract that includes electron beam welding of a number of materials. B-120 VCA titanium is among them, also fully hard cold-worked stainless steel. This work is now in progress.

T. H. Burns We have, Dr. Hartbower, found that there is a tremendous amount of reduction in the coarsening tendency normal for a TIG type weld in B-120 VCA compared to that coming from the electron beam process. As a matter of fact, this factor of crystal size is a matter of great importance. The physical properties resulting from this lack of coarsening are surprising. Elongation values many times those coming from Heliarc welds have been received. I would like to ask Mr. Jones if GE has done any room temperature deformation of 30 to 40 percent reduction of martensite?

E. S. Jones We have done some experiments on cold rolling semi-austenitic steels in various conditions of micro-structure. I guess the closest thing that we have done in respect to your question is some rolling of AM 355 type alloys, where you have martensitic plus austenitic duplex structures, and also on a structure leaning more toward the martensitic than austenitic.

T. H. Burns We have done some of this at Thiokol. On the 4340 steels we were able to get as high a yield strength as 310,000 psi with 350,000 psi ultimate coming out of them at 45 percent reductions of area.

W. A. Backofen What was the condition of this material?

T. H. Burns Tempered martensite C Rc 50-52.

E. S. Jones Very good. I have a question for fellow-panel member Hartbower. In his description of M.I.G. versus T.I.G. welding, he has some other information that I think would be of interest to the group, and that is the results of analyses for atmospheric contamination and also of grain size, which I think is quite important.

C. Hartbower In welding with the relatively high-energy-input tungsten inert-gas-shielded (TIG) process, we anticipated higher interstitial content than with the low-energy-input consumable-electrode (MIG) process but chemical analysis of the weld deposits did not substantiate this. Another possibility for explaining the greater notch toughness generally realized in the MIG welds is less grain growth. The rapidly cooled MIG welds had decidedly finer structure than the high-energy-input TIG welds.

N. L. Reed I have a question on why there is a broad spread between the yield and ultimate strength?

E. S. Jones We are looking for a fair amount of plastic deformation once the yield has been exceeded, or putting in another way, we want to have ample opportunity to dissipate stress concentrations before we reach the fracture stress. It is hard to maintain a large spread between yield and tensile if you emphasize high yield strength. Another explanation for why we got such a large difference I think was in the retained austenite which we definitely did have. The last slide I showed gave the results of refrigeration on some samples and it resulted in a decided boost in yield strength. In other words the difference between yield and ultimate was decreased appreciably. So part of that difference is due to retained austenite.

A. Hurlich As usual I would like to express a contrary point of view. If you have a wide spread between yield and ultimate, you are wasting a lot of strength because if you design to a given yield strength design allowable, what advantage does it provide if you have 400,000 psi ultimate but you have to limit the design to the 200 to 250,000 psi yield strength that you get. I would advocate having a reasonably small spread between yield and ultimate.

W. A. Backofen I would like to make an observation here. It seems to me that Mr. Hurlich's view is a "having your cake and eating it too" point of view. It may be argued quite convincingly, as I tried to indicate in the opening talk that an over-all, more persistent rate of strain hardening, which means in effect a higher tensile-to-yield ratio, is useful in building up fracture toughness. Some day we have to come to grips with the problem of what is to be done metallurgically to regulate this quality of fracture toughness. A good case can be made for the belief that ability to strain harden would contribute to fracture toughness by giving the essential requirement of a large plastic volume at the crack tip. But, what has been suggested is that as soon as a gap exists between yield and tensile, we close this gap in some way by elevating the yield strength. The result may be a higher yield stress for design purposes, but the price is quite likely to be reduced fracture toughness. Undoubtedly there is something of a balance to be struck there.

H. Bernstein I think we ought to try to agree on why there is a big spread between yield and tensile strength. If it is retained austenite, we ought to avoid it like the plague because the motor case will be subjected to prestressing prior to service use. We will get a strain induced transformation of austenite to martensite. The toughness of the martensite is very low.

W. A. Backofen But do we know that this is bad?

H. Bernstein Well, all of our data have shown that the higher the matrix strain, the lower the toughness, and as you temper back you increase the toughness. If you are going to have areas of untempered martensite, you will have very low-fracture toughness areas.

FOURTH SESSION

"Fracture, Crack Initiation and Propagation"

CURRENT VIEWS AND THEORIES ON FRACTURE,

CRACK INITIATION AND PROPAGATION

By
Volker Weiss
Syracuse University

It is the objective of this session to present to this conference a summary of the current views, concepts, and theories of fracture, crack initiation and crack propagation. An up-to-date review of the subject is the main topic of this introductory talk. Then, several of the most recent advances in theory and experiment, pertinent to a more basic understanding of fracture mechanics, will be discussed by the panel members of this session.

This conference is mainly concerned with the engineering aspects of the broad fracture problem. The desired goal is the establishment of reliable design criteria on the basis of which it would be possible to achieve maximum utilization of currently existing materials to advanced design systems. In most hopeful and general terms, the question before us is: "What physical material constants and parameters determine fracture and how can these constants (if any) be used to accurately predict fracture for a given applied stress system?" In answer to this question we require a basic understanding of the cohesive strength of crystalline materials and of the effects of impurities and applied stress system on the cohesion. It has often been pointed out that strength properties are hard to define, in terms of physical constants, as these are extremely structure sensitive. It is also well known that properties depending on energy values are far less structure sensitive, i.e. heat of fusion, heat of evaporation, specific heat etc. For this reason great efforts have been made to develop fracture concepts along the path (or detour) of energy balance principles. However, such an analysis requires the use of quantities which are structure sensitive (surface tension) and not much is gained compared to a direct approach.

That the energy balance approach might be a detour can be seen from the analysis of the fracture problem on an ideal material. The material in question has a linear stress-strain relationship to fracture. Separation occurs when the applied force equals the cohesive strength: the fracture stress is a materials constant. Thus the Lame-Navier fracture concept proposed in 1828 (1)*. Even if the fracture strength were not a universal material constant but depended upon the stress system (biaxiality, triaxiality), this dependence could be determined.

* (1): The Lame-Navier fracture concept does not make reference to an ideally elastic material, but was intended for metals. Ludwick (2) proposed a similar concept by postulating the existence of a critical brittle fracture stress.

There are two basically different approaches to the fracture problem: the macroscopic approach and the microscopic approach. The latter tells us how well the assumptions made in the former are justified.

The presently accepted macroscopic approach is the Griffith Brittle Fracture Concept (3) proposed in 1921 and modifications based thereon (4, 5, 6). It is an energy balance concept expressed in terms of the crack length, the applied stress and material constants. It has been shown that it applies not only to glass and other ideally brittle materials but also to metals showing moderate plastic flow at the tips of the crack (4). The existence of cracks is postulated. This postulate is necessary as it is the only explanation for the discrepancy between observed and theoretical strength.

Fracture concepts which do not make use of the energy balance principle have also been proposed for metals. One of these concepts which deserves particular attention was proposed by Beeuwkes (7) at the Third Sagamore Research Conference. It is based on the stress-strain characteristics of actual materials up to fracture. Beeuwkes has shown that a straight line relationship between stress and strain to fracture is obtained when the true stress is plotted against the hyperbolic true strain, as shown in Fig. 1. He postulates the existence of a "fracture corner", the location of the termination points of the stress-strain curves. Brittle fracture, in a loose terminology, is defined by a constant fracture stress while ductile fracture is determined by a constant fracture strain. He also found that in this representation the stress-strain curves for face centered cubic metals investigated are parallel while those for body centered cubic metals intersect each other at one point, as shown in Fig. 2.

As the main portion of this paper deals with macroscopic fracture concepts, it appears desirable to discuss briefly the microscopic foundation of some of the macroscopic concepts. This of course involves dislocation mechanics applied to the formation of cracks.

The problem is how the conversion from glide dislocations to cavity dislocations takes place. Four possible models are shown in Fig. 3 taken from Cottrell (8). The mechanisms illustrated are: 1) pile-up of edge dislocations, 2) pile-up in a slip band of edge dislocations against a grain boundary, 3) shear on two intersecting slip bands and 4) slip band crossing a tilt boundary. In order for any of these systems to work it is necessary that the elastic energy which the dislocations bring with them is not dispersed through plastic flow in the nearby material. In materials having only one or two easy slip systems, the mechanisms are feasible - the brittleness of hexagonal metals can be explained on this basis, see Fig. 4. For cubic crystals with good slip systems in several directions, Mott (9) and Stroh (10) pointed out that a yield drop is required for the mechanism to work. Such a phenomenon gives rise to dislocation avalanches which run together and form a crack before nearby dislocation sources can start working. To delve further into the details of dislocation theory and its application to the fracture problem would be beyond the scope of this conference. An excellent up to date summary of the atomic mechanisms of fracture was presented in the 1959 Swampscott Conference on Fracture (11). Let it suffice

to say that the assumption of the existence of cracks appears justified. With the help of these micromechanisms for crack formation, and the Griffith concept, Cottrell (12) and Petch (11) were able to define fracture in terms of the yield strength, the dislocation pinning strength and the surface tension by the well known equation:

$$\sigma_y k_y d^{1/2} = \beta \mu \gamma$$

where σ_y is the yield strength, d the grain size, β a constant (=2 for torsion, =1 for tension and = 1/3 in the plastically constrained zone at the root of a notch) μ the shear modulus and γ the surface tension. $k_y = \sigma_D \ell^{\frac{1}{2}}$ where σ_D is the unpinning stress for the temperature and time concerned and ℓ the spacing of the dislocation sources. This equation gives information on both brittle and ductile fracture. When the left hand side exceeds the right hand side, the yield stress is more than sufficient to propagate the microcracks. On the other hand, when the right hand side is larger than the left hand side, the yield stress does not suffice to propagate the microcracks. The equality sign defines the condition for fracture transition. It is interesting to note, that the surface energy finds its way into the above equation via the Griffith concept. Thus far there was no information available concerning the effect of surface tension. Recent experiments which Dr. Rostoker will discuss in this session constitute, to my knowledge, the first experimental test of the Griffith concept with respect to its fundamental constant, the surface energy.

THE GRIFFITH CRACK CONCEPT

The Griffith concept states that an existing crack of length 2c will propagate cataclysmically if the strain energy release due to the crack is larger than the surface energy gain, i.e. if the total free energy of the system is lowered by an increase of c. Although the concept is well known and understood it appears useful to review it in terms of Irwin's $\mathcal{G}$ values.

Let the change in the total system energy of an elastic solid due to a crack of length 2c in an otherwise uniform stress field σ in the direction normal to the plane of the crack be

$$\Delta W = \Delta E + \Delta T$$

where T is the change in surface energy (area of the crack times the surface tension per unit area, A · T) and Δ E the change in elastic strain energy due to the presence of the crack. The change in elastic strain energy can be expressed by an intergral

$$E = -\int_0^c \mathcal{G}.1(c)\, dc$$

where is the elastic strain energy release rate per unit edge length of the crack and l(c) the edge length of the crack. The strain energy release rate is a function of both the applied stress and the geometrical variables of the crack. Instability, and cataclysmic crack propagation occurs if

$$\frac{\delta(\Delta\omega)}{\delta_c} = 0$$

or

$$\mathcal{G}_c \ell_{(c)} = \frac{\delta\ (T, A)}{\delta_c}$$

It should be noted that for all crack forms thus far investigated

$$\mathcal{G}_c = \frac{1}{\ell_{(c)}} \cdot \frac{\delta\ (T, A)}{\delta_c} = 2\ T$$

which means that the assumption of a constant surface energy term is synonymous to the assumption to a constant $S = \mathcal{G}_c$.

Orowan (4) has shown, for an elastic solid, that the Griffith condition for crack propagation is not only a necessary but also a sufficient condition for brittle fracture. He has pointed out that the stress at the tip of a Griffith crack equals the cohesive strength of the material and that the stored elastic energy for both the fixed grip and the fixed load condition is more than sufficient to propagate the crack. But he has also shown that for metals the discrepancy between the apparent and the true surface energy is several orders of magnitude. This is due to plastic flow at the root of the notch which consumes a certain part of the liberated elastic energy thus making it unavailable for the propagation of the crack. He suggested that Griffith's equation be modified to include an energy term for plastic work P which is assumed to be a constant for a given material. This concept is applicable to metals as long as the plastic zone near the root of the notch is small compared to the crack length. In accordance with the experimental results on "semiductile" metals the energy balance principle may be expressed by the equation

$$\mathcal{G}_c = \frac{1}{\ell_{(c)}} \frac{\delta f\ (T+P) \cdot A]}{\delta_c}$$

which, if $\mathcal{G}$ is known as a function of the crack geometry and the applied stress, defines the fracture strength of metals in the presence of cracks.

An analytic determination of requires a knowledge of the stress distribution in the materials surrounding the crack. The stress field equations, most easily applicable to this problem, were developed by Westergaard (13) based on a two-dimensional stress analysis are for either plane stress or plane strain, and are given below

$$\sigma_y = \frac{K}{\sqrt{2\pi r}} \cos\frac{\theta}{2}\left[1 + \sin\frac{\theta}{2}\sin\frac{3\theta}{2}\right]$$

$$\sigma_x = \frac{K}{\sqrt{2\pi r}} \cos\frac{\theta}{2}\left[1 - \sin\frac{\theta}{2}\sin\frac{3\theta}{2}\right] - \sigma_{ox}$$

where y is the direction normal to the plane of the crack, r the radial distance from the tip of the crack and θ the angle between r and x, see Fig. 5. In completing the intergration to determine the strain energy release rate it turns out that $\mathcal{G} = K^2/E$ where E is Young's modulus. Both $\mathcal{G}$ and K are of course functions of the stress and the crack length. The early work on fracture mechanics by Irwin and his coworkers cf. (6) employed the Griffith energy balance principle to a phenomenological description of the fracture process by postulating that a material's resistance to sudden fracture is characterized by a critical $\mathcal{G}_c$ value. If the strain energy release rate exceeds this critical value, sudden fracture occurs. As the underlying stress analysis is two dimensional, it is not surprising that experimental $\mathcal{G}_c$ values depend upon the sheet thickness.

Recently it was recognized (14,15) that the Westergaard stress field equations can also be utilized in a phenomenological description of the fracture process (without the detour over an energy balance principle) with the help of the Sachs elastic strain distribution concept (16) also expressed by Lubahn's congruency principle (17), according to which the fracture strength of specimens having the same stress distribution at and near the root of a notch or crack is a material constant. This stress distribution for sharp cracks in plane stress or plane strain is completely defined by the stress intensity factor, K, appearing in Westergaard's equations. The material's resistance to sudden crack propagation can now be characterized by a maximum stress intensity K_c which it will withstand. The fact that $\mathcal{G}$ and K are related by the modulus of elasticity, and that their relationship for the Westergaard analysis is independent of the applied stress and the crack length, makes the two fracture descriptions identical as far as a fracture stress crack length dependence is concerned.

The equation for $\mathcal{G}$ and K for the infinite plate, the finite plate and the three dimensional case are shown on Table I.

Methods and procedures for determinations of K_c for sheet materials are discussed in great detail by the ASTM Committee Report of Fracture Testing of high strength sheet materials (18).

It has been demonstrated, that for most metals an existing crack propagates first at a slow speed and that only after a critical crack length is reached does the transition to sudden fracture take place. Realistic ς_c or K_c or corrected surface tension values can only be obtained if the stress and the crack length at this moment of transition is accurately known. It also implies that specimens of sufficient size have to be used and they become rather large as the ductility of the material in question is above a certain value. However, it is maintained that this transition takes place for all materials as long as the size is sufficiently large (6).

It has to be understood, however, that the above mentioned analytical methods to derive equations for K are based on a two dimensional elastic stress analysis which cannot be expected to account for effects of sheet thickness and plasticity. Dr. Irwin will discuss the effects of plasticity and plate thickness and present a correction method whereby these effects can be incorporated into two-dimensional elastic fracture mechanics.

Fast fracture occurs not only in the form of a flat tensile crack but also in the form of an oblique shear crack (19). One must assume that the energy absorptions for these two fracture modes are different. Often a transition between the two modes takes place during isothermal testing of sheet specimens. The ratio of flat to shear portion of a fracture surface depends upon the test temperature and is used as one index for the transition to brittle behavior of a material. An analysis of these phenomenal will be presented by Mr. Srawley.

Now the question arises: can the modified Griffith concept be used as a design criterion? Winnie and Wundt (20) claim that it is possible to classify forgings by the degree of their susceptibility to brittle fracture in the presence of discontinuities by means of ς_c values. Irwin and his coworkers (14) have suggested to relate the ς_c or K_c value of a material in consideration to the yield strength or the ultimate tensile strength and determine a critical crack size. The design and the material should be chosen in such a way that cracks of critical size can be detected on inspection. Such a design criterion, which places the major responsibility on inspection procedures, has several shortcomings: a) it puts a severe penalty on mild notches which could withstand a much higher stress than determined by the modified Griffith theory, b) it hopefully assumes that critical cracks, be they only approximately a hundred atomic dimensions wide, can be detected, and c) it involves assumptions concerning the growth of cracks of subcritical size to critical size, which are at present not clarified.

THE NEUBER CONCEPT

Neuber's Theory of Notch Stresses (21) is well known and has been utilized for many years in the design of parts having notches, grooves, fillets,

and so forth. The stress distributions for a great number of geometrical configurations and applied stress systems at locations of stress concentration are analyzed. As a consequence of this analysis, stress concentration factors are determined which relate the existing maximum stress σ_{max} to the applied average stress σ_N by the equation

$$K = \frac{\sigma_{max}}{\sigma_N}$$

Stress concentration factors for a wide variety of geometrical configurations and stress systems can be found in e.g. Peterson (22). Therefore, a brittle fracture concept can be formulated with the help of Neuber's stress concentration factors and the Lame-Navier concept which assumes σ_{max} to be a material constant. This concept would be expected to hold for brittle materials where all deformation to fracture is elastic, and for mild notches for which K does not exceed 6 or 8. The material constant σ_{max} has to be determined by extrapolation of σ_N vs. K curves to K = 1. Even for the most brittle materials investigated, this extrapolation does not lead to the atomic cohesive strength but to a considerably lower value, which, if desired, could be used to make guesses about the size and distribution of microcracks. Mr. Sessler will present data obtained at Syracuse which indicate that the adoption of the above fracture concept is certainly feasible to describe fracture in a brittle metal. For other than almost ideally brittle materials, this concept is very conservative as can be shown on the basis of the many notch strength/tensile strength ratio vs. K curves available for technical materials (23,24,25,26).

Before going to Neuber's theory of pointed notches, mention should be made of a rather neglected subject: the stress gradient at the root of a notch, and the section size effect which is intimately related to the stress gradient. It is generally recognized that more than just the maximum stress at the notch root should be considered in an analysis of fracture phenomena. The Griffith concept does this indirectly by integrating over the entire portion of the stress field to obtain the elastic energy release. With the help of Neuber's equations concerning the stress distribution in the proximity of notches, it is possible to obtain a mathematical expression for the stress gradient in terms of stress concentration factor and notch root radius. Within an error of not more than 10 percent, the stress gradient for edge notched and centrally notched sheet specimens is given by

$$\left.\frac{\delta\sigma_y}{\delta x}\right|_{\sigma = \sigma_{max}} = \Gamma = \frac{2\sigma_{max}}{r} = \frac{2K\sigma_N}{r}$$

where r is the notch root radius, σ_N the average notch stress and K the stress concentration factor, (27, 28, 29). That this gradient is related to the size of the specimen can be seen by keeping K constant and increasing the size of the specimen. The gradient decreases with size if the notch depth is kept constant. The loss of strength with increasing size can thus be related to stress gradient. No theoretical concepts concerning such relationships are available yet, although experimental evidence indicates that this is feasible. In Figure 6 are plotted the notch strength values of several tests on an extremely brittle Ti-2.5Al-16V sheet against the overall size and the crack length c. Three test sequences are reported: a) low stress concentration K = 4 constant, constant percent notch depth, increasing size, b) low stress concentration K = 5 and stress gradient constant, increasing size variable notch depth and c) extremely high stress concentration (r = 0.001 in), constant percent notch depth, increasing size. The modified Griffith concept for sequence c) predicts $\sigma\sqrt{b}$ = constant. However, it appears that the observed size effect for sheet materials is less than predicted. The Neuber fracture concept predicts no size effect at all for series a). However, again a size effect similar to that observed in series c) is obtained while no size effect at all is observed in series b) for which not only K but also stress gradient was kept constant. This suggests an amendment of the Neuber-Lame-Navier fracture concept to include the stress gradient as well. Extensive further testing will be required, to arrive at such a concept. The results point to a fracture criterion proposed several years ago by Sachs (16) that: the fracture strength of specimens having the same stress state (stress concentration factor and stress gradient) at the root of the notch is a material constant.

Another interesting by-product of our study on the effects of stress gradient concerns the degree of biaxiality at the notch root. By an analogy to the stress distribution of smooth bend specimens for which the biaxiality is determined by the width to thickness ratio (30) as shown in Fig. 7, it could be shown that the biaxiality developed at the root of a notch in a flat sheet depends on the thickness to root radius ratio, see Fig. 8. Thus full biaxiality, i.e. the ratio of hoop stress to membrane stress equals 1/2, is predicted for specimens for which the thickness to notch root radius ratio exceeds the value 8. The experimental results obtained by Loetsch (31) have recently confirmed this thesis to the extent that full biaxiality is developed at the center of a notch for all t/r ratios larger than 10. No data are available at present for specimens having smaller t/r ratios.

For stress concentration factors larger than 8, Neuber's original theory becomes unrealistic (21). For extremely sharp notches K would assume values proportional to $2\sqrt{17/r}$. In order to arrive at realistic values for K, the finite size of the structural units has to be considered. The differential equations used to solve the continuum -mechanics problem for mild notches have to be replaced by difference equations corresponding to the finite size of the structural units as soon as the root radius approaches the size of these units. However, the failure of the classical theory of elasticity concerns only the region of high stress gradient at the notch root. A small finite particle of the size η is introduced at the notch root. The particle is small enough

to justify the assumption of constant stresses at its bounding surfaces. The new stresses are obtained by forming the average value of the "old" stresses on the bounding surfaces of the particle. This particle has often erroneously been referred to as the "plastic particle" an inference which has to be rejected because it merely is used as a means to introduce a discontinuum mechanics correction to a continuum mechanics approach. It has nothing to do with a plastic zone. The result of this calculation is that the stress concentration factor is now not only a function of the notch geometry (r and c) but also of η which is assumed to be a material constant. For sharp elliptical cracks of length 2c at the center of a plate the stress concentration factor is now given by

$$K = 1 + 2\sqrt{\frac{c}{r_1}}$$

where the corrected root radius r_1 is now a function of the true root radius r and of η . For a notch angle of 0 degree, r_1 is given by

$$r_1 = r + 2\eta$$

and K by

$$K = 1 + 2\sqrt{c/(r + 2\eta)}$$

Increasing the notch angle to 60 degrees has, for all technical purposes, a vanishingly small effect.

The above introduced Neuber-Lame-Navier fracture concept can now be applied to pointed notches. Replacing K by σ_{max}/σ_N neglecting the term $\sqrt{r + 2\eta}$ as small compared to the term $2\sqrt{c}$ and rearranging the equation yields, for the notch strength at fracture,

$$\sigma_N = \frac{\sigma_{max}\sqrt{r + 2}}{2\sqrt{c}}$$

which has the same functional dependence on c, i.e., as the Griffith concept. This concept is graphically illustrated in Fig. 9 which gives several $\sigma_N - K_c$ curves as a function of η . The major differences between the two fracture concepts are a) the above concept is derived directly from maximum stress considerations without any energy balance principles and b) while the Griffith concept is a one-parameter concept (the parameter being the surface tension) the above is a two-parameter concept (the parameters being σ_{max} and η). One decisive advantage of

the above concept is the fact that it applies not only to sharp notches but to mild notches as well. Experimental evidence as to the applicability of this concept will also be given by Mr. Sessler in his presentation during this session.

In order to account for the effects of plasticity on the basis of the stress concentration factor concept a mathematical analysis would have to make use of the non-linearity of the stress-strain curves for metals. This approach is now being taken up by Prof. Neuber in Germany also under contract with the WADD, (32). Such an analysis, although too complicated to be treated within the framework of the present conference, can ultimately be expected to yield most of the basic information required to adequately describe the fracture process of any material for which the stress-strain curve is known.

In the meantime "plasticity corrections" have to be utilized to account for the experimentally observed phenomena. Such a correction adapted to the stress concentration factor concept has been suggested by Stowell (33) and was followed up by Hardrath (34). It related the observed stress concentration factor K_p to the elastic stress concentration factor K_e by means of the ratio of the secent moduli at the notch root and at a large distance from the notch root, $E_{sn}/E_{s\infty}$ according to the equation

$$K_p = 1 + (K_e - 1) \frac{E_{sn}}{E_{s\infty}}$$

Using values obtainable from the stress-strain curve, the notch strength σ_{max}/K_p can be similarly expressed as follows:

$$K_p = K_e \frac{\varepsilon_e}{\varepsilon_t} + \frac{\varepsilon_p}{\varepsilon_t}$$

where ε_p is the (true) fracture strain or ductility of a smooth specimen, ε_e is the elastic strain at the (true) failure stress, or $\varepsilon_e = \sigma_{max}/E$, and $\varepsilon_t = \varepsilon_e + \varepsilon_p$. This equation contains only quantities obtainable from a smooth test although the stress state must be considered for the failure strain. It is identical to Hardrath's and Ohman's equation if the yield strength of the metal is high and $E_{s\infty} = E$. The notch strengthening due to plastic constraint is not considered. The above equation can be interpreted to mean that the stress concentration factor for a material showing plasticity is made up of two parts: the percentage of "elasticity" of the material, expressed by the ratio $\varepsilon_e/\varepsilon_t$ = e times the elastic stress concentration factor, plus the percentage of plasticity of the material, expressed by the ratio $\varepsilon_p/\varepsilon_t$ times the plastic stress concentration factor 1.

Fig. 10 shows a family of $1/K_p$ vs. K_e curves for several e ratios. The curves were calculated on the basis of the shallow notch equations for K_e assuming an equivalent particle sizeη = 0.0017 in. A similarity between the theoretical and experimentally observed data represented in the same fashion, i.e. notch strength ratio vs. K, is observed. The general effect of increasing plasticity is to displace the theoretical curve $1/K_e$ vs. K_e to the right and to decrease its slope. It can also be observed, that moderate amounts of plasticity, up to e = 0.5 have only little effect on the general shape of the theoretical curve.

In order to arrive at more fundamental knowledge concerning the deformation at and near the notch root more elaborate plasticity treatments have been made in Russia (35, 36). The use of double notched specimens is also practiced in the USSR (37). In such specimens fracture only occurs between one pair of notches leaving the remaining portion of the specimen containing an identical notch for analysis of the strain state just prior to fracture. Tests on such specimens are now also being conducted at Syracuse University (38) in order to study the deformation characteristics of various materials and notch geometries.

Thus the Neuber stress concentration concept of fracture can account for most of the pertinent features of fracture in the presence of notches and cracks. With consideration of the effect of the stress gradient it will no doubt become possible, to account for the observed width and size effects as well.

GRIFFITH NEUBER COMPARISON

The two approaches discussed can be compared on the basis of relative agreement or disagreement with experimental data and also on the basis of the interrelationships of the parameters involved.

Experimental agreement is obtained for both concepts when the discontinuities are sharp cracks as long as $c \gg r$. The Griffith-Irwin Fracture Mechanics is not intended for mild notches but it also breaks down for metals as soon as the crack length becomes small enough, for which case it predicts far too high strength values, Fig. 11a. Better agreement is obtained with the help of Irwin's plasticity correction (18) which introduces yield strength of the material as an additional parameter and is expressed by the equation

$$K_c^2 = \frac{\pi \sigma^2 c}{1 - 0.5(\sigma / \sigma_y)}$$

where σ_y is the yield strength of the material. Unfortunately this correction extrapolates to $\sigma = \sqrt{2\sigma_y}$ for $c \rightarrow o$ for the infinite sheet case. The results of this correction are also shown in Fig. 11a. Wundt (39) has arrived at similar curves for cylindrical notched bars by using experimental data which indicate notch strengthening in the ductile range.

The proposed Neuber brittle fracture concept is in agreement with experimental data even for very shallow notches as can be seen in Fig. 11b, where the relationship $\sigma\sqrt{c}$ is examined for the Neuber concept.

For simplicity the interrelationship of the strength parameters is examined for the infinite plate case originally treated by Griffith, i.e. an elliptical crack of length 2c in an infinite plate. The stress for onset of brittle fracture according to Griffith is given by

$$\sigma = \frac{2E(T+P)}{\pi c} = \frac{E\mathcal{G}_c}{\pi} = \frac{K}{\sqrt{\pi c}} = \frac{\chi}{\sqrt{c}}$$

where the symbols are the same as used above except that K is the Westergaard stress intensity factor which equals $\sqrt{E}$ and is $K/\sqrt{\pi}$. According to Neuber's brittle fracture concept the stress at fracture is given by

$$\sigma = \frac{\sigma_{max}\sqrt{r+2\eta}}{2\sqrt{c}}, \quad (r+2\eta) \ll 4c$$

A relationship between the constants and the parameters of both concepts is obtained by equating the two fracture conditions and results in

$$\sigma_{max}\sqrt{r+2\eta} = 2\sqrt{\frac{2E(T+P)}{\pi}} = 2\frac{E\mathcal{G}_c}{\pi} = \sqrt{\frac{2K_c}{\sqrt{\pi}}} = 2\chi$$

It can be seen that the corrected surface tension of the Griffith concept $(T+P)$, or the critical energy release rate of Irwin, etc., have their analog in the term $(r+2\eta)$ of the Neuber concept. If it is assumed that the "equivalent particle size" is a material constant then the material constant of the Griffith approach becomes a function of r of the type

$$(T+P) = A \cdot r + B$$

which only assumes a constant value when r vanishes.

It was mentioned that in contrast to the one parameter Griffith approach the Neuber approach is a two-parameter concept. This is only true in the strict mathematical sense. If looked at with a Griffith viewpoint,

the Neuber approach is a three-parameter concept, the root radius being the third parameter, which is just another way of saying that $(T \pm P)$ becomes a function of r and that the fundamental relationship $\sigma\sqrt{c}$ = constant holds not only for extremely sharp notches but also for notches having moderate root radii, provided that r is kept constant and $(r + 2\eta)$ 4c.

The equivalence of the two concepts for the condition of vanishingly small root radii and the experimental agreement obtained for the Neuber concept for both mild and sharp notches justify the hope that it is possible to develope a unified macroscopic fracture concept for the entire range of brittle fracture i.e. not only for cracks but also for milder notches. This unified concept will probably not be the Neuber concept in its presented form. It will have to include the effect of stress gradient, perhaps to the extent that σ_{max} becomes a function of the stress gradient, in order to account for the observed size effect.

CRACK PROPAGATION

The above treatment concerned fracture initiation. However, the theoretical means used pertain to crack propagation i.e. the growth of a crack through its velocity transition point. A proper treatment of crack initiation belongs in the field of the micromechanism of fracture which goes beyond the scope of this session. It is, however, justifiable to treat fracture initiation with a crack propagation concept because the energies involved in bringing the crack towards its critical size are, in real materials, plastic flow contributions which are in all likelyhood related to the material only. A totally elastic solid would only fracture under the cohesive strength. Cracks present in such solids would not propagate (at absolute zero) until the stress at the tip of the crack equals the cohesive strength, or until the Griffith condition is fulfilled (for which the true surface tension T has to be used).

In macromechanic terms, the question of crack propagation relates to the velocity of a spreading crack before and after the occurrence of instability. For an ideally elastic solid, not much can be said about the crack extension prior to the velocity transition point except that thermal energy fluctuations might be sufficient to cause some slight extension of the crack. These have been calculated and are found to contribute little for ordinary temperatures of interest. In order to obtain an estimate of the crack velocity after the transition to fast fracture assumptions concerning the kinetic energy have to be made. With the help of such assumptions Mott (40) calculated the velocity of a Griffith crack as

$$v = \left[\frac{E}{\gamma}\left(\frac{4\pi}{K} - \frac{8E^2T}{cK\sigma\gamma}\right)\right]^{1/2}$$

where ζ is the density of the material and k a dimensionless constant. For metals the plastic work factor P may be introduced rigorously by simply adding it to the surface tension T. Thus, for metals, once a fast crack has started it can only come to a stop if a sudden increase in P occurs. This has been verified by Tipper (41) who intitiated a sudden fracture in a brittle area and had it propagate into a ductile area. The crack stopped in the ductile area with considerable plastic deformation and generation of heat. Similar experiments were made by Robertson (42) in order to study crack propagation transition temperature. As v approaches the velocity of sound, Mott's analysis (static elasticity) breaks down. Yoffe (43) has shown that at high velocities (1/2 the velocity of elastic shear waves) a shock wave builds up in front of the running crack causing a nearly equal stress distribution over a wide arc in front of the running crack. This causes the crack to branch, a phenomenon frequently observed (44). Studies have also shown that P decreases with increasing crack velocity (5). Wells and Post (45) have shown with the help of photoelasticity that little change is observed in the stress system ahead of a running crack as compared to a static crack. Frankland (46) in his calculations however, points out that the degreee of biaxiality increases with crack velocity which in turn increases the plastic constraint ahead of the crack and thus increases the stress required for the occurrence of yielding. Later in this session Mr. Bluhm will present new and interesting experimental results concerning crack propagation and the effect of a changing stress state on such propagation.

Recently, Newhouse and Wundt (47) have devised a test which is intended to reveal a material's susceptibility to crack propagation only. In their proposed test easy fast-crack initiation is facilitated by nitriding the notched section of a Charpy-type impact test bar or a notched tensile test bar. The energy absorption of such tests is then largely due to the energy consumed for crack propagation.

So much for crack propagation once the velocity transition has occurred. While little can be said for an elastic solid about the propagation of an existing crack prior to the velocity transition, it is known that slow propagation always precedes sudden fracture in technical materials. This is due to the ductility of such materials. The energy available to cause plastic flow and the creation of cavity dislocation, i.e. the development of cracks, is proportional to the elastic strain energy release due to the presence of a crack. This energy release $\mathcal{G}$, a function of the applied stress and the crack geometry, can also be interpreted as causing the force which tends to spread the crack. It may therefore be assumed that constant rate of slow propagation of a crack is obtained if $\mathcal{G}$ or K is held constant by continuously decreasing the applied stress by amounts proportional to the square root of c. The value of $\mathcal{G}$ selected for such experiments must be less than the critical strain energy release rate $\mathcal{G}_c$ which defines the onset of sudden crack propagation. Professors Corten and Carpenter are presently investigating the validity of such assumptions for the slow growth of fatigue cracks. The results of these studies will be presented here by Dr. Corten.

It is hoped that the review presented covered the major fields of interest to this group in a critical and unbiased fashion. Much of the experimental evidence in support or disproof of the concepts presented had to be deleted in order to keep within the time limits allotted. If some of the well known and widely discussed aspects of Dr. Irwin's contributions were treated only briefly it is because the author feels that the lesser known European work is badly in need of discussion.

Finally, it appears that the long and hard efforts by distinguished research workers in this area are bearing fruit and that much progress has been made towards the goal of establishing design criteria for optimum utilization of presently existing materials.

This paper was prepared with the help of Dr. George Sachs and Mr. J. G. Sessler to whom the author is deeply indebted. Some of the experimental and theoretical work referred to was conducted at Syracuse University under the sponsorship of the following government agencies: U. S. Navy Bureau of Weapons, Atomic Energy Commission and Wright Air Development Division.

BIBLIOGRAPHY

1. Lame, Navier, Memoire Sur l'equilibre interieu des corps solides homogenes; Paris Mem. Par. divers savants. t. 4 (1833).

2. Ludwik, P., Elemente der Technologischen Mechanik, Berlin (1909).

3. Griffith, A. A., The Phenomenon of Rupture and Flow in Solids, Phil. Trans. Roy. Soc., Series A, Vol. 221, p. 163 (1921).

4. Orowan, E., Energy Criteria of Fracture, Weld. Res., Vol. 20, p. 157-S (1955).

5. Hall, E. O., The Brittle Fracture of Metals, Mech. Phys. Solids, Vol. 1, No. 4, p. 227 (1953).

6. Irwin, G. R., Fracture, in book Handbuch der Physik, Band VI, Elastizitaet und Plastizitaet, Springer Verlag, p. 551-580 (1958).

7. Beeuwkes, R. Jr., Plasticity and Fracture, Proc. of the Third Sagamore Conference on Materials Evaluation in Relation to Component Behavior, p. 89-152 (1956).

8. Cottrell, A. H., Theoretical Aspects of Fracture, in book Fracture Technology Press, p. 20-53 (1959).

9. Mott, N. F., Fracture in Metals, J. Iron Steel Inst. Vol. 183, p. 233-243 (1956).

10. Stroh, A. N., A Theory of the Fracture of Metals, Advances in Physics, Vol. 6, p. 418-465 (1957).

11. Averbach, B. L., Felbeck, D. K., Hahn, G. T. and Thomas, D. A. (Editors), Fracture, Technology Press (1959).

12. Cottrell, A. H., Theory of Brittle Fracture in Steel and Similar Metals, Trans. Met. Soc. A.I.M.E., Vol. 212, p. 192-203 (1958).

13. Westergaard, H. M., Bearing Pressures and Cracks, Trans. A.S.M.E. Vol. 61, p. A.49-A.53 (1939).

14. Irwin, G. R. and Kies, J. A., Fracture Theory as Applied to High-Strength Steels for Pressure Vessels, Golden Gate Metals Conference, San Francisco, (1960).

15. Irwin, G. R. and Kies, J. A., Fracture Theory Applied to High-Strength Steels, Metal Progress, Vol. 78, p. 73-78 (1960).

16. Lubahn, J. D., On the Applicability of Notch Tensile Data to Strength Criteria in Engineering Design, Trans. ASME, Vol. 79, p. 111 (1957).

17. Lubahn, J. D., Correlation of Tests Using the Congruency Principle, Proc. A.S.T.M., Vo. 58, p. 678-684 (1958).

18. Fracture Testing of High-Strength Sheet Materials; A Report of a Special A.S.T.M. Committee; A.S.T.M. Bulletin, p. 29-51,Jan. and Feb. (1960).

19. Srawley, J. E. and Beachem, C. D., Crack Propagation Tests of Some High-Strength Sheet Steels, N.R.L. Report 5263 (1959).

20. Winne, D. H. and Wundt, B. M., Application of the Griffith-Irwin Theory of Crack Propagation to the Bursting Behavior of Disks, Including Analytical and Experimental Studies, Trans. A.S.M.E. Vol. 80, p. 1643-1658 (1958).

21. Neuber, H., Kerbspannungslehre, Springer Verlag (1958).

22. Peterson, R. E., Stress Concentration Design Factors, John Wiley (1953).

23. Sachs, G. and Sessler, J. G., Effect of Stress Concentration on Tensile Strength of Titanium and Steel Alloy Sheet at Various Temperatures, Am. Soc. Testing Mats. Preprint 76a (1960).

24. Sachs, G., Weiss, V. and Klier, E. P., Effects of a Number of Heat-Treating and Testing Variables on the Notch Strength of 4340 Steel, Trans.Am.Soc.Test.Mats. (1956)

25. Sachs, G., Sessler, J. G., Pray, R. F. and Yeh, T. H., Relations Between the Notch Tensile Strength of Cylindrical and Prismatic Specimens of Titanium Alloys and Heat-Treated Steel, Basic Engr., June (1960).

26. Sachs, G., Sessler, J. G. and Brown, W. F. Jr., Influence of Stress Concentrations at Elevated Temperature, Am. Soc. Test. Mats. STP 260 (1959).

27. Weiss, V., Sessler, J. G., Packman, P. and Sachs, G., The Effect of Several Geometrical Variables on the Notch Strength of 4340 Steel Sheet Heat-Treated to Three Strength Levels, WADD Tech. Rep. 60-310 (1960).

28. Yen, C. S. and Dolan, T. J., A Critical Review of the Criteria for Notch Sensitivity in Fatigue of Metals, University of Illinois Engineering Experiment Station, Bulletin Series No. 398 (1952).

29. Wolf, H., The Determination of the Stress Gradient Index for Notched Structures, Forschungsarbeit, Ver. Deutsch. Ing. Vol. 25, p. 63 (1959).

30. Sachs, G., Gerberich, W. W. and Weiss, V., Low Cycle Fatigue of Pressure Vessel Materials, submitted to Am. Soc. Test. Mats. (1960).

31. Lotsch, K., Contribution to the Mechanics of Stresses During Constrained Deformation (German), Oesterr, Ingenieur Archiv., Vol. 13, p. 191 (1959).

32. Neuber, H., Research on the Distribution of Tension in Notched Construction Parts, Final Report WADD No. AF 61(514)-1111.

33. Stowell, E. L., Stress and Strain Concentration at a Circular Hole in an Infinite Plate, NACA TN 2073 (1950).

34. Hardrath, H. F. and Ohman, L, A Study of Elastic and Plastic Stress Concentration Factors Due to Notches and Fillets in Flat Plates, NACA TN 2566 (1951).

35. Grubin, A. N. and Likhachev, V. I., Analysis of Stresses Developing in the Stage of Large Plastic Deformations in Tension Tests of Cylindrical Specimens with Circular Notches, Zhurnal Teknicheskay Fiziki, Vol. 25, p. 512-528 (1955).

36. Uzhik, G. V., Tensile Strength of Metals (1950) in Russian.

37. Mirkin, I. L. and Trunin, I. I., An Investigation of Creep and Failure of Steel in Zone of Stress Concentration, Trudy Tsentral 'nyy Nauchno - Issledovatel 'skiy, Institut Teknologii i Mashinostroenii, Vol. 79, p. 24-35 (1957).

38. Sessler, J. G., Grewal, K. S., Weiss, V., Sachs, G., Investigation of the Effects of Stress Concentrations and the Cracking Tendency of Heat-Treated Titanium and Steel Sheet Alloys, Bur. Aer. No. NOas 58-855C, Progress Rep. 5, October (1959).

39. Wundt, B. M., A Unified Interpretation of Room-Temperature Strength of Notched Specimens as Influenced by Their Size, Am. Soc. Mech. Eng., Paper 59-Met.-9 (1959).

40. Mott, N. F., Fracture of Metals: Theoretical Considerations, Engineering, Vol. 165, p. 16-18 (1948).

41. Tipper, C. F., Unpublished, Admiralty Ship-Welding Committee Report (1951).

42. Robertson, T. S., Propagation of Brittle Fracture in Steel, J. Iron Steel Inst. (London), Vol. 175, p. 361-374 (1953).

43. Yoffe, E. H., The Moving Griffith Crack, Phil. Mag. Ser. 7, Vol. 42, p. 739-750 (1951).

44. Orowan, E., Fundamentals of Brittle Behavior in Metals, Fatigue and Fracture of Metals, John Wiley, p. 139-167 (1952).

45. Wells, A. A. and Post, D., The Dynamic Stress Distribution Surrounding a Running Crack - A Photoelastic Analysis Proc. Soc. Exp. Stress Analy., Vol. 16, p. 69-96 (1958).

46. Frankland, J. M., Triaxial Tension at the Head of a Rapidly Running Crack, Trans. Am. Soc. Mech. Eng., Appl. Mech. Paper No. 59-APM-11.

47. Newhouse, D. L. and Wundt, B. M., A New Fracture Test for Alloy Steels, Metal Progress, Vol. 78, p. 81 (1960).

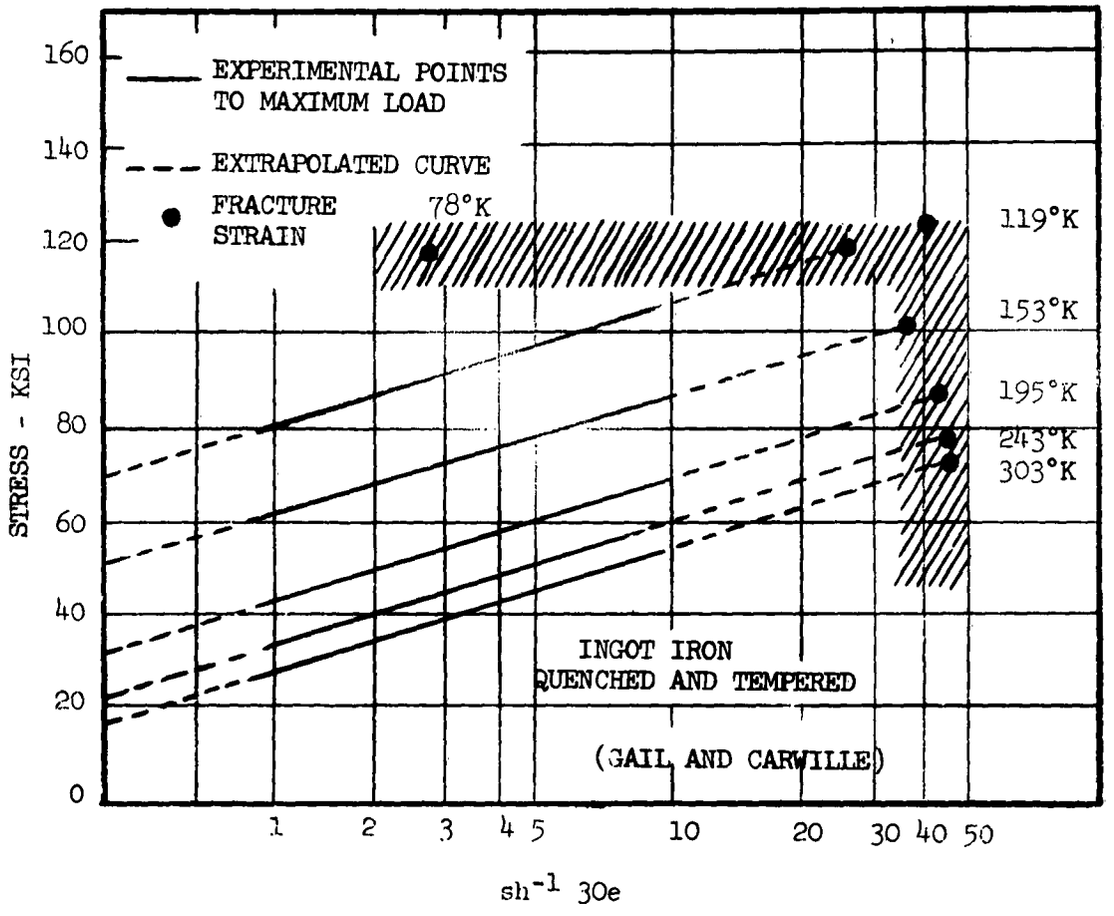


FIG. 1 STRESS-STRAIN-FRACTURE DIAGRAM FOR INGOT IRON, QUENCH TEMFERED

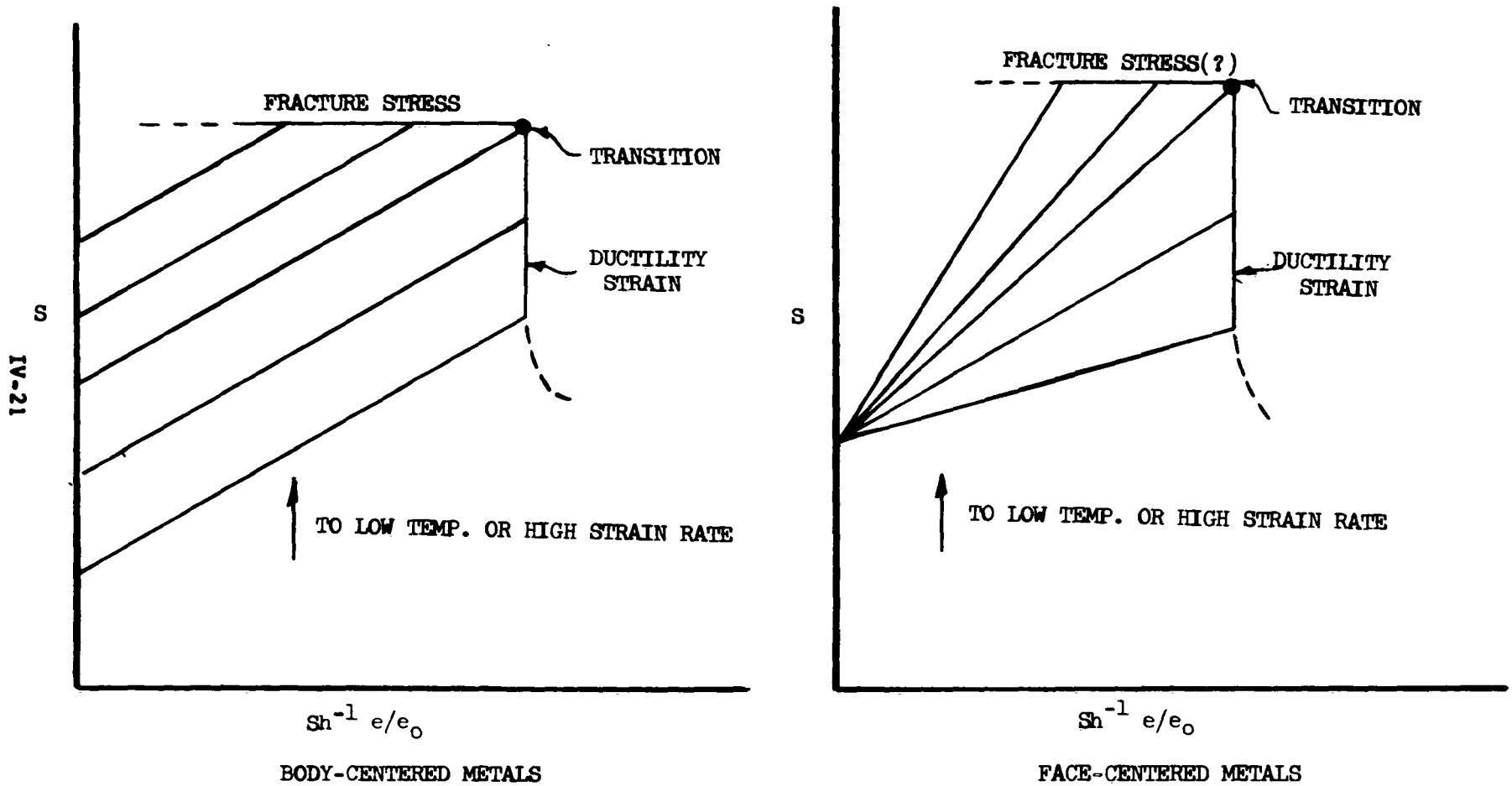


FIG. 2 TRUE STRESS-STRAIN CURVES

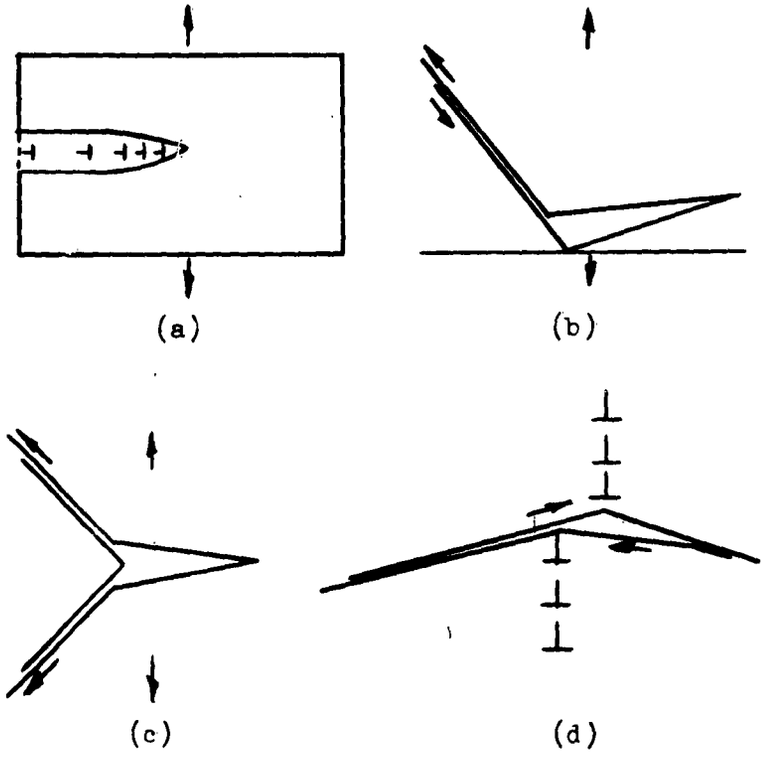


FIG. 3 DISLOCATIONS AND CRACKS (a) ELASTIC CRACK REGARDED AS PILE-UP OF EDGE DISLOCATIONS (b) CRACK FORMED FROM PILE-UP AGAINST A BOUNDARY (c) CRACK RESULTING FROM SHEAR ON TWO BANDS (d) CRACK FORMED AT A TILE BOUNDARY

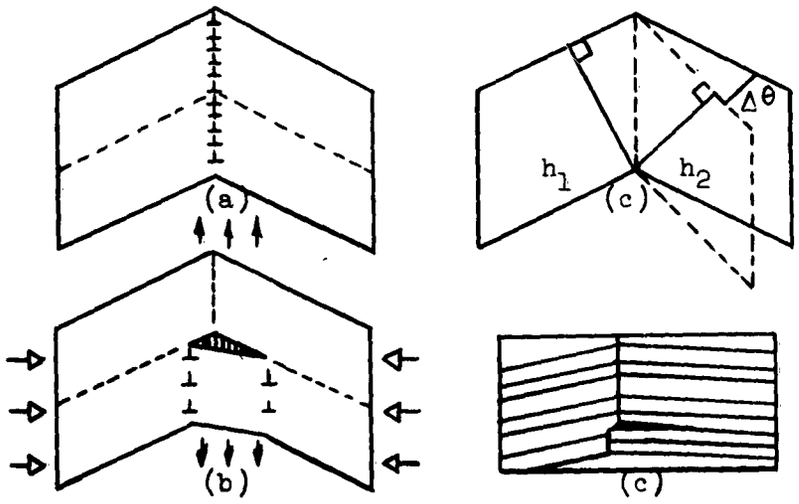
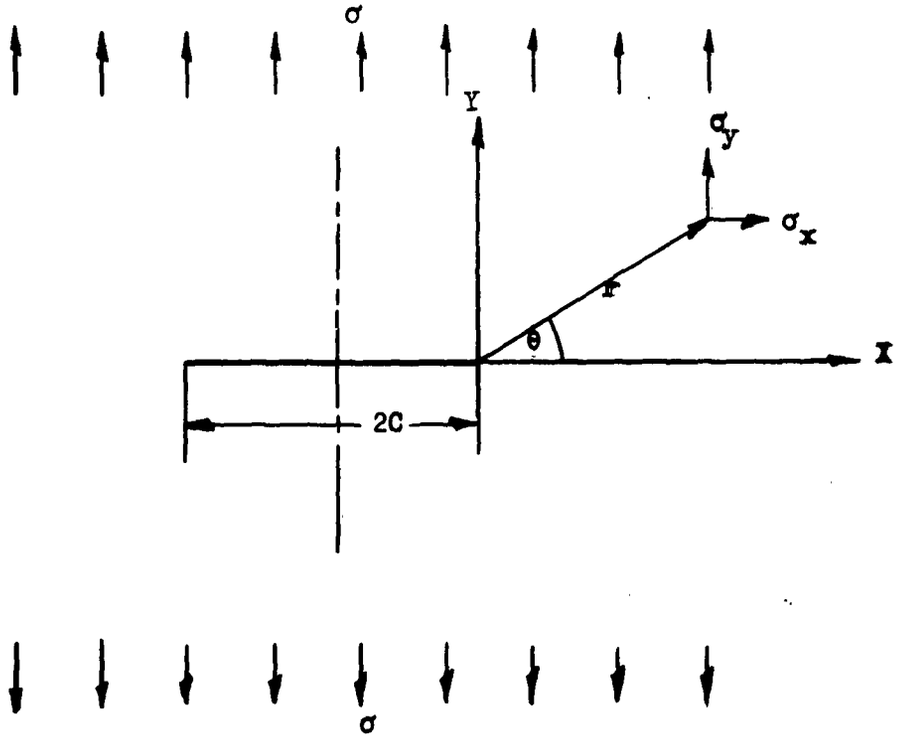


FIG. 4 FORMATION OF CRACKS AT KINK PLANES IN ZINC



$$\sigma_y = \frac{K}{\sqrt{2\pi r}} \cos\frac{\theta}{2}\left[1 + \sin\frac{\theta}{2}\sin\frac{3\theta}{2}\right]$$

$$\sigma_x = \frac{K}{\sqrt{2\pi r}} \cos\frac{\theta}{2}\left[1 - \sin\frac{\theta}{2}\sin\frac{3\theta}{2}\right] - \sigma_{ox}$$

FIG. 5 CRACK GEOMETRY AND STRESS DISTRIBUTION ACCORDING TO WESTERGAARD

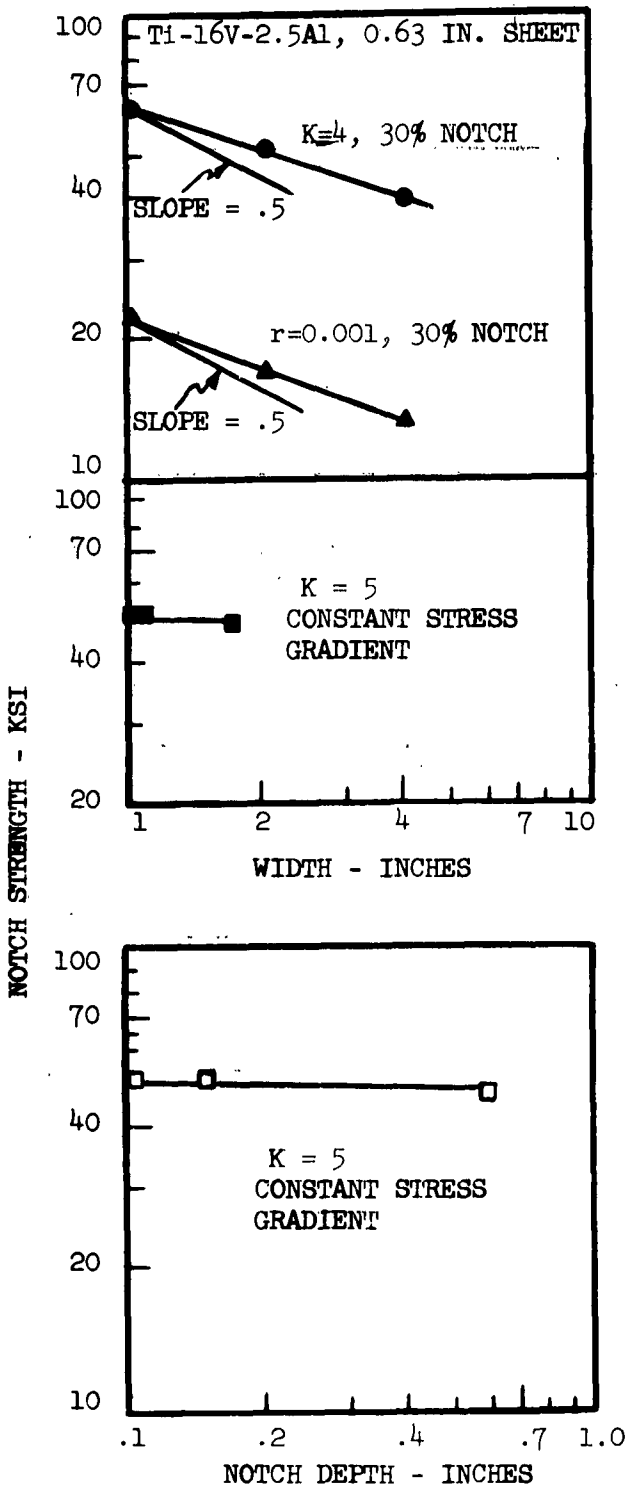


FIG. 6 EFFECT OF SPECIMEN WIDTH ON THE NOTCH STRENGTH OF A BRITTLE TITANIUM ALLOY

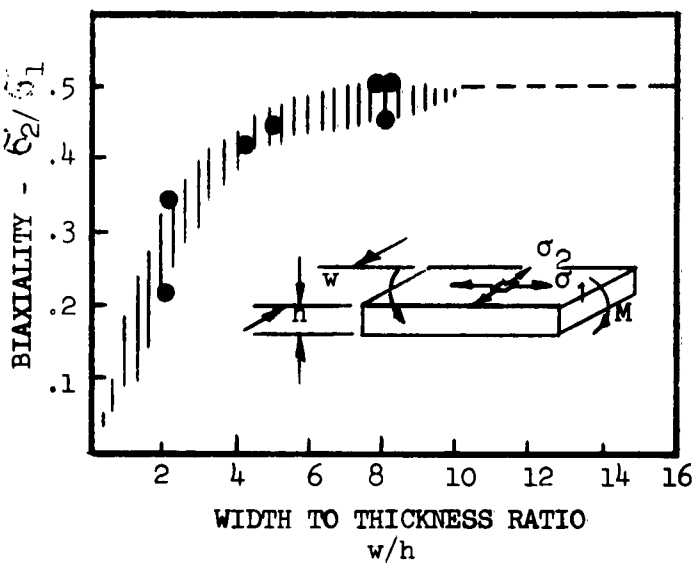
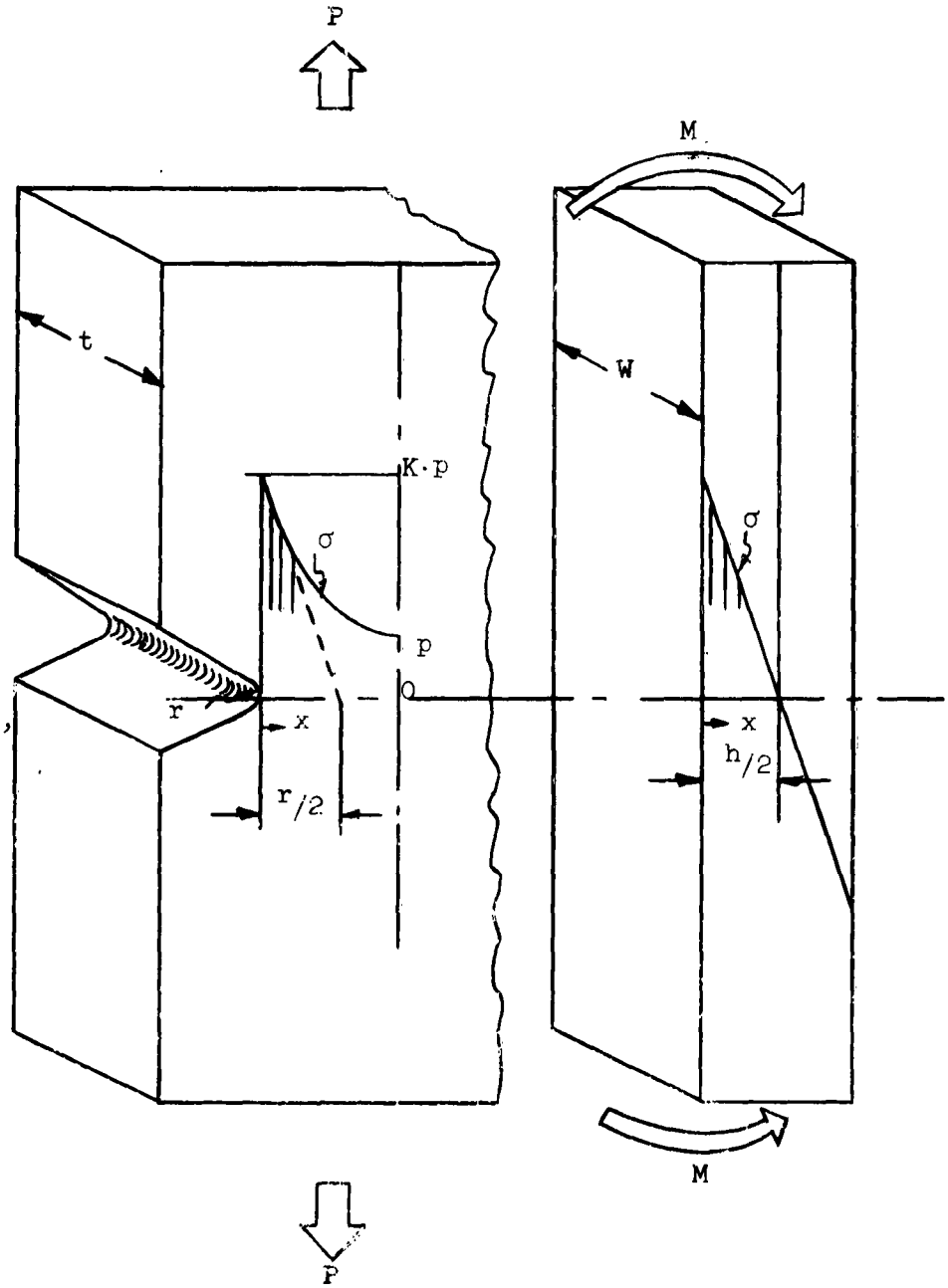


FIG.7 EFFECT OF WIDTH TO THICKNESS RATIO ON THE BIAXIALITY OF BEND SPECIMENS



$$\frac{\delta\sigma}{\delta x} = \frac{\sigma_{max}}{r/2} \qquad \frac{\delta\sigma}{\delta x} = \frac{\sigma_{max}}{h/2}$$

BIAXIALITY DEPENDS ON	t/r	w/h

FIG. 8 ANALOGY BETWEEN THE STRESS STATES IN SMOOTH BEND AND NOTCH TENSILE SPECIMENS TO ESTIMATE STRESS BIAXIALITY AT CENTER OF NOTCH ROOT

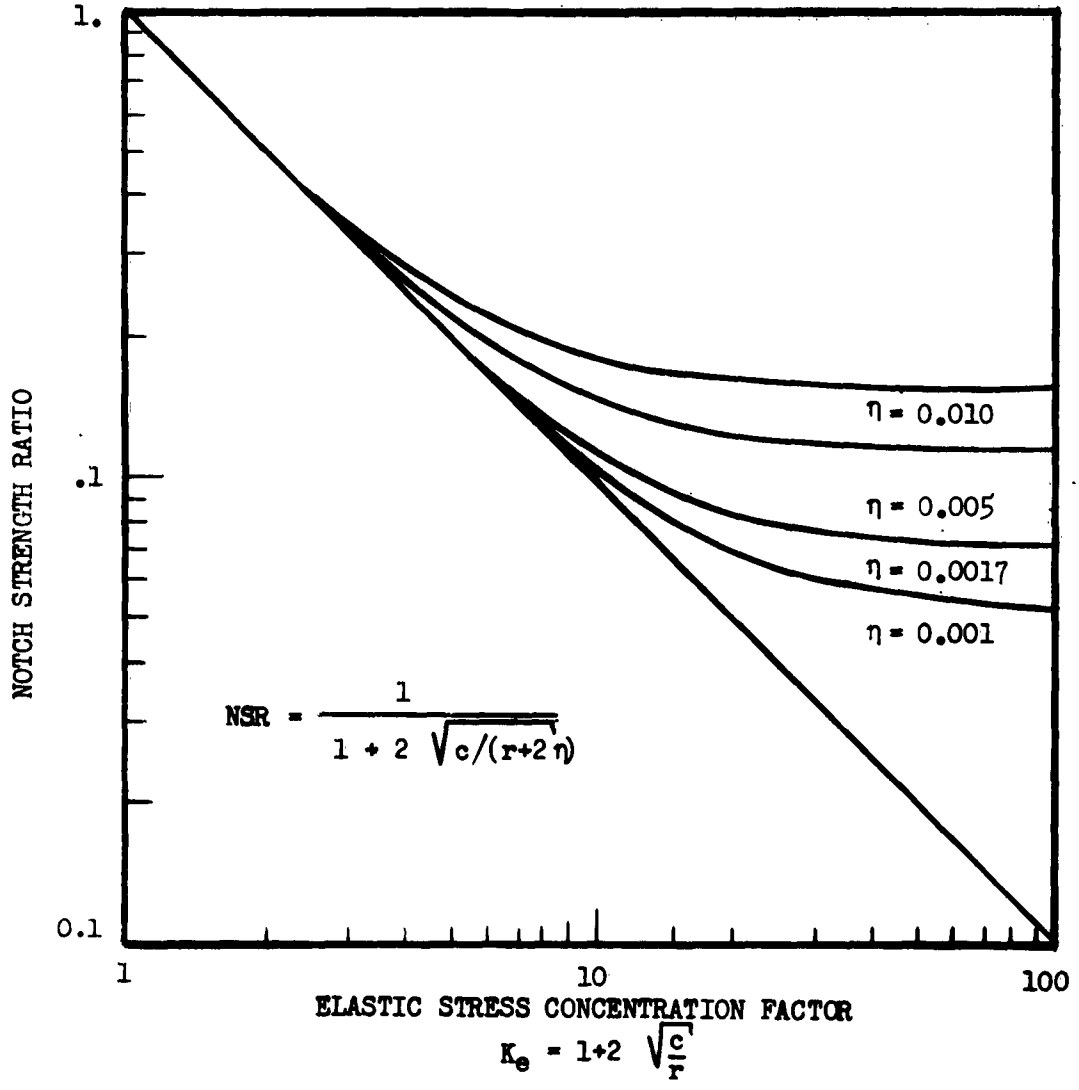


FIG. 9 EFFECT OF THE EQUIVALENT PARTICLE SIZE η ON THE NSR VS. K CURVE OF A BRITTLE MATERIAL -(CALCULATED)

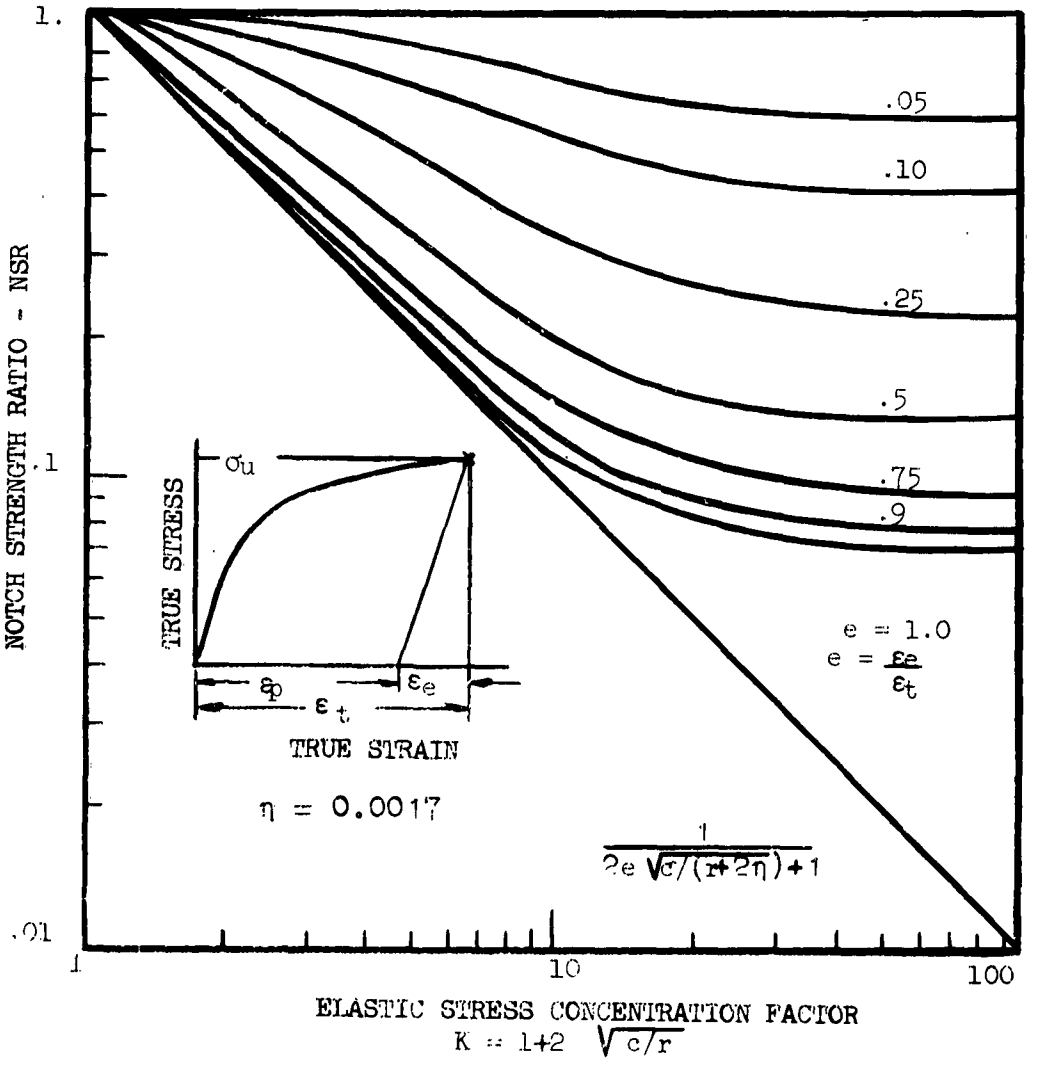


FIG. 10 EFFECT OF PLASTICITY CORRECTION ON THE NSR VS. K CURVE. EQUIVALENT PARTICLE SIZE η AS INDICATED.

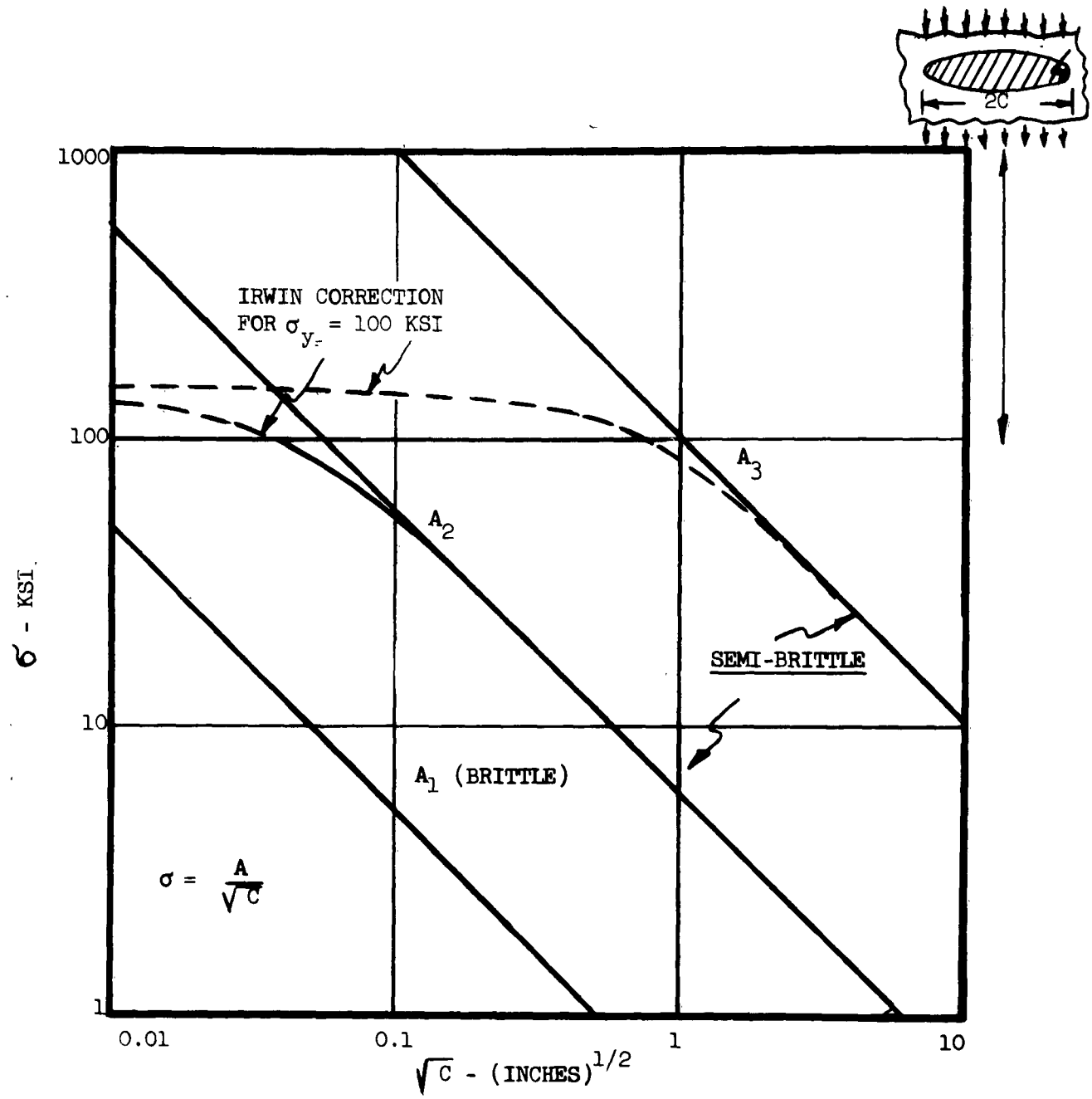


FIG. 11a GRAPHIC REPRESENTATION OF SUGGESTED RELATIONS BETWEEN STRENGTH OF AN INFINITE PLATE WITH AN ELLIPTICAL CRACK OR HOLE

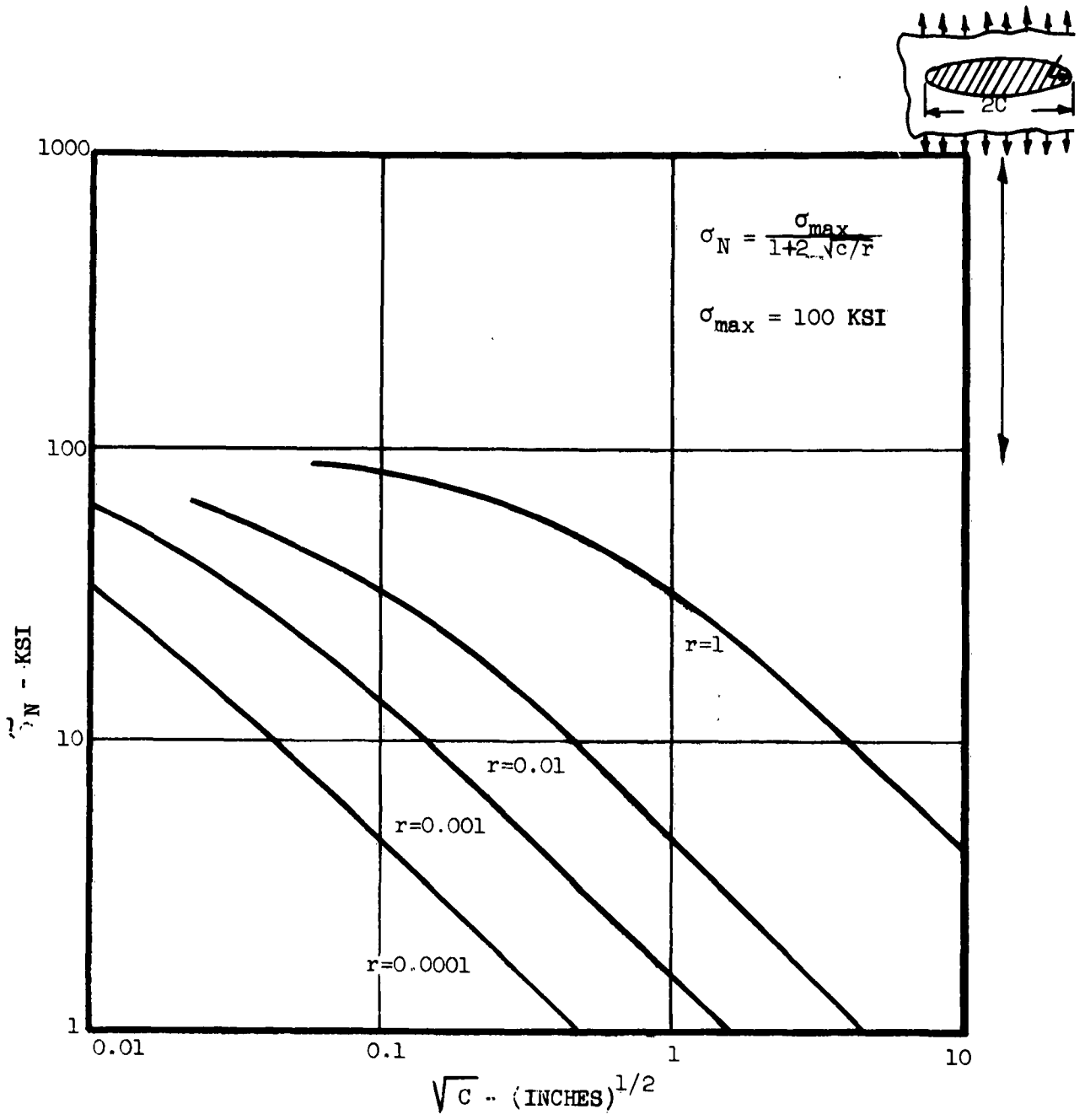


FIG. 11b GRAPHIC REPRESENTATION OF SUGGESTED RELATIONS BETWEEN STRENGTH OF AN INFINITE PLATE WITH AN ELLIPTICAL CRACK OR HOLE

TABLE I

GRIFFITH - IRWIN FRACTURE MECHANICS

INFINITE PLATE	$\mathcal{G} = \frac{\pi\sigma^2 c}{E}$	$K = \sigma\sqrt{\pi c}$
FINITE PLATE	$\mathcal{G} = \frac{\sigma^2 b}{E} \tan\frac{\pi c}{b}$	$K = \sigma\sqrt{b \tan\frac{\pi c}{b}}$
PENNY - SHAPED CRACK	$\mathcal{G} = \frac{\sigma^2 c \, 4(1-\nu^2)}{\pi E}$	$K = \sigma\sqrt{\frac{4c(1-\nu^2)}{\pi}}$

BEHAVIOR OF A BRITTLE METAL

John G. Sessler
Syracuse University

Analyses of the behavior of solids based on the theory of elasticity assume the existence of an "idealized material" which is presumed to be isotropic, homogeneous and perfectly elastic. It is known, however, that the engineering metal alloys presently available for structural use are not idealized materials. They seldom exhibit complete isotropy and even the strongest alloys are far from being perfectly elastic at room temperature.

In the presence of stress concentrations, even a small amount of plastic flow prior to failure may cause a considerable readjustment of the initial elastic stress distribution and thereby influence the fracture strength. Therefore, the application of concepts based on the theory of elasticity to predict the failure strength of these alloys must necessarily be subject to modifications or plasticity correction factors.

To date, there is little evidence available on how closely a metal may approach a perfectly elastic and fully brittle state under certain conditions. This state is somewhat difficult to determine, since brittleness depends not only on the basic properties of the material but also on other factors such as the state of stress or strain, stress gradient, section size, strain-rate, temperature, and possibly on other factors as yet unrecognized. High strength steel sheet alloys appear to approach an extremely brittle state, at very low temperatures if their ultimate tensile strengths exceed about 300,000 psi, and possibly also at room temperature if untempered or high in carbon. Refractory metals and cermets are also known to be brittle under most conditions. The behavior of such materials, particularly in the presence of stress concentrations, is of considerable interest to both metallurgists and engineers.

In this paper, experimental notch strength data acquired for materials differing widely in ductility will be presented and analyzed according to some of the theoretical concepts discussed by Dr. Weiss.

Recently, at Syracuse University, some of the heat treatable titanium sheet alloys were found to be extremely sensitive to the strength-reducing effects of stress concentrations when tested in critically aged conditions. The most sensitive alloy investigated was Ti-2.5Al-16V, aged at 700F for 8 hrs.* It was decided to further explore the behavior

---

* Normally this alloy is used in an overaged condition obtained by aging at 990F for 4 hrs.

of this alloy for various stress concentrations to determine how closely it would conform to the maximum principal stress theory combined with Neuber's theory of finite stress concentrations (1).

Four series of tensile tests were conducted on 1 in wide sheet specimens aged at 700F for either 4 or 8 hrs. Three series were performed on 0.063 in sheet and the fourth series on 0.125 in sheet. Stress concentrations were introduced by means of two symmetrical edge-notches with 60 degree flank angles, constant notch depths of 30 percent, and various root radii from 0.001 to 0.070 in. A few smooth specimens and very mild notched specimens were also tested. The geometries employed resulted in theoretical elastic stress concentration factors (K_t) from unity to about 17, according to Neuber's equations for arbitrary notches (1) (2).

Neuber's Concepts

If the maximum principal stress theory is assumed to be valid, the strength values for elastic materials should conform to the following relationship

$$\sigma_N = \frac{\sigma_u}{K_t} \qquad [1]$$

where σ_N = average stress at failure or "notch strength"

σ_u = a constant, equivalent to the strength of a smooth specimen

K_t = Neuber's elastic stress concentration factor for an arbitrary notch, as given by Peterson (2).

The conformance of the test data to Equation [1] is best illustrated in a log-log representation of notch strength (σ_N) versus K_t, where the equation is represented by 45 degree parallel straight lines. Fig. 1 presents the test data for the four presumably brittle alloy conditions, differing slightly in chemistry and heat treatment. Three of these conditions (Heats A and C, aged 8 hrs and Heat B, aged 4 hrs) appear to conform to Equation [1] for the range of stress concentration values from unity to about 8.

At K_t values greater than 8, the notch strength remains substantially constant. A possible explanation for this deviation from a straight line at high K_t factors is the concept proposed by Neuber (3) for "pointed notches", which was previously discussed by Dr. Weiss. Neuber has recognized the inability of metals to retain

extremely high stress concentrations and has suggested the addition of a material constant η to the radius, r, to account for the reduction in K. Values of η between 0.001 and 0.002 in were found to correct the data reasonably well for the entire range of K factors.

Since the data for mild and intermediate notches seem to conform to Equation [1], it is believed that these alloys approach the behavior of an elastic solid more closely than any metal investigated to date.

The test data for one of the four alloy conditions investigated (Heat A, aged 4 hrs) also deviates from Equation [1] in the range of mild and intermediate notches, and exhibits higher notch strength values. A tentative explanation for these variations is that relatively small changes in aging temperature or time appear to result in a material that is underaged, with a corresponding increase in ductility.

Engineering structural alloys are considerably more ductile at room temperature than the alloys represented in Fig. 1, and their notch strength is substantially higher. This is illustrated in Fig. 2a for several titanium sheet alloys*. The N.S.R.** versus K curves for these alloys form a rather uniform family of curves which aids in simplifying the analyses.

To explain the notch strength behavior of relatively ductile materials, first a correction should be applied for ductility. Second, it must be recognized that the uniaxial stress state in a smooth tensile test is replaced by biaxiality and triaxiality in the notched section. These factors must be combined with the previously discussed "pointed notch" correction.

A plasticity correction is obtained theoretically by replacing the elastic stress concentration by a smaller value, the difference in the two values depending on the ratio of elastic deformation to total deformation. A family of theoretical plasticity correction curves for a given value of η are shown in Fig. 2b.

---

* Heat treated titanium sheet was chosen for this representation for it has been shown that they do not normally exhibit the sharp transition with temperature observed for many high strength steels. At temperatures close to the transition, the effects of strain-rate and biaxiality are greatly magnified and these tend to further complicate the overall shape of the σ_N versus K curves.

** Ratio of notch strength to ultimate tensile strength or "notch-strength-ratio".

A comparison of Fig. 2a with 2b still indicates considerable differences at low and intermediate K factors. To explain these, the effects of the shift from uniaxial to multiaxial stress states with increasing K factors should be analyzed.

Griffith's Concept

According to the concept proposed by Griffith in 1920 (4), the condition for spontaneous crack extension is given by the relationship

$$\sigma = \sqrt{\frac{2ET}{\pi c}} \qquad [2]$$

where σ = applied average stress at a distance from the crack

c = one-half the initial crack length

T = surface tension per unit area

E = Young's modulus

This concept was also discussed previously by Dr. Weiss.

Equation [2] suggests that the fracture stress of a specimen containing a crack length 2c is inversely proportional to the square root of c, provided that the crack length is small when compared to the specimen width.

Two series of tests were performed to determine if the brittle titanium sheet alloys (Heat A, aged for 4 hrs and 8 hrs, respectively) would conform to Equation [2]. The specimens employed for these series were 1 inch in width and contained different initial crack lengths from 0.005 to 0.350 inch. Cracks were simulated by edge-notches with 0.001 in. root radii.

The test results are presented in Fig. 3 as σ versus $\sqrt{c}$. The data for both aged conditions fall on a straight line as predicted by Equation [2], except for crack lengths exceeding one half the specimen width.

Based on the limited data obtained in these studies, the behavior of the sheet alloy, Ti-2.5Al-16V (aged at 700F for 8 hrs), appears to be in general conformance with the concepts for elastic materials as proposed by Neuber and Griffith. Neuber's concepts may be applied to the entire range of stress concentration factors.

It is recognized that the behavior of materials, in the presence of stress concentrations, is also influenced by many factors such as stress gradient, section size, section thickness, strain-rate, temperature, and other factors not considered in these investigations. Close agreement between theoretical concepts and experimental data for all alloys cannot be expected until the effects of all these pertinent parameters are well established.

REFERENCES

1) H. Neuber, "Theory of Notch Stresses", Springer, Berlin, (1937).

2) R. E. Peterson, "Stress Concentration Design Factors", John Wiley and Sons, New York, (1953).

3) H. Neuber, "Theory of Notch Stresses", Springer, Berlin, 2nd Ed., (1958) in German.

4) A. A. Griffith, "The Phenomenon of Rupture and Flow in Solids", Phil. Trans. Roy. Soc. of London, Ser. A221 (1920) pp 163-198.

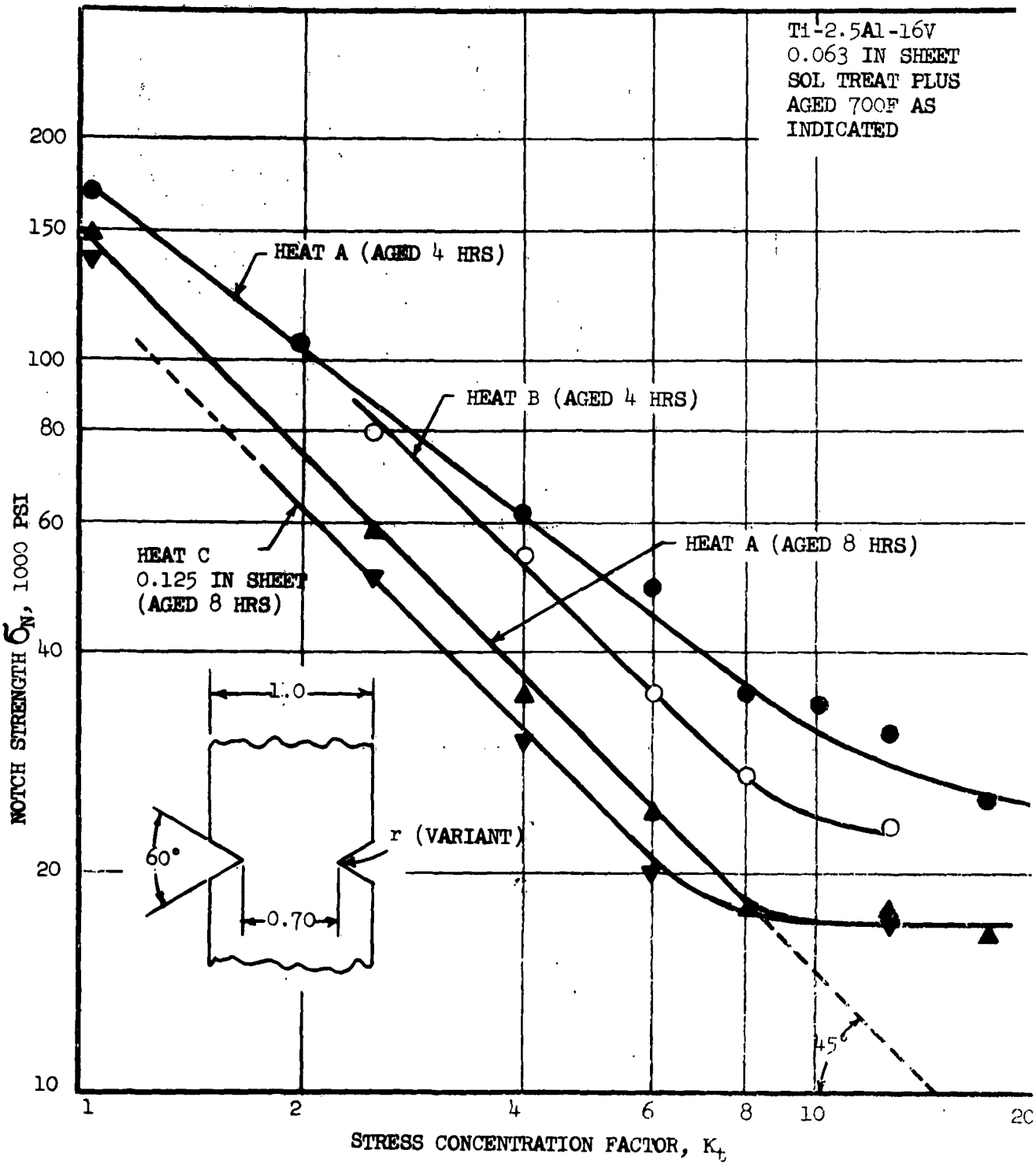


FIG. 1 NOTCH STRENGTH OF BRITTLE TITANIUM ALLOYS AT VARIOUS K_t FACTORS (LOG-LOG REPRESENTATION)

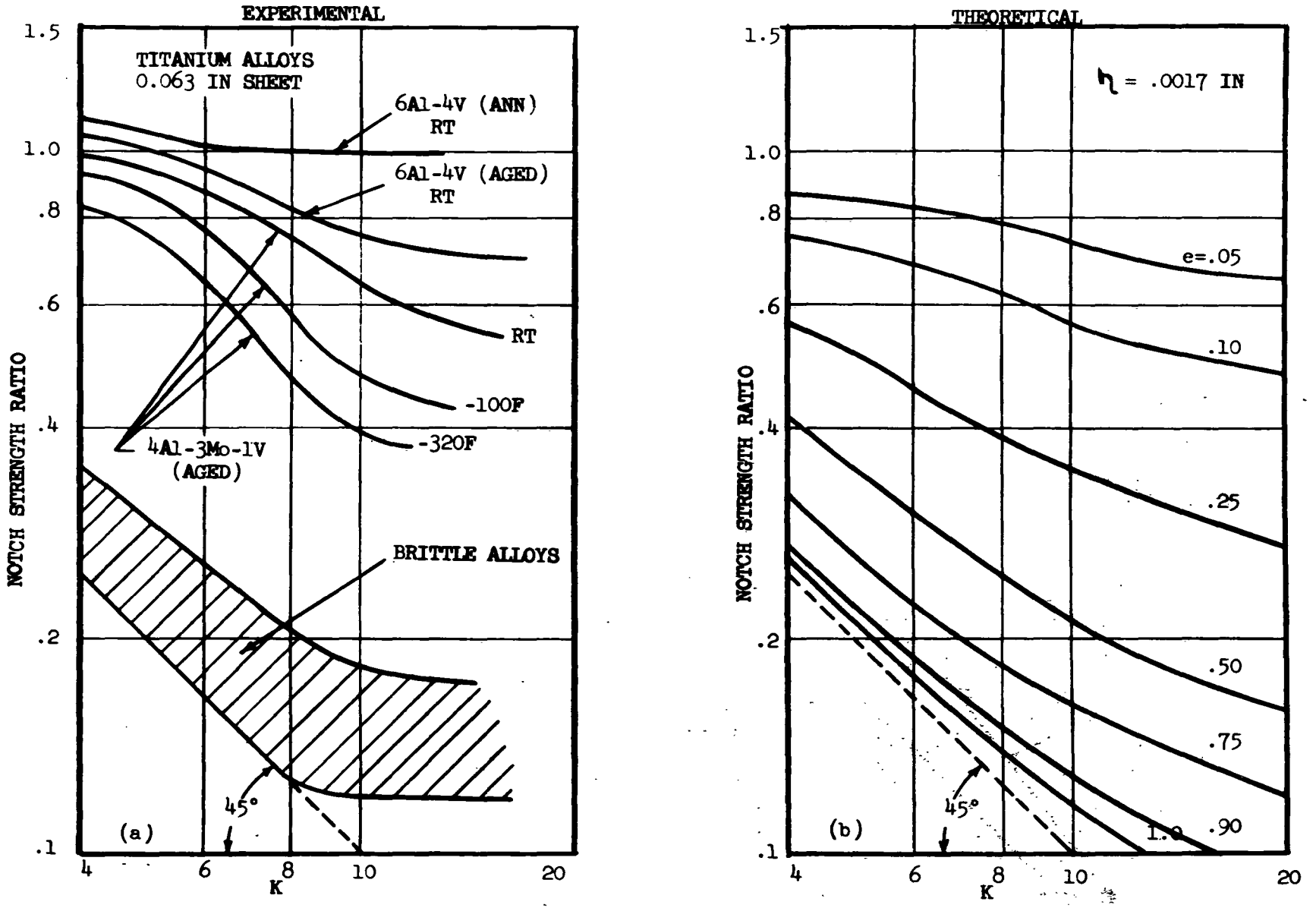


FIG. 2 COMPARISON OF EXPERIMENTAL CURVES AND THEORETICAL CURVES (LOG-LOG REPRESENTATION

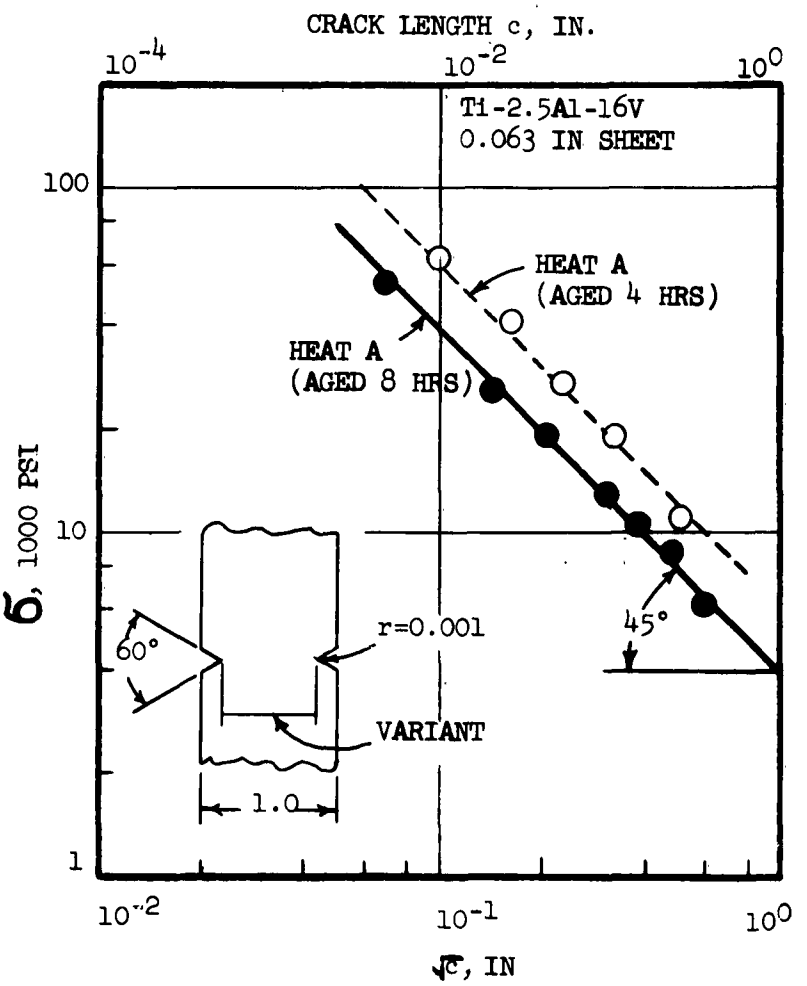


FIG. 3 σ VERSUS $\sqrt{c}$ FOR BRITTLE TITANIUM SHEET

FRACTURE APPEARANCE OF HIGH STRENGTH STEELS AND OTHER ALLOYS

J. E. Srawley
U. S. Naval Research Laboratory
Washington 25, D. C.

Study of fractured surfaces is undoubtedly a very ancient method for judging the quality of materials and for attempting to assess the extent to which material factors contributed to structural failures. Rational interpretation of fracture features has advanced considerably during the present century, but we are still far from being able to derive the maximum of useful information from them. We shall be mainly concerned here with one particular macroscopic characteristic which is known to be related to fracture toughness.

Fracture appearance has been found to be particularly useful as an indicator of the temperature range over which the susceptibility to brittle fracture changes markedly in certain important engineering materials, notably mild steels. Pronounced temperature sensitivity occurs in some high strength sheet and thin plate materials and the relationship between fracture appearance and resistance to fracturing (in terms of load-bearing capability), as these vary with temperature for a given material, is a matter of considerable interest and potential usefulness.

Full scale high strength sheet structures are rarely tested to destruction deliberately, and most of the available systematic information on fracture appearance relates to small laboratory specimens. Failures by fracture under loads insufficient to cause noticeable deformation occur because of the occurrence or development of stress intensifying flaws; in order to produce fractures resembling those observed in pressure vessels or other sheet structures that failed at low levels of nominal stress, it is necessary to use sharply notched tensile specimens. The familiar edge-notched type, with machined notches of near maximum sharpness, is suitable and widely used (1,2,3). However, the data presented here were obtained with an alternative, centrally-notched type, essentially a strip with a narrow transverse slot, symmetric about the centerline. To ensure sharpness, short fatigue cracks are provided at each end of the slot by tension-tension repeated loading. The slot and cracks together are regarded as the equivalent of a single transverse crack extending from one fatigue crack tip to the other. The most efficient ratio of total crack length to specimen width for measurement of

fracture resistance is about one third. This type of specimen is less sensitive than the edge-notched type to unintentional asymmetric loading during testing, as has been demonstrated with photo-elastic models by G. R Irwin. However, this need not be a serious problem when using edge-notched specimens if suitable alignment arrangements are made

Another type of specimen that is used is provided with a transverse surface crack in place of the slot with end cracks. Hydrogen embrittlement or stress corrosion conditions are employed in forming these cracks, which have roughly semi-elliptical boundaries with the major axis at the specimen surface.

Transverse and Oblique Shear Modes of Fracture

Examination of fracture surfaces of sharply notched sheet specimens suggests a major distinction between two modes of fracture: transverse,and oblique shear. These terms refer to the general inclination of the surfaces of separation to the direction of the maximum nominal tensile stress - in this case the direction of the major axis of the specimen - not to the inclinations of individual fracture facets. In a theoretical discussion of fracturing, G. R. Irwin has shown that three modes of crack extension are required for full generality, which he terms the opening mode and the first and second sliding modes (4). The observed transverse mode corresponds to Irwin's opening mode, while the oblique shear mode may correspond to either of the sliding modes, usually the second. None of these terms is intended to imply any particular relationship between fracture path and crystal structure; a transverse fracture might equally well be transgranular cleavage, or intergranular, or a mixture of the two.

Examples of transverse and oblique shear fractures of center-cracked specimens, and of an intermediate case are shown in Fig. 1. Each fracture propagated from the fatigue crack at the right to the edge of the specimen at the left. There is a similar fracture on the other side of each specimen which is not shown in the photographs. One feature of the transverse fracture at the bottom which is not very clear in the illustration is the characteristic chevron markings, pointing back to the origin, which are quite plain when the specimen is viewed directly. In examining service failures these are used to track down the origin of the fracture. There is an alternative type of oblique shear fracture to the one shown in the top photograph, which is quite common in specimens of this type. Instead of a single inclined surface, there may be two surfaces inclined in opposite directions and

intersecting along the centerline to form a trough or a ridge. In some specimens the fracture is of one type on one side and the other type on the other side. Long runs of shear fracture, as in thin-walled pressure vessel failures, usually consist of consecutive segments of the single surface type, the surfaces being inclined in opposite directions in adjacent segments.

A full shear fracture does not develop immediately from a transverse fracture origin, there is a transition zone in which the transverse fracture occupies a diminishing proportion of the thickness of the specimen - the triangular region at the right in the example in Fig. 1. During the course of testing a specimen, when the crack first starts to extend from the original fatigue crack front, the constraint is high and the ratio of shear stress to normal stress consequently low at positions close to the crack front, except in the immediate vicinity of the specimen surfaces. This favors the transverse mode of fracturing within the specimen but not at the surfaces, where plastic deformation occurs and relieves the constraint. The advancing crack front therefore assumes the well-known parabolic shape. With increasing load, the depth at which the shear stress is high enough to cause plastic deformation and reduce the constraint also increases, so that the advancing transverse crack front is progressively constricted. If the properties of the material are favorable,notably if the yield strength is low enough in relation to what we might loosely call the fracture strength, the constriction will continue to the limit and the transverse fracture tongue will narrow down to a point. Shear separation of the plastically deformed material on either side of the transverse fracture tongue appears to lag behind. It probably occurs along narrow oblique bands in which the plastic deformation is highly concentrated. The length of the initial transverse fracture triangle which precedes a full shear fracture seems to be less the tougher the material, but no very definite relationship has yet been established.

If the material properties are not favorable for the eventual development of a full shear fracture, the constriction of the advancing transverse fracture ceases short of the limit. This mode of fracture is then maintained within a central band of quite constant width, bounded by plastically deformed zones in which shear separation follows slightly behind. This is the intermediate case in Fig. 1. The fully transverse fracture is, of course, simply the extreme case where the shear borders are negligible.

A convenient quantitative index of fracture appearance is the percentage of the specimen thickness occupied by the shear borders - the percent shear. This is best determined in practice by measuring the average width of the transverse fracture band, subtracting this from the thickness, and expressing the difference as a percentage of the specimen thickness. Measurements are made at some distance from the origin, at positions where the shear borders are uniform. This requires that the specimens be of sufficient width; generally it is possible to make satisfactory measurements if the run of fracture exceeds 5 times the thickness, corresponding to a minimum width to thickness ratio of about 16.

Temperature, Thickness and Notch Sharpness

In many materials, the fracture mode changes from entirely transverse to full shear over a range of temperature characteristic of the material, condition and thickness. This is, of course, a consequence of the temperature dependence of the significant properties of the material and reflects a change in the balance between these quantities. Figure 1 illustrates the variation in percent shear with temperature for a low alloy steel, 0.075" thick, quenched and tempered at 1000°F to have a yield strength at room temperature of 200 ksi. The abrupt decrease from 100 percent shear to about half that value over a very narrow range of temperature is typical of steels that have high fracture toughness at temperatures above the full shear temperature (the lowest temperature at which the fracture mode would be entirely shear).

At a given temperature the percent shear may be strongly dependent on the thickness. This is to be expected on the basis of the previous remarks on the development of shear borders since the proportion of the thickness of the specimen which is critically constrained will be greater the greater the thickness, other things being equal. An example of the effect of thickness is shown in Fig. 2, where percent shear is plotted against testing temperature for sheets of four different thicknesses, all rolled from the same heat of AMS 6434 steel. It is clear that if a closely spaced series of thicknesses were tested at a particular temperature there would be a sharp transition with increasing thickness, analogous to the transition with decreasing temperature for a given thickness. For materials of this order of thickness, any effect due to the greater degree of hot working of the thinner sheets can probably be discounted, the important factor is the geometrical constraint.

Thickness is a basic factor in the fracture of sheet materials and resistance to fracturing may be markedly less in a thick section than in a thin one. In fact it is not inconceivable that increasing the thickness of a structural member to reduce the stress under given loading conditions might result in enhancing rather than reducing the risk of fracture.

The requirement that a sufficiently sharply notched specimen should be used in order to obtain a characteristic fracture appearance was mentioned earlier. Both the percent shear and, more markedly, the strength of the specimen are affected by notch sharpness. In Fig. 3, the percent shear as a function of temperature is compared between specimens which had central transverse slots ending in drilled holes of 0.02" radius, and specimens with slots ending in fatigue cracks. The third set of data points in this Figure is for specimens having transverse surface cracks formed by stress corrosion cracking, these results being in between those for the other two types of specimen. The influence of the type of stress-concentrator on the percent shear at a given temperature is quite appreciable, but it should be noted that the full shear temperature is not appreciably influenced within the scatter of results. The differences between fracture strengths for the different types of specimen were much more pronounced than the differences between percent shear values, and it is considered that it is the level of nominal stress at which the fracture propagates that influences the percent shear value at a particular temperature. Hence the relatively small stress corrosion cracks, as well as the blunt slotes, resulted in higher percent shear values than the crack-slots. In another group of tests, comparing specimens with slots of end radii of about 0.003" with specimens with slots ending in fatigue cracks, there were no apparent differences in percent shear and the differences in specimen strength were relatively small. In general, specimens having notches which are sufficiently sharp for satisfactory fracture toughness or fracture strength measurements will provide consistent values of percent shear.

The fractures of ordinary sheet tensile specimens generally do not show any simple correspondence with those of sharply notched specimens broken at the same temperatures. The two extremes of full shear fracture and transverse fracture do occur at appropriate temperatures, but no method has yet been devised for systematizing the various intermediate types. Necking occurs before fracture, usually obliquely and frequently at more than one position. Fracture may follow the neck in a ragged fashion, or may initiate as a transverse

fracture at some point along the neck, often at the intersection of two necks, and then be completed by shear tearing. It is possible that further study will suggest useful interpretations of such fractures; however, the conditions of fracture of a sheet tensile specimen are quite different to those prevailing in the failure of a sheet structure under a stress lower than the yield strength.

Fracture Appearance and Resistance to Fracturing

The correspondence between decrease in percent shear and decrease in resistance to fracturing as the temperature decreases is most clearly shown by heat treated steels. Two contrasting examples are given in Fig. 4, where resistance to fracturing is represented by the nominal net fracture stress of 1.5" wide, centrally-notched specimens, (i.e., the maximum load sustained in the test divided by the product of the thickness and the difference between the width and the initial crack length. This corresponds to the "notch strength" of an edge notched specimen. It is a useful comparative measure for results from specimens of equal dimensions, but is obviously dependent upon specimen width and crack length.) These examples are both low alloy steels, hardened and tempered to yield strengths of 193 ksi for X1, and 220 ksi for C2b/1, at room temperature (Table 1). The tempering temperature for C2b/1 was selected in order to provide an embrittled condition, and resulted in a full shear temperature of about 300°F; that for the X1/1 was selected to favor toughness at the expense of some yield strength, and resulted in a full shear temperature of -50°F. In each case the net fracture stress reaches a maximum at about the full shear temperature, but the net fracture stress changes much more gradually for the C2b/1 than for the X1/1. In general, the net fracture stress usually reaches a maximum at some temperature close to the full shear temperature and then declines with further increase in temperature in fair accordance with the decline in yield strength. Also, transitions tend to be sharper and to occur at lower temperatures the lower the yield strength to which the steel is tempered.

Comparison of the relationship between net fracture stress and percent shear with varying temperature for different materials is facilitated if one is plotted directly against the other, as in Fig. 5. Data points have been omitted for clarity, each curve representing the mean trend for a particular low alloy steel in a particular condition as the temperature changes over the range up to the full shear temperature. The curves are all similar in general form, the net fracture stress decreasing relatively gradually

as the fracture changes from full shear to somewhat less than 50 percent shear, and then quite rapidly with further decrease in percent shear. It may be added that with further decrease in temperature, beyond the point at which the shear borders are no longer distinguishable, the decline in net fracture stress is gradual. Thus the major change in net fracture stress occurs in the range between about 5 and about 50 percent shear. Nevertheless, since the temperature range between 50 and 100 percent shear is often quite narrow, the full shear temperature is an appropriate indication of the range of marked temperature dependence of fracture toughness.

It is clear that the full shear temperature is not a sufficient basis for selection, since the resistance to full shear fracturing differs considerably among materials, and between different conditions of a given material, for instance C6a/2 and C5a/3 in Fig. 5. Its main value is as a safeguard against the selection of a material which is highly temperature sensitive in the range in which it may be used. In addition, there is a broad negative correlation between full shear temperature and maximum level of net fracture stress, the former tending to increase and the latter to decrease with increasing yield strength. The upper four curves in Fig. 5 represent steels with relatively low yield strengths (Table 1).

In Fig 6, curves of net fracture stress versus percent shear are shown for cold rolled type 301 stainless steel (Y1/1), aluminum alloys 2024.T3 (AA), and 7075.T6 (AB), and the titanium 13-V-11Cr-4Al beta alloy in the solution treated condition (T1/1), and after aging for 100 hours at 900°F (T1/2). The curves for the two low alloy steels X1/1 and C2b/1 from Fig. 5 are shown as dashed lines for comparison. The percent shear values for the stainless steel and the titanium and aluminum alloys were estimated visually because the fractures were too irregular for measurement. The transverse and oblique fracture modes do occur in materials such as these, but the shear borders of intermediate fractures are ragged and somewhat obscured by the general roughness of the fractures. In some cases it is not possible even to estimate the percent shear, but in these examples the estimates could be made well enough to establish the trends with confidence.

For the two aluminum alloys the net fracture stress is almost independent of percent shear, and this is probably true also for the type 301 stainless steel, though the data for this does not extend below 40 percent shear and therefore leaves some doubt. The net fracture stress exceeded the yield strength for the 2024, but was less than the yield strength

for the 7075 and much less for the type 301. The behavior of the age-hardened titanium alloy (T1/2) is very similar to that of the steel (C2b/1), whereas in the solution treated condition (T1/1) the net fracture stress decreases almost linearly with percent shear. Considering the low density of titanium, the resistance to fracturing at the full shear temperature for the solution treated condition is very impressive. Unfortunately, the net fracture stress is highest at the full shear temperature of about -175°F and then decreases in close correspondence with tensile strength to 135 ksi at room temperature. On the other hand, the full shear temperature in the aged condition is above 400°F and the net fracture stress at room temperature about 70 ksi (20 percent shear). The optimum condition should be somewhere between these extremes.

The resistance to fracture may be alternatively expressed in terms of a quantity having a less restricted significance than the net fracture stress. This quantity is the fracture toughness, K_c, proposed by G. R. Irwin as a consequence of his stress analysis approach to the problem of fracture*. In principle, and subject to certain requirements for a satisfactory test, K_c is independent of specimen dimensions other than thickness. It is a measure of the intensity of the elastic stress field near the tip of a propagating crack when the rate of propagation reaches a critical value, and is proportional to the nominal stress normal to the crack and to the square root of the effective size of the crack. Different methods of calculating K_c from the results of tests of notched sheet specimens are distinguished in Reference (1) by subscript numbers; the values which are used here are those referred to as K_{c3} values (centrally notched specimen, indirect estimate of critical crack length).

Curves of K_{c3} versus percent shear are shown in Fig. 7 for the low alloy steels of Fig. 5 and for three other hardenable steels, for which the results were obtained with 0.5" wide specimens. The increase of K_{c3} with percent shear is more uniform than that of the net fracture stress. There is a wide spread of fracture toughness values at the full

*See Reference (1). $K_c = \sqrt{E\mathcal{G}_c}$, where E is Young's Modulus and $\mathcal{G}_c$ is Irwin's critical strain energy release rate.

shear temperature, but the spread decreases with decreasing percent shear. Thus a material which has relatively high fracture toughness for full shear fracturing does not necessarily have any advantage in fracture toughness for predominantly transverse fracturing.

In. Fig. 8, curves of K_{c3} versus percent shear are shown for the titanium and aluminum alloys and the type 301 stainless steel, together with curves for the low alloy steels X1/1 and C2b/1 (dashed). The comparative behavior of the different materials is very similar to that for the net fracture stress in Fig. 6.

General Remarks

In testing other titanium alloys (6Al-4V, 16V-2.5Al, and 4Al-3Mo-1V), it has not been possible to classify fracture appearances in terms of percent shear, nor, as yet, to find an alternative classification that is roughly quantitative. The fracture appearances do change with temperature, and the transverse and oblique shear modes of fracture do occur, but the intermediate cases take a variety of forms. One complication is that the direction of propagation, instead of remaining normal to the tension axis, may change at some point to become oblique to the axis. The distance from the origin at which the change in direction occurs is greater the lower the temperature and the effect is clearly due to the finite width of the specimen. With these alloys so-called transitions in the dependence of net fracture stress and fracture toughness on temperature do occur, and it may be possible when enough examples have been studied to find a related fracture appearance index.

The texture of transverse fracture regions changes with temperature as well as differing between one alloy and another. While this is hardly a suitable attribute for macroscopic measurement, it would clearly be a most interesting subject for detailed study at high magnification. As far as is known no such study of high strength materials has yet been reported.

Occasionally fractures of sheet materials are found which have a markedly laminated appearance. Splitting occurs on planes of weakness parallel to the sheet surfaces, apparently in advance of fracturing. This may be quite beneficial as far as fracture toughness is concerned because these internal free surfaces reduce the constraint and inhibit transverse fracturing in favor of shear separation. The sheet behaves rather like a loosely bonded pack of much thinner sheets and benefits from the thickness effect that was mentioned earlier.

Summary

A fundamental distinction may be made between transverse and oblique shear modes of fracture, referring to macroscopic orientation. In many sheet materials mixed fractures take a simple form which can be described in terms of a percent shear index. The temperature dependence of this index is characteristic of the material, its condition and its thickness, and is closely related to the temperature dependence of the fracture toughness in terms of load-bearing capability. A simple concept is to regard the material as having separate and independent properties of transverse or "plane strain" fracture toughness, and shear or "plane stress" fracture toughness (the terms in quotes are due to G. R. Irwin). Thus, the change in observed fracture toughness with temperature, over the range in which the fracture appearance changes, is due to the change in relative contributions of the two types of fracture toughness. For some materials these differ widely, resulting in a marked transition in observed fracture toughness with temperature. For other materials they may differ hardly at all, and the observed fracture toughness then varies only gradually with temperature. Changes in the individual values of the two types of fracture toughness with temperature are thought to be gradual; in fact, the fracture toughness for full shear fracturing usually decreases with increasing temperature, contrary to the behavior of the observed fracture toughness in the transition range.

For materials which do suffer a radical change in fracture toughness over a narrow, transition range of temperature, it is important to know where this range is in relation to the temperature at which the material will be in service. The full shear temperature is a useful index in this respect, and appears to have the advantage of being independent of specimen width. However, the resistance to full shear fracturing varies widely among different materials so that fracture appearance is not, in itself, a sufficient criterion of suitability of a material.

References

(1) Report of the Special Committee on Fracture Testing of High Strength Sheet Materials, ASTM Bulletin, Jan-Feb 1960, pp 29-51.

(2) Espey, G. B., Jones, M. H., and Brown, W. F., Jr., "The Sharp Notch Tensile Strength of Several High Strength Sheet Alloys", Proceedings ASTM, Vol 59, Part II, 1959.

(3) Sachs, G., and Sessler, J. G., "Effect of Stress Concentration on Tensile Strength of Titanium and Steel Alloy Sheet", to be published by ASTM (1960 Preprint 76a).

(4) Irwin, G. R., Article on Fracture, Handbuch der Physik, Vol VI, pp 551-589, 1958.

TABLE 1 - DETAILS OF MATERIALS

	Material	Nominal Thickness (in.)	Specimen Width (in.)	Condition	Tensile Strength* (ksi)	Yield Strength* (ksi)	Full Shear Temp. (°F)
	Steels						
C2b/1	300M	0.063	1.500	Temp. 800°F	260	220	320
C5a/2	300M(CEVM)	0.063	1.500	Austempered 600°F	225	157	-10
C5a/3	300M(CEVM)	0.063	1.500	Temp. 600°F	294	240	110
L2a/2	X200(CEVM)	0.063	1.500	Temp. 1000°F	232	197	100
L2a/3	X200(CEVM)	0.063	1.500	Temp. 700°F	296	246	80
P9/6	AMS 6434	0.125	1.500	Temp. 400°F	250	196	0
X1	D6a	0.100	1.500	Temp. 1100°F	206	193	-50
U1	H-11 (5% Cr)	0.025	0.500	Temp. 1025°F	245	200	50
J1	Type 422	0.025	0.500	Temp. 1000°F	219	160	55
B	12MoV	0.010	0.500	Temp. 1050°F	213	164	-90
Y1	Type 301	0.021	1.500	Cold Rolled XXFH	279	259	-200 to -100
	Titanium						
T1/1	13V-11Cr-4Al	0.063	1.500	Solution Treated	135	129	-175 to -150
T1/2	13V-11Cr-4Al	1.500	1.500	Aged 900°F for 100 hr	189	178	400 to 500
	Aluminum						
AA	2024.T3	0.050	1.500	T3	68.4	46.8	Above 90
AB	7075.T6	0.053	1.500	T6	79.8	71.3	250 to 300

* At Room Temperature

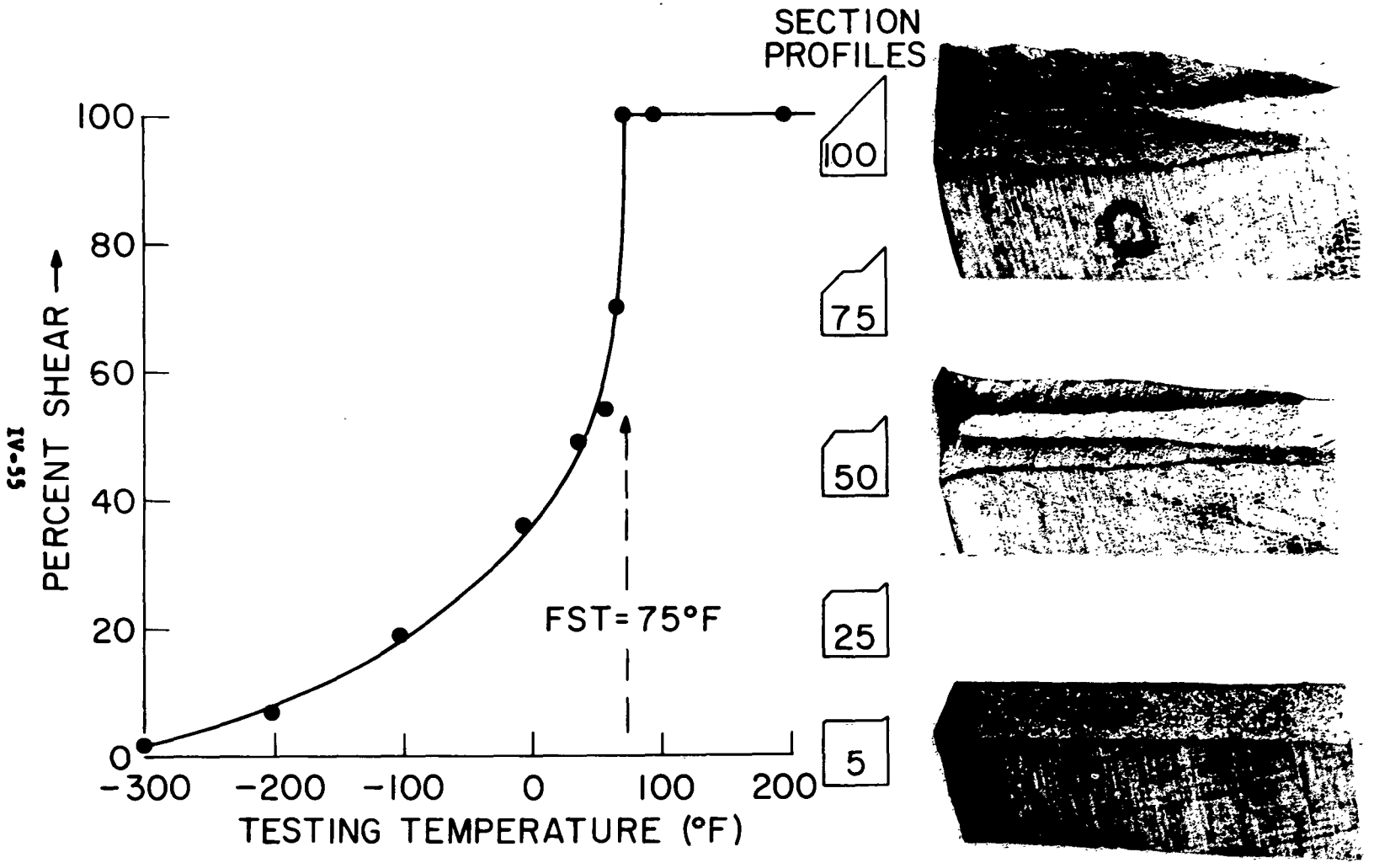


Fig. 1 - Percent shear versus testing temperature for high-strength low-alloy steel, 0.075 in. thick. Examples of full shear, 50% shear and transverse fractures.

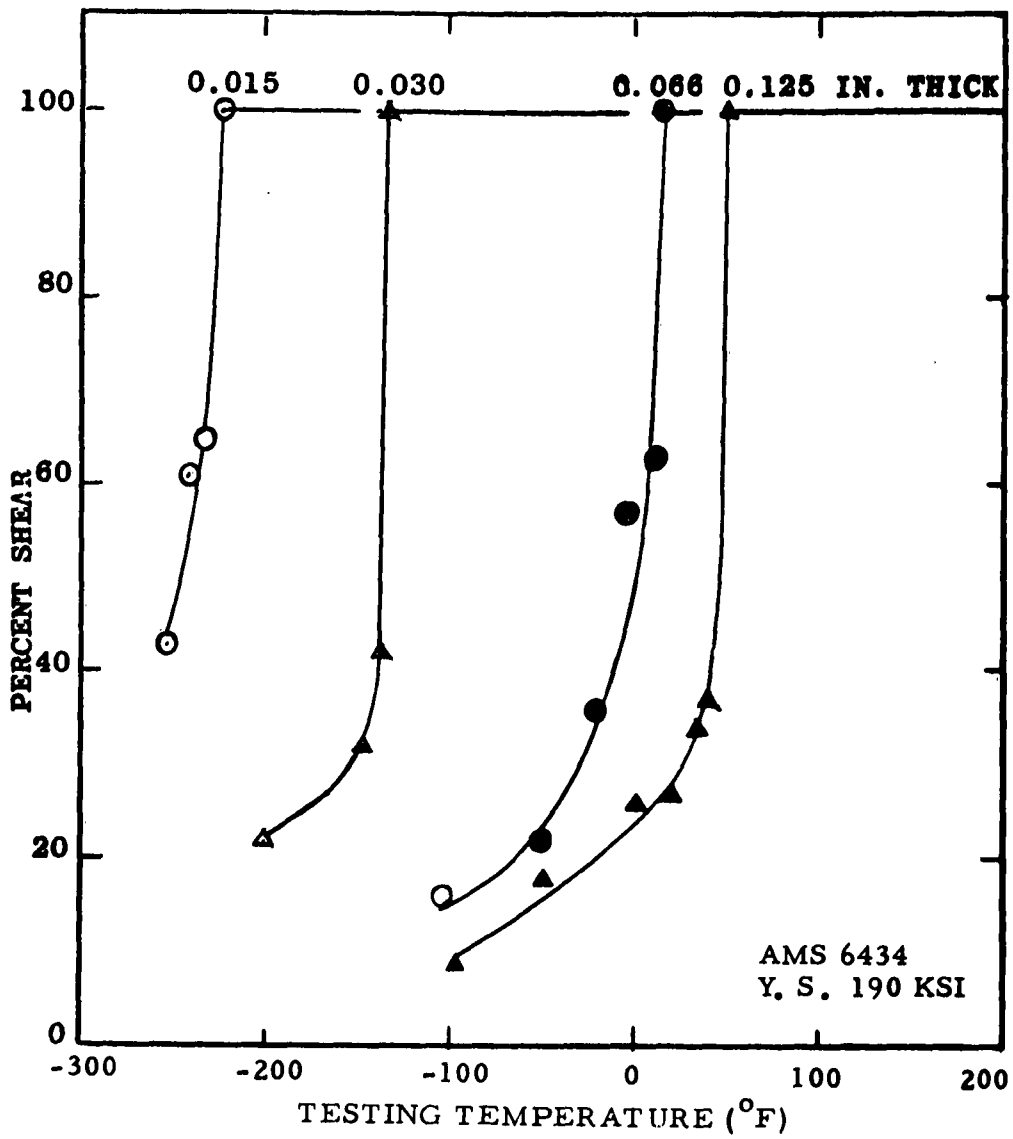


FIG. 2 - EFFECT OF THICKNESS ON PERCENT SHEAR FRACTURE FOR A LOW ALLOY STEEL.

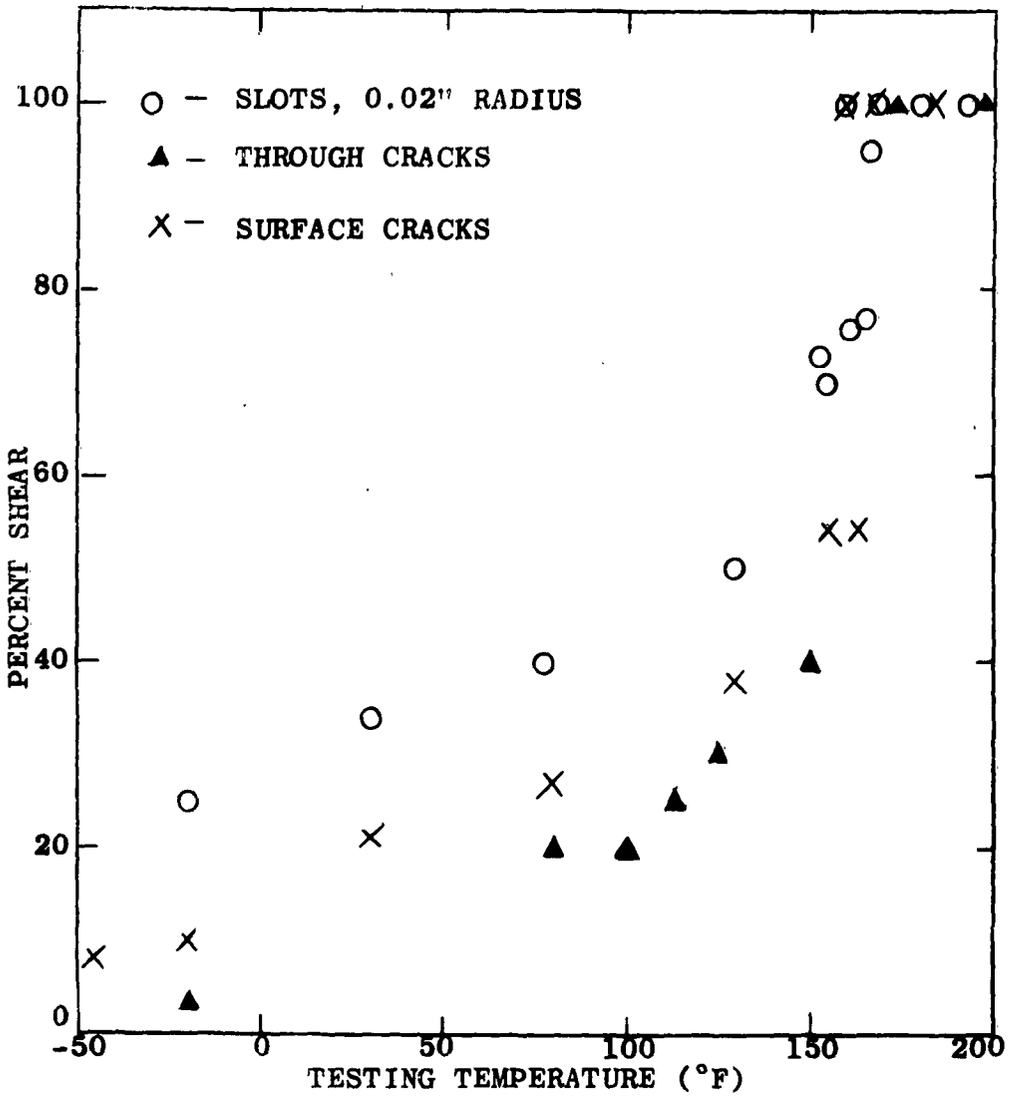


FIG. 3 - EFFECT OF "NOTCH" SHARPNESS ON PERCENT SHEAR FRACTURE FOR HARDENED AND TEMPERED 12% Cr STAINLESS STEEL.

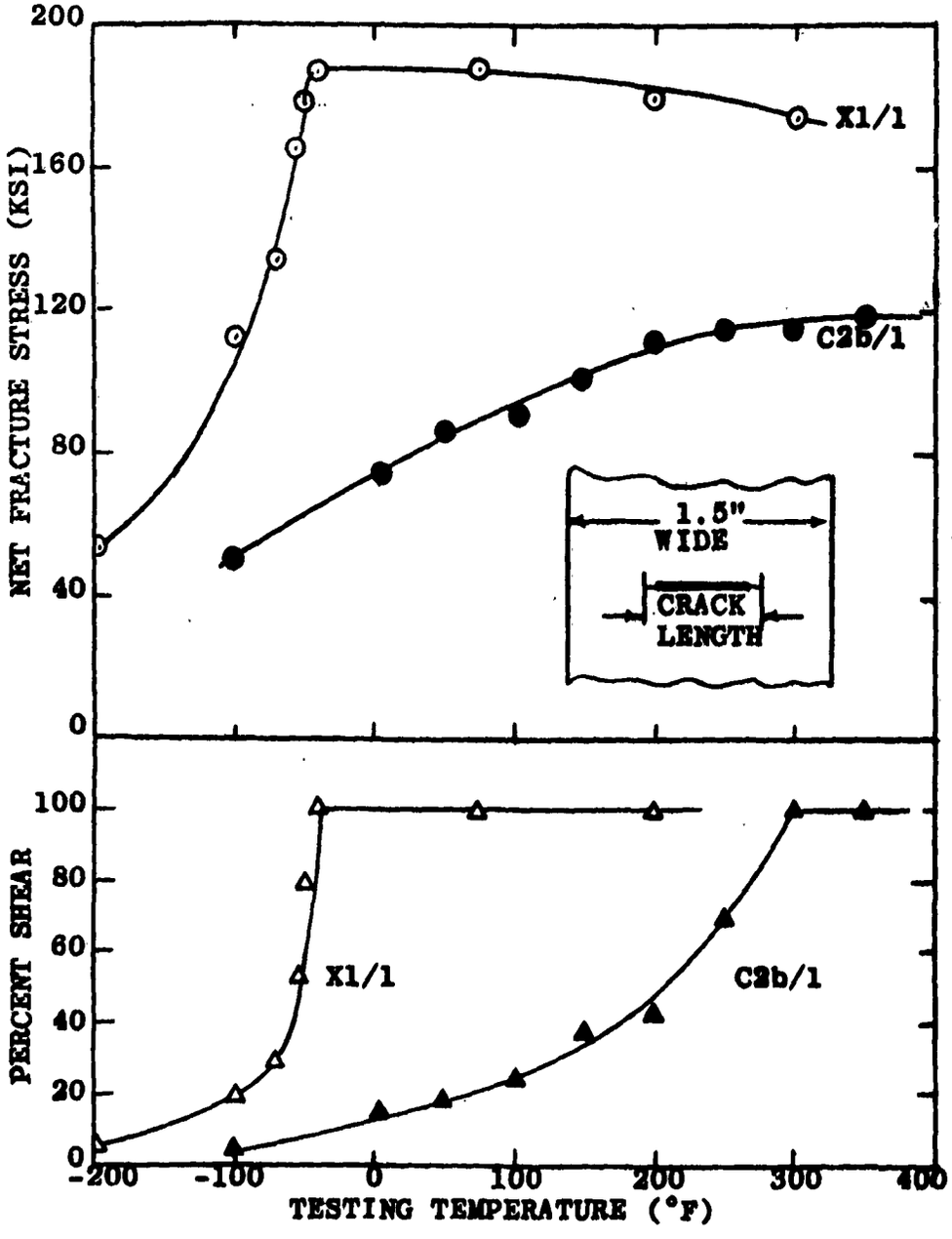


FIG. 4 - NET FRACTURE STRESS AND PERCENT SHEAR FOR TWO LOW ALLOY STEELS. RATIO OF CRACK LENGTH TO WIDTH BETWEEN 0.35 and 0.4.

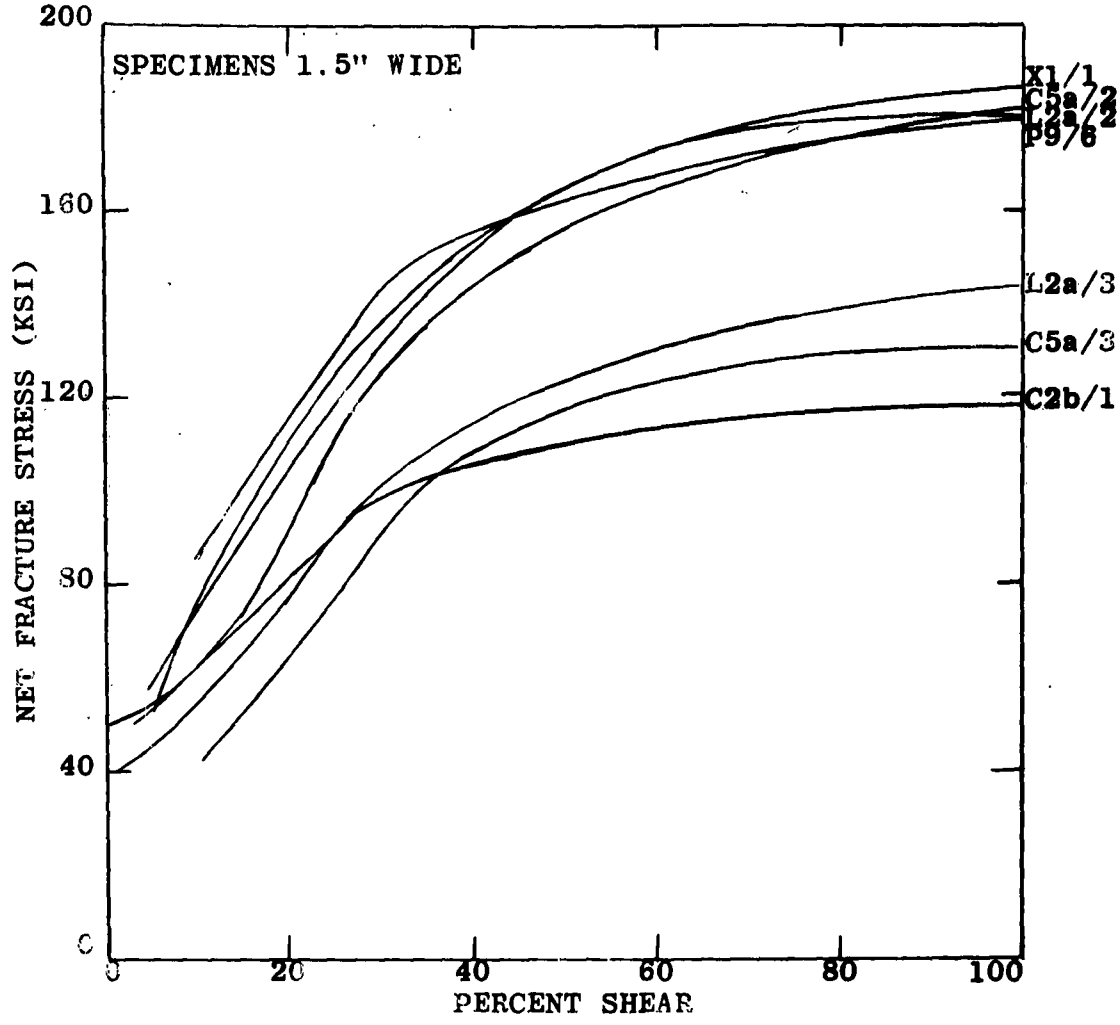


FIG. 5 - RELATIONSHIP BETWEEN NET FRACTURE STRESS AND PERCENT SHEAR WITH VARYING TEMPERATURE FOR SEVERAL LOW ALLOY STEELS. (SEE TABLE 1).

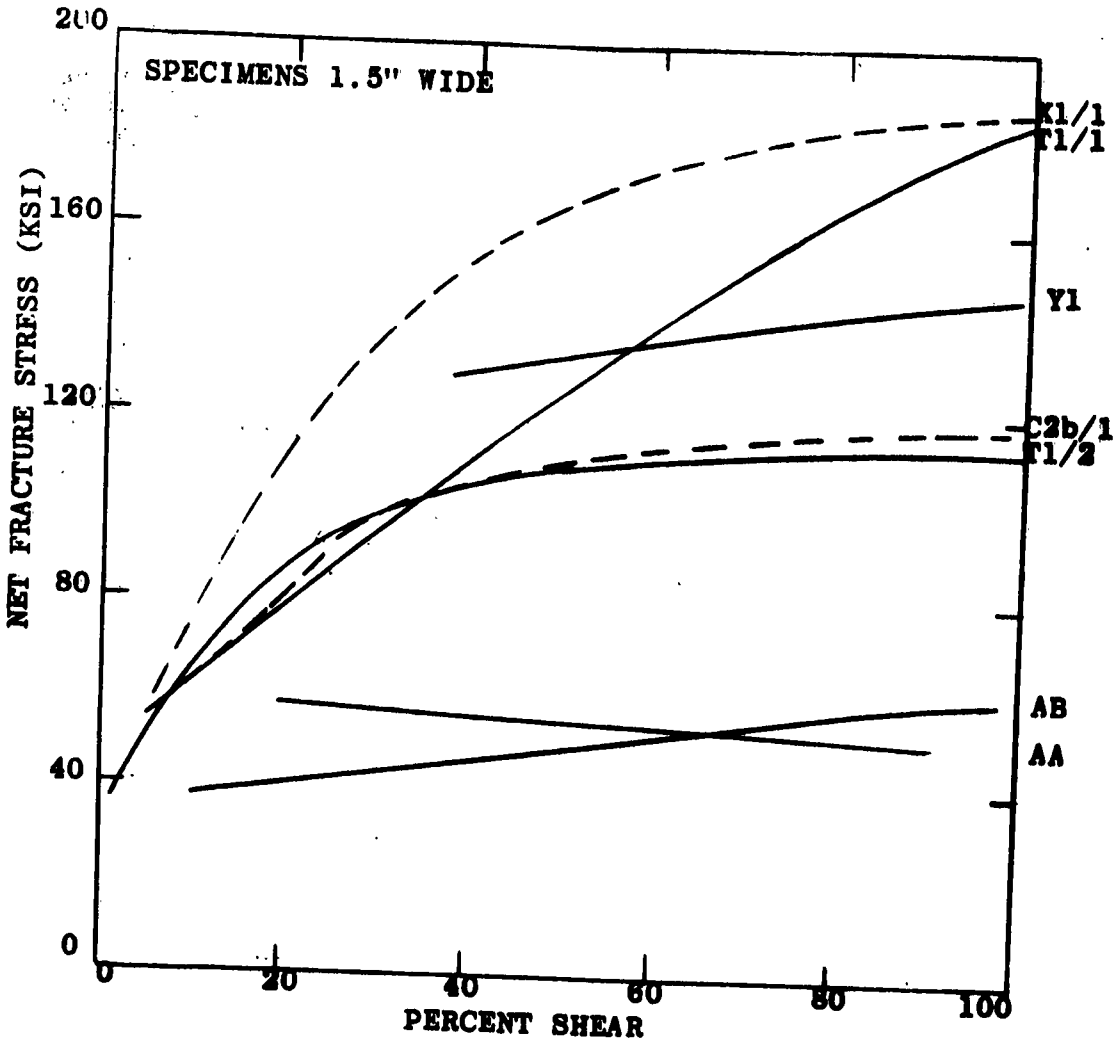


FIG. 6 - RELATIONSHIP BETWEEN NET FRACTURE STRESS AND PERCENT SHEAR WITH VARYING TEMPERATURE FOR ALUMINUM ALLOYS, AA AND AB, TITANIUM ALLOY, T1/1 AND T1/2, COLD ROLLED STAINLESS STEEL, Y1, COMPARED WITH LOW ALLOY STEELS. (SEE TABLE 1.)

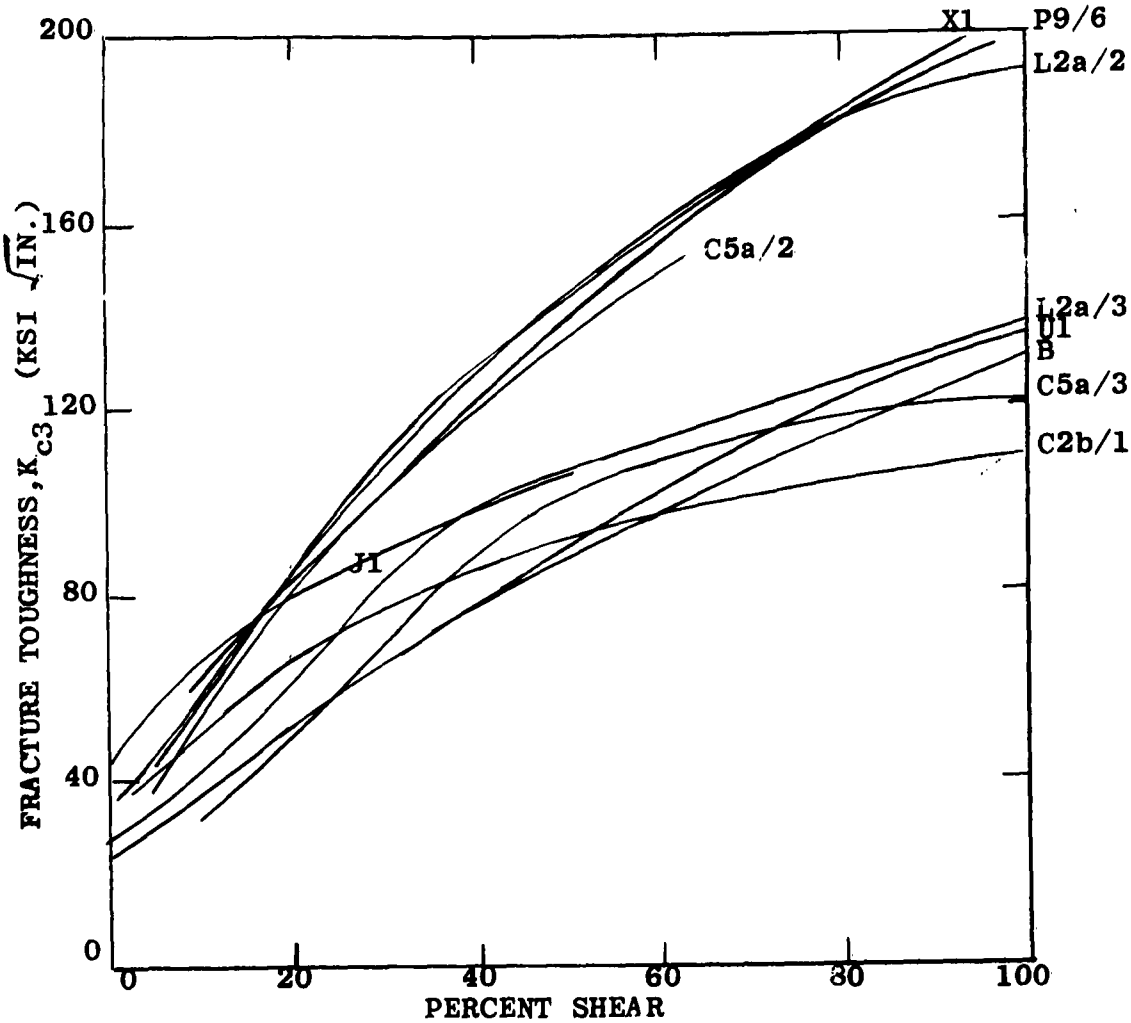


FIG. 7 - RELATIONSHIP BETWEEN FRACTURE TOUGHNESS, K_{c3}, AND PERCENT SHEAR WITH VARYING TEMPERATURE FOR SEVERAL HEAT TREATED STEELS. (SEE TABLE 1.)

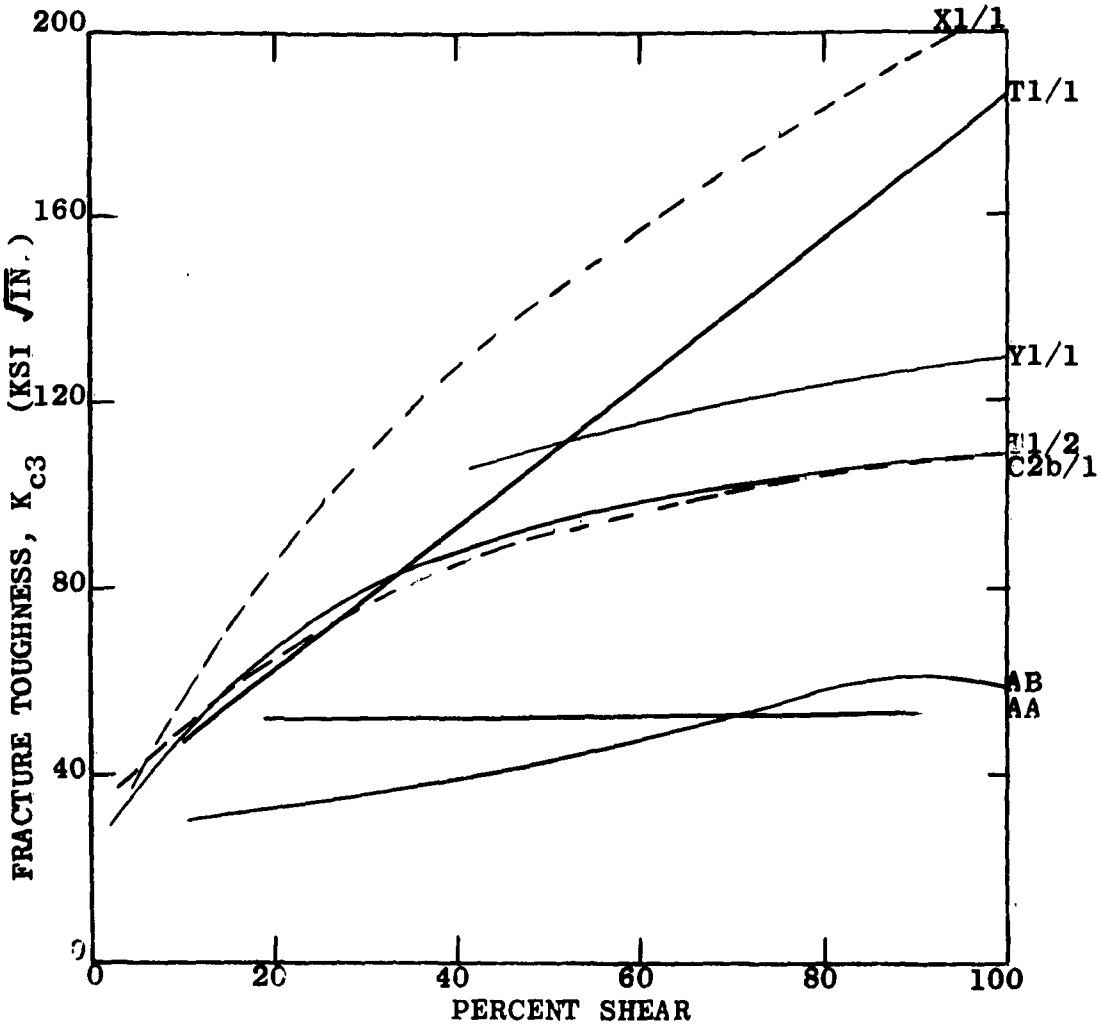


FIG. 8 - RELATIONSHIP BETWEEN FRACTURE TOUGHNESS, K_{c3}, AND PERCENT SHEAR WITH VARYING TEMPERATURE FOR ALUMINUM ALLOYS, AA AND AB, TITANIUM ALLOY, T1/1 AND T1/2, COLD ROLLED STAINLESS STEEL, Y1, COMPARED WITH LOW ALLOY STEELS. (SEE TABLE 1.)

PLASTIC ZONE NEAR A CRACK AND FRACTURE TOUGHNESS

by

G. R. Irwin
U. S. Naval Research Laboratory
Washington 25, D. C.

Introduction

In order to discuss fracture in terms of stresses we need a descriptive terminology related to the stresses near the leading edge of the crack. One might term the simplest method for doing this, a one-parameter method. A natural and appropriate characterization of the one-parameter type is provided by the crack-extension force $\mathcal{G}$ or equivalently by the stress intensity factors K and $\mathcal{K}$. These terms are related as follows (1):

$$K^2 = E\mathcal{G} = E\mathcal{K}^2 = \begin{cases} \mathcal{G}E & \text{(plane stress)} \\ \dfrac{\mathcal{G}E}{1-\nu^2} & \text{(for plane strain)} \end{cases} \quad - - - \quad (1)$$

E is Young's modulus and ν is Poisson's ratio.

As an example of the descriptive use of these stress field parameters, one can apply tension to a test specimen containing a starting crack and observe the value of the stress parameter for onset of rapid crack extensions. The special values of the parameters obtained in this way are designated K_c, $\mathcal{K}_c$, and $\mathcal{G}_c$. When carefully done, this testing procedure results in a useful, reproducible and quantitative measurement of fracture toughness (2).

Normally in fracture tests of this type the stress field parameter value is not obtained from an experimental stress analysis. Instead the length of the slow crack is marked with a staining procedure and an appropriate theoretical analysis in terms of crack length 2a, gross section stress σ, and specimen width W is used to calculate the stress field parameter. For example, in the case of the centrally-notched specimen, Figure 1, the recommended computation procedure is based upon the equations:

$$K^2 = \sigma^2 W \tan u \quad - - - - - - - - - - - - - - - - \quad (2)$$

$$\text{and} \quad u = \frac{\pi}{W}\left(a + \frac{K^2}{2\pi\sigma_{YS}^2}\right) \quad - - - - - - - - \quad (3)$$

where σ_{YS} is the uniaxial tensile yield stress.

The stress analysis basic to equations (2) and (3) is derived from a mathematical model which differs from the real specimen principally in just two ways. One difference is that the mathematical

model corresponds to a specimen subject to relatively small normal stresses on the side boundaries. In the test situations of practical interest this difference from the real test specimen has a negligible influence on the value of K and is not of interest in this discussion. The second, and more significant difference stems from the fact that the mathematical model is based entirely on equations of linear elasticity. The allowance for zones of plastic strains at the crack ends, illustrated by the term added to a in equation (3), merely assumes the influence of stress relaxation in the plastic zones is equivalent to additional crack length in the simple way shown.

The existence of a difference between the real test situation and the idealized mathematical model employed for test analysis purposes is a universal characteristic of physical measurements. Sometimes the difference is recognized but ignored, in other instances an approximate correction procedure is employed. An example like the crack stress field problem in some respects can be given from another field if one allows going back some years in time, back to the period when the study of resonance frequencies of open and closed tubes was of considerable interest. It was noted the tubes resonated as if the effective length exceeded the actual length. Intuitively it seemed that a length equal to half the tube diameter added at each open end would be about the right correction. Use of an end effect correction of this amount was suggested by such authorities as Rayleigh and Lamb and served a useful purpose in this application for many years. I have been informed some theoretical calculations during the past 15 years have been made which show the proper end effect correction is very nearly but not exactly equal to half the tube diameter.

As was true of the acoustic tube end-effect so also in the case of the plastic zone correction there are simple considerations which suggest an approximate answer to the problem.

Notched Sheets in Tension

The elastic theory stress analysis for the end region of a long crack in an infinite plate predicts the tension normal to the crack, σ_y, acting across the line of expected crack extension is given by

$$\sigma_y = \frac{K}{\sqrt{2\pi r}} \qquad \text{- - - - - - - - -} \qquad (4)$$

where r is the distance from the end of the crack. By solving for r with σ_y put equal to the uniaxial yield stress σ_{YS} one obtains

$$r_{YS} = \frac{1}{2\pi}\left(\frac{K}{\sigma_{YS}}\right)^2 \qquad \text{- - - - - - -} \qquad (5)$$

Since stress relaxation in the plastic zone means more stress must be carried beyond this zone it is clear the actual zone of plastic strains must extend to a greater distance than r_{YS} from the end of the crack. On the other hand our problem does not actually require knowing the size and shape of the plastic zone or

the stresses within this zone. What we need is an estimate of the additional crack length such that the elastic stress field for the lengthened crack would correspond closely to the real stress field in regions beyond the zone of plastic strains. This added crack length should be smaller than the actual plastic zone size and might, in fact, be nearly equal to r_{YS}. The situation is shown schematically in Figure 1.

Consider next the net-section stress expected from equations (2) and (3). One can derive from equation (2) and (3) the relation

$$\frac{1}{W}\left(\frac{K}{\sigma_{YS}}\right)^2 = \left(\frac{\sigma_N}{\sigma_{YS}}\right)^2 \left(1 - \frac{2a}{W}\right)^2 \tan\left[\frac{\pi a}{W} + \frac{1}{2W}\left(\frac{K}{\sigma_{YS}}\right)^2\right] \quad - \quad (6)$$

Taking the square root of both sides of equation (6) one has

$$\left(\frac{K}{\sigma_{YS}}\right)\frac{1}{\sqrt{W}} = \left(\frac{\sigma_N}{\sigma_{YS}}\right)\left(1 - \frac{2a}{W}\right)\left\{\tan\left[\frac{\pi a}{W} + \frac{1}{2W}\left(\frac{K}{\sigma_{YS}}\right)^2\right]\right\}^{1/2} \quad - - - \quad (7)$$

Using the term on the left of equation (7) as the abscissa variable and $\left(\frac{\sigma_N}{\sigma_{YS}}\right)$ as the ordinate, Figure 2 shows essentially the predicted variation of net-section stress with inverse square root of specimen width. Curves for two fixed values of a/W are shown. As the specimen width becomes smaller, conditions on the next section approach those of general yielding. Because of this one expects measured values of net-section stress would fall below proportionality to $1/\sqrt{W}$ and approach some value in the yield-tensile strength range as specimen width is decreased. If we use only the region of positive slope, equation (7) predicts a behavior of the type expected.

Now, if the plastic zone correction factor had been taken to be

$$r_p = \frac{p}{2\pi}\left(\frac{K}{\sigma_{YS}}\right)^2 \quad - - - - - - - - - - - - \quad (8)$$

the effect of the proportionality factor p is to multiply the number scales of ordinate and abscissa by $1/\sqrt{p}$. By taking p to be unity the net-section stress predicted by equation (7) has a maximum value of σ_N nearly equal to 1.15 σ_{YS}, a plausible value in the yield-tensile strength range. This maximum occurs when the size of r_p is nearly half of the unbroken ligament of the specimen.

From equations (4) and (5) one can see that, as an estimate of the plastic zone correction factor, r_{YS} is unlikely to be wrong by as much as a factor of two. From Figure 2 and equation (7) it is clear the proportionality factor, p, must be selected to be in the range 0.75 to 1.3 in order to predict a leveling off of net-section stress in the range of 1.0 to 1.3 σ_{YS}.

The value of K is determined by stress level and by crack length. In the above discussion the plastic zone correction was discussed only in terms of an adjustment to the crack length. A more accurate though more complex correction procedure can be developed

by use of a stress level correction term in addition to the crack length correction term. The latter is not, in this case, as large, and the relative magnitudes of the two correction terms can be adjusted to give an improved fit to the actual stress field in the specimen.

As an illustration consider again the centrally-notched sheet tensile specimen. The K value of equation (2) is derived from a stress analysis which predicts the stresses σ_y along the line of expected crack extension are given by

$$\sigma_y = \sigma \left\{ 1 - \left(\frac{\sin u}{\sin \frac{\pi x}{W}} \right)^2 \right\}^{-1/2} \quad \text{- - - - - - - - -} \quad (9)$$

$$\text{with} \quad u = \frac{\pi a}{W} + \frac{p_1}{2W} \left(\frac{K}{\sigma_{YS}} \right)^2 \quad \text{- - - - - - - - -} \quad (10)$$

Assume that the crack length is half the specimen width, the value of β is 2π where

$$\beta = \frac{K^2}{B\sigma_{YS}^2}, \quad \text{- - - - - - - - -} \quad (11)$$

and W/B is 16. In this event selection of a plastic strain correction equal to r_{YS} has the effect of increasing K by about 10 percent. A similar increase of K would occur by addition to σ of a stress correction term equal to 10 percent of σ. Alternatively one could add $r_{YS}/2$ to a and increase σ only 5 percent. All three corrective procedures would predict the same K value to within 1 percent. However, the agreement of equation (9) with an experimental stress analysis across the net section along the x-axis is sensitive to these alternatives.

A program of experimental stress measurements to explore this situation was initiated at the Naval Research Laboratory last year. The experiment employed a 12 inch wide sheet of 1/8-in. thick 7075-T6 Al alloy with a central slot and a photoelastic coating on each side. The central slot ended in 3/16-in. diameter holes to deter crack formation. The experiment consisted in application of a series of increasing tensile loads and the determination, at each load, of the corrective factors to the applied gross section stress σ and to the crack length.

Replacing σ in equation (9) by $(\sigma + \sigma_1)$, for each of the tensile loads σ, it was possible to find a pair of values, σ_1 and p_1, such that σ_y from equation (9) (thus modified) fitted the measured values of σ_y along the x-axis throughout the region of elastic strains. Values of p were then found using the relation

$$\tan\left(\frac{\pi a}{W} + \frac{pK^2}{2W\sigma_{YS}^2} \right) = \left(1 + \frac{\sigma_1}{\sigma} \right)^2 \tan\left(\frac{\pi a}{W} + \frac{p_1 K^2}{2W\sigma_{YS}^2} \right) \quad \text{--(12)}$$

The experimental values of pr_{YS} are shown on figure 3 as a function of r_{YS}. At light loads the circular opening at each end of the slot had a strong influence on the results. However, the measured crack length correction appeared to approach r_{YS} as the load was increased and it was not possible within experimental uncertainties to conclude that a significant difference of p from unity was indicated by these measurements.

From the equation for K as influenced by σ, and p, r_{YS} the effect of these corrections decreases as specimen width increases. Thus a study of K as a function of specimen size should assist finding best values for the correction terms. Theoretically this procedure might seem the basic method for their determination. In practice there are many pitfalls. At specimen widths exceeding 50 times the sheet thickness (for steel) it is often necessary to use buckling restraints on the test sheet to insure a flat sheet test situation at onset of fast fracture. If an oblique shear mode of fracture occurs, too much restraint interferes with transverse displacements natural to the shear fracture and too little restraint allows an undesirable deviation from sheet flatness. For heat treated high strength sheet steels some residual stress may exist in the specimen and affect test results in a way dependent upon specimen size. The latter effect can be avoided by use of test specimens cut from a large sheet of 7075 T-6 Aluminum. Figure 4 shows results for such specimens. Restraints to prevent buckling were necessary for W/B greater than 80. In addition 24 frames per second movies instead of ink staining was the method used for estimating crack length at onset of rapid fracture in all but two of the results shown. The calculations assumed p equal to unity. From the appearance of the results a different choice of p would not have improved uniformity of K_c as a function of specimen width. In fact, as shown on Figure 4, the largest shift of a plotted point by removing the plastic strain correction is smaller than variation of K_c due to causes not related to plastic strain.

Plane Strain Stress Conditions

Measurements of crack toughness in terms of the K_c value designated K_{Ic} are conveniently made using a round tensile bar with a circumferential notch of sharp root radius (3). In several respects these tests are less complex than crack toughness measurements of sheet material. Because of notch sharpness there are no shear lips growing at the side boundaries of the initial crack to assist stable slow crack extension and the separation due to slow crack extension normally is so small it seems permissible to neglect this factor in calculating results. Thus ink staining of the slow crack is not required. In addition the plane strain stress conditions at the edge of the sharp notch result in an effective notch depth substantially less than r_{YS} because of the increased elastic constraint. Comparing plane stress and plane strain stress conditions from the crack edge elastic stress equations for equal K value, one finds the average of the square of the largest shearing stress is less for plane strain than for plane stress by a factor of 0.39. If

one chooses as the effective increase of notch depth the value $r_{YS}/2\sqrt{2}$ ($\approx 0.35\, r_{YS}$), the use of this 10 percent smaller factor permits some simplification in the numbers appearing in the K value equation for a specimen notched so as to make the net section area half of the cross section area. The equation for K then becomes

$$K\left[1 - \frac{K^2}{2\pi D \sigma_{YS}^2}\right]^2 = 0.233\sqrt{\pi D}\,\sigma_N \quad \text{- - - - - - - -} \quad (13)$$

where D is the cross diameter of the specimen and σ_N is the net section stress at fracture.

Equation (13) is of the form

$$x\left[1 - (1/2)\,x^2\right]^2 = 0.233\,\frac{\sigma_N}{\sigma_{YS}} \quad \text{- - - -} \quad (14)$$

where $x = \dfrac{K}{\sqrt{\pi D}\,\sigma_{YS}}$

Figure 5 shows the values of ratio σ_N/σ_{YS} as a function of x from equation (14). At values of x approaching 0.63 equation (14) predicts a pronounced departure of σ_N from proportionality to inverse square root of specimen size and a trend toward a maximum value of $1.74\,\sigma_{YS}$. Data points from tests of 7075-T6 aluminum (squares) and tests of a rotor steel (circles) are also shown.

The plastic zone correction factor of $r_{YS}/2\sqrt{2}$ is an intermediate choice relative to the data shown and is consistent with the plane stress correction factor from approximate analysis of the influence of elastic constraint. In view of the fact that plastic yielding near a crack is also influenced by strain hardening, stress gradient, and other significant details it seems pointless to attempt more than a rough estimate of the plastic strain corrections in terms of their proportionality to $(K/\sigma_{YS})^2$. From the considerations discussed above the plastic strain correction factor should be in the range $0.8r_{YS}$ to $1.3r_{YS}$ for conditions of plane stress and should be in the range $0.3r_{YS}$ to $0.5r_{YS}$ for plane strain. Given any selections in these ranges, materials and test conditions could probably be found for which the selected corrections would seem correct.

Fracture Mode Transition and a Minimum Toughness Criterion

Plastic yielding near the leading edge of a crack was discussed above in terms of its influence upon the stress analysis applied to test specimens. For a crack traversing of a plate one can observe that a change from flat-tensile to oblique shear fracture can be introduced by reduction of plate thickness (4). This fracture mode transition correlates with the ratio of r_{YS} to plate thickness B in such a way that mid-range conditions of fracture transition occur when

$$2r_{YS} = B \quad \text{- - - - - - - - - - -} \quad (15)$$

or

$$\beta_c = \frac{K_c^2}{B \sigma_{YS}^2} = \pi \text{ - - - - - - - - - - } (16)$$

Figure 6 shows illustrative data for 7075-T6 Al. The dashed line represents equation (16).

Intuitively one feels use of a sheet material tough enough so that full shear fracturing is observed should bring a substantial measure of protection from fracture failure due to small flaws. For high strength sheet steels the percent shear for a running crack is consistently above 50 percent for $\beta_c \geq 2\pi$. A β_c value of 2π has been suggested as a minimum toughness criterion for such structures (5). Figure (7) provides some support for this idea.

Commonly fracture failure of a high strength steel pressure vessel occurs by the spread through the wall thickness of a small crack and the subsequent lateral propagation of the crack after local severing through the wall has occurred. The computations shown on this figure are intended to represent the stress (in fraction of yield stress) required for crack propagation at various stages of this process. The movement of the leading edge of the crack assumed in the calculations is shown on the figure by dashed lines.

To the left the curves refer to extension of a partial crack from one surface through the plate. To the right the curves refer to extension of a through crack. Three levels of toughness are represented, as indicated by the β_c numbers on the curves to the right. The same three levels of toughness, but expressed in terms of β_{Ic} values, appear on the graph at the left. β_{Ic} is defined by the equation

$$\beta_{Ic} = \frac{K_{Ic}^2}{B \sigma_{YS}^2} \text{ - - - - - - - - - - -(17)}$$

To obtain values of β_{Ic} corresponding to β_c use was made of the empirical relation

$$\beta_c = \beta_{Ic} \ (1 + 1.4 \ \beta_{Ic}^2) \text{ - - - - - -(18)}$$

In terms of percent shear the assumptions were intended to correspond approximately to 80, 50, and 5 percent shear in the appearance of the running crack. For the lower two toughness levels the stress required for propagation is generally less than 80 percent of the yield stress and decreases steadily with no indication of an arrest tendency as the crack completes through the thickness. For $\beta_c = 2\pi$ a stress equal to the yield stress is required both for the half depth crack and for the through crack of half length equal to the plate thickness. Hence there is a suggestion that fracture arrest may occur. With moderate additional toughness stresses greater than the yield stress would be required throughout the partial crack extension process.

Fracture mode transition is a general thing occurring in low carbon steel and soft metals as well as in high strength metals. The meaning, however, of the fracture appearance is somewhat different because the running crack fracture appearance is determined by a relative plastic zone size based upon dynamic rather than the static yield properties. For high strength metals there is relatively little dynamic elevation of the yield stress. A mild steel structure would be expected to bear loads less than those required for general yielding with reference to the yield stress for slow loading, a stress level probably less than 40,000 psi. However, for rapid loading yielding occurs at a stress level higher by a factor of 2 to 3 depending upon loading speed. Thus in terms of percent of dynamic yield stress a stress level sufficient to arrest a crack in the first through-crack position shown in Figure 7 is, for low carbon structural steel, unlikely to exceed the lowest of the three curves and corresponds to less than 10 percent shear lip in the running crack fracture appearance. Assuming there is no dynamic overstressing and that engineers usually estimate design loads in a conservative manner for mild steel structures, a fracture toughness criterion of the mil-ductility type means, in most such structures, about the same degree of crack propagation safety as one has in a high strength rocket chamber for which the wall toughness corresponds to $\beta_c = 2\pi$ and the fracture appearance is nearly 100 percent shear.

Summary

The effect of plastic strains on the crack edge stress field, on fracture mode transition, and on the toughness necessary for arrest of a short through-crack can be estimated approximately in terms of a length r_{YS} given by

$$r_{YS} = \frac{1}{2\pi} \left(\frac{K}{\sigma_{YS}} \right)^2$$

In each case the estimate is only of the rough approximation type. However, it should be noted in support of these estimates that substantial improvements will require solution of complex multi-parameter problems. Within the framework of a simple one-parameter representation of the stress elevation near the leading edge of a crack, exact answers to these problems do not exist. In addition, each of the problems discussed is affected by other uncertainty factors of comparable magnitude which are not representable in terms of an elastic-plastic stress analysis problem.

References

(1) G. R. Irwin, J. A. Kies, H. L. Smith, "Fracture Strengths Relative to Onset and Arrest of Crack Propagation," Proc. ASTM, Vol. 58, p. 640, 1958

(2) ASTM Committee Report, "Fracture Testing of High Strength Sheet Materials," ASTM Bulletin, p. 29-40, Jan. 1960

(3) G. R. Irwin, "Dimensional and Geometric Aspects of Fracture," ASM Conf. on Fracture of Eng. Mat'ls, Troy, N. Y., August 24-25, 1959

(4) G. R. Irwin, "Fracture Mode Transition for a Crack Traversing a Plate," Trans. ASME, Vol. 82, Series D, p. 417 (1960)

(5) G. R. Irwin, J. A. Kies, "Fracture Theory as Applied to High Strength Steels for Pressure Vessels," Golden Gate Metals Conf., San Francisco, Calif., Feb. 4-6, 1960

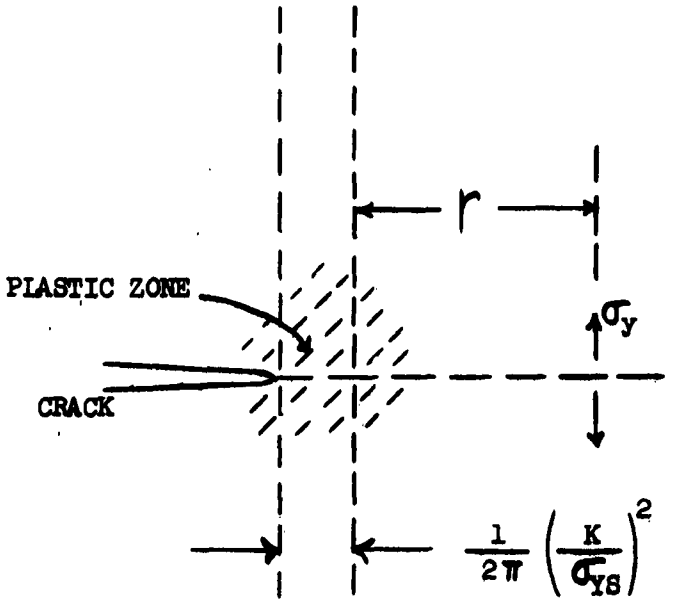


Fig. 1 - The distance r from the effective edge of the crack to the position of the normal tensile stress σ_y. The size of the plastic zone correction is shown schematically relative to the plastic zone size.

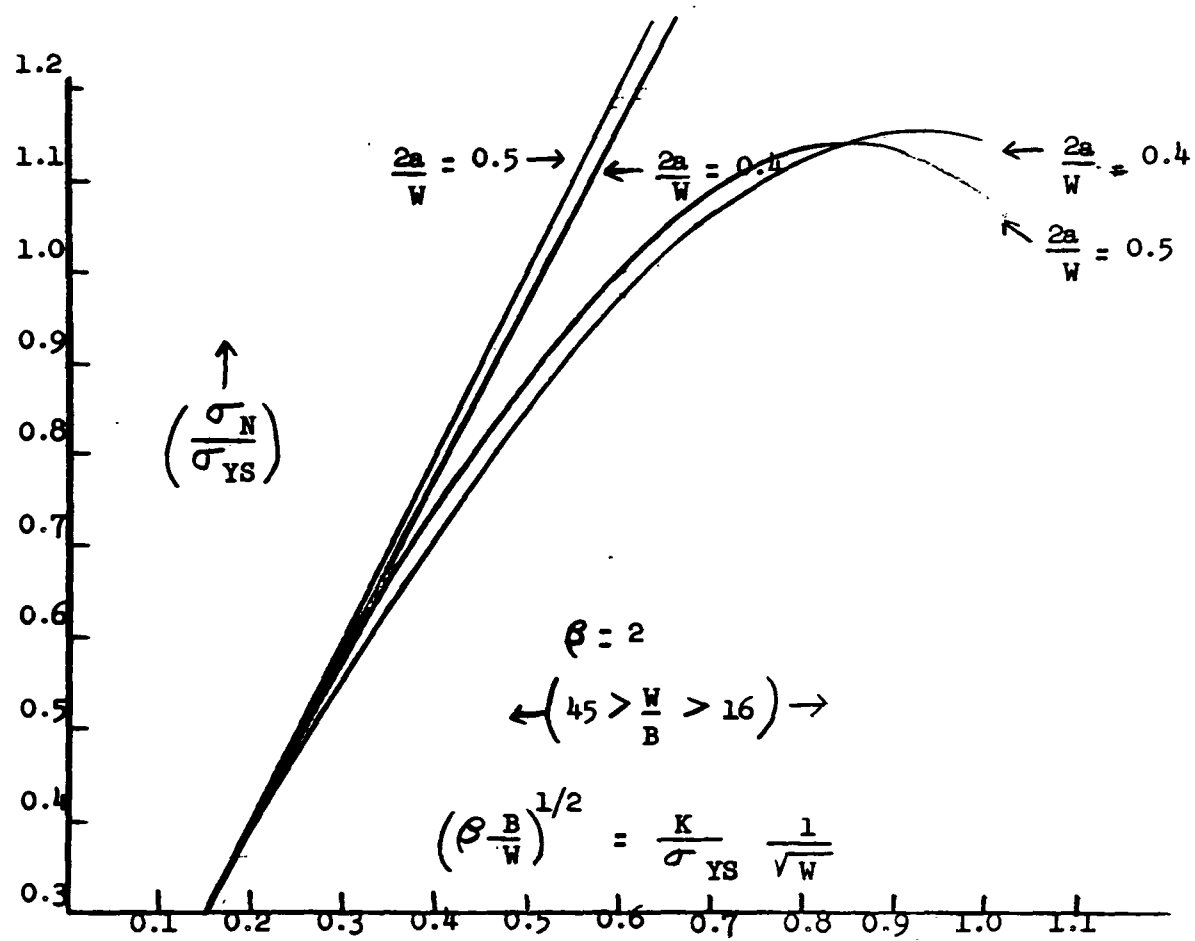


Fig. 2 - Influence of the added crack length r_{YS} upon the relation of net section stress to inverse square root of specimen width for geometrically similar centrally notched sheet tensile specimens as predicted by equation (7).

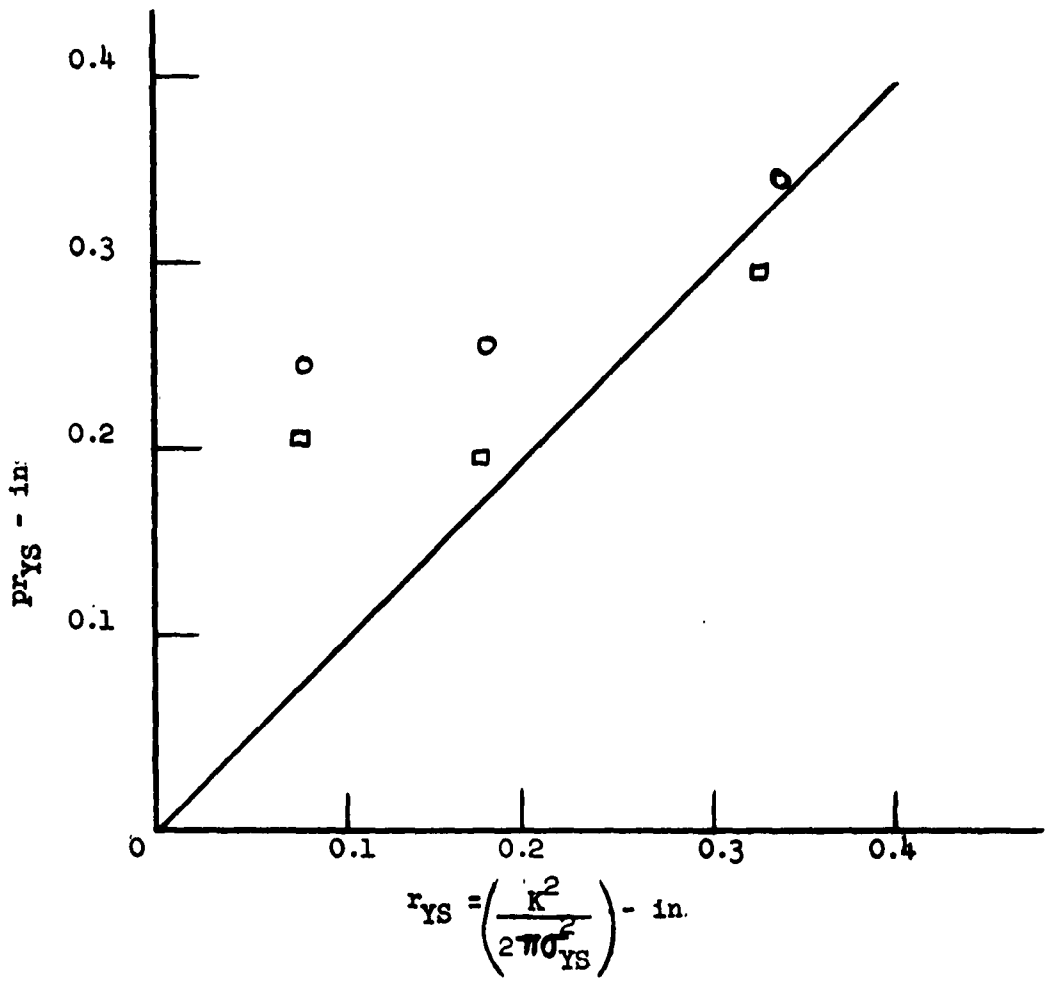


Fig. 3 - Experimental stress analysis measurements of pr_{YS} plotted against r_{YS} for a 1/8" thick centrally slotted sheet tensile specimen of 7075 T-6 aluminum.

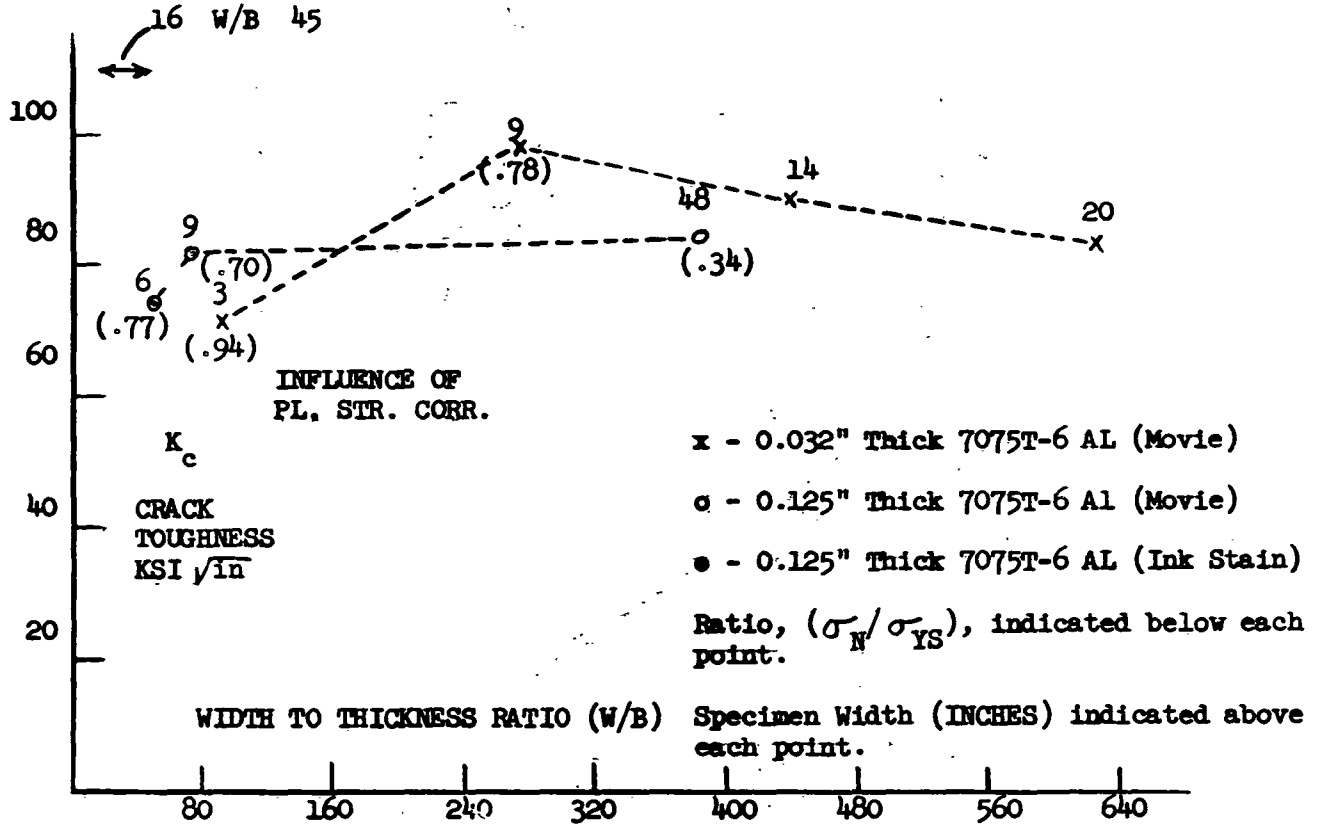


Fig. 4 - Values of K_c from centrally notched sheet tensile specimens of 7075T-6 aluminum plotted as a function of the ratio of sheet width to sheet thickness.

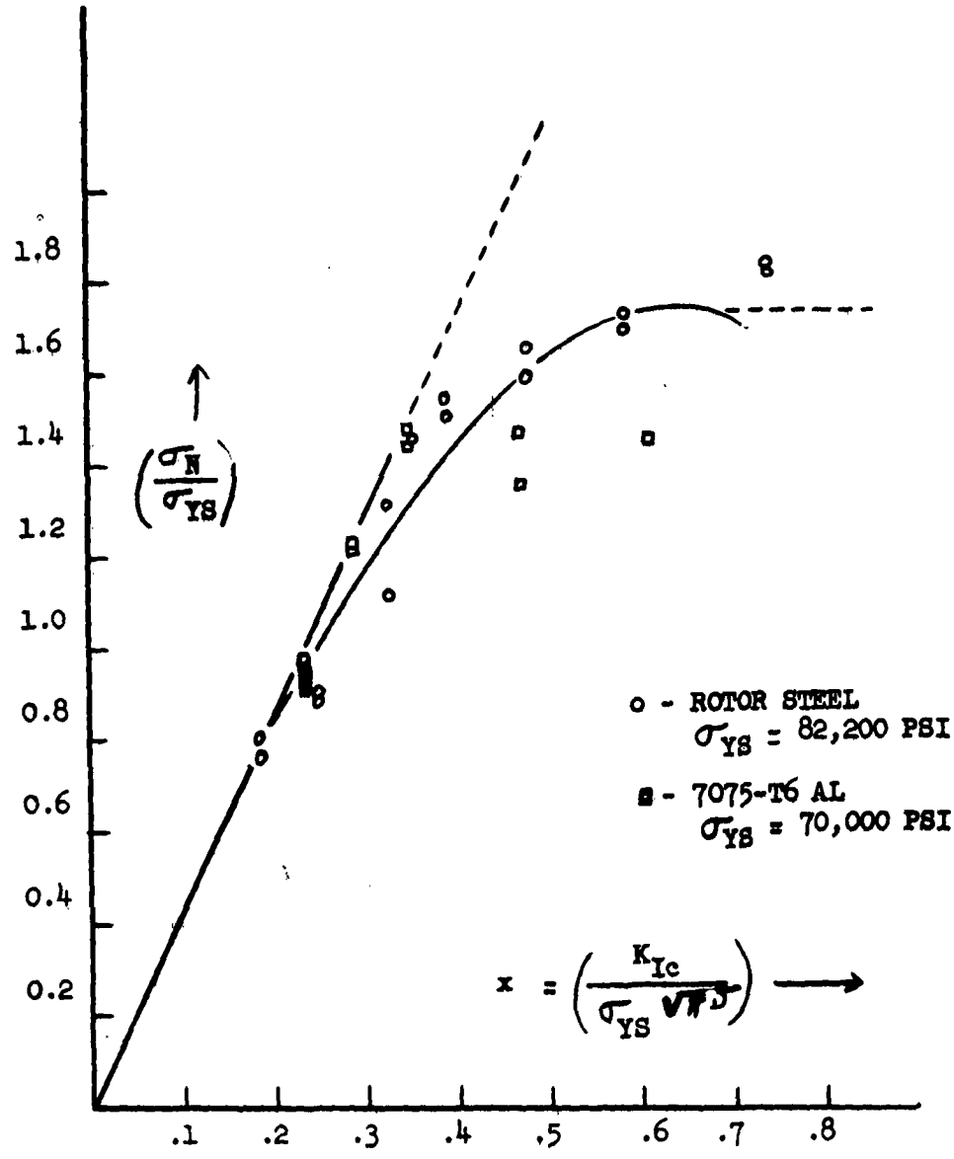


Fig. 5- Influence of the added effective notch depth ($r_{YS}/2\sqrt{2}$) upon the relation of net section stress to inverse square root of specimen diameter for circumferentially notched round tensile bars as predicted by equation (13). Shown on the figure are experimental points for a rotor steel and for 7075-T6 aluminum.

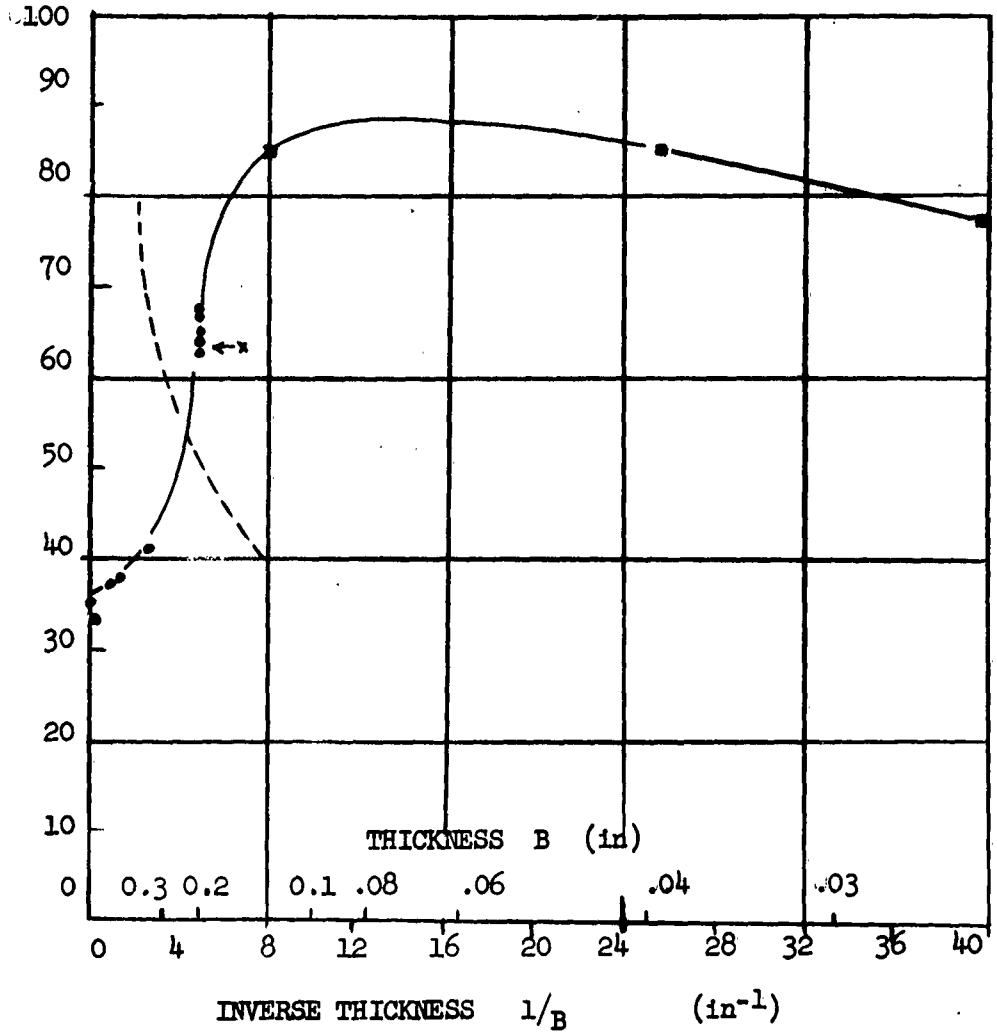


Fig. 6 - K_c as a function of reciprocal sheet thickness (1/B) for 7075-T6 aluminum alloy. Dashed line is the $\beta_c = 2.4$ locus

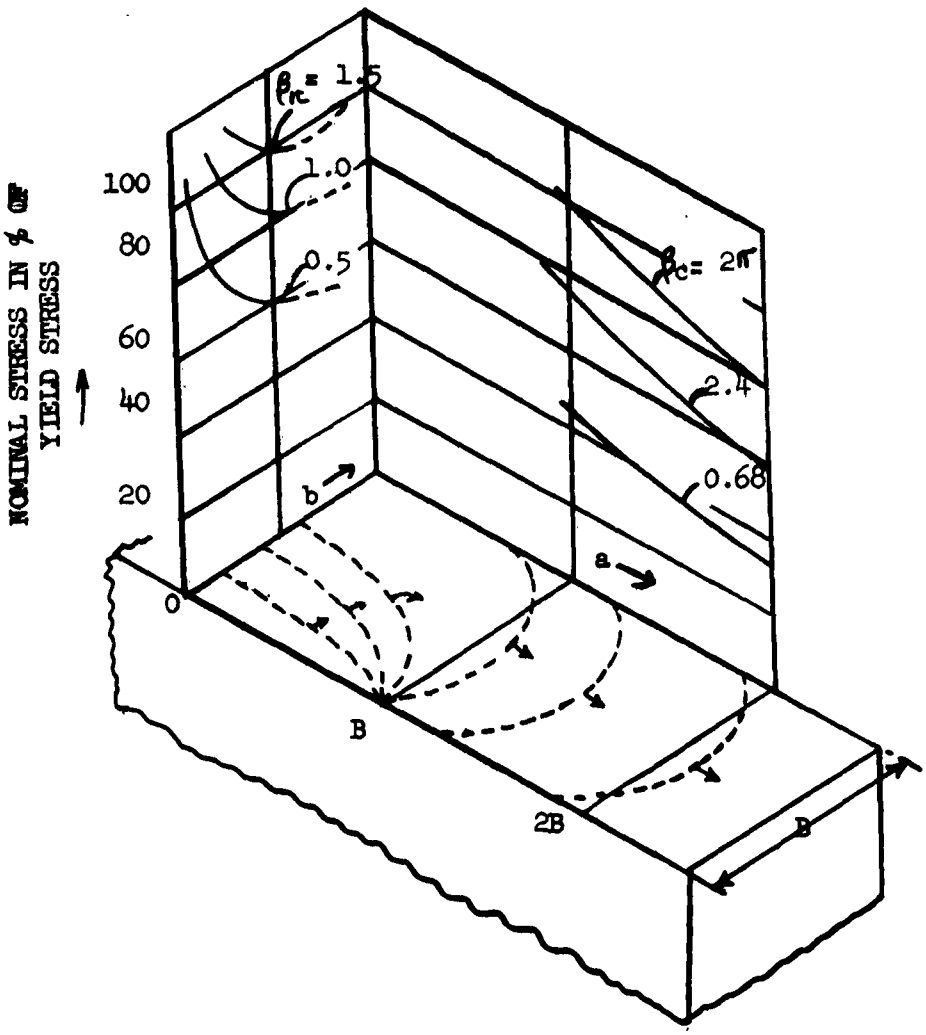


Fig. 7 - Right background graph shows relative stress for propagation of through-cracks. Three levels of toughness are represented corresponding to β_c values of 2π, 2.4, and 0.68. Left background graph shows relative stress for propagation of partial cracks. Computations were based upon plane strain β_{Ic} values estimated as equivalent to the through-crack β_c values.

FRACTURE ARREST IN PRESSURE VESSELS

BY

JOSEPH I. BLUHM

and

MILTON M. MARDIROSIAN

ABSTRACT

A technique is developed for the experimental evaluation of the elastic energy release rate in a pressure vessel and is applied to plastic models. The feasibility of effecting crack arrest is demonstrated and the prediction of the arrested crack length is schematically indicated.

I. INTRODUCTION

The risk of catastrophic or rapid fracture in a structural component can be minimized in a number of ways. Obviously, first considerations tend toward optimization of the material selection such as to utilize a material having as high a "toughness" as possible, consistent with the strength levels required and operating temperatures involved. All too frequently, however, weight considerations dictate such a high strength level that the toughness levels available in even the best materials is only marginal.

A second alternative is to use materials at a lower than otherwise optimum strength level. This, of course, entails a weight sacrifice though an appreciable gain in toughness may be effected.

Finally, one can approach the problem by consideration of design innovations which might be employed. Consider the case where even the best of the materials tentatively selected, has inadequate toughness and that crack initiation is highly probable. Can the designer then employ some design device to minimize the consequences of the anticipated rapid fracture?

It is proposed that if a crack, which has started to propagate, is halted prior to a functional failure of the materiel, then in effect the hazards associated with the fracture are minimized and limited propagation consequently may be tolerated. Obviously, a small crack in a liquid fuel container may permit escape of fuel and possible consequent ignition and self-destruction or other malfunction. In such applications, even the initiation of a crack must be prevented. But what of the case of a solid fuel rocket motor casing, for example? Leakage is not a primary problem. If a crack which has initiated can be arrested, i.e. brought to a halt, prior to a functional failure, then a finite crack might be tolerated.

It is then the express purpose of the present study to examine the feasibility of designing for crack arresting in such vessels and to provide some basis for a design procedure.

II. BASIC CONSIDERATIONS

The classic paper by Griffith (1)[1] lays the foundation for the development of our current thinking on fracture. This work aimed at explaining the discrepency between the theoretical and observed strengths of glass (a very brittle material), established the energy balance criterion for the instability of a crack as follows:

$$dG/dA \geq dS/dA \qquad (a)$$

where dG/dA is the rate of release of elastic strain energy per unit increase in crack surface and dS/dA is the rate of energy absorbed per unit increase in crack surface as surface tension. This equation implies that for a fixed specimen having a crack as the load is increased, a critical load will be reached such that the rate of release of strain energy is just equal to the rate of surface energy absorbtion. If the load is increased slightly, the crack will become unstable and propagate.

The extension of this basic equation to structural metals has been discussed in the literature (2) and in effect replaces the surface energy term dS/dA by a plastic work term dP/dA. Then the instability criterion becomes

$$dG/dA \geq dP/dA \qquad (b)$$

These equations though applicable to the onset of rapid fracture, require some insight for practical application in view of the uncertainties relating to the actual plastic stress state near the crack root (3). The applicability of these equations has been implied similarly (4) for the "arrest" criterion. It is not believed that these equations are generally valid as an arrest criterion without due consideration of the kinetic energy changes, dK/dA which occur; more generally, for "arrest" one might use

$$dG/dA \leq dP/dA + dK/dA \qquad (c)[2]$$

Since at the present time analyses of the dynamics of the growing crack are not available, the use of quasi-static criterion, i.e. Equation (b), for the arrest condition has generally been adopted (4) (5).

---

[1] *Numbers in parentheses refer to bibliography at the end of the paper.*

[2] *More generally, the energy balance is written as follows:*

$$dG/dA + dF/dA \leq dS/dA + dP/dA + dK/dA$$

where dF/dA is the rate of work of the external forces; for rapid fracture of large specimens, this work term can be ignored in both the onset and arrest criteria. In small specimens, this term must be taken into account.

III. THE EXPERIMENTAL PROGRAM

A. General

A series of tests are performed in which plastic pressure vessels containing longitudinal cracks and a set of crack arrestors are loaded with internal pressure. The present program is aimed at determining the feasibility of designing a cylindrical pressure vessel to a crack "arrest" condition. An experimental procedure was initially adopted because of the inherent difficulties associated with the sufficiently detailed and accurate stress analysis necessary for a calculation of the required "energy release rates". Although calculable energy release rates are available for simple configurations such as a "cracked" flat sheet under tension or a cylinder with radial cracks under internal pressure or notched bend specimens, no such exact solutions are available for a "cracked" cylindrical pressure vessel. The principal difficulty arises in attempting to determine the stress state in the neighborhood of the lip formed at the crack.

A further difficulty arises in the case of a ring reinforced pressure vessel. Ignoring for the moment the aforementioned "lip" problem, any attempt to utilize flat sheet criteria in lieu of the developed cylinder must recognize the significant discrepancy which arises because of the departure in the loading of the reinforced cylinder from "uniform tension field" remote from the crack. The uniform stress field case is the classic case; the finite width plate and non-uniform tension due to the bulging in a reinforced pressure vessel impose challenging problems to the analyst. An experimental procedure on the other hand precludes the difficulties and includes these effects in a routine fashion.

Since the elastic energy release rate is a function only of the geometry, loading and the elastic properties of the specimen, a scale model with known elastic properties may be used to determine the release rate. Use of plastic models, in particular, provides the advantage that low pressures are used, thus decreasing the hazards associated with pressure testing; the deformations are large and accurately measurable and the models are simple to machine and cost very little. Extension of the model results to prototype materials and/or sizes may readily be effected by consideration of the pertinent Buckingham π factors, i.e.

$$\pi_1 = \frac{1}{E\ell} \frac{dG}{dA}$$

and

$$\pi_2 = P/E$$

where the terms on the right side are defined later.

Experimental techniques for determination of the elastic energy release rate have been described in detail by Lubahn (6) for the flat sheet and notch bar in bending and/or tension. These procedures require careful load-deformation measurements. In the present study, the equivalent quantities are pressure p and volume V. The stored elastic energy, E_{stored}, is merely given by the integral.

$$E_{stored} = \int p \, dV$$

By determination of the stored elastic energy as a function of pressure and crack length, it is possible to derive the rate of release of elastic strain energy.

The principal difficulty in the present problem is in the measurement of the volumetric changes of the test specimen. Direct measurements of the fluid being pumped into the test specimen leaves unresolved the problems of gas being trapped in the specimen, and compressibility of the fluid and the actual volume measurement. These seemed relatively insurmountable. By way of contrast a relatively simple scheme consists of submerging the pressurized vessel within a filled second chamber and causing the fluid in this latter chamber, which is displaced by the expansion of the test specimen, to rise into a precision tube of sufficiently small diameter to provide the anticipated accuracy and sensitivity. Figure 6 shows this scheme in detail. This scheme eliminates any difficulties associated with either gas which is trapped in the pressure vessel or with compressibility of the fluids. The fluid in the outer chamber (the volumetric measuring chamber) is at atmospheric pressure.

B. The Materials and Models

Plastic models were made in accordance with Figure 1 using both Plexiglas and Micarta. The stress strain curves of both materials are shown in Figures 2 and 3 respectively. Non-linear behavior was negligible in either material at the maximum working stresses used. (i.e. approximately 1500 psi and 100 psi pressure) Creep though evident, was minor at the temperature of the test, i.e. 20°C., but was nevertheless compensated for by the load unload test cycle used, (see Test Procedure).

The test cylinders were plugged internally at both ends by a set of stainless steel caps and constrained on the outside by a set of stainless steel restrainers. In effect, the cylinder was provided very closely with a "clamped-clamped" edge condition. "Rigid"[1] crack arrestors of stainless steel were provided. These could be moved to predetermined positions. Figure 4 shows the detail of the test specimen assembly.

[1] *"Rigid" i.e. relative to the plastic cylinder. Steel arrestors were utilized initially. It is intended later to investigate the effect of arrestor flexibility in optimizing the design and to make possible "scaling" from model to prototype.*

Final machining techniques involved the cutting of the crack with .004-inch thick circular saws and removing the radii at the ends of kerf with a .004-inch thick straight saw blade. The cutting edge of this latter blade provided the .002-inch radius at the ends of the cracks.

Specimens were used repeatedly with successively longer cracks, as long as a failure did not interrupt the sequence of tests. No effect of the prior loading on subsequent test behavior was anticipated, though this is being checked in detail.

C. The Test Procedure

After machining the "crack" to the desired length, a seal was placed in the inner surface of the specimen against the crack to prevent leakage in the subsequent pressure tests. The seal was effected by bonding a piece of thin, flexible, inner tube patching rubber over the crack area. One stainless steel cap and restrainer was then attached so that sealing on the "O" ring occurred, (see Figure 4). The test specimen was then filled with the pressurizing fluid in an upright position to the upper threads and the upper stainless steel cap and restrainer were screwed on and seated against the upper "O" ring. The excess fluid was permitted to escape through either the pressure readout tap hole or the pump inlet.

It was necessary to attach the crack arrestors prior to applying the upper cap because of clearances. Final spacing of the arrestors was accomplished after assembly by screwing the arrestors along the exterior thread of the caps.

After complete assembly of the test specimen, as shown in Figure 4, the assembly was affixed to the manifold head (an aluminum cover plate--see Figure 5) and connected to the pressure pump. At this stage, the specimen assembly was pressurized to 3 psi and, with the pressure maintained, the outer surface of the specimen over the crack area was sealed similarly to the inner surface. This was necessary to preclude the possibility of fluid being sucked into the test specimen upon unloading. After this outer seal was applied, the assembly was inserted in the volumetric measuring chamber (the Plexiglas housing of Figure 6) and affixed to it by a series of 4 tie rods. These tie rods permitted the cover and base plate and the Plexiglas housing to be drawn together against "O" rings, thus achieving the necessary seal. The pressure gage, a volumetric displacement measuring capillary tube, and thermometers were then inserted and the necessary plumbing tightened. Figure 6 shows the entire test ensemble in schematic form for the "Energy Release Rate Determination." Figure 7 shows the test ensemble.

Although the entire test program was conducted in a temperature and humidity controlled room, the temperature fluctuations were sufficient to warrent further refinement and it was necessary to immerse the test ensemble in a large vat of water. With this setup, the temperature varia-

tions during the period of a test were always less than .05°C and more frequently of the order of .01°C. The temperature sensitivity of the test ensemble using Micarta specimens was determined and is shown in Figure 8.

Pressure was applied in increments of 2 psi to a maximum pressure dependent on the crack length. The volumetric changes were observed by the rise (or fall) of the fluid level in the precision volumetric capillary tube and was measured to the nearest milli-meter using a standard meter stick. The bore of the measuring tube was specified by the manufacturer to be .125± .0002 inches corresponding to a calibration of .00793 cc per mm.

Only minor creep of the specimen occurred and volumetric changes observed by different types of loading cycles led to identically the same results. The final procedure adopted was to record initial data, apply a small increment of pressure, record the pressure, temperature, and volume change, then unload rapidly (to avoid the creep effects) to zero pressure and again record the basic data. The specimen was then reloaded to the next higher increment of pressure and this process was repeated till the ultimate pressure was achieved.

Pressures were measured by means of a Control Engineering Pressure Gage Type EP-400 and an SR4 Type N strain indicator.

IV. RESULTS AND DISCUSSION

The limited data available on Plexiglas specimen is shown in Figure 9. Here the raw, unmodified pressure-expansion data is plotted for a series of cylinders having crack lengths from 0 inches to 2 inches, and a crack arrestor spacing of 3 inches. Figure 10 shows these "curves" modified and shifted for low pressure errors such as backlash and for temperature correction. Figure 12 shows a plot of the slope of these "curves" as a function of the crack length. Figures 11 and 13 show the corresponding data for Micarta specimens.

If the shape of this slope curve can be represented as a single cosine curve, a rather trivial analysis can be carried out. This analysis permits the determination of the critical fracture toughness "$\mathcal{G}_c$" from the results of a series of model tests and an observation of the pressure and crack length at which catastrophic fracture takes place in the actual prototype material. In addition this analysis provides a basis for predicting the influence of the ring stiffener on crack arrest. Schematic details of this procedure are given in the Appendix. This procedure is not restricted obviously to the use of the idealized slope curve demonstrated. In any real case the actual curve may be used and the procedure indicated in the Appendix will be valid.

Figure 14 shows an actual test cylinder of Plexiglas which contained an initial crack of approximately 1/2 inch and had arrestors at 3 inch spacing. It will be noted that the crack propagated to the crack arrestors. It will be further noted that the cracks turned 90° at the arrestor position. This shift in direction of the crack is considered to be attributable to the high bending moments at this section due to the arrestor constraints. An additional specimen which had only the arrest action of the end clamps permitted the crack to propagate closer to the cylinder ends where the crack again turned some 90°. This is shown in Figure 15. The turning of the crack in this case is again associated with the regions of maximum bending stresses.[1]

These latter specimens certainly demonstrate the feasibility of achieving crack arrest by design. The prediction of crack arrest can be carried out using the procedure schematically outlined in Figures A1 through A7 of the Appendix.

The experimental techniques described, though requiring some further refinement, appear entirely suitable for the determination of the energy release rates of pressure vessels. The use of plastic models entails considerable advantage over tests using prototype materials for the energy release rate measurements.

---

[1] *The maximum bending moment occurs at the clamped edge but due to a filleted thickness variation in this region, the maximum stresses occur further inboard. The variance in the location of the turn at either end of the crack may be associated with the rather slow variation in the maximum stresses in this general region.*

The procedure furthermore provides a basis for, and tends to substantiate this basis for, determining the arrested length of the crack. The problem of whether a crack, arrested or not, can be tolerated must be answered on an individual case basis.

V. CONCLUSION AND RECOMMENDATION FOR FURTHER RESEARCH

On the basis of the work described in this report, it is concluded that:

1. It is entirely feasible to effect crack arrest in pressure vessels by appropriate design innovation.

2. It is feasible to utilize plastic models of complex structural configurations to obtain the energy release rates associated with "cracks", and that specifically in the case of pressure vessels sufficient precision is possible in the volume measurement by the technique described.

3. Crack arrest can be predicted in complex configurations by use of plastic model results and a single test on prototype material.

It is recommended that further work be carried on aimed at the following areas of interest:

a. The influence of the kinetic energy term in the arrest criteria.

b. The analyses of the flat sheet under biaxial non-uniform tension (to take into account actual distribution in ring reinforced cylinders).

c. The determination of $\mathcal{G}_c$ under axial as against biaxial loading ($\mathcal{G}$ is not expected to be effected - but $\mathcal{G}_c$ is).

d. The analysis of the "lip" problem for pressure vessels.

e. Optimization of ring-cylinder design for maximum strength consistent with an arrested crack.

BIBLIOGRAPHY

(1) GRIFFITH, A. A. "The Phenomenon of Rupture and Flow in Solids" Royal Soc. Phil. Trans. A 221:163-198 (1920).

(2) OROWAN, E. "Fundamentals of Brittle Behavior in Metals" Article in Book "Fatigue and Fracture in Metals" Published by MIT, Technology Press and Wiley & Sons, 1952, pp 139-167. See also Orowan, E. and Felbeck, D. K. "Experiments on Brittle Fracture of Steel Plates" Welding Jl. Res. Supp. Nos 1955 pp 570s-575s.

(3) IRWIN, G. R. "Fracture Mechanics" Contributed to the First Symposium on Naval Structural Mechanics August 11-14, 1958, at Stanford University.

(4) IRWIN, G. R., KIES, J. A. & SMITH, H. L. "Fracture Strength Relative to Onset and Arrest of Crack Propagation" Naval Res. Lab. Report NRL 5222 dated 20 Nov. 1958.

(5) ROMUALDI, J. P. & SANDERS, P. H. "Fracture Arrest by Riveted Stiffeners" Proc. 4th Annual Conference on Solid Mechanics held at University of Texas, Austin, Texas, September 1959.

(6) LUBAHN, J. D. "Exp. Det. of Energy Release Rate for Notch Bending and Notch Tension" ASTM-80-1959 Preprint.

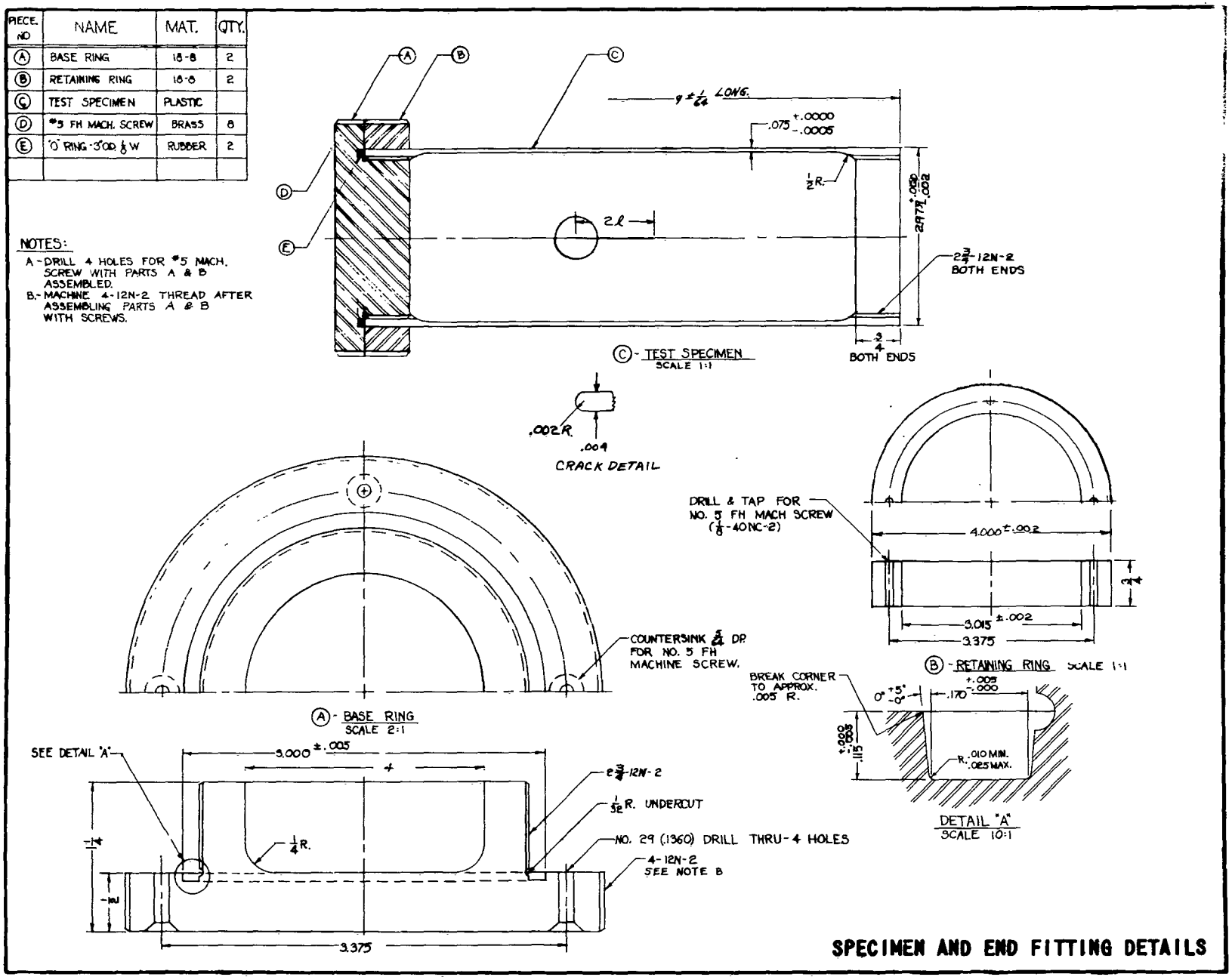

PIECE NO
NAME
MAT.
QTY.
Ⓐ BASE RING 18-8 2
Ⓑ RETAINING RING 18-8 2
Ⓒ TEST SPECIMEN PLASTIC
Ⓓ #5 FH MACH. SCREW BRASS 8
Ⓔ 'O' RING-3"OD ⅛"W RUBBER 2
NOTES:
A - DRILL 4 HOLES FOR #5 MACH. SCREW WITH PARTS A & B ASSEMBLED.
B - MACHINE 4-12N-2 THREAD AFTER ASSEMBLING PARTS A & B WITH SCREWS.
9 ± 1/64 LONG.
.075 +.0000 -.0005
1/2 R.
2ℓ
2.978 +.000 -.002
2 3/4-12N-2 BOTH ENDS
3/4 BOTH ENDS
Ⓒ - TEST SPECIMEN SCALE 1:1
.002 R.
.004
CRACK DETAIL
DRILL & TAP FOR NO. 5 FH MACH SCREW (1/8-40NC-2)
4.000 ± .002
3/4
3.015 ± .002
3.375
Ⓑ - RETAINING RING SCALE 1:1
COUNTERSINK 5/64 DP. FOR NO. 5 FH MACHINE SCREW.
Ⓐ - BASE RING SCALE 2:1
BREAK CORNER TO APPROX. .005 R.
0° +5° -0°
.170 +.003 -.000
.115 +.003 -.000
R. .010 MIN. .065 MAX.
DETAIL "A" SCALE 10:1
SEE DETAIL 'A'
3.000 ± .005
2 3/4-12N-2
1/32 R. UNDERCUT
1/4 R.
NO. 29 (.1360) DRILL THRU-4 HOLES
4-12N-2 SEE NOTE B
3.375
SPECIMEN AND END FITTING DETAILS

FIGURE 1

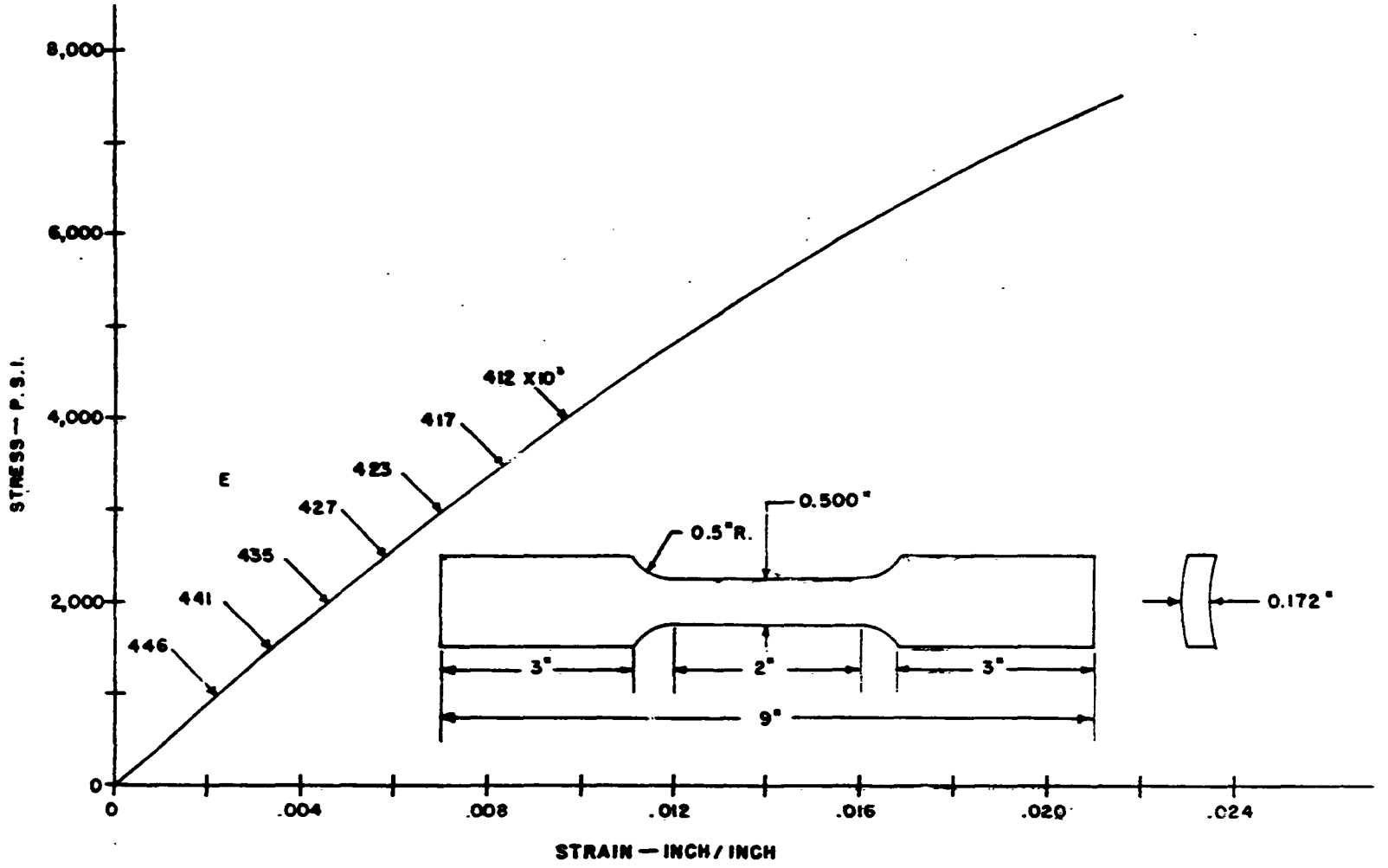


FIGURE 2. STRESS—STRAIN CURVE FOR PLEXIGLAS

AM 2230

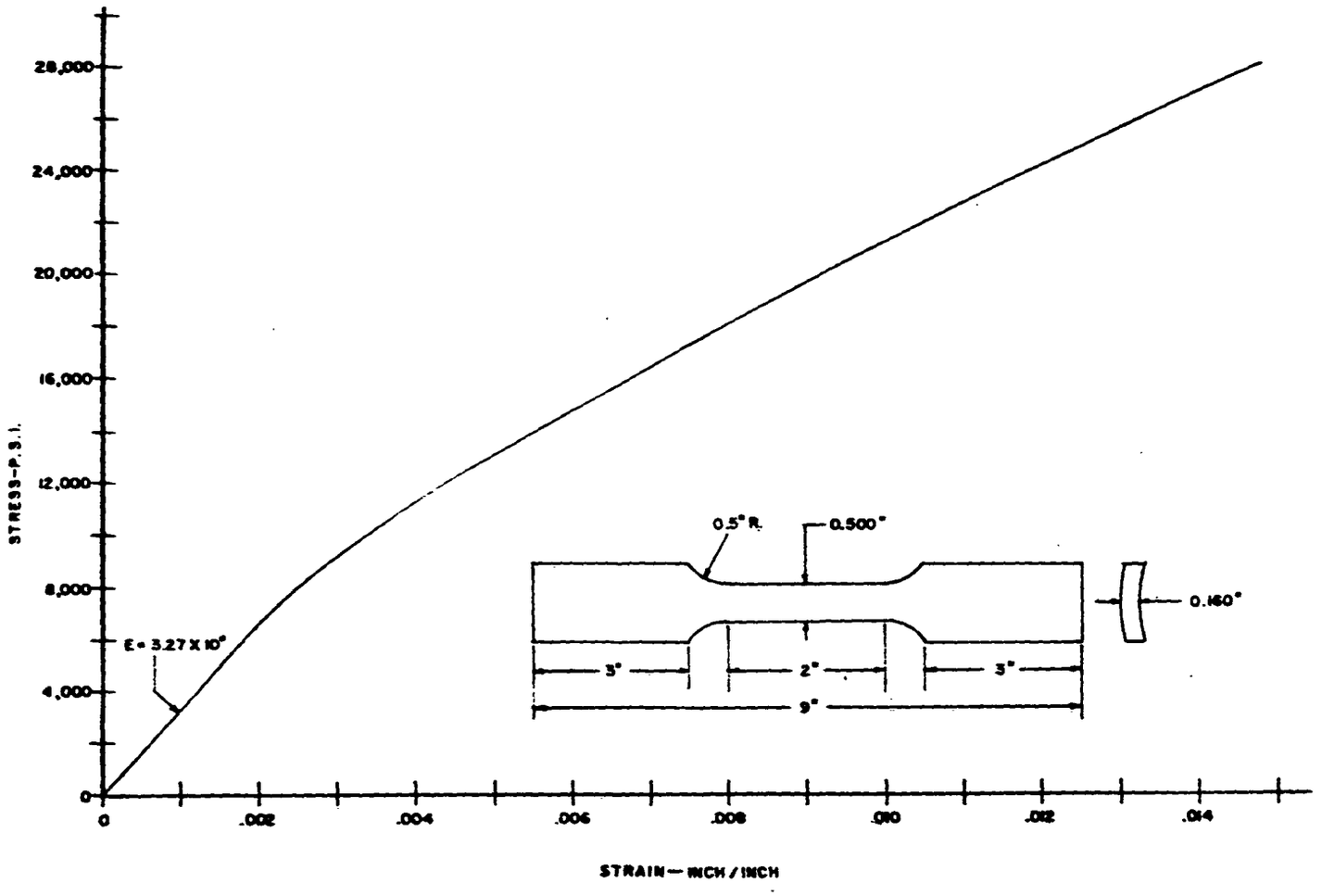
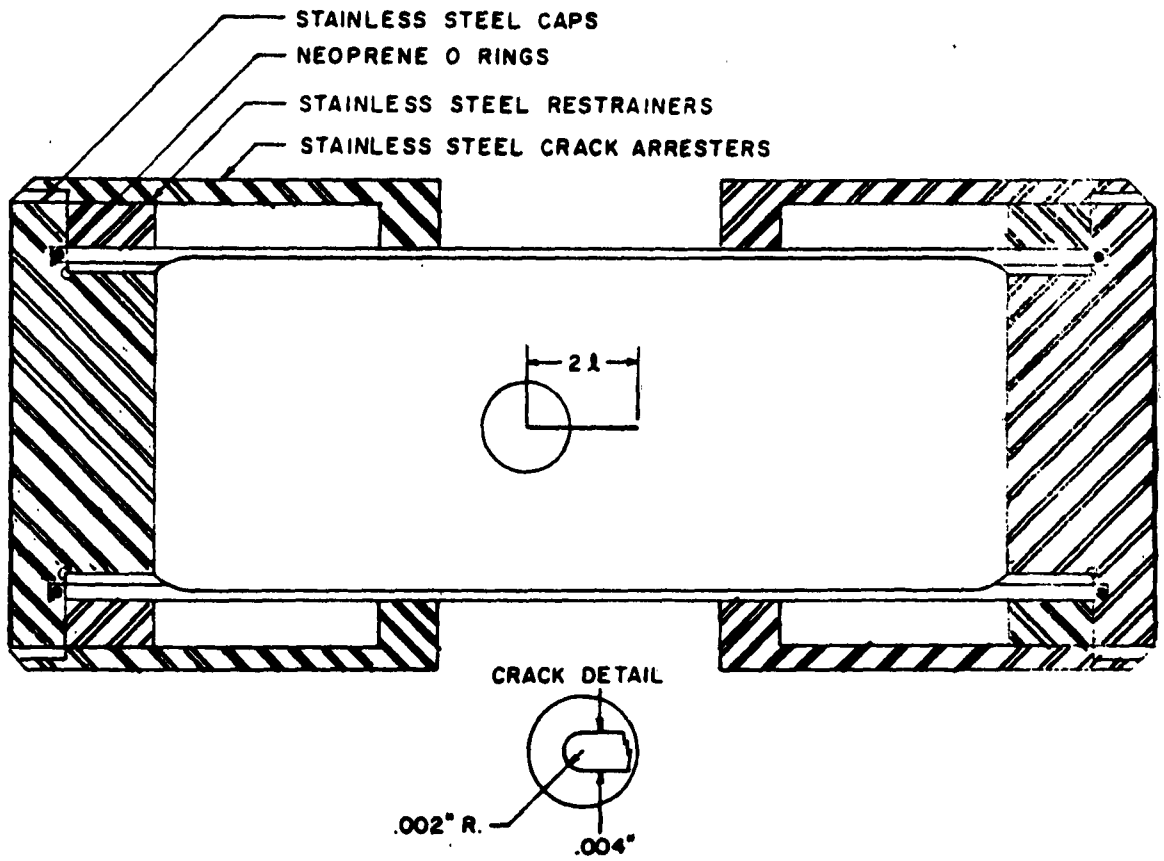


FIGURE 3

STRESS—STRAIN CURVE FOR MICARTA GMG

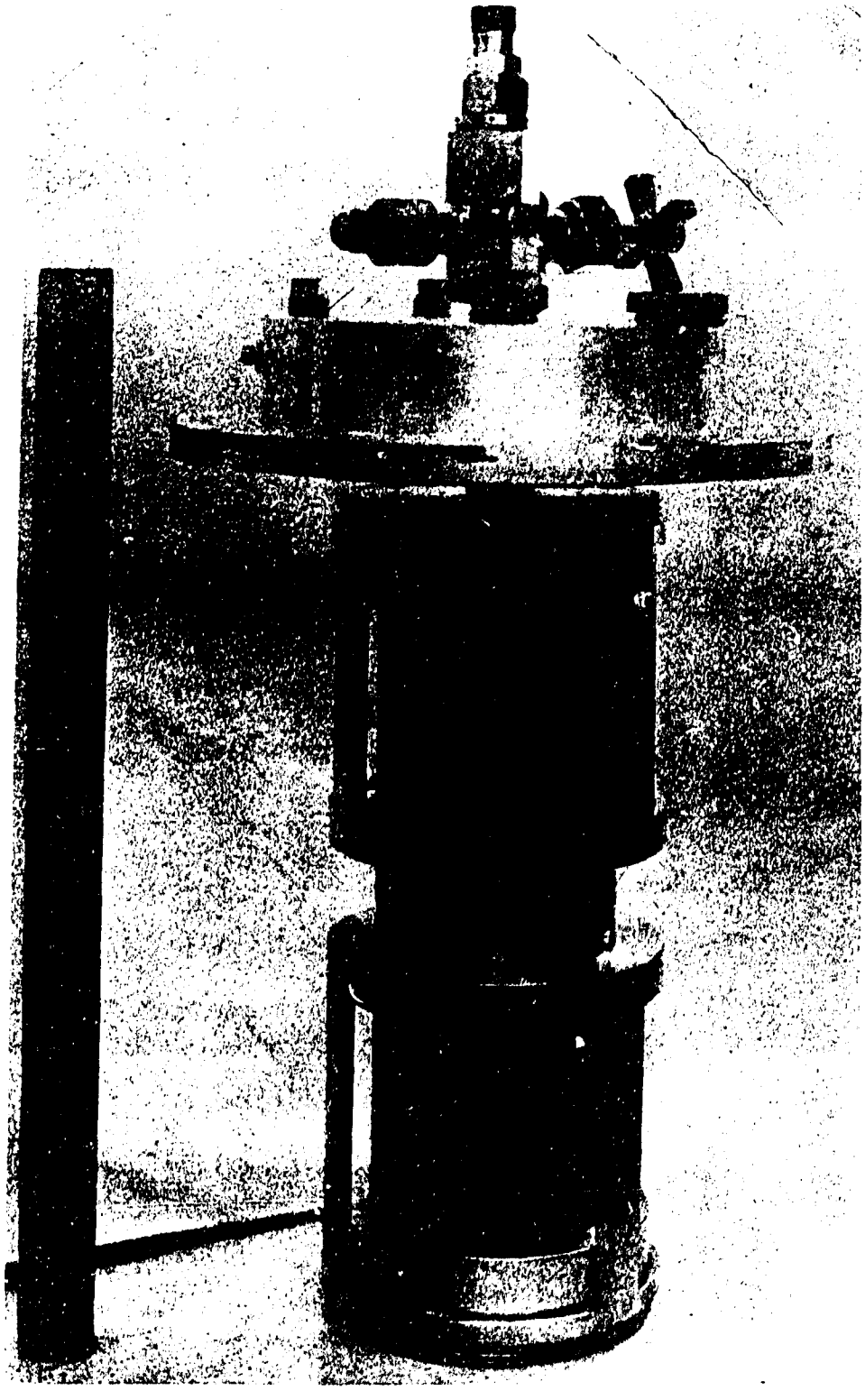
AM 2234



TEST SPECIMEN ASSEMBLY SHOWING CRACK DETAIL

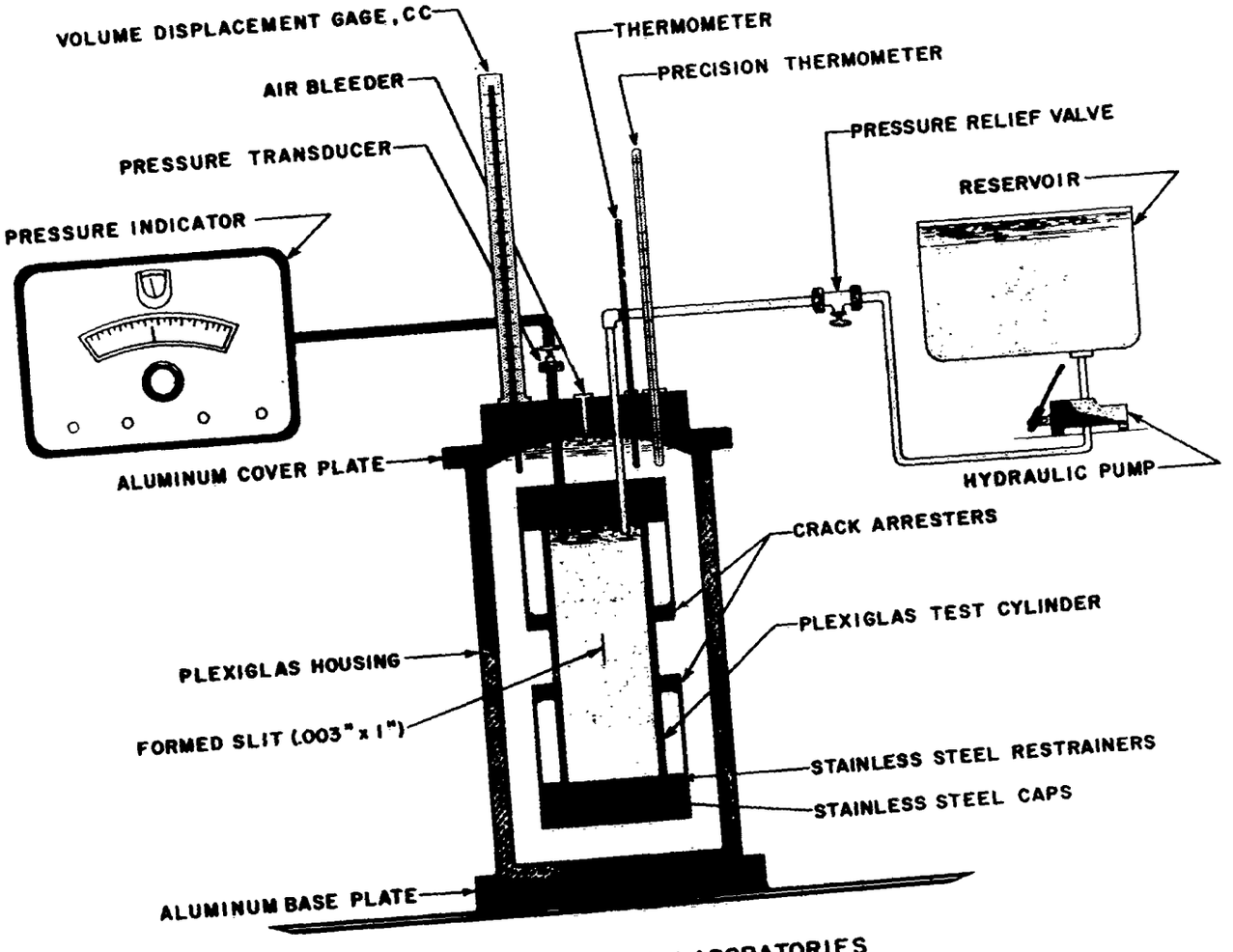
AM 2232

FIGURE 4



SPECIMEN ASSEMBLY AFFIXED TO ALUMINUM COVER PLATE

FIGURE 5



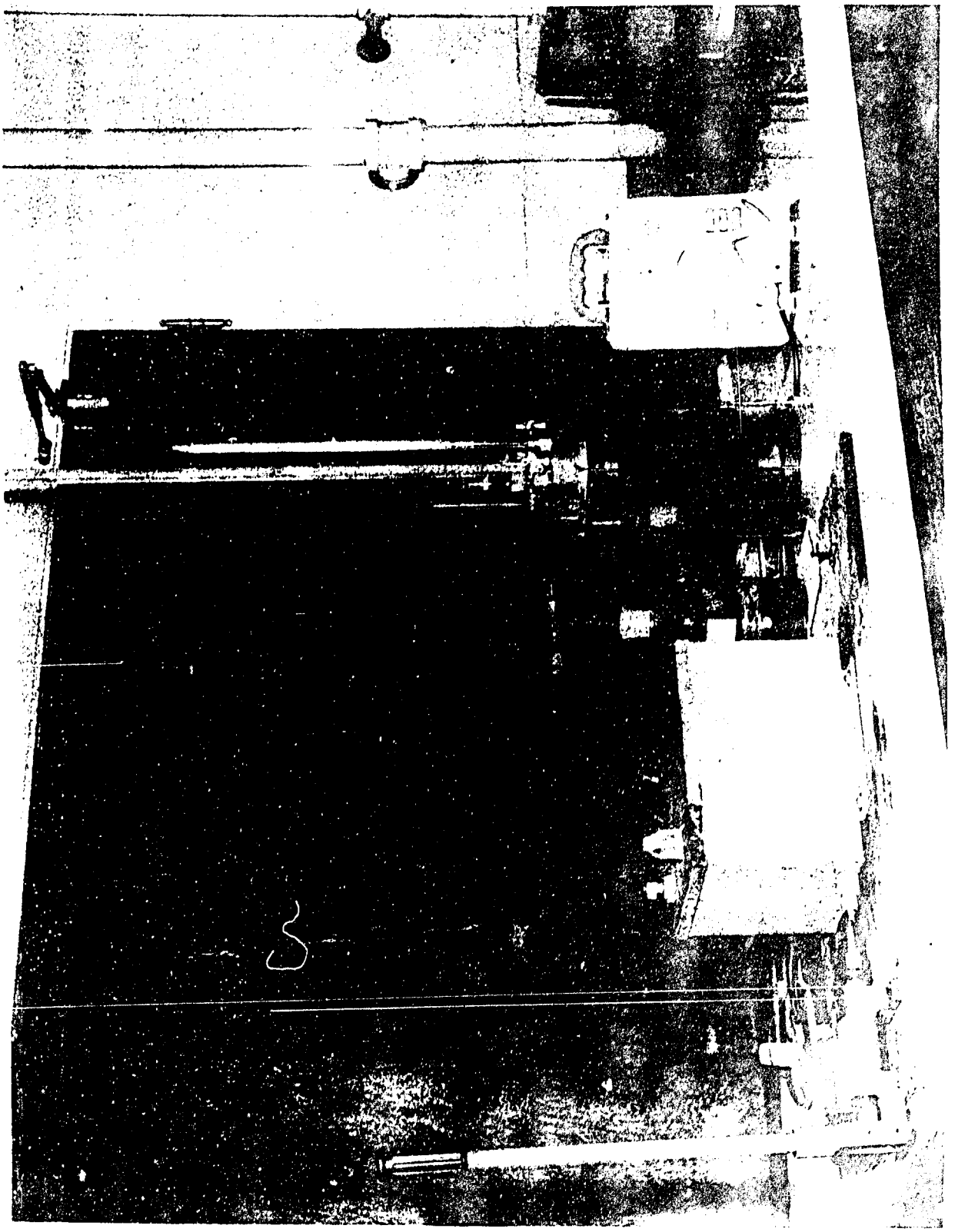
WATERTOWN ARSENAL LABORATORIES

ENERGY RELEASE RATE DETERMINATION

19-066-1276/ORD-60

FIGURE 8

IV-93



TEST ENSEMBLE

FIGURE 7

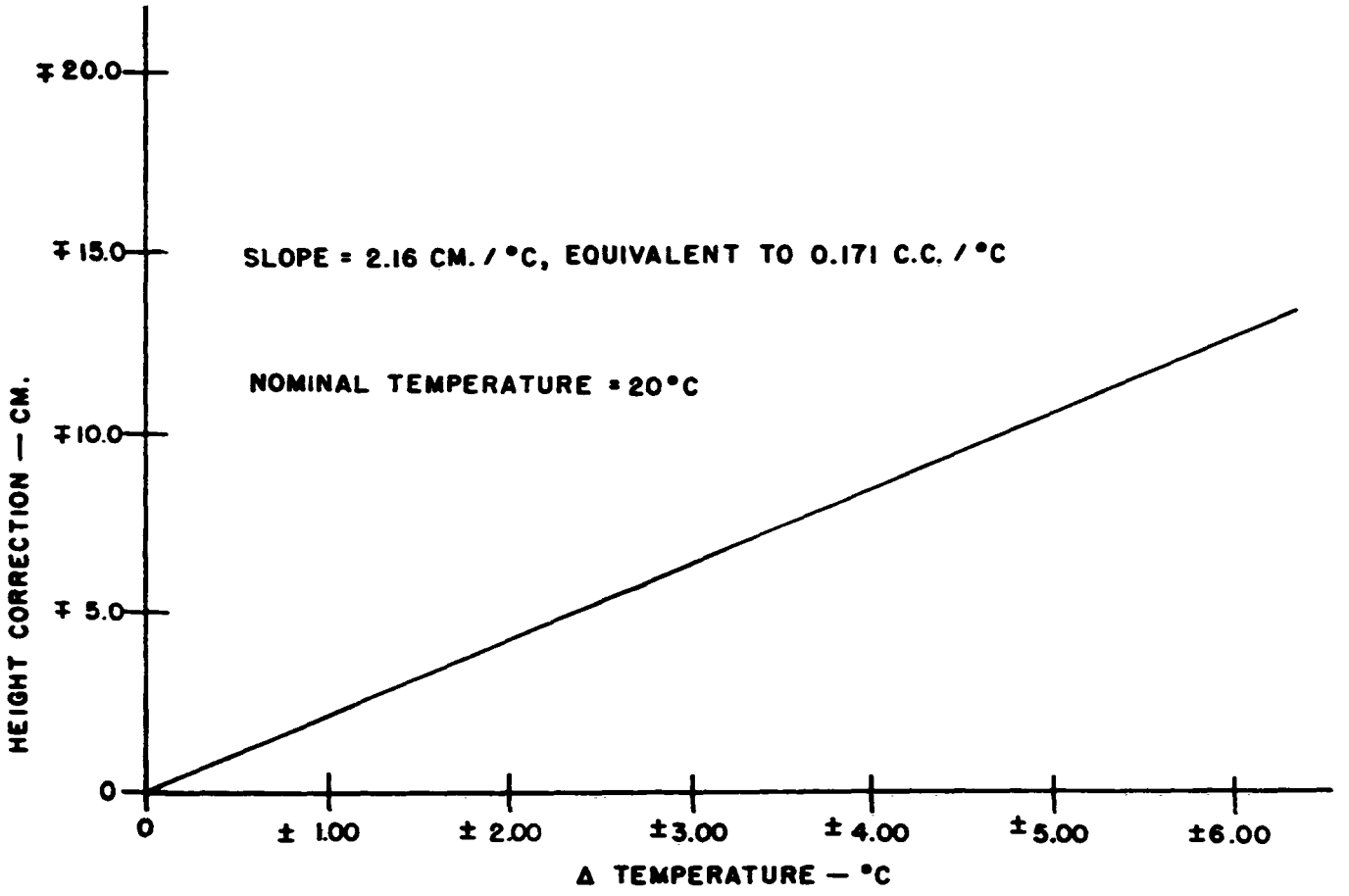
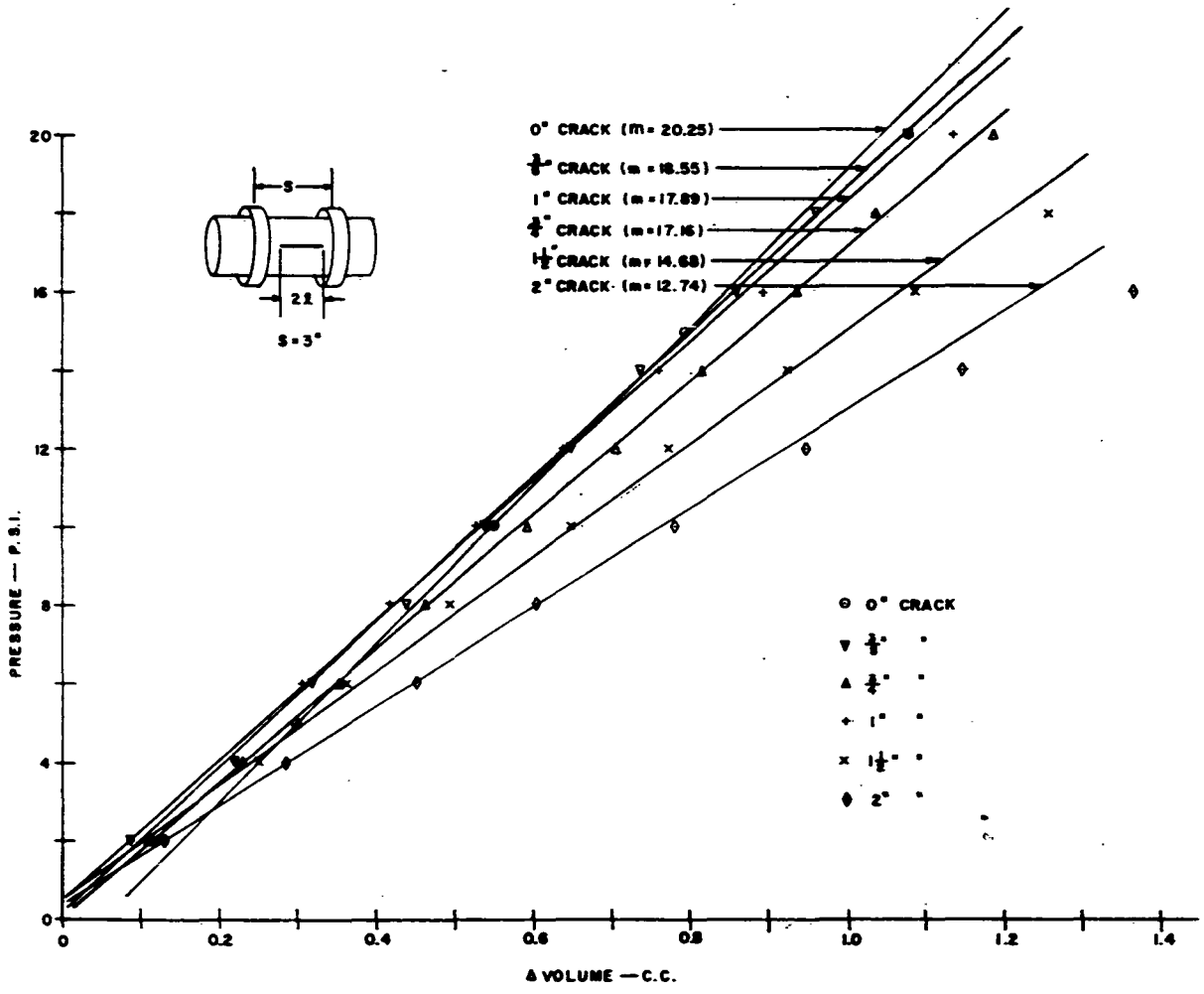


FIGURE 8

TEMPERATURE CORRECTION FOR MICARTA TYPE GMG

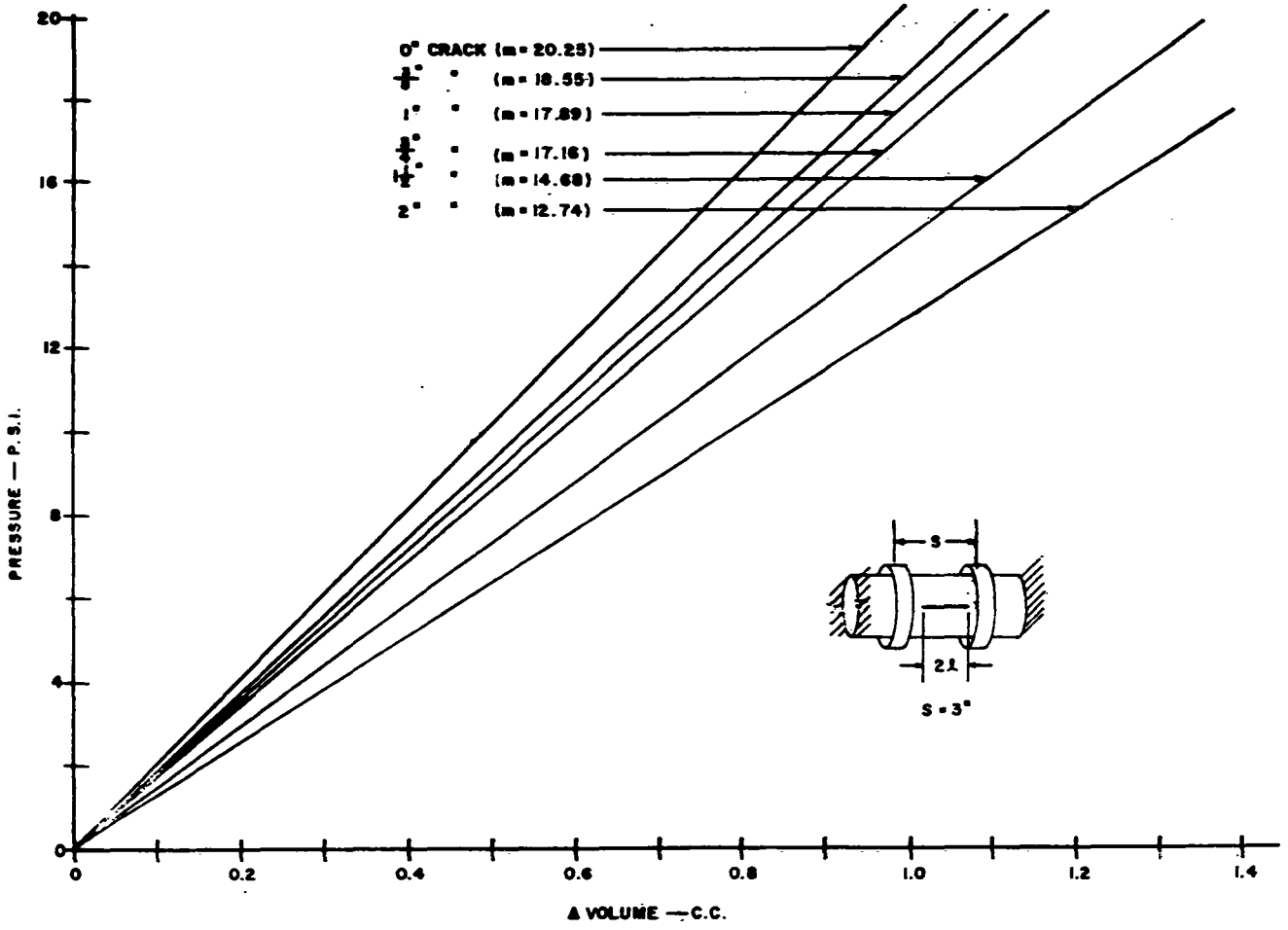
AM 2233



ORIGINAL TEST DATA — PLEXIGLAS SPECIMENS

AM 2234

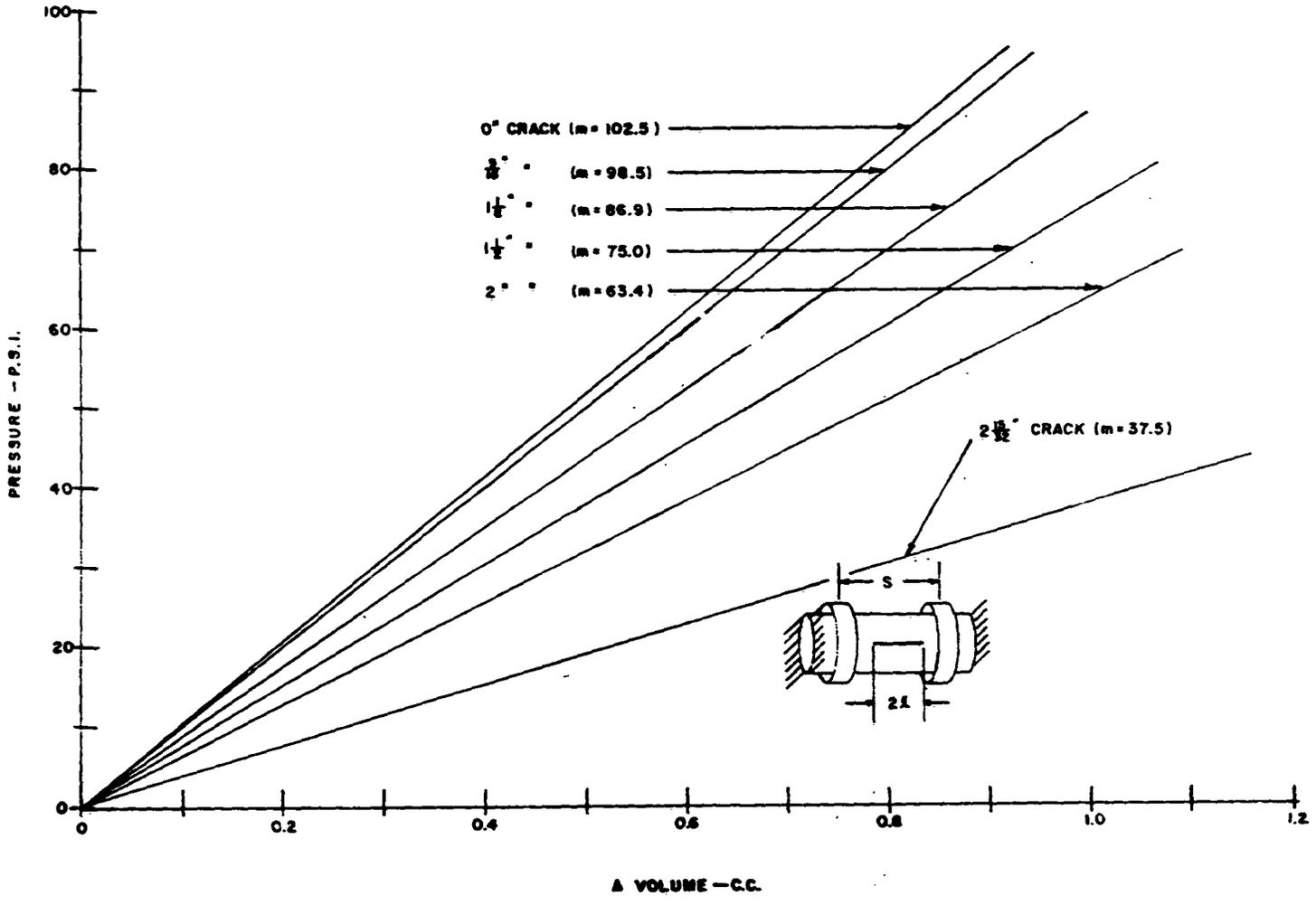
FIGURE 9



CORRECTED TEST DATA — PLEXIGLAS SPECIMENS

AM 2235

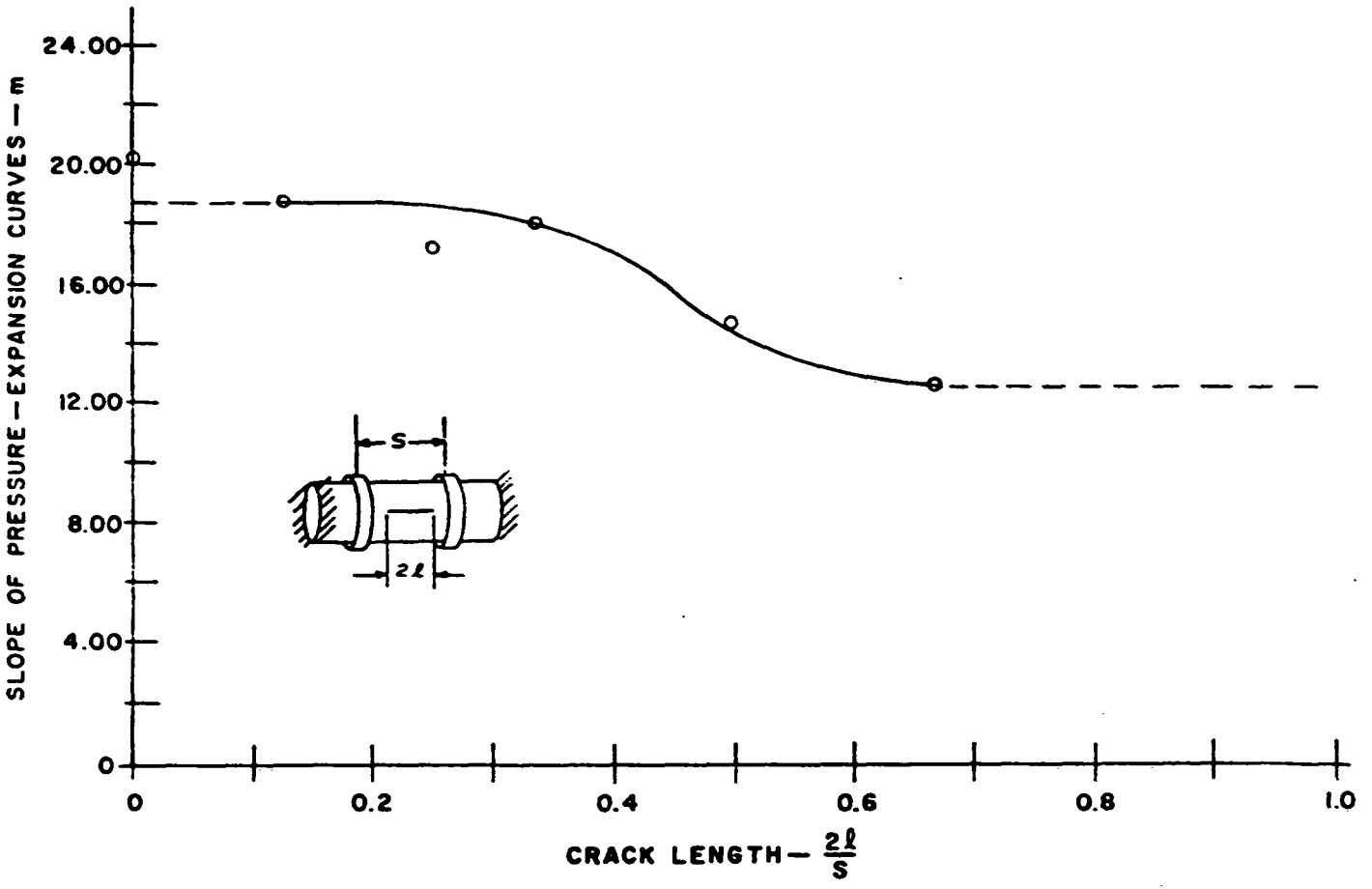
FIGURE 10



CORRECTED TEST DATA — MICARTA SPECIMENS

AM 2237

FIGURE 11

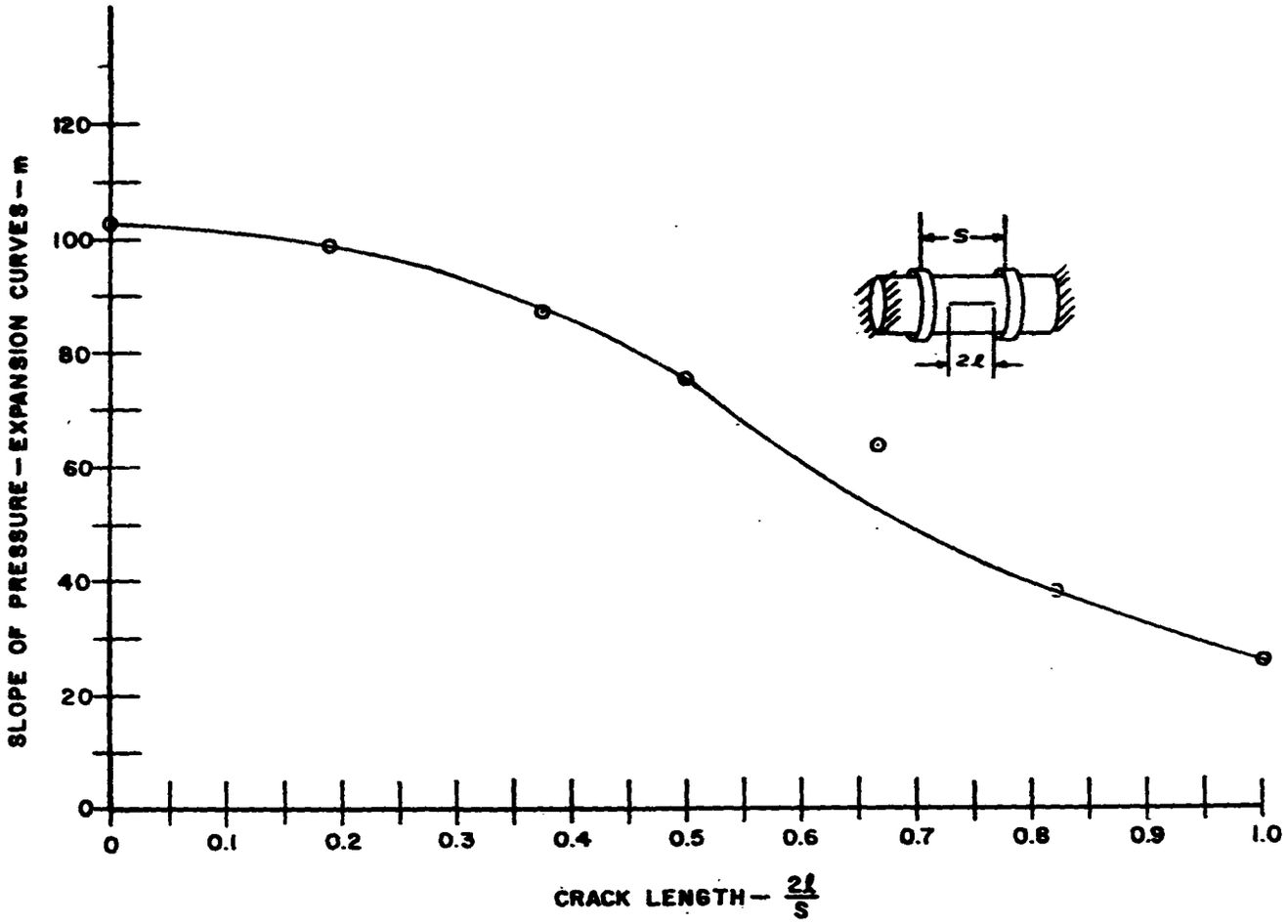


SLOPE OF PRESSURE – EXPANSION CURVES VS. CRACK LENGTH

PLEXIGLAS SPECIMENS

AM 2236

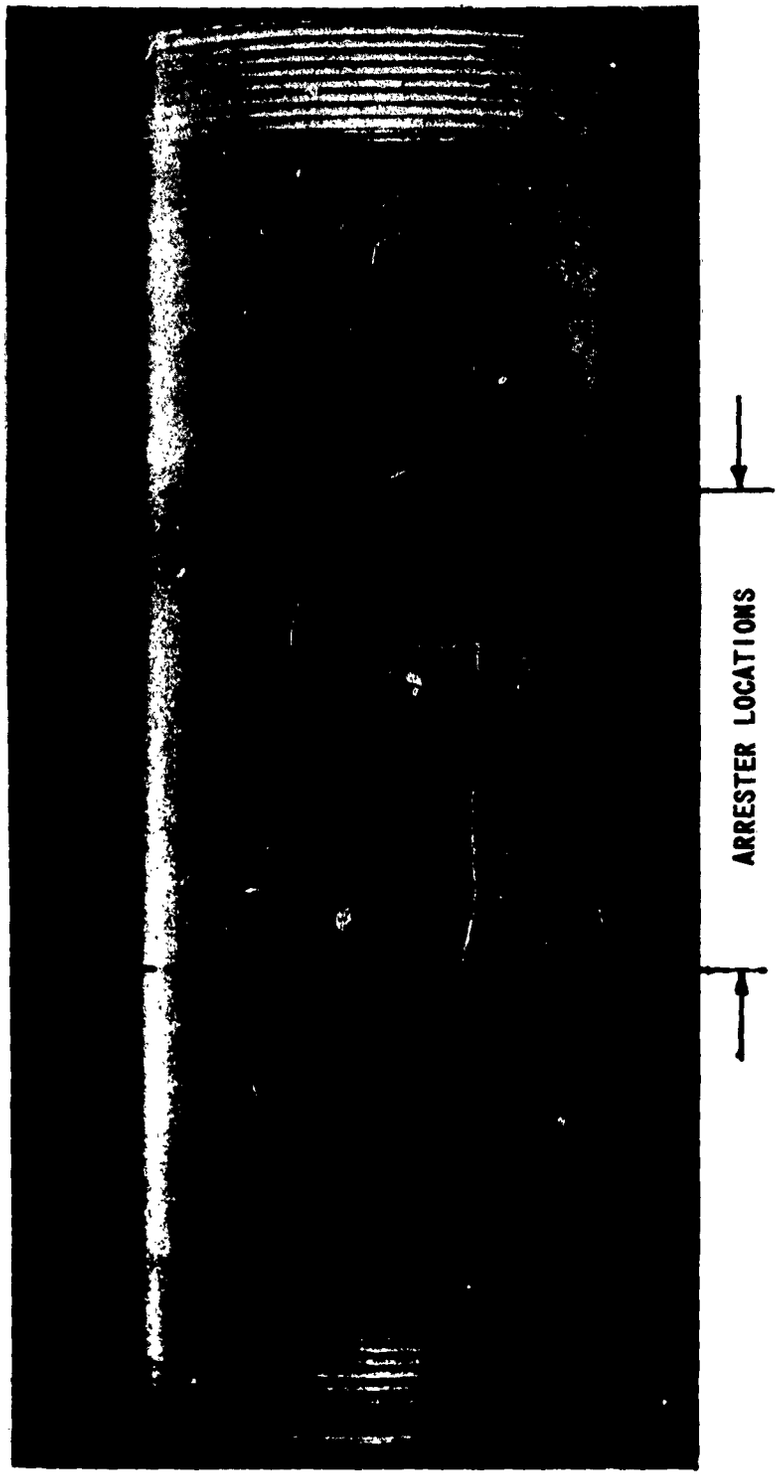
FIGURE 12



SLOPE OF PRESSURE—EXPANSION CURVES VS. CRACK LENGTH
MICARTA SPECIMENS

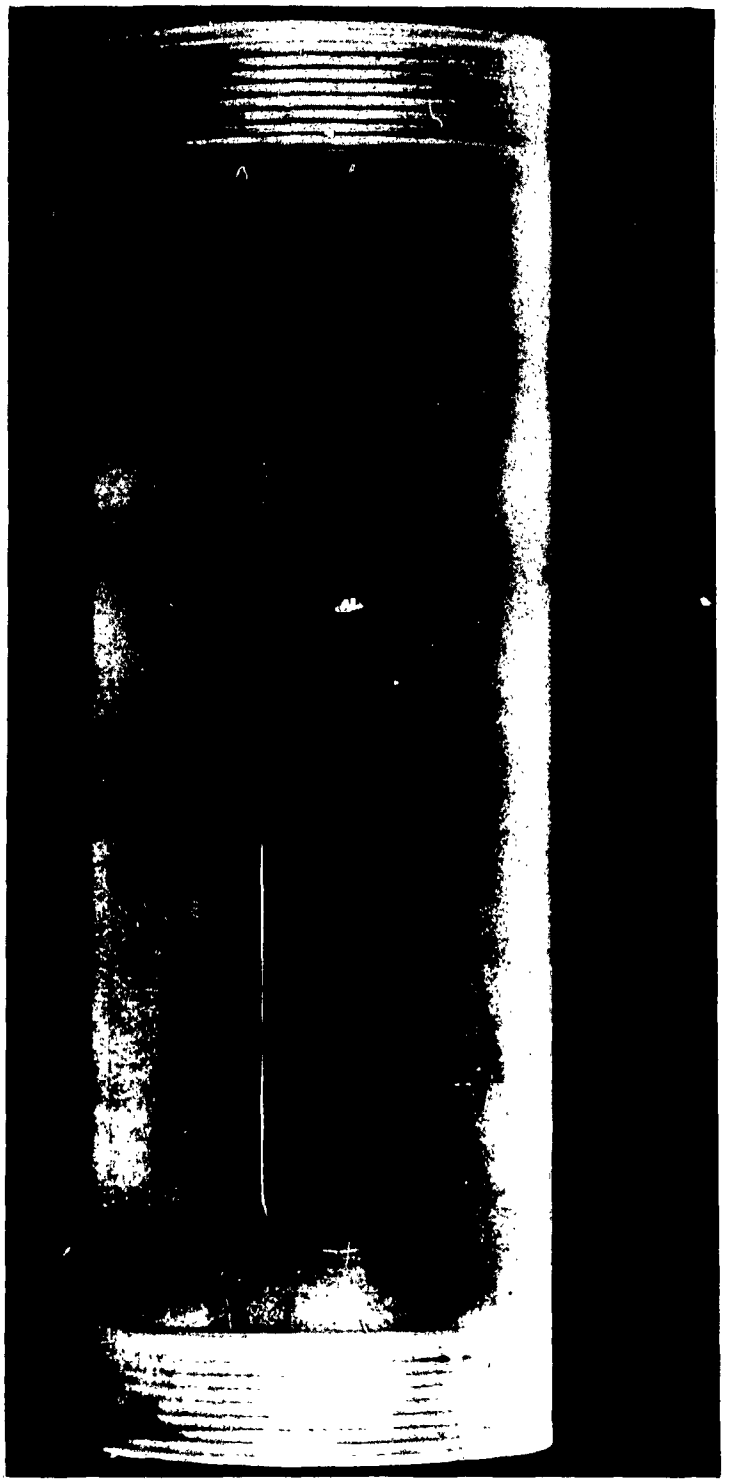
AM2238-1

FIGURE 13



TEST SPECIMEN SHOWING CRACK ARREST AND TURN 3-INCH ARRESTER SPACING

FIGURE 14



TEST SPECIMEN SHOWING CRACK ARREST AND TURN 7-1/2 INCH CLEAR LENGTH

FIGURE 16

APPENDIX

SEMI-EMPIRICAL DETERMINATION OF THE ELASTIC ENERGY RELEASE RATE

The experimental data (see Figure 12 suggests the following approximate analytical expression for the slope m of the pressure-expansion curves

$$m = k + A \left\{ 1 + \cos \frac{2\pi \ell}{S} \right\} \qquad (a)$$

where k and A are as indicated in Figure A2, 2ℓ is the crack length and S is the arrestor spacing. The slope "m" is defined by the relation

$$p = m (V - V_o) = m \Delta V \qquad (b)$$

The elastic energy stored in a specimen[1] under pressure is given by

$$E_{\text{stored}} = \int_{V_o}^{V} p \, dV \qquad (c)$$

and by substituting Equation (a) and Equation (b) into this, one obtains

$$E_{\text{stored}} = \left[\frac{k + A \left\{ 1 + \cos \frac{2\pi \ell}{S} \right\}}{2} \right] \Delta V^2. \qquad (d)$$

For a zero crack length

$$E_{o\ \text{stored}} = \left[\frac{k + 2A}{2} \right] \Delta V^2 \qquad (e)$$

The energy released, G, in propagating from a zero crack length to a crack length $2\ell/S$ is then given by the difference of Equation (d) and (e). i.e.

$$G = E_{o\ \text{stored}} - E_{\text{stored}}$$

or

$$G = \frac{A}{2} \left\{ 1 - \cos \frac{2\pi \ell}{S} \right\} \Delta V^2 \qquad (f)$$

[1] *It should be cautioned, of course, that the energy values obtained in the plastic models must not be applied directly to the prototype without due regard for the pertinent scale factors as discussed under Part III, Section A.*

The rate of energy release with respect to crack area, dG/dA, may be determined directly from Equation (f)

$$\frac{dG}{dA} = \frac{dG}{d(2\ell t)} = \frac{1}{2t}\frac{dG}{d\ell} = \frac{\pi A \Delta V^2}{2tS} \sin\frac{2\pi\ell}{S}$$

or using the more common notation for dG/dA we have

$$\mathcal{G} \equiv \frac{dG}{dA} = \frac{\pi A}{2tS}\Delta V^2 \sin\frac{2\pi\ell}{S} . \qquad (g)$$

Here t is the sheet thickness.

The critical value of $\mathcal{G}$, namely $\mathcal{G}_c$, can now be determined by observing in a specimen of the prototype material the pressure and crack length at which rapid propagation occurs. Noting, for example, that from Equation (b) we have $\Delta V = p/m$ and substituting this into Equation (g) and using the observed critical values of p and 2ℓ at instability, we get for $\mathcal{G}_c$.

$$\mathcal{G}_c = \frac{\pi A}{2tS}\left[\frac{P_{cr}}{k + A\left\{1 + \cos\frac{2\pi\ell_{cr}}{S}\right\}}\right]^2 \sin\frac{2\pi\ell_{cr}}{S} \qquad (h)$$

For small crack lengths, i.e. $2\ell/S << 1$ this reduces to

$$\mathcal{G}_c \approx \frac{A\pi^2}{t[k + 2A]^2 S^2} P_{cr}^2 \ell_{cr} . \qquad (i)$$

Hence, by the judicious use of models and appropriate application of the π factors and a single prototype test, the energy release and the critical energy release rate (or fracture toughness) can be determined for a given material.

In addition, it is possible to anticipate the crack length at which arrest takes place based on the foregoing results. The elastic release rate $\mathcal{G}$ is (Equation (h).

$$\mathcal{G} = \frac{\pi A}{2tS}\left[\frac{P}{k + A\left\{1 + \cos\frac{2\pi\ell}{S}\right\}}\right]^2 \sin\frac{2\pi\ell}{S}$$

The critical release rate is (Equation (h).

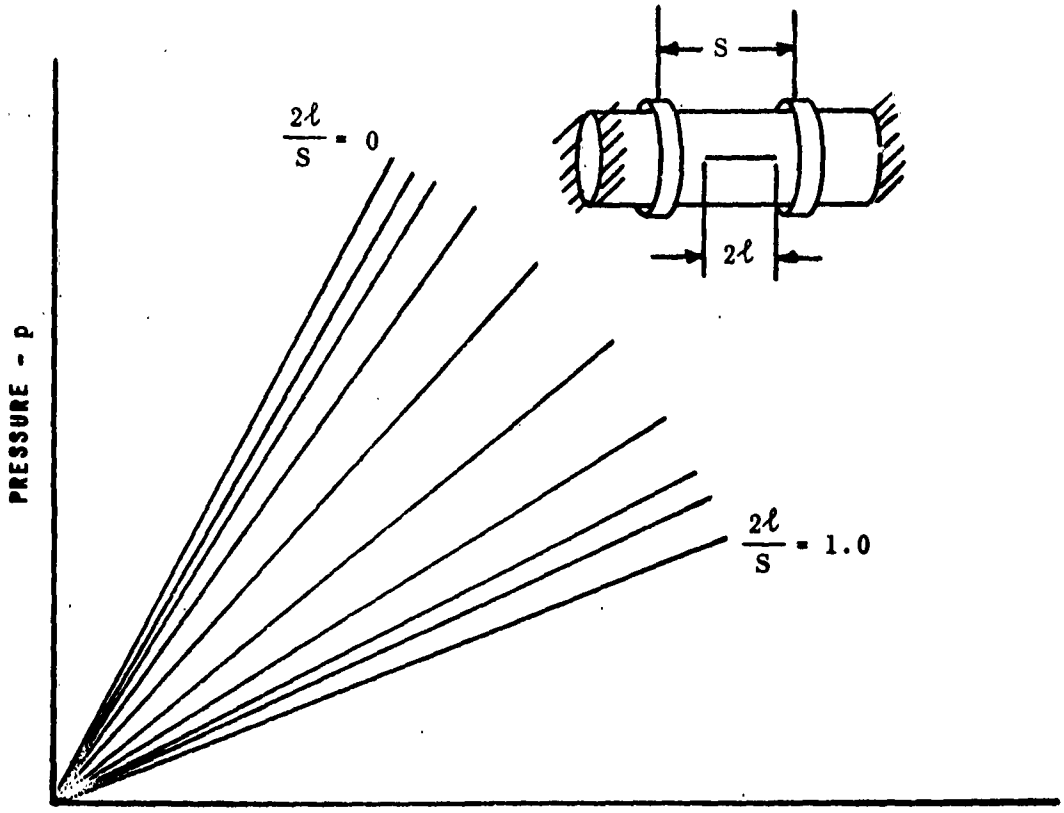
$$\mathcal{G}_c = \frac{\pi A}{2tS}\left[\frac{P_{cr}}{k + A\left\{1 + \cos\frac{2\pi\ell_{cr}}{S}\right\}}\right]^2 \sin\frac{2\pi\ell_{cr}}{S} .$$

Equating these, we obtain

$$\left[\frac{p}{k + A\left\{1 + \cos\frac{2\pi\ell}{S}\right\}}\right]^2 \sin\frac{2\pi\ell}{S} = \mathcal{G}_c = \text{constant} .$$

Solution of this equation then provides the "arrested crack length."

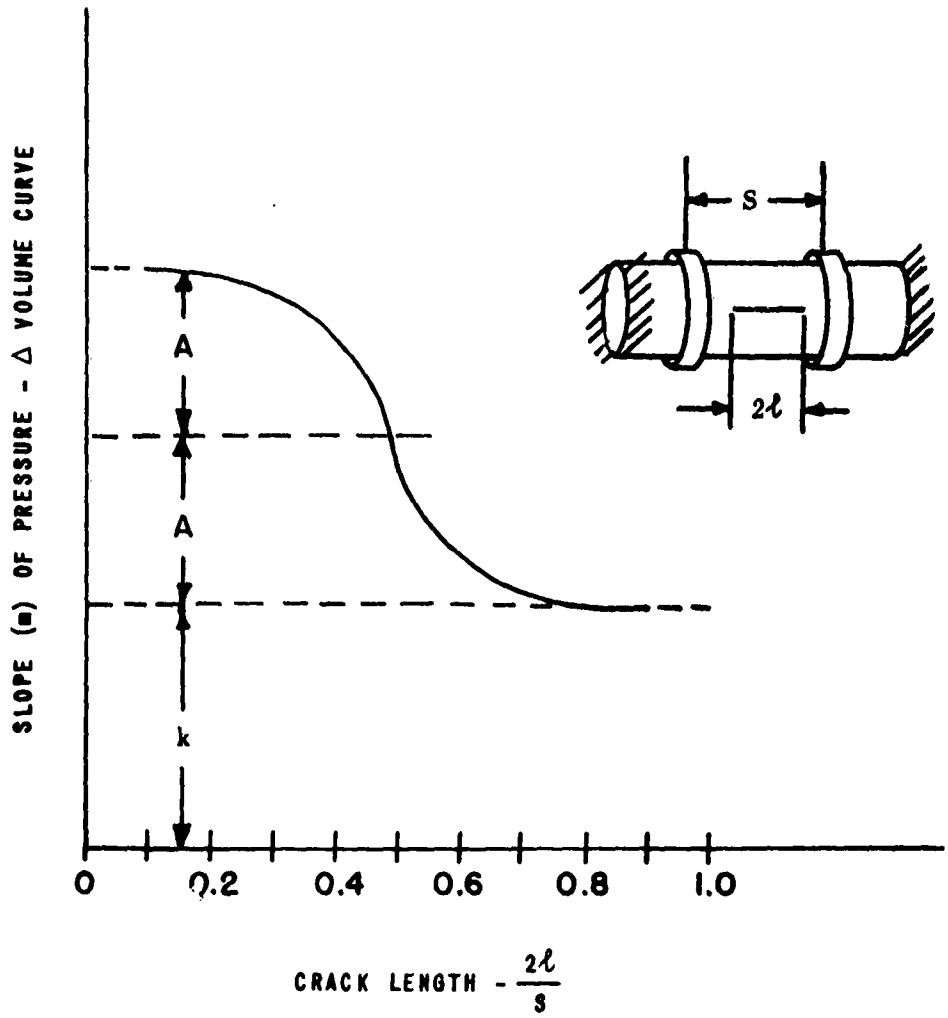
The procedure demonstrated in this Appendix stems from an idealization as a cosine curve, of the slope curve of the p-V relations for "cracked" cylinders. Though the idealization may not be valid, the basic scheme used should be applicable to any slope curve having an inflection point. Figures A1 through A7 demonstrate schematically, step by step, the application as it might apply to any pressure vessel and do not require further elaboration except as follows: Figure A2 indicates an anti-symmetric configuration such as a cosine curve but this is only for the purpose of definition of the terms used in the text of this Appendix. Figure A1 is the "corrected" plot of the original pressure expansion data; Figure A2 shows the slopes of these curves; Figures A3 and A4 are the areas under the curves of Figure A1 for fixed ΔV or p respectively; Figure A5 is obtained as a curve plot of Figure A3 at the specific change in volume ΔV_o; Figure A6 is obtained directly from Figure A5 and finally, Figure A7 is merely the first derivative curve of Figure A6.



PRESSURE EXPANSION CURVES - SCHEMATIC

AM 2222

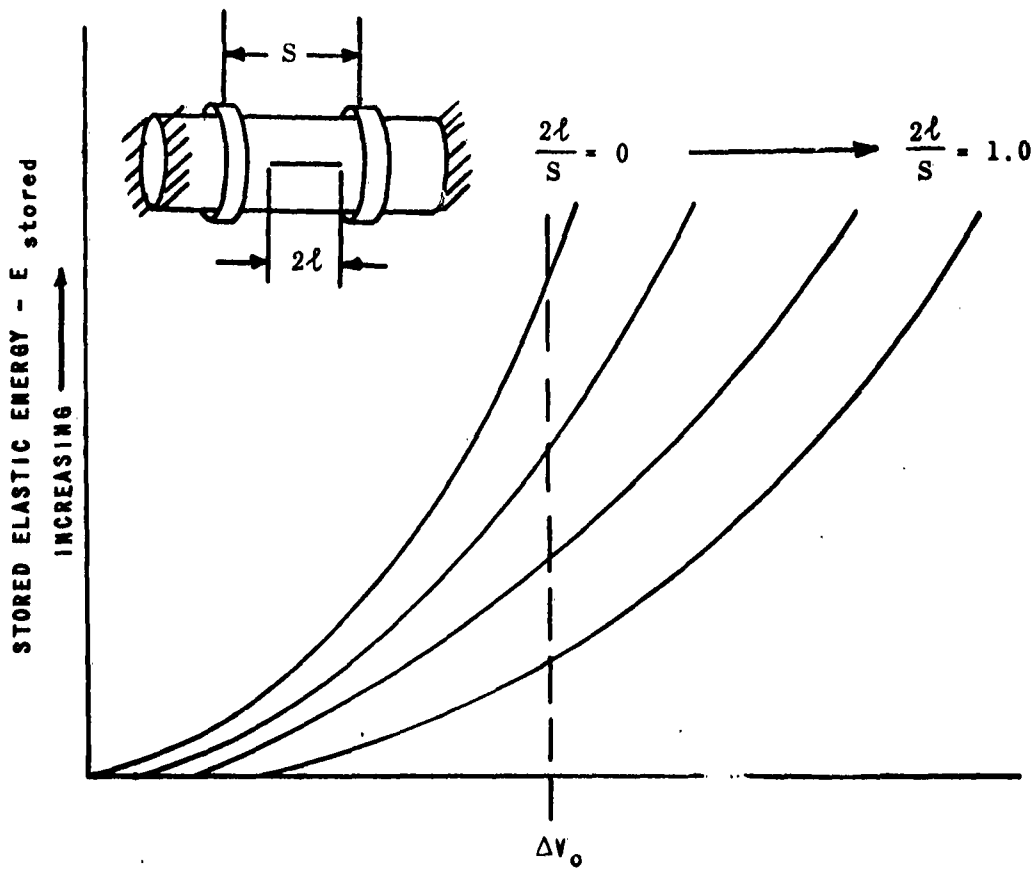
FIGURE A1



SLOPE OF PRESSURE EXPANSION CURVES - SCHEMATIC

AM 2223

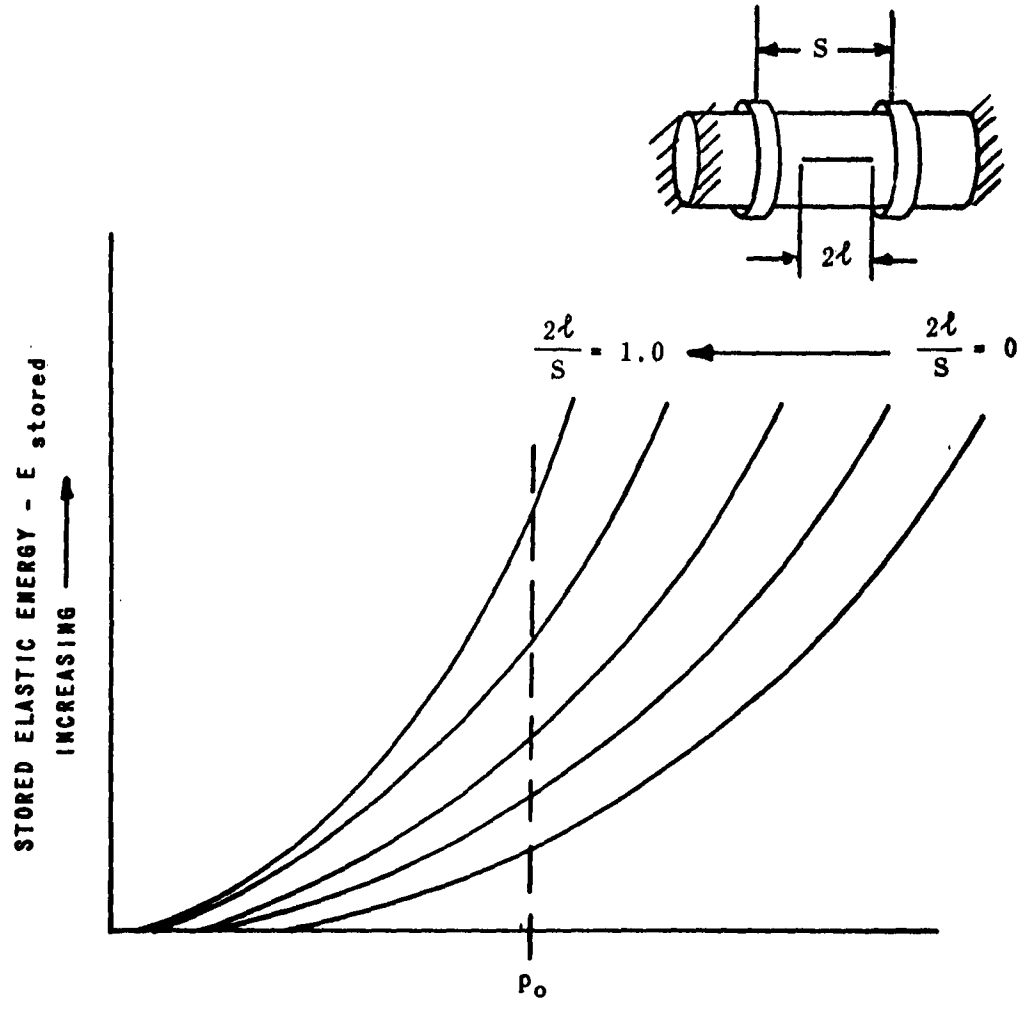
FIGURE A2



STORED ELASTIC ENERGY VERSUS VOLUME CHANGE

AM 2224

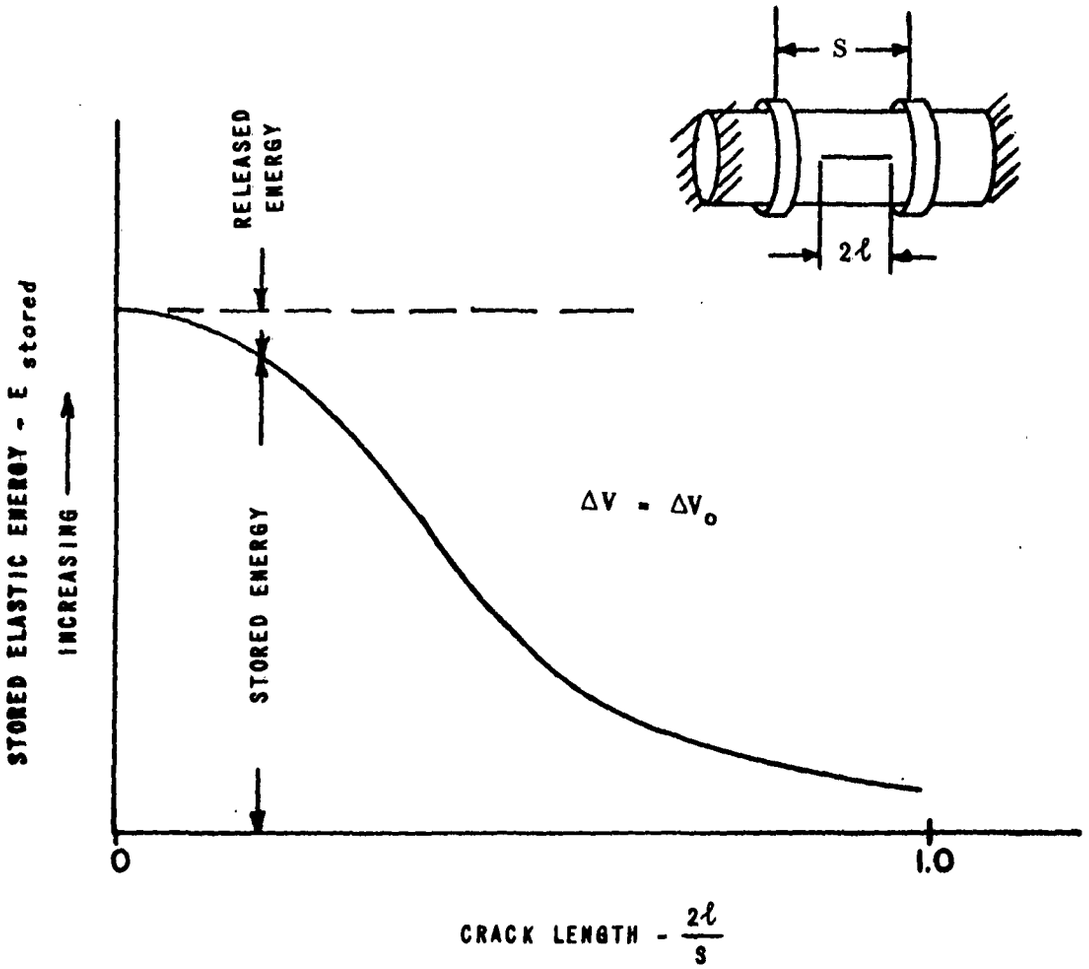
FIGURE A3



STORED ELASTIC ENERGY VERSUS PRESSURE

AM 2225

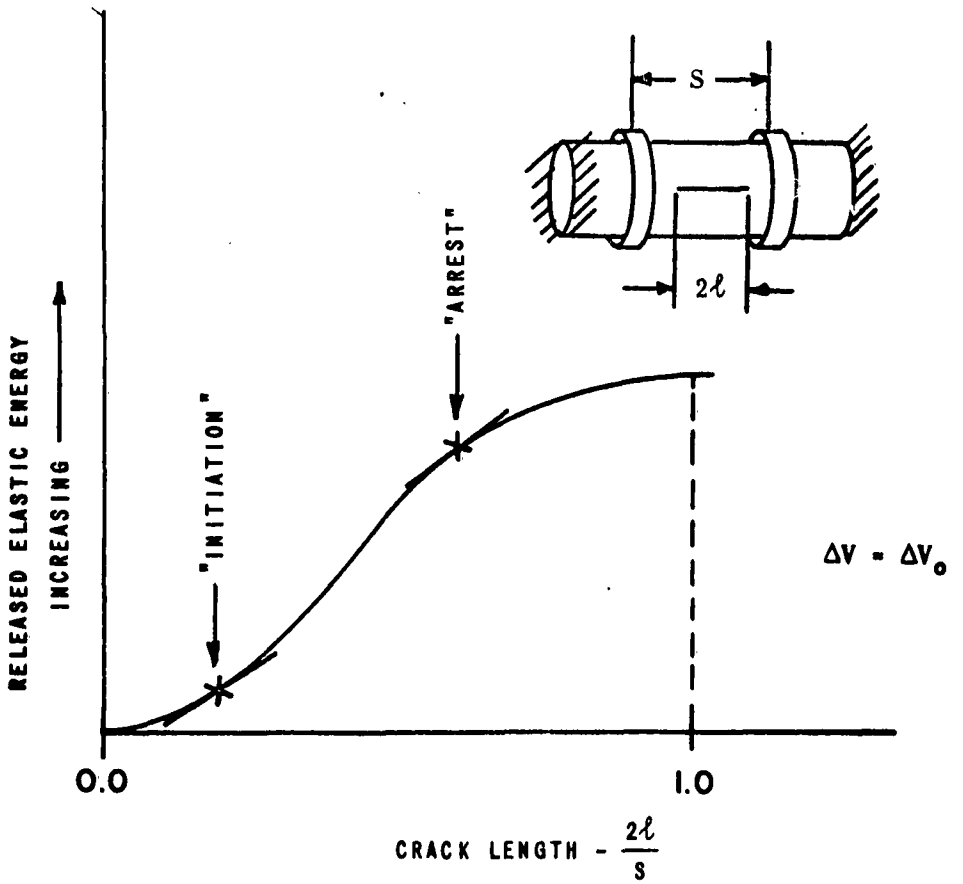
FIGURE A4



STORED ELASTIC ENERGY VERSUS CRACK LENGTH FOR SPECIFIC CHANGE IN VOLUME - ΔV_o

AM 2226

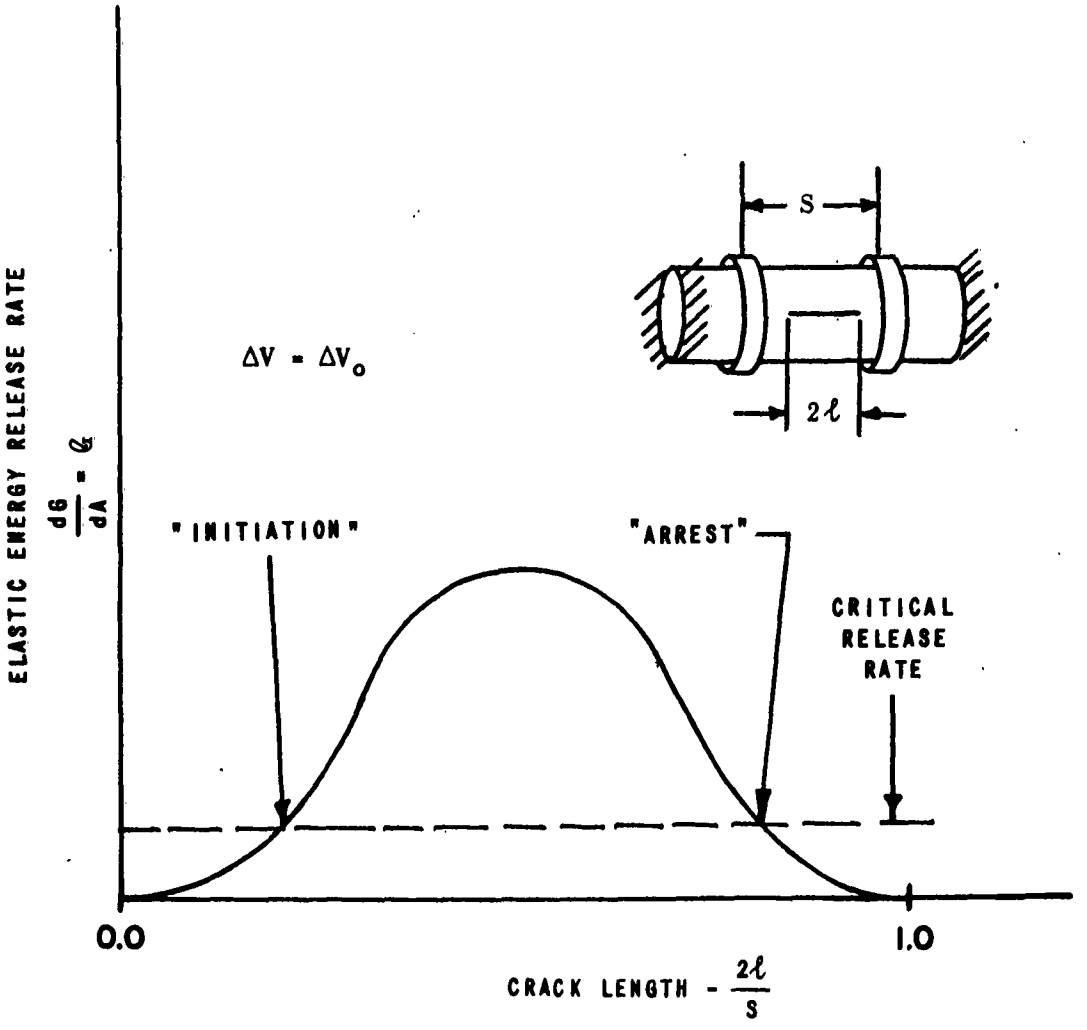
FIGURE A5



RELEASED ELASTIC ENERGY VERSUS CRACK LENGTH FOR SPECIFIC CHANGE IN VOLUME - ΔV_o

AM 2227

FIGURE A6



RATE OF RELEASE OF ELASTIC ENERGY VERSUS CRACK LENGTH FOR SPECIFIC CHANGE IN VOLUME - ΔV_o

AM 2228

FIGURE A7

SLOW CRACK EXTENSION IN HIGH STRENGTH STEELS

by H. T. Corten
University of Illinois

Introduction. Quality pressure vessels made of high strength steel for use as solid propellent missile motor cases are desired which exhibit 100 per cent reliability. Hydrotesting, that is, several cycles of pressurization with water to peak firing pressure, is used as a means of insuring reliability in the finished motor case. Experience with hydrotesting shows, however, that while the first cycle of hydrotesting singles out many defective motor cases, each subsequent cycle of hydrotest also causes failure of a small percentage of motor cases. This evidence strongly suggests that something less than 100 per cent reliability has been insured for the firing cycle by previous cycles of hydrotesting.

Failure of motor cases during hydrotesting occurs by rapid fracture. The fracture origin can frequently be traced to a small flaw or crack in the vessel. Analysis employing fracture mechanics (1)* offers a means of estimating the maximum allowable crack size in order to avoid rapid fracture. However, it is observed that small cracks which are subcritical in size before hydrotesting, grow by slow extension and may reach critical size as a result of one or more cycles of hydrotest. Thus, to estimate the size of the maximum allowable crack for purposes of inspection, it is necessary to reduce the critical crack size as estimated from fracture mechanics, by the amount of slow crack growth that the crack experiences in all cycles of hydrotest.

Purpose. This investigation was undertaken to study slow crack extension which precedes rapid fracture. The immediate goals were to provide a means of estimating slow crack extension and to recommend an optimum hydrotest procedure. These problems were approaches by exploring and isolating the important parameters governing slow crack growth.

Approach to Problem. Fracutre mechanics stress analysis of the region around the tip of a crack was employed. The stress intensity factor, K, is a one parameter description or measure of the elevation of the stress field around the crack tip. For a large thin plate loaded in axial tension and containing a small crack as shown in Fig. 1, K is given by

$$K = \sigma\sqrt{\pi a} \qquad (1)$$

where σ is the gross section stress away from the crack and a is one-half of the crack length. For elastic behavior, the stress in the y direction at any point along the x axis, is given by

$$\sigma_y = \frac{K}{\sqrt{2\pi r}} \qquad (2)$$

---

* Numbers in parentheses refer to list of references.

where r is equal to the x coordinate of the point.

The stress field represented by the stress components σ_x, σ_y, and τ_{xy} at any point near the crack tip, may be represented in terms of K and the coordinates of the point.

As a basis for studying slow crack extension, the following hypothesis was employed: at two different stages of slow crack extension in a given plate, the same amount of slow crack extension per cycle should occur if the plate was loaded to produce the same value of K. (2) This hypothesis assumes that in a particular material, the rate of slow crack extension is a function only of the stress field elevation around the tip of the crack. That is

$$\frac{d(2a)}{dN} = f(K) \tag{3}$$

For different materials, it is expected that the resistance offered by the material to slow crack extension will be different. Thus an extension by Eq. (3) to include some measure of the resistance of the material to slow crack extension is required. For the present problem, a convenient material property is K_c, the stress intensity factor associated with rapid fracture. Thus, K_c will be introduced into Eq. (3) to give

$$\frac{d(2a)}{dN} = f(K, K_c) \tag{4}$$

Equation (4) suggests a basis for an experiment to determine the significant parameters governing slow crack extension.

Experimental Program. A modified SAE 4335 steel, designated M-255 with a chemical composition as shown in Table I, was used in this investigation. Unwelded sheets, 0.188-in. thick, were cut to standard 3-in. by 12-in. central notched tensile specimens. Slots about 1/8-in. by 7/8-in. were machined in the specimens and the regions around the slots were surface ground to permit accurate visual observation of the crack length. The specimens were austenitized at 1650°F in a neutral atmosphere and oil quenched. Four series of thirteen specimens each designated L, were cut parallel to the direction of rolling and three series of specimens designated T, were cut perpendicular to the rolling direction. The tempering temperatures and the resulting mechanical properties are given in Table II. After heat treatment, the specimens were subjected to completely reversed cycles of repeated bending stress in a Krouse plate fatigue machine to induce sharp fatigue cracks at the corners of the slot to act as crack starters. The fatigue cracks are clearly visible on the fracture surface as shown in Fig. 2

Fracture appearance indicated that both a flat fracture and 45° shear lip were present as illustrated in Fig. 2. Ink staining indicated that the flat crack was always longer than the surface crack. A series

of specimens for each heat treatment were ink stained and/or heat tinted at various stages of crack extension to obtain the relation between the internal flat crack length and the surface crack length. The results for the T4 series of specimens are shown in Fig. 3. The "adjusted crack length" was computed by dividing the area of the actual crack by the thickness of the specimen. The "adjusted crack length" was employed to compute values of K. For each of several series of specimens it was found that the "adjusted crack lengths" could be represented as a constant proportion of the surface crack lengths, as shown in Fig. 4.

Using the "adjusted crack length" and the stress analysis for a finite width specimen, including the plastic zone correction factor (1), experiments were conducted in which K was adjusted to a constant value at the beginning of each cycle of load. This was done by using the adjusted crack length at the end of the previous cycle, and solving Eq. (5) (1) for σ.

$$K^2 = \sigma^2 W \tan \left(\frac{\pi a}{W} + \frac{K^2}{2W \sigma_{ys}^2}\right) \qquad (5)$$

The load was maintained constant during each cycle and was held for a 3 minute interval.

Experimental Results. Typical data from one experiment is shown in Fig. 5 for specimen T4 R4. The important quantities, the gross-section stress σ, the value of K at the beginning and end of each cycle, and the surface crack length are shown for each cycle of load through 15 cycles. Note that the desired value of K was not reached until the fourth cycle. A progressively increasing value of K was employed on cycles 1, 2, and 3 in an attempt to control the initial crack growth and the value of K that developed at the end of each cycle. Note that on cycle 4, the final value of K is the highest value attained because of the extensive slow crack growth on cycle 4. Large crack growth during the first several cycles is associated with the development of shear lips. Starting from the fatigue cracks, flat fracture commences during loading at approximately 75 per cent of the maximum load on cycle 1, and produces a crack in which the flat region is longer than the surface crack. The major resistance to slow crack growth appears to be caused by the shear lips. Until the shear lips reach a characteristic size, full resistance to slow crack growth is not developed and thus the first few cycles of load cause rather large amounts of slow crack growth.

Starting with cycle 4 in Fig. 5, the shear lip is well developed and slow crack growth on each subsequent cycle is approximately constant for the remaining cycles. Thus, in accordance with the original hypothesis, the rate of crack growth caused by a constant value of K is approximately constant with cycles of load after the shear lips are developed. *

---

* There is some indication that the shear lips gradually increase in size as the crack grows and the rate of crack growth gradually decreases.

Crack growth data for similar experiments using different values of K are shown in Fig. 6. The solid points indicate the cycle when the desired value of K was reached. While some variability in rate of crack growth is present, it is possible to assign an average rate of crack extension to each curve, that is, to each value of K.

In Fig. 7 the rate of crack extension per cycle, $\delta (2a)/\delta N$ is shown as a function of K. While the scatter is considerable, it is evident that the rate of slow crack extension increases with the applied value of K for each of the three groups of data. Within each group the yield strength and fracture toughness are similar. From Fig. 7, it is obvious that to produce the same rate of slow crack growth in each group of specimens, K increases as the value of K_c increases.

From data of the type shown in Figs. 5 and 6, it is clear that the rate of slow crack extension is a function of K, the stress intensity factor. In addition, the change in mode of fracture, starting from a flat fracture and proceeding to the development of shear lips, produces a large influence on the rate of crack extension. This change in resistance to slow crack extension was not initially included in Eqs. (3) and (4) but obviously must be introduced.

Because ink staining was employed to study crack shape at various stages of crack extension, direct determination of K_c using ink stain to indicate the crack length at instability, was not possible. Indirect determination of K_c, namely, K_{c_3}, (1) employing the per cent shear, is being made. However, these data are incompletely analyzed.

The Mechanism of Slow Crack Extension. Since both cycling and time at maximum load form part of the hydrotest specifications, it appears important to separate the effects of these two variables. A series of experiments were performed in which K values identical to those used in the cycling experiments were used except that the specimens were not cycled. The specimens were loaded to the appropriate value of K and held for 3 minutes. At the end of the first, and each subsequent 3 minute interval, the load was adjusted, if necessary, to maintain K at the appropriate constant value. The results of a cycling and non-cycling series of experiments are compared in Figs. 8a and 8b, respectively. In Fig. 8b, the number of 3 minute intervals are directly comparable with the number of cycles in Fig. 8a. It is clear that cycling is necessary to produce continued slow crack extension.

To further investigate the influence of load cycling, a series of experiments were performed in which the load was reduced to a lower value, one-fourth or one-half of maximum load, and then increased to maximum load again. The results of these experiments are shown in Fig. 9. From these data it is evident that slow crack extension is a function of the amplitude of K as well as the maximum value of K.

During loading the stress at the tip of the crack, as given by Eq. (2) exceeds the tensile yield strength of the material and a small zone of plastic deformation is formed. The residual stresses that result from unloading can be simply determined by noting that unloading is

equivalent to superimposing a compressive load on the tensile load, and superimposing the stress distribution caused by the compressive load upon that caused by the tensile load. The resulting residual stress distribution is shown schematically in Fig. 10. Upon unloading, the residual stresses near the tip of the crack reach the compressive yield strength of the material, and again cause plastic deformation. Upon reloading in tension, yielding again occurs at the tip of the crack, this time in tension. Thus, each cycle of loading and unloading causes cyclic plastic strain at the tip of the crack. In the experiments reported in Fig. 9, the plastic strain that occurred upon unloading and reloading was controlled by the extent of unloading. Less cyclic plastic strain occurred when the load was reduced to one-half the maximum load than when the load was reduced to zero. These experiments constitute very low cycle fatigue experiments. Each cycle of load causes damage at the tip of the cracks and slow extension of the cracks toward critical size.

With regard to hydrotest, it must be expected that the present procedure, that is 1 to 5 cycles of pressurization, each to peak firing pressure, does not insure 100 per cent reliability of motor cases, and that a small percentage of vessels will fracture on the next cycle, either pressurization or firing, as a result of slow crack growth. This conclusion has been suspected for some time, however the evidence herein reported established the fact.

Prediction of Slow Crack Extension. An expression for the amount of slow crack extension per cycle of load has been developed based on the following three concepts: (a) in low cycle fatigue the relation between the fatigue life N and the plastic strain per cycle is given by

$$\Delta\epsilon_p \, N^{1/2} = 2\epsilon_f \qquad (6)$$

where $\Delta\epsilon_p$ is the increment of plastic strain per cycle, N is the number of cycles to fracture, and ϵ_f is the true fracture strain in a static tension test, (b) the fact that the plastic strain is approximately equal to the computed elastic strain in the region near the tip of the crack, and (c) the amount of shear lip which provides resistance to slow crack extension, increases rapidly in the early stages of crack growth. The resulting empirical expression contains a number of approximations and one undetermined constant which must be evaluated from slow crack growth data. At this stage of the development it appears unwise to do more than report that effects are being made in this direction.

Because the problem of rapid fracture requires an immediate answer, the following approach to the hydrotest procedure is recommended (3).

A Hydrotest Procedure to Insure Reliability. As noted previously, current hydrotest procedures consist of from 1 to 5 cycles of pressurization, each to peak firing pressure. Because this is really a very low cycle fatigue test, each hydrotest cycle causes damage and slow crack extension of any small cracks that may be present. It must be expected that

upon each subsequent cycle of pressurization to the same peak pressure, the probability is finite that some vessels contain cracks which will reach critical crack size and cause rapid fracture.

Consider a motor case containing a distribution of crack sizes as shown schematically in Fig. 11. It is assumed that the number of large cracks is small and the number of smaller cracks increases as the size decreases. The critical crack size for the pressure involved is indicated by $(2a)_c$. The first cycle of hydrotest causes the existing cracks to grow to lengths indicated by the dashed line distribution. If the longest crack represented by the dashed line does not reach the critical size, the vessel will not fail on cycle 1. Since crack growth on cycle 1 may be expected to be the largest, cycle 2 may also be safe as indicated by the dash-dot line. However, on the third cycle in this illustration, the longest crack would reach the critical size, causing rapid fracture, Three factors, the relative position of the initial crack size distribution, the critical crack size $(2a)_c$, and the rate of slow crack growth, determine when rapid fracture occurs. Obviously the curve for the initial crack size distribution can be moved to the left by improved fabrication techniques, and particularly by careful nondestructive inspection. These procedures should increase percentage of usable motor cases. Also an increase of K_c moves the value of $(2a)_c$ to the right, if other factors remain constant. Each of these factors may be viewed as contributing to increased reliability of motor cases. However, to insure 100 per cent reliability, hydrotesting was introduced. The fact that the current hydrotest does not accomplish this purpose means that the test procedure must be modified.

A hydrotest procedure that will insure optimum reliability consists of one cycle of pressurization to a pressure that exceeds the firing pressure by a small percentage, possibly 110 per cent. The basis for this recommendation is as follows: Consider a motor case in which the maximum stress in the wall during the firing cycle is σ. The initial length of the largest crack will be denoted by $(2a)_i$. The hydrotest cycle will involve a higher stress, $\alpha\,\sigma$, where α is the ratio of the hydrotest pressure to the firing pressure. During hydrotest the longest cracks will grow from $(2a)_i$ to $(2a)_j$. If the vessel does not fail, it is then known that $(2a)_j$ is less than $(2a)_c$, the critical crack length. Thus, as the limiting condition, $(2a)_j \leq (2a)_c$. Similarly, it is known that the value of K during hydrotest was less than K_c. In the limiting condition, K, during hydrotest was

$$K = \alpha\sigma\sqrt{\pi a_j} \leq K_c \qquad (7)$$

During the firing cycle, the stress will be σ and the longest initial crack length will be $(2a)_j$. Thus, during the firing cycle the initial value of K will be

$$K = \sigma\sqrt{\pi a_j} \qquad (8)$$

This is less than the minimum possible value of K_c given by Eq. (7). To approach the minimum value of K_c, the longest crack must grow by slow extension from $(2a)_j$ to $(\alpha^2\ 2a_j)$ during the firing cycle. In effect, the minimum critical crack length is increased to $\alpha^2\ 2a_j$ on the firing cycle when it is known from hydrotest that the longest crack present did not initially exceed $(2a)_j$. Thus, by making the value of α greater than 1.0, it is possible to adequately allow for slow crack growth with certainty that the vessel will not fracture.

At the beginning of the hydrotest cycle, the longest crack is $(2a)_j$ and the value of K is given by Eq. (8). At the stress σ, the crack of length $(2a)_j$ may safely increase by slow growth, Δa_j to the value of K, given by Eq. (7). Throughout this period of slow crack growth, the motor case is safe. The increasing value of K is given by

$$K = \sigma \sqrt{\pi(a_j + \Delta a_j)} \tag{9}$$

Setting K in Eq. (9) equal to K in Eq. (7), establishes a limiting safe relation between α and Δa_j, and gives

$$\alpha^2 a_j = a_j + \Delta a_j \tag{10}$$

Solving for $\Delta a_j / a_j$ gives

$$\frac{\Delta a_j}{a_j} = \alpha^2 - 1 \tag{11}$$

The quantity Δa_j in Eq. (10) and (11) is the amount of slow crack extension that will cause the value of K, during the firing cycle, to be equal to the value of K reached during the hydrotest cycle. If slow crack extension in the motor case is smaller than Δa_j, given by Eq. (11), then the value of K during the firing cycle remains less than K during the hydrotest cycle and 100 per cent reliability may be expected.

An appropriate value of α, for use in hydrotest, requires knowledge of the rate of slow crack growth. From experiments of the type reported in Fig. 5, information on slow crack growth for various values of α may be obtained. For example, the stress on the fourth cycle in Fig. 5 is 63,800 psi and the stress was reduced to 61,100 psi on the fifth cycle in order to maintain K constant. Crack extension on the fifth cycle was 0.02-in. A value of α was computed as the ratio of the stress on the fourth cycle to the stress on the fifty cycle, or $\alpha = 1.045$. Similar data from a number of specimens are shown in Fig. 12. For values of α from 1.0 to 1.05, considerable slow crack growth occurred in at

least a few specimens. However, for all values of α above 1.05, the maximum slow crack extension indicated by the ratio $\delta(2a)/2a$, was less than .04 on the cycle following the high stress.

For comparison, Eq. (11) is also plotted in Fig. 12. For values of α of about 1.04 and larger, the slow crack extension data are all well below the limiting value of $\Delta a/a$ given by Eq. (11).

Obviously, the number of hydrotest failures will increase as α is increased, and the minimum value of α that will insure 100 per cent reliability upon firing must be determined. From the data in Fig. 12, it appears that $\alpha = 1.10$ should provide 100 per cent reliability and that a smaller value of α may be adequate when additional data are available.

It should be remembered that all of the data shown in Fig. 12 are for unwelded specimens of M-255 steel. Experiments on other materials and on welded specimens are necessary to further evaluate the required magnitude of α.

Concluding Remarks. Many phases of this work are incomplete and work is currently underway to fill these gaps. It appears appropriate to mention several important aspects.

In specifying a steel for use in motor cases, the concept of a minimum fracture toughness, K_c, has been introduced based on rapid fracture. Because of the importance of slow crack growth, Professor Carpenter of Swarthmore College (4) has suggested that a more realistic value for design should be based on slow crack growth. He has introduced the term "Sub-Critical Crack Driving Force, $\mathcal{G}_{sc}$, "($\mathcal{G}E = K^2$) which defines a value of $\mathcal{G}$, less than $\mathcal{G}_c$, which produces insufficient slow crack growth to cause rapid fracture within three cycles of load. The ratio $\mathcal{G}_{sc}/\mathcal{G}_c$ is under investigation as a design criterion, however the available data are insufficient for adequate evaluation of the concept.

A method of estimating slow crack growth is under development in order that a realistic flaw size may be estimated for use in nondestructive inspection of motor cases.

A study of the transition from slow crack growth to rapid fracture is in progress. Preliminery results (5) indicate that the critical crack length, $(2a)_c$, is not sharply defined. As the condition for rapid fracture is approached, that is as (2a) approaches $(2a)_c$ by slow propagation under conditions of constant load, the time interval during which a crack of length (2a) remains stable decreases as (2a) approaches $(2a)_c$. Thus, the phenomena of "slow crack growth" and "rapid fracture" are connected by a "transition zone" in terms of crack length.

The recommendation made in the previous section that the pressure used in a 1 cycle hydrotest exceed the peak firing pressure by 10 per cent ($\alpha = 1.10$) was based on the uncertainty connected with this transition.

From the data in Fig. 12, it appears that slow crack growth does not exceed $(\Delta 2a/2a) = 0.04$ but the allowable slow growth is $(\Delta 2a/2a) = 0.21$ at $\alpha = 1.10$. This difference was intended to account for the transition region from slow crack growth to rapid fracture.

References

1. Fracture Testing of High-Strength Sheet Materials: A Report of a Special ASTM Committee, ASTM Bulletin, January, 1960.

2. This approach to the problem was proposed by Dr. G. R. Irwin, Naval Research Laboratory.

3. The recommended hydrotest procedure was proposed by Dr. H. W. Liu, University of Illinois

4. S. T. Carpenter, "Low Cycle Fatigue and Fracture Strength of High Strength Steels," NRL Project 62R19-05, Technical Memo No. 123, May 20, 1960.

5. H. W. Liu, "Effect of Water on the Fracture Strength of Specimens with a Central Notch," NRL Project 62R19-05, Technical Memo. No. 123, August 1, 1960.

Table I

Chemical Composition of M-255 Steel

C	Mn	P	S	Si	Cr	Ni	Al	Mo	Cu	Va
.36-	.68-	.008-	.009-	.45	.68-	1.72-	.010-	.33-	.048	.20-
.39	.76	.011	.010	.56	.89	1.84	.010	.37	.077	.22

Table II

Tempering Temperatures and Mechanical Properties of the Seven Series of Specimens

Specimen Series	Tempering Temperature	Hardness Rc	Yield Strength 0.2% offset lb/in^2	Ultimate Strength	Reduction of Area per cent
L5	400	51.3	228,000	236,000*	3
L6	550	49.1	220,000	250,000	28**
L7	550	50.3	218,000	251,000	7
L8	725	47.7	205,000	232,000	11
T2	550	52.5	230,000	260,000	24**
T3	750	48.2	205,000	232,000	30**
T4	750	48.5	210,000	246,000	25**

* Fractured in pin hole used to load specimen.

** Specimens were surface ground.

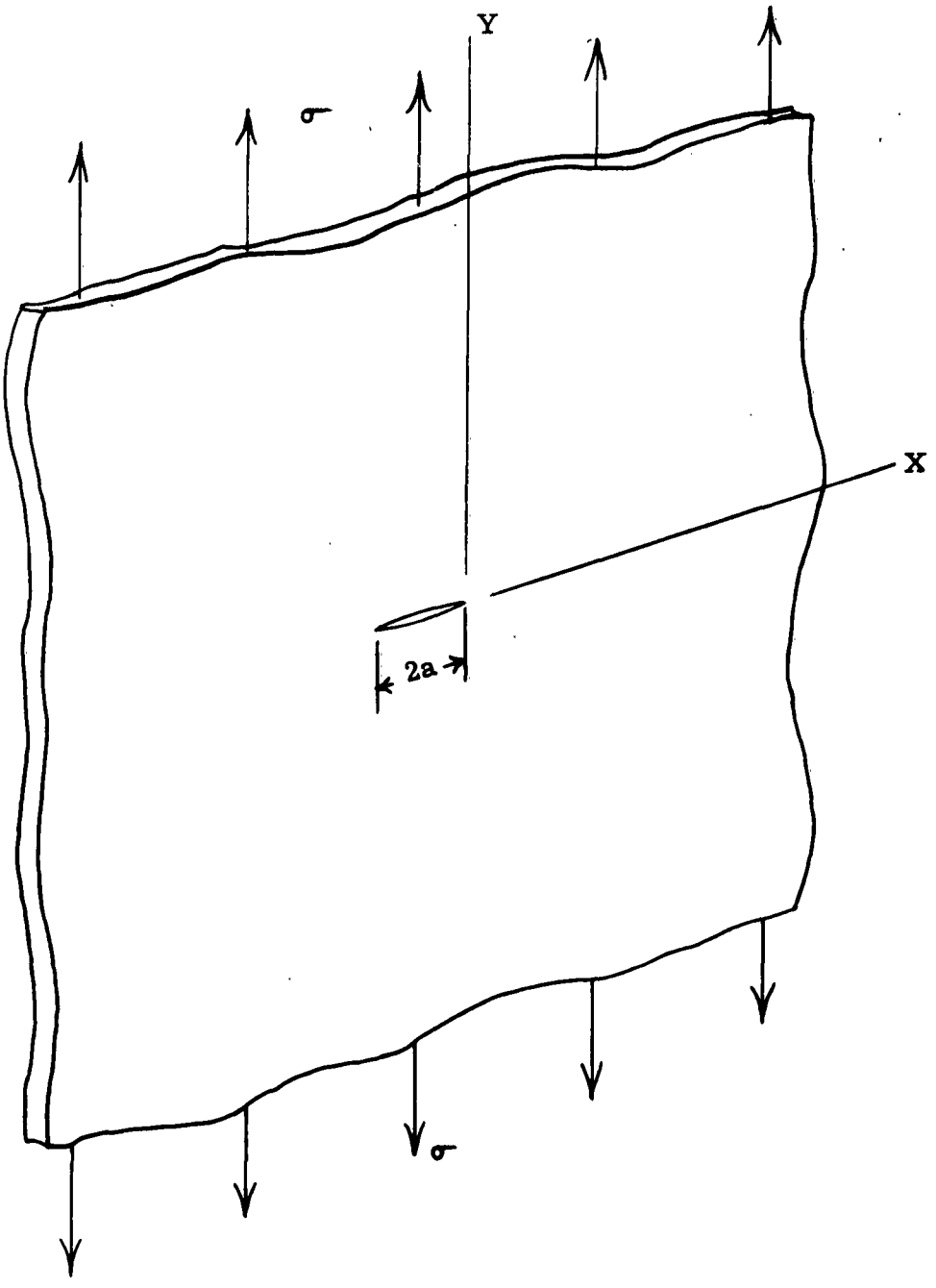


Fig. 1 Large Thin Plate Containing a Crack of Length 2a

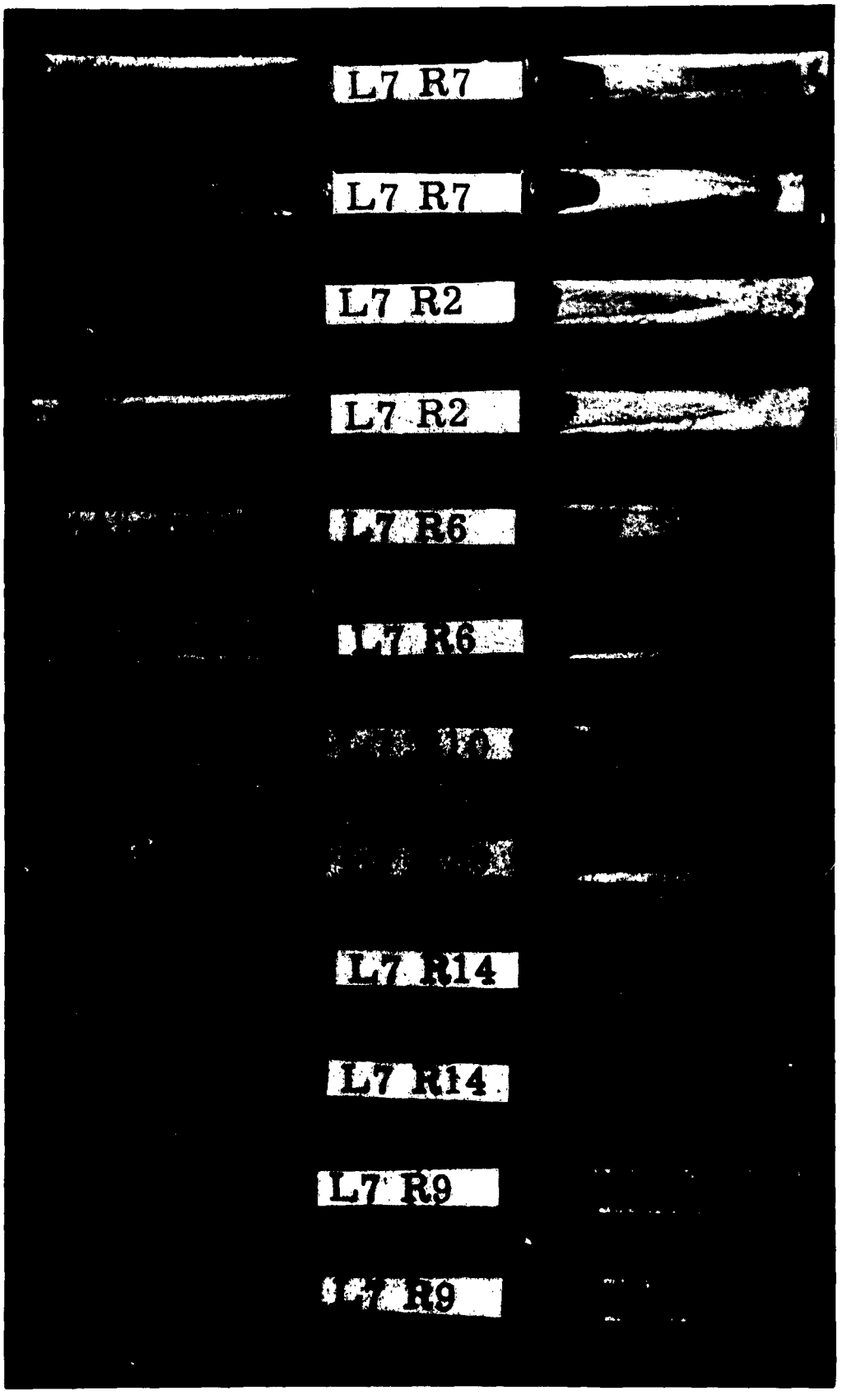


Fig. II Study of Crack Shape for AMS 255 Steel, 0.188 in. Thick, σ_y=220,000 psi, Tempering Temp.-550°F, Heat Tinted at 400°F for 2 hr.

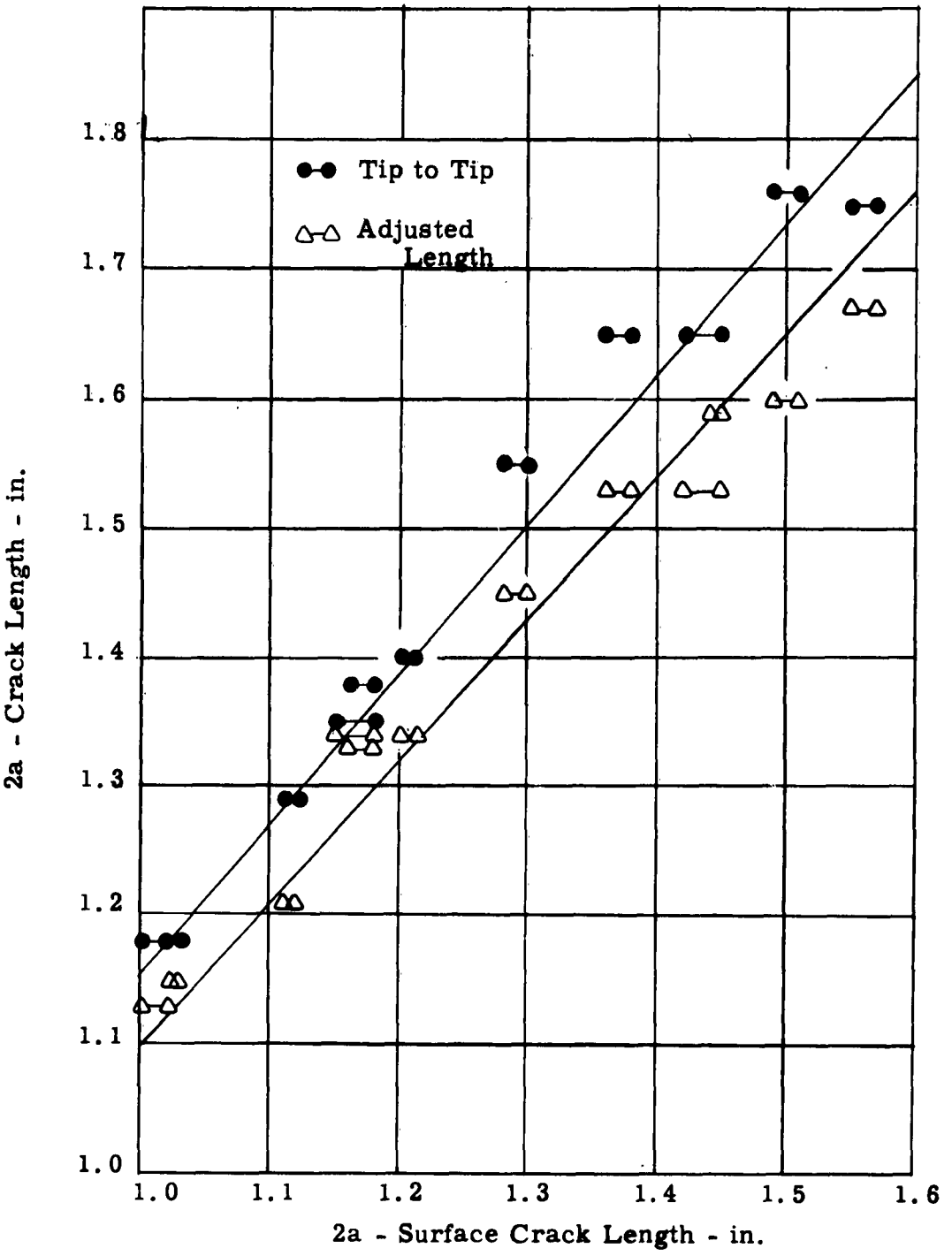


Fig. 3 Relation Between Tip to Tip Crack Length, Adjusted Crack Length and Surface Crack Length for T4 Specimens.

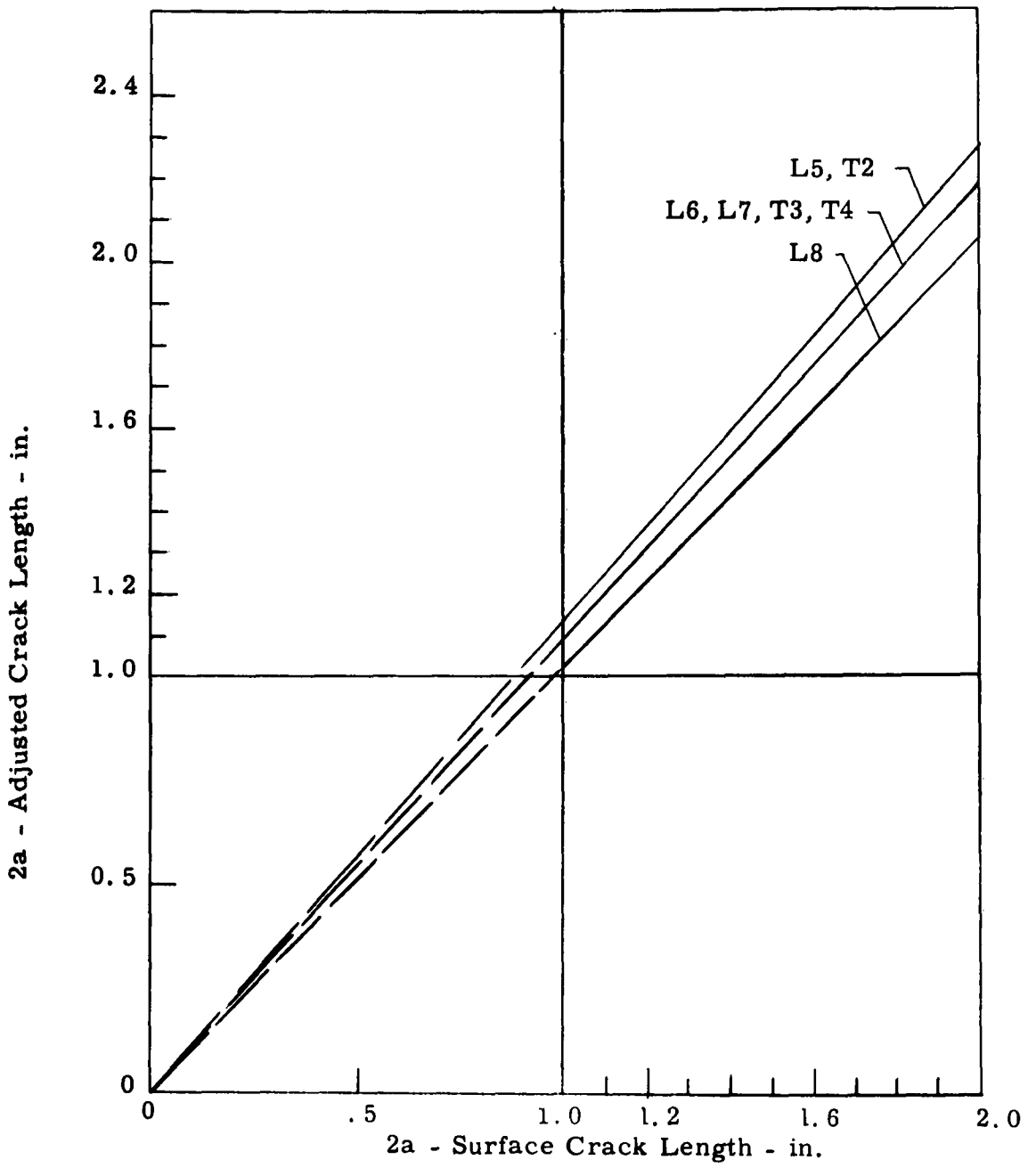


Fig. 4 Relation Between Surface Crack Length and Adjusted Crack Length

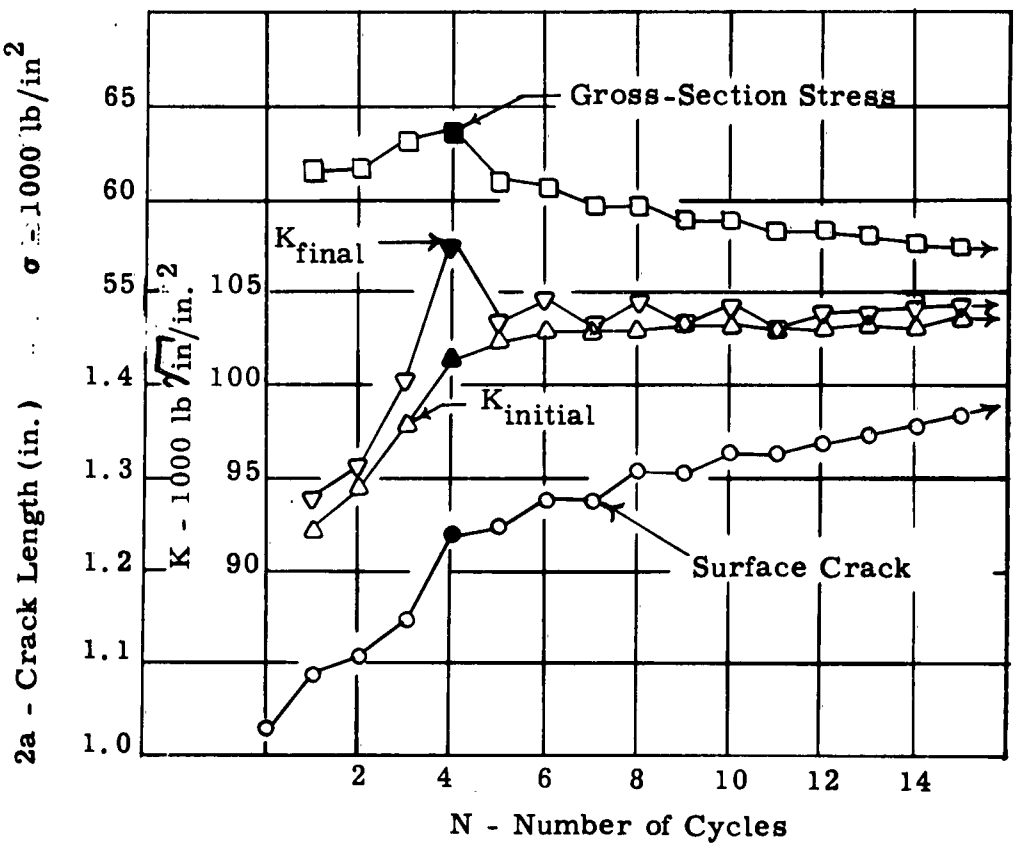


Fig. 5 Slow Crack Extension Data for Specimen T4 R4

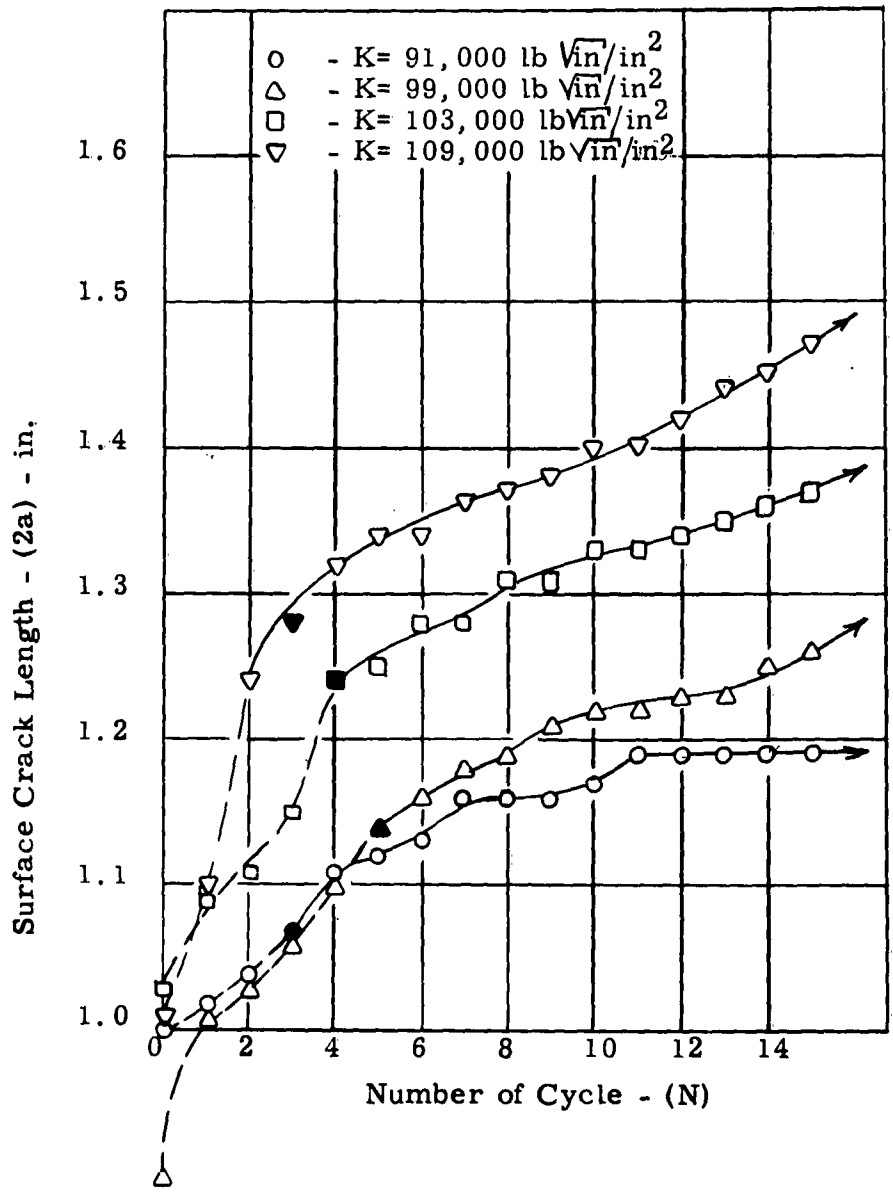


Fig. 6 Slow Crack Extension of T4 Specimens

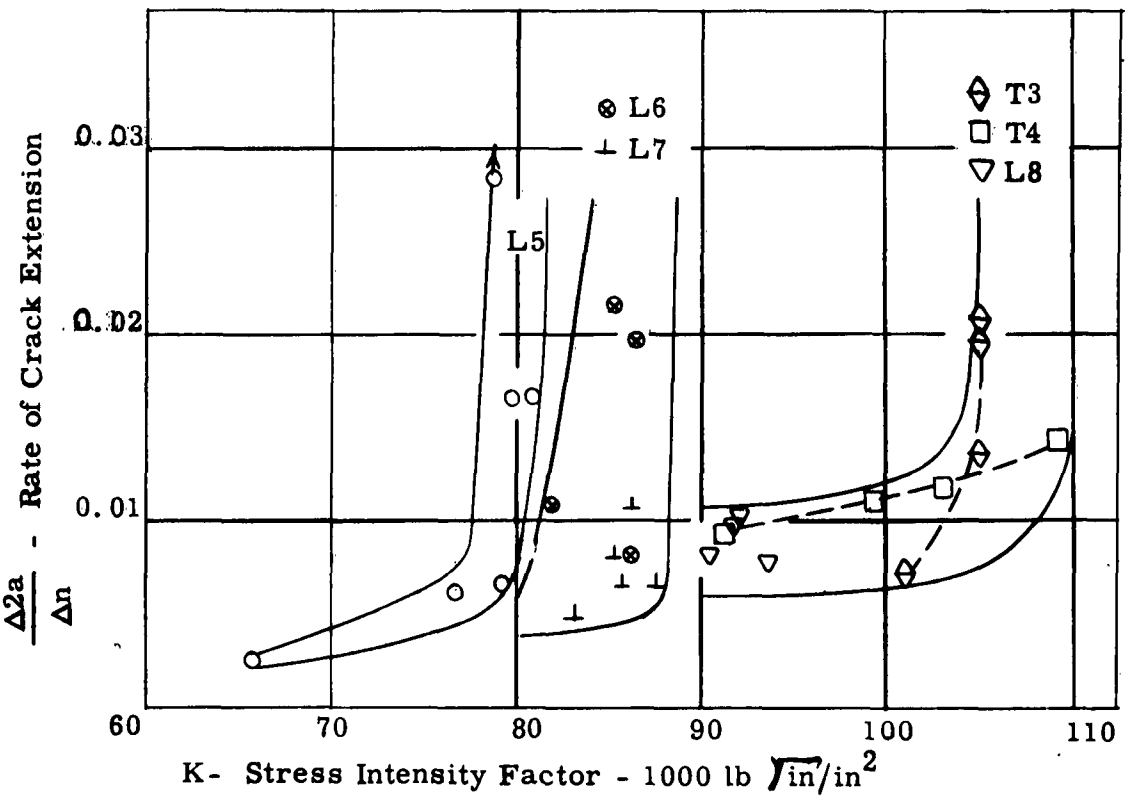


Fig. 7 Influence of Stress Intensity Factor on Rate of Crack Extension

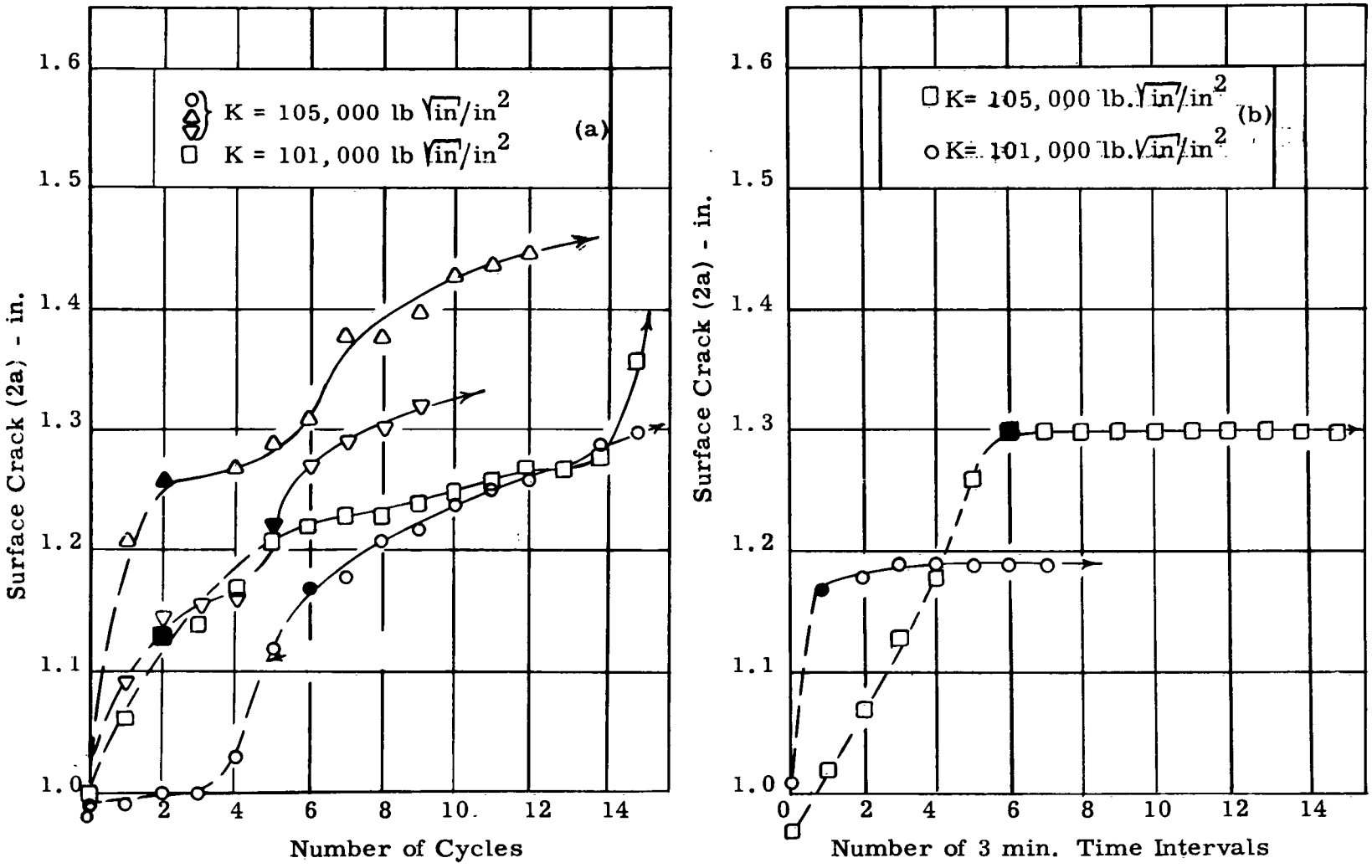


Fig. 8 **Slow Crack Extension Caused by (a) Zero to Maximum Cycling and (b) Without Cycling. T3 Specimens.**

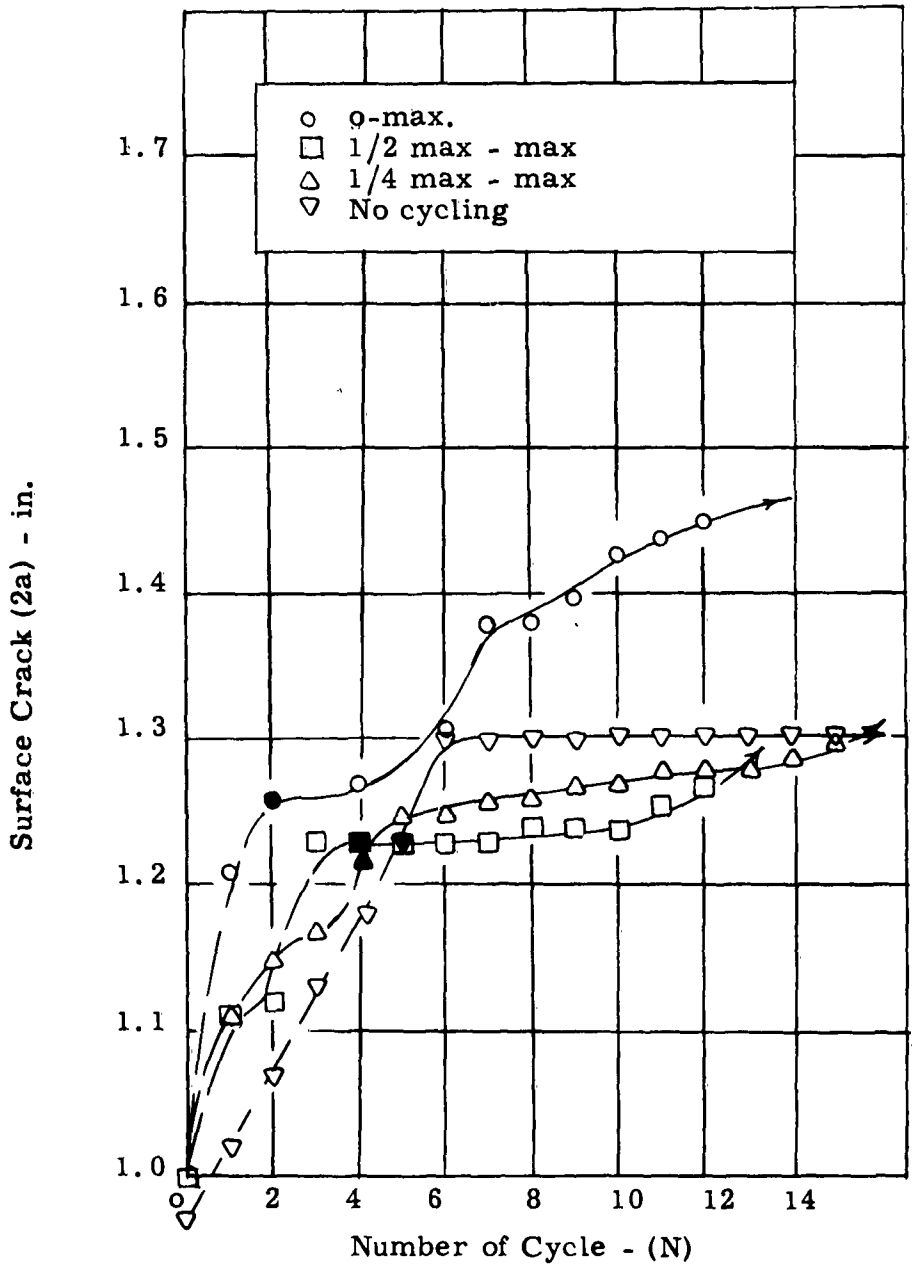


Fig. 9 Influence of Amplitude of Loading on Slow Crack Extension. At Maximum Load, $K = 105,000$ lb $\sqrt{\text{in}}/\text{in}^2$ for All Specimens.

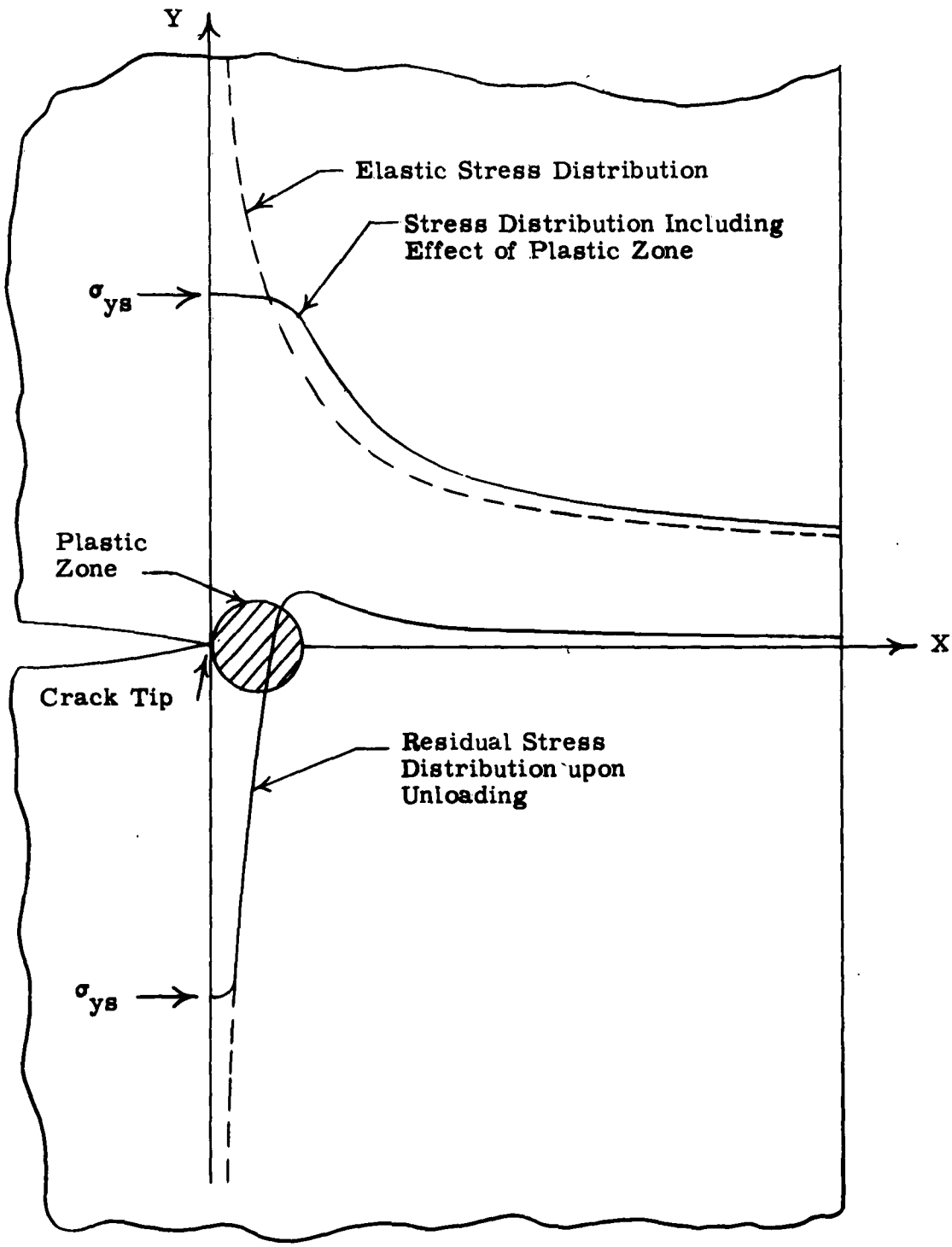


Fig. 10 Stress Distribution Illustrating the Accumulation of Plastic Strain Both Upon Loading and Unloading

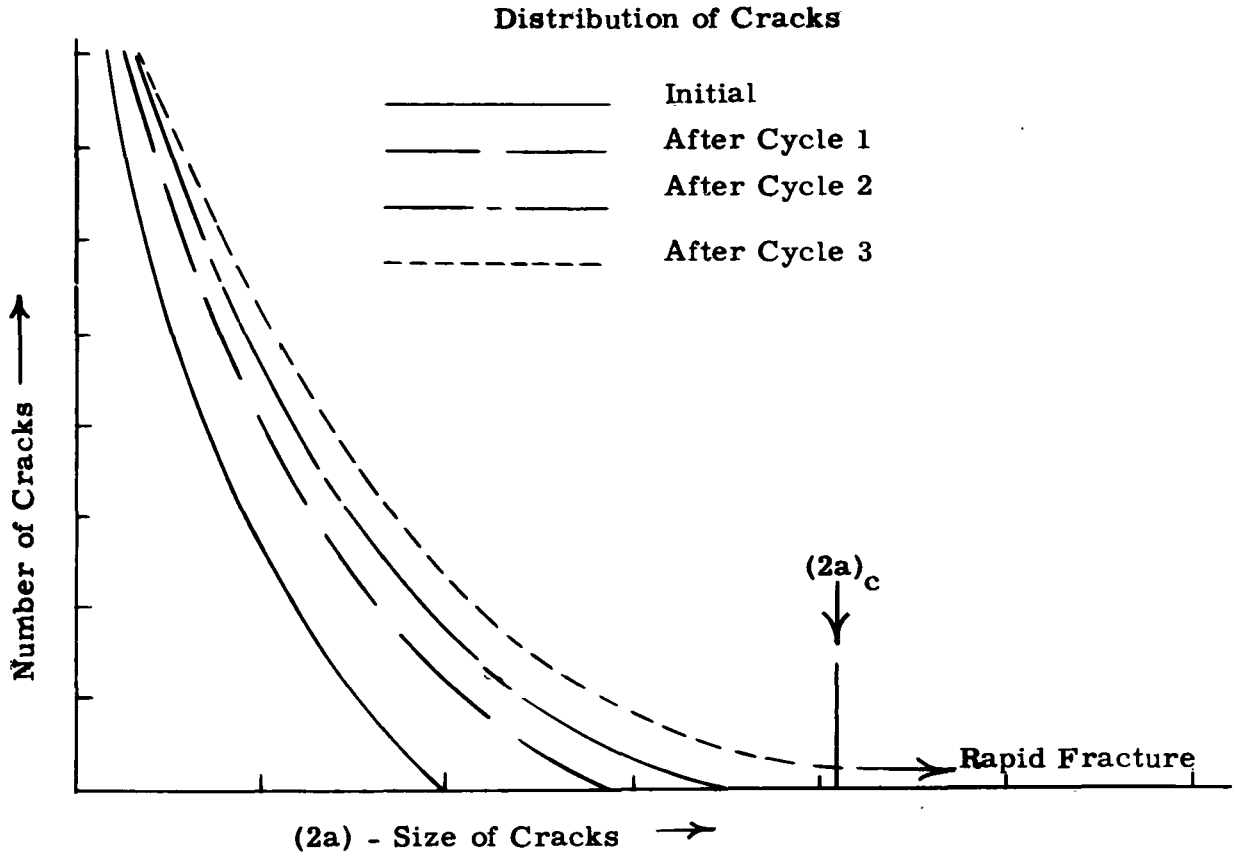
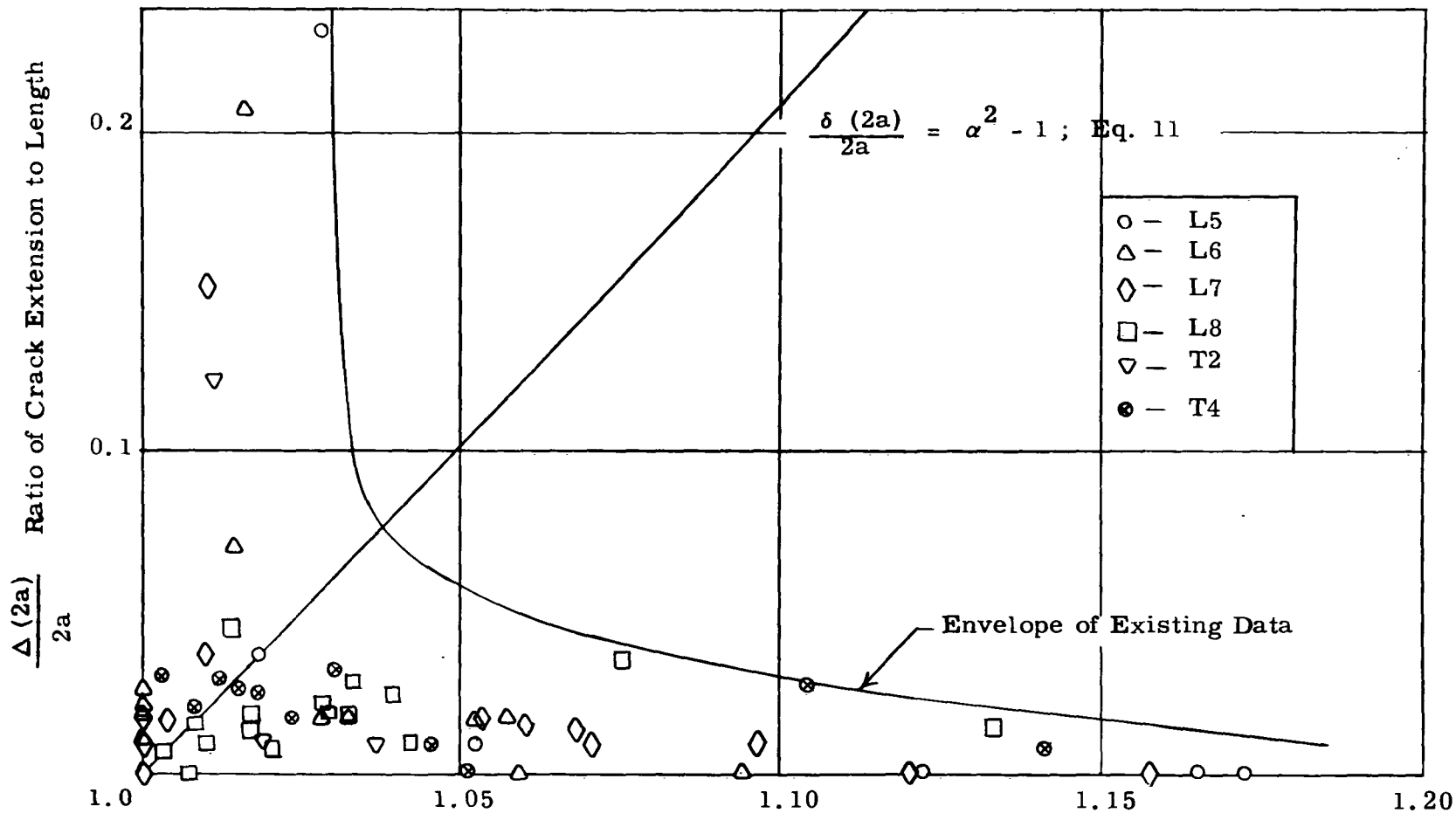


Fig. 11 Schematic Crack Size Distributions Illustrating Inevitability of Rapid Fracture Resulting From Repeated Cycles of Hydrotesting



α - Ratio of High Stress to Low Stress, or Ratio of Hydrotest Pressure to Pressure upon Firing.

Fig. 12 Slow Crack Extension When the Ratio of the Stress on the Preceding Cycle to the Stress on the Current Cycle is α .

ERRATA SHEET

Pages IV-137 thru IV-158 withdrawn.
Pages duplicated on pages IV-115 thru IV-136.

EMBRITTLEMENT BY LIQUID METALS

by

W. Rostoker*

It is important at the outset to distinguish various forms of embrittlement by liquid metals. Many liquid metals, during prolonged exposure to a solid metal of higher melting point, will diffuse into the body of the latter, producing brittle coatings which impair the ductility of the whole section. Steel immersed for long times in molten tin or zinc may be affected in this manner. Certain liquid metals will penetrate intergranularly into a polycrystalline solid metal given sufficient time at a high enough temperature. The envelope developed around each grain will engender brittleness. For instance, molten bismuth will intergranularly penetrate into polycrystalline copper and permanently reduce or destroy its ductility. Intergranular penetration is symptomatic of a very low dihedral angle relationship between liquid bismuth and the grain boundaries of copper. The envelope structure is a natural consequence of the driving force to reduce the interfacial energy of the system.

These two embrittlement processes are easily observed and easily rationalized. The rates of both processes are increased by increasing temperature. By contrast, a third and much more catastrophic embrittlement can occur whose nature and origin are not at all obvious. Embrittlement can occur under the circumstance that a liquid metal has wetted, or, in other words, has established a true interface with the solid metal in jeopardy. Cracking initiates at that interface and propagates in a general direction normal to the axis or axes of principal tensile stresses. The conjoint existence of a liquid-solid interface and of a critical magnitude of stress is the necessary condition for the generation of fracture. The stress may be dynamic in origin as in the simple uniaxial tensile test, static as under dead weight loading, residual from prior thermal-mechanical history, or alternating.

It is appropriate at this point to list some of the characteristics of this form of embrittlement by liquid metals:

(a) Not every liquid metal will embrittle every structural metal, even with the establishment of a true interface. For instance, high-strength aluminum alloys are embrittled by Hg, Ga, Na, In, and Sn above their melting points, but not by Li, Bi, Pb, or Cd.

(b) Neither the area wetted nor the amount of liquid present need be large. However, the extent of cracking measured by length and number depends on the amount of liquid available.

(c) Fractures in recrystallized metals are invariably intercrystalline except when the grain structure is elongated.

---

* Metals Division, Armour Research Foundation, Chicago, Illinois

However, transcrystalline cracking can be produced in heavily cold-worked metals and in certain single crystals or coarse grains.

(d) Embrittlement can be encountered in all degrees--from slight reduction in total ductility to brittle fracture well below the engineering yield point. This is illustrated in Figure 1 by the tensile behavior of cold-rolled copper wetted by a series of Bi-Pb alloys. It is to be noted that wetting by a liquid metal does not influence the yield point.

(e) Brittle fracture is potential at the moment of wetting if the stress is high enough. At lower stresses, a finite delay time is associated with fracture. The delayed failure of a hardened AISI 4130 steel wetted with lithium is illustrated in Figure 2.

(f) Brittle fracture associated with wetting by a liquid metal is temperature dependent--disappearing abruptly at some elevated temperature. The ductility-temperature curve appears as the ductile-brittle transition ordinarily encountered in body-centered cubic metals as shown in Figure 3. Reiterating an earlier remark, this is opposite to the two other processes of embrittlement by liquid metals.

(g) The fracture stress in the wetted condition is dependent on the hardness of the metal. A two-fold trend is found. At low hardnesses, the fracture stress follows the yield stress and, above some critical hardness level, fracture stress is progressively less than the engineering yield stress. This is illustrated in Figure 4.

With this necessarily brief introduction to phenomenology, it is appropriate to begin a discussion of present views of the nature of the process. First, it is important to establish that the ductile-brittle transition encountered is basically the same as that encountered in body-centered cubic metals. This point has been explored. It has been shown that the transition temperature of 70/30 brass wetted with mercury is related to grain size in the same fashion as mild steel--that is, the transition temperature is proportional to the logarithm of the grain size. As also with mild steel, increasing strain rate of testing has been shown to raise the transition temperature of an aluminum alloy wetted with mercury, according to a logarithmic function.

From the Cottrell-Petch condition for the occurrence of a ductile-brittle transition:

$$\sigma_y \cdot K_y \cdot d^{1/2} = \beta G \gamma$$

where σ_y = yield stress; K_y = slope of the σ_y vs. $d^{-1/2}$ function; d = grain size; β = a numerical factor; G = modulus of rigidity; γ = surface energy associated with fracture.

One can surmise that the surface energy term γ is most likely the factor influenced by the presence of a liquid-solid interface. Thus, one can expect an interplay between σ_y and γ.

This has been demonstrated. Cold worked copper wetted with a series of Bi-Pb alloys at 350°C shows a transition to failure below the yield point at about 70% Bi. When the copper is annealed (and σ_y thereby reduced), the same transition occurs at pure Bi. This is consistent with the trend of interfacial energies between copper and Bi-Pb alloys in which γ varies from 250 ergs/cm^2 (Bi) to 350 ergs/cm^2 (Pb).

Taking the position that surface adsorption of the liquid metal lowers the energy of formation of crack nuclei, one can explore the magnitude of the reduced surface energy by two definitive experiments. The first was devised by Petch(1) to rationalize a mechanism of hydrogen embrittlement of steel. He argued that the value of K ought to be depressed by the presence of hydrogen, where

$$K = \frac{\sigma_f - \sigma_o}{d^{-1/2}} = \sqrt{\frac{6\pi G \gamma}{1-\nu}}$$

σ_f = fracture stress; σ_o = an intercept; ν = Poisson's ratio.

According to Petch's data, γ for mild steel is reduced by dissolved hydrogen from about 1600 to about 600 ergs/cm^2--in good agreement with independent measurements by another method.

One can demonstrate similar behavior in specimens wetted by an appropriate liquid metal. Even when ductile face-centered cubic metals do not normally provide a clear linear dependence of σ_f on the grain size function, $d^{-1/2}$, they do when wetted by a liquid metal. Computed values of effective surface energy are 730 ergs/cm^2 for mild steel wetted with molten lithium, and 280 ergs/cm^2 for brass wetted with liquid mercury. Both of these values are well within the range expected for brittle behavior.

The very low surface energies derived suggest that liquid metals can produce almost ideal brittle fracture. Under more normal circumstances, as Orowan and Felbeck(2) have shown, there is still a very large energy term associated with microplastic deformation so that the apparent surface energy is of the order of 10^6 ergs/cm^2.

An experimental evaluation of the constants in the Griffith equation for crack propagation provides another method of estimating the effective surface energy associated with brittle fracture induced by wetting with a liquid metal. It has been discovered that crack propagation in 70/30 brass sheets wetted with mercury can be arrested by rapid unloading. Accordingly, it is possible to "walk" a crack across a wide sheet specimen. This permits

multi-point determinations of fracture re-initiation stresses, σ_i, according to the Griffith equation:

$$\sigma_i = \sqrt{\frac{E\,\gamma}{C}}$$

where E = Young's modulus; C = initial crack length.

By wetting with mercury on only one side, one can get a mixture of brittle and ductile fracture which, when plotted as in Figure 5, yields an estimated effective surface energy of about 10^6 ergs/cm^2. By wetting on both sides, the data as plotted in Figure 6 yield an effective surface energy of about 1000 ergs/cm^2 or less.

The results of experiments cited indicate that the shear-stress-activated dislocation pile-up model for fracture nucleation is applicable to the phenomenon of liquid metal embrittlement. However, inasmuch as fracture initiates at the liquid-solid interface, it is necessary to modify the model to treat only dislocation pile-ups at a surface. That such do in fact exist has been amply demonstrated by etch pit studies, particularly by Low and Guard(3) on silicon ferrite (Fe + 3%Si). The "dislocation decoration" process reveals the emergence of dislocation lines to a free surface, and the arrays of etch pits observed show that slip line pile-ups do occur at grain boundaries. Since the grain boundary is the most effective pile-up barrier, it is not surprising that cracks appear to be largely intergranular. However, intersecting slip bands are known to be capable of producing crack nuclei in certain metals, particularly body-centered cubic, and so one should expect that in certain cases it is possible to initiate cracking in the center of a grain. Experiments with very coarse-grained silicon ferrite, in which only the centers of grains were wetted with molten lithium, have demonstrated that cracking can be induced and propagated without the association of a grain boundary. This reinforces the conclusion brought out earlier--that prior penetration of the liquid metal is not implicit in the mechanism of brittle fracture.

This work was performed under contract to Frankford Arsenal.

REFERENCES

1. N. J. Petch, Phil. Mag., 1- (1956),331.

2. E. Orowan and D. K. Felbeck, Welding Journal, Res. Suppl., 34 (1955),570S.

3. J. Low and R. Guard, Acta Metallurgica, 7 (1959),171.

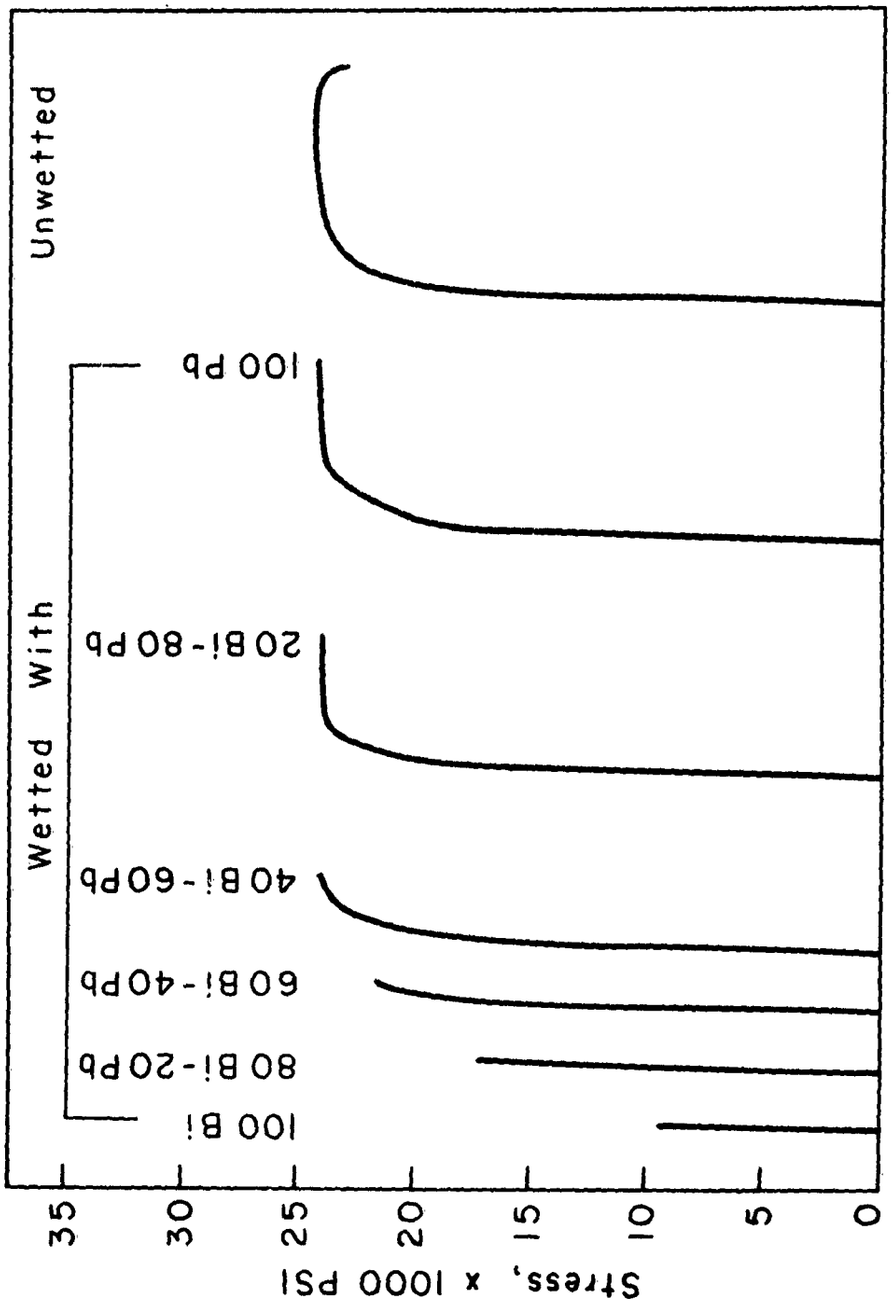


FIG. 1 - Stress-strain curves of hard rolled copper wetted with various Bi-Pb alloys at 350°C.

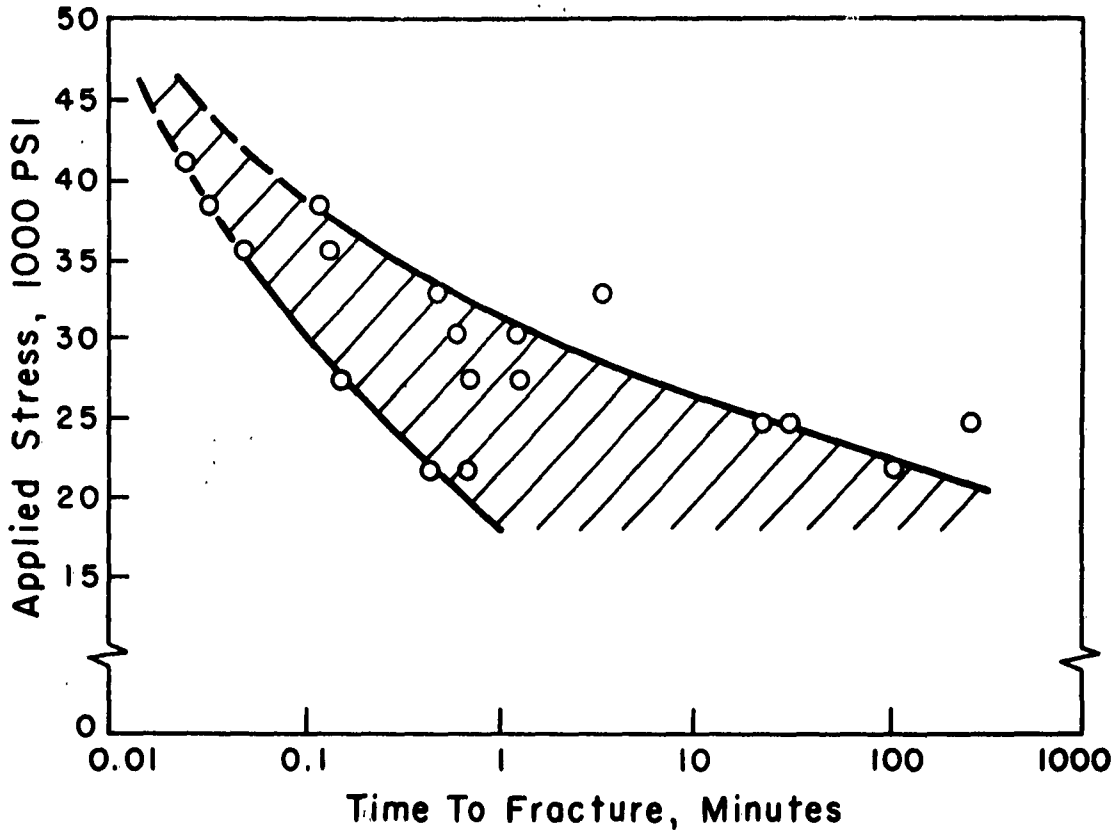


FIG. 2 - Delayed failure or static fatigue of SAE 4130 steel at a tempered hardness of R_c44 when wetted with molten lithium at 205°C.

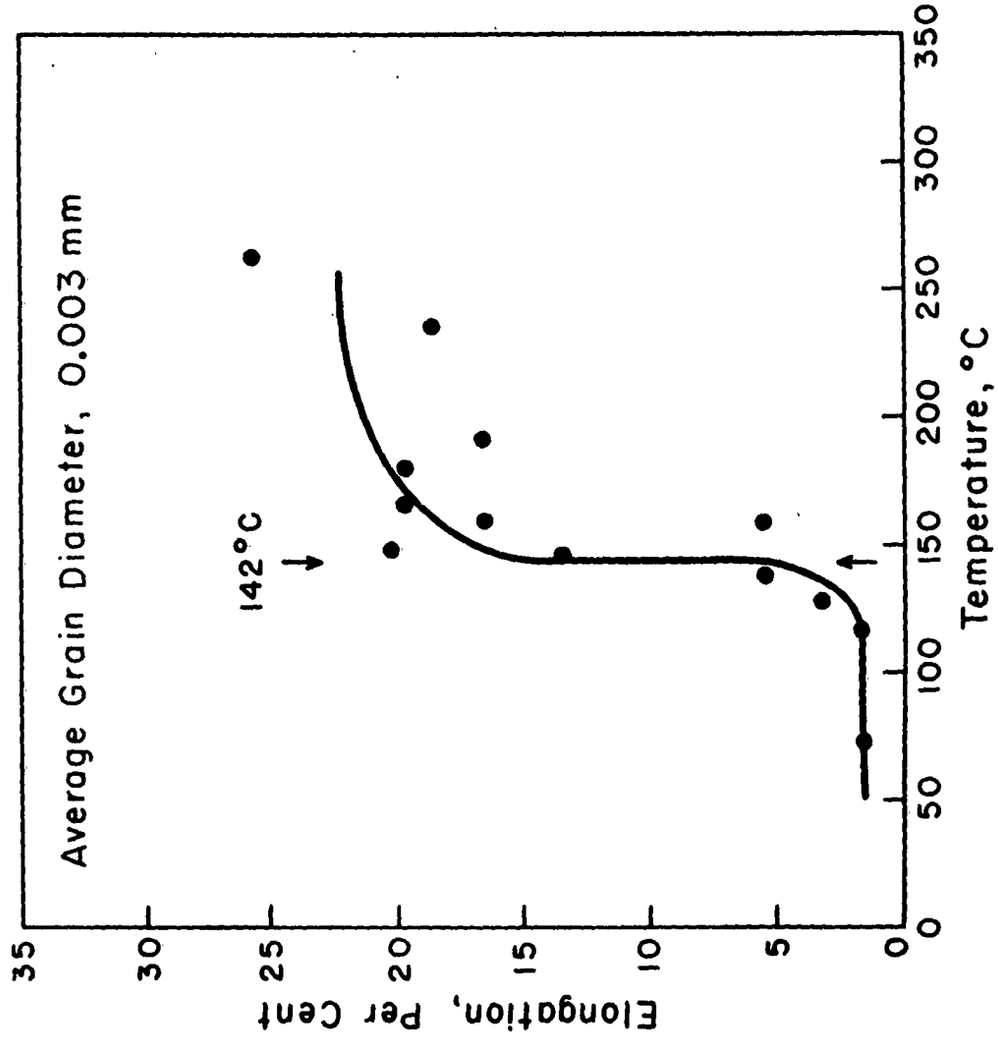


FIG. 3 - Ductile-brittle transition in 70/30 brass wetted with mercury.

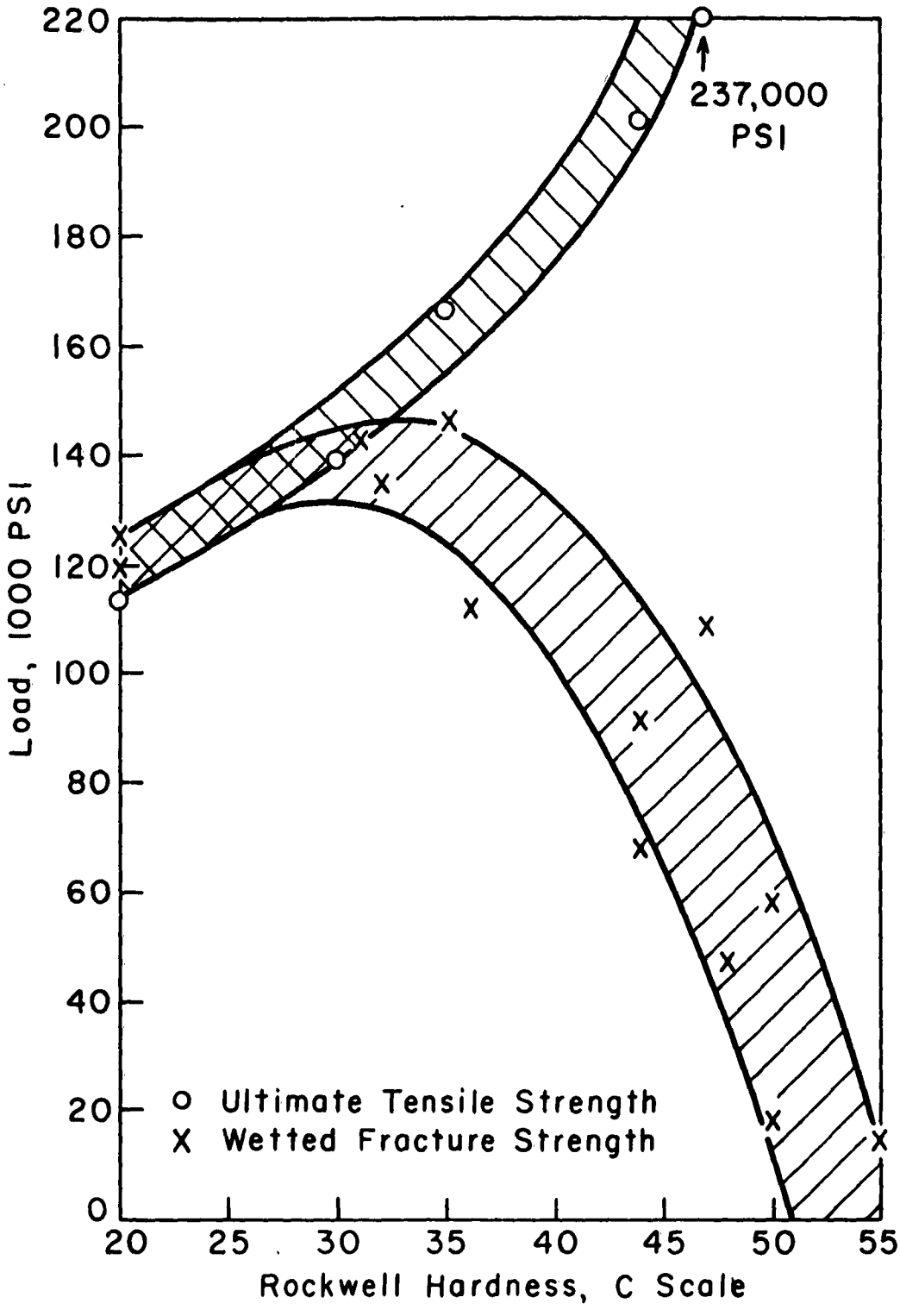


FIG. 4 - Correlation between hardness and tensile strength (wetted with molten lithium at 200°C and unwetted) for an SAE 4130 steel.

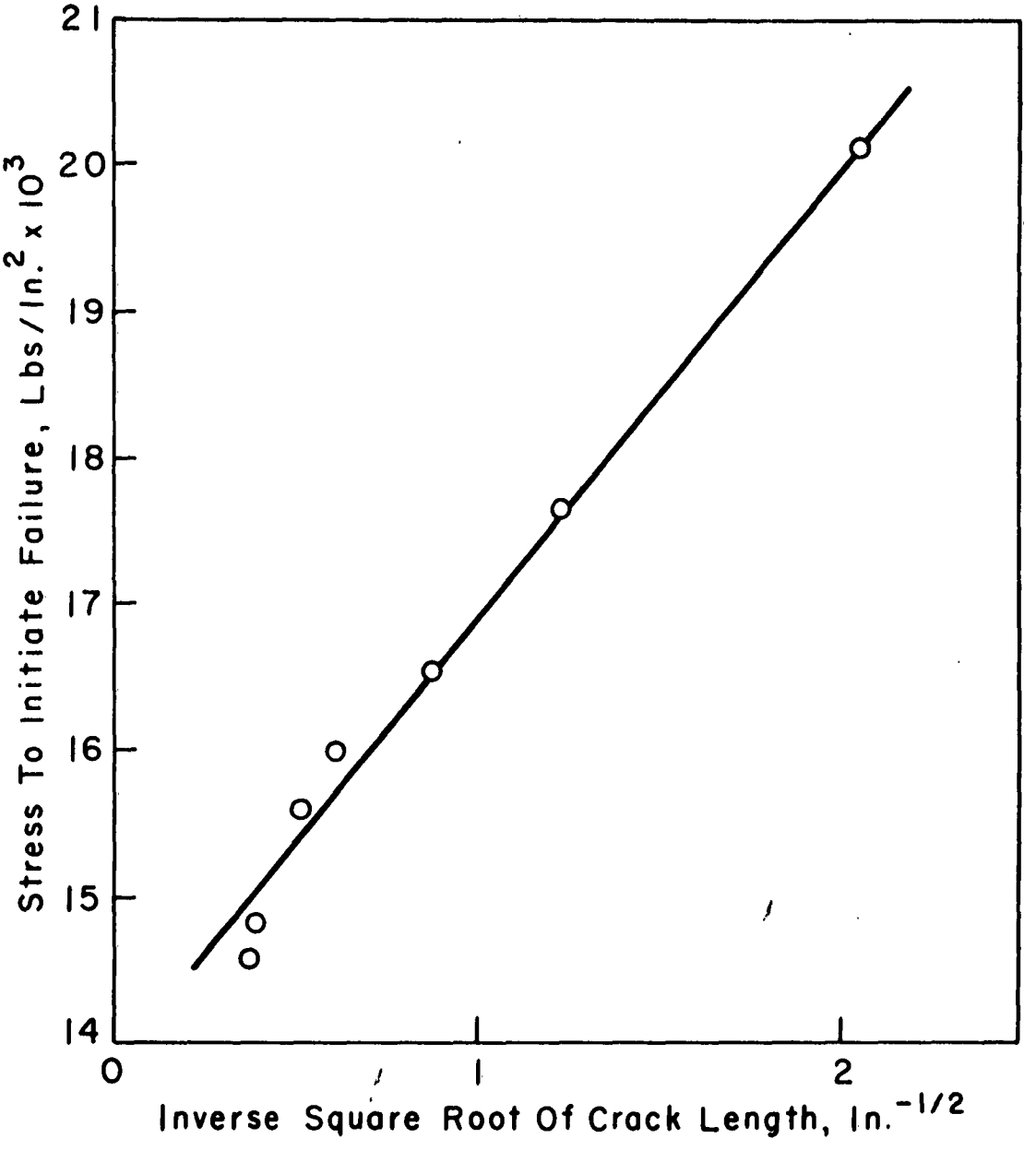


FIG. 5 - Stress to propagate a crack as a function of carck length. 70/30 brass sheet wetted on one side with mercury.

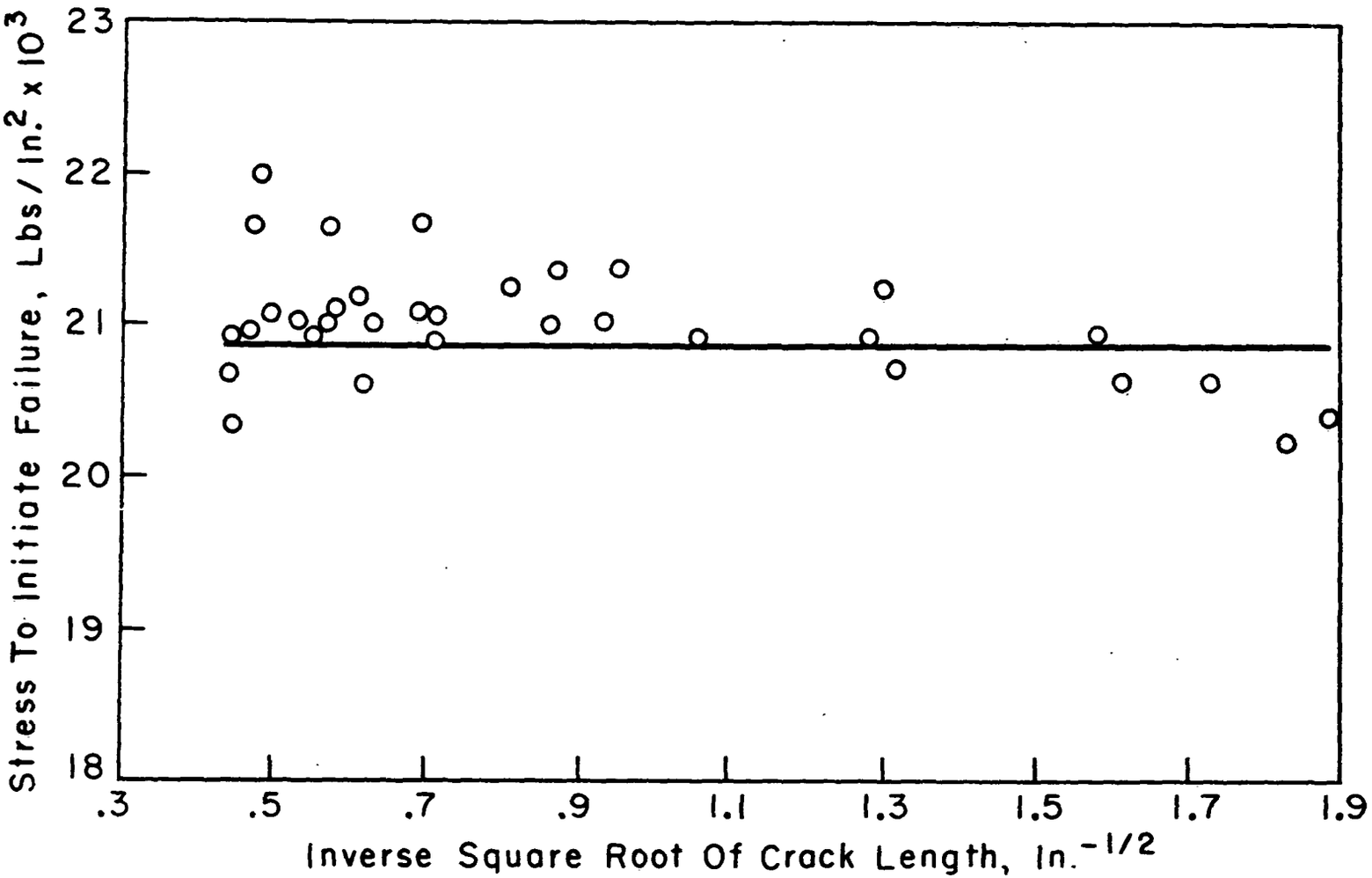


FIG. 6 - Stress to propagate a crack as a function of crack length. 70/30 brass sheet wetted on both sides with mercury.

PREPARED DISCUSSION - FOURTH SESSION

The Effect of Small Surface Cracks on Strength

prepared by
J. E. Srawley and C. D. Beachen*

Tensile crack propagation tests of sheet materials are usually conducted on specimens with sharp notches or slots which are quite large in comparison with the sheet thickness. We feel that there is a need for experimental data on the effect of the size of small cracks which do not penetrate through the thickness of the sheet. We have been able to introduce such cracks into specimens by controlled hydrogen embrittlement cracking, and believe that the results obtained so far with these specimens will be of some interest to those at this Conference.

Specimens 1 in wide were obtained from a sheet of X200 steel, about 0.07 in thick, and were air hardened and tempered at 700 F to have a yield strength of 228 ksi and an ultimate tensile strength of 274 ksi at room temperature. These were provided with central, transverse cracks of semi-elliptical shape, the smallest being about 0.01 in deep and 0.05 in long. After cracking, the specimens were baked to remove hydrogen and tested in tension.

Results for three testing temperatures are shown in Figure 1, in terms of the crack strength ratio (nominal net fracture stress divided by ultimate tensile strength) versus relative crack size (area of the original crack divided by specimen thickness). The points at the right which are circled refer to specimens with crack-ended central slots which were tested for comparison. At room temperature the effect of the smallest cracks is very slight, but the strength decreases very rapidly as the relative crack size increases in the range 0.01 to 0.05 inches. For example, a crack of relative area 0.037, which was about 0.11 in long and 0.03 in deep, reduced the strength to less than the yield strength. The results in general suggest that there is a lower limit to the size of crack which will have an appreciable influence on strength, and that this limit decreases markedly with temperature. Beyond the borderline crack size, the decrease in strength as the crack size increases is very pronounced The strength is decreased further by a decrease in temperature (or the material becomes more brittle).

* Metallurgy Division, U. S. Naval Research Laboratory, Washington 25, D. C.

Some further tests were conducted at room temperature to investigate a possible effect of environment on the results. The cracks in some specimens were filled with water or with india ink during testing, while other specimens were first dehydrated in a vacuum dessicator and subsequently protected during testing by adhesive patches enclosing particles of a dessicant. The results are shown in Fig. 2 (which is on a much larger scale than Fig. 1). Thetriangular points, representing water or india ink, do appear to be significantly lower, on average, than the others, though the effect is only of the same order as the general scatter of results. These tests were each completed in a few minutes, and it is quite possible that larger effects would be observed in more prolonged tests. It is also very likely that the sensitivity to environment varies with material and condition. The material used here was fairly tough at room temperature (K_C about ksi · inches $^{1/2}$ full shear fracture), and a more brittle material might be considerably more sensitive.

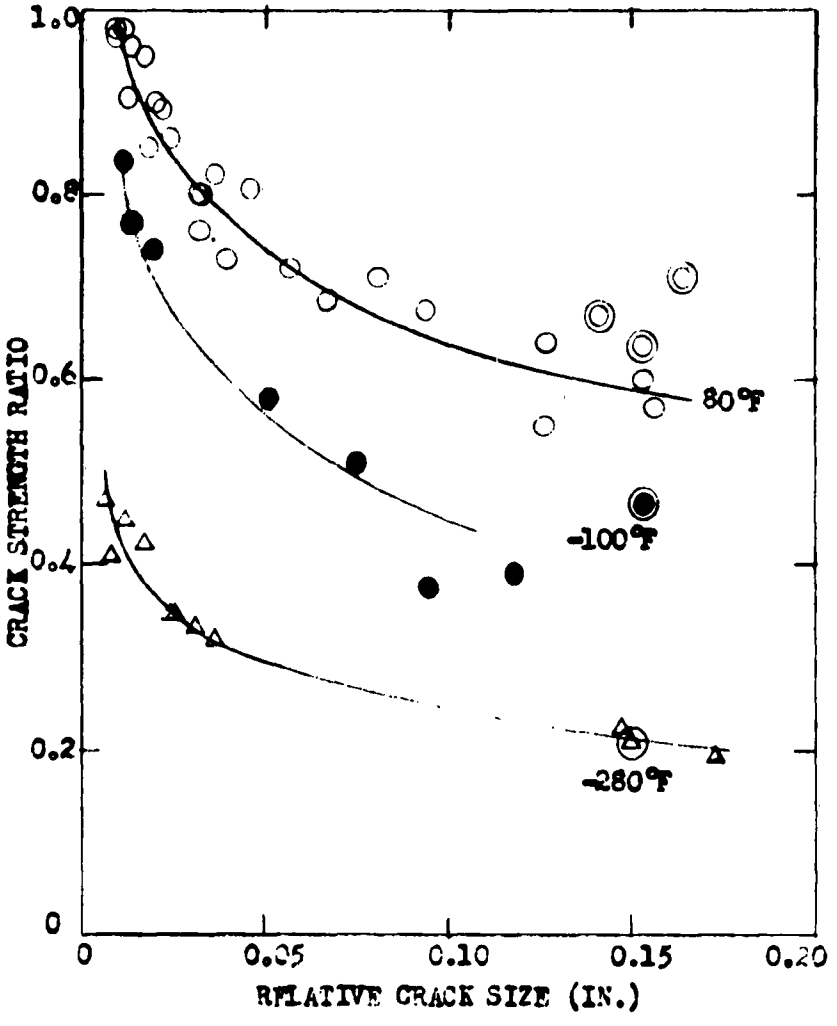


Figure 1. Effect of Crack Size on Crack Strength Ratio (Nominal Net Fracture Stress/Ultimate Tensile Strength) at Three Temperatures

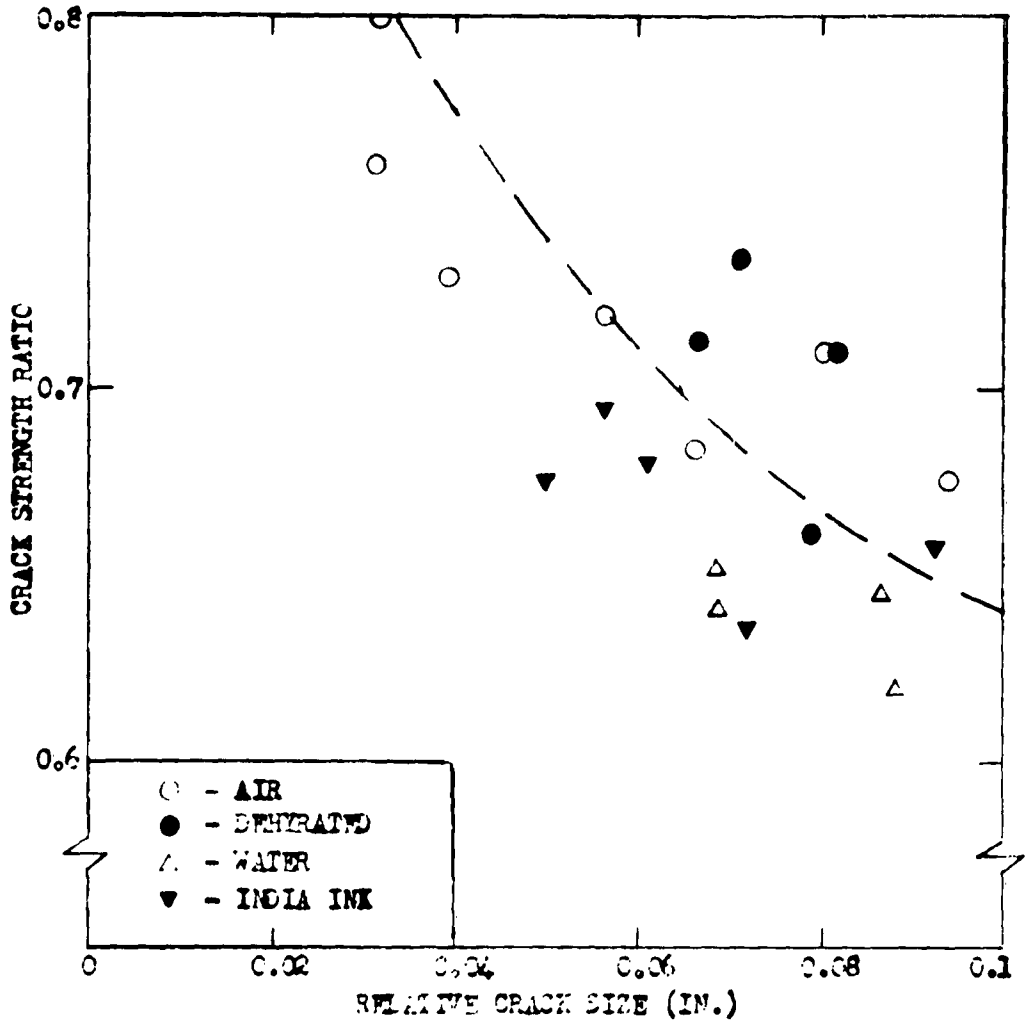


Figure 2. Effect of Environment on Crack Strength Ratio at 80°F

PREPARED DISCUSSION - FOURTH SESSION

Discussion of Paper

"Plastic Zone Near a Crack and Fracture Toughness"

by
G. Irwin

prepared by
George Sachs, Syracuse University

The merit of Dr. Irwin's work is undisputed. However, I would like to take strong exception to the philosophy which he expressed. If we do not know how to drive an automobile we may be forced to use a wheelchair. However, if we start to equip the wheelchair with powerbrakes and powersteering we might as well learn to drive an automobile.

My background is to a considerable extent in Applied Mechanics. For me, stress concentration effects, as defined by the theory of elasticity and calculated by Neuber, are more readily understandable than Dr. Irwin's calculations. I have discussed this problem with a number of scientists and have frequently been asked to act as council for defending the stress concentration approach. Griffith's theory is a thermodynamical approach and circumvents stress distributions. According to my way of thinking, its combination with stress distribution calculations is not permissible and does not lead to clearly definable conclusions.

Griffith's theory is expressed by the equation $\sigma = A/\sqrt{c}$, where σ is the gross stress and **A** a compound material constant identical to the gross stress for c = 1 where c is the crack length. It postulates, for a brittle metal, that instability occurs for a given combination of σ and c. It also postulates the pre-existence of an extremely sharp crack. The constant **A**, according to Griffith's initial concept which involves surface tension, is very small, perhaps .01 or .001 of actually observed values. To explain these, Orowan increased the constant **A** to include a plasticity energy term. This equation still remains the basic single-parameter equation, and $\mathcal{G}_c$ is only another form of the constant. Further leading refinements by Irwin to a two-parameter equation to account for plasticity make use of arbitrary and non-permissible calculations. These lead to a maximum strength, for infinitely small cracks, at a value $\sqrt{2}$ times the yield strength. There is a very peculiar assumption hidden in such an approach. Finally, a correction for finite specimen size is introduced from Westergaard's calculations. Although, this procedure appears valid, the correction for practical conditions turns out to be only a few percent and can be usually neglected. Therefore, there is no need for the use of the resulting complicated equations. Furthermore, the final result is very similar to that derived from the Neuber's concept of

finite stress concentrations, which is much simpler, and this has been discussed in detail by Dr. Weiss.

Griffith's theory is also not applicable to the effect of section size, as recognized early in this game, nor does it lead to any conclusions relating to such phenomena as a fast rate of crack propagation, critical crack length and so forth. A plausible theory for a distinction between slow and fast rate of crack propagation does not exist. If the claim is made that these phenomena can be explained on the basis of a modified Griffith's theory, this becomes a matter of religion, rather than of science: you either believe it or you do not believe it.

PREPARED DISCUSSION - FOURTH SESSION

Discussion of Paper

"Embrittlement by Liquid Metals"

by
W. Rostoker

prepared by
J. M. McCaughey, Frankford Arsenal

Dr. Rostoker has presented some studies undertaken on the embrittlement of certain solid metals by liquid metals. His paper has been primarily centered on brass, copper and steel and he has shown conclusively that liquid metal fracture is definitely "brittle" in nature. Several relationships also have been determined for the embrittlement of aluminum alloys by liquid metals, and I believe, they would be of interest to this group.

First, it has been suggested that a demonstration of liquid metal embrittlement would be appropriate at this time.

This first specimen is an alclad strip of 2-24-T3 aluminum alloy and as you know, it may be easily bent without experiencing any cracking or failure. However, if a similar specimen has a small amount of amalgam placed on it prior to bending, fracture will take place immediately. No permanent deformation has taken place prior to failure, indicating the stress required was lower than the yield stress. The amalgam used is primarily mercury but with some additives to make it pasty for ease in handling, and also to enhance the embrittlement phenomenon.

One additional demonstration can be made to show this effect. An 1/8 inch thick 2024-T3 plate has an indentation in the center to give large residual stresses. If some amalgam is now applied to this area, fracture will take place without the necessity of the application of an external stress.

Several relationships have been determined for liquid metal embrittlement of 2024-T3 aluminum alloy and these are shown in the following figures.

Figure 1 shows the role of intrinsic strength on the embrittling capability of a liquid metal. This plot is essentially for dry fracture strength versus wet fracture strength (fracture strength when wet by a liquid metal), and it indicates that for alloys with an ultimate tensile strength greater than 60,000 psi, the wet strength is less than the dry strength. The alloys with this high strength are 2024-T4, 7075-T6, and

7001-T6 and the stress required for fracture (wet) for these alloys is actually much lower than the normal yield stress. The other alloys are also embrittled but the stress required is above the yield stress.

Figure 2 shows the quantity of liquid metal required for cracking. This is for a specimen 1/2 inch thick by 3 inch wide stressed to 10 percent of its ultimate tensile strength and then wetted by the liquid metal. This figure indicates that 4 grains of the amalgam are required for complete fracturing of the test specimen. Smaller amounts also produce cracking but incomplete failure of the specimen.

Figure 3 gives an indication of the role of stress on the embrittlement phenomenon. The lower radiograph shows a typical crack when wet by mercury while stressed to 10 percent of the ultimate strength. There is usually one long crack at right angles to the stress direction, and then extensive branching at the ends of the crack. As the stress level is increased prior to crack initiation, the single crack decreases in length and the branching increases. It is believed the reason for this is that with the higher stresses, there are more components above the threshold value for crack initiation.

Figure 4 is a plot showing the effect of temperature on mercury embrittlement of an aluminum alloy. If one strain rate is followed, it will be seen that greater ductility is achieved prior to fracture, indicating a reduction in the embrittling propensity with increasing temperatures. This figure shows also the relationship for strain rate. As the strain rate is increased, the ductility decreases, thus indicating that liquid metal embrittlement is enhanced with increasing strain rates.

Figure 5 shows a similar delayed failure curve for aluminum alloys as Dr. Rostoker has presented for SAE 4130 steel. At a high stress level, failure is immediate, but at lower levels, a finite time is required for failure. There also exists a threshold stress below which failure will not take place. An interesting feature of this relationship is that if the stress and liquid metal are removed prior to fracture, no harmful effects remain on the specimen. That is, if it were now tested, the tensile strength would be the same as for a conventional specimen.

Figures 6 and 7 are radiographs of cracks in 2024-T4 aluminum alloy specimens when stressed and wetted with mercury. The first is for uniaxial tension and in this case the crack has extended for approximately 12 inches. The second is for biaxial tension and again the crack has extended for a long distance.

Thus, it is evident that liquid metal embrittlement is not restricted to only one solid metal-liquid metal combination. The possibility exists that any stressed metal may be made to fracture in a brittle fashion if wetted by the appropriate liquid metal.

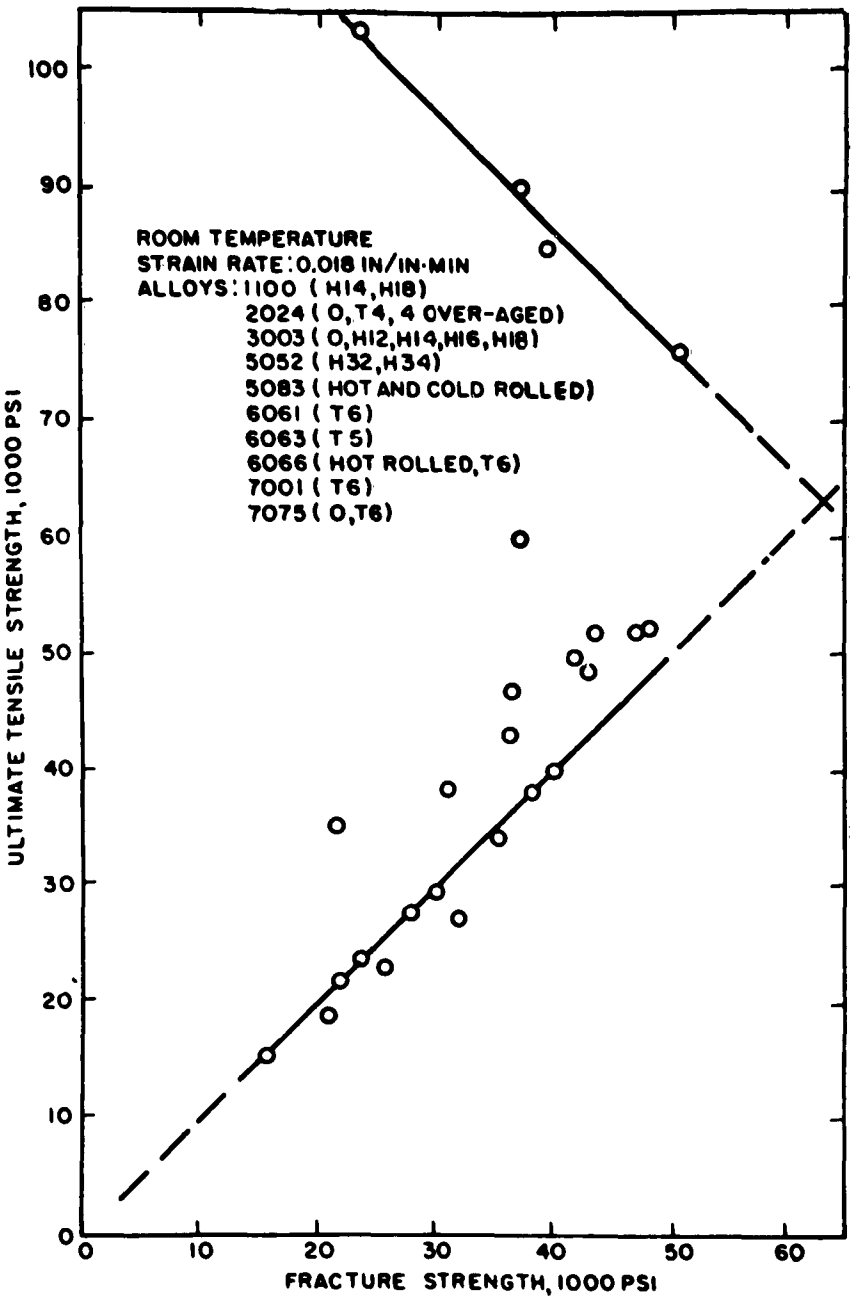


Figure 1. Relationship Between Normal Tensile Strength of Commercial Aluminum Alloys and Their Fracture Strength When Wetted with a Mercury Amalgam

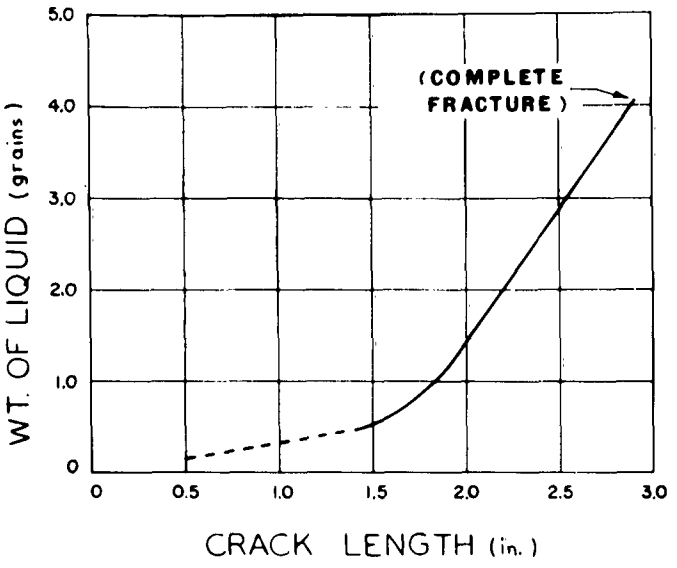


Figure 2. Crack Length as a Function of Amount of Liquid Amalgam Used

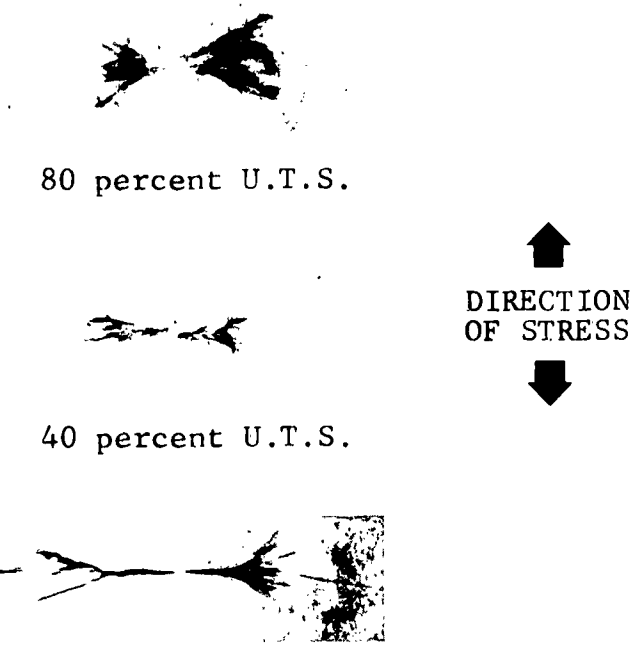


Figure 3. Crack Pattern in Aluminum Alloy Plate (2024-T3) as a Function of the Applied Stress

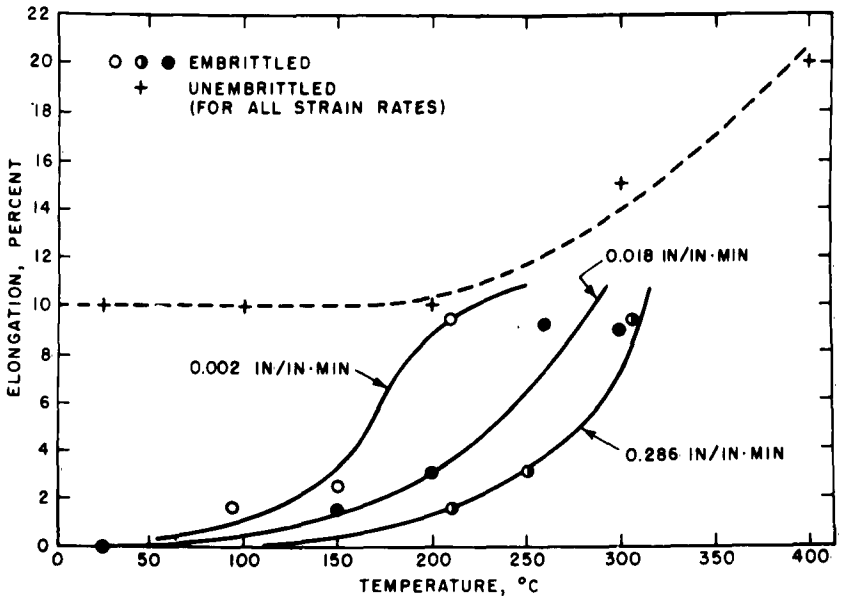


Figure 4. Correlation of Temperature and Strain Rate with Ductility of 2024-T4 Aluminum Alloy Wetted with a Liquid Amalgam

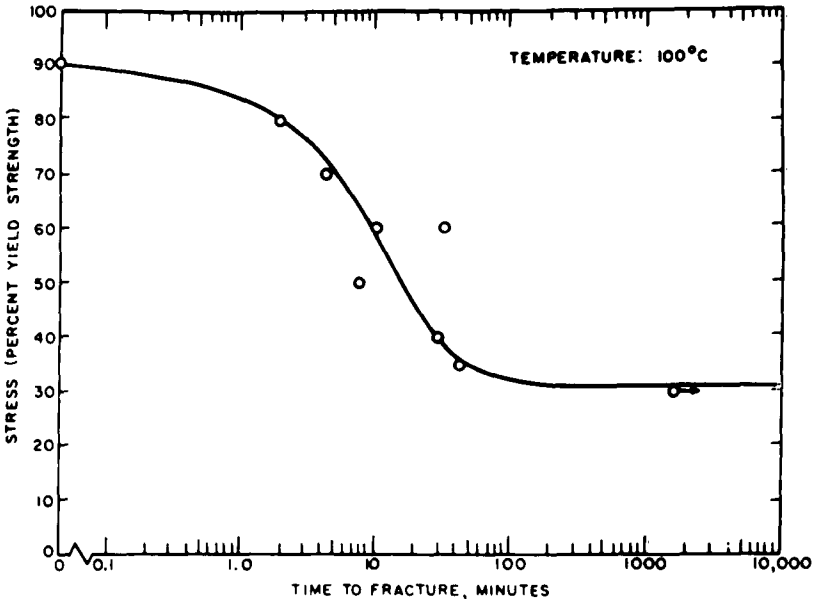


Figure 5. Time to Failure for a 2024-T4 Aluminum Alloy Wetted with an Amalgam as a Function of Statically Applied Stress

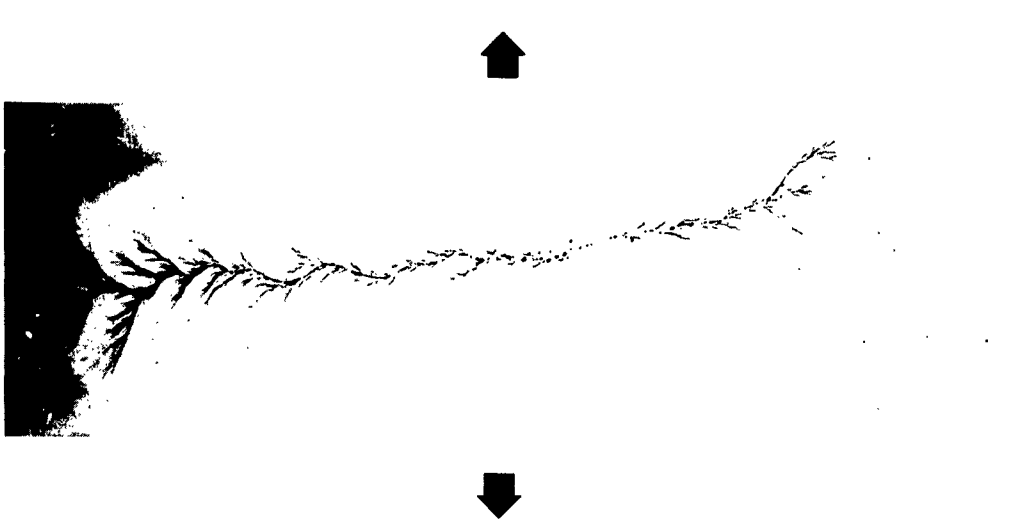


Figure 6. Radiograph of Crack in Aluminum Specimen Stressed Uniaxially and Wetted with Mercury. (Crack Approx. 12 inches Long)

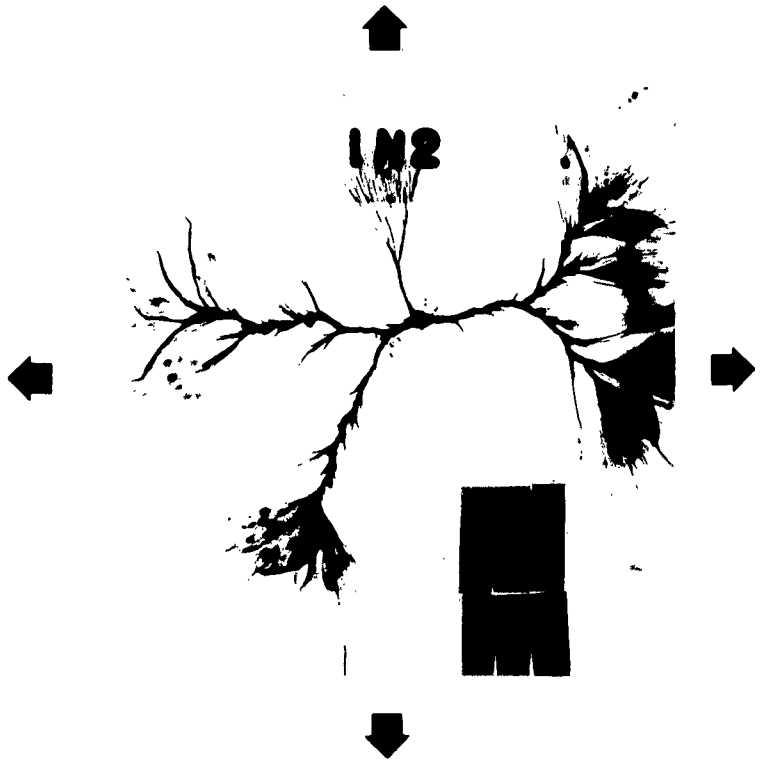


Figure 7. Radiograph of Crack in Aluminum Specimen Stressed Biaxially and Wetted with Mercury.

A. Hurlich I would like to suggest to Mr. Srawley that he apply his technique of surface cracking test specimens to pin down the problem of decarburization. I venture to predict that a decarburized surface will permit a much larger flaw to exist before we have a measurable decrease of the fracture strength of the material. I think this might be a good experimental technique to nail this point down. In respect to Mr. Corten's talk, I would like to make a comment because I think that his statement was extremely pertinent to a development that has been occurring over the last two years. In the aerospace industry and in the Air Force it has become very popular to bandy about the word "reliability". I think this word is a semantically unclear one, though a very glamorous one, and as a consequence we have seen the growth of large reliability groups now in the missile companies. In fact, in some companies there are more people in the reliability group that are evaluating the reliability of the missile than there are people designing the missile. Fortunately, a lot of these reliability people do nothing more innocuous than collect statistics from service failures. Unfortunately, however, a large number of them insist on earning their money by demanding extensive reliability testing and they are immune to the argument that reliability testing is often performed at the expense of reliability. In as much as missiles, because of weight limitations, operate at stress levels high up in the finite life portion of the S-N fatigue diagram, the more reliability testing one does, the more one extracts from the remaining life of the rocket motor casing or other critically stressed components. I think the people in the solid propellant missile industry are fairly lucky because once you touch the match to the motor, it has gone off and you cannot do much about it. We who are in the liquid propellant missile business, however, are less fortunate because our engines can be turned on and off and operated time and again. Consequently, by the time a liquid propellant missile reaches the firing pad, it has already undergone a very large number of reliability tests. The propulsion system, the pneumatic system, the guidance system, and all other types of systems have been tested to a point where they probably have a very good chance of failing on the missile launch because we have extracted so much of the reliability from the structure. I would like to suggest to Mr. Corton that he could do the nation a real benefit by travelling around to the various industries and speaking to reliability people and urging them to cease some of this horrible reliability testing that I see going on. Also, if a pressure vessel is designed to operate at a certain pressure, proof testing it at a very much higher pressure not only does not assure that it will subsequently perform reliablity at the design pressure, but may have actually caused the extension of flaws such that it is now prone to fracture at lower pressures. I am gratified that Mr. Corton has pointed out the dangers inherent in proof testing pressure vessels at unreasonably high "over-pressures". This danger becomes progressively more severe

in the high strength, relatively brittle materials.

The strength and fatigue performance of pressure vessels made from soft, ductile and tough materials can actually be improved by over-pressure testing as a result of slight deformations which remove eccentricities and produce some cold working, but this cannot be extrapolated to the high strength, brittle materials being used for rocket motor cases.

B. M. Wundt Dr. Weiss' paper is a rational attempt to summarize concisely the current views on theories of fracture. In this he has succeeded well. I would like to add a few comments which may help to elucidate the problem. Pertaining to Neuber's particle sizeη it may he of interest that an English physicist, C. Gurney, had suggested in 1946 (ref. 1W) an interesting treatment for high stress concentration factors in sharp ended cracks. He assumed that cracks degenerate from notches which have an elliptic shape, In order to obtain an "effective" stress concentration, an "average stress" over a small area of dimension Δ at the end ofthe major axis, 2a, of the ellipse is computed. This "effective" stress concentration which is computed in terms of $\sqrt{(a/r)}$ is shown in Gurney's Fig. 2 as a function of the ratio Δ/r, where r is the radius of curvature at the end of the major axis. Gurney points out that in a particularly important case, when $r/\Delta = 1$, i.e. when the radius of curvature is equal to the particle size (atomic dim.), the "effective" stress concentration factor is only about half of the maximum stress concentration which otherwise occurs at the boundary of the elliptical hole. When the radius of curvature is made to approach zero and when the minor axis of the ellipse, 2b, vanishes, Gurney's formulae yield for the "effective" stress concentration factor for a sharp ended crack of length 2a, $1.8\sqrt{(a/\Delta)}$. For "particle size" $\Delta = 0.001$ in., 0.0025 in. or 0.010 in., the "effective" stress concentration factor is 57, 36 and 18 respectively; when the central crack length 2a = 2in.

In connection with the stress intensity coefficient, it should be noted that Dr. Irwin has pointed out (ref. W2 eq. 10) that it may be obtained as a limit of the following expression when the radius of curvature approaches zero:

$$K = \left(\frac{E\gamma}{\pi}\right)^{1/2} = \lim \; 1/2 \left[\sigma_{max} \sqrt{r}\right]$$

as $r \to 0$

but

$$\sigma_{max} = K_t \; \sigma_N$$

and

$$\chi = \frac{1}{2}\ \sigma_N \quad \text{Lim} \quad [\, K_t \sqrt{r}\,] \qquad \text{as } r \to 0$$

In order to obtain K_t for a given configuration it is necessary to know the theoretical stress concentration factor K_t as a function or radius of curvature r and plot the product $K_t \sqrt{r}$ as a function of r. Its value for r = 0 is obtained by extrapolation. The discussor has used this procedure with the help of Peterson's book.

Dr. Weiss points out that the Griffith-Irwin fracture mechanics breaks down as soon as the crack length becomes small. This is inherent in the formula, but for practical purposes the correct strength behavior may be easily approximated by the application of the known boundary conditions. This is shown clearly in Fig. 11 of the discussor's paper (39) and in reference W4.

Dr. Weiss mentioned the work which Prof. Neuber is doing under contract with WADD. The discussor doubts if the extension of the theory of stress concentration will help to solve the problems of notch-strength variation connected with the fracture appearance transition temperature. For instance, in Fig. 6 of ref. W3, the average notch-strength of large flat specimens of constant geometry, equipped with pre-existing cracks, is shown as a function of temperature. This figure indicates a most significant notch-strength behavior, at temperatures above 150 F the notch-strength is about 120,000 psi, but at temperatures below 125 F the notch-strength is only 60,000 psi. In the transition range between 125 F and 150 F there is a rapid change in notch-strength. The strength and ductility properties of smooth tension specimens from the same steel are shown in Fig. 4 of ref. W3. It is seen that the strength behavior in the temperature range between 125 and 150 F is not at all indicative of the change which occurs in the notch-strength behavior. The discussor cannot understand how Prof. Neuber's extension of the theory of stress concentrations, based on true stress-strain diagrams of smooth specimens, will be helpful in the analysis of behavior of cracked or very-sharp notched specimens near the temperature transition range. I also fail to see how Neuber's finite particle η, as discussed by Dr. Weiss, could be used to attack the above problem.*

---

* References for Wundt's Discussion:

W1 C. Gurney, The Effective Stress Concentration at the End of a Crack in Materials having Atomic Constitution, Ph. Mag. 7, 39 (1948) pp 71-76

W2 G. R. Irwin, J. A. Kies, H. L. Smith, Fracture Strength Relative to Onset and Arrest of Crack Propagation, Proceedings ASTM Vol. 58 (1958) pp 640-660

W3 E.T. Wessel, The Influence of Pre-Existing Sharp Cracks on Brittle Fracture of a Nickel-Molybdenum-Vanadium Forging Steel, Trans. Am. Soc. for Metals (1960) pp 277-306

W4 Discussion of W3 by B. M. Wundt, pp 300-302

I would like to suggest to Prof. Corten that if he would like to initiate a crack very easily, a nitrided case 5 mm thick at the apex of the notch will do it. Also, nitriding of the specimen surfaces will probably eliminate shear lips which interfere with crack propagation.

I would like to ask Dr. Rostoker if the surface adsorption theory which was studied for some time by Prof. Rebinder in the USSR, is the same phenomenon which he is describing?

W. Rostoker This surface energy concept in mechanical properties is similar to Prof. Rebinder's. The approaches to validating the concepts as presented here, however, are new.

V. Weiss With respect to Mr. Wundt's first comment pertaining to and C. Gurney's work, I would like to point out that Gurney's Δ is equivalent to Neuber's η for an elliptical hole, axes a and b and radius of curvature $r = \frac{a}{b^2}$ at $x = a$ the stress concentration factor is given by $K = 1 + 2\frac{a}{b}$ or for sharp cracks $2\frac{a}{b} = 2\sqrt{\frac{a}{r}}$. After assuming an average stress over a particle of size η Neuber finds for 0° notch angle, $K = 2\sqrt{\frac{a}{r+\frac{1}{2}\eta}}$ which yields for $r = \eta$, $K = \frac{2}{\sqrt{3}}\sqrt{\frac{a}{\eta}} = 1.15\sqrt{\frac{a}{\eta}}$ or $1.15\sqrt{\frac{a}{b}}$ and for $r = 0$, $K = \frac{2}{\sqrt{2}}\sqrt{\frac{a}{\eta}} = \sqrt{2}\sqrt{\frac{a}{\eta}}$ versus Gurney's $K = 1.1\frac{a}{b}$ and $1.8\sqrt{\frac{a}{\Delta}}$ for the same assumptions, respectively.

Mr. Wundt's second comment pertains to the relationship between the stress concentration and the stress intensity factor. It appears to me that there is no reason why for sharp notches, the limit of the above expression cannot be formed with the help of Neuber's η, i.e.

$$\mathcal{K} = \lim_{r \to 0} \frac{1}{2} [\sigma_{max}\sqrt{r}] = \frac{1}{2}\sigma_{max}\sqrt{2\eta} = \sigma_{max}\sqrt{\frac{\eta}{2}}$$

which is identical to equation (9) in ref. (W2).

On the other hand the stress intensity factor can also be expressed in terms of σ_N and the crack length, as shown below

$$\mathcal{K} = \frac{1}{2}\sigma_N \lim_{r \to 0} [K_t\sqrt{r}] =$$

$$\mathcal{K} = \frac{1}{2}\sigma_N \lim_{r \to 0} \left[2\sqrt{\frac{a}{r+2\eta}} \cdot \sqrt{r+2\eta}\right] = \sigma_N\sqrt{a}$$

With regard to the third question relating to fracture appearance transition temperature, it is obvious that all present macroscopic fracture concepts measure the consequences of the occurrence of such a transition rather than to predict it.

Only Cottrell's and Petch's work points towards the possiblity of predicting the ductility transition phenomenon on the basis of the yield point and the dislocation unpinning stress. Although critical experiments will have to decide the feasibility of such an approach, there is no reason why, with a knowledge of the stress-strain curves of smooth specimens, the ductility transition behavior for various notch configurations cannot be predicted. I completely agree with the last statement as I have repeatedly pointed out that η has nothing whatsoever to do with plasticity.

G. Sachs I would like to make a few additional remarks which I hope will help to clarify the divergencies in opinion. Neuber assembles in his book, the knowledge of the effects of stress raisers on the stress distribution under elastic conditions. In addition, he advances the hypothesis that a sharp crack does not exist, apparently based on some previous tests that the theory of elasticity predicts stresses which are too high for very high stress concentrations. The hypothesis leads to the result that a crack acts like a notch having a certain radius which depends on the metal involved. This explains, why a simple V-notch with a very small radius has the same effect as a crack, but the radius must be very small. In other words, the assumed elastic stress concentration must be very high to lead to a minimum notch strength. The shape of an "Eloxed" notch, as used by Irwin, does appear to me to possess too large a radius in this respect. Actual cracks, on the other hand, lead to the suspicion that their production introduces some changes in the material quite different from those resulting from a running crack in static loading.

Regarding a plasticity correction, the fact which must be explained numerically is the reduction of stress concentration caused by plastic flow. Hardrath, et al. at Langley Research Center have found that modifying the elastic value to include both plastic and elastic strains, yields a practically useful equation. We find that a similar approach also explains the fracture values or notch-strength of semi-brittle materials, as presented by Dr. Weiss. A similar approach has been used by Gerard at N.Y.U. The relations obtained appear considerably more realistic and lucid than those based on Orowan's and Irwin's modifications of Griffith's theory.

Regarding comparison of experimental data, it must be kept in mind (a) that the section size effect is not a subject of Griffith's theory, but that only the length of the notch appears in this theory and (b) that full understanding of the relation presupposes that the effects of other pertinent variables, in particular those of biaxiality and section size or stress gradient, on the ductility are known. Gross effects in metallurgy, unfortunately, are found generally to result from a combination of several basic effects. Although, some empirical relation may be applicable to a limited amount of test data no generalization is permissible and full success cannot be expected until each physical phenomenon involved is fully recognized and evaluated.

J. Sohn I would like to ask Dr. Rostoker to comment on the antithesis of the surface tension being lowered by a liquid wetting it, in other words, the cases where surface tension is raised by some liquids. An example would be the raising of fatigue strength by coating the surface with oil.

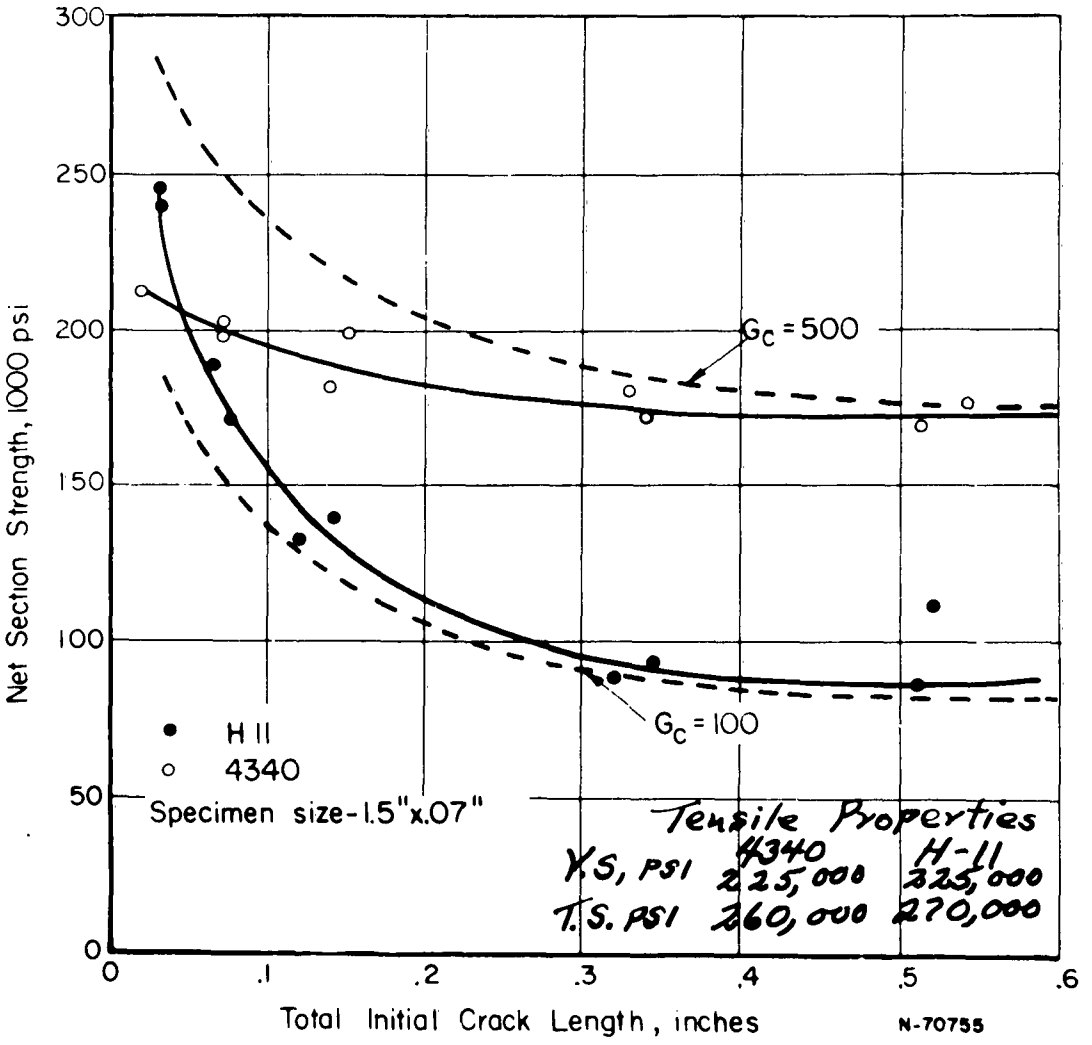
W. Rostoker The effect of raising fatigue strength by a liquid metal is rare. It is not, however, impossible to rationalize. Remember that all metals are clothed by their oxides. An interfacial energy system exists between the metal and its oxide which may be less than the interfacial energy between the metal and another liquid.

G. K. Manning Battelle made two series of center-cracked tests in which the only variable was the initial crack length. One series was made of 4340 steel, the other of H-11 steel. The specimens of each series were from the same sheet and the heat treatment was identical for all the specimens within a series. The initial cracks were produced by tension-tension fatigue of specimens containing a small center hole. The hole diameter never exceeded 50 percent of the intial crack length. The fatigue cracks were formed before heat treating in a controlled-atmosphere furnace.

The figure shows the net section strength versus the initial crack length (Irwin's $2a_o$). Note that the two solid lines representing the H-11 and 4340 data cross one another at a crack length of about 0.05 inch.

There are two points worth considering. First, it would appear that if one is evaluating steels on the basis of a long crack but expects only very short cracks to be present in a motor case, there is the possibility of being misled. On the basis of net section strength in the presence of, for example, a half-inch center crack, 4340 appears to be very much superior to H-11. However, on the basis of net section strength in the presence of a crack only one-thirty-second of an inch long, H-11 appears to be superior.

Second, the curves shown here provide an opportunity to experimentally test the mathematical model that Dr. Irwin referred to in his talk. In this respect, the results are discouraging because it is obvious that the effect of crack length cannot be accounted for by use of a single equation. The results suggest that if we are to rationalize the data, we not only need to use different G_c values but also a different equation form for each of these materials.



Net Section Strength vs Initial Crack Length
(4340 vs H-11)

F. R. Larson I would like to make a few comments about fracture surface appearance. In running tests on cylindrical specimens and studying different strength levels and heat treatments in 4340 steel over a range of testing temperatures, it becomes quite apparent that there are many features in the surface appearance of the broken bars which may give information to the quite interesting search for the mechanism of how the fracture actually occurs. Fig. 1 illustrates some of these features. Aside from the cleavage cracking phenomenon on which quite a bit has been said, one could say that there are three different fracture zones. The origin, which is obviously a conical shaped area with an inclusion on top of it is enclosed by an area which could be described as being made up of circumferential ridges. As you move out from the center of the bar, you find a transition zone and these circumferential ridges disappear and a set of radial markings appear. The radial nature of these markings depend a great deal on the location of the center of the origin. If the center of the origin is slightly off-center, you get an unbalance in the stresses associated with the propagation of these radial markings and they tend to have a curved nature much as you would see in the so called herring-bone fracture, as it propagates along a sheet. Finally, we find the shear-lip on the edge of the specimen. There are certain characteristics that change with changing testing temperatures. First, as we decrease the testing temperature, we go from the case of circumferential markings (which can engross the whole center section except for the shear-lip) to the appearance of the radial markings and then the shear-lip decreases markedly and seems to be associated somewhat with the size or the height of the radial markings. As we further lower the testing temperatures, the circumferential markings continue to decrease until they disappear. The only thing that remains at the fracture origin then is an inclusion. The inclusion is the origin of fracture in both cases, but the propagation from the inclusion is quite different in each case. The conical nature of the origin in the circumferentially marked area refutes any kind of splitting or radial stresses which might arise from necking, causing a longitudinal split. However, it was reported by Marshall and Shaw that it was a shear stress in the shear plane that initiate the fracture down the side of a cone from the inclusion origin. The primary emphasis they made was that the shear stress was modified by the normal stress on the shear plane. I would like to suggest that the normal stress had much greater influence than they proposed. Finally, as we move into the radial areas, we find considerable longitudinal splitting. This is probably due to the high tangential stress in the small plastic zone associated with the rapidly moving crack in this general area. I would like to suggest that if people want to have a very interesting piece of detective work, they can spend many hours in studying fracture surfaces.

PREPARED DISCUSSION - FOURTH SESSION

The Effect of Small Surface Cracks on Strength

prepared by
J. E. Srawley and C. D. Beachen*

Tensile crack propagation tests of sheet materials are usually conducted on specimens with sharp notches or slots which are quite large in comparison with the sheet thickness. We feel that there is a need for experimental data on the effect of the size of small cracks which do not penetrate through the thickness of the sheet. We have been able to introduce such cracks into specimens by controlled hydrogen embrittlement cracking, and believe that the results obtained so far with these specimens will be of some interest to those at this Conference.

Specimens 1 in wide were obtained from a sheet of X200 steel, about 0.07 in thick, and were air hardened and tempered at 700 F to have a yield strength of 228 ksi and an ultimate tensile strength of 274 ksi at room temperature. These were provided with central, transverse cracks of semi-elliptical shape, the smallest being about 0.01 in deep and 0.05 in long. After cracking, the specimens were baked to remove hydrogen and tested in tension.

Results for three testing temperatures are shown in Figure 1, in terms of the crack strength ratio (nominal net fracture stress divided by ultimate tensile strength) versus relative crack size (area of the original crack divided by specimen thickness). The points at the right which are circled refer to specimens with crack-ended central slots which were tested for comparison. At room temperature the effect of the smallest cracks is very slight, but the strength decreases very rapidly as the relative crack size increases in the range 0.01 to 0.05 inches. For example, a crack of relative area 0.037, which was about 0.11 in long and 0.03 in deep, reduced the strength to less than the yield strength. The results in general suggest that there is a lower limit to the size of crack which will have an appreciable influence on strength, and that this limit decreases markedly with temperature. Beyond the borderline crack size, the decrease in strength as the crack size increases is very pronounced. The strength is decreased further by a decrease in temperature (or the material becomes more brittle).

* Metallurgy Division, U. S. Naval Research Laboratory, Washington 25, D. C.

Some further tests were conducted at room temperature to investigate a possible effect of environment on the results. The cracks in some specimens were filled with water or with india ink during testing, while other specimens were first dehydrated in a vacuum dessicator and subsequently protected during testing by adhesive patches enclosing particles of a dessicant. The results are shown in Fig. 2 (which is on a much larger scale than Fig. 1). Thetriangular points, representing water or india ink, do appear to be significantly lower, on average, than the others, though the effect is only of the same order as the general scatter of results. These tests were each completed in a few minutes, and it is quite possible that larger effects would be observed in more prolonged tests. It is also very likely that the sensitivity to environment varies with material and condition. The material used here was fairly tough at room temperature (K_C about ksi · inches $^{1/2}$ full shear fracture), and a more brittle material might be considerably more sensitive.

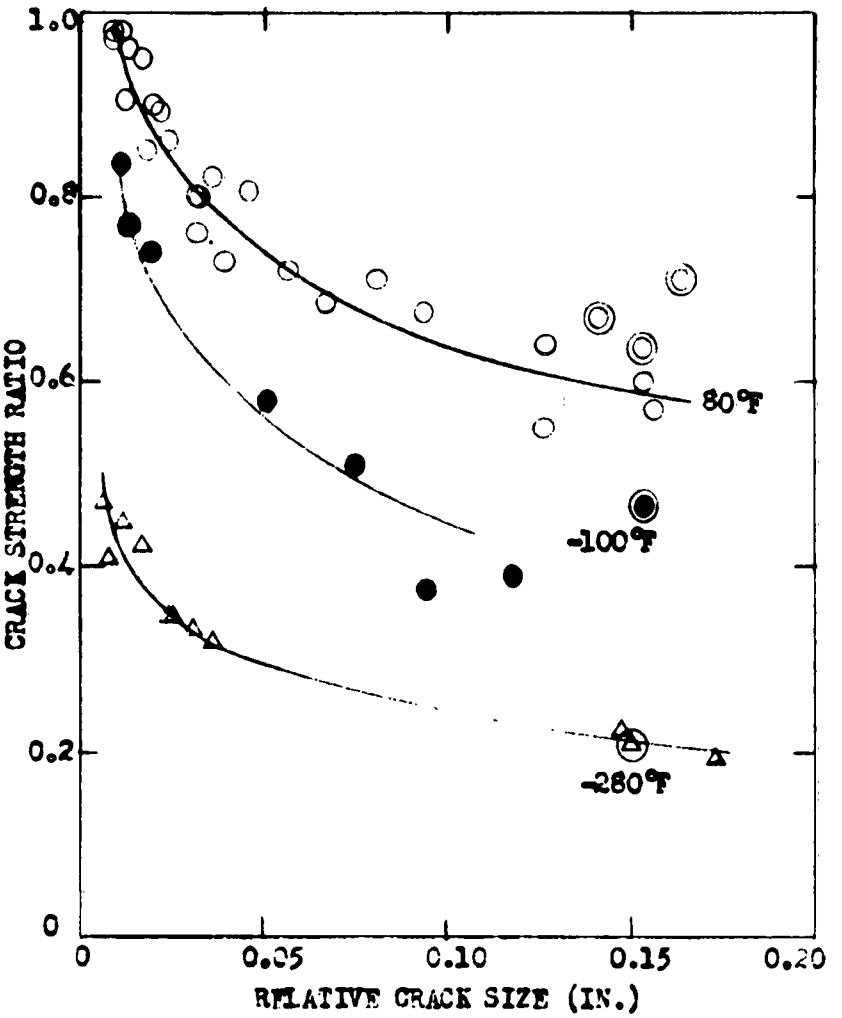


Figure 1. Effect of Crack Size on Crack Strength Ratio (Nominal Net Fracture Stress/Ultimate Tensile Strength) at Three Temperatures

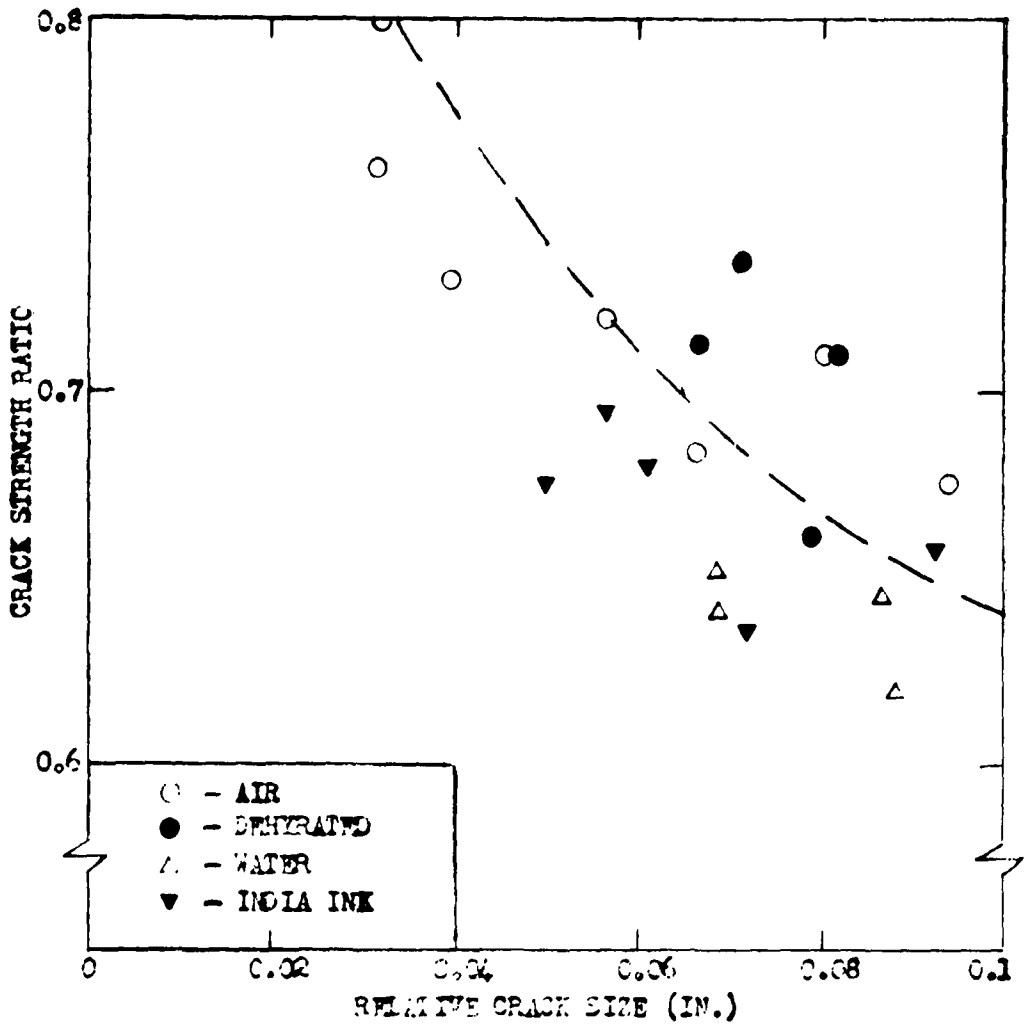


Figure 2. Effect of Environment on Crack Strength Ratio at 80°F

PREPARED DISCUSSION - FOURTH SESSION

Discussion of Paper

"Plastic Zone Near a Crack and Fracture Toughness"

by
G. Irwin

prepared by
George Sachs, Syracuse University

The merit of Dr. Irwin's work is undisputed. However, I would like to take strong exception to the philosophy which he expressed. If we do not know how to drive an automobile we may be forced to use a wheelchair. However, if we start to equip the wheelchair with powerbrakes and powersteering we might as well learn to drive an automobile.

My background is to a considerable extent in Applied Mechanics. For me, stress concentration effects, as defined by the theory of elasticity and calculated by Neuber, are more readily understandable than Dr. Irwin's calculations. I have discussed this problem with a number of scientists and have frequently been asked to act as council for defending the stress concentration approach. Griffith's theory is a thermodynamical approach and circumvents stress distributions. According to my way of thinking, its combination with stress distribution calculations is not permissible and does not lead to clearly definable conclusions.

Griffith's theory is expressed by the equation $\sigma = A/\sqrt{c}$, where σ is the gross stress and A a compound material constant identical to the gross stress for c = 1 where c is the crack length. It postulates, for a brittle metal, that instability occurs for a given combination of σ and c. It also postulates the pre-existence of an extremely sharp crack. The constant A, according to Griffith's initial concept which involves surface tension, is very small, perhaps .01 or .001 of actually observed values. To explain these, Orowan increased the constant A to include a plasticity energy term. This equation still remains the basic single-parameter equation, and $\mathcal{G}_c$ is only another form of the constant. Further leading refinements by Irwin to a two-parameter equation to account for plasticity make use of arbitrary and non-permissible calculations. These lead to a maximum strength, for infinitely small cracks, at a value $\sqrt{2}$ times the yield strength. There is a very peculiar assumption hidden in such an approach. Finally, a correction for finite specimen size is introduced from Westergaard's calculations. Although, this procedure appears valid, the correction for practical conditions turns out to be only a few percent and can be usually neglected. Therefore, there is no need for the use of the resulting complicated equations. Furthermore, the final result is very similar to that derived from the Neuber's concept of

finite stress concentrations, which is much simpler, and this has been discussed in detail by Dr. Weiss.

Griffith's theory is also not applicable to the effect of section size, as recognized early in this game, nor does it lead to any conclusions relating to such phenomena as a fast rate of crack propagation, critical crack length and so forth. A plausible theory for a distinction between slow and fast rate of crack propagation does not exist. If the claim is made that these phenomena can be explained on the basis of a modified Griffith's theory, this becomes a matter of religion, rather than of science: you either believe it or you do not believe it.

PREPARED DISCUSSION - FOURTH SESSION

Discussion of Paper

"Embrittlement by Liquid Metals"

by
W. Rostoker

prepared by
J. M. McCaughey, Frankford Arsenal

Dr. Rostoker has presented some studies undertaken on the embrittlement of certain solid metals by liquid metals. His paper has been primarily centered on brass, copper and steel and he has shown conclusively that liquid metal fracture is definitely "brittle" in nature. Several relationships also have been determined for the embrittlement of aluminum alloys by liquid metals, and I believe, they would be of interest to this group.

First, it has been suggested that a demonstration of liquid metal embrittlement would be appropriate at this time.

This first specimen is an alclad strip of 2-24-T3 aluminum alloy and as you know, it may be easily bent without experiencing any cracking or failure. However, if a similar specimen has a small amount of amalgam placed on it prior to bending, fracture will take place immediately. No permanent deformation has taken place prior to failure, indicating the stress required was lower than the yield stress. The amalgam used is primarily mercury but with some additives to make it pasty for ease in handling, and also to enhance the embrittlement phenomenon.

One additional demonstration can be made to show this effect. An 1/8 inch thick 2024-T3 plate has an indentation in the center to give large residual stresses. If some amalgam is now applied to this area, fracture will take place without the necessity of the application of an external stress.

Several relationships have been determined for liquid metal embrittlement of 2024-T3 aluminum alloy and these are shown in the following figures.

Figure 1 shows the role of intrinsic strength on the embrittling capability of a liquid metal. This plot is essentially for dry fracture strength versus wet fracture strength (fracture strength when wet by a liquid metal), and it indicates that for alloys with an ultimate tensile strength greater than 60,000 psi, the wet strength is less than the dry strength. The alloys with this high strength are 2024-T4, 7075-T6, and

7001-T6 and the stress required for fracture (wet) for these alloys is actually much lower than the normal yield stress. The other alloys are also embrittled but the stress required is above the yield stress.

Figure 2 shows the quantity of liquid metal required for cracking. This is for a specimen 1/2 inch thick by 3 inch wide stressed to 10 percent of its ultimate tensile strength and then wetted by the liquid metal. This figure indicates that 4 grains of the amalgam are required for complete fracturing of the test specimen. Smaller amounts also produce cracking but incomplete failure of the specimen.

Figure 3 gives an indication of the role of stress on the embrittlement phenomenon. The lower radiograph shows a typical crack when wet by mercury while stressed to 10 percent of the ultimate strength. There is usually one long crack at right angles to the stress direction, and then extensive branching at the ends of the crack. As the stress level is increased prior to crack initiation, the single crack decreases in length and the branching increases. It is believed the reason for this is that with the higher stresses, there are more components above the threshold value for crack initiation.

Figure 4 is a plot showing the effect of temperature on mercury embrittlement of an aluminum alloy. If one strain rate is followed, it will be seen that greater ductility is achieved prior to fracture, indicating a reduction in the embrittling propensity with increasing temperatures. This figure shows also the relationship for strain rate. As the strain rate is increased, the ductility decreases, thus indicating that liquid metal embrittlement is enhanced with increasing strain rates.

Figure 5 shows a similar delayed failure curve for aluminum alloys as Dr. Rostoker has presented for SAE 4130 steel. At a high stress level, failure is immediate, but at lower levels, a finite time is required for failure. There also exists a threshold stress below which failure will not take place. An interesting feature of this relationship is that if the stress and liquid metal are removed prior to fracture, no harmful effects remain on the specimen. That is, if it were now tested, the tensile strength would be the same as for a conventional specimen.

Figures 6 and 7 are radiographs of cracks in 2024-T4 aluminum alloy specimens when stressed and wetted with mercury. The first is for uniaxial tension and in this case the crack has extended for approximately 12 inches. The second is for biaxial tension and again the crack has extended for a long distance.

Thus, it is evident that liquid metal embrittlement is not restricted to only one solid metal-liquid metal combination. The possibility exists that any stressed metal may be made to fracture in a brittle fashion if wetted by the appropriate liquid metal.

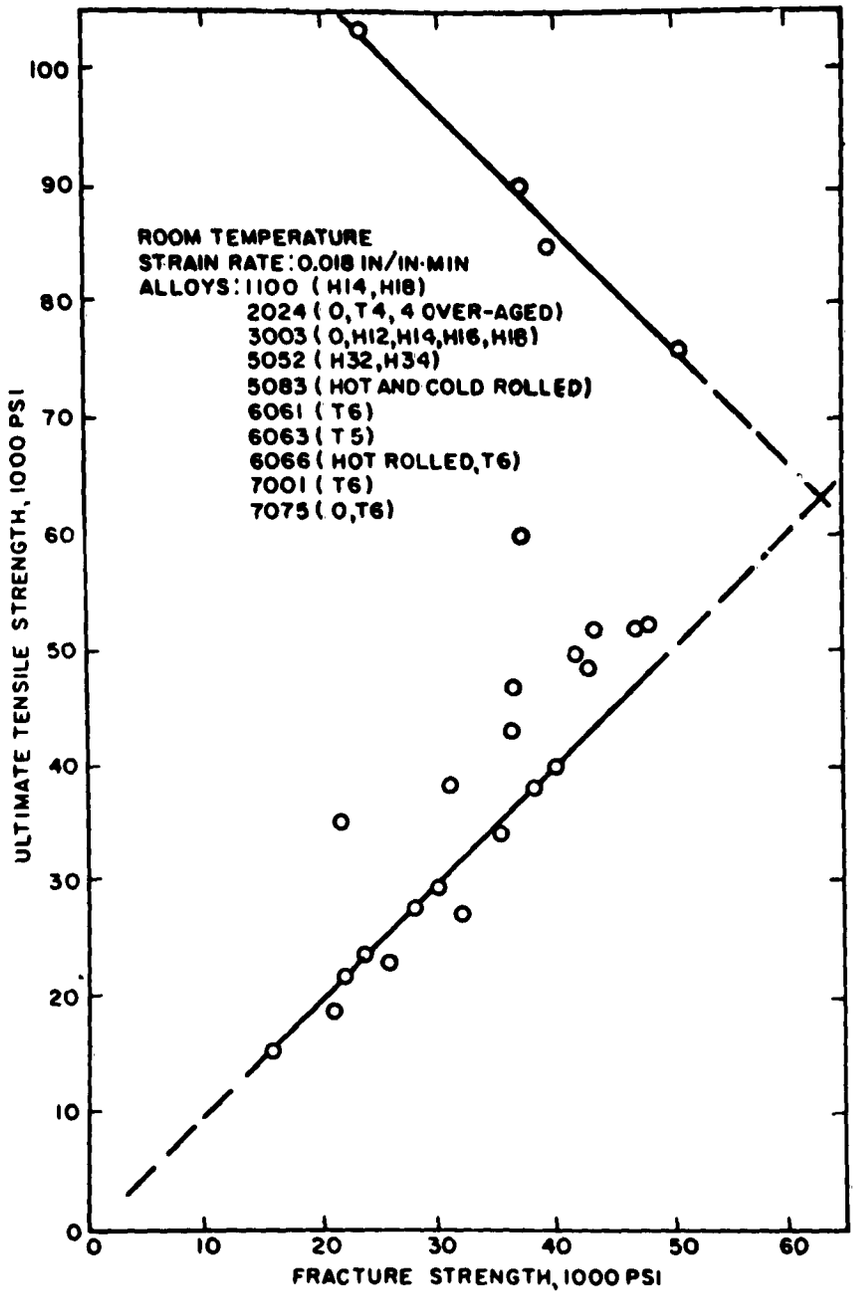


Figure 1. Relationship Between Normal Tensile Strength of Commercial Aluminum Alloys and Their Fracture Strength When Wetted with a Mercury Amalgam

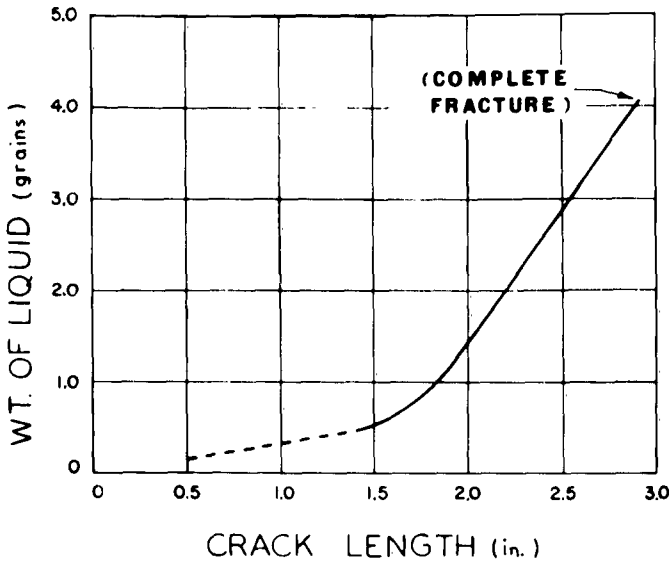
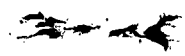


Figure 2. Crack Length as a Function of Amount of Liquid Amalgam Used



80 percent U.T.S.



DIRECTION OF STRESS

40 percent U.T.S.



10 percent U.T.S.

Figure 3. Crack Pattern in Aluminum Alloy Plate (2024-T3) as a Function of the Applied Stress

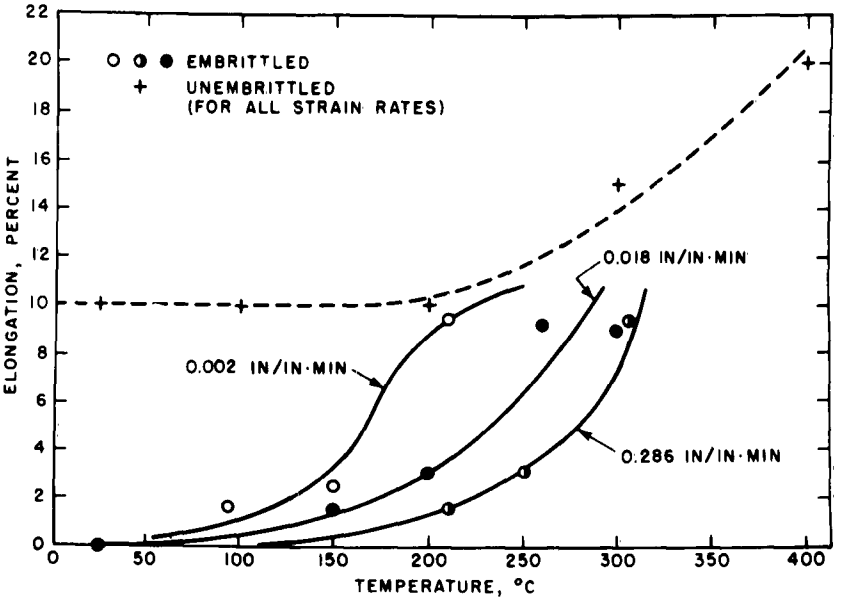


Figure 4. Correlation of Temperature and Strain Rate with Ductility of 2024-T4 Aluminum Alloy Wetted with a Liquid Amalgam

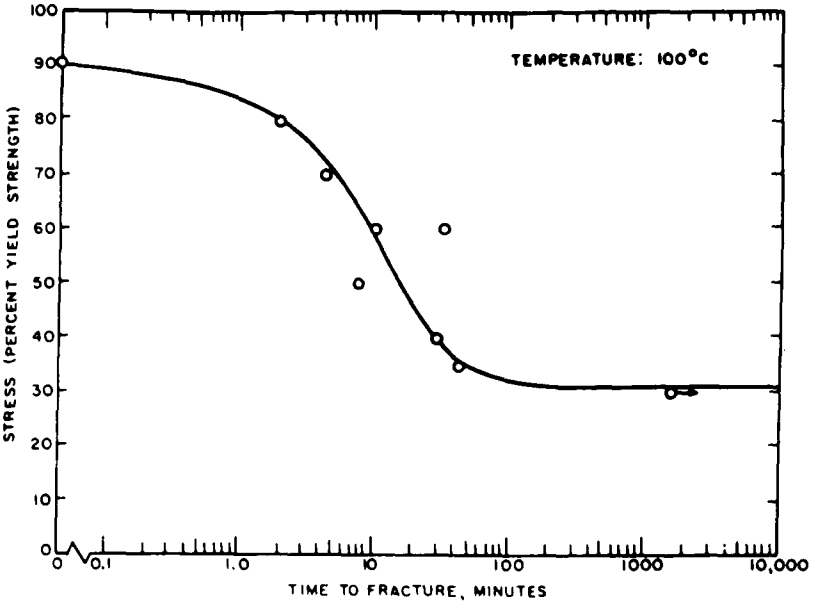


Figure 5. Time to Failure for a 2024-T4 Aluminum Alloy Wetted with an Amalgam as a Function of Statically Applied Stress

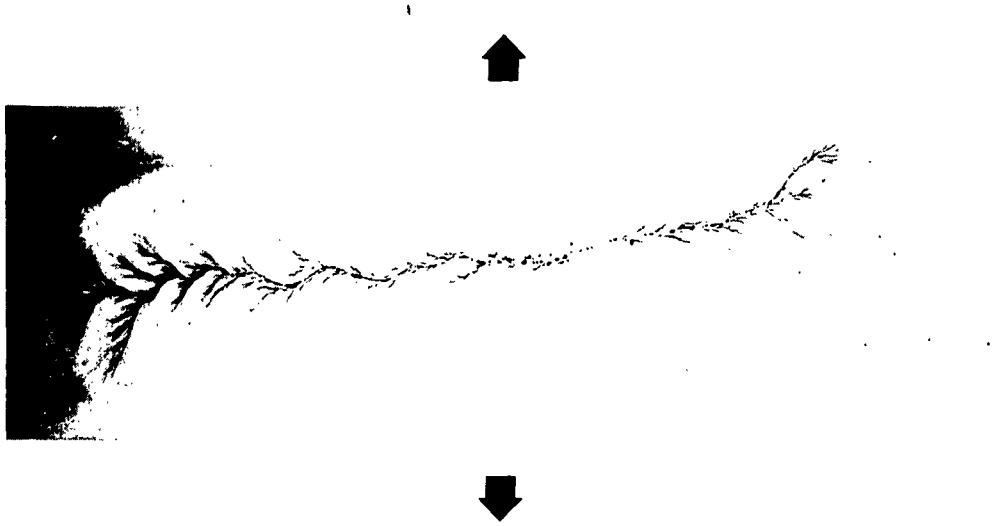


Figure 6. Radiograph of Crack in Aluminum Specimen Stressed Uniaxially and Wetted with Mercury. (Crack Approx. 12 inches Long)

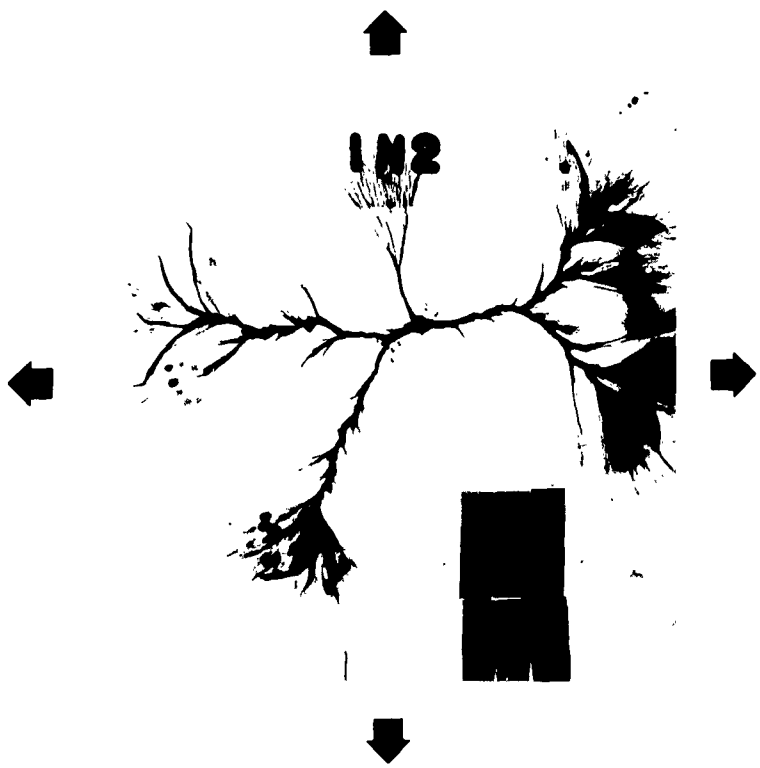


Figure 7. Radiograph of Crack in Aluminum Specimen Stressed Biaxially and Wetted with Mercury.

A. Hurlich I would like to suggest to Mr. Srawley that he apply his technique of surface cracking test specimens to pin down the problem of decarburization. I venture to predict that a decarburized surface will permit a much larger flaw to exist before we have a measurable decrease of the fracture strength of the material. I think this might be a good experimental technique to nail this point down. In respect to Mr. Corten's talk, I would like to make a comment because I think that his statement was extremely pertinent to a development that has been occurring over the last two years. In the aerospace industry and in the Air Force it has become very popular to bandy about the word "reliability". I think this word is a semantically unclear one, though a very glamorous one, and as a consequence we have seen the growth of large reliability groups now in the missile companies. In fact, in some companies there are more people in the reliability group that are evaluating the reliability of the missile than there are people designing the missile. Fortunately, a lot of these reliability people do nothing more innocuous than collect statistics from service failures. Unfortunately, however, a large number of them insist on earning their money by demanding extensive reliability testing and they are immune to the argument that reliability testing is often performed at the expense of reliability. In as much as missiles, because of weight limitations, operate at stress levels high up in the finite life portion of the S-N fatigue diagram, the more reliability testing one does, the more one extracts from the remaining life of the rocket motor casing or other critically stressed components. I think the people in the solid propellant missile industry are fairly lucky because once you touch the match to the motor, it has gone off and you cannot do much about it. We who are in the liquid propellant missile business, however, are less fortunate because our engines can be turned on and off and operated time and again. Consequently, by the time a liquid propellant missile reaches the firing pad, it has already undergone a very large number of reliability tests. The propulsion system, the pneumatic system, the guidance system, and all other types of systems have been tested to a point where they probably have a very good chance of failing on the missile launch because we have extracted so much of the reliability from the structure. I would like to suggest to Mr. Corton that he could do the nation a real benefit by travelling around to the various industries and speaking to reliability people and urging them to cease some of this horrible reliability testing that I see going on. Also, if a pressure vessel is designed to operate at a certain pressure, proof testing it at a very much higher pressure not only does not assure that it will subsequently perform reliablity at the design pressure, but may have actually caused the extension of flaws such that it is now prone to fracture at lower pressures. I am gratified that Mr. Corton has pointed out the dangers inherent in proof testing pressure vessels at unreasonably high "over-pressures". This danger becomes progressively more severe

in the high strength, relatively brittle materials.

The strength and fatigue performance of pressure vessels made from soft, ductile and tough materials can actually be improved by over-pressure testing as a result of slight deformations which remove eccentricities and produce some cold working, but this cannot be extrapolated to the high strength, brittle materials being used for rocket motor cases.

B. M. Wundt Dr. Weiss' paper is a rational attempt to summarize concisely the current views on theories of fracture. In this he has succeeded well. I would like to add a few comments which may help to elucidate the problem. Pertaining to Neuber's particle sizeη it may be of interest that an English physicist, C. Gurney, had suggested in 1946 (ref. 1W) an interesting treatment for high stress concentration factors in sharp ended cracks. He assumed that cracks degenerate from notches which have an elliptic shape, In order to obtain an "effective" stress concentration, an "average stress" over a small area of dimension Δ at the end ofthe major axis, 2a, of the ellipse is computed. This "effective" stress concentration which is computed in terms of $\sqrt{(a/r)}$ is shown in Gurney's Fig. 2 as a function of the ratio Δ/r, where r is the radius of curvature at the end of the major axis. Gurney points out that in a particularly important case, when $r/\Delta = 1$, i.e. when the radius of curvature is equal to the particle size (atomic dim.), the "effective" stress concentration factor is only about half of the maximum stress concentration which otherwise occurs at the boundary of the elliptical hole. When the radius of curvature is made to approach zero and when the minor axis of the ellipse, 2b, vanishes, Gurney's formulae yield for the "effective" stress concentration factor for a sharp ended crack of length 2a, $1.8\sqrt{(a/\Delta)}$. For "particle size" $\Delta = 0.001$ in., 0.0025 in. or 0.010 in., the "effective" stress concentration factor is 57, 36 and 18 respectively; when the central crack length 2a = 2in.

In connection with the stress intensity coefficient, it should be noted that Dr. Irwin has pointed out (ref. W2 eq. 10) that it may be obtained as a limit of the following expression when the radius of curvature approaches zero:

$$K = \left(\frac{E\gamma}{\pi}\right)^{1/2} = \lim \; 1/2 \; [\sigma_{max} \sqrt{r}\,]$$

as $r \to o$

but

$$\sigma_{max} = K_t \; \sigma_N$$

and

$$\chi = \frac{1}{2} \sigma_N \quad \text{Lim} \quad [K_t \sqrt{r}] \qquad \text{as } r \to 0$$

In order to obtain K_t for a given configuration it is necessary to know the theoretical stress concentration factor K_t as a function or radius of curvature r and plot the product $K_t \sqrt{r}$ as a function of r. Its value for r = 0 is obtained by extrapolation. The discussor has used this procedure with the help of Peterson's book.

Dr. Weiss points out that the Griffith-Irwin fracture mechanics breaks down as soon as the crack length becomes small. This is inherent in the formula, but for practical purposes the correct strength behavior may be easily approximated by the application of the known boundary conditions. This is shown clearly in Fig. 11 of the discussor's paper (39) and in reference W4.

Dr. Weiss mentioned the work which Prof. Neuber is doing under contract with WADD. The discussor doubts if the extension of the theory of stress concentration will help to solve the problems of notch-strength variation connected with the fracture appearance transition temperature. For instance, in Fig. 6 of ref. W3, the average notch-strength of large flat specimens of constant geometry, equipped with pre-existing cracks, is shown as a function of temperature. This figure indicates a most significant notch-strength behavior, at temperatures above 150 F the notch-strength is about 120,000 psi, but at temperatures below 125 F the notch-strength is only 60,000 psi. In the transition range between 125 F and 150 F there is a rapid change in notch-strength. The strength and ductility properties of smooth tension specimens from the same steel are shown in Fig. 4 of ref. W3. It is seen that the strength behavior in the temperature range between 125 and 150 F is not at all indicative of the change which occurs in the notch-strength behavior. The discussor cannot understand how Prof. Neuber's extension of the theory of stress concentrations, based on true stress-strain diagrams of smooth specimens, will be helpful in the analysis of behavior of cracked or very-sharp notched specimens near the temperature transition range. I also fail to see how Neuber's finite particle η, as discussed by Dr. Weiss, could be used to attack the above problem.*

---

* References for Wundt's Discussion:

W1 C. Gurney, The Effective Stress Concentration at the End of a Crack in Materials having Atomic Constitution, Ph. Mag. 7, 39 (1948) pp 71-76

W2 G. R. Irwin, J. A. Kies, H. L. Smith, Fracture Strength Relative to Onset and Arrest of Crack Propagation, Proceedings ASTM Vol. 58 (1958) pp 640-660

W3 E.T. Wessel, The Influence of Pre-Existing Sharp Cracks on Brittle Fracture of a Nickel-Molybdenum-Vanadium Forging Steel, Trans. Am. Soc. for Metals (1960) pp 277-306

W4 Discussion of W3 by B. M. Wundt, pp 300-302

I would like to suggest to Prof. Corten that if he would like to initiate a crack very easily, a nitrided case 5 mm thick at the apex of the notch will do it. Also, nitriding of the specimen surfaces will probably eliminate shear lips which interfere with crack propagation.

I would like to ask Dr. Rostoker if the surface adsorption theory which was studied for some time by Prof. Rebinder in the USSR, is the same phenomenon which he is describing?

W. Rostoker This surface energy concept in mechanical properties is similar to Prof. Rebinder's. The approaches to validating the concepts as presented here, however, are new.

V. Weiss With respect to Mr. Wundt's first comment pertaining to and C. Gurney's work, I would like to point out that Gurney's Δ is equivalent to Neuber's η for an elliptical hole, axes a and b and radius of curvature $r = \frac{a}{b^2}$ at $x = a$ the stress concentration factor is given by $K = 1 + 2\frac{a}{b}$ or for sharp cracks $2\frac{a}{b} = 2\sqrt{\frac{a}{r}}$. After assuming an average stress over a particle of size η Neuber finds for 0° notch angle, $K = 2\sqrt{\frac{a}{r+2\eta}}$ which yields for $r = \eta$, $K = \frac{2}{\sqrt{3}}\sqrt{\frac{a}{r}} = 1.15\sqrt{\frac{a}{r}}$ or $1.15\sqrt{\frac{a}{b}}$ and for $r = 0$, $K = \sqrt{2}\sqrt{\frac{a}{\eta}} = \sqrt{2}\sqrt{\frac{a}{\eta}}$ versus Gurney's $K = 1.1\frac{a}{b}$ and $1.8\sqrt{\frac{a}{\Delta}}$ for the same assumptions, respectively.

Mr. Wundt's second comment pertains to the relationship between the stress concentration and the stress intensity factor. It appears to me that there is no reason why for sharp notches, the limit of the above expression cannot be formed with the help of Neuber's η, i.e.

$$\mathcal{K} = \lim_{r \to 0} \frac{1}{2} [\sigma_{max}\sqrt{r}] = \frac{1}{2}\sigma_{max}\sqrt{2\eta} = \sigma_{max}\sqrt{\frac{\eta}{2}}$$

which is identical to equation (9) in ref. (W2).

On the other hand the stress intensity factor can also be expressed in terms of σ_N and the crack length, as shown below

$$\mathcal{K} = \frac{1}{2}\sigma_N \lim_{r \to 0} [K_t\sqrt{r}] =$$

$$\mathcal{K} = \frac{1}{2}\sigma_N \lim_{r \to 0} \left[2\sqrt{\frac{a}{r+2\eta}} \cdot \sqrt{r+2\eta}\right] = \sigma_N\sqrt{a}$$

With regard to the third question relating to fracture appearance transition temperature, it is obvious that all present macroscopic fracture concepts measure the consequences of the occurrence of such a transition rather than to predict it.

Only Cottrell's and Petch's work points towards the possiblity of predicting the ductility transition phenomenon on the basis of the yield point and the dislocation unpinning stress. Although critical experiments will have to decide the feasibility of such an approach, there is no reason why, with a knowledge of the stress-strain curves of smooth specimens, the ductility transition behavior for various notch configurations cannot be predicted. I completely agree with the last statement as I have repeatedly pointed out that η has nothing whatsoever to do with plasticity.

G. Sachs I would like to make a few additional remarks which I hope will help to clarify the divergencies in opinion. Neuber assembles in his book, the knowledge of the effects of stress raisers on the stress distribution under elastic conditions. In addition, he advances the hypothesis that a sharp crack does not exist, apparently based on some previous tests that the theory of elasticity predicts stresses which are too high for very high stress concentrations. The hypothesis leads to the result that a crack acts like a notch having a certain radius which depends on the metal involved. This explains, why a simple V-notch with a very small radius has the same effect as a crack, but the radius must be very small. In other words, the assumed elastic stress concentration must be very high to lead to a minimum notch strength. The shape of an "Eloxed" notch, as used by Irwin, does appear to me to possess too large a radius in this respect. Actual cracks, on the other hand, lead to the suspicion that their production introduces some changes in the material quite different from those resulting from a running crack in static loading.

Regarding a plasticity correction, the fact which must be explained numerically is the reduction of stress concentration caused by plastic flow. Hardrath, et al. at Langley Research Center have found that modifying the elastic value to include both plastic and elastic strains, yields a practically useful equation. We find that a similar approach also explains the fracture values or notch-strength of semi-brittle materials, as presented by Dr. Weiss. A similar approach has been used by Gerard at N. Y. U. The relations obtained appear considerably more realistic and lucid than those based on Orowan's and Irwin's modifications of Griffith's theory.

Regarding comparison of experimental data, it must be kept in mind (a) that the section size effect is not a subject of Griffith's theory, but that only the length of the notch appears in this theory and (b) that full understanding of the relation presupposes that the effects of other pertinent variables, in particular those of biaxiality and section size or stress gradient, on the ductility are known. Gross effects in metallurgy, unfortunately, are found generally to result from a combination of several basic effects. Although, some empirical relation may be applicable to a limited amount of test data no generalization is permissible and full success cannot be expected until each physical phenomenon involved is fully recognized and evaluated.

J. Sohn I would like to ask Dr. Rostoker to comment on the antithesis of the surface tension being lowered by a liquid wetting it, in other words, the cases where surface tension is raised by some liquids. An example would be the raising of fatigue strength by coating the surface with oil.

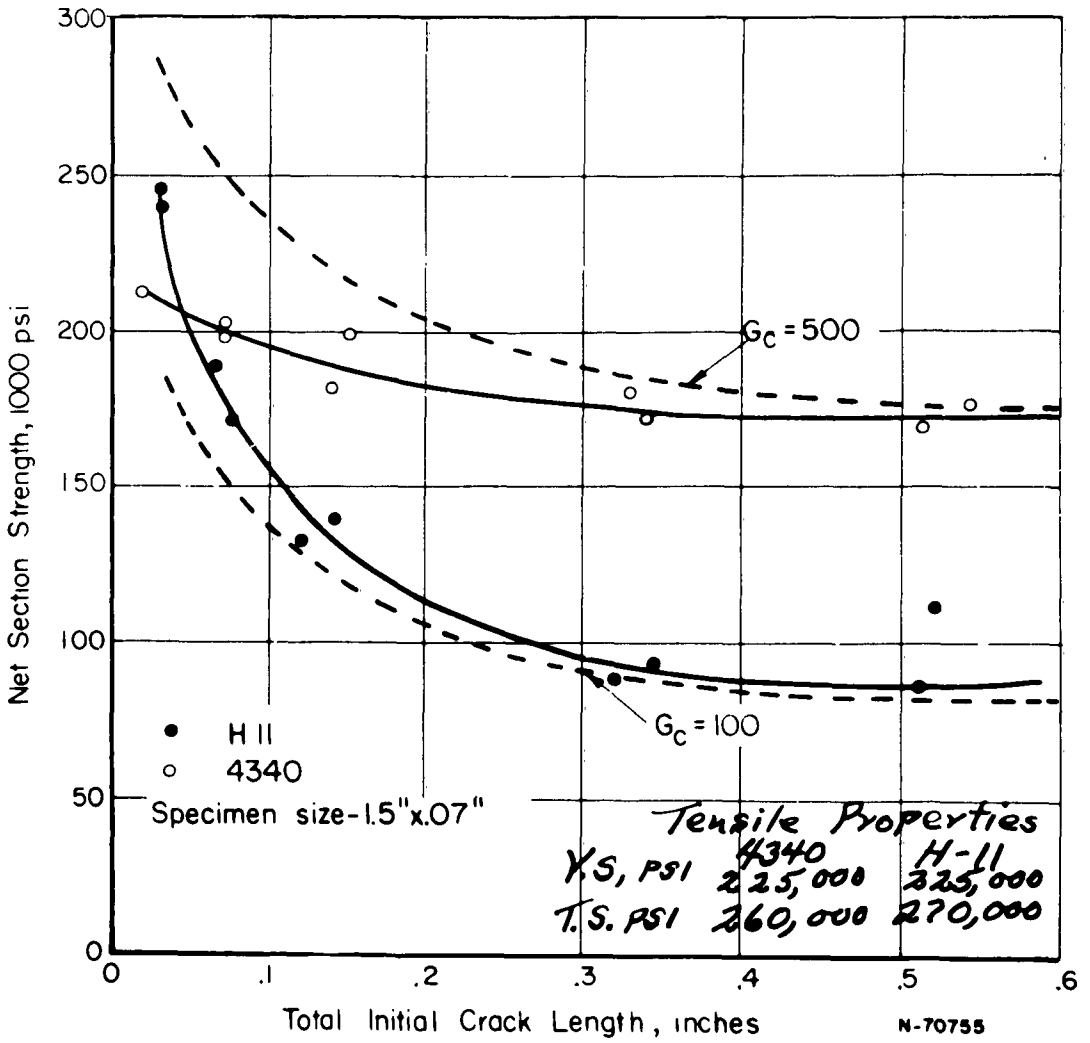
W. Rostoker The effect of raising fatigue strength by a liquid metal is rare. It is not, however, impossible to rationalize. Remember that all metals are clothed by their oxides. An interfacial energy system exists between the metal and its oxide which may be less than the interfacial energy between the metal and another liquid.

G. K. Manning Battelle made two series of center-cracked tests in which the only variable was the initial crack length. One series was made of 4340 steel, the other of H-11 steel. The specimens of each series were from the same sheet and the heat treatment was identical for all the specimens within a series. The initial cracks were produced by tension-tension fatigue of specimens containing a small center hole. The hole diameter never exceeded 50 percent of the intial crack length. The fatigue cracks were formed before heat treating in a controlled-atmosphere furnace.

The figure shows the net section strength versus the initial crack length (Irwin's $2a_o$). Note that the two solid lines representing the H-11 and 4340 data cross one another at a crack length of about 0.05 inch.

There are two points worth considering. First, it would appear that if one is evaluating steels on the basis of a long crack but expects only very short cracks to be present in a motor case, there is the possibility of being misled. On the basis of net section strength in the presence of, for example, a half-inch center crack, 4340 appears to be very much superior to H-11. However, on the basis of net section strength in the presence of a crack only one-thirty-second of an inch long, H-11 appears to be superior.

Second, the curves shown here provide an opportunity to experimentally test the mathematical model that Dr. Irwin referred to in his talk. In this respect, the results are discouraging because it is obvious that the effect of crack length cannot be accounted for by use of a single equation. The results suggest that if we are to rationalize the data, we not only need to use different G_c values but also a different equation form for each of these materials.



Net Section Strength vs Initial Crack Length (4340 vs H-11)

F. R. Larson I would like to make a few comments about fracture surface appearance. In running tests on cylindrical specimens and studying different strength levels and heat treatments in 4340 steel over a range of testing temperatures, it becomes quite apparent that there are many features in the surface appearance of the broken bars which may give information to the quite interesting search for the mechanism of how the fracture actually occurs. Fig. 1 illustrates some of these features. Aside from the cleavage cracking phenomenon on which quite a bit has been said, one could say that there are three different fracture zones. The origin, which is obviously a conical shaped area with an inclusion on top of it is enclosed by an area which could be described as being made up of circumferential ridges. As you move out from the center of the bar, you find a transition zone and these circumferential ridges disappear and a set of radial markings appear. The radial nature of these markings depend a great deal on the location of the center of the origin. If the center of the origin is slightly off-center, you get an unbalance in the stresses associated with the propagation of these radial markings and they tend to have a curved nature much as you would see in the so called herring-bone fracture, as it propagates along a sheet. Finally, we find the shear-lip on the edge of the specimen. There are certain characteristics that change with changing testing temperatures. First, as we decrease the testing temperature, we go from the case of circumferential markings (which can engross the whole center section except for the shear-lip) to the appearance of the radial markings and then the shear-lip decreases markedly and seems to be associated somewhat with the size or the height of the radial markings. As we further lower the testing temperatures, the circumferential markings continue to decrease until they disappear. The only thing that remains at the fracture origin then is an inclusion. The inclusion is the origin of fracture in both cases, but the propagation from the inclusion is quite different in each case. The conical nature of the origin in the circumferentially marked area refutes any kind of splitting or radial stresses which might arise from necking, causing a longitudinal split. However, it was reported by Marshall and Shaw that it was a shear stress in the shear plane that initiate the fracture down the side of a cone from the inclusion origin. The primary emphasis they made was that the shear stress was modified by the normal stress on the shear plane. I would like to suggest that the normal stress had much greater influence than they proposed. Finally, as we move into the radial areas, we find considerable longitudinal splitting. This is probably due to the high tangential stress in the small plastic zone associated with the rapidly moving crack in this general area. I would like to suggest that if people want to have a very interesting piece of detective work, they can spend many hours in studying fracture surfaces.

FIFTH SESSION

"Mechanical Screening Tests"

MECHANICAL SCREENING TESTS

FOR SHEET ALLOYS

By W. F. Brown Jr.*

INTRODUCTION

A screening test is one that will permit the sorting of materials in relation to some property measured under a given set of conditions. In this respect the conventional tensile test is a screening test in that materials may be rated according to their tensile or yield strengths at some particular test temperature. However, for high strength alloys the conventional tensile test does not yield strength values that are always realizable in service. The service strength is frequently limited by the presence of so-called "brittle" fracture which may occur at a fraction of the yield strength in the presence of high stress concentrations such as cracks or crack-like flaws. In this case there is need for a test which will measure resistance to this brittle fracture.

In selecting a suitable screening test several requirements should be kept in mind: (1) The test should incorporate the essential features of the stress field surrounding a crack. (2) The sensitivity of the test should be sufficient to reveal changes in material brittleness as influenced by composition and heat treatment. (3) The test should permit rapid evaluation of a large number of alloys and alloy conditions with a minimum expenditure of time, money and material. (4) The test should be easily conducted even by those with minimum training in stress analysis or metallurgy.

CLASSIFICATION OF SCREENING TESTS

A large number of tests have been used to assess the relative brittleness of sheet alloys. Some of these were developed for other purposes and have been adapted to sheet testing while some were developed specifically for screening sheet materials.

With few exceptions these tests incorporate some form of stress raiser such as a natural crack or notch. However, many different notch configurations have been employed and both tensile or bending loads are applied either statically or dynamically.

*Chief, Strength of Materials Branch, NASA Lewis Research Center, Cleveland, Ohio

The various tests may be conveniently classified according to specimen geometry and method of loading, as follows: (1) center notch tensile tests, (2) edge notch static or impact tensile tests, (3) edge notch static or impact bend tests, (4) notched impact bulge tests and (5) tests on unnotched specimens. Information concerning these tests is given in figures 1 to 9 which show the essential geometrical features, method of loading and data most commonly reported. In addition, the persons or organizations primarily concerned with the test development are indicated. Certainly this list is not complete but does include the tests most commonly employed for screening alloys. The following discussion will briefly describe the various tests and where possible discuss some of their advantages and limitations. Later the screening tests recommended by the ASTM Special Committee on the Fracture Testing of High Strength Sheet Materials will be considered in more detail. Our panel members will also further discuss certain other of the more widely used specimens.

Center notched tensile tests: The basic specimen type is shown in Figure 1 and consists of a sheet with some type of central slot. It will be noted that a wide range of widths and various slot configurations have been used. However, the slot length to width ratio is generally between 0.3 and 0.5. In most cases there is an attempt to sharpen the end of the slot, the ultimate sharpness being obtained with a natural crack used by Srawley at NRL. (1) (2) In the case of Eloxed slots it is very difficult to reduce the end radius below about 0.002 inch. With saw cuts the slot widths are limited to greater than about 0.005 inch. Generally the larger slot end dimensions have been only used on the very wide specimens. The specimen proposed by Kattus and Morrison (3) has a cold worked area at the "shear crack" tip and for some alloy conditions a natural crack may be present at this location. This test appears to have certain advantages and Mr. Morrison will describe it further.

Edge notch static or impact tensile tests: The basic specimen type is shown in Figure 2. The edge notches are machined into the sheet and with care radii less than 0.0007 inch can be consistently produced. The notch angle has generally been either 45° or 60° and the ratio of total notch length to specimen width in the range between 0.3 and 0.4. There is some question as to the necessity for impact loading and this point will be discussed more fully by Mr. Brothers. It is to be emphasized that very sharp notches are necessary to yield meaningful results.

Edge notch static or impact bend specimens: The basic specimen type, Figure 3, is a sheet with one edge notch which is subjected to bending moments in the sheet plane with the notch on the tension side. A variation of this type is the edge notch modified Kahn test which is a sharply notched eccentrically loaded tension specimen. The Charpy impact is a sheet specimen with the plane dimensions of a standard Charpy bar. Both it and the slow bend test (Boeing) have a mild notch (0.010 inch radius). Tests with such mild notches have the disadvantage that considerable plastic energy may be used in initiating a crack at the notch root and therefore the test may not reveal brittleness that could occur in the presence of an initial crack.

The taper notch specimen developed by Hartbower and Orner (4) at Watertown Arsenal has the desirable feature of providing very good crack starting characteristics without the machining of an extremely sharp notch. This results from the presence of a feather edge at the junction between the two notches at the top of the specimen.

There appear to be no particular advantages of the slow bend tests in Figure 3 over the notched tensile tests previously described. The impact test, of course, has the advantage of testing equipment simplicity if only the energy to fracture is measured and it is quite rapid to perform. On the other hand, the testing of a thin sheet edge notch specimen in bending requires special precautions to avoid buckling. In addition, the energy absorbed by the very brittle conditions may be so low that special impact machines with low pendulum mass must be used to obtain accurate values. The analysis of such specimens to obtain K_c values is possible; however additional instrumentation is necessary and limits on the geometry have not been established.

The Douglas tear test was developed by Schapiro and recently described by Vigor and Hornaday (5). This test has been used to predict the formability of titanium sheet with particular reference to H_2 embrittlement. The test starts as a one-inch square with a 1/16-inch hole at its center. A saw cut connects this hole to one edge forming a slot. The ears are formed by 90° bends located approximately one-quarter inch from the central hole. After bending the test piece is torn by means of hooks engaged in the large holes. Generally, the work to produce a crack of a given length (about 1/4 inch) is measured, this being determined from an oscillographic load versus time graph. This test has proven quite successful in detecting H_2 embrittlement in Ti alloy sheet. However, from the geometry of the specimen, it is not clear as to how the test can represent the action of an initially present crack. It would seem that a very sharp ended slot would improve the situation in this respect.

Notch impact bulge tests: The basic type of specimen, Figure 4, is a square sheet generally containing a central stress raiser. Loading is by impact rubber bulging (Puzak (6)) or by dropping a weighted ball onto the slotted area (Rayan Aero.).

In the case of Puzak's test a small inert gas arc fusion weld (without filler) is made at the plate center. A notch is then ground longitudinally into the surface of this brittle weld. The specimens are brought to temperature either in a furnace or in a liquid low temperature bath. The specimen is then quickly transferred to the impact bulger shown in Figure 5, and a 300 to 500 pound weight dropped on the ram from a height of about 8 feet. A crack starts at the weld notch and propagates across the sheet. Some examples of the fractures are given in Figure 6 for four steels at a hardness level of 53 - 54 Rc tested at -32°F. After the test the fracture surface is examined to determine the percent shear. This measurement is made about one-half inch outside the weld heat affected zone. Tests are made over a range of temperatures in order to develop

the shear transition temperature (Figure 7). The transition temperature so defined appears to agree with that determined using center cracked tensile tests (Figure 8). Puzak's test has also been suggested to evaluate weldments. The specimen is then made up of two halves welded together, and the amount of plastic strain controlled by limiting the bulge height by means of a die cup. The fractures will presumably initiate at weld defects and run along brittle zones. This impact die bulge seems to have considerable promise for rapid screening both parent materials and weldments. Unfortunately, very little data has been obtained with this test.

The drop ball impact test has been used primarily as a measure of crack initiation rather than propagation, the highest impact value which will not cause a visible crack being reported. The test is relatively simple to perform but the results will undoubtedly be affected by small variations in the slot end radius.

Unnotched specimens: Unless a natural crack is formed at areas of high strain gradients during rising load a test without a notch cannot give meaningful information regarding resistance to brittle fracture. However, there has been a belief by some that the presence of biaxial stresses per se, such as exist in the wall of a pressurized missile tank, can induce brittle fracture at stresses much lower than encountered in a tensile test. With this in mind, static bulge tests were made. This test involves deformation by oil pressure of a sheet clamped under a die with a circular opening (Figure 9). The test gives balanced biaxial tension at the pole and fracture will occur in this area if the die is designed correctly. Data from this type of test does not reveal any embrittlement associated with biaxiality per se. Low fracture stresses when observed in these tests are explained by the presence of crack-like defects associated with welds or to stress concentrations associated with the die radius or with methods employed to clamp the specimen. Furthermore, there appears to be no evidence that tube or bulge tests are better suited to investigate weld embrittlement than tensile tests containing welds.

The Allison test is essentially a three point bend test on a specimen sufficiently wide to develop full biaxiality. As indicated in Figure 9, a bend parameter is derived which relates to the difference in elastic outer fiber stress at maximum load (σ_m) and that existing at the start of rapid fracture (σ_1). The test has the advantage of employing a very simple specimen and in addition gives an indication of the plane strain fracture toughness. It has two notable disadvantages; if the material is very brittle, σ_1 will be essentially equal to σ_m and the test becomes insensitive. On the other hand, if the specimen is too ductile it may not crack clear through even when bent 180°; in such cases the parameter cannot be determined. Mr. Sipple will describe this test later in further detail.

ATTEMPTS AT STANDARDIZATION

From the foregoing it is little wonder that increasing pressures for standardization arose. These pressures reached a peak when difficulties with brittle failures were encountered in the solid propellant rocket program. Early in 1959 the ASTM, at the suggestion of the Department of Defense, organized an Ad Hoc committee to review testing methods and to make recommendations regarding a standard method for evaluating high strength sheet materials regarding their resistance to brittle fracture. At about the same time the Aerospace Industries Committee considered the problem through the action of the ARTC-W-97 Committee. Both these groups have arrived at tentative recommendations. Those of the ASTM have been published (7) and the following will describe some of this work in detail. Mr. Stapleton, Chairman of the W-97 Committee, will describe the activities and conclusions of that group. As will be seen, there are many points of agreement.

The general philosophy of the ASTM Committee was that brittle service failures could be traced to unstable rapid fracture having its origin in a pre-existing crack or crack-like flaw. With this in mind it seemed only logical to require that the screening specimen reproduce the essential characteristics of the stress field surrounding a crack. Furthermore, the specimen requirements previously mentioned were to be satisfied. In order to reproduce the action of cracks it was agreed that the specimen must contain either a natural crack or a very sharp notch. It appeared that a tensile specimen offered the advantage of ready availability of test equipment and ease of making the necessary measurements. A rather large amount of data was already available using both the sharp edge notch tensile test and the center crack tensile test. Both these tests seemed to meet the sensitivity requirements. The Committee then set about examining the parameters which influence the strength values of such specimens with the object of designing a suitable specimen. In the following we will consider the influence of some of these parameters.

Notch radius: There is no quarrel with the fact that a natural crack is ideally suitable. However, the production of such cracks requires the use of equipment and personnel which may in some cases not be available. On the other hand, the production of a sharp edge notch is strictly a machining job requiring the application of standard equipment and tools. The question arises as to the necessary sharpness of the machined notch. The effect of notch radius on several alloys is illustrated in Figure 10, which shows the notch tensile strength ratio* as a function of radius. It will be noted that while the embrittlement increases with decreasing radius, the effect varies with the alloy. It is important to note that for some materials, notably H-11 Mod. and

* The notch tensile strength ratio is obtained by dividing the nominal notch strength (max. load divided by min. initial area in the notch plane) by the conventional tensile strength. A decrease in the ratio indicates increasing brittleness.

4-3-1-Ti, there is a considerable increase in brittleness when the radius is reduced from 0.002 to 0.0007 inch. Furthermore, where comparative data is available it appears that edge notches of less than 0.001 in radius provide embrittlement sufficiently close to that obtained with natural fatigue cracks in 1-inch wide center notch specimens.**

Notch angle: Limited data for the effect of notch angle on the edge notch strength are given in Figure 11. The results are rather unexpected in that a slight minimum in strength occurs at about 60° for transverse tests on AISI 301 (70%CR.) and at about 45° for H-11 Mod. (1000°F temper). Thus, a small increase in the sensitivity of the edge notch test may be possible by the selection of an optimum flank angle. However, this apparently is an unknown function of the material.

Notch depth: Data obtained by Sachs et al, Figure 12, indicate that a broad minimum in the edge notch tensile strength ratio occurs between about 20 to 40 percent notch depth. This range of maximum sensitivity is also indicated by Irwin's (7) stress analysis.

Thickness effect: Data obtained by Srawley (1), Figure 13, and that obtained by Romine (8) on a different alloy indicate the notch strength decreases with increasing thickness for constant width and notch length. The magnitude of this effect depends on the alloy. It increases with increasing strength level and appears to fade out as the thickness increases. The observed effects probably contain a metallurgical (structural) component that would tend to make the material having the greatest total reduction the toughest.

Specimen width: The selection of the specimen width for a constant percentage notch depth and root radius sets the sensitivity of the test, in that for notch sensitive conditions the wider the specimen the lower the strength. This is, of course, expected on theoretical grounds (7). In order for the test to be sensitive to metallurgical or other factors controlling the embrittlement it is necessary that the notch strength be below the tensile strength and preferably below the yield strength. An example is given in Figure 14 for H-11 Mod. It will be noted that at the 1110°F temper the sharp edge notch strength of one-inch wide specimens is above the yield strength while the corresponding strength values for three-inch wide, but otherwise similar specimens, is below the yield strength.

Testing speed: Missile cases are pressurized very rapidly (small fraction of a second) in service. However, most laboratory screening

**For equal toughness edge cracks should give notch strengths roughly 5 percent lower than center cracks. The edge notch strength of 300 M is lower than the center crack strength by a much greater factor. The author has no explanation for this unexpected difference. Both center crack and edge notch specimens were taken from the same sheet and had equal width and $\frac{2a_o}{W}$ values.

tests are conducted at relatively slow speeds. Few notch data are available for defining the speed effect. Srawley (7) has obtained some data for fatigue center cracked specimens of a low alloy steel tested at loading rates of 1000 and 200,000 psi per second. These tests carried out over a range of temperatures, Figure 15, show no effect of this speed variation. However, the upper rate is much lower than encountered in some service applications and the data were obtained for low alloy tempered steel where only small rate effects might be expected (9). In addition, as will be discussed later, environmental influences may affect the slow crack growth and notch strength for some alloys if the loading rate is sufficiently slow.

Recommendations for a screening specimen: On the basis of the previously described data the ASTM Special Committee on the Fracture Testing of High Strength Sheet Materials recommended the edge notch tensile specimen shown in Figure 16 for screening of sheet alloys having a strength to density ratio above 700,000. It was also recognized that a fatigue center crack specimen of the same width and total notch length would be equally suitable. However, the strength values determined with these two specimens are likely to be different.

It will be noted that the notch radius was selected as 0.001 inch maximum and the notch depth 30 percent. These values are well established by the previously discussed data. The width was selected as one inch. A large amount of data (7), (10), (11), (12) obtained with specimens very similar to those shown in Figure 16 have shown this width to yield sufficient sensitivity for alloys of interest. Regarding notch angle, 60° was recommended, again on the basis that a large amount of data has been obtained using this angle and because relatively slight differences were noted for variations between 30° and 90°. In the absence of additional data on testing speed the recommended loading rate was 1000 to 10,000 psi (net section stress) per second. There is no question that the alloy to be evaluated should be tested in the thickness to be used in service and that different alloys be compared at the same thickness.

It will be noted that pin loading is recommended to reduce eccentricities and that careful attention is given to machining tolerances so that the loading axis passes through the mid-point between the notch tips and is perpendicular to a line joining these points.

Specimen preparation and procedure have been covered in two papers (7) (13) and these references should be consulted for details. Heat treatment is recommended following finish machining. This has the advantage that the specimen machining is usually easier and that cracks in components resulting from welding are frequently subjected to a heat treating atmosphere. In any case the heat treating atmosphere for the specimen should be identical to that used for the service component.

Reporting results: On the basis of the evidence available the nominal notch strength and a measure of the fracture appearance (percent shear) should be reported along with the smooth ultimate and 0.2 percent yield strength. The smooth specimens should be heat treated in exactly the same manner as the notch specimens. It was recommended that at least duplicate, but preferably triplicate notch tests be made for each metal condition investigated. One suitable index of embrittlement in the presence of cracks is the ratio between the nominal notch strengths and the tensile strength. This ratio is a measure of utilization of the strength potential in the presence of the sharp notch employed. Thus, the notch strength ratio may be used to rate materials regarding their resistance to brittle crack propagation at a particular strength level. Values equal to unity indicate a highly tough metal condition, but unless the ratio is below unity the notch screening test is not sensitive to embrittling factors.

It should be emphasized that the quantitative values of fracture toughness, K_c, could equally well serve to rate materials. However, it is felt that the narrow screening specimen (one inch wide) complicates the accurate determination of slow crack extension and at least three-inch wide specimens are recommended for K_c determinations.

In conclusion, it should be noted that the Aerospace Industries ARTC W-97 Committee accepted the majority of the ASTM recommendations, as will be described by Mr. Stapleton.

NASA - NRL COOPERATIVE PROGRAM

One purpose of this program is to examine the room temperature strength values derived from several different types of sharply notched tensile specimens in order to determine whether one offers any particular advantage over the other for screening purposes. The various specimen types are indicated in Figure 17. It will be noted that one- and three-inch nominal widths are considered and all specimens have a crack length to width ratio $\left(\frac{W}{2a_o}\right)$ of about 0.3. The program includes several sheet alloy types, namely a 5 percent Cr tool steel (H-11 Mod.), β titanium alloy (B 120 VCA) and AISI 301 cold rolled 70 percent. With the exception of AISI 301 several levels of toughness are being investigated for each material. The thickness in all cases is 0.063 inch, heat treating is done after machining, and at least triplicate tests are made for each condition.

At present, results are available for H-11 Mod. tempered over a wide range of temperatures. The results are in Figures 18 and 19 for the one-inch and three-inch specimens respectively. These representations show the spread of values obtained with each specimen type as well as a few data, to be discussed later, obtained using 0.002-inch radius one-inch wide edge notch specimens.

Considering first the one-inch wide specimens, Figure 18, it will be noted that the results obtained using either shear cracked or fatigue cracked center notches are identical within the limits of scatter. The sharp edge notch tests (0.007-inch radius) yield somewhat higher strength values at 1000°F and 1075°F temper. All these tests define the same tempering temperature at which notch strength and yield strength are equal and also agree in that the notch sensitivity increases with decreasing tempering temperature. In addition, the region of greatest alloy variability is established to be at tempering temperatures between about 1075° and 1100°F.

The results for the three-inch wide specimens, Figure 19, establish essentially the same general trends of notch strength with tempering temperature as were observed for the one-inch wide specimens. It would be expected that the values would be lower for the larger specimens. This is noted for the sharp edge notch and the center shear cracked tests which give equivalent values within the limits of scatter. However, the three-inch center Elox slot yields values at tempering temperatures from 900° to 1075°F which are nearly as high as obtained with one-inch edge notched specimens. However, all three-inch wide specimens establish the same tempering temperature at which the notch strength equals yield strength. It will be noted that this is about 20°F higher than established with the one-inch wide tests.

The high values for the three-inch center Eloxed tests, Figure 19, may be explained by the fact that the notch radius was too large to accurately simulate the action of a natural crack. It is known that the one-inch wide edge notch strengths of this alloy, tempered at 1000°F, are strongly affected by the radius (see Figure 10). With this in mind 0.002-inch radius one-inch wide notch specimens were tested and according to Figure 18 the larger radius does, indeed, raise the notch strength at tempering temperatures below about 1100°F.

The program is not sufficiently far along to permit drawing any definite conclusions. However, for the one alloy tested it would appear that all the specimens provide sufficient sensitivity, this being increased with a decrease in the notch radius. The shear center crack specimen is attractive from the point of view that it can be produced rather easily. However, considerable more experience with this specimen type on a variety of alloys will be necessary before it can be established as an alternate to the screening tests proposed by the ASTM.

ALLOY SELECTION

It would be desirable if the data from a screening test could be used as a guide in selecting materials for a given service application. If the flaw sizes are known then, of course, the laboratory measured K_c values are a direct aid in this respect. However, in most cases these sizes are not even approximately established until considerable fabrica-

tion experience has been accumulated. The question then is, what is a safe yield strength level to use when fabricating the initial series of components? Past experience with service failures and screening tests provides some criteria in this respect. However, there are a number of factors which were not considered in the formulation of any of these criteria.

First there must be reasonable assurance that the metallurgical surroundings of the notch in the screening specimen correspond to those of a crack in the component. Thus, if welds are involved, the screening test must consider the properties of the weld metal and heat affected zone. This may be accomplished by locating the notches at various positions in relation to the weld centerline in order to establish the area of lowest toughness. This procedure has been followed by Romine et al (14) using Eloxed center slotted specimens. Another important consideration is that the loading history and environment in the laboratory test should approximate that of the service component. Thus, if the component is subjected to repeated loading an attempt should be made to simulate this in the screening test. The criteria for alloy selection which have been so far proposed do not take into account all these factors. However, there appears to be no reason why they could not do so, at least in a qualitative fashion.

Fracture mechanics approach: The concepts of Irwin (7) yield one criterion. Essentially this is based on the assumption that small, probably undetectable cracks are imbedded in the sheet. These are assumed to propagate to the surface at very low applied stresses. When such cracks reach the surface, they have an extent approximately equal to double the plate thickness. The criterion for acceptance is then that the material must have a K_c value at least equal to that necessary to prevent the catastrophic propagation of a twice the thickness through crack at the operating stress. A further development of this idea considers Irwin's (7) β factor which attempts to relate the relative plastic zone size $R_y = \frac{K_c^2}{2\pi \sigma_y^2}$, to the plate thickness as follows:

$$\beta = \frac{K_c^2}{B \sigma_y^2}$$

where K_c is the fracture toughness, σ_y is the uniaxial yield strength, and B the sheet thickness. It can be shown (7) that if the tank operating stress is set at the uniaxial yield strength and the flaw size equal to 2B, then B must at least equal 2π for the flaw in the tank to be stable.

Empirical criteria: Several purely empirical criteria have been suggested. One is that the notch strength of the one-inch wide screening specimen should at least exceed the yield strength. A similar but more conservative criterion is that the sharp edge notch tensile strength ratio be at least unity. The best that these two criteria can offer is a measure of assurance that the structure will be safe in the presence of severe defects. This is indeed an important consider-

ation. However, it must be assumed that the notch in the specimen is at least as severe as any that will occur in a reasonably designed and fabricated missile tank. On the basis of experience, this is probably true for the specimen shown in Figure 16.

Another empirical criterion is that the fracture appearance of the screening test should be 100 percent shear at the operating temperature. This is based on a considerable amount of data obtained by Srawley (1) (2) (15) which shows the fracture appearance transition temperature defined in terms of percent shear to be somewhat higher than that defined by the notch strength equal to the yield strength. An example of such behavior is illustrated in Figure 20 for a low alloy steel tested by Srawley (2) over a range of temperatures. On the basis of other results it would appear that this is a necessary but not sufficient condition for tough behavior. Thus, according to Figure 21, 300 M tempered at 400° to 550°F exhibits 100 percent shear in center crack tests but has a notch strength well below the yield strength. Irwin (7) has suggested that the β factor may be correlated with the percent shear such that $\beta = 2\pi$ corresponds to a shear value between 80 and 100 percent. However, as more data is accumulated (18), Figure 22, it appears that while the β value does increase with increasing percent shear, there is no definite or useful relation between these quantities.

It should be realized that all these criteria do not give the same answer. The conditions based on the notch strength of the ASTM screening specimen, equal to yield strength (or tensile strength) are more conservative than $\beta = 2\pi$ for thicknesses equal to or less than about 0.063 inch. On the basis of general experience it is indicated that materials selected in accordance with the former criteria may be fabricated into welded structures with normal care. With extreme care it has been possible to fabricate large, circumferentially welded vessels of H-11 Mod. tempered to 225,000 psi yield strength level where β is considerably less than 2π (16). Such vessels burst at circumferential stresses above the unaxial yield strength.

Partial thickness cracks: In many cases a component may contain cracks either imbedded in the sheet or extending from one surface partially through the thickness. These cracks may then slowly grow under the operating stress to an unstable size. This slow growth may produce through-the-thickness cracks or in very brittle alloys the condition of instability might be reached before the crack completely penetrates the thickness. The screening tests so far discussed all employ through-the-thickness cracks. The question arises as to whether or not such specimens might yield an unconservative estimate of the relative toughness for a given alloy if partial cracks are present in service.

It is not known how to produce imbedded cracks in specimens. However, recently Srawley (17) has obtained very interesting data for a series of one-inch wide X-200 specimens (0.069-inch thick) with surface cracks extending partially through the thickness. The technique

is essentially to subject a specimen to low bending stresses and to hydrogen embrittle a small area of the surface by cathodic charging. By varying the area exposed to hydrogen and the charging time it was possible to control both length and depth of an elliptically shaped crack.

Selected data is given in Figure 23 which compares results obtained over a range of test temperatures, for specimens having through cracks with those having surface cracks. An attempt was made to select surface cracked specimens with the crack length ($2a_o$) in a range which bracketed the through crack lengths.

It will be noted that at all testing temperatures 140-180 mil long surface cracks yield higher notch strength ratios than 150 mil through cracks. At room temperature no through crack data are available to compare with the 292-327 mil length surface cracks. However, data for sharp edge notches with a 300 mil total notch length (from a different heat of the same thickness) yields a notch strength ratio far lower than the surface cracks. It is also to be noted that for approximately equal percent crack depths (thickness penetration) the notch strength ratio follows essentially the same trend with testing temperature (ductility level).

On the basis of this limited data it would appear that for practical purposes materials may be screened using through the thickness notches or cracks and that different ratings would not be obtained using specimens containing surface cracks. Additional tests are necessary, particularly for shallow surface cracks, to verify this observation.

QUALITY FACTOR CONSIDERATIONS

The consideration of alloys other than steels has introduced a density variation into the picture. It has been general practice to form the ratio between tensile strength (or yield strength) and density and to then compare the fracture toughness of various alloys at a constant value of this ratio. In this way the advantages of low density are taken into account. Kies et al (18) have made the suggestion that a quality factor might be formed as follows:

$$Q.F. = \frac{K_c}{K_{c\ min}} \times \frac{\sigma_y}{\rho} \qquad (1)$$

where $\frac{\sigma_y}{\rho}$ is yield strength to density, K_c is the value measured for the material in question and $K_{c\ min}$ is that value necessary to withstand a through crack of given length in a pressure vessel stressed to the unaxial yield strength, σ_y.

In the case of a large thin walled cylindrical tank

$$K_{c\ min} = 2\pi\sigma_y^2\ a_o \qquad (2)$$

where a_o is the observed initial flaw dimension. If a_o = B where B is the sheet thickness, then this is the previously discussed acceptance criterion proposed by Irwin.

An example calculation is useful in examining the application of this quality factor. Consider the aluminum alloy 2024T3 for which $K_c \sim 130 \times 10^3$ psi $\sqrt{in}$, $\sigma_y = 46 \times 10^3$ psi, B = 0.050 in., and ρ = 0.1 lbs./in.^{3}. From equation (2), $K_{c\ min} = 25.8 \times 10^3$ psi $\sqrt{in}$. The quality factor from equation (1) is then:

$$Q.F. = 5.05 \times 46 \times 10^4 = 2.32 \times 10^6 \qquad (3)$$

This may be compared with H-11 Mod. steel tempered to σ_y = 200,000 psi where $K_c = 175 \times 10^3$ psi $\sqrt{in}$. and $\rho = 0.284$. Now $K_{c\ min} = 112 \times 10^3$ psi $\sqrt{in}$. and the quality factor

$$Q.F. = 1.56 \times 700 \times 10^4 = 1.09 \times 10^6 \qquad (4)$$

Thus, according to equation (1) aluminum has a higher quality factor than the steel. This does not seem consistent with practical considerations. The steel has a higher strength to density ratio permitting a lighter structure and has a 50 percent safety factor in toughness. The difficulty, of course, lies in the fact that the very large ($5.05\ K_c/K_{c\ min}$) value for the aluminum has been given too much weight in formulating its quality factor. Apparently the σ_y/ρ must be balanced against the available toughness in as yet an undetermined manner. It would appear that material selection can best be made with the aid of plots of K_c (or sharp notch strength ratio) vs σ_y/ρ. These parameters are complex functions of one another and different for different alloys.

ENVIRONMENTAL INFLUENCES

Screening tests are normally conducted in the room atmosphere and fracture occurs at most in a few minutes. On the other hand, a component may be subjected to damaging environmental influences during its life. An example is the hydrotesting of solid propellant cases, where both stress and water may be applied for several hours. Under such conditions it has been suggested by Shank et al (19) that hydrogen embrittlement can occur. Certainly, an additional factor is stress corrosion due to dissolved oxygen or other corrosive substances in the water. If stress corrosion does occur the magnitude of slow crack growth might be profoundly affected and time dependent. Likewise, it might be expected that screening tests would exhibit increased slow crack growth and reduced notch strength in the presence of certain media.

Very little is known so far about stress corrosion of high strength alloys in the presence of sharp notches or cracks. Irwin (20) has shown some data which indicate the notch strength of a low alloy steel, heat treated to a brittle condition, was reduced 50 percent if loaded slowly

in the presence of water. On the other hand, a more ductile alloy did not show a similar effect. Some additional data has been obtained in the author's laboratory. The results are preliminary and represent a mixture of both materials and testing conditions.

It was desired to establish whether the room temperature sharp edge notch strength of one-inch wide screening specimens would be influenced by the presence of a number of media: (1) distilled water, (2) distilled water plus a commonly used corrosion inhibitor ($Na_2 Cr_2 O_7$), (3) transformer oil and (4) India ink. These media were applied directly to the notch in much the same manner as normally employed with India ink in K_c testing, care being taken to have enough fluid present to completely fill any slow crack. In addition, a test run in water was protected by coating with Cosmoline No. 1060 applied at about 200°F. Both a normal loading rate (30,000 psi notch section stress per minute) and a slow loading rate (1500 psi notch section stress per minute) were employed for selected conditions.

The data are presented in Figure 24 for two low alloy sheet steels and two titanium alloys. The numbers shown represent the percentage the notch strength was changed by the indicated media. The reference value is taken as the median notch strength of replicate specimens tested at the normal rate in air, or with India ink in the notch. While the data are not complete in this respect, it would appear from results obtained with 300 M (E) that the presence of India ink does not change the notch strength over that obtained in air when normal test speeds are employed. The percentage figures refer to tests on single specimens and no effect (zero) is reported unless the percentage exceeds the normal scatter of ± 10 percent.

A number of interesting observations may be made on the basis of the data available:

1. There is little or no reduction in notch strength when specimens are tested at slow rates in air.

2. Tests carried out at normal loading rates with India ink show no reduction in notch strength.

3. The notch strength of the high yield strength level steels is reduced by slow loading in distilled water. This effect is larger for 300 M (up to 60 percent) than for H-11 Mod. A similar but smaller effect is noted with India ink.

4. The notch strength of the low yield strength level steels and of the fully heat treated titanium alloys is not reduced by slow loading in distilled water.

5. The addition of $Na_2 Cr_2 O_7$ appears to effectively inhibit the deleterious effect of distilled water in slow tests.

6. Transformer oil does not reduce the notch strength of steels heat treated to high yield strength levels.

7. Cosomiline 1060 effectively protects the steels against distilled water.

The one encouraging aspect of these results is that a simple corrosion inhibitor, $Na_2 Cr_2 O_7$, effectively protected the notch brittle steels against water. The immunity of the titanium alloys to water may be due to their inherently high corrosion resistance in this media. In steels the deleterious effect of water is apparently a function of the tendency to form slow cracks at relatively low loads. Thus, the H-11 Mod. at 223,000 psi yield strength level tends to form very little slow crack in a normal rate test in air while 300 M forms considerably longer slow cracks under the same conditions. In this connection it is interesting to note that the slow crack length of 300 M (C) is increased up to 30 percent when tested slowly with India ink. When the steels are heat treated to low yield strength levels, slow cracking does not start until after gross yielding and the water would not be expected to have an effect.

BIBLIOGRAPHY

1. J. E. Srawley and C. D. Beachem: "Crack Propagation Tests of High Strength Sheet Steels Using Small Specimens." NRL Report No. 5727, NRL, April 9, 1958

2. J. E. Srawley and C. D. Beachem: "Crack Propagation Tests of Some High Strength Sheet Steels." NRL Rept. No. 5263, NRL, Jan. 10, 1959

3. J. D. Morrison, J. B. Preston, and J. R. Kattus: "An Investigation of Methods for Determining the Crack Propagation Resistance of High Strength Alloys." Bimonthly Progress Rept. No. 1, Southern Research Institute, Birmingham, Ala., Dec. 1959

4. G. M. Orner and C. E. Hartbower: "Notch Sensitivity in High Strength Sheet Materials." Rept. of Progress, Watertown Arsenal Lab's., Watertown, Mass., May 16, 1960

5. C. W. Vigor and J. R. Hornaday, Jr.: "Tear Test for Titanium Sheet." Metal Progress, April, 1958, p. 103

6. P. P. Puzak and J. Stoop: "Simple Laboratory Bulge Tests for Sheet Metal Fracture - Transition Studies and for Weldment Performance Evaluation." NRL Rept. No. 5347, NRL, Aug. 4, 1959

7. "Fracture Testing of High Strength Sheet Materials -- a Report of a Special ASTM Committee." ASTM Bulletins, 1960, Jan., p. 29-40, and Feb., p. 18

8. H. E. Romine: "Critical Crack Extension Force in AMS 6434 Steel Sheets from Stock at the Aerojet General Corp. Intended for Large Solid Propellant Rocket Casings. Thicknesses of 0.063, 0.125 and 0.188 Inch Heat Treated to Yield Strengths of 170,000, 190,000 and 210,000 psi." Tech. Memo. No. 87, NRL Project 62R1905, U.S. Naval Proving Ground, Dahlgren, Virginia, July 1959.

9. G. R. Irwin, J. A. Kies and H. L. Smith: "Fracture Strengths Relative to Onset and Arrest of Crack Propagation." Proc. ASTM, Vol. 58, 1958, p. 640

10. G. B. Espey, M. H. Jones and W. F. Brown, Jr.: "The Sharp Notch Tensile Strength of Several High Strength Sheet Alloys." Proc. ASTM, Vol. 59, 1959, p. 837

11. G. B. Espey, A. J. Repko and W. F. Brown, Jr.: "Effect of Cold Rolling and Stress Relief Heat Treatment on the Sharp Edge Notch Tensile Characteristics of Austenitic Stainless Steel Sheet Alloys." Proc. ASTM, Vol. 59, 1959, p. 816

12. G. B. Espey, M. H. Jones and W. F. Brown, Jr.: "Sharp Edge Notch Tensile Characteristics of Several High Strength Titanium Sheet Alloys at Room and Cryogenic Temperatures." ASTM Prep. 76b, 1960.

13. J. L. March, W. J. Ruprecht and George Reed: "Machining of Notched Tension Test Specimens." ASTM Bulletin, Feb. 1960, p. 52

14. H. E. Romine: "Fracture Toughness Tests on Welded Titanium Alloys Being Considered for the Chambers of Solid Propellant Rockets: Ti-13V-11 Cr-3AL and Ti-6Al-4V Alloys from Company C." Tech. Memo No. 121, NRL Project 62R1905, U.S. Naval Proving Ground, Mar. 1960

15. J. E. Srawley and C. D. Beachem: "Crack Propagation Tests of High-Strength Sheet Materials, Part III: Low Alloy Air Hardening Steel." NRL Rept. No. 5348, NRL July 30, 1959

16. R. C. Powell: "Notes on Steel Selection for Pressure Vessels." Rocket Motor Case Symposium, Pratt & Whitney Aircraft Corp., Sept. 29, 1959

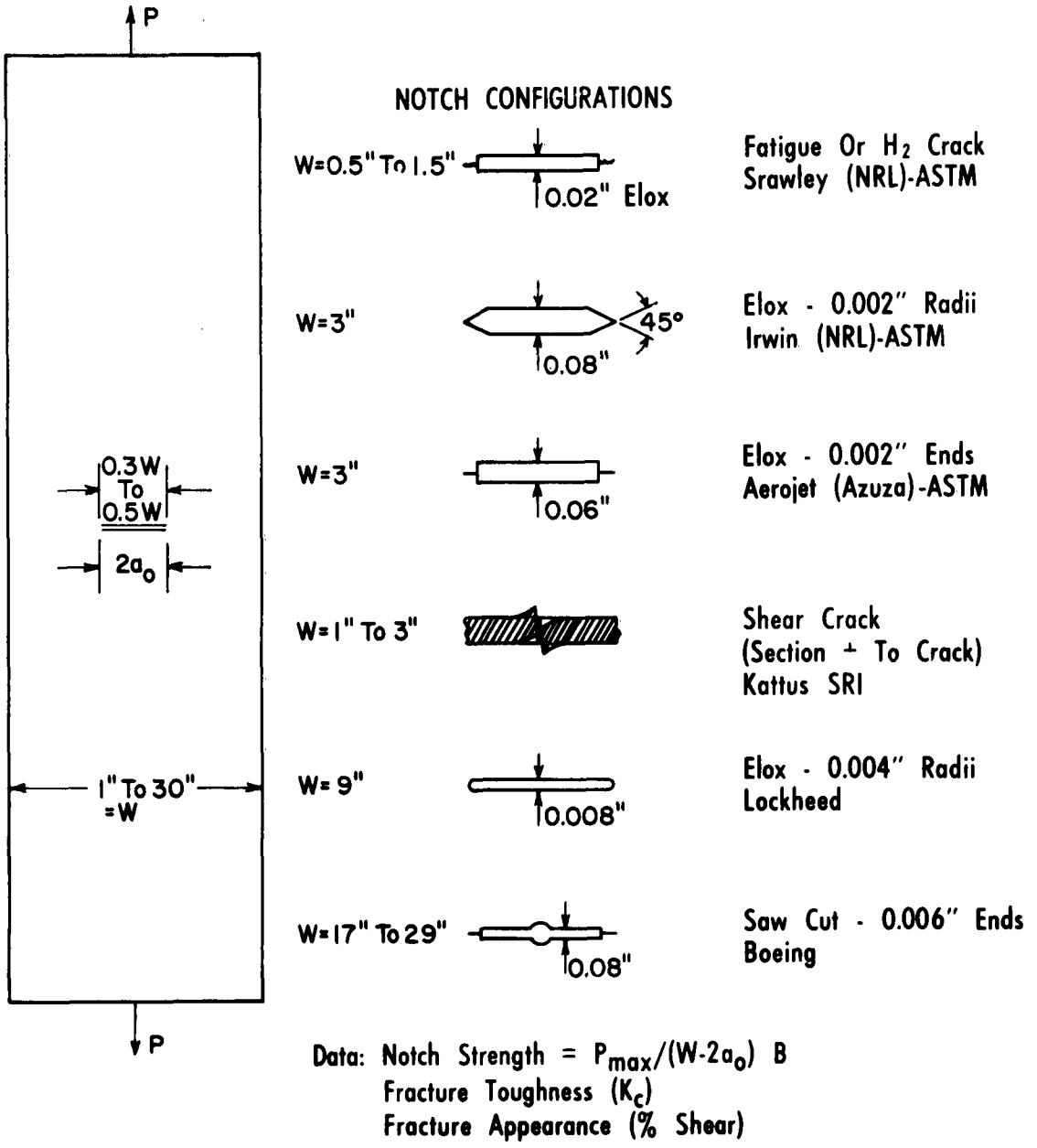
17. J. E. Srawley: Communication to the ASTM Committee on Fracture Testing of High Strength Sheet Materials, 1960

18. J. A. Kies, H. Romine, H. L. Smith and H. Berstein: "Minimum Toughness Requirements for High Strength Steel Sheet." ASME Metals Engineering Division Conference, Los Angeles, April 25-29, 1960

19. M. E. Shank, C. E. Spaeth, V. W. Cooke and J. E. Coyne: "Solid Fuel Rocket Chambers for Operation at 240,000 psi and Over." Rocket Motor Case Symposium, Pratt and Whitney Aircraft Corp., Sept. 29, 1960.

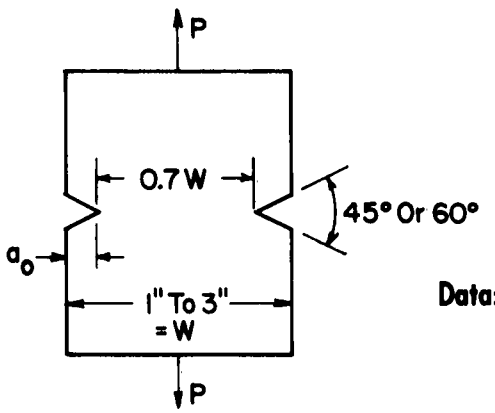
20. G. Irwin: Communication to the ASTM Committee on Fracture Testing of High Strength Sheet Materials, 1960.

E-1043



Data: Notch Strength = $P_{max}/(W-2a_o)$ B
Fracture Toughness (K_c)
Fracture Appearance (% Shear)

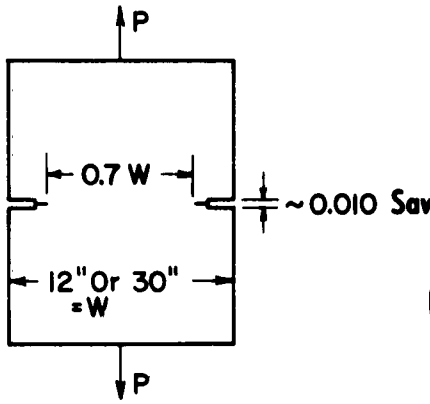
Figure 1. - Center notch tensile tests showing various slot configurations.



STATIC Sachs (SURI)
Brown (NASA)

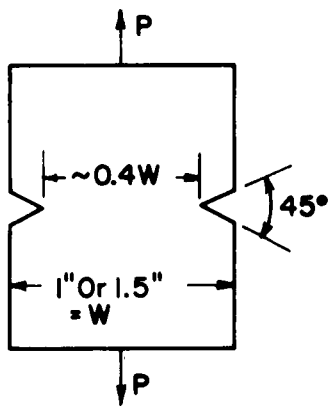
Notch Radii: <0.010"
0.001" Max - ASTM

Data: Notch Strength = $P_{max}/(W - 2A_o)$ B
Fracture Toughness (K_c) For Sharp Notches
Fracture Appearance (% Shear)



STATIC Irwin And Smith (NRL)

Data: Notch Strength
Fracture Toughness (K_c)
Fracture Appearance (% Shear)

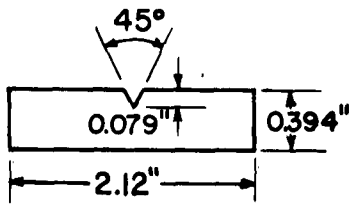


Notch Radii: 0.001" - JPL
0.010" - WAL

Data: Impact Energy
Fracture Appearance (% Shear)

Figure 2. - Edge notch static and impact tensile tests.

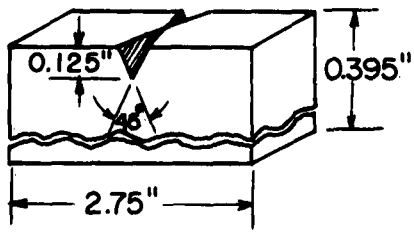
E-1043



CHARPY IMPACT (Sometimes Laminated)

0.010" Radius

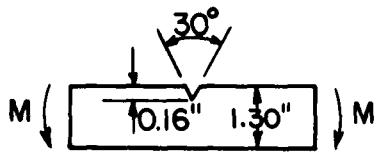
Data: Impact Energy
Fracture Appearance



TAPER NOTCH IMPACT Hartbower & Orner (WAL)

0.010" Radii

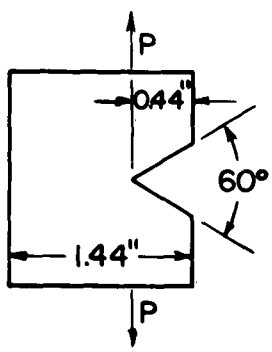
Data: Impact Energy



SLOW BEND (Boeing)

0.010" Radius

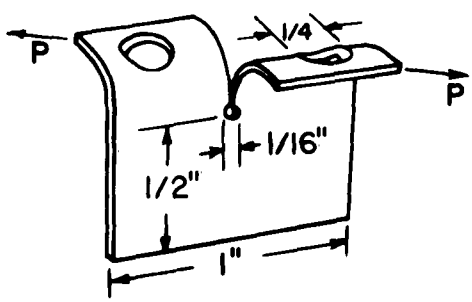
Data: Energy/Unit Crack Area
Strain At Notch Root



MODIFIED KAHN (Alcoa, Convair)

<0.001" Radius

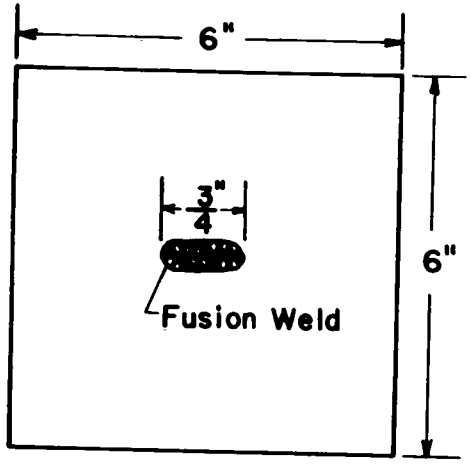
Data: Energy From Load Vs. Gross Extension Plot
a. To Initiate Crack
b. To Propagate Crack To Failure
c. Total Energy



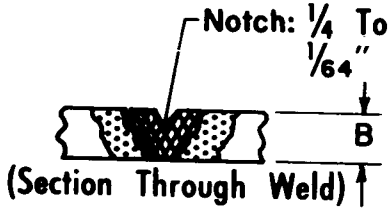
DOG-EARRED TEAR Schapiro

Data: Energy To Produce A Crack
¼" Long From Load Vs.
Gross Extension Plot

Figure 3. - Edge notch static and impact bend tests.

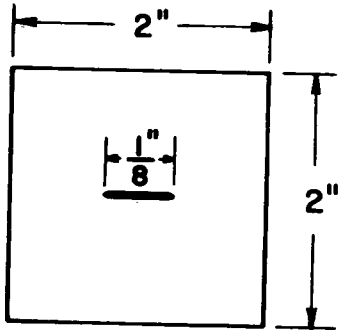


WELD BEAD IMPACT Puzak (NRL)

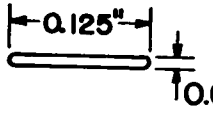


Specimen Impact Rubber Formed Into 5-Inch Diameter Circular Die

Data: Fracture Appearance (% Shear) As Function Of Test Temperature



DROP BALL IMPACT Ryan Areo.



Elox 0.002" Radii

Data: Maximum Energy (1/2" Diam. Ball Weight X Drop Height) That Will Not Cause Crack Visible At 40X With Single Impact

Figure 4. - Notched impact bulge tests.

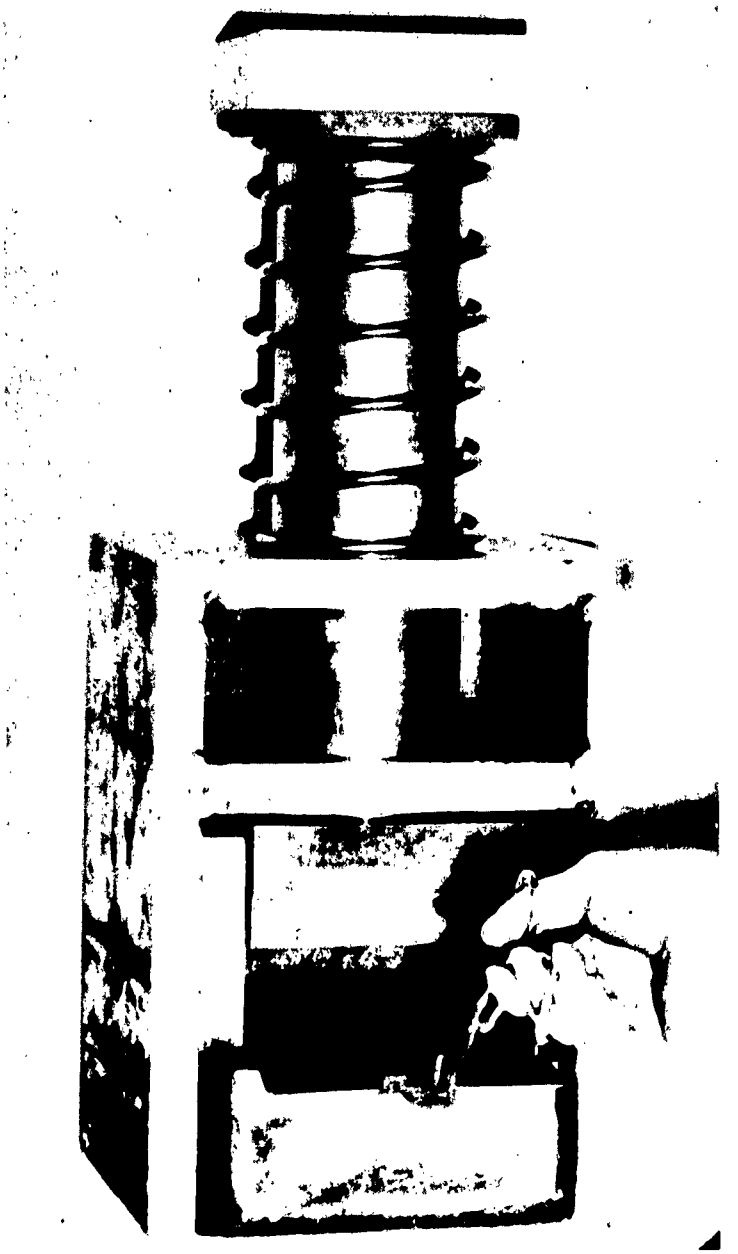


Figure 5. - NRL impact bulge apparatus (Pusak, ref. 6).

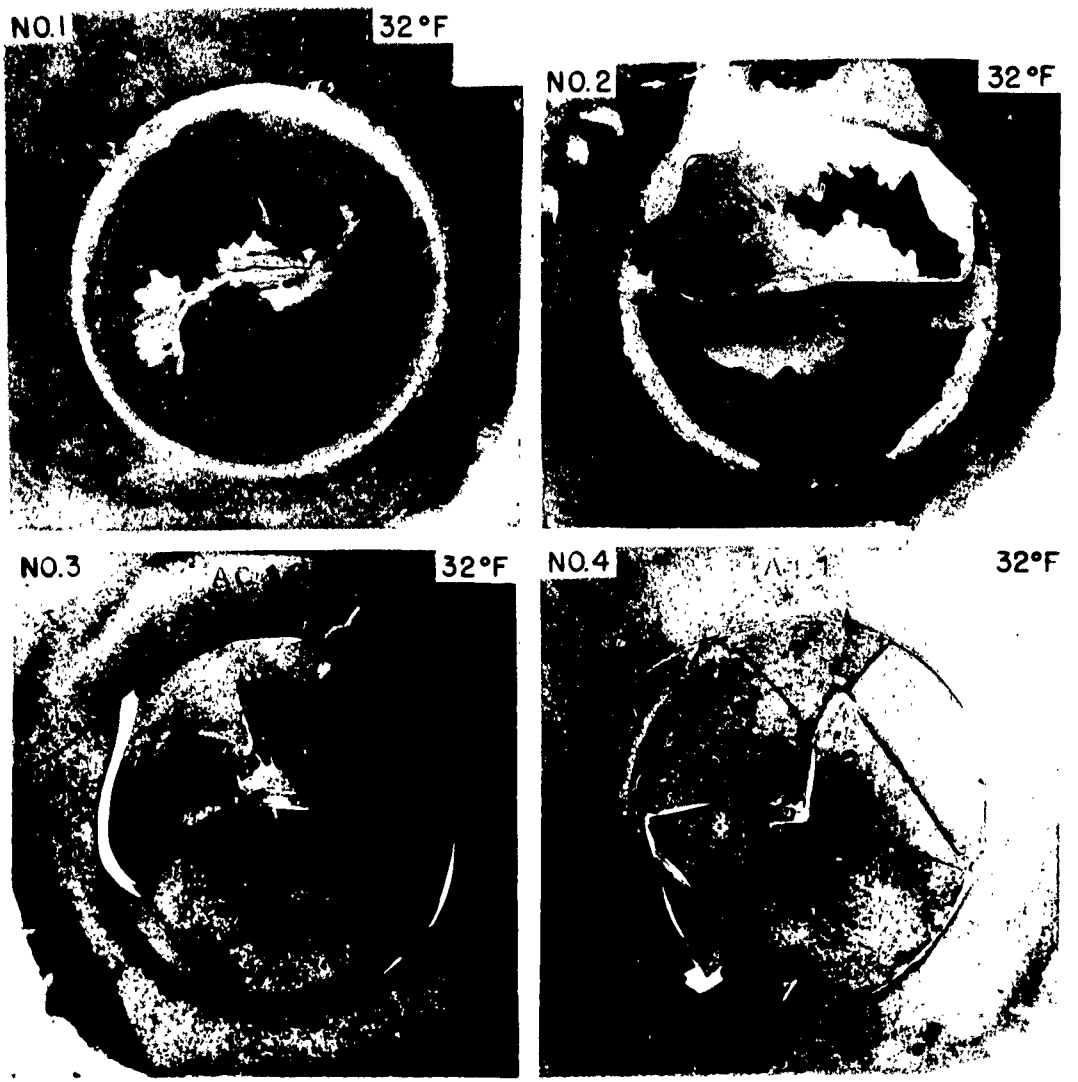


Figure 6. - Examples of fractures obtained by NRL impact bulging of high strength sheet steel (Pusak, ref. 6).

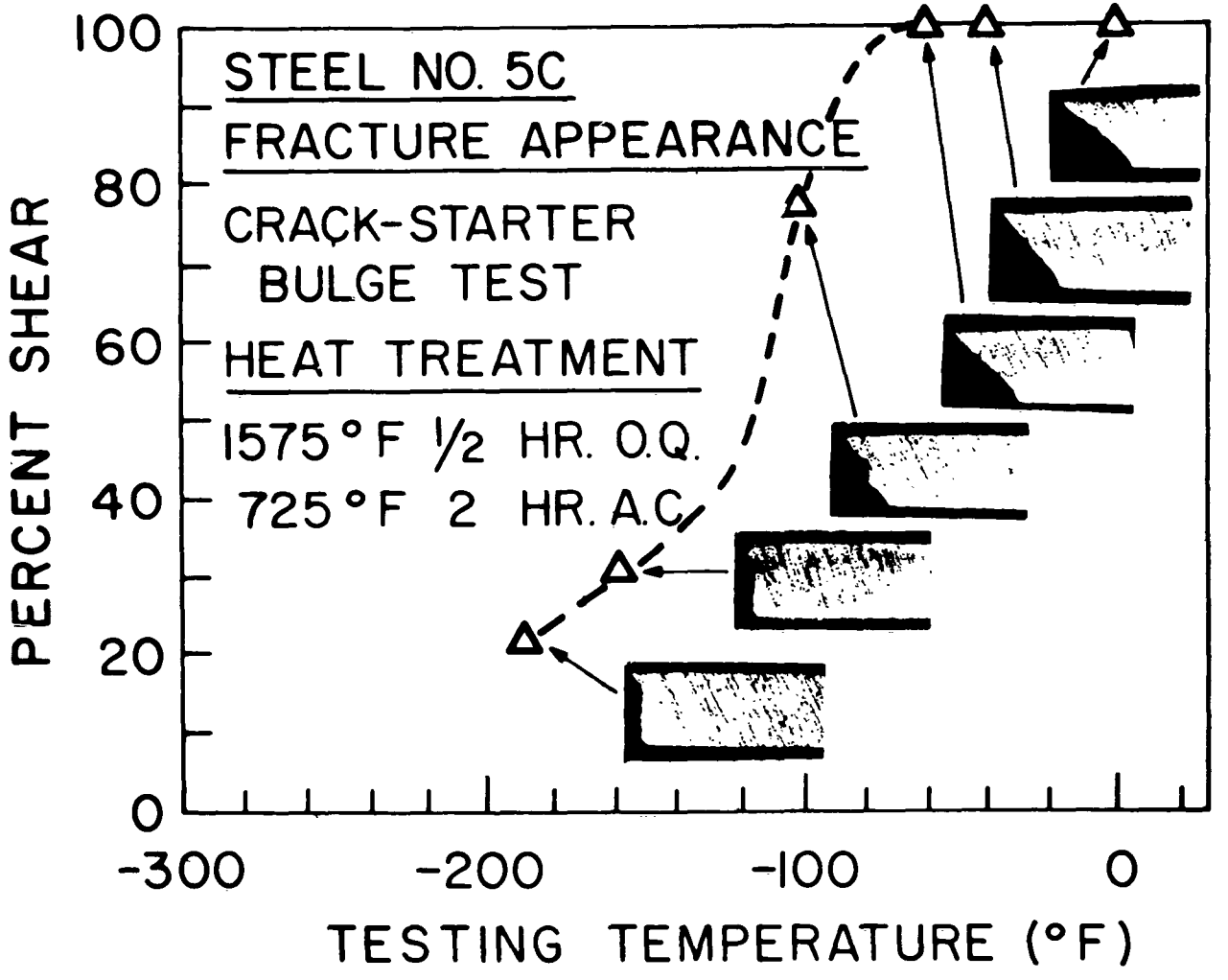


Figure 7. - Fracture appearance transition curve and representative fractures obtained by NRL impact bulging of a high strength sheet steel (Pusak, ref. 6).

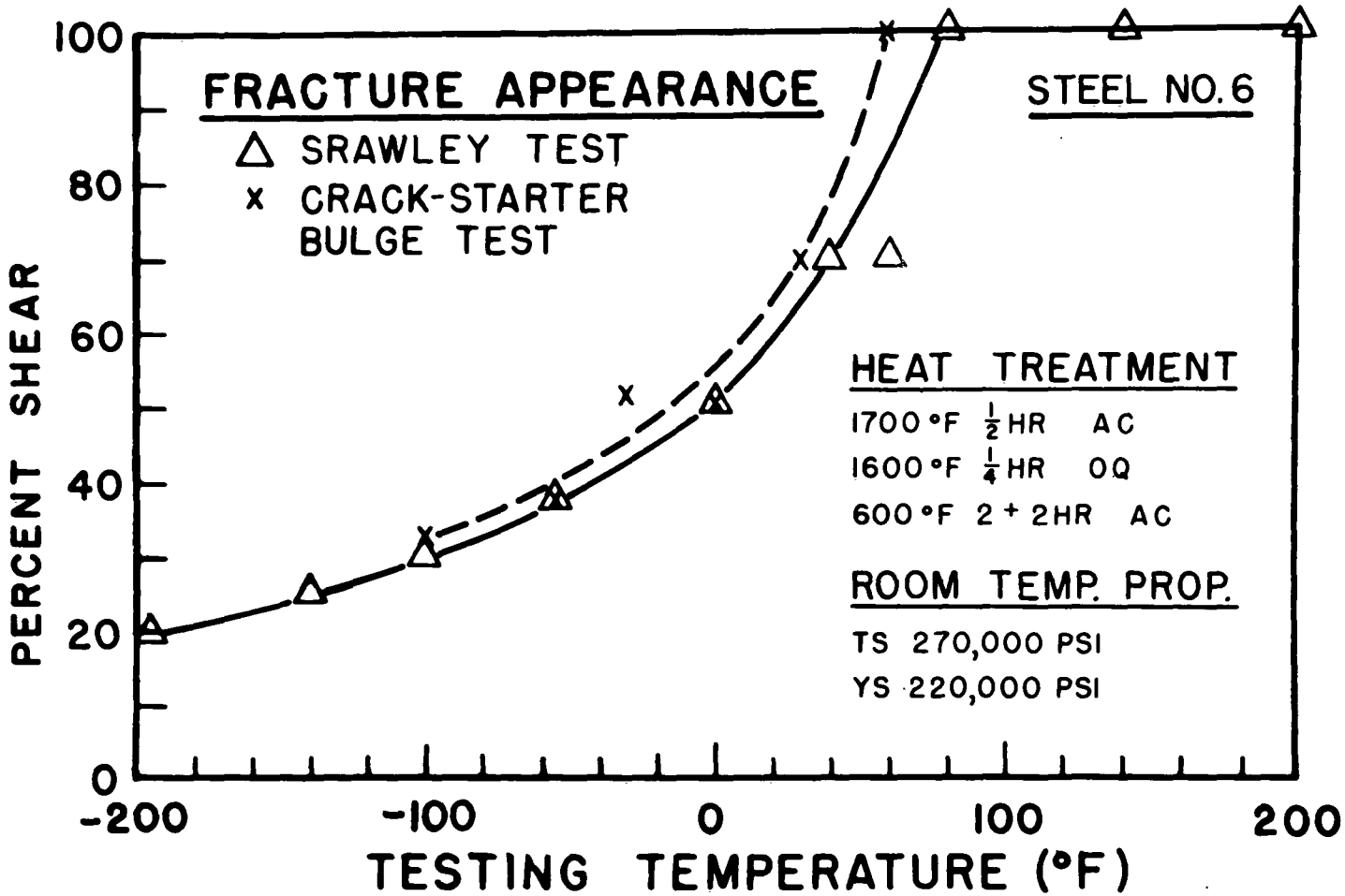
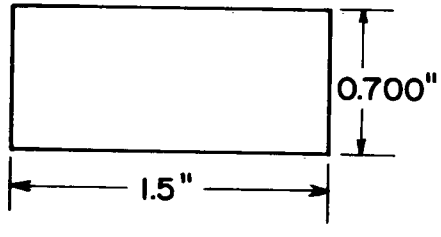


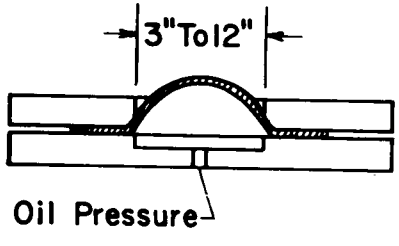
Figure 8. - Comparison of fracture appearance (percent shear) as a function of testing temperature for NRL impact bulge tests and center cracked tensile tests for the same high strength steel sheet (Pusak, ref. 6).



UNNOTCHED BEND Hannik (Allison)

Three Point Bend Over 1/8" Radius With 1/4" Diam. Support Pins At 1" Span

Data: P_{max} And P_1 (Load At Onset Of Rapid Cracking)



HYDRAULIC CIRCULAR BULGE

Data: Pressure
Plate Deflection
Strain Distribution

Armour Inst. Aerojet (Sacremento)

Figure 9. - Unnotched screening tests.

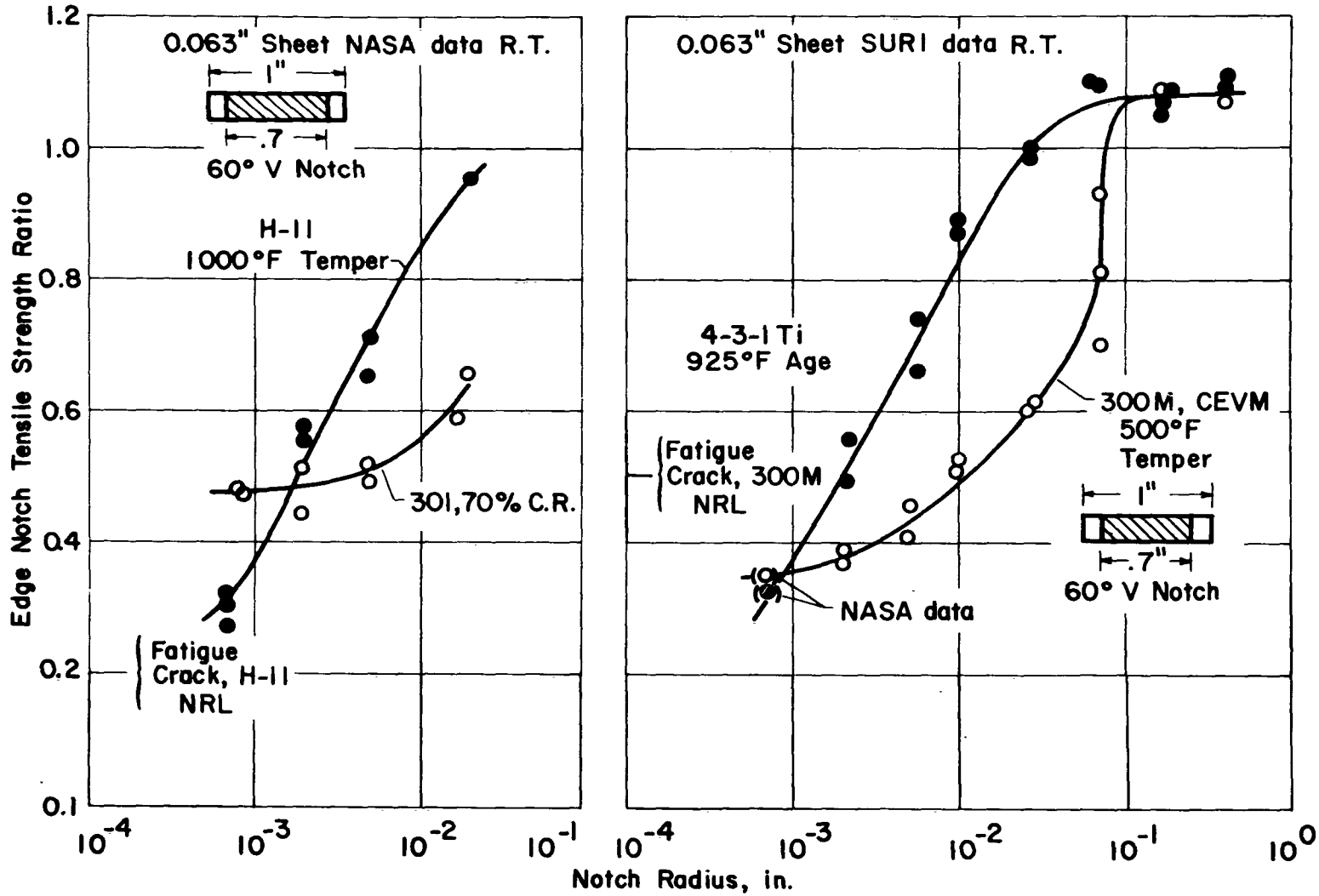


Figure 10. - Effect of notch radius on the edge notch strength ratio for several alloys (Brown, ref. 7).

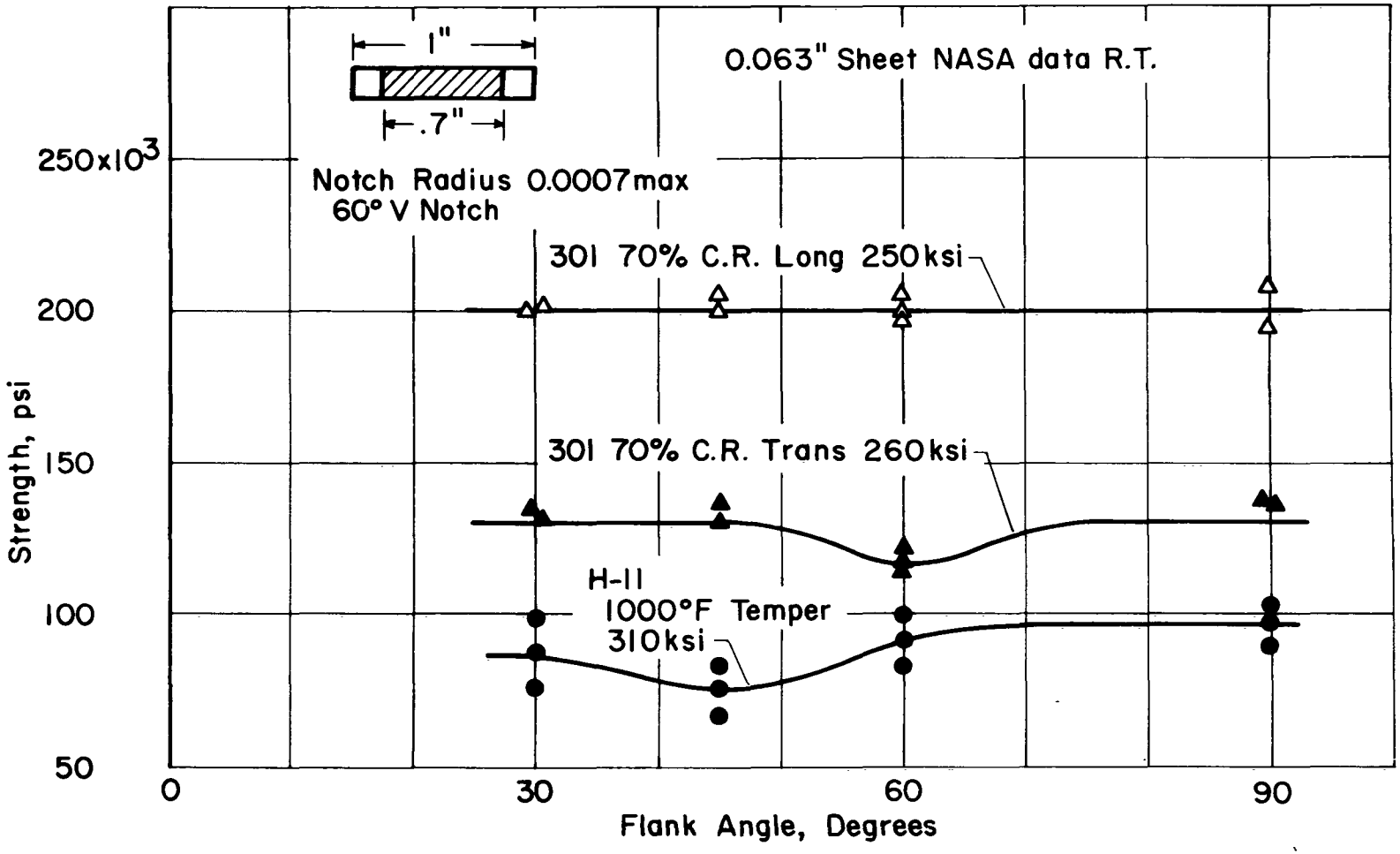


Figure 11. - Effect of flank angle on sharp edge notch strength of two alloys (Brown, ref. 7).

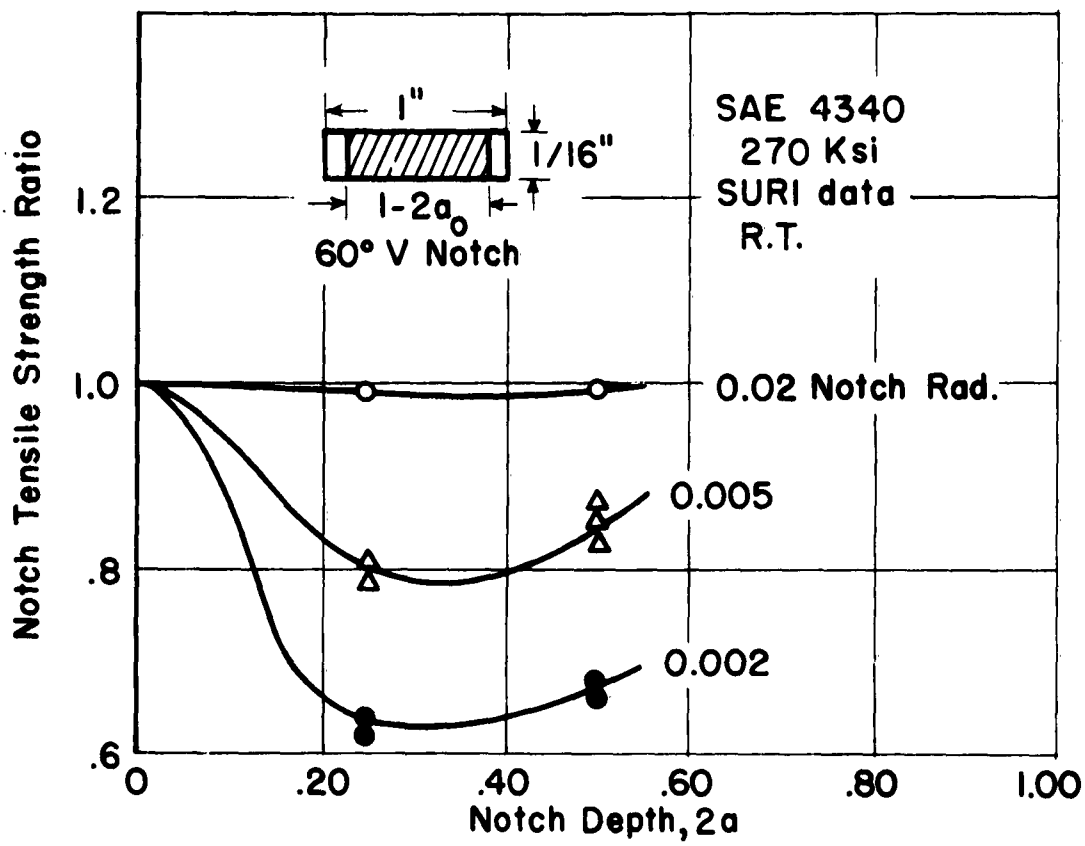


Figure 12. - Effect of notch depth on the edge notch strength ratio for several notch radii (Sachs, ref. 7).

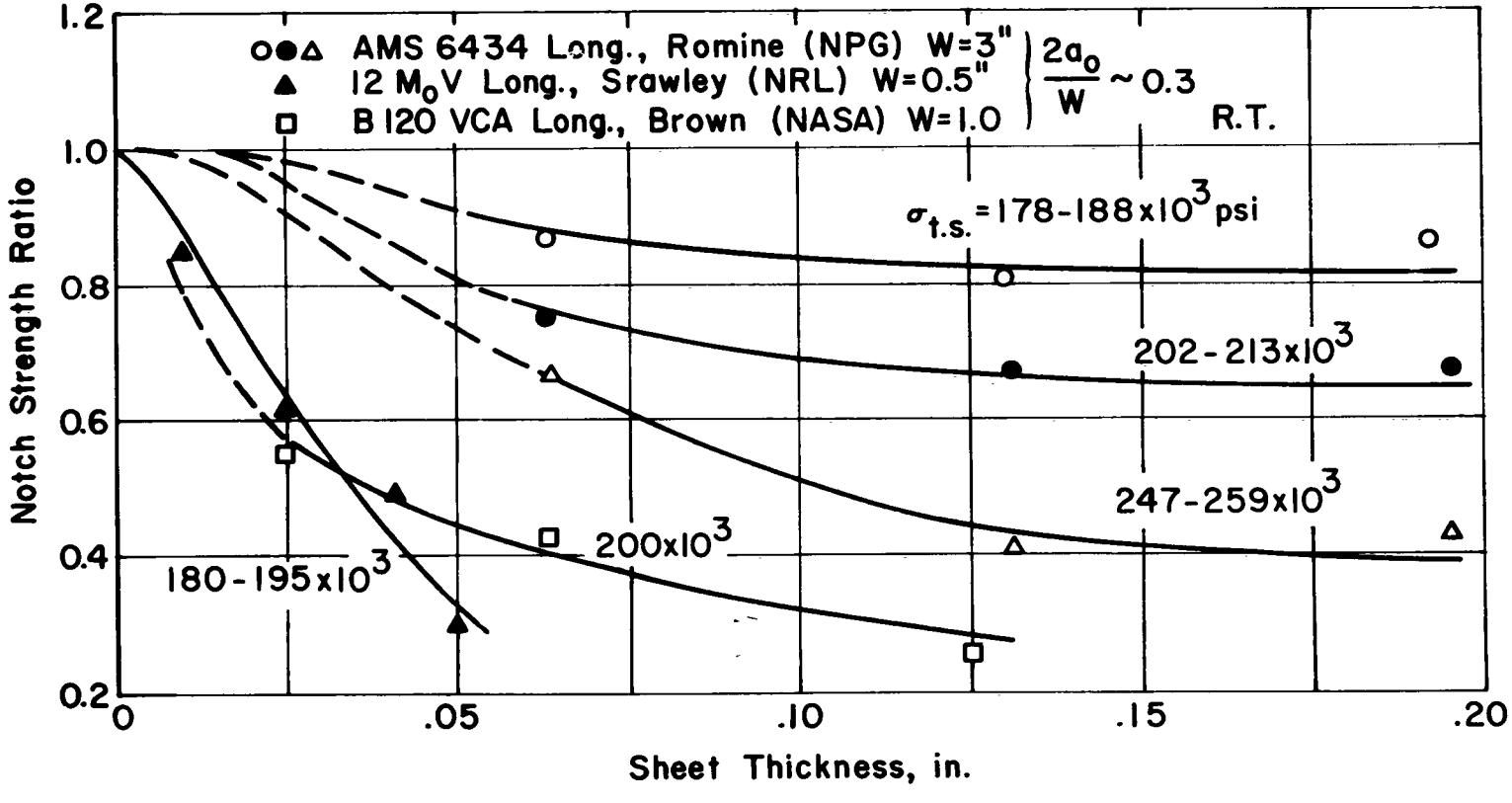


Figure 13. - Effect of sheet thickness on the strength of center cracked specimens.

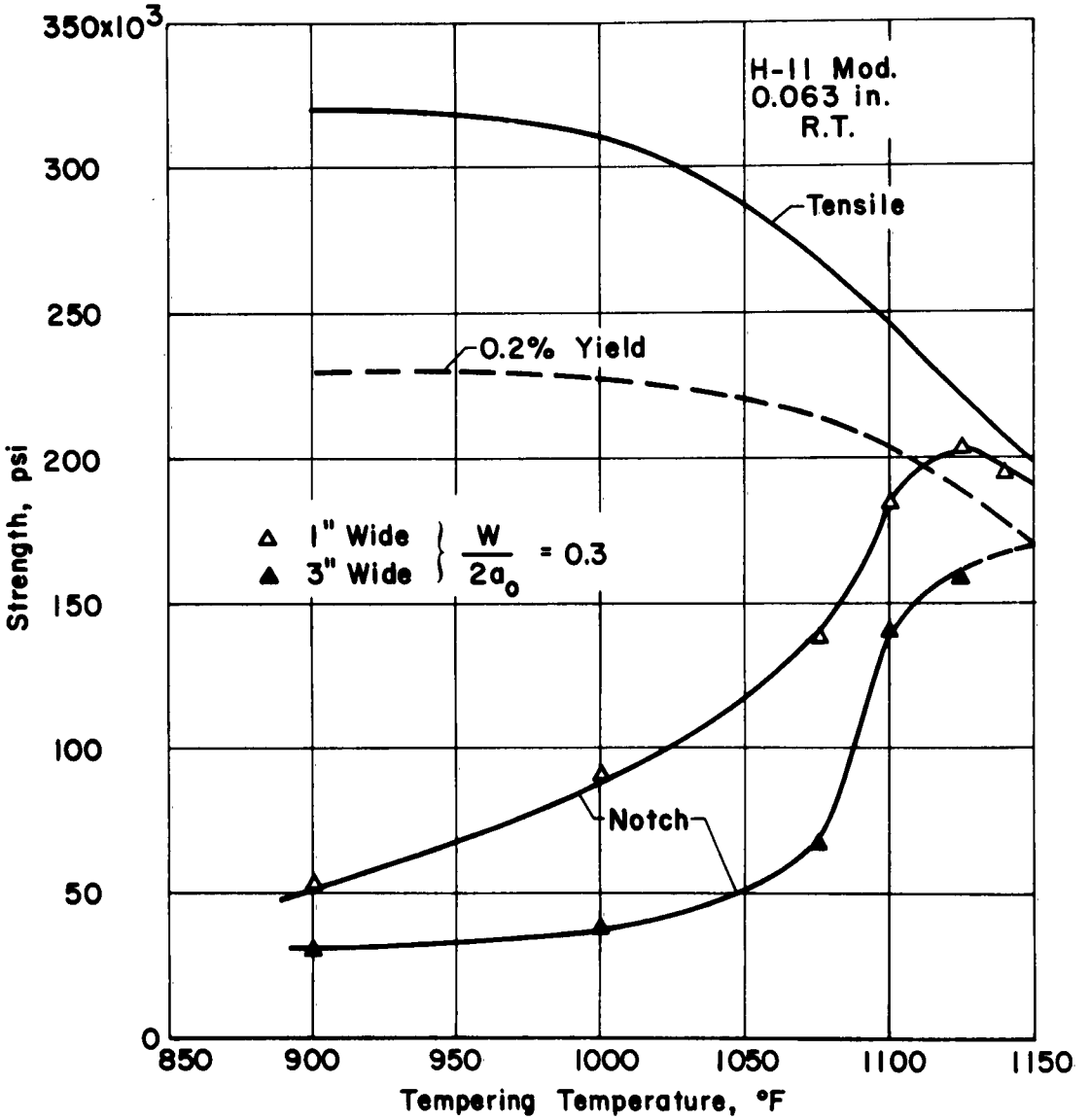


Figure 14. - Sharp edge notch tensile strength of H-11 Mod as a function of tempering temperature for one-inch and tree-inch wide specimens (Brown, NASA).

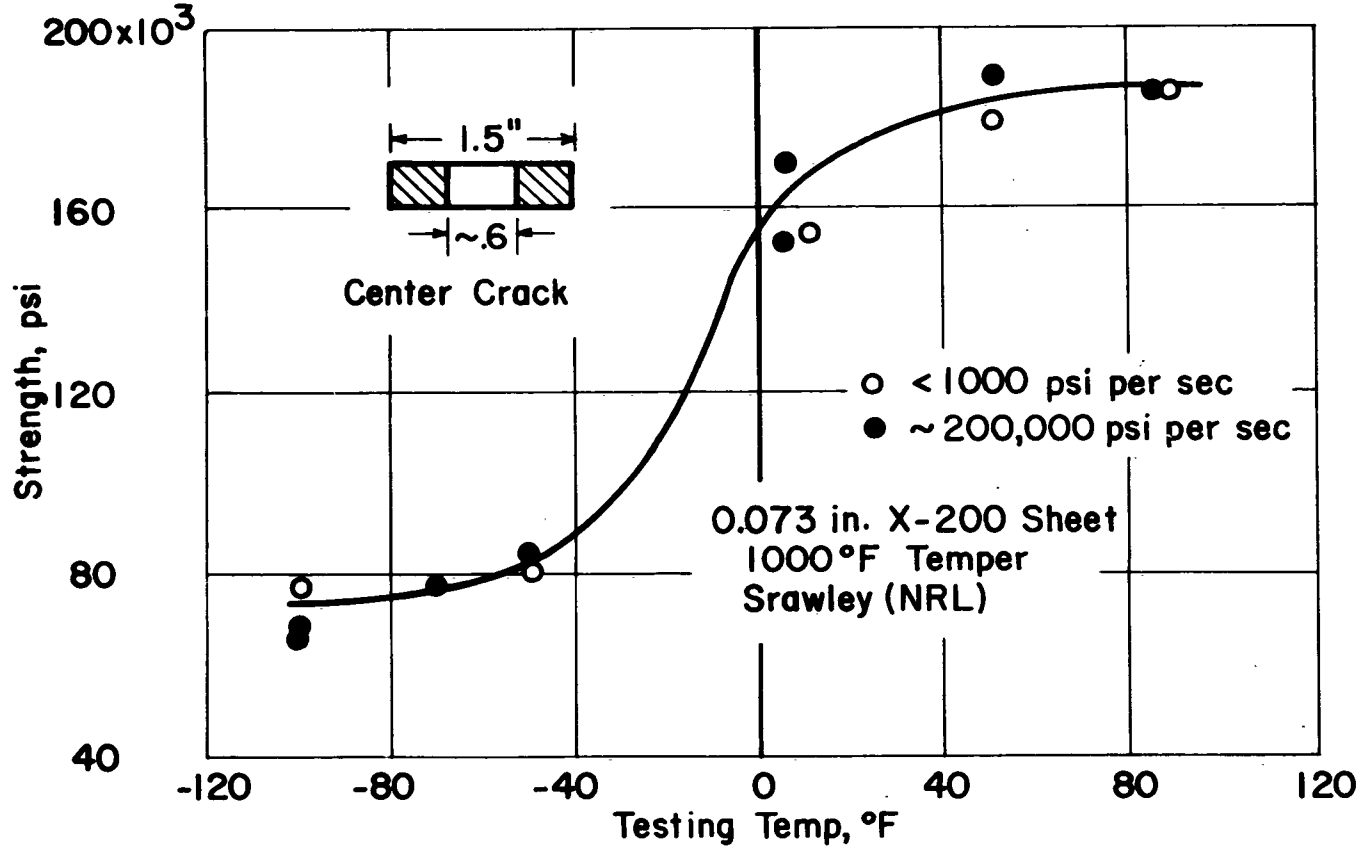
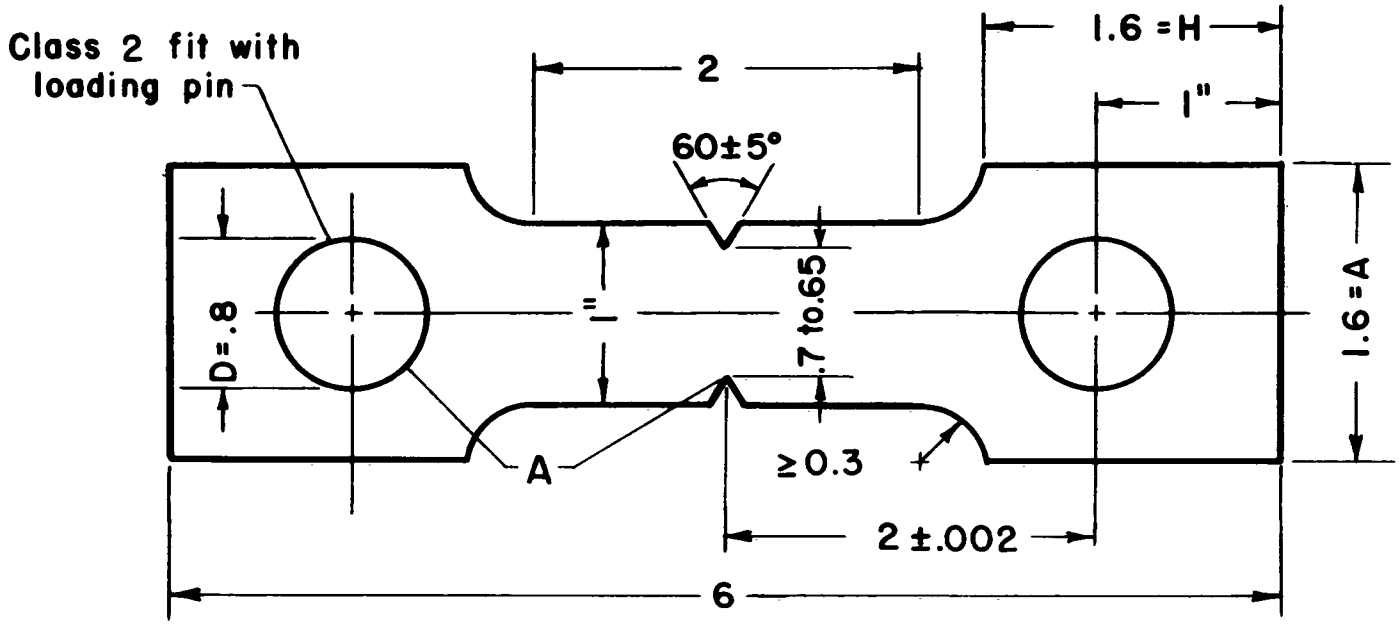


Figure 15. - Strength of center crack specimens as a function of testing temperature at two loading rates (Srawley, ref. 7).



A - Surface true to ℄ within 0.001 in.

Notch root radius = 0.001 max.

Unless otherwise noted, dimensions may vary ±1/32.

Figure 16. - ASTM proposed sharp edge notch screening test (ref. 7).

SPECIMENS EMPLOYED IN NASA-NRL COOPERATIVE PROGRAM

NOTCH TYPE	INVESTIGATOR	WIDTH, W IN.	$2a_o/W$
EDGE, 60^o; V; 0.0007 IN. RAD	BROWN (NASA)	1	0.3
		3	0.3
CENTER, SHEAR CRACK	KATTUS AND MORRISON (SRI)	1.2 & 1.3	0.37 & 0.34
		3	0.34
CENTER, FATIGUE CRACK	SRAWLEY (NRL)	1	0.3
CENTER, ELOX SLOT, 0.002 IN. RAD.	IRWIN (NRL)	3	0.3

NOTE: ALL SPECIMENS PIN LOADED

Figure 17.

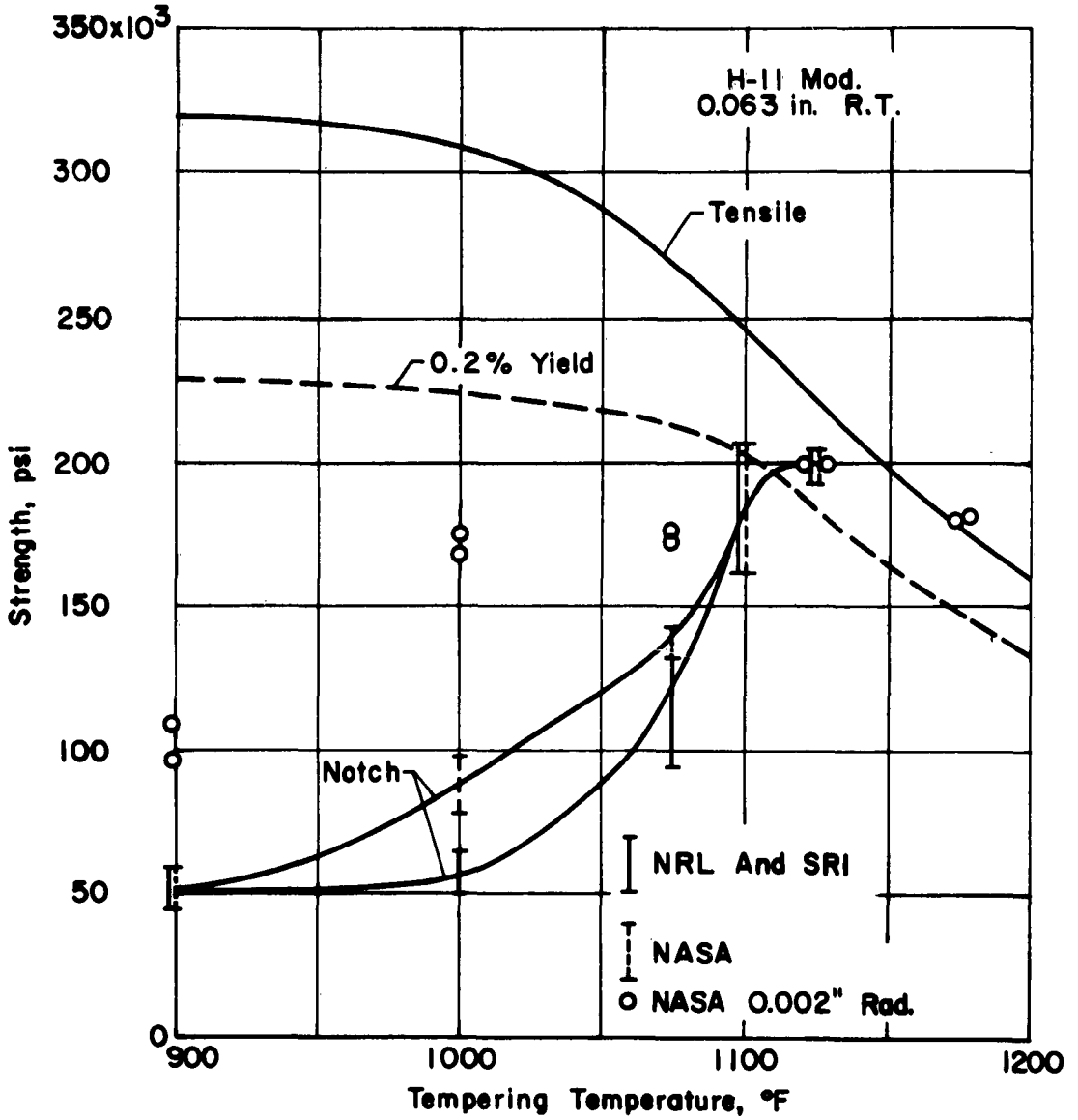


Figure 18. - Notch strength of various one-inch wide specimens as a function of tempering temperature for H-11 Mod (Brown, NASA).

E-1043

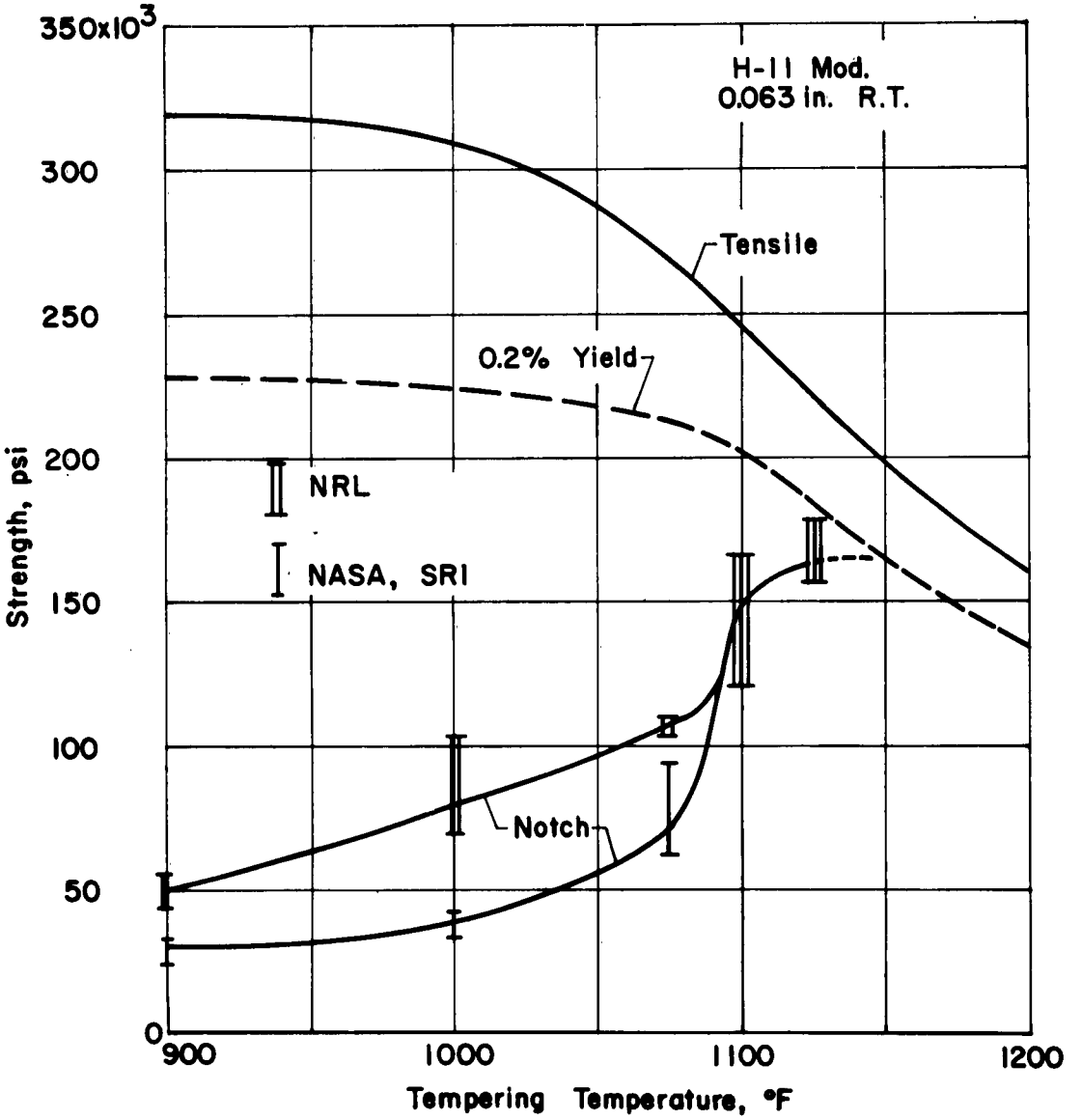


Figure 19. - Notch strength of various three-inch wide specimens as a function of tempering temperature for H-11 Mod (Brown, NASA).

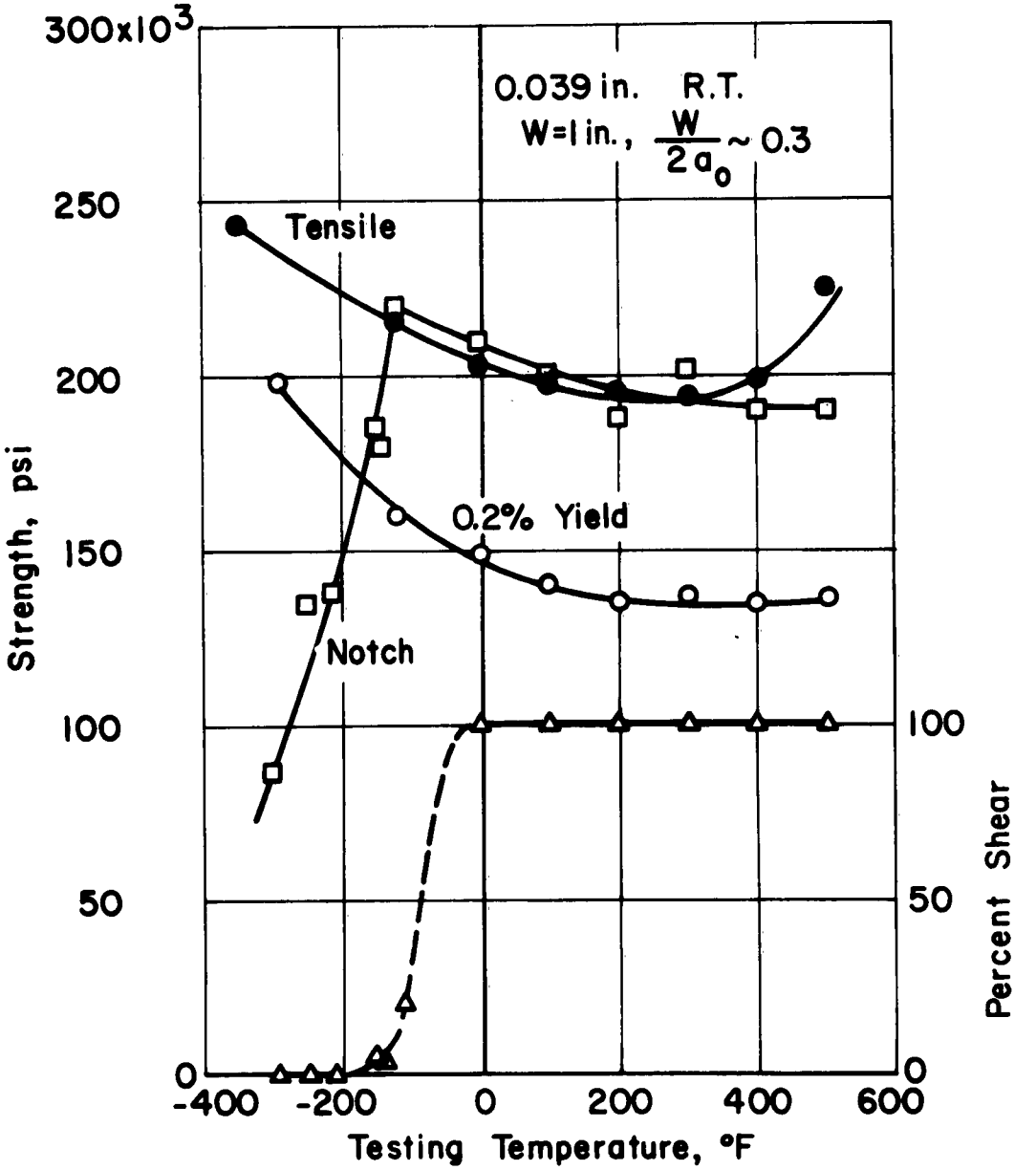


Figure 20. - Strength of NRL center crack specimens and fracture appearance (percent shear) as a function of testing temperature for AISI 410 steel sheet (Srawley, ref. 2).

E-1043

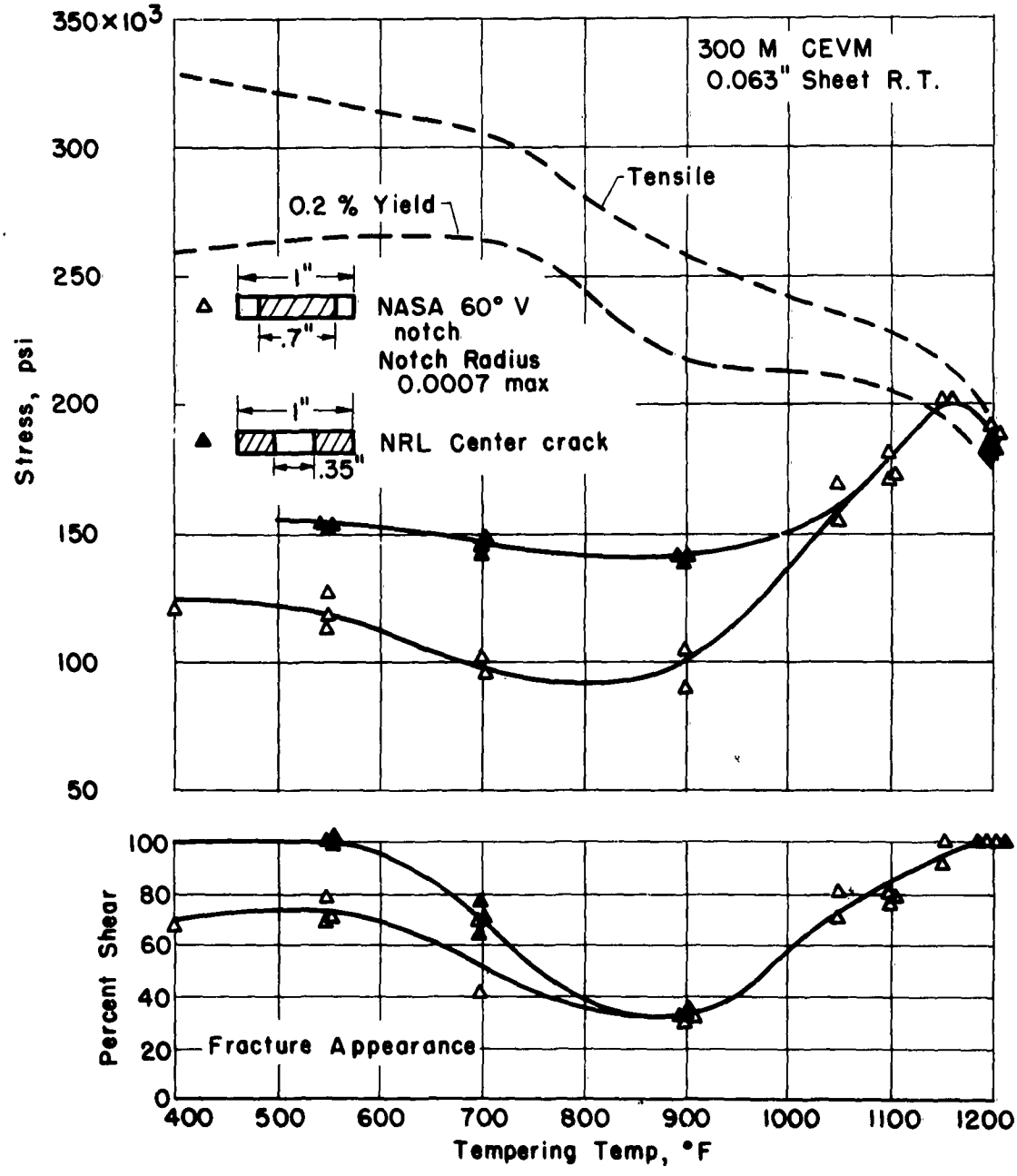


Figure 21. - Sharp edge notch strength, center crack strength and fracture appearance (percent shear) for 300 M tempered at various temperatures (Srawley and Brown, ref. 7).

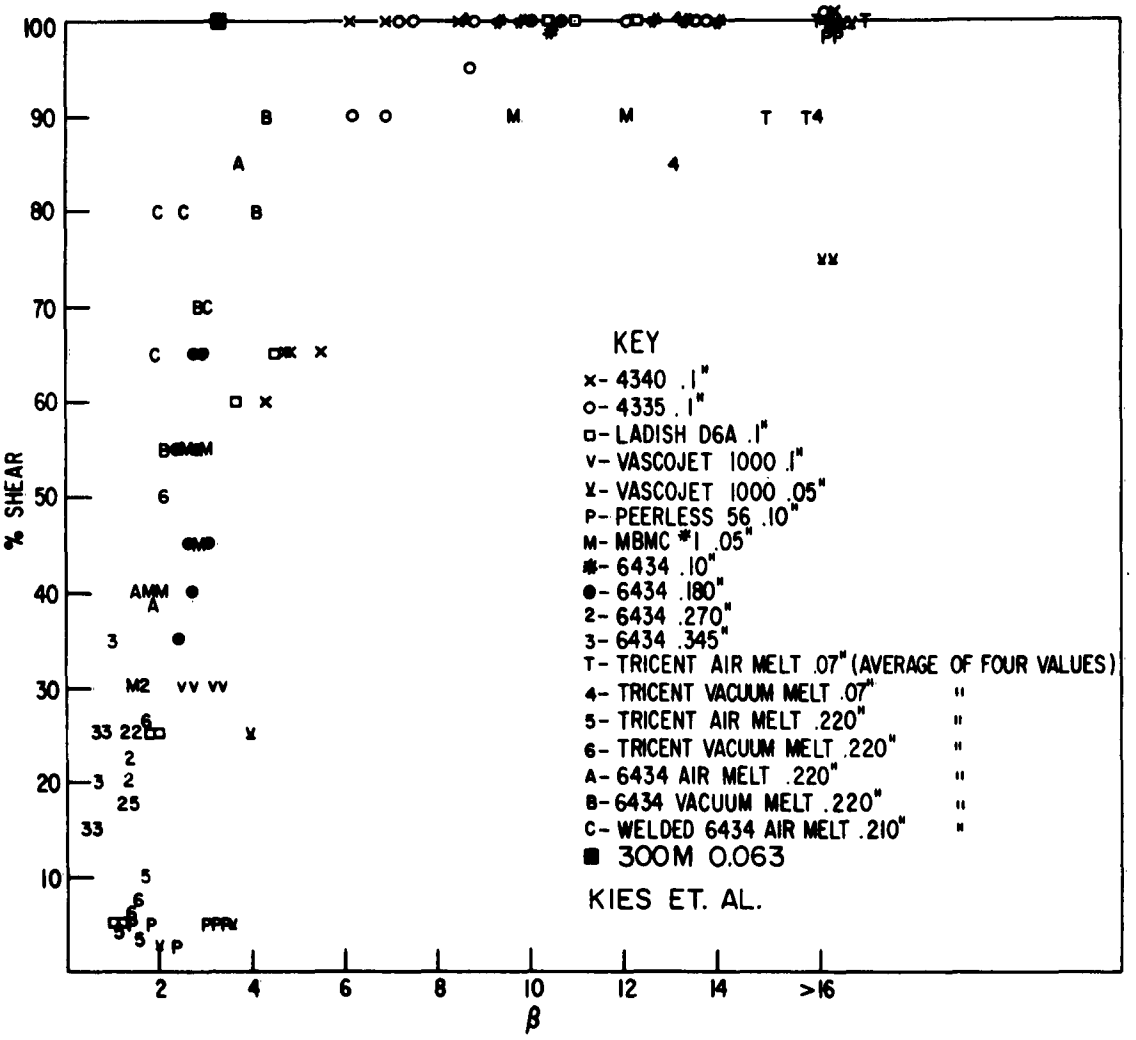


Figure 22. - Percent shear vs. the β factor for various steels tested at room temperature (Kies, ref. 18).

E-1043

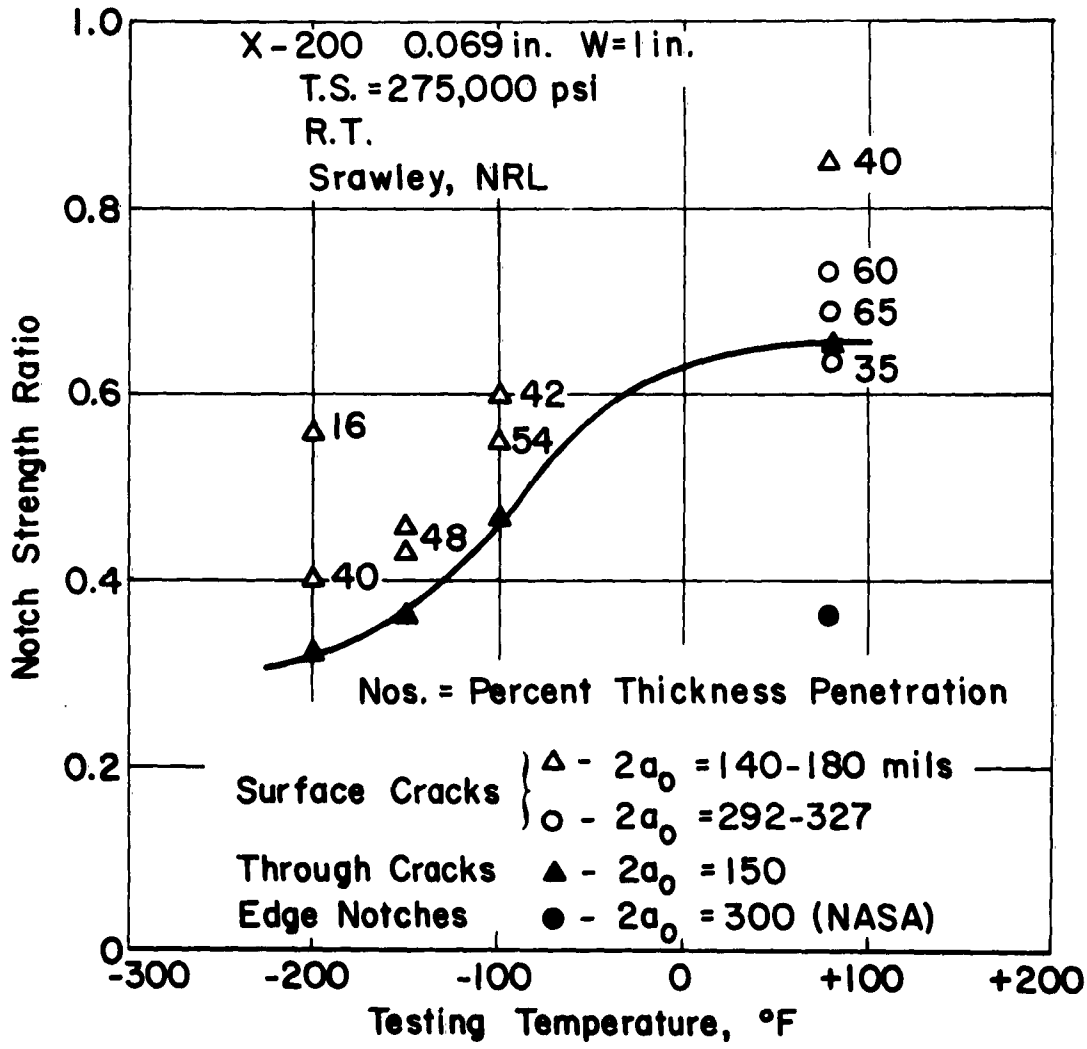


Figure 23. - Notch strength ratio as a function of testing temperature for specimens of a high strength steel provided with through the thickness cracks and cracks on one surface (Srawley, ref. 17).

ALLOY	YIELD STRENGTH $\times 10^3$, PSI	LOAD RATE	AIR	DISTILLED H_2O	INDIA INK	DISTILLED H_2O + $Na_2Cr_2O_7$ [3]	TRANS-FORMER OIL	COSMOLINE 1060 + H_2O
300M(C)	265	N [1]			85,000*			
		S [2]	-16%	-60%	-34%	0%	+13%	
300M(E)	242	N	117,000*		0%			
		S	0%	-40%	-18%			0%
300M(CEVM)	268	N			120,000*			
		S		-26%		+17%		
	195	N			195,000*			
		S		0%				
H-11 MOD.	223	N	80,000*					
		S	0%	-13%		0%		
	165	N			165,000*			
		S		0%				
6A1-4V-Ti AGED	160	N	110,000*					
		S		0%				
B120VCA AGED	195	N			67,000*			
		S		0%				

1. N - NORMAL LOADING RATE (30,000 PSI NOTCH SECTION STRESS PER MIN).
2. S - SLOW LOADING RATE (1500 PSI NOTCH SECTION STRESS PER MIN).
3. 2 OUNCES PER GALLON WATER.

* NOTCH STRENGTH REFERENCE LEVEL.

FIG. 24. - THE EFFECT OF VARIOUS MEDIA ON THE ROOM TEMPERATURE SHARP EDGE NOTCH STRENGTH OF SEVERAL 0.063-INCH THICK SHEET ALLOYS TESTED AT A NORMAL AND SLOW LOADING RATE.

NASA-CLEVELAND, OHIO E-1043

STANDARDIZATION OF TEST PROCEDURE FOR TEAR RESISTANCE OF METALLIC SHEET MATERIAL

By
T. J. STAPLETON
Lockheed Aircraft Corporation, Burbank, California

INTRODUCTION

Material limitations are increasingly becoming the critical factor in aircraft and space vehicle designs. The temperature developed both in the propulsion system and in the external structure due to aerodynamic heating preclude the use of lightweight aluminum and in many cases, titanium also. Refractory materials are therefore mandatory. Unfortunately, with very few exceptions, the refractory metals (steel, nickel, molybdenum tungsten, etc.) are 3 to 6 times denser than aluminum. For aircraft and space vehicles, the importance of developing the highest possible working stresses in these materials is evident. Metallurgists have recently made significant strides in this direction. Stainless steels are now available with ultimate tensile strengths in the 300,000 psi range. Unfortunately, these high strengths are almost inevitably associated with lower ductility and "notch sensitivity". The result is that a small, almost imperceptible crack, could precipitate complete failure of a structure at a stress well below the nominal tensile strength of the material. For tensile loaded structures, this resistance to crack propagation failure rather than tensile ultimate strength is therefore very frequently the criterion for the selection of both the material and the design allowable stresses.

ARTC Project W-97 was established with the objective of standardizing on a test procedure to evaluate a sheet material's susceptibility to "crack propagation" failure. At the outset, the project decided that design data could not be obtained from small "screening" specimens and that two types of specimen are required

1.) Screening Specimen
2.) Design Specimen

Immediate efforts were concentrated on the "screening" specimen and several such specimens were presented to the project for consideration. Although a considerable amount of data had been accumulated with these methods, the data were not on identical materials and experience indicated that "crack resistance" is very dependent on sheet thickness, grain direction, heat treatment and heat of material. To provide a reliable comparison of these methods, it was decided to conduct these tests on identical sheets of material. Several "typical" materials were selected to be evaluated by each of these methods. To provide a basis for comparison, large cracked specimens were fabricated from the same sheets of material. Close liaison was established with the ASTM Fracture Committee and several members of that group volunteered to perform further tests on these materials. The following individuals participated in the Project Activity.

ARTC Participants

Boeing		Convair	
E. J. Zapel	(Seattle)	T. T. Tanalski	(Astronautics)
W. R. Thurtle	(Wichita)	H. C. Turner	(San Diego)
G. B. Wadsworth	(Wichita)	G. D. Lindeneau	(San Diego)

ARTC Participants (cont.)

Douglas
- C. S. Yen (Santa Monica)
- P. R. McGowan (Long Beach)
- J. D. Cuzzolina Jr. (Long Beach)
- D. S. Warren (Long Beach)
- J. S. Supancic (Long Beach)

Lockheed
- R. W. Parcel (Missiles & Space Div.)
- F. R. Steinbacher (" " ")
- J. Rebman (Burbank)
- R. D. Schwartz (")
- T. J. Stapleton (" Chairman)

North American
- T. R. Dutko (Los Angeles)
- D. C. Riot (" ")
- W. A. Reinsch (" ")
- G. Fitch (" ")
- H. C. Ihsen (Downey)

Northrop
- W. H. McCarthy
- K. E. Kuschell (Norair)

Ryan
- A. F. Hofstatter

Other Participants

Naval Research Laboratory
- B. F. Brown
- G. R. Irwin
- K. R. McKinney
- H. L. Smith
- J. E. Srawley

Jet Propulsion Laboratory
- L. D. Jaffe
- A. J. Brothers
- H. E. Martens

NASA-Lewis Laboratory
- W. F. Brown, Jr.
- G. B. Espey

Rohr
- E. L. Kunz

Allegheny Ludlum
- F. K. Lampson

INTRODUCTION (Continued)

Other Participants (cont.)

Armco
- W. W. Rohde

Battelle
- W. P. Achbach
- E. W. Cawthorne
- J. E. Campbell
- H. B. Goodwin

Aerojet - General
- R. A. Rawe

Allison Division - General Motors
- D. K. Hanink

PURPOSE

The purpose of this report is to:

1. Present the Results and Conclusions of the industry-wide program sponsored by ARTC Project W-97 to evaluate various "screening" test methods for "tear resistance" of metallic sheet materials.

2. Describe the test method recommended by the Project.

CONCLUSIONS & RECOMMENDATIONS

1. A recommended notched specimen for screening purposes is described in Appendix "A". This is basically the same as the edge notched tensile coupon recommended by the ASTM Fracture Committee (Ref. 1).

2. It is recommended that this test be limited to evaluating the effect of the following variables on material "Tear Resistance".

   a. Test temperature
   b. Sheet thickness
   c. Process variables
   d. Variations in composition within a particular "class" of materials.

3. Within the variations of the notch specimens used in the program, the test data appear to verify the conclusion of the ASTM Committee that the notched-unnotched strength ratio is a fairly consistent material property provided that $K_t \geq 18$.

4. Based on available evidence, this sharp notched-unnotched ratio appears to provide as dependable an indication of a material's static crack resistance as any other small screening specimen.

5. The notched-unnotched tensile ratio is universally useful for screening purposes since anyone doing serious work will be running tensile tests and little additional equipment is needed.

6. However, no one test procedure is uniquely suited to measure a material's crack sensitivity. Each test provides additional information about a material's behavior (e.g., notched impact resistance, resistance to fatigue crack growth, etc.).

7. The material "Fracture Toughness" ($K_c = \sqrt{E \frac{dW}{da}}$) should be determined when close choices are to be made. For many materials under consideration, the small screening specimen will result in net failure stress $\geq$ yield stress. In this case, the K_c value obtained will be only a "minimum" value and a wider specimen will be required for a more accurate evaluation.

CONCLUSIONS & RECOMMENDATIONS (Continued)

8. It is recommended that another project be organized with the aim of establishing a standard test procedure for determining design criteria for tear resistance of metallic sheet material. There are now several methods in use for analyzing a structure to insure its resistance to crack propagation failure. Among these are the "Energy Method" (Ref. 1), the "Stress Concentration Factor Method" (Ref. 2), and also an effective width concept (Ref. 3). It will first of all be required to review these methods to establish which material parameter or parameters are required. Following this, it should be possible to standardize a test specimen and procedure.

SCOPE OF TEST PROGRAM

Thirteen proposed "screening" specimens were used to evaluate five materials:

2024-T3	Bare Aluminum Alloy
7075-T6	" " "
AM350 CRT850	Stainless Steel
AM350 CRT1050	" "
301XX Full Hard	" "

Relatively large (up to 30 in. wide) cracked specimens were fabricated from the same sheets of material and tension loaded to failure to provide a basis of comparison.

The two aluminum alloys were selected since the relative crack resistance of these two materials has been well established from service experience. (Because of its greater crack resistance, 2024-T3 has replaced 7075-T6 for the skins of pressurized fuselages.) Three typical high strength stainless steels were selected which, it was anticipated, would provide a relatively wide variation in crack resistance. It was not required that the "screening" specimens be able to rate all five materials collectively, but only that it rank the 2 aluminums in their correct relationship and likewise the 3 stainless steels.

For economy's sake, tests were basically limited to one grain direction (transverse) and one temperature (room temperature). The materials selected were known to be relatively insensitive to temperature in this region.

DESCRIPTION OF MATERIALS

The two aluminum alloys, 2024-T3 and 7075-T6, have both been used extensively in aircraft structures for many years and are now furnished with an extremely small range of variations in properties. The chemical compositions, as determined at Lockheed, are listed in Table I with the heat treatments in Table III. These materials were procured from Lockheed Production stores.

For the steel alloys, the chemical compositions, as furnished by the producer are included in Table II with the heat treatments listed in Table IV. The AM350 was procured from Lockheed stores and the 301XX FH sheet was furnished by Allegheny-Ludlum.

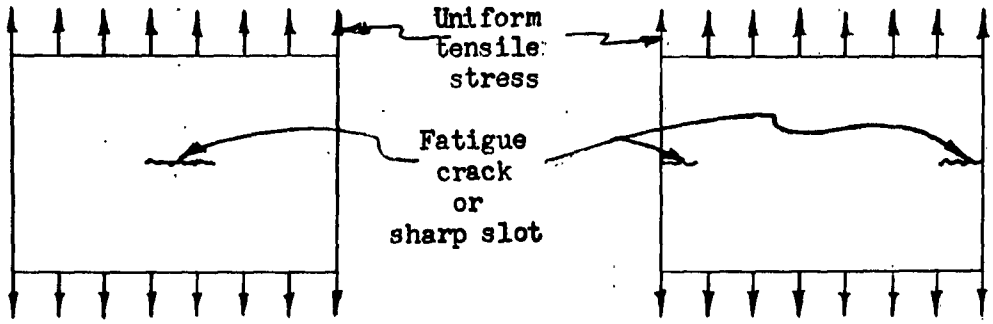
All materials were tested in the "as received" condition except the AM350 CRT1050. The "overaging" at 1050°F was performed at Lockheed.

The conventional tensile coupon properties of all the materials are listed in Table VII. Typical elongation vs. gage length curves for the 5 materials are included in Fig. 10.

TEST METHODS

"Control" Specimens"

The control specimens were all relatively large, (9 in to 30 in wide) sheet specimens in which either a central or edge crack was induced. This may either be a very sharp slot or a fatigue crack.



The specimens were loaded to failure in increments, while a record of the crack length was obtained. In a test of this type, after a certain load is reached, the crack begins to grow stably with increasing load. At a somewhat higher load and corresponding crack length, the crack will begin to grow "spontaneously" without any additional load. Depending on the material and the inertia of the loading mechanism, the specimen will either fail instantaneously at this point, or the load will slowly drop off as the crack progresses across the specimen. In either event, this maximum load and corresponding crack length are used as the bases of comparing the crack resistance of materials.

The results were interpreted in terms of the "Energy" Method (Ref. 1). As originally proposed by A. A. Griffith for brittle materials (Ref. 4) this theory stated that a constant quantity of energy was absorbed as a crack progressed through a particular material. It is now known that this energy varies considerably with various factors, including crack length and specimen size. For metallic materials, most of this energy is expended in the plastic deformation at the crack surface. The source of this energy is the elastic stored energy in the surrounding material which becomes available as the stress is released due to the crack growth. When the rate at which the elastic energy is released becomes equal to the required energy rate to propagate the crack, the crack will grow "spontaneously". The rate at which energy is absorbed with crack growth is expressed as "$\frac{dw}{da}$" $\left(\frac{\text{in - lbs}}{\text{in}^2}\right)$ which may be thought of as the work expended in forming a unit area of cracked surface. Another material property involved is the modulus of elasticity "E". The significant material parameter then is E $\frac{dw}{da}$ which is a measure of a material's crack resistance.

Neglecting secondary effects, which unfortunately in practice cannot be ignored, it may be shown that

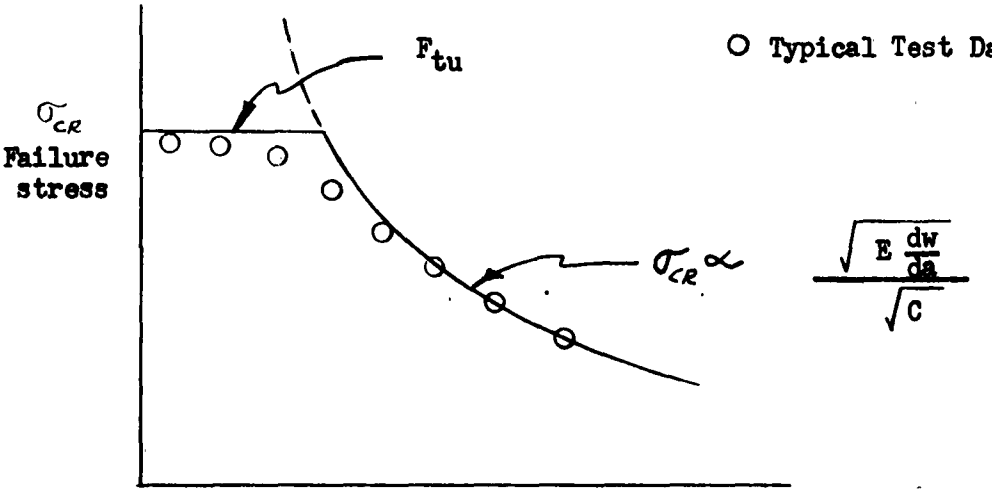
$$\sigma_{cR} \propto \frac{\sqrt{E \frac{dw}{da}}}{\sqrt{c}} \qquad \text{Eq. 1}$$

where
- σ_{cR} = critical gross area stress (psi)
- E = modulus of elasticity (psi)
- c = critical crack length (in)
- $\frac{dw}{da}$ = rate at which energy is absorbed in expanding a crack per unit area $\left(\frac{\text{in-lbs}}{\text{in}^2}\right)$

TEST METHODS (Continued)

There are at least two pronounced "correction factors" to this equation. First, in the region of the crack, the material is strained far into the plastic region and the ordinary linear relationship between stress and strain upon which Eq. 1 is based is not valid. Second, all specimens and structures have finite geometries, and these "boundary conditions" enter the picture. Unfortunately, the magnitude of these effects vary considerably depending upon the material. A graphical method of accounting for these factors quantitatively is presented by Dr. Irvin of the Naval Research Laboratory in Ref. 1. Dr. Irvin uses $K_c = \sqrt{E \frac{dw}{dA}}$ which he terms the "Fracture Toughness" as a measure of a material's crack resistance. The control specimen results are interpreted on the basis of this method.

An examination of Eq. 1 will give an indication of the difficulty in obtaining reliable "K_c" values from small "screening" specimens. A small specimen, can only have a short crack. Optimum results seem to come when the crack length is in the order of 1/4 to 1/3 of the specimen width. From Eq. 1, as the crack length decreases, a higher σ_{cr} results. Consequently a minimum length crack is required to avoid a net tension failure.



In practice, when the net fracture stress is greater than the material yield strength, the "K_c" value obtained is only considered as a "minimum" value for the material, and a larger specimen is used if a closer approximation of "K_c" is desired.

"Screening" Specimens

With two exceptions, the "screening" specimen results are interpreted in terms of either a non-dimensional notched-unnotched strength ratio, or an energy absorption value. Energy is either measured by a notched impact test or by slowly "tearing" a specimen and measuring the area under the load-head travel curve.

SCREENING SPECIMENS

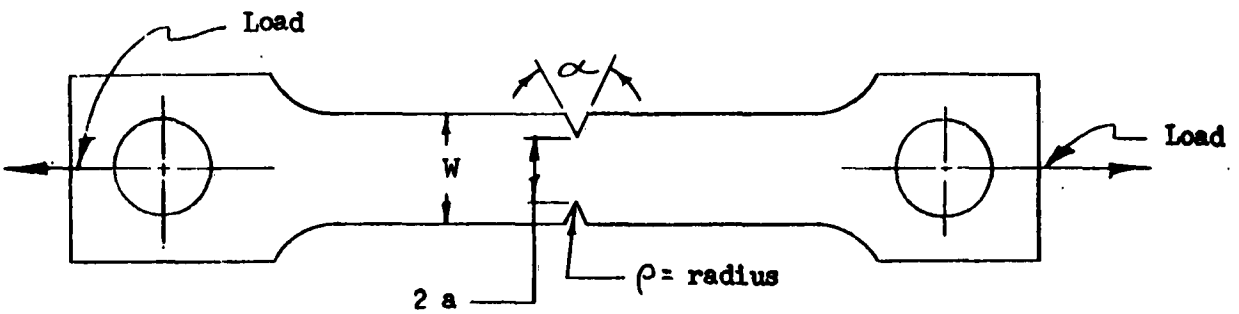
Notched-Unnotched Ratio Criterion	Energy Criterion		Others
	Notched Impact Tests	"Tear" Tests	
Douglas Notched Tensile Coupon	Drop Ball Impact	Kahn Tear Test	Fatigue Crack Growth Rate
Convair Notched Tensile Coupon	Charpy Impact	Douglas Tear Test	Unnotched Bend Test
NASA Notched Tensile Coupon	Notched Tensile Impact		
JPL Notched Tensile Coupon			
NRL Notched Tensile Coupon			
4" Wide Cracked Specimen			

TEST METHODS (Continued)

In addition, it is possible to interpret the notched tensile coupon results in terms of an energy parameter " K_c " by the method of Ref. 1. Unfortunately, for most of the materials under consideration, these small notched tensile coupons result in net fracture stresses greater than the material yield strength and the " K_c " values obtained may only be considered as "minimum" values.

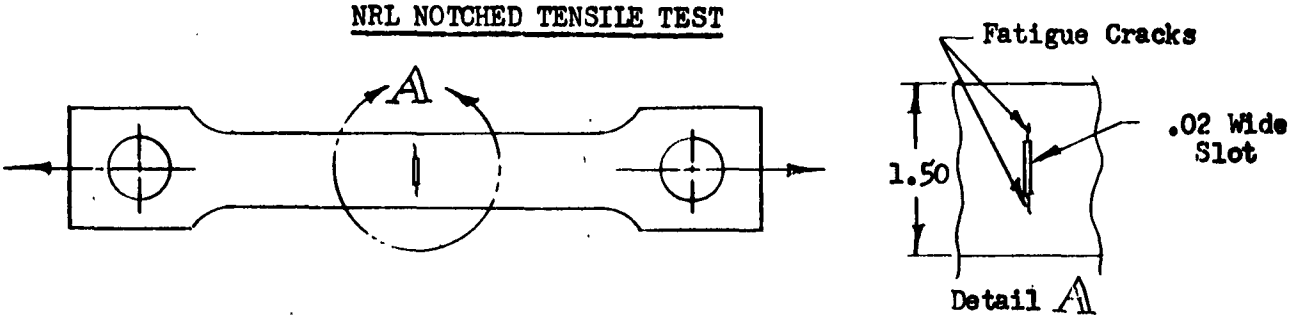
A very brief description of the various test methods is given below. Further details can best be obtained by contacting the appropriate individuals directly.

DOUGLAS, CONVAIR, NASA, & JPL NOTCHED TENSILE TESTS



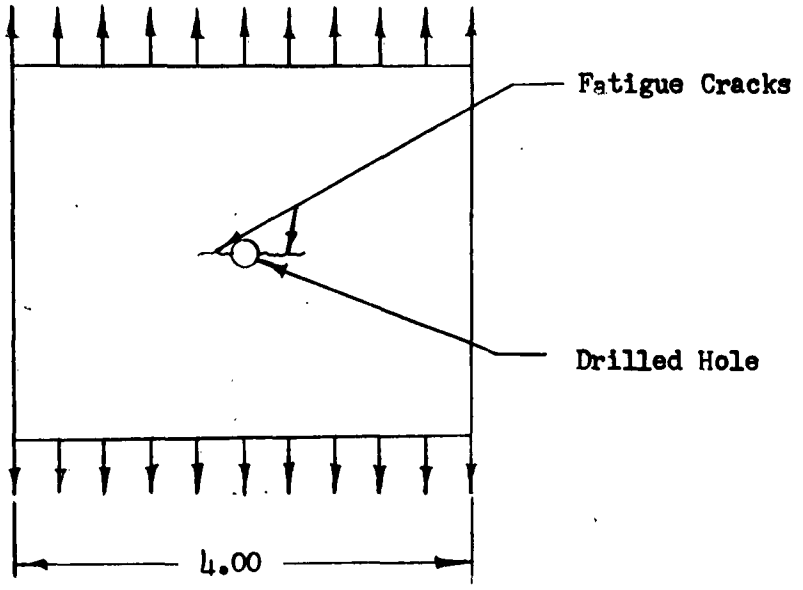
SPECIMEN	α	W (in)	ρ (in)	2 a (in)	$=\sqrt{\frac{a}{\rho}}$
Douglas	60°	.75	.002-.003	.53	10.0
Convair (for Alum)	45°	1.00	.001	.66	18.7
Convair (for Steel)	45°	1.00	.0035	.66	9.1
NASA	60°	1.00	.001 Max.	.70-.65	18.0
JPL	45°	1.50	.002 Max.	.886	15.0

NRL NOTCHED TENSILE TEST



This specimen is first fatigued until the desired length of fatigue crack is obtained (32 to 40% of the specimen width). Static tensile load is then applied to failure. Since the specimen is so small, the length of the fatigue crack is used as a basis of evaluation rather than attempting to measure the stable crack growth which is very slight. The net area notched tensile strength is compared to the unnotched tensile ultimate strength.

FATIGUE CRACK GROWTH TEST (Douglas)

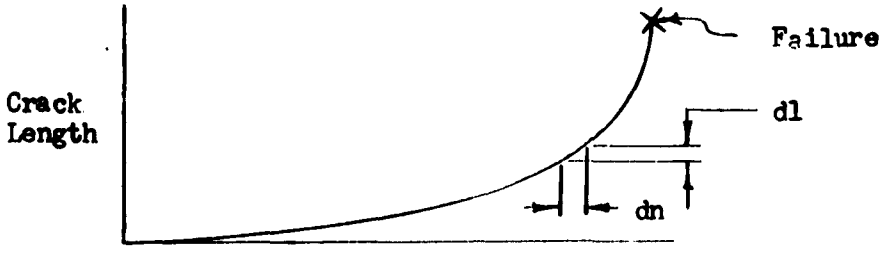


The specimen is fatigue loaded at 1 g $\pm \frac{2}{3}$ g

where

1 g gross area stress = 39.9 KSI for Steel
1 g gross area stress = 13.3 KSI for Aluminum

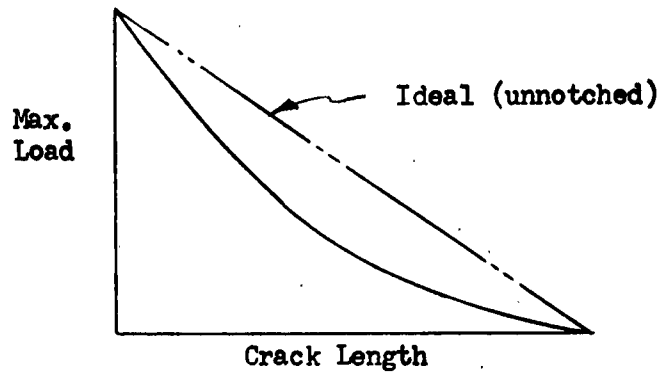
Crack growth is recorded to failure and plotted



TEST METHODS (Continued)

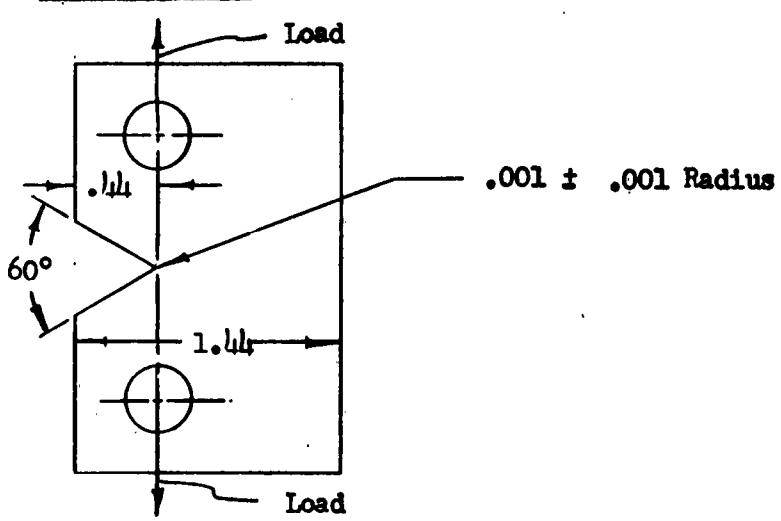
The slope of the curve, $\frac{dl}{dn}$, at a crack length of 1 inch is used as the quantitative measure of fatigue crack growth resistance; the lower the $\frac{dl}{dn}$ value, the better the material.

The Notched-Unnotched Strength of 4 inch Wide Cracked Specimens is obtained using the Douglas fatigue crack growth specimen. The test procedure is the same except that after the fatigue crack reaches a predetermined length, the fatiguing is stopped and the specimen is statically loaded to failure with crack growth measurements being taken. The maximum load and corresponding crack length are plotted

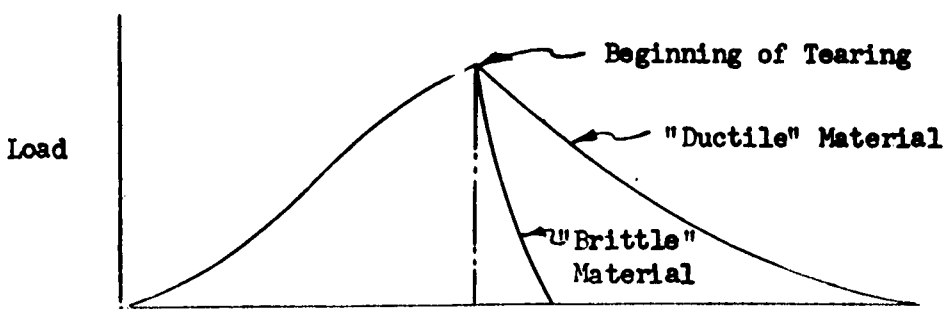


For quantitative evaluation, the notched-unnotched ratio when the sheet is cracked to 20% of its width is reported as a measure of crack resistance

KAHN TEAR TEST (Convair)

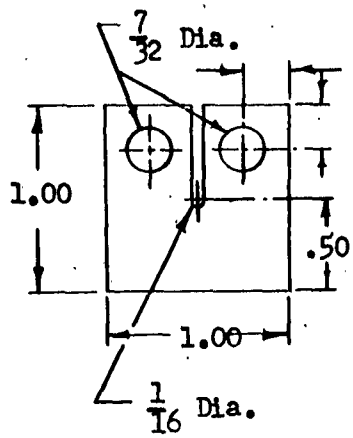


The specimen is continuously loaded to failure and a plot of load vs machine head travel is obtained

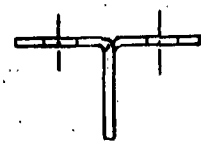


The area under this curve after tearing begins (ie maximum load) is a measure of the energy required to propagate the crack.

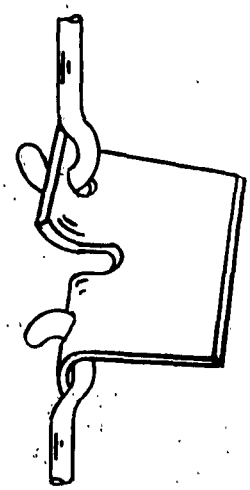
DOUGIAS TEAR TEST



FLAT PATTERN OF SPECIMEN



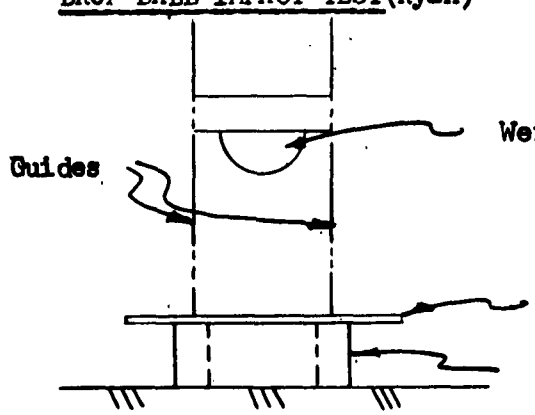
SPECIMEN WITH EARS BENT



SPECIMEN READY FOR TEST

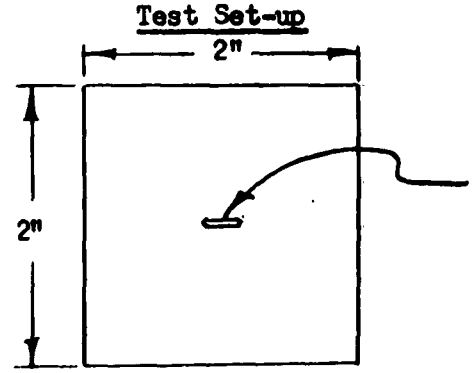
The test procedure is basically the same as for the Kahn Test with a plot of load vs. machine head travel being obtained. Once again the area under the curve after maximum load is used to measure "tear resistance".

DROP BALL IMPACT TEST(Ryan)



WT = 5.25 lbs.
Dia. = ½" dia.

Test Set-up



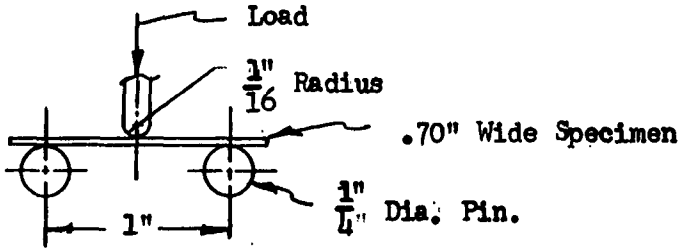
Specimen

TEST METHODS (Continued)

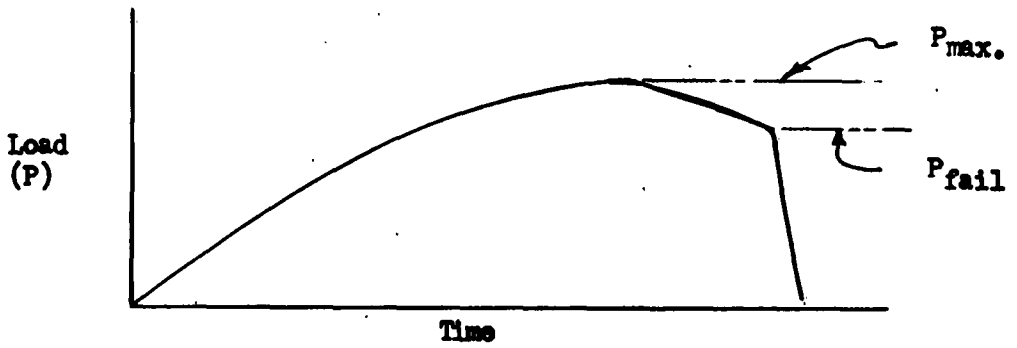
The weighted ball is dropped from successively higher levels until a crack develops at the ends of the elox slot. Each specimen is only struck once after which it is replaced. The potential energy of the ball at the highest level from which it may be dropped without cracking the specimen is used as the criterion of crack resistance. Several drops are made around this level to verify the results.

The Notched Tensile Impact Specimen (JPL) was the same as the JPL notched specimen Pg. 10 . Special fixtures were used to mount the specimen in a conventional impact testing machine so that axial impact load was applied to the specimen. Material comparisons are made on the basis of the energy absorbed in failing the specimen.

Allison Unnotched Bend Test



The specimen is loaded to failure at a constant crosshead speed of approximately 5 in/min. A record of load vs. time is obtained



The load reaches a maximum and then slowly drops off to a certain point at which time complete failure occurs. Observation of the specimen shows that at maximum load, P_{max}, a crack develops in the surface and slowly progresses through the section until P_{fail} when complete failure occurs. These loads are converted to corresponding bending stresses σ_{max} & σ_{fail} and the difference $\sigma_{max} - \sigma_{fail}$ is used as a criterion of crack resistance.

TEST METHODS (Continued)

Charpy Impact Test (Boeing)

These were standard "V" notch simple beam impact specimens except for thickness, since the sheet gages were considerably under the standard. (Ref. ASTM Standards Vol. 3) Steel doublers were bonded onto the ends of the specimens to bring them up to the standard width at the ends.

TEST RESULTS

A summary of the test results is presented in Table VII. For the most part, the "screening" test results are the average of 5 specimens and the "control" results of 2 specimens.

The Fracture Toughness values "K_c" are summarized in Table VIII which includes a tabulation of the maximum valid "K_c" values for various specimen widths based on the $F_{NET} = F_{TY}$ limitation (Ref. 1). These results are presented graphically in Fig. 1 and Fig. 2.

Both the Naval Research Laboratory and the Jet Propulsion Laboratory also furnished data on the percent shear lip observed, which are presented in Table V. A 100% shear lip indicates a completely "ductile" or "shear" failure, whereas 0% designates a completely "brittle" or "cleavage" failure.

In the case of the relatively wide centrally cracked specimens, buckling was observed. This is caused by the high shear stresses as the load is transferred around the ends of the crack. To evaluate the effect of this buckling, the NRL also furnished a comparison of "K_c" values obtained from specimens in which buckling occurred with those in which buckling was prevented by supporting the specimen against lateral deflection. These results are included in Table VI, which indicates that the effect of buckling on apparent "K_c" values was not excessive for the 12 in. wide specimens, varying from approx. 0 to 8%. However, this reduction may be expected to increase rapidly with specimen width and for this reason, all specimens wider than 12 in. were stabilized against buckling.

Centrally notched tensile tests were also conducted at the NRL to determine the effects of temperature on the subject materials. These data are presented graphically in Fig. 5 through Fig. 9.

DISCUSSION OF RESULTS

"Control" Specimens

An examination of Fig. 1 and Fig. 2 indicates a noticeable variation of "K_c" with specimen width. There does not appear to be a consistent pattern to this variation. For three materials, "K_c" increases with specimen width, in one case it remains relatively constant and in one it decreases. Although this variation is not excessive, it is sufficient to prevent any close quantitative correlation between the small "screening" specimens and the large "control" specimens. The ranking of the materials is, however, quite well defined by the "control" specimens viz.

Aluminum Alloys	Stainless Steels
2024-T3	AM350 CRT850
7075-T6	AM350 CRT1050
	301XX FH

The "screening" specimens were therefore compared primarily on the basis of the order in which they ranked the materials.

"Screening"Specimens

Most of the "screening" specimens ranked the materials in the same order as the "control" specimens. The exceptions were the 3 impact tests and the rate of growth of a fatigue crack, which reversed the rating of the tempering temperatures of AM350 CRT. This does not mean that these tests are unreliable, but rather it appears that they are evaluating a somewhat different material property or properties. These properties, particularly the rate of fatigue crack growth are certainly significant in materials evaluation.

Three of the materials proved too "tough" to be evaluated by either the Allison Bend Test or the "K_c" values from the notched tensile coupon. The latter does, however, provide a "minimum" K_c value which may be useful for "screening" purposes.

All the notched-unnotched tensile strength ratios as well as the KAHN and Douglas Tear Tests ranked the materials in the same order as the large "screening" specimens, although in the KAHN Test, one material (AM350 CRT1050) proved too tough to be evaluated quantitatively. This is curious since the large "control" specimens indicated that the 850 temper was even tougher than the 1050, although the KAHN test could evaluate it. Numerous unpublished data from ALCOA Research Laboratories indicate a close correlation between the KAHN Test and "K_c" values from 16 in. wide cracked panels for aluminum alloys with relatively low "K_c" values. However, for relatively tough aluminum alloys, there was no consistent correlation. **On the basis of presently available evidence, it therefore appears that the KAHN Test is primarily useful for distinguishing relatively "brittle" materials.**

DISCUSSION OF RESULTS (Continued)

"Screening" Specimens (cont.)

The effect of temperature on the materials' "notch toughness" is shown in Fig. 5 through Fig. 9 based on the NRL notched specimen. Included in these figures and also in Table V are fracture appearance data. These data are of particular interest when a material undergoes a "ductile" to "brittle" transition. However measurement of percent shear very often requires a considerable amount of judgement on the part of the observer and for this reason it does not lend itself to an industry-wide standard "screening" test.

The notched-unnotched tensile ratios are plotted vs. stress concentration factor K_t in Fig. 3 and Fig. 4. In view of the very considerable differences among the various specimens (notch angle, specimen width, method of notching, etc.) the scatter in results is not excessive. It appears that for high K_t values, the notched-unnotched ratio is a reasonably constant material property. The ASTM Fracture Committee in Ref. 1 concluded that there was little decrease in notched-unnotched ratio when K_t is increased beyond $K_t = 18$ (see coupon Fig. I-1). Figs. 3 & 4 tend to bear out this conclusion.

The notched-unnotched tensile strength was selected by the Project for the following reasons:

1. The ASTM Fracture Committee has tentatively adopted this method (specifically the NASA configuration) for "screening" specimens.

2. The specimen preparation and testing are relatively simple and most laboratories would not require any more equipment than is used for a conventional tensile test.

3. Within the variations of the notch specimens used in the program, these data appear to verify the conclusion of the ASTM Committee that the notched-unnotched ratio is a fairly consistent material property provided that the $K_t \geq 18$.

4. Based on available evidence, the sharp edge notched tensile coupon appears to provide as dependable an indication of a material's "crack resistance" as any other small "screening" specimen.

It is not meant to imply that this test should replace all the existing "screening" tests. As indicated previously, each test provides additional information about a material's behavior. In addition, it is recognized that the data accumulated to date are not sufficient to "conclude" the question of a "screening" specimen.

Since the notched-unnotched ratio is a non-dimensional reduction factor, its primary usefulness is for comparison of materials of approximately the same tensile strengths. It is suggested that the notched-unnotched ratio be used only as a preliminary "screening" test to evaluate the effects of:

DISCUSSION OF RESULTS (Continued)

"Screening" Specimens (cont.)

a. Test temperature
b. Sheet thickness
c. Process variables
d. Variations in composition within a particular "class" of materials.

For predicting quantitatively the behavior of materials in service, more sophisticated tests are required. It is therefore recommended that another project be organized with the aim of establishing a standard test procedure for determining the design criteria for tear resistance of metallic sheet material.

Scope of Proposed Design Project

It will first be required to review the methods now in use for analyzing structures to insure against crack propagation failures. As well as the "Energy Method" already mentioned, there are several other approaches currently in use. One of these is the "Stress Concentration Factor Method (Ref. 2). This factor is defined by an effective radius(ρ) at the crack tip in addition to a plasticity correction factor (η) both of which may be combined into a single material parameter ($\frac{\eta}{\rho^{1/2}}$).

Another method (Ref. 3) is to assume that the load being shed by the material in the cracked area is transferred to an "effective width" of material (ω_e) in front of the crack. Failure results when this full effective width is worked to the material ultimate strength. In this case, a material's crack resistance is expressed in terms of the effective width which is considered a basic material property.

A logical initial step would appear to be a survey of the industry to determine if there is sufficient agreement on the design parameters required. If the results are affirmative, it should then be possible to standardize on a test method or methods.

REFERENCES

1. Fracture Testing of High-Strength Sheet Materials: A Report of a Special ASTM Committee. ASTM Bulletin, Jan. and Feb., 1960.

2. A. J. McEvily, Jr., W. Illg and H. F. Hardrath "Static Strength of Aluminum Alloy Specimens Containing Fatigue Cracks", NACA TN3816, October 1956.

3. W. J. Crichlow, Lockheed Aircraft Corporation, "Ultimate Strength of Damaged Structures - Analysis Methods and Correlating Test Data" ICAF-AGARD Symposium on Full Scale Aircraft Fatigue Testing, June 9,10,11, 1959; Amsterdam, Netherlands.

4. A. A. Griffith "The Phenomena of Rupture and Flow in Solids" Philosophical Transactions of the Royal Society of London, England, Vol. 221, p. 163, 1920.

TABLE I

CHEMICAL COMPOSITIONS OF ALUMINUM ALLOYS

Material	Cu	Mg	Mn	Fe	Sg	Cr	Zn	Ti	Al
2024-T3	4.41	1.20	0.67	0.39	0.24	Nil	0.085	0.03	Rem.
7075-T6	1.25	2.25	Nil	0.35	0.19	0.19	5.10	0.093	Rem.

TABLE II

CHEMICAL COMPOSITIONS OF STAINLESS STEELS

Material	Heat Number	Chemical Composition									
		C	Mn	P	S	S_1	Cr	N_1	Mo	N	Cu
AM350	79726	.092	.83	.025	.011	.43	16.78	4.24	2.82	.092	.14
301	79284	.11	.78	.022	.017	.25	17.62	6.90	-	-	-

TABLE III

HEAT TREATMENTS OF ALUMINUM ALLOYS

Material	Solution Treatment	Quench	Ageing	Cold Work
2024-T3	910-930°F for 30 min.	Water	Room Temp.	Stretched
7075-T6	860-880°F for 30 min.	Water	245-255°F for 24 hrs.	None

TABLE IV

HEAT TREATMENTS OF STAINLESS STEELS

Material	Cold Rolled	Temper
AM350CRT850	Yes	850°F
AM350CRT1050	Yes	850°F 1050°F for 1 3/4 hrs.
301XXFH	Yes	None

TABLE V

FRACTURE APPEARANCE

Material	Percent Shear Lip						
	NRL Notched Tensile Coupon	JPL Notched Tensile Coupon		NRL Crack Propagation Spec.			
				30" Wide		12" Wide	
		Static Test	Impact Test	Center Crack	Edge Crack	Center Crack	Edge Crack
.050 2024-T3 Al. Alloy	90	100	100	100	100		
.050 7075-T6 Al. Alloy	70	90	90			68	67
.025 AM350CRT850 St.St'l	100	100	100			100	100
.025 AM350CRT1050 St.St'l	100	100	100			100	100
.020 301XXFH St. St'l	100	100	100			100	100

TABLE VI

EFFECT OF BUCKLING ON 12 IN. WIDE CRACKED SPECIMENS

(Mat'ls Evaluated in Longitudinal Grain Direction)

Crack Location	Material	K_c $\left(10^3 \frac{psi}{in^{\frac{1}{2}}}\right)$		% Drop in K_c Due to Buckling
		With Buckling Prevented	With Buckling Permitted	
Center	.025 AM350CRT850	374	361	3.5
Center	.025 AM350CRT1050	315	290	7.9
Center	.021 301XXFH	168	155	7.7
Edge	.025 AM350CRT850	395	398	0.8(increase)
Edge	.025 AM350CRT1050	354	331	6.5
Edge	.021 301XXFH	181	176	2.8

TABLE III

ARTC PROJECT W-57

SUMMARY OF RESULTS OF TEST PROGRAM TO EVALUATE "SCREENING" TEST METHODS

TYPE OF TEST	STANDARD TENSILE COUPON			"SCREENING" SPECIMENS																"CONTROL" SPECIMENS									
				NOTCHED TENSILE COUPON						ALLISON BEAD TEST	DROP BALL IMPACT	KAHN TEAR TEST	CHARPY IMPACT TEST	FATIGUE CRACK GROWTH	DOUGLAS TEAR TEST	4" WIDE CRACKED SPECIMEN	NOTCHED TENSILE IMPACT	NOTCHED TENSILE COUPON		UNIAXIAL TENSION "CRACK PROPAGATION" SPECIMENS									
SOURCE & AFFILIATION	F_u, F_y & % ELONG. AVERAGE OF ALL REPORTED DATA				YEU DOUGLAS	TAULBEE CONAIR		BROWN NASA	MARTENS JPL	SRAWLEY LRC	HAVILUK GEN. MOT.	HOFFATTER RYAN	TURNER CONVAIR	ZAPEL BOEING	YEU DOUGLAS	YEU DOUGLAS	YEU DOUGLAS	MARTENS JPL	MARTENS JPL	SRAWLEY LRC		SCHWARTZ LOCKHEED	SMITH LRC				ZAPEL BOEING			
				SPEC. WIDTH (IN.) NOTCH LOCATION NOTCH RADIUS K_t	.75 EDGES .002-.003 10	.100 .001 187	.100 .0005 5.1	1.00 EDGES .001 MAX. 18	1.50 EDGES .002 MAX. 15	1.50 CENTER EDGES* 2.2*																			
																					APPROX. SPEC. WIDTH (IN.)	5	30	30	12	12	25	24	20	17
																					CRACK LOCATION	CENTER	CENTER	EDGES	CENTER	EDGES	CENTER			
QUANTITY MEASURED	F_u KSI	F_y KSI	% ELONG. IN 2"	NOTCHED-UNNOTCHED STRENGTH RATIO						STRESS DROP BET. MAX. LOAD & FAIL (PSI)	ENERGY TO CRACK NOTCHED SHEET (IN.-LBS.)	ENERGY TO PROPAGATE CRACK (IN.-LBS) (IN²)	IMPACT ENERGY (FT.-LBS.)	FATIGUE CRACK GROWTH RATE (IN/N) (CYCLES)	WORK FOR TEARING (IN.-LBS) (IN²)	CRACKED UNCRACKED $\frac{F_{cy}}{F_y}$	IMPACT ENERGY (FT.-LBS)	$K_c = \sqrt{E\frac{G}{2A}}\left(10^3 \frac{PSI}{IN^2}\right)$ ◆		$K_c = \sqrt{E\frac{G}{2A}}\left(10^3 \frac{PSI}{IN^2}\right)$ ◆								
250 2024 T-3 AL. ALLOY	68.0	46.0	17.7		.78	.81		.80	.78	.75	∞	15.75	573	662	87	11052	.56	5.1	> 68.5	> 54		82.2	12.9*	15.5*				102.0*	101.8*	45.0*
250 7075 T-6 AL. ALLOY	80.7	71.5	9.5		.72	.76		.72	.68	.71	$.02 \cdot 10^6$	10.5	54	1.07	433	582	.42	6.8	52.3	5.38		51.8								
225 AM 350 CRT 850 ST. STL.	204.0	172.0	22.8		1.04		.97	.97	.97	.85	∞	14.44	1090	8.77	76	3132	.68	15.8	> 237.9	> 180		260			47.3	47.3			276*	
225 AM 350 CRT 1050 ST. STL.	201.1	185.1	11.1		.84		.71	.75	.72	.66	∞	47.25	——	10.0	27	2570	.54	17.1	> 175.6	> 135		205			374*(L)	395*(L)			262*	
220 301 KX FH ST. STL.	276.8	246.4	3.2		.51		.42	.52	.49	.50	$.25 \cdot 10^6$	5.45	313	1.14	1805	1477	.28	8.7	121.0	12.10		855			318*(L)	354*(L)	58.4*			
																									168*(L)	181*(L)				

NOTE:

1. ALL MATERIALS EVALUATED IN TRANSVERSE GRAIN DIRECTION EXCEPT THOSE INDICATED BY (L) WHICH WERE EVALUATED IN THE LONGITUDINAL GRAIN DIRECTION.
2. ◆ K_c VALUES DETERMINED BY METHOD OF ASTM BULLETIN, JANUARY 1960, PAGE 28.
3. * SPECIMEN CLAMPED TO PREVENT BUCKLING

V-66

TABLE VIII

ARTC Project W-97

FRACTURE TOUGHNESS K_c FOR VARIOUS SPECIMEN WIDTHS

Material	Maximum valid K_c for various widths at this strength level[1]	Measured K_c Smith NRL 30" wide	Zapel Boeing 20" wide	Smith NRL 12" wide	Schwartz Lockheed 9" wide	Srawley NRL 1½" wide	Martens JPL 1½" wide
2024 T3 0.050" thick	155 - 30" width 127 - 20" width 85 - 9" width 33 - 1½" width	129-133	102	—	82	(>54)[5]	(>69)
7075 T6 0.050" thick	190 - 20" width 150 - 12" width 130 - 9" width 54 - 1½" width	—	49[2]	47	52	51	52
AM350CRT850 0.025" thick	470 - 20" width 315 - 9" width 129 - 1½" width	—	276	—[3]	250	(>180)	(>238)
AM350CRT1050 0.025" thick	359 - 20" width 240 - 9" width 98 - 1½" width	—	262	—[3]	209	(>135)	(>176)
301XXFH 0.020" thick	690 - 20" width 460 - 9" width 189 - 1½" width	—	58[4]	—[3]	85	121	121

1 Determined as explained in ASTM Bulletin, January, 1960, page 32.
2 Specimen width 17 inches
3 Tests made in longitudinal direction, but results not compared with tests made in transverse direction
4 Specimen width 29 inches
5 Minimum value only, since specimen width inadequate

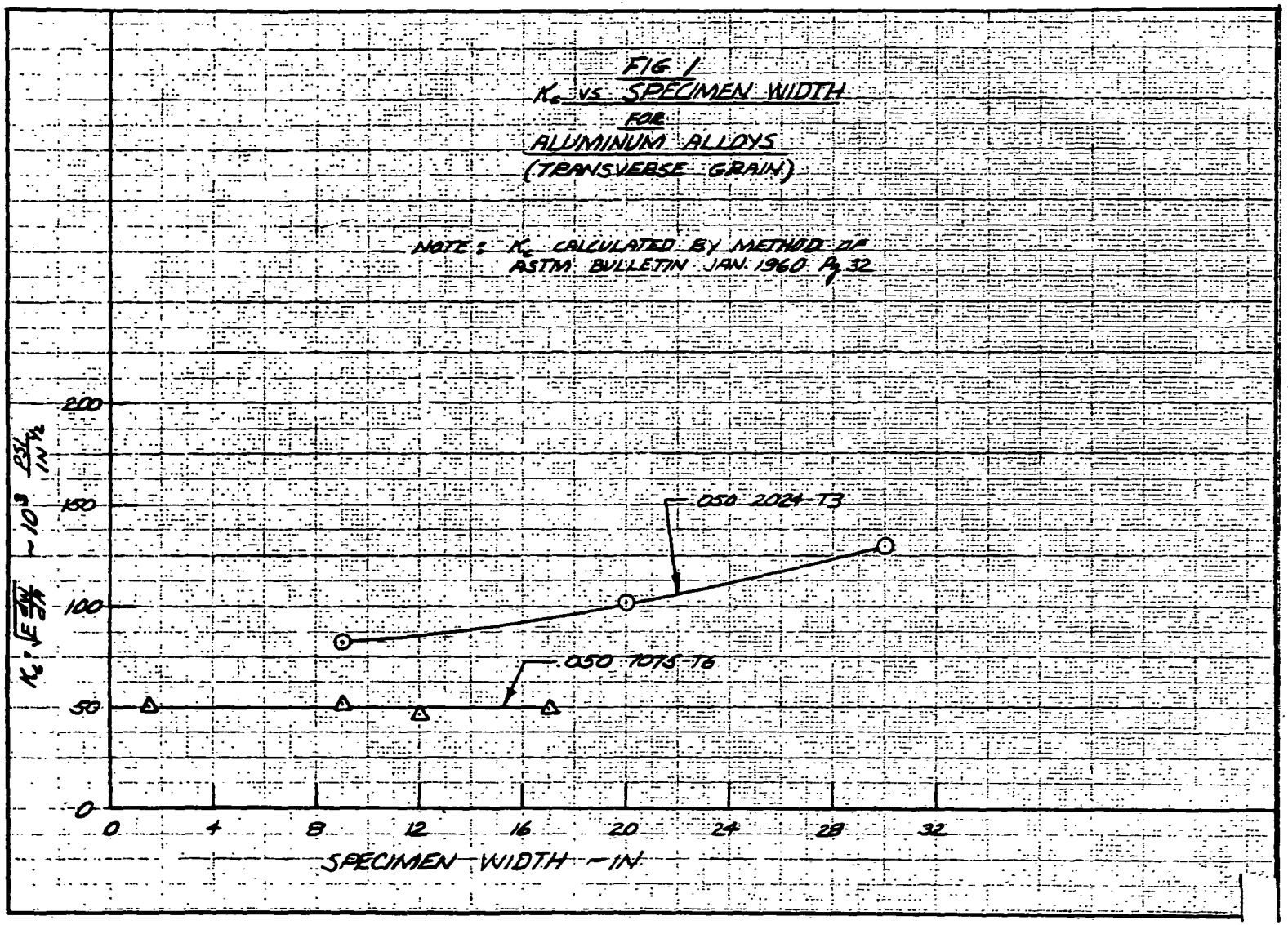

FIG. 1
K_c VS SPECIMEN WIDTH
FOR
ALUMINUM ALLOYS
(TRANSVERSE GRAIN)
NOTE: K_c CALCULATED BY METHOD OF ASTM BULLETIN JAN. 1960 Pg 32
050 2024-T3
050 7075-T6
$K_c \sqrt{\pi a} \sim 10^3$ PSI $\sqrt{IN}$
200
150
100
50
0
0
4
8
12
16
20
24
28
32
SPECIMEN WIDTH - IN

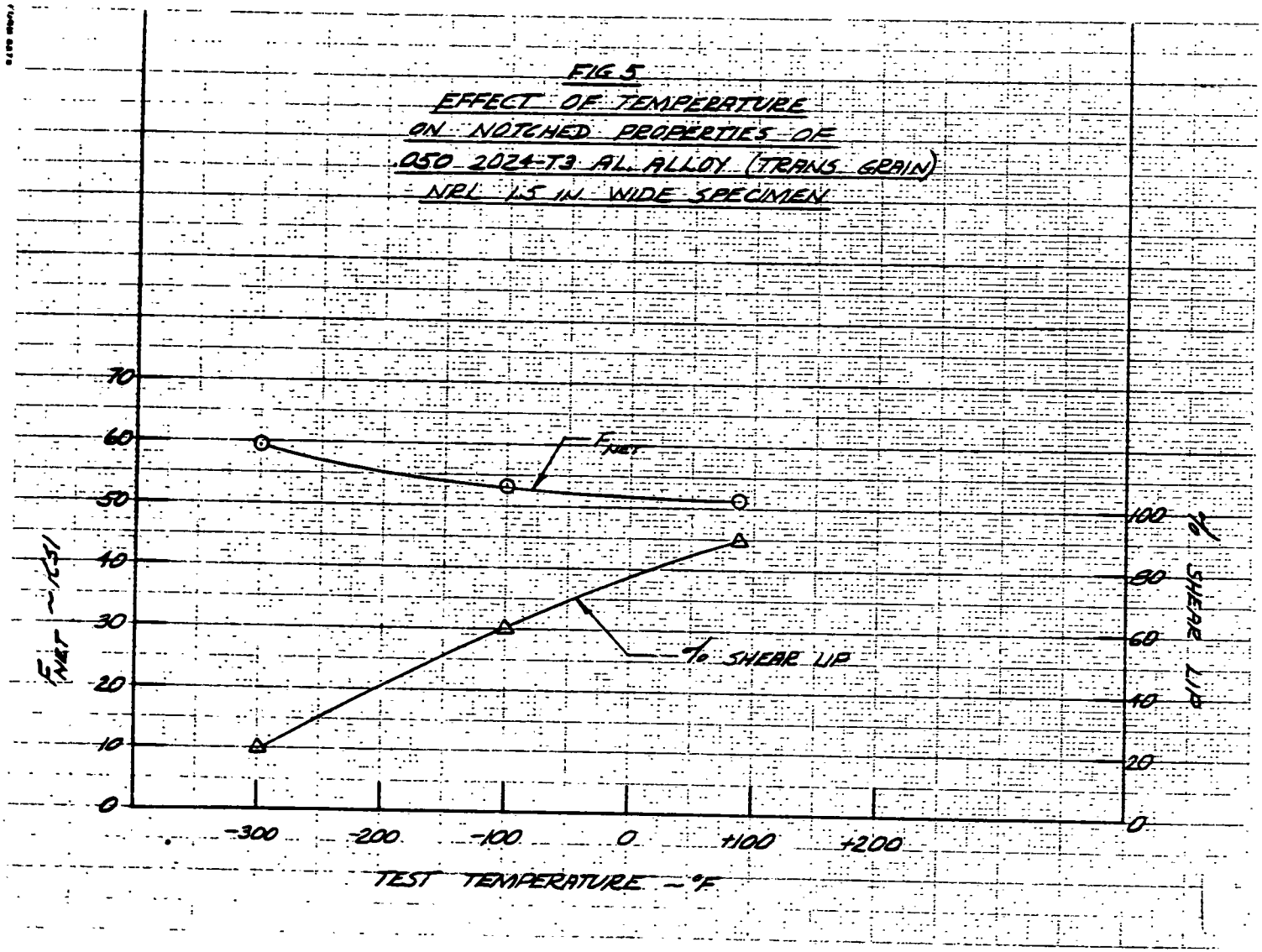
FIG. 2
K_c VS SPECIMEN WIDTH
FOR
STAINLESS STEELS
(TRANSVERSE GRAIN)
.025 AM350 CRT 850
.025 AM350 CRT 1050
.020 301 ANNEAL
K_c - ksi $\sqrt{in}$
NOTE:
K_c CALCULATED BY METHOD OF ASTM BULLETIN, JAN 1960 p 32
SPECIMEN WIDTH - IN
0
4
8
12
16
20
24
28
32
300
250
200
150
100
50

FIG 3
VARIATION OF NOTCHED/UNNOTCHED RATIO WITH K_t FOR ALUMINUM ALLOYS

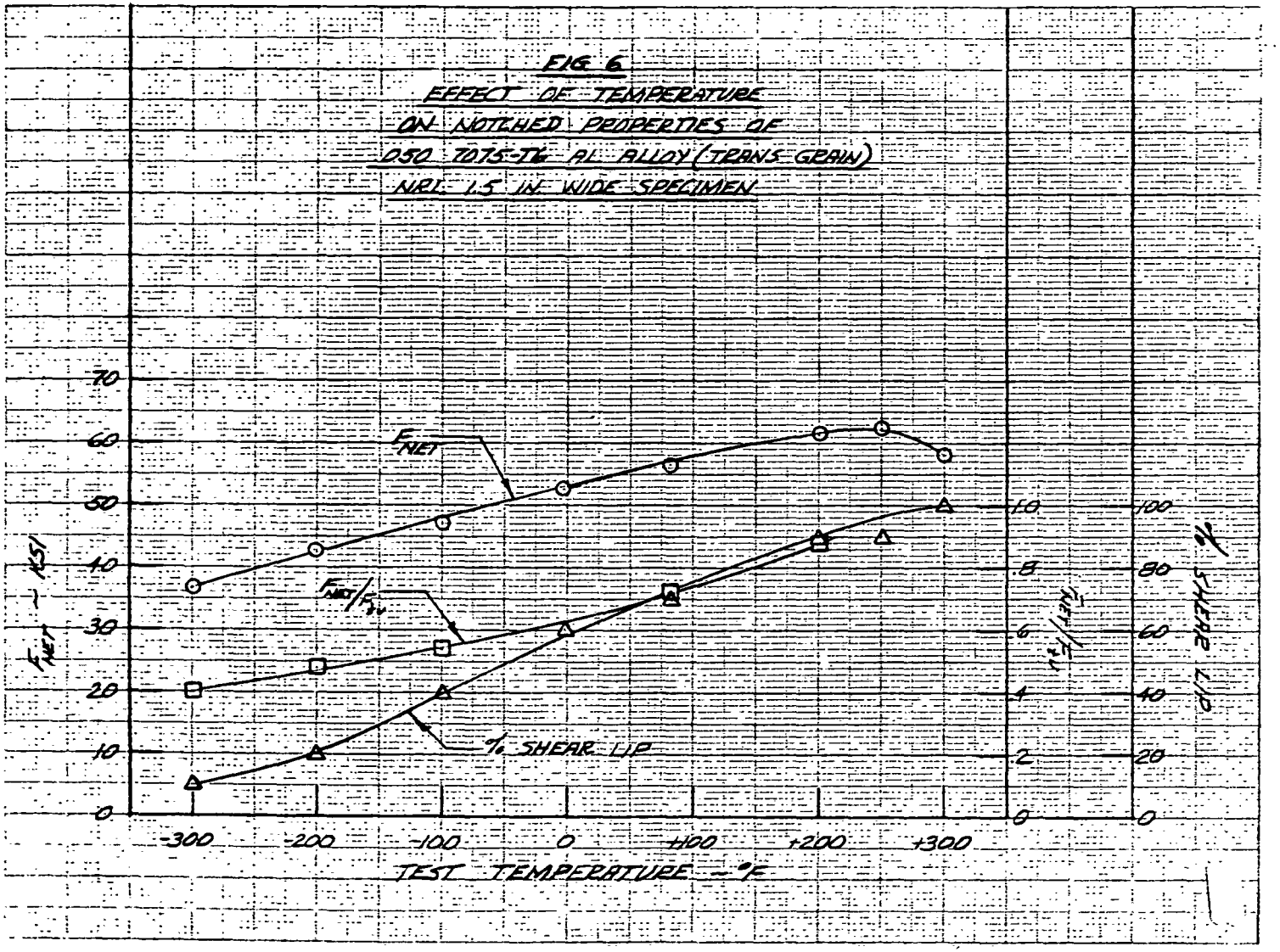
FORM 0270

68

NOTCHED/UNNOTCHED STRENGTH RATIO
0 1 2 3 4 5 6 7 8 9 10 11
0 2 4 6 8 10 12 14 16 18 20 22 24 26
K_t
STEELS
ALUMINUM ALLOYS
TITANIUM ALLOYS
STAINLESS STEELS
MAGNESIUM ALLOYS
ANNEALED
AGED
SOLUTION TREATED AND AGED
SOLUTION TREATED
ANNEALED
AGED
SOLUTION TREATED AND AGED
SOLUTION TREATED
ANNEALED
AGED
SOLUTION TREATED AND AGED
SOLUTION TREATED


FIG 5
EFFECT OF TEMPERATURE
ON NOTCHED PROPERTIES OF
.050 2024-T3 AL. ALLOY (TRANS. GRAIN)
NRL 1.5 IN. WIDE SPECIMEN
F_{NET}
% SHEAR LIP
F_{NET} ~ KSI
% SHEAR LIP
70
60
50
40
30
20
10
0
100
90
60
40
20
0
-300
-200
-100
0
+100
+200
TEST TEMPERATURE ~ °F

V-70


FIG 6
EFFECT OF TEMPERATURE
ON NOTCHED PROPERTIES OF
.050 7075-T6 AL ALLOY (TRANS GRAIN)
NRI. 1.5 IN. WIDE SPECIMEN
F_{NET} ~ KSI
F_{NET}
F_{NET}/F_{tu}
% SHEAR LIP
F_{NET}/F_{tu}
% SHEAR LIP
0
10
20
30
40
50
60
70
0
2
4
6
8
10
0
20
40
60
80
100
-300
-200
-100
0
+100
+200
+300
TEST TEMPERATURE — °F

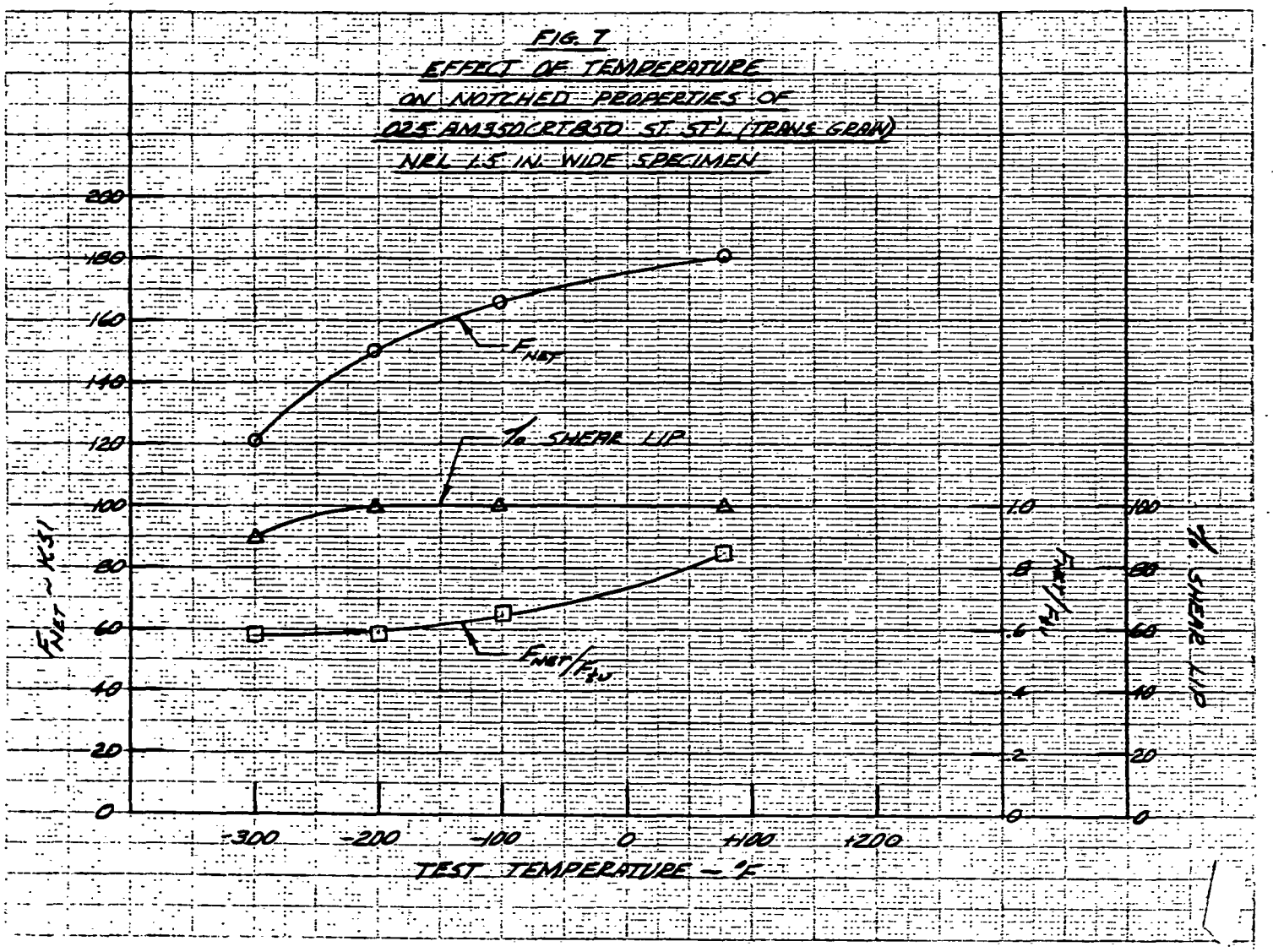
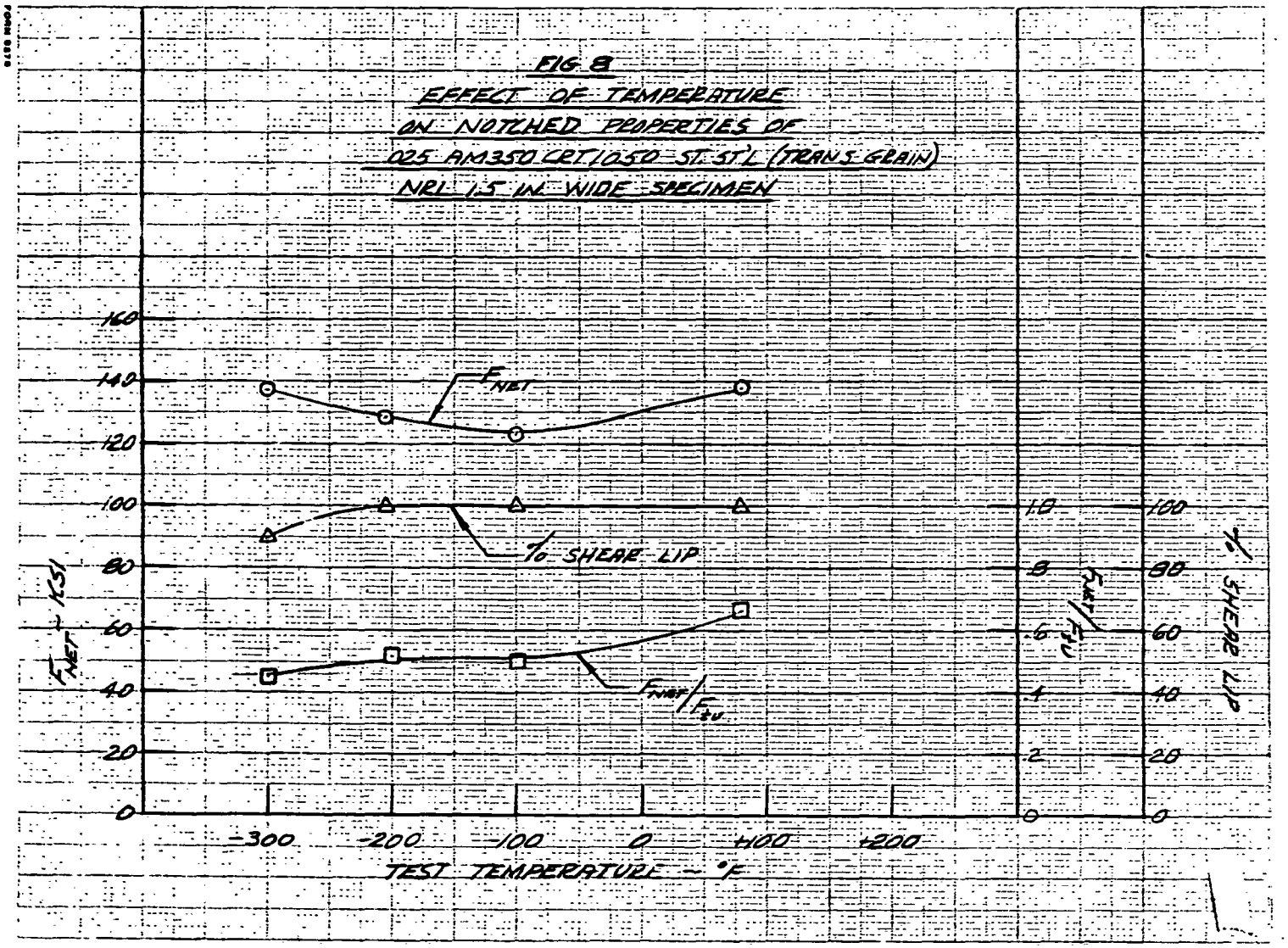
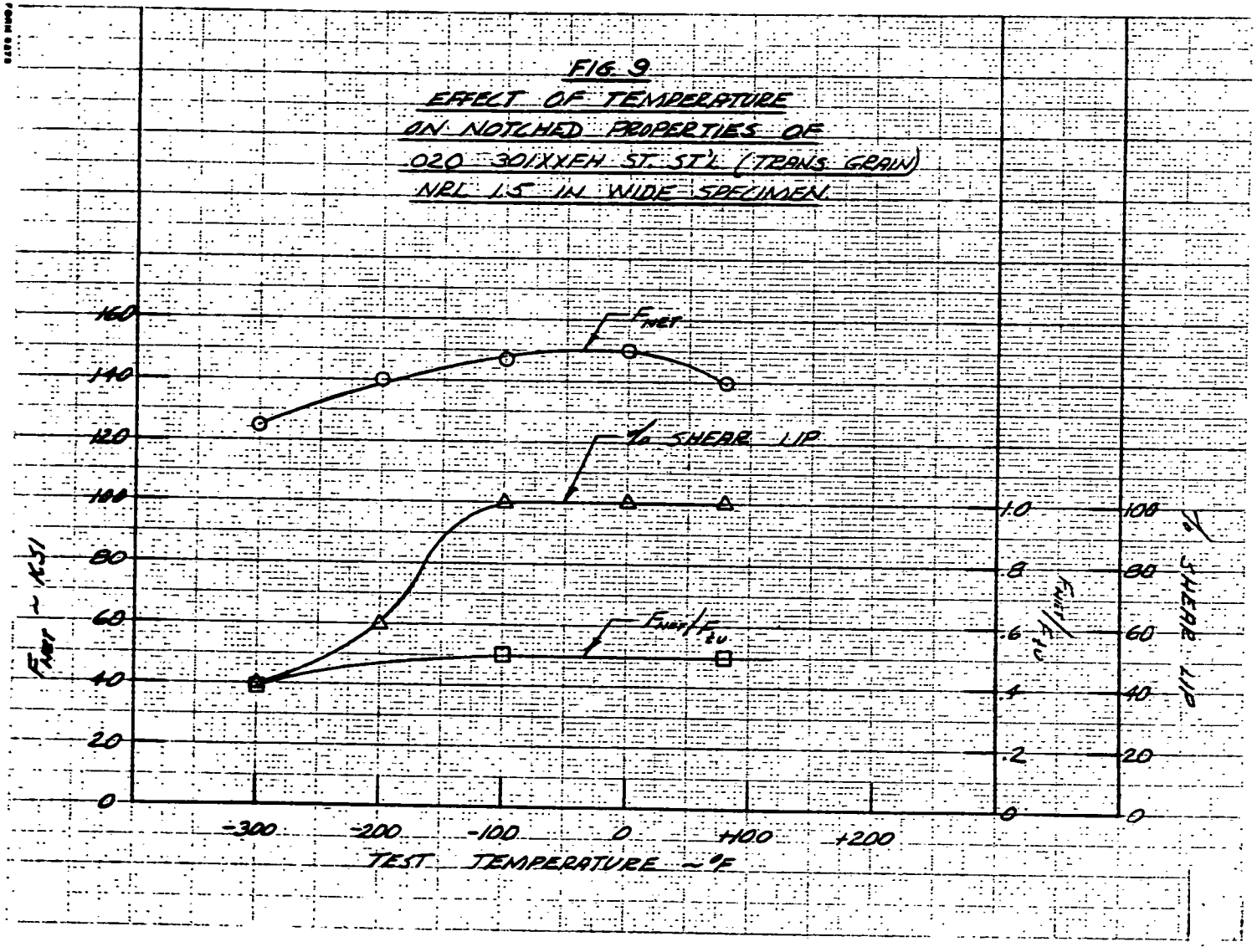

FIG. 7
EFFECT OF TEMPERATURE
ON NOTCHED PROPERTIES OF
.025 AM350CRT850 ST. ST'L. (TRANS GROW)
NRL 1.5 IN. WIDE SPECIMEN
200
180
160
140
120
100
80
60
40
20
0
F_{NET} ~ KSI
F_{NET}
% SHEAR LIP
F_{NET}/F_{tu}
1.0
.8
.6
.4
.2
0
100
80
60
40
20
0
% SHEAR LIP
-300
-200
-100
0
+100
+200
TEST TEMPERATURE — °F

FIG. 8

EFFECT OF TEMPERATURE ON NOTCHED PROPERTIES OF .025 AM350 CRT 1050 ST. ST'L (TRANS. GRAIN) NRI 1.5 IN. WIDE SPECIMEN




FIG 9
EFFECT OF TEMPERATURE
ON NOTCHED PROPERTIES OF
.020 301XXFH ST. ST'L (TRANS GRAIN)
NRL 1.5 IN WIDE SPECIMEN
F_{NET}
% SHEAR LIP
F_{NET}/F_{tu}
F_{NET} ~ KSI
F_{NET}/F_{tu}
% SHEAR LIP
TEST TEMPERATURE ~ °F
160
140
120
100
80
60
40
20
0
1.0
.8
.6
.4
.2
0
-300
-200
-100
0
+100
+200

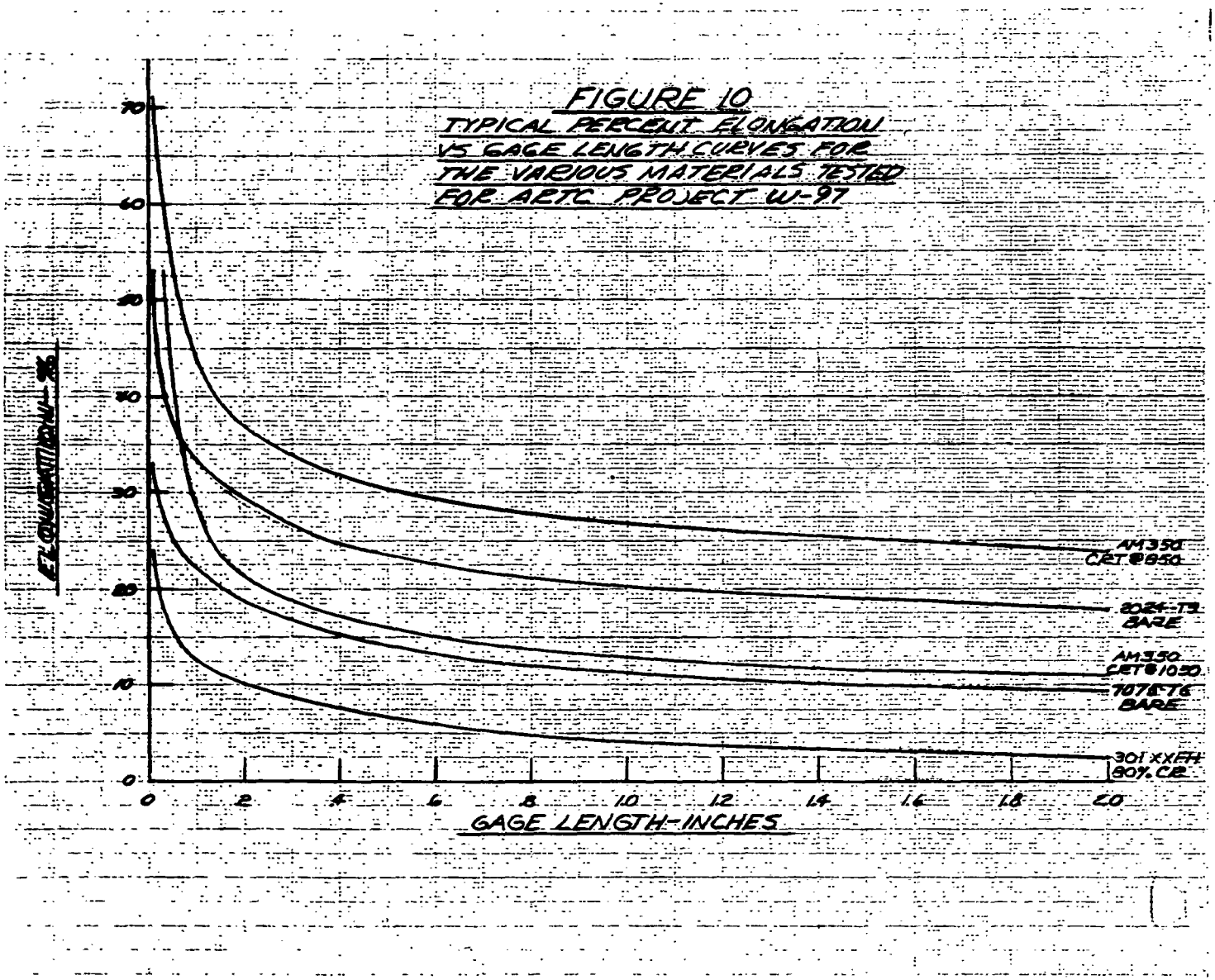
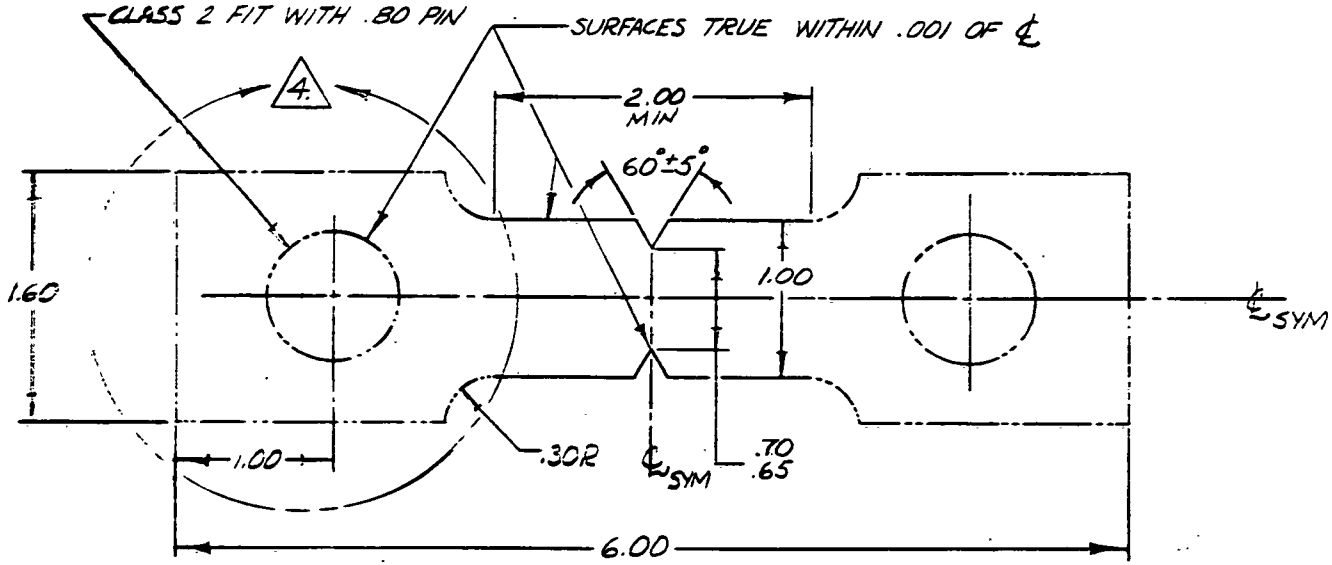


FIGURE 10
TYPICAL PERCENT ELONGATION VS GAGE LENGTH CURVES FOR THE VARIOUS MATERIALS TESTED FOR ARTC PROJECT W-97

FIG A-1
EDGE NOTCHED TENSILE COUPON



NOTE
1. NOTCH RADIUS .001 MAX.
2. NOTCH SYMMETRICAL ABOUT BOTH ℄'S WITHIN .001
3. ALL TOLERANCES ±.032 EXCEPT AS NOTED
4. END DETAILS OPTIONAL

APPENDIX A

EDGE NOTCHED TENSILE TEST

DESCRIPTION OF SPECIMEN

A diagram of the suggested specimen is shown in Figure I-1. The end details are the type used by the NASA; any satisfactory pin loaded arrangement may be use This specimen size is recommended for sheet materials up to .063 thick. For thicker materials, the specimen width should be increased to provide a minimum width to thickness ratio of 16.

Except for the notch, the machining of the specimen may be accomplished by conventional methods. It has been found most satisfactory to perform all the machining operations before heat treatment. The preparation of the notch requires special techniques, the method recommended by the ASTM (Ref. 1) being as follows:

A surface grinder is used to produce a root radius from 0.005 to 0.007 in. A 1/2-in. thick A120J alundum wheel is dressed to a 60-deg angle, dead sharp for this operation. Roughing to approximately 0.005 in. of final depth can be done with two or three redressings. Coolant is applied to the wheel. The final radius is produced by fixing a carbide tool in the head of a milling machine and by drawing the specimen under the tool by movement of the bed. Generally, only one specimen can be worked at a time. The tool is diamond ground to a point and to within ±1 deg of the notch angle produced by the previous grinding. Several cuts and tool regrinding operations may be necessary to produce a radius of 0.001 in. maximum. During this procedure, the notch radius must be frequently examined with an optical comparator preferably of 100 X magnification. When replacing the tool, particular attention should be given to proper alignment with respect to the notch. This can best be accomplished with a low-power microscope mounted on the milling machine.

TEST APPARATUS & PROCEDURE

The test apparatus and procedure are basically the same as used for conventional tensile coupons. A loading rate of 1,000 to 10,000 psi (net sectio stress) per sec. is recommended.

REPORTING OF RESULTS

The net area notch strength ($\sigma_{N.S.}$) should be recorded together with the corresponding smooth ultimate (σ_{ULT}) and 0.2% yield strength ($\sigma_{Y.P.}$) and the notched unnotched ratio $\frac{(\sigma_{N.S.})}{(\sigma_{ULT})}$.

The net area notch strength is defined as -

$$\sigma_{N.S.} = \frac{P_{max.}}{B\,(W - 2a_o)}$$

where
- $P_{max.}$ = maximum load (lbs.)
- B = Sheet thickness
- W = Specimen width (in.)
- $2a_o$ = Total initial notch depth (in.)

DYNAMIC NOTCHED SCREENING TEST

by

Alfred J. Brothers[1] and Howard E. Martens[2]

Abstract

The procedures, criteria, and limitations of dynamic notched tests currently in use for sheet material are reviewed. The effect of notch acuity on dynamic test results is demonstrated. Some recommendations for conducting and interpreting the results of sheet impact tests are described. A comparison of the results of various notched-impact tests and the NASA and K_c-type static notched-tensile tests show that the impact tests are mutually consistent, but in some materials do not correlate with the results of the static tests.

The most promising dynamic notched screening test is the precracked-notch sheet Charpy test employed by Orner and Hartbower.

---

[1]Applied Research Metallurgist, formerly with the Jet Propulsion Laboratory and now with the Large Steam Turbine-Generator Department, General Electric Company, Schenectady, New York

[2]Assistant Chief, Materials Research Section, Jet Propulsion Laboratory, California Institute of Technology, Pasadena, California

I. INTRODUCTION

The current interest in the fracture resistance of high strength sheet material has generated a great amount of experimentation to determine the properties which quantitatively define or correlate with resistance to low stress service fracture. Experience derived from notched tests of plate materials and consideration of anticipated service conditions has resulted in the development of a number of notched screening tests. Among these are test procedures which utilize dynamic or impact loading.

It has been suggested that the apparent lack of strain rate sensitivity of high strength ferrous alloys makes a dynamic test unnecessary. However, this should not be considered as a critical limitation. If through experience the results of a simple, economical dynamic test procedure correlates with other tests or preferably, service behavior, its use is justified.

For simplicity and clarity, the various dynamic test procedures have been grouped into three classes; (1) notch-bend impact, (2) notch-tensile impact, and (3) drop-weight type tests. Following a brief description of each type test including its limitations, the results of these tests, their mutual correlatibility and general usefulness as screening tests will be described.

II. NOTCH-BEND IMPACT TESTS

Two notched bend tests derived from the conventional V-notched Charpy impact tests are the laminated sheet Charpy specimen used by Arnold[1] of Watertown Arsenal Laboratory and the single sheet sub-thickness edge-notched Charpy test employed by Orner and Hartbower[2] of the same Laboratory. These test specimens in their original form are shown in Figure 1. Arnold, to simulate more closely the standard Charpy specimen, to obtain greater test termperature control and to increase absorbed energy values, stacked and riveted sheets to obtain the conventional plate Charpy thickness. For simplicity and economy, Orner and Hartbower test only a single sheet thickness. Orner has recently modified his specimen design to obtain a precrack as a notch radius; this is described later in the report.

The primary criterion for both these tests is absorbed energy measured in a conventional or modified impact machine. To account for slight differences in thickness, Orner and Hartbower express energy as ft.-lbs. per 0.1 inch thickness.

Since both these notch tests are loaded in bending, they are difficult to perform on sheet thicknesses less than about 0.040". Also, at these thicknesses the absorbed energy values or single sheet thicknesses are about 0.10 to 5 ft.-lbs. Although these low energy values can be measured accurately on modern or subsize impact machines, the generally low level reduces confidence in their significance.

III. NOTCH TENSILE IMPACT TEST

To develop a sheet tensile impact test for use over a wide range of thickness, notch tensile impact specimens have been employed. One of these, used by the authors at the Jet Propulsion Laboratory, is shown in Figure 2. The pin-loaded specimen rests in a fixture mounted in a conventional impact machine; these details are shown in Figure 3. For these tests, it is necessary to use doublers or stiffiners to prevent deformation near the loading pins. Other procedures for notch tensile impact tests of sheet have been used at Armour Research Institute[3] and Watertown Arsenal Laboratory[4].

If from consideration of lack of strain rate sensitivity, dynamic test procedures are considered unnecessary, little advantage is obtained in using notch tensile impact tests. The specimen shown in Figure 2 requires as much material as a static notch tensile test, it is as difficult to machine as the NASA sharp notch specimen and ultimately provides energy results which are believed to be a more complex quantity than strength.

IV. DROP-WEIGHT IMPACT TEST

To determine the fracture resistance of very thin high-strength sheet steels, a notched drop-ball or drop-weight impact test has been developed at the Ryan Aeronautical Company.[5] The Ryan test, using the specimen shown in Figure 4 determines the minimum energy required to initiate a crack at the end of an elox or shear formed crack. This figure shows a specimen before and after testing in the apparatus shown in Figure 5. The specimen is placed over a hole of 5/8" diameter and a weight containing a 1/2" diameter ball is dropped from increasingly higher positions to determine the minimum energy required to crack the specimens. This procedure has been used to compare materials as thin as .007".

V. DYNAMIC TEST CRITERIA

The primary test criterion of all the above tests is energy. Generally, it is assumed that for a given temperature and sheet thickness, the absorbed energy value is proportional to the resistance to crack propagation. Orner and Hartbower through considerations of available stored elastic energy have proposed an empirical relationship between Charpy energy per unit thickness and K_c, the fracture toughness described by Irwin and his associates[6].

The fracture appearance determined by the relative amounts of cleavage and shear is useful only in defining the temperature below which a material will fail with very low fracture toughness. The usefulness of this criterion is limited to those materials which (a) exhibit shear-to-cleavage transition and (b) in which full shear fracture is accompanied by high fracture

toughness. It should be emphasized that some ferrous and non-ferrous sheet materials fracture with low static notch ratios although the fractures exhibit complete oblique shear. An example of this low stress shear fracture behavior is demonstrated in a recent report by Srawley and Beachem[7].

To date there is insufficient information to determine conclusively whether materials exhibiting low stress shear fracture will also fracture with low energy in an impact test. Until more data is available, it is apparent that both the fracture appearance and energy criterion for these materials should be interpreted with caution.

Since absorbed energy is an integral quantity which includes both the initiation and propagation aspects of fracture, it is apparent that those variables affecting crack initiation will be reflected in the measured energy. Of most significance is the effect of notch acuity. Figure 6 shows the effect of notch radius on sub-thickness Charpy tests results of three high strength steels, the properties of which are shown in Table I. These properties include K_c, the fracture toughness, which was measured on nine inch wide panels containing a 1.5" long central slot terminating in a fatigue crack. The values shown in Figure 6 indicate that in the presence of a blunt, i.e., 10 mil radius notch that a material of very low fracture toughness may exhibit high absorbed energy. This figure also shows that the notch radius affects the energy level of materials at each of the K_c levels investigated. Decreasing the notch radius from .010 to .0015 lowered the absorbed energy 2-8 fold.

Figure 7 shows the effect of notch acuity on the correlation of sub-thickness Charpy properties and G_c, a quantity proportional to K_c, the fracture is toughness. This data, from Orner, shows that scatter is minimized and the correlation improved by using a sharp crack rather than the standard .010" radius. The precrack in these specimens was obtained by compressively prestraining a tapered notch at liquid nitrogen temperatures and permitting the crack to form spontaneously under conditions of high residual tension stresses. The details of this specimen are shown in Figure 8 and described in Reference (2). Recent correspondence from Orner indicates that fatigue cracking is also a feasible method of precracking Charpy specimens.

VI. COMPARISON OF TEST PROCEDURES

As part of a recent experimental program by the W-97 Panel of the ARTC, several sheet alloys were evaluated using a number of static and dynamic test procedures including most of the tests described in this report. A summary of these are shown in Table II. For comparison purposes, the table includes conventional fracture properties measured in static notch tensile tests with the NASA sharp notch test specimen and wide center slotted specimens suitable for determining reliable values of K_c, the fracture toughness. Each of the dynamic tests rate the materials in the same order and with the exception of the AM350 alloy are

consistent with the results of the static notched tests. The apparent lack of correlation between dynamic and static tests of the AM350 alloy may, for the edge-notch Charpy and JPL notch-tensile impact test, be attributed to test data scatter. The difference in energy values as measured in the drop-weight test indicates an obvious difference, the meaning of which remains to be clarified.

VII. CONCLUSIONS

From consideration of the above described test procedures and results, the following conclusions have been drawn:

1. The results of the W-97 Panel Correlation Program has indicated the mutual correlatibility of each of the dynamic test procedures described above. Proof of a practical correlation between dynamic and static test results remains uncertain.

2. From the limited data presently available, the edge-notch precracked Charpy test used by Orner and Hartbower appears to be the most promising of the currently available dynamic test procedures. However, the great affect of notch acuity on absorbed energy values suggests caution in the use of this or any of the dynamic test procedures.

3. For specimen thicknesses less than about 0.040, all of the test procedures described above offer little obvious advantage over the currently established static notch tensile tests. Subsequent to further experimentation, the Ryan drop-weight test may prove a simple and economical test procedure for very thin sheets.

REFERENCES

1. S. V. Arnold, "A Proposed Method For Impact Testing of Sheet Metal," Watertown Arsenal Laboratory Report WAL 112/90, ASTIA Doc. AD104577.

2. G. M. Orner and C. E. Hartbower, "Notch Sensitivity in High Strength Sheet Materials," Progress Report 16, May, 1960.

3. R. F. Domagala and H. L. Nurnberg, "How to Impact Test Sheet Materials," The Iron Age, November 15, 1956.

4. G. M. Orner and C. E. Hartbower, "Notch Sensitivity in High-Strength Sheet Materials," Welding Journal Res. Supplement, April 1960

5. Minutes of First and Second Meeting, Aircraft Industries Association, ARTC Panel W-97 "Standardization of Test Procedure for Tear Resistance of Metallic Sheet Material," July 16 and November 20, 1958.

6. "Fracture Testing of High-Strength Sheet Materials": A report of a Special ASTM Committee, ASTM Bulletin, January-February, 1960.

7. J. E. Srawley and C. D. Beachem, "Crack Propagation Tests of High-Strength Sheet Materials," Part IV - The Effect of Warm Pre-Straining, U. S. Naval Research Laboratory Report No. 5460, April 18, 1960.

TABLE I

ROOM TEMPERATURE TENSILE AND FRACTURE

PROPERTIES OF 0.050 INCH THICK STEEL SHEETS*

	H-218	17-7PH (TH1075	AM350SCT
Tensile Properties			
Tensile Strength, kpsi	250.0	209.0	213.0
0.2% Yield Strength, kpsi	210.0	199.0	180.0
Elong. in Two Inches, %	6.0	6.0	15.0
Fracture Properties**			
Gross Section Fracture Stress, kpsi	34.6	60.4	85.5
Crack Length at Fracture, inch	1.50	1.55	1.98
Fracture Toughness, K_c, kpsi in.	54	96	153

NOTES: *Transverse properties
**Nine inch wide center slotted specimen with fatigue crack

TABLE II

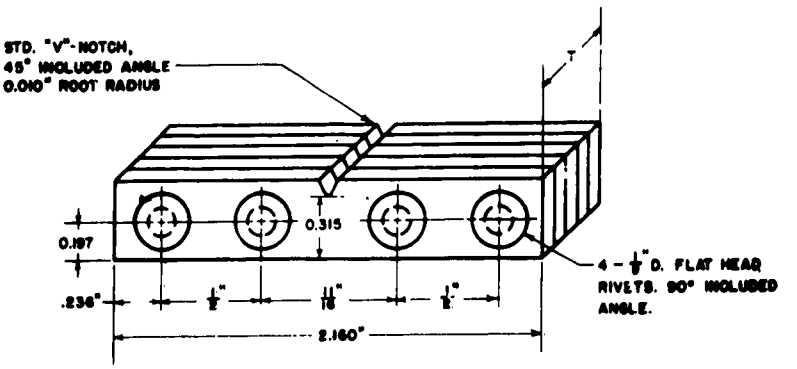
COMPARISON OF DYNAMIC NOTCH-TEST RESULTS*

Material	Thick (in)	0.2% Yield Strength (kpsi)	Ultimate Tensile Strength (kpsi)	Elong in 2" (%)	0.010 in Rad. Edge-Notch Charpy (ft.-lbs)	JPL Notch Tensile Impact (ft.-lbs.)	RYAN Drop-weight Test (in.-lbs.)	NASA NSR	K_c** (kpsi $\sqrt{in.}$)
2024S-T6	.050	46.6	68.4	18.5	6.6	9.1	15.8	.80	82
7075S-T6	.053	69.8	80.0	10.1	1.1	6.8	10.5	.72	52
Type 301XXFH	.022	239.6	272.6	2.9	1.0	5.7	9.5	.52	85
AM350CRT(850)	.025	172.4	208.8	24.0	8.8	15.8	14.4	.97	250
AM350CRT91050)	.025	123.8	204.8	10.9	10	17.1	47.3	.75	209

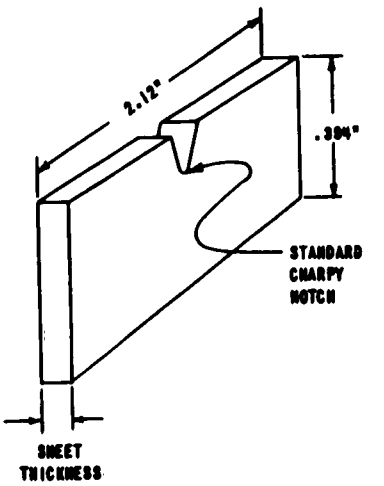
V-82d

NOTES: *All values are average of five tests

**Determined using 9" wide center slotted specimen with fatigue crack



Laminated-Sheet Charpy Test Specimen (Arnold)



Sub-Thickness Edge Notched Charpy Specimen (Orner)

FIGURE 1 CHARPY TYPE SHEET TEST SPECIMENS

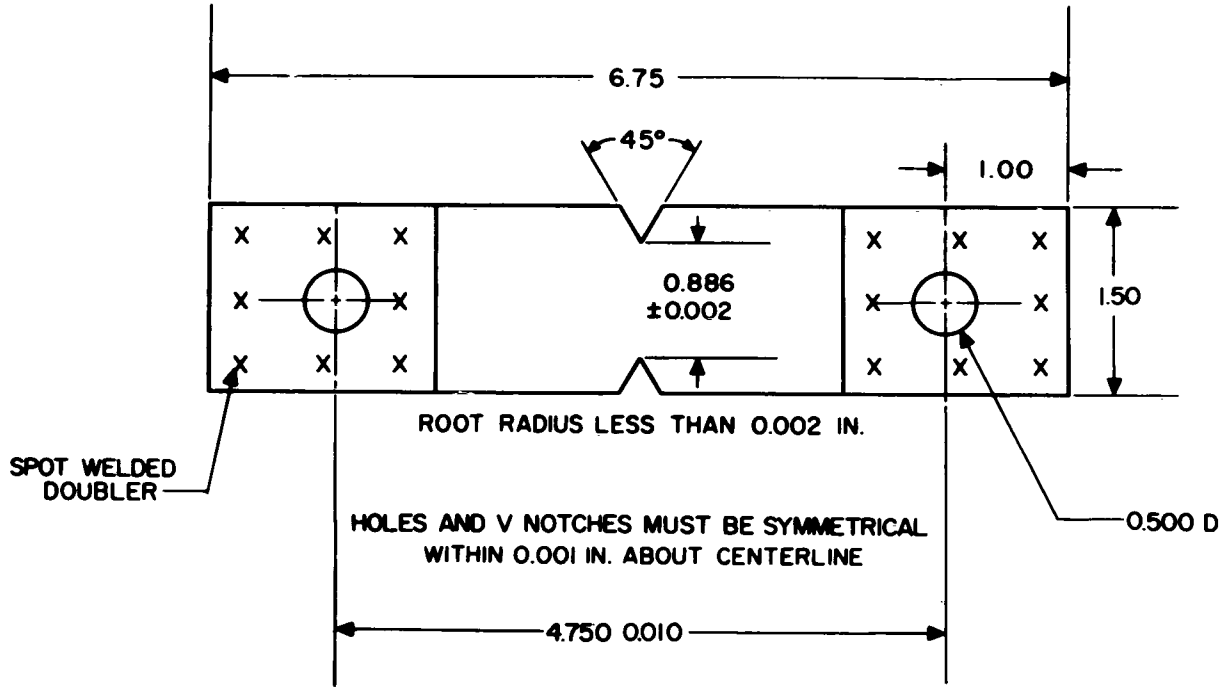


FIGURE 2 NOTCH TENSILE IMPACT SPECIMEN

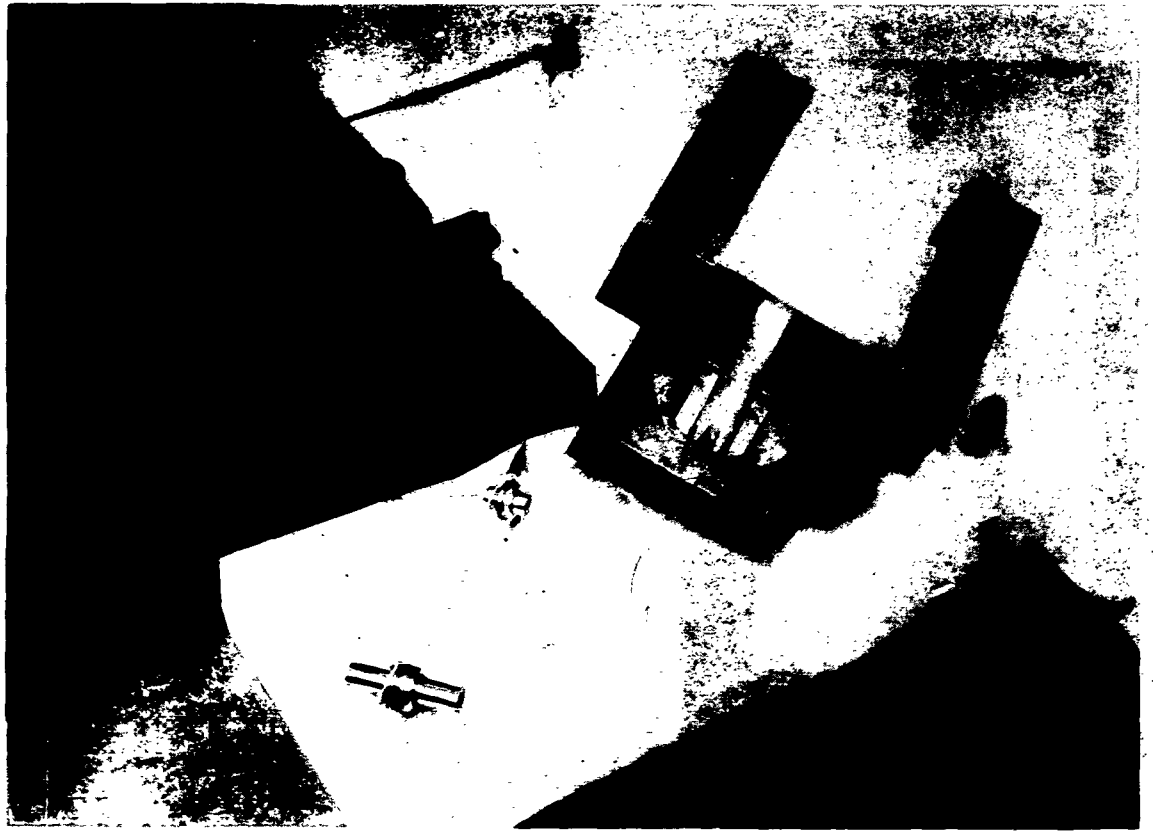


FIGURE 3 NOTCH-TENSILE IMPACT TEST FIXTURE

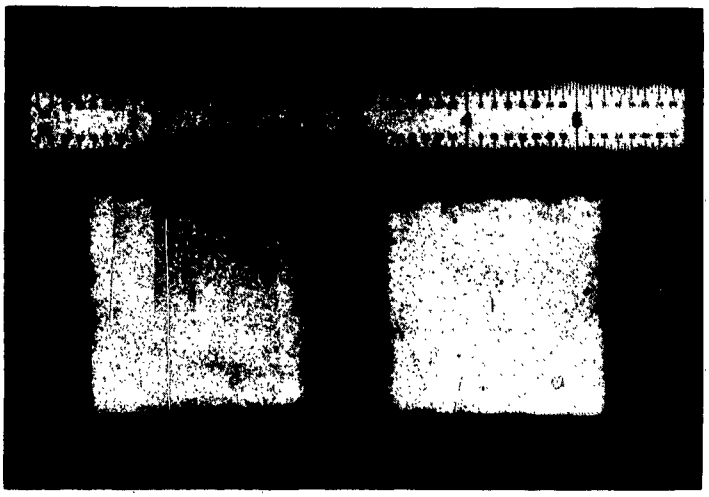


FIGURE 4 RYAN DROP-WEIGHT TEST SPECIMEN

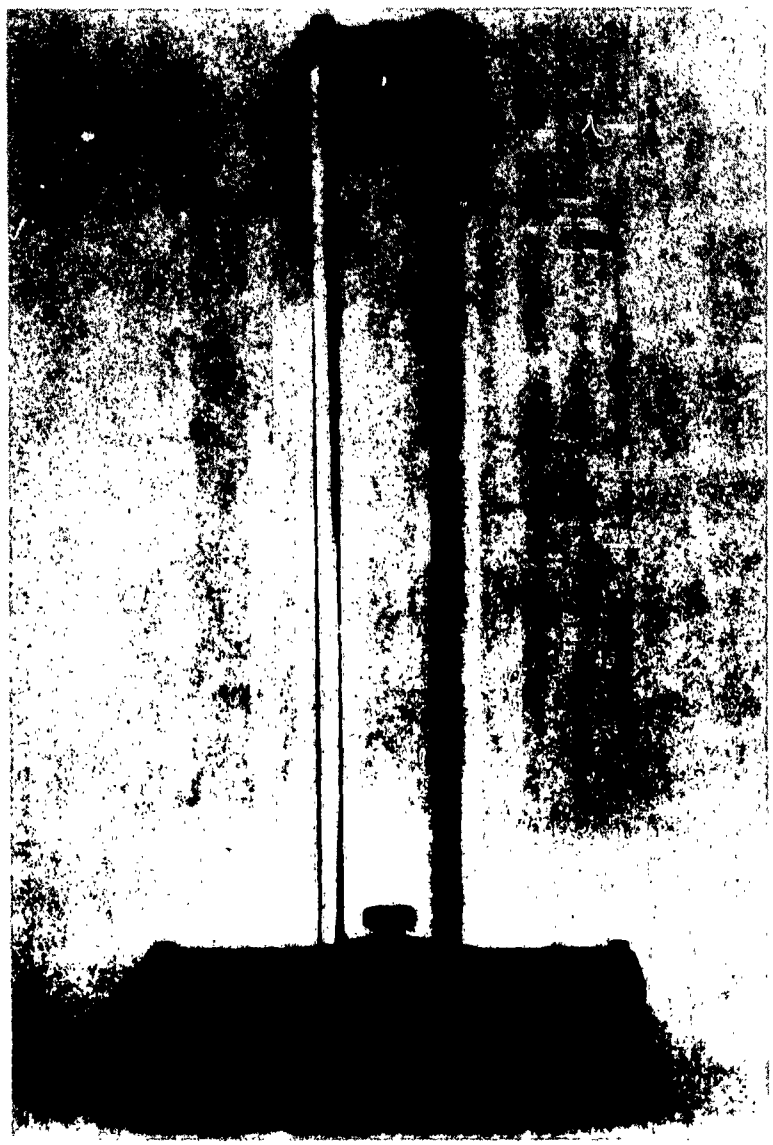


FIGURE 5 RYAN DROP-WEIGHT TEST FIXTURE

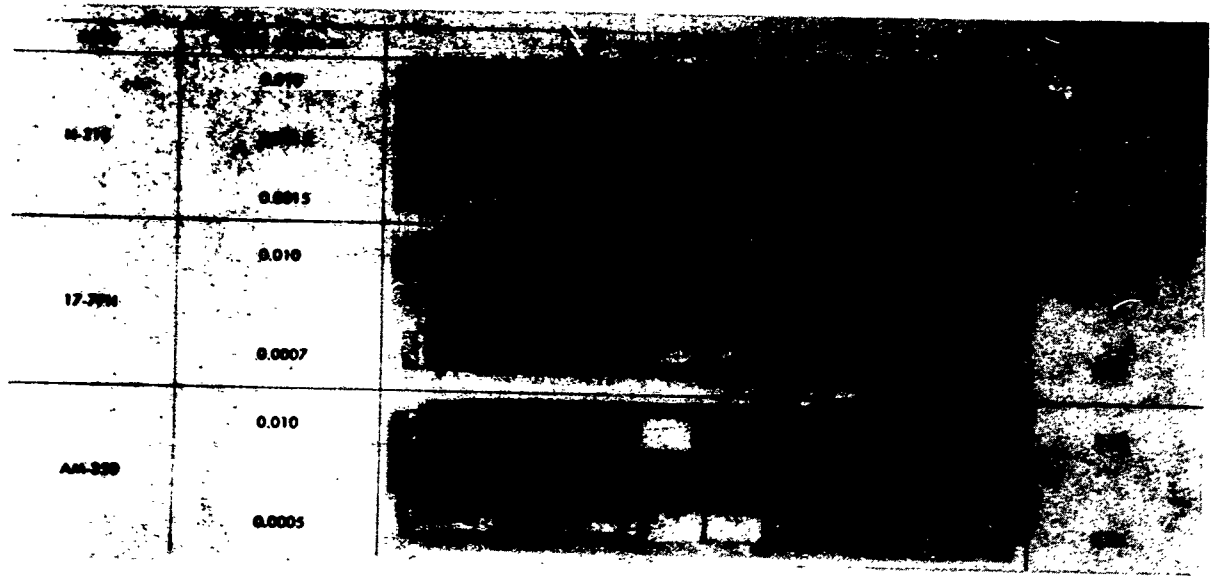


FIGURE 6 EFFECT OF NOTCH RADIUS ON SUB-THICKNESS CHARPY PROPERTIES OF 0.050 INCH THICK HIGH STRENGTH STEEL SHEET

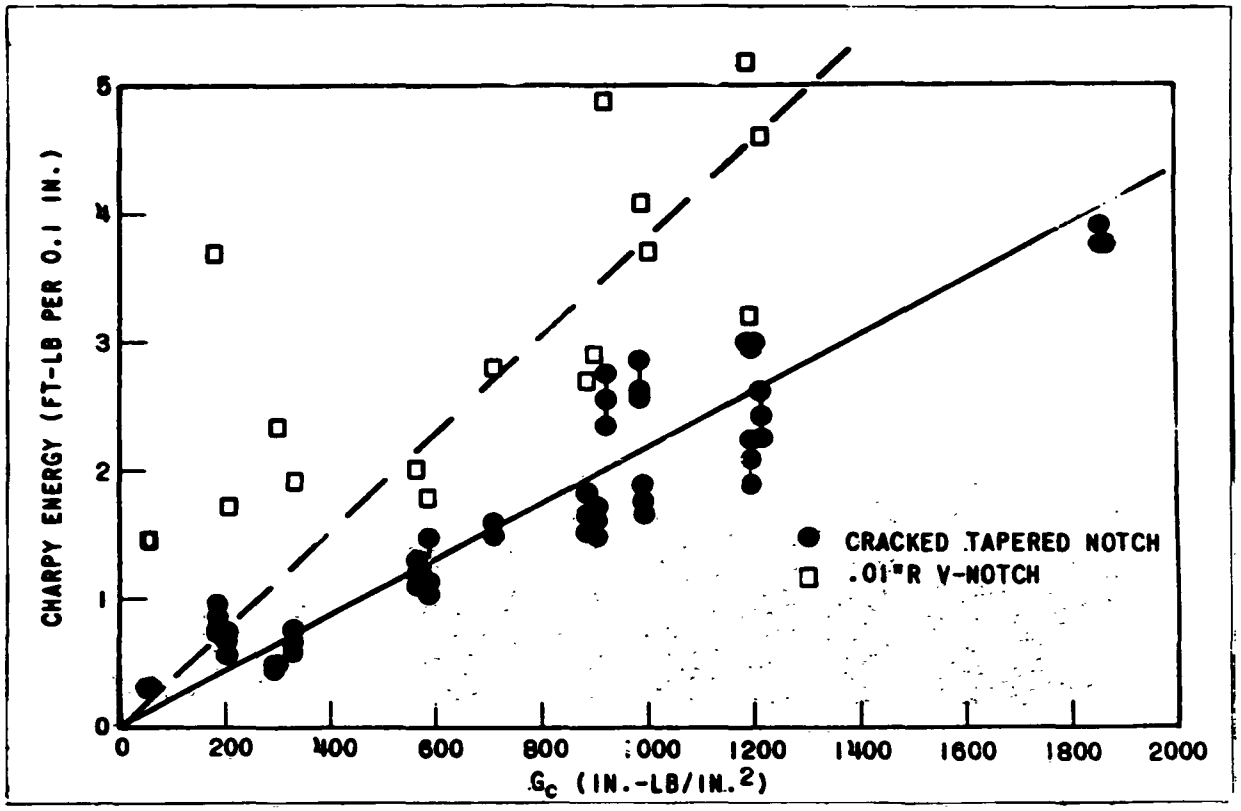


FIGURE 7 RELATIONSHIP BETWEEN CRACKED TAPERED CHARPY ENERGY PER 0.1 INCH THICKNESS AND G_c (Orner)



FIGURE 8 TAPER NOTCHED SPECIMEN AND TYPICAL INK STAINED CRACKS (Orner)

INSTRUMENTED BEND TESTS APPLIED TO PRESSURE VESSEL RELIABILITY

By

R. McPhee*, K. E. Muszar*, G. R. Sippel**, G. L. Vonnegut***

Abstract

A method for evaluation of rocket motor case materials and processes, involving uniaxial strength and crack propagation resistance, is discussed. The Instrumented Bend Test provides a simple and inexpensive test for measurement of the crack propagation parameter values. A description of the test and its correlation with other crack propagation tests and pressure vessel behavior is presented. Instrumented Bend Test results show a good degree of correlation when obtained in different laboratories on the same lots of samples.

Data on three high strength rocket motor case steels are presented showing that elevated temperature embrittlement occurs in these materials when tempered below 800° F.

I. Method for Evaluation of Rocket Motor Case Materials and Processes

The two main properties of a material, which determine its behavior in pressure vessel applications, are the uniaxial strength and crack propagation resistance. In general, these two properties vary inversely one to the other; i.e., the higher the strength, the lower the crack propagation resistance. It is the balance of these two opposing properties that provides the optimum condition of a material for pressure vessel applications, such as a rocket motor case.

A plot of crack propagation resistance and uniaxial strength for air melt D6 steel is shown in Figure 1. In addition to the uniaxial yield strength, the corresponding biaxial yield strength as determined on 24" diameter pressure vessels, is also plotted. Based on pressure vessel behavior, there is a minimum crack propagation resistance

* Experimental Metallurgist; Materials Research Lab., Allison Div., General Motors Corporation.

** Asst. Plant Metallurgist - Research; Materials Research Lab., Allison Division, General Motors Corporation.

***Supervisor Alloy Development; Materials Research Lab., Allison Division, General Motors Corporation.

which must be attained in order to have consistent reliable behavior. When the crack propagation resistance is below this minimum, the vessel behavior is not reliable and premature failure may occur far below the uniaxial properties of the material, as indicated on the graph. Above this minimum crack propagation resistance value, the uniaxial tensile properties govern the biaxial behavior of pressure vessels.

Obviously, it is desirable to process a material so as to impart the highest possible strength with the highest possible crack propagation resistance. In order to evaluate materials or processes for rocket motor case applications, one should construct such crack propagation resistance - uniaxial strength curves and choose the material or process whose curve lies toward the upper right corner of the chart. In addition, materials should never be processed so as to give crack propagation resistance below the minimum level and place the material in the area of questionable reliability.

There are a number of tests which provide crack propagation resistance parameters. Three such tests have recently been fully covered by a Special ASTM Committee[1] publication.

NRL Center Notch Tensile Test
NASA Edge Notch Tensile Test
Allison Instrumented Bend Test

The first two tests require the use of rather large specimens and are difficult to prepare. The particular crack propagation resistance test used in all of the rocket motor case work at Allison is the Instrumented Bend Test developed by the Allison Materials Research Laboratory.

The Instrumented Bend Test provides a crack propagation resistance parameter ($\sigma_m - \sigma_1$) which lends itself very well to the construction of evaluation curves due to its simplicity to test and ease of sample preparation.

II. Description of Instrumented Bend Test

The Allison Instrumented Bend Test is a crack propagation test, wherein a small, unnotched, rectangular specimen is biaxially stressed to failure by bending as a simple beam, using a three point loading system. This test provides a crack propagation resistance parameter which correlates with other types of crack propagation tests and with pressure vessel behavior.

(1) "Fracture Testing of High Strength Sheet Materials; A Report of a Special ASTM Committee" ASTM Bulletin January 1960.

Specimen

Most of the Instrumented Bend Test data have been obtained using a specimen 0.052 x 0.700 x 1.5 inches. These dimensions were chosen for two reasons.

a. This size sample can easily be obtained from subscale as well as full scale rocket motor cases after burst testing.

b. The width to thickness ratio of approximately 14 provides an adequate 2:1 biaxial stress area approximately 1/2 inch in width.

Specimens of other thicknesses and widths may be used, but a minimum width to thickness ratio of 10 is recommended. The width and thickness should remain constant when comparing results of different materials or processes.

All specimens are ground to the finished dimension without breaking sharp edges. The surface finish is not critical as long as grinding burns are avoided, with the normal surface finish ranging from 10 to 20 RMS. Surface finishes ranging from 10 to 150 RMS do not essentially change the test results. No mechanical notches or cracks of any kind are necessary in the preparation of these test specimens.

Equipment and Instrumentation

The test basically consists of bending the specimen as a simple uniform rectangular beam supported at two points by 1/4 inch rounds and loaded through a 1/8 inch round at the center of a 1 inch span as shown in Figure 2.

All components of the bend test fixture are made from tool steel hardened and tempered to R_C 60. The rate of deflection is maintained constant at a tensile machine cross-head speed of 0.5 inch per minute. This value is not critical within the range of 0.1 to 2.00 inches per minute. The load on the specimen is sensed during the test by a resistance strain gauge load cell (1000 pound capacity) which is placed between the bend test fixture and the lower platen of the tensile machine. The output of the load cell is fed into a strain gauge amplifier and recorder. It is important that the recorder have sufficient pen speed response to accurately track the load on the specimen without lag. An oscillographic type recorder with a frequency response of 60 cycles per second or higher is recommended. Potentiometer type recorders with 1/4 second full scale deflection have also been successfully used. The strain gauge load cell and the recorder are calibrated against the tensile machine so that each division of the recorder strip chart is usually equivalent to 20 or 25 pounds load.

The chart paper is usually driven at 5 millimeters per second. The strip chart of the recorder thus furnishes a continuous record of the specimen load as a function of time during the test.

Interpretation and Calculation of Test Results

Typical load-time curves, obtained from Instrumented Bend Tests conducted on a high strength steel heat treated to uniaxial 0.2% yield strength levels of 235,000 psi (Ex. A) and 205,000 psi (Ex. B), are shown in Figure 3.

All curves show the same general behavior, in that the load increases to maximum value and then decreases at a relatively slow rate until a lower load is reached at which time there is a sharp and rapid change in the rate of unloading. The maximum load is indicated by P_m and the load at which the rapid change in rate of unloading begins is denoted by P_l.

Observation of the tension face of specimens during the test has shown that the first cracks appear in the center biaxially stressed area at the P_m load and progress by slow crack propagation until P_l load is reached, when rapid crack propagation occurs. Figure 4 shows ink stain fractures demonstrating slow crack progression as the load decreases from P_m to P_l.

The first step in the calculation of the Instrumented Bend Test Parameter is to pick P_m and P_l from load-time curves. A sharp change in the slope of the load-time curve is required to accurately pick the P_l load. When materials approach low strength levels, the P_l point is not distinct, and reliable parameter calculations cannot be made. These loads are corrected for small dimensional differences in the thickness and width of different samples, by converting to maximum outer fiber stress, σ_m and σ_l, by means of the beam formula:

$$\sigma = \frac{3PL}{2wt^2}$$

Where:

σ = maximum outer fiber stress in psi
P = load in pounds
L = distance between supports (1.00 inch)
t = thickness of specimen (0.052 inch nominal)
w = width of specimen (0.700 inch nominal)

The difference between σ_m and σ_1 then represents the reduction in the calculated highly localized outer fiber stress in the specimen, due to slow crack progression, before rapid crack progression occurs. The Instrumented Bend Test Parameter is defined as $(\sigma_m - \sigma_1)$. The values calculated from the two curves, shown in Figure 3, were 0.00×10^5 psi for Ex. A, and 1.01×10^5 psi for Ex. B.

III. Correlation of $(\sigma_m - \sigma_1)$ With Other Crack Propagation Tests

The Instrumented Bend Test Parameter $(\sigma_m - \sigma_1)$ has been correlated with the results of center notch tensile tests conducted on H-11 steel, heat treated to various strength levels, as shown in Figure 5. A direct correlation of $(\sigma_m - \sigma_1)$ with K_{c_1}, G_c, % Shear and notch-strength ratio $\frac{(NFS)}{(UTS)}$ is shown in Figure 6. Each point is the average of 4 to 6 tests. Since the Instrumented Bend Test Parameter correlates with K_c and other parameters derived from the more complex center notch tensile test, it serves as a simple, rapid and valid screening test for crack propagation resistance of high strength materials.

IV. Correlation of $(\sigma_m - \sigma_1)$ Values in Different Laboratories

It is highly desirable that crack propagation parameter values obtained by different laboratories on the same lot of samples show good correlation when tested by the same screening test. Such a correlation study has been made using the Instrumented Bend Test. Identical lots of samples from two high strength precipitation hardening stainless steels in various heat treat conditions were tested by two laboratories using different Instrumented Bend Test equipment. Laboratory A used an oscillographic recorder in conjunction with a strain gage AC amplifier and recorder, while Laboratory B used a 1/4 second full scale potentiometer recorder with a DC bridge. The degree of correlation between the parameter values obtained by the two laboratories can be seen in Figure 7. These data show good correlation with each point being the average of 4 tests for each laboratory.

Some of the same data are presented in Figure 8 where the correlation between Laboratory A and B is shown for each alloy and heat condition, when tested in both the longitudinal and transverse direction of the sheet. This data shows the high sensitivity of the Instrumented Bend Test to anisotropy in high strength materials as well as the ability of different laboratories to rate materials in the same order of merit by use of this test.

V. Correlation of $(\sigma_m - \sigma_1)$ With Pressure Vessel Behavior

Crack propagation resistance tests conducted in a laboratory would have very little meaning if the test values did not correlate with pressure vessel behavior.

Instrumented Bend Test results have been correlated with the pressure test results of a number of 24" diameter vessels fabricated from D6 steel forgings. Uniaxial tensile and Instrumented Bend Test specimens were removed from the vessels after pressure testing approximately 90° from the longitudinal failures. A plot of burst strength to uniaxial tensile strength ratio as a function of $(\sigma_m - \sigma_1)$ is shown in Figure 9. It can be seen from the data points, representing twenty (20) pressure vessels, that reliable behavior was obtained when the $(\sigma_m - \sigma_1)$ values were 0.5×10^5 psi or higher. Reliable behavior is denoted here by attainment of burst strengths higher than the uniaxial tensile strength ($\frac{\text{Burst}}{\text{UTS}}$ ratio > 1.0) due to the 2:1 biaxial stress field advantage of approximately 15 - 20 per cent.

When the $(\sigma_m - \sigma_1)$ values fall below 0.5×10^5 psi premature failures were observed at approximately 0.6 of the uniaxial tensile strength. Figure 1, previously seen, shows a similar behavior for the biaxial yield strength.

As a result of the correlation of $(\sigma_m - \sigma_1)$ with reliable pressure vessel behavior, the Instrumented Bend Test in conjunction with the uniaxial tensile test is being used today for quality control of material and heat treatment for Minuteman First Stage Rocket Motor Cases fabricated by Allison.

VI. Elevated Temperature Embrittlement

Solid propellant rocket motor cases are subject to environments during firing that result in a metal temperature rise from ambient or below to as high as 350°F or 400°F. This temperature rise may be due to firing from a pit and/or aerodynamic heating. In any event this temperature range is traversed while the steel case is stressed to full firing pressure, so that it is important to know the strength and crack propagation resistance of a case material in its final condition throughout this temperature range.

The Instrumented Bend Test lends itself very well to elevated and subzero temperature testing. The effect of test temperature on $(\sigma_m - \sigma_1)$ from -100°F to +600°F for D6 steel sheet is shown in Figure 10. The material was tested with both a 600°F and 1000°F temper. The 600°F

temper curve shows an increase in fracture toughness from -100°F to +100°F, but an elevated temperature embrittlement at 300°F - 400°F with the (σ_m - σ_1) values decreasing to zero (0.0) in this temperature range. Above 400°F the fracture toughness very rapidly increases with temperature. The same basic behavior is observed with the 1000°F temper but the degree of embrittlement at 350°F is not so severe. A similar "350°F embrittlement" has been reported by Southern Research Institute[2] for Tricent and AMS 6434 when using the center shear crack specimen test.

A further study of this elevated temperature embrittlement of high strength steels has recently been made by the Allison Materials Research Laboratory using the Instrumented Bend Test. Three high strength steels, were heat treated by hot salt quenching from the appropriate austenitizing temperature (marquenching) and double tempering for two hours at 500°F - 1100°F. The steels used were D6C forging, H-11 bar, (double vacuum melted) and UCX2 sheet. All materials were tested in the longitudinal direction at 80°F and 350°F. The results of these tests on D6C, H-11 and UCX2 are shown in Figures 11, 12, and 13, respectively.

All three steels tempered at 500°F show extreme embrittlement at 350°F even though the 80°F test gave acceptable (σ_m - σ_1) values of 0.5×10^5 psi. It appears that the 350°F embrittlement in all three steels can be eliminated by tempering higher than 800°F. The H-11 material should be tempered higher than 1000°F to eliminate brittleness at both 80°F and 350°F.

Additional work is required to determine the degree of embrittlement at test temperatures other than 80°F and 350°F as a function of tempering temperature for these and other materials for application as pressure vessels in this temperature range. The exact mechanism of this 350°F embrittlement is not known but is believed to be associated with strain aging. Preliminary tests have indicated:

1. Samples heated to 350°F and then tested at 80°F do not show embrittlement.

2. Material plastically deformed at 80°F, exposed to 350°F and then tested at 80°F show embrittlement.

(2) "An Investigation of Methods for Determining the Crack Propagation Resistance of High Strength Alloys"; Progress Report No. 1, Dec. 30, 1959; Bu. Nav. Weapons. Contract NOas 60-6040c.

A few preliminary attempts have been made to show the 350°F embrittlement on the UCX2 material tempered at 500°F, by means of the center fatigue crack test. However, the 80°F and 350°F tests both showed 100% shear with K_{c3} values of 133 and 121 Ksi $\sqrt{in.}$ and notch-strength ratios of 0.53 and 0.50, respectively. While these center fatigue crack tests consisted of only 2 samples at each test temperature, it appears that this type of embrittlement may not be readily detected by this type of test.

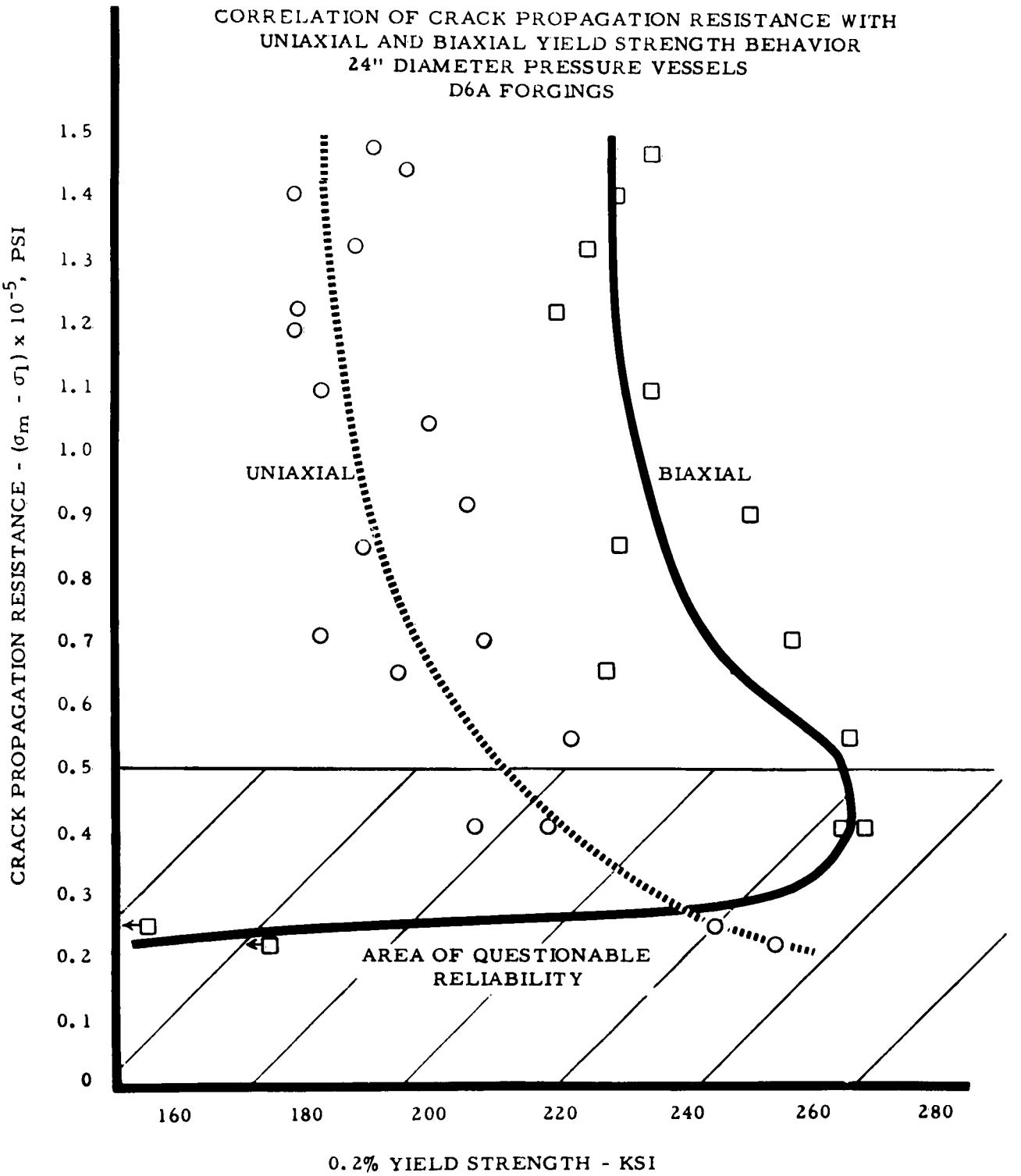

CORRELATION OF CRACK PROPAGATION RESISTANCE WITH
UNIAXIAL AND BIAXIAL YIELD STRENGTH BEHAVIOR
24" DIAMETER PRESSURE VESSELS
D6A FORGINGS
CRACK PROPAGATION RESISTANCE - $(\sigma_m - \sigma_1) \times 10^{-5}$, PSI
1.5
1.4
1.3
1.2
1.1
1.0
0.9
0.8
0.7
0.6
0.5
0.4
0.3
0.2
0.1
0
UNIAXIAL
BIAXIAL
AREA OF QUESTIONABLE
RELIABILITY
160
180
200
220
240
260
280
0.2% YIELD STRENGTH - KSI

FIGURE 1

SCHEMATIC - INSTRUMENTED BEND TEST

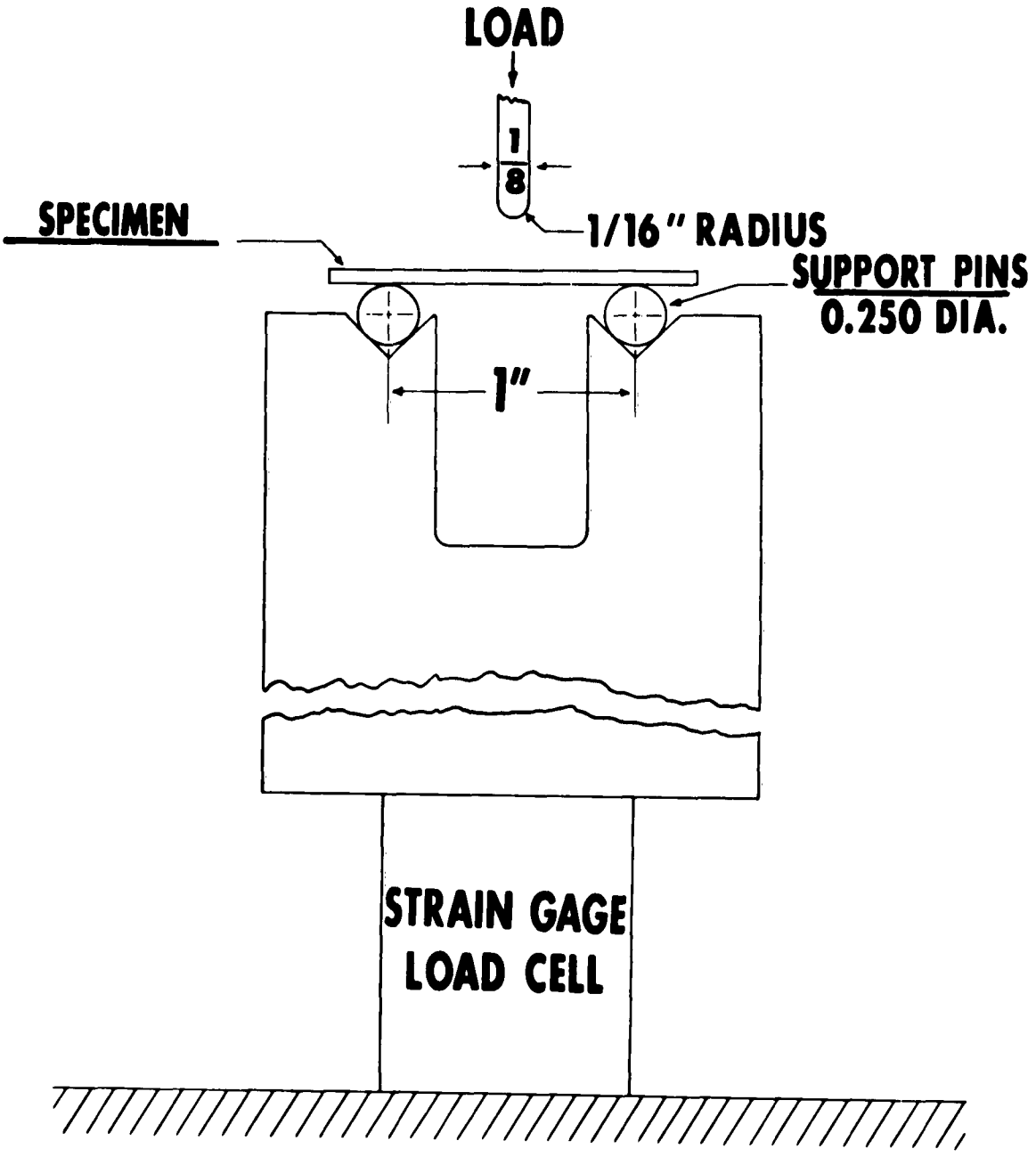


FIGURE 2

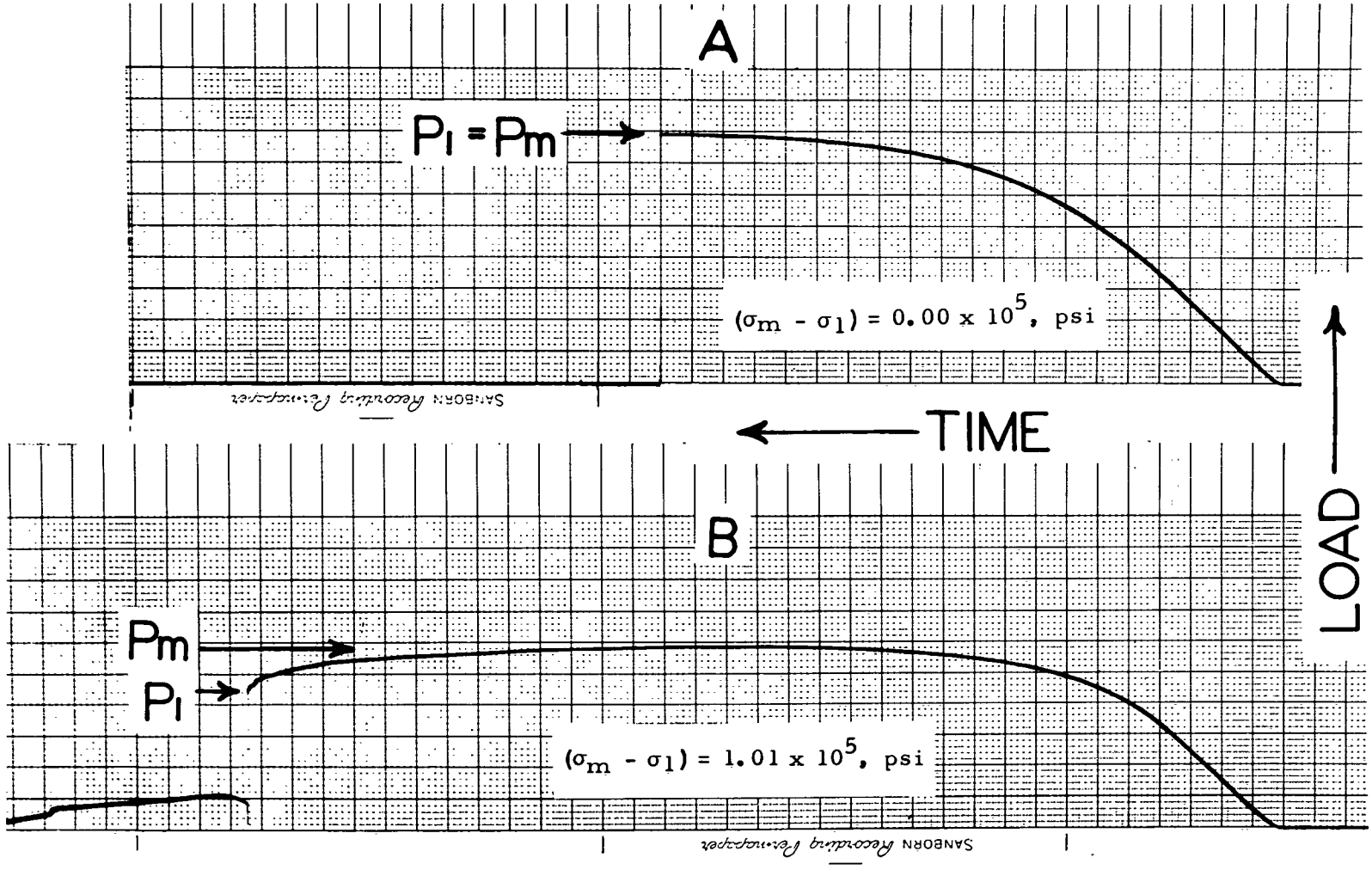

A
$P_I = P_m$
$(\sigma_m - \sigma_1) = 0.00 \times 10^5$, psi
SANBORN Recording Equipment
TIME
LOAD
B
P_m
P_I
$(\sigma_m - \sigma_1) = 1.01 \times 10^5$, psi
SANBORN Recording Equipment

FIGURE 3

CRACK PROPAGATION
INSTRUMENTED BEND TEST

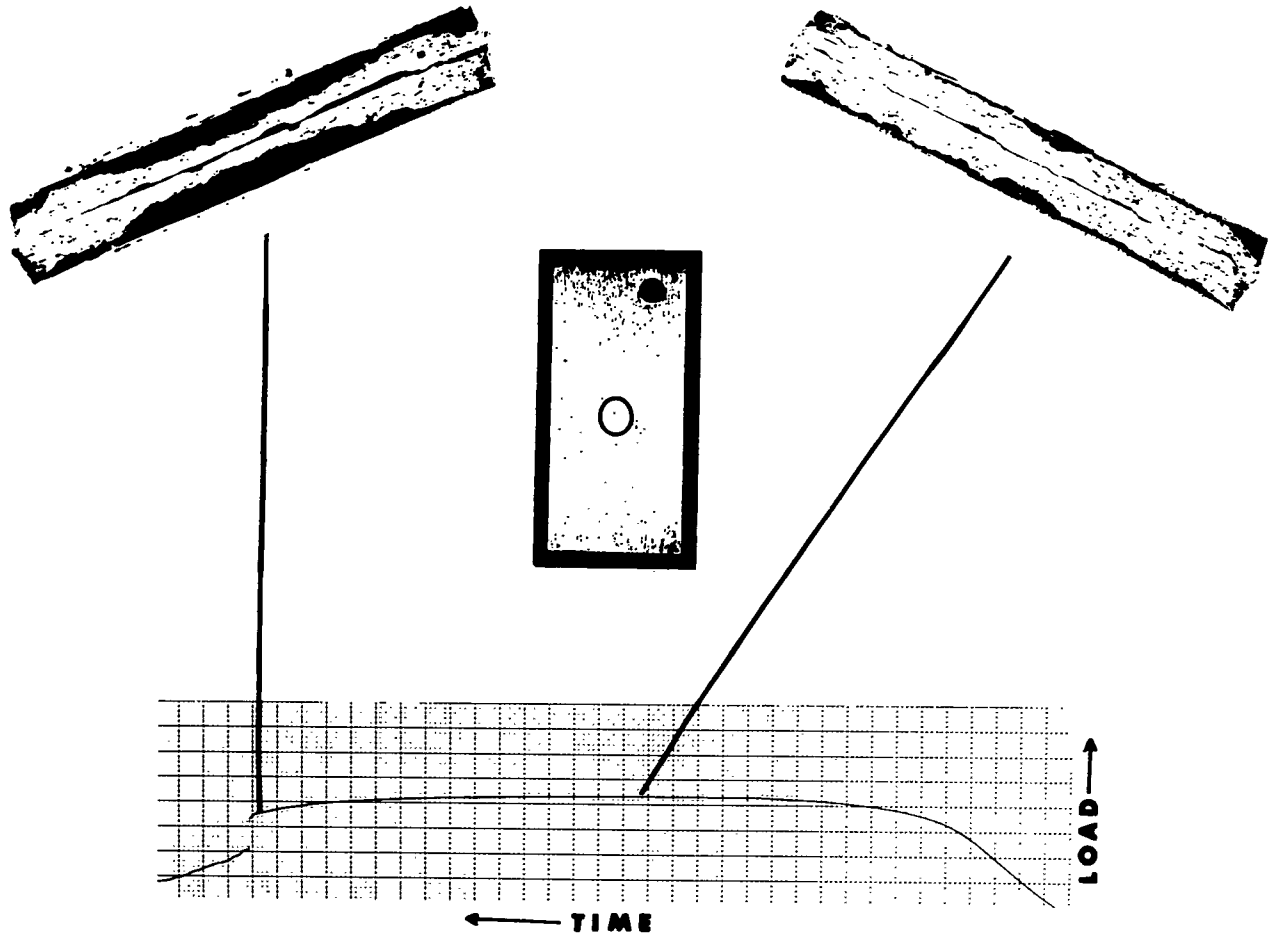


FIGURE 4

CORRELATION OF INSTRUMENTED BEND TEST PARAMETER ($\sigma_m - \sigma_1$) WITH CENTER NOTCH TEST H-11 SHEET (0.095")

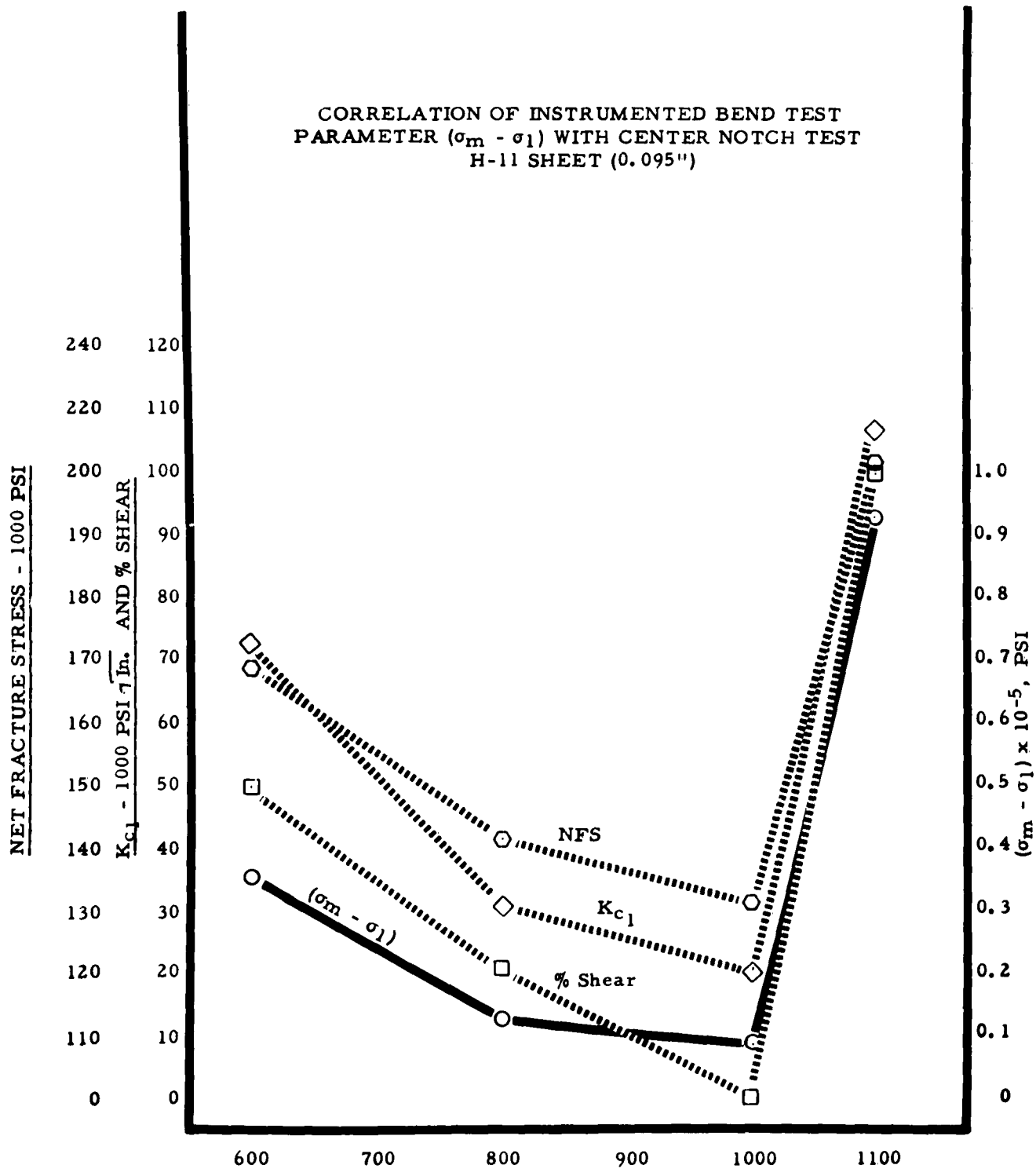


FIGURE 5

CORRELATION BETWEEN INSTRUMENTED BEND TEST PARAMETERS
AND CENTER CRACK TENSILE TEST VALUES
FOR H-11 SHEET (0.095")

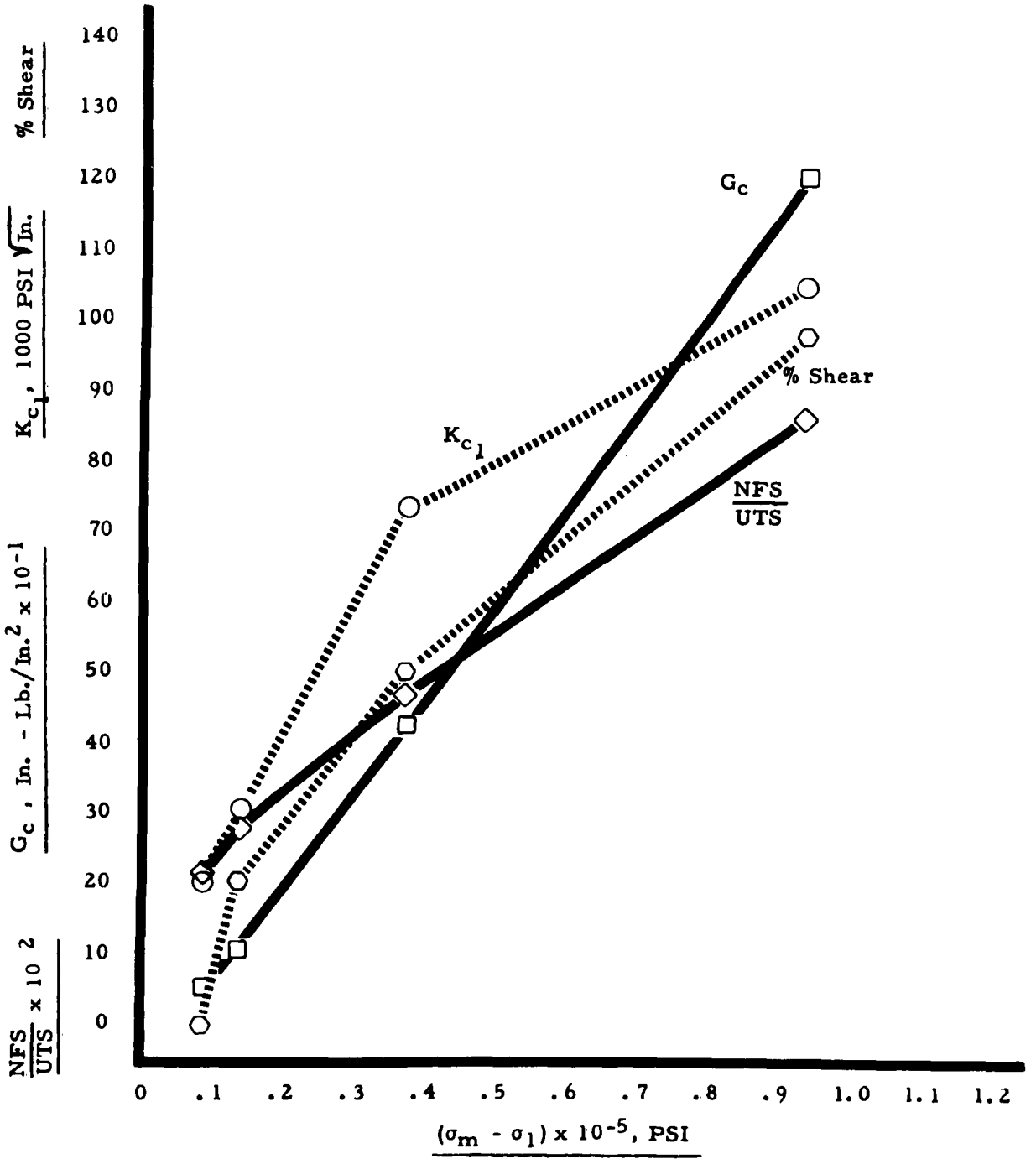


FIGURE 6

CORRELATION OF INSTRUMENTED BEND TEST PARAMETERS OBTAINED IN TWO DIFFERENT LABORATORIES FOR IDENTICAL SAMPLES OF HIGH STRENGTH STEELS

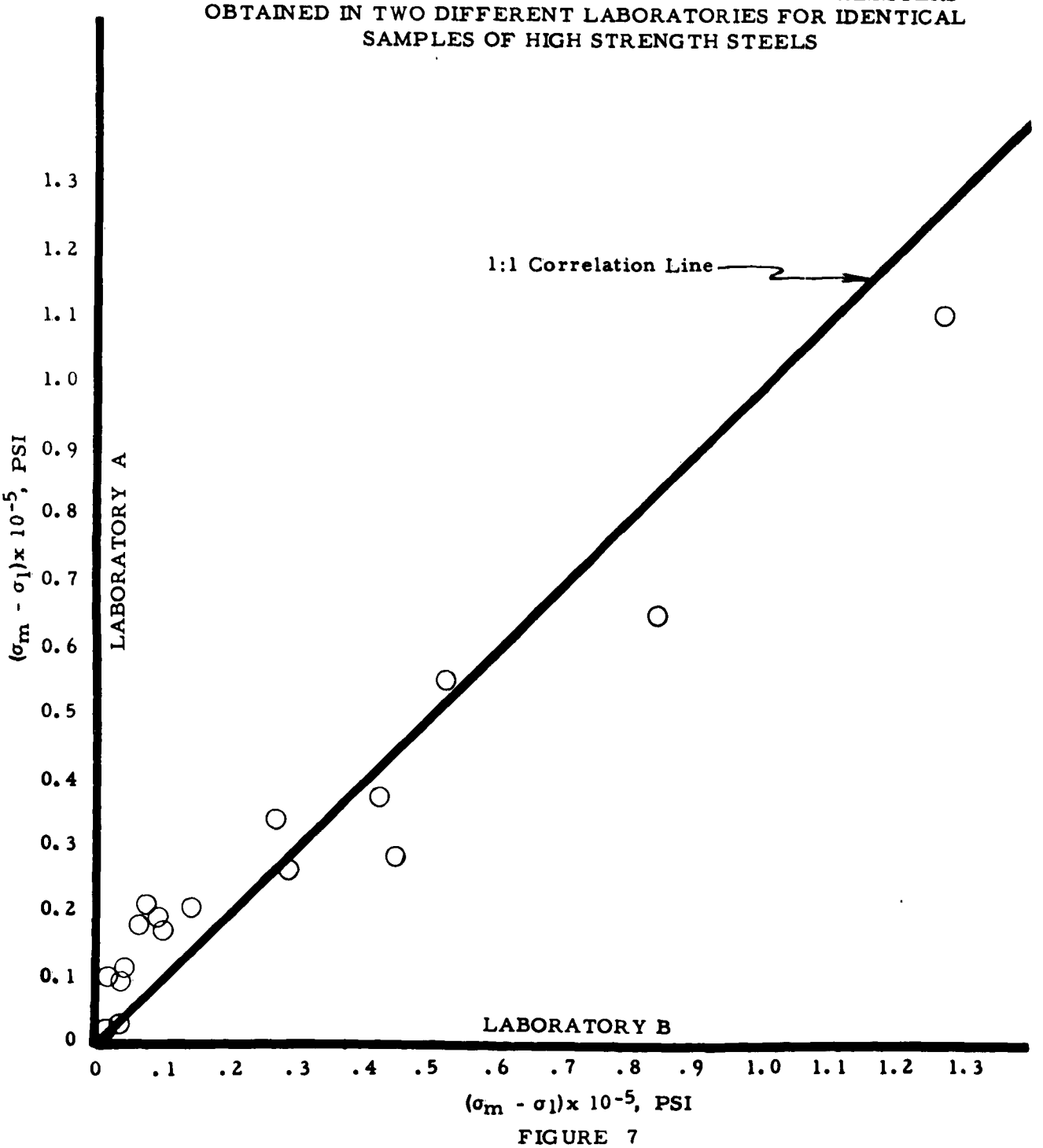


FIGURE 7

CORRELATION OF INSTRUMENTED BEND TEST PARAMETERS
OBTAINED IN TWO DIFFERENT LABORATORIES

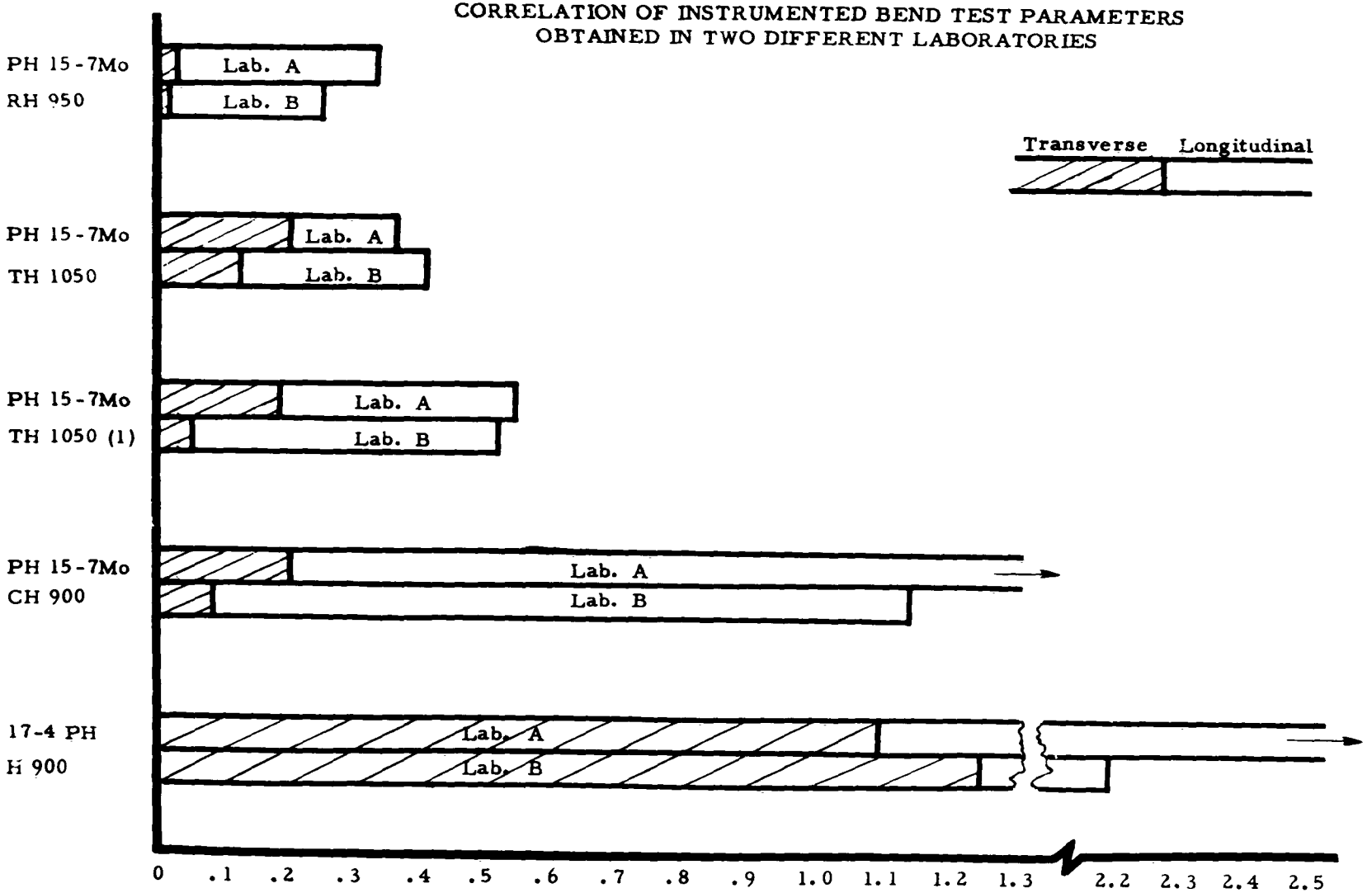


FIGURE 8

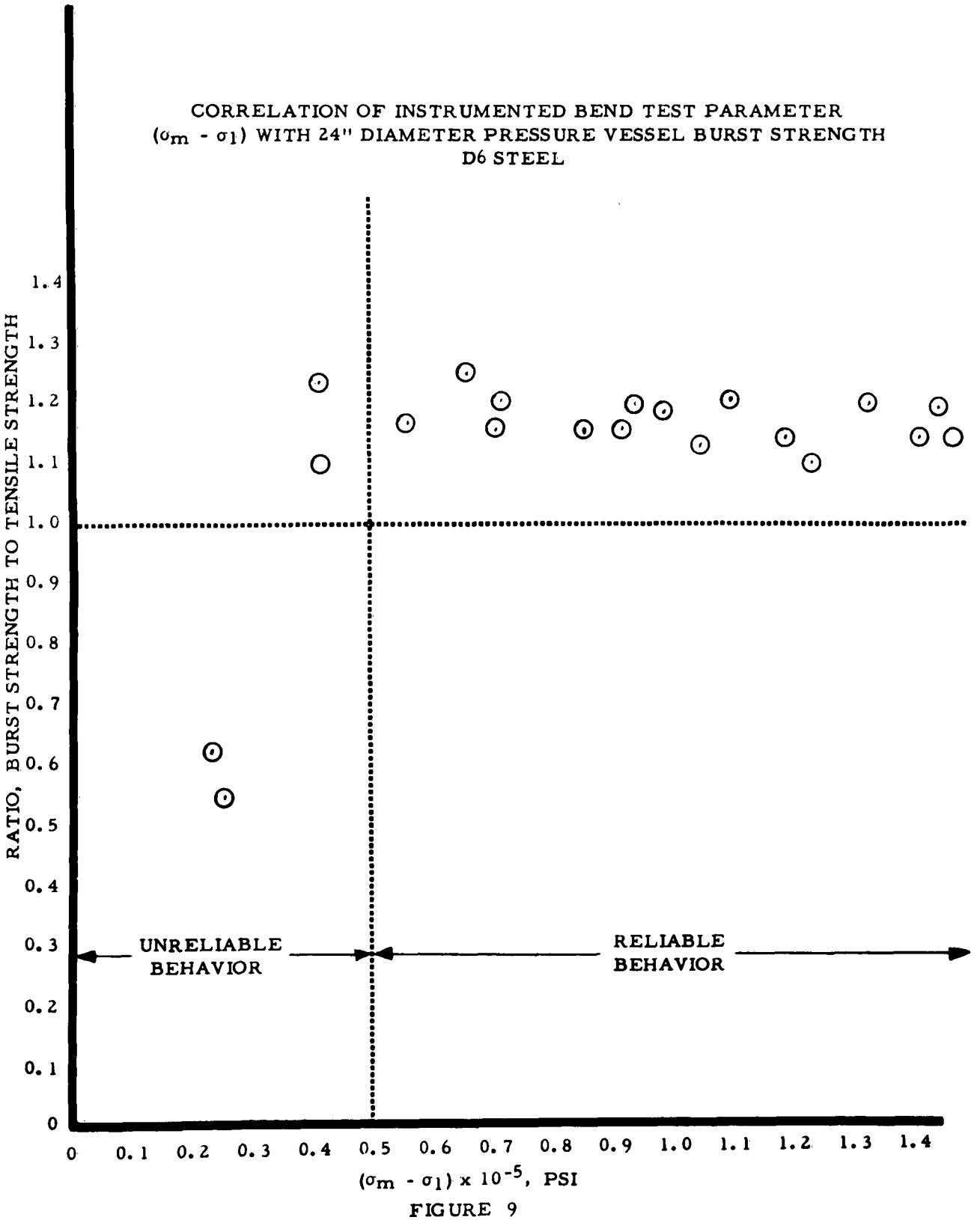

CORRELATION OF INSTRUMENTED BEND TEST PARAMETER
(σ_m - σ_1) WITH 24" DIAMETER PRESSURE VESSEL BURST STRENGTH
D6 STEEL
RATIO, BURST STRENGTH TO TENSILE STRENGTH
1.4
1.3
1.2
1.1
1.0
0.9
0.8
0.7
0.6
0.5
0.4
0.3
0.2
0.1
0
UNRELIABLE BEHAVIOR
RELIABLE BEHAVIOR
0 0.1 0.2 0.3 0.4 0.5 0.6 0.7 0.8 0.9 1.0 1.1 1.2 1.3 1.4
(σ_m - σ_1) x 10^{-5}, PSI

FIGURE 9

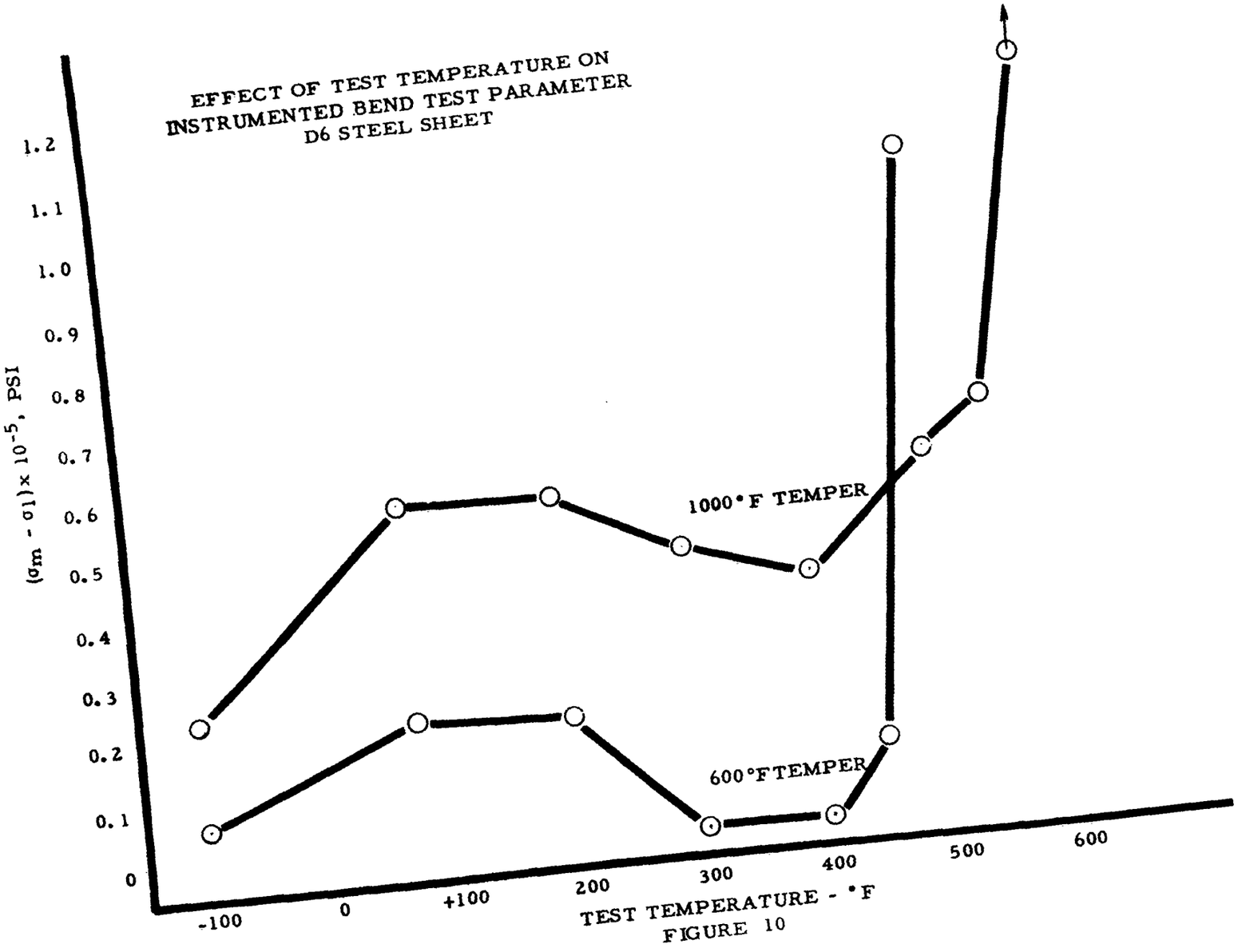

EFFECT OF TEST TEMPERATURE ON
INSTRUMENTED BEND TEST PARAMETER
D6 STEEL SHEET
1.2
1.1
1.0
0.9
0.8
0.7
0.6
0.5
0.4
0.3
0.2
0.1
0
$(\sigma_m - \sigma_1) \times 10^{-5}$, PSI
1000°F TEMPER
600°F TEMPER
-100
0
+100
200
300
400
500
600
TEST TEMPERATURE - °F

FIGURE 10

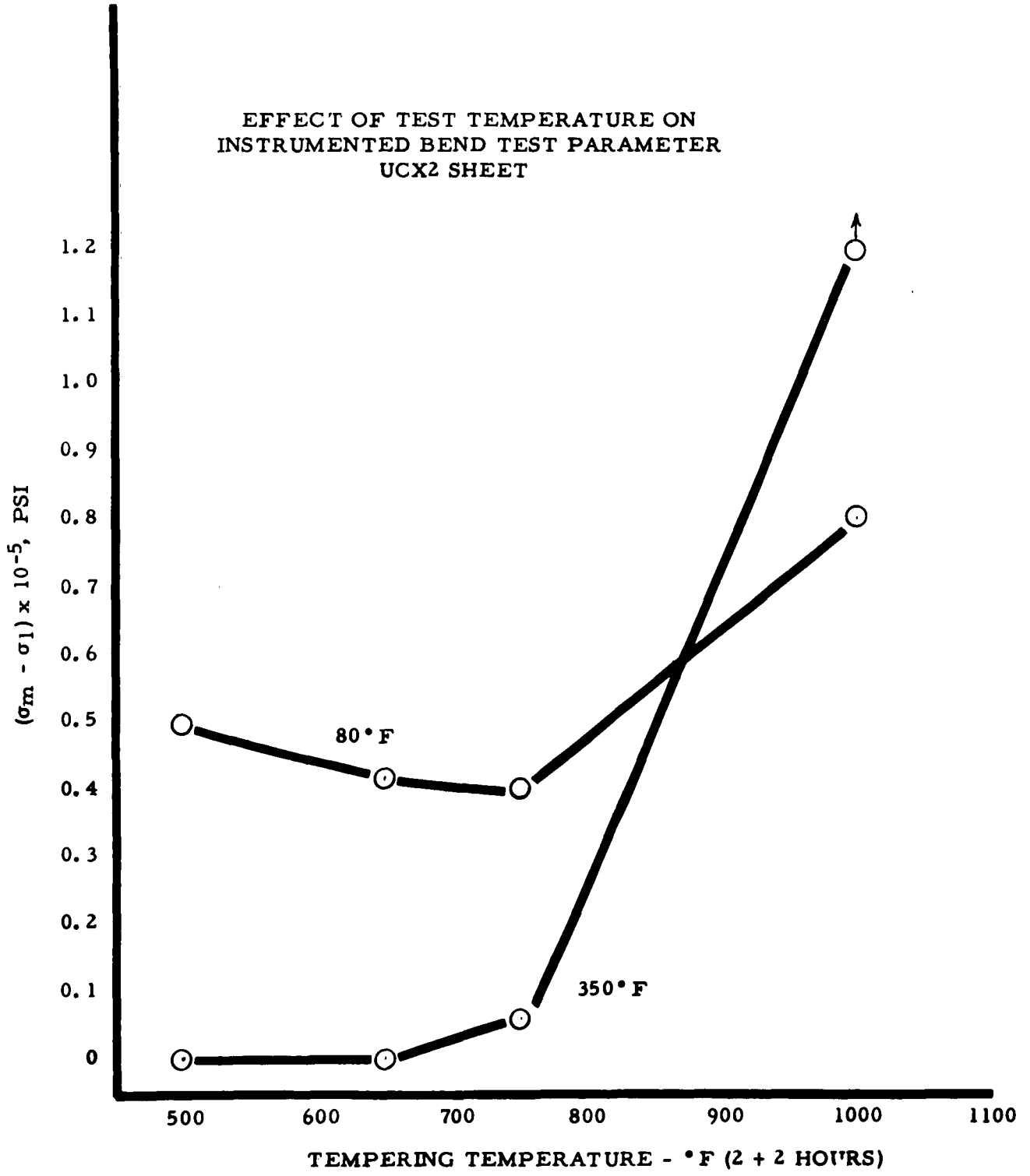

EFFECT OF TEST TEMPERATURE ON
INSTRUMENTED BEND TEST PARAMETER
UCX2 SHEET
1.2
1.1
1.0
0.9
0.8
0.7
0.6
0.5
0.4
0.3
0.2
0.1
0
$(\sigma_m - \sigma_1) \times 10^{-5}$, PSI
80° F
350° F
500
600
700
800
900
1000
1100
TEMPERING TEMPERATURE - °F (2 + 2 HOURS)

FIGURE 11

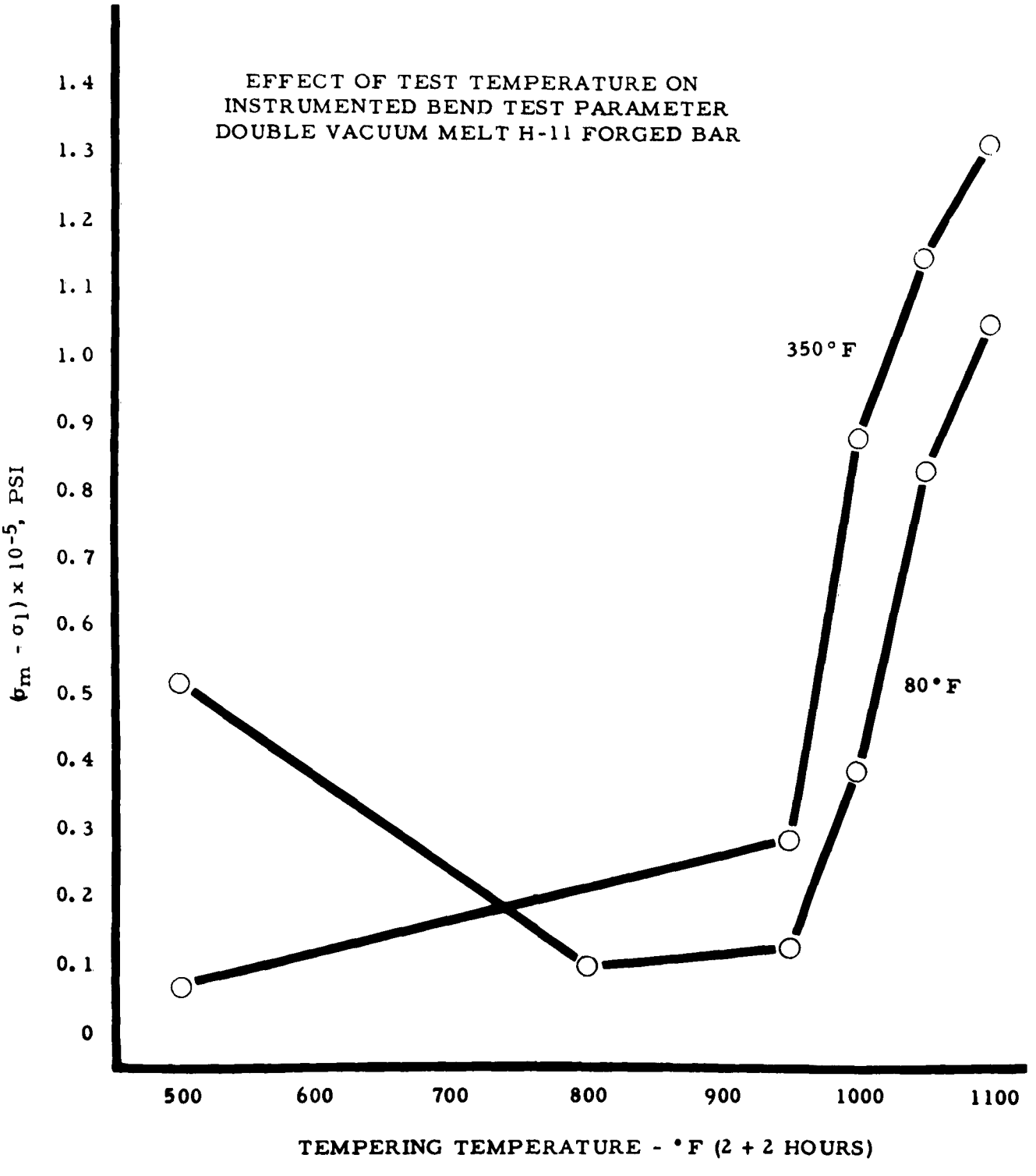

EFFECT OF TEST TEMPERATURE ON
INSTRUMENTED BEND TEST PARAMETER
DOUBLE VACUUM MELT H-11 FORGED BAR
350°F
80°F
$(\sigma_m - \sigma_1) \times 10^{-5}$, PSI
1.4
1.3
1.2
1.1
1.0
0.9
0.8
0.7
0.6
0.5
0.4
0.3
0.2
0.1
0
500
600
700
800
900
1000
1100
TEMPERING TEMPERATURE - °F (2 + 2 HOURS)

FIGURE 12

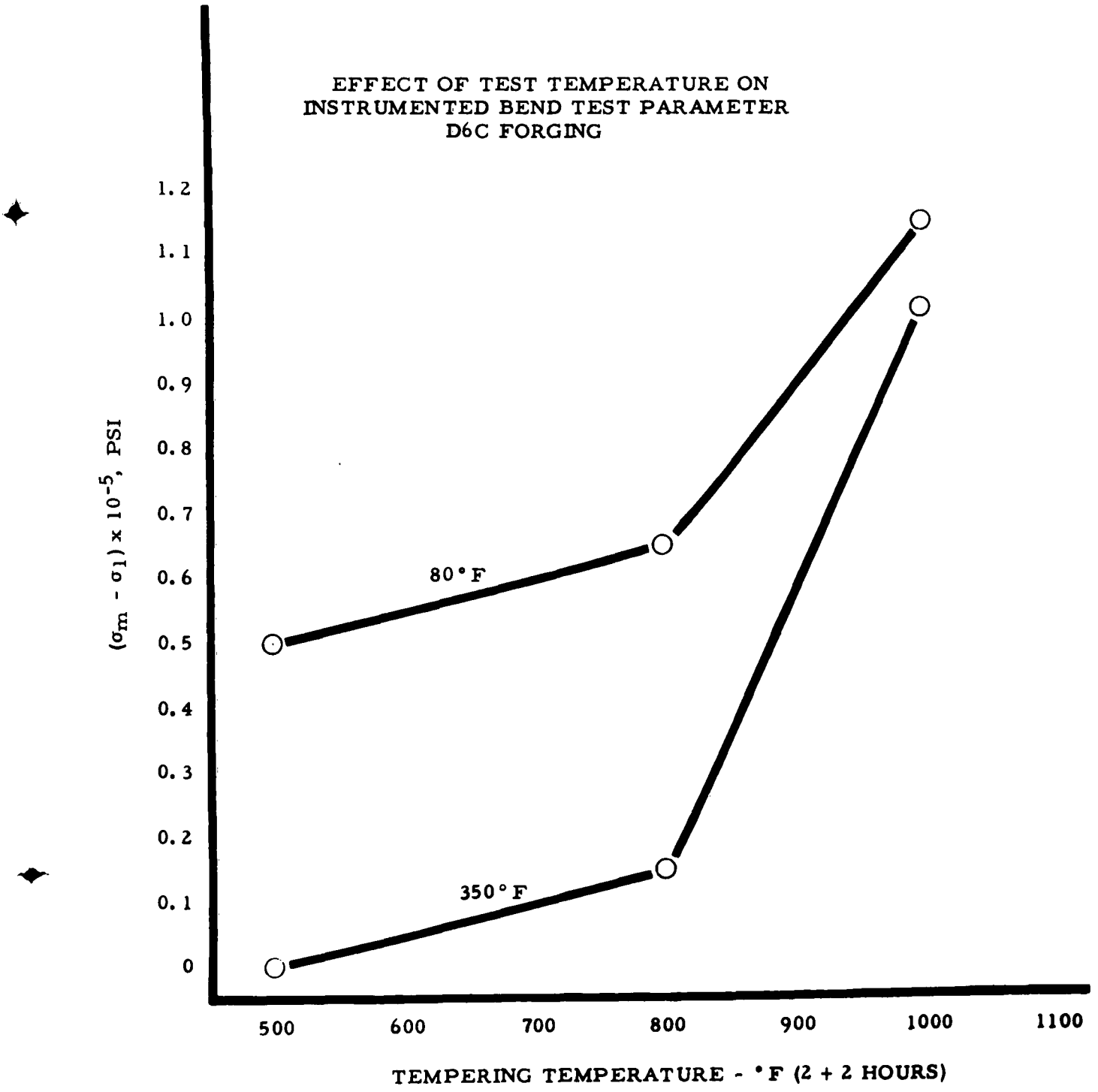

EFFECT OF TEST TEMPERATURE ON
INSTRUMENTED BEND TEST PARAMETER
D6C FORGING
1.2
1.1
1.0
0.9
0.8
0.7
0.6
0.5
0.4
0.3
0.2
0.1
0
$(\sigma_m - \sigma_1) \times 10^{-5}$, PSI
80° F
350° F
500
600
700
800
900
1000
1100
TEMPERING TEMPERATURE - °F (2 + 2 HOURS)

FIGURE 13

THE EFFECT OF SPECIMEN GEOMETRY ON DETERMINATION OF ELONGATION IN SHEET TENSILE SPECIMENS

by

Eric B. Kula
Norbert H. Fahey
Watertown Arsenal Laboratories

INTRODUCTION

The current interest in sheet material has emphasized the need for a more accurate understanding of the significance of ductility of materials. This is especially true of elongation, which is the most common means of assessing the ductility of sheet materials. Unfortunately, elongation values depend on such geometrical factors as specimen thickness and width in addition to gage length and the inherent ductility of the material itself. As a convenience, a constant gage length and specimen width are used as the A.S.T.M. standard sheet tensile specimen[1], but this means that the elongation of specimens of different thicknesses are not strictly comparable. If an interrelationship between elongation, gage length, specimen width, and specimen thickness could be determined, either analytically or empirically, it would be possible to correlate ductility for materials of widely different size and shape.

It was recognized that elongation values can be affected by end restraint, type of fracture, etc., but that elongation is more dependent on specimen size, and hence the primary purpose of this report is to obtain a greater understanding of elongation as a measure of the ductility of plate and sheet materials as affected by specimen size and gage length. These other variables were studied, together with the influence of specimen geometry on yield and tensile strength, and will be reported at a later date.

LITERATURE REVIEW

There has been considerable interest in the effects of specimen geometry on tensile properties and especially elongation in the past The older European literature has been reviewed in Handbuch der Werkstoffprüfung[2], whereas much of the American literature is reviewed in a recent NMIC report[3].

Quantitative relations between elongation and gage length and or cross-section geometry generally take two forms:

a. variation of elongation with gage length for specimens of a given cross-section, and

b. variation of elongation with specimen area in specimens with differing cross-section size and/or geometry but with the same gage length.

Equations relating elongation and gage length have been important because of the great number of gage lengths in common use and the

desirability of comparing elongation values. Throughout the world, the gage lengths used for determining elongation vary from 3.54 to 10 times the specimen diameter for round specimens[2] (4 to 11.3 times the square root of the area for flat specimens). Even in the same country, two or more gage lengths may be used. Some of the equations relating elongation and gage length are:

Martens[4] $$E - E_u = \frac{E_o}{L} \quad (1)$$

Bach[5] $$E - C = \frac{B}{\sqrt{L}} \quad (2)$$

Gallik[2] $$E - E_u = \frac{D_o}{L} \frac{C}{\sqrt{1 + E_u}} \left[RA(1 + Eu/100) - E_u\right] \quad (3)$$

Krisch and Kuntze[6] $$E - E_u = (E_o - E_u)a^{\frac{100}{}} (L/D_o)^{2n} \quad (4)$$

Bauschinger[7] $$E - E_u = \frac{Q\sqrt{A}}{L} \quad (5)$$

Bertella[8] $$E - C = \frac{A^{m/2}}{L^m} \quad (6)$$

where

E = per cent elongation
E_u = per cent elongation measured on an infinitely long gage length

E_o = per cent elongation measured on a zero gage length
RA = per cent reduction in area
L = gage length
D_o = original diameter
A = original area

B,C,Q,
a,m,n, = constants

In all the equations it is recognized that the elongation decreases to some limiting value as the gage length approaches infinity. This is generally termed the infinite gage length elongation. In some cases the limiting elongation for zero gage length is used. This can be calculated from the reduction in area if constancy of volume is assumed. Between these limiting values the elongation decreases with increasing gage length, in a complex exponential manner according to Krisch and Kuntze, or with an exponential function of the reciprocal of the gage length. This exponent is 1 according to Martens, Gallik, and Bauschinger, 2 according to Bach, and arbitrary according to Bertella.

The dependence of elongation on specimen cross-section area has always been recognized. This can be seen by the designation of gage length as some multiple of specimen diameter. Even for rectangular specimens, gage lengths have been specified as a multiple of the square root of the area. Since the elongation depends on the area and not the dimensions, the cross-section shape apparently is not important. Templin reported similar elongation values for various shaped specimens, in-

cluding tubular[9], of the same area. Some of the equations relating elongation in a fixed gage length and specimen cross-section area are:

Bauschinger[7] $$E = E_u + \frac{Q}{L}\sqrt{A} \quad (5)$$

Bertella[8] $$E = C + \frac{L}{L^m} A^{m/2} \quad (6)$$

Templin[9] $$E = C A^n \quad (7)$$

where the terms have the same meaning as before. All three equations show that the elongation increases with some exponential function of the area. Templin's equation does not consider variations in both gage length and area, so the term E_u does not appear.

Malmberg studied the effect of various factors on tensile elongation.[10] By measuring the strain distribution along the length of a bar during straining, he showed that the strain is fairly uniform until just before maximum load, except near the shoulders. When necking occurred, the parts of the bar outside the neck still continued to deform, until just before the fracture load was reached. On round tensile bars varying in size from 5 to 25 mm. diameter, the same variation of elongation with gage length was found for all bars between gage lengths of 2 d to 20 d. This supports the importance of the quantity $\sqrt{A}/L$ in determining elongation. Tensile bars with rectangular cross sections and width-to-thickness ratios varying from 1 to 20 and areas from 25 to 1500 square mm. were studied. In contrast to the results on the round bars, here it was found that the elongation in a certain gage length expressed as a multiple of the square root of the area did depend on area, and tended to decrease with increasing area. Finally, the effect of length of reduced section was studied on round bars. It was found that the shoulders have an effect over a length 1.5 to 3 times the diameter. Beyond this distance from the shoulder, the strain distribution was independent of specimen length.

Miklowitz studied the strain distribution in various size flat tensile bars.[11] He concluded that because of shoulder restraints, straining is non-uniform from the very onset of yielding. In line with this, he maintained a constant ratio of reduced section length to specimen width. He also studied in detail the local strains occurring during necking. Aronofsky also studied necking in flat tensile bars[12]. He studied the effect of width to thickness ratio on the formation of the oblique neck that forms under certain conditions.

Low and Prater studied the effect of various geometries on tensile elongation[13]. They showed that the ratio of reduced section length to specimen width determined the length restrained by the shoulders, and hence the length under simple tension. The influence of lateral restraint in reducing the elongation of bars of width to thickness ratios greater than 6 was pointed out.

PROCEDURE

Since contributions to elongation can ideally be considered to

come from two sources, the uniform elongation and the extension associated with the neck, the effect of specimen geometry on these quantities was to be determined. This was accomplished by photogridding the specimens with a grid spacing of twenty to the inch along the reduced section and analyzing the distribution of strain throughout this region, with particular emphasis placed on the necked region. With this in mind the materials used were selected because of their differences in uniform strain values. The materials used, each of which were individual heats, were hard drawn and annealed copper, AISI 1020 steel, and H 11 tool steel. The copper and steel were obtained as 1/2" thick by 2 1/2" wide bar in random lengths and the H 11 was supplied in 1/8" sheet. After insuring the homogeneity of the material by macroetching and hardness surveys, tensile specimens of various thicknesses and widths were prepared from the 1/2" bar by slicing to the approximate thickness and then careful grinding to size. Specimen thicknesses from 0.010 to 0.500 inches were prepared, with widths ranging from 1/8 to 2 inches, see Figure 1. This resulted in specimen width to thickness ratios of from 1:1 to 200:1 and areas ranging from 0.0013 to 1.00 square inch.

Tensile properties of the various materials used are summarized in Table I.

TABLE I

Material	0.2% Yield Strength psi	Tensile Strength psi	Reduction of Area, %	Elongation, Total, %	Elongation, Uniform %	Specimen Type
Copper, hard drawn	34,800	37,000	69.2	30.0	7.0	.357" D
Copper, Annealed	8,900	31,000	70.4	37.9	26.5	.357" D
1020 Steel	32,300	55,900	63.0	37.1	25.0	.357: D
H 11 Tool Steel	231,000	250,900	----	8.8	5.0	1/2" X 1/8"

The copper was received in the hard drawn condition, and testing was carried out after machining and an anneal of 2 hours at 400°F. The annealed copper was obtained by annealing the as-received material for one hour at 1200°F. It too was given an anneal of 2 hours at 400°F after machining. The AISI 1020 hot rolled steel was normalized at 1700°F prior to machining and annealing at 750°F for 2 hours. The H 11 tool steel was machined to size, austenitized in a salt pot at 1800°F for 20 minutes (after preheating at 1450°F), quenched in still air, and tempered twice, 1 hour each time, at 1050°F.

Since the specimens were of various sizes, a good range in load capacities was necessary and three different tensile testing machines were utilized. The head speed of the machines was regulated so that all specimens were strained at an initial rate of 0.01 inches per inch of gage length up to the yield and then at 0.02 inches per inch of gage length to fracture.

All the specimens had been photogridded prior to testing with the grids spaced at twenty to the inch. Grids were put on the width surface for specimen thicknesses of 1/8" or less and on both the width and thickness surfaces for specimen thicknesses of 1/4" and 1/2", see Figure 2. As shown on this figure, two local strains, namely the width and longitudinal strains, could easily be measured on all specimens and the thickness strain could be measured on the larger specimens. On the thinner specimens the average thickness strains could be measured directly, with a micrometer. Furthermore, any one strain can be calculated from the other two, since because of constancy of volume, the sum of the principal strains is zero.

RESULTS AND DISCUSSION OF RESULTS

Since the distance between grids on a longitudinal line running along the center of the bar was measured, the elongation for any gage length could be determined. Plots of elongation versus various combinations of gage length and area were constructed and observations are made. The idealized picture of tensile deformation is that a test piece contracts uniformly in the transverse directions as it elongates. This uniform deformation continues until a maximum in the load is reached. At this point, further deformation becomes limited solely to a restricted portion of the test piece termed the neck. The size of this necked region depends on the specimen dimensions. The results will be discussed in terms of this simplified picture.

A. Effect of Gage Length on Elongation

Typical results showing the dependence of elongation on gage length for the four materials are shown in Figures 3a to d.

In each case the elongation decreases as the gage length increases, due to the decrease in the fraction of the gage length representing the necked region. There are three features of each curve which are worthy of further discussion. These are the zero gage length elongation, the infinite gage length elongation, and the variation of elongation with gage length between these two values.

The zero gage length elongation does not seem to be a constant value for a given material, but seems to decrease with specimen area. The smallest gage length measured is 0.1 inches however, and closer agreement might have been obtained if the zero gage length elongation had been calculated from measured transverse and thickness strains. It was not possible to obtain accurate values of thickness strain at the fracture however, since the fracture surface often cut through the region of minimum thickness at an oblique angle. Furthermore, all elongation values, measured along the center line of the specimen, include a gap that forms between the two halves of the specimen as the

fracture propagates from the center outward. This gap is normally included in standard elongation values obtained by placing the broken halves of the specimen together and is generally greater the greater the specimen thickness. Finally, there is no indication that bars of different geometries fracture at a constant value of longitudinal strain. Results by Miklowitz[11] suggest that the conditions for fracture are more nearly a constant thickness strain.

The infinite gage length elongation is the elongation that a bar infinitely long would exhibit, and where the contribution of the neck would be effectively zero. This could also be considered to be the maximum uniform extension. This value should be independent of specimen size. The actual results for the longest gage lengths measured do not show this. If infinitely long specimens had been used, no doubt this would have been observed, but the restraining effects of the shoulders tend to reduce the elongation in this region. Of some interest are the very low elongations displayed by the 0.010" specimens, which are even less than the strains at maximum load as determined from true stress-strain tests on round bars. The reason for this must lie in non-uniformity of the original test piece. Even a variation in thickness of 0.0005", which represents 5% variation in area for a 0.010" specimen, would tend to strongly localize deformation from the start of straining, with accompanying low elongation.

The variation of elongation between zero and infinite gage length has been expressed by several of the equations presented earlier. It should be pointed out that in no case is there a sound fundamental reason for deriving any of the equations, beyond recognizing the significance of zero and infinite gage length elongation.

To check some of these equations, elongation has been plotted versus $1/L$ and $1/\sqrt{L}$ in Figures 4 and 5 for each material at one size. The results show that either relationship is valid over short ranges of L, but that neither holds over a large range of gage lengths. In some cases, one or the other relationship does give a reasonably straight line, but for another material or size similar results are not found. It has been noted that extrapolations of the curves to infinite gage lengths do not yield a constant value, and in some cases yield negative values, which points out the inadequacy of the relationships. Plots of the same data on log-log coordinates, Figure 6, do not show a straight line either, showing that Bertella's equation (Eq. 6), is not correct.

After considering the fact that there is no known theoretical basis for expecting a simple relationship, coupled with experimental conditions such as end effects, possible non-homogeneity of material and specimens, and the occurrance of double necks, it is not surprising that no one equation adequately predicts the actual variation of elongation with gage length.

B. Effect of Specimen Area on Elongation in a Fixed Gage Length

The results plotted in Figure 7 show that over a range of sizes, there is a linear relationship between log of elongation in 2" and log of area. There is considerable scatter. However, and at low areas

there is a deviation from the linear behavior. These points represent the thinnest specimens, where dimensional variations would have the greatest effect. As discussed earlier, many of the elongation values are lower than the strain at maximum load, which supports the viewpoint of the non-homogeneity of strain because of dimensional variations.

Three equations, Eqs.5, 6, and 7, mentioned earlier, relate elongation to some power of the area. It must be realized that for a specimen with an area approaching zero, the elongation approaches the uniform elongation, and for very large specimens, the elongation in 2 inches approaches the zero gage length elongation. None of the equations approach these limits at zero or infinite gage length, which emphasizes their empirical nature. Bauschinger's and Bertella's equations do approach a finite value at zero area however. In figures 8a to d are plotted log ($El - El_u$) versus log area. The uniform elongations were determined from true stress-strain tests. It can readily be seen that a straight line can be drawn here also, although from a practical viewpoint Templin's equation is to be preferred since the amount of scatter for the lower elongations is seemingly reduced.

GENERAL DISCUSSION

There are two questions concerning the observed relationship between elongation and area which are of interest. The first is concerned with the significance of area, rather than width-to-thickness ratio or reduced section length-to-width ratio in determining elongation, and the second with the slope of the straight line portions of the curves in Figure 7.

A. Significance of Specimen Area

Figure 9 shows a plot of the distribution of local elongation, measured over gage lengths of one grid spacing. It can readily be shown that the elongation over a two inch gage length can be represented on such a plot by a horizontal line drawn such that the area under it is the same as the area under the curve. Figure 9 shows a plot of strain distribution for three bars of the same cross-section geometry, but different areas. The shapes of the curves are generally the same, except that as the specimen area gets larger, the curve gets broader which is an indication of the larger extent of the necked region. There is an effect of size on the maximum strain. Here again, the arguments advanced in the earlier discussion are valid, in which it was pointed out that the true zero gage length elongation was not determined. Further the local strain at the extremities of the gage length section is greater for the larger area bar, because of the closer proximity to the neck. All in all however, the greater elongation in 2 inches (area under the curve) for the larger area bars can be attributed to the larger extent of necked region.

Figure 10 shows similar plots of local strain for three bars having the same area. Within experimental accuracy, these bars have the same elongation, and hence the same area under the curve. Notice now that the shapes of the curves are quite different. At a width-to-thickness ratio (w/t) of 1, the local strain decreases uniformly with distance from the fracture. As w/t increases, there is a tendency for

a more rapid decrease of strain with distance in a very narrow range in the vicinity of the fracture, with a change to a more gradual decrease at larger distances from the fracture. The height of the curve for high w/t ratios is such that at intermediate distances from the fracture it lies below, and at large distances from the fracture it lies above the curve for a square specimen, with the net result being the same area under the curve.

Because of the constancy of volume, it is possible to break the longitudinal strains into a component of transverse or width strain and thickness strain. Further insight into the shape of the curves can possibly be found by considering the effect of width-to-thickness ratio separately on width and thickness strains. Some results are plotted in Figure 11, where true strains have been used, since here the sum of the width and thickness strain should equal the longitudinal strain. The width strains were determined over a one grid length (0.05"), whereas the thickness strains were determined over the whole thickness.

The results clearly show the differing behavior for the various w/t's. For a w/t of 1, the width and thickness strains are almost equal. (The hard drawn copper is actually slightly anisotropic, by virtue of having a preferred orientation arising from cold working.) As w/t increases, there is a restraint in the width direction and the ratio of the thickness strain to the width strain increases at the fracture, so that most of the elongation at this point arises from the contribution of the thickness strain.

B. Significance of Exponent "n" in Templin's Equation

Of some importance is the slope of the curves in Figure 7, which is characterized by the exponent "n" in Templin's equation, Eq. 7. The importance of this lies in the fact that it is a measure of the sensitivity of elongation values to thickness changes. It would tell, for example, whether two materials which have the same elongation value at a thickness of 1/8" would also have the same elongation at some other thickness. One is tempted to look upon the exponent "n" as a material property, which can be determined and tabulated. A little reflection on the problem will show the fallacy of such an approach.

Consider the case of the same materials used in this investigation, but fracturing at a lower strain. The curves of percent elongation versus gage length, Figure 3, would then have a different shape. This has in effect been done by pulling various size bars to as constant a strain as possible at the center of the neck, but below the fracture strain, and measuring the strain distribution. These results are plotted in Figures 12a to c together with strain distributions from the fractured bars. It is readily apparent that at small gage lengths the elongations are much lower for the bars not fractured, but that as the gage lengths increase, the elongations for the two cases approach each other, and for an infinite gage length they would presumably be the same. Note further that for some intermediate gage length, say 2 inches, the spread in elongation values between the smallest and largest areas is less for the bars pulled to a strain

less than the fracture strain than for the bars pulled to fracture. If these values of elongation are plotted versus area as formerly, the results such as in Figure 13 are obtained. Allowing for experimental scatter and for the fact that all bars were not pulled to exactly the same strain, it can be seen that a straight line is obtained, but with a lower slope than for the bars pulled to fracture. In fact, in an extreme case, if the bars were all pulled to or fractured at or before the limit of uniform strain the elongation would be the same for all bars over all gage lengths, and the slope would be zero on a log-log plot of elongation versus gage length.

From these considerations, it can be seen that the exponent "n" in Templin's equation is not a general material property which can be tabulated, but rather depends on the ductility of the specific lot of material being tested. For two different materials with the same uniform strain, the one having the higher fracture strain would have the greater value of the exponent "n". Similarly, for a constant fracture strain, the lower the uniform strain the higher the value of this exponent. The quantity, determinable from a single tensile test, which best correlates with Templin's exponent "n" is probably the ratio of the fracture to the uniform strain. Unfortunately, the high strength sheet materials of current interest do have a low value of uniform strain with moderate fracture strains, so that their elongation values are quite sensitive to variations in thickness.

C. Prediction of Per Cent Elongation

In many cases, it would be desirable to be able to predict the elongation for any arbitrary size specimen. Lacking complete data for many specimens which would allow an interpolation to be made, there is a method which suggests itself. This is based on the concept that a constant elongation is obtained if $\sqrt{A}/L$ is maintained constant, as suggested by Bauschinger's equation, Eq. 5. Malmberg found this to be valid for round bars, but not for rectangular bars. The results of this investigation support Malmberg and show that this is not generally true. Nevertheless, under some conditions it is a good approximation. If it is valid, then at a constant value of elongation:

$$\frac{L_1}{\sqrt{A_1}} = \frac{L_2}{\sqrt{A_2}}$$

where L and A are the gage lengths and area of two different bars 1 and 2. To determine the elongation in a length L_2 on a bar with an area A_2 from measurements on a bar with area A_1, simply measure the elongation on bar 1 over a gage length $L_1 = L_2 \sqrt{A_1/A_2}$. From this relation, the elongation in a fixed gage length for any area bar can be calculated from measurements over different gage lengths on one bar.

Some results using this method have been calculated for several size bars of the various materials, and are plotted in Figure 14 with the experimentally determined results from Figure 7. In some cases, the points do not lie on the experimentally determined curve, since the standard 2 inch elongation for the bar used lie off the curve. In general the results are good, and the slopes of the experimental and

calculated curves are the same. Deviations are noted when the elongation must be measured over such a long gage length that either a second necked region or end restraints are encountered.

In a practical sense, this principle could be applied to standard 1/2" wide specimens. Suppose for example one had available and knew the properties of 1/8" sheet, what elongation could then be expected from 0.080" thick sheet? From the above relation, one can determine that the elongation measured on $L = 2\sqrt{\frac{.125}{.080}} = 2.5$ of the 1/8" sheet is the same as the elongation in 2 inches on 0.080" sheet. Accurate values should be obtained if the areas do not differ appreciably.

SUMMARY

A study has been made of the effect of specimen gage length, width and thickness on the elongation as determined in a tensile test. Hard-drawn copper, annealed copper, 1020 steel, and H 11 steel were studied.

Although a number of relationships have been proposed to explain the variation of elongation with gage length, the results show that no one relationship adequately describes the course of the curves.

The elongation in 2 inches is found to vary approximately linearly with the specimen area on a log-log plot, showing agreement with Templin's equation. The reason for the dependence of elongation on specimen area rather than width-to-thickness ratio, can be seen from a study of the local width, thickness and longitudinal strains.

The sensitivity of elongation to specimen area or thickness, as measured by the exponent "n" in Templin's equation, $El = CA^n$, is dependent on the fracture strain as well as the uniform strain, and hence varies from heat to heat of material. This exponent is most closely related to the ratio of fracture strain to uniform strain.

If $L/\sqrt{A}$ is maintained constant, the elongation will be approximately constant. Using this relation, it is possible to estimate the elongation for any size bar from measurements made on one bar.

REFERENCES

1. Tentative Methods of Tension Testing of Metallic Materials (E8-57T), 1958 Book of ASTM Standards.

2. SIEBEL, E., "Die Prüfung der Metallischen Werkstoffe," Vol 2, Handbuch der Werkstoffprüfung, Julius Springer, Berlin, p. 69, 1955.

3. "The Influence of Sheet Thickness on Tensile Properties of Metal Sheet," Defense Metals Information Center Memorandum 5, January 23, 1959

4. MARTENS, A., "Handbuch der Materialienkunde für den Maschinenbau," Vol I, Springer, Berlin, p 94, 1898.

5. BACH, C., VDI-Forschungs Heft, Vol 29, p. 69, 1905

6. KRISCH, A. and KUNTZE, W., Archiv f. d. Eisenhüttenwesen, Vol 7, p. 305, 1933/34.

7. BAUSCHINGER, J., Mitteilungen des mechanish-techn. Laboratoriums des Kgl. techn. Hochschule, München, Vol 21, p. 22

8. BERTELLA, C. A., "Sulle Prove de Tensions dei Metalli", Giornale del Genio Coville, Vol 60, p. 343, 1922.

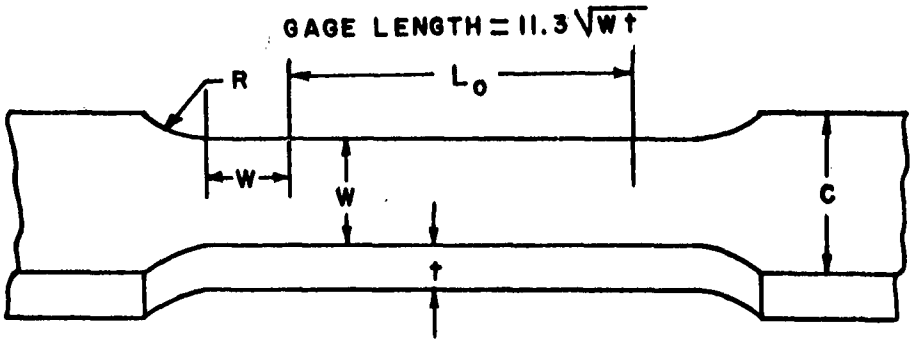
9. TEMPLIN, R. L., "The Effect of Size and Shape of Test Specimens on the Tensile Properties of Sheet Metal," Proceedings, Am. Soc. Testing Mats., Vol 26, Part 2, p. 378, 1926.

10. MALMBERG, G.," Provstavsformens Inverkan på Forlängningen vid Dragprov," Jernkontorets Annaler, Vol 128, p. 197, 1944.

11. MIKLOWITZ, J., "The Influence of the Dimensional Factors on the Mode of Yielding and Fracture in Medium-Carbon Steel-I," Jour. Applied Mechanics, Trans. Am. Soc. Mech. Eng., Vol 70, p. 274, 1948.

12. ARONOFSKY, J., "The Formation of a Necked Region and Fracture Along an Oblique Line in Flat Tensile Bars," Proceedings of the First U. S. National Congress of Applied Mechanics, Am. Soc. Mech. Eng. p. 521, 1952.

13. LOW, J. and PRATER, T., "Measurement of Ductility in Sheet Metals" Symposium on Deformation of Metals as Related to Forming and Service, Am. Soc. Testing Mats. Special Technical Publication No. 87, p. 53, 1948.



WHERE

W: 1/8", 1/4", 1/2", 1", 1-1/2", AND 2"

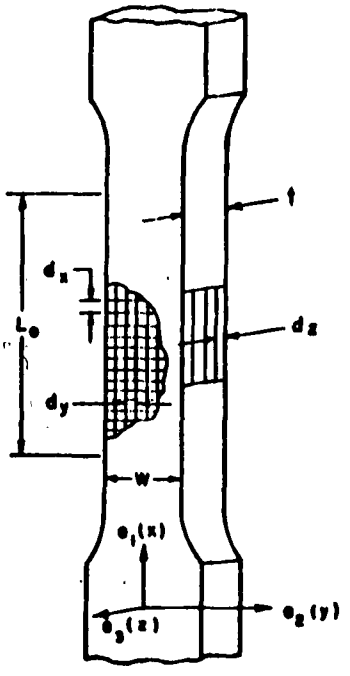
t: 0.010", 0.020", 0.040", 0.080", 0.125", 0.250", AND 0.500"
(IN NO CASE WAS W/t < 1)

C: 1/2" FOR W = 1/8" AND 1/4", 1" FOR W = 1/2", 2" FOR W = 1", AND 2-1/2" FOR W = 1-1/2" AND 2"

R: 1" RADIUS IN ALL CASES

L_o: 11.3 $\sqrt{Wt}$, BUT MINIMUM 2"

FIGURE 1: FLAT TENSILE SPECIMEN



RELATIONS:

LOCAL STRAINS:	AVERAGE STRAINS:	WHERE:
$e_1 = \frac{d_x' - d_x}{d_x}$	$e_1 = \frac{L - L_o}{L_o}$	d_x', d_y', d_z', L, W, and t are the strained values of d_{x_o}, d_{y_o}, d_{z_o}, L_o, W_o, and t_o
$e_2 = \frac{d_y' - d_y}{d_y}$	$e_2 = \frac{W - W_o}{W_o}$	
$e_3 = \frac{d_z' - d_z}{d_z}$	$e_3 = \frac{t - t_o}{t_o}$	

FIGURE 2: STRAIN DIRECTIONS IN TENSILE SPECIMEN

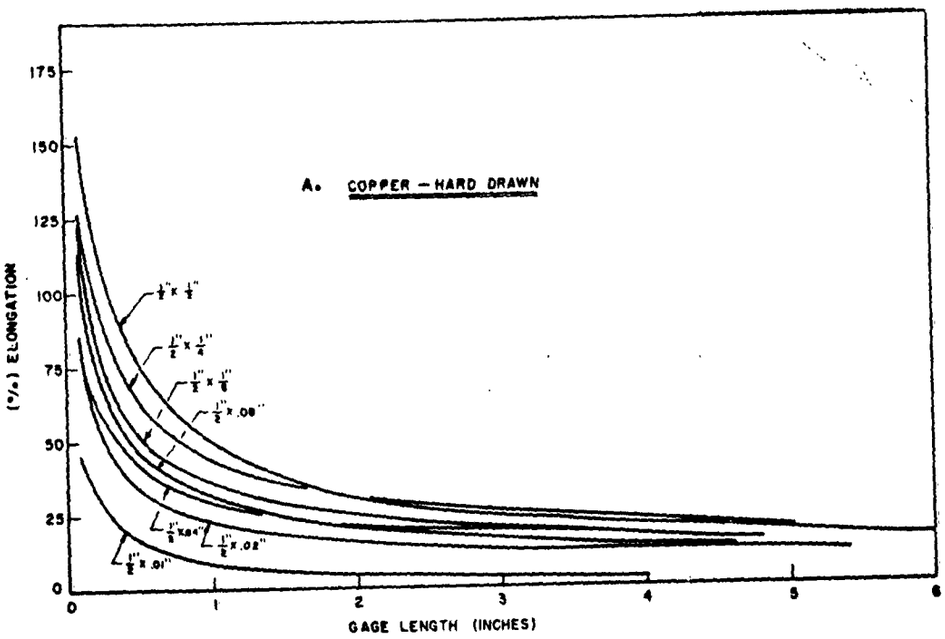


FIGURE 3A

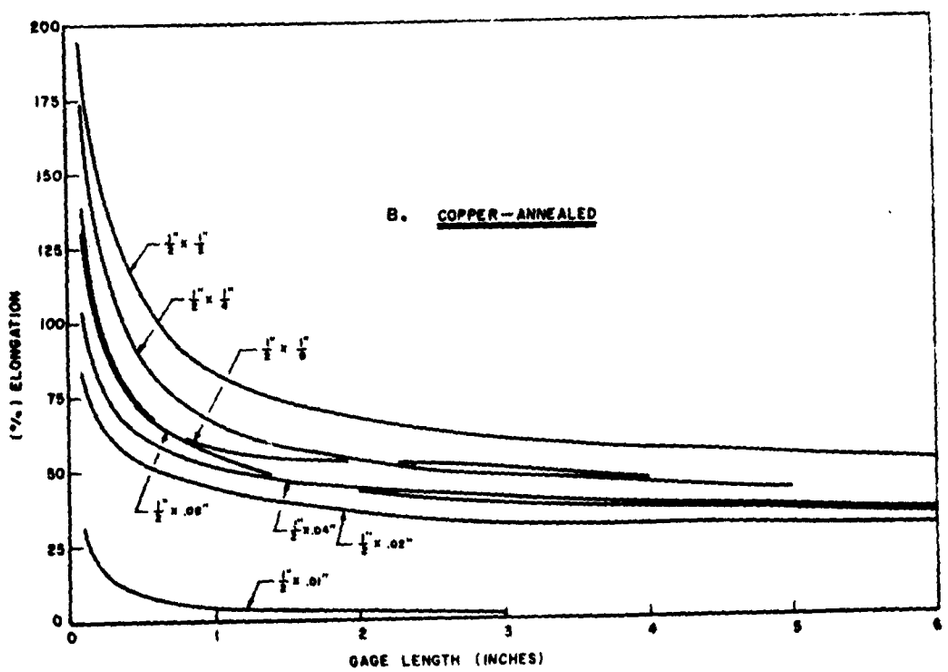


FIGURE 3B

VARIATION OF ELONGATION WITH GAGE LENGTH

FIGURES 3A & 3B

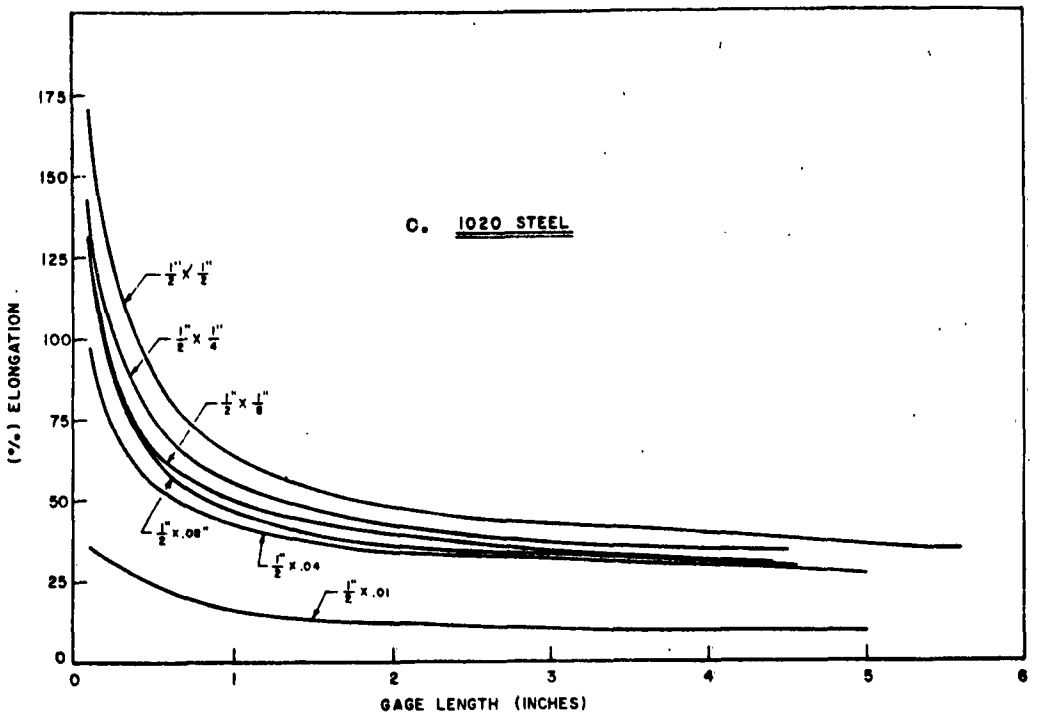


FIGURE 3C

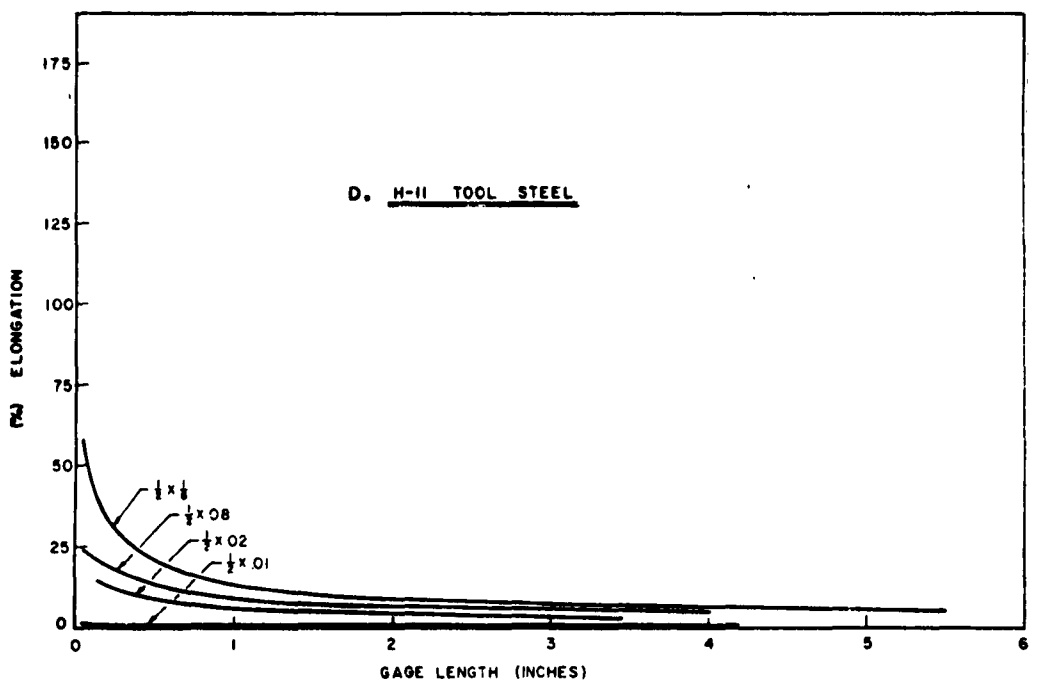


FIGURE 3D

VARIATION OF ELONGATION WITH GAGE LENGTH

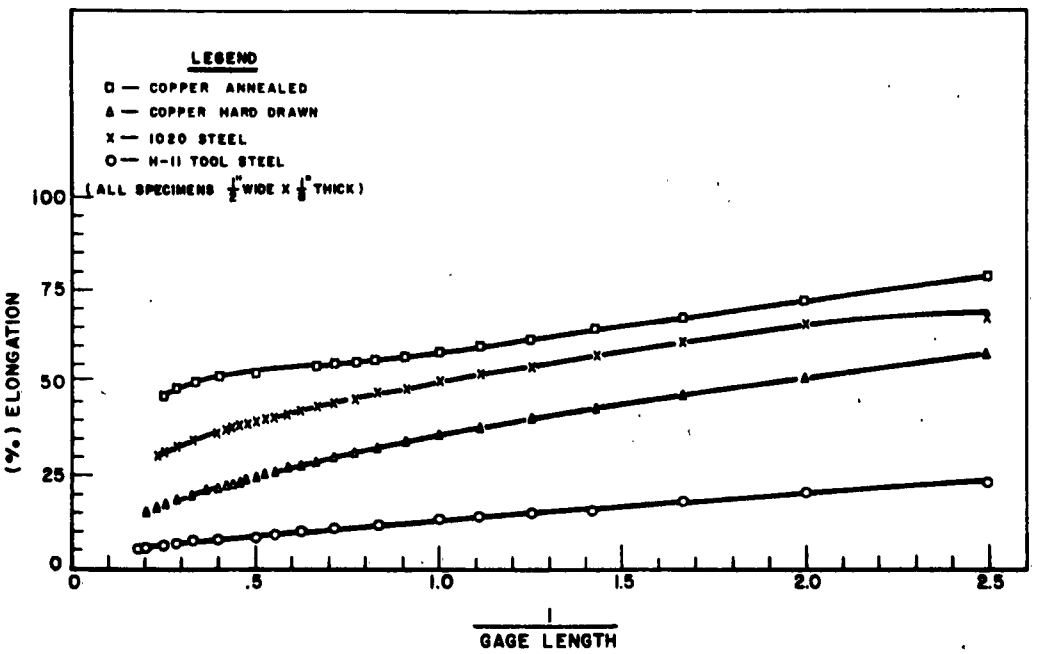


FIGURE 4: VARIATION OF ELONGATION WITH 1/GAGE LENGTH

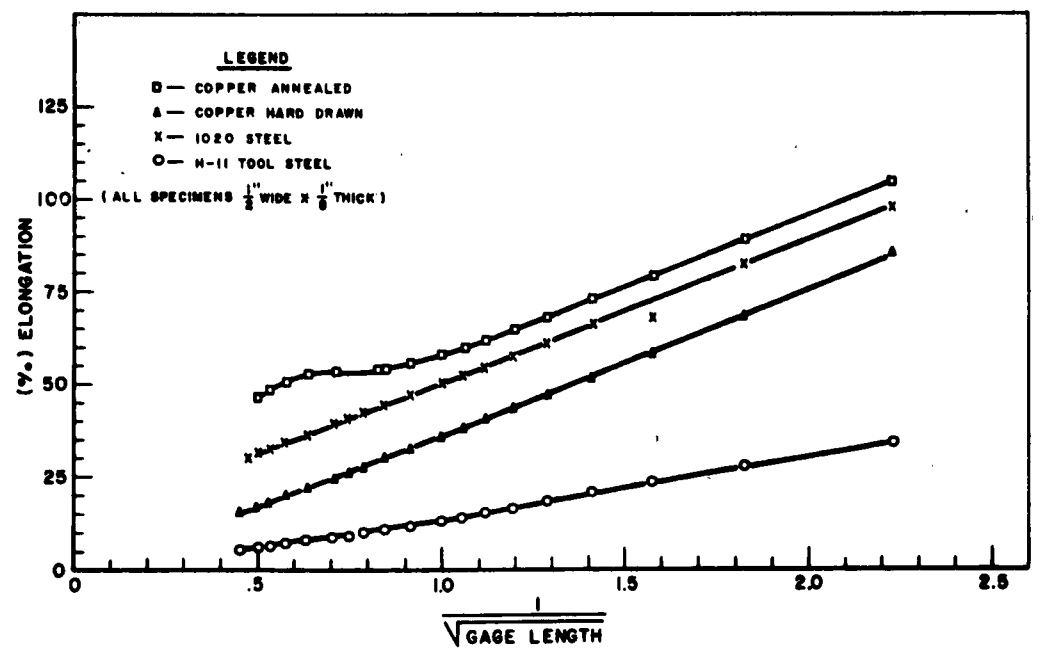


FIGURE 5: VARIATION OF ELONGATION WITH 1/ $\sqrt{\text{GAGE LENGTH}}$

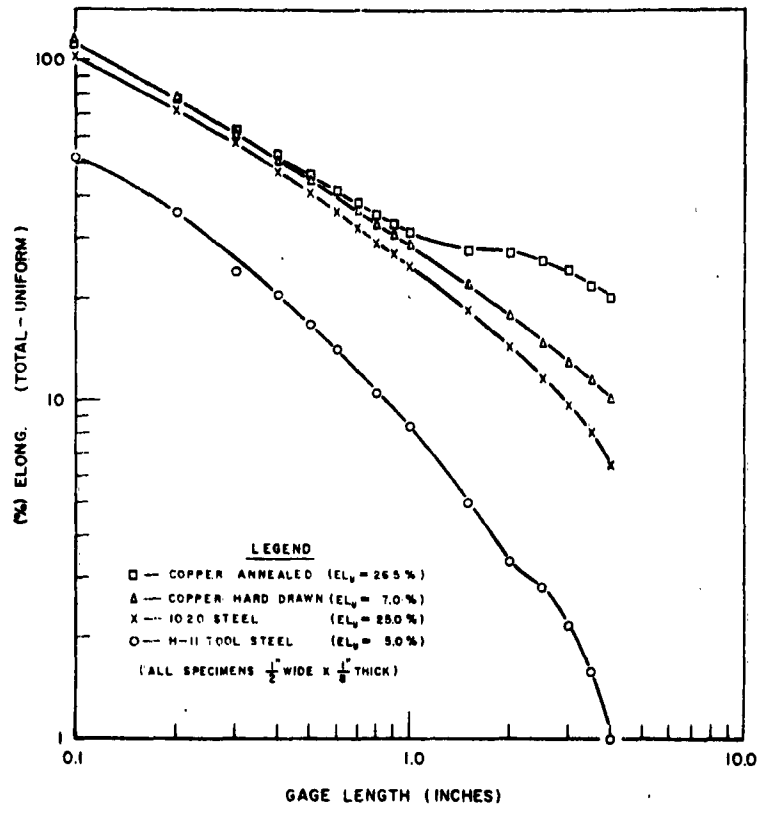


FIGURE 6: VARIATION OF TOTAL-UNIFORM ELONGATION WITH GAGE LENGTH

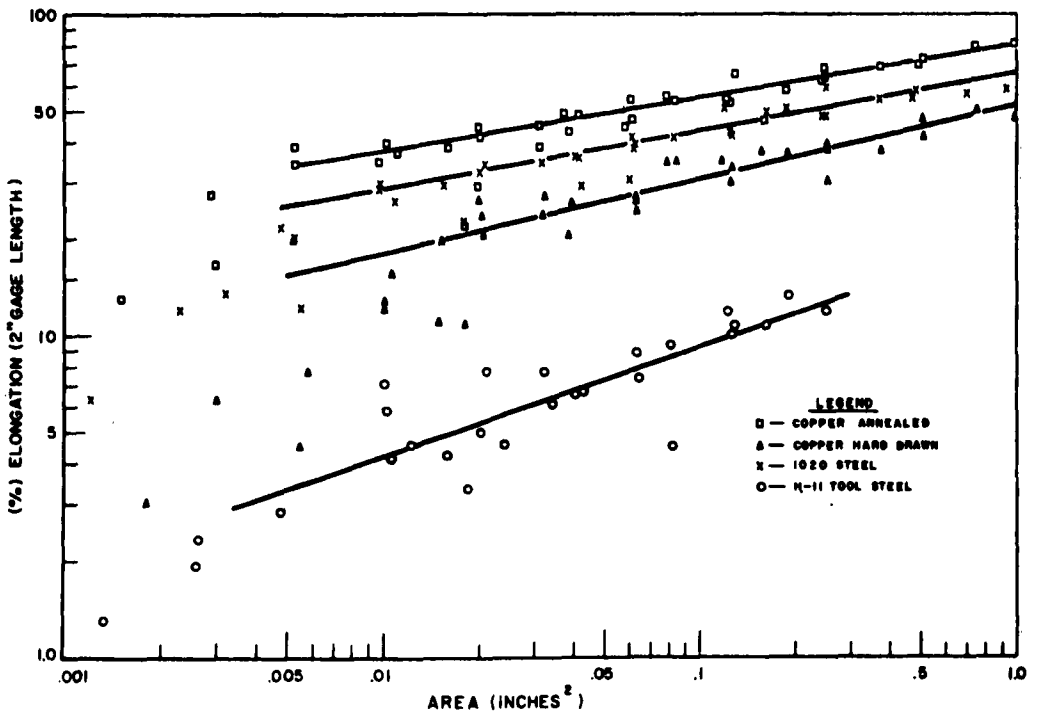


FIGURE 7: EFFECT OF SPECIMEN AREA ON ELONGATION IN 2 INCHES

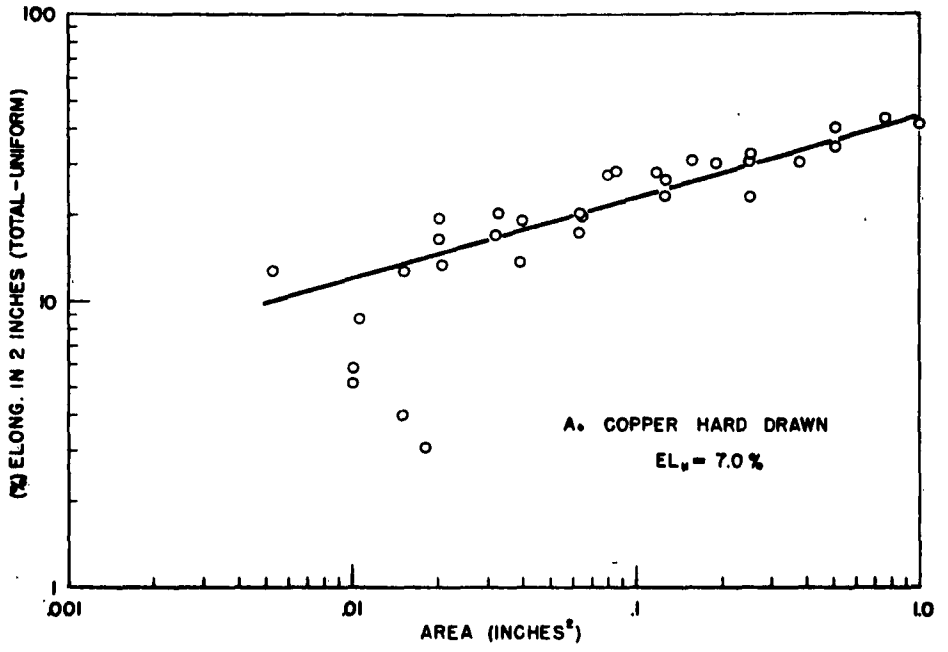


FIGURE 8A

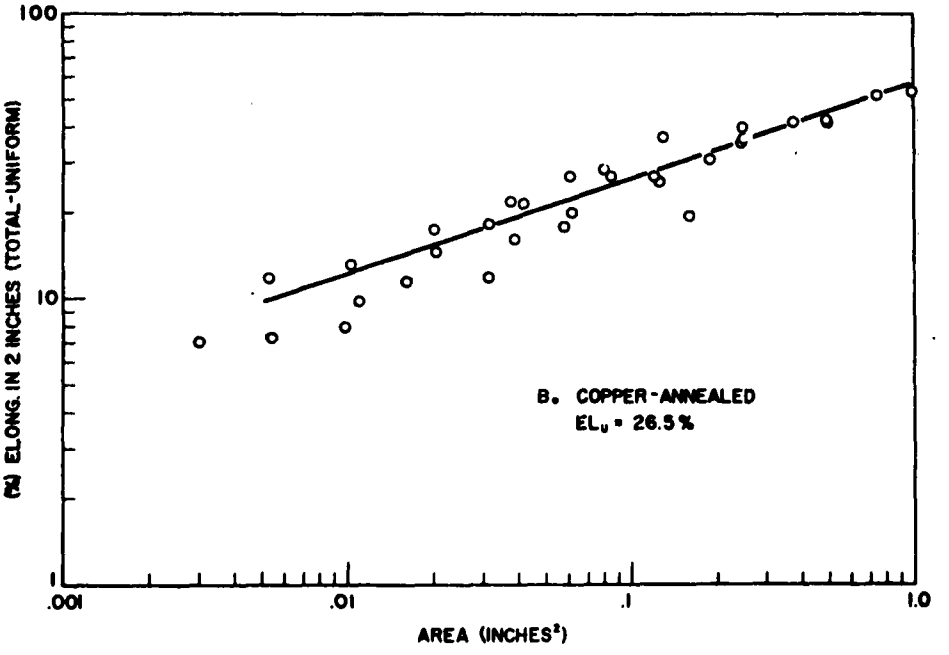


FIGURE 8B
EFFECT OF SPECIMEN AREA ON TOTAL-UNIFORM ELONGATION

FIGURES 8A & 8B

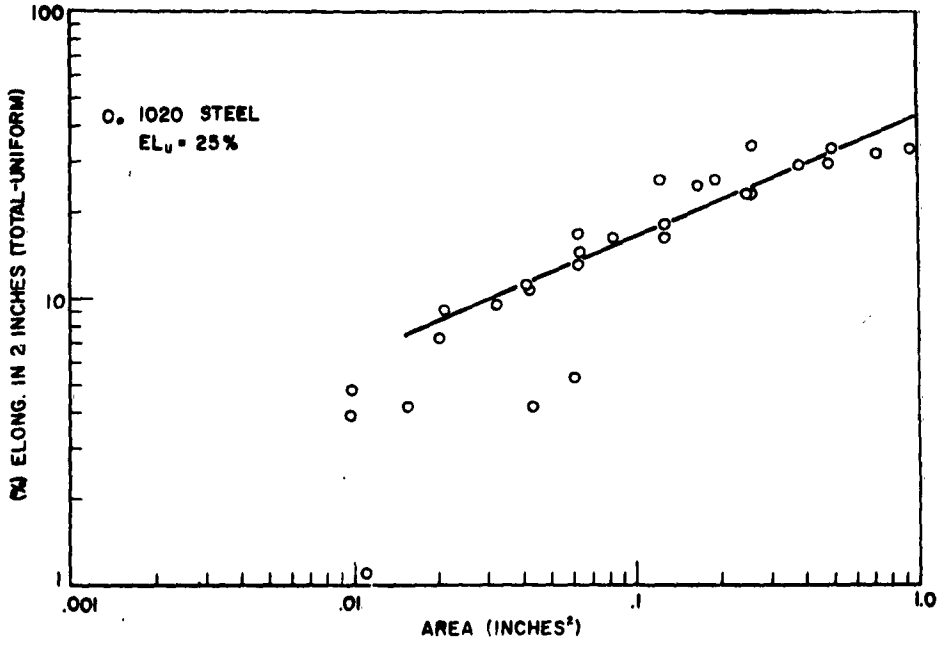


FIGURE 8C

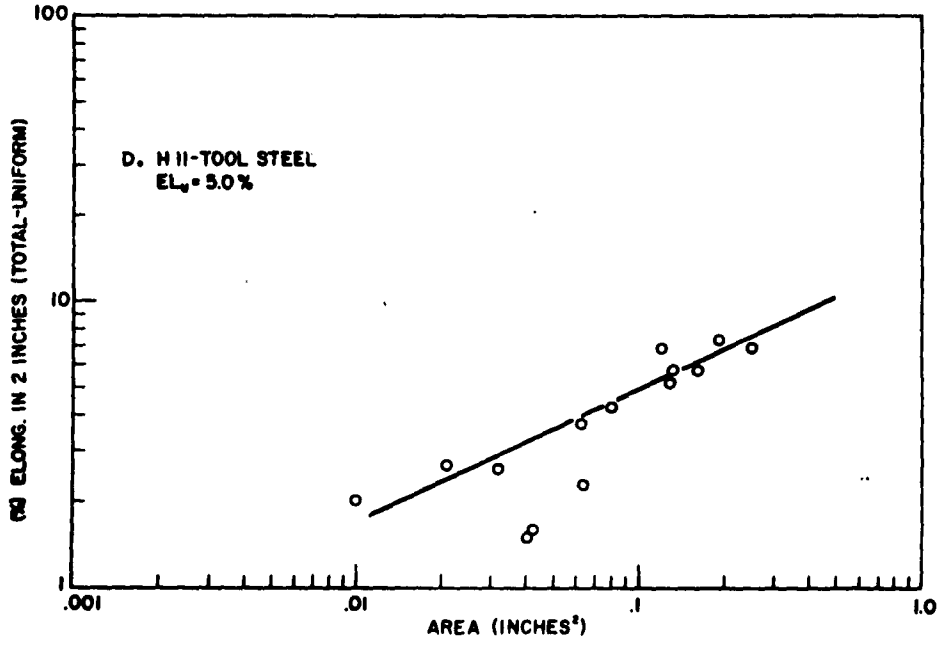
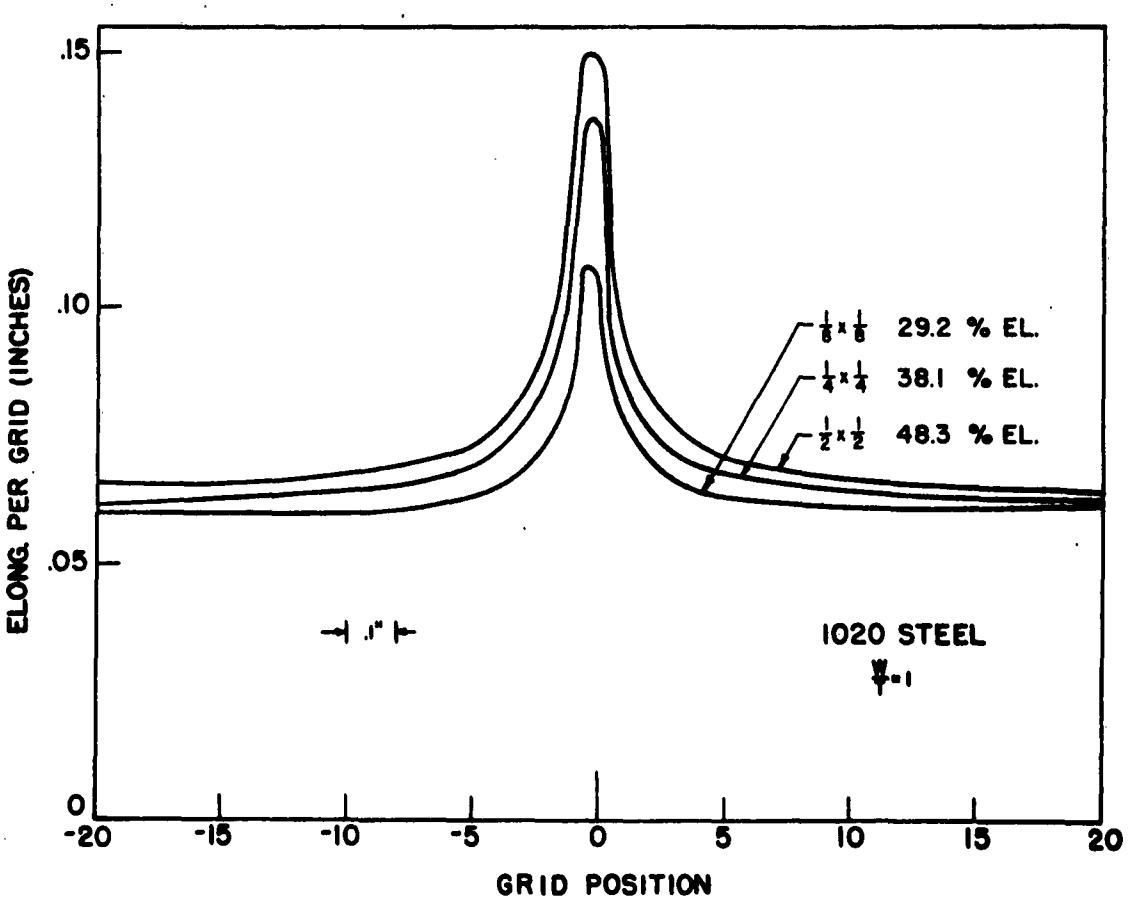


FIGURE 8D

EFFECT OF SPECIMEN AREA ON TOTAL-UNIFORM ELONGATION



LONGITUDINAL STRAIN DISTRIBUTION IN GAGE LENGTH SECTION FOR BARS OF DIFFERENT AREA

FIGURE 9

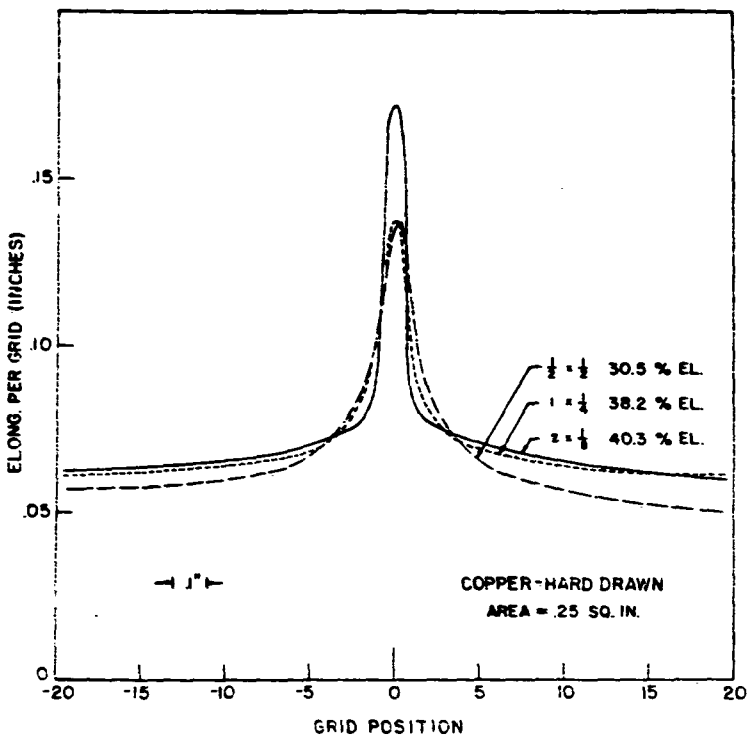


FIGURE 10: LONGITUDINAL STRAIN DISTRIBUTION IN GAGE LENGTH SECTION FOR BARS OF SAME AREA BUT DIFFERENT GEOMETRY

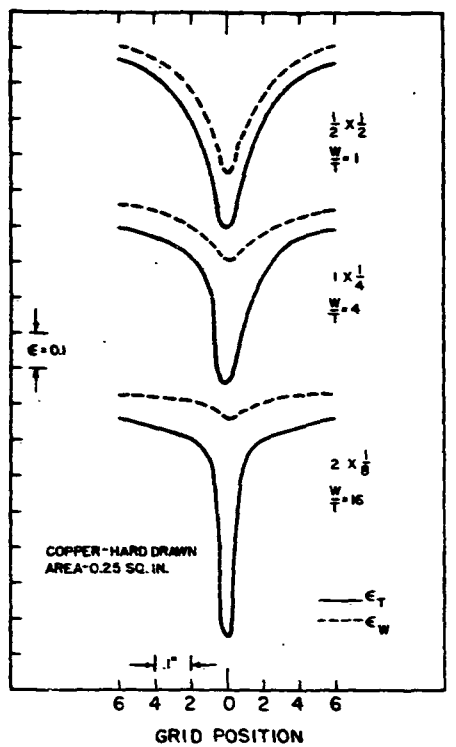


FIGURE 11: WIDTH AND THICKNESS STRAIN DISTRIBUTION IN GAGE LENGTH SECTION FOR BARS OF SAME AREA BUT DIFFERENT GEOMETRY

FIGURES 10 & 11

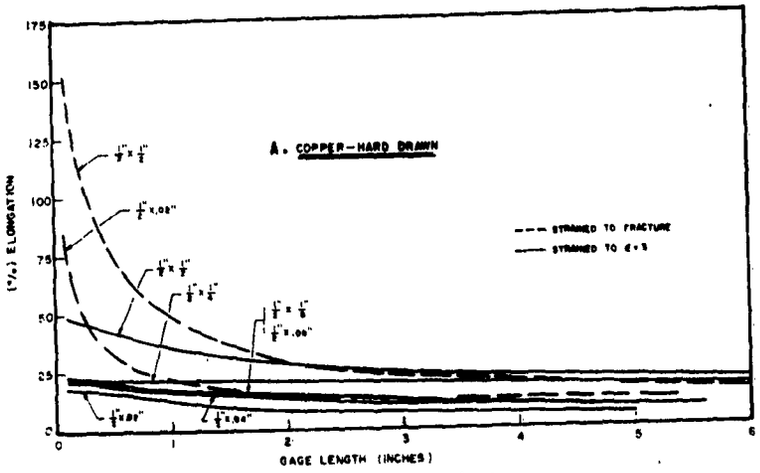


FIGURE 12A

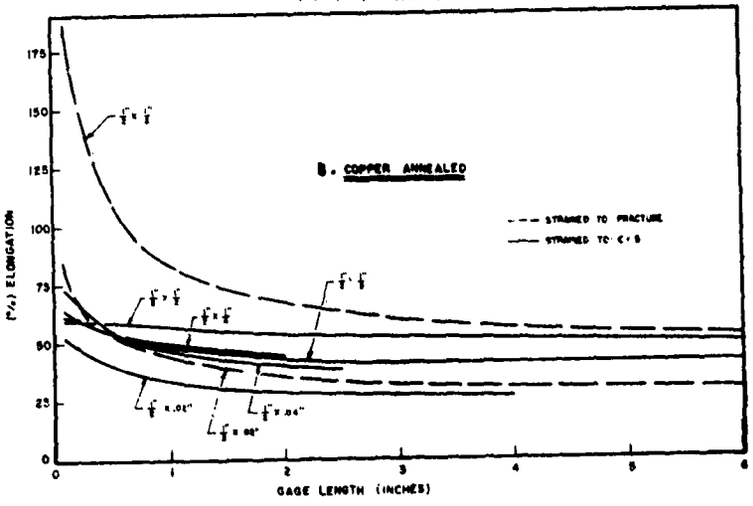


FIGURE 12B

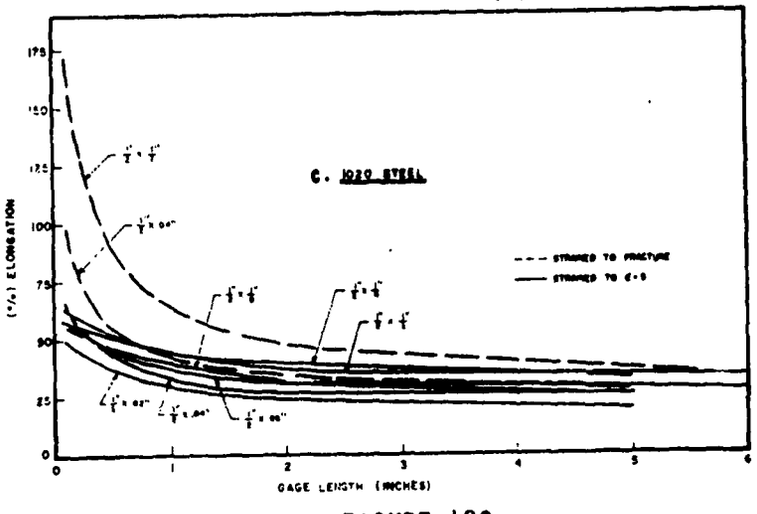


FIGURE 12C
VARIATION OF ELONGATION WITH GAGE LENGTH

FIGURES 12A, 12B & 12C

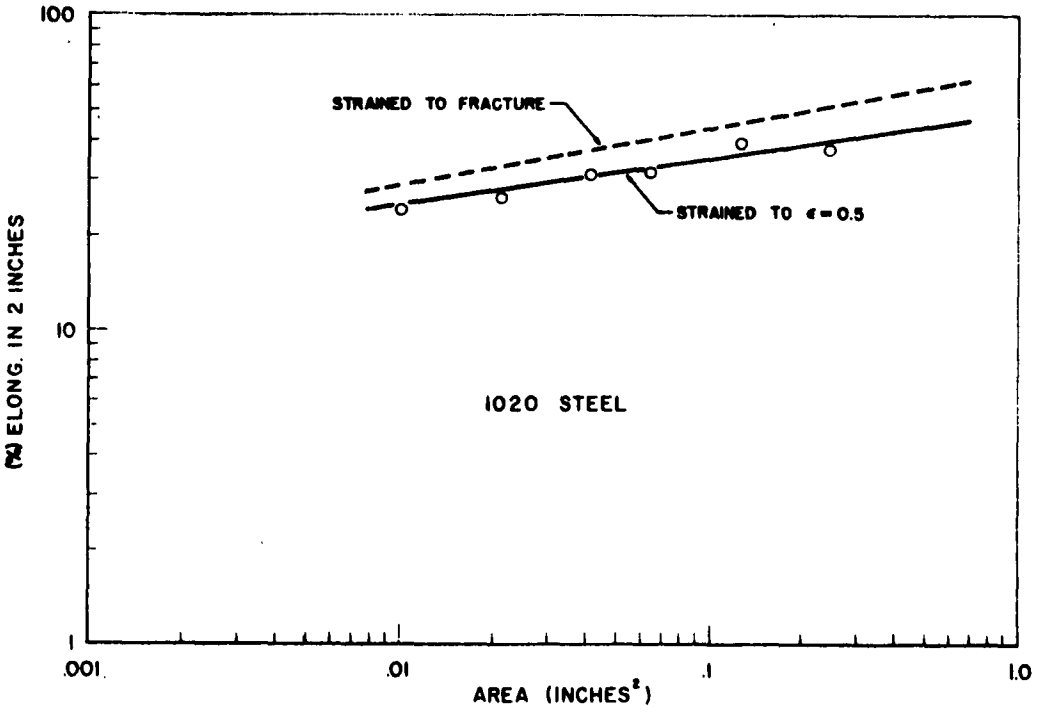


FIGURE 13: VARIATION OF ELONGATION IN 2 INCHES WITH SPECIMEN AREA

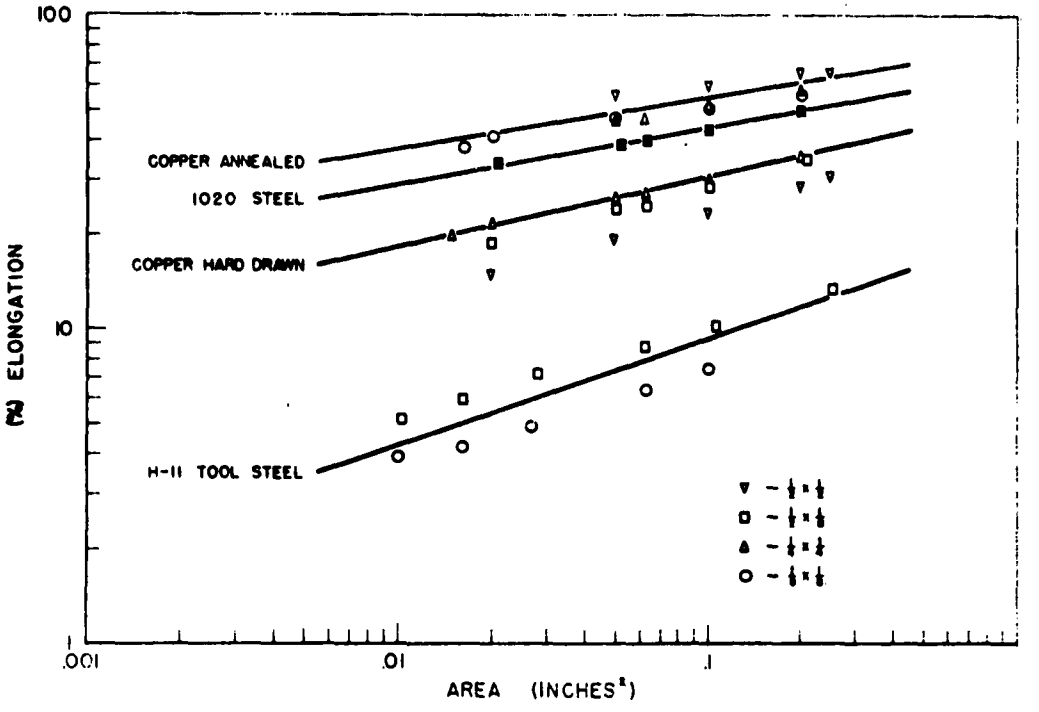


FIGURE 14: CALCULATED VARIATION OF ELONGATION IN 2 INCHES WITH SPECIMEN AREA

THE USE OF SHEAR-CRACKED SPECIMENS FOR EVALUATION OF SHEET MATERIALS

By J. D. Morrison and J. R. Kattus

ABSTRACT

A description is given of a special tensile specimen, the shear-cracked specimen, which was designed for use in the evaluation of fracture toughness of sheet materials. The shear-cracked specimen, which is geometrically similar to the central fatigue-cracked specimen, is prepared rapidly and economically in quantity by means of special punch-and-die fixtures. In the limited comparisons made so far, it has been found that fracture data obtained with shear-cracked specimens are very similar to the fracture data obtained with fatigue-cracked or sharp edge-notched specimens of the same material. Some results are presented of investigations, with shear-cracked specimens, of the effect of experimental variables on fracture toughness. An attempt to correlate fracture-toughness characteristics with the burst properties of model pressure vessels is also described.

INTRODUCTION

In the recent report of the ASTM Committee on Fracture Testing of High Strength Sheet Materials, two sorts of special tensile specimens were recommended for determining the fracture toughness of sheet materials, these specimens having either very sharp edge notches or central fatigue cracks. The production of a quantity of uniform specimens of either of these two types generally requires the use of techniques that are rather time-consuming or expensive or both.

It seemed desirable, therefore, to devise a valid fracture specimen that could be produced rapidly and cheaply in quantity for use in large-scale evaluation programs. We believe that the shear-cracked specimen described in this paper meets these requirements.

This research was supported in whole by the Navy Department, Bureau of Naval Weapons, under Contract NOas 60-6040c.

SPECIMEN PREPARATION

The shear-cracked specimen is geometrically similar to the central fatigue-cracked specimen. The shear crack is produced by means of a punch-and-die fixture that makes a transverse cut of the desired length through the center of the specimen, the ends of the cut terminating in a tear. A typical shear-cracked specimen is shown in Fig. 1. Two offset punches operate from opposite sides of the specimen, each punch penetrating half the specimen thickness. The punches are adjustable, by means of shims, so that a range of specimen thicknesses can be shear-cracked.

The sides of the punches are rounded to a radius of 0.090 in. The rounded sides of the punches account for the projecting points in the crack-plane of the specimen.

Punch-and-die fixtures are available in four sizes, producing shear-crack lengths of about 0.20 in., 0.35 in., 0.60 in., and 1.00 in. The shear-crack lengths obtained with a given fixture will vary slightly, depending upon the particular specimen thickness. This range of shear-crack lengths is suitable for specimen widths up to 3 in. The large fixture will accommodate sheet thicknesses up to 0.125 in. Specimen width and crack length are selected for the particular sheet thickness, in accordance with the recommendations of the ASTM Fracture Committee.

Specimens of quench-hardenable materials are shear-cracked in the annealed condition before heat treatment. Work-hardenable materials, such as the austenitic stainless steels, have been shear-cracked after as much as 50% cold-reduction. The hardness of Type 301 material in this condition was about R_C 45, and the standard tensile elongation, 2.5% in 2 in. Beta-titanium samples, 0.100 in. thick, have been shear-cracked after aging to 180,000 psi nominal yield strength. The probable upper limit of hardness for shear cracking, without excessive damage to the punches, is believed to be about R_C 50.

MATERIAL EVALUATIONS WITH SHEAR-CRACKED SPECIMENS

In the material evaluations made with shear-cracked specimens so far, it has been the practice to obtain net-fracture-strength data and fracture-appearance data for each material over a range of temperatures from about -200° F to 600° F. These temperature limits can be extended if necessary. The loading rate usually employed causes fracture within about 2 min. Tensile yield-strength and ultimate-strength properties are obtained in the same temperature range with standard specimens of each material for comparison with crack-propagation properties. As is the case for fatigue-

cracked and edge-notched specimens, the fracture-strength parameter, K_{C_3}, may be calculated for shear-cracked specimens from initial crack-length measurements and percent-shear values. By means of measurements of critical crack length, K_{C_1} values may be obtained. For specimens fractured at near ambient temperatures, critical crack length is measured by the ink-stain method. The progress of slow crack extension, and hence an indication of critical crack length, can also be recorded by means of an electrical-resistance method. This method can be used under any conditions in which plastic flow causes little or no reduction of area in the fracture plane. In the electrical-resistance method, a small direct current is passed through the specimen, and the potential-drop across the crack is recorded as a function of time while the specimen is loaded to failure. The calibration standards for the method are shear-cracked specimens of varying crack lengths. A typical recording of an electrical-resistance measurement of crack extension is shown in Fig. 2, which is a recording for a shear-cracked specimen of AM 350 stainless steel fractured at -200° F. In this plot, crack-length values, obtained by means of the calibration, have replaced potential-drop values in the abscissa. The short, stepwise crack extensions just prior to fracture were also manifested by audible "cracking."

The results of an evaluation of 0.064-in. thick AMS 6434 steel, hardened and tempered at 400° F, are shown in Fig. 3. Shear-cracked specimens of 1.5 in. over-all width were used. The full-shear transition temperature for this material was -100° F. The fracture surfaces of the specimens are shown in Fig. 4. A rather pronounced "maximum" in standard tensile strength properties, occurring at about 350° F, correlates with a decrease in net fracture stress at this temperature. These effects are thought to be associated with strain-aging of the AMS 6434 material.

COMPARISON OF SHEAR-CRACKED SPECIMENS WITH OTHER FRACTURE SPECIMENS

The acceptance of the shear-cracked specimen as a valid crack-propagation specimen must be justified by a direct comparison with other specimens now in general use, namely, the fatigue-cracked specimen and the sharp edge-notched specimen. Such a comparison is being made at Southern Research Institute between shear-cracked and fatigue-cracked specimens. Some limited comparative data have been obtained. In Fig. 5, fracture data obtained with shear-cracked and fatigue-cracked specimens of aged AM 350 stainless steel sheet are compared. The fracture specimens, all of which were of 1.5 in. over-all width, were machined from 0.040-in.-thick sheet. Standard tensile properties of the alloy are also shown. Both types of fracture specimens indicated a full-shear transition temperature of -100° F for the AM 350. Net-fracture-strength values were in fairly good agreement, showing the transition temperature to be between -50° F and -100° F.

A comparison of fracture properties of Vascojet-1000 sheet, obtained with sharp edge-notched specimens and with shear-cracked specimens, has been made at the NASA Lewis Research Center. This comparison was made with specimens of five different strength levels and of two over-all widths. Generally, good agreement was found for net fracture stress, K_c, and percent shear between the two types of specimens of the same over-all width and at the same strength level.

EFFECTS OF EXPERIMENTAL VARIABLES ON FRACTURE PROPERTIES

The effects of several experimental variables on crack-propagation characteristics are presently being investigated with shear-cracked specimens. Such variables include rate of loading, nominal strength level, and sheet thickness.

The effects of loading rate on the fracture properties of aged AM 350 sheet are shown in Fig. 6. Two loading rates were used: the slow rate causing fracture in about 2 min, and the fast rate causing fracture in about 0.1 sec. The specimen dimensions and the heat treatment were identical with those used in the work on AM 350 already described. Apparently, the effect of greatly increasing the loading rate was to lower the transition temperature. This effect was evident for both the fracture appearance and the net fracture stress. As a check on these results, fracture data were obtained at the fast loading rate with fatigue-cracked specimens of the AM 350. These data were in close agreement with the fast-loading rate data obtained with shear-cracked specimens as is shown in Fig. 7. Additional work now in progress indicates that the effects of strain rate on transition temperature may depend upon the type of alloy, increasing strain rate effecting a decrease in transition temperature in some materials and an increase in other alloys.

CORRELATION WITH BURST STRENGTH OF MODEL PRESSURE VESSELS

Another phase of the investigation of fracture toughness with shear-cracked specimens consists of an attempt to correlate crack-propagation properties with burst strength of model pressure vessels. Two steels—SAE 4130 and SAE 4340—are included in this program. Results for the SAE 4130 material, heat treated to a nominal strength level of 200,000 psi, will be described; similar work on the 4340 vessels has not yet been completed. The 4130 vessels, which were seamless gas cylinders of 205 cu. in. capacity, were evaluated over a range of temperatures from -160° to 364° F. Evaluations of the fracture toughness of shear-cracked sheet

specimens of the same thickness as the finished-vessel wall thickness (nominally 0.100 in.) were made over the same temperature range. Standard tensile properties were also determined for this material.

The three types of data are compared in Fig. 8. Fracture-appearance data for the vessels and fracture-appearance and fracture-stress data for the shear-cracked specimens indicate that, at temperatures somewhat below -50° F, the vessels could have failed at lower applied stresses if stress-concentrating defects of sufficient severity had been present.

Values of the fracture-strength parameter, K_{C3}, were calculated from the initial-crack-length and fracture-appearance data for the shear-cracked specimens. For two shear-cracked 4130 specimens, one fractured at 75° F and one at -150° F, K_{C1} values were calculated from critical crack-lengths. For the specimen fractured at 75° F, critical crack-length was measured by the ink-stain method and by the electrical-resistance method, identical values being obtained with the two methods. For the specimen fractured at -150° F, the critical crack-length was measured by the electrical-resistance method. These data are shown in Fig. 9, where it is seen that both criteria—fracture appearance and K_C values—indicate the same brittle-to-ductile transition temperature, -50° F.

CONCLUSIONS

Work completed so far indicates that shear-cracked specimens are quite suitable for determining the fracture toughness of sheet metals under wide conditions of temperature, strain rate, and specimen size. Present and future work will give additional insight into the usefulness of specimens of this type for predicting service performance of engineering structures.

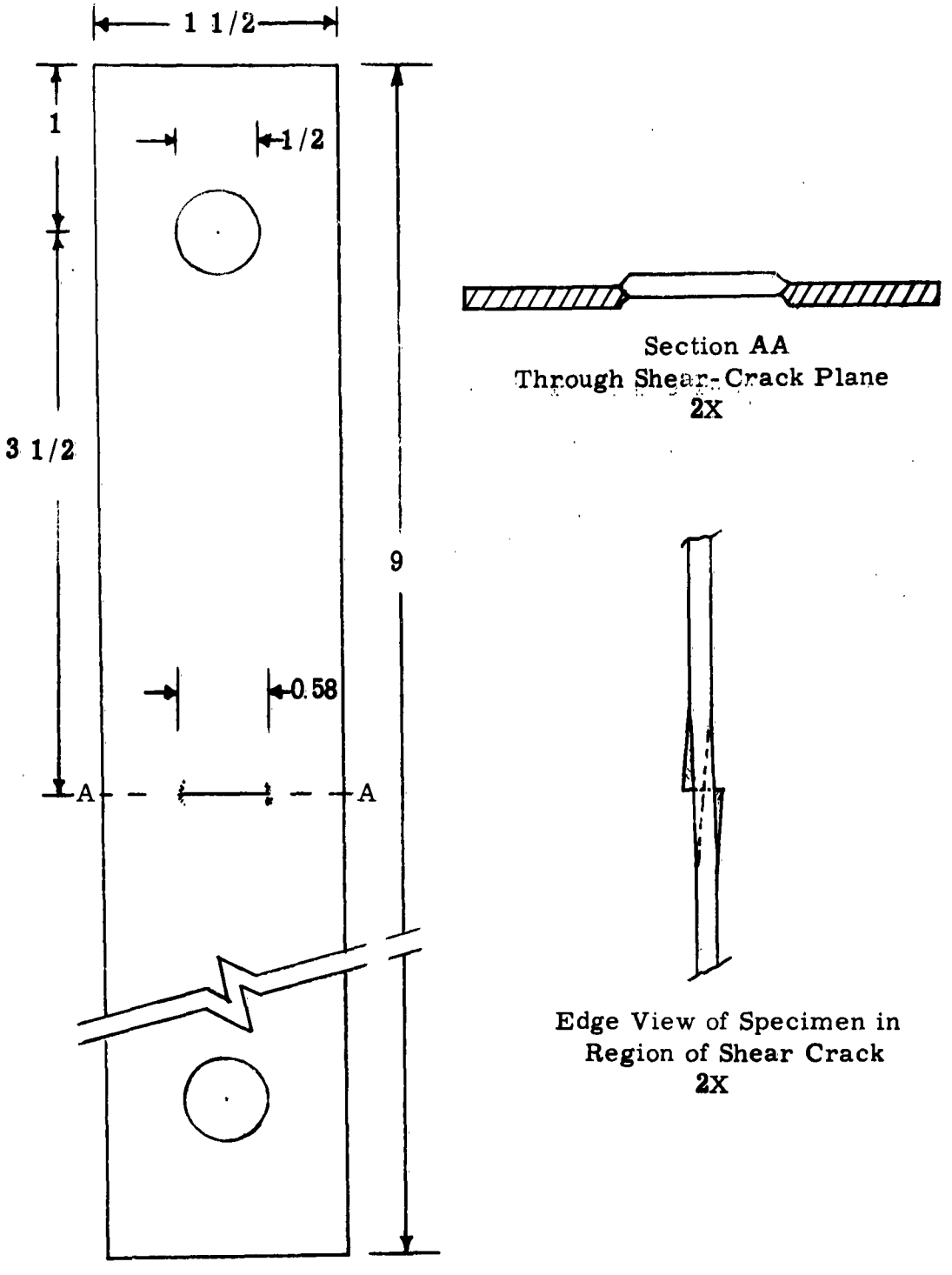


Figure 1. Typical shear-cracked specimen

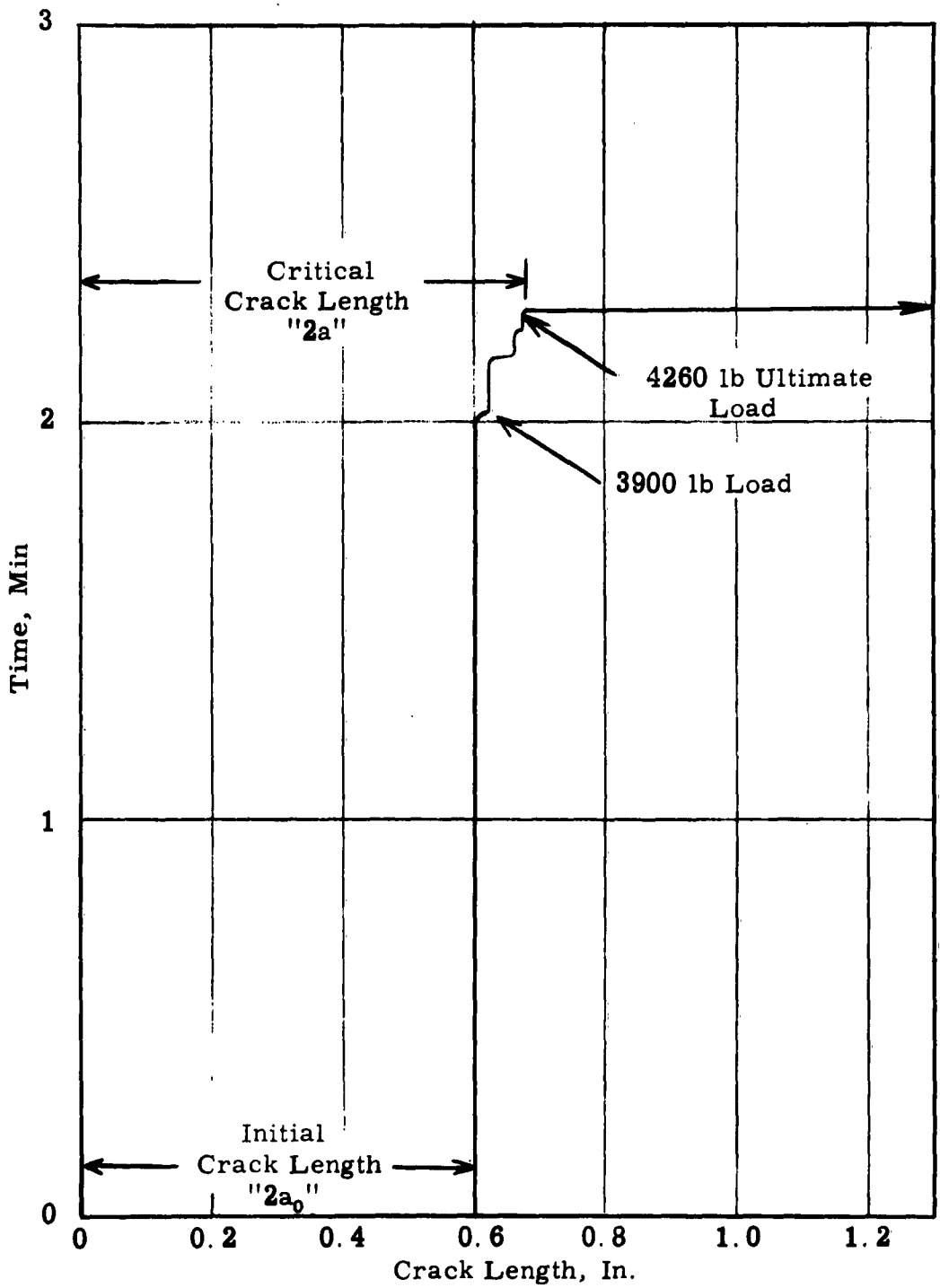


Figure 2. Measurement of crack extension obtained by means of the electrical-resistance method for a shear-cracked specimen of AM 350 stainless steel fractured at -200° F.

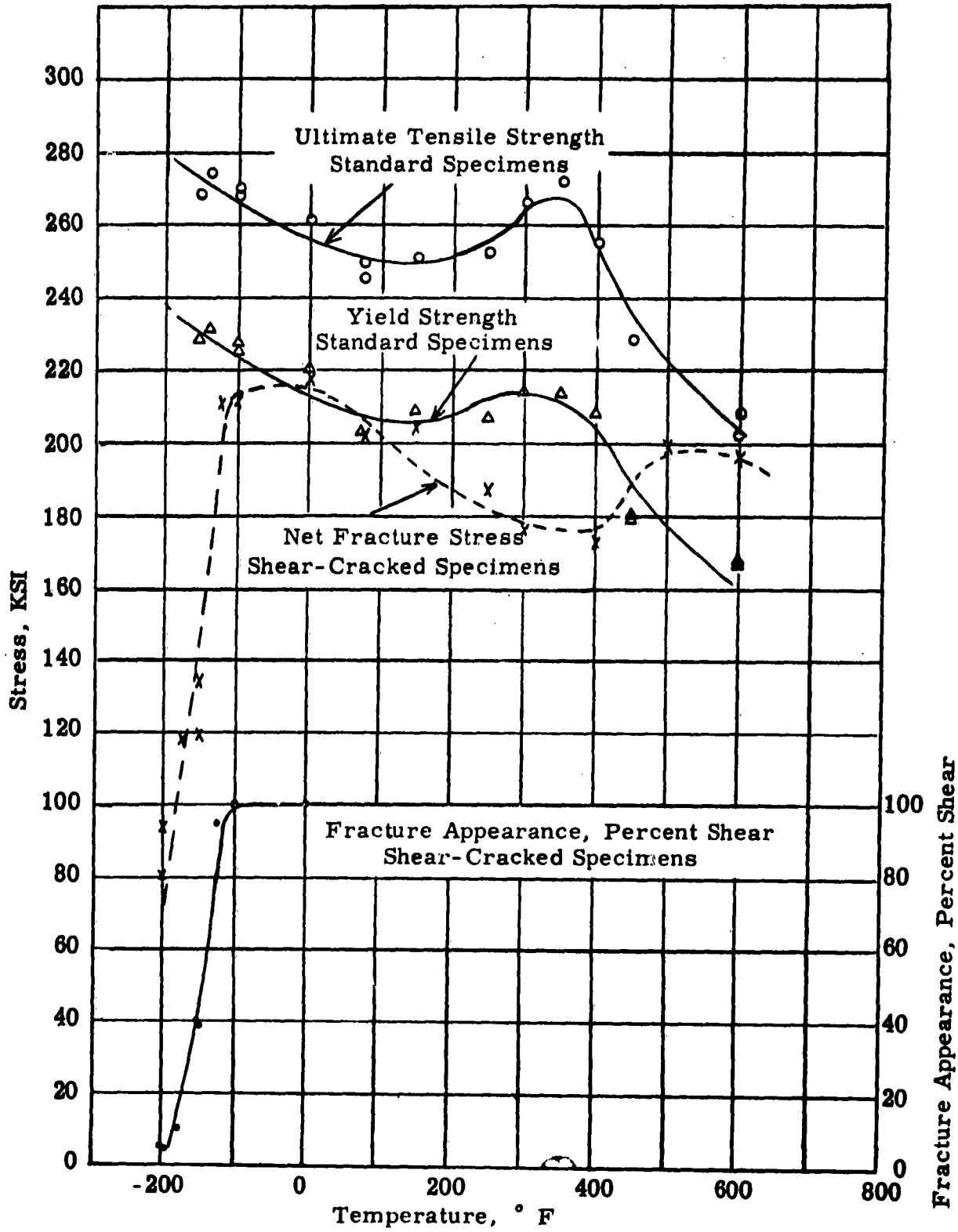


Figure 3. Effect of temperature on the standard-tensile properties and fracture properties of heat-treated[1] longitudinal specimens of AMS 6434 steel sheet.

[1] Austenitized at 1620° F for 30 min (argon), oil-quenched; tempered at 400° F for 2 hr.

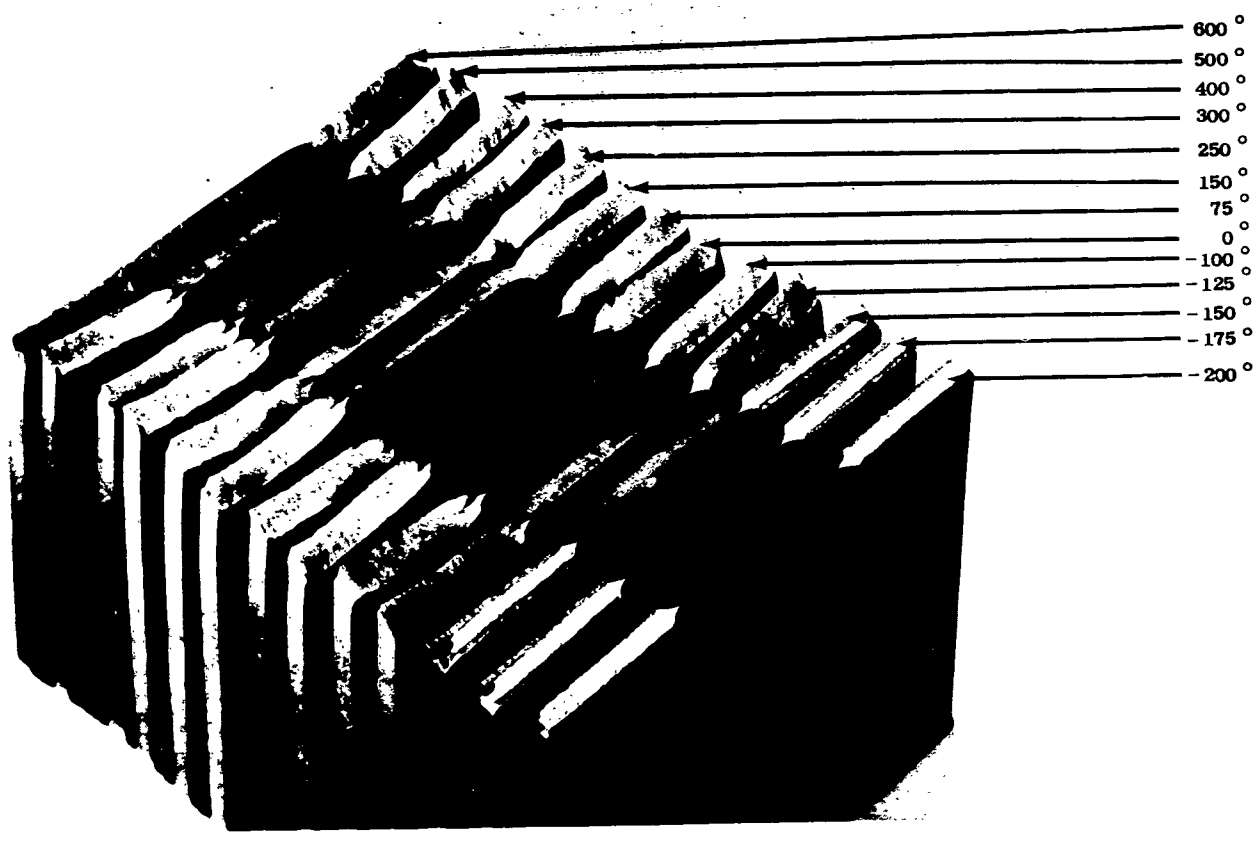


Figure 4 Appearance of fracture surfaces of shear-cracked AMS 6434 steel sheet loaded to failure at temperatures from -200° F to 600° F.

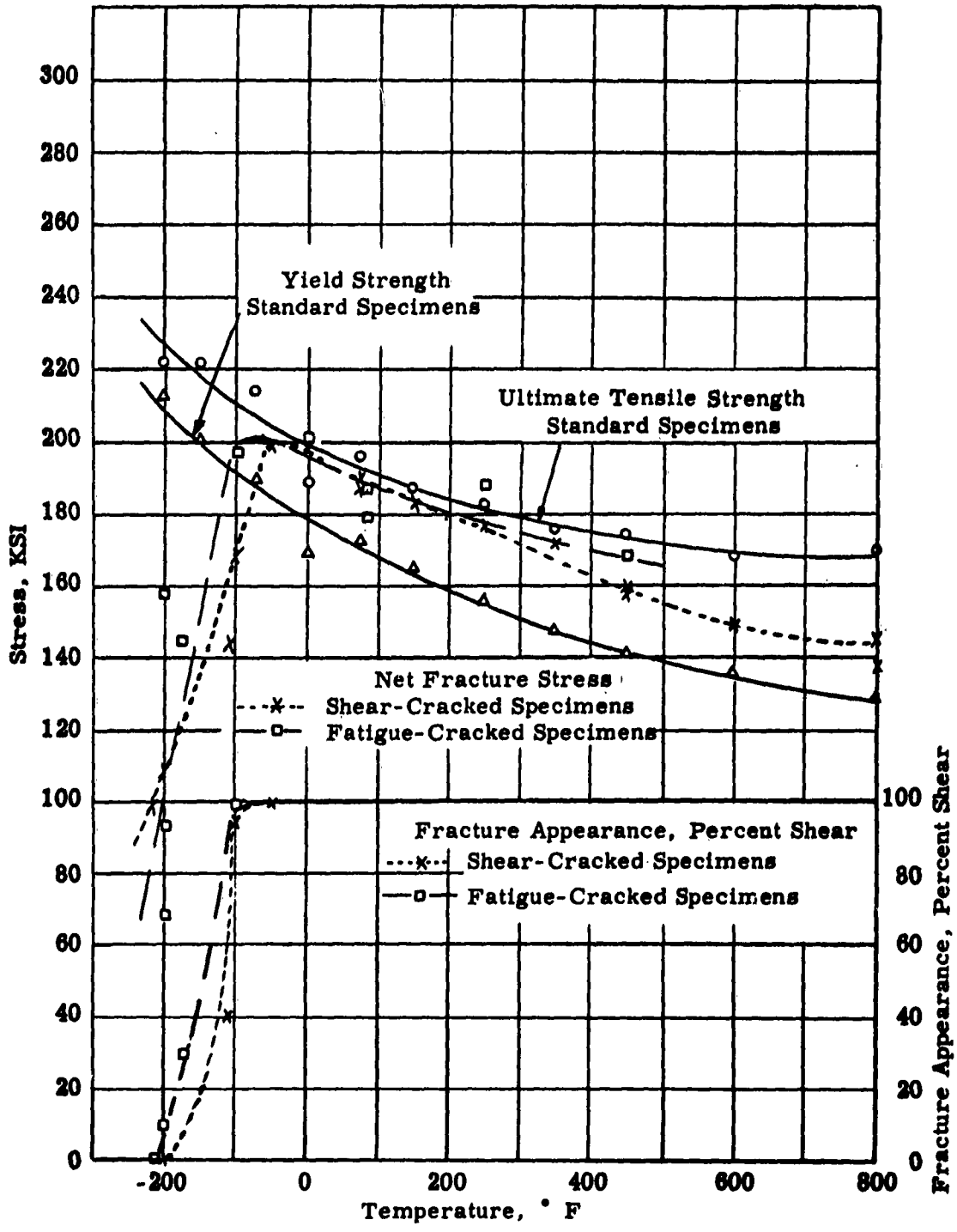


Figure 5. Effect of temperature on the standard tensile properties and fracture properties of heat-treated[1], longitudinal specimens of AM 350 stainless steel sheet, loaded to fracture in 2 min.

[1] Solution treated at 1725° F for 30 min (argon), water quenched; refrigerated at -105° F for 3 hr; aged at 850° F for 3 hr.

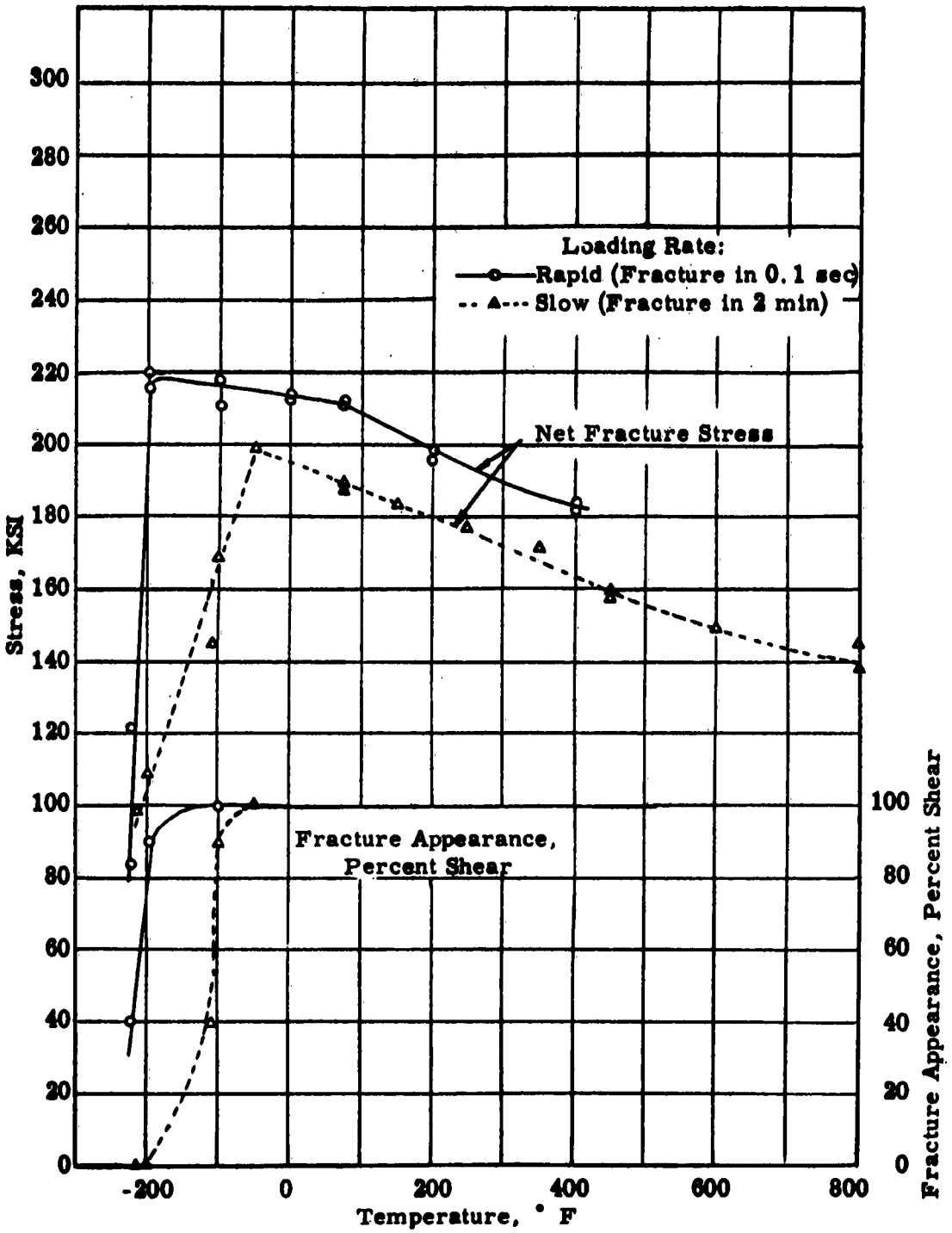


Figure 6. Effect of loading rate on the fracture properties of longitudinal, shear-cracked, AM 350 stainless steel sheet[1] at various temperatures.

[1] Solution treated at 1725° F 30 min (argon), water-quenched; refrigerated at -105° F 3 hr; aged at 850° F 3 hr.

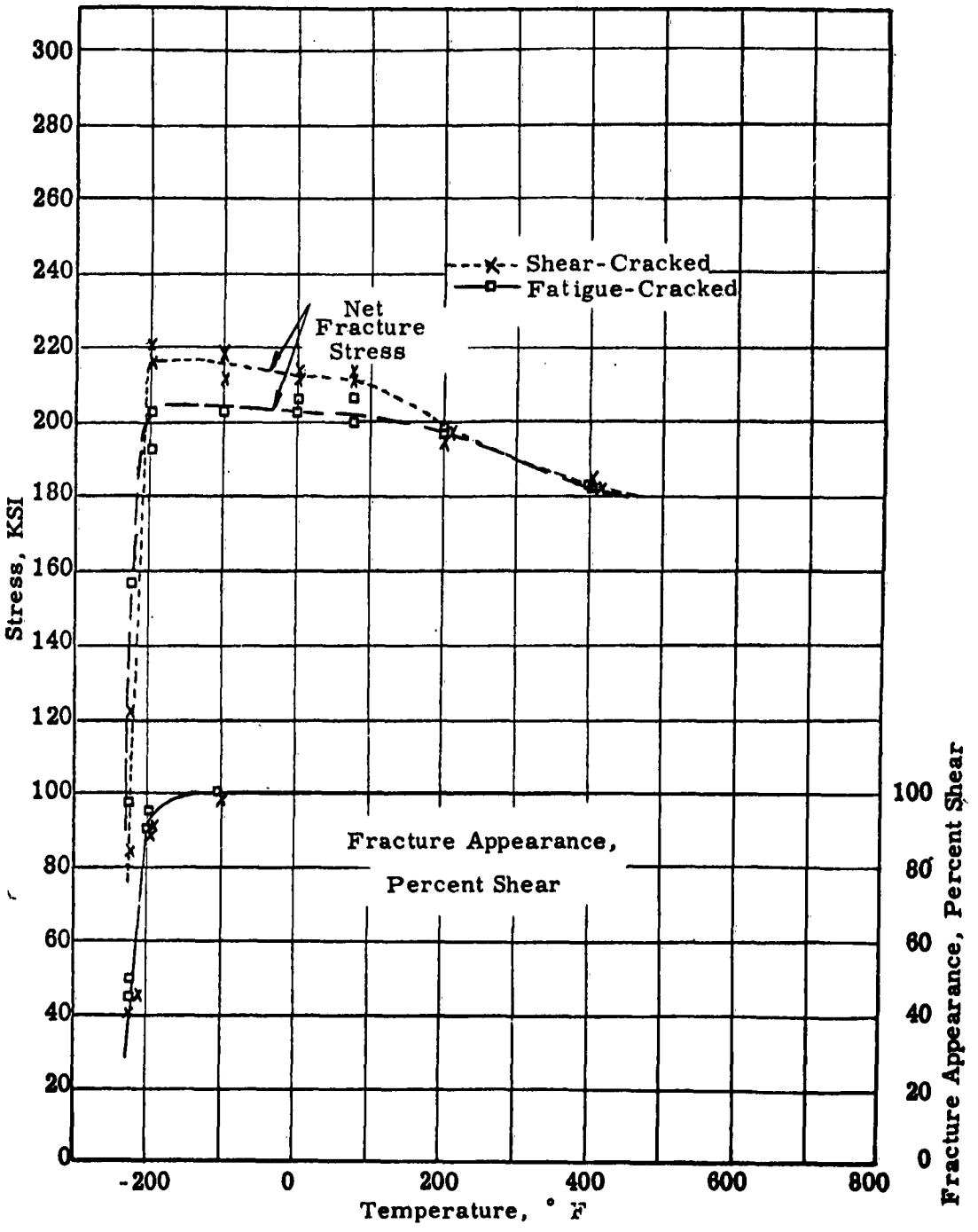


Figure 7. Effect of temperature on the fracture properties of longitudinal shear-cracked and fatigue-cracked specimens of AM 350 sheet[1], loaded to fracture in 0.1 sec.

[1] Solution treated at 1725° F 30 min (argon), water-quenched; refrigerated at -105° F 3 hr; aged at 850° F 3 hr.

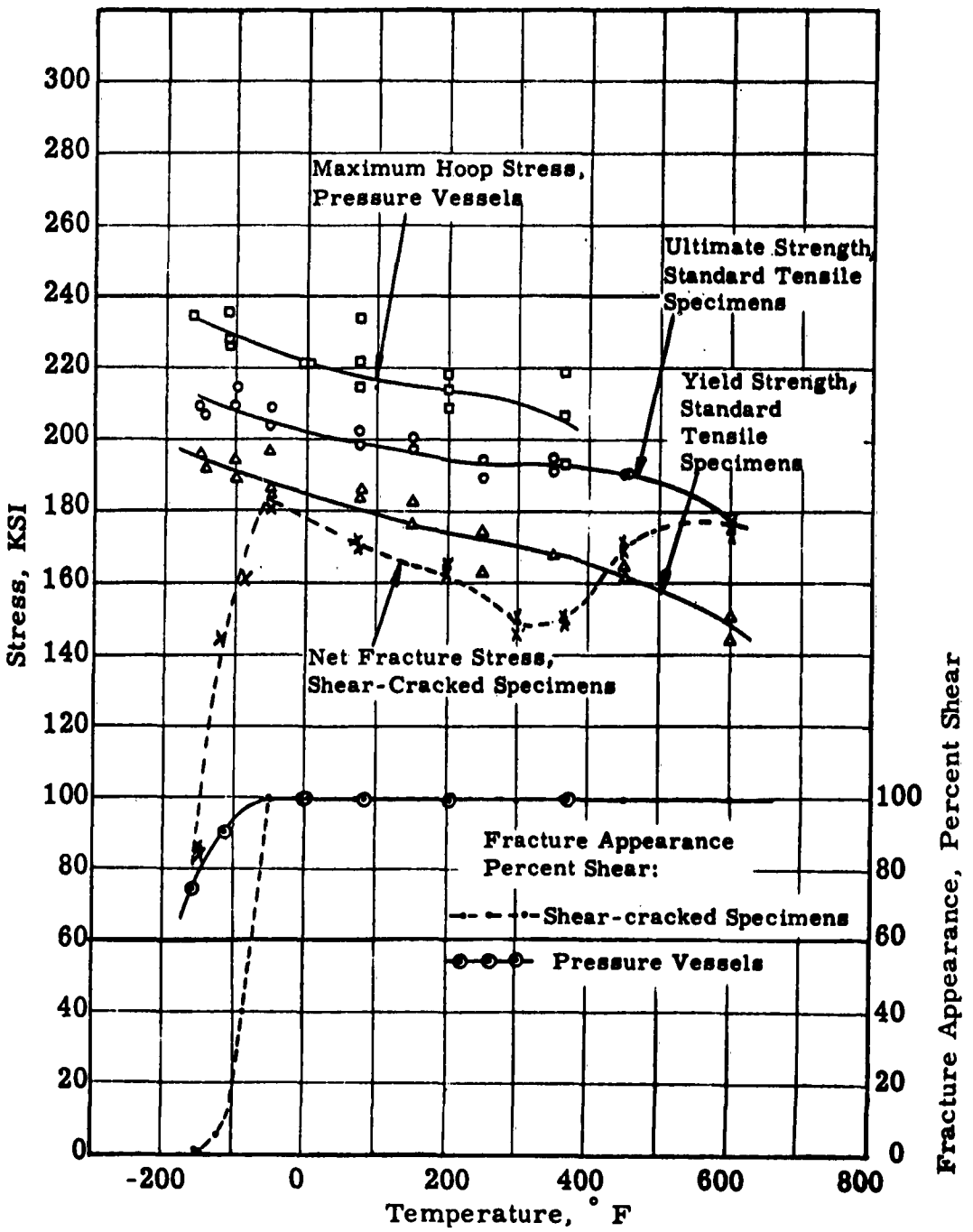


Figure 8. Effect of temperature on the fracture properties of SAE 4130 steel vessels[1] and on the standard tensile properties and fracture properties of SAE 4130 steel sheet specimens[1].

[1] Heat treated as follows: Austenitized at 1700° F for 68 min, oil-quenched; tempered at 825° F for 1 hr.

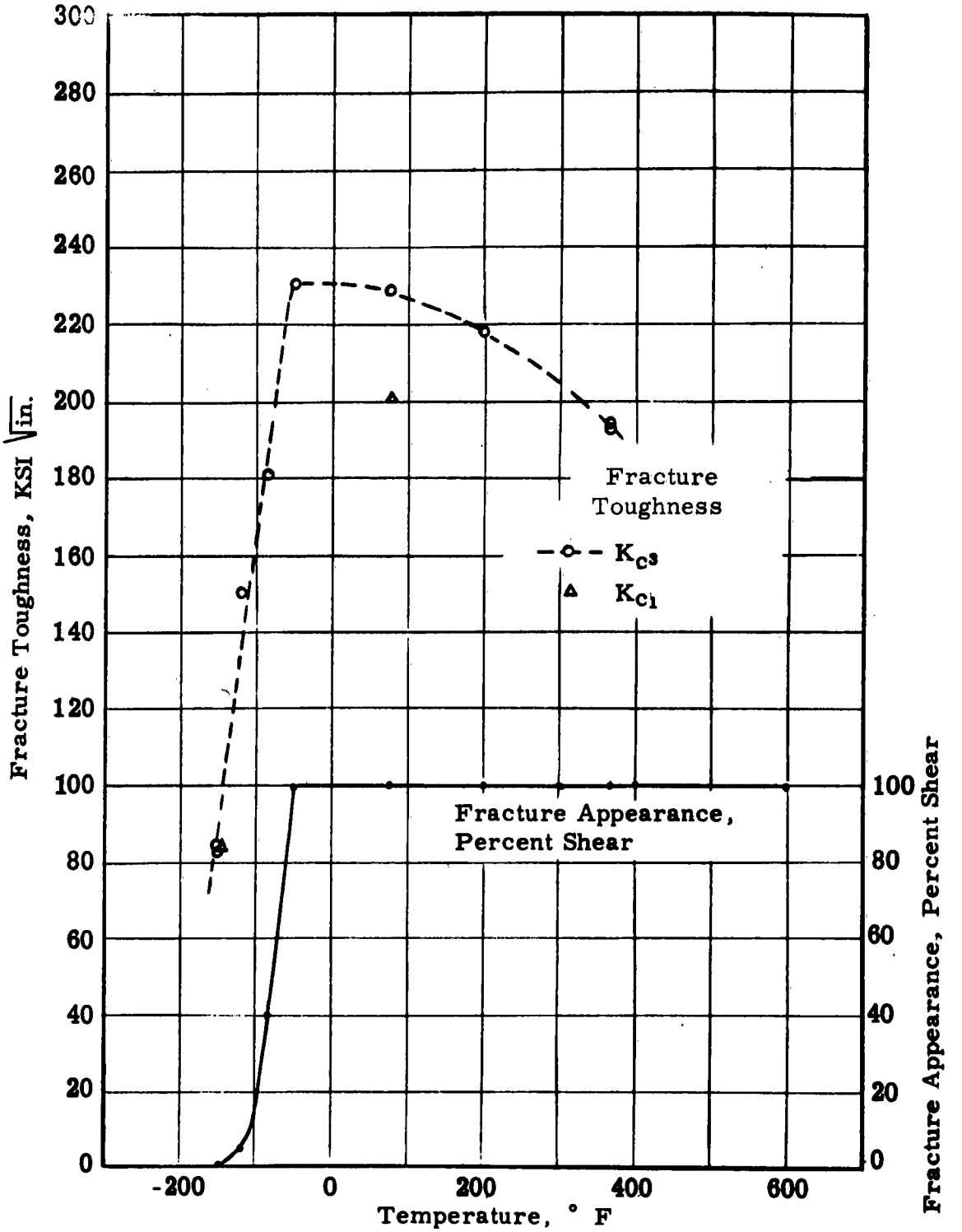


Figure 9. Effect of temperature on the fracture toughness and fracture appearance of shear-cracked specimens of SAE 4130 steel sheet.[1]

[1] Heat treated as follows: Austenitized at 1700° F for 68 min, oil-quenched; tempered at 825° F for 1 hr.

SCREENING TESTS FOR NOTCH TOUGHNESS OF SHEET

Elliot W. Brady
(Presented by E.R. Mertz, Aerojet General Corp.)

The problem of screening material for rocket motor usage has received concentrated attention during the past five years; and the basic problem of avoiding brittle failures in structures has been studied intensively for the last twenty years, having been accelerated by the ship failures and the failures of aircraft landing gear. Work on the latter problem has helped by showing the need for sensitive tests and the necessity for the modification of alloy composition and treatment. Alloy development has continued and very attractive strength levels have been achieved.

Therefore, materials with attractive strength-density properties must be screened to find which ones have potential for rocket cases. Suitable screening tests may be used to determine the highest strength compatible with acceptable toughness for a given material or to compare materials to determine which has the best fracture toughness at a given strength level. The properties of a promising material can be optimized by determining the effect of variables in composition, manufacture, and heat treatment upon strength and toughness by means of suitable tests.

There is no lack of tests. In fact, the multiplicity of tests and the many criteria for interpreting each test has added to the problem of evaluating materials. For instance, center-notch tensile data is not all comparable; results may vary by a factor of 3 depending on the specimen used. Values for G_c have been given without specifying the specimen used, the test procedure, or the method of calculation. Other laboratories have adopted the name "NRL test" to dignify a test which is similiar only in name. And notch strengths obtained with large radius notches ($K_t = 5$) are still used to prove the toughness of each new wonder metal. In many cases an individual investigator is wedded to a given test because (a) he developed the test, (b) he has had expensive jigs made for machining, inspecting, and testing his own specimen, and (c) he has accumulated a great deal of test data. Actually, the selection of screening tests should be relatively simple; if the test is used only for comparison we can avoid all the controversy about what the criteria should be, or what toughness is required.

What are the criteria for a suitable screening test? Obviously, the first requirement is that the test be capable of distinguishing between materials which vary in toughness, and that it be sensitive enough to indicate small differences with good reproducibility. However, the test should also be economical of material and time; considering machining, inspecting, testing, and interpretation time. It should be equally well suited to steel, titanium alloy, and aluminum alloy. The test should permit investigation of toughness over a wide range of temperatures.

A critical review of the screening tests currently being used is beyond the scope of this paper; however, some generalizations can be made. In general, the un-notched specimen tests are not sensitive enough to reveal changes in specimen brittleness as influenced by variables in composition or heat treatment. The pressure tests, such as bulge, flanged-hemisphere (or hat), cylinder, sphere, semisphere, or sub-scale chamber are also too expensive to fabricate, instrument, and test to be considered as screening tests. Other tests--such as the impact bulge and instrumented bend test--are very attractive because of low specimen and testing cost, but apparently result in excessive spread in results for some materials, possibly because the bending stress exaggerates the effect of surface conditions.

Tensile tests with sharp notches or transverse cracks were a logical development, since similiar stress concentrations have been found to be the cause of many pressure vessel failures. In evaluating bar and forgings, the value of sharply-notched tensile specimens has long been recognized. [1,2] Flat specimens containing zero-radius notches resembling artificial cracks were investigated many years ago. [3] More recently, the center-notched and center-cracked specimens have been developed. The center-notch tensile test is one of the most valuable for evaluation, but specimen preparation is quite time consuming where notching by spark-discharge machining is required, or if cracking by hydrogen embrittlement or fatigue is required. Southern Research Institute is investigating a center-notched specimen in which a transverse crack is produced by shearing action, using a die set. If this specimen is found to give reproducible results it should result in an excellent screening test.

One of the most attractive screening tests is the edge-notch tensile test. An excellent specimen design has been recommended by the ASTM Committee[4] and extensive data has been developed which proves the sensitivity of the test. Numerous attempts have been made to simplify specimen fabrication by using a larger notch radius, but the evidence to date indicates that radii resulting in notch factors lower than $K_t = 12$ fail to give the required sensitivity. Another approach is to use a wider specimen, since with a 3 inch width a notch radius as large as 0.007 inches will result in $K_t = 12$. This approach, however, sacrifices the advantage of the crack or sharp notch. Probably additional development will simplify the machining of the 0.0007 inch radius (maximum) notch, perhaps by use of one of the newer machining methods, such as electrolytic grinding.

It is the opinion of the writer that a test similiar to the edge-notch tensile of Reference 4 should be adopted as a Tentative Standard as soon as possible, since its wider usage by producers and users of sheet materials would result in enormous savings of time and money in rocket motor case development.

Superscripts refer to the reference list on page 5.

REFERENCES

1. G. Sachs, J. D. Lubahn and L. J. Ebert, "Notched Bar Tensile Test Characteristics of Heat Treated Low Alloy Steels," Trans. ASM, vol. 33, 1944, p. 340.

2. G. Sachs, J. D. Lubahn and L. J. Ebert, "The Effects of Notches of Varying Depth on the Strength of Heat Treated Low Alloy Steels," Trans. ASM, vol 35, 1945, p. 517.

3. C. P. O'Haven and J. P. Harding, "Studies of Plastic Flow Problems by Photo Grid Methods." Proceedings of the Society of Experimental Stress Analysis, vol. 2, No. 2, October 1944.

4. Evaluation of Fracture Toughness of Sheet Materials, ASTM Bulletin, January 1960.

PREPARED DISCUSSION - FIFTH SESSION

"Comments on Future Higher Strength Materials"

By
J. C. Hamaker

Perhaps it is blasphemous to discuss future higher strength materials in view of the problems encountered with the materials currently available. However, since alloy development has not been mentioned in the program, I thought you might like to hear what is anticipated in the future to help guide your thinking as far as notch sensitivity is concerned.

Figure 1 constitutes an addendum to the Lockheed report presented by Dr. Schapiro which pointed out that strength levels of structural aircraft parts are considerably above those of current missile manufacture. This is the major carry-through structure in the tail frame of the North American A3J Vigilante, a production twin jet Naval attack bomber. It is made from Modified H-11 steel, heat treated to 280-310,000 psi ultimate. The assembly is approximately 14 feet across with individual parts as long as 7 feet. Sections vary from about 5 inches in diameter on the three spindles which support the tail surfaces, to only .060 inches in the web and frame structure. The manufacturer reports that extremely close tolerances are held by the air hardening heat treatment, with no surface removal other than blasting required after heat treatment in controlled atmosphere. Furthermore, multiple tempering at 1000 F to the 280-310,000 psi ultimate strength level results in less than 1 percent retained austenite by X-ray diffraction, along with maximum removal of residual stresses and any detrimental effects of final surface protection treatments.

These parts have been fabricated in a number of ways. The first few were machined hog-outs, employing billets 28 x 8 inches in cross section, 18 x 5 inches, 12 x 12 inches, etc., which were hand forged to a very approximate shape and then simply whittled to the extremely thin sections shown. You can well imagine how much reliability was required in the center of a billet when some of the material remaining after the hogging-out operation was only .060 inches thick in that location. Subsequent parts have been made by fusion welding or pressure welding from die forged and/or sheet components.

A number of other critically stressed parts on the A3J are also made from Modified H-11 at 280-310 ksi, including catapult and arresting gear components, support lugs, etc., all with excellent reliability. One incident, involving a crash due to a system failure, gave an indication of reliability at this strength level. When the aircraft was dug up for examination (it was one of those 50 foot hole jobs) the

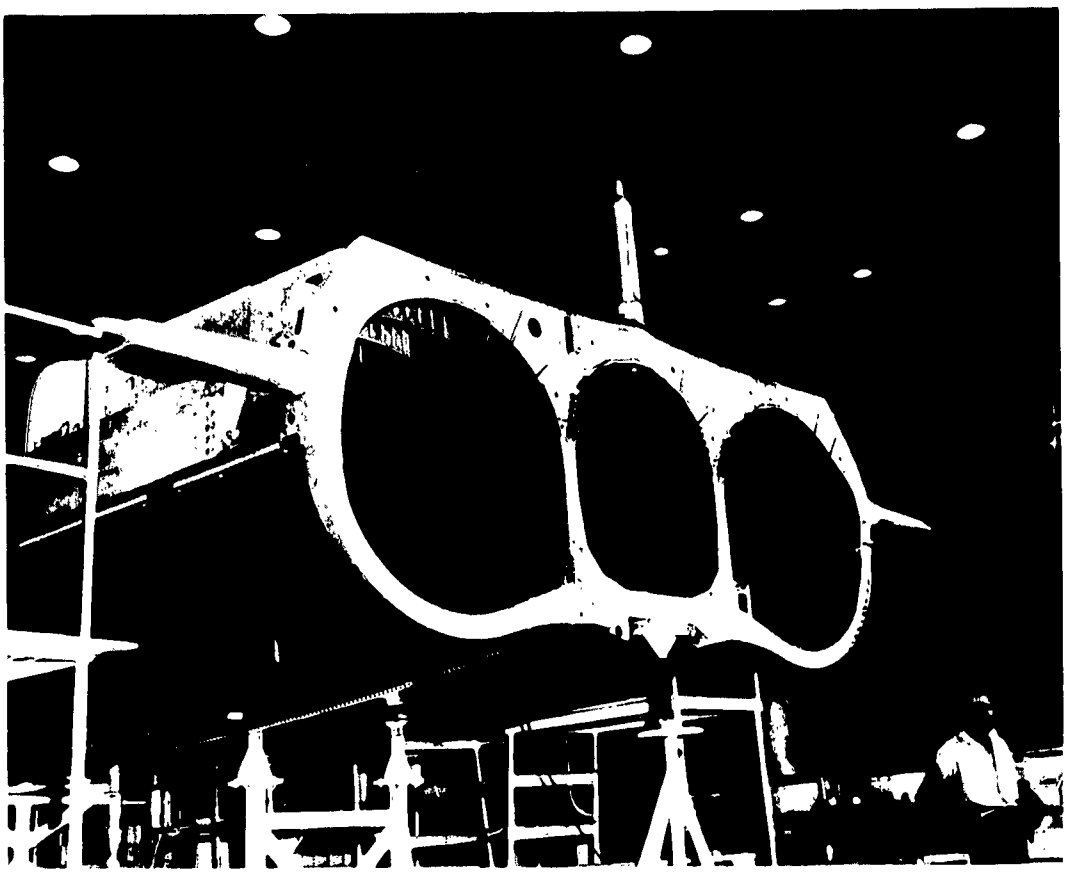


Figure 1. Carry-Through Structure in Tail Frame of A3J Vigilante Naval Attack Bomber

largest pieces of the airplane were found to be this tail frame structure. This is quite remarkable considering that aluminum, titanium, and other supposedly more ductile materials were also on the aircraft.

A few other outstanding applications might be mentioned. On the Convair B-58 Hustler bomber, the elevon hinges support all of the control surfaces on the delta wing and thus are extremely critical parts. When made from titanium, these were called the "Cadillac parts"; by changing to a H-11 Modified steel at 260 ksi, the cost was reduced to approximately one-fifth of the original, and very satisfactory weldability, heat treatment, and performance have been reported. The new B-70 Valkyrie bomber is another major application of this steel at the 280,000 psi minimum strength level for landing gear, hydraulic system, and major air frame components.

So much for aircraft applications at strength levels above and beyond those currently used in missiles; we all recognize that missile design problems and safety factors are much more restrictive.

Let us now consider future higher strength trends. Figure 2 shows estimated strength capabilities of low and medium alloy steels extrapolated to the year 1975 for a recent Materials Advisory Board standing Committee reviewing the DOD Metals Research and Development Program. The slopes beyond 1960 are, of course, strictly conjecture, but the strength levels indicated for 1975 have already been obtained on a laboratory scale. These include 465,000 psi ultimate in ausformed steel, and 425,000 psi ultimate with 365,000 yield in conventionally heat treated steel. To achieve these values, it was necessary to increase the carbon content from the .40 percent currently used in ultra high strength steels to approximately .60 percent, balanced by a total of 8 to 11 percent alloying elements.

Alloy development studies to date indicate a definite need for increased alloy content for higher strengths; carbon alone is insufficient for the purpose. Figure 3, from a 1957 ASM paper on bend testing, illustrates this trend. Low alloy steel S1 and medium alloy steel 07 each achieve maximum bend yield strength at intermediate hardness levels; attempting to heat treat them to higher than their optimum hardness results in a decided strength decrease. The high alloy steels M2 and T1, on the other hand, maintain proportionality of strength and hardness up to nearly the maximum hardness obtainable by conventional heat treatment. Thus far, the high speed steels, similar to M2 and T1, have proved to be the strongest heat treatable compositions, and modifications of these steels have produced all of the conventional heat treated strength values in the 375-425,000 psi range. Secondary hardening, as obtained in high speed steels and hot work die steels, appears particularly important above 300,000 psi because the high tempering temperatures (1000 F and above) permit maximum stress relief and hydrogen removal, as well as transformation of unstable retained austenite by multiple tempering.

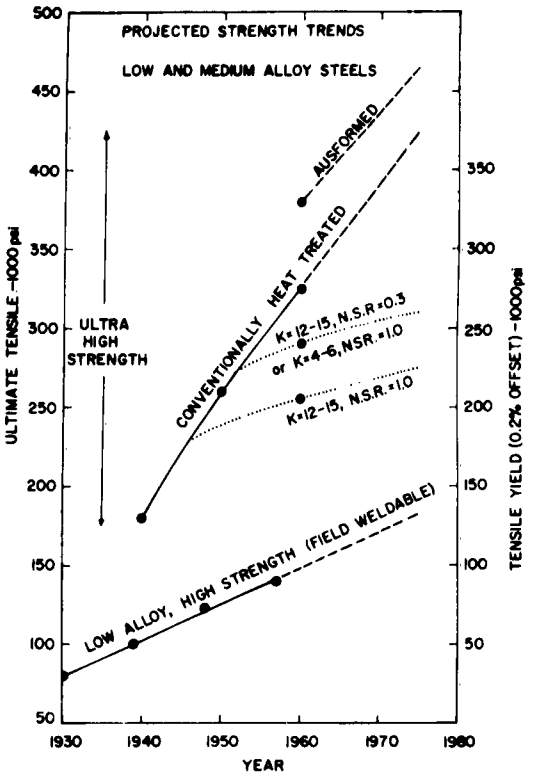


Figure 2

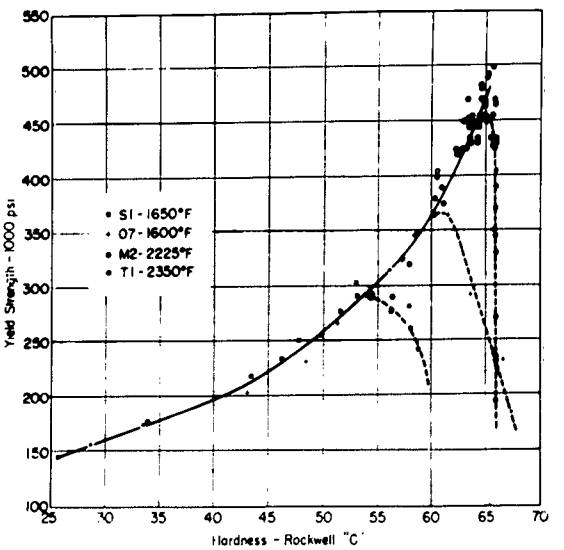


Figure 3

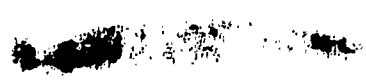
These trends to higher carbon and alloy contents for higher strength materials will, of course, mean inherently less ductility. Let us refer again to Figure 2. In 1940 aircraft designers considered 180,000 psi to be the maximum safe strength level for aircraft design. Today, they are using 300,000 and 325,000 psi materials, taking advantage of improved design and fabrication techniques, and improved quality of materials. Each step upward along this curve has necessitated extensive reliability evaluation of the lower ductilities inherent with the higher strengths, and has presented momentary plateaus until new and daring breakthroughs have been achieved.

Similar plateaus, based on notch sensitivity or crack propagation, appear to be currently facing the missile industry. These are indicated by the dotted lines in Figure 2. The lower dotted line shows the current 200-220,000 yield strength limitation based on notch toughness criteria requiring G_c = 800-1000, or a notch strength ratio of 1.0 with very sharp notches.

This relationship of sharp notch strength to heat treated strength level has been demonstrated in slides throughout this conference and extensively reported in the literature. Figures 4 and 5, from Aerojet-General studies on a number of materials, clearly indicate the marked dependence of G_c on the heat treated yield strength. Values as high as 3000 have been reported at yield strengths below 220,000 psi in consumable vacuum melted material, but slightly higher yield strengths result in consistently low G_c values for all materials. The data of Brown et al (Figure 6) similarly show increasing notch sensitivity with increasing strength level, with a fairly narrow band for steels strengthened by widely different mechanisms. Their recent data for titanium alloys indicate a similar band, but a slightly higher strength-to-density ratios indicating some promise from that source.

In any event, the evidence consistently points to definite plateaus in usable strength levels of all materials based on sharp notch criteria.

The dotted lines in Figure 2 have been drawn with relatively small slopes because the intensive development and testing programs of the past several years have failed to indicate a significant breakthrough toward increasing strength without sacrificing ductility and corresponding sharp notch toughness. Although consumable vacuum melting has provided 200-300 percent improvement in transverse ductility of large billets for landing gear and major air frame sections, it has shown very small improvements in sharp notch properties by the various test methods. Extensive testing of existing alloys and alloy development programs in many research laboratories have similarly produced no significant change in sharp notch properties compared with existing steels. We are, of course, continuing our programs in the hope of developing such a fabulous material, but feel that conservatism is necessary in extrapolating future potentials.



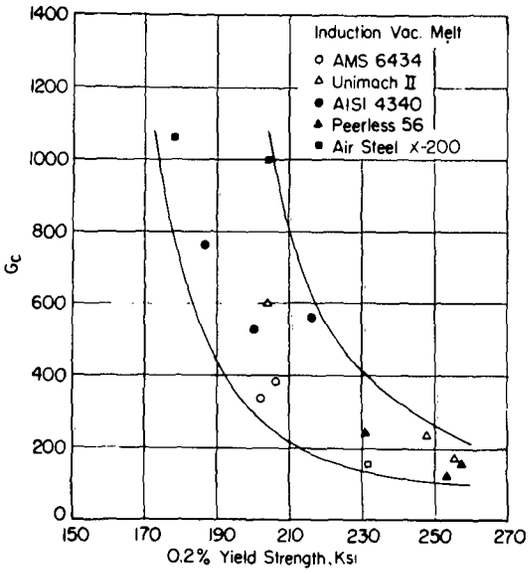


Figure 4

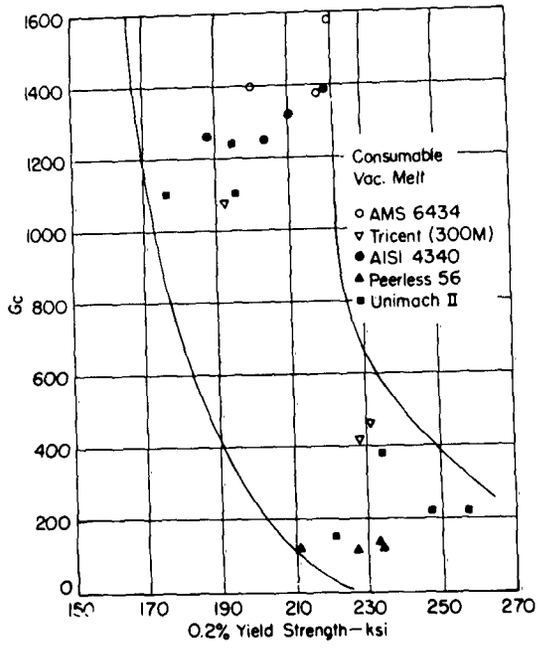


Figure 5

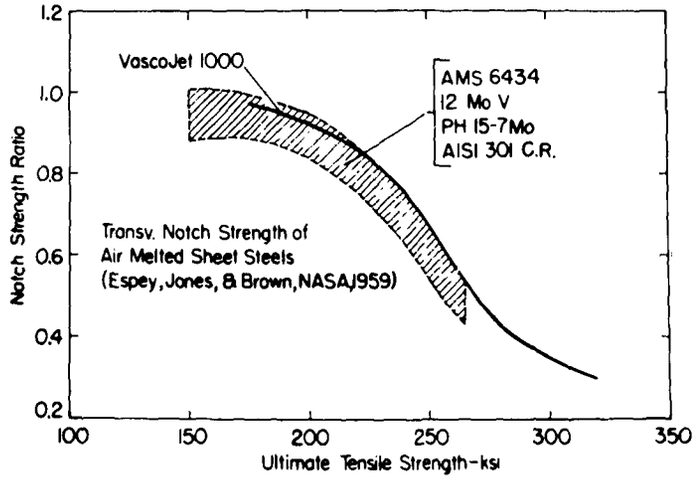


Figure 6

If, through improved design, fabrication, and inspection procedures, lower notch strength ratios can be accommodated, or, similarly, milder notch criteria are acceptable, the usable strength level is increased as shown by the upper dotted line of Figure 2. This potential has been demonstrated by Pratt and Whitney in the rocket cases they have been describing, and by the milder notch data of Dr. Sachs and his associates. And, proceeding on up the ultra high strength curve, it does not seem too unreasonable to expect a series of new plateaus accompanying various notch criteria. According to Mr. Jones' report here, ausformed steels also are exhibiting low sharp notch properties with their extremely high strength potential.

Perhaps, with extremely clean steels, and optimum design, fabrication, and inspection, crack initiation rather than crack propagation will become the important consideration. High speed steels and cold work die steels have been heat treated to extremely high hardness and strength levels for many years and, if free of cracks or corresponding design defects to start with, they remarkably withstand shock and stress during extended service.

In summary then, from the present state of the art, it appears that higher strength levels in rocket cases may be best achieved by improvements in design, fabrication, and inspection procedures, to accommodate the greater notch sensitivity apparently inherent in materials capable of achieving these strengths.

PREPARED DISCUSSION - FIFTH SESSION

NRL-NASA-SRI COOPERATIVE STUDY OF HIGH STRENGTH SHEET SPECIMENS INTENDED FOR MEASURING DESIGN VALUES OF FRACTURE TOUGHNESS

By
A. G. Holms

INTRODUCTION

Recent proposals for the geometry of specimen types to be used for screening high strength materials are described in references 1 and 2. In addition, some proposals concerning specimens to be used for determining quantitative values of fracture toughness (K_c) were described by the ASTM Committee on Fracture Testing of High Strength Sheet Materials (ref. 3). The work to be discussed herein was done with specimens that are essentially in accord with the recommendations of reference 3. This investigation is intended to provide further information on what geometrical characteristics specimens should have for determination of K_c values. The program was started as a cooperative effort by NRL and NASA and now includes a specimen geometry that was developed at Southern Research Institute.

Three basic designs of specimen are being used and two sizes of specimens are being tested within each basic design. These six combinations of size and shape are listed in Fig. 17 of reference 1. Additional description of the Southern Research Institute specimens is given in reference 4.

The work in progress includes static tensile testing at room temperature to measure fracture toughness for (1) H-11 modified; (2) AISI 301 with 70 percent cold reduction, and (3) beta titanium, BC 120 VCA. Each material is tested in conditions varying from tough to relatively brittle. Heat treatment is carried out at NASA before notching or cracking. NRL specimens are tested at NRL. NASA and SRI specimens are tested at NASA. Almost all the testing of the H-11 modified and the AISI 301 is complete. Decisions on heat treatments for the titanium are still to be made.

SAMPLING

All specimens of a given alloy were obtained from a single heat of material. The AISI 301 specimens were taken from a single sheet in a manner such that all specimen designs were stratified equally with respect to longitudinal and transverse positions in the sheet. Specimens of H-11 were taken from three sheets, and no particular sampling plan was employed. However, specimen hardness measurements shown in Table I indicate very uniform response to the various tempering treatments employed. The numbers given in the table are averages of two to four impressions on a single specimen.

Within any tempering, the hardness varied at most by one or two points. This uniformity in hardness suggests that a corresponding uniformity should occur in the fracture characteristics. For example, the notch properties of a given heat of H-11 modified are known to be a unique (but nonlinear) function of the tensile strength, and tensile strength is a function of hardness.

RESULTS WITH H-11 MODIFIED

The end purpose of the tests was the measurement of fracture toughness, K_c. As part of this measurement, an ink stain technique was used to determine the crack length at the start of rapid fracture. The maximum load divided by the uncracked area at the start of rapid fracturing is called the net fracture stress, σ_a. The calculation for K_c presented by the ASTM Fracture Committee was recommended for design purposes only when the ratio of net fracture stress to yield strength, σ_a / σ_{ys}, is less than unity.

The ratio σ_a / σ_{ys} is shown as a function of tempering temperature in Fig. 1. All specimen shapes and sizes met the condition of $\sigma_a / \sigma_{ys} \leq 1$ for all tempers up to 1075 F. At 1100 F, only the large NASA and SRI specimens met this condition, and at 1125 F, only the large NASA specimen satisfied this condition.

The K_c values for all specimens that met the condition of $\sigma_a / \sigma_{ys} \leq 1$ are shown in Fig. 2. The points are averages obtained from triplicate tests.

The differences in K_c values shown in Fig. 2 can be interpreted from two points of view; namely, a difference might or might not be important and separately it might or might not be significant. An important difference is one that represents practical differences in component performance. The designer or project engineer must be the judge of whether a difference is important. A significant difference is one that is larger than any difference that might be expected from a chance combination of small random errors. The mechanical metallurgist or the statistician must be the judge of whether a difference is significant. Because the point of view of the designer or project engineer is not immediately available, the data will be interpreted from the point of view of differences that are real when compared with the random scatter, that is, differences that are significant.

The K_c values obtained from the NASA 1-inch specimens and the K_c values obtained from the NRL 3-inch specimens were significantly high, as shown by Fig. 2. These two specimens were qualitatively similar in that they did not possess natural cracks at the beginning of the static test. The small NRL specimens did have a natural crack at the start of the test and the SRI specimens possessed punch and die shear cracks that, according to the results, served as well as natural cracks for this material. Apparently the large NASA

specimen was wide enough to be sufficiently embrittled by the very sharp notch, where as the NASA small specimen was not so embrittled by the same radius notch.

The designer wants to know what errors in predicted loads result from applying the K_c concept to qualitatively different structures. The specimens listed in Fig. 2 represent qualitatively different structures (although the range of size variation cannot be considered as large as that which would occur in actual engineering structures such as rocket motor casings). The errors of prediction of critical loads for the availabe specimens were examined as follows:

The estimated "true fracture toughness" of H-11 modified at each tempering temperature was obtained by averaging the K_c values for those specimens that seemed to have natural cracks, namely, the small NRL specimens and the large and small SRI specimens. The low crack lengths observed in all the actual specimens were averaged over several tests for particular designs, size and heat-treatment combinations to represent the "critical crack length in the structure." These slow crack lengths and the estimates of "true fracture toughness" were then used in the K_c equations to calculate predicted gross stresses for the various specimen types. Ratios of gross stresses as observed for each specimen to the gross stress predicted for the group of replicates were then plotted as a function of tempering temperature in Fig. 3. With the exception of the large NRL and small NASA specimens, the results for all the individual specimen show a scatter of not more than +23 percent and -19 percent about the desired ratio of unity. Clearly the K_c concept has provided predictions well within the range of experimental scatter for these specimens. Excessively high K_c values were shown for the large NRL and small NASA specimens in Fig. 2. Comparison of observed and predicted loads for the large NRL specimens showed observed values in excess of predictions from 42 to 194 percent. The ratios of observed to predicted loads for the small NASA specimens showed deviations varying from 12 percent to 88 percent high.

RESULTS WITH AISI 301, 70 PERCENT COLD REDUCED

Results of testing AISI 301 stainless steel supplied as 70 percent cold reduced sheet are given in Table II, and average values of K_c are plotted in Fig. 4. This work hardened steel is seen to vary in embrittlement with specimen orientation as shown in Fig. 4 by the lower K_c values for tension applied in the direction transverse to rolling.

The transverse specimen K_c data show no significant differences among specimen designs except that both sizes of the SRI specimens evidenced a tougher condition. The behavior of the SRI specimen is in contrast to that oberserved when testing H-11 steel. As was discussed previously, tests on H-11 showed good agreement between data obtained with the SRI specimens and the NRL 1-inch center fatigue cracked specimen. The reason for this

difference in behavior of the SRI specimen with change in material is not known. However, it should be noted that the slow crack growth ratios (values of a/a_0) in Table II suggest that while the other specimens were experiencing slow crack growth during rising load, the SRI specimens were experiencing a stress redistribution making these specimens less severe tests of the material.

The comment that is suggested is that ease of fabrication may make the SRI specimen particularly efficient in production control (for example, in the heat-to-heat sampling of H-11) but its use for the purpose of making absolute measurements of K_c must first be validated for a given material by checking against some specimen that is known to be suitable.

SUMMARY

In summary, we are testing two types of specimens that were recommended by the ASTM Special Committee on Fracture Testing of High Strength Sheet Materials (Ref. 3), together with a type of specimen proposed by Kattus and Morrison (Ref. 4). Instances have been found in which some of the specimens with K_c computed according to the methods outlined in reference 3 may not be suitable for quantitative work. We hope that the addition of titanium alloy data will enable the ASTM Fracture Testing Committee to define more accurately the specimen types most suitable for K_c determination.

ACKNOWLEDGEMENTS

The writer is indebeted to Dr. G. R. Irwin and to Dr. John Srawley for the cooperation received from NRL and to J. D. Morrison and J. R. Kattus for cooperation received from Southern Research Institute. Mr. W. F. Brown, Jr., of NASA furnished a mine of data on the behavior of the materials and largely guided the selection of the materials and their heat treatments. Mr. M. H. Jones of NASA was particularly helpful with ink stains and their interpretation.

REFERENCES

1. Brown, W. F., Jr., Mechanical Screening Tests for Sheet Alloys, Seventh Sagamore Ordnance Materials Research Conference on Mechanical and Metallurgical Behavior of Sheet Materials, Aug.1960.

2. Stapleton, T. J., Final Report of ARTC Project W-97, Standardization of Test Procedure for Tear Resistance of Metallic Sheet Material, ATC Report No. ARTC-24 Aerospace Industries Association, Los Angeles, California, July 7, 1960.

3. ASTM Committee on Fracture Testing of High Strength Sheet Materials, Fracture Testing of High-Strength Sheet Materials, ASTM Bulletin No. 243, pp. 29-40. Jan. 1960, and No. 244, pp. 18-28, Feb. 1960.

4. Morrison, J. D. and Kattus, J. R., The Use of Shear-Cracked Specimens for Evaluation of Sheet Materials, Seventh Sagamore Ordnance Materials Research Conference on Mechanical and Metalurgical Behavior of Sheet Materials, Aug. 1960.

TABLE I. - SPECIMEN AVERAGE HARDNESS VALUES, H-11 MOD.

Triple tempering temperature, F	900	1000	1075	1100	1125
Number of specimens	17	17	17	20	17
Min. Rockwell-C	57.4	56.3	51.7	49.0	46.9
Max. Rockwell-C	58.5	57.9	53.7	51.2	48.5
Range Rockwell-C	1.1	1.6	2.0	2.2	1.6

TABLE II. - SLOW CRACK EXTENSION, NET STRESS RATIOS, AND CRACK TOUGHNESS VALUES

FOR SPECIMENS OF AISI 301, 70 PERCENT COLD REDUCTION

Specimen type	Nominal width, in.	Longitudinal, σ_{ys} = 220.3 kpsi				Transverse, σ_{ys} = 227.2 kpsi			
		Specimen number	a/a_0	σ_a/σ_{ys}	K_c	Specimen number	a/a_0	σ_a/σ_{ys}	K_c
NRL fatigue center crack	1.5	7HLSL1	1.531	1.106	196.3	7HLST1	1.643	0.807	120.0
		7HLSL2	1.511	1.072	183.2	7HLST2	1.686	.823	122.7
		7HLSL3	1.291	.961	157.0	7HLST3	1.547	.749	112.3
		Mean	1.444	1.046	178.8	Mean	1.625	0.793	118.3
NRL Elox center crack	3.0	7HLL1	1.663	0.966	216.1	7HLLT1	1.522	0.560	117.1
		7HLL2	1.326	.897	201.6	7HLLT2	1.293	.528	110.8
		7HLL3	1.500	.952	216.5	7HLLT3	1.522	.560	116.6
		Mean	1.496	0.938	211.4	Mean	1.446	0.549	114.8
NASA sharp edge notch	1.0	7HASL1	1.498	1.051	157.1	7HAST1	1.495	0.717	94.6
		7HASL2	1.445	1.082	169.0	7HAST2	1.403	.817	112.3
		7HASL3	1.608	1.211	-----	7HAST3	1.518	.718	94.4
		Mean	1.517	1.115		Mean	1.472	0.751	100.4
NASA sharp edge notch	3.0	7HALL1	1.441	0.753	169.9	7HALT1	1.318	0.449	99.0
		7HALL2	1.269	.790	183.1	7HALT2	1.322	.466	103.1
		7HALL3	1.297	.770	176.9	7HALT3	1.282	.435	95.9
		Mean	1.336	0.771	176.6	Mean	1.307	0.450	99.3
SRI shear center crack	1.3	7HISL1	1.268	1.202	-----	7HIST1	1.419	1.095	186.6
		7HISL2	1.185	1.160	-----	7HIST2	1.347	1.045	170.5
		7HISL3	1.261	1.205	-----	7HIST3	1.490	1.109	190.0
		Mean	1.238	1.189		Mean	1.419	1.083	182.4
SRI shear center crack	3.0	7HILL1	1.066	0.954	221.0	7HILT1	1.116	0.719	157.3
		7HILL2	1.072	.834	183.2	7HILT2	1.123	.750	165.3
		7HILL3	1.066	.890	200.1	7HILT3	1.140	.741	162.8
		Mean	1.068	0.893	201.4	Mean	1.126	0.737	161.8

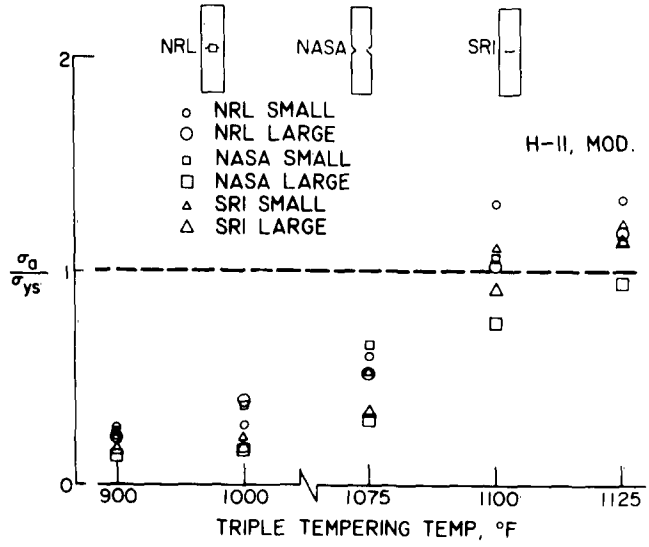


Figure 1. Ratios of Net Stress to Yield Strength for Data Generally Averaged from Three Specimens

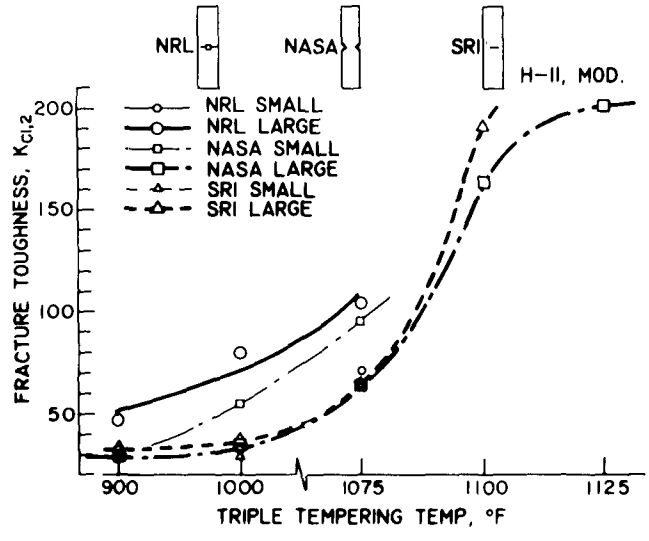


Figure 2. Fracture Toughness Values at Stated Tempers as Determined from Average of About Three Specimens

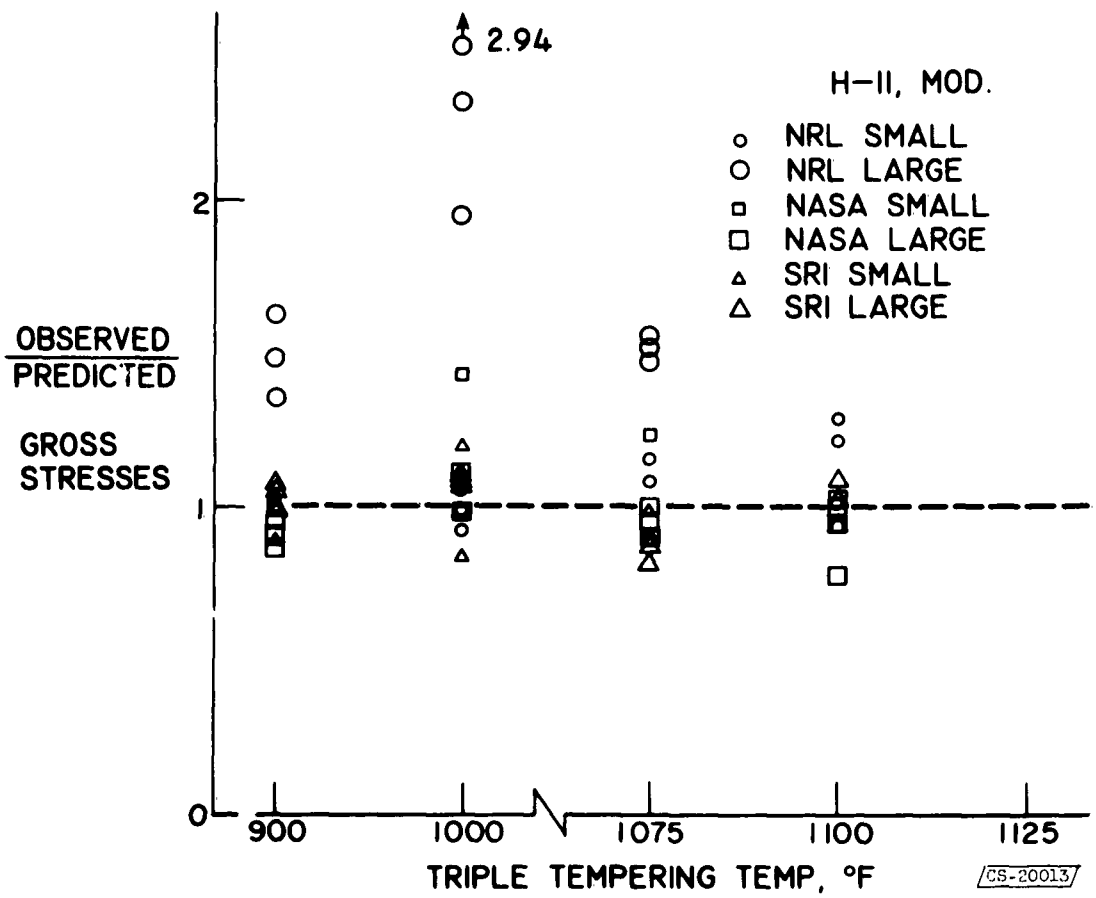


Figure 3. Ratios of Observed to Predicted Gross Stress as Function of Tempering Temperature for H-11 Modified

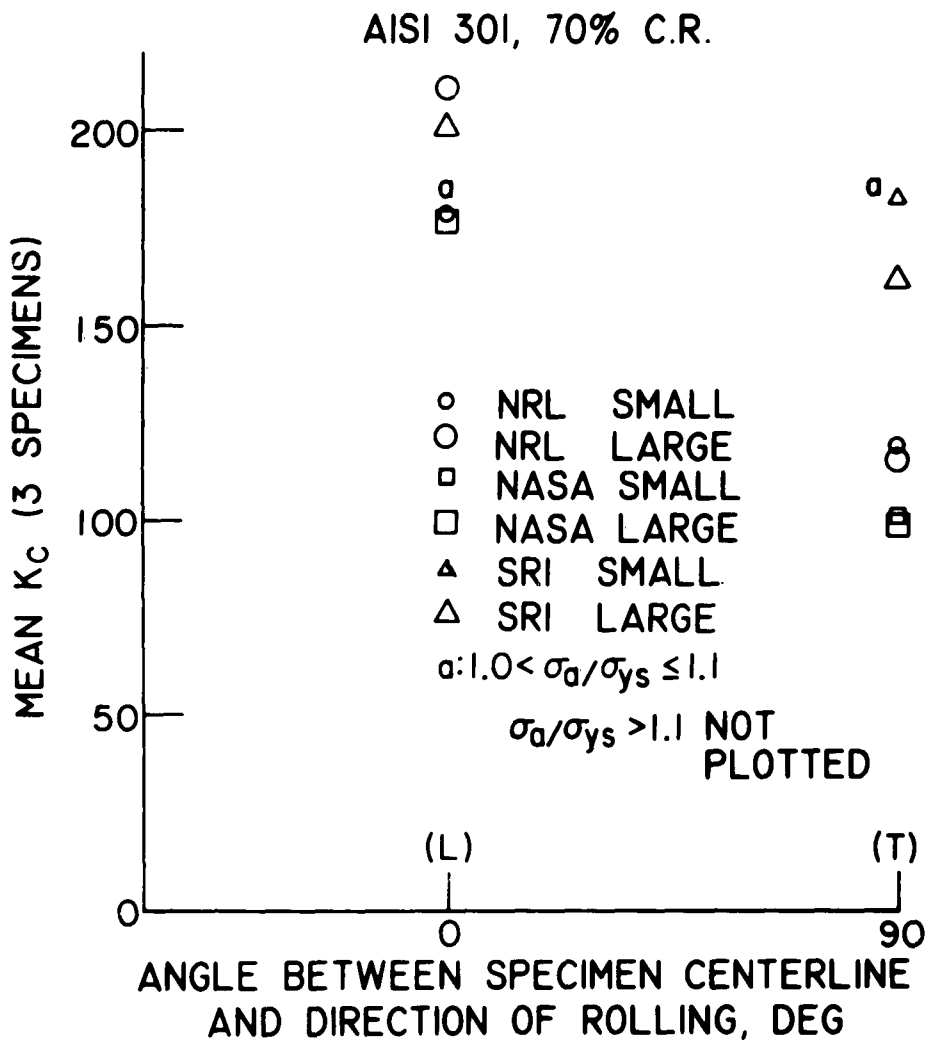


Figure 4. Fracture toughness Measurements with AISI 301 Stainless Steel

J. F. Watson There are two questions I would like to ask Mr. Sippel regarding the bend test. First, what is the range of sheet thickness that can be tested with this apparatus? As you know, in steel pressure vessels, skin gauges may go down to .010 or .012 inches, while in aluminum gauges may exceed .100 inches. Thus we need a test that will cover at least this range of thickness.

Second, can you, or have you applied the bend test to welded joints? When subjecting a weld joint to a notched tensile test, it is difficult to make up identical samples. The question always arises as to where to put the notch; i.e. in the weld metal, the heat effected zone, or at some intermediate point. It seems that the bend test would offer a solution to this problem by offering an "integrated" test that would test all of these areas simultaneously.

G. R. Sippel In answer to your first question about thickness range, we have had very limited experience in the thickness ranges below 0.050 inches. We have tested a few specimens of AM 350 and Type 301 at the 0.020 inches thickness level where we were able to get satisfactory tests when the crack propagation resistance of the material was low. When the crack propagation resistance is high, these thin cross sections allow very high specimen deflections with a 1 inch span and as a result we do not get sharp breaks in the load-time curves. I believe, however, that by changing the span distance to less than one inch we can get satisfactory results on thin samples.

In answer to the second part of your question concerning the testing of welds, we regularly check welds by means of the instrumented bend test. In fact, some of the bend test parameters which I showed for the 24 inch diameter pressure vessels were obtained from the weld areas of those vessels whose failure origins were in the welds. The test works equally well for longitudinal or transverse weld test, although we normally use specimens wherein the bend axis is transverse to the weld, simulating girth welds in a vessel. In these specimens, the fusion zone and the heat affected zone are both biaxially stressed to the same degree and we actually have an integrated type of test.

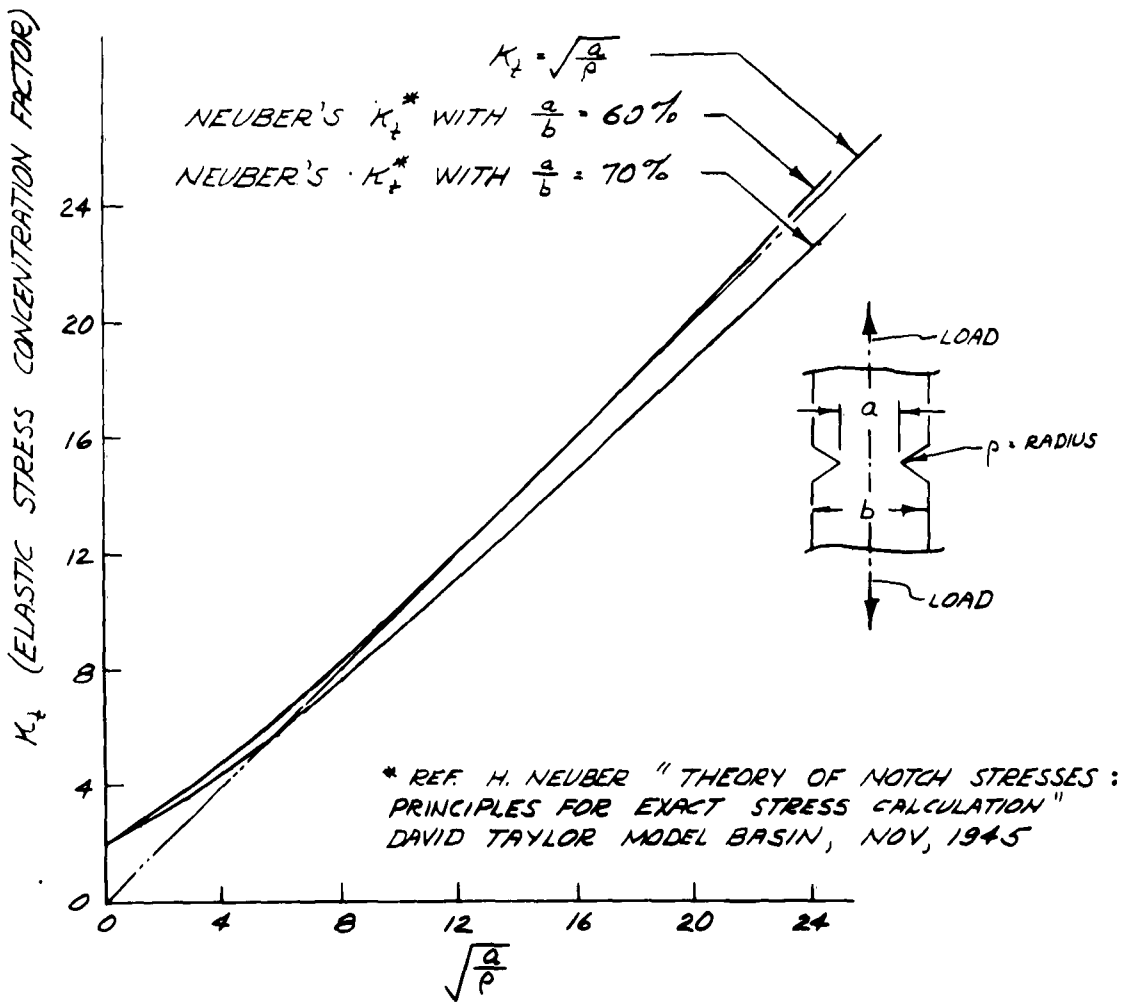
A. Hurlich With respect to Jack Hamaker's most recent pronouncements, I would say "God help the United States if we make it a national policy to believe that by means of design and fabrication ingenuity we can make critically stressed engineering structures out of brittle materials."

H. Bernstein I would like to report the results of some recent environmental tests we made. The material was M255 which is used in the POLARIS motor cases, also known as AMS16434. The yield strength level was 200,000 psi, thickness about 100 mils, fracture toughness about 900 to 950 ipsi (this is high toughness). The environments were air, India ink, water, water plus an inhibitor which is used in the hydro tests, and lastly 0.1 N hydrochloric acid. Specimens were precracked to insure that a natural crack was present before the introduction of the environment. We used a 3 inch specimen with a central notch. It was first pulled in tension until a natural crack appeared at the notch edges, the load was then released and the environment introduced. We compared the loads to failure, assuming constant toughness, and found no difference.

One explanation for the difference in behavior between AMS16434 and the Tricent data reported by Mr. Brown of NASA is that the phenomenon may be chemistry sensitive. Tests made at NRL have also demonstrated the sensitivity of Tricent to environment. The other factor may be toughness level. Mr. Brown's data showed that the lower strength, tougher material was not as sensitive and I think this may be a contributing factor.

V. Weiss I would like to point out that the stress concentration factors quoted by Mr. Stapleton are not identical to the stress concentration factors defined by the ratio of the maximum stress at the notch root divided by the average stress at the notched section. However, the correct stress concentration factors can be determined from the quoted values of $\sqrt{a/\rho}$ from Peterson's book.

T. J. Stapleton $\sqrt{a/\rho}$ is used as an approximation for K_t by a number of the airframe companies. A comparison of this method with the "exact" method of Neuber for a notch of arbitrary depth is presented in the accompanying figure. The accuracy of this approximation is a function of the ratio of specimen net width to gross width ($\frac{a}{b}$). The range of notch geometries included in the subject paper are all between the two curves plotted ($\frac{a}{b}$ = 60 and 70 percent). For the purpose of this investigation, the $\sqrt{a/\rho}$ approximation is considered sufficiently accurate.



Comparison of $\sqrt{\frac{a}{\rho}}$ with Neuber's "Exact" K_t

R. D. Lula I would like to add some more hopeful information to that given by Mr. Hamaker. It appears that if you have to select a steel based on the present toughness criteria, there is a limitation in the usable strength level of the low alloy hardenable steels. However, there are types of higher alloyed steels which are quite promising and have a good chance to raise the present strength level of rocket case materials. I want to mention two of them. One type is the 20 and 25 percent Ni PH steels developed recently by International Nickel. Though they are just in their development stage and the first production heats are now being made, these steels are capable of developing between 250 and 300,000 psi yield strength with good ductility. Another family of steels which are in a more advanced stage of development and for which a certain amount of notch toughness information is available, are the AM 355 and AM 357 PH steels. These steels can develop strength from 250 up to 370,000 psi in the work-hardened condition. These strengths can be achieved either by cold rolling or by shear spinning. These work-hardening methods restrict fabrication to the ribbon-wrap and the shear spinning method where spinning is used not only to give the shape but also to work-harden the material. The notch properties of AM 357, based upon a limited amount of information, indicate that this steel could provide a good rocket case material up to approximately 300,000 psi tensile strength.

S. V. Arnold Mr. Brown, I was rather surprised to see that when you were comparing these various candidate notch sheet specimens, you did so on the basis of various tempering temperatures. Would it not have been more significant to do this on the basis of various testing temperatures so that you would have a comparison of transition curves?

W. F. Brown We could have done it on the basis of test temperature. However, if you do it on this basis, it becomes difficult to measure slow crack extension because the liquids freeze at low temperatures. What we are mainly interested in doing is to provide a range of fracture toughness and that can be done either by varying the tempering temperatures or it can be done by varying the testing temperature. If the testing temperature is varied, then the ink staining can not be used to determine slow crack extension.

S. V. Arnold This points out, with certain exceptions, what seems to be a shortcoming of current notch, sheet tensile testing practice; namely, you do not explore the temperature variable. I think it is an important variable and that is one reason why we at Watertown are sticking with the dynamic test which, although it is not so readily interpretable for design purposes, does explore the temperature variable rather simply.

W. F. Brown That comment neglects the work done by John Srawley. He is doing a very thorough job of exploring the temperature variable and other people do this too. There is no reason why you cannot use tensile specimens for that purpose If we are going to do a thorough job, at very low temperatures down to that of liquid hydrogen, then we should develope means for measuring slow crack growth when the specimen is immersed in cold liquid. This is not an easy job to do but I think it is a problem that has to be attacked.

B. M. Wundt This shear-cracked specimen test is of interest and I would like to make a comment. Fig. 3 of the paper indicates that the transition temperature was minus 100 or minus 150 F. I also assume that the shear crack is produced at room temperature.

W. F. Brown For tests used in the NASA-NRL cooperative program the punching was performed at room temperature with the metal in a soft condition.

B. M. Wundt That means that the crack has a fibrous teat at the end of the crack and the operation of punching may include hot pre-stressing. This may result in strengthening when tested at temperatures below room temperatures. I suggest therefore, that the specimen be shear-cracked at temperatures below the transition temperature. This will result in a crack which has cleavage characteristics and which will be much easier to initiate. Such specimens may result in considerably lower notch-strength values and in lower stress intensity coefficients.

W. F. Brown Let me make one comment, before you go further. The specimens of H-11 steel were prepared for us by the Southern Research Institute and they were, as you say, punched at room temperature. However, the results from these specimens, if I recall correctly, agreed quite well with the natural fatigue crack specimens that were produced by John Srawley. So, for that particular alloy I do not think that shear cracking at low temperature is necessary. Perhaps a natural cleavage crack was present at the tips of the punched notch. When these specimens were tested, pings were heard at very low loads. We would guess therefore, that the cold-worked area at the notch tip may result in the extension of a crack early in the test. In type 301, 70 percent cold-reduced material, the shear cracked specimen did not provide embrittlement because of the dimpling mentioned by Mr. Holms. Shear cracking at low temperature probably would not have eliminated this difficulty. Your suggestion may be a good one in some cases, however, the data available do not indicate where it would be of benefit.

F. Richmond I think the standardization of specimen design discussed this afternoon has been very good. Something has to be done to straighten out this system of testing. What bothers me is that all the emphasis is on the design of specimens and types of testing, but there does not seem to be much emphasis on the preparation of specimens or the sequence of machining and heat treating. I realize that ASTM has recommended that machining be done prior to heat treatment. If, what Pratt & Whitney has found about decarburization is so, this could cause a terrific amount of variation, even though you standardize specimen geometry and test procedures.

W. F. Brown What you say is partly true. The specimen used to test a given material had better represent that material which is put into the structure, and if the structure is decarbed, the specimen should be decarbed in a similar manner. However, we use the notch test as a tool for investigating factors that influence the embrittlement such as tempering temperature and alloy composition. Since we do not want to introduce any extraneous

variables, we make sure that decarb is absent. The sheet we obtain is not decarbed and we do not decarb the specimens when we heat treat them. The ASTM committee recommended machining before heat treatment mainly because it is much easier to produce sharp notches in soft metal. A notch radius of less than .001 inches can be produced by grinding in very hard material but this is more difficult and introduces the possible effect of grinding stresses. Of course, it should be remembered that fatigue cracks can be produced in very hard specimens using "Eloxed" crack starters as done by John Srawley. Now we will go back to the question of machining before or after heat treatment. We have made a few tests which indicate that it does not make any difference whether the machining is done before or after notching. John Srawley has similar information for X200 steel which appears in the report of the ASTM Fracture Committee. I do not want to imply that we should forget this variable, but the little information that we do have does not give cause to worry. Decarburization could be investigated rather easily by machining prior to heat treating and heat treating in different types of atmospheres to produce different depths of decarburization.

F. R. Larson I would like to make a few comments about the various specimen designs and some results that have been known for quite a while about general metallic materials. Contrary to what the "plasticians" would like to think, these metallic materials are not isotropic. We should not hope to make exact correlation between specimens of different design. This cannot be done because of the introduction of different stress systems into the material where the fracture zone is occurring. You can through some little mental gyrations, show quite a marked difference between two very similar specimens, the edge crack and the center crack specimens. All you have to do is think about the normal anisotropy which I illustrated in the titanium materials and you will see very quickly that there is quite a bit of difference here. Now where does that leave us? If we cannot think about our materials as being isotropic and we have laboratory testing such as screening tests or fracture toughness measurements, then I think we still have to go back to the old story, make the hardware and try it.

W. F. Brown I do not understand your argument, specifically as applied to these sheet specimens where edge notches or central cracks go all the way through the sheet. Would you care to explain that a little more thoroughly?

F. R. Larson I think possibly that one of the reasons why we have not run into too much trouble along these lines to date is because the anisotropy in the steel material is usually small and it is weaker in the thickness direction than it is in the width direction. My remarks will be clarified by a simple little illustration. I would like to emphasize the exact opposite case where the material is stronger in the thickness direction than in the width direction. Now, if you compare the edge notch and the center notch specimen you see that the plastic zone that develops in the general yielding case is a shear band of a configuration as illustrated in figure 1.

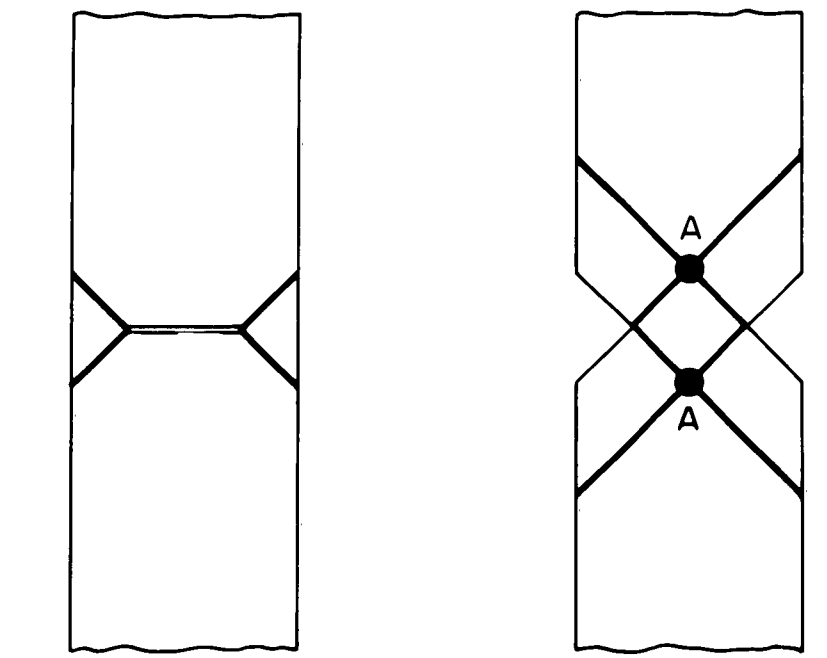


Figure 1. Front View of Edge and Center Notched Sheet Tension Specimens

In the edge notch case, the strengthening effect due to the opposing stresses at the centerline of the specimen is such that you can develop, if the anisotropy is very strong, a strengthening effect much like you could in cylindrical bar because you force your plastic flow up in area "A" and possibly penetrate up through the entire section. You could conceivably, if the anisotropic behavior of the material was extreme, reach the notch strengthening effects for a cylindrical bar. That is just one example where two very similar specimens can give quite widely different results.

W. F. Brown Well I think for a long time to come we will probably have steel sheets which are weaker in the thickness direction. Therefore, your argument will not apply.

F. R. Larson I do not think we ought to have them, though.

W. F. Brown No we ought not to, but I think this is inherent in the rolling process. The more reduction, probably the worse it is.

K. S. Grewal Prestraining in torsion greatly reduces both ductility and fracture stress in tension (1, 2). Effects of such prestraining persists even after annealing. Thus, the production of a crack by shearing would greatly reduce the tensile ductility and fracture stress in the vicinity of the crack tip. This might be beneficial in the study of fracture toughness (3). On the other hand, since the effect of local prestraining in shear will vary with different alloys and with sheet thickness for the same alloy, notch strength data obtained with this test are not likely to be as consistent as those obtained with fatigue cracked specimens or machined edge-notched specimens.*

C. Hartbower Mr. Brown, with regard to Mr. Arnold's question, I believe that Mr. Arnold's point was that it is important to test over a range of temperatures and I am sure he did not mean to imply that no one is doing this with a tensile test. We know that people are doing it, but the point is that it is much easier and much more economical with the Charpy test. For screening purposes, the Charpy test lends itself to testing over a range of temperatures, whereas the tensile test is more difficult and much more expensive to run as soon as you get away from room temperature.

---

* Reference

1. H. W. Swift, Tensional Effects of Torsional Overstrain in Mild Steel, J. Iron and Steel Inst. Vol. 140 (1939) p. 181
2. W.A. Backofen and B. B. Hundy, Mechanical Anisotropy in Some Ductile Metals, J.Inst. Metals, Vol. 81 (1952-53) p. 433
3. D. L. Newhouse and B. M. Wundt, A New Fracture Test for Alloy Steels, Metal Progress, Vol. 78 (1960) p. 81

J. E. Srawley Since we do a lot of tensile testing over a range of temperatures, I guess, I should comment. It is undoubtedly easier to break a Charpy specimen at low or high temperature than it is to break a tensile specimen. The same applies to room temperature, it is easier to break a Charpy specimen at room temperatures than a tensile specimen. Charpy is just not such an elaborate test as the tensile test. But I think you are exaggerating a little bit about the difficulties of making tensile tests, crack propagation or regular tests, at high or low temperatures. We find it no problem, we control the temperatures within plus or minus 2 F. One operator can run anywhere from 8 to 16 or 20 tests a day which I think is pretty good going, although it is not nearly the rate at which you can test Charpy specimens. We think we get more information from tensile testing; by tensile I mean both standard tensile testing and crack propagation testing. I think it is a good thing that you and I do these two different kinds of tests, we get both kinds of information, and we might one day be able to understand what they both mean. While I am on my feet I might make one more comment directed at Mr. Brown. Again about the question of difficulty, I do not think it is so much more difficult to prepare a fatigue notched specimen than it is to prepare a specimen which has a very sharp machined notch. In fact I would think the costs were somewhat comparable. However, I fully realize, that nobody is going to write specifications involving fatigue cracked specimens. So that it is inevitable that we will be using machined notches in specification tests. But I would not like people who might want to use fatigue cracked specimens, or corrosion cracked specimens for that matter, to be discouraged by the idea that it is so very difficult. Our fatigue cracked specimens are fatigue cracked by a foundry molder. He is about 60 years old and wears glasses. He does a wonderful job although he has not been doing it for very long.

C. Hartbower I agree that fatiguing is quite feasible. We are now fatigue cracking Charpy specimens which permits us to do away with the tapered notch (illustrated by Mr. Brothers). The tapered notch was adopted as a matter of expediency because when we tried to produce a natural crack under the standard .010 inch Charpy V-notch by a low energy blow, the crack tended to be skewed so that special notching was necessary. But in the last few weeks we have been fatiguing cracks at the base of the standard Charpy V-notch. We found a fatigue machine in the test laboratory that was not being used too much. With instrumentation, designed by Mr. Orner, the fatigue machine is shut off automatically when the crack get to a predetermined depth. We believe that we can now easily produce controlled reproducible fatigue cracks at the base of standard Charpy V-notches in high-strength sheet materials.

W. F. Brown I would like to make a comment on both those comments. I think it is really useless to pursue the argument much longer. I have no objection to fatigue cracks, they are natural cracks and that is what we are trying to simulate. The only advantage the edge-notch has is that some people may not have the necessary fatigue equipment.

J. Goodman This is in connection with burst test of miniature pressure vessels by STL. Instrumented bend tests were conducted on coupons heat treated with the vessels. These test results show a sensitivity to process history, for the coupons were made from machined tubes, split and flattened, with an extra anneal. According to Dean Hanink these results are therefore too low. For the sake of argument, however, we would like to point out that the trend is definitely down with decreasing tempering temperatures, while burst tests, as shown in the slide, obviously increase with lower tempering temperatures. There are no premature failures or evidence of unreliability even in the 320,000 psi UTS range. Question: Even if the I.B.T. data shown were displaced down by the coupon treatment, does this not indicate an inverse correlation with burst strength?

G. R. Sippel The instrumented bend test parameter, like all crack propagation resistance parameters, shows an inverse correlation with strength as shown in Figure 1 of my paper. As the strength of a material increases, the crack propagation resistance decreases, and therefore the data which you have presented, showing a decrease of bend test parameter with decreasing tempering temperature (increasing strength), is exactly what is expected.

You show an increase in burst strength of the 2 inch diameter D6 vessels with decreasing tempering temperature (increasing strength), without premature failures and this is perfectly in agreement with the data and method for evaluation of rocket motor case materials and processes presented in my paper.

It has been shown that the biaxial yield and burst strength of a pressure vessel is governed by the uniaxial tensile yield and ultimate strengths as long as the crack propagation resistance is above a certain value. Below this value the pressure vessel behavior is unreliable and premature failures may occur, while at the same time there is also some statistical probability that the biaxial behavior will still be governed by the uniaxial properties. This value of the lower limit of crack propagation resistance is dependent on a number of factors including pressure vessel design, fabrication procedure, inspection and quality control levels. The lower limit of crack propagation resistance will be lowered as these factors are improved through experience and improvement in the state of the art.

In the case of your 2 inch diameter pressure vessel tests, premature failures were not observed even at very low levels of crack propagation resistance due to the fact that your miniature vessel approaches an "ideal" vessel in that there are no welds, the geometry is very simple and easy to accurately fabricate and inspect. These factors reduce the lower limit of crack propagation resistance for your particular vessel to a very low value. If a weld were added to your cylindrical section, the lower limit of crack propagation resistance would undoubtedly increase to some higher value.

SIXTH SESSION

"Mechanical Model Testing"

Paper Presented at
7th Sagamore Ordnance Materials
Research Conference, Raquette Lake,
New York 12-19 August 1960

"MECHANICAL MODEL TESTING"

By A. Hurlich*

The Sixth Session of this Conference is concerned with the validity, usefulness, and limitations of model testing. It is obvious that the very high costs of fabricating and testing full scale missile propellant tanks, rocket motor cases, and other large thin-walled pressure vessels prohibit the extensive testing of full scale components. Although some full scale testing is always conducted to establish the performance characteristics, reliability, fatigue resistance, or other behavior of finished products, full scale testing is generally uneconomical and often impossible to consider when evaluating and selecting among candidate materials, processing, and fabrication techniques prior to establishing the final design and production procedures to be used for the end items.

The uneconomical aspects of full scale testing is especially pertinent at this time when a large number of recently developed materials and novel production methods are clamoring for attention and evaluation. New titanium alloys, high strength steels of the martensitic, cold worked and heat treated austenitic and semi-austenitic types, metallic wire, glass filament, and plastic laminate materials are all being considered for application in large light-weight, thin-skinned pressure vessels. Also, a large variety of welding processes; forging, roll,-spin,-and explosion-forming techniques; sprial wrapping of thin strip and bonding by means of adhesives, spot-welding, and brazing; wire and non-metallic filament winding and plastic adhesive bonding and many other fabrication procedures have specific economic, weight, ease of fabrication, and other advantages and merit serious consideration for application to present and future rocket, missile, and space-craft design.

With this super abundance of materials and fabrication processes requiring evaluation, model testing, whenever applicable, permits rapid and relatively inexpensive assessments to be made. Obviously,

---

*Research Group Engineer, Materials Research Group, Convair-Astronautics Division, General Dynamics Corporation, San Diego, California.

model testing is most valuable when it yields quantitative data comparable to that obtained from the test of full scale components. Less valuable, but quite significant data can be obtained from scale model testing when deformation and fracture mechanisms and phenomena reproduce those obtained from full scale testing. It is very important that the experimenter determines, in advance of testing, whether or not the type and conditions of testing permit scale model structures to behave exactly as the full scale structures would under similar test conditions.

This point is well illustrated by the results of a series of tests which were performed by the Convair-Astronautics Division several years ago during the development of the Atlas missile. The Atlas is characterized by the fact that its propellant tanks are large, thin-skinned monocoque vessels with no internal or external supporting trusses, longerons, or other reinforcing structure. As a result of internal pneumatic pressurization, the tank skins are maintained under uniform tension stresses and are rigid enough to support heavy loads and withstand large bending forces without becoming unstable.

Inasmuch as after assembly, and during transport, storage, and erection of the missile, it is necessary to maintain internal pressurization at all times to keep the tanks rigid and unwrinkled, the question arose as to the damage which might be sustained by the missile and the hazard to personnel caused by an accidental puncture of the tank skins such as might result from a bullet or other high speed penetrating object.

To develop a feel for this problem, small 24" diameter tanks 3 feet in length were fabricated from the same sheet material which is employed for the missile and these tanks were internally pressurized to develop a range of skin stresses. Calibor .22 bullets were fired into the tanks to observe the effect of the level of internal pressurization and skin stresses upon their fracture behavior. At low stress levels, the tank skins were simply punctured, with a small hole developed which could be readily repaired by a patch seam and spot welded over the hole. When, however, the wall stress exceeded approximately 20% of the ultimate tensile strength of the material, the tanks failed with explosive violence; the skin rupturing into fragments which were hurled for some distance from the tank location.

Following these scale model tests, a 12 foot diameter tank, 75 feet in lenght was fabricated from the same sheet material and was fired at with caliber .22 bullets. Initially, the tank was pressurized to low stress levels and then the pressure raised for subsequent tests. At low pressures, the tank was again simply punctured and each puncture was repaired by a small readily applied patch. When the pressure was raised to the point where the skin stresses again exceeded approximately 20% of the tensile strenght of the material, the large tank failed catastrophically, with pieces thrown for great distances and with massive fracture and failure of the tank. The results of these tests are shown in Table 1 and indicate the excellent correlation obtained between the results of scale model and full scale tests when the factors being investigated were fracture phenomena and crack propagation.

It was interesting to note that while explosive rupture occurred at a wall stress level of 20% of the tensile strength under bullet impact, it required a stress level of 50% of ultimate to cause explosive rupture when a chisel with a sharp cutting edge was forced into the tank. When a blunt piercing tool (Phillips-head screw driver) was forced into the tank no explosive rupture occurred at stresses up to 70% of the ultimate tensile strength, only simple puncture resulted.

Inasmuch as the bullets, chisel, and Phillip-head screw driver each produced cracks of different lenghts, it was possible to determine critical crack lengths for catastrophic tank failure as a function of internal pressure and wall stress in the 24" diameter tanks. Because of the exact correlation developed between the scale model and full scale tanks, it was possible to calculate the critical crack lengths for total failure of the large tanks for various levels of internal pressurization. An accident which occurred with an R & D missile at a test base completely confirmed these calculations.

In the tests described above, the 24" diameter tanks, while having thin side wall sections, were fitted with heavy flat plates bolted into the ends to form pressure tight vessels. The large tank, on the other hand, had thin formed sheet bulkheads welded to the side wall sections. Since the bullets were fired at the side walls and failure initiated at the bullet penetrations, the fracture phenomena were not affected by the differences in end attachments and relative rigidities, and both types of tanks behaved identically under this test condition.

Cyclic fatigue tests were also performed on the smae type of 24" diameter tanks and on large 10 foot diameter tanks, with stresses applied by almost filling the tanks with water and then applying cyclic loads with air pressurization. This time, the scale model tank tests failed dismally to reproduce the results of the full scale tests. Because of the rigidity of the end attachments, much higher stresses were developed in the 24" diameter tanks at the joint between the end plates and the side wall section, leading to failure developing in this location in as few as 60 cycles when the stress levels alternated between 0 and 90% of the material's yield strength. The greater flexibility of the bulkhead-to-side wall joint in the 10 foot diameter tanks permitted much more uniform stress distribution in this critical region and the development of much superior fatigue resistance; the large tanks withstanding up to 1500-1800 cycles of stress before failure occurred.

Thus, one must be careful when designing scale model tests to insure that differences in stress discontinuities, relative rigidities, and other factors do not intervene to render scale model meaningless.

While evaluating the fatigue characteristics of large, thin skinned welded tanks of the type employec in the Atlas missile,

it has been found possible to develop four inch wide axially loaded welded joint specimens which reasonably well reproduce the fatigue behavior of the large tanks both qualitatively and quantitatively. This specimen is shown in Figure 1, and incorporates the same weld joint as the vertical splice joint in the Atlas missile; namely, an inert gas tungsten arc butt weld, with the weld roll planished flat and the joint reinforced with a 4" wide doubler sheet of the same thickness as the base metal resistance spot welded with staggered rows of spots on each side of the butt weld.

The results of ambient temperature fatigue tests on both the axially loaded 4" wide specimen and full scale 10' diameter tanks are shown in Table 2 and demonstrate the usefulness of the fatigue test specimen in assessing and predicting the fatigue resistance of the large tanks. The cost of fabricating and fatigue testing the full scale tanks ran into tens of thousands of dollars, especially when test were performed at -320°F by filling the tanks with liquid nitrogen and cyclically pressurizing them with helium gas. In all cases, fracture of both the specimens and the tanks occurred in the same location, starting at the outer row of spot welds at the heat affected zones and progressing from spot weld to spot weld.

The fatigue resistance of both the specimens and the tanks increased significantly at -320°F as compared to ambient temperature tests since the strength of the base metal and the welded joints increased considerably at the sub-zero temperature while the fatigue stress level remained constant. The low temperature fatigue tests were therefore performed at stresses representing a lower percentage of yield and tensile strength, and the fatigue life increased by thousands of cycles. At the low testing temperatures, the results of specimen and tank fatigue tests were still as comparable as they were at room temperature.

It should be pointed out that photostress techniques were employed during the development of the 4" wide axially loaded weld joint specimen to insure that the stress distribution across of width of the specimen uniform and comparable to that across the similar weld joint in the full-scale tank. Again, it cannot be overemphasized that the model test must duplicate the full scale stress distribution and test conditions to yield comparable results.

The above fatigue test specimen has been successfully employed to evaluate the behavior of a large number of candidate high strength steel and titanium sheet alloys at temperatures down to -423°F (liquid hydrogen). The outdoor fatigue test facility and chambers for testing specimens at liquid nitrogen and liquid hydrogen temperatures are shown in Figures 2 and 3. The specimens are pin loaded and are stressed by means of load cells at a rate of 6 stress cycles per minute in tension, from 0 or any predetermined tensile stress to a higher tensile stress.

While this test is not strictly classifiable as a model test, it does indicate how an element of a full scale test can be broken down to a relatively inexpensive small size test specimen and used to screen materials and investigate weld joint designs and welding procedures in a

much more simple and much less costly manner than is possible in full scale testing.

There are many features of full scale pressure vessels which cannot be reproduced in model structures. If a full scale 6 to 10 foot diameter vessel has a wall thickness of 0.025" to 0.050", it would be necessary to employ practically foil gauges in scale model vessels. Such thin gauge materials may prove impossible to procure in some alloys or may be excessively difficult to handle, weld, or otherwise process into the finished product.

In addition, resorting to very thin gauges in model structures will change the stiffness characteristics, particularly at joints and discontinuities, and therefore produce stress fields different from those encountered in full scale vessels.

In scale model fabrication, it is feasible to hold dimensions to very close tolerances. A 12" diameter bulkhead or cylinder can be made to $\pm$ 0.001", but this would be well-nigh impossible in a 10 foot diameter vessel. Dimensional variations in large structures may lead to eccentricities in stress distribution and premature failure in large structures as compared to small models. Explosive forming of small bulkheads poses no serious problems; the application of this same technique to 6 to 10 foot diameter components may involve lengthy and costly development programs.

The papers which follow will present the pros and cons of model testing as experienced by a number of companies and research facilities which have had extensive experience in both scale model and full scale pressure vessel testing.

TABLE I

COMPARISON OF FRACTURE CHARACTERISTICS OF SCALE MODEL AND FULL SCALE THIN-SKINNED TANKS

Caliber .22 bullets fired at internally pressurized tanks

Internal Pressure, psi	Wall Stress, Percent of Ultimate Tensile Strength	Result
24 in. diameter tanks, 3 feet long		
50	18.2	simple puncture
55	19.3	" "
60	21.3	tank fragmented
75	23.2	" "
12 foot diameter tank, 75 feet long		
10.9	19.7	simple puncture
12.9	23.4	tank fragmented

TABLE 2

CORRELATION OF FATIGUE TESTS ON LARGE TANKS* WITH FATIGUE TESTS ON AXIALLY LOADED WELDED TEST SPECIMENS**

ITEM	CYCLIC FATIGUE STRESS RANGE-PSI	NO. OF CYCLES TO INITIAL LEAK	NO. OF CYCLES TO FAILURE
4 in. wide specimen	0-144,000	430	1208
10 ft. diam. tank	0-144,000	637	1762
4 in. wide specimen	66,000-144,000	1170	2375
10 ft. diam. tank	66,000-144,000	1910	2355

---

* Tank fabricated from three segments of cold-rolled Type 301 stainless steel sheet approximately 3' wide. Each segment formed into hoop, with ends heliarc butt welded, roll planished, and reinforced with doubler sheet of same thickness spot-welded on both sides of the butt weld. Adjacent segments are overlapped approximately 1" and roll seam welded and reinforced with spot-welds on each side of roll seam weld.

** 4" wide specimen has same weld joint as vertical splice weld of tank-butt weld with spot-welded doubler.

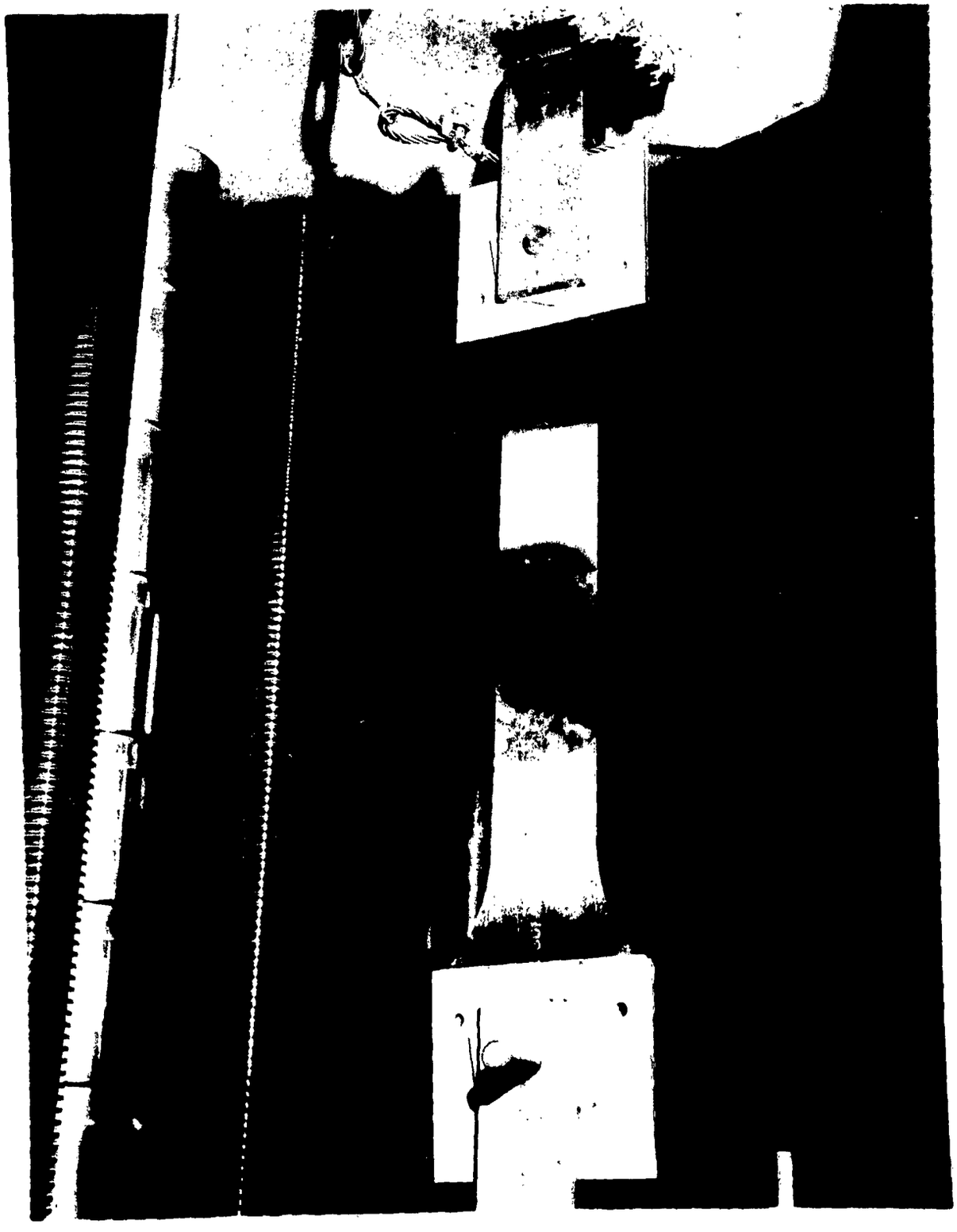


Fig. 1 4" Wide Welded Joint Specimen Employed in Tensile And Fatigue Tests to Evaluate Full Scale Tank Performance

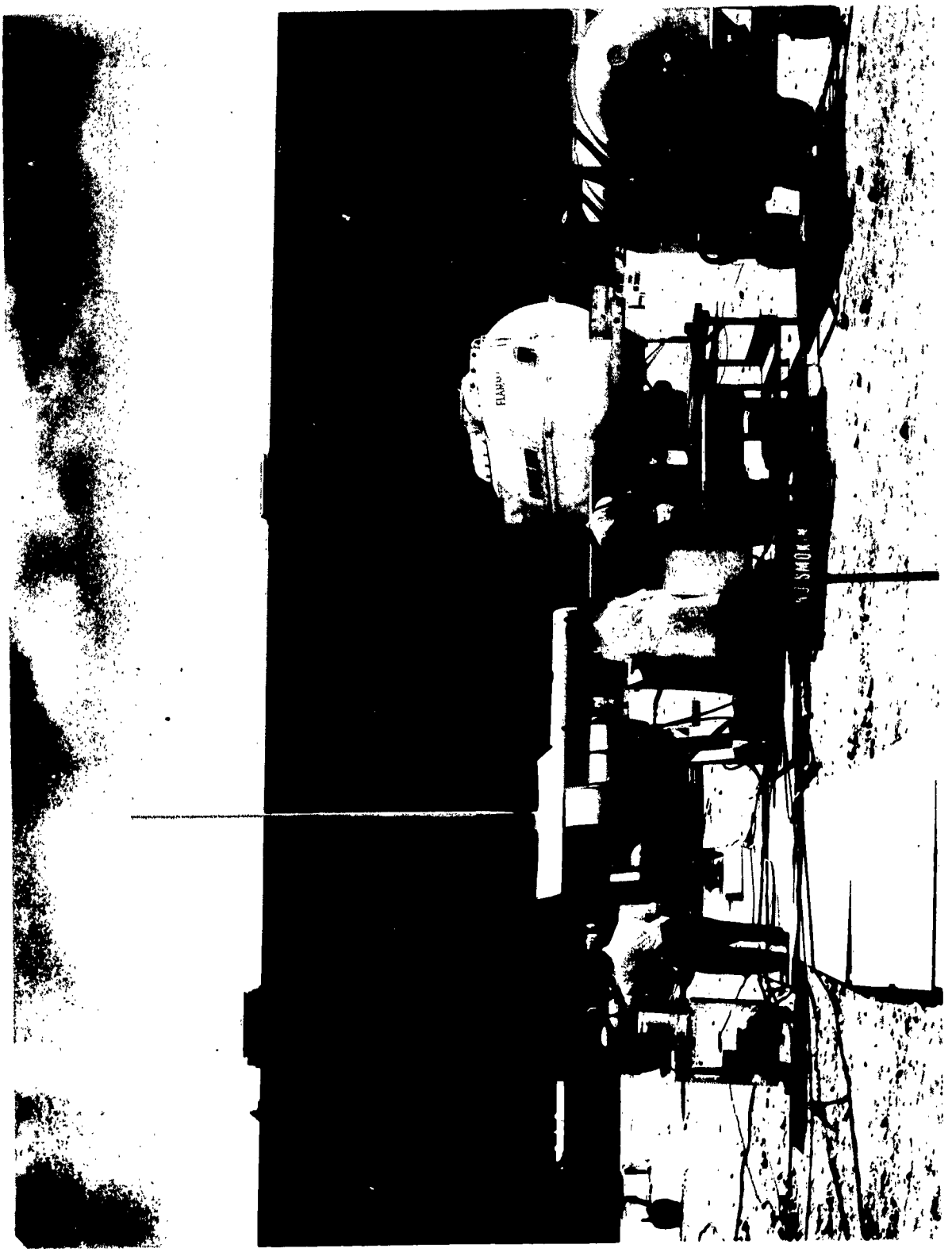


Fig. 2 Outdoor Test Facility For Fatigue Testing of Specimens at Cryogenic Temperatures



Fig. 3 Cryogenic Chambers And Load Cells For Fatigue Testing of Welded Joint Specimens

HYDRODYNAMIC TESTING OF THIN-WALLED CYLINDERS

K. H. ABBOTT

Watertown Arsenal Laboratories

Introduction

Watertown Arsenal has a long history of research, development, and manufacture of heavy gun barrels. As a part of the research and development effort, a high pressure hydraulic facility was installed in the Laboratory during World War II for research on autofrettage of gun barrels. The facility includes high-pressure pumps, intensifiers, accumulators, and piping capable of generating and transporting hydraulic pressures of up to 200,000 psi. Approximately two years ago, Laboratory personnel developed a pneumatic operated high-speed valve which can transfer hydraulic pressure from one line to another very rapidly. Since many Ordnance components are subjected to rapid rates of loading in service, and since weight minimization programs in Ordnance have led to fabrication of very thin-walled components, attempts have recently been made to utilize the high-pressure equipment for dynamic loading of test specimens and components. This brief report covers some of the initial tests performed to demonstrate the feasibility and characteristics of the apparatus.

Preliminary Test Results

A schematic sketch of a general equipment arrangement used to test thin-walled cylindrical components is contained in Figure 1. Here the hydraulic fluid is pumped from the reservoir to the intensifier with a bleed line through a pneumatic valve back to the reservoir. The fluid then passes through another pneumatic valve and through the high-speed transfer valve to the accumulator. When the specimen is to be tested, the second pneumatic valve is closed, and the fluid is switched from the accumulator to the specimen by actuation of the high-speed transfer valve. Baldwin pressure cells as well as manganin wire pressure cells are usually positioned as shown, although gage No. 2 can be positioned inside the specimen if desired. The specimen end closures are constrained in a press and connected inside the specimen with a heavy rod so that the specimen is constrained at the ends only by the packing.

Figure 2 is a crude sketch of the high-speed transfer valve. The valve stem is moved quickly to the right by a pneumatic cylinder allowing the fluid to flow from the high-pressure Line C to the low-pressure Line D. The complex detail of the valve has been omitted to reveal the simple principle of operation.

Figure 3 contains some selected initial slopes of strain-time curves obtained with an arrangement such as that of Figure 1. All data shown were obtained with wire resistance strain gages recorded on an eight channel Strainalyser. Although the initial parts of the curves

are all smooth, in many cases reflected pressure waves caused undulations in later stages of the curve. The specimens used to obtain the data were either hollow cylinders or simple-compression specimens. The curves are intended only to show the variation in initial strain rates which can be obtained by suitable manipulation of hydraulic pressure in the accumulator, the pneumatic pressure used to actuate the high-speed transfer valve, and the sizes of piping and discharge orifices. The hydraulic line pressures for these tests varied from about 5,000 psi to about 75,000 psi, with the higher pressures being applied to the compression specimens. Initial strain rates varied from approximately 2.5×10^{-4} per second to about 5.5 per second, or a factor of about 10,000. Lower strain rates can be readily obtained, and it is believed that strain rates up to about 10-100 times greater than the maximum shown can be achieved. In general, when a specimen is to be tested to destruction dynamically at a high-rate of strain, the pressure-transfer parameters can be adjusted so that the specimen fails before the pressure wave undulations appear on the strain-time or load-time diagrams; and the stress-strain-time curves can be computed when the specimen geometry is simple.

The specimen shown in Figure 4 is a section of an Ordnance component which is dynamically loaded in service with a pressure-rise time in the low millisecond range. The specimen ends have been altered for accommodation of hydraulic packing. A three-inch diameter filler bar was inserted centrally in the specimen to reduce the fluid volume. Because of the complex specimen shape, no attempts were made to compute stress-strain data. The static load-strain curve for two transverse gage locations are contained in Figure 5. Notice that the proportional limit occurs at a load of about 4000 psi corresponding to about 3500 microinches per inch strain, and that the specimen failed at a load of 9400 psi (other specimens of this type failed at 7500-10,000 psi). The component, manufactured from a vanadium-silicon modified 4330 steel, was designed by Frankford Arsenal to operate at a service pressure of 5400 psi. Several specimens were loaded statically to 5400 psi and exhibited no measurable permanent set after release of the load.

A specimen was then subjected to a dynamic fatigue test with a 5400 psi load transfer, and the specimen unloaded as soon as the pressure in the specimen reached 5400 psi. A reproduction at half of the strain-time trace for one of these cycles is contained in Figure 6. The relaxation part of the curve takes approximately as long as the first half so that a complete cycle occurs in about 30-35 milliseconds. Both load-time and strain-time data for the dynamic cycles were recorded on Visicorders so that records are on permanent file. For these tests a time lag occurred between cycles since instrumentation to permit automatic cycling was not available. A total of 400 dynamic cycles were made during the initial tests of this specimen with no measurable permanent set in evidence. A number of strain-time records were selected randomly, and the maximum strain for the gages selected is plotted against the number of cycles in Figure 7. It is obvious by inspection that the maximum strain was reproduced very well from cycle to cycle. Variations in maximum load (hydraulic pressure) between any two cycles were less than

100 psi or less than 2%. Such variation is acceptable for most contemplated tests, but a new electronic control panel arrangement to be installed next month will permit a decrease in the amount of variation.

A final specimen of the group was subjected to dynamic cycling in identical fashion to the previous one except that the maximum load was 7800 psi per cycle. The load-time and strain-time traces occurred with the same order of variation as existed with the previous specimen. However, since the permanent set was of prime interest for these "over-pressure" cycles, the data is presented in Figure 8 with the outside diameter plotted against the number of cycles run. After fifteen cycles, diameter measurements were made on every fifth cycle. Notice that yielding occurring during the first 10-20 cycles results in sufficient strain hardening so that no additional yielding occurs. On cycle number 33, an equipment malfunction resulted in static loading of the specimen. The static load resulted in a relatively large amount of yielding and a further increase in permanent set. However, no increase in permanent set occurred during the following 39 dynamic cycles. A second static test resulted in a small increase in permanent set, four dynamic cycles gave no increase, and a third static cycle resulted in another small increase in permanent set.

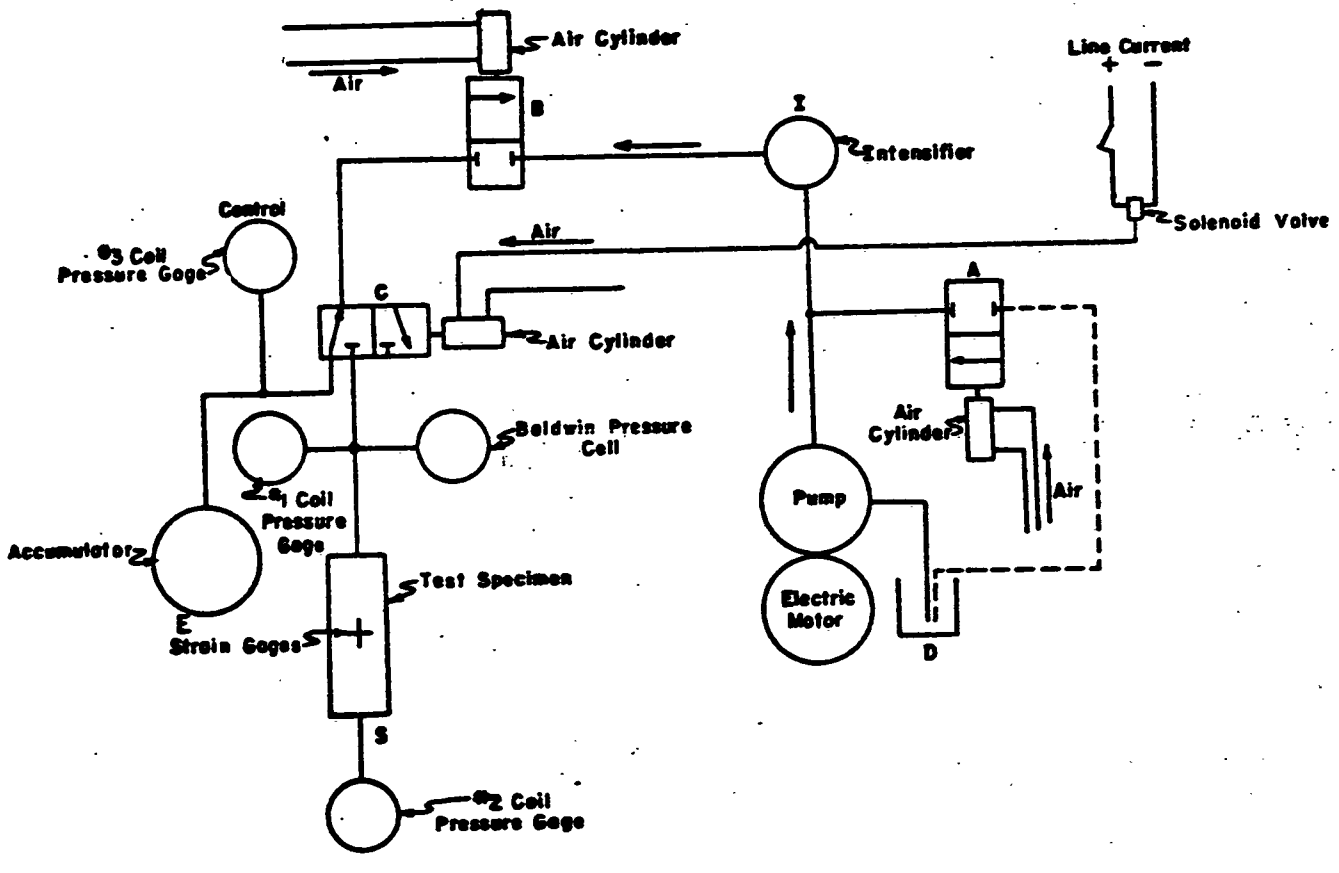
This vanadium-silicon modified 4330 steel in a cylindrical specimen of about .090" wall thickness had been heat treated to an initial yield strength of 200,000 psi. All specimens loaded hydrostatically to failure exhibited very ductile fractures with large amounts of deformation. All failures were longitudinal. What is perhaps most significant is the additional strengthening apparent from the data in Figure 8. The actual increase in yield strength during testing cannot be reported since the specimen has not yet been cut into tensile specimens. Instead it will be subjected to from 2000-20,000 additional dynamic-load cycles when the new control panel is installed. Suffice to say that this particular steel will find many uses in Ordnance equipment.

A number of thin-walled cylinders of a titanium alloy (6Al-6V-2.5Sn) at 180,000 yield strength have also been subjected to dynamic-load tests. Although the test results cannot be released, it is pointed out that the dynamic tests of these cylinders were conducted under nearly the same conditions as the 4330 steel cylinders or about .5 inches per inch per second. The test results were satisfactory in relation to the component design requirements.

Lastly, with the aid of a suitable fixture, standard .252" uniaxial tensile specimens of the 6Al-6V-2.5Sn titanium alloy and of 4340 steel have been tested dynamically at various strain rates from static to about 50 inches/inch/second. Difficulty was encountered in breaking dynamically the steel specimens which had a static ultimate strength of 250,000 psi. However, the titanium alloy exhibited a static ultimate strength of 200,000 psi with 7% elongation and 15% R. A. As the strain rate was increased to about .01 per second the ultimate strength increased to 230,000 psi with 12% elongation and 35% R. A. As the strain rate was increased to 50 per second, the ultimate strength remained constant. However, the elongation decreased uniformly to about 9-10%

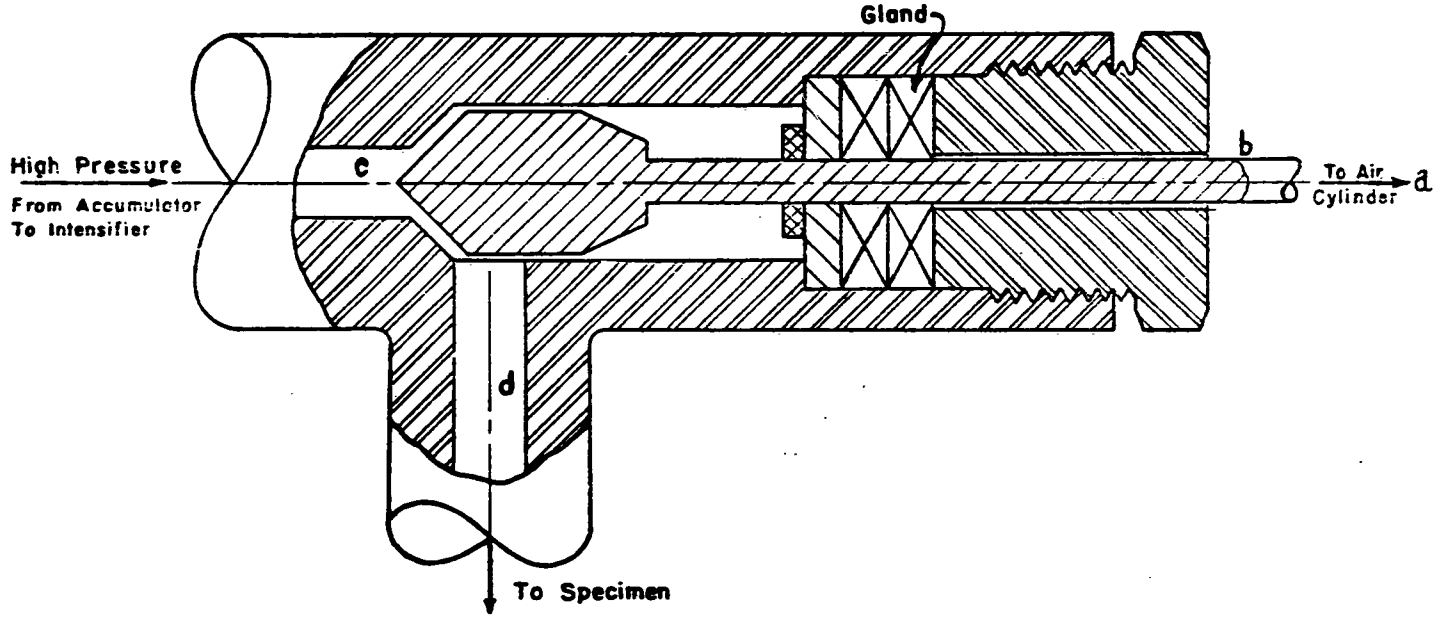
and the reduction of area to about 25%. No conclusions can be made from these very limited tests, but the feasibility of testing is established, and additional specimens will be tested in the near future.

Due to the difficulty encountered in developing the proper synchronization of all parts of the testing and recording equipment, the above limited tests are all that have been accomplished to date. It is believed, however, that the feasibility of dynamic testing, in both uniaxial and biaxial testing with the Watertown Arsenal Laboratories high-pressure hydraulic equipment, has been quite firmly established. After the new electronic control and recording system is installed in September 1960, it is expected that efficient techniques will be available for conducting a large amount of dynamic testing of specimens and Ordnance components.



GENERAL ARRANGEMENT OF HIGH PRESSURE EQUIPMENT

FIGURE 1



FAST ACTING LOADING VALVE IN HIGH PRESSURE SYSTEM

FIGURE 2

STRAIN-TIME CURVES GENERATED FROM HYDRODYNAMIC LOADING OF THIN-WALLED CYLINDERS & TENSILE SPECIMENS.

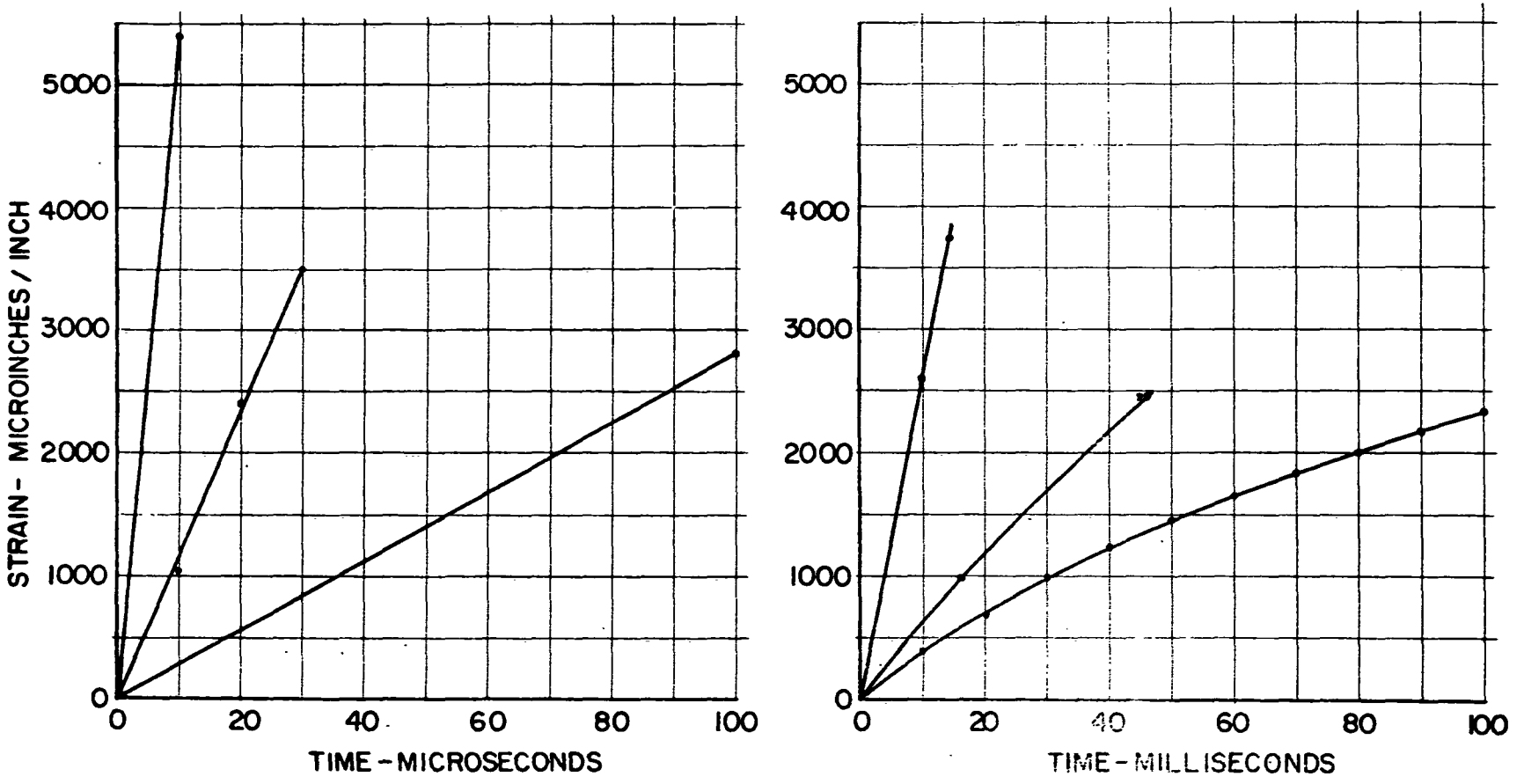
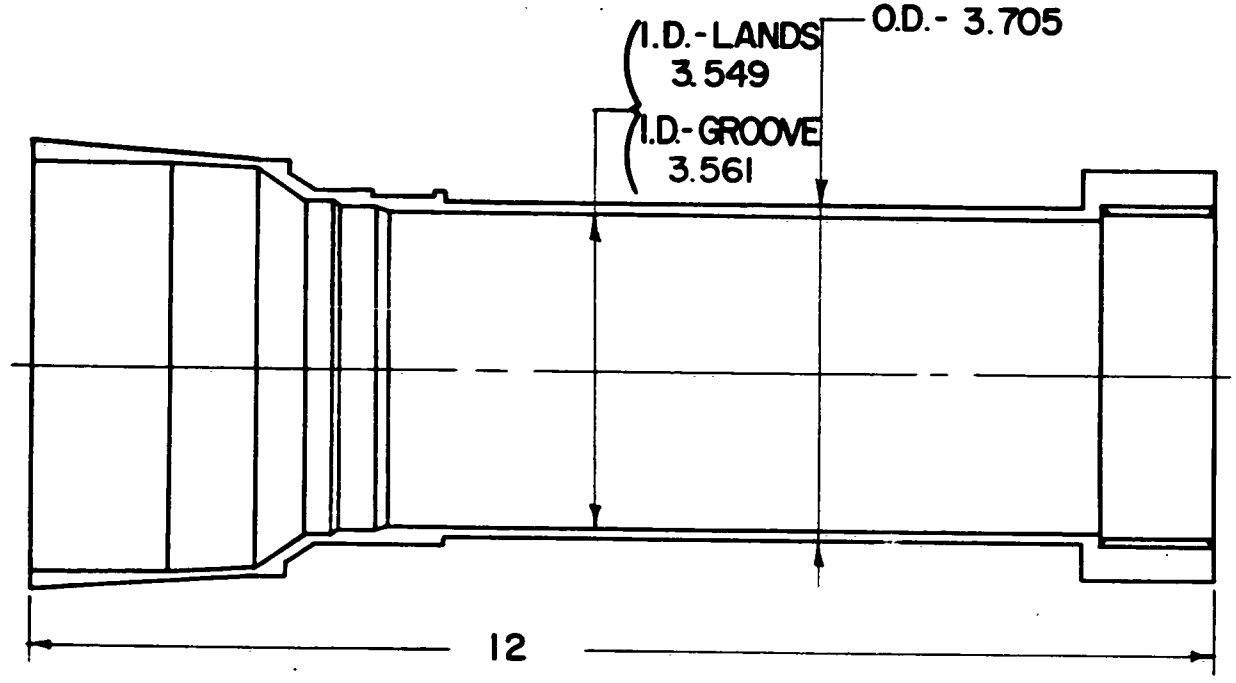


FIGURE 3



SPECIMEN FOR HYDRAULIC TESTING OF RECOILLESS RIFLE SECTION

FIGURE 4

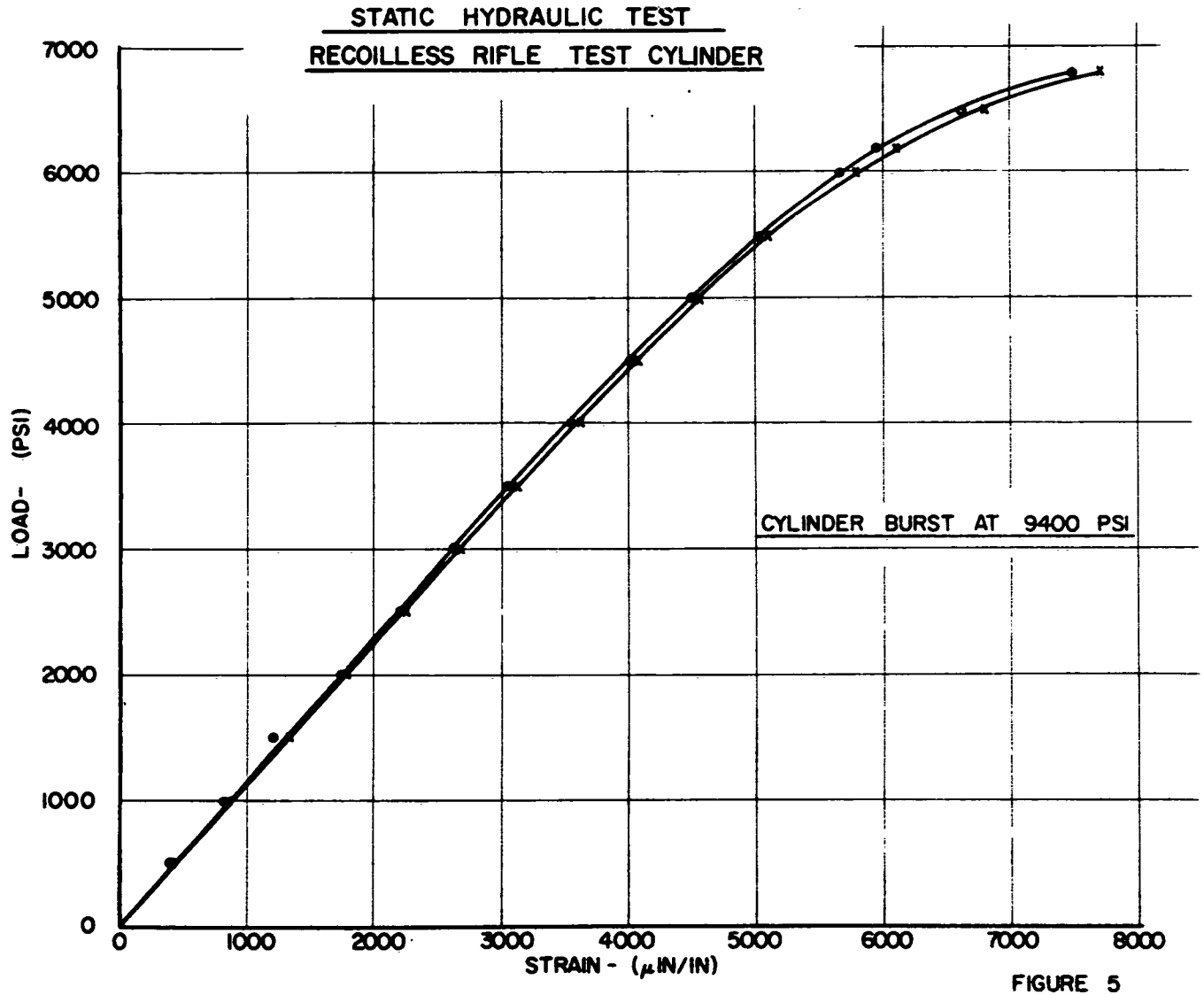

STATIC HYDRAULIC TEST
RECOILLESS RIFLE TEST CYLINDER
LOAD- (PSI)
7000
6000
5000
4000
3000
2000
1000
0
0
1000
2000
3000
4000
5000
6000
7000
8000
STRAIN - (μIN/IN)
CYLINDER BURST AT 9400 PSI

FIGURE 5

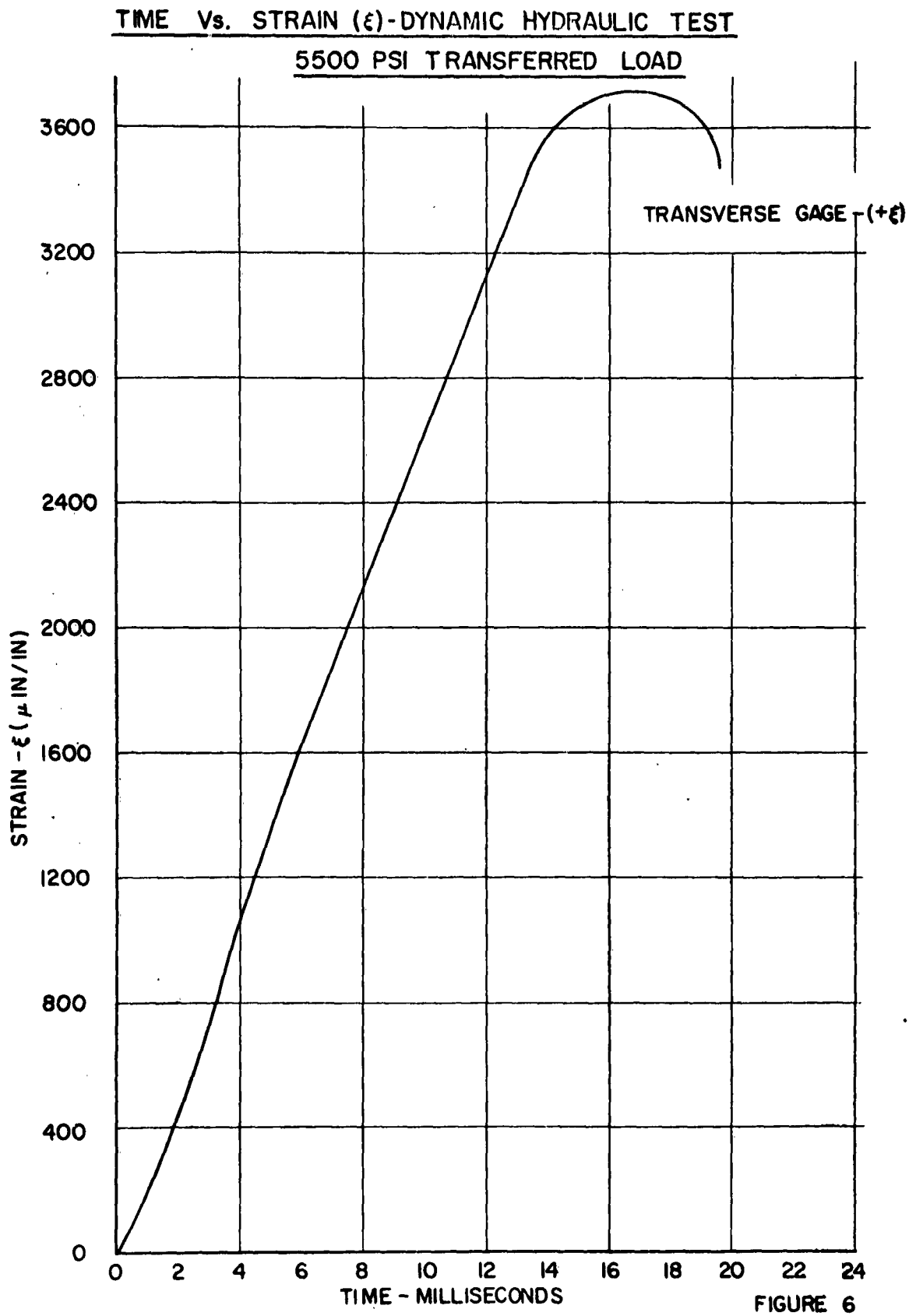

TIME Vs. STRAIN (ε)-DYNAMIC HYDRAULIC TEST
5500 PSI TRANSFERRED LOAD
TRANSVERSE GAGE -(+ε)
STRAIN -ε (μ IN/IN)
3600
3200
2800
2400
2000
1600
1200
800
400
0
0 2 4 6 8 10 12 14 16 18 20 22 24
TIME - MILLISECONDS

FIGURE 6

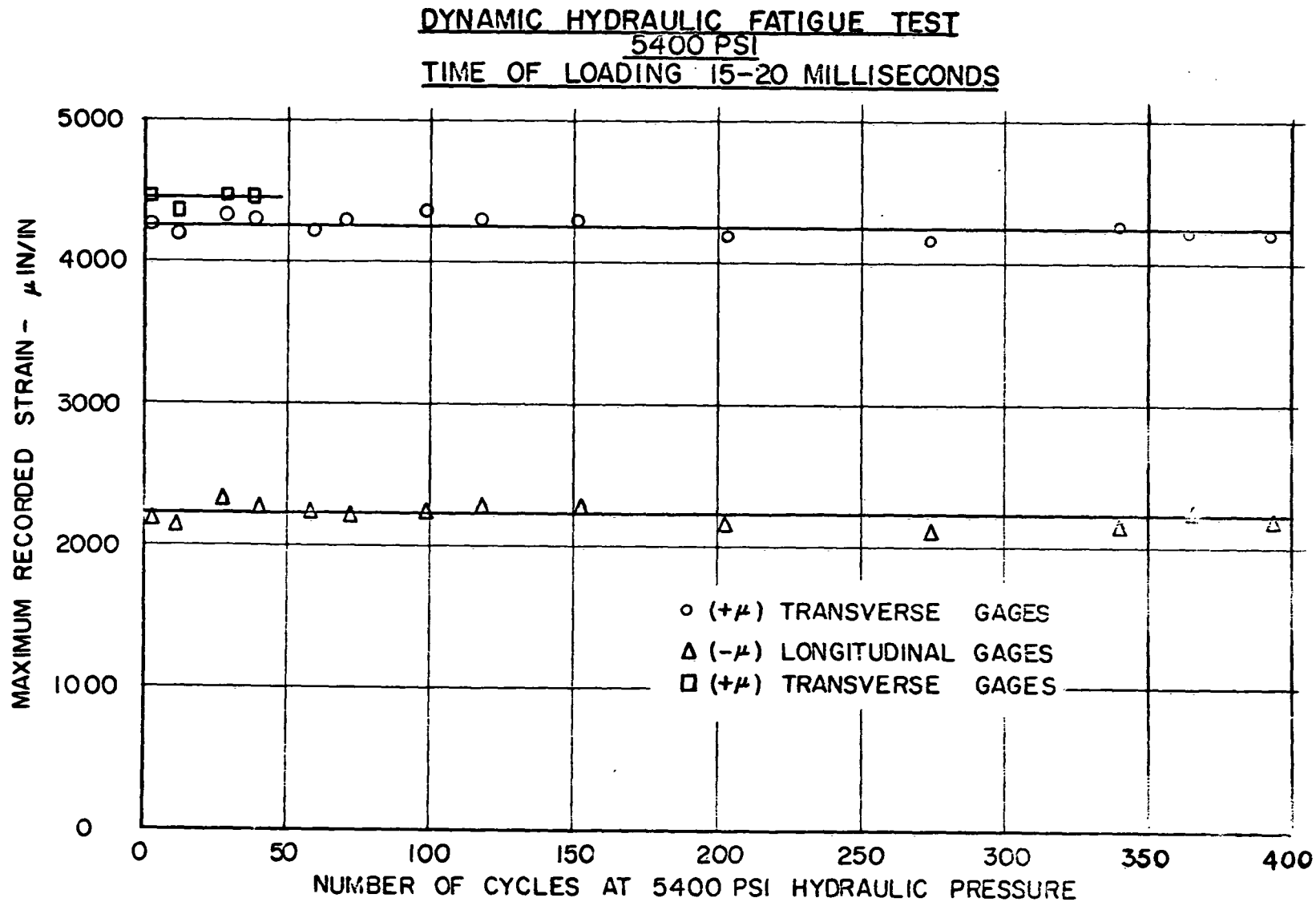

DYNAMIC HYDRAULIC FATIGUE TEST
5400 PSI
TIME OF LOADING 15-20 MILLISECONDS
MAXIMUM RECORDED STRAIN - μ IN/IN
5000
4000
3000
2000
1000
0
0
50
100
150
200
250
300
350
400
NUMBER OF CYCLES AT 5400 PSI HYDRAULIC PRESSURE
o (+μ) TRANSVERSE GAGES
Δ (-μ) LONGITUDINAL GAGES
□ (+μ) TRANSVERSE GAGES

FIGURE 7

DYNAMIC HYDRAULIC FATIGUE TEST (7800 PSI)

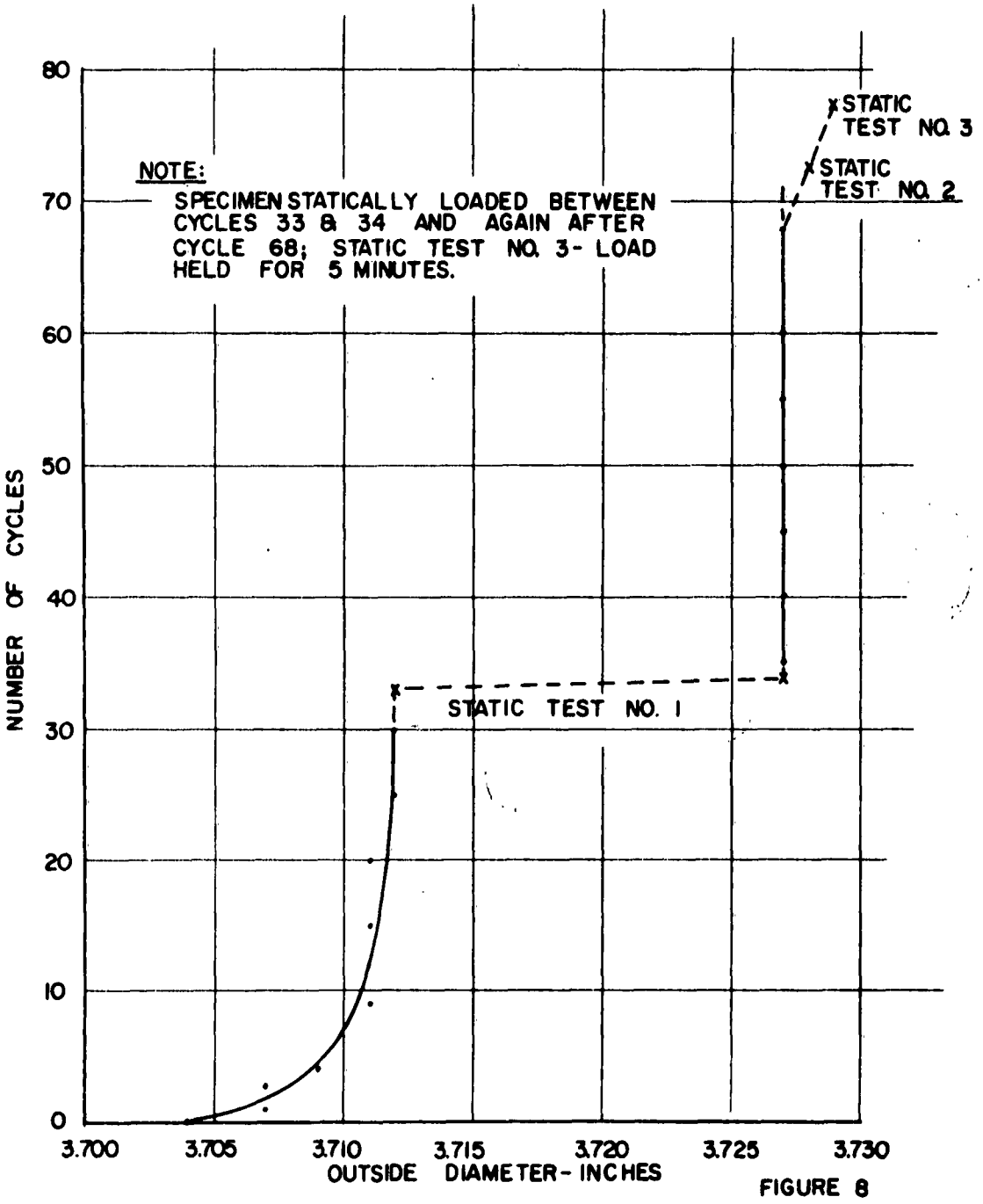


FIGURE 8

EVALUATION OF BIAXIAL PROPERTIES OF ROCKET MOTOR CASE MATERIAL USING SUB-SCALE SPECIMENS

By

G. K. BHAT
D. V. LINDH

Mellon Institute, Pittsburg, Pa.

ABSTRACT

This paper describes a method, using deep drawn cups and welded and unwelded cylindrical vessels, for evaluating the biaxial properties of rocket motor case materials. Data are presented showing the relationship between uniaxial and biaxial properties which can be successfully utilized in the selection of the most suitable material for a particular missile system.

The paper discusses and suggests how various material properties and design limits presently determined by separate tests for each property can be evaluated by simple biaxial tests. A few of these are:

(1) Selection of the highest possible biaxial strength level without loss of biaxial ductility.

(2) Establishment of a maximum allowable decarburization limit in order to decrease susceptibility towards notch embrittlement due to surface imperfections.

(3) Evaluation of embrittling ranges found at some tempering temperatures.

(4) Susceptibility of a material toward notch sensitivity.

(5) Detection of internal defects and undesirable conditions such as banding, unusual segregation, level of inclusion content, and heterogeneity caused by non-uniform rolling and other processing conditions.

INTRODUCTION

The premature failure, in a brittle manner, of high-performance motor cases has become a matter of primary concern within the past few years. The cause of these failures has been attributed to the sensitivity of materials heat treated to high strength levels (above 190 ksi) to defects within the material, to defects caused in handling and fabrication, and to high local tensile stresses.

Many screening techniques have been used for the purpose of qualifying materials for missile motor case application with various degrees of success. It has, however, been considered desirable that any such evaluation technique be capable of yielding the following information which is of importance to missile motor case designers and fabricators:

(1) Selection of the highest possible biaxial strength level without loss of biaxial ductility.

(2) Establishment of a maxinum allowable decarburization limit in order to decrease susceptibility toward notch embrittlement due to surface imperfections.

(3) Evaluation of embrittling ranges found at some tempering temperatures.

(4) Determination of the susceptibility of a material toward notch sensitivity.

(5) Detection of internal defects and undesirable conditions, such as banding, unusual segregation, level of inclusion content, and heterogeneity caused by non-uniform rolling and other processing conditions.

This paper describes a material evaluation technique, first evolved at Mellon Institute, which attempts to accomplish all of the above requisites and furthermore to correlate the results with those of scale model and full-scale chambers, as well as others, such as the edge-notched tensile tests.

EQUIPMENT AND PROCEDURE

This technique uses a specimen or a "cup" of the configuration shown in Figure 1, which is produced by cold drawing sheet material. The drawn cups are heat treated and then tested in the fixture shown sectionally in Figure 2. Figure 3 shows the experimental set-up along with several fractured cups.

The experimental procedure consists of hydrostatically pressurizing a cup having a biaxial strain gage attached to its apex, and taking strain readings at various pressures until severe yielding is observed, and then pressurizing until rupture occurs. Following this, the cup is taken from the fixture and thickness readings are taken along the fractured edge for the purpose of assessing the ductility of the material under biaxial conditions.

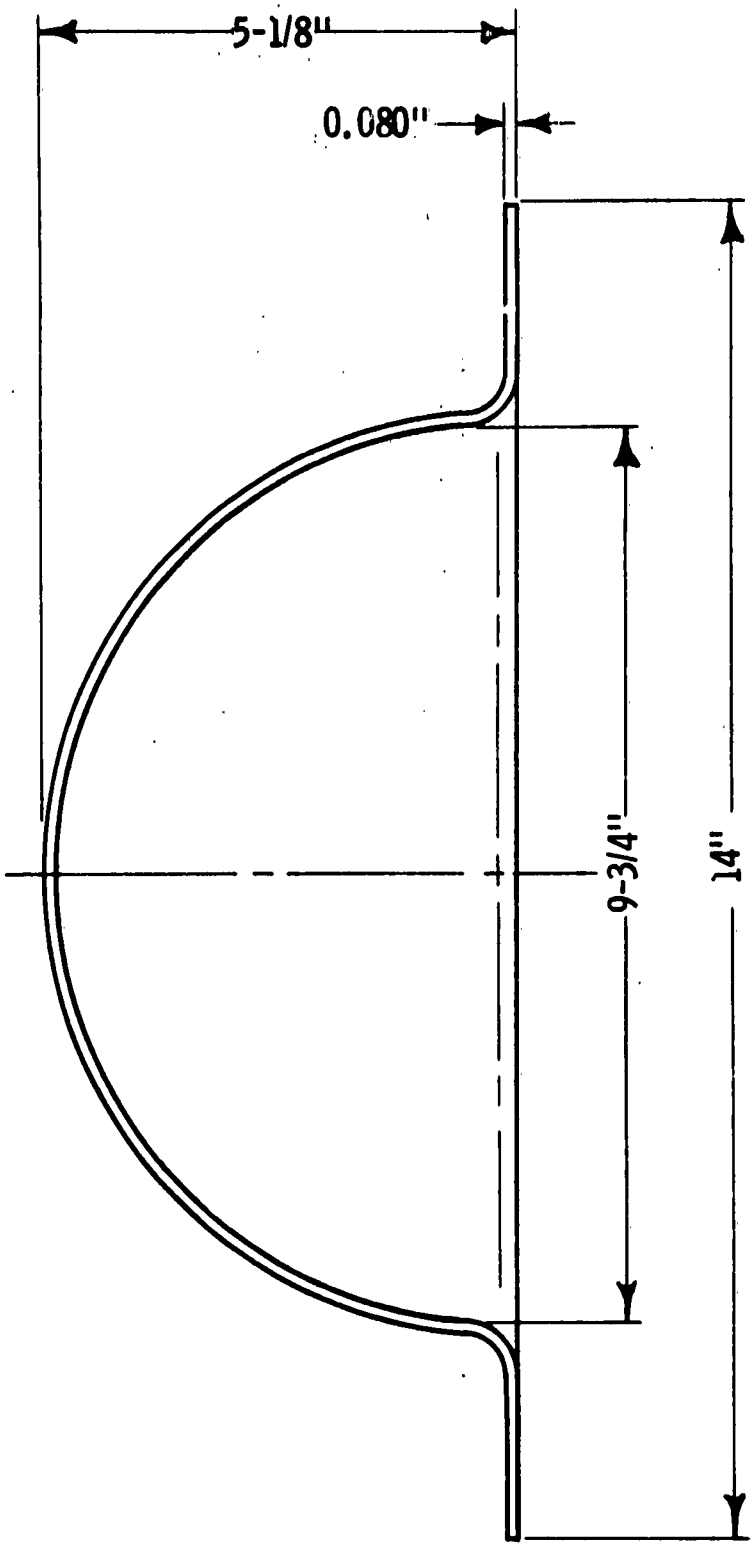


Figure 1 - Sectional Schematic View of a Hemispherical Cup Specimen

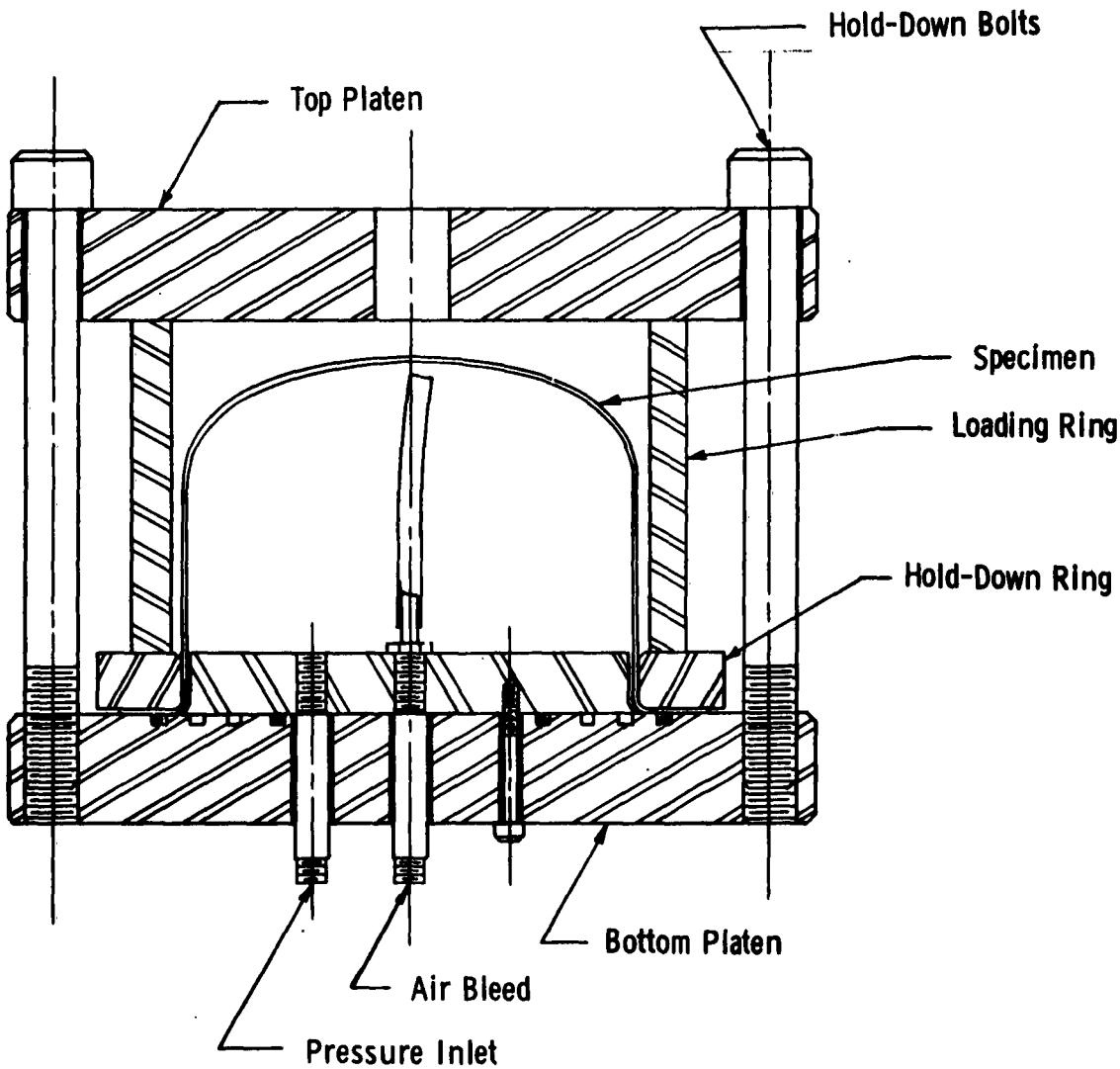


Figure 2 - Sectional Schematic View of Cup Test Fixture



Figure 3 - Disassembled Cup Test Fixture and Support Equipment

RESULTS

The principal stresses at various pressures, calculated from the strain readings obtained are tabulated for a sample material[1] in Table I and shown graphically in Figure 4. From this plot, the biaxial yield strength and biaxial rupture strength are determined. The yield strength is determined by the intersection of the stress-pressure curve and a line parallel to and offset 10,000 psi from the linear part of it. This offset, which is shown in Figure 4, corresponds to approximately .03% principal strain.[2] The biaxial rupture strength is determined by extrapolation of the pressure-stress plot on to the rupture pressure. This is also shown in Figure 4.

By plotting biaxial strength properties against the conditions of the independent variable, the effect of the independent variable on the properties can be observed. An example of this is shown in Figure 5, the data of which are tabulated in Table II. In this chart the independent variable is tempering temperature.

A measure of biaxial ductility is obtained by calculating the maximum reduction in head thickness, given by the following equation:

$$\% \text{ Reduction in Head Thickness} = \frac{t_o - t_f}{t_o} \times 100$$

t_o = original thickness at apex

t_f = final minimum thickness along fracture edge

---

[1]The steel used to obtain the data presented through this report is 4137 Co having the following chemical composition except when indicated otherwise: C 0.39%, Mn 0.70%, Si 1.00%, P 0.01%, S 0.01%, Cr 1.10%, Mo 0.25%, V 0.15%, Co 1.00%.

[2]Principal strain = Principal Stress/E

TABLE I

Values of Principal Head Stress[a,b] at

Various Pressures for a 4137 Co Cup Specimen[c,d]

Pressure psig	Principal Stress ksi
0	0
500	25
1000	49
2000	96
3000	147
3200	155
3500	168
3700	177
4000	193
4200	203
4500	221
4700	231
5000	250
5200	263
5500	287

(a) Principal stress at the apex of the specimen.

(b) Principal stress values are increasingly too large beyond the elastic range of the material.

(c) Austenitized at 1700 F for 30 min., quenched in oil and double tempered at 550 F.

(d) Initial sheet thickness 0.080". Minimum cup head thickness 0.064".

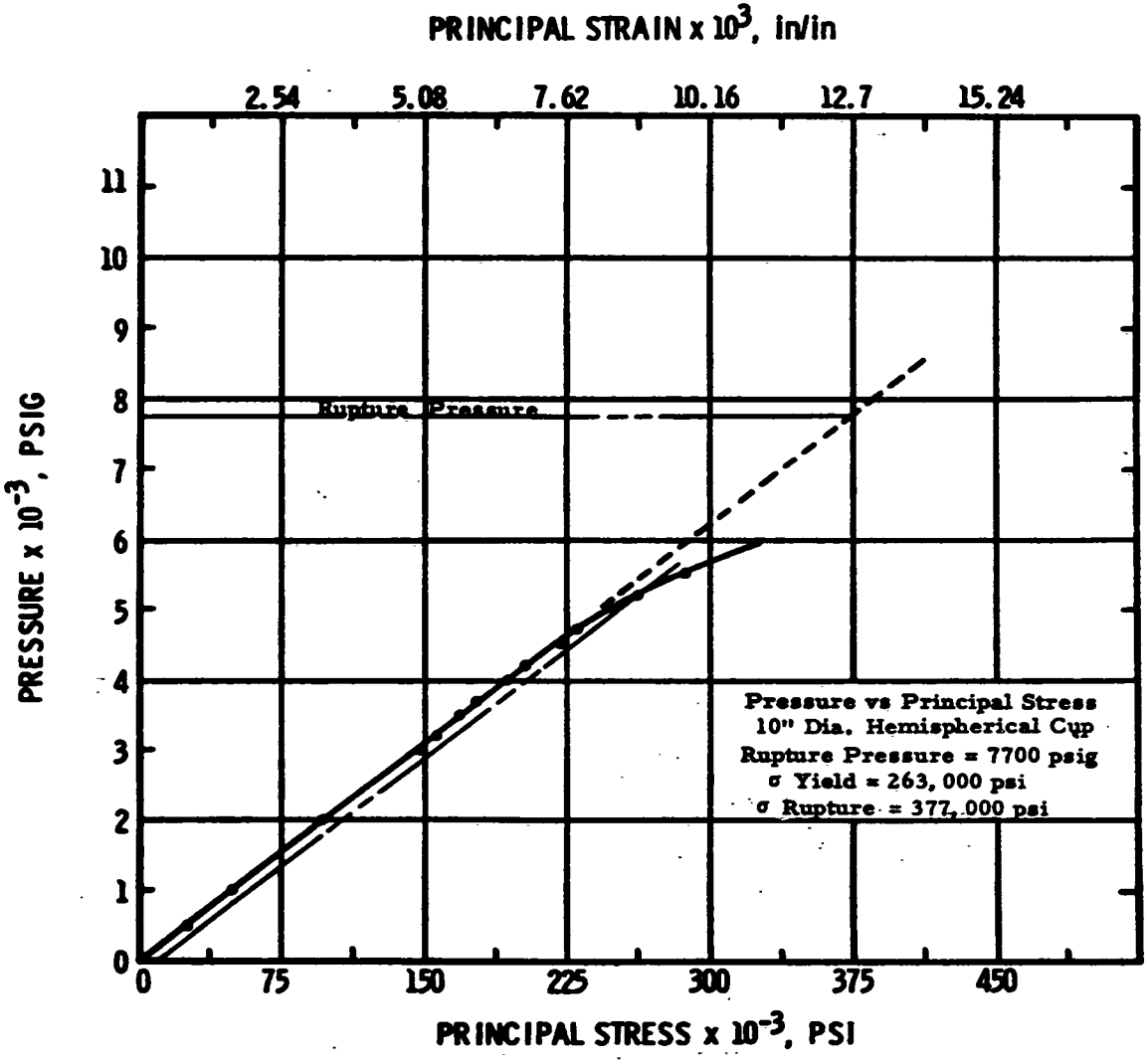


Figure 4 - Principal Head Stress vs. Pressure Graph of a Sample Cup Showing Method Used to Determine Biaxial Yield and Rupture Strength.

TABLE II

Room Temperature Biaxial Mechanical Strength Properties of 4137 Co

Tempering[a] Temperature F	Biaxial[b] 0.03% offset Yield Strength ksi	Biaxial[b] Extrapolated Rupture Strength ksi
400	249	389
450	264	377
500	270	380
550	268	376
600	255	320
650	262	266
750	229	306
800	221	-
900	221	293
1000	213	264

(a) Austenitized at 1700 F for 30 min., quenched in oil and tempered as indicated.

(b) Biaxial Ratio = 1:1.

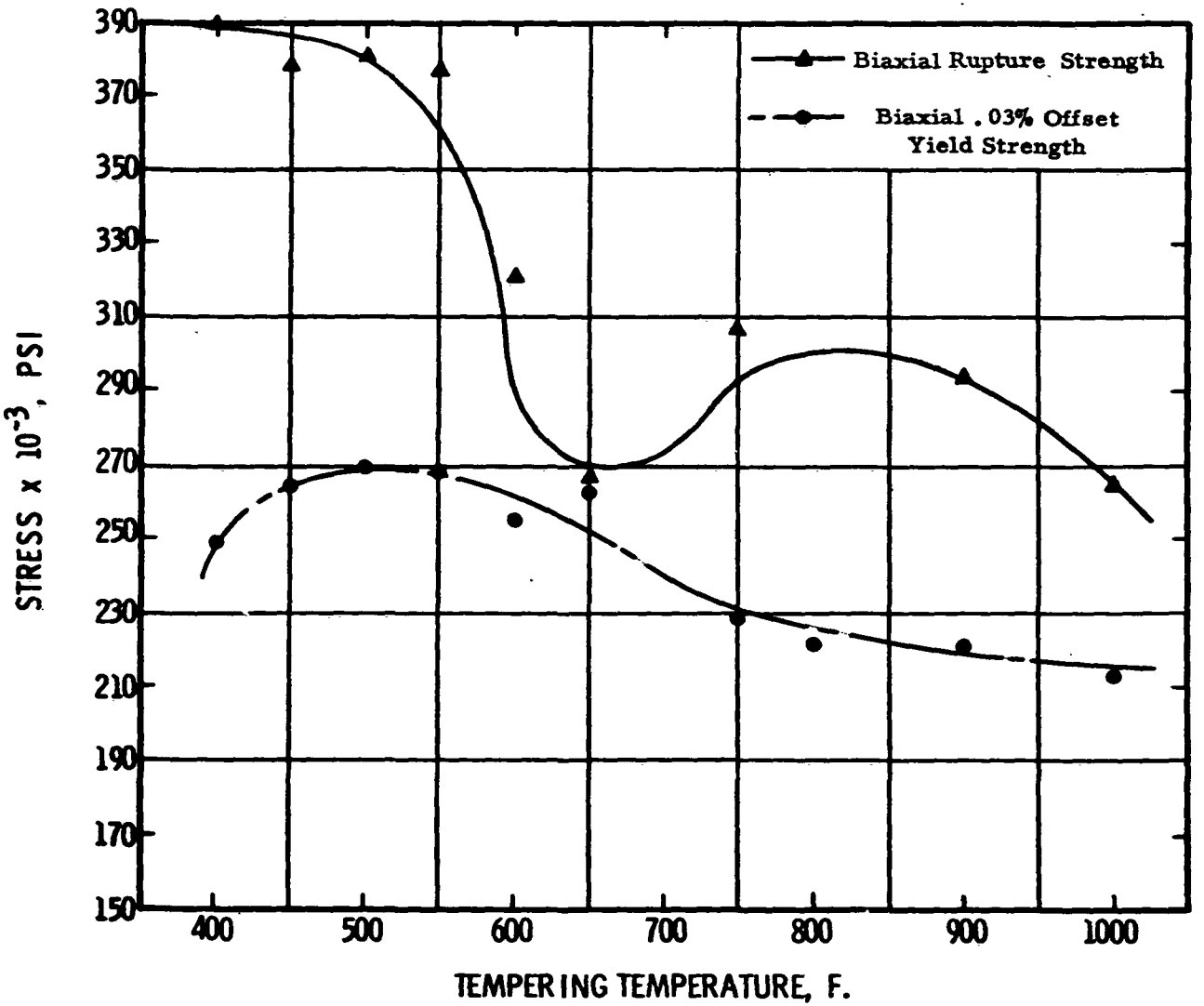


Figure 5 - Biaxial Mechanical Strength Properties Plotted Against Tempering Temperature.

An example of this with the results compared against the independent variable is given in Table III and Figure 6. The independent variable is again tempering temperature.

INTERPETATION OF RESULTS

It should now be possible to indicate how this technique can be used to evaluate, under biaxial conditions, many material properties affecting its strength, such as the influence of heat treatment, gas content, size and distribution of inclusions and other defects.

Selection of Highest Possible Biaxial Strength Without Sacrifice of Ductility

Selection of the highest possible biaxial strength without loss of ductility is best accomplished by comparing uniaxial and biaxial strength and uniaxial and biaxial ductility parameters over a range of tempering temperatures. This is done for a sample material in Table IV and Figures 7 and 8.

From Figure 7, it is evident that the maximum uniaxial and biaxial yield strengths occur at tempering temperature of approximately 550 F and at this point both uniaxial ultimate strength and biaxial rupture strength are near their maximum values. Furthermore, it can be seen that the biaxial rupture strength is much greater than the corresponding uniaxial value, a condition that must exist if brittle failure is to be avoided. Data in support of this are given in Table V.

TABLE III

Reduction in Head Thickness of 4137 Co

Tempering[a] Temperature F	Reduction in Head Thickness %
400	11.0
450	11.0
500	9.4
550	12.5
600	0
650	0
750	18.0
900	21.8
1000	21.8

(a) Austenitized at 1700 F for 30 min., quenched in oil and tempered as indicated.

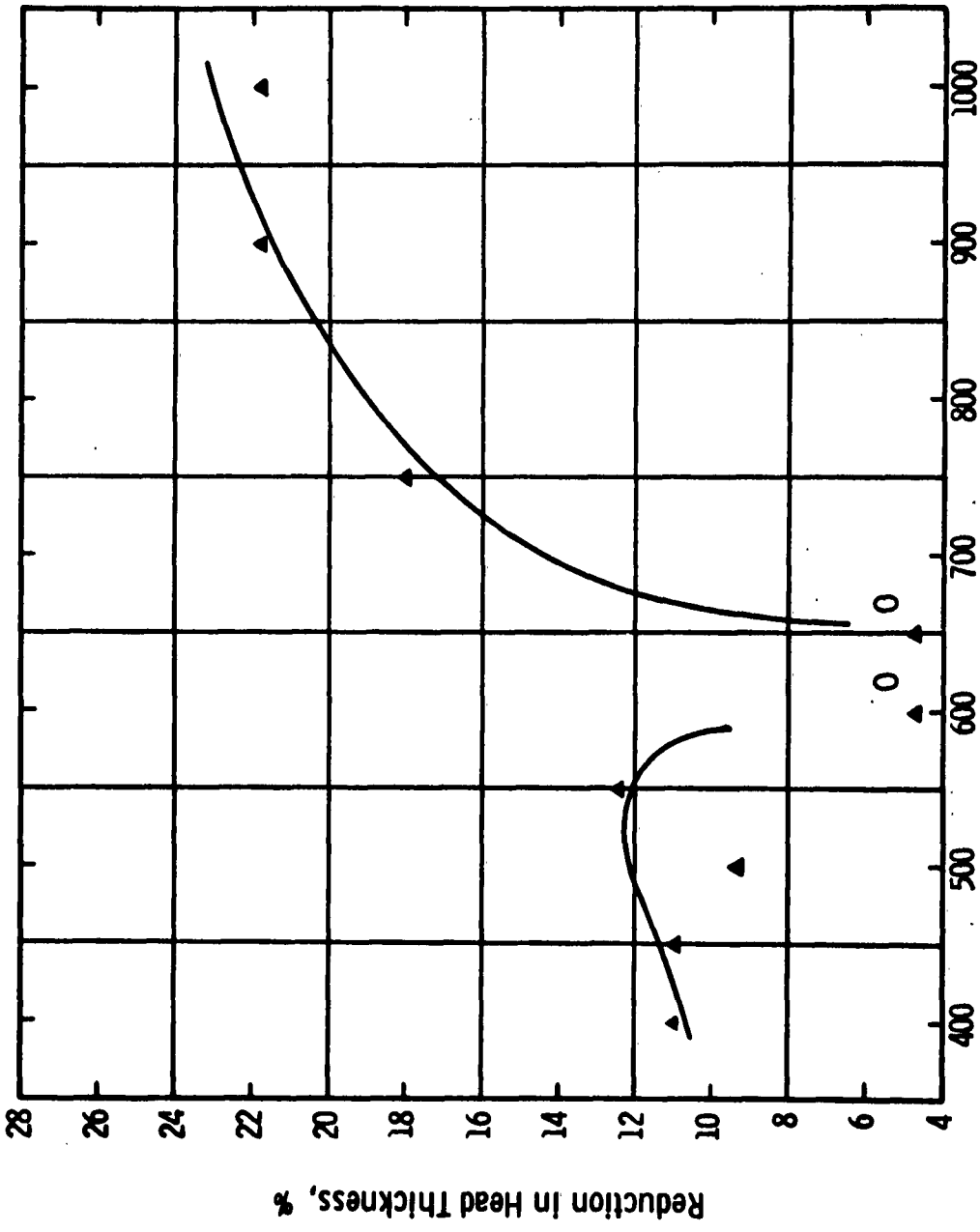


Figure 6 - Biaxial Ductility Parameter Plotted Against Tempering Temperature.

TABLE IV

Room Temperature Uniaxial and Biaxial Mechanical Properties of 4137 Co

Tempering[a] Temperature F	Uniaxial Properties			Biaxial Properties[b]		
	0.2% offset Yield Strength ksi	Ultimate Strength ksi	Reduction in Area %	0.03% offset Yield Strength ksi	Extrapolated Rupture Strength ksi	Reduction in Head Thickness %
400	242	302	20.5	249	389	11.0
450	237	293	19.2	264	377	11.0
500	237	287	21.5	270	380	9.4
550	244	292	24.5	268	376	12.5
600	234	282	22.0	255	320	0
650	229	274	22.2	262	266	0
750	206	241	28.0	229	306	18.0
800	203	236	17.7	221	-	-
900	195	218	-	221	293	21.8
1000	186	208	28.0	213	264	21.8

(a) Austenitized at 1700 F for 30 min., quenched in oil and tempered as indicated.

(b) Biaxial Ratio = 1:1.

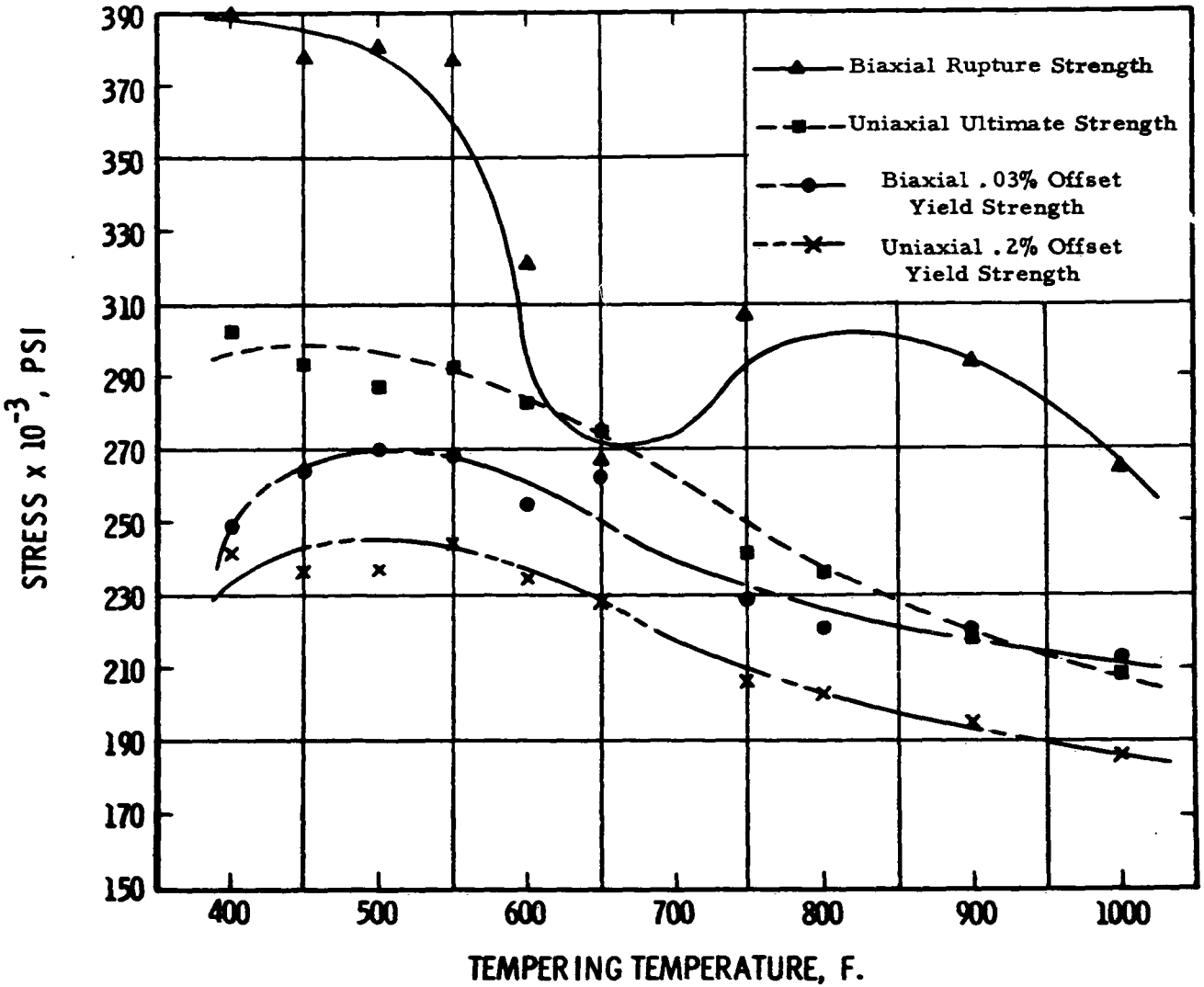


Figure 7 - Comparison of Uniaxial and Biaxial Mechanical Strength Properties.

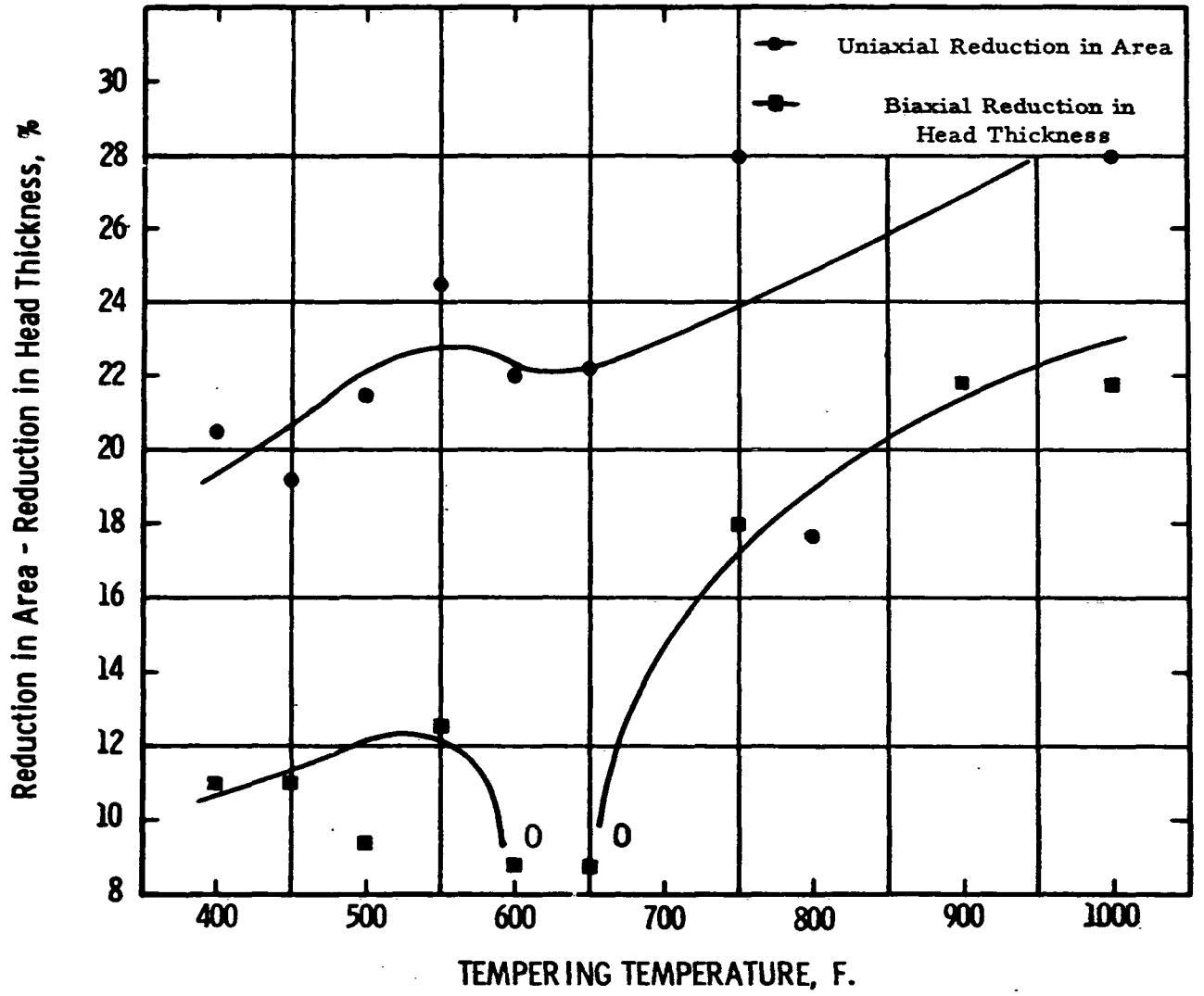


Figure 8 - Comparison of Uniaxial and Biaxial Ductility Parameters

TABLE V

Correlation of Cup Test Results With Vessel Results

Steel	Target Uniaxial 0.2% offset Yield Strength ksi	Uniaxial Properties		Biaxial Properties		
		.01% offset Yield Strength ksi	Ultimate Strength ksi	Threshold[a,b] Yield Strength (6" dia. Vessel) ksi	Ultimate[b] Strength (6" dia. Vessel) ksi	Extrapolated[c] Rupture Strength (12" dia. Cup) ksi
4137 Co	240	219	283	246	275	460
	230	200	279	240	270	415
	220	186	267	236	259	375
H-11	240	202	296	No yielding observed	200	260
	230	172	286	191	312	360
	220	159	263	188	308	350

(a) Threshold yield strength is equivalent to a 0.01% offset yield strength.

(b) Biaxial Ratio = 2:1.

(c) Biaxial Ratio = 1:1.

Figure 8 shows that the biaxial ductility parameter, reduction in head thickness, nearly parallels the uniaxial ductility parameter, reduction in area, indicating that the material does not tend to become brittle under a biaxial stress field and especially at a tempering temperature of 550 F.

Establishment of a Maximum Allowable Decarburization Limit

The criterion for selection of the maximum allowable surface decarburization in sheet material is permissible loss in strength. The multiaxial strength evaluation technique can be used to determine the average biaxial strength of a material at different tempering temperatures and with various depths of surface decarburization. An example of the effect of surface decarburization is given in Table VI and shown graphically in Figure 9.

The steel used to obtain the data of Figure 9 had an initial amount of decarburization on each surface. The values corresponding to a decarburization depth of 0.003 inches were obtained from specimens heat treated in salt while the remaining data were obtained from specimens heat treated in air. As it can be seen, an additional 0.003 inches in surface decarburization depth causes considerable loss in both uniaxial and biaxial strength while no appreciable gain in ductility is noted. An interesting point to note is the fact that this data indicates that decarburization depth should be minimized as it decreases strength considerably while having very little effect on ductility parameters. However, there is evidence to show that surface decarburization could help minimize failures which originate at surface flaws.

TABLE VI

Effect of Surface Decarburization Depth on the Room Temperature Uniaxial and Biaxial Mechanical Properties of 4137 Co[a]

Decarburization[b] Depth x 10^3 In.	Uniaxial Properties				Biaxial Properties[c]	
	0.2% offset Yield Strength ksi	Ultimate Strength ksi	Elongation in 2 in. %	Reduction in Area %	0.03% offset Yield Strength ksi	Extrapolated Rupture Strength ksi
3.0	244	294	5.0	24.5	268	376
5.8	215	257	6.5	23.0	220	364
6.0	194	232	6.0	27.6	220	360
6.2	211	254	6.5	26.0	225	358
6.3	224	259	5.5	26.0	222	352

(a) Austenitized at 1700 F for 30 min., quenched in oil and double tempered at 550 F.

(b) Measured by microhardness technique.

(c) Biaxial Ratio = 1:1.

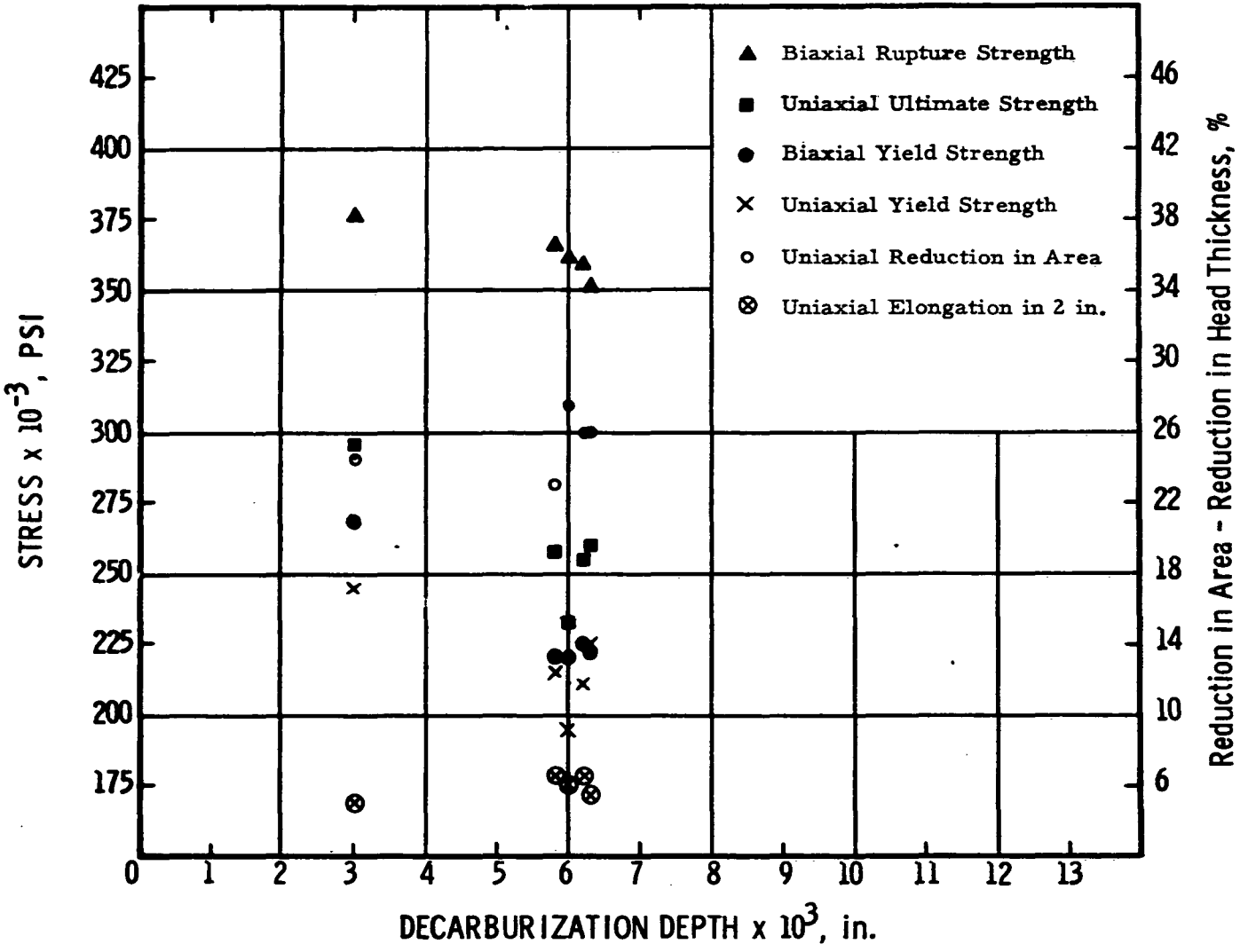


Figure 9 - Effect of Surface Decarburization Depth on Uniaxial and Biaxial Mechanical Properties.

Location of Embrittling Ranges

The effect of an embrittling temperature range on the results of the material evaluation technique being discussed is quite evident from Table VII and Figures 10 and 11.

Figure 10 compares uniaxial ultimate strength, uniaxial edge notch ultimate strength and biaxial rupture strength over a range of tempering temperatures. It can be readily seen from the notch strength and biaxial rupture strength curves that a tendency toward embrittlement exists around a tempering temperature of 650 F. The important point, however, is that this technique points out the embrittling range and points it out much more clearly than the results of edge notched tensile tests.

A comparison of uniaxial and biaxial ductility parameters, as shown in Figure 11, also exhibits clearly the existence of a temper embrittlement region. The advantages of using a multiaxial strength evaluation technique thus becomes obvious.

Determination of the Susceptibility of a Material Toward Notch Sensitivity

The susceptibility of a material toward notch sensitivity has been successfully predicted through interpetation of the cup test results. An example of this for a notch sensitive steel[1] is given in

---

[1]The steel used to obtain the data given in Table VIII is Rocoloy 250 of the following nominal chemical composition: C 0.41%, Mn 0.79%, Si 0.99%, Cr 1.15%, Mo 0.59%, V 0.15%, Co 1.19%.

TABLE VII

Uniaxial Notched and Unnotched Mechanical Properties Compared with Biaxial Mechanical Properties of 4137 Co

Tempering[a] Temperature F	Uniaxial Properties				Biaxial Properties[c]		
	0.2% offset Yield Strength ksi	Unnotched Ultimate Strength ksi	Notched[b] Ultimate Strength ksi	Reduction in Area %	0.03% offset Yield Strength ksi	Extrapolated Rupture Strength ksi	Reduction in Head Thickness %
400	242	302	306	20.5	249	389	11.0
450	237	293	-	19.2	264	377	11.0
500	237	287	-	21.5	270	380	9.4
550	244	292	302	24.5	268	376	12.5
600	234	282	-	22.0	255	320	0
650	229	274	-	22.0	262	266	0
750	206	241	254	28.0	229	306	18.0
800	203	236	-	17.7	221	-	-
900	195	218	-	-	221	293	21.8
1000	186	208	237	28.0	213	264	21.8

(a) Austenitized at 1700 F for 30 min., quenched in oil and tempered as indicated.

(b) K_t = 5. 50 per cent notch.

(c) Biaxial Ratio = 1:1.

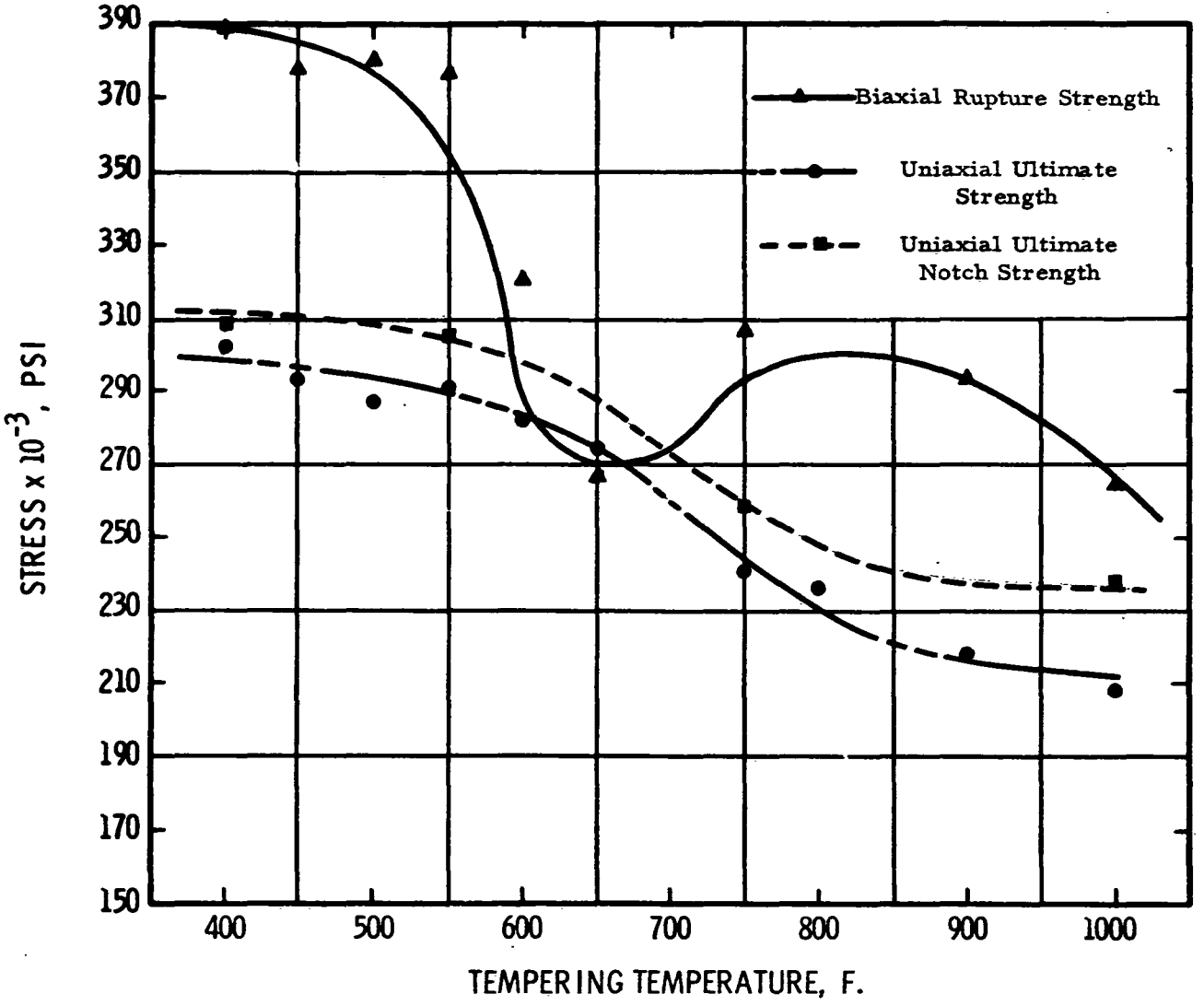


Figure 10 - Effect of Temper Embrittlement on the Uniaxial Notch Strength, Uniaxial Unnotched Ultimate Strength and Biaxial Rupture Strength.

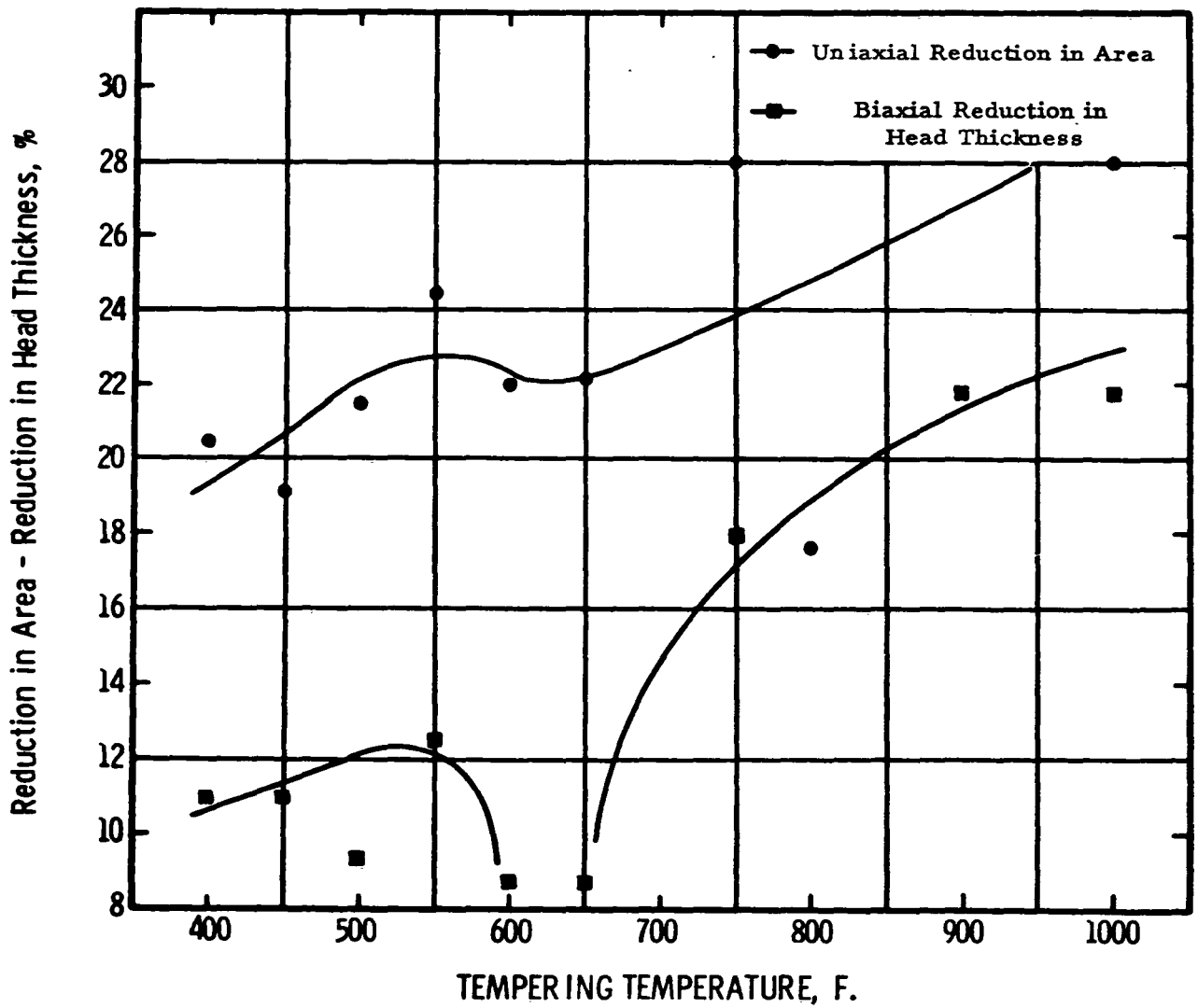


Figure 11 - Comparison of Uniaxial and Biaxial Ductility Parameters

Table VIII and in Figures 12 and 13. The steel is deliberately given an embrittling treatment by using a lower austenitizing temperature prior to quenching.

Figure 12 compares the uniaxial ultimate strength, uniaxial edge notch ultimate strength and biaxial rupture strength over a range of tempering temperature. It is readily seen from this figure that the biaxial rupture strength decreases well below the notch ultimate strength and uniaxial ultimate strength above a tempering temperature of 600 F, indicating brittle behavior or a notch sensitivity.

Figure 13 also reflects the brittle behavior of the material due to a drastic drop in the biaxial ductility parameter. The uniaxial ductility also, but not as markedly, reflects the brittle behavior in the continual but gradual decrease in the reduction in area as tempering temperature increases.

CONCLUSION

A material evaluation and screening technique has been described and data of consequence in the selection and application of a material for rocket motor case have been presented. It has been clearly indicated that the multiaxial cup test is capable of yielding the following information:

(1) Selection of the highest possible biaxial strength level without loss of biaxial ductility.

TABLE VIII

Uniaxial Unnotched and Notched Mechanical Properties

Compared with Biaxial Mechanical Properties of Rocoloy 250

Tempering[a] Temperature F	Uniaxial Properties				Biaxial Properties[c]		
	0.2% offset Yield Strength ksi	Unnotched Ultimate Strength ksi	Notched[b] Ultimate Strength ksi	Reduction in Area %	0.03% offset Yield Strength ksi	Extrapolated Rupture Strength ksi	Reduction in Head Thickness %
400	237	295	306	28.0	267	404	9.3
450	245	296	-	27.5	250	358	12.3
500	237	288	-	23.5	-	-	-
550	243	288	308	27.6	247	358	10.8
600	241	287	-	25.3	259	303	4.6
650	231	274	-	25.2	No yielding	140	-
700	227	270	-	28.0	No yielding	100	-
750	217	258	283	27.2	No yielding	155	0
900	-	-	-	-	No yielding	190	0
1000	-	-	261	-	-	-	-

(a) Austenitized at 1700 F for 30 min., quenched in oil and tempered as indicated.

(b) K_t = 5. 50 per cent notch.

(c) Biaxial Ratio = 1:1.

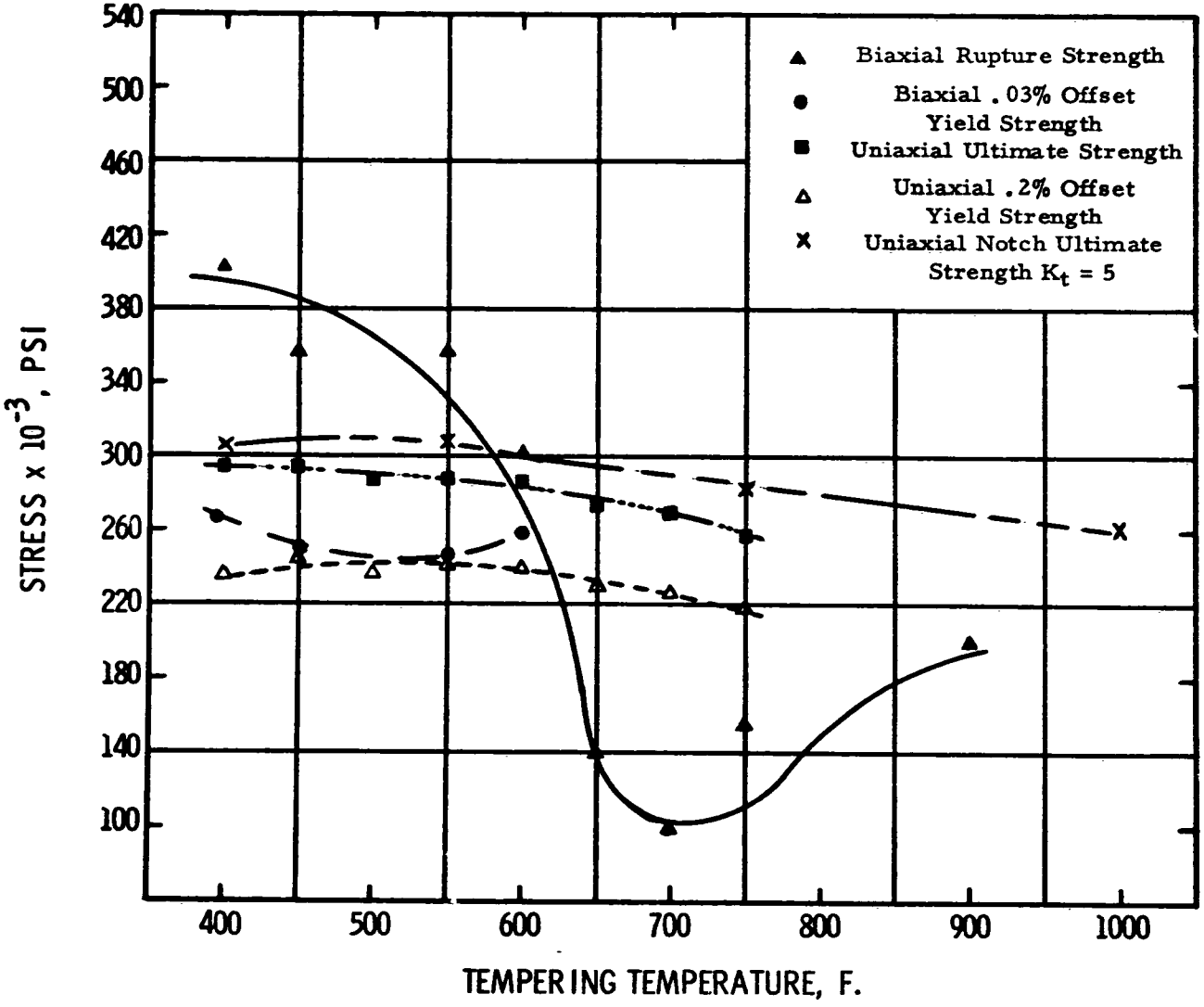


Figure 12 - Effect of Notch Sensitivity on the Uniaxial Notch Strength, Uniaxial Unnotched Ultimate Strength and Biaxial Rupture Strength of Rocoloy 250.

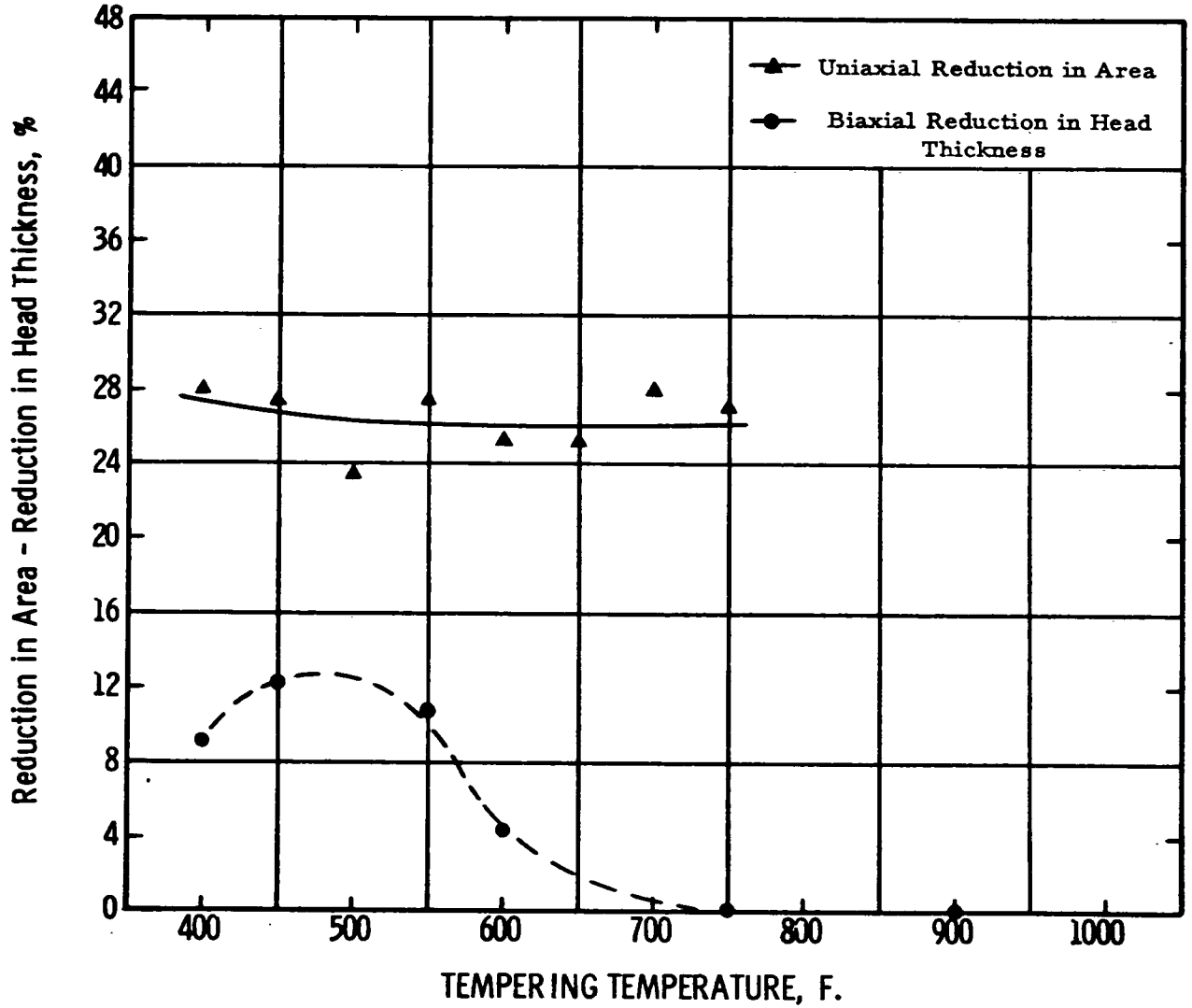


Figure 13 - Effect of Notch Sensitivity on the Uniaxial and Biaxial Ductility Parameters of Rocoloy 250.

(2) Establishment of a maximum allowable decarburization limit in order to decrease susceptibility toward notch embrittlement due to surface imperfections.

(3) Evaluation of embrittling ranges found at some tempering temperatures.

(4) Determination of the susceptibility of a material toward notch sensitivity.

(5) Detection of internal defects and undesirable conditions, such as banding, unusual segregation, level of inclusion content, and heterogeneity caused by non-uniform rolling and other processing conditions.

The results obtained through the use of this technique have been compared with the results of various other tests employed to select missile materials. This hydrostatic cup test has been shown to be more sensitive in delineating even the smallest deficiencies in a missile material.

As a final remark on the reliability of this technique, it would be appropriate to mention that the multiaxial cup test provides consistent and reproducible results. Furthermore, it appears possible to directly correlate the yield strength and rupture strength data of the cup test with similar results obtained by hydrostatic testing of scale model and full-scale rocket motor chambers. Data presented in Table IX support the above statement.

TABLE IX

Comparison of Cup Data with Scale Model
and Full-Scale Rocket Motor Chamber Data

Test Specimen[a]	Biaxial Threshold Yield Strength ksi	Biaxial Ultimate Strength ksi
10" dia. hemispherical[b] head cup	245	377*
Falcon motor case[c] 0.050" wall	246	275
Falcon motor case[c]	230[d]	270
Full-scale Polaris[c] A-1 second stage motor chamber	e	269

(a) All specimens heat treated to a 0.2% offset uniaxial yield strength level of 230,000 psi and a uniaxial ultimate strength level of 270,000 psi.

(b) Biaxial Ratio = 1:1.

(c) Biaxial Ratio = 2:1.

(d) Case successfully fired at this stress level.

(e) No yielding observed after three pressurization cycles to a stress level of 147 ksi.

* Extrapolated rupture strength.

ACKNOWLEDGEMENTS

The subject material for this paper is extracted from various progress reports submitted to Bureau of Naval Weapons Code SP-271 under Prime Contract NOrd 18169.

The authors express their gratefulness to Mellon Institute for permission granted to present this paper and the Special Projects Office of the Naval Bureau of Weapons for their sponsorship of this research work.

Dr. H. L. Anthony III of Mellon Institute acted as technical adviser.

THE CORRELATION OF LABORATORY SPECIMEN AND STRIP WOUND PRESSURE VESSEL TESTS

by

Robert J. Voth
Ryan Aeronautical Co.
San Diego, California

INTRODUCTION

Research and development of resistance welded strip wound pressure vessels has been conducted continuously for the past two and one-half years by the Ryan Aeronautical Company at their main plant in San Diego. Notable achievements have resulted from this research, in the quest of higher strength-to-density ratio rocket motor cases. One of the milestones of the program occurred when a laminated cylinder first achieved a hoop stress in excess of 300,000 psi, a value which has subsequently been surpassed several times. A second rewarding experience was the graduation of the program from sub-scale model testing to a full scale production case. A hoop stress of 291,000 psi was achieved on the first attempt.

Much of the success of the program can be attributed to the thousands of specimen tests conducted prior to chamber fabrication.

DESIGN FEATURES

The RyanWrap concept of pressure vessel design incorporates the usage of high strength foil gage metals helically wound on a cylindrical mandrel. A sufficient number of laminations are added to achieve the desired wall thickness. These layers are subsequently resistance welded together to form a cylindrical shell. End closures are added by resistance welding through a lap joint configuration. This versatile concept permits almost unlimited variation of material, chamber size, number of laminations, gage of each lamination and total wall thickness. The elimination of fusion welding permits the usage of simplified inspection procedures and allows fabrication without subsequent heat treatment. These many advantages, including greater resistance to notch sensitivity and "fail-safe" features, can be obtained using a minimum of production facilities and make the concept exceptionally attractive.

MATERIAL EVALUATION

As reported in reference 1, seven materials were initially screened to select an optimum alloy for strip wound cylindrical pressure vessels. The screening tests included tear, tensile, spotweld degradation, drop ball impact (reference 2), and G_c (references 3, 4, 5, 6) specimens. Figure 1 shows the results of the spotweld degradation tests; Figure 2, the G_c ratings; and Figure 3, the drop ball impact test results. Summarizing the results of these tests, the materials were rated in the following order:

TABLE I

Material Evaluation Ratings

	G_c	Degradation	Drop Ball
1.	AM355 CRT	AM355 CRT	AM355 SCCRT (30% CR)
2.	PH15-7MO	AM355 SCCRT (70% CR)	H. S. -25
3.	301 EFH	PH15-7MO	AM355 CRT
4.	HS -25	AM355 SCCRT (30% CR)	17-7 PH
5.	AM355 SCCRT (70% CR)	301- EFH	AM355 SCCRT (70% CR)
6.	AM355 SCCRT (30% CR)	17-7 PH	PH15-7MO
7.	17-7PH	H. S. - 25	301 EFH

From the screening tests including strength-to-density determination, the AM355 CRT material was selected as the best. It also offered the best potential for future improvement in properties by modifying the tempering or percentage of cold reduction. One gage, .008, common to all materials was tested in this evaluation program. Limited quantities of B120-VCA, all beta titanium, have been tested in addition to some 6AL-4V titanium. The results of the all beta tests are not encouraging, while the 6AL-4V tests are not complete.

RESISTANCE WELD FRACTURES

To fully understand the many problems involved in the design of a resistance welded pressure vessel, the modes of failure of this structure must be comprehended. Three basic types of fracture exist. The first, spotweld shear, as shown in Figure 4, is caused by insufficient nugget diameter or an inadequate number of welds. The second,

shear out or tear out, as shown in Figure 5, is caused by excessive penetration in the outer sheets, excessive weld spacing or insufficient edge distance. The third mode of failure, of utmost importance in wrapped chamber design, is degradation of the parent metal. It is analogous to a net section failure in a bolted connection. Too many bolts in the joint are often more detrimental than too few. Of significance in the degradation failure is the continued analogy to the bolted connection. The spotweld nugget acts as a shear pin in a hole, and the failure propagates around the nugget in the heat affected zone created when the nugget is cast. Figures 6 and 7, a pair of unique photomicrographs, show areas of imminent failure in test specimens. Figure 6 is of a single loaded layer specimen which contained a four-layer spotweld by use of tabs on the top and bottom of the test section. The tabs were loose, indicating that a failure had occurred around the spotweld nugget. When the tabs were pried off, the nugget was like a loose pin in a hole. Stress lines had started to form, originating at the edge of the hole, and were progressing outward toward the edge of the specimen. Figure 7 is of a spotweld through 20 layers of .008 steel. This, too, was a single loaded layer specimen; the additional 19 layers were tabs in the test section. In the laminate which was subjected to tension loads, a fracture can be seen in the heat affected zone around the nugget, indicating that failure in this area was imminent. Ultimate failure of the specimen had previously occurred in parent metal outside of the spotweld test area. From Figures 6 and 7 it is apparent that a degradation failure starts by a failure around the spotweld in the heat affected zone and that stress concentrations at the edge of the resulting hole create a crack which progresses outward to the edge of the specimen. This accounts for the critical effect of edge distance on the stress level achieved.

SPOTWELD DIAMETER

Some of the tangible parameters to consider in resistance welding through many laminations are the number of interfaces, the resistance of each interface, the gage of each laminate, the material, and the required shear stress of the welds. The nugget diameter requirements must be matched to the appropriate resistance welding machine. In addition, the skill and ingenuity of the welding research engineer are taxed to develop the best possible welds. Included in this research are choices of electrode shape and material, current density, wave shape and cyclic post heat and chill. Specimens were tested (reference 7) to determine the degrading effects on parent material in 4, 8, 12, 16 and 20 layers of .008" AM355 CRT with various spotweld diameters. Figure 8 shows the results of these tests. Eight laminations were required to achieve the required internal design pressure. Further testing efforts were concentrated on this configuration.

SPOTWELD SPACING

Circumferential spotweld spacing has little effect on the allowable hoop stress in a wrapped cylinder, as indicated on Figure 9. However, the axial stress in the cylinder must be transferred from layer to layer across the discontinuities in adjacent strips (reference 8). The highest stress in an axial type of specimen is obtained when a balance is achieved between tear out and degradation types of failure. Figure 10 shows these test results.

EDGE DISTANCE

As pointed out in the discussion of the modes of failure, the edge distance of the rows of circumferential spotwelds adjacent to the edges of the strip contributes significantly to the stress level which can be achieved in the hoop direction. Of additional significance is the eccentricity of the row of welds in the specimen. Two types of specimens were constructed to show this effect. The first group had a variable width test section with the row of welds down the center of the specimen. The second group held the width of test section constant; and the rows of welds, parallel to the direction of stress, were placed at variable distances from the edge of the specimens to the center line. Figure 11 shows the results of this investigation.

CYLINDER CORRELATION WITH SPECIMEN TESTS

As in the case of any research program, models were built to check specific variables and to verify analytical development. Direct correlation cannot be expected between tensile specimens and wrapped cylinders, since two very important parameters affecting wrapped cylinder performance are difficult to reproduce in tensile specimens. These two parameters are biaxial stress distribution and pre-stress of the laminations. If the trend, shown in the specimen tests, is duplicated by the results of the burst tests of the cylinders which were designed from the specimens, then conclusions can be drawn regarding the effects of the uncontrolled variables. Figures 12 and 13 show the correlation of the cylinders to the trend established in the specimen tests and the magnitude of the difference to be expected.

CYLINDER TO END CLOSURE JOINT

Many methods of joining end closures to a laminated cylinder were evaluated in specimen tests. These methods included fusion welded joints, mechanical fasteners, and four types of resistance welded joints. The specimen tests served as a rough screening operation, despite the fact that discontinuity stresses which are present in an actual joint could not be accurately reproduced in the specimen tests.

Chambers were fabricated incorporating the most promising of four of the basic designs. The joints on one of these chambers used mechanical fasteners, another chamber was fusion welded, and two resistance welded designs were included on other chambers. Measurements of the radial deflections in the area of the joints while the chambers were pressurized were subsequently graphed. The resulting deflection curves after differentiating twice yielded the $\frac{M}{EI}$ diagrams of the structure. Estimation of the material resisting bending then permitted relatively accurate calculation of the discontinuity bending stresses in the end closure attachment. It then was a relatively easy task to choose the most efficient joint. Both quarter scale and full size chambers were fabricated utilizing the optimum joint. A comparison between the bending moments for the quarter scale and full size model is shown in Figure 14 (reference 9). The validity of the analysis and the assumptions made were demonstrated by hydrostatic burst tests of twelve successive chambers incorporating this joint in which failures always originated in the cylinder body.

CONCLUSIONS

It is relatively meaningless to compare circumferential spotweld spacing specimens loaded in the axial direction to the burst strength of a cylinder, unless the failure of the cylinder occurred because of axial stress. As long as the specimens show that a strength level in excess of half the expected hoop stress can be transmitted in the axial direction, the design, using these specimen test results, should yield a hoop stress failure in the cylinder.

The excellent results achieved by the method of joint analysis discussed permits the designer to calculate the PL/AE deformations of any of his head attachment designs and convert these deflections to bending stresses. Model tests of these designs can then be extrapolated to determine full size chamber requirements.

Specimen and model tests have proven extremely valuable in establishing trends for the many variables associated with strip wound pressure vessel design. These trends have indicated areas of research to be abandoned as well as fields which merit further consideration.

BIBLIOGRAPHY

1. Voth, R. J., "The Behavior of 300,000 PSI Thin Sheet Steels, With and Without Spotwelds, Subjected to Tensile Loads", SESA Paper #554, May 1959.

2. Hausner, Paul H., "Impact Testing of Sheet Material", Ryan Aeronautical Company Metallurgical Report #59-5.

3. Ewing, H. O., "G_c Toughness Measurements on Three Materials Supplied by Ryan Aeronautical Co.", U. S. Naval Research Laboratory Technical Memo #40, 19 November 1958.

4. Ewing, H. O., "G_c Toughness Measurements on Two Materials Supplied by Ryan Aeronautical Co.", U. S. Naval Research Laboratory Technical Memo #72, 19 March 1959.

5. Ewing, H. O., and Kies, J. A., "Toughness and Strength Measurement on 17-7 PH Steel Strip With and Without Spotwelds", U. S. Naval Research Laboratory, 20 August 1958.

6. Ewing, H. O., "Toughness Measurements (G_c) on Three Coils of Thin Strip Material Received from Ryan Aeronautical Co.", U. S. Naval Research Laboratory, 28 October 1958.

7. Voth, R. J., and Rubisch, M. G., "Interim Report - Development of Spotweld Method for Fabrication of Strip Wound Rocket Motor Cylinders", Ryan Report G-17-102 (Confidential), 1 June 1959.

8. Voth, R. J., "Hydrostatic Testing of StripWound Rocket Motor Chambers", American Ordnance Association Paper, April 1960.

9. Rubisch, M. G., and Sakamoto, N. S., "Final Report - Development of Spotweld Method for Fabrication of Strip Wound Rocket Motor Cylinders", Ryan Report G-17-108 (Confidential), 1 April 1960.

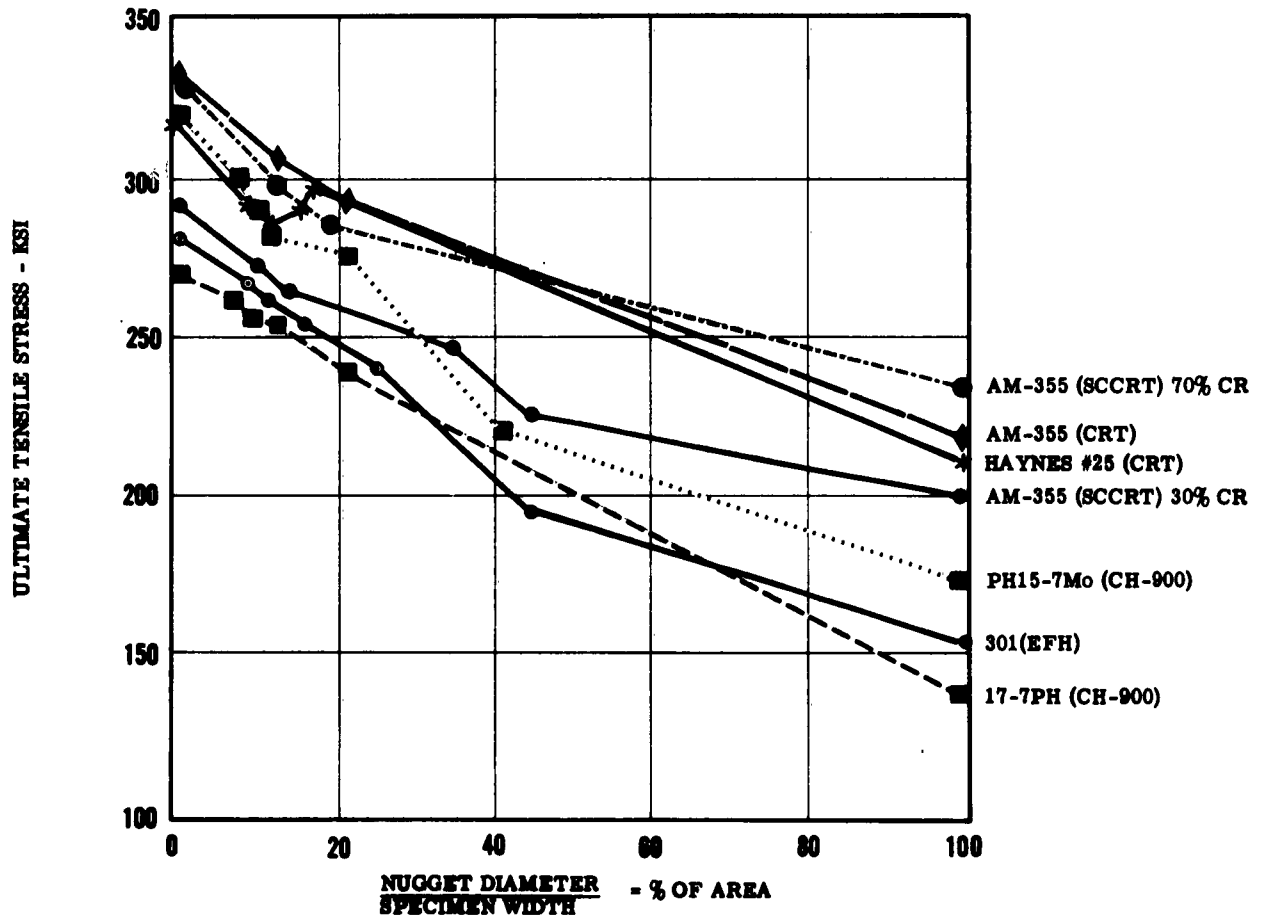


Figure 1 Ultimate Tensile Strength Reduction Due to Presence of Spotwelds

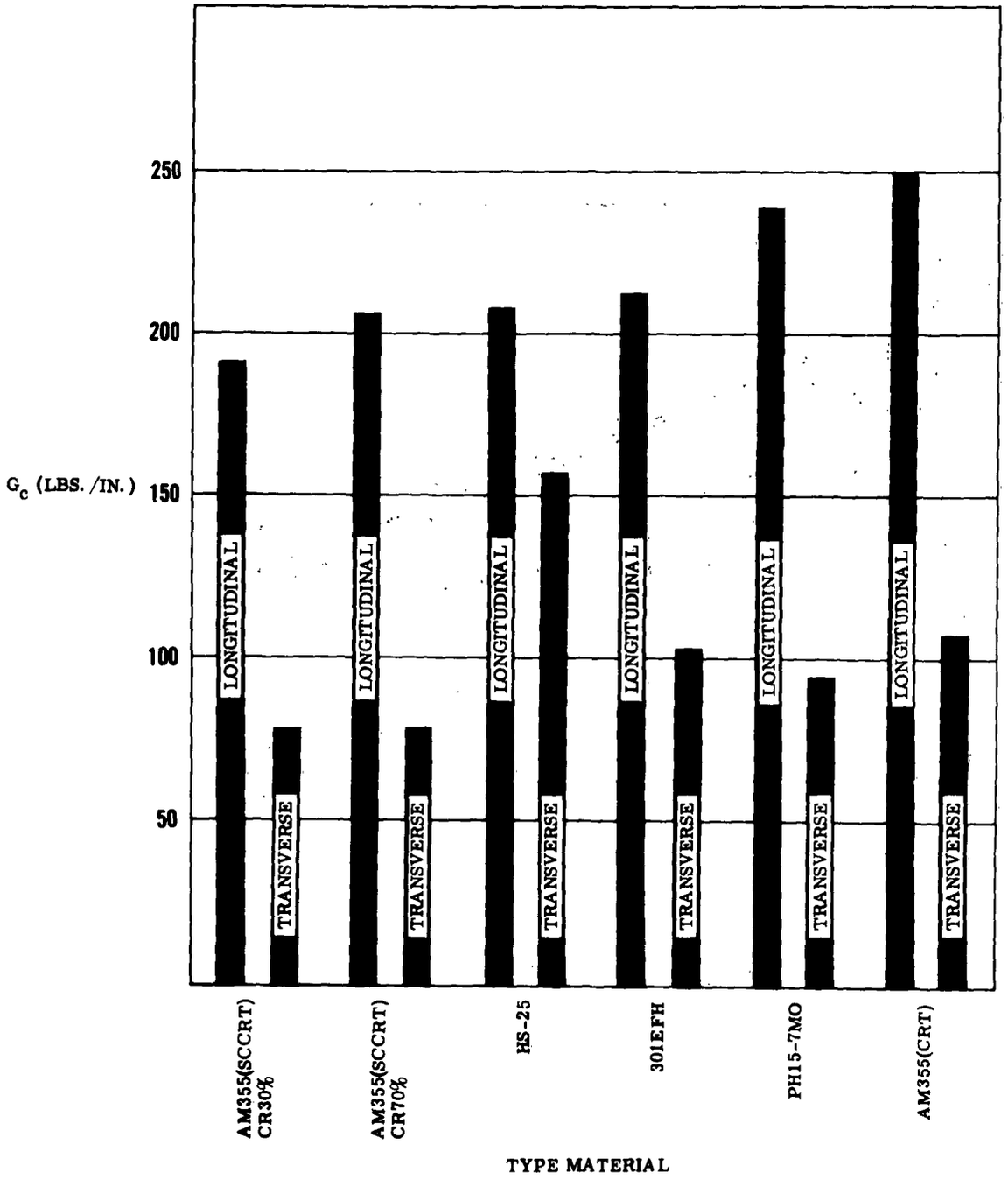


Figure 2 G_c Ratings

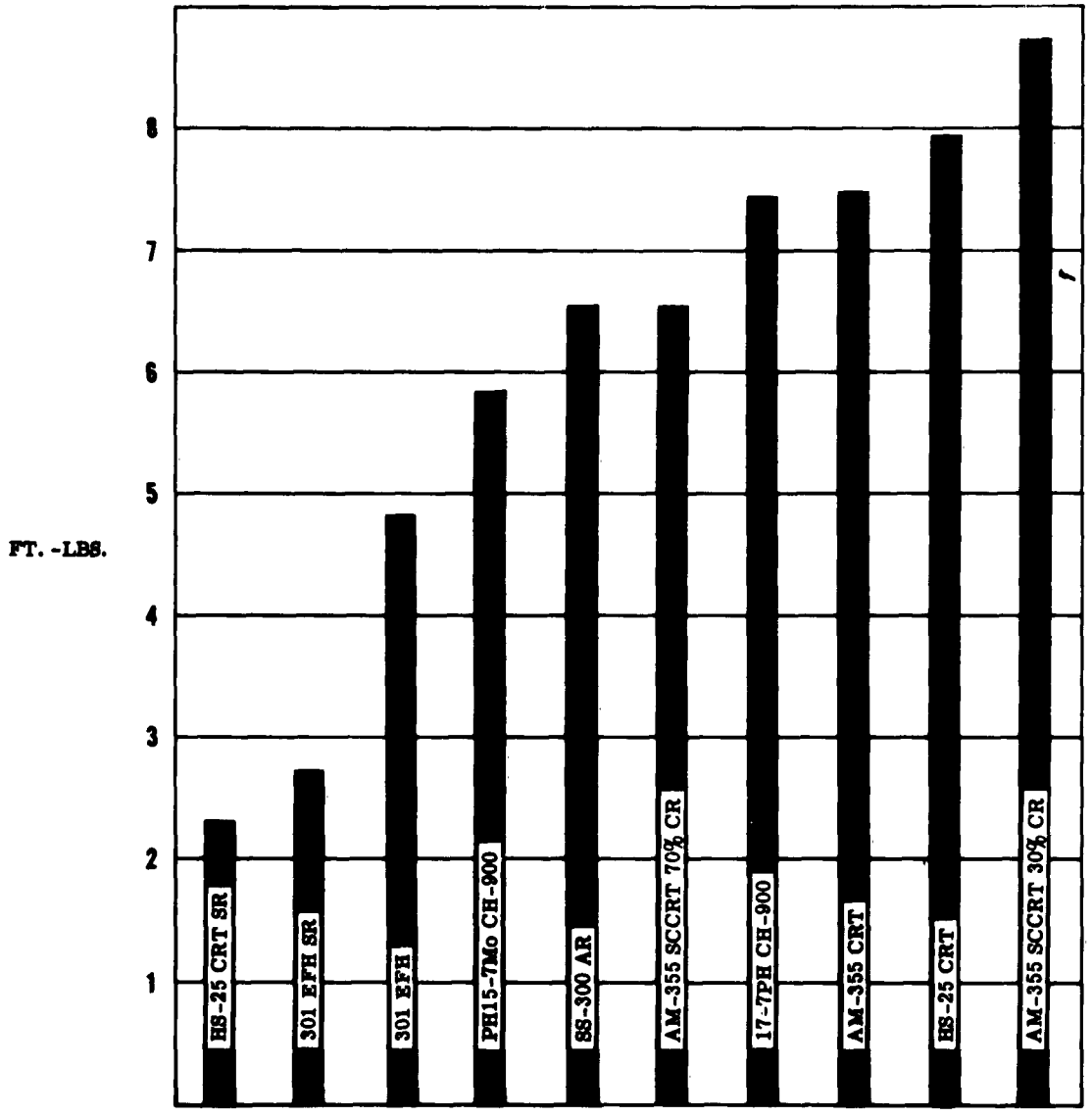
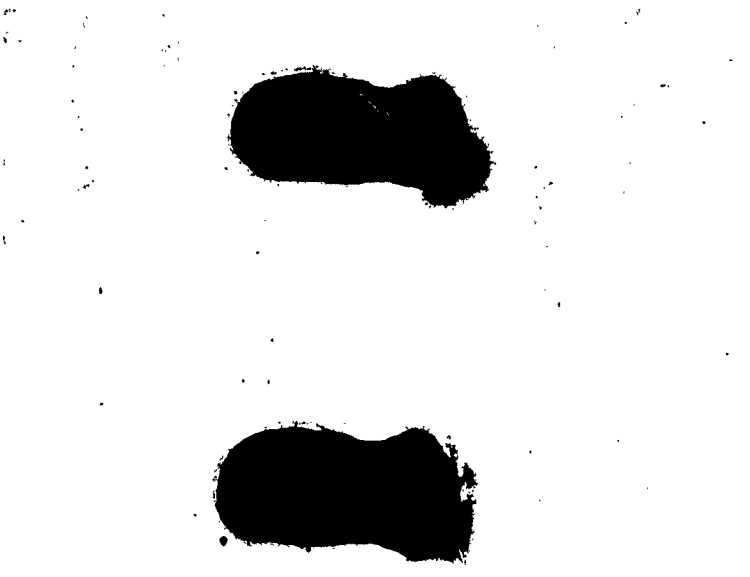


Figure 3 Impact Loads to Point of Fracture



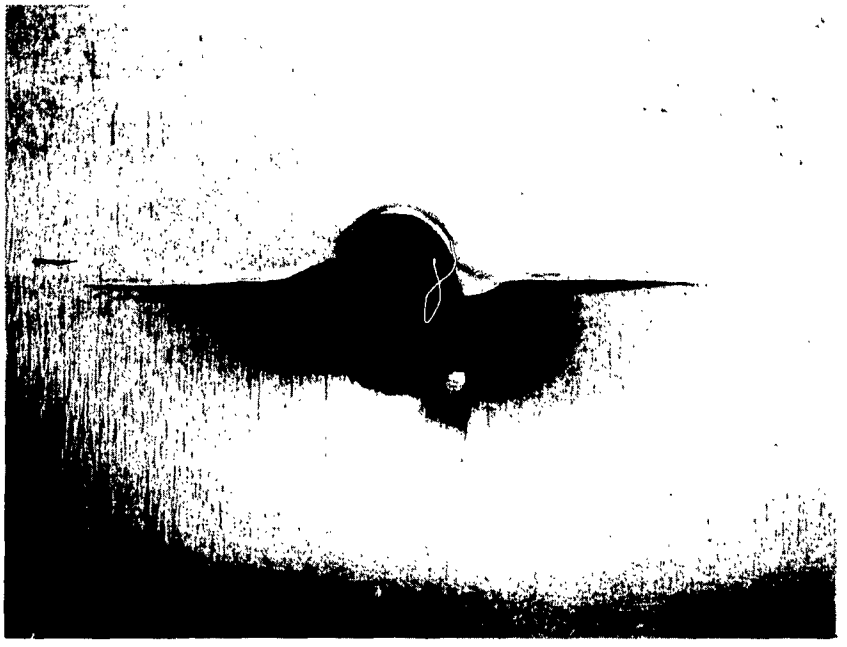
Magnification
10 X

Figure 4 Sheared Spotweld



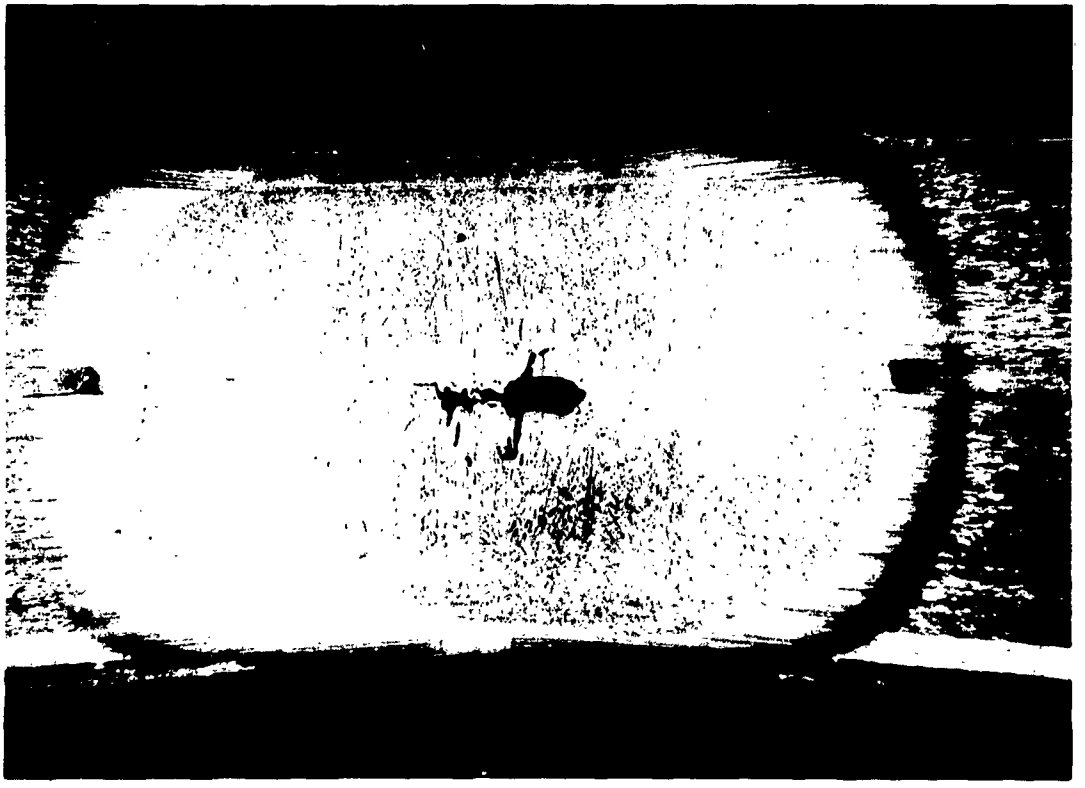
Magnification
10 X

Figure 5 Spotweld Tear-out



Magnification
8 X

Figure 6 Spotweld Degradation



Magnification
25 X

Figure 7 Spotweld Degradation

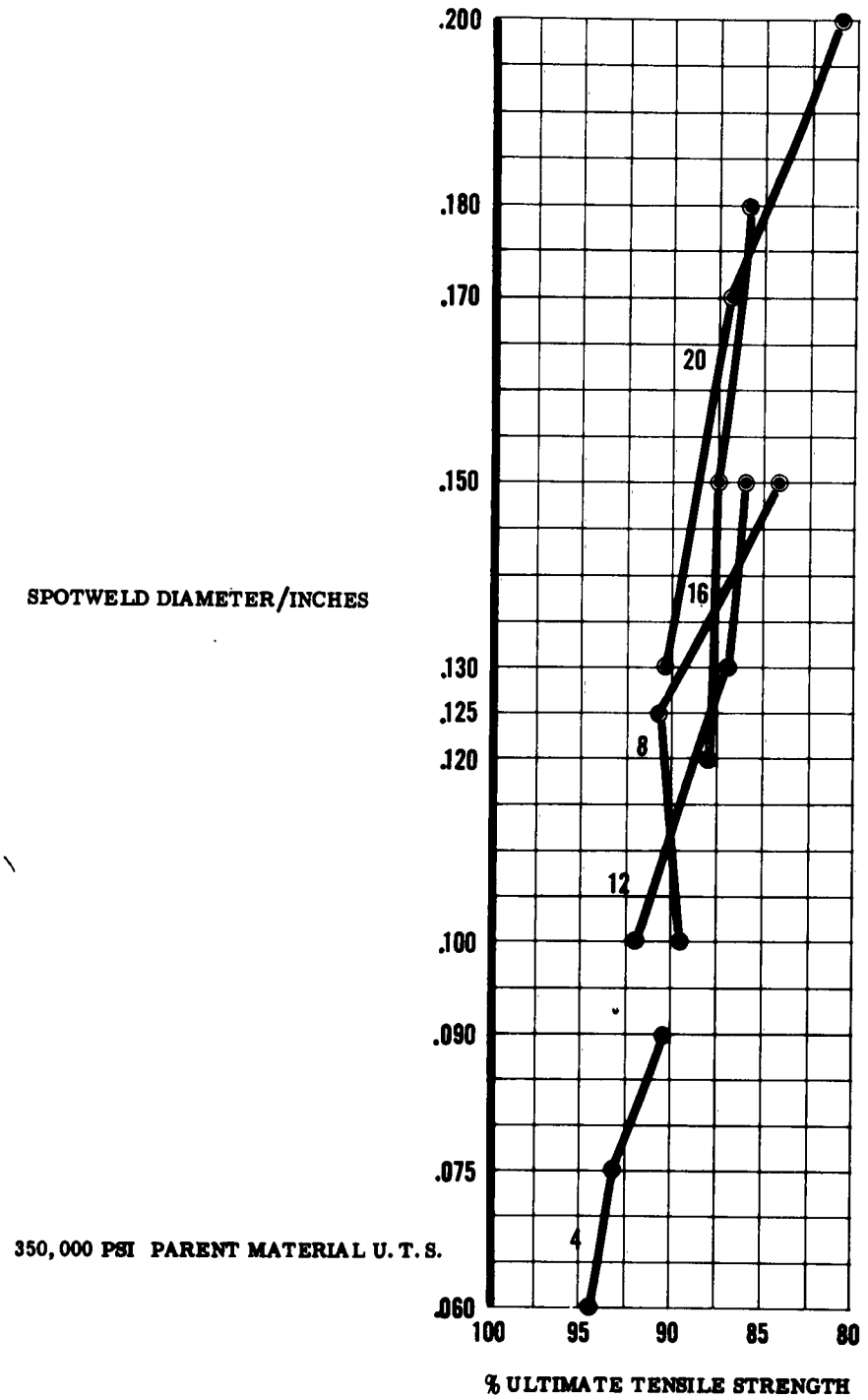


Figure 8 % Parent Material Strength V. S. Spotweld Diameter in 4, 8, 12, 16, 20, Laminations of . 008 AM355 CRT with . 50 Edge Distance

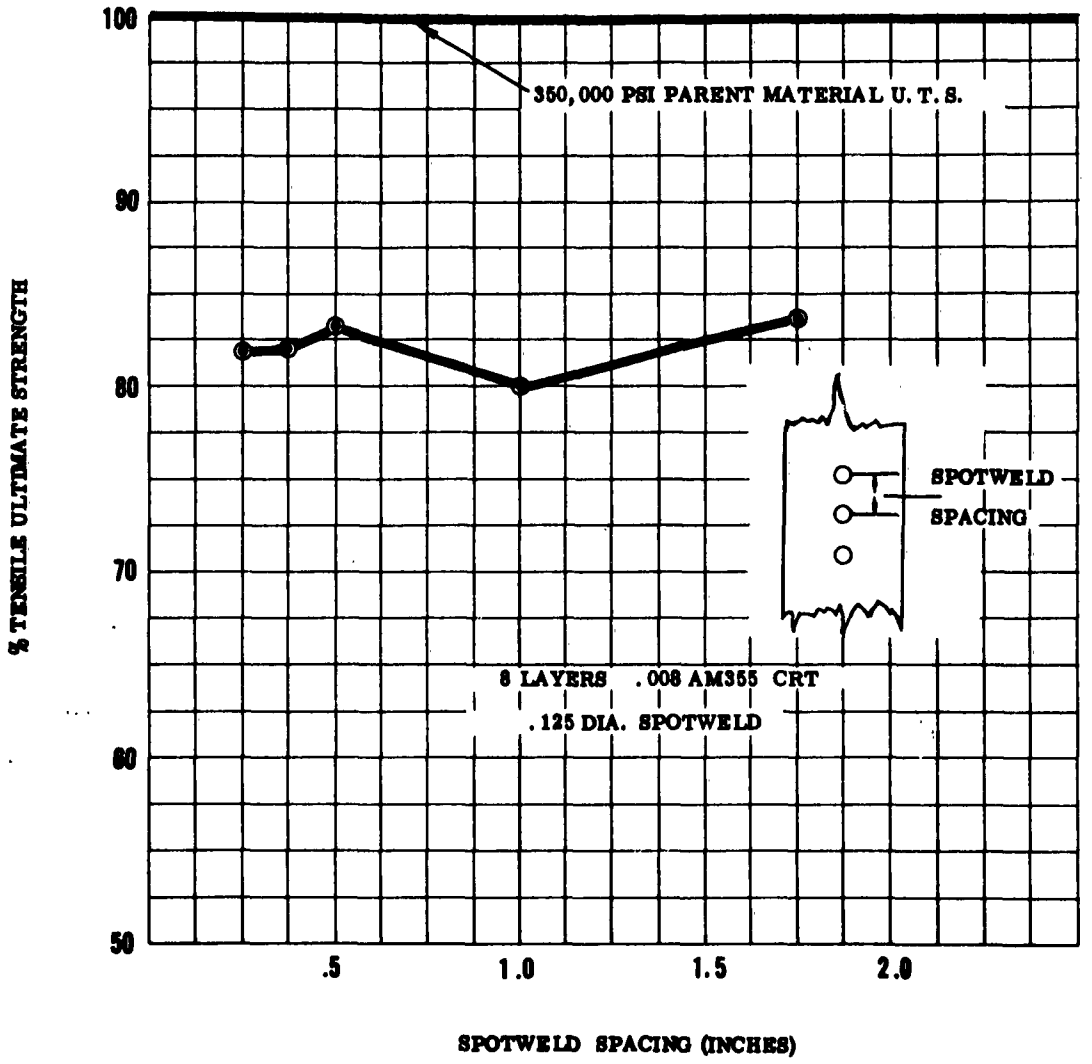


Figure 9 Allowable Hoop Stress Vs Circumferential Spot Spacing

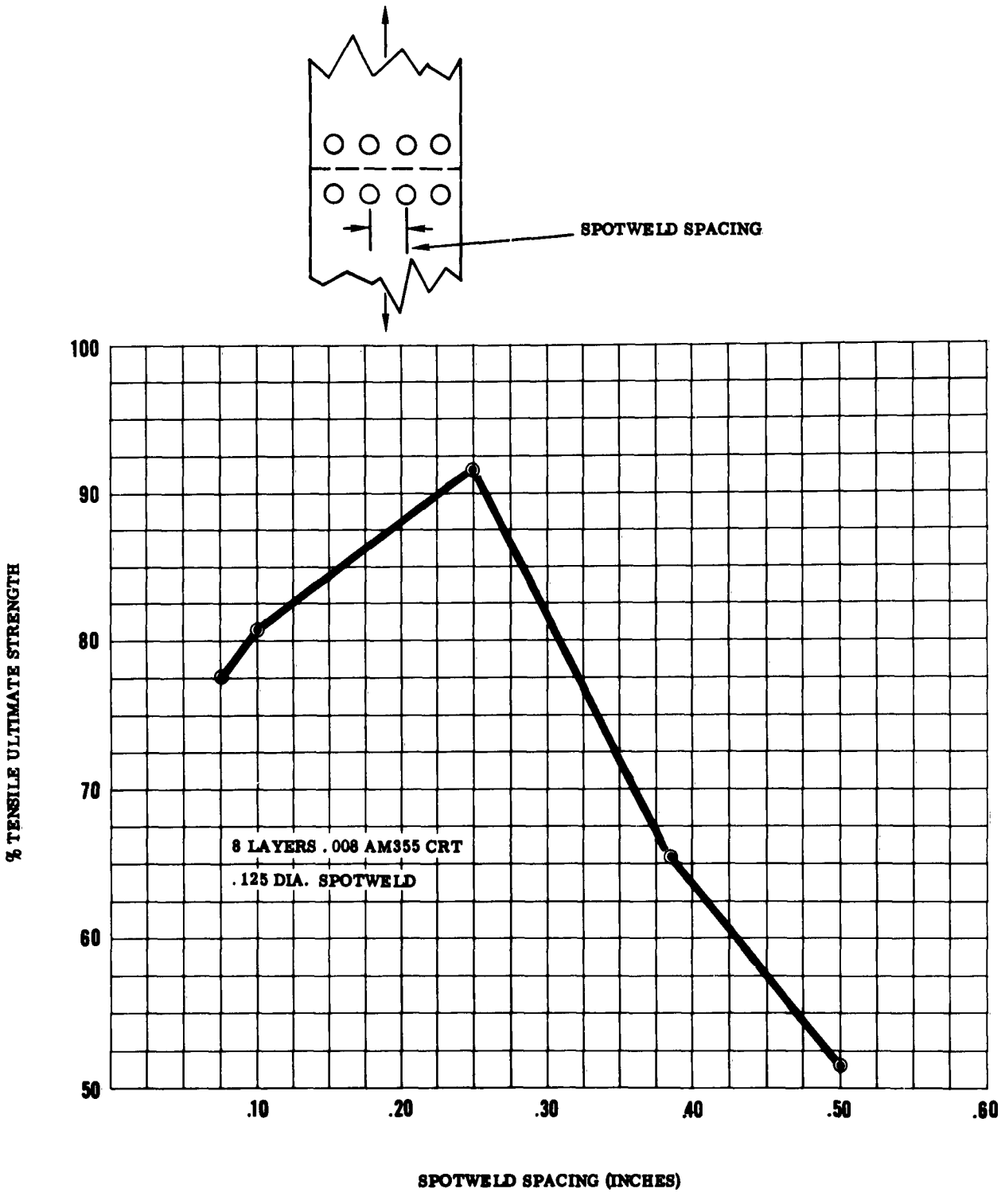


Figure 10 Allowable Axial Stress Vs Circumferential Spot Spacing

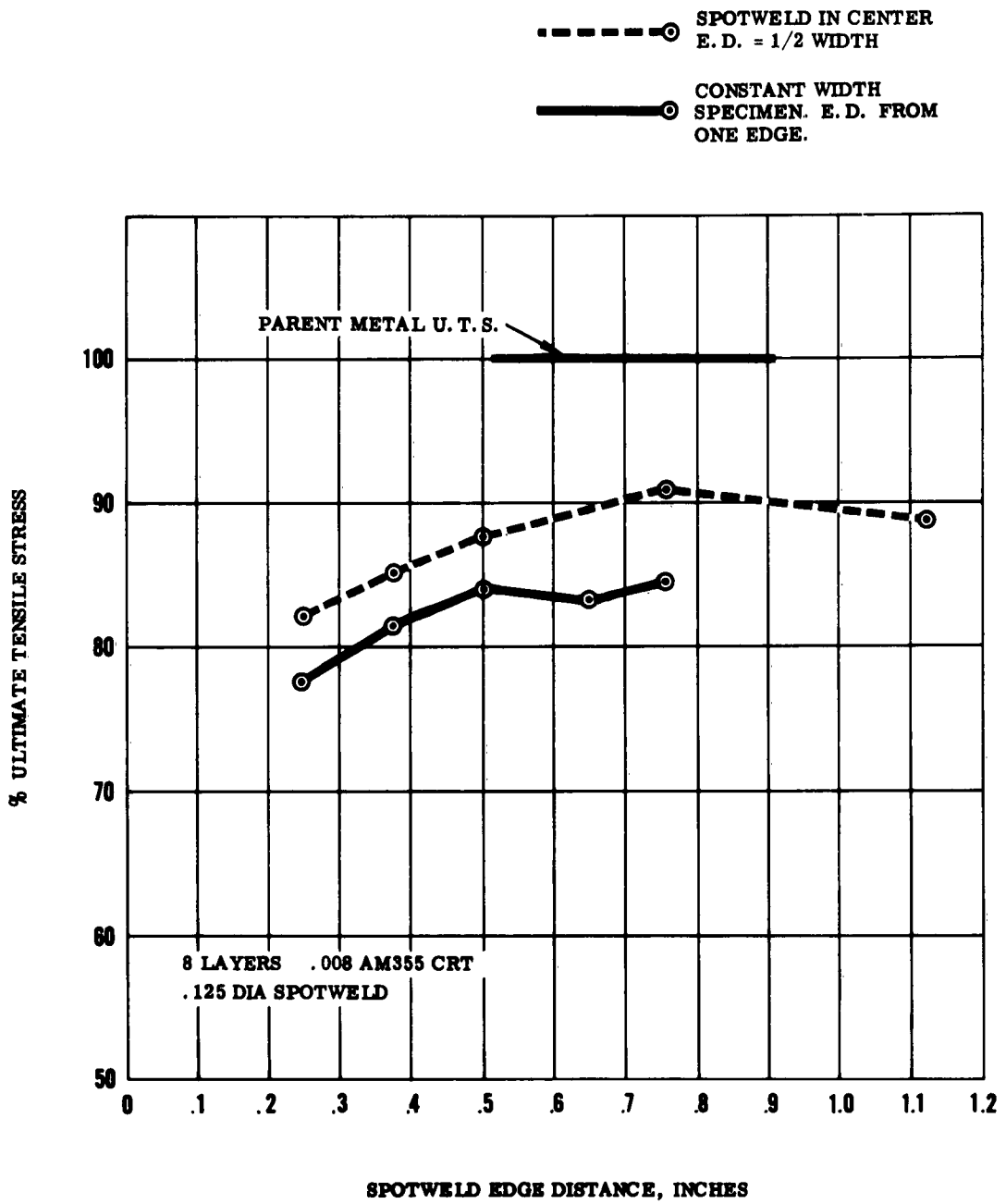


Figure 11. Variation of Ultimate Tensile Stress (Hoop Direction) with Spotweld Edge Distance

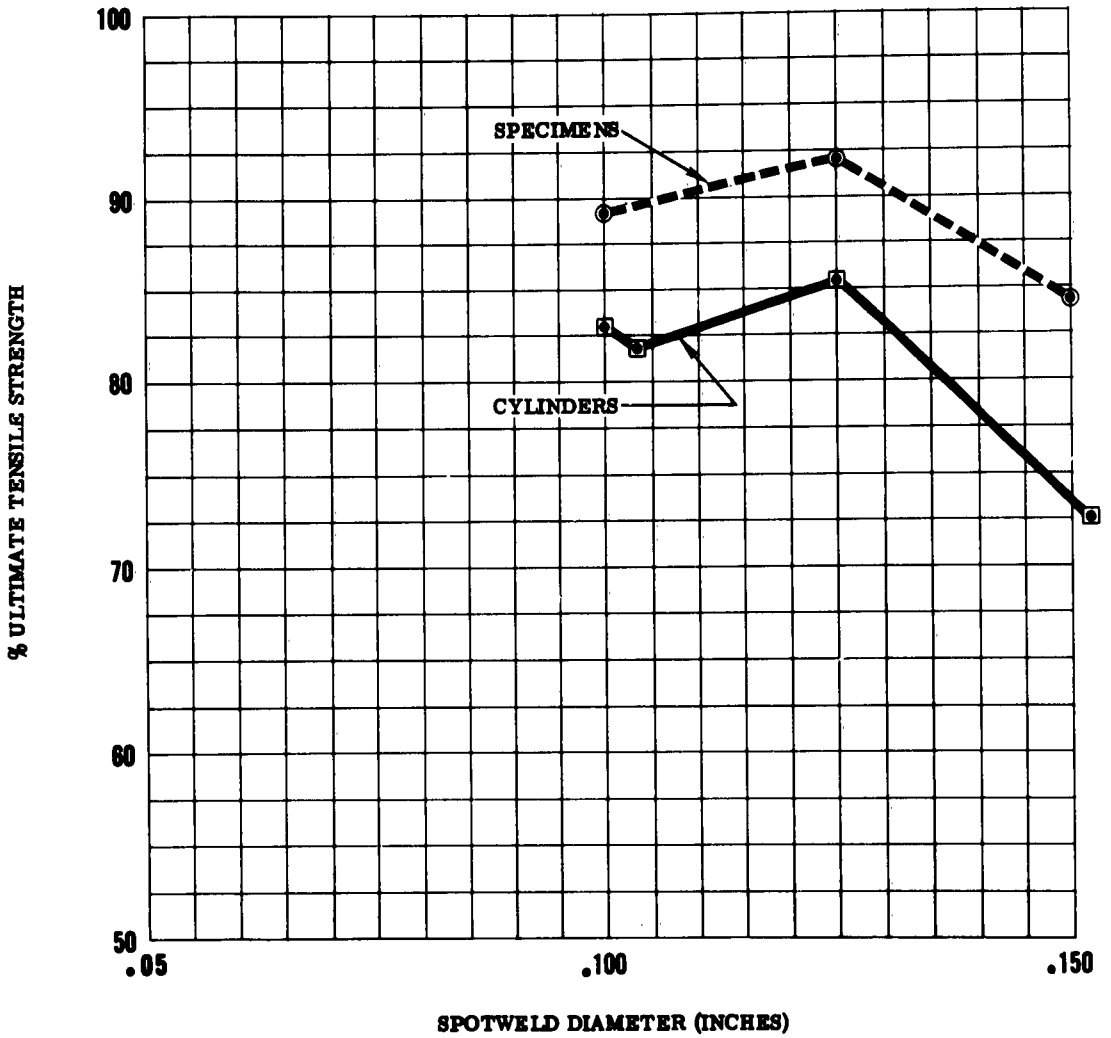


Figure 12 Spotweld Diameter Vs Hoop Stress

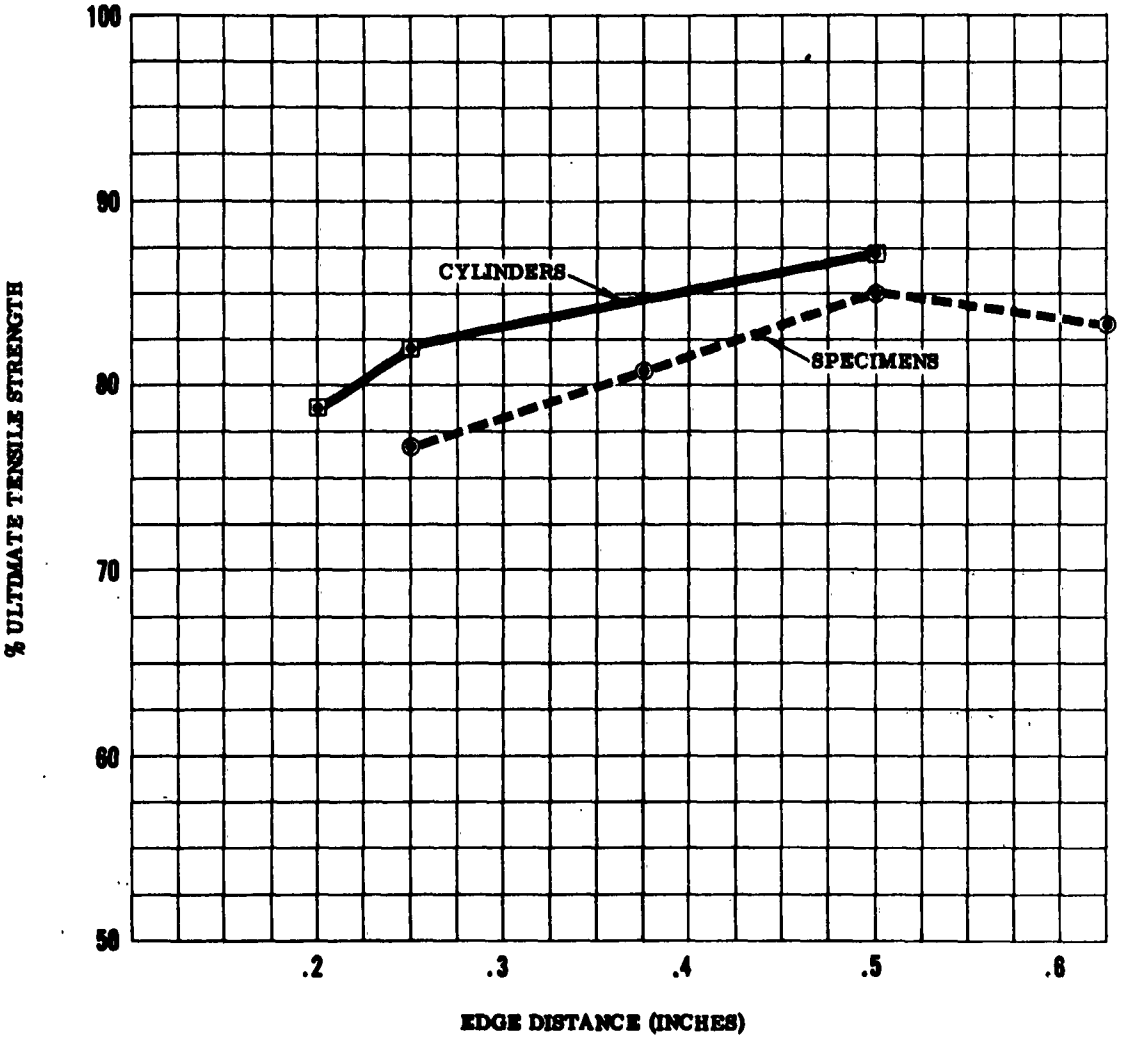


Figure 13 Spotweld Edge Distance Vs Hoop Stress

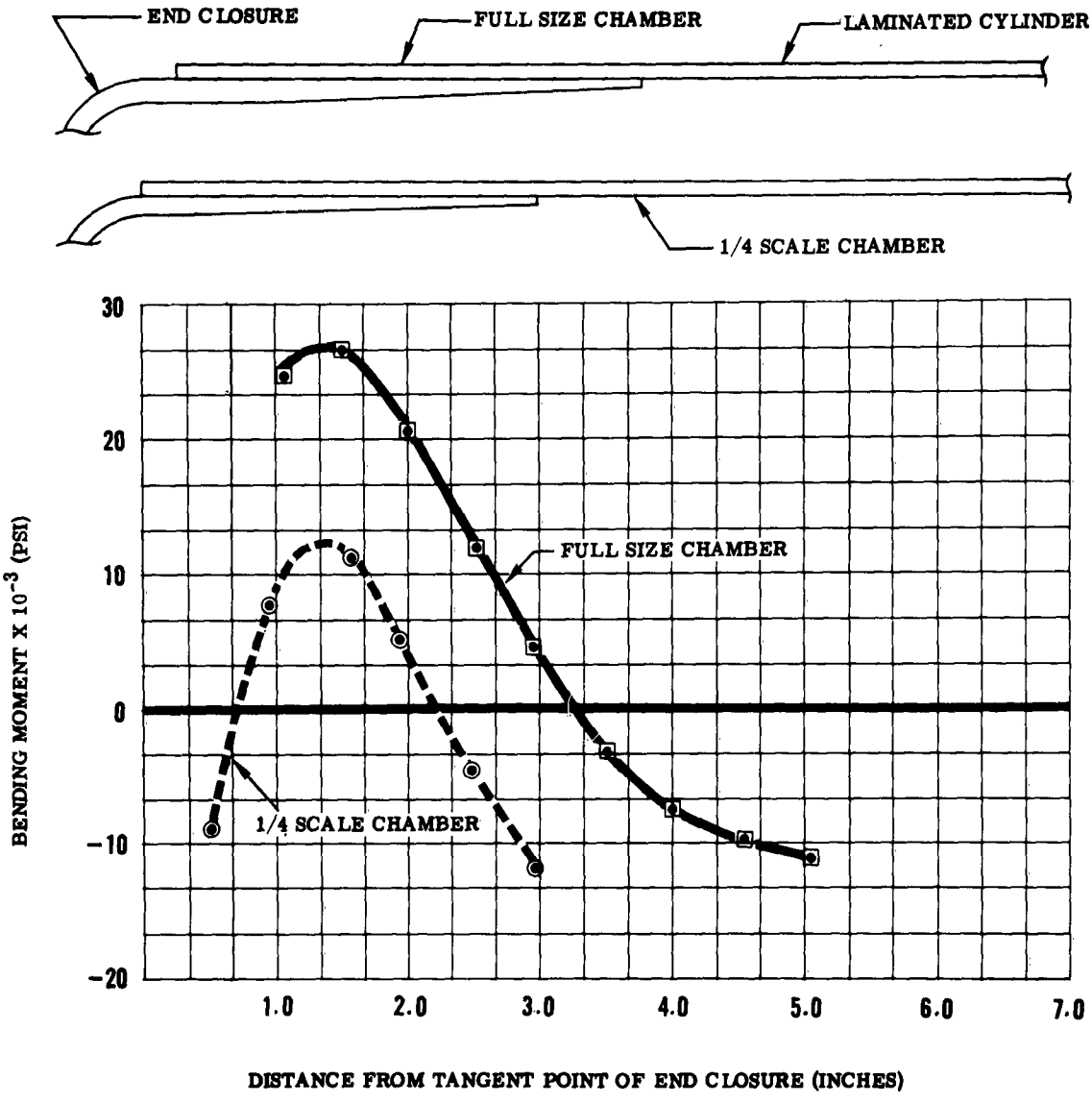


Figure 14 Bending Moment Comparison at End Closure Joint of Full Size and Quarter Scale Models

ABSTRACT

FULL SCALE PERSHING MOTOR CASE BURST TESTS (TITANIUM AND STEEL)

C. A. Tidwell, Jr.
Propulsion Laboratory
Marshall Space Flight Center
National Aeronautics and Space Administration
Redstone Arsenal
Huntsville, Alabama

The results of burst testing one full scale 2nd stage titanium (BIZOVCA) motor case, one full scale 1st stage steel (H-11) motor case and three full scale 2nd stage steel (H-11) motor cases are presented. Comparisons are made between uniaxial yield strength and biaxial strength, as well as between uniaxial ultimate strength and actual hoop stress at failure.

MODEL (SUBSCALE) TESTING AND SIGNIFICANCE

E.C. Schneider
Senior Design Engineer
Pratt & Whitney Aircraft
E. Hartford, Conn.

Presented at the
Seventh Sagamore Ordnance Materials
Research Conference

Raquette Lake, New York
August 16-19, 1960

ABSTRACT

The use of subscale pressure vessels in the development of modern solid propellant rocket cases is reviewed. Their place in a coordinated engineering program ranging from simple tensile testing to the completed case is discussed. Results of various programs aimed at evaluating and developing materials, fabrication techniques and establishing design parameters are presented. Problems encountered in the evaluation of subscale pressure vessel testings are also discussed. Applying subscale results to large cases is shown to be valid and the application of subscale vessels to future problems is mentioned.

Introduction

In general the development of high performance solid propellant rocket cases requires an extensive material, design and fabrication background. Even though these cases are relatively simple mechanical structures, the high stress levels they operate at and stringent reliability requirements makes them expensive pieces of hardware. Consequently, even though a final configuration must be evaluated on full scale parts, economical means must be developed to provide answers which insure the satisfactory functioning of the resultant design. One such tool is a subscale model. These models can range from simple pressure vessels designed to evaluate failure mechanisms on material behavior to more complicated models duplicating in every detail the design of the full size unit. The purpose of this paper is to review the use of these subscale models in developing a solid propellant rocket case and present results obtained during various development programs.

Approach

Much can be learned from fairly simple pressure vessels. One such vessel is shown in Fig 1. Commenly called a Watermelon, for reasons of its size and shape, pressure vessels of this type have been successfully used to evaluate material capabilities and failure mechanisms as well as fabrication techniques. These vessels are normally manufactured by hydroforming sheet stock into a spherical dome and cylindrical skirt. Two of these parts are girth welded together while the addition of a pressurizing plug completes the test vessel. Modifications of this procedure consist of flow-turning the skirt or the addition of intermediate cylinders to form longer vessels. The length of the vessel is important in evaluating the material strength and will be discussed in a later paragraph.

A further refinement, providing additional flexibility but increased cost, is obtained by using machined end domes welded to floturned center cylinders. (Fig. 2). Vessels of this type are used when dimensional changes unobtainable with sheet stock are required or selective fabrication techniques are being investigated.

The final refinement of course consists of detailed parts duplicating, at a reduced scale, flanges, igniter bosses, etc. These test vessels are normally used to evaluate particular designs or develope design techniques. One such test dome to evaluate thrust termination ports is shown in Fig. 3.

Results

A-Simple Models

Initially Pratt and Whitney Aircraft utilized the watermelon test vessels to evaluate material behavior under biaxial loading and establish welding techniques. Fig. 4a shows the chronological results of an initial series of tests. The early results were poor until weld techniques improved and more attention was paid to simple matters such as the welded in pressurizing plug. Two failures originated in this area and this weld problem was solved by eliminating it and resorting to a mechanical joint. While these test vessels are difficult to inspect, this series of tests proved very clearly that not only could much be learned regarding the behavior of a particular material but considerable fabrication experience could be gained at minimum cost.

A further series of tests (Fig. 4b) evaluated the fabrication variables involved in welding together hardened details. While the previous vessels had been made by first welding and then heat treating, these next series of tests were made by heat treating the individual details, welding and then locally tempering the weld zone. The low point resulted from a 50% mismatch in the weld. It is also interesting to note the last two points; the points noted U and O were under and over tempered respectively. Even though the over tempered weld was, in theory, considerably weaker its resultant strength was far superior to the harder under tempered weld.

Another series of tests was conducted utilizing a slightly different heat treatment. The results noted in Fig. 5 indicate a further refinement introduced in this series of testing. In evaluating burst strengths a considerable amount of non-linear bulging is normally noted. This effect can be compensated for and the true material burst strength determined by carefully measuring the resultant carviture of the burst vessel. This series of tests was considered highly successful despite the low burst values of vessel #5 which failed at a weld defect and vessel #6 which failed as a result of a 30% mismatch in the weld zone. These defects were readily inspectable and would not occur in a full scale case.

B-Modified Models

The results shown in Fig. 6 are indicative of testing requiring a slightly more sophisticated subscale vessel than those discussed above. This particular series of tests required a cylinder, cold worked by flow turning, which was welded to machined and heat treated end domes. Since different heat treatments were required for the cylinders and domes (resulting in different strengths) greater dimensional control had to be maintained. This series of tests yielded satisfactory results and it is interesting to note the fairly close correlation with prior uniaxial data. Additional information was also obtained regarding the behavior of this particular material. Fig. 2 shows one of burst vessels and the brittle nature in which it failed. Because of the extreme brittleness of this material and its sensitivity to stress corrosion (Fig. 7). This material was considered unsuitable for high strength cases.

C-Detailed Model

The strain gaged dome shown in Fig. 3 and the burst dome shown in Fig. 8 are indicative of the more complex model required to evaluate specific design, develope design techniques or fabrication details. By utilizing applicable stress-coat and strain gage techniques the dome shown in Fig. 2 contributed greatly to an understanding of the stress distribution around non symmetrical igniter bosses. This dome was reoperated following pressure testing within the elastic range of the material. Utilizing this technique considerable data was obtained from one "test specimen". In a similar manner the dome shown in Fig. 8 was tested to evaluate forging techniques and their effect upon the resultant strength of the material. The uniform failure of this model indicate that the initial estimates of its material properties and stress distribution were reasonably accurate.

Pitfalls

The fundamental question which usually arises in any discussion of subscale results revolves about their applicability to the full scale rocket cases. Questions of weld control, dimensional tolerances, etc. are obvious-the full scale rocket case will only be as good or as bad as its smaller predecessors. One of the major problems which must be carefully guarded against however is any change in the fundamental dimensions of subscale model relative to the full scale case (eg. L/D ratio). Biaxial effects in theory will increase the yield strength of a cylinder by 15%, while distortions due to yielding have increased the apparant burst strength by as much as 25% over a nominal strength level calculated by $^{Pr}/_{t}$. Fig. 9 shows a typical correction curve for a 10" dia cylinder as a function of bulge radius.

Application

The proof of the pudding as I have previously stated lies in the final testing of the complete rocket case. The full size case usually has a least two advantages over subscale models 1) it is larger, therefore more accessable and more readily inspected and 2) fabrication is usually more closely controlled than in experimental models. Considering these advantages it is not surprising that all of the P&WA full size cases tested to date have bettered or equalled the results of the subscale testing without "low" scatter points. The excellent results obtained with the large cases can be attributed to learning well the lessons taught by the small scale cases. In the future the use of these subscale vessels can be extended to include storage and handling problems as well as the more fundamental development problems.

Conclusions

All the results of a number of subscale programs correlated to full size case results indicate that model tests are perfectly feasible method of predicting the behavior of and economically developing large solid rocket cases.



9.4" DIAMETER B-120 VCA PRESSURE VESSEL
AFTER BURST TEST

Fig. 1

17-7 STAINLESS STEEL PRESSURE VESSEL WHICH RUPTURED IN PRESSURE TEST IN BRITTLE MANNER



PRATT & WHITNEY AIRCRAFT
DIVISION OF UNITED AIRCRAFT CORPORATION

VI-81

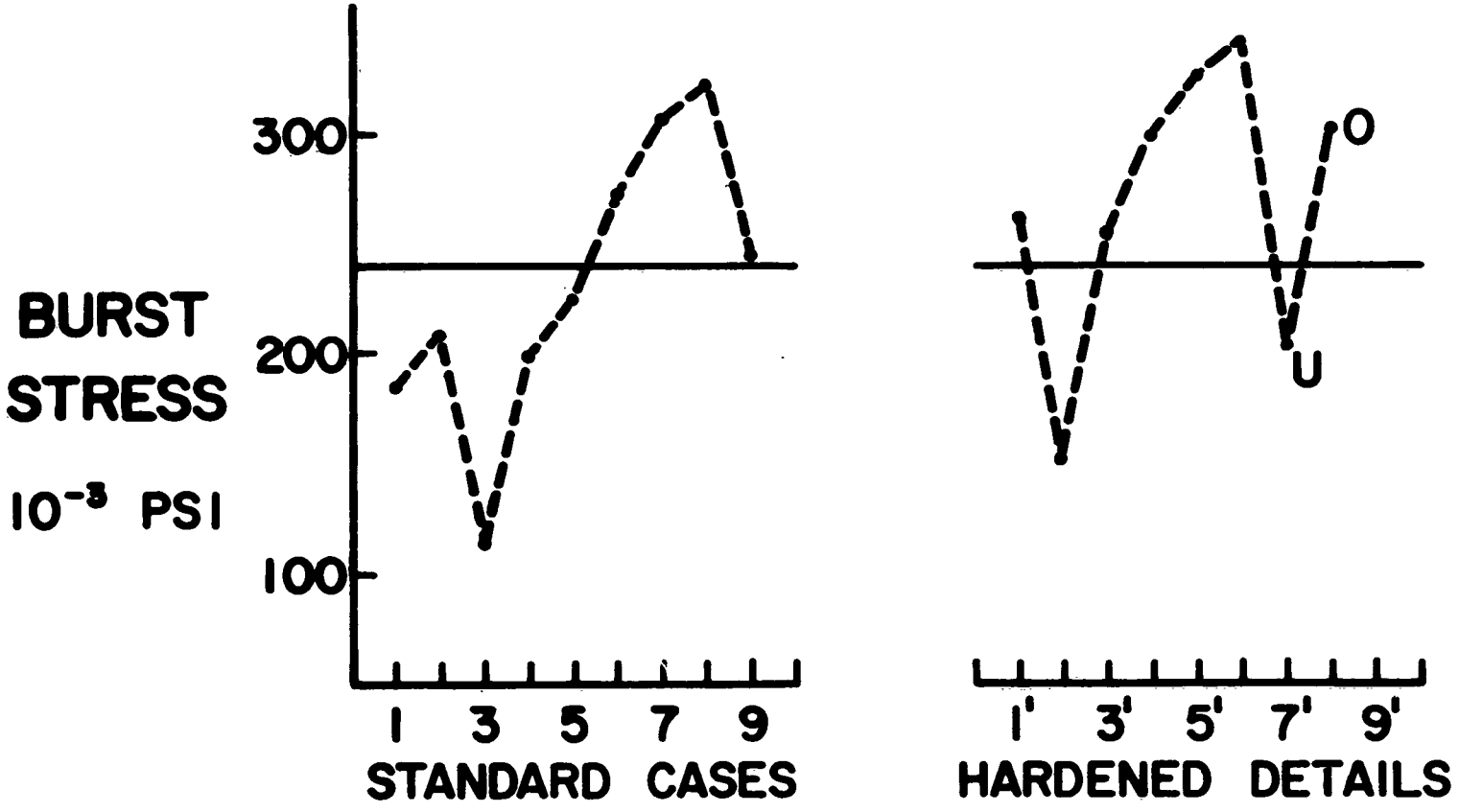
FIG. 2

STRAIN GAGED
MULTIPLE BOSS
DOME

PRATT & WHITNEY AIRCRAFT
DIVISION OF UNITED AIRCRAFT CORPORATION

Fig. 3

CHRONOLOGICAL WATERMELON BURST RESULTS
H-11 STEEL



9-18-59

VI-83

Fig. 4

PRATT & WHITNEY AIRCRAFT
DIVISION OF UNITED AIRCRAFT CORPORATION

WATERMELON BURST RESULTS
H-11 STEEL



Fig. 5

CASE BURST RESULTS & UNIAXIAL STRENGTH (17-7PH) vs COLD REDUCTION RATIO

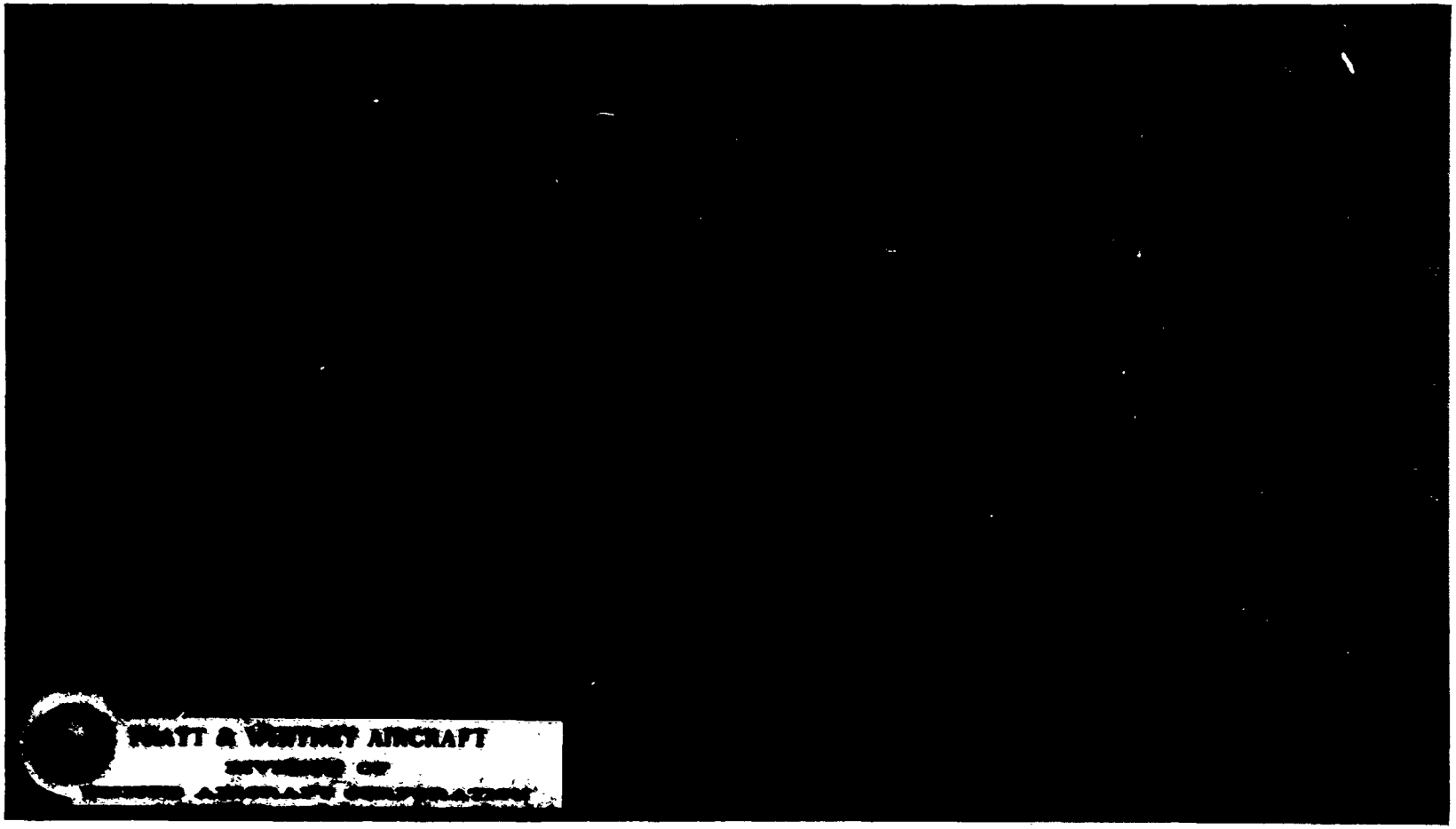


Fig. 6

17-7 PH CYLINDER AFTER 88 HRS.
IN SALT SPRAY ATMOSPHERE

PRATT & WHITNEY AIRCRAFT
DIVISION OF UNITED AIRCRAFT CORPORATION

Fig. 7

14" DIAMETER DOME FORGING RUPTURED IN BURST TEST; WALL STRESS AT 223,000 psi

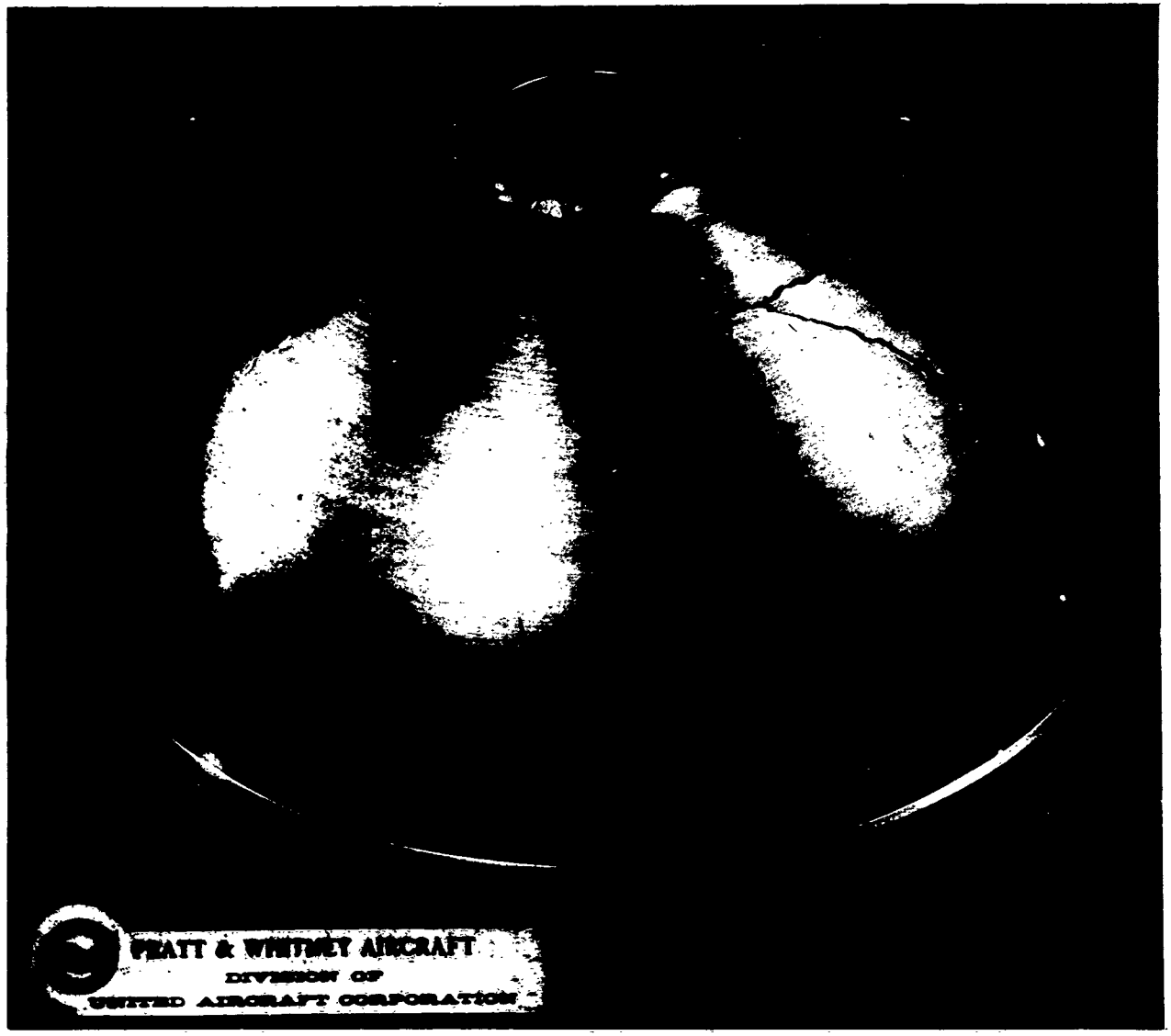


Fig. 8

HOOP STRESS CORRECTION CURVE
FOR
10" DIAMETER TEST VESSEL
PRATT & WHITNEY AIRCRAFT
DIVISION OF
UNITED AIRCRAFT CORPORATION

Fig. 9

Rocket Casing Behavior Predicted by Laboratory Tests

By

J. D. Marble
General Electric Company
Evendale, Ohio

ABSTRACT*

The behavior of a full-size Minuteman solid-fuel rocket casing is reviewed and compared to the behavior in 6-inch diameter cylinder tests and laboratory tests (primarily a flat-plate bulge test). The bulge tests were conducted with three different stress ratios, produced by three different geometrical configurations of bulging die. Primary conclusion is that yielding is a function not only of stress state, but also of geometry. Even though the cylindrical section of the full-size casing and the sub-scale cylinders obeyed the von Mises criterion for yielding, the heads of the casing did not behave similarly. The heads required much higher than predicted stresses to produce yielding. Overall geometrical instability acted as the criterion for failure in many of the six-inch diameter cylinders. However, localized thinning did not produce local instability in either the cylindrical or ellipsoidal (head) section of the casing, or in bulge-test plates simulating a 30 percent loss in thickness under each stress field. The stresses at yielding were considerably different in the different stress-states even on material heat-treated identically, and were much higher than would have been predicted by the von Mises criterion.

These seemingly anomalous behaviors of the material in the rocket casing were predicted by laboratory flat-plate bulge tests made with various stress fields applied to the plates. The differing behaviors are explained by the different geometrical instabilities applicable and the manner of strain buildup (slip-line field generation) over the entire structure to make it possible to achieve a specific level of strain at a local area. Welded panels constituted much of the experimental work, being done primarily to simulate behavior in a girth weld. When the geometry of the bulge specimen was sufficiently stable, minor weld defects controlled failure level - rather than its being controlled by structural instability. These minor defects were measured as to their severity and correlated with fracture pressure level. Analysis was made of each type of test. Primarily this was a comparison of stress-strain behavior in the various stress states, using the von Mises criterion for determining effective stress-effective strain curves for specific examples of the various tests. On this basis, the cylindrical section of the casing, the small cylinders, and the bulge-test with stress-ratio of approximately 0.5 were in good agreement with each other and with uniaxial tensile tests. However, the domes of the full-scale rocket casing and the two bulge tests simulating portions of the domes

* The complete paper has not been released for these proceedings up to the date of printing. If and when this becomes available, a supplement will be prepared and distributed.

with stress-ratios of approximately 0.85 and 1.0, deviate considerably from the stress-strain behavior predicted by the von Mises criterion. These deviations are explained as being primarily a geometrical phenomenon.

Simulated Service Evaluations of Steels for Solid-Propellant Missile Motor Cases*

By
K. E. Caine, J. M. Hodge, R. D. Manning, W. J. Murphy, H. J. Nichols and H. M. Reichhold

Approved by
P. W. Marshall, Assistant Director

ABSTRACT**

To establish the performance of 0.40 percent carbon martensitic alloy steels under conditions more nearly simulating those encountered in service than can be obtained with laboratory tests, and to obtain further information as to the relationships between laboratory tests and performance under simulated service conditions, model pressure vessels were carefully fabricated from such steels and hydrostatically tested to destruction. Five vessels were fabricated from each of five steels: AISI 4130, Airsteel X200, 300M, MBMC No.1, and H-11. Sandwichrolled sheets of these steels of a nominal thickness of 0.080 inch were roll formed and welded into 12-inch-diameter pressure vessels under closely controlled fabricating conditions. The fabricated vessels were heat-treated by commercial heat-treating companies in vertical controlled-atmosphere furnaces and were carefully inspected for flaws by X-ray and Magnaflux. Laboratory evaluations on the materials from which the vessels were fabricated included cross-section microhardness tests for decarburization, tension tests, and fracture-toughness tests. After burst testing, tension tests, fracture-toughness tests, and cross-section microhardness tests were made on samples cut from the failed vessels, and the fracture initiation sites were critically examined. The results of this program can be summarized as follows:

1. The vessels fabricated from AISI 4130 steel with yield strengths in the range of 173,000 to 186,000 psi and with high fracture toughness all showed excellent burst-test performance with burst stresses ranging from 218,000 to 255,000 psi.

2. Three vessels each of the X200, 300M and MBMC No. 1 steels, which were decarburized during heat-treatment and had yield strengths of 204,000 to 216,000 psi and relatively high fracture-toughness values, showed excellent burst-test performance with burst stresses ranging from 242,000 to 278,000 psi.

* (Progress Report) (ARL 40.02-070) (2) (TD-263) (a-AS-NP-26)

**The complete paper has not been released for these proceedings up to the date of printing. If and when this becomes available, a supplement will be prepared and distributed.

3. Two vessels each of X200, 300M, and MBMC No. 1 steels with yield strengths of 234,000 to 251,000 psi and with relatively low fracture toughness exhibited very low burst stresses, ranging from 92,000 to 187,000 psi.

4. The vessels fabricated from H-11 steel with yield strengths ranging from 226,000 to 244,000 psi and with low fracture toughness exhibited a brittle burst-test behavior, shattering into many pieces on bursting, and failing at stresses of from 206,000 to 225,000 psi.

Thus, the results of this program indicate that when steels of relatively high fracture toughness (a K_c value of at least 150,000 psi $\sqrt{\text{in.}}$) and yield strengths up to 220,000 psi are used to fabricate pressure vessels of the type used in this program, satisfactory hydrostatic test performance can be expected.

PREPARED DISCUSSION - SIXTH SESSION

By

Jack Sweet

I have attempted to summarize some of the data related to the application of tear tests to aircraft design considerations. About a year ago, Boeing ran a series of tests to evaluate the tear resistance of PH15-7 Mo steel. The material was given a simulated braze cycle, and aged at 950 F, which treatment produces a minimum ultimate tensile strength of 225,000 psi. This is the proposed treatment for the PH15-7 Mo to be used in sandwich structure. There were 15 center-notched 18-inch wide specimens tested adequately supported by bonded doublers. The tear tests indicated that with a gross area stress of a 100,000 pounds per square inch, 0.040 inch material had a typical critical crack length of 0.4 inch at 70 F; 0.020 inch material had a typical crack length of 0.2 inch at 70 F; and 0.020 inch material had a typical critical crack length near 0.1 inch at minus 65 F. The lowest test value indicated the critical crack length less than 0.05 inch.

The following is concluded from this test:

(1) The tear resistance of PH15-7 Mo, RH950 (braze cycle) sheet is so low that undetectable cracks could reduce the allowable tensile strength below 100,000 psi.

(2) The presence of any hole or other source of fatigue cracks presents a potential hazard.

(3) Tear resistance of PH15-7 Mo, heat-treated by the RH950 braze cycle, increases with increasing temperature, increasing sheet thickness, and decreasing gross area stress within the range tested.

(4) An improved heat treatment for PH15-7 Mo should be selected, and resulting tear resistance determined. The determination should concentrate in lower temperature environment.

Two braze heat treatments, involving a simulated braze cycle, were tested. A treatment we designated as RH 1100 (modified), which gave a tentative minimum ultimate of 176,000 psi, and TH 1050 (modified), which gave a tentative minimum ultimate of 188,000 psi, were selected for test. There were 34 specimens tested at a gross area stress of

100,000 psi, at a temperature of minus 65 F. The minimum critical crack length for the TH 1050 (modified) treatment was one inch and that for the RH 1100 (modified) treatment was somewhat greater.

It was concluded from this series of tear tests that:

(1) The RH 1100 condition is 25 percent more tear-resistant than the TH 1050 condition.

(2) Both conditions are in the order of 10 times as tear-resistant as the RH 950 condition.

(3) Tear resistance at 550 F is approximately equal to that at minus 65 F in both the RH 1100 condition and the TH 1050 condition.

(4) Tear resistance is reduced in panels loaded transverse to rolling direction.

(5) Tear resistance is reduced in lighted gages.

(6) Cracks longer than 1.0 inch may be critical at 100,000 psi gross area stress if the material is in the TH 1050 condition.

You may have noticed last night in one of the slides presented by Dr. Stack that the old braze heat treatment cycle for the B70 was designated with the 950 F aging, and the new braze heat treat cycle was designated with the 1050 F aging, which would result in material with a much better tear resistance. This type of tear data serves to aid the designer in deciding when he should reduce ultimate for appreciable increase in tear resistance.

PREPARED DISCUSSION - SIXTH SESSION

"Interpretation of Model Tests from the Point of View of Fracture Mechanics"

By
H. Bernstein

A great deal can be learned from burst tests on small pressure bottles. Admittedly, fabrication problems increase by some order of magnitude when full scale vessels are manufactured, but they are costly experimental models. Experimentation with small bottles is a more practical approach.

One program utilized the 5 percent Cr hot die steel. The bottles were 6 inches in diameter x 13 inches long with 0.06 inch wall. The cylindrical sections were welded from rolled sheet. The heads were drawn and attached to the cylinders by circumferential welds. The bottles were carefully inspected and it is assumed that the flaw level was uniform. The bottles were heat-treated to a range of strength levels, along with tensile coupons. The results of the burst and tensile tests are shown in Figure I. Hoop stresses at burst exceeded the uniaxial tensile strength at tensile levels below 265,000 psi. Above this strength level, burst stresses were below tensile strength and demonstrated a good deal of scatter. We know that toughness varies inversely with strength level i.e., the high strength material had low fracture toughness, which increased as the strength decreased. At the 225,000 psi strength level, the pressure bottles had sufficient toughness to demonstrate ductile, predictable behavior. However, as the strength level increased, the toughness fell off and the flaws became critical at the 265,000 psi level. Above this, unpredictable fracture behavior predominated, as shown by the rapid fall off in burst stress.

We can shift the crossover point in the direction of higher burst strengths in two ways - one, by increasing the toughness of the material at the higher strength levels, and the other by reducing the flaw size. As a matter of fact, if flawless pressure vessels could be made, we would expect the hoop stresses at burst to parallel tensile behavior. Such a relationship is shown in Figure 2 for Ladish D6aC. The vessels were simple cylinders, 10 inches in diameter x 20 inches long, fabricated by machining forged rings. The ends of the cylinders were plugged for testing. The data show that the burst stress was usually equal to 115 percent of the uniaxial strength. It would be unrealistic to claim that there were no flaws in the Ladish cylinders. There certainly were small inherent flaws in the parent metal such as inclusions. However, there were no welds and the fabrication flaws evidently did not attain critical dimensions.

If flawless pressure vessels could be made, then the only test required would be the simple tensile test. The experiences of those who have examined hydrotest failures indicate that the day of perfection is a long way off. What then can we do to improve the reliability of high strength pressure vessels? There are three approaches to this problem. First, we need more toughness at high strength levels. However, in view of the limited progress that has been made in this direction in the past two years, we would be overoptimistic to expect a toughness breakthrough via a new formulation or heat treatment. Second, we need new inspection techniques and better inspection to eliminate flaws. Third, we have to learn how to handle brittle materials. It is apparent by now that the demands for higher strengths and higher toughness will continue to outpace the supply. If metals are to continue to dominate in pressure vessel applications, all three approaches must be vigorously pursued.

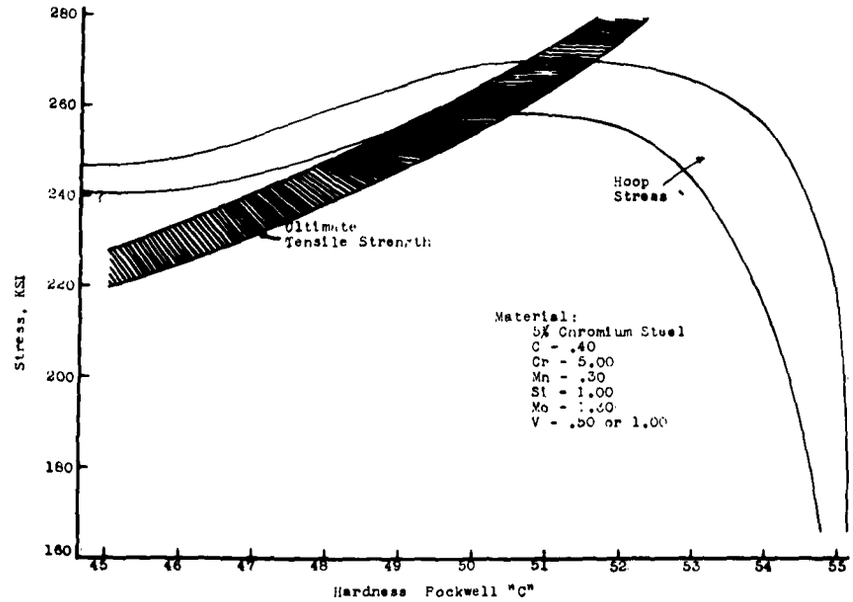


Figure 1

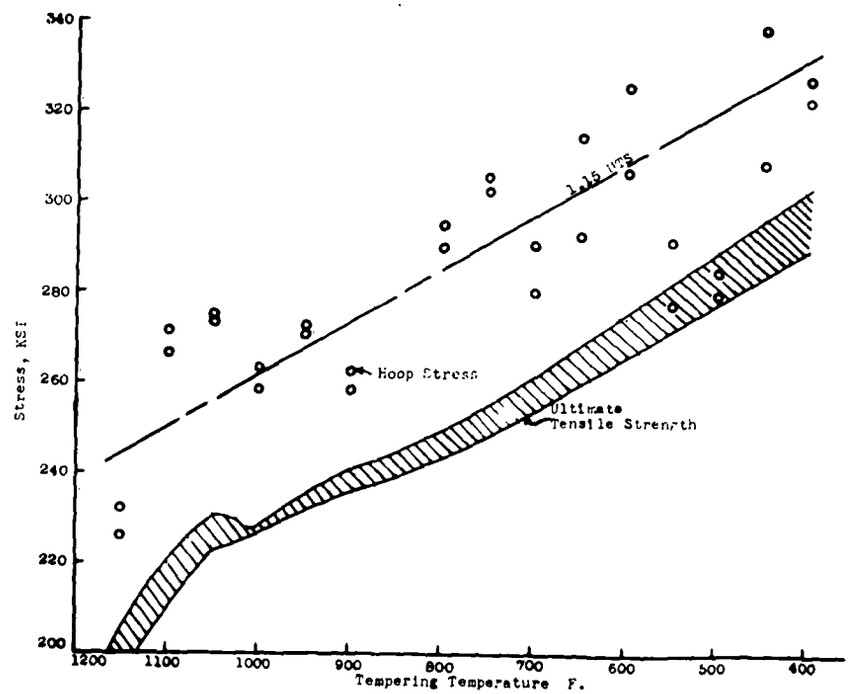


Figure 2

BIAXIAL STRESS TESTS OF MINIATURE PRESSURE VESSELS

(Discussion offered by J. W. Goodman, STL, at the Seventh Sagamore Ordinance Materials Research Conference on Properties of Sheet Materials, August 19, 1960.)

I. INTRODUCTION

The biaxial stress tests reported herein arose from a program at Space Technology Laboratories aimed at the development of Pressure Vessel Design Criteria, in connection with rocket cases and gas storage bottles. Although the brittle fracture problem was recognized, primary information desired from the burst tests was the behavior of pressure vessels if "premature failure" were somehow avoided. The upper limit on strength is, of course, tensile instability in which the true stress in the material increases faster than the pressure; evidence of the attainment of this limit and determination of the instability stress were sought.

In the beginning of the program, the emphasis was not on burst tests at all, but rather on local ductility and the effects of discontinuities. A uniaxial specimen with a simulated weld mismatch, but no weld, underwent extensive tests with 4340 sheet. These results and fracture strains from wide bend tests indicated fairly high local ductility for the material tested and we began to look elsewhere for causes of low burst stresses in large pressure vessels. A logical starting point was a subscale vessel; a miniature specimen was devised and systematic biaxial stress testing began in 1959.

The first material tested was 4340 airmelt bar stock at seven (7) strength levels because: (a) it might be possible to correlate burst data with the previous work and (b) it was a well known material. Ladish D6AC was then becoming prominent and the second series of tests used this steel at nine (9) strength levels. On a much smaller scale were investigations of 6Al-4V titanium alloy and 7178 aluminum alloy

II. TEST METHOD

The specimen shown in Figure 1 was selected because it offered economy of manufacture, adaptability to various stress fields, freedom from welds and other discontinuities, and simplicity of required test equipment. The vessel is 2" in diameter, with an .050" wall thickness and has internal and external shoulders to accomodate externally applied end loads. Coupons heat treated with the vessels were cut from flattened tubes and included tensile, wide bend, and Allison Instrumented Bend test specimens. Apparently because of the flattening, these coupons were not representative of the material in the vessels.

The various stress fields were obtained by varying the ratio of end load to internal pressure thereby achieving axial-to-circumferential stress ratios of 1:0 (uniaxial tension), 2:1, 1:1, 1:2 (pressure only) and 0:1 (hoop tension only). A close fitting internal plug reduced the energy stored in the hydraulic medium. Two post yield strain gages were installed on each specimen: their putputs were combined with signals from a pressure transducer to feed x-y plotters. The end product was full range biaxial stress-strain curves as shown in Figure 2.

III. TEST RESULTS

A natural base point for presenting the results of burst tests is the uniaxial strength, based on tensile tests (1:0) of the vessel itself. As shown in Figure 3 the strength-hardness relations of 4340 and D6AC coincide. The hardness, of course, is not absolute, especially since measurements were made on buttons cut from the .050" walls of the vessels.

Figure 4 shows the nominal ultimate strengths of 4340 bar stock in several stress fields. The uniaxial strength is designated 1:0 and tests with internal pressure only are the 1:2 band. Discrepancy between 1:2 burst strength and 2:1 is due in part to anisotropy and in part to the different instabilities of the cylinder in different stress fields. The 1:1 strength is generally slightly below uniaxial. The G group of specimens is noticeably out of line due to apparent variation in composition. The obvious feature of these results is the erratic behavior above 280/KSI/UTS as shown by the "fan". The cause of these premature failures is not known; the vessels show no difference in microstructure, number of defects, or mode of fracture (shear) from those vessels which reached full strength.

Figure 5 shows the contrasting behavior of vacuum melted Ladish D6AC vessels machined from individually extruded forgings. The same relative sequence of strengths is seen; 2:1, 1:2, 1:0 and 1:1. Note first that no abnormally low failures occurred, although some scatter is present. (The black points represent variations from the basic heat treatment and are not related to the scatter bands). The 1:2 burst stresses above 300 KSI suggest that some materials in geometrically and metallurgically clean vessels might be able to use this range.

About eight (8) each 7178-T6 aluminum and 6Al-4V titanium vessels were tested in the various stress fields. In general the titanium showed very high 2:1 properties but low strain capability in the 1:2 and 1:1 fields presumably because of forging defects. The aluminum was very anisotropic and no appreciable increase of biaxial over uniaxial strength is present in either direction.

IV. COMMENTS AND CONCLUSIONS

The upper limit on strength of a pressure vessel is tensile instability, the attainment of which may be construed as one measure of the merit of the material and the design of a given vessel. The tabulation in Figure 6 shows the contrasting behavior of vacuum melted D6AC and aircraft quality 4340.

The achievement of tensile instability was judged from the experimental biaxial stress-strain or pressure-strain diagrams solely on the presence of a horizontal tangent. Of course, specimens which failed early include a few markedly premature failures, before or at yield, as well as some which exhibited considerable plastic flow but did not quite reach instability. The D6AC vessels reached instability far more frequently than the 4340 and it appears that no 1:2 tests of 4340 got there because of the limited transverse ductility of this air melted bar stock.

Whereas during the past year or so our effort has been mainly on testing, our activity in the near future will be analytical, beginning with an incremental elastic-plastic solution to instability of a pressure vessel, based on the uniaxial stress-strain curve.

The immediate conclusions to be drawn from these tests are as follows:

1. The miniature pressure vessel is an excellent vehicle for the determination of plastic behavior of materials and strength characteristic of the tensile instability mode of failure in biaxial stress fields.

2. If premature fractures, before or at yield, occur in miniature vessels of a given material, full scale pressure vessels would be even more susceptible to this type of failure.

V. REFERENCES

This work is being conducted for the Air Force under contract no. AF 04 (647) - 309 and the following reports have been issued:

1. Fitzgibbon, D., "Semiannual Report on Pressure Vessel Design Criteria for Period of 1 July 1958 to 31 December 1958". Space Technology Laboratories, Inc., 31 December 1958.

2. Fitzgibbon, D., "Semiannual Report on Pressure Vessel Design Criteria for Period of 1 January 1959 to 30 June 1959". Space Technology Laboratories, Inc., 30 June 1959.

3. Fitzgibbon, D. and Goodman J., "Semiannual Report on Pressure Vessel Design Criteria for Period of 1 July 1959 to 31 December 1959". Space Technology Laboratories, Inc., 31 December 1959.

4. Fitzgibbon, D., "Experimental Method for Testing Materials in Biaxial Stress Fields". Space Technology Laboratories, Inc., 25 February 1960.

5. Goodman, J., "Semiannual Report on Pressure Vessel Design Criteria for Period of 1 January 1960 to 30 June 1960". Space Technology Laboratories, Inc., 30 June 1960.

JWG:sh



Figure 1. Miniature Pressure Vessel

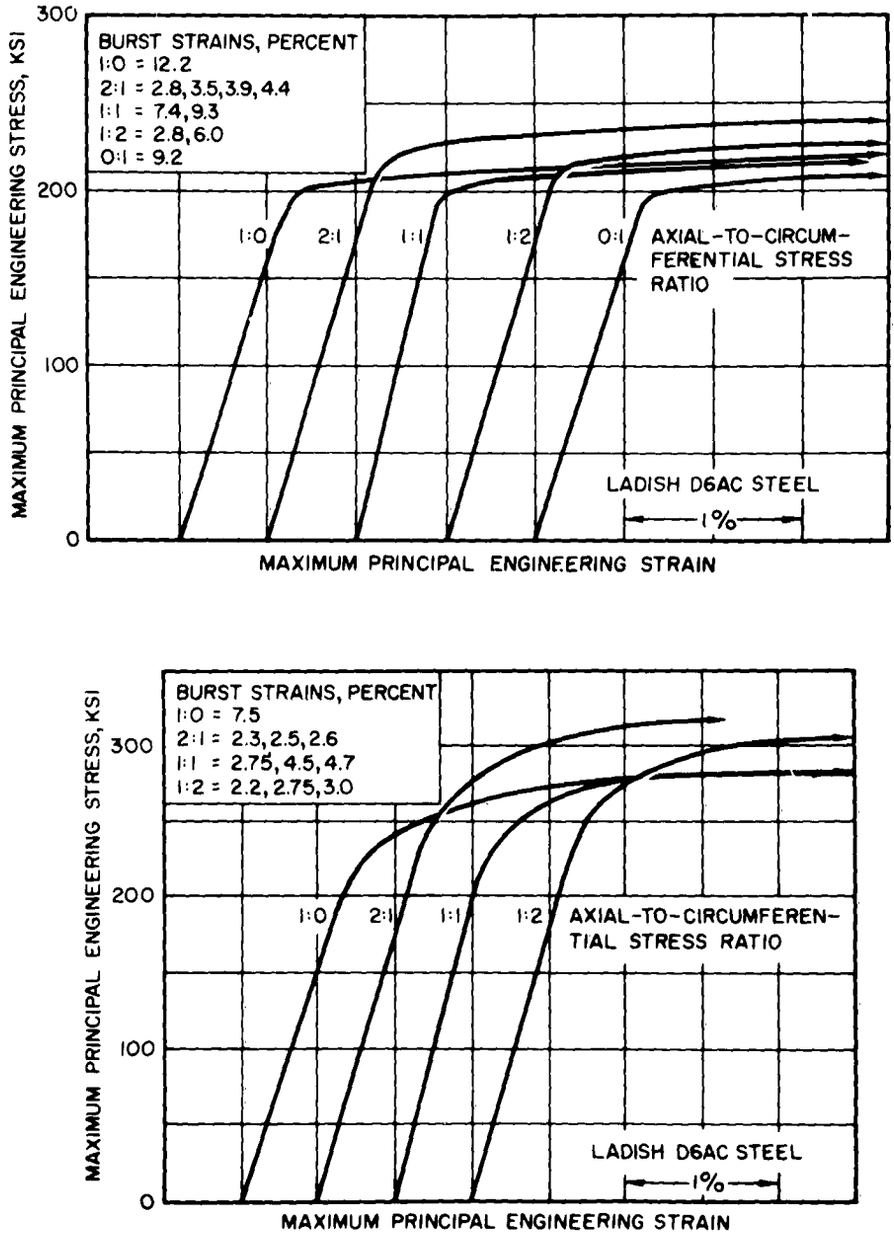


Figure 2. Biaxial Stress-Strain Curves for D6AC Tempered at 1075°F (Above) and 400°F (Below)

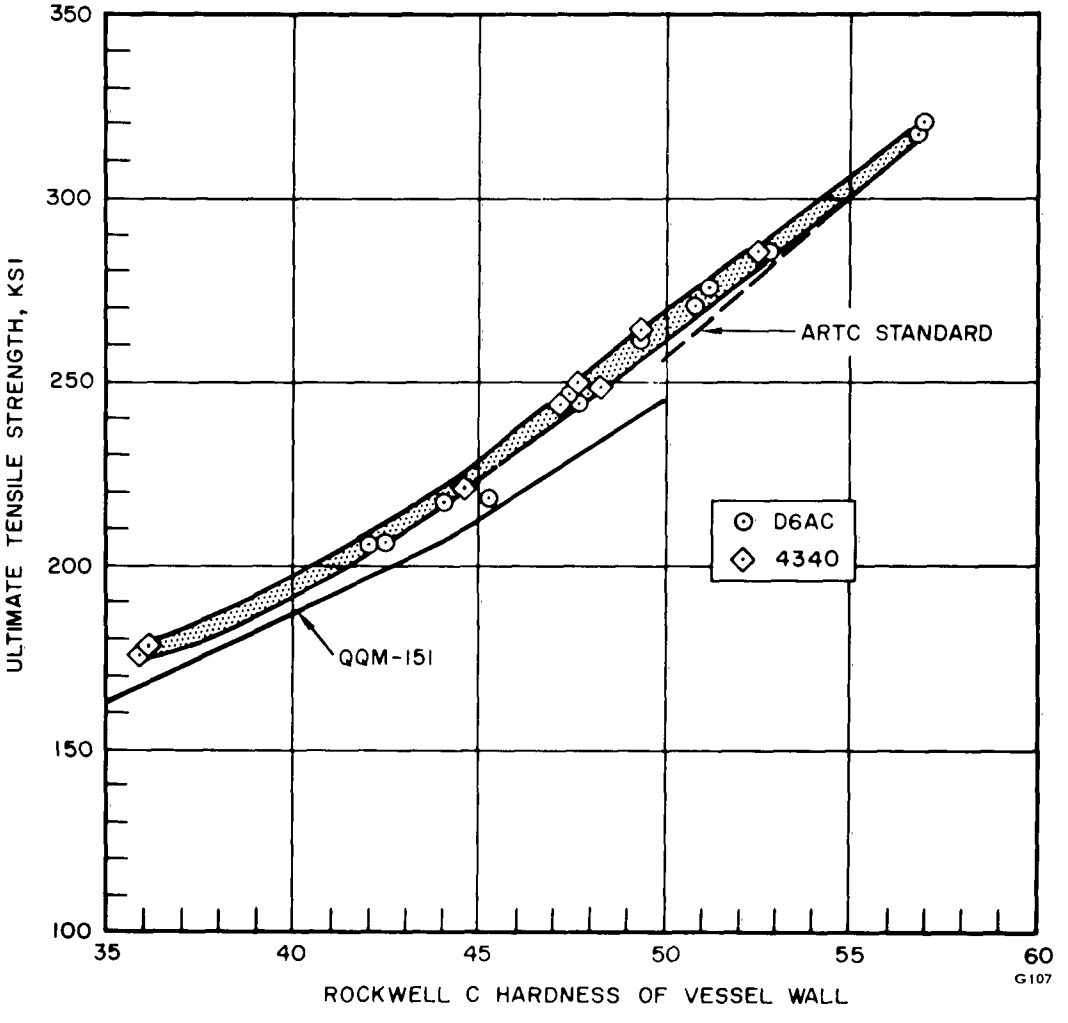


Figure 3. Hardness-Tensile Strength Correlation for 4340 and D6AC Steel from 1:0 Tests of Pressure Vessel Specimens

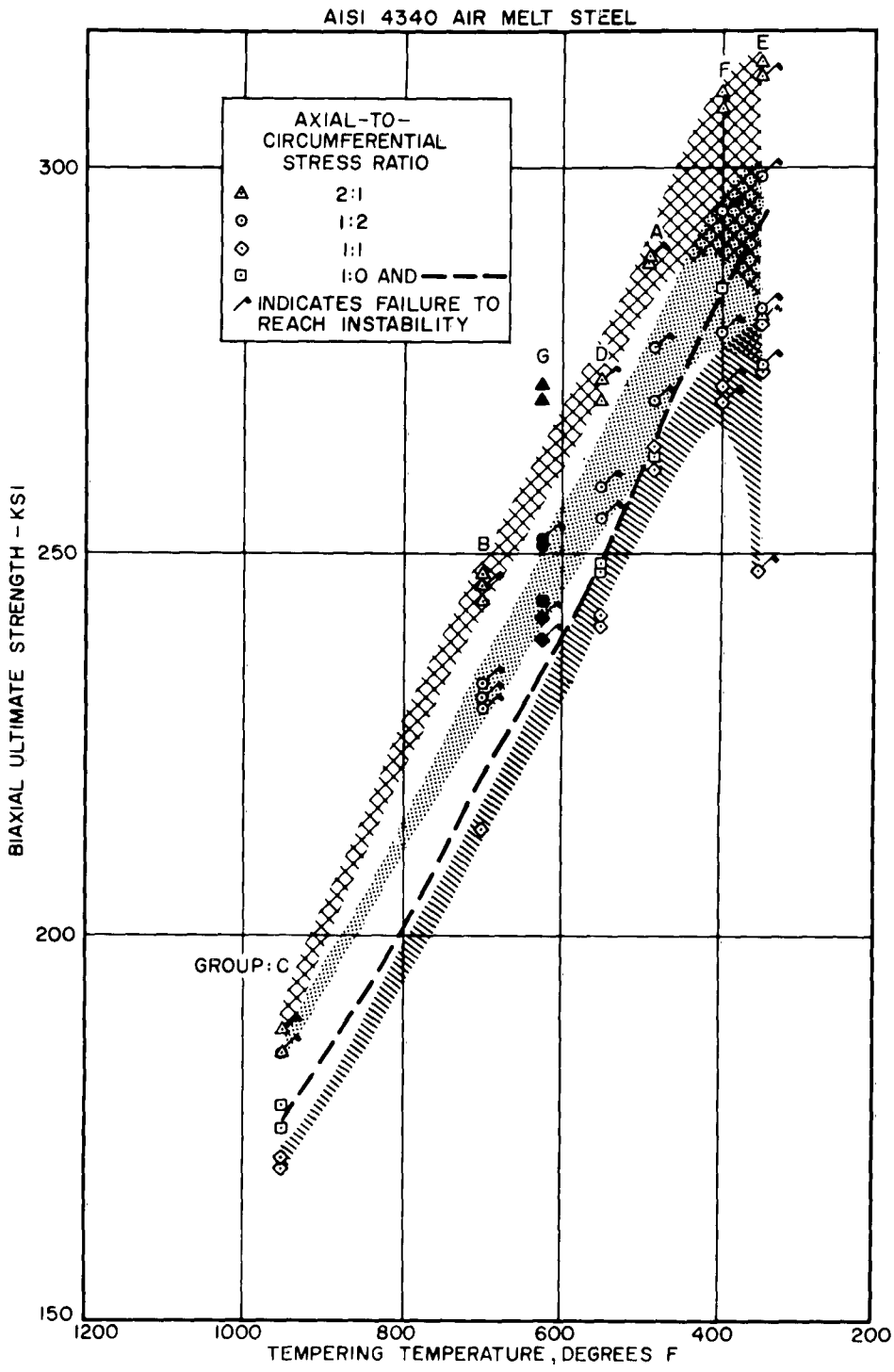


Figure 4. Nominal Ultimate Strength in Various Axial-to-Circumferential Biaxial Stress Fields for Air Melt AISI 4340 Steel

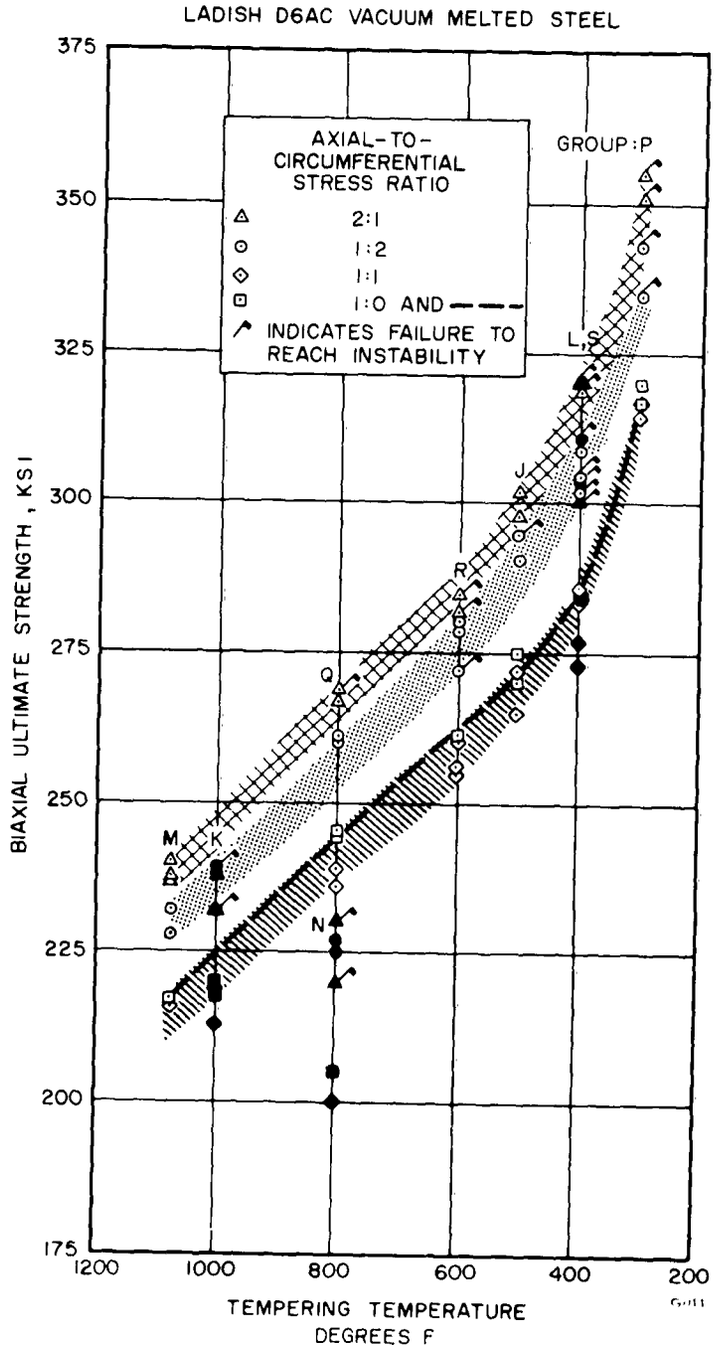


Figure 5. Nominal Ultimate Strength in Various Axial-to-Circumferential Biaxial Stress Fields for Vacuum Melted D6AC Steel

NUMBER OF SPECIMENS ACHIEVING TENSILE INSTABILITY (ANALYTIC MAXIMUM ON ENGINEERING STRESS-STRAIN DIAGRAM)				
STRESS FIELD AXIAL:CIRCUM-FERENTIAL	AIRMELT 4340 STEEL		VACUUM MELT D6AC STEEL	
	YES	NO	YES	NO
2:1	16	13	7	15
1:2	0	39	15	9
(PURE PRESSURE)				
1:1	16	8	19	0
1:0	6	0	12	0
(UNIAXIAL)				
0:1	3	2	1	0

Figure 6. Comparison of Air Melt 4340 and Vacuum Melt D6AC Steels on Attainment of Tensile Instability in Biaxial Stress Fields

J. D. Marble In relation to this question about flaw size, I can state that a 0.010 inch dia. pore in a 0.075 inch wall thickness (where the weld had been benched to equal thickness with the wall) was tolerated at a stress level of 300,000 psi, with no apparent change in size of the pore as revealed by x-ray before and after test.

J. E. Srawley Concerning Mr. Marble's remark about flaw size and this question of inspection, I would like to point out one thing, which I think we all realize. That is, for a given size flaw, the more nearly spherical it is the easier it is to find by inspection, and the less damaging it is. The more damaging it is, the more difficult it is to find by inspection. In other words, a round, blunt flaw is easy to find by inspection, while a tight, sharp crack of the same diameter is difficult to find by inspection.

A. G. Holms I believe that Dr. Srawley refers to the ability of X-rays to detect a relatively harmless class of defects, namely round pores, and that a more harmful class, namely cracks, are more difficult to detect. I would like to add that the methods of nondestructive testing are complimentary and that sonic and penetrant inspections are relatively poor for detecting pores but they become especially efficient for detecting cracks.

J. D. Marble I certainly agree upon this point of difficulty of inspection. One thing we have done, as you know, is to develop an ultrasonic procedure which did pick out the items which were harder to find by radiographic inspection. We have found in a few instances that defects which passed by our special ultrasonic inspection, did result in reduced fracture strength.

J. E. Srawley In regard to the notch tests which failed to show the 650 F tempering embrittlement, were these sharp notch tests?

G. K. Bhat These are K5, 8 and up to 12.5 we could not get to 17.5.

J. E. Srawley The second question relates to the high values shown by the biaxial tests at lower tempering temperatures, at least that's what it seemed to show to me. How would you interpret this with relation to the question of retained austenite which was discussed earlier in this conference?

G. K. Bhat We have tried to assess the amount of retained austenite. In the first place, we have designed the steel in such a manner that the Ms and M temperatures are high enough, and in the second place, the X-ray evidence showed that we have less than 1 percent retained austenite. As a matter of fact, the tests were negative. In all of our program we are at least making an attempt to keep the M temperature high enough so that we obviate the possibility of retained austenite.

G. Sachs It appears from this and other talks that many people attempt to obtain pertinent information from some test other than uniaxial tension; such as some spherical heads or bulges formed from flat sheet. A head is, of course, similar to a preformed bulge, and the stress state for both is near 1 to 1. The major interest, however, relates to the cylindrical portion of the case or the stress state 2:1. In addition to the rather expensive testing of model cases, a number of simpler tests are available and may be suitable for investigating the 2 to 1 stress state, such as a bead; a sheet specimen, stretch formed or otherwise laterally restrained, a preformed cup, etc.

A. Hurlich May I try to answer part of that. Because I limited myself to 15 minutes at the beginning, I just have time to cover some of these points that Dr. Sachs raised. I did point out that in our tests we did fatigue tests and rupture tests on full scale tanks and got basic data on the performance of the large structure. This is all well and good but it is too expensive to do very extensive tests of this type. We then went to the 4-inch wide axially loaded fatigue test specimen, using the same gauges and materials as we did on the full scale tanks, and duplicated the missile weld joint design. We did reproduce the fatigue behavior and the fracture characteristics that we got on the full-scale tanks at room temperature, at liquid nitrogen temperature, and at liquid hydrogen temperature. Then, because it cost about $50 to make the specimen and about $500 to run a complete test, we looked around for a still cheaper test method that would give us useful data to screen candidate materials and evaluate their applicability to this type of pressure vessel. What we now use are notched and unnotched tensile specimens and we employ the notched-unnotched tensile ratio as a criterion. Our notched specimen has somewhat different dimensions than Bill Brown's but gives generally the same type of data. We use the stress concentration factor calculated from the square root of A over R as 6.3, but by the new Neuber method it is 13.6, twice that plus one. We find that we correlate the notched-unnotched tensile ratio with the fatigue performance at the same testing temperature. When we have a notched-unnotched ratio that was essentially unity or higher, we had a predictably high fatigue life. When we had a low notched-unnotched ratio, the fatigue life was low, and the lower it was, the poorer was the fatigue life. We use the notched-unnotched tensile ratios as the first screening test and then conduct the fatigue test on the 4-inch wide specimen on the more promising materials. So I think this answers the question that Dr. Sachs raised. This recounts the development of a series of laboratory tests which can be used to evaluate the end product quite satisfactorily, at least in our thin-skinned tanks of the Atlas missile.

J. D. Marble As Dr. Sachs noted, he previously used some bulge tests which did simulate the 2:1 biaxial stress ratio. We have also used this type bulge test very successfully. I am sorry that I cannot describe our results; some of them are in the paper that I was expecting to give. There is a part of Dr. Sachs' question that I'd like to ask Dr. Bhat. Did not the 1:1 biaxial stress ratio tests which he performs exhibit the same yielding behavior and strengths as were recorded in the head of the full-scale rocket case made of the same alloy? Are you allowed to discuss that?

G. K. Bhat I think it does. We have actually two tests, one using these domes. In order to give you people who are cost conscious some idea of the cost, this test cost us less than a notch test. Actually the cost is about $7 with the strain gages on the dome, excluding manpower costs. We have also used the 5.7 inch, 27 inches long vessel to get our 2:1 and this test costs us about $30.

J. D. Marble I don't think you quite answered the question that I asked. The question was: How similar is the stress-strain and the yielding behavior in the full-scale rocket case dome to your hemispherical bulge test?

G. K. Bhat The full-scale vessel had too many openings, the Polaris 2nd stage case, but if you take strain gauge readings particularly at the apex, it did compare very well with the biaxial dome test. But if you take strain readings some other place it did not.

E. R. Mertz I noticed that in your cup test, what started out as something hemispherical ended up as something rather short-nosed. Did you make correction for this change in contour in calculating stresses?

G. K. Bhat We are attempting to make these corrections for ellipsoidal head shapes. This is why we have used this extrapolated values. In the hemispherical cup this correction is not indicated. We are talking to the stress analysts and trying to use some of the corrections they have informed us of.

N. L. Reed In your figure 9, Dr. Bhat, you show some results of testing after decarburization. I understand that you have either decarburized 0.003 or 0.006 inches. I would judge therefore, that the decarburization is from both sides of the sheet so that the metal, unaffected by decarburization, drops down to either 0.074 or 0.068 inches from the nominal thickness of 0.080 inches. Am I interpreting your graph correctly?

G. K. Bhat Yes.

J. Sheehan What function does cobalt play in the formulation of your steel?

G. K. Bhat I would like to defer that as to the next paper we are presenting shows the effect of cobalt. In the first place we believe that cobalt gives us a real fine structural matrix, and in order to do any high strength alloy development work, particularly increasing carbon, the need for cobalt in the matrix seems obvious

L. Schapiro Mr. Voth, among the many advantages you listed for the strip wound vessel was that three-D machining was not necessary. Since it is my understanding that three-D machining is not being applied to the cylindrical body of anybody's vessel but only to the end members, I assume that you inferred that there was not any three-D machining of end members required. Will you illustrate how the strip winding makes the end member?

R. J. Voth I don't recall putting that in the paper. The contemplated method of head fabrication is explosive forming of Chem-milled blanks to achieve the integral bosses, then resistance welding these heads to the cylindrical portion.

S. V. Arnold Do you coat the strip prior to the winding operation or coat the vessel afterwards?

R. J. Voth Never.

S. V. Arnold It occurred to me that you have what amounts to capillary passages between the strips. I wondered whether these might not channel moisture to the residually stressed areas around the spot welds and so promote stress corrosion cracking. Have you encountered this or checked for it?

R. J. Voth We have done no checking on this. There has been no evidence, to my knowledge, of stress corrosion cracking resulting in any ultimate failure at a value which we would consider a premature failure. Once the many parameters of variables had been ironed out, we had a variation in burst strength of approximately 6 to 7 percent in the latter stages of the program. The lowest, I think, in the last twelve chambers was a 269,000 psi hoop stress burst strength which I don't feel can be considered as a premature failure.

A. Hurlich With respect to Mr. Arnold's comments, faying surface stress corrosion does occur even in stainless steel and is a serious problem. I would anticipate that this could be a serious problem in wrapped cases that would have to be solved by applying a protective coating on the outside that would not permit any moisture to get in between the various layers.

J. F. Watson In addition to the advantages you mentioned, we have found one other very important advantage in the spiral wrap process when dealing with cold rolled materials. This advantage is that it is possible to cold roll the thinner gauges. Consider a .080 inch thick pressure vessel where you could use either eight layers each .010 inch thick in the spiral wrap concept, or one layer .080 inch thick in the more usual

technique. In the 300 series cold rolled stainless steels as well as grades such as AM 350 and AM 355, it will be found that the .010 inch thickness can be obtained at a much higher strength level than the .080 inch material.

J. A. Kies In hydrotests, where the burst pressure or burst stress is given, we are not told what the bulging or plastic deformation is. At the time of burst, the chamber usually has already had so much plastic strain that it would be inoperable. Therefore we ought to specify when we make these tests what the real criterion for usefulness is. A great deal of bulging prior to fracture may seem reassuring but it is probably not useful in service.

R. T. Voth This is true. I don't know whether anyone has ever tried to bulge razor blades before, but this material which we are using - is probably more brittle than razor blades. I will say that the elongation, as well as we could measure, was less than half of one percent. In this particular instance you will get the PL/AE stretch of the material under stress but you will get no plastic yielding because the material is not plastic. So in that instance you can design to ultimate strength of the material in as much as the yield and ultimate are identical.

J. A. Kies You said that this material is brittle and has less than 1 percent elongation. These two terms do not mean the same thing. This may be a notch tough material but one with a low static elongation.

R. T. Voth In addition to this particular question, we have seen that the G_c values of the material in other monolithic cases have had to be somewhere in the range of 900 to 1,000 to achieve good burst strength and to achieve the multiaxial strength in excess of the uniaxial tensile strength. The material in which we are working had a G_c value only of approximately 250, and maybe because of or in spite of this value we are still achieving burst strengths in the 300,000 psi range.

E. R. Mertz One point you just mentioned which I think is very worthwhile is the good dimensional control in the strip winding procedure. We have in the past used a similar type of thing and it has excellent concentricity, that is, the accuracy of the final product is as accurate as you can machine the mandrel. Inasmuch as the lathe turning operations can be within a few thousandths of an inch in concentricity, you can expect this in the final case since you get no heat-treating distortion and no warpage thereafter.

H. A. Jahnle There are methods of preventing stress corrosion around the weld. There are processes for metals such as AM 355 recommended by Allegheny Ludlum. These consist of post tempering treatments after welding. Another method we use is the planishing the weld zones immediately after welding, that is, a cold forging operation. There are a number of coatings available which will do an excellent job.

On bend ductility, although in a tensile coupon elongations of 1, 2 or 5 percent may be obtained in a 350,000 psi ultimate material, we can bend this material to a 3 or 4 t radius. This is fairly good.

I have one question about the multiple wrap. What problems do you have in localized buckling between resistance welds? How do you know that the seven or eight sheets are resisting the internal pressure equally at all times?

R. T. Voth I think you noticed on the first slide, that there was a considerable difference between inside and outside layers stress level. This has been attributed to deflection of the wrapping mandrel due to the wrap tension which is applied. We are using approximately 10,000 psi wrapping tension and we have not as yet worked out the final variation in wrapping tension from layer to layer to achieve uniform distribution of stress. We are sure that by either analytical means or by testing, we will be able to come up with a variation in this wrapping tension to achieve uniform distribution through the many laminations.

A. Hurlich I can add something to that because we've made a number of 4-ply vessels out of cold-rolled 301 and after fracture you can see the Lüders lines and plastic deformation around each spot weld. If you break apart the four layers you will see exactly the same deformation pattern around each and every spot weld so that every layer and every spot weld is carrying a pretty uniform load compared to all the other spot welds in the structure.

H. A. Jahnle We have also made multiple wrapped cases where buckling has been of concern. Test results have been fairly good, though. One of the problems here is in making sure that you have a good resistance weld through more than 2 thicknesses of metal. We use an automatic control, Monautronic, which guarantees a good weld.

R. D. Lula I would like to make a short comparison between cold rolled Type 301 and the cold rolled Ph steels. The cold rolled Ph steels can develop much higher strength than Type 301. In fact, the highest strength attainable in the Ph steels is at least 100,000 psi higher than in Type 301. The same strength can be attained in Ph steels with the smaller amount of reduction which is a definite processing advantage. Elongation of cold rolled Ph steels also is considerably higher than in Type 301.

R. J. Voth On the next to the last slide your burst strengths of approximately 350,000 psi were corrected for bulging, but were there any corrections made for the length consideration of the cylinder? You mentioned earlier in your talk that the diameter on watermelon cylinders was about 9.4 and the length of the cylinder was about 9.5 and with a hemispherical head this would make it nearly a sphere with a PR/2t rather than a PR/t stress. Do you have that correction in there?

E. C. Schneider This correction is in there. One thing I would like to tell you is this. This bulge radius sometimes will follow the full length of the cylindrical section, other times it will not. You cannot take this bulge as applying basically the L/d of the vessel. You have to look at the bulge itself, sometimes the length of the bulge will only occur over half the cylinder length, so this correction is in there and compensated for the particular vessel.

L. Schapiro Referring to that same table of eight values, were all of them the same type vessel?

E. C. Schneider Yes, they were all the same diameter vessels. The length was not exactly the same in each one. They probably varied, give or take, an ich or two, with girth welds at the center.

L. Schapiro Did the bulge span this weld or did it occur on one side or the other, or both sides?

E. C. Schneider The bulge did not uniformly span the girth weld. At the girth weld the thickness of the vessel was increased. The entire length of the cylinder, including the girth weld, bulged in some cases while in others it only bulged between the weld and the dome.

J. Hamaker Perhaps we should recall a point that Mr. Powell mentioned in his report. The H-11 welding wire is lower in carbon content than the sheet; this was worked out several years ago. It is the problem that Prof. Adams touched on the other day: we should match the welding wire properties and not the composition. This has been done for H-11.

L. Schapiro In connection with this I assume the weld bead is not uniformly the same thickness as the wall in spite of the ductility that you are speaking of, and this is why I assume that there might be some rigidity there.

G. Sachs I have looked carefully at the relations between notch test data and burst pressure presented by the speaker. It is clearly revealed that these fall into two distinctly different groups, namely for the heavily decarburized and only slightly decarburized cases, respectively. While these notch test data and burst tests correlate reasonably well for the slightly decarburized steels, they fail to do so for the heavily decarburized steels (see Fig. 15 of my talk). For these, high burst

strength is still associated with a low notch strength. This is explained by the lack of decarburization in the notch bottom. The decarb consequently considerably reduces the burst strength but only slightly reduces the notch strength.

W. J. Murphy First of all, in the tests that we run in our laboratory for the measurement of fracture tougness, notching is done after heat-treatment so that even when we are testing for the effect of decarburization we do not have decarburization at the notch roots. In these tests the decarburization on the sheet surfaces across which the crack is running will produce an increase in fracture toughness. In the second place, in the vessels tested, extensive slow crack growth occurred prior to the onset of unstable crack propagation. And obviously, if you have slow crack growth you do not have decarburization at the tips of the crack leading to unstable crack propagation. Therefore, the fracture situation in the model pressure vessels was, in my opinion, very similar to that in the laboratory center-notch tension tests.

W. F. Brown It escapes me as to why all these tests are being made. From one standpoint I realize that the development of a particular pressure vessel has to be preceded by some model testing. However, from this model testing has come very little, if any, fundamental information regarding the use of proposed fracture mechanics concepts for finding safe working stresses in pressure vessels. This is true even when the tests were presumably designed specifically for this purpose. I want to ask the present speaker if he made any attempt to determine the initial flaw sizes or estimates of slow crack growth which might have occurred. If this was done, were attempts made to calculate the fracture toughness from the pressure vessel tests and to compare the values with those of laboratory specimens? I have another question which may come out of your answer to the first. Could you or could you not have found any defects by your careful inspection technique?

W. J. Murphy The report which you received includes a very large section on the examination of the fracture initiation sites in the model pressure vessels. In most cases fracture initiation could be traced back to a defect of some sort. I can list several of them: we had three vessels which failed at magnaflux arc burns, we had about 12 vessels which failed in the weld metal of the longitudinal or the girth welds, and we had a peculiar case in one vessel in which some austenitic material on the inside sheet surface of one of these vessels initiated failure. On examining these initiation sites, most of which were relatively small, we could observe an area of plane strain fracture which occured as a result of a slow crack growth from these small defects. Using the length of this plane-strain crack and the burst stress, I was able to calculate a K_C for some of the vessels. I then compared these K_C's with the K_C's obtained from the laboratory center notch tension tests and I did obtain a rough correlation. In only one case was a detectable defect responsible for

initiating failure and that was missed when the X-ray films were read. In all other cases the defects were metallurgical in nature and not detectable by nondestructive inspection methods. For example, a magnaflux arc strike will not necessarily be revealed by X-ray inspection.

A. Hurlich I would like to discuss something at this point because I just cannot restrain myself. I made the plea last night when I said God help the United States if we use brittle materials. There have been many experiences in the rocket motor casing development where, after something has failed, we go back to the original X-rays defect and say this caused the failure; but this pinpoint escaped the best, most careful nondestructive inspection method we now possess. I think this again highlights the fact that brittle materials kill you. We do have suitable inspection methods today that will weed out the minute defects which prove so catastrophic in nucleating fracture in brittle materials. I am also reminded of the fact that during World War II, in the production of Armor-piercing shot, these .60 carbon steel armor-piercing shot were heat treated to Rockwell C-55 and higher. They were then carefully inspected and found free of all flaws, loaded into ammunition and put into storage and then sent around the world for use by troops. We had serious epidemics of fracture of these shot in storage. The noses would suddenly pop off due to the build up of the residual stresses and their relief by fracture nucleating at an inclusion or at an interface between carbide and martensite and things of this sort. I am willing to stake my bottom dollar that many of these good cases we are making of the ultra high-strength steels that we carefully inspect and put in storage, if we have to take them out within five years and use them we will have a significant percentage of cracked cases.

J. Hamaker I would like to point out that current ultra high strength steels are much more sophisticated than those used in shot. These new steels, which I was discussing yesterday are air hardened not quenched, and have secondary hardening characteristics. We are pretty well convinced that in order to go up to higher strength levels, we will have to take advantage of these characteristics. Thus, tempering will always be above 1000 F, for any strength level, at which temperatures stress relief is very adequate, up to 90 percent. This is entirely diferent from low alloy materials liquid quenched and tempered at 400, 500, or 600 F for similar strength levels. Residual hardening and other stresses may be as much as 50 percent of the yield strength. Secondary hardening also permits transformation of unstable retained austenite, thorough baking out of hydrogen and other means of potential embrittlement. The successful H-11 rocket cases you have been hearing about this morning were all tempered above 1000 F.

F. Richmond In answering Dr. Sachs's question about the decarburization of the test samples versus the decarb existing in samples cut from the vessel, the principle of cutting specimens out of the case after failure was defended by Mr. Murphy by the statement that in fast crack propagation, it does not matter whether you decarburize or not. But this means that all this talk about stress concentration factors, in specimen design is relatively unimportant since if all you are interested in is fast crack propagation, the stress concentration factor is the same - or nearly so - at the base of the running crack. But is not the slow crack propagation which eventually results in a flaw large enough to generate the fast crack also important? Would not this slow crack propagation be affected by the depth of decarburization existing in the test specimen or case?

W. J. Murphy I do not think there is any question about the fact that the slow crack propagation phase of this thing is important and that decarburization may have an effect on slow crack growth. I think that the fact that this is being given careful attention has been brought out in some of the papers that have been presented this week.

E. C. Schneider In all these cases there is a longitudinal weld as well as a girth weld, and the question I have is this since so many of these cases fail near the longitudinal weld, either in the weld or close to the weld and we know that any mismatch or peaking in the longitudinal weld will cause very high normal stress increases. Do you think that the results you obtained would have been grossly changed if you had eliminated the longitudinal weld and made a vessel with only girth welds? I would like to comment on Mr. Brown's question before. The value of the subscale vessel is also quite important from the fabrication point of view in establishing what defects you get from those vessels during fabrication. When you talk to production people and mention the G_c values and crack lengths all you get is a completely blank stare. So that you have to run these tests and find out statistically and practically what you do get and how these materials will behave when handled in a shop.

W. H. Sharp During this three day conference, we have primarily discussed steels which are known to show brittle behavior at high strength levels. It seems to me that those attending this conference should be more concerned about where we are going with materials of more ductile behavior. Two materials which display a higher measure of ductility at the higher strength levels are: (1) the 20-25 percent nickel (iron base) alloys recently developed by Bieber and (2) the titanium alloys.

E. R. Mertz From the comments expressed during the course of this conference, one is inclined to conclude that high burst strength is the major criteria for solid rocket cases. This is likely to be misleading, because certainly in a solid rocket that is loaded with propellant

we cannot accommodate much deformation without loss of bond between the propellant and the case, so that our real criterion is elastic behavior and not plastic behavior.

G. Sachs I would like to suggest that we start to worry about the ground rules for model testing. In order to discuss this problem, I would like to suggest two items, namely:

(1) The wall of the model should be preferably the same as that of the full size case.

(2) The case should be large enough to be "thinwalled", i.e. the wall thickness should not exceed a few percent of the diameter.

APPENDIX A

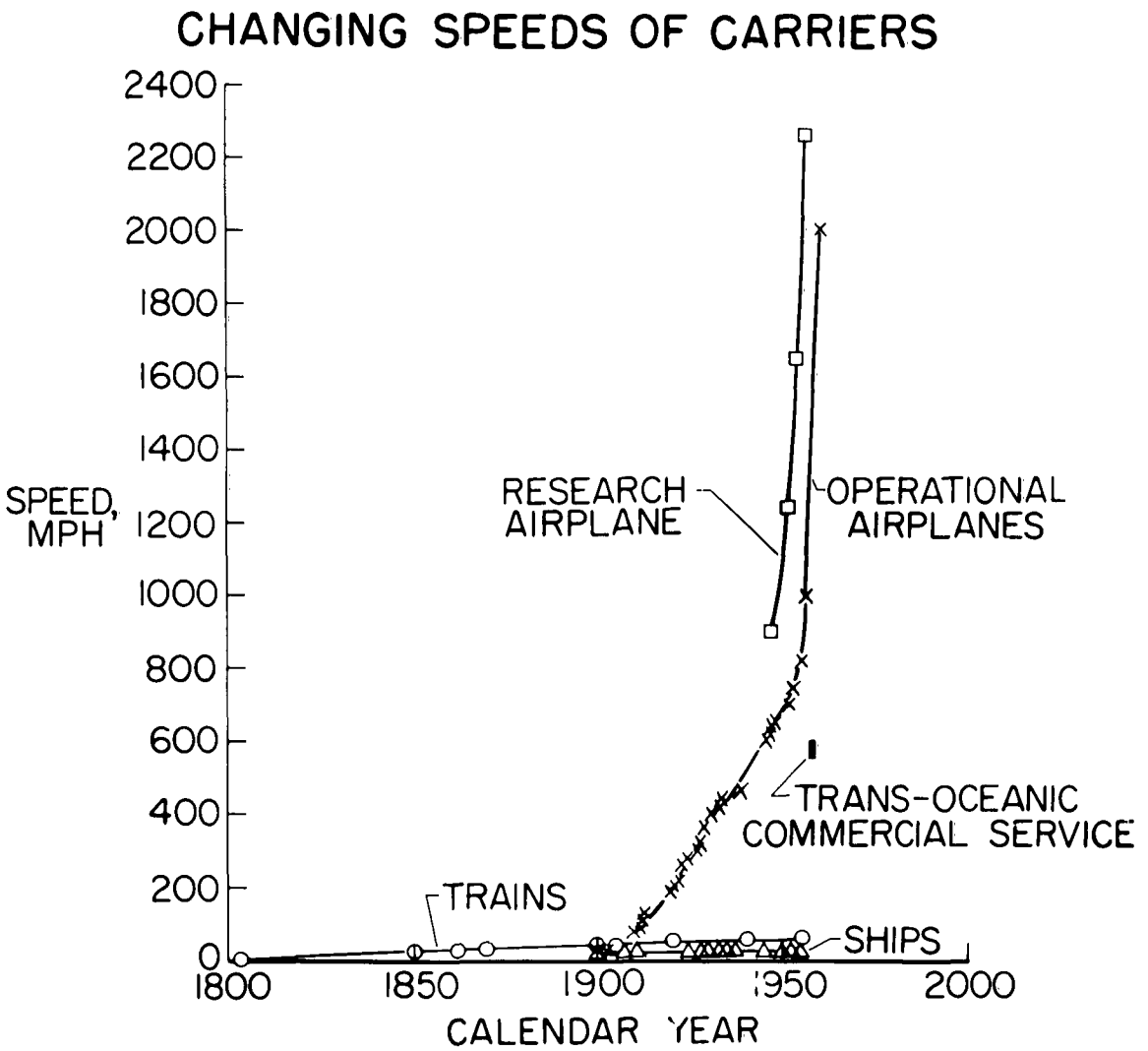

CHANGING SPEEDS OF CARRIERS
2400
2200
2000
1800
1600
1400
1200
1000
800
600
400
200
0
SPEED, MPH
RESEARCH AIRPLANE
OPERATIONAL AIRPLANES
TRANS-OCEANIC COMMERCIAL SERVICE
TRAINS
SHIPS
1800
1850
1900
1950
2000
CALENDAR YEAR

Figure 1

THE MATERIALS PROBLEMS OF THE SUPERSONIC TRANSPORT

John Stack
NASA Langley Research Center

Transportation is so much a primary lubricant for modern technological development we must constantly seek to the improvement of its various forms in terms of performance and efficiency. The rate of technological development parallels closely the rate of performance improvement in commercial transport. Figure 1 illustrates the rate of performance improvement with commercial transport since the period of about 1800, the beginning of the industrial revolution. It is immediately apparent that the surface modes of transportation had been fully exploited performancewise by about the period of 1900. One might ask immediately why has there been no performance improvement in the surface modes of transport. Could it have been that the rise of the airplane had halted development, or was there something fundamental that prevented the further development? I rather think it is because there is something fundamental in the modes of surface transport that prevented their further performance improvement. The land vehicle is dependent upon the wheel. Its driving and control forces must be transmitted through surface contact of the wheel with the ground. It is this need for fairly firm contact between the surface vehicle and the ground that imposes a rather fundamental performance limit. As the speed is increased, dynamic disturbances due to unevenness of the surface effectively reduce the firmness of the contact between the wheel and the surface so that both control and driving power become limited and finally aerodynamic forces become so large as to become the controlling factor. The practical upper limit speed for land transport is shown by the figure to have been reached late in the last century. Similarly, the surface vessel has the same type of performance history as the land vehicle. The fundamental limit is encountered in the so-called hump speed. At this speed, the wave patterns set up absorb so much power that the practical speed limit is reached. With these fundamental limits, it appears that transport performance would have been limited to about the speed performance of 1900 had it not been for the airplane. The speed performance increase of the airplane, as you can see from this chart, has been extremely rapid. It has, of course, been fostered by military developments occasioned by the need for survival in the two major wars in this century. This military sponsorship of technological development is not new to our times. One needs only to recall that the principles of road building developed by the Romans did not come about so that the populace could take a Sunday drive in their chariots!

Speed performance becomes very important when the transport of valuable goods is concerned, and by this I mean people and goods which have a large amount of high-skill man-hours involved in their production. Goods where the raw material becomes a smaller part of the cost and are rather expensive because of the high input of the

energy of man are the classes of things that require high-speed performance for transport.

From the shape of the curve of aircraft speed performance, we apparently are not against any fundamental limits in terms of the commercial air transport, military operational aircraft having already achieved substantially better performance than the best of our modern commercial transports. The speed of the modern jet transports is shown by the small block.

There is a major difference, however, between the military application and the commercial transport. The high cost of such vehicles requires that, in commercial service, they have a long, useful life. The fact that they must operate in and out of commercial areas imposes additional limitations not present for the military vehicle. The military vehicle can usually be a specialized single design point vehicle. The bomber, for example, is required to deliver a particular load the greatest distance at the highest speed. It does not have to operate in and out of densely populated commercial areas. The military machine is one which is used primarily for training and held in readiness, except for training needs, against the day it is needed for actual combat operations. In this sense it is like the equipment of a fire department rather than like the commercial truck on the highway. The commercial transport must be operable at a low cost, on the order of 2 cents per seat mile direct operating cost. The military machine has no such limits imposed. At these operating costs, the commercial machine must have a useful life in actual flying service of the order of 30,000 hours at least, and preferably 50,000 hours. The long life requirement imposes on the commercial transport a far more serious materials problem than need be the case for the military machine of equal speed.

Before discussing these materials problems, however, it is well to examine the state-of-the-art in other areas. Only if the state-of-the-art in the other areas is sufficiently advanced do the materials problems become critical. Figure 2 illustrates the factors affecting flight efficiency. These are the energy per pound of fuel, the structural weight, the propulsion efficiency, and the aerodynamic efficiency. I will treat these in the reverse order. The status with respect to aerodynamic efficiency is shown in figure 3, which is a plot of the lift-to-drag ratio against the cruise Mach number. Now the overall aerodynamic efficiency is represented by the product of the lift-to-drag ratio and the speed or Mach number. The present-day subsonic jets have lift-to-drag ratios on the order of 22 at Mach numbers on the order of 0.8. The product is 17.6. We cannot hope to meet the commercial operating costs unless we achieve an aerodynamic efficiency at least this good. I say at least this good because the supersonic machines will cost substantially more than the present jets. They should be better. There is shown on the figure the lift-to-drag ratios of the present-day supersonic aircraft. These are types now flying, and quite obviously these values are not adequate for a commercial

FACTORS AFFECTING FLIGHT EFFICIENCY

ENERGY PER POUND OF FUEL

STRUCTURAL WEIGHT

PROPULSION EFFICIENCY

AERODYNAMIC EFFICIENCY

Figure 2

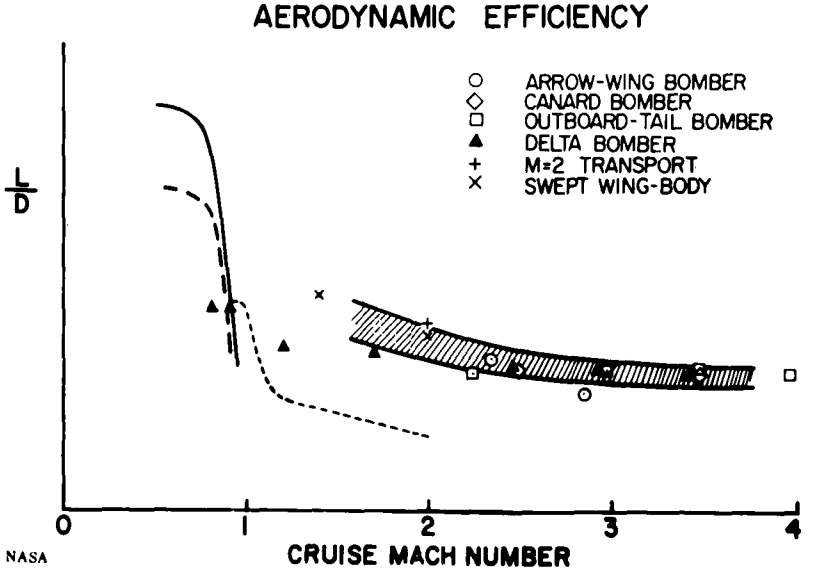


Figure 3

machine. However, in the last 6 to 8 years, as a result of extensive research, the lift-to-drag ratios have been raised to the area shown by the shaded band. A very large number of configurations have been investigated seeking to determine what are the properties that lead to a sufficiently high lift-to-drag ratio to become commercially interesting as well as militarily useful from a range-radius viewpoint. If you examine this figure in terms of the product of lift-to-drag ratio times Mach number, you see immediately that at Mach numbers of 1.5 the lift-to-drag ratio—Mach number product is significantly less than that achieved by the present jets. Obviously, this cannot do.

Because of the relatively small variation of the lift-to-drag ratio with Mach number at the supersonic values of the Mach number, it is apparent that sufficiently high values of the aerodynamic efficiency factor can be achieved if the cruise Mach number chosen is high.

On this basis, then, we can establish that the Mach number for the transport should be in the range of 2 to 3. To conclude that the Mach number should be between 2 and 3 is a general but very insufficient conclusion because the particular Mach number can influence the type of configuration. For example, figure 4 illustrates a class of configuration that offers extremely high aerodynamic efficiency in the Mach number range around 2 and below. One notes the high sweep of the wings, the arrow-like configuration, the imbedded engines in the highly area-ruled body-wing juncture. This kind of a configuration has a wave drag that is very nearly as low as the wave drag for the idealized streamline body of the same effective fineness ratio. As Mach number is increased, however, the low drag properties of the wing are lost as the Mach waves approach the same slope as the wing leading edge. One must then look for other types of configuration. In the research that has been done to date, figure 5 illustrates the type of configuration suitable in the Mach number range 2.5 and above, perhaps, let us say, up to 4. Beyond Mach number 4, figure 6 illustrates a possible type of configuration. You will note immediately that these three classes of configurations bear little in common structurally. There are many other difficulties with these configurations related to their landing and their take-offs which I shall discuss a little later.

The state-of-the-art with respect to propulsion efficiency is fairly well advanced. This is illustrated by figure 7. The turbojet or turbofan engines fit the speed range to Mach numbers of the order of 3. As Mach number 4 is approached, the dynamic compression of the air is so great the compressor cannot be used and the engine becomes a pure ramjet, and auxiliary means would be required for landing and take-off. The important point here, however, is that when the engine is optimized for its cruise Mach number we can obtain propulsion efficiencies exceeding those now being obtained. Again, because of the high cost of these machines, it is not safe for us to sit back and assume that the advantage in propulsion efficiency can offset some of the other disadvantages. I must

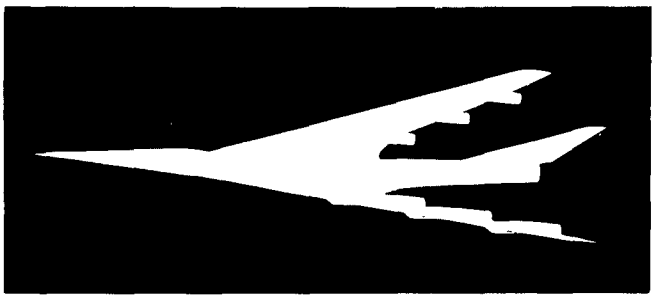


Figure 4

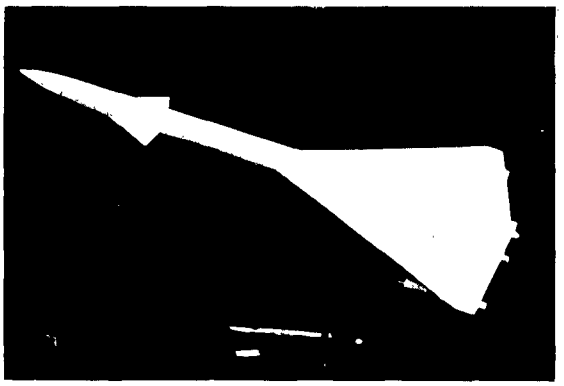


Figure 5

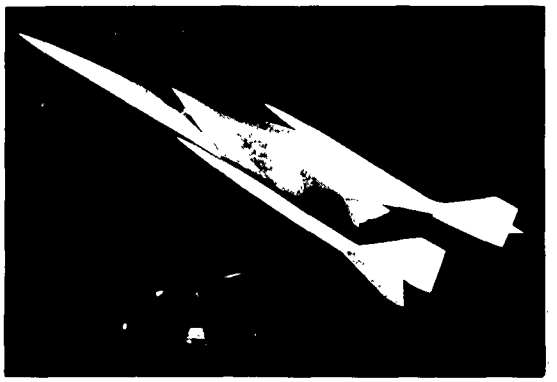


Figure 6

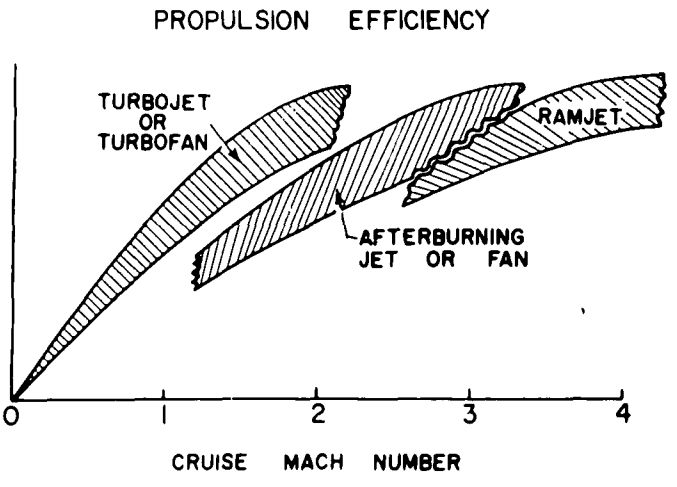


Figure 7

emphasize that better overall propulsion and aerodynamic efficiencies than those for present jet aircraft should be and are achievable.

A typical flight plan of such an airplane on the New York to Paris run is illustrated in figure 8. The airplane will take off and climb to a high altitude at subsonic speeds and then accelerate through Mach number 1, and finish the climb to its cruise speed and altitude for the journey. On approach to destination, the engines would be throttled back and the airplane would use a maximum ground gaining descent. The actual descent would probably be started 400 or more miles away from destination. The airplane may be required to hold for a substantial period, perhaps on the order of 30 minutes, at a low altitude near its destination dependent upon weather or traffic conditions. We cannot neglect the problems of take-off and climb to cruise speed and altitude and the problems of letdown. We are in rather poor position when one considers climbout problems and the holding and landing problems. The configurations so far developed lack acceptable properties for these "off-design" conditions.

Supersonic aircraft emit, as you know, a shock wave, the so-called sonic boom. Substantial pressures occur in this shock wave. These pressures are capable of doing great damage to buildings when the flight at supersonic speeds is at too low an altitude. All of the existing information indicates that we shall probably have to climb at subsonic speeds until we reach 45,000 feet. Some of the configurations that I have shown you are incapable of subsonic flight above 30,000 feet, and this is simply because the drag associated with the production of lift at the high angles of attack required is too great. There are other problems, too, associated with the landing. These types of configurations have a low lift-curve slope, that is, a low slope of the lift plotted against angle. Landing angles sufficiently great to permit full realization of the maximum lift of the wings cannot be obtained because of striking the tail on the ground. This means that the landing speeds go up enormously. Similarly, the take-off speeds in such configurations would be high. Landing and take-off speeds approaching 200 knots could be required. Entirely apart from the safety of landing and take-off at such speeds, the length of airport runways would become prohibitive and the land required at each end of the runway would be of the order of 5 miles.

It is interesting to examine the fuel requirements for such configurations as we have just discussed. Figure 9 shows the percentage of total fuel consumed and the fuel flow rates in pounds per hour for the various segments of the Mach 3 New York-Paris flight plan. Looking first at total fuel consumed, you can see immediately that 40 percent of the total fuel onboard is consumed in the first 350 miles of the trip. This is merely the take-off and climbout to attain cruise speed and altitude. In this part of the flight, fuel pumping rates exceeding 200,000 pounds per hour would occur.

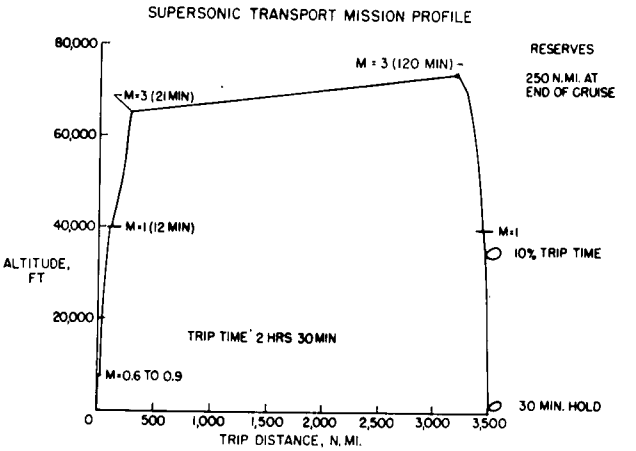


Figure 8

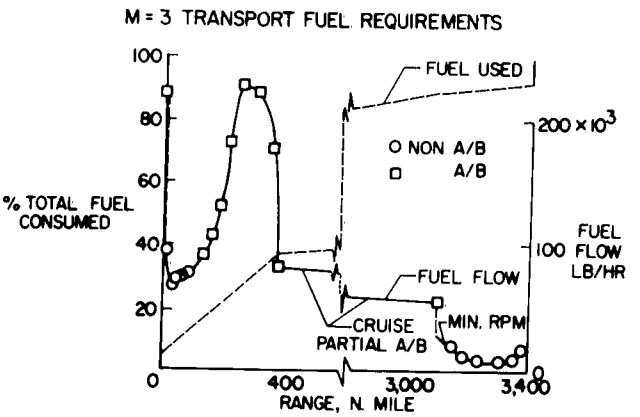


Figure 9

We can cruise with overall flight efficiencies perhaps better than we are obtaining with the present jet transport, but we are not meeting any of the other requirements, the so-called "off-design" requirements, as landing and take-off. If we had one engine out at midrange, we would have to come down to low altitudes, perhaps on the order of 30,000 feet, and cruise at subsonic speed. This "off-design" is very costly on fuel because it is "off design" for both airplane and engine. Under certain conditions, one could not consider proceeding to the ultimate destination but would have to seek an alternate.

At this point, the position in terms of the state-of-the-art might be briefly summarized by saying that if the mission involved flight at design supersonic speed and altitude only, and no emergencies occurred, intercontinental ranges of commercial interest and importance can be readily achieved. The ladders by which the airplane climbs to its supersonic cruise speed and altitude and descends therefrom, however, have broken or weak rungs. It is the "off-design" operation that creates a large part of the remaining difficulties, and the principal characteristic of this "off-design" area is the necessity for operation of optimized supersonic configurations at subsonic speeds.

There are solutions to these problems, and perhaps the best way to introduce the idea of the type of solution is to consider the configuration characteristics required by subsonic flows as compared to those required by supersonic flows. At subsonic speeds, drag is produced by two sources: skin friction and drag due to lift, called induced drag. When one considers skin-friction drag, one looks for the largest volume for the minimum surface area. From simple geometry this comes out, of course, to be a sphere. Now it is well known that the sphere is a shape that has high peak pressures followed by high recovery pressures on the aft end. Because of the energy taken out in the skin-friction layer, the airstream does not have sufficient energy to achieve the theoretical recovery pressures on the aft end and the flow separates; a very disturbed wake and very high drag occur. To correct this, the sphere is stretched in the direction of flight, doing enough stretching to reduce the peak pressures so that the flow adheres to the surface. An elongated sphere, the streamline body with which you are all familiar, is then the suitable body shape. At subsonic speeds, the optimum fineness ratio of this body, that is, the length divided by its diameter is in the range of 3 up to 6.

The drag due to lift is a consequence of the downward component of velocity imparted to the air by the wings, as the reaction to the lift force. When the airplane passes any given point, it leaves in the atmosphere a downward component of velocity. The kinetic energy represented by this downward component of velocity is energy that is not recoverable to the system and appears in the system as drag. The energy being a velocity square function, it is necessary to keep that downward component of velocity as small as possible, and we do this

by leaning on as large a mass of air as possible so that the downward component of velocity is a minimum. This leads to wings of great span that reach out to contact a large mass of air. So at subsonic speed, now, we have an overall configuration that is in the fineness-ratio range of 3 to 6, with wings of great span.

On approaching or exceeding Mach number 1, it is necessary now to strike a balance between three drag-producing sources: skin friction as before, drag due to lift as before, and now shock-wave drag. Shock-wave drag is proportional to the thickness squared. Now to reduce the shock-wave drag, the thickness ratio must be reduced. To accomplish this, the fuselage is further stretched in the flight direction, and we continue this stretching process until we reach a point where any further stretching would give a skin-friction addition that is more than the wave-drag reduction obtained by the thinning due to the stretching out process. Theory and experiment have shown that the optimum fineness ratio for the supersonic speed is of the order of 11 to 14 as compared to the 3 to 6 values for subsonic speed. Similarly, the wing thickness ratios must be reduced. The reduction of the wing thickness ratio reduces the depth available for structure so that it becomes necessary to reduce the wing-root bending moments. The wing-root bending moments are reduced by reducing the span, and the thickness ratio is reduced by increasing the chord. A considerable amount of sweepback is used which effectively reduces the aerodynamic thickness ratio. The supersonic machine, thus, is one that has fineness ratios on the order of 12 to 14 with wings of small span, very large chord, and high sweepback. The subsonic machine ideally is one that has fineness ratios of the order of 3 to 6 and wings which stretch out to great span. There is then an incompatibility of configuration for the two flow regimes.

The problem then becomes one of making the configuration compatible with the flow laws. It quite obviously requires variable geometry of the configuration. Now at first glance, variable geometry of the configuration might seem like a very radical idea. We have, however, been using variable geometry in aircraft for many, many years as witness the tremendous flaps on our present jet transports. This form of variable geometry has been used to reduce landing and take-off speeds to safe, reasonable values. A different kind of variable geometry appears to be required, and this form of variable geometry is variable sweep of the wings. A first step in this direction is illustrated by figure 10. The supersonic configuration is shown in the upper part. The landing take-off and subsonic climb configuration is shown in the lower part. The swept forward position corresponds to the "off-design" flight regime.

Variable sweep is not new. Two such aircraft have been built and flown. One was the research airplane X-5. This airplane varied its wing sweep from 30° to 60° and has been

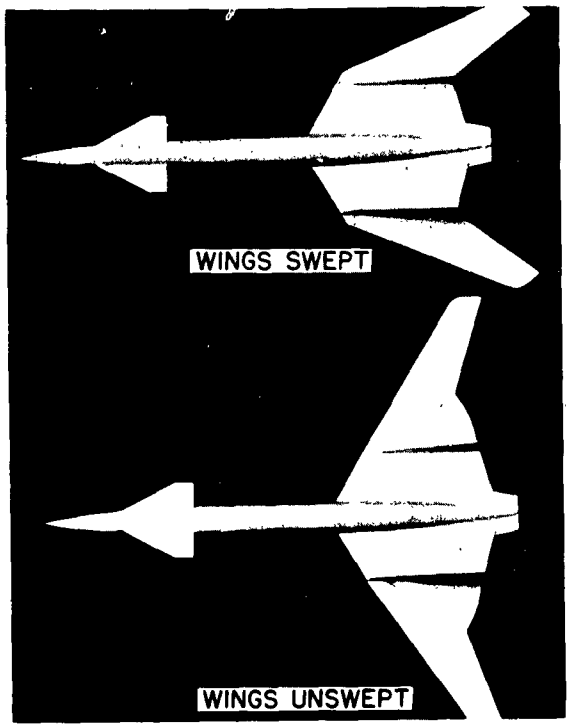


Figure 10

STRUCTURAL AND MATERIALS PROBLEMS

1. TYPE OF CONSTRUCTION

2. AVAILABLE MATERIALS

3. GENERAL PROBLEM AREAS
   (a) FATIGUE
   (b) CREEP

4. SPECIAL PROBLEM AREAS
   (a) AIR CONDITIONING
   (b) CONSTRUCTION COSTS

Figure 11

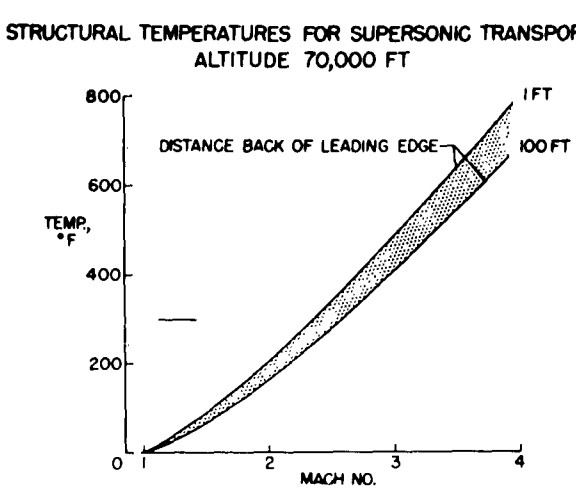


Figure 12

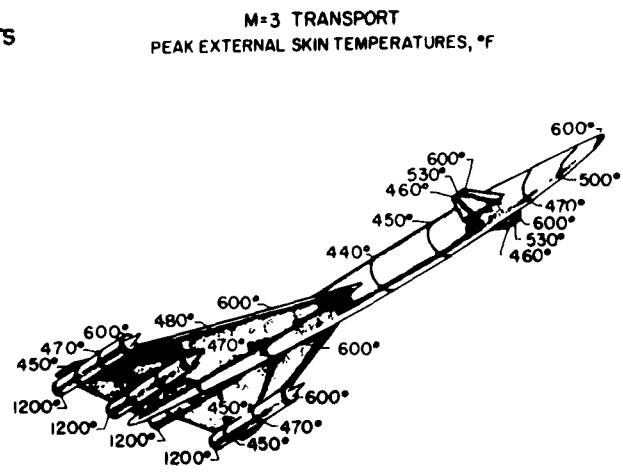


Figure 13

through extensive flight tests. Another was a Navy airplane, F-10F. This was built as an operational airplane. At the time it was built, the engine thrusts were not really adequate to provide supersonic velocity. Afterburner development was not very advanced. The machine was essentially a subsonic machine and as such had only small need for this class of variable geometry. However, both of these machines demonstrated the feasibility of variable sweep in flight. One practical difficulty occurred with both of these machines. It was necessary to move the wing fore and aft as the sweep changed in order to maintain the correct relation of the center of gravity and center of pressure of the airplane for stability. Through recent research, this difficulty has been overcome so that proper stability can now be maintained without fore and aft movement of the wings. With variable sweep of the wings as illustrated here, and with turbofan engines, we can meet the take-off, the climbout, the landing, and the holding requirements every bit as well as they are presently being met with subsonic aircraft, and we can achieve the configuration that is needed for the supersonic cruise.

The structural and materials problems of this type aircraft are really new. While an enormous amount of work has been done with high-temperature materials, much of the work has been concentrated on the problems within the engines and, more recently, with the problems of reentry. The area for the commercial supersonic transport needs considerably more work. Figure 11 lists some of the problem areas. These are: type of construction; the available materials; the general problem areas, such as fatigue and creep; and then special problem areas which have to do with air conditioning, construction costs, and so forth. To fix the range of temperatures with which we are concerned, figure 12 gives a plot of temperature against Mach number for an altitude of 70,000 feet. It varies from the nose to the tail of the airplane by a significant amount as indicated by the shaded band. The upper limit is the temperature about 1 foot back of the nose, the lower limit about 100 feet back of the nose. The horizontal line on the chart illustrates the temperature at 300°, a kind of presumed limit for aluminum, and this corresponds to a Mach number of 2.3.

Temperature contours for a typical configuration at cruise altitudes and Mach number 3 are illustrated in figure 13. The highest temperatures occur, of course, in the engine and at the rear of the engine installation structure. We have a considerable experience background with this problem because the temperatures in these areas are not too different from those existing for the similar parts of existing machines. For the main airframe structure, however, for which the temperatures encountered in steady flight will attain values of 450° to 600° F and with consequent temperature gradients, there is no experience background.

The design conditions for the supersonic transport differ in important respects from those for the subsonic machines in current

use. Figure 14 illustrates some of these differences. The supersonic machine will be substantially larger and heavier. It will be subjected to operation over very much greater speed and altitude ranges, and totally new and different is the wide materials temperature range.

Various types of construction have been studied. Neglecting for the moment the special problem areas associated with a long life requirement such as fatigue, creep, and loss of strength on prolonged exposure to high temperatures, figure 15 illustrates the relative weights of structure for some of the considered materials as the weights are affected by temperature. All weights are shown relative to aluminum at room temperature. The type of construction assumed is the familiar skin-stringer construction. Above 200° aluminum begins to deteriorate. This temperature corresponds roughly to a Mach number of 2.

The data for beryllium are included as a matter of general interest. Beryllium is presently in short supply, very little is known about fabrication methods, and it is known to be toxic. It does, however, promise such a large weight advantage that considerable research should be initiated, particularly so because the supersonic transport is not the sole area of technological interest.

The data on this slide are not for long-time exposure or cyclic exposure to temperature changes such as will occur. Some data on aluminum, illustrated in figure 16, are not encouraging. With exposure of 10,000 hours at 350°, the aluminum alloy has lost 40 percent of its room-temperature strength. With a minimum 30,000-hour life requirement for the commercial transport, the use of aluminum would force the Mach number to values probably well below 2, where the aerodynamic efficiency is becoming too low to be of interest.

It appears now that the choice of materials will be steel with some use of titanium. In using the high-strength materials, skin-stringer construction will likely be replaced by sandwich construction for structural efficiency reasons. Figure 17 illustrates the relative weights for sandwich-type construction using the various materials previously discussed. All of the high-strength materials are superior to aluminum when sandwich construction is used. As with the skin-stringer construction, beryllium is the best and its relative advantage appears greater the higher the temperature.

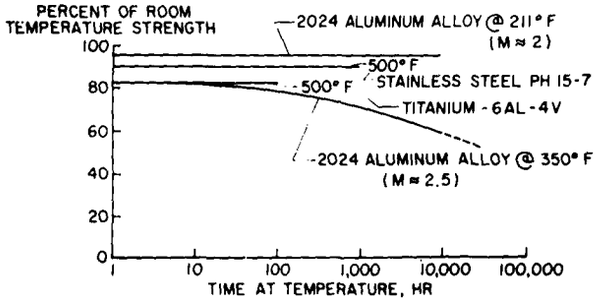
At this point, it is fair to state that we have a very considerable knowledge in the materials area. However, not much of this has been obtained under the environment or conditions under which the material must necessarily exist and exist for long lifetime. The environment in which the material must survive for the minimum required 30,000 hours of flight time is further illustrated by figure 18. Economic operation will require four or more flights as a daily average yielding not less than 8 and preferably up to 12 hours average daily flight time. The aircraft structure will thus make on the average four daily temperature cycles as illustrated by figure 18.

DESIGN CONDITIONS

	SUBSONIC JET	SUPERSONIC JET
ALTITUDE, FT	40,000	75,000
M.	.95	2 TO 3
DYN. PRESS.	600	1400
WEIGHT, LB	300,000	400,000 TO 600,000
TEMP.	COLD	500° F
MATERIAL	ALUMINUM	ALUM. OR STEEL
CONFIGURATION		

Figure 14

STRENGTH DETERIORATION OF TYPICAL METAL ALLOYS



NASA

Figure 16

STRUCTURAL WEIGHT SKIN-STRINGER CONSTRUCTION

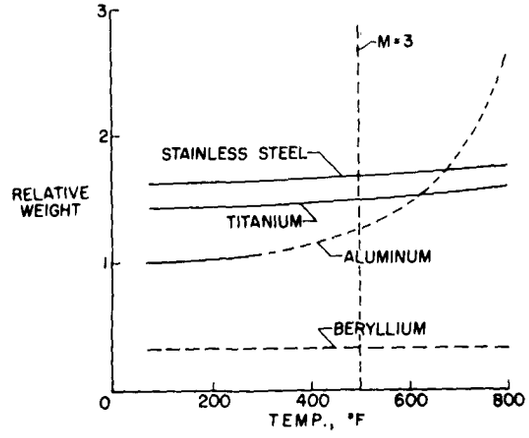


Figure 15

STRUCTURAL WEIGHT SANDWICH CONSTRUCTION

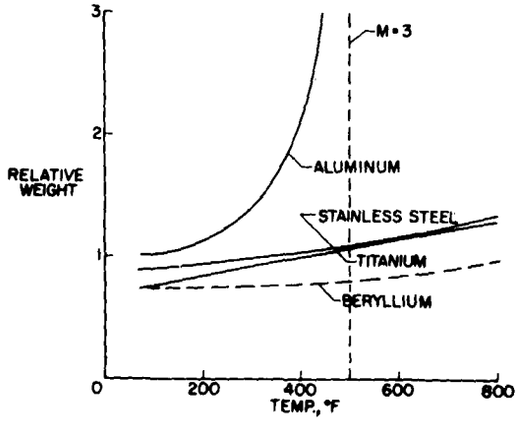


Figure 17

There are other special problem areas about which little is known and on which considerable research is necessary. Some of these are listed in figure 19.

Fatigue is perhaps the most important structural problem associated with present-day aircraft. Increasing aircraft speeds into the supersonic range is expected to compound the complexity of the fatigue problem (including sonic fatigue) because an additional parameter, temperature, is introduced. Comparatively little information is available on the fatigue behavior of materials at elevated temperature and practically no information is available on fatigue of aircraft structural components. Research into this field will undoubtedly accelerate when the environmental conditions and types of construction are more clearly defined. One problem associated with fatigue that will continue to be of concern is the problem of explosive failure of pressurized fuselages. Research into this problem at room temperature has been under way for several years. Very few studies of this type have been made to extend the knowledge to the temperatures associated with the supersonic transport.

Creep, in general, is not expected to be a problem of major concern in supersonic transports for titanium-alloy or stainless-steel construction. Some studies have shown that creep will not occur at the working stresses to which the structures will be subjected at elevated temperatures. The exception to this may occur if aluminum-alloy structures are used at temperatures above 300° F for long periods.

Air conditioning will be of special concern in flight at supersonic speeds. Special attention to insulation and air conditioning of spaces for the passengers, crew, and cargo will be required, and at the high Mach numbers heat-protection systems for the fuel will be necessary. If conventional insulation and air-conditioning systems are employed to maintain cabin temperature at, say, 70° F, sufficient weight may be involved to effectively increase fuselage weight as much as 50 percent. New concepts in maintaining satisfactory temperatures within the aircraft are being considered, and these indicate that efficient and relatively lightweight cooling systems may be obtained.

One of the major items of concern regarding the supersonic transport is construction cost. Two types of construction have been discussed here. Of these, the skin-stringer type is considerably cheaper than the sandwich-plate construction. Skin-stringer construction utilizing conventional aluminum alloys costs approximately $25 per pound of structure. For sandwich construction utilizing brazed honeycomb, this cost may approach $200 per pound of structure. Because of such large differences in construction costs, many studies will be needed to determine the type of construction to be used. The high cost of sandwich construction coupled with the substantial saving in structural weight will be compared with cheaper methods of construction

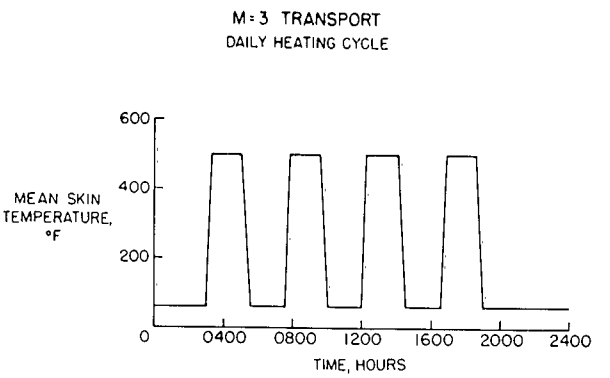


Figure 18

PROBLEM AREAS

1. FATIGUE
   (a) MATERIALS AND STRUCTURES
   (b) SONIC (NOISE) FATIGUE
   (c) EXPLOSIVE FAILURE

2. CREEP

3. AIR CONDITIONING

4. CONSTRUCTION COSTS
   (a) SKIN-STRINGER ($25 PER LB.)
   (b) SANDWICH PLATE ($200 PER LB.)

Figure 19

that result in increased structural weights. At the present time, it cannot be said which type of construction will be favored. The predicted overall economy of the aircraft will obviously be a major factor in the selection of the type of construction.

APPENDIX B

SEVENTH SAGAMORE ORDNANCE MATERIALS RESEARCH CONFERENCE

AUGUST 16, 17, 18 and 19, 1960

ATTENDEE LIST

Abbott, Kenneth H.	Watertown Arsenal, Watertown 72, Mass.
Achbach, Wm. P.	Battelle Memorial Institute, 505 King Ave., Columbus, Ohio
Adams, C. M.	Massachusetts Institute of Technology, Cambridge, Mass.
Angerman, R.	Special Project Dept. Borg-Warner Corp., Kalamazoo, Mich.
Anthony, H. L.	Mellon Institute, 4400 Fifth Ave., Pittsburgh 13, Pa.
Arnold, S. V.	Watertown Arsenal, Watertown 72, Mass.
Backofen, W. A.	Massachusetts Institute of Technology, Cambridge, Mass.
Barrett, John C.	Office of Director Defense Research & Engineering, Pentagon, Washington, D. C.
Beeuwkes, R. Jr.	Ordnance Materials Research Office, Watertown 72, Mass.
Bernstein, H.	Special Projects Office, Dept. of the Navy, Washington 25, D. C.
Bhat, G. K.	Mellon Institute, 4400 Fifth Ave., Pittsburgh 13, Pa.
Bluhm, J. I.	Watertown Arsenal, Watertown 72, Mass.
Brothers, A. J.	Materials & Processes Lab., Bldg. No. 6-145, General Electric Co., 1 River Rd., Schenectady, N. Y.
Brown, Wm. F. Jr.	Lewis Research Center, National Aeronautics & Space Admin. 21000 Brookpark Rd. Cleveland, Ohio
Burke, John	Ordnance Materials Research Office, Watertown 72, Mass.
Burns, T. H.	Thiokol Corp., Huntsville, Alabama
Carman, C. M.	Frankford Arsenal, Philadelphia 37, Pa.
Corten, H. T.	321a Talbot Laboratory, University of Illinois, Urbana, Ill.
Culp, Neil J.	Carpenter Steel Co., Front & Bern Sts., Reading, Pa.
Darcy, G. A.	Watertown Arsenal, Watertown 72, Mass.
Dawson, John	Office of Ordnance Research, Box CM, Duke Station, Durham, N. C.
Duerr, Thomas	Army Rocket & Guided Missile Agency, Propulsion Laboratory - OML Division Redstone Arsenal, Huntsville, Alabama
England, D. E.	USAF-AFFTC, Edwards Air Force Base, California
Esgar, J. B.	Lewis Research Center, National Aeronautics & Space Admin. 21000 Brookpark Rd., Cleveland, Ohio
Furgason, C.	Ladish Co., Cudahy, Wisc.
Galbraith, R. A.	Syracuse University, College of Engineering, Syracuse 10, N. Y.
Goodman, J.	Space Tech. Laboratories, Inc. P. O. Box 95001, Los Angeles, Cal.
Graae, A.	Allegheny Ludlum, Watervliet, N. Y.
Grewal, K. S.	Syracuse Research Institute, Syracuse 10, N. Y.
Hall, T. H.	British Joint Services Mission, 1800 K. St., N. W., Washington, D. C.

Hamaker, J.	Vanadium Alloys Steel Co., Latrobe, Pa.
Hartbower, C.	Watertown Arsenal, Watertown 72, Mass.
Hendricks, P. L.	Materials Central, Wright Air Development Division, Wright-Patterson Air Force Base, Ohio
Hoffman, Oscar	Missiles & Space Division, Lockheed Aircraft Corp., Palo Alto, Cal.
Holmes, A. G.	Lewis Research Center, NASA, 21000 Brookpark Rd., Cleveland, Ohio
Hurlich, A.	Convair Astronautics, 5001 Kearny Mesa, San Diego 12, Cal.
Irwin, G. R.	Naval Research Laboratory, Washington 25, D. C.
Jahnle, H.	Budd Co., 2450 Hunting Park Ave., Philadelphia 32, Pa.
Jones, A. F.	Ordnance Materials Research Office, Watertown 72, Mass.
Jones, E. S.	Flight Propulsion Laboratory Dept., General Electric Co., Cincinnati, Ohio
Jones, J. P.	Ordnance Tank Automotive Command, Detroit Arsenal, Center-line, Michigan
Kalpakcioglu, Serope	Cincinnati Milling Machine Co., Cincinnati 9, Ohio
Kearns, T. F.	Bureau of Naval Weapons, Washington 25, D. C.
Keller, D. V.	Syracuse University Research Institute, Syracuse 10, N. Y.
Kies, J. A.	Naval Research Laboratory, Code 6210, Washington 25, D. C.
Kinsey, D. W.	U.S. Steel Co., 525 William Penn Pl., Pittsburgh, Pa.
Koehler, R. B.	Office of Chief of Ordnance, ORDTB, Washington, D. C.
Korman, S.	Republic Aviation Co., Farmingdale, L. I.
Kosting, P. R.	Office of Ordnance Research, Box CM, Duke Station, Durham, N. C.
Kula, Eric B.	Watertown Arsenal, Watertown 72, Mass.
Larson, F. R.	Watertown Arsenal, Watertown 72, Mass.
Latorre, J. V.	Syracuse University Research Institute, Syracuse 10, N. Y.
Lindh, D. V.	Mellon Institute, 4400 Fifth Ave., Pittsburgh 13, Pa.
Lula, R. D.	Allegheny Ludlum Steel Co., Research Labs., Brackenridge, Pa.
Manning, George	Battelle Memorial Institute, 505 King Ave., Columbus, Ohio
Marble, J. D.	Flight Propulsion Laboratory Dept., General Electric Co., Cincinnati, Ohio
Markus, Harold	Frankford Arsenal, Philadelphia 37, Pa.
Martin, J. L.	Ordnance Materials Research Office, Watertown 72, Mass.
Matesky, S. J.	Bureau of Naval Weapons, Missile Propulsion Division (RMMP-2), Rm. 2223 Munitions Bldg., Washington, D. C.
McCaughey, J. M.	Pitman-Dunn Labs., Frankford Arsenal, Philadelphia 37, Pa.
Mertz, E. R.	Aerojet General Corp., P. O. Box 1168, Sacramento, Cal.
Minkler, W. W.	Titanium Metals Corp. of America, 233 Broadway, New York 7, N. Y.
Morrison, J. D.	Southern Research Institute, Birmingham, Alabama
Murphy, W. J.	U.S. Steel Co., Applied Research Labs., Monroeville, Pa.

Norem, A. G.	Institute for Defense Analysis, Pentagon, Washington, D. C.
Powell, Ross C.	Pratt & Whitney Aircraft Division, United Aircraft Corp., 400 Main St., E. Hartford, Conn.
Pschera, K. G.	Marshall Space Flight Center, NASA, Redstone Arsenal, Alabama
Reed, N. L.	Ordnance Materials Research Office, Watertown 72, Mass.
Richmond, F.	Universal Cyclops Steel Corp., Bridgeville, Pa.
Rostoker, W.	Armour Research Foundation, 10 W. 35th St., Chicago, Ill.
Rustay, A.	Wyman-Gordon Co., Grafton Plant, 105 Madison St., Worcester 1, Mass.
Sachs, G.	Syracuse University Research Institute, Syracuse 10, N.Y.
Salter, C. B.	Ordnance Tank Automotive Command, Detroit Arsenal, Centerline, Mich.
Scavuzzo, J.	Picatinny Arsenal, Dover, N.J.
Schapiro, L.	Missiles & Space Division, Lockheed Aircraft Corp., Palo Alto, Cal.
Schneider, E. C.	Pratt & Whitney Aircraft Division, United Aircraft Corp., E. Hartford, Conn.
Sessler, J. G.	Syracuse University Research Institute, Syracuse 10, N.Y.
Sharp, W. H.	Pratt & Whitney Aircraft Division, United Aircraft Corp. E. Hartford, Conn.
Sheehan, J.	Armour Research Foundation, 10 W. 35th St., Chicago, Ill.
Sippel, G. R.	Allison Division, General Motors, Indianapolis 6, Ind.
Sohn, J.	Wright Aeronautical Division, Curtiss-Wright Corp., Wood-Ridge, N.J.
Spaeth, C. E.	Pratt & Whitney Aircraft Division, United Aircraft Corp., E. Hartford, Conn.
Srawley, J. E.	Naval Research Laboratory, Washington 25, D.C.
Stack, John	Langley Research Center, NASA, Langley Field, Va.
Stapleton, T. J.	Lockheed Aircraft Corp., Burbank, California
Stark, Philip	Manufacturing Laboratories, Cambridge, Mass.
Sullivan, J. F.	Watertown Arsenal, Watertown 72, Mass.
Sweet, J. W.	Boeing Airplane Co., Seattle, Wash.
Tarr, A.	Army Research Office, Pentagon, Washington 25, D.C.
Tidwell, C.	Marshall Space Flight Center, NASA, Redstone Arsenal, Huntsville, Alabama
Voth, R. J.	Ryan Aeronautical Co., P.O. Box 311, San Diego, Cal.
Wallace, P.B.	Thiokol Corp., Huntsville, Alabama
Watson, J. F.	Convair Astronautics, 2612 Deerpark Dr., San Diego, Cal.
Weiss, Volker	Syracuse University Research Institute, Syracuse 10, N.Y.
Werner, F.	Westinghouse Electric Co., Research Labs., Beulah Rd. Churchill Boro, Pittsburgh 35, Pa.
Wilson, W. J.	Kaiser Fleetwing, Bristol, Pa.
Wundt, B.M.	Large Steam Turbine Division, General Electric Co., Schenectady, N. Y.